ENG.20070115.0006

QA: QA

ANL-SSD-GE-000001 REV 00

January 2007

Subsurface Geotechnical Parameters Report

Prepared for:
U.S. Department of Energy
Office of Civilian Radioactive Waste Management
Office of Repository Development
1551 Hillshire Drive
Las Vegas, Nevada 89134-6321

Prepared by:
Bechtel SAIC Company, LLC
1180 Town Center Drive
Las Vegas, Nevada 89144

Under Contract Number
DE-AC28-01RW12101

DISCLAIMER

This report was prepared as an account of work sponsored by an agency of the United States Government. Neither the United States Government nor any agency thereof, nor any of their employees, nor any of their contractors, subcontractors or their employees, makes any warranty, express or implied, or assumes any legal liability or responsibility for the accuracy, completeness, or any third party's use or the results of such use of any information, apparatus, product, or process disclosed, or represents that its use would not infringe privately owned rights. Reference herein to any specific commercial product, process, or service by trade name, trademark, manufacturer, or otherwise, does not necessarily constitute or imply its endorsement, recommendation, or favoring by the United States Government or any agency thereof or its contractors or subcontractors. The views and opinions of authors expressed herein do not necessarily state or reflect those of the United States Government or any agency thereof.

BSC	Scientific Analysis Signature Page/ Change History Complete only applicable items.	Page iii 1. Total Pages: 664

2. Scientific Analysis Title

Subsurface Geotechnical Parameters Report

3. DI (including Rev. No.)

ANL-SSD-GE-000001 Revision 00

	Printed Name	Signature	Date
4. Originator	Fei Duan (Lead)		1/10/07
5. Checker	David Tang		1/10/07
6. QER	Dan Tunney		1/10/2007
7. Responsible Manager/ Lead	Fei Duan		1/10/07
8. Responsible Manager	Robert Saunders		1/10/07

9. Remarks

Authors of this document are as follows:

Sections 1 through 5	J.B. Cho, F. Duan, M. Mrugala
Section 6.1	D. Suarez
Section 6.2	J.B. Cho, F. Duan
Section 6.3	F. Duan, M. Mrugala
Section 6.4	J.B. Cho, M. Mrugala, D. Suarez
Section 6.5	F. Duan (The information presented in Section 6.5 was provided by J. Leem).
Section 6.6	F. Duan, M. Mrugala
Section 6.7	F. Duan, M. Mrugala
Section 7	F. Duan, M. Mrugala
Section 8 and DIRS	J.B. Cho
Appendices and CD	J.B. Cho, M. Mrugala

Total Number of Pages for Appendices: 182 plus 1 CD

Appendix A: 31

Appendix B: 16

Appendix C: 32

Appendix D: 55

Appendix E: 14

Appendix F: 23

Appendix G: 9

Appendix H: 2 plus 1CD

Change History

10. Revision No.	11. Description of Change
REV 00A	Initial Issue 800-K0C-WIS0-00400-000-00A
ANL-SSD-GE-000001 REV 00	Revised Initial Issue 800-K0C-WIS0-00400-000-00A

INTENTIONALLY LEFT BLANK

EXECUTIVE SUMMARY

General—This report, *Subsurface Geotechnical Parameters Report*, Revision 00 and referred as SGPR REV 00, provides a summary of geotechnical data developed to support engineering design and performance assessment. Activities documented in this report involve thoroughly searching and identifying all geotechnical source data existing in the Technical Data Management System, systematically checking and verifying the data entries, analytically and empirically deriving the site-specific mechanical properties of the rock mass, and performing calculations and statistical analyses to determine the ranges and magnitude distributions of the existing laboratory and field data. Site geology, stratigraphy, stratigraphic nomenclature, and lithostratigraphic structural features are included to provide a framework for presentation of the properties for both the intact rock and rock mass.

SGPR REV 00 focuses on assessment of intact rock physical, mechanical, time dependent and thermal properties; rock mass quality estimates; and estimated rock mass physical, thermal, and mechanical properties. Data for each parameter are summarized and implications of the geotechnical data impact on engineering design and performance assessment are reviewed. This report evaluates the data variability and the level of data completeness to support repository design and performance assessment.

Data available through March 2006 was used herein. A major portion of the revision effort was expended on evaluating and sorting the above-mentioned Technical Data Management System data according to significant rock material conditions (e.g., size, temperature, saturated or dry, etc.) and methods of testing. Although SGPR REV 00 contains a summary of all geotechnical data available, the inclusion of all aspects of data analyses was not always practical. In effect, three separate calculations were prepared that address the intact rock property data, results of the field mapping and rock mass quality ratings, and lithophysal rock mass mechanical properties, respectively. These individual calculations function as topical reports to support the development of SGPR REV 00.

New Work Completed Since Initial Edition of *Subsurface Geotechnical Parameters Report* (SGPR REV 00A)—During development of the SGPR REV 00A, a large portion of intact rock data still required a thorough checking to verify the data correctness and, to the extent possible, to eliminate errors and enhance data integrity and traceability to data sources. A separate calculation, *Intact Rock Mechanical Properties of Yucca Mountain Stratigraphic Units*, was completed where the entire population of intact rock data was assembled, computations and statistical analyses were performed, and results were compiled to provide one location where traceable data can be obtained. The appropriate statistical data analyses of the acquired and developed parameter database were performed, and by combining all qualified and analyzed test data in one central location, comprehensive tables of intact rock mechanical parameters were prepared (Section 6.4.2).

The initial scope of work to develop rock mass parameters for the nonlithophysal rock only using conventional rock mass rating approach was extended to include the entire sequence of Yucca Mountain rock units from the surface to the repository host horizon. This decision was dictated by the need for developing one methodology that would serve as a benchmark for all rock units. It was also supported by the practical need to tie the laboratory and numerical analyses to the

readily verifiable field evidence—the existing system of underground openings (Exploratory Studies Facility, Enhanced Characterization of the Repository Block Cross-Drift, and heated drift) and observation of their performance. It was apparent that a "reality check" would be beneficial for reconciling results generated while applying different approaches. A "reality check" was performed to verify the representativeness of rock mass properties by comparing them to the results obtained from closed-form calculations (Section 6.4.4.4.1.2). The check to revealed that, in some cases, overly conservative test conditions adopted in the laboratory testing program resulted in low estimates of rock mass strength. While the data presented in SGPR REV 00A focused primarily on the lithophysal and nonlithophysal rock units of the repository host horizon, SGPR REV 00 provides additional data characterizing other lithostratigraphic units located at and above the repository host horizon (Section 6.4.4 4.1).

The qualified laboratory rock strength data, results of the field mapping, and rock mass quality and rock mass rating estimates were analyzed in *Rock Mass Quality Ratings and Classifications of the Combined ESF, Heated Drift and ECRB Cross Drift*. These data were used to estimate properties of the rock mass. The previous approach of treating each lithostratigraphic unit as one of the major thermal-mechanical units was enhanced by developing a more refined rock mass property database including information on each distinct rock strata (Section 6.4.4 4.1). Also, mechanical properties for the rock above and below the repository host horizon have been evaluated in a consistent manner, which was not done previously.

The unique characteristics of lithophysal rock units and the need to better understand their response to the repository-induced stress and temperature environments led to significant effort spent on the description and the demonstration of the applicability of alternative numerical simulation techniques. These techniques, when used in combination with laboratory data, enhance engineers' understanding of rock behavior and processes occurring within the lithophysal rock mass units.

A new Section 6.4.2.4, summarizing tests on time-dependent behavior of tuff was added. Test data include the latest results on tuff creep obtained between January 2, 2004, and February 25, 2005. For nonlithophysal rock, the temporal variation in mechanical rock mass behavior relates to the degradation of the fracture strength parameters. The data presented in this section will be used to address the impact of time-dependent behavior on drift degradation and to address a set of issues related to the postclosure behavior of tuff. Time-dependent numerical simulation and residual fracture strength characterization are planned activities for the near future in a separate effort related to investigating drift degradation.

The qualified data included in this report are representative, however, a large portion of density and porosity data still remain to be qualified. Completion of the qualification process for the remaining data will be completed during the LA defense period, which will further enhance the existing density and porosity database for the RHH rock units. In addition, it will also enlarge the database to cover the strata above the RHH, resulting in a better representation of rock property spatial variability and a further enhancement of licensing defensibility. The qualified data on dry bulk density and matrix porosity pertaining mainly to the RHH units are included in Section 6.4.1.

***Data Summary*—**SGPR REV 00 provides a summary of all available and qualified geotechnical parameters required for design of underground facilities. These design parameters include the following:

- ***Physical properties***: density and porosity
- ***Mechanical properties of the intact rock***: Young's modulus and Poisson's ratio, uniaxial (unconfined) compressive and tensile strengths, cohesion, internal angle of friction, and confined compressive strength. Also included for parameters are their dependency on size, location (spatial), and time (temporal)
- ***Mechanical properties of the rock mass***: Young's modulus and Poisson's ratio, uniaxial (unconfined) compressive and tensile strengths, cohesion, internal angle of friction, and compressive strength. Also included are their dependency on size, location (spatial), and time (temporal), and their associated uncertainty
- ***Mechanical properties of joints/fractures***: normal and shear stiffness, cohesion, friction angle, dilation angle, and strength degradation
- ***Index properties of rock mass***: rock quality designation, rock mass rating, and rock mass quality
- ***Thermal properties***: thermal conductivity, specific heat, coefficient of thermal expansion, and also including their depending on temperature porosity and moisture content.

These parameters have always constituted key inputs to repository opening stability evaluations, ground support design analyses, and rockfall predictions throughout project development phases such as viability assessment, site recommendation and current licensing application. SGPR REV 00 provides not only a location for geotechnical parameters at, above, and below the repository host horizon, but also an anchor for assessing data transparency, traceability, and completeness. The design engineer is presented with a single document containing the complete set of qualified data and their sources needed to pursue design activities. From the designers' perspective this data is considered adequate and is sufficient for subsurface design in support of a license application.

SGPR REV 00 provides the foundation of a living document that will be updated periodically as dictated by additional geotechnical testing data, further field measurements and observations, improved data analysis techniques, and special project needs, such as licensing defense and performance confirmation support. The need for additional rock property data will gradually diminish as further testing, simulation, and confirmation activities are carried out. As underground facilities are constructed, additional information will be obtained, allowing the subsurface geotechnical parameter database and general level of understanding to continue to expand with the advance and maturation of the project.

Performance Confirmation Program— The Performance Confirmation Program is intended to confirm baseline information regarding the response of the natural system to the design system and monitoring of the baseline data for changes that could affect performance of the designed subsurface openings during the preclosure period to ensure, in part, retrievability. The Performance Confirmation Program will serve multiple functions including: (1) recording instrument readings, (2) evaluating the performance of underground structures, and (3) reporting discrepancies observed during the course of subsurface facility development and operation. Existing geotechnical data must be systematically compiled for traceability, checked for accuracy, organized for transparency, analyzed for adequacy, stored for ready access, and managed for ready receipt of, objective appraisal on, and timely communication of new data. SGPR REV 00 serves as a significant milestone towards achieving this goal.

Data Enhancement—In conjunction with Section 6.7.4 on further data enhancements, it is suggested that a Geographic Information Systems-type relational database including spatial coordinates as key parameters be considered. Development of this new database and verification and summary of data therein should be accomplished with active participation of personnel specializing in both database design and development and personnel well versed in rock property testing and rock parameter usage in design. Once developed, this relational database should be controlled and become the sole source of data for all appropriately acquired and derived subsurface rock parameters.

Future revisions of this report will point to further enhancement of the existing data, allowing for higher-level derivations of parameters to be performed with even greater confidence. In effect, more informed descriptions of parameters including uncertainties and spatial and temporal variabilities will be developed. Future revisions of this document will ensure that additional data and analyses become available to all interested parties, and that information will be maintained current for use by the different scientific and engineering groups developing assessments and designs for the repository.

The advantage of using numerical simulations of lithophysal rock mass behavior using Particle Flow Code and Universal Distinct Element Codes has been demonstrated and preliminary results from some of these simulation efforts are discussed in this report. Further work is needed to describe and demonstrate the range of applicability of these preliminary, alternative numerical simulation techniques, which when used in combination with limited laboratory and/or field data, enhance engineers' understanding of rock behavior. Numerical simulation is particularly useful in work related to investigation of time-dependent degradation of rock properties.

Initial steps were taken on the development of a Geographic Information Systems-relational database. It is recommended that this work be assigned a high priority as there is great potential benefit of making not only geotechnical but other Yucca Mountain Project-related data widely accessible, traceable, transparent, and easy to update. All properly reviewed data on the Project can be placed in this database.

Monitoring and periodical analysis of Exploratory Studies Facility and the Enhanced Characterization Repository Block Cross-Drift tunnel deformation monitoring, steel sets monitoring, and gathering of any construction records should continue and should be used to augment site-specific evaluation of the performance of rock mass.

It is understood that this subsurface geotechnical parameters report is a living document. As the Yucca Mountain Project enters a new stage leading to construction and access to the new sections of the future repository block, new revisions of this report will become necessary to accommodate the flow of new data.

Data Uncertainty, Spatial Variability and Adequacy—The extent to which geotechnical parameters, based on measurements from a finite set of samples, can be used to characterize in situ conditions of lithostratigraphic units at Yucca Mountain is affected by uncertainties associated with the available data and in the parameters used to characterize the units. The uncertainty and variability in the data, and therefore, the determination of geotechnical parameters are due, in part, to the natural variability and heterogeneity in subsurface geologic conditions. For example, uncertainty is affected by natural variations in geotechnical parameters within and between the lithostratigraphic units, including the precise nature and extent of the fracture network and presence, size, and extent of lithophysae, as well as other naturally occurring variations in the rock mass. Additional uncertainty can be introduced through the selection of sampling and testing methodologies, time dependencies, and up-scaling effects. Uncertainty in data produces corresponding uncertainty in the description of resulting geotechnical models and processes.

Due to the naturally occurring spatial variation in the thickness and extent of the lithostratigraphic units at Yucca Mountain and the accessibility of units to sampling, the number of samples available to characterize various units can vary significantly. As a result, quantification of uncertainties presents challenges specific to the lithostratigraphic unit and the representative sample population. Therefore, the sample size, as well as natural and introduced uncertainties, contributes to the overall assessment of data and parameter uncertainties derived to characterize each lithostratigraphic unit.

When using geotechnical parameters derived from relatively small sample specimens to describe the strength of the rock mass with associated voids, fractures, and all other natural variabilities, scaling effects must be considered. Even the relatively populous data set available for lithostratigraphic units of the repository host rock must be treated with caution while this relationship between size and scale is being defined. The presence and size of lithophysal voids, which can exceed sample size within the rock mass, presents a unique challenge when up-scaling parameter assessments derived from the sample scale. Since the effects of these large voids can not be directly assessed due to sample size limitations, computer simulations are used to assess the nature and mechanisms impacting the strength and performance of the rock mass and associated uncertainties. Computer simulation can be used to assess the impact of parameters spanning the range of uncertainty by examining a variety of hypothetical scenarios.

The design of underground excavations may also require consideration of time-dependent effects on the rock mass and ground support materials that result from environmental parameters, e.g., ground saturation, variable temperature, ground chemistry, and seismic ground motion input. The time factor included in an analysis and associated time-dependent properties of rock introduce additional variables that will contribute to the overall uncertainty characterizing the final design product.

The consequence of the representativeness of the data must be judged in the context of the potential contribution from the uncertainties on the intended use in subsurface design products, e.g., tunnels, shafts, or other subsurface openings. In effect, the user of geotechnical data and rock parameters presented in this analysis is advised to exercise caution while using any and all data presented herein. The details pertaining to each data set should be consulted to verify the potential ranges of each parameter considering the number of tests, test attributes and the purpose of the particular calculations or analysis. Throughout this analysis, wherever appropriate, potential types of uncertainties and identification of their sources is provided to benefit subsequent quantification by the users of this data.

CONTENTS

Page

CONTENTS (Continued)

Page

CONTENTS (Continued)

Page

CONTENTS (Continued)

Page

CONTENTS (Continued)

Page

INTENTIONALLY LEFT BLANK

FIGURES

Page

FIGURES (Continued)

Page

FIGURES (Continued)

Page

FIGURES (Continued)

Page

FIGURES (Continued)

Page

FIGURES (Continued)

Page

FIGURES (Continued)

Page

INTENTIONALLY LEFT BLANK

TABLES

Page

TABLES (Continued)

Page

TABLES (Continued)

Page

TABLES (Continued)

Page

ACRONYMS AND ABBREVIATIONS

ACRONYMS

AMR	Analysis and Modeling Report
ASTM	American Society for Testing and Materials
BSC	Bechtel SAIC Company, LLC
CR	Condition Report
CRWMS	Civilian Radioactive Waste Management System
CTE	coefficient of thermal expansion
DIRS	Document Input Reference System
DOE	U.S. Department of Energy
DST	drift scale test
DTN	data tracking number
ECRB	Enhanced Characterization of the Repository Block
EPA	U.S. Environmental Protection Agency
ESF	Exploratory Studies Facility
GIS	Geographic Information Systems
GSI	Geologic Strength Index
HD	heated drift
ITS	important to safety
JRC	joint roughness coefficient
KTI	Key Technical Issue
LVDT	linear variable differential transformer
MPBX	multi-point borehole extensometer
NRC	U.S. Nuclear Regulatory Commission
NRG	North Ramp Geologic (boreholes associated with north access ramp)
NWPA	Nuclear Waste Policy Act
PFC	Particle Flow Code (software)
QA	quality assurance
RDTME	Repository Design and Thermal-Mechanical Effects
REKA	rapid evaluation of K and Alpha (thermal probe method)
RH	relative humidity

ACRONYMS AND ABBREVIATIONS (Continued)

RHH	repository host horizon
RMR	rock mass rating
RQD	rock quality designation
SC	Safety Category
SCC	stress corrosion cracking
SCFZ	Solitario Canyon Fault Zone
SGPR	*Subsurface Geotechnical Parameters Report*
SGR	Site Geotechnical Report
SHT	single heater test
SNL	Sandia National Laboratories
TBM	tunnel boring machine
TDMS	Technical Data Management System
TSPA	total system performance assessment
UCS	unconfined compressive strength
UDEC	Universal Distinct Element Code
UE	underground exploratory
USBR	United States Bureau of Reclamation
USGS	United States Geological Survey
VPP	vapor phase partings
YMP	Yucca Mountain Project
YMRP	Yucca Mountain Review Plan

ABBREVIATIONS

CHn	Calico Hills nonwelded hydrogeologic unit
CHn1	Calico Hills and lower Paintbrush nonwelded thermal-mechanical unit
CHn2	Calico Hills and lower Paintbrush nonwelded thermal-mechanical unit
dam	decameter
HQ	borehole with core diameter of approximately 63.5 mm
kgf	kilogram force
kW	kilowatt
lbf	pound (mass) per foot
L/D	length to diameter (ratio)
PTn	Paintbrush nonwelded hydrogeologic unit Paintbrush nonwelded thermal-mechanical unit

ACRONYMS AND ABBREVIATIONS (Continued)

Tac	Calico Hills Formation
TCw	Tiva Canyon welded hydrogeologic unit Tiva Canyon welded thermal-mechanical unit
Tm	Timber Mountain Group
Tmbt1	pre-Rainier Mesa Tuff bedded tuff
Tmr	Rainier Mesa Tuff
Tp	Paintbrush Group
Tpbt1	pre-Topopah Spring Tuff bedded tuff
Tpbt2	pre-Pah Canyon Tuff bedded tuff
Tpbt3	pre-Yucca Mountain Tuff bedded tuff
Tpbt4	pre-Tiva Canyon Tuff bedded tuff
Tpbt5	post-Tiva Canyon Tuff bedded tuff
Tpc	Tiva Canyon Tuff
Tpc_un	Tiva Canyon Tuff—undifferentiated
Tpcpll	Tiva Canyon Tuff crystal-poor lower lithophysal zone
Tpcpln	Tiva Canyon Tuff crystal-poor lower nonlithophysal zone
Tpcpmn	Tiva Canyon Tuff crystal-poor middle nonlithophysal zone
Tpcpul	Tiva Canyon Tuff crystal-poor upper lithophysal zone
Tpcpv	Tiva Canyon Tuff crystal-poor vitric zone
Tpcr	Tiva Canyon Tuff crystal-rich member
Tpcrl	Tiva Canyon Tuff crystal-rich lithophysal zone
Tpcrn	Tiva Canyon Tuff crystal-rich nonlithophysal zone
Tpcrv	Tiva Canyon Tuff crystal-rich vitric zone
Tpk	rhyolite of Comb Peak
Tpp	Pah Canyon Tuff
Tpt	Topopah Spring Tuff
Tptp	Topopah Spring Tuff crystal-poor member
Tptpll	Topopah Spring Tuff crystal-poor lower lithophysal zone
Tptpln	Topopah Spring Tuff crystal-poor lower nonlithophysal zone
Tptpmn	Topopah Spring Tuff crystal-poor middle nonlithophysal zone
Tptpul	Topopah Spring Tuff crystal-poor upper lithophysal zone
Tptpv	Topopah Spring Tuff crystal-poor vitric zone
Tptpv1	Topopah Spring Tuff crystal-poor vitric zone nonwelded subzone
Tptpv2	Topopah Spring Tuff crystal-poor vitric zone moderately welded subzone
Tptpv3	Topopah Spring Tuff crystal-poor vitric zone densely welded subzone
Tptr	Topopah Spring Tuff crystal-rich member
Tptf	Topopah Spring Tuff lithic- rich zone
Tptrl	Topopah Spring Tuff crystal-rich lithophysal zone
Tptrn	Topopah Spring Tuff crystal-rich nonlithophysal zone
Tptrv	Topopah Spring Tuff crystal-rich vitric zone
Tptrv1	Topopah Spring Tuff crystal-rich vitric zone densely welded subzone
Tptrv2	Topopah Spring Tuff crystal-rich vitric zone nonwelded to moderately welded subzone
Tptrv3	Topopah Spring Tuff crystal-rich vitric zone nonwelded subzone
Tpy	Yucca Mountain Tuff

ACRONYMS AND ABBREVIATIONS (Continued)

TSw	Topopah Spring welded hydrogeologic unit
TSw1	Topopah Spring welded, lithophysal-rich thermal-mechanical unit
TSw2	Topopah Spring welded, lithophysal-poor thermal-mechanical unit
TSw3	Topopah Spring welded, vitrophyre thermal-mechanical unit
UO	Undifferentiated overburden thermal-mechanical unit

1. PURPOSE

1.1 BACKGROUND

In 1997, the U.S. Department of Energy (DOE) issued *Yucca Mountain Site Geotechnical Report* (SGR) (CRWMS M&O 1997 [DIRS 103564]). The purpose of SGR was to integrate the available qualified geotechnical data and nonqualified (corroborative) data gathered to support engineering design, safety analysis and performance assessment. Included in SGR are the data resulting from field and laboratory testing that were available through June 1996.

Most of the data in SGR (CRWMS M&O 1997 [DIRS 103564]) were derived from surface-based testing activities, primarily surface mapping and borehole exploration. In addition, SGR included some subsurface data references and a limited amount of the actual Exploratory Studies Facility (ESF) geologic mapping data from the North Ramp and from the Main Drift that were available through mid-March of 1997. Subsequent reviews and use of SGR information revealed the need for additional rock testing and updating the data, such as the need to better characterize lithophysae-rich lithostratigraphic zones. Subsequent activities have focused on acquiring the additional data considered necessary to support the License Application (LA). These characterization activities include field measurements, laboratory testing, in situ testing, numerical analysis and analytical assessment.

In July 2002, the U.S. Nuclear Regulatory Commission (NRC) published *Integrated Issue Resolution Status Report* (NRC 2002 [DIRS 159538]). Included in the NRC report were the Repository Design and Thermal-Mechanical Effects (RDTME) Key Technical Issues (KTIs). Geotechnical agreements were formulated to resolve a number of KTI subissues, in particular, RDTME KTIs 3.04, 3.05, 3.07, and 3.19 that relate to the physical, thermal and mechanical properties of the host rock (NRC 2002 [DIRS 159538], pp. 2.1.1-28, 2.1.7-10 to 2.1.7-21, A-17, A-18, and A-20).

The initial edition of *Subsurface Geotechnical Parameters Report* (SGPR), referred hereinafter as SGPR REV 00A (BSC 2003 [DIRS 166660]), was developed under AP-3.12Q, *Design Calculations and Analyses,* issued in December 2003 to present an account of available geotechnical information that helped respond to NRC comments on the closure of geotechnical parameters-related KTI subissues. This report, *Subsurface Geotechnical Parameters Report*, REV 00A, analyzed and summarized available qualified geotechnical data that existed in the Yucca Mountain Project (YMP) Technical Data Management System (TDMS) database through July 2003.

Subsurface Geotechnical Parameters Report, REV 00, is conceptualized to be a living document that will be updated as a result of newly acquired and developed information, as well as enhanced data reduction methodologies through the preclosure life of the repository. This revision of SGPR, referred as SGPR REV 00, incorporates data available in the TDMS database through March 2006. In addition, the corroborative data obtained from tests performed by non-BSC organizations and considered as non-qualified was discussed to reinforce conclusions derived based on the qualified data.

1.2 OBJECTIVES

As is stated in *Technical Work Plan for Subsurface Geotechnical Parameters Report* (BSC 2006 [DIRS 178063]), the objectives of SGPR REV 00 are to derive, analyze, summarize, and update thermal-mechanical properties for the rock mass within the repository footprint, with emphasis on enhancing both data transparency and traceability. It further evaluates the sufficiency and quality of data existing in the TDMS database as of March 2006, including some of the corroborative data obtained from tests performed by non-BSC organizations to support engineering design, performance assessment, and response to NRC follow-up actions on RDTME KTI closure (i.e., RDTME 3.04, 3.05 and 3.07). In addition, this SGPR REV 00 includes necessary content to address a number of geotechnical data issues and concerns that have been raised since the completion of SGPR REV 00A (BSC 2003 [DIRS 166660]). Overall, SGPR REV 00 is to:

- Provide an up-to-date summary of site-specific subsurface geotechnical parameters on the YMP
- Assess the quality of the source technical data
- Summarize important contextual information associated with particular parameters in order to ensure appropriate use of the parameters by users
- Systematically identify and quantify the uncertainties and spatial and temporal variability of the geotechnical parameters
- Evaluate the adequacy of data for license application activities.

1.3 SCOPE

The general work scope of SGPR REV 00 is outlined in *Technical Work Plan for Subsurface Geotechnical Parameters Report* (BSC 2006 [DIRS 178063]). During preparation of this SGPR REV00, it was determined that some of the criteria listed in technical work plan (BSC 2006 [DIRS 178063] are no longer relevant for this SGPR.REV 00 The revised criteria are provided in Sections 4.2.2 and 4.3.3.2. Activities documented in this revision involve developing rock property data, using analytical methods, and performing calculations and statistical analyses to determine the ranges and magnitude distributions of the existing laboratory and field data. SGPR REV 00 provides a summary of geotechnical data developed to support engineering design and performance assessment. Site geology, stratigraphy, stratigraphic nomenclature, and lithostratigraphic structural features are included to provide a framework for presentation of the rock and rock mass property data.

SGPR REV 00 focuses on physical rock property data; intact rock mechanical and thermal parameters; rock mass quality estimates; and estimated rock mass physical, thermal, and mechanical properties. In addition, in situ field testing data are discussed in this report. Specifically, geotechnical data for subsurface design have primarily involved the following parameters:

- Physical properties for the intact rock: density and porosity
- Mechanical properties for the intact rock: elastic properties (Young's modulus and Poisson's ratio), strength parameters (confined and unconfined compressive and tensile strengths), Mohr-Coulomb strength parameters (cohesion and internal friction angle), and rock mechanical properties dependency on size, location (spatial variations), and time (temporal variations)
- Mechanical properties for the rock mass: elastic properties (Young's modulus and Poisson's ratio), strength parameters, Hoek-Brown parameters, Mohr-Coulomb strength parameters (cohesion and internal friction angle), and rock mechanical properties dependency on size and location (spatial variations)
- Mechanical properties for joints/fractures: normal and shear stiffness, fracture strength (cohesion (c) and internal friction angle (ϕ)), dilation angle, and strength degradation
- Rock mass index properties: rock quality designation (RQD), rock mass rating (RMR), and rock mass quality (Q); these methods are sometimes referred as the RQD, RMR and Q indexes for rock classification
- Rock thermal properties: thermal conductivity, specific heat, and coefficient of thermal expansion (CTE).

For the SGPR REV 00A (BSC 2003 [DIRS 166660], data for each parameter are summarized, and implications of the geotechnical data impact on engineering design and performance assessment are reviewed. This SGPR REV 00 presents an evaluation of the data variability and the level of completeness to support repository design and repository performance assessment. The scope of work involved in developing SGPR REV 00 includes:

- Compiling relevant subsurface geotechnical data from the TDMS needed to develop the identified rock parameters
- Evaluating and sorting relevant geotechnical data according to significant rock material and testing conditions (e.g., size, temperature, saturated or dry, etc.)
- Performing computations and analyses of the compiled geotechnical data to determine the rock parameters supporting the license application
- Performing the appropriate statistical data analyses of the acquired and developed geotechnical parameters

- Providing comprehensive reference tables of geotechnical parameters by presenting relevant qualified and analyzed test data in one central location

- Describing and demonstrating the range of applicability for the alternative numerical simulation techniques, which when used in combination with available data will enhance the engineers' understanding of rock behavior, processes, and descriptions

- Developing a combined statistical and engineering judgment-based approach for assessment of data uncertainty, variability, and representativeness that will be used to produce recommended statistical values, ranges and distributions for subsurface rock parameters.

Providing a preliminary definition and assessment of data adequacy for the license application.

SGPR REV 00 intends to provide a common source of geotechnical parameter data to be used by various engineering disciplines in the process of designing underground components of the repository.

1.4 ANALYSIS APPLICABILITY AND LIMITATIONS

SGPR REV 00A (BSC 2003 [DIRS 166660]) focused primarily on parameters of the lithophysal and nonlithophysal rock units of the repository host horizon (RHH) existing in the TDMS as of July 2003. SGPR REV 00 summarizes all the existing geotechnical data for lithostratigraphic rock units above, at and below the RHH, and includes data available in the TDMS database through March 2006.

The geotechnical data summarized in SGPR REV 00 are considered to be valid and are appropriate for license application design activities in accordance with the design criterion provided in Section 4.2.1. All data presented in this report are qualified, except where specifically stated otherwise (i.e., corroborative data).

2. QUALITY ASSURANCE

The technical work plan (BSC 2006 [DIRS 178063], Section 8.1) determined that this activity was subject to the requirements of *Quality Assurance Requirements and Description* (DOE 2006 [DIRS 177092]). Generally, the work performed by the Bechtel SAIC Company, LLC (BSC) is now subject to the requirements of the BSC *Quality Management Directive* (BSC 2006 [DIRS 177655]). The technical work plan did not specify a quality level for this activity. However, this activity of developing the SGPR REV 00 involves items and barriers which are expected to be classified as Safety Category. Accordingly, this activity is considered Quality Level 1 in accordance with EG-PRO-3DP-G04T-00905, *Determination of Quality Levels*, Section 3.2.1. The subsurface rock descriptions and parameters developed and presented in SGPR REV 00 will be used as inputs in a number of analysis and modeling activities that support performance assessment, and in design of ground support systems in emplacement drifts and all other underground openings. Some of these activities are associated with the emplacement and retrieval system and the engineered barrier system, which were classified as Safety Category (SC) systems in *Q-List* (BSC 2005 [DIRS 175539], p. A-7), and with some Subsurface Facility openings classified as SC components in *Q-List* (BSC 2005 [DIRS 175539], p. A-11). This work also supports the characterization of the natural barriers important to waste isolation that were classified as SC on *Q-List* (BSC 2005 [DIRS 175539], pp. A-8 and A-12). These categories were determined in accordance LS-PRO-0203, *Q-List and Classification of Structures, Systems, and Components*. It is noted that the current *Q-List* has been cancelled recently. However, the results of this SGPR REV 00 are not impacted because it has not been used as direct input.

The SGPR REV 00 was guided by a technical work plan (BSC 2006 [DIRS 178063]) prepared in accordance with LP-2.29Q-BSC, *Planning for Science Activities*, and was developed in accordance with procedures LP-SIII.9Q-BSC, *Scientific Analyses*, IT-PRO-0011, *Software Management*, and PA-PRO-0301, *Managing Technical Product Inputs*. SGPR REV 00 was reviewed following PA-PRO-0601, *Document Review*. The electronic management of data is controlled in accordance with Section 8.4 of the technical work plan.

INTENTIONALLY LEFT BLANK

3. USE OF SOFTWARE

All software documented in this section is appropriate for applications used in this document. The software is managed under IT-PRO-0011, *Software Management*, and was obtained from Software Configuration Management in accordance with IT-PRO-0011.

3.1 LEVEL 1 SOFTWARE

Level 1 software was not directly used to prepare this document.

3.2 LEVEL 2 SOFTWARE

Level 2 software used in this document includes Microsoft® Excel® 2000 SP-3 (STN: 003743-E), JMP™ Version 5.1 (STN: 610337), and RocLab® Version 1.020 (STN: 611192). These software programs were used to perform support calculation activities and visual representation as described in Section 6, and associated Appendices.

Commercially available software such as support software (i.e., systems software and software tools), word processors, spreadsheets, database managers, and other types of automated office support systems are Level 2 software products in accordance with IT-PRO-0011, Attachment 12. Accordingly, Excel® 2000 SP-3, JMP™ Version 5.1, and RocLab® Version 1.020 are Level 2 software applications. All software in this category was performed on personal computers with a Pentium® microprocessor and Microsoft® Windows® 2000 operating system. All supporting excel files are archived on a CD-ROM included as part of Appendix H.

Excel® 2000 was used to perform data manipulation and some arithmetic and statistical calculations. Standard functions of Excel® were used in Section 6.

JMP™ was used to perform statistical analysis of the intact rock mechanical properties data.

RocLab® was used to perform the analysis of rock mass strength. RocLab is a product of RocScience Inc. and is a software program for determining rock mass strength parameters based on the generalized Hoek-Brown failure criterion. Only standard built-in functions of RocLab® were used and the results are not dependent on the use of RocLab®.

The results of calculations from Level 2 software were verified by performing arithmetic analysis.

3.3 INDIRECT LEVEL 1 SOFTWARE

Other qualified software are cited in SGRP REV 00, such as Particle Flow Code (PFC) PFC2D (V.2.0, STN: 10828-2.0-00 [DIRS 161950]; V.2.0, STN: 10828-2.0-01 [DIRS 169930]) and PFC3D (V.2.0, STN: 10830-2.0-00 [DIRS 160612]; V.2.0, STN: 10830-2.0-01 [DIRS 169931]), Universal Distinct Element Code (UDEC) (V.3.1 Sub-Release 3.10.109, STN: 10173-3.1-00 [DIRS 161949]) and FRACMAN V2.512 [DIRS 160577] are cited in this document; however, these codes are not used directly in this document. PFC 2D and 3D and UDEC codes were used in the calculation *Lithophysal Rock Mass Mechanical Properties of the Repository Host Horizon* (BSC 2004 [DIRS 172334]), which supports this document. Details of

these codes are presented by BSC (2004 [DIRS 172334]) and are summarized in the following paragraphs.

The PFC simulation represents rock as a number of small, rigid, spherical grains that are bonded together at their contacts by tensile and shear strengths, as well as a grain-to-grain friction if the contact bond is broken due to loading. Details on the mechanics of the PFC programs are provided in *Itasca Software–Cutting Edge Tools for Computational Mechanics* (Itasca Consulting Group 2002 [DIRS 160331]).

The UDEC program simulates the response of discontinuous media subjected to thermal, static, or dynamic loading. In UDEC, a discontinuous medium is numerically represented as an assemblage of discrete blocks. The discontinuities such as joints and fractures between blocks are treated as boundaries that are governed by force-displacement relations. Both normal and shear displacements take place at these boundaries. UDEC was used to help examine the behavior of the lithophysal rock within the RHH.

FRACMAN (V.2.512, STN: 10114-2.511-00 [DIRS 160577]) was used to replicate the fracture geometry observed in the ESF to develop a representative volume of jointed rock mass in *Drift Degradation Analysis* (BSC 2004 [DIRS 166107]), which supports this document. Details of this code application in fracture study are presented in BSC 2004 [DIRS 166107], Section 6.1.6).

4. INPUTS

4.1 DIRECT INPUTS

Inputs are used for preparation of this document include calculations, technical reports, and qualified data tracked with data tracking numbers.

4.1.1 Calculations

The primary geotechnical calculations used as direct source for this revision are included in Table 4-1. These calculations function like topical reports addressing specific data areas respectively. Therefore, it is appropriate to use these calculations as primary source for the development of SGRP REV 00.

Table 4-1. List of Calculations Used as Direct Source

Calculation	Document ID No.	Section Used
Lithophysal Rock Mass Mechanical Properties of the Repository Host Horizon (BSC 2004 [DIRS 172334])	800-K0C-SS00-00200-000-00A	6.4.4
Intact Rock Mechanical Properties of Yucca Mountain Stratigraphic Units (BSC 2005 [DIRS 176611])	800-K0C-SS00-00800-000-00A	6.4.2
Rock Mass Quality Ratings and Classifications of the Combined ESF, Heated Drift and ECRB Cross-Drift (BSC 2004 [DIRS 176608])	800-K0C-SS00-00700-000-00A	6.4.4

4.1.2 Supplementary Technical Reports

In addition to the calculations listed in Table 4-1, technical reports used to support this document include *Drift Degradation Analysis* (BSC 2004 [DIRS 166107]) and *Thermal Conductivity of the Potential Repository Horizon* (BSC 2004 [DIRS 169854]). The use of these Analyses and Modeling Reports (AMRs) has been approved by their inclusion on an information exchange drawing, *IED Geotechnical and Thermal Parameters II* (BSC 2006 [DIRS 178277]). These documents include the latest information or parameters such as drift stability analysis, bulk densities, and porosities, which are not discussed in calculations listed in Table 4-1. These documents were prepared under applicable quality assurance (QA) procedures; therefore, the information contained in these documents is considered appropriate to use as direct input for this document.

4.1.3 Data Tracking Numbers

4.1.3.1 Qualified Data

Both acquired and developed data used in this document are obtained from the TDMS database. Table 4-2 lists sources data tracking numbers (DTNs) of qualified data used as direct input in this document. The use of these DTNs has been approved by their inclusion on an information exchange drawing, *IED Geotechnical and Thermal Parameters II* (BSC 2006 [DIRS 178277]). These data are qualified data and therefore are appropriate for use in this document.

Table 4-2. Source DTNs for Qualified Data

Parameters	Source DTN
Density and Porosity	MO0109HYMXPROP.001 [DIRS 155989], GS980808312242.014 [DIRS 106748], MO0010CPORGLOG.002 [DIRS 155229], MO0010CPORGLOG.003 [DIRS 155959], SNL02030193001.027 [DIRS 108410], SNL01A05059301.007 [DIRS 108980]
Material Abundances	SN0305L0207502.005 [DIRS 163373], SN0305L0207502.006 [DIRS 165747], SN0301F4102102.008.[DIRS 165431], SN0302F4102102.010.[DIRS 165436], SN0303F4102102.012 [DIRS 165440]
Compressive Strength	MO0311RCKPRPCS.003 [DIRS 166073], SN0208L0207502.001 [DIRS 161871], SN0211L0207502.002 [DIRS 161872], SN0302L0207502.003 [DIRS 165014], SN0305L0207502.004 [DIRS 165013], SN0306L0207502.008 [DIRS 165015], SNL02030193001.001 [DIRS 120572], SN0505L0212303.005 [DIRS 174956]
Static Elastic Properties, Young's modulus and Poisson's ratio	SN0208L0207502.001 [DIRS 161871], SN0211L0207502.002 [DIRS 161872], SN0302L0207502.003 [DIRS 165014], SN0305L0207502.004 [DIRS 165013], SN0306L0207502.008 [DIRS 165015], SNL02030193001.001 [DIRS 120572], SN0505L0212303.005 [DIRS 174956], MO0402DQRIRPPR.003 [DIRS 168901]
Indirect Tensile Strength with Porosity Data	MO0401DQRIRPTS.003 [DIRS 168905]
Static Fatigue and Creep Test Data	SNL02071596001.001 [DIRS 162205], SN0406L0212303.002 [DIRS 170289], SN0505L0212303.004 [DIRS 174955]
Jointed Rock Mechanical Properties	SNL02112293001.001 [DIRS 161629], SNL02112293001.002 [DIRS 108411], SNL02112293001.003 [DIRS 108412], SNL02112293001.005 [DIRS 108413], SNL02112293001.006 [DIRS 159992], SNL02112293001.007 [DIRS 108414], GS031083114222.002 [DIRS 177299]
Heat Capacity	SNL01C12159302.002 [DIRS 148289], SN0208F3504502.019 [DIRS 161883], SN0206F3504502.013 [DIRS 159146], SN0307T0510902.003 [DIRS 164196], SN0206F3504502.012 [DIRS 159145], SN0206F3504502.011 [DIRS 165270]
Thermal Conductivity	SNL22080196001.001 [DIRS 109722], SNL22100196001.006 [DIRS 158213], SN0203L2210196.007 [DIRS 158322], SN0209L01A1202.001 [DIRS 163601], SNL01A05059301.005 [DIRS 109002], SNL22100196001.002 [DIRS 153138], SNL22080196001.003 [DIRS 119042], SN0206F3504502.012 [DIRS 159145], SN0208F3504502.019 [DIRS 161883], SN0206F3504502.013 [DIRS 159146], SN0404T0503102.011 [DIRS 169129], SN0303T0503102.008 [DIRS 162401], UN0106SPA013GD.004 [DIRS 159116], UN0201SPA013GD.007 [DIRS 159119]
Coefficient of Thermal Expansion	SNL22080196001.001 [DIRS 109722], SN0203L2210196.007 [DIRS 158322], SNL22100196001.002 [DIRS 153138], SNL22080196001.003 [DIRS 119042], SNL01B05059301.006 [DIRS 129168], SN0208L01B8102.001 [DIRS 165211], SN0211L01B8102.002 [DIRS 165218], SNL01B02019501.001 [DIRS 177308]
Detailed Line Survey and Full-Periphery Geotechnical Map Data	GS950508314224.003 [DIRS 107488], GS000608314224.005 [DIRS 166002], GS960408314224.001 [DIRS 168135], GS960408314224.003 [DIRS 168136], GS960708314224.009 [DIRS 168137], GS000608314224.006 [DIRS 152572], GS960908314224.015 [DIRS 108372], GS960908314224.016 [DIRS 108373], GS960908314224.017 [DIRS 108376], GS970108314224.002 [DIRS 107490], GS970208314224.004 [DIRS 107492], GS970808314224.009 [DIRS 107494], GS970808314224.011 [DIRS 107495], GS970808314224.013 [DIRS 107497], GS990408314224.003 [DIRS 108404], GS990408314224.004 [DIRS 108405], GS990408314224.005 [DIRS 108408], GS990408314224.006 [DIRS 108409], GS970608314224.007 [DIRS 158430], GS971108314224.025 [DIRS 106025], GS960708314224.008 [DIRS 105617], GS000608314224.004 [DIRS 152573], GS960708314224.010 [DIRS 106031], GS960908314224.014 [DIRS 106033], GS971108314224.028 [DIRS 106047], GS970208314224.003 [DIRS 106048], GS970808314224.010 [DIRS 106050], GS960908314224.020 [DIRS 106059]

Table 4-2. Source DTNs for Qualified Data (Continued)

Parameters	Source DTN
Rock Mass Modulus Data from PLT	SN0011F3912298.023 [DIRS 158399], SN0310F3912298.054 [DIRS 168527], SNF35110695001.010 [DIRS 158300], SN0207F4102102.001 [DIRS 165429], SN0208F4102102.002 [DIRS 161874], SN0212F4102102.003 [DIRS 165432], SN0212F4102102.004 [DIRS 161875]
Tunnel Convergence and MPBX Data	SN0405F3312393.015 [DIRS 177261]
Hydraulic Fracturing Stress Measurements	SNF37100195002.001 [DIRS 131356]
Lithostratigraphic Contacts	MO0004QGFMPICK.000 [DIRS 152554]
GFM2000 Representation	MO0309MWDVCNGR.001 [DIRS 166600]

4.1.3.2 Corroborative Data – Non Qualified

Corroborative data is used to reinforce conclusions derived based on the qualified data. Corroborative data were obtained by non-BSC organizations, such as the Nevada System of Higher Education, formerly the University and Community College System of Nevada, and NRC and are considered non-qualified data. Table 4-3 lists the source DTNs for corroborative data.

Table 4-3. Source for Corroborative Data

Parameters	Source
Physical Properties of Intact Rock	MO0302UCC027BA.006 [DIRS 177311]; MO0311UCC018LM.001 [DIRS 177313]; Tien et al. 1985 [DIRS 102096]
Intact Rock Mechanical Properties	MO0302UCC027BA.006 [DIRS 177311]; MO0311UCC018LM.001 [DIRS 177313]; MO0311UCC018LM.003 [DIRS 177314]; MO0311UCC018LM.002 [DIRS 177315]

4.2 CRITERIA

Project Design Criteria Document (BSC 2006 [DIRS 178308]) provides the design criteria necessary to support the development of preliminary and detailed design for all repository structures, systems, and components. Section 4.5 of the Project Design Criteria addresses the geotechnical design criteria, which includes applicable codes and standards and ground support design criteria.

4.2.1 Project Geotechnical Design Criteria

The ground support shall be based on the site-specific geotechnical rock property data that: (1) are obtained from the laboratory and field investigations of the rock from or at the Yucca Mountain site; (2) comply with the requirements for traceability and transparency; (3) account for spatial variability of rock strata; and (4) provide a representative geotechnical characterization of the rock mass and in situ environment.

The following definitions are provided to help implement this criterion:

- **Geotechnical Data**: Data that include: intact rock and rock mass strength parameters, elastic modulus, Poisson's ratio, porosity, density, thermal-mechanical properties (specific heat, thermal conductivity, and the coefficient of linear thermal expansion) and their dependence on time and temperature.

- **Data Traceability**: The ability to trace the history, original testing conditions, application, qualification status, or location of data and parameters using recorded documentation.

- **Data Transparency**: A data process that is sufficiently detailed as to purpose, data gathering, analysis and interpretation methodology, data quality appraisal, storage, and record keeping so that a person technically qualified in the subject can understand the process and its supporting documentation, and verify data adequacy without recourse to the originator or the originating organization.

- **Spatial Variability**: A data attribute that must be taken into account to ensure data representativeness for engineering application to the design of repository.

- **Representativeness**: A quality measure of the adequacy of data for engineering application.

4.2.2 Technical Acceptance Criteria

This SGPR REV 00 will address the following technical aspects as part of acceptance criteria (BSC 2006 [DIRS 178063], Section 3.5.2):

- Provide an executive summary of the thermal-mechanical properties (based on measured and derived data) of both the intact rock and the rock mass for the repository footprint. The data set will serve as a unified data source for subsurface design.

- Provide technical information to respond to the NRC's comments related to closure of RDTME KTIs 3.04, 3.05, and 3.07 (Note: specific follow-up actions stated in a letter from the NRC to the DOE, dated January 11, 2005, titled "Pre-Licensing Evaluation of Agreements in 'Technical Basis Document Number 4, Mechanical Degradation and Seismic Effects' and Three Other Associated Agreements" (Kokajko 2005 [DIRS 176613]).

- Support issuing new DTNs needed to streamline a complex system of existing geotechnical data sources; for example, some existing DTNs are inconsistent, overlapping, and lacking correlation among data entries.

4.3 CODES, STANDARDS, AND REGULATIONS

A number of statutory and regulatory requirements, as well as guidance from regulatory agencies involved with YMP, were reviewed as part of this effort to update the project's summary of subsurface geotechnical parameters. This section presents the requirements and guidance and a brief discussion of their relevancy to the subsurface geotechnical parameters information.

4.3.1 Statutory Background

The Atomic Energy Act of 1954 [DIRS 103817] and the Energy Reorganization Act of 1974 [DIRS 152452] established the general authority of the NRC to promulgate rules and regulations to govern the possession and use of special nuclear material, source material, and by-product material, as the NRC may deem necessary to protect public health and safety or promote the common defense and security.

The Nuclear Waste Policy Act of 1982 (NWPA) [DIRS 100014], as amended in the Nuclear Waste Policy Amendments Act of 1987 [DIRS 100016], directed the DOE to investigate Yucca Mountain, Nevada exclusively to determine whether it is a suitable site for locating the Nation's first geologic repository for spent nuclear fuel and high-level radioactive waste. The NWPA established the framework for evaluating the suitability of the Yucca Mountain site, and designated the following responsibilities to federal agencies: the DOE will site, construct, operate, and close the repository; the U.S. Environmental Protection Agency (EPA) will set public health and safety standards for releases of radioactive materials from the repository; and the NRC will promulgate regulations governing the construction, operation, and closure of the repository.

In addition to the NWPA, the Energy Policy Act of 1992 (Public Law No. 102-486 [DIRS 100017]) provided additional direction to the EPA in establishing public health and safety standards for the protection of the public from possible releases of radioactive materials stored in a repository at Yucca mountain; the specific direction was to ensure that the standards are consistent with the findings and recommendations of the National Academy of Sciences. The Energy Policy Act of 1992 also provided direction to the NRC to modify its licensing regulations so as to be consistent with the established EPA standards.

4.3.2 EPA Safety Standard Requirements

In response to the NWPA, as amended in the Nuclear Waste Policy Amendments Act of 1987 [DIRS 100016], and the Energy Policy Act of 1992 [DIRS 105989], the U.S. Environmental Protection Agency promulgated 40 CFR Part 197, Protection of Environment: Public Health and Environmental Radiation Protection Standards for Yucca Mountain, Nevada [DIRS 175755] to establish the environmental radiation protection standards for Yucca Mountain for the protection of the public from releases of radioactive materials. These standards apply to the storage and management of radioactive materials above and below ground at the site, during both the preclosure and postclosure periods.

Preclosure Requirement—40 CFR 197.4, Subpart A [DIRS 175755], requires that no member of the public in the general environment receive an annual committed effective dose (as defined in the regulation) of more than 15 millirem.

Postclosure Requirement—40 CFR 197.20, Subpart B [DIRS 175755], requires that DOE use a performance assessment to demonstrate that there is a reasonable expectation that for 10,000 years following disposal, the reasonably maximally exposed individual would receive no more than an annual committed effective dose equivalent of 15 millirem from releases from the undisturbed Yucca Mountain disposal system. Separate groundwater protection standards have been incorporated into 40 CFR 197.35, Subpart B. Also, separate standards for radiation exposures as a result of inadvertent human intrusion into the repository have been included in 40 CFR 197.25, Subpart B.

The foregoing EPA safety standards have been incorporated by NRC into Subparts K and L of 10 CFR Part 63, Energy: Disposal of High-Level Radioactive Wastes in a Geologic Repository at Yucca Mountain, Nevada [DIRS 176544] for regulating repository licensing requirements. At the present time, the 10,000-year duration for the postclosure EPA standard has been litigated and found by a federal court to be void because it was not of sufficient length to comply with the recommendations of the National Academy of Science. Consequently, the 10,000-year duration for this standard is subject to possible future change. A current draft of the proposed changes to the EPA standard defines two levels of postclosure dose compliance: a similar dose limit as for the voided standard applicable up to 10,000 years, and a higher dose limit applicable between 10,000 and 1,000,000 years.

4.3.3 NRC Licensing Requirements and Guidance

4.3.3.1 10 CFR Part 63

In response to the NWPA, as amended in 1987 [DIRS 100016], and to the Energy Policy Act of 1992 [DIRS 105989], the NRC promulgated 10 CFR Part 63 [DIRS 176544] to regulate licensing requirements for the disposal of high-level radioactive waste in a geologic repository at Yucca Mountain, Nevada. Among other topics, this regulation specifies the preclosure and postclosure performance objectives of the geologic repository operations area that must be met for licensing the repository.

Sections of 10 CFR Part 63 [DIRS 176544] that are directly relevant to geotechnical parameters that might affect repository design and performance are the following:

- 10 CFR 63.21(c)(1)(ii) requires that information regarding the geomechanical properties and conditions of the host rock be included in the Safety Analysis Report of the License Application.

- 10 CFR 63.111(d) requires that the Performance Confirmation Program be implemented within the geologic repository operations area in conformance with requirements stated in 10 CFR Part 63, Subpart F.

- 10 CFR 63.132(a) states that a specific requirement of this Performance Confirmation Program is to provide a continuing program of surveillance, measurement, testing, and geologic mapping during repository construction and operation to confirm geotechnical and design parameters, and to ensure that appropriate action is taken to inform the Commission of design changes needed to accommodate actual field conditions encountered.

- 10 CFR 63.132(b) states that subsurface conditions must be monitored and evaluated against design assumptions.

- 10 CFR 63.132 (c) states that specific geotechnical and design parameters to be measured or observed, including any interactions between natural and engineered systems and components, must be identified in the performance confirmation plan.

- 10 CFR 63.132(d) states that the measurements and observations of geotechnical and design parameters must be compared with the original design bases and assumptions. If significant differences exist between the measurements and observations and the original design bases and assumptions, the need for modifications to the design or construction methods must be determined and these differences, their significance to repository performance, and the recommended changes must be reported to the Commission.

The foregoing requirements would include monitoring of ground support performance parameters such as opening convergence, ground support and rock temperatures, and ground support loads.

4.3.3.2 Yucca Mountain Review Plan (Rev. 2)

Yucca Mountain Review Plan, Final Report (YMRP), NUREG-1804 (NRC 2003 [DIRS 163274]), establishes a format for the review of the YMP license application. Its objective is to ensure quality and uniformity of the individual NRC staff licensing reviews. It presents the areas of review, review methods, acceptance criteria, evaluation findings, and references that the staff will use for its review. Consequently, this document provides guidance in regards to what constitutes an acceptable technical content for a successful license application. This document supports determining compliance with specific regulatory requirements from 10 CFR Part 63 [DIRS 176544], and with the final rules of the U.S. Environmental Protection Agency applicable to Yucca Mountain.

Specific items in NUREG-1804 (NRC 2003 [DIRS 163274]) that are directly relevant to subsurface geotechnical parameters are described in the following sections. These acceptance criteria are addressed throughout the report.

4.3.3.2.1 Site Characterization

- The following acceptance criteria are based on meeting the requirements of 10 CFR 63.21(b)(5) [DIRS 176544], relating to the description of site characterization work provided in the “General Information” section of the License Application.

YMRP (NRC 2003 [DIRS 163274], Section 1.5.3)—Acceptance Criterion 1—The "general information" section of the license application will contain an adequate description of site characterization activities and results.

YMRP (NRC 2003 [DIRS 163274], Section 1.5.3)—Acceptance Criterion 2—The "general information" section of the license application will contain an adequate description of site characterization results.

4.3.3.2.2 Preclosure Safety Analysis

YMRP (NRC 2003 [DIRS 163274], Section 2.1.1)—The safety analysis report section of the license application will contain a preclosure safety analysis. The preclosure safety analysis is a systematic examination of the site, the design, the potential hazards and initiating events and their consequences, and the potential dose consequences to workers and the public due to nuclear operations during the preclosure period. As part of developing a risk-informed, performance-based review plan for preclosure safety evaluation, preclosure safety analysis considers the probability of potential hazards, taking into account the range of uncertainty associated with the data that support the probability calculations. The adequacy of the site description will be assessed in the context of the information required to conduct the preclosure safety analysis and to design the geologic repository. The following acceptance criterion is based on meeting the requirements of 10 CFR 63.112(c) [DIRS 176554] relating to the site description as it pertains to the preclosure safety analysis.

YMRP (NRC 2003 [DIRS 163274], Section 2.1.1.1.3)—Acceptance Criterion 5—: The License Application contains descriptions of the site geology and seismology adequate to permit evaluation of the preclosure safety analysis and the geologic repository operations area design.

- Site characterization data adequately include rock mechanics properties based on in situ and laboratory test results for the rock formations where major construction activities will take place. Collection and processing of these data are based on accepted industry techniques.

- Rock mechanics testing data adequately support the license application analyses of the stability of subsurface materials.

5. ASSUMPTIONS

Assumptions are used in this report, in the absence of directly confirming data or evidence, to develop this document. These assumptions are presented in the various individual calculations and are summarized in this section.

5.1 INTACT ROCK

5.1.1 Base Case Testing Conditions

Assumption: A base case is identified amongst various testing conditions under which mechanical properties of the intact rock were obtained. The following laboratory testing conditions are selected and considered to be the base case representative for individual lithostratigraphic rock zones:

- Where available, both tensile and compressive strength data are utilized
- Specimen size (diameter) equal to or greater than 50 mm with exceptions as noted
- Length to diameter (L:D) ratio: approximately 2 to 1
- Specimen saturation: saturated with exceptions as noted
- Testing temperature: ambient/room temperature
- Strain rate: 0.5×10^{-5} to 5×10^{-5} per second
- Confining pressure and pore pressure: as noted.

This assumption is used throughout the document.

Rationale: Over the course of the YMP characterization, several hundred laboratory tests have been conducted on the rock samples obtained from the boreholes at or in the vicinity of the YMP site, surface outcrops, and underground tunnels (i.e., ESF and Enhanced Characterization of the Repository Block (ECRB) Cross-Drift). The laboratory tests were conducted on various specimen sizes ranging from 25 mm to about 300 mm under different test conditions in terms of saturation, temperature, strain rate, and confining pressure. It is commonly known that the laboratory testing under different test conditions with varying specimen sizes will yield a wide range of intact rock strength data as documented in Section 6.4.2. The base case conditions selected for analysis in this document encompass the most common rock test conditions and represent largest test populations.

These testing conditions represent the most common standard in rock testing; therefore, it is considered reasonable to use the base case conditions as previously stated. Furthermore, the intact rock mechanical property data used in this document provide a benchmark for comparison between the base rock mass property data and rock mass data derived using other testing procedures. The base case assumption does not preclude application of intact rock mechanical property results from other testing conditions.

5.1.2 Statistical Characteristics of the Intact Rock Mechanical Property

Assumption: The intact rock mechanical property variability for each distinct lithologic unit is characterized by a "normal distribution" and it is therefore appropriate to use an arithmetic mean and standard deviation for statistical analysis of intact rock mechanical property data.

This assumption is used in Section 6.4.

Rationale: The distribution characteristic of the intact rock mechanical property data (strength and static elasticity parameters) for each lithostratigraphic zone is examined in *Intact Rock Mechanical Properties of Yucca Mountain Stratigraphic Units* (BSC 2005 [DIRS 176611], Section 6.3). Although it would be desirable that each test type would be represented by the population of at least seven test specimens, however, test populations containing even as few as one test of particular kind are included for the sake of completeness.

The use of this assumption is appropriate for this document and does not require further validation. Confirmation of this assumption is considered an on-going activity. Once the fieldwork resumes, gathering of rock property data from various lithostratigraphic zones at multiple locations and depths throughout the repository will increase the population of the test results available for analyses. This will result in an increased confidence in the accuracy of rock strata characterization.

5.1.3 Isotropy of Intact Rock Elastic Properties

Assumption: The intact rock samples have isotropic properties.

This assumption is used in Sections 6.3.1.1 and 6.4.2.2.

Rationale: As reported in *Intact Rock Mechanical Properties of Yucca Mountain Stratigraphic Units* (BSC 2005 [DIRS 176611], Section 6.3.5.4), dynamic tests were performed for P- and S-wave velocities in three orthogonal directions. From these velocities, dynamic elastic properties (Young's modulus and Poisson's ratio) were calculated with the assumption that the intact rock is isotropic.

Several studies (Olsson and Jones 1980 [DIRS 102940]; Price et al. 1984 [DIRS 106604]; Price et al. 1991 [DIRS 161289]; Martin et al. 1992 [DIRS 160028]; Price 2004 [DIRS 170894]) have investigated the effect of direction on both the dynamic and static Young's modulus and Poisson's ratio in tuffs from Yucca Mountain. The results of these studies have indicated no significant elastic anisotropy (Price 2004 [DIRS 170894], p. 9). In the most recent study by Price (2004 [DIRS 170894]), a maximum anisotropy of less than 10% in Young's modulus and about 6% in the Poisson's ratio were observed in 55 samples with a nominal diameter of 50.8 mm. Based on these studies, it is reasonable to assume that the intact rock is isotropic.

The use of this assumption is appropriate for this document and does not require further validation.

5.2 ROCK MASS

5.2.1 Lateral Continuity of Lithostratigraphic Zones

Assumption: This document is developed based on the bounding assumption that properties of the individual rock units are laterally continuous, such that data obtained from samples taken at a particular lithostratigraphic zone from boreholes in and around the repository block are representative of that rock unit in the repository block itself. Therefore, statistical parameters derived from all boreholes in the immediate area of the repository block also define the bounding limits of the rock within the repository block.

This assumption is used throughout the document.

Rationale: The majority of the rocks contained at Yucca Mountain were deposited during explosive volcanic eruptions originating from the north. On a regional scale, there is lateral variability in the thickness and characteristics of the rock units as documented in *GFM2000 Representation in the VULCAN Software System* (BSC 2003 [DIRS 165802]). Generally, the units are thinner towards the south away from the source and east and west from the main channel of flow. Some units thin out away within the YMP area and become nonexistent towards the south. However, the rock property data obtained from testing rock samples from individual units were found having similar properties throughout the area of the repository in all lateral units of the same lithostratigraphy. Results of extensive mapping performed within YMP underground excavations and on the surface provide strong support to this rationale.

Confirmation of this assumption can be made by comparing data from smaller (25.4 or 50.8 mm diameter) specimens obtained from the same lithostratigraphic zones at different boreholes located within the area of the repository (BSC 2005 [DIRS 176611], Table 6-4).

5.2.2 Variation of Lithophysal Porosity in the Tptpll Lithostratigraphic Zone

Assumption: It is assumed that the lithophysal rock in the repository area is both similar in geologic structure and laterally continuous, having formed under similar depositional, pressure, and temperature conditions. More specifically, the lithophysae data that was developed from the ECRB Cross-Drift measurements of the Tptpll lithostratigraphic zone provides an adequately representative and statistically reliable sampling of the horizontal and vertical spatial variation of lithophysal porosity across lithophysal rock in the Tptpll zone (BSC 2004 [DIRS 172334], Assumption 5.1).

This assumption is used in Sections 6.4.4.3 and 6.4.4.4.

Rationale: The Topopah Spring Tuff was created by the cooling and welding of regionally extensive and large volume (about 1200 km^3) of pyroclastic flow deposits that derived from a massive caldera eruption located north of the repository site, which occurred approximately 12.8 million years ago (BSC 2004 [DIRS 169734], pp. 3-8, 2-11, 2-12, 3-18, 3-19, and 3-29; Sawyer et al. 1994 [DIRS 100075], pp. 1305 and 1306; Sawyer et al. 1995 [DIRS 104580], p. 18; Schuraytz et al. 1989 [DIRS 107248], p. 5927). This assumption is based on the following conditions:

1. Given the distance from the volcanic source and a repository footprint length (north-south direction) of approximately 5 km (3 mi) (BSC 2003 [DIRS 165572], Table 7 and Figure 10), it is likely that the pyroclastic flow material deposited over the repository area was relatively homogeneous in composition (BSC 2004 [DIRS 169734], pp. 2-12 and 2-13).

2. The following geologic concepts pertaining to the thickness of the Topopah Spring Tuff and its lithostratigraphic zones are deemed suitable (BSC 2004 [DIRS 170029], Section 6.4.1, p. 6-19): (1) volcanogenic rocks generally thin away from their sources; (2) the major volcanic deposits at Yucca Mountain generally filled in preexisting topography, so that the top of a formation may have been originally more planar than the base; (3) the top of a formation may have eroded after deposition; (4) the lower vitric zones of the Topopah Spring Tuff blanketed preexisting topography and began the process of filling in topographic lows; and (5) the Topopah Spring Tuff lithophysal and nonlithophysal rocks were produced by multiple processes and, although approximating a stratiform geometry, these lithostratigraphic zones may have irregular thickness distributions.

3. The bulk of the pyroclastic flow material that formed the repository units was rhyolite (a vitric rock) with estimated temperatures of ranging from about 700°C to 800°C (Schuraytz et al. 1989 [DIRS 107248], pp. 5933 and 5934).

4. The scientific principles of causality and admissibility dictate that the same physical laws of nature governing the processes of welding (material consolidation under pressure), crystallization, formation of lithophysae, vapor movement, and fracturing were active throughout the entire pyroclastic deposit during creation of the Topopah Spring Tuff. Buesch and Spengler (1998 [DIRS 101433], pp. 20 and 21) describe some of these processes and the development of lithostratigraphic features in lithophysal and nonlithophysal zones and subzones.

Consideration of these conditions reveals that spatial variation of ignimbrite (volcanic pyroclastic rock, e.g., rhyolite) material properties, boundary conditions, and loading forces occur primarily in the vertical direction. There is no reason to suspect significant spatial variation of any of these conditions laterally, or accordingly, in the final resulting rock formation.

This assumption is valid for the Topopah Spring Tuff formation in the repository footprint only. The use of this assumption is appropriate for this document and does not require further validation.

5.2.3 Distribution and Variation of Lithophysal Porosity in the Upper Lithophysal Zone (Tptpul)

Assumption: For determining a suitable range of lithophysal rock mechanical properties, the quantified lithophysae abundance data obtained by mapping the Tptpll zone is assumed to be statistically similar to the distribution and spatial variation of lithophysal porosity of the Tptpul zone (BSC 2004 [DIRS 172334], Assumption 5.2).

This assumption is used in Sections 6.3.4, 6.3.5, 6.4.4.3, and 6.4.4.4.

Rationale: Sensitivity results of the analysis indicate that porosity variation within lithophysal units is insignificant.

Assessment of the spatial variation of the rock mass properties in lithophysal rock, conducted in *Scoping Analysis on Sensitivity and Uncertainty of Emplacement Drift Stability* (BSC 2003 [DIRS 166183], Section 7.1.3) was based on simulated lithophysal porosity. The overall rock mass response around the drifts at various locations are predicted to be compatible with those of the base case Rock Mass Category 3 (average) rock.

Further analysis of drift stability indicates that considering the lithophysal rock mass with spatial variation resembling the median rock mass quality category, the degradation of rock mass around the opening during the preclosure is insignificant.

Therefore, the use of this assumption is appropriate for this document and does not require further validation.

5.2.4 Composition of Lithophysal Rock

Assumption: It is assumed that the lithophysal rock is conceptualized as being a composition of (1) solid matrix and (2) air-filled lithophysal voids (lithophysae). In terms of the mechanical behavior of the rock matrix, the explicit presence of fractures and spot and rim features in the lithophysal rock are ignored (BSC 2004 [DIRS 172334], Assumption 5.3).

This assumption is used in Section 6.4.4.

Rationale: Based on available physical characterization of rock samples and for simplicity and ease of numerical analysis, a two-component material simulation is adopted (solid matrix and voids) for preliminary characterization of lithophysal rock mass behavior. Accordingly, lithophysal rock mechanical behavior, ignoring fractures, is based primarily on the geometry of matrix rock with lithophysal voids.

Although the material simulation ignores rock fractures, rims, and spots; small fractures and rim and spot material may be present in tested rock specimens, and so their effects on mechanical behavior are included as part of laboratory characterization. To the extent that these effects are represented in the laboratory mechanical characterization, they are represented in the numerical analysis since simulation calibration was based on laboratory testing. For this reason, it is considered acceptable to ignore fractures and spot and rim in the mechanical characterization of lithophysal rock.

Since the lithophysal rock mass mechanical behavior is based on the laboratory testing of intact rock and numerical analysis calibrated to the same intact rock testing, then it is potentially affected by any bias in the laboratory data. However, because of spatial heterogeneity considerations (one does not observe meter-size spot and rim material) at the drift scale and smaller, the bias or uncertainty of underrepresenting fractures, rims and spots in the mechanical characterization of intact rock is not considered to be large or significant. Therefore, the use of this assumption is appropriate for this document and does not require further validation.

5.2.5 Laboratory Lithophysal Rock Mass Mechanical Behavior

Assumption: It is assumed that the estimated range of mechanical rock properties of lithophysal rock at the 1 m and larger scale can be suitably estimated from the available large-core (approximately 0.3 m or 12 –in. diameter) specimen laboratory testing results. This assumes that the dominant mechanical failure mechanism in a lithophysal rock mass is the creation and/or reactivation of matrix-ground mass fractures that weaken the intact blocks of tuff (as observed in laboratory testing and numerical analysis), and not slip along preexisting fracture planes that form the boundaries of strong intact blocks of tuff (analogous to the dominant failure method expected for a nonlithophysal rock mass) (BSC 2004 [DIRS 172334], Assumption 5.4).

This assumption is used in Section 6.4.4.

Rationale: Laboratory results (Section 6.4.4.4.2.3) indicate that there is a scaling effect of mechanical properties at the laboratory scale (ranging from diameters of 25 to 290 mm). However, due to the limited number of mechanical tests, uncertain specimen porosities, the presence of fractures and other imperfections (lithophysae, rims, and spots), and testing over a range of environmental conditions (moisture content and rock temperature), there is a large amount of scatter in the laboratory results. It is assumed that this scatter can capture the property scaling effect present in rock mass up to dimensions of about 3 m. The approximate relationship of strength and specimen size is discussed in Section 6.4.4.4.3. The numerically simulated laboratory testing of meter-size specimens (Section 6.4.4.4.2.5.2) is generally within the property bounds estimated for large-core testing.

5.2.6 The Spatial Variability Analysis Developed for Lithophysal Porosity

Assumption: It is assumed that the simulation developed to represent the spatial variability of lithophysal porosity (BSC 2004 [DIRS 172334], Appendix A) can be applied to other uncertain simulation parameters (e.g., Young's modulus, E, and unconfined/uniaxial compressive strength (UCS). In other words, the spatial variation of lithophysal porosity, defined by field mapping techniques, can be used to indirectly determine the spatial variation of rock mass mechanical parameters, based on correlations between specimen lithophysal porosity and the mechanical parameters determined from these tested rock specimens (BSC 2004 [DIRS 172334], Assumption 5.5).

This assumption is used throughout Section 6.4.4.3.

Rationale: The assumption of using rock lithophysal porosity as a surrogate for simulating the spatial variability of other variables is described in Section 6.4.4.4.2.1. The spatial variability of the elastic Young's modulus and UCS cannot be developed directly because only a small number of mechanical laboratory tests have been carried out on rock specimens containing lithophysal voids.

The repository horizon layers are similar in mineralogical composition (BSC 2003 [DIRS 164670], Table 6.2) and differ primarily in terms of matrix ground mass and lithophysal porosity percentages. Because the mineralogical abundance and chemical composition for these zones are similar, the mechanical behavior of the matrix ground mass material in all zones should be similar.

As demonstrated in Section 6.4.4.4.2.3, sample porosity is the primary factor controlling the mechanical behavior in compression testing. The significance of this key controlling factor is confirmed by the validation provided by the numerical analysis of mechanical lithophysal rock behavior discussed in Sections 6.4.4.4.2.5 and 6.4.4.4.2.7.

5.3 TIME-DEPENDENCY

No assumption is used.

5.4 THERMAL PROPERTIES OF LITHOSTRATIGRAPHIC ROCK UNITS

5.4.1 Intact Thermal Conductivity Measurements

Assumption: Intact rock thermal conductivity from laboratory measurements is calculated from Fourier's law of heat conduction with the following assumptions: (1) the heat flow is one-dimensional, (2) the testing material is homogeneous and isotropic, and (3) the thermal conductivity is independent of the small changes in temperature and moisture content.

This assumption is used in Section 6.5.3.1.2.

Rationale: Thermal conductivities were measured from small specimens of right circular cylinders, cored to nominal dimensions of 50.8 mm in diameter and 12.7 mm in length (Brodsky et al. 1997 [DIRS 100653], Table 2-1). These rock specimens usually contain few voids or fractures, and behave like an intact rock. Therefore, the results from the laboratory thermal conductivity measurements using these small rock specimens can be considered to represent properties of intact rock.

The conditions assumed are generally achievable in laboratory measurements by controlling heat flow in one-dimension, using small right circular cylindrical specimens, and measuring heat transfer rate over a small temperature change. In field measurements, these ideal conditions are difficult to achieve. Therefore, the use of this assumption is appropriate for this document and does not require further validation.

5.4.2 Rock Mass Thermal Properties

Assumption: Thermal properties of rock mass can be determined based on field measurements at various locations of the unit of interest. The locations of the field thermal properties

measurement should be chosen carefully to represent the unit of interest, and is assumed to be representative to the unit of interest.

This assumption is used in Section 6.5.

Rationale: Field measurements of thermal properties assume background (in situ) conditions of the rock mass, such as temperature, that remain unchanged during a short time period. Measurement values of field thermal properties are corrected based on available information regarding the background conditions. For example, an estimation of thermal conductivity (k) and thermal diffusivity (α) using data from field thermal conductivity measurements taken by REKA probes, assumes that rock mass will behave in a homogeneous and isotropic manner. The assumption is reasonable since REKA probe measurements pertain to a relatively small volume of rock mass, about 0.6 m in length with an estimated radius of 0.1 m and does not require further validation.

5.4.3 Saturation of Rock Matrix

Assumption: The rock matrix is assumed fully saturated to calculate matrix and lithophysal porosity from petrophysical measurements of the four repository horizon units.

This assumption is used in Section 6.5.3.

Rationale: The assumption is reasonable since the measured in situ saturation value is over 90% (BSC 2004 [DIRS 169900], Table 6.2.2.5-2) and does not require further validation.

5.4.4 Data Representation

Assumption: Data from available measurements of core specimens and borehole petrophysical logs are assumed to be representative of the geological units in Yucca Mountain.

This assumption is used in Section 6.5.3.

Rationale: The assumption is reasonable since the specimens and boreholes are well spaced and located within the footprint of the repository (BSC 2004 [DIRS 169854], Figure 4-1) and does not require further validation.

5.4.5 Water Saturation

It is assumed that the water saturation decreases linearly from its initial value to zero over the 19°C temperature range during the trans-boiling phase, 95°C to 114°C.

This assumption is used in Section 6.5.3.

Rationale: The assumption is based on observations of rock moisture content as a function of temperature (BSC 2004 [DIRS 169900], Figure 6.3.2.3-2) and does not require further validation.

6. SCIENTIFIC ANALYSIS AND DISCUSSION

6.1 GEOLOGICAL OVERVIEW

Understanding the regional geologic setting and the local geology of the Yucca Mountain area is necessary to fully understand the development of the different geotechnical properties exhibited by the various tuffaceous rock units comprising Yucca Mountain. This section of the report presents an overview of the regional geologic framework and local geology of Yucca Mountain, as well as some terminology definitions of observed lithostratigraphic features.

6.1.1 Regional Geology at Yucca Mountain

The geologic framework of the Yucca Mountain region is described in detail in Section 3 of *Yucca Mountain Site Description* (BSC 2004 [DIRS 169734]), and some salient aspects are summarized in this section.

Yucca Mountain, in southwest Nevada, lies in the south-central part of the Great Basin that forms the northern subprovince of the Basin and Range physiographic province. More specifically, Yucca Mountain occupies part of the Walker Lane belt, a major structural lineament considered to be a zone of transition between (1) the central and southeastern parts of the Great Basin, characterized by dip-slip normal faulting and typical basin and range topography; and (2) the southwestern Great Basin, typified by both dip-slip and strike-slip faulting and irregular topography. Yucca Mountain itself is situated on the south flank of the southwestern Nevada volcanic field, which consists of a series of volcanic centers from which large volumes of pyroclastic flow and fallout tephra deposits were erupted from about 14.0 to 11.4 million years (Ma) ago. Accordingly, the mountain and the adjacent landforms carry the imprint of the area's extensive volcanic history, as well as its deformational history (BSC 2004 [DIRS 169734], Section 3.2.1).

Yucca Mountain is an irregularly shaped upland, 3 to 8 km wide and about 35 km long that stretches from near Beatty Wash at the northwest end to near the north edge of the Amargosa Desert at the south end. The crest of the mountain reaches elevations of 1,500 to 1,930 m, about 125 to 275 m higher than the floors of adjacent washes and lowlands. The dominantly north-trending pattern of structural blocks characterizing this prominent upland area is controlled by high-angle block-bounding faults with vertical displacements of several hundred meters in places. The fault blocks, composed of volcanic rocks of Miocene age, are tilted eastward, so that the fault-bounded west-facing slopes are generally high and steep, in contrast to the more gentle and commonly deeply dissected east-facing slopes. The valleys are generally narrow and V-shaped along their upper and middle reaches, but locally contain flat, alluviated floors in their lower reaches. Valley morphology ranges from shallow, straight, steeply sloping gullies and ravines to relatively deep, bifurcating, gently sloping valleys and canyons (BSC 2004 [DIRS 169734], Section 3.2.1).

The structural geology of Yucca Mountain and vicinity is dominated by a series of north-striking normal faults along which Tertiary volcanic rocks were tilted eastward and displaced hundreds of meters, predominantly down-to-the-west primarily during a period of extensional deformation in middle-to-late Miocene time. These block-bounding faults are spaced 1 to 5 km apart and include, from east to west within the site area, the Paintbrush Canyon, Bow Ridge, Solitario Canyon, Fatigue Wash, and Windy Wash faults (BSC 2004 [DIRS 169734], Section 3.5).

6.1.2 Lithostratigraphy of Yucca Mountain

The lithostratigraphy of the Yucca Mountain site is described in detail in *Yucca Mountain Site Description* (BSC 2004 [DIRS 169734], Section 3.3), and some major aspects are summarized in this section. The general stratigraphic column of Yucca Mountain is presented in Figure 6-1.

6.1.2.1 General

In the Yucca Mountain area, separation of formations into subunits is based on macroscopic features (for example, degree of welding) of the rocks as they appear in exposures and borehole cores. Their identification is augmented by quantitative mineralogy, borehole geophysics, rock properties such as density and porosity, and geochemical composition (BSC 2004 [DIRS 169734], Section 3.3.3).

Three primary stratigraphic systems have been developed to investigate the distribution of lithostratigraphic, hydrogeologic, and thermal-mechanical units at Yucca Mountain. Common to all these systems are the properties of bulk rock density, grain density, and porosity. Changes in these rock properties result in commensurate changes in many of the associated hydrogeologic and thermal-mechanical properties that define units whose boundaries coincide with a particular stratigraphic contact (BSC 2004 [DIRS 169734], Section 3.3.6). Table 6-1 lists the lithostratigraphic sequence comprising Yucca Mountain and how the lithostratigraphic zones correlate with defined thermal-mechanical units based on the thermal and mechanical properties of the rock units, and with the defined hydrogeologic units based on the hydrologic or groundwater-transmitting properties of the rock units.

Important lithologic and rock-property criteria for differentiating volcanic rock units include:

- Variations in grain size and sorting
- Relative abundance of volcanic glass (vitric versus devitrified)
- Degree of welding
- Types and degree of crystallization
- Relative abundance of lithophysae
- Amount and types of glass alteration
- Fracture characteristics.

Table 6-1. Lithostratigraphic, Thermal-Mechanical and Hydrogeologic Unit of Yucca Mountain

Lithostratigraphic Units [a, b, c, d]		Thermal-Mechanical Units [a, e]	Hydrogeologic Units [f]
TIMBER MOUNTAIN GROUP (Tm)	Rainier Mesa member (Tmr) (02_UO_Tmr)	Undifferentiated overburden (UO)	Unconsolidated surficial materials (UO)
	Pre-Rainier Mesa bedded tuff (Tmbt1)		
PAINTBRUSH GROUP (Tp)			
	rhyolite of Comb Peak (Tpk); includes the pyroclastic flow deposit (Tpki) that is informally referred to as tuff unit "X" (Tpki) (**03_UO_Tpki**)		
	post-Tiva Canyon bedded tuff (Tpbt5)		
Tiva Canyon Tuff (Tpc)	crystal-rich member (Tpcr) vitric zone (Tpcrv) -nonwelded subzone (Tpcrv3) -moderately welded subzone (Tpcrv2) -densely welded subzone (Tpcrv1) nonlithophysal zone (Tpcrn[g]) (**04_TCw_Tpcrn + 05_TCw_Tpcrn2 + 06_TCw_Tpcrn1**) lithophysal zone (Tpcrl)	Tiva Canyon welded (TCw) [h]	Tiva Canyon welded (TCw) [h]
	crystal-poor member (Tpcp) upper lithophysal zone (Tpcpul) (**07_TCw_Tpcpul**) middle nonlithophysal zone (Tpcpmn) (**08_TCw_Tpcpmn**) lower lithophysal zone (Tpcpll) (**09_TCw_Tpcpll**) lower nonlithophysal zone (Tpcpln) (**10_TCw_Tpcpln**) -hackly subzone (Tpcplnh) -columnar subzone (Tpcplnc) vitric zone (Tpcpv) -densely welded subzone (Tpcpv3) (**11_TCw_Tpcpv3**) -moderately welded subzone (Tpcpv2) (**12_TCw_Tpcpv2**) -nonwelded subzone (Tpcpv1) (**13_PTn_Tpcpv1**)		
	pre-Tiva Canyon bedded tuff (Tpbt4) (**14_PTn_Tpbt4**)		
Yucca Mountain Tuff (Tpy)	Yucca Mountain Tuff (Tpy) (**15_PTn_Tpy**)	Paintbrush nonwelded (PTn)	Paintbrush nonwelded (PTn)
	pre-Yucca Mountain bedded tuff (Tpbt3) (**16_PTn_Tpbt3**)		
Pah Canyon Tuff (Tpp)	Pah Canyon Tuff (Tpp) (**17_PTn_Tpp**)		
	pre-Pah Canyon bedded tuff (Tpbt2) (**18_PTn_Tpbt2**)		
Topopah Spring Tuff (Tpt)	crystal-rich member (Tptr) vitric zone (Tptrv) -nonwelded subzone (Tptrv3) (**19_PTn_Tptrv3**) -moderately welded subzone (Tptrv2) (**20_PTn_Tptrv2**) -densely welded subzone (Tptrv1) (**21_TSw1_Tptrv1**) nonlithophysal zone (Tptrn) (**22_TSw1_Tptrn**) lithophysal zone (Tptrl) (**23_TSw1_Tptrl**) lithic-rich zone (Tptf) (**24_TSw1_Tptf**)	Topopah Spring welded lithophysae-rich (TSw1)	Topopah Spring welded (TSw)
	crystal-poor member (Tptp) upper lithophysal zone (Tptpul) [upper part]		
RHH	upper lithophysal zone (Tptpul) [lower part] (**25_TSw1_Tptpul**) middle nonlithophysal zone (Tptpmn) (**26_TSw2_Tptpmn**) lower lithophysal zone (Tptpll) (**27_TSw2_Tptpll**) lower nonlithophysal zone (Tptpln) (**28_TSw2_Tptpln**)	Topopah Spring welded lithophysae-poor (TSw2)	

Table 6-1. Lithostratigraphic, Thermal-Mechanical and Hydrogeologic Unit of Yucca Mountain (Continued)

Lithostratigraphic Units [a, b, c, d]		Thermal-Mechanical Units [a, e]	Hydrogeologic Units [f]
	vitric zone (Tptpv) -densely welded subzone (Tptpv3) (**29_TSw3_Tptpv3**) -moderately welded subzone (Tptpv2) (**30_CHn1_Tptpv2**) -nonwelded subzone (Tptpv1) (**31_CHn1_Tptpv1**)	Topopah Spring welded vitrophyre (TSw3)	Topopah Spring basal vitrophyre (TSbv)
	pre-Topopah Spring bedded tuff (Tpbt1) (**32_CHn1_Tpbt1**)	Calico Hills and lower Paintbrush nonwelded (CHn1)	Calico Hills Nonwelded (CHn)
CALICO HILLS GROUP (Tac)	Calico Hills Formation (Tac) (**33_CHn1_Tac**)		
	pre-Calico Hills bedded tuff (Tacbt) (**34_CHn1_Tacbt**)	Calico Hills and lower Paintbrush nonwelded (CHn2)	

Source: Modified from *Yucca Mountain Site Description* (BSC 2004 [DIRS 169734], Table 3.5). The numbered lithostratigraphic zones are used in Section 6.4.4.

NOTES: [a] Buesch et al. 1996 [DIRS 100106], Table 4

[b] SGR (CRWMS M&O 1997 [DIRS 103564], Table 3-1)

[c] Moyer et al. 1995 [DIRS 103777]

[d] Geslin et al. 1995 [DIRS 103330], Table 2

[e] Ortiz et al. 1985 [DIRS 101280], Table 1

[f] Arnold et al. 1995 [DIRS 101423], Table 2-1

[g] This unit includes Tpcrn1 and Tpcrn2 that were identified during the ESF and ECRB Cross-Drift geologic mapping

[h] Where preserved, the base of the crystal-poor densely welded subzone (Tpcpv3) forms the base of the TCw thermal-mechanical and hydrogeologic units (Buesch et al. 1996 [DIRS 100106], Table 4).

These rock properties are the combined products of the primary processes of eruption and deposition, the secondary processes of cooling and crystallization of some pyroclastic flows, and post-eruptive processes, such as alteration by infiltrating aqueous solutions and by fracturing and faulting from tectonism. Two of these lithologic and rock-property criteria are especially important for distinguishing zones and subzones within the volcanic sequences. One is the presence or absence of lithophysae (spherical to oblate cavities), which is a condition that is used to define some of the principal zones, particularly within the Tiva Canyon Tuff and Topopah Spring Tuff, and is closely associated with variously welded units. The other criterion is the degree of welding, a property that distinguishes many subzones and also provides a principal means of separating hydrogeologic and thermal-mechanical units based on whether they are nonwelded, partially welded, or densely welded zones. Such zones are vertically distributed in a single cooling unit of ash-flow tuff, with nonwelded rocks at the top and bottom of the deposit and increasingly welded rocks toward the center. Relatively thick deposits, such as the Tiva Canyon Tuff and the Topopah Spring Tuff, may have the complete welding range, both laterally and vertically, but thin deposits may lack the more welded parts. In general, the degree of welding controls porosity, which ranges from 45% to 65% for nonwelded rocks, 25% to 45% for partially welded rocks, 10% to 25% for moderately welded rocks, and less than 10% for densely welded rocks (BSC 2004 [DIRS 169734], Section 3.3.3.1).

Mineralogy plays an important role in differentiating lithostratigraphic zones, as distinct crystallized and altered zones commonly form in ash-flow tuffs. Four such recognized zones are (BSC 2004 [DIRS 169734], Section 3.3.3.2):

Vitric zones—These are created where the original glassy components remained as glass after the period of high-temperature crystallization and final cooling of the deposit had ended.

High-temperature devitrification zones—The process of high-temperature devitrification forms rocks composed mostly of feldspar and silica minerals (quartz, cristobalite, tridymite) with minor amounts of other minerals, which texturally form the ground mass that has crystallized within the former glass particle sites.

Vapor-phase zone—This zone can be divided into (1) vapor-phase corrosion, whereby glass is corroded to form secondary porosity, and (2) vapor-phase mineralization, which occurs as the temperature cools and minerals, such as tridymite or cristobalite and sanidine, precipitate.

Alteration and crystallization zones—These are zones in which high porosity and permeability facilitate alteration of glass, producing sillar textures, and iron oxidizes in the glass to form variegated red and orange colors. Common low-temperature alteration products include smectite and the zeolitic minerals, clinoptilotite and mordenite.

Volcanic rocks at Yucca Mountain show systematic variations in their chemical and isotopic compositions resulting from differentiation and assimilations in the magma chamber that lead to zonation within the erupted ash flows. The most abundant chemical constituents of both vitric and devitrified tuffs are SiO_2 and Al_2O_3. Analysis of the chemical composition data of the Yucca Mountain rock units show that (1) the Calico Hills Formation, Yucca Mountain Tuff, and crystal-poor members of the Tiva Canyon Tuff and the Topopah Spring Tuff are predominantly high-silica rhyolites; (2) Pah Canyon Tuff consist of low-silica rhyolites; and (3) the crystal-rich members of the Tiva Canyon Tuff and Topopah Spring Tuff are largely quartz latites (BSC 2004 [DIRS 169734], Section 3.3.3.3).

The lithostratigraphic sequence at Yucca Mountain also illustrates some systematic variations in the distribution and concentrations of rare earth and trace elements with stratigraphic position. Variations in these elements, reflecting differences in magma sources and differentiation histories, are useful for stratigraphic correlation and for the identification of altered zones (BSC 2004 [DIRS 169734], Section 3.3.3.3).

6.1.2.2 Description of Lithostratigraphic Zones

The following descriptions pertain to the lithostratigraphic sequence at Yucca Mountain, which is presented in Tables 6-1 and 6-2. The individual units range in age from the youngest Timber Mountain Group (approximately 11.5 Ma) at the top of the sequence to the oldest Calico Hills Formation (approximately 12.9 Ma) at the base of the sequence (BSC 2004 [DIRS 169734], Sections 3.3.4.6 and 3.3.4.8).

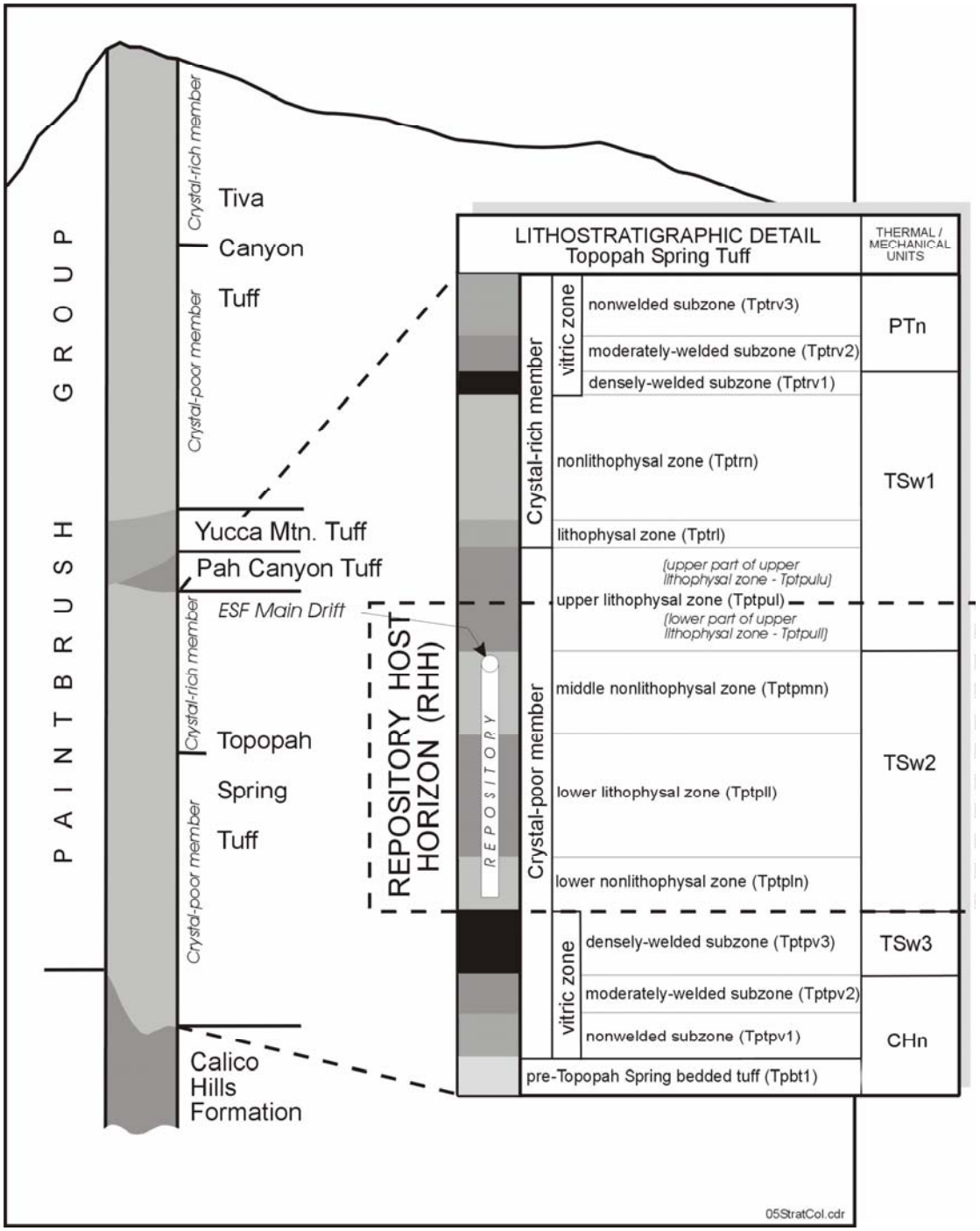

Source: Modified from *Determination of Available Volume for Repository Siting* (CRWMS M&O 1997 [DIRS 100223], Figure 5).

NOTES: The detailed lithostratigraphic and thermal-mechanical nomenclatures are shown for the Topopah Spring Tuff, including lithostratigraphic positions of the RHH, the ESF Main Drift, and the repository.

Figure 6-1. General Stratigraphic Column for Yucca Mountain

6.1.2.2.1 Timber Mountain Group (Tm)

A sequence of pyroclastic flow and fallout tephra deposits occurs between the top of the Tiva Canyon Tuff(Tpc) and the base of the Rainier Mesa Tuff (Tmr) of the Timber Mountain Group (Tm) in the vicinity of Yucca Mountain (post-Tiva Canyon tuff bedded tuff (Tpbt5), rhyolite of Comb Peak (Tpk), and pre-Rainier Mesa tuff bedded tuff (Tmbt1)). Rocks in this stratigraphic position occur in the subsurface beneath alluvial deposits in Midway Valley, on the east flank of Yucca Mountain (BSC 2004 [DIRS 169734], Section 3.3.4.8).

The overlying Timber Mountain Group includes all of the quartz-bearing pyroclastic flow and fallout tephra deposits that were erupted from the Timber Mountain caldera complex. The oldest unit of the Timber Mountain Group is the Rainier Mesa Tuff . This unit is a compositionally zoned compound-cooling unit consisting of high-silica rhyolite tuff overlain with a partial cooling break by a considerably thinner quartz latite tuff that is restricted to the vicinity of the Timber Mountain caldera. The unit does not occur across much of Yucca Mountain, but is locally present on the downthrown blocks of large faults in valleys on either side of the mountain. In localities near Yucca Mountain, a maximum thickness of 240 m (787 ft) for the Rainier Mesa Tuff was observed in the southwestern part of Crater Flat. Thicknesses reported from studies of boreholes on the east side of Yucca Mountain are generally less than 30 m (100 ft) (BSC 2004 [DIRS 169734], Section 3.3.4.8.1).

The pre-Rainier Mesa Tuff bedded tuff consists of nonlithified fallout-tephra and pyroclastic-flow deposits. The sequence occupies intervals of about 17 m as observed in boreholes, and is characterized by moderately well-sorted white pumice lapilli and volcanic lithic clasts (BSC 2004 [DIRS 169734], Section 3.3.4.8.1).

6.1.2.2.2 Paintbrush Group (Tp)

The Paintbrush Group (Tp) consists of four formations. In descending order, the formations include the Tiva Canyon Tuff (Tpc), Yucca Mountain Tuff (Tpy), Pah Canyon Tuff (Tpp), and Topopah Spring (Tpt) Tuff. This group is one of the most widespread and voluminous caldera-related assemblages in the southwestern Nevada volcanic field. The Paintbrush Group is dominated volumetrically by the Tiva Canyon Tuff and Topopah Spring Tuff. The Yucca Mountain Tuff and Pah Canyon Tuff are volumetrically minor units, but are of potential hydrologic importance because of their high-matrix porosity compared to the Tiva Canyon Tuff and Topopah Spring Tuff, which are largely densely welded with low-matrix porosity. The welded tuffs also have higher fracture abundance and connectivity, providing stratified contrasts in unsaturated zone hydrologic properties in the Paintbrush Group rocks above the repository (BSC 2004 [DIRS 169734], Section 3.3.4.7).

Table 6-2. Yucca Mountain Stratigraphy as Used in *Geologic Framework Model (GFM2000)*

Thermal Mech. Unit	Group	Formation	Member	Zone	Subzone	Abbreviation	Geologic Framework Model Unit	Subsequent Item Number	Lithostratigraphic Units Used in This Analysis	Lithostratigraphic Units Mapped in YMP Underground Excavations Used in This Analysis
		Alluvium and Colluvium				Qal, Qc	Alluvium	1	1	01_UO
	Timber Mountain Group					Tm		2		
		Rainier Mesa Tuff				Tmr		3	2	02_UO_Tmr
	Paintbrush Group					Tp		4		
			Post tuff unit "x" bedded tuff			Tpbt6		5		
			Tuff unit "x"			Tpki (informal)	**Crystal-Rich**	6	3	03_UO_Tpki
			Pre-tuff unit "x" bedded tuff			Tpbt5	**Tiva and**	7		
TCw		**Tiva Canyon Tuff**				Tpc	**Post-Tiva**	8		
			Crystal-Rich Member			Tpcr		9		
				Vitric zone		Tpcrv		10		
					Nonwelded subzone	Tpcrv3		11		
					Moderately welded subzone	Tpcrv2		12		
					Densely welded subzone	Tpcrv1		13		
				Nonlithophysal zone		Tpcrn		14	4	04_TCw_Tpcrn
					Subvitrophyre transition subzone	Tpcrn4		15		
					Pumice-poor subzone	Tpcrn3		16		
					Mixed pumice subzone	Tpcrn2		17	5	05_TCw_Tpcrn2
					Crystal transition subzone (not always present)	Tpcrn1		18	6	06_TCw_Tpcrn1
				Lithophysal zone		Tpcrl		19		
					Crystal transition subzone (not always present)	Tpcrl1		20		
			Crystal-Poor Member			Tpcp	**Tpcp**	21		
				Upper lithophysal zone		Tpcpul		22	7	07_TCw_Tpcpul
					Spherulite-rich subzone	Tpcpul1		23		
				Middle nonlithophysal zone		Tpcpmn		24	8	08_TCw_Tpcpmn
					Upper subzone	Tpcpmn3		25		
					Lithophysal subzone	Tpcpmn2		26		
					Lower subzone	Tpcpmn1		27		
				Lower lithophysal zone		Tpcpll		28	9	09_TCw_Tpcpll
					Hackly-fractured subzone	Tpcpllh		29		
				Lower nonlithophysal zone		Tpcpln		30	10	10_TCw_Tpcpln
					Hackly subzone	Tpcplnh		31		
					Columnar subzone	Tpcplnc	**TpcLD**	32		
				Vitric zone		Tpcpv		33		
					Densely welded subzone	Tpcpv3	**Tpcpv3**	34	11	11_TCw_Tpcpv3
PTn					Moderately welded subzone	Tpcpv2	**Tpcpv2**	35	12	12_PTn_Tpcpv2
					Nonwelded subzone	Tpcpv1	**Tpcpv1**	36	13	13_PTn_Tpcpv1
			Pre-Tiva Canyon bedded tuff			Tpbt4	**Tpbt4**	37	14	14_PTn_Tpbt4
		Yucca Mountain Tuff				Tpy	**Yucca**	38	15	15_PTn_Tpy
			Pre-Yucca Mountain bedded tuff			Tpbt3	**Tpbt3_dc**	39	16	16_PTn_Tpbt3
		Pah Canyon Tuff				Tpp	**Pah**	40	17	17_PTn_Tpp
			Pre-Pah Canyon bedded tuff			Tpbt2	**Tpbt2**	41	18	18_PTn_Tpbt2
		Topopah Spring Tuff				Tpt		42		
			Crystal-Rich Member			Tptr		43		
				Vitric zone		Tptrv		44		
					Nonwelded subzone	Tptrv3	**Tptrv3**	45	19	19_PTn_Tptrv3
					Moderately welded subzone	Tptrv2	**Tptrv2**	46	20	20_PTn_Tptrv2
TSw1					Densely welded subzone	Tptrv1	**Tptrv1**	47	21	21_TSw1_Tptrv1
				Nonlithophysal zone		Tptrn		48	22	22_TSw1_Tptrn
					Dense subzone	Tptrn3		49		
					Vapor-phase corroded subzone	Tptrn2		50		
					Crystal transition subzone (not always present)	Tptrn1	**Tptrn**	51		
				Lithophysal zone		Tptrl		52	23	23_TSw1_Tptrl
					Crystal transition subzone (not always present)	Tptrl1	**Tptrl**	53		
			Crystal-Poor Member			Tptp		54		
				Lithic-rich zone		Tptpf or Tptrf	**Tptf**	55	24	24_TSw1_Tptf
							Tptpul			
				Upper lithophysal zone		Tptpul	**RHHtop**	56	25	25_TSw1_Tptpul
TSw2				Middle nonlithophysal zone		Tptpmn		57	26	26_TSw2_Tptpmn
					Nonlithophysal subzone	Tptpmn3		58		
					Lithophysal-bearing subzone	Tptpmn2		59		
					Nonlithophysal subzone	Tptpmn1	**Tptpmn**	60		
				Lower lithophysal zone		Tptpll	**Tptpll**	61	27	27_TSw2_Tptpll
				Lower nonlithophysal zone		Tptpln	**Tptpln**	62	28	28_TSw2_Tptpln
				Vitric zone		Tptpv		63		
TSw3					Densely welded subzone	Tptpv3	**Tptpv3**	64	29	29_TSw3_Tptpv3

Table 6-2. Yucca Mountain Stratigraphy as Used in *Geologic Framework Model (GFM2000)* (Continued)

Thermal Mech. Unit	Group	Formation	Member	Zone	Subzone	Abbreviation	Geologic Framework Model Unit	Subsequent Item Number	Lithostratigraphic Units Used in This Analysis	Lithostratigraphic Units Mapped in YMP Underground Excavations Used in This Analysis
CHn1					Moderately welded subzone	Tptpv2	Tptpv2	65	30	30_CHn1_Tptpv2
					Nonwelded subzone	Tptpv1	Tptpv1	66	31	31_CHn1_Tptpv1
			Pre-Topopah Spring bedded tuff			Tpbt1	Tpbt1	67	32	32_CHn1_Tpbt1
		Calico Hills Formation				Ta	Calico	68	33	33_CHn1_Tac
CHn2			Pre-Calico Hills bedded tuff			Tacbt	Calicobt	69	34	34_CHn2_Tacbt
CHn3	Crater Flat Group					Tc		70		
		Prow Pass Tuff				Tcp		71		
				Prow	Pass Tuff upper vitric nonwelded zone	Tcpuv	Prowuv	72	35	35_CHn3_Tcpuv
				Prow	Pass Tuff upper crystalline nonwelded zone	Tcpuc	Prowuc	73	36	36_CHn3_Tcpuc
				Prow	Pass Tuff moderately densely welded zone	Tcpmd	Prowmd	74	37	37_CHn3_Tcpm
				Prow	Pass Tuff crystalline nonwelded zone	Tcplc	Prowlc	75	38	38_CHn3_Tcplc
				Prow	Pass Tuff lower vitric nonwelded zone	Tcplv	Prowlv	76	39	39_CHn3_Tcplv
			Pre-Prow Pass Tuff bedded tuff			Tcpbt	Prowbt	77	40	40_CHn3_Tcpbt
		Bullfrog Tuff				Tcb	Tcb	78		
					Bullfrog Tuff upper vitric nonwelded zone	Tcbuv	Bullfroguv	79	41	41_CHn3_Tcbuv
					Bullfrog Tuff upper crystalline nonwelded zone	Tcbuc	Bullfroguc	80	42	42_CHn3_Tcbuc
					Bullfrog Tuff welded zone	Tcbmd	Bullfrogmd	81	43	43_CHn3_Tcbm
					Bullfrog Tuff lower crystalline nonwelded zone	Tcblc	Bullfroglc	82	44	44_CHn3_Tcblc
					Bullfrog Tuff lower vitric nonwelded zone	Tcblv	Bullfroglv	83	45	45_CHn3_Tcblv
			Pre-Bullfrog Tuff bedded tuff			Tcbbt	Bullfrogbt	84	46	46_CHn3_Tcbbt
		Tram Tuff				Tct		85		
					Tram Tuff upper vitric nonwelded zone	Tctuv	Tramuv	86	47	47_CHn3_Tctuv
					Tram Tuff upper crystalline nonwelded zone	Tctuc	Tramuc	87	48	48_CHn3_Tctuc
					Tram Tuff moderately densely welded zone	Tctmd	Trammd	88	49	49_CHn3_Tctm
					Tram Tuff lower crystalline nonwelded zone	Tctlc	Tramlc	89	50	50_CHn3_Tctlc
					Tram Tuff lower vitric nonwelded zone	Tctlv	Tramlv	90	51	51_CHn3_Tctlv
			Pre-Tram bedded tuff			Tctbt	Trambt	91		
			Lava and flow breccia (informal)			Tll		92		
			Bedded tuff			Tllbt		93		
		Lithic Ridge Tuff				Tr		94		
			Bedded tuff			Tlrbt		95		
			Lava and flow breccia (informal)			Tll2		96		
			Bedded tuff			Tllbt		97		
			Lava and flow breccia (informal)			Tll3		98		
			Bedded tuff			Tll3bt	Tund	99		
			Older tuffs (informal)			Tt		100		
					Unit a (informal)	Tta		101		
					Unit b (informal)	Ttb		102		
					Unit c (informal)	Ttc		103		
			Sedimentary rocks and calcified tuff (informal)			Tca		104		
			Tuff of Yucca Flat (informal)			Tyf		105		
	Pre-Tertiary sedimentary rock							106		
		Lone Mountain Dolomite				Slm		107		
		Roberts Mountain Formation				Srm	Paleozoic	108		

Source: MO9510RIB00002.004 [DIRS 103801], CRWMS M&O 1997 [DIRS 100223], pp. 43-50, GS980608314221.002 [DIRS 107024].

NOTE: Shaded rows indicate header lines for subdivided units

Tiva Canyon Tuff—The Tiva Canyon Tuff (Tpc) is a large-volume, regionally extensive tuff sequence that forms most of the rocks exposed at the surface of Yucca Mountain. The unit is compositionally zoned, ranging from a high-quartz rhyolitic glass at its base upward to a quartz latite. The thicknesses of the formation penetrated in boreholes or observed in outcrops range from less than 50 m to as much as 175 m (165 to 575 ft). The formation is divided into a lower crystal-poor member (Tpcp) and an upper crystal-rich member (Tpcr*/*), which in turn are further divided into zones and subzones based on lithophysal content and degree of welding (BSC 2004 [DIRS 169734], Section 3.3.4.7.5).

Yucca Mountain Tuff—The Yucca Mountain Tuff (Tpy) is a simple cooling unit that is nonwelded throughout much of the Yucca Mountain area, but is partially to densely welded where it thickens in the northern and western parts. The formation is thickest in the northern part of the project area, but thins to zero to the south. Although typically vitric in most locations in the central part, the tuff is increasingly devitrified where it is thick. The formation is nonlithophysal throughout Yucca Mountain, but contains lithophysae where densely welded in northern Crater Flat. The formation is chemically similar to the high-silica rhyolites of the Tiva Canyon and Topopah Spring Tuffs. It contains both plagioclase and sanidine crystal-fragments. The pre-Yucca Mountain Tuff bedded tuff (Tpbt3) consists of pumiceous, vitric, nonwelded pyroclastic-flow deposits (BSC 2004 [DIRS 169734], Section 3.3.4.7.4).

Pah Canyon Tuff—The Pah Canyon Tuff (Tpp) is a simple cooling unit composed of multiple-flow units that are poorer in silica content than the high-silica rhyolites of several of the other volcanic-rock units. The formation reaches its maximum thickness of about 79 m (260 ft) in the northern part of Yucca Mountain, and thins southward to zero. The Pah Canyon Tuff varies from nonwelded to moderately welded and, throughout much of the area, vitric pumice clasts are preserved in a nondeformed matrix that was sintered or lithified by vapor-phase mineralization. Throughout much of the area, vitric pumice clasts are preserved in a nondeformed matrix that was sintered or lithified by vapor-phase mineralization. Crystal fragments in the matrix and in large pumice clasts constitute 5% to 10% of the rock, with a larger proportion of feldspars relative to mafic minerals (biotite and clinopyroxene). Lithic clasts of devitrified rhyolite (as much as 5% of the rock) are common, and clasts of porphyritic obsidian occur in some horizons. Shards occur either as poorly preserved clear glass or as devitrified material. Because of the relatively impermeable upper vitrophyre of the underlying Topopah Spring Tuff, the alteration of the Pah Canyon Tuff (typically to smectite) is generally more extensive than that of the overlying Yucca Mountain Tuff. The pre-Pah Canyon bedded tuff (Tpbt2), about 3 to 10 m thick, consists of moderately well-sorted pumiceous tephra with thin layers of lithic-rich fallout and very fine-grained ash at the base (BSC 2004 [DIRS 169734], Section 3.3.4.7.2).

Topopah Spring Tuff—The Topopah Spring Tuff (Tpt) includes the host rock units for the repository. As such, its characteristics are of direct importance to repository design, unsaturated zone hydrologic flow and radionuclide transport, and TSPA. Consequently, it is probably the most extensively characterized unit of the lithostratigraphic sequence at Yucca Mountain. The Topopah Spring Tuff is 0 to 381 m (0 to 1,250 ft) thick in the YMP area. The formation is divided into a lower crystal-poor member and an upper crystal-rich member. Vitric rocks form zones at the top and bottom of the formation, and alternating lithophysal and nonlithophysal zones characterize the remaining parts of the two members. The Topopah Spring Tuff is

compositionally zoned, with an upward chemical change from high-silica rhyolite in the crystal-poor member to quartz latite in the crystal-rich member. The two members are clearly distinguishable on the basis of mineralogy and trace element concentrations. The lower part of the formation, which is the repository horizon, is one of the most chemically homogeneous rock types in the region. The crystal-poor member, characterized by 3% or less of felsic crystal fragments, is divided into vitric rocks of the vitric zone near the base and (in ascending order) devitrified rocks of the lower nonlithophysal, lower lithophysal, middle nonlithophysal, and upper lithophysal zones. The vitric zone is divided primarily on the basis of degrees of welding, which ranges upward from a nonwelded to partially welded subzone at the base, through a moderately welded subzone, to a densely welded subzone at the top. The vitric, densely welded subzone, commonly referred to as the vitrophyre (Tptpv3), is identified as an important subunit within the Topopah Spring welded thermal-mechanical unit (TSw3) (BSC 2004 [DIRS 169734], Section 3.3.4.7.1).

6.1.2.2.3 Calico Hills Formation (Tac)

The Calico Hills Formation (Tac), which underlies the Paintbrush Group, is a complex series of rhyolite tuffs and lavas. Five pyroclastic units, overlying a bedded-tuff unit and a locally occurring basal sandstone unit, have been distinguished in the Yucca Mountain area. The formation thins southward across the repository area, from composite thicknesses of as much as 460 m (1,500 ft) to only about 15 m (50 ft) (BSC 2004 [DIRS 169734], Section 3.3.4.6).

The basal volcaniclastic sandstone unit of the Calico Hills Formation is interbedded with rare reworked pyroclastic flow deposits. Thicknesses of the unit range from 0 to 5.5 m (0 to 18 ft). The overlying bedded tuff (unit Tacbt), 9 to 39 m thick, is composed primarily of pyroclastic fall deposits. Each of the five pyroclastic units forming the bulk of the Calico Hills Formation (units Tac1 to Tac5) consists of one or more pyroclastic flow deposits separated by locally preserved fall horizons. Ash-fall and ash-flow deposits beneath the repository block give way to lava flows to the north and east (BSC 2004 [DIRS 169734], Section 3.3.4.6).

There is an abundance of authigenic zeolites in all units of the Calico Hills Formation. The presence of zeolitized zones within the Calico Hills Formation has important implications with respect to paleohydrologic interpretations and the potential development of natural barriers to contaminant (radionuclide) movement by groundwater (BSC 2004 [DIRS 169734], Section 3.3.4.6).

6.1.3 Geology at Repository Footprint

The rock strata underlying Yucca Mountain have been divided according to geologic criteria into lithostratigraphic zones and subzones that are stratiform (laterally continuous) on a repository scale, but locally may vary (Section 6.1.2.1). The RHH is the body of rock, in which the repository excavations are planned, and it spans four lithostratigraphic zones (the lower part of the Tptpul, Tptpmn, Tptpll, and Tptpln) as part of the Topopah Spring Tuff formation (Figure 6-1)[1]. The repository will cover about 5.0 km^2 (1.9 mi^2) within the Topopah Spring Tuff Formation, as shown in Figure 6-2. Approximately 66 km (41 miles) of the emplacement drifts

[1] The word "tuff" is a term of formal stratigraphic nomenclature but also carries the connotation of a mappable ashflow cooling unit that was emplaced in an instant of geologic time (Byers et al. 1976 [DIRS 104639], p. 2).

(BSC 2003 [DIRS 165572], Table 8) will be located primarily within the Tptpll (red shading in Figure 6-2; 81%), and the Tptpmn (green shading in Figure 6-2; 12%). The remaining geological units comprise about 7% (Tptpul about 4% and Tptpln about 3%) of the emplacement drift area. Overall, the nonlithophysal rocks comprise approximately 15% of the emplacement area, whereas the lithophysal rocks comprise approximately 85%. Details of the repository layout are presented in *Underground Layout Configuration* (BSC 2003 [DIRS 165572], Section 8.4 and Table II-2).

A detailed description of Topopah Spring Tuff formation is presented by Buesch et al. (1996 [DIRS 100106], pp. 19 to 21) and in *Yucca Mountain Site Description* (BSC 2004 [DIRS 169734], Section 3.3), and its major features are summarized in Section 6.1.3.1.

6.1.3.1 Topopah Spring Tuff Characteristics

The rocks of the RHH are within the crystal-poor member of the Topopah Spring Tuff, and geochemically these rocks have a very uniform geochemical composition of rhyolite. Lithostratigraphic features in the crystallized rocks of the Topopah Spring Tuff include the matrix-ground mass, lithophysal cavities, rims (developed on lithophysal cavities and some fractures), spots, vapor-phase mineral coatings or linings, and vapor-phase corroded or mineralized areas (Figure 6-3). The matrix-ground mass is a combination of sedimentary and igneous petrologic terms applicable to crystallized pyroclastic-flow deposits (or ignimbrites). The term “matrix” is used as a sedimentological term that refers to the finer-grained material between larger grains. In ignimbrites, the matrix material has vitroclastic textures formed by shards, crystal, pumice, and lithic clasts that are typically less than a few millimeters in size, and this material is between the larger clasts of pumice, lithic, and even crystal fragments. The term “ground mass” is used as an igneous term that refers to the fine-grained interstitial minerals between coarse-grained minerals. The “high” temperature crystallization of ignimbrites (typically about 550°C to 900°C, depending on the geochemical composition) results in fine-grained textures of feldspar and quartz (or cristobalite). Lithophysae are the gas cavities in a rock formed where the vapor pressure was great enough to inflate a cavity; most lithophysae have various components including the cavity, rim, and a vapor-phase mineral coating (or lining). A spot is similar in texture and mineralogical composition to a rim, except there is not a cavity. Some spots have “cores” of crystal fragments, lithic clasts, or small areas of crystallized matrix-ground mass.

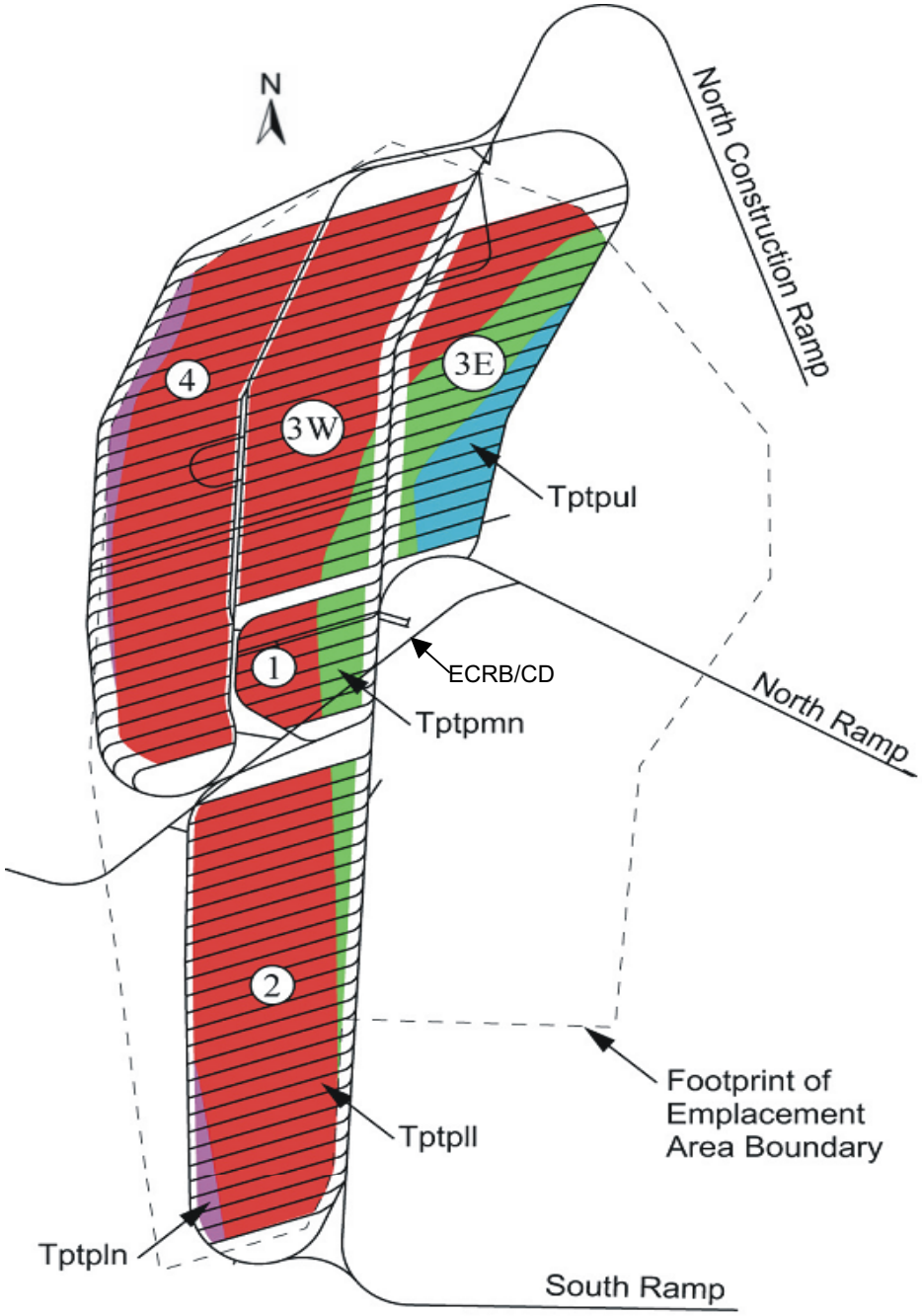

Source: Modified from *Underground Layout Configuration* (BSC 2003 [DIRS 165572], Figure II-3).

NOTES: Footprint of emplacement area boundary is shown as a dashed line. This footprint represents the currently characterized area in which emplacement drifts can be located. Circled numbers are Construction Panel Numbers.

Figure 6-2. Plan View of Repository Layout Showing an Overlay of the Lithostratigraphic Rock Units at the RHH

Unlike the earliest assessments, the current understanding is that the majority of fractures and associated features mapped underground at Yucca Mountain are cooling joints; however, there also are localized tectonic fracture zones related to faults. Some cooling joint fractures and incipient fractures are characterized by four major features, depending on the size, type of rock and fracture described: veinlets, streaks, stringers, and vapor-phase partings. Early cooling fractures may have formed while the rock was still glassy, and some cooling fractures served as pathways that transferred vapor during cooling and welding of the ignimbrite. These pathways led to either porous rim material along the open fractures or, later in time, surface deposits of vapor phase minerals. The sub-horizontal vapor phase partings are relatively continuous structures seen throughout the Tptpmn (see BSC 2004 [DIRS 166107], Figure 6-9). This continuous, not anastamosing fractures are subparallel to the foliation of the rock unit, and are filled with concentration of vapor-phase minerals (primarily tridymite and critobalite). The surface are rough on a small scale and, as a results of mineral filling, they have cohesion (unlike the sub-vertical fractures).

Changes in the numbers and roughness of fractures typically coincide with the boundaries of lithophysal and nonlithophysal zones. In general, although nonlithophysal zones have vapor phase parting fractures, the zones are dominated by high-angle fractures with smooth surfaces. In contrast, lithophysal zones contain some low-angle fractures with rough surfaces, except possibly near zone boundaries (BSC 2003 [DIRS 166660], Section 5.3.3.2).

6.1.3.2 Repository Host Horizon Rock Units

Site-specific characteristics of the rock units of the Topopah Spring Tuff that constitute the host rock at the repository horizon have been described in detail through the geologic mapping of those units in both the ESF tunnel and the ECRB Cross-Drift. These studies, which have been summarized for the ESF (Beason et al. 1996 [DIRS 101191]; Barr et al. 1996 [DIRS 100029]; Albin et al. 1997 [DIRS 101367]; Eatman et al. 1997 [DIRS 157677]), and for the ECRB Cross-Drift (Mongano et al. 1999 [DIRS 149850]), are the sources for the site-specific unit descriptions presented here. The locations of the ESF tunnel and ECRB Cross-Drift, and the lithostratigraphic units excavated by the tunnel and drift, are illustrated in the geologic cross section shown in Figure 6-4. The units that comprise the host rocks of the repository horizon are all zones of the crystal-poor member (Tptp) of the Topopah Spring Tuff. In descending order, the host rocks consist of the lower part of the Tptpul of the TSw1 unit, and all of the TSw2 unit, which includes the Tptpmn, Tptpll, and the Tptpln. In terms of the repository layout design (Figure 6-2), it has been determined that the emplacement drifts would be located primarily within the Tptpll and the Tptpmn zones (Board 2003 [DIRS 165036], Section 4).

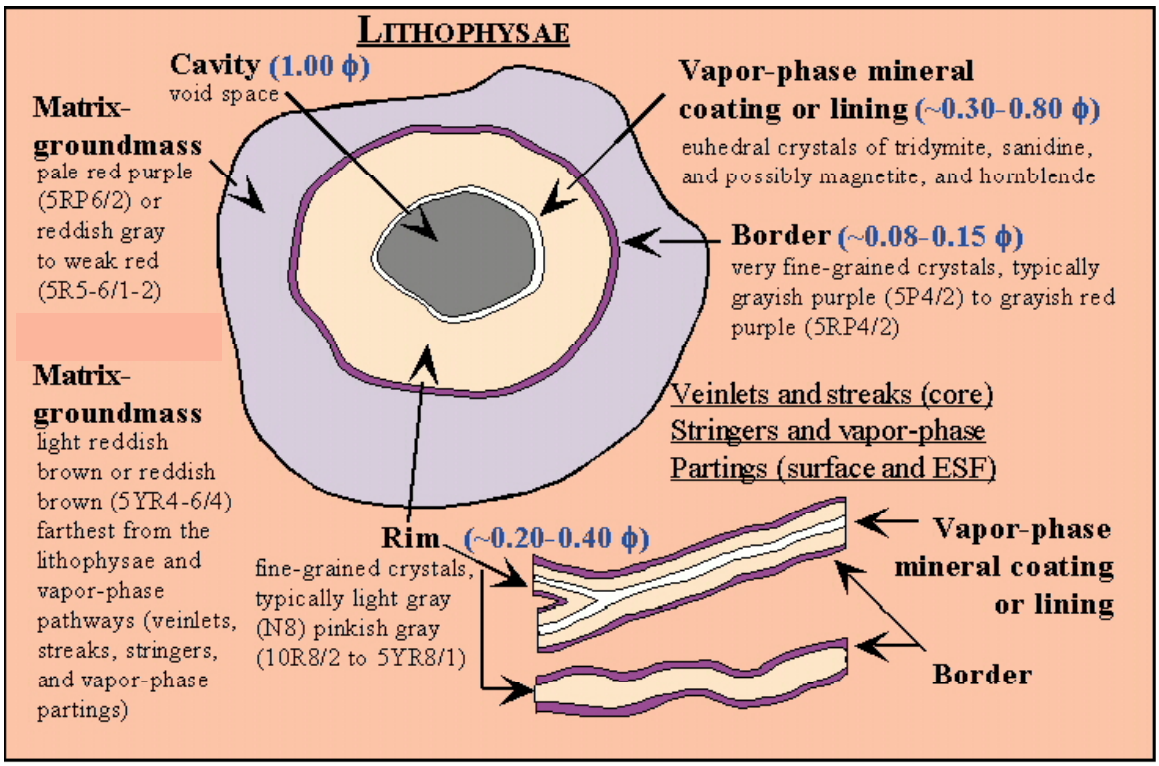

Source: Modified from *Proposed Stratigraphic Nomenclature and Macroscopic Identification of Lithostratigraphic Units of the Paintbrush Group Exposed at Yucca Mountain, Nevada* (Buesch et al. 1996 [DIRS 100106], Figure 3).

NOTES: Porosity values (ϕ) for rims, borders, and vapor-phase mineral coatings are estimates by Buesch (2003 [DIRS 162271]). Note that there are two types of matrix-ground mass. The nomenclature for color (e.g., pale red purple – 5RP6/2) is based on soil color charts (Munsell Color Company 1994 [DIRS 106399]).

Figure 6-3. Typical Lithostratigraphic Features Related to Lithophysae and Fractures

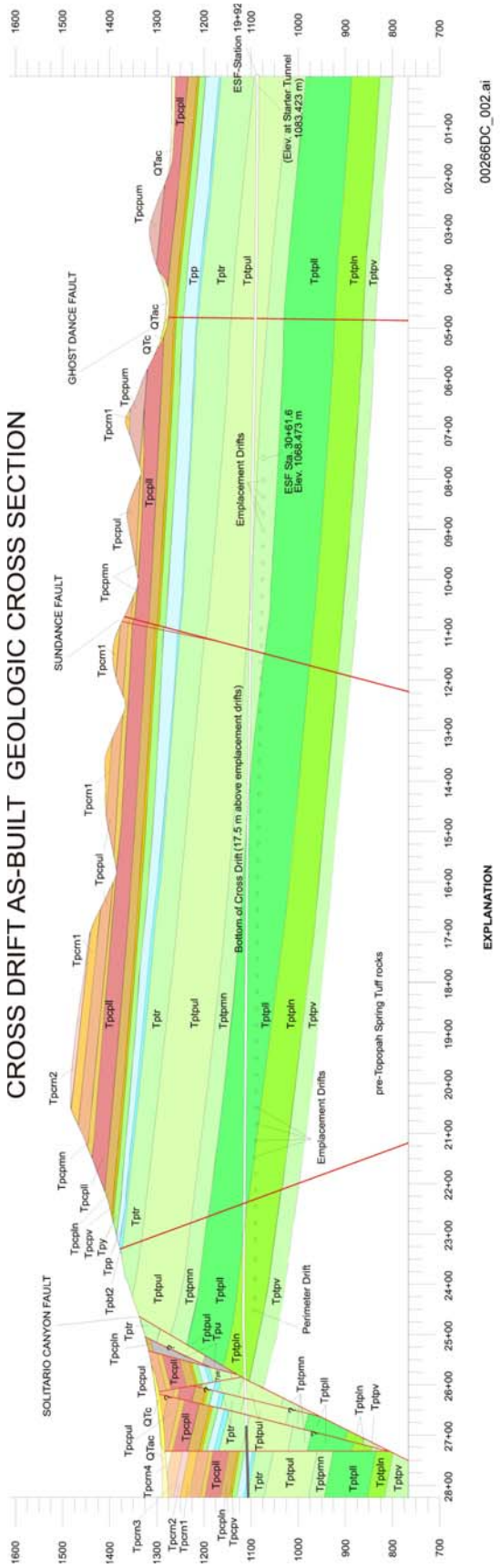

Source: Modified from *Geology of the ECRB Cross Drift—Exploratory Studies Facility, Yucca Mountain Project, Yucca Mountain, Nevada* (Mongano et al. 1999 [DIRS 149850], Drawing OA-46-345).

Figure 6-4. Geologic Cross Section through the ECRB Cross Drift (approximately Northeast-Southwest, Looking Northwest)

Based on the report by Mongano et al. (1999 [DIRS 149850]), the site-specific characteristics of the repository horizon zones from tunnel mapping are summarized as follows:

Tptpul: The crystal-poor upper lithophysal zone is exposed in both the ESF tunnel and ECRB Cross-Drift. The ECRB Cross-Drift begins in the upper central portion of the zone and it exposes rocks of the central and lower portions of the zone from Station 0+00 to 10+15. The upper portion of the upper lithophysal zone is also exposed in the hanging wall of the eastern strand of the Solitario Canyon fault zone from Station 25+90 to 26+57.5. In both exposures, the zone is moderately to densely welded, devitrified, and vapor-phase altered. In general, the rock appears grayish red-purple (5RP4/2) and contains 10% to 40% vapor-phase spots, stringers, and partings. The central and lower parts of the zone (Station 0+00 to 10+15) are composed of 0% to 15% pumice, 1% to 3% phenocrysts, 0% to 5% lithic fragments, 10% to 60% lithophysae, and 40% to 90% matrix. The upper part of the zone (Station 25+90 to 26+57.5) is composed of 5% to 15% pumice, 2% to 5% phenocrysts, less than 1% lithic fragments, 3% to 20% lithophysae, and 60% to 90% matrix.

Tptpmn: The ESF tunnel is excavated in the middle nonlithophysal zone from Stations 27+21 to 57+29, from 58+78 to 63+08, and from 70+58 to 71+68. The ECRB Cross-Drift exposes the middle nonlithophysal zone from Station 10+15 to 14+44. In general, the moderately to densely welded, devitrified and variably vapor-phase altered zone is composed of less than 5% to 10% pumice (locally 25% to 35%), 1% to 2% phenocrysts, 1% to 2% lithic fragments, 0% to 1% lithophysae, and 85% to 93% matrix. Vapor-phase spots, stringers, and partings comprise from 1% to 15% of the rock. Smooth, high-angle fractures are typical of the zone, but it also contains occasional low-angle, continuous shears and cooling joints. Another feature characteristic of the Tptpmn is the presence of low-angle concentrations of vapor-phase minerals. These features appear as continuous partings subparallel to the dip of the zone.

Tptpll: The ESF tunnel exposes a small portion of the upper contact of the lower lithophysal zone from Station 57+29 to 58+78. The lower lithophysal zone is exposed along the ECRB Cross-Drift from Station 14+44 to 23+26. In general, the moderately to densely welded, devitrified, and vapor-phase altered zone is composed of 3% to 7% pumice (locally 10% to 35%), 1% to 2% phenocrysts, 1% to 5% lithic fragments (locally 12% to 15%), 5% to 30% lithophysae (locally 1% to 5%), and 56% to 90% matrix. Lithophysae vary in size from ten centimeters to greater than 1 m in diameter. Throughout most of the zone, vapor-phase spots, stringers, and wisps comprise between 3% and 12% of the rock. In several intervals, however, vapor-phase alteration products form 15% to 40% of the rock.

Tptpln: The Tptpln, exposed only in the ECRB Cross-Drift from Station 23+26 to 25+85, comprises moderately to densely welded, devitrified pyroclastic-flow material. It is generally composed of 3% to 20% pumice, 1% to 2% phenocrysts, 3% to 7% lithic fragments, 0% to 5% lithophysae, and 66% to 93% matrix. Vapor-phase alteration products form a minor component of the rock in some portions of the zone. Rocks of the lower nonlithophysal zone vary from a heterogeneous mix of grayish red and grayish orange pink (5YR7/2) to comparatively homogeneous pale red, light brown, pale brown, or grayish brown (5YR6/4). Near the Solitario Canyon fault zone, this zone is brecciated and altered. In this area, the breccia matrix varies from moderate reddish brown to grayish orange pink to pale red; breccia clasts are locally bleached to very light gray adjacent to the fault plane.

Rock Mass Structural Features—Internal structures within the tuffaceous host rocks of the repository horizon are among the most important features in determining their thermal-mechanical properties, their geotechnical strength, and their structural response to repository-related stresses. Among the most important internal structures are fracture characteristics and lithophysal content (and associated porosity). These structures have been extensively mapped in the ESF tunnel and the ECRB Cross-Drift (CRWMS M&O 1998 [DIRS 102679], Section 7.4; Mongano et al. 1999 [DIRS 149850], pp. 12 to 46), and various relationships have been observed (Figures 6-3, 6-5, and 6-6).

The two basic types of repository host rock units are nonlithophysal zones (Tptpmn, Tptpln) and lithophysal zones (Tptpul, Tptpll), based on their relative proportion of lithophysal cavities (Figure 6-5). The nonlithophysal zones are generally hard, strong, fractured rocks with matrix porosities of 10% or less. Fractures that formed during the cooling process are the primary structures in these zones. In contrast, the lithophysal zones have significantly fewer fractures of significant continuous length (i.e., trace length greater than 1 m), but have relatively uniformly distributed porosity in the form of lithophysal cavities. Lithophysal porosity in the Tptpul and Tptpll is on the order of 10% to 30% by volume. The ground mass that makes up the rock matrix in the lithophysal zones is heavily fractured with small scale (lengths on the order of 1 cm) inter-lithophysal fractures in the Tptpll, but is relatively fracture-free in the Tptpul (Board 2003 [DIRS 165036], Section 5.2).

As shown in Figure 6-6, detailed line mapping in the ECRB Cross-Drift (Mongano et al. 1999 [DIRS 149850], p. 76 and Figure 13) has demonstrated an inverse relationship between fracture density and lithophysal porosity in the repository host rock units. The density of fractures with trace length greater than 1 m is significantly higher in the Tptpmn and Tptpln (20 to 35 fractures per 10 m), as compared to five fractures per 10 m or less in the Tptpul and Tptpll where lithophysal porosities are higher. The fractures and lithophysae are among the dominant rock structures that will probably largely determine the thermal-mechanical responses of the rock mass during repository construction and operation.

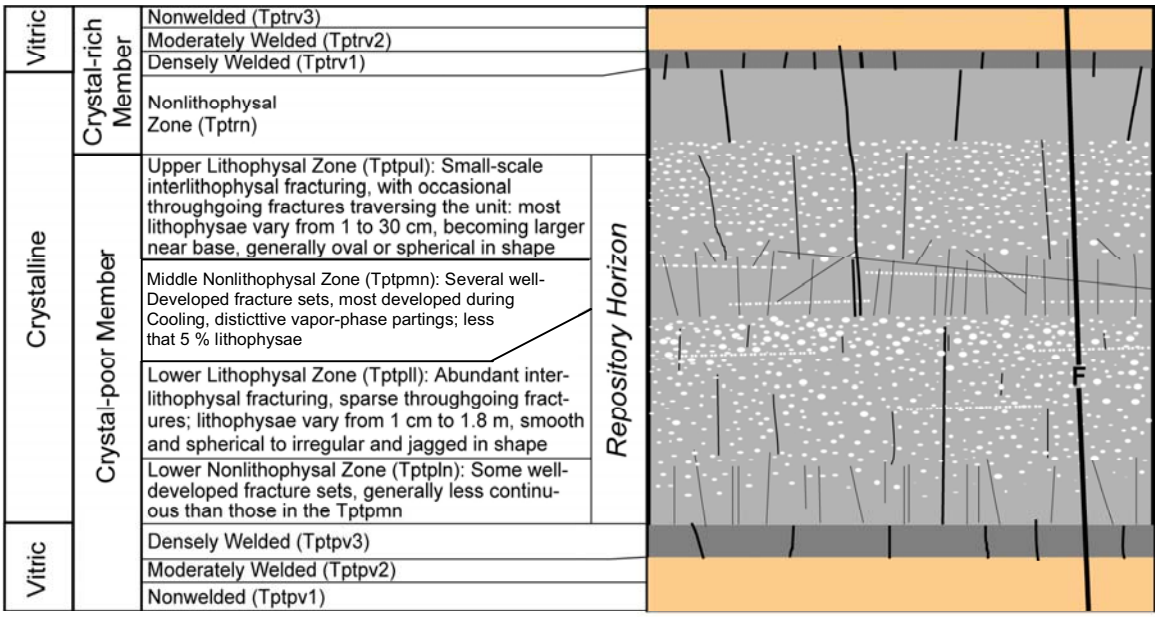

Diagrammatic Cross Section of the Topopah Spring Tuff Illustrating Relative Discontinuity Densities and Orientations: This figure indicates how fractures, faults, and lithophysae are typically distributed through the ignimbrite.

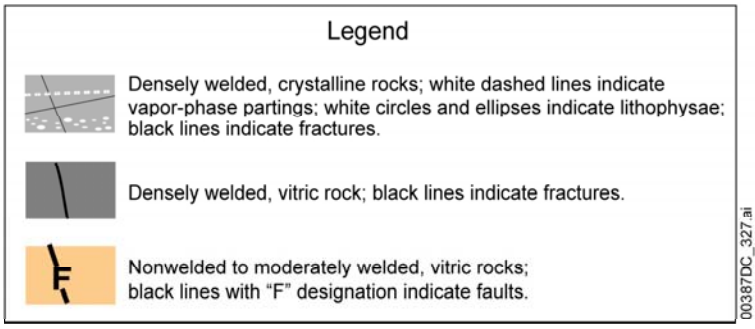

Source: Modified from *Drift Degradation Analysis* (BSC 2004 [DIRS 166107], Figure 5).

Figure 6-5. Schematic Illustration of the Structure of the Topopah Spring Tuff

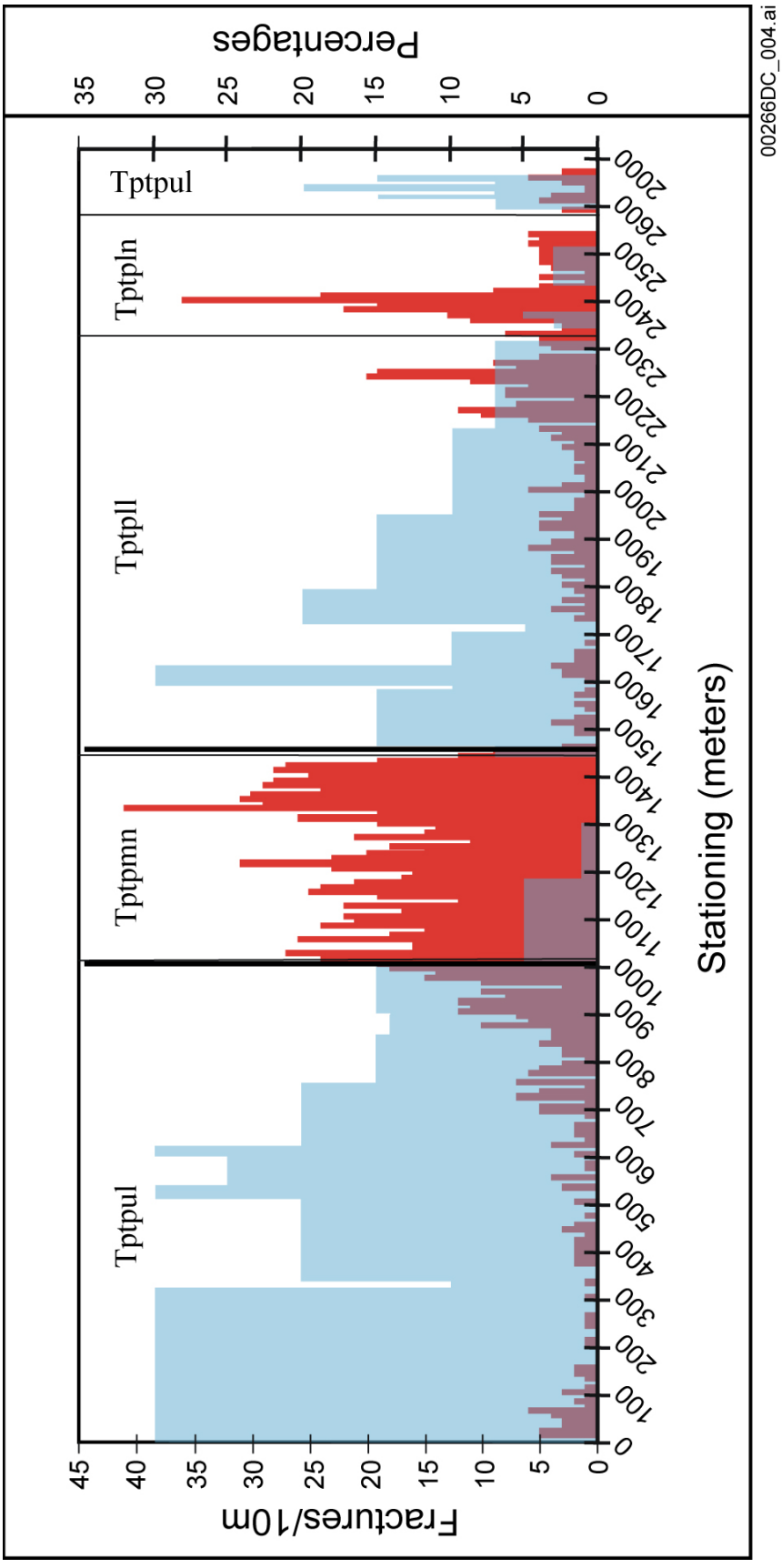

Source: Mongano et al. 1999 [DIRS 149850], Figure 13.

NOTE: Observe the inverse relationship within individual lithostratigraphic zones.
Light blue indicates lithophysal porosity and red indicates fracture frequency per 10 m.

Figure 6-6. Composite Plot of Fracture Frequency and Lithophysal Porosity as a Function of Distance along the ECRB Cross Drift

6.1.3.2.1 Emplacement Areas

The Topopah Spring Tuff (Tpt) encompasses the host rock zones for the repository, and its characteristics have been studied in detail. A detailed description of this formation is presented in *Proposed Stratigraphic Nomenclature and Macroscopic Identification of Lithostratigraphic Units of the Paintbrush Group Exposed at Yucca Mountain, Nevada* (Buesch et al. 1996 [DIRS 100106], pp. 19 to 21) and in *Yucca Mountain Site Description* (BSC 2004 [DIRS 169734], Section 3.3).

The Topopah Spring Tuff (Tpt) is divided into a lower crystal-poor member (Tptp) and an upper crystal-rich member (Tptr) as illustrated in Figure 6-5. Each member is divided into numerous zones, subzones, and intervals based on variations in depositional features, such as crystal content and assemblage, lithophysal content, size and abundance of pumice and lithic clasts, distribution of welding and crystallization zones, and fracture characteristics.

The Topopah Spring Tuff is compositionally zoned, with an upward change from high-silica rhyolite in the crystal-poor member to quartz latite in the crystal-rich member; these two members are also clearly distinguishable on the basis of mineralogy and trace element concentrations. The lower crystal-poor member (Tptp) of the Topopah Spring Tuff, which encompasses the repository horizon, is one of the most chemically homogeneous rock types in the region. The homogeneity of the major-element chemistry within the high-silica rhyolite also extends to trace elements. Somewhat greater chemical variability is seen in the quartz latites. These characteristic chemical differences result in variable devitrification, vapor-phase, and low-temperature alteration minerals that account for differences in rock texture and mineralogy between the rhyolitic and quartz-latitic rocks.

The crystal-poor member (Tptp), which is characterized by less than 3% felsic phenocrysts, is divided into vitric rocks of the vitric zone near the base (Tptpv) and devitrified rocks of the Tptpul, Tptpmn, Tptpll, and Tptpln zones; the latter four zones form the host rock for the repository. The vitric zone (Tptpv) is divided into three subsystems primarily on the basis of degrees of welding, which range upward from a nonwelded subzone (Tptpv1) at the base, that includes partially welded rocks near the top, through a moderately welded subzone (Tptpv2), to a densely welded subzone (Tptpv3) that caps the sequence. The vitric, densely welded subzone (Tptpv3), commonly referred to as the vitrophyre, is also identified as an important thermal-mechanical unit (TSw3).

Within the repository host rock units (i.e., the devitrified, rhyolitic portion of the Topopah Spring Tuff), crystal fragments are minor constituents (less than 5%) of the rock, with the remaining more than 95% consisting of fine-grained devitrification minerals. These devitrification products are principally feldspars plus a variable combination of the silica polymorphs tridymite, cristobalite, and quartz. The silica polymorph distributions are particularly important because of their thermal stability, dissolution properties, and properties as inhalation hazards.

A transitional zone, commonly referred to as the vitric-zeolitic transition, extends downward from the base of the Tptpln into the crystal-poor vitric zone (Tptpv) through a stratigraphic interval ranging from about 3 to 30 m in thickness.

In many parts of Yucca Mountain, the moderately welded and nonwelded subzones at the base of the crystal-poor vitric zone are overprinted by zeolite alteration zones. Accordingly, a vitric-zeolitic boundary can be drawn that varies within a narrow range of stratigraphic positions, but generally coincides closely with the contact between the moderately welded subzone and the overlying densely welded subzone.

The crystal-rich member (Tptr) is characterized by greater than 10% crystal fragments, with a crystal-transition subzone at the base where the abundance of phenocrysts increases upward from 3% to 10%. In ascending order, the crystal-rich member is divided into lithophysal (Tptrl), nonlithophysal (Tptrn), and vitric (Tptrv) zones. Rocks in both the lithophysal and nonlithophysal zones are devitrified, and the division is based on the presence or absence of lithophysae. The vitric zone (Tptrv), which caps the member, is distinguished by preservation of the volcanic glass to form rocks with a vitreous luster that typically grade upward from densely welded (Tptrv1) to nonwelded (Tptrv3). This vitric zone is a particularly important geochemical subunit because it is relatively impermeable.

The repository will consist of four emplacement panels (Panels 1-4) within the Topopah Spring Formation, as shown in Figure 6-2. Emplacement drifts will have a diameter of 5.5 m (18 ft) and are found primarily within the Tptpll (red areas, 81%), and the Tptpmn (green areas, 12%) zones. The remaining geological units comprise about 7% (Tptpul about 4% and Tptpln about 3%) of the emplacement drift area. Overall, the nonlithophysal rocks comprise approximately 15% of the emplacement area, whereas the lithophysal rocks comprise approximately 85% (BSC 2003 [DIRS 165572], Section 8.4 and Table II-2).

6.1.3.2.2 Non-emplacement Areas

The non-emplacement openings for the repository underground layout (Figure 6-2) are located above, within, and below the host rock horizon.

Excavations to be located mostly above the host rock horizon include the portals, the access ramps, and ventilation shafts and raises. The stratigraphy for rock formations that host the non-emplacement openings has been extensively characterized for the ESF. The ESF tunnel traversed all the formations of interest from the surface to the emplacement horizon. Stratigraphy crossed by the North Ramp, the main access way to the repository, is included in Figure 6-7. The North Ramp descends at a maximum grade of 2.15% from the North Portal to the approach curve into the ESF main drift (Station 21+87), where the tunnel turns into a mild uphill grade to meet the ESF main drift at Station 28+04. The North Ramp starts at the North Portal (Station 00+00 in Figure 6-7) at an invert elevation of 1122.56 m and it ends at Station 28+04 at elevation 1065.00 m (BSC 2003 [DIRS 165572], Figure 3).

Stratigraphic interpretations between Stations 00+00 and approximately 4+50 are difficult because of the effects of the Bow Ridge Fault and the Daylight Valley Faults A and B (see Figure 6-8). This section of the North Ramp crosses the alluvium and some units of the Timber Mountain Group (Rainier Mesa Tuff—Tmr, and Pre-Rainier Mesa bedded tuff—Tmbt1), and some of the uppermost units of the Paintbrush Group (pyroclastic flow deposit—Tpki also known as tuff unit "X", and the Tiva Canyon Tuff units Tpcrn and Tpcpul) (Brechtel et al. 1995 [DIRS 101493], Section 4.3). Stations 4+00 to 8+69 of the North Ramp expose units of the Tiva

Canyon Tuff from the crystal-rich nonlithophysal zone to the base of the formation. The Tiva Canyon Tuff is composed of multiple pyroclastic-flow units that are distinguished by swarms of pumice clasts or laminated horizons of crystal-rich material. A prominent zone of argillic alteration occurs within the Tiva Canyon Tuff at the contact between the crystal-poor lower nonlithophysal zone and crystal-poor vitric zone. A thin ground layer composed of coarse pumice and lithic clasts marks the base of the formation. Stations 8+69 to 10+76 expose a series of nonwelded reworked deposits, pumice-fall deposits and pyroclastic-flow deposits that include the Yucca Mountain Tuff and Pah Canyon Tuff. Cross lamination, substrate erosion, and other textural features clarify the depositional histories of these units, which were locally altered to zeolite minerals (the lower Pah Canyon Tuff and underlying reworked deposits). A localized zone of intense argillic alteration occurs within the pre-Pah Canyon Tuff bedded tuffs at the contact between reworked deposits and pumice-fall deposits (approximately Stations 10+20 to 10+45). This region has a complex geologic history that reflects a period of fumarolic/hydrothermal alteration associated with cooling of the underlying Topopah Spring ignimbrite.

Exposures in Alcove 4 illustrate the limited extent of this dramatic feature. Stations 10+76 to 28+00 expose pyroclastic-flow units of the Topopah Spring Tuff from the crystal-rich vitrophyre to the crystal-poor middle nonlithophysal zone. The Topopah Spring Tuff is composed of multiple pyroclastic-flow units that are distinguished by swarms of pumice clasts. The exposure in the North Ramp clarifies and confirms many lithostratigraphic relationships within the Topopah Spring Tuff that were previously inferred from studies of drill core, downhole video, and hydrologic observations. Included are a zone of intense vapor-phase alteration within the crystal-rich nonlithophysal zone (Stations 12+75 to 13+36), the cavernous lithophysal subzone of the crystal-poor upper lithophysal zone (Stations 17+97 to 19+06), and a flow unit containing blocks of quartz latite pumice in the crystal-poor lithophysal zone (Stations 19+06 to 20+80), all of which are features with stratigraphic significance in the North Ramp.

Lithophysae, which is present in both the Tiva Canyon Tuff and the Topopah Spring Tuff vary in size and internal characteristics within each unit. Contacts between lithophysal and nonlithophysal rock are gradational over a few meters. Lithophysae are lined with vapor-phase minerals, locally including specular hematite; they locally have calcite and opal as secondary minerals (Barr et al. 1996 [DIRS 100029], pp. 20 and 126 to 128).

The fracture network in the North Ramp from Stations 4+00 to 21+87 can be divided into three sets by cluster analysis. The first set includes cooling fractures that occur mostly in the Tiva Canyon Tuff and Topopah Spring Tuff. This set of cooling joints dips steeply, and strikes east-west, with a mean orientation of 254 to 258 degrees. The second set, which is the dominant tectonic set of fractures, occurs in all rock units, including the bedded tuffs. These features strike northeast-southwest, and dip steeply to the west. Although the frequency of tectonic fractures is lower in the bedded tuffs than in the welded ash-flow deposits, this set is the only set that is well represented in the bedded tuffs. The mean orientation of this set is 215 to 219 degrees, although there is a wide scatter in the data, ranging from 132 to 230 degrees. All of the continuous faults with significant offset observed in the North Ramp fall within this set. The third set of fractures is the shallowly dipping, subhorizontal features such as vapor-phase partings. These, as with the first set, occur primarily in the Tiva Canyon and Topopah Spring Tuffs. The mean orientation of

this set is approximately 016 to 025 degrees, although the orientation of these fractures scatters widely around the horizontal plane (Barr et al. 1996 [DIRS 100029], pp. 126 to 128).

Non-emplacement excavations located within the host rock horizon include all the turnouts (one for each emplacement drift), the access and exhaust mains that are aligned along the perimeter of the emplacement areas, intake and exhaust shaft access drifts, and the observation drift that is located a few meters below the Panel 1 emplacement drifts invert elevations. There are no planned repository excavations into the lower units of the Paintbrush Group such as into the vitric zone (Tptpv).

Ventilation shaft and raise excavations for the repository will traverse either all or majority of the rock units discussed in this section. They will range in depth from approximately 248 to 428 m (BSC 2003 [DIRS 165572], Table 7). Figure 6-9 illustrates the stratigraphic column for a location east of Panel 1 and about half way between Exhaust Raise #2 and Intake Shaft #3, and provides representative thicknesses of the different rock units to be traversed by a non-emplacement vertical excavation in the general area.

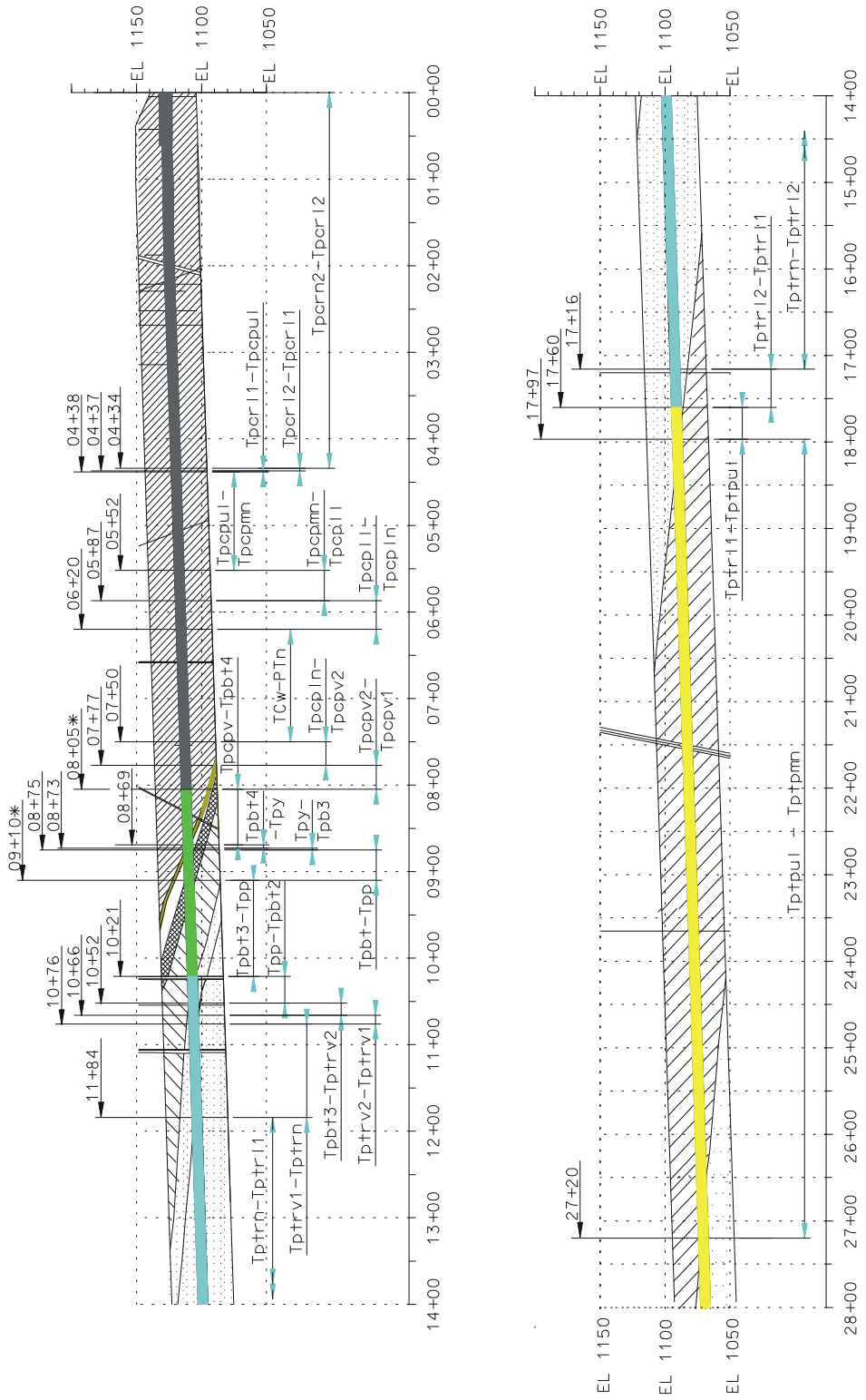

Source: Modified from *Geology of the North Ramp — Stations 4+00 to 28+00, Exploratory Studies Facility, Yucca Mountain Project, Yucca Mountain, Nevada* (Barr et al. 1996 [DIRS 100029], Table 1).

Figure 6-7. North Ramp Stratigraphy

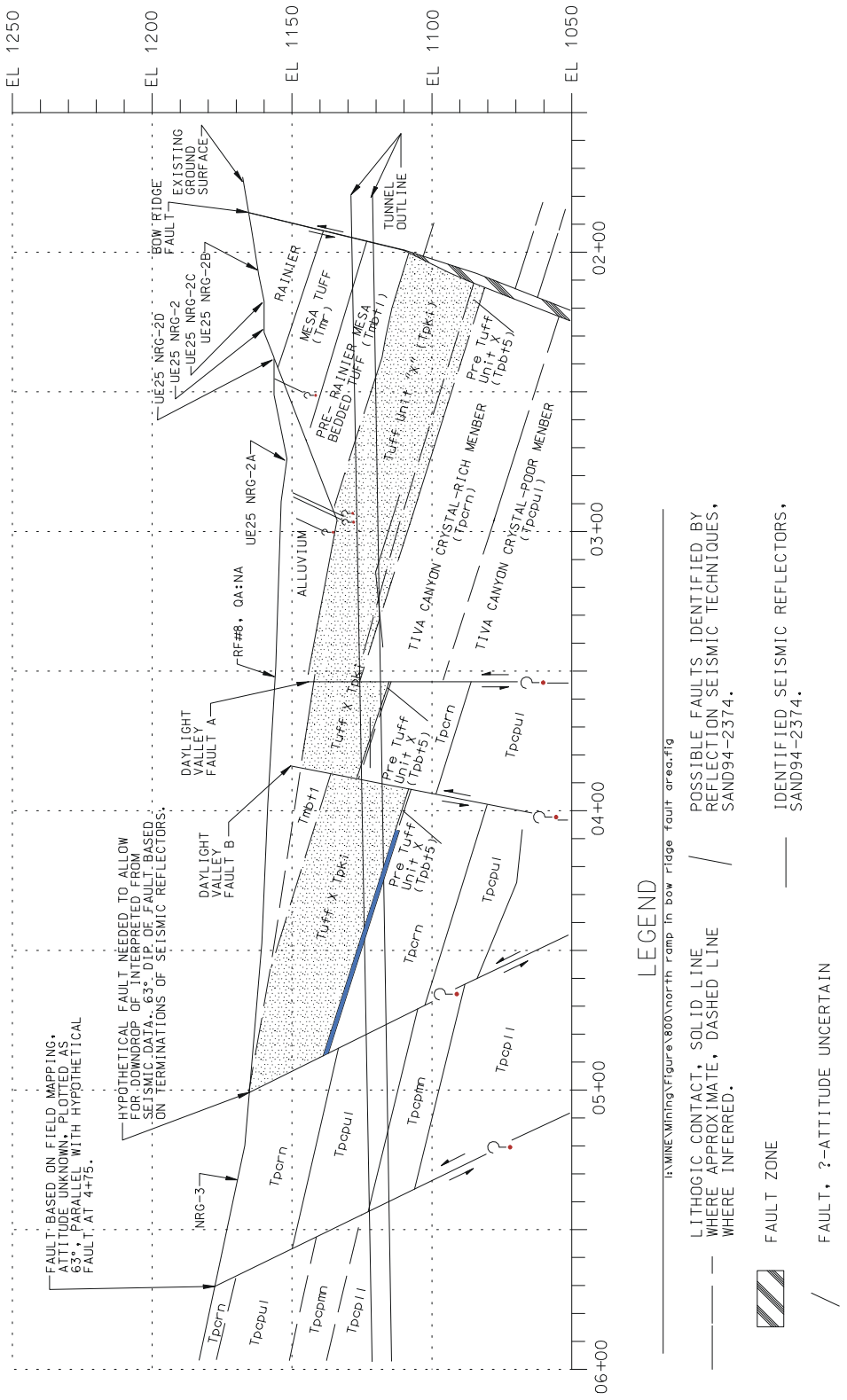

Source: Modified from *Geotechnical Characterization of the North Ramp of the Exploratory Studies Facility* (Brechtel et al. 1995 [DIRS 101493], Figure 4-5).

Figure 6-8. North Ramp in Bow Ridge Fault

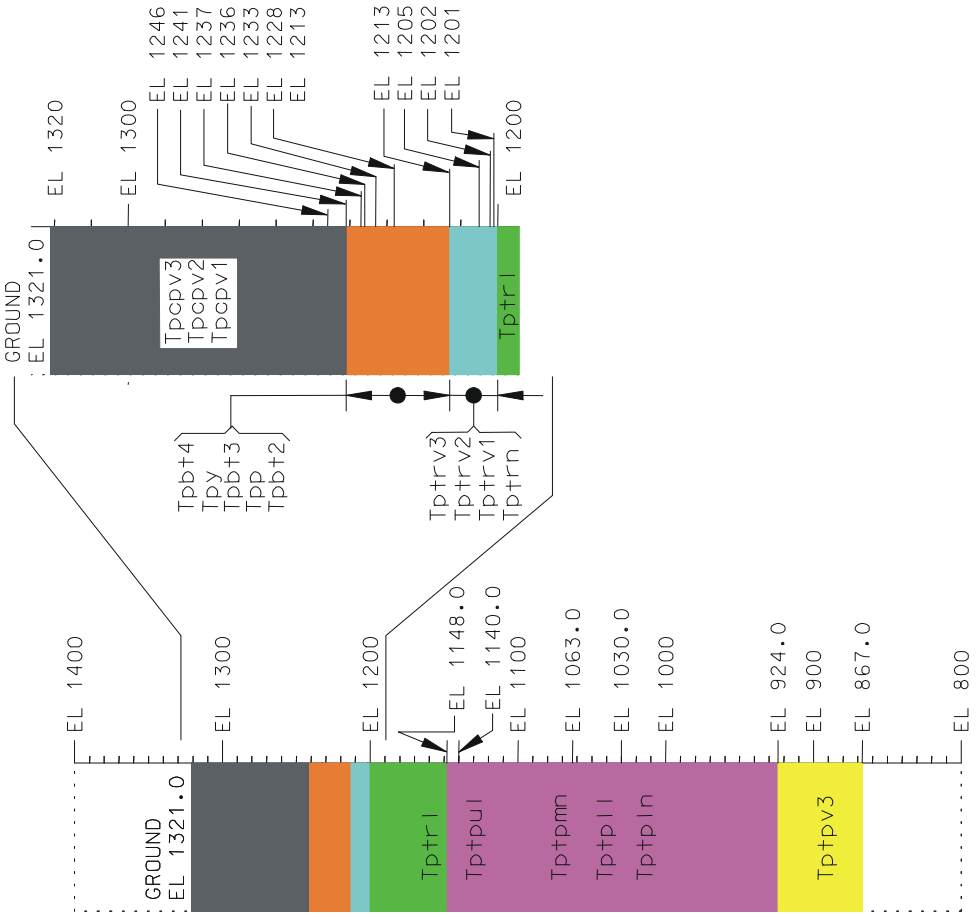

SOURCE:

ELEVATION, m	HORIZON	DEPTH, m	THICKNESS, m
1321.0	GROUND	0	0
1246.0	Tpcpv3	75	75
1246.0	Tpcpv2	75	0
1241.0	Tpcpv1	80	5
1237.0	Tpb+4	84	4
1236.0	Tpy	85	1
1233.0	Tpb+3	88	3
1228.0	Tpp	93	5
1213.0	Tpb+2	108	15
1205.0	Tptrv3	116	8
1202.0	Tptrv2	119	3
1201.0	Tptrv1	120	1
1200.0	Tptrn	121	1
1148.0	Tptrl	173	52
1140.0	Tptpul	181	8
1063.0	Tptpmn	258	77
1030.0	Tptpll	291	33
924.0	Tptpln	397	106
867.0	Tptpv3	454	57

I:\WINE\Mining\Figure\800\typ stratigraphic col for shaft riser.fig

Source: Modified from CRWMS M&O 1999 [DIRS 107475].

Figure 6-9. Typical Stratigraphic Column for a Shaft

Impact of Lithophysae on Geotechnical Characterization

From the rock mechanics perspective, the presence of lithophysae in lithophysal zones makes their impact somewhat more problematic to characterize. Discussed below are some issues that contribute to this problem.

Standard Characterization Issues—Typically a set of simple tensile, uniaxial, and triaxial compressive strength tests are used to obtain the intact rock material characteristics. These tests are performed on a typical NX core, on 54 mm diameter specimens. Commonly, the core quality is assessed in terms of core RQD index. This index is defined as a percentage calculated as a ratio of the sum of lengths of core pieces greater that 10 cm (4 in.) per one meter of the core run.

Figure 6-10 shows the difference between evaluating an RQD Index for nonlithophysal rock and lithophysal rock. Any two parallel boreholes drilled in nonlithophysal fractured rock are likely to intercept similar number of discontinuities and produce a relatively consistent RQD. A similar procedure applied to lithophysal rock may produce substantially different RQD results as the number of intercepted voids will be different in each case producing two different values of RQD Index. In addition, the fractures counted from the broken core do not necessarily indicate that the rock is fractured at these locations.

Fracture Characterization—Fractures are common features in the hard rock mass, causing rock mass strength degradation. Their impact is assessed in terms of such factors as fracture frequency, surface roughness, aperture, presence and type of infilling, orientation, and the presence of water. Generally a standardized mapping procedure results in a relatively consistent account of all important fracture parameters.

In lithophysal rock, however, the fracturing is somewhat less evident. Large fractures are relatively few while shorter fractures terminating at bridges and voids are more abundant and their traces are more difficult to locate as they follow a rather convoluted path through solid bridges separating adjacent lithophysae. The fractures in the lithophysal strata vary by unit. In the Tptpul, there are not many fractures, while in Tptpll there are ubiquitous, closely-spaced fractures, but are not continuous and rarely intersect lithophysae (Figure 6-5).

Impact of Discontinuities on Strength—Typically strength of rock material (intact rock strength) is assessed from tests on cylindrical specimens obtained from the solid portion of the rock core machined to specific dimensions (e.g., of the length-to-diameter ratio of 2:1). In lithophysal rock this requirement cannot be easily satisfied for typical small-diameter specimens. The proximity of lithophysae results in difficulty obtaining a solid standard specimen. Also the question arises on how to treat lithophysae – are they to be treated as discontinuities or are they a part of rock material structure? If an attempt is made to quantify the effect of lithophysae on rock strength in a way similar to that of discontinuities then the relationship expressing this "equivalency" must be established first. By treating lithophysae as a part of rock structure it is necessary to test a specimen that contains the representative number of lithophysae in its volume.

Using the Tptpul strata as an example, the diameter of a typical lithophysae is on the order of 5 to 10 cm (2 to 4 in.). Considering five lithophysae as a reasonable number of such voids across the specimen diameter and adding a number of bridges in between and of the same order, one

obtains a minimum specimen diameter ranging from 50 to 100 cm (20 to 40 in.). Specimens in this size range, considering an average tuff unit weight of 22,000 N/m^3 will weigh between about 430 and 3500 kgf (950 to 7,700 lbf).

In order to assess the impact of lithophysae on rock strength, a new approach was developed utilizing the numerical simulation (software codes: PFC and UDEC). This new approach is discussed in Section 6.4.4.4.2.

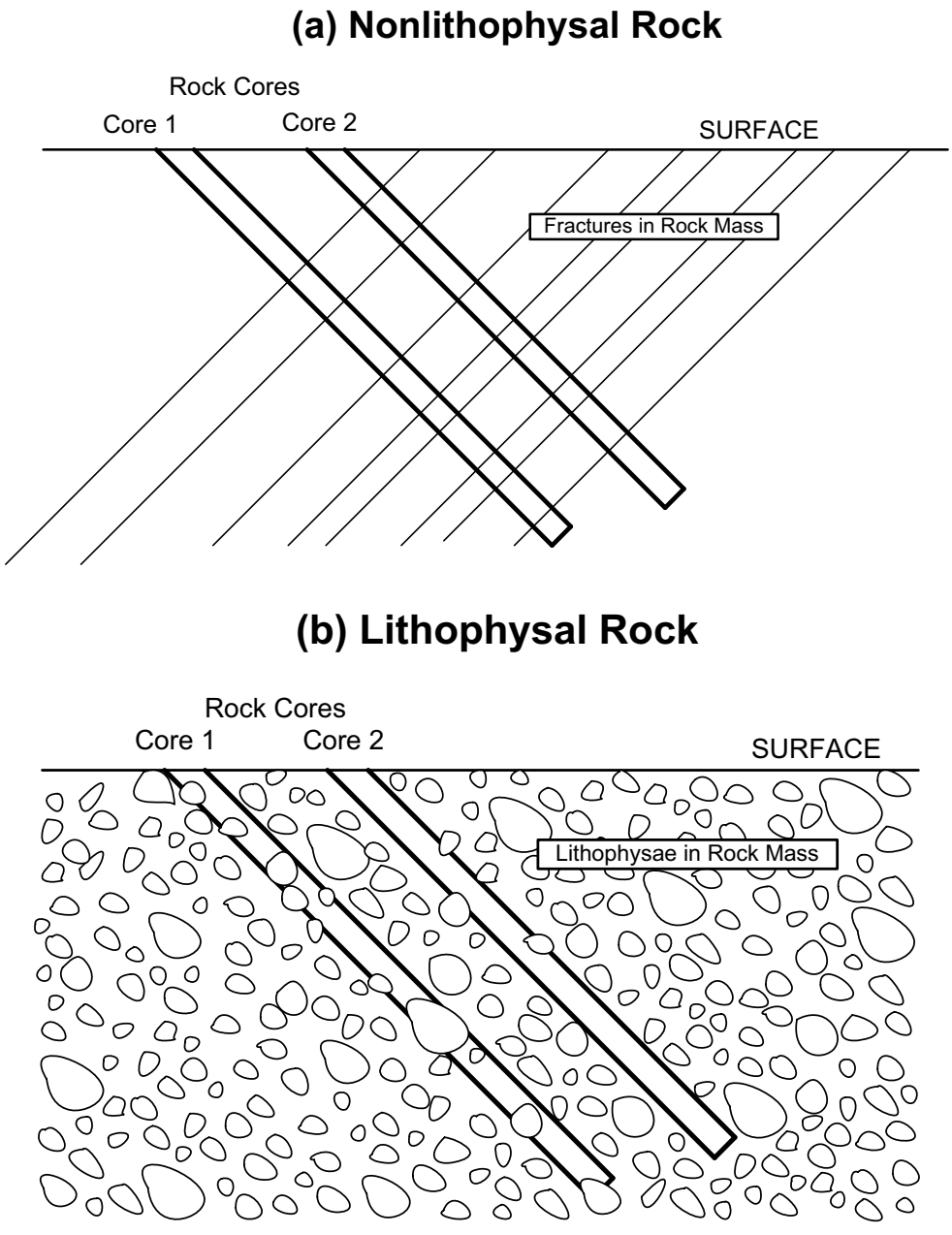

Figure 6-10. Illustration of Differences between Results of Evaluating RQD for (a) Nonlithophysal Rock and (b) Lithophysal Rock

6.2 GEOTECHNICAL DATA NEEDS

This section provides a brief overview of various project needs for geotechnical data.

6.2.1 Subsurface Engineering Design

The subsurface repository facility consists of four underground emplacement panels (Panels 1-4) and auxiliary openings. Engineering design of these openings requires the whole suite of geotechnical data mentioned in Section 1.3.

6.2.1.1 Excavation Types

The subsurface repository design includes the following types of openings: emplacement drifts, turnouts, access ramps and access mains, exhaust mains, shafts, portals, and other ancillary openings. These openings have either a circular or horseshoe-shaped cross-section, range in size from approximately 5.5 to 8 m in diameter or width, and will be excavated in various rock formations by using either tunnel boring machine (TBM), roadheader, drill-and-blast, raise borer, or combinations of these methods.

6.2.1.2 Pillar Sizing

As is illustrated in *Underground Layout Configuration* (BSC 2003 [DIRS 165572]), there are a number of pillars between repository openings. A typical example is the wedge-shaped pillar between the access main and emplacement drift turnout. Another example is the horizontal pillar between twin exhaust mains shared by Panels 3W and 4. The vertical separation between the performance confirmation drift and emplacement drift in Panel 1 is another example of the pillars. In a broad term, all the spacing between parallel emplacement drifts are pillars in essence. Proper sizing of these pillars relies on rock mechanic principles that in turn call for a realistic estimate of rock mass mechanical properties and strength parameters in particular. SGPR provides a consistent source for rock mass mechanical properties needed for pillar design.

6.2.1.3 Drift Stability Analysis

A thorough analysis of the stability of each repository opening is essential to adequately design ground support systems. Such an analysis requires a good knowledge of mechanical properties of the rock mass and its inherent joints and other discontinuities as part of important design input parameters. Recognizing that determination of rock mass properties and parameters involves uncertainties in terms of spatial variability, sample size representativeness, insufficient data, and data reduction, it is often necessary to carry out a systematic sensitivity analysis taking into account data uncertainties to bound the design. In this respect, this document provides a comprehensive summary of geotechnical data availability, variability, and limitation for subsequent licensing supporting activities and detailed ground support design.

6.2.2 Support of Preclosure Safety Analyses

Adequate prediction of rockfall scenarios during preclosure provides essential input to preclosure safety analyses and waste package design, particularly in all emplacement drifts, and in those non-emplacement openings that will be used for waste package transportation. Since both waste

package and transporter are classified as being important to safety (ITS), an upper bound prediction of rockfall without even taking credit for the presence of ground support is carried out. An adequate determination of mechanical properties of the rock mass and discontinuities is essential to making rockfall computations as realistic as possible. In essence, such predictive analyses require the same input as those for engineering design of the repository openings.

6.2.3 Support of Procurement and Construction

Typically, the cost and method of excavation are derived utilizing a range of geotechnical data. The progress of excavation and associated excavation schedule are determined utilizing the rock property data. In addition, the cost of tunneling largely depends on the type and quantities of ground support components. These are determined considering both the type and size of excavation and the amount of maintenance foreseen as reasonable for the type of designed excavation. Accurate geotechnical data for each rock unit provides a basis of more accurate cost and schedule predictions. The geotechnical data available and included in this report provide a basis for preparation of the baseline case for construction cost and schedule estimates.

6.2.4 Support of Repository Operations

In addition to the activities to be supported as part of the performance confirmation monitoring and testing as described in Section 6.2.6, geotechnical support will be provided during operation of the facility. This construction support will consist of assessment of special locations or conditions encountered where ground support may have to be specifically prescribed to fit better local conditions. This type of support may be more prevalent in the nonemplacement openings where excavation methods and opening configurations may be more variable, and rock conditions less known. Geotechnical support during operation will also be needed for locating and anchoring structures such as invert structures and bulkheads to the drift floor and walls. Some of the isolation barriers will be in place throughout the preclosure period, so their location selection and anchoring will be critical to their longevity.

Shafts also have an expected service life of up to 100 years, and maintenance of the non-accessible exhaust shafts is expected to be minimal or not required except as a contingency. These expectations place a lot of emphasis on adequate specification of the liner designs, and on design adaptations or modifications where unfavorable rock conditions are encountered. Geotechnical support will be available throughout the shaft construction phase to analyze specific rock conditions encountered, prescribe additional testing as needed, and provide advice on required design modifications.

Geotechnical support during operations will be critical to help ensure that evolving drift instability problems and ground support component failures are detected, monitored, tested, and remediated on a timely basis before they impact the repository operations. This support is also necessary to maintain the repository in optimal condition so that the option of retrievability is not impacted.

6.2.5 Support of Postclosure Performance Assessment

Specific support offered by this report to performance assessment of the repository during postclosure is to provide a most updated geotechnical data source to be used for performing the drift degradation analysis and its future revisions. Such an analysis has to first step though the preclosure period during which the same geotechnical parameters will be used for both engineering design and drift degradation analysis. *Drift Degradation Analysis* (BSC 2004 [DIRS 166107]) provides an assessment of the amount of drift degradation anticipated in repository emplacement drifts for discrete events and time increments extending throughout the repository's postclosure period of performance. The analysis results presented mainly in the forms of rockfall quantity, size, velocity, and dynamic energy support the license application.

6.2.6 Support of Performance Confirmation

The requirements for confirmation of geotechnical parameters during construction and operation until permanent closure of the repository are described in 10 CFR 63.132 [DIRS 176544]. Guidelines for such activities are described in the YMRP (NRC 2003 [DIRS 163274]).

The SGPR functions as a basis of initial conditions for the performance confirmation program. The geotechnical parameters presented in this report will be used in determining stresses, displacements, rockfall, and safety margins for the design of repository openings. In addition, the field measurements and observations made by the performance confirmation program during the construction and operational phases of the repository will be used either to verify the design or to confirm geotechnical parameters through a back analysis technique. Therefore, SGPR technically supports the performance confirmation program, although confirmation of geotechnical parameters is only a part of the performance confirmation program.

As is widely adopted by the tunneling industry, a specific geotechnical instrumentation program will accompany the excavation of repository openings to provide the timely geotechnical information on performance of excavations and ground support for engineering, construction, client, regulator, and the public. Such a geotechnical instrumentation program will closely integrate with the performance confirmation program.

6.3 METHODOLOGY OF GEOTECHNICAL DATA ACQUISITION AND ENHANCEMENT

6.3.1 Introduction

As outlined in Section 6, an outstanding issue for license application is the production of an adequate summary of thermal-mechanical properties that are needed for subsurface design, pre-closure repository safety analysis, and repository safety analysis after permanent closure. An intimately related outstanding issue is the development of numerical rock behavior simulators and approaches to adequately capture: (1) the sample size (scale) dependency of rock properties and prediction of parameters at the rock mass scale, (2) the spatial variation or heterogeneity of rock parameters across the proposed repository storage volume, and (3) the predicted variation of rock behavior and parameters over the proposed post-closure period of 10,000 years.

The methodology of resolving these issues was progressively developed from a series of Geotechnical Review Panel meetings held in 2001 and 2002, and from work proposals prepared and reviewed by its participants. The Review Panel consisted of BSC personnel as well geomechanics experts from Sandia National Laboratories (SNL), United States Bureau of Reclamation (USBR), U.S. Geological Survey (USGS), University of Nevada – Las Vegas, University of Nevada – Reno, New England Research, and consultants from the Itasca Consulting Group and Nick Barton and Associates. The general YMP approach for resolving these geomechanical issues are summarized in the *Resolution Strategy for Geomechanically-Related Repository Design and Thermal-Mechanical Effects (RDTME)* (Board 2003 [DIRS 165036], Section 2.2.1).

The overall approach for resolving these geomechanical issues consists of utilizing a combination of analyses, studies and calculations to maximize site-specific data: 1) Evaluation and geotechnical analysis of the existing, extensive geological mapping and geotechnical characterization data from surface and underground mapping of lithology, structure, and rock quality; 2) Additional laboratory and in situ thermal-mechanical testing, primarily of lithophysal rocks, to provide information for confirmation of the numerical rock simulators and property ranges to be used in design and performance sensitivity studies; 3) Development, calibration and validation of numerical rock simulators capable of representing the thermal-mechanical behavior of lithophysal and nonlithophysal rocks; 4) Use of the validated numerical rock simulators to supplement the material properties database and explore the impact of geologic variability (porosity, lithophysae shape and distribution, and fracture density) on the geomechanical response, primarily of lithophysal rocks; and 5) To perform numerical rock simulators sensitivity studies to further explore the impact of parameter uncertainty on pre-closure ground support and post-closure drift degradation and seismic stability issues (Board 2003 [DIRS 165036], Section 2.2.1).

6.3.1.1 Scaling of Rock Properties – Size Effect

When discussing mechanical and thermal properties of rock, it is important to include a discussion of the scale or size of the rock under consideration for property determination. Three useful categories of rock can be distinguished for mechanical and thermal testing purposes: rock matrix, bulk rock, and rock mass. Larger size rock samples typically behave differently than smaller size rock samples due to the presence of lithophysae, discontinuities and other features.

The rock matrix scale represents behavior of the tuff matrix-groundmass (ranging from cm^3 to m^3 for nonlithophysal rock and cm^3 to dm^3 for lithophysal rock). Properties or parameters reported at the rock matrix scale are idealized to be free of any large features causing anisotropy or nonhomogeneity such as varying mineral type, lithophysae, rims, spots, and fractures. The ignimbrite matrix material contains shards, crystal, pumice, and lithic clasts that are typically less than a few millimeters in size. Matrix-groundmass material typically has a mean of 0.10 cm^3/cm^3 (10%) total porosity and ranges from approximately 0.08 to 0.13 cm^3/cm^3 (BSC 2003 [DIRS 166660], Section 8.2.3).

Bulk rock is a term referring to whole tuff rock at a laboratory or field scale (bulk rock is generally not used for nonlithophysal rock and ranges from cm^3 to m^3 for lithophysal rock). Bulk rock properties represent the behavior of rock samples that may include lithophysae, rims

and spots, yet still exist as an "intact" piece of rock. In general, bulk rock data excludes tests of rock samples known to have fractures or planes of weakness that would influence the property being tested. Since all reported properties are assumed to be of isotropic and homogeneous rock (Assumption 5.1.3), ideally, bulk rock properties should be tested at an appropriate representative elementary volume or tests performed on a specimen of critical size, which is large enough to include a sufficient number of representative lithophysae, rims and spots. On the other hand, since such a large representative elementary volume size is not practical for either sampling or laboratory testing, an approach has been adopted to test a sufficient number of the largest intact rock samples feasible to collect and test. Experimental data indicate that a number of mechanical and thermal properties correlate well with porosity, therefore, the total and lithophysal porosity of these samples are measured and reported with the bulk rock properties.

Rock mass properties apply to a scale large enough to include all the rock imperfections present in the field at the scale of interest, including rock fractures (ranging from m^3 to dm^3 for both lithophysal and nonlithophysal). The structure of the rock mass plays what is perhaps the most important role in defining the structural response of the repository to thermal and mechanical loading. In particular, fractures and the lithophysal porosity are the primary geologic structures of importance. For a given lithostratigraphic zone of rock, which is typically idealized to be isotropic and homogeneous, the rock mass properties are the appropriate and representative scale to use for design and analysis work. For the homogeneous case, the spatial variability in rock mass properties is included as part of the uncertainty associated with a given rock mass property. For lithostratigraphic zones simulated as nonhomogeneous rock, the vertical and horizontal spatial variability of the rock properties are described explicitly and separately, usually as a function of porosity. The volume of rock tested as part of in situ field tests may not be adequate to represent the rock mass representative elementary volume. In such cases, further analysis or application of empirical methods will be necessary to estimate rock mass properties that appropriately consider joint sets or other appropriate large-scale features.

6.3.1.2 Approach for Nonlithophysal Rock Parameter Data Analysis

A relatively large number of laboratory tests have been performed on intact samples of nonlithophysal rock. In the field, a large database of meter-scale fracture geometry and rock quality data was produced from extensive mapping of the ESF and ECRB tunnels. Although evaluation and geotechnical analysis of these data needs to be carried out, the general mechanical and thermal behavior of nonlithophysal rock is considered to be adequately understood, along with the geometry of representative fracture patterns. Still lacking was an adequate characterization of the mechanical behavior of fractures by fracture set, a characterization of the small-scale fractures in nonlithophysal rock, and the effect of these small-scale fractures on rock mass behavior.

The rock mass behavior of nonlithophysal rock is controlled largely by the fracture geometry that separates the relatively strong and stiff blocks of intact rock. Even though the fracture geometry was well known along the two mapped tunnels, it was realized that a representative fracture simulation of the repository site was needed for design purposes. Time-dependent degradation of rock fracture properties still requires better understanding.

6.3.1.3 Approach for Lithophysal Rock Parameter Data Analysis

The need to better understanding the behavior of lithophysal rock became apparent with the realization that most of the repository would reside in lithophysal rock and that nonlithophysal and lithophysal rock behaviors were significantly different. Several important mechanical and thermal rock properties are strongly dependent on rock porosity and sample size. Deformability of rock, rock strength parameters and thermal conductivity were some of the key parameters identified for further study. Additional site-specific testing at the laboratory and field scales was undertaken to better characterize the porosity and size dependencies on these properties. However, because of practical limitations, these effects could not be fully studied in the field and laboratory. It was considered necessary to supplement this testing with numerical testing of lithophysal rock, where behavioral mechanisms could be carefully studied along with the full range of the sample size effect.

Before the spatial variability of these properties could be quantified, it was necessary to simulate the variation of rock porosity in the field. Once a picture emerged of how porosity varied across the site, property correlations could be used to predict the spatial variation of rock parameters at the site for use in design and safety analysis. The rock mass behavior of lithophysal rock is controlled largely by stress conditions and lithophysae in the rock that can lead to failure of the bulk lithophysal rock.

6.3.1.4 Field Characterization Program

For nonlithophysal rock, the major component of the field characterization program consisted of adequate mapping of RHH, fracture geometries from tunnels, boreholes and outcrops. A secondary aspect of the program was to collect rock quality data for rock classification purposes in RHH units and perform limited index testing across the site. The existing database will be supplemented by large-scale field roughness estimates that will be used in empirical relations for estimating shear strength and dilation for each major joint set.

For lithophysal rock, the primary aspect of field characterization was an adequate mapping of the shape, size and abundance of lithophysae, spots and rims in RHH lithophysal rock. This mapping could be carried out along the ESF and ECRB tunnels, in existing site boreholes, and where RHH rock unit outcrops have been located. A secondary component of lithophysal rock field characterization is an adequate mapping of RHH fracture geometries.

For all lithostratigraphic zones, an additional field characterization activity carried out was geophysical logging of boreholes to indirectly determine vertical variation of bulk density and porosity data. This existing data will be further evaluated and summarized.

6.3.2 Laboratory Testing Program

A large number of thermal-mechanical tests have been performed on intact small cores of RHH nonlithophysal rock and other rock units from outside the RHH. The mechanical testing program using samples from boreholes scattered around the repository site is considered adequate for project purposes in describing the behavior of intact nonlithophysal rock. However, to better understand the effect of various physical and environmental factors known to impact thermal-mechanical properties, the existing set of laboratory test results needed to be broken

down and analyzed. The required additional data included better estimates of fracture shear constitutive behavior. The fracture shear response was augmented by conducting laboratory direct shear tests on large and small samples of nonlithophysal rock by joint set.

For lithophysal rocks within the RHH, a fairly extensive testing program was required based on testing of large diameter core samples. Subsequently, a laboratory thermal-mechanical testing program was carried out on large diameter core samples (from 30.5 cm [12 in.] boreholes) that contain many lithophysae. Due to difficulties in obtaining such large drill cores, a rather limited number of samples were tested in the laboratory. Nevertheless, these large laboratory samples not only provided useful information regarding porosity and size effects, but also allowed for calibrating the numerical simulations of mechanical lithophysal rock behavior.

One aspect that requires closer examination is determining how the mechanical and thermal properties of the rock change as a function of time. Of most importance is the time-related mechanical degradation of intact rock and fractures under expected stress and thermal loading conditions.

6.3.3 In Situ Testing Program

The next step beyond laboratory testing was gathering as much in situ site-specific rock behavior information as possible. This program extends from the small-scale borehole testing of thermal and mechanical behaviors to meter-scale mechanical and thermal testing of rock blocks (e.g., single heater test (SHT), plate loading tests, and slot tests) to drift scale tests (DST) in both RHH nonlithophysal (DST) and lithophysal rock. In particular, it was necessary to carry out in situ testing in lithophysal rock to help confirm simulations and ranges of behavior. Rock mass scale testing of both nonlithophysal and lithophysal rock was also required under thermal loading conditions to validate numerical simulations and empirical approaches to characterizing behavior. Some long-term mechanical loading tests of meter-scale rock were also deemed useful for characterizing time effects.

Another aspect of the in situ testing program is the information gathered from TBM pressure and mining rate data as well as periodic surveying of the ESF and ECRB tunnels and drifts to study tunnel deformation over time.

6.3.4 Numerical Approaches to Enhance Understanding of Rock Behavior and Provide Geostatistical Evaluation of Key Rock Features

Even after conducting all the testing in the above two sections, only a limited database will exist relative to thermal and mechanical lithophysal rock behavior. The approach adopted to extrapolate the mechanical behavior to a larger-size scale was to perform additional testing using numerical simulations capable of representing lithophysal rock behavior. These numerical simulations must be developed, calibrated, and validated by using the site-specific laboratory and field-testing of lithophysal rock. Two- and three-dimensional numerical simulations have the advantage of allowing a rock sample to be created and tested at any scale considered necessary. The numerically simulated lithophysal holes of any convenient size and shape can then be inserted at any desired location within the rock sample. These numerical approaches have also been shown to reproduce observed complex rock behavior, such as allowing for the development

of interlithophysal fracturing; thus, providing a methodology for representing and understanding the basic mechanical response of lithophysal rocks through back-analysis of actual testing.

This full methodology involves five steps: (1) development of approach to simulate cavities within existing numerical codes, (2) calibration of the numerical simulator by adjusting its numerical simulator properties to reproduce the behavior of actual laboratory and field tests, (3) use of the software to further study and understand mechanisms of behavior by simulating tests at the laboratory and field scale to ensure that all significant aspects of lithophysal rock behavior have been reasonably reproduced, (4) use of the software to extrapolate lithophysal rock behavior by simulating samples at larger spatial scales, and (5) validation of the simulation in steps (3) and (4), to the extent possible, by predicting the behavior of boundary-value in situ tests and other analyses. The validated numerical simulations, based on PFC (BSC 2003 [DIRS 166660], Section 9.1) and UDEC software (BSC 2003 [DIRS 166660], Section 9.2), will be judiciously used to supplement site-specific test data by relying on professional judgment that is explained by means of documented technical reasoning. Any limitations in approach will also be clearly stated, such as that Tptpul (upper lithophysal) and Tptpll (lower lithophysal) rock behavior is identical, even though the Tptpll is much more fractured (most likely due to higher in situ stresses found at the Tptpll depth) (Assumption 5.2.3).

In addition, time-dependent strength properties (i.e., static fatigue) need to be determined for both nonlithophysal and lithophysal rock. Again, the pertinent rock-testing database will be limited, so a program similar to the one used for simulation of size effects will be carried out to understand and enhance the time-related mechanical behavior of nonlithophysal and lithophysal rock.

The conceptual and numerical simulation of thermal behavior of lithophysal rock is more established. This effort has continued to be refined in order to gain an acceptable level of understanding of thermal behavior and characterization of thermal parameters.

Evaluation of the extensive existing database of the tunnel full-periphery structure maps will produce a statistical database, by fracture set, of fracture geometry data such as fracture orientation, spacing, and trace length. Geostatistical approaches will be applied to this tunnel database, borehole fracture data, and outcrop fracture measurements as a basis for the development of statistically representative fracture volumes using the FRACMAN software program (BSC 2003 [DIRS 166660], Section 9.3). These fracture volumes will contain fracture geometry data by RHH units that adequately capture the ranges of fracture geometry parameters expected at the site.

Finally, a simplified geostatistical approach will also be used to simulate lithophysae volumes (BSC 2003 [DIRS 166660], Section 9.4) in the repository area. The simplified geostatistical analysis considers only the mapped lithophysal tunnel data, but a more complete geostatistical treatment will also include borehole geophysics data, mapped borehole lithophysal data, and outcrop data. Like the fracture volumes, these lithophysal volumes will describe the spatial variation of lithophysal cavities expected across the site at various degrees of reliability. This variation will then be translated into a variation of mechanical and thermal properties as described in *Subsurface Geotechnical Parameters Report* (BSC 2003 [DIRS 166660], Section 10.2).

6.3.5 Empirical Approaches to Characterize and Estimate Rock Behavior

Nonlithophysal behavior at the rock mass scale cannot be studied in the laboratory; rather, traditional empirical rock characterization techniques are usually relied upon to describe the mechanical rock mass behavior. However, these empirical approaches have never been applied to a lithophysal rock mass. The originator of the Q rock characterization system (Barton et al. 1974 [DIRS 101541]), Nick Barton, has suggested modifications to the Q rock characterization technique in order to extend the Q technique to lithophysal rocks (Duan 2003 [DIRS 163586], Sections 1 and 3). During the development of Yucca Mountain tunnels and other underground excavations, a detailed mapping was performed and a full set of mapping data necessary for the conventional rock mass quality estimates are available. Empirical approaches provide a practical and common methodology in mining and tunneling industries as a way of determining rock mass mechanical properties.

6.3.6 Program to Integrate Data, Confirm Parameter Ranges, and Simulate Rock Performance

The final step in the characterization effort is to sufficiently evaluate and integrate all of the above sources of rock behavior data using geotechnical judgment. For example, the numerical simulation program must be intimately tied to the testing programs to be justifiable. This global analysis of the data must be carried out for all rock parameters in order to produce defensible parameter summaries that include discussions on parameter ranges or distributions, uncertainty, spatial variability, and temporal variability. Professional judgment is required to assess and combine the considerably different sources of data into one coherent picture of the state of current knowledge. Judgment is also required to assess whether parameter descriptions are adequate for project purposes. Part of this objective is doing what can be practically accomplished to understand and then reduce the level of uncertainty in the geomechanical parameters, particularly those for the RHH strata.

Related to the above, confidence must be demonstrated that the thermal-mechanical behaviors of the rock, at all scales of interest, are sufficiently understood. In particular, a number of numerical simulations and empirical methods and approaches are being relied upon heavily to understand and describe rock behavior and parameters.

6.4 SUBSURFACE GEOTECHNICAL DATA AND PARAMETERS

Since the late 1970's, a large quantity of data has been collected on the mechanical properties of intact rock from site characterization efforts at Yucca Mountain, Nevada. The majority of data collected has been determined from rock specimens obtained from the Topopah Spring Tuff formation. These efforts were focused on maximizing data and information about the lithostratigraphic rock units located within the RHH. The analyses of the intact rock mechanical properties presented in this section primarily focus on the RHH zones (Tptpul, Tptpmn, Tptpll, and Tptpln), but also includes other non-RHH zones.

The subsurface geotechnical data presented in this report are based on the data tables presented in Appendix A. The data tables were developed by the Geotechnical Group of the YMP Subsurface Project organization following the checking and corrections of all available existing geotechnical data available in the TDMS database through March 2006.

Several studies to determine mechanical properties of rock were performed and have indicated that there is some lateral and vertical variability in the elastic and strength properties of the tuff units, which are predominantly a function of porosity (Price and Bauer 1985 [DIRS 106590]; Price 1993 [DIRS 160023]). The primary importance of porosity on mechanical properties and related geomechanical issues led to a normalizing procedure of establishing test conditions considered to be baseline conditions and then noting the effect of changes to those conditions.

The baseline conditions were defined in the early 1980's. As an example, sizes/conditions are considered to be nominal. Individual samples could vary from the baseline. For an unconfined compression test specimen, a baseline is established as a right-circular cylinder with a diameter of 25.4 mm (1 in.) and an L:D ratio of 2:1, saturated, and tested at room temperature, ambient pressure, and at an axial strain rate of 10^{-5} s^{-1}. In the mid 1980s larger samples were available, and the baseline diameter was changed to 50.8 mm (2 in.) at that time. For many years, this baseline data was considered appropriate because the repository was being planned to be located in the middle nonlithophysal zone of the Topopah Spring tuff and, in general, the variability of these rocks from the baseline was small. However, the current selected location of the RHH consists of the entire TSw2 unit (Tptpmn, Tptpll, and Tptpln zones) and the lower part of the TSw1 unit (Tptpul zone). The RHH includes two lithophysal zones: Tptpul and Tptpll. When data from the lithophysal zones were analyzed, greater variability of individual samples from the baseline conditions was noted, primarily due to the presence and relative size of lithophysal cavities within these rock zones.

The baseline test analysis was established as follows: The stress or strength is calculated by dividing the applied axial load by the specimen's cross-sectional area. The displacements from the elastic and permanent deformation of the sample in an axial direction are measured, with the axial strain calculated by dividing the displacement by the initial length over which the deformation is measured. In most cases, a similar measurement is made in a lateral (diametral) direction for the determination of lateral strain. In addition, the sample dimensions, saturation, temperature, confining and pore pressures, and time, are recorded.

Factors Affecting Mechanical Properties of Intact Rock

In general, the geomechanical properties of an intact rock will change in response to variations in physical and environmental conditions. Examples of physical characteristics are bulk properties (mineralogy, grain density, bulk density, and porosity), sample size, and anisotropy. Environmental conditions include degree of saturation, temperature, confining pressure, and strain rate. The effect of these conditions on the variability of test results is well documented in previous studies (Boyd et al. 1996 [DIRS 101491], Section 3; [DIRS 101492], Section 3; Martin et al. 1994 [DIRS 104760], Section 3; Martin et al. 1995 [DIRS 104761]; Nimick et al. 1985 [DIRS 105195]; BSC 2005 [DIRS 176611]).

Porosity: Porosity is an important aspect of simulation for the extent and magnitude of inherent variability (location specific variability for a specific parameter), as well as the variability resulting from a change in location (i.e., positional variability) for repository geotechnical parameters. It has been noted that the total porosity is associated with the magnitude of Young's modulus and unconfined compressive strength. Therefore, the variability and distribution of porosity is a good index of changes in geo-mechanical properties.

Sample Size: Scale effect is a key factor in the evaluation of test data and relates to the relationship between properties of the laboratory test samples to the in situ properties of the Yucca Mountain rock mass. Small specimens are expected to exhibit different test results compared to large specimens. The effects of scale can be understood by testing differently sized samples in order to make correlations with the properties of the host rock mass. In certain situations, full-scale in situ testing and performance monitoring is practical and appropriate.

Sample Orientation (Anisotropy): The variation in mechanical properties in relation to the axis of the test specimen is a measure of the mechanical anisotropy of a material. The depositional processes of tuff (ash fall and ash flow) imparts anisotropic properties in tuff. The mechanical anisotropic properties of the rock mass are important input parameters for numerical simulation and design engineering.

Saturation: The proposed repository horizon within Yucca Mountain consists of rock units that are partially saturated. However, as the repository is excavated and exposed to air circulation and increased temperatures resulting from the stored nuclear waste, the rock mass will begin to dry out. The drying process will change the geomechanical properties of the host rock, which will affect the engineering design of the repository openings.

Temperature: Because of the emplacement design of the nuclear waste repository, the host rock mass will be subjected to thermal loading. Therefore, the effects of temperature on mechanical properties are important.

Confining Pressure: Most of the laboratory testing was conducted on unconfined samples. Numerical simulation and subsequent design engineering will require test data that demonstrates the effects of confinement within the repository rock mass.

Rate or Time-Scale: It is noted that laboratory testing was performed in a relatively short span of time (on the order of 30 minutes), whereas the repository is designed to be temperature stable over an extensive period of residence related to the half-life of the nuclear waste. Methods need to be developed to simulate the long-term behavior of the tuff, based on extrapolation of results from short duration testing.

Laboratory Test Code

A code system is introduced to examine the variations in testing or environmental conditions. Table 6-3 describes the code system that includes sample diameter, saturation, temperature, L:D ratio, strain rate, and confining pressures. The combination of these codes is assigned to each test result. A code combination of 231221 is set for baseline conditions, and the effect of changes in strength and elastic properties are noted. In addition to the test parameters in Table 6-3, the effect of porosity and sample orientation (anisotropy) are presented in *Intact Rock Mechanical Properties of Yucca Mountain Stratigraphic Units* (BSC 2005 [DIRS 176611], Section 6).

Table 6-3. Description of Code System for Intact Rock Testing Conditions

Code	Test Parameter					
	Size, Diameter (mm)	Saturation	Temperature (ºC)	L/D Ratio	Strain Rate (S^{-1})	Effective Confining Pressure (MPa)
1	< 38	Dry (oven dry)	Room-temperature	<1.8	< 0.5E-05	~0
2	38-70	Ambient (room dry)	125 or up	1.8 to 2.2	0.5E-05 to 5.0E-05	~5
3	>70	Saturated	NA	> 2.2	> 5.0.E-05	6-15
4	Rectangular, (~190 x ~215 mm)	NA	NA	NA	NA	>15

NOTES: Baseline testing conditions are set to a code combination of 231221 and are highlighted in green.

NA: Not Applicable

Code 4 in Size represents block samples with size about 190 (W) x 215 mm (L). Other samples are cylindrical.

Account of Tests on Intact Rock

The laboratory test results are required as input in the process of developing rock mass properties. Prior to performing more detailed analyses, it was considered important to provide a general account of all tests performed on intact rock, considering the origin of test specimens and number of specimens tested at each location. As shown in Table 6-4, the total number of specimens is equal to 1,106. These specimens were obtained either from drill cores or rock samples recovered from 39 locations. A relatively large sample population originates from Busted Butte (245 specimens) and borehole USW G-1 (200 specimens). Figure 6-11 shows the planar view of specimen locations relative to the ESF Main Loop tunnel. The majority of sampling points originate from borings located in the vicinity of the North Ramp.

Not displayed in this figure is the location of the G-Tunnel. At the earlier Project stage the test results obtained from the G-Tunnel were used to supplement a relatively small population of samples originating from the repository area. As the Project progressed and the additional test data became available, the G-Tunnel data became the corroborative data. For purposes of this report, the decision was made not to include the G-Tunnel data; thus, potentially avoiding the need to validate data similarity/equivalency between this relatively small group of specimens (20 tests) and the bulk of other data originating from Yucca Mountain or its proximity. Also not included are the data from the Calico Hills Group units, which are located below the RHH, as there are no planned underground openings below the RHH.

Listed in Table 6-4 and shown in Figure 6-11 are locations of boreholes from which laboratory test specimens used in current analysis were obtained. Summarized in Appendix A are all laboratory-test specimens and test conditions under which they were tested. Table 6-5 shows the general summary of test conditions under which the specimens were tested. A set of tests performed at a particular test condition on specimens prepared from a specific lithostratigraphic zone is called a test group. Data for each lithostratigraphic zone is represented by test groups, which vary in numbers. The number of test groups is larger for RHH strata as the number of

tests performed for this zone is the largest. Details provided in Appendix B provide a detailed summary of tests arranged according to the test groups designated by the appropriate test code (Table 6-5).

The detailed account of intact rock strength and laboratory test data available for the YMP are summarized in *Intact Rock Mechanical Properties of Yucca Mountain Stratigraphic Units* (BSC 2005 [DIRS 176611]). A summary of laboratory strength properties, Young's modulus, and Poisson's ratio data are summarized in Appendix B. The data provided in the appendix also includes information about the tests group codes and associated statistics.

Table 6-4. Summary of Rock Strata Sampling Locations

Sample Location Number	Sample Location		Thermal-mechanical Unit	Lithostrati-graphic Zone	No. of Specimens Tested	Total Numbers for Location	Coordinates (ft)	
	General	Specific					X_COORD (NV State Plane Central)	Y_COORD (NV State Plane Central)
	Busted Butte	Busted Butte	TSw1	Tptpul	10	-	573947.00	742105.00
	Busted Butte	Busted Butte	TSw2	Tptpll	125		-	-
	Busted Butte	Busted Butte	TSw2	Tptpmn	110		-	-
1	Busted Butte	Busted Butte	-	-	-	245	-	-
2	ESF/ECRB/Borehole	ESF 19+22.2 & ESF 19+28.7	TSw2	Tptpll	6	6	-	-
3	ESF/ECRB/Borehole	ESF 63+60.5 to 63+96	TSw1	Tptpul	13	13	-	-
4	ESF/ECRB/Borehole	ESF-AOD-HDFR1	TSw2	Tptpmn	4	4	562650.00	767600.00
	ESF/ECRB/Borehole	ESF-GTEC-CS1250	TSw2	Tptpmn	1	-	-	-
	ESF/ECRB/Borehole	ESF-GTEC-CS1900	TSw2	Tptpll	1	-	-	-
	ESF/ECRB/Borehole	ESF-GTEC-CS1922	TSw2	Tptpll	1	-	-	-
	ESF/ECRB/Borehole	ESF-GTEC-CS1928	TSw2	Tptpll	1	-	-	-
	ESF/ECRB/Borehole	ESF-GTEC-CS2150	TSw2	Tptpll	2	-	-	-
	ESF/ECRB/Borehole	ESF-GTEC-CS2200	TSw2	Tptpll	3	-	-	-
	ESF/ECRB/Borehole	ESF-GTEC-CS6350	TSw1	Tptpul	1	-	-	-
	ESF/ECRB/Borehole	ESF-GTEC-CS6500	TSw1	Tptpul	7	-	-	-
5	ESF/ECRB/Borehole	ESF-GTEC (All locations)	-	-	-	17	562500.00	756700.00
6	ESF/ECRB/Borehole	ESF-SDM-MPBX-1	TSw2	Tptpmn	5	5	562500.00	767650.00
7	ESF/ECRB/Borehole	ESF-SDM-MPBX-2	TSw2	Tptpmn	4	4	562400.00	767700.00
8	ESF/ECRB/Borehole	ESF-SDM-MPBX-3	TSw2	Tptpmn	3	3	562350.00	767750.00
9	ESF/ECRB/Borehole	ESF-TMA-BJ-1	TSw2	Tptpmn	4	4	562000.00	767700.00
10	ESF/ECRB/Borehole	ESF-TMA-H1	TSw2	Tptpmn	3	3	562000.00	767700.00
11	ESF/ECRB/Borehole	ESF-TMA-MPBX-1	TSw2	Tptpmn	3	3	562000.00	767700.00
12	ESF/ECRB/Borehole	ESF-TMA-MPBX-2	TSw2	Tptpmn	3	3	562000.00	767700.00
13	ESF/ECRB/Borehole	ESF-TMA-MPBX-3	TSw2	Tptpmn	3	3	562000.00	767700.00
14	ESF/ECRB/Borehole	ESF-TMA-MPBX-4	TSw2	Tptpmn	6	6	562000.00	767700.00
15	ESF/ECRB/Borehole	ESF-TMA-PTC-1	TSw2	Tptpmn	2	2	562000.00	767700.00
16	ESF/ECRB/Borehole	ESF-TMA-PTC-2	TSw2	Tptpmn	1	1	562000.00	767700.00
17	ESF/ECRB/Borehole	ESF-TMA-PTC-4	TSw2	Tptpmn	7	7	562000.00	767700.00

Table 6-4. Summary of Rock Strata Sampling Locations (Continued)

Sample Location Number	Sample Location		Thermal-mechanical Unit	Lithostrati-graphic Zone	No. of Specimens Tested	Total Numbers for Location	Coordinates (ft)	
	General	Specific					X_COORD (NV State Plane Central)	Y_COORD (NV State Plane Central)
18	ESF/ECRB/Borehole	ESF-TMA-PTC-H-1	TSw2	Tptpmn	3	3	562000.00	767700.00
19	ESF/ECRB/Borehole	ESF-TMA-PTC-MPBX-1	TSw2	Tptpmn	1	1	562000.00	767700.00
20	ESF/ECRB/Borehole	USW NRG-2	TCw	Tpcpln	8	8	569162.44	765763.75
	ESF/ECRB/Borehole	UE-25 NRG #2a	TCw	Tpcrn	11	-	-	-
	ESF/ECRB/Borehole	UE-25 NRG #2a	UO	Tpki	7	-	-	-
21	ESF/ECRB/Borehole	UE-25 NRG #2a	-	-	-	18	569001.06	765699.94
22	ESF/ECRB/Borehole	UE-25 NRG #2b	UO	Tmr	5	5	569214.56	765765.25
	ESF/ECRB/Borehole	UE-25 NRG #3	TCw	Tpcpll	3	-	-	-
	ESF/ECRB/Borehole	UE-25 NRG #3	TCw	Tpcpmn	15	-	-	-
	ESF/ECRB/Borehole	UE-25 NRG #3	TCw	Tpcpul	5	-	-	-
	ESF/ECRB/Borehole	UE-25 NRG #3	TCw	Tpcrn	7	-	-	-
23	ESF/ECRB/Borehole	UE-25 NRG #3	-	-	-	30	568316.13	766250.63
	ESF/ECRB/Borehole	UE-25 NRG #4	PTn	Tpbt2	3	-	-	-
	ESF/ECRB/Borehole	UE-25 NRG #4	PTn	Tpp	5	-	-	-
	ESF/ECRB/Borehole	UE-25 NRG #4	TSw1	Tptrl	3	-	-	-
	ESF/ECRB/Borehole	UE-25 NRG #4	TSw1	Tptrn	26	-	-	-
24	ESF/ECRB/Borehole	UE-25 NRG #4				37	566820.00	767080.19
25	ESF/ECRB/Borehole	UE-25 NRG #5	TSw2	Tptpmn	8	8	564769.88	767889.63
	ESF/ECRB/Borehole	UE-25 NRG-1	TCw	Tpcpmn	7	-	-	-
	ESF/ECRB/Borehole	UE-25 NRG-1	TCw	Tpcpul	7	-	-	-
	ESF/ECRB/Borehole	UE-25 NRG-1	TCw	Tpcrn	3	-	-	-
26	ESF/ECRB/Borehole	UE-25 NRG-1	-	-	-	17	569803.35	765359.03
	ESF/ECRB/Borehole	UE-25 a #1	CFUn	Tcbm	3	-	-	-
	ESF/ECRB/Borehole	UE-25 a #1	CFUn	Tcbuc	1	-	-	-
	ESF/ECRB/Borehole	UE-25 a #1	CFUn	Tcplc	1	-	-	-
	ESF/ECRB/Borehole	UE-25 a #1	CFUn	Tcplv	1	-	-	-
	ESF/ECRB/Borehole	UE-25 a #1	CFUn	Tcpm	3	-	-	-
	ESF/ECRB/Borehole	UE-25 a #1	CFUn	-	-	9	-	-
27	ESF/ECRB/Borehole	UE-25 a #1	CHn	Tac	5	-	-	-

Table 6-4. Summary of Rock Strata Sampling Locations (Continued)

Sample Location Number	Sample Location		Thermal-mechanical Unit	Lithostrati-graphic Zone	No. of Specimens Tested	Total Numbers for Location	Coordinates (ft)	
	General	Specific					X_COORD (NV State Plane Central)	Y_COORD (NV State Plane Central)
	ESF/ECRB/Borehole	UE-25 a #1	PTn	Tpbt4	1	-	-	-
	ESF/ECRB/Borehole	UE-25 a #1	TCw	Tpcpln	4	-	-	-
	ESF/ECRB/Borehole	UE-25 a #1	TSw2	Tptpln	3	-	-	-
	ESF/ECRB/Borehole	UE-25 a #1	TSw2	Tptpmn	2	-	-	-
27	ESF/ECRB/Borehole	UE-25 a #1				15	566349.88	764901.00
	ESF/ECRB/Borehole	USW G-1	CFUn	Tcbbt	4	-	-	-
	ESF/ECRB/Borehole	USW G-1	CFUn	Tcblv	8	-	-	-
	ESF/ECRB/Borehole	USW G-1	CFUn	Tcbm	24	-	-	-
	ESF/ECRB/Borehole	USW G-1	CFUn	Tcbuc	18	-	-	-
	ESF/ECRB/Borehole	USW G-1	CFUn	Tcbuv	11	-	-	-
	ESF/ECRB/Borehole	USW G-1	CFUn	Tcpbt	8	-	-	-
	ESF/ECRB/Borehole	USW G-1	CFUn	Tctlc	4	-	-	-
	ESF/ECRB/Borehole	USW G-1	CFUn	Tctlv	29	-	-	-
	ESF/ECRB/Borehole	USW G-1	CFUn	Tctm	4	-	-	-
	ESF/ECRB/Borehole	USW G-1	CFUn	Tctuc	4	-	-	-
	ESF/ECRB/Borehole	USW G-1	CFUn	Tctuv	7	-	-	-
	ESF/ECRB/Borehole	USW G-1	CFUn	-	-	121	-	-
	ESF/ECRB/Borehole	USW G-1	CHn	Tac	56	-	-	-
	ESF/ECRB/Borehole	USW G-1	CHn	Tacbt	8	-	-	-
	ESF/ECRB/Borehole	USW G-1	TSw2	Tptpll	8	-	-	-
	ESF/ECRB/Borehole	USW G-1	TSw2	Tptpln	7	-	-	-
28	ESF/ECRB/Borehole	USW G-1	-	-	-	79	561001.06	770501.63
	ESF/ECRB/Borehole	USW G-2	CHn	Tpbt1	7	-	-	-
	ESF/ECRB/Borehole	USW G-2	TSw1	Tptf	8	-	-	-
	ESF/ECRB/Borehole	USW G-2	TSw1	Tptrn	5	-	-	-
	ESF/ECRB/Borehole	USW G-2	TSw2	Tptpll	12	-	-	-
	ESF/ECRB/Borehole	USW G-2	TSw3	Tptpv3	4	-	-	-
29	ESF/ECRB/Borehole	USW G-2	-	-	-	36	560503.94	778825.94
30	ESF/ECRB/Borehole	USW G-4	CHn	Tptpv1	14	-	-	-

Table 6-4. Summary of Rock Strata Sampling Locations (Continued)

Sample Location Number	Sample Location		Thermal-mechanical Unit	Lithostrati-graphic Zone	No. of Specimens Tested	Total Numbers for Location	Coordinates (ft)	
	General	Specific					X_COORD (NV State Plane Central)	Y_COORD (NV State Plane Central)
	ESF/ECRB/Borehole	USW G-4	TSw2	Tptpll	18	-	-	-
	ESF/ECRB/Borehole	USW G-4	TSw2	Tptpln	5	-	-	-
	ESF/ECRB/Borehole	USW G-4	TSw2	Tptpmn	19	-	-	-
30	ESF/ECRB/Borehole	USW G-4	-	-	-	56	563081.75	765807.50
	ESF/ECRB/Borehole	USW G-3/GU-3	CHn	Tptpv2	3	-	-	-
	ESF/ECRB/Borehole	USW G-3/GU-3	TSw1	Tptpul	2	-	-	-
	ESF/ECRB/Borehole	USW G-3/GU-3	TSw1	Tptrn	9	-	-	-
	ESF/ECRB/Borehole	USW G-3/GU-3	TSw2	Tptpll	2	-	-	-
	ESF/ECRB/Borehole	USW G-3/GU-3	TSw2	Tptpln	7	-	-	-
	ESF/ECRB/Borehole	USW G-3/GU-3	TSw2	Tptpmn	10	-	-	-
	ESF/ECRB/Borehole	USW G-3/GU-3	TSw3	Tptpv3	2	-	-	-
31	ESF/ECRB/Borehole	USW G-3/GU-3	-	-	-	35	558483.31	752779.63
	ESF/ECRB/Borehole	USW NRG-6	PTn	Tpbt2	3	-	-	-
	ESF/ECRB/Borehole	USW NRG-6	PTn	Tpbt3	2	-	-	-
	ESF/ECRB/Borehole	USW NRG-6	PTn	Tpbt4	1	-	-	-
	ESF/ECRB/Borehole	USW NRG-6	PTn	Tpcpv2	2	-	-	-
	ESF/ECRB/Borehole	USW NRG-6	PTn	Tpp	2	-	-	-
	ESF/ECRB/Borehole	USW NRG-6	TCw	Tpcpll	16	-	-	-
	ESF/ECRB/Borehole	USW NRG-6	TCw	Tpcpln	5	-	-	-
	ESF/ECRB/Borehole	USW NRG-6	TSw1	Tptpul	3	-	-	-
	ESF/ECRB/Borehole	USW NRG-6	TSw1	Tptrn	27	-	-	-
	ESF/ECRB/Borehole	USW NRG-6	TSw2	Tptpll	6	-	-	-
	ESF/ECRB/Borehole	USW NRG-6	TSw2	Tptpmn	8	-	-	-
32	ESF/ECRB/Borehole	USW NRG-6	-	-	-	75	564187.00	766726.50
	ESF/ECRB/Borehole	USW NRG-7a	PTn	Tpbt2	1	-	-	-
	ESF/ECRB/Borehole	USW NRG-7a	PTn	Tpbt3	1	-	-	-
	ESF/ECRB/Borehole	USW NRG-7a	PTn	Tpbt4	1	-	-	-
	ESF/ECRB/Borehole	USW NRG-7a	PTn	Tpcpv1	3	-	-	-
33	ESF/ECRB/Borehole	USW NRG-7a	PTn	Tpcpv2	2	-	-	-

Table 6-4. Summary of Rock Strata Sampling Locations (Continued)

Sample Location Number	Sample Location		Thermal-mechanical Unit	Lithostrati-graphic Zone	No. of Specimens Tested	Total Numbers for Location	Coordinates (ft)	
	General	Specific					X_COORD (NV State Plane Central)	Y_COORD (NV State Plane Central)
	ESF/ECRB/Borehole	USW NRG-7a	PTn	Tpp	4	-	-	-
	ESF/ECRB/Borehole	USW NRG-7a	PTn	Tptrv3	1	-	-	-
	ESF/ECRB/Borehole	USW NRG-7a	PTn	Tpy	3	-	-	-
	ESF/ECRB/Borehole	USW NRG-7a	TCw	Tpcpln	5	-	-	-
	ESF/ECRB/Borehole	USW NRG-7a	TSw1	Tptpul	7	-	-	-
	ESF/ECRB/Borehole	USW NRG-7a	TSw1	Tptrl	1	-	-	-
	ESF/ECRB/Borehole	USW NRG-7a	TSw1	Tptrn	30	-	-	-
	ESF/ECRB/Borehole	USW NRG-7a	TSw2	Tptpll	3	-	-	-
	ESF/ECRB/Borehole	USW NRG-7a	TSw2	Tptpln	7	-	-	-
	ESF/ECRB/Borehole	USW NRG-7a	TSw2	Tptpmn	20	-	-	-
33	ESF/ECRB/Borehole	USW NRG-7a	-	-	-	89	562984.00	768880.13
	ESF/ECRB/Borehole	USW SD-12	PTn	Tpbt2	1	-	-	-
	ESF/ECRB/Borehole	USW SD-12	PTn	Tpbt3	2	-	-	-
	ESF/ECRB/Borehole	USW SD-12	PTn	Tpcpv2	1	-	-	-
	ESF/ECRB/Borehole	USW SD-12	PTn	Tpp	1	-	-	-
	ESF/ECRB/Borehole	USW SD-12	TCw	Tpcpln	9	-	-	-
	ESF/ECRB/Borehole	USW SD-12	TCw	Tpcpmn	4	-	-	-
	ESF/ECRB/Borehole	USW SD-12	TSw1	Tptrn	8	-	-	-
	ESF/ECRB/Borehole	USW SD-12	TSw2	Tptpln	6	-	-	-
	ESF/ECRB/Borehole	USW SD-12	TSw2	Tptpmn	4	-	-	-
	ESF/ECRB/Borehole	USW SD-12	TSw3	Tptpv3	3	-	-	-
34	ESF/ECRB/Borehole	USW SD-12	-	-	-	39	561605.63	761956.56
	ESF/ECRB/Borehole	USW SD-9	CHn	Tac	2	-	-	-
	ESF/ECRB/Borehole	USW SD-9	CHn	Tpbt1	1	-	-	-
	ESF/ECRB/Borehole	USW SD-9	PTn	Tpbt2	1	-	-	-
	ESF/ECRB/Borehole	USW SD-9	PTn	Tpcpv1	1	-	-	-
	ESF/ECRB/Borehole	USW SD-9	PTn	Tpp	1	-	-	-
	ESF/ECRB/Borehole	USW SD-9	PTn	Tptrv3	1	-	-	-
35	ESF/ECRB/Borehole	USW SD-9	PTn	Tpy	2	-	-	-

Table 6-4. Summary of Rock Strata Sampling Locations (Continued)

Sample Location Number	Sample Location		Thermal-mechanical Unit	Lithostrati-graphic Zone	No. of Specimens Tested	Total Numbers for Location	Coordinates (ft)	
	General	Specific					X_COORD (NV State Plane Central)	Y_COORD (NV State Plane Central)
	ESF/ECRB/Borehole	USW SD-9	TSw1	Tptpul	1	-	-	-
	ESF/ECRB/Borehole	USW SD-9	TSw1	Tptrn	3	-	-	-
	ESF/ECRB/Borehole	USW SD-9	TSw2	Tptpln	4	-	-	-
	ESF/ECRB/Borehole	USW SD-9	TSw2	Tptpmn	23	-	-	-
35	ESF/ECRB/Borehole	USW SD-9	-	-	-	40	561818.00	767998.50
36	ESF/HD	ESF-HD-WH-38	TSw2	Tptpmn	1	-	-	-
37	ESF/HD	ESF-HD-WH-39	TSw2	Tptpmn	1	-	-	-
38	ESF/HD	ESF-HD-WH-40	TSw2	Tptpmn	2	-	-	-
39	ESF/HD	ESF-HD-WH-44	TSw2	Tptpmn	1	-	-	-
40	ESF/HD	ESF-HD-WH-49	TSw2	Tptpmn	1	-	-	-
	ESF/HD	-	-	-	-	6	562605.00	767900.00
41	Fran Ridge	Fran Ridge	TSw2	Tptpmn	30	30	-	-
42	G-Tunnel, Block 1	G-Tunnel, Block 1	NA	NA	20	20	-	-
Total Number of Specimens					**1106**	**1106**	-	-
Total Number of Specimens excluding CFn unit and G-Tunnel					**956**	**956**	-	-

NOTES: The coordinates of Busted Butte and ESF boreholes are estimated to show the specimens location plan as presented in Fig ure 6-11 and may not represent actual coordinates. These coordinates are presented here for illustration purpose only.

NA = not available

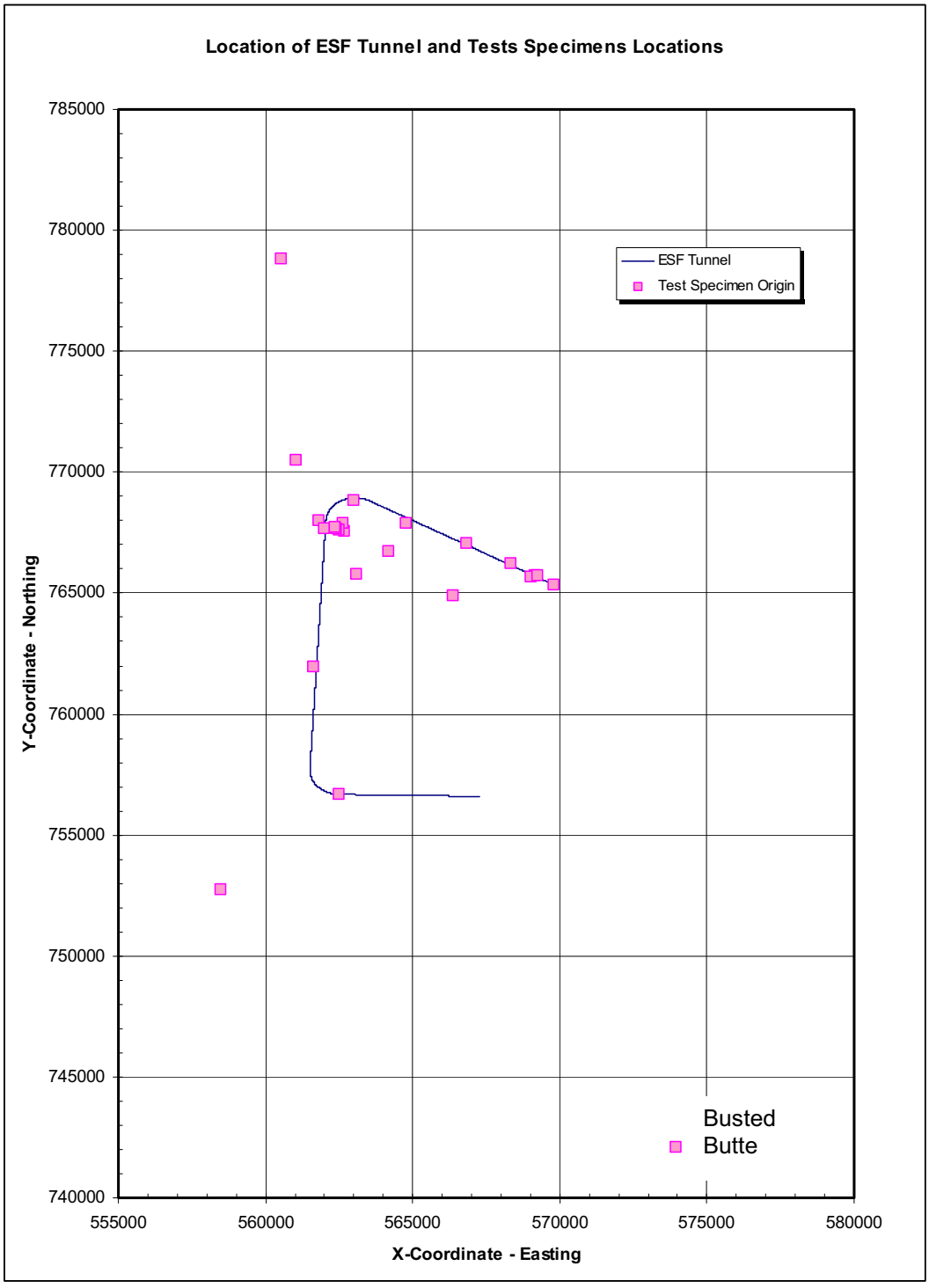

NOTES: Approximate test specimen locations are plotted based on the coordinates in Table 6-4. Actual coordinates of ESF boreholes and the Busted Butte area may differ from those in Table 6-4. This figure is developed based on Table 6-4.

Figure 6-11. Overall View of General Tests Specimens Locations

Table 6-5. Summary of Number of Tests and Test Types for Each Lithostratigraphic Zone

TM	Litho-stratigraphic Zone	Compres-sive Strength Tests Total	Base Case Tests Only	Indirect Tensile Strength Tests	Diameter—mm				Temperature condition		Saturation Level			Uni-axial	Triaxial—Confining Pressure—MPa				Total	Total (%)	TM Unit (%)
					<38	40-70	71-150	>150	Amb.	Elev.	Amb.	Dry	Sat.		<10	10 - 14	15 - 19	>20			
UO	01_UO	0	0	0	0	0	0	0	0	0	0	0	0	0	0	0	0	0	0	0	
	02_UO_Tmr	5	5	3	0	5	0	0	5	0	0	0	5	5	0	0	0	0	5	0.52	
	03_UO_Tpki	7	7	6	0	7	0	0	7	0	0	0	7	7	0	0	0	0	7	0.73	1.26
TCw	04_TCw_Tpcrn	21	18	24	0	22	0	0	21	0	3	0	18	21	0	0	0	0	21	2.20	
	05_TCw_Tpcrn2	0	0	0	0	0	0	0	0	0	0	0	0	0	0	0	0	0	0	0.00	
	06_TCw_Tpcrn1	0	0	0	0	0	0	0	0	0	0	0	0	0	0	0	0	0	0	0.00	
	07_TCw_Tpcpul	12	5	23	0	12	0	0	12	0	7	0	5	9	0	0	1	2	12	1.26	
	08_TCw_Tpcpmn	26	8	16	8	18	0	0	26	0	7	0	19	12	6	5	1	2	26	2.72	
	09_TCw_Tpcpll	19	5	3	12	7	0	0	19	0	0	0	19	9	5	5	0	0	19	1.99	
	10_TCw_Tpcpln	31	20	19	0	31	0	0	30	1	0	0	27	21	3	5	0	2	31	3.24	
	11_TCw_Tpcpv3	0	0	0	0	0	0	0	0	0	0	0	0	0	0	0	0	0	0	0.00	
	12_TCw_Tpcpv2	5	4	4	0	5	0	0	5	0	0	0	5	4	0	1	0	0	5	0.52	11.92
PTn	13_PTn_Tpcpv1	4	4	1	0	4	0	0	4	0	0	0	4	4	0	0	0	0	4	0.42	
	14_PTn_Tpbt4	3	1	0	0	3	0	0	3	0	2	0	1	3	0	0	0	0	3	0.31	
	15_PTn_Tpy	5	5	1	0	5	0	0	5	0	0	0	5	5	0	0	0	0	5	0.52	
	16_PTn_Tpbt3	5	2	1	0	5	0	0	5	0	2	0	3	4	1	0	0	0	5	0.52	
	17_PTn_Tpp	13	10	13	0	13	0	0	13	0	2	0	11	12	0	1	0	0	13	1.36	
	18_PTn_Tpbt2	9	6	5	0	9	0	0	9	0	3	0	6	9	0	0	0	0	9	0.94	
	19_PTn_Tptrv3	2	2	0	0	2	0	0	2	0	0	0	2	2	0	0	0	0	2	0.21	
	20_PTn_Tptrv2	0	0	0	0	0	0	0	0	0	0	0	0	0	0	0	0	0	0	0.00	4.29
TSw1	21_TSw1_Tptrv1	0	0	0	0	0	0	0	0	0	0	0	0	0	0	0	0	0	0	0.00	
	22_TSw1_Tptrn	108	53	53	34	74	0	0	108	0	5	0	103	68	21	19	0	0	108	11.30	
	23_TSw1_Tptrl	4	3	7	0	4	0	0	4	0	0	0	4	3	1	0	0	0	4	0.42	
	24_TSw1_Tptf	8	1	0	7	1	0	0	8	0	0	0	8	8	0	0	0	0	8	0.84	12.55
	25_TSw1_Tptpul	44	8	19	13	0	8	23	40	4	14	4	26	41	2	1	0	0	44	4.60	
TSw2	26_TSw2_Tptpmn	293	42	14	107	162	21	2	247	46	55	60	178	224	26	32	5	6	293	30.65	
	27_TSw2_Tptpll	188	15	24	54	88	35	11	175	13	112	20	56	181	3	4	0	0	188	19.67	
	28_TSw2_Tptpln	39	10	13	17	22	0	0	38	1	5	0	34	30	3	4	1	1	39	4.08	59.00
TSw3	29_TSw3_Tptpv3	9	1	3	4	5	0	0	9	0	2	0	7	3	1	5	0	0	9	0.94	0.94
CHn1	30_CHn1_Tptpv2	3	0	0	2	1	0	0	3	0	1	0	2	3	0	0	0	0	3	0.31	
	31_CHn1_Tptpv1	14	0	0	14	0	0	0	14	0	0	0	14	10	2	2	0	0	14	1.46	
	32_CHn1_Tpbt1	8	1	0	7	1	0	0	8	0	0	0	8	8	0	0	0	0	8	0.84	
	33_CHn1_Tac	63	2	0	56	7	0	0	63	0	9	0	54	44	0	10	0	9	63	6.59	

Table 6-5. Summary of Number of Tests and Test Types for Each Lithostratigraphic Zone (Continued)

TM	Litho-stratigraphic Zone	Compres-sive Strength Tests Total	Base Case Tests Only	Indirect Tensile Strength Tests	Diameter—mm				Temperature condition		Saturation Level			Uni-axial	Triaxial—Confining Pressure—MPa				Total	Total (%)	TM Unit (%)
					<38	40-70	71-150	>150	Amb.	Elev.	Amb.	Dry	Sat.		<10	10 - 14	15 - 19	>20			
CHn 1	34_CHn1_Tacbt	8	0	0	8	0	0	0	8	0	0	0	8	8	0	0	0	0	8	0.84	10.04
Total		956	238	252	343	513	64	36	891	65	229	84	639	758	74	94	8	22	956	100.0	100.0

Source: Appendix C.

Amb. = ambient; Elev. = elevation; Sat. = saturated; TM = thermal-mechanical.

6.4.1 Physical Properties of Intact Rock

Physical properties of intact rock include density and porosity. Typically two types of densities are determined: (1) grain or matrix density and (2) bulk density. While the first accounts for solid particles of rock material only, the second density includes intergranular voids and variance from the baseline dimensions of the sample. As indicated earlier, rock porosity is an important index property that serves as an indicator of a significant number of rock parameters. Porosity usually accounts for microscopic and macroscopic voids within the rock structure. Typically, there are pores existing within the rock matrix that may also include fractures common to the specific rock type. In addition to these two common types of material discontinuities or voids, the Topopah Spring Tuff includes vapor-phase alterations and lithophysae.

Lithophysae is used in this report to refer only to air-filled large-scale voids. Vapor-phase alterations or other mineral deposits commonly associated with lithophysae, such as rims and spots, are conceptualized as matrix. Void spaces characterized as matrix may be either water or air-saturated. Lithophysae are treated as air-saturated under all conditions since the rock units being studied are all located above the water table in the region of interest, and the relatively strong capillary forces of the matrix and fractures will, under virtually all conditions, preferentially retain any moisture present in the rock (BSC 2004 [DIRS 169854], Section 1).

The Topopah Spring Tuff upper and lower lithophysal zones include an abundance of lithophysae, and their presence necessitates an assessment of bulk density and porosity to develop a better understanding of the behavior of the lithophysae-rich Topopah Spring tuff. In this regard, bulk density and porosity related to scale factor is significant to the measurement of rock properties. Accurate estimates of in situ bulk density and porosity for the various subsurface rock units in the repository area of Yucca Mountain are required for site evaluation, numerical simulation, engineering design, and performance assessment. Current estimates of rock density and porosity have been developed in the laboratory from analyses of cores collected from North Ramp Geologic (NRG), systematic drilling, and unsaturated zone boreholes. Because of the relative size of the laboratory specimens to void size, test results reflect the properties of matrix rock but do not adequately take into account the contribution from lithophysae. Therefore, results from laboratory core analysis do not truly represent in situ bulk density and porosity of the total rock mass.

Borehole geophysical logging provides an assessment of a larger volume of the rock. These measurements provide better estimates of bulk density and porosity of the in situ rock mass than the laboratory analyses.

The following sections present a summary of the density and porosity of the lithostratigraphic zones at Yucca Mountain estimated from laboratory core analyses and geophysical logs, as well as from estimates based on statistical analyses.

6.4.1.1 Density

A recent analysis of the borehole data, *Thermal Conductivity of the Potential Repository Horizon* (BSC 2004 [DIRS 169854]), analyzed data for boreholes located within and in the immediate vicinity of Yucca Mountain (Figure 6-12). Laboratory core measurements of particle density from the following boreholes were analyzed: (1) USW SD-7, USW SD-9, USW SD-12,

USW NRG-7/7a, USW UZ-7A, USW NRG-6, and USW UZ-16/USW UZ-14 (DTN: MO0109HYMXPROP.001 [DIRS 155989]); and (2) USW SD-6 (DTN: GS980808312242.014 [DIRS 106748]) (BSC 2004 [DIRS 169854], Section 4.1). Histogram plots of particle density derived from these core measurements are presented in Figure 6-13. These plots illustrate that particle density gradually increases with depth over the four RHH zones, with mean values of 2.51, 2.53, 2.55, and 2.55 g/cc for the Tptpul, Tptpmn, Tptpll, and Tptpln zones, respectively (BSC 2004 [DIRS 169854], Section 6.1.6). These mean values look reasonable when compared with grain density values of 2.53, 2.53, 2.56, and 2.56 g/cc reported in previous analyses (CRWMS M&O 1996 [DIRS 111105], pp. 5-30 and 5-31) for the same lithostratigraphic zones.

In lieu of direct measurements of bulk density for the lithophysal zones, the analysis *Thermal Conductivity of the Potential Repository Horizon* (BSC 2004 [DIRS 169854]) presents a methodology for calculating bulk density by using data for particle density, matrix porosity, and lithophysal porosity that uses Equation 6-1 below. Dry bulk density, ρ_{bd}, is defined as the mass per unit volume of an air-saturated porous rock. In lithophysae bearing units, ρ_{bd} can be expressed as a function of matrix porosity, ϕ_m; lithophysal porosity, ϕ_L; and particle density, ρ_g:

$$\rho_{bd} = (1 - \phi_L)(1 - \phi_m)\rho_g \qquad \text{(Eq. 6-1)}$$

Table 6-6 presents the results for calculated dry bulk densities for the RHH zones.

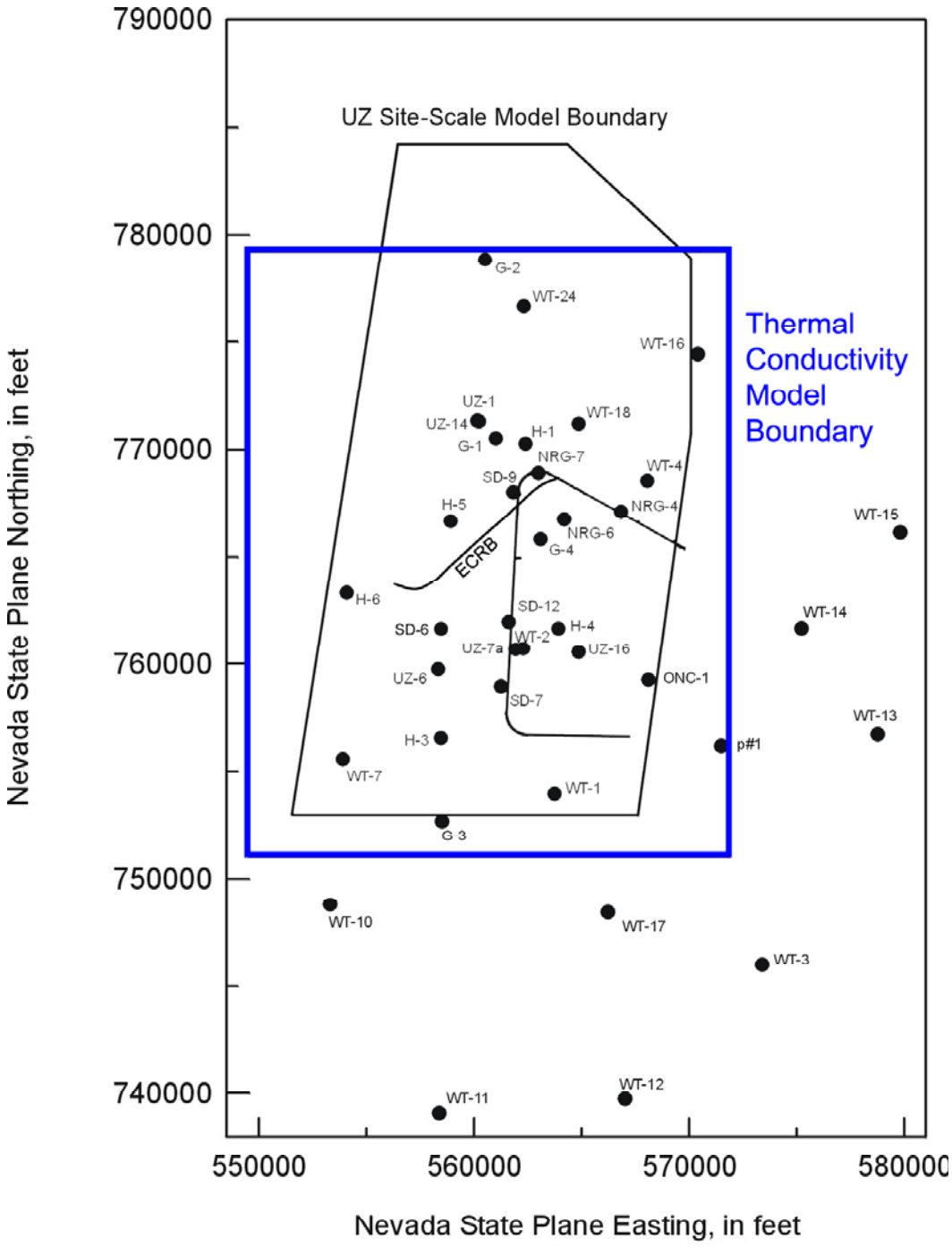

Source: BSC 2004 [DIRS 169854], Figure 4-1.

Figure 6-12. Yucca Mountain Boreholes that Penetrate the Tptpul Zone

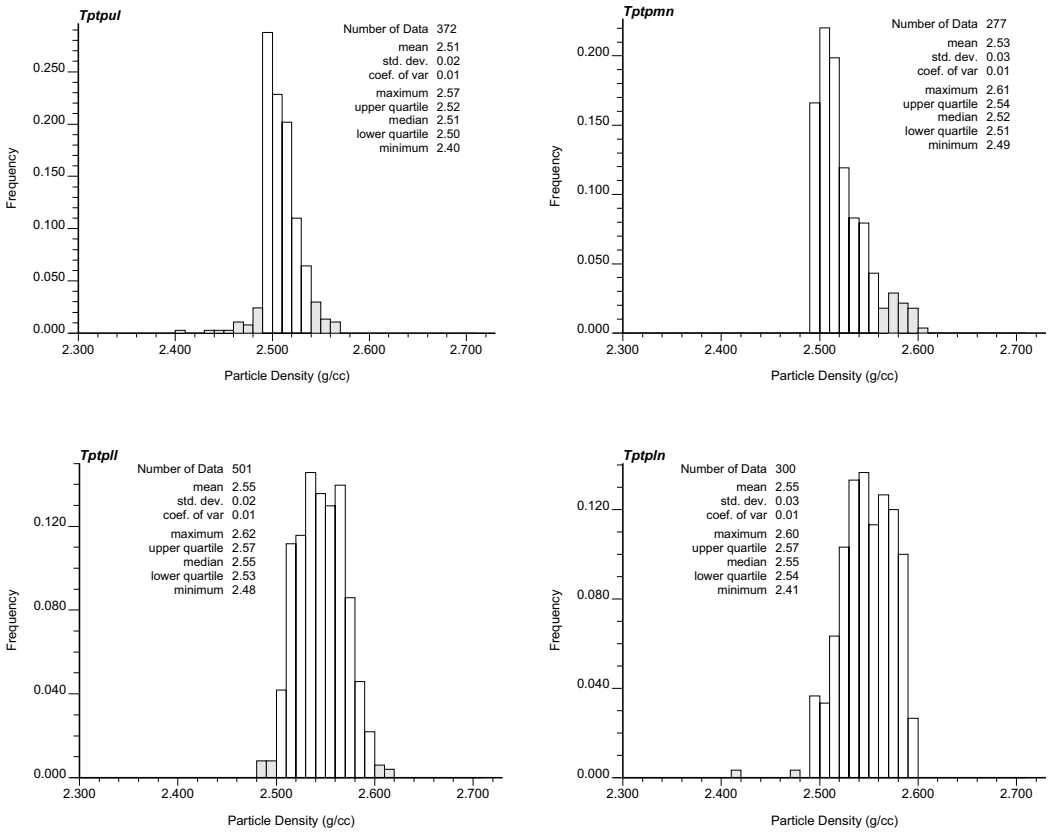

Source: BSC 2006 [DIRS 178277], Figure 4.

Figure 6-13. Histogram Plots of Particle Density for RHH Lithostratigraphic Zones

Table 6-6. Bulk Densities and Porosities for RHH Zones

Lithostratigraphic Zone	Matrix Porosity		Lithophysal Porosity		Dry Bulk Density [g/cc]	
	Mean	Standard Deviation	Mean	Standard Deviation	Mean	Standard Deviation
Tptpul	0.1667	0.0412	0.1228	0.0613	1.8344	0.1496
Tptpmn	0.1287	0.0323	0.0254	0.0225	2.1483	0.0932
Tptpll	0.1486	0.0340	0.0883	0.0540	1.9793	0.1381
Tptpln	0.1058	0.0264	0.0302	0.0253	2.2114	0.0857

Source: BSC 2006 [DIRS 178277], Table 1.

6.4.1.2 Porosity

The tuffaceous rock units at Yucca Mountain contain two components of porosity: matrix and macroscopic lithophysae. To estimate the matrix and lithophysal porosity values primarily from geophysical logs, computation methods were developed and presented in *Thermal Conductivity of the Potential Repository Horizon* (BSC 2004 [DIRS 169854], pp. 6-12 and 6-13 and Appendix A). Three methods were presented in *Thermal Conductivity of the Potential Repository Horizon* for calculating matrix and lithophysal porosity, based primarily on core analysis results (Method A); based mostly on geophysical log data (Method B); and based on

computation without benefit of test data (Method C). The calculations of matrix and lithophysal porosities are based on the data presented in DTNs: MO0010CPORGLOG.002 [DIRS 155229] and MO0010CPORGLOG.003 [DIRS 155959]. A summary of the input sources for the calculations in Methods A through C is listed in Table 6-7.

Table 6-7. Sources for Porosity and Petrophysical Data

Data Source Description	Source DTNs
Laboratory Core Physical Properties Data: Particle Density, Water Saturation, and Porosity	MO0109HYMXPROP.001 [DIRS 155989] [a] GS980808312242.014 [DIRS 106748] [b]
Petrophysical Data: Neutron Porosity and Bulk Density	MO0010CPORGLOG.002 [DIRS 155229] MO0010CPORGLOG.003 [DIRS 155959]

[a] Boreholes: USW SD-7, USW SD-9, USW SD-12, USW NRG-7/7a, USW UZ-7a, USW NRG-6, and USW UZ-16/USW UZ-14.

[b] Borehole: USW SD-6.

Borehole petrophysical measurements of bulk density and neutron porosity were used to make quantitative estimates of matrix and lithophysal porosity. These data provide substantial information regarding the spatial heterogeneity of porosity across the entire site (Figure 6-12) (BSC 2004 [DIRS 169854], Section 4.1.2).

6.4.1.2.1 Matrix Porosity

Matrix porosity is the normal porosity of a rock created by small-scale void space situated between the rock grains. It is normally calculated from laboratory analysis using small samples from core material. Matrix porosity can be further divided into the matrix ground mass and vapor-phase altered material, also referred to as rims and spots. The rims and spots have higher porosity than the matrix ground mass because of the altered condition. There is no way to differentiate the components in the matrix using the calculation methods, so the calculations treat the rims, spots, and matrix ground mass together as a matrix.

Geostatistical representations of matrix porosity are developed based on laboratory core and well-log petrophysical measurements. Matrix porosity can be calculated either by comparing saturated and dry bulk densities or by comparing dry bulk and grain densities. Reports of laboratory core measurements produced for the YMP generally include two values of dry bulk density determined using two testing methods. Using method 1, the dry density was obtained by drying the sample in a 60°C oven at 65% relative humidity (RH). Using the method 2, the dry density value was obtained by drying the sample in the oven at 105°C and ambient but very low RH. The porosity data calculated based on the dry density value determined using method 2, are almost always greater than those obtained using method 1. The most likely reason is that the higher test temperature and low humidity causes water to evaporate, thus leaving the pore space empty. The lower temperature and higher RH (method 1) causes that water still remains within the rock volume bound to minerals, or otherwise trapped in unconnected pores.

A method of calculating matrix porosity from bulk density and neutron porosity is presented as follows. Equation 6-2 gives an expression for evaluating matrix porosity, ϕ_m, from knowledge

of the grain density, ρ_s, bulk density, ρ_b, matrix water saturation, S_w, and volumetric water content, V_{wc} (BSC 2006 [DIRS 178277], Figure 5).

$$\phi_m = \frac{\rho_s}{S_w\left(\frac{\rho_b}{V_{wc}} - \rho_w\right) + \rho_s} \quad \text{(Eq. 6-2)}$$

This equation is applied at locations where petrophysical data are available but core data are not. Where core data are available, matrix porosity is measured directly from the core; therefore, it is unnecessary to calculate.

Histogram plots of the composite matrix porosity data set that resulted from analyses for each of the four RHH lithostratigraphic zones are illustrated in Figure 6-14 (BSC 2004 [DIRS 169854], Section 6.1.5). The histogram plots yield a matrix porosity means of 0.1639, 0.1256, 0.1481, and 0.1045 for the Tptpul, Tptpmn, Tptpll, and Tptpln zones, respectively.

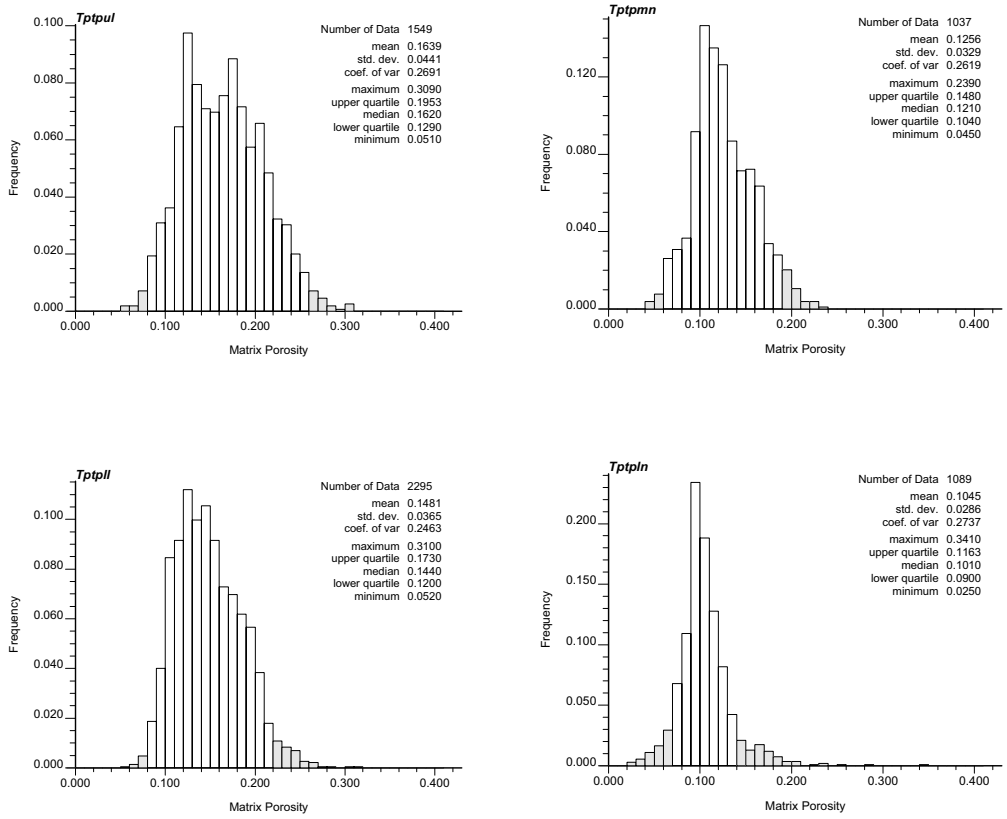

Source: BSC 2006 [DIRS 178277], Figure 3.

NOTE: The histograms in this figure combine matrix porosity data from core measurements and estimates based on petrophysical logging (Method B using Equation 6-2).

Figure 6-14. Histogram of Matrix Porosity for the RHH Lithostratigraphic Zones

6.4.1.2.2 Lithophysal Porosity

Lithophysal porosity is the measure of large-scale (macroscopic) voids present in the host rock unit as gas-derived voids called lithophysae, which range from centimeter to meter-size. Within the RHH zone, lithophysae are concentrated in the lithophysal lithostratigraphic zones (Tptpul and Tptpll), but they may be present in the nonlithophysal zones (Tptpmn and Tptpln) as smaller and less uniform voids. Lithophysae are gas filled because capillary action tends to distribute the water in small matrix pore spaces and fractures.

Mappings in the ECRB Cross-Drift show that lithophysae vary in size, shape, and abundance throughout all four lithostratigraphic layers of the RHH (Mongano et al. 1999 [DIRS 149850], pp. 16 to 35; BSC 2003 [DIRS 166660], Section 5.3.3.3; BSC 2004 [DIRS 166107], Appendix O). The abundance of lithophysae, as suggested by their given names, is greater in the upper and lower lithophysal zones than in the middle and lower nonlithophysal zones. The lithophysae in the Tptpul generally tend to be smaller, roughly 1 cm to 10 cm in diameter, than the lithophysae in the Tptpll, which tend to have lithophysae that are highly variable in size. The lithophysae found in the Tptpll range from less than 1 cm to 1.8 m in size. The lithophysae in the Tptpul tend to be more uniform in size and distribution than the lithophysae in the Tptpll, which tend to have shapes that are highly variable and are of simple geometry to irregular, cuspate, and merged. The lithophysae exhibit varying infilling and rim thicknesses. The lithophysae in both zones have a volume that varies consistently and predictably with stratigraphic position.

Bulk density is the principal petrophysical measurement used to calculate lithophysal porosity. In theory, petrophysical measurements of bulk density account for all contributions of mass to the system (liquid, solid, gas). Lithophysal porosity can be calculated directly from bulk density when certain properties of the matrix (porosity and saturation) have been established through direct measurement (i.e., core samples). Depending on the availability of direct measurements, one of three methods is used, which is summarized as follows (BSC 2004 [DIRS 169854], Section 6.1.4 and Appendix A):

- **Method A**: In boreholes where core samples were collected and measurements of matrix porosity obtained, depth-matched bulk density values are linearly interpolated from the smoothed bulk density data set (BSC 2004 [DIRS 169854], Section 4.1.2). Lithophysal porosity is calculated using Equation 6-3 (BSC 2006 [DIRS 178277], Figure 5).

$$\phi_L = 1 - \frac{\rho_b}{\phi_m S_w \rho_w + (1 - \phi_m)\rho_s} \qquad \text{(Eq. 6-3)}$$

  Where,

  ρ_b: interpolated bulk density
  ϕ_m: core matrix porosity
  S_w: matrix water saturation
  ρ_w: water density
  ρ_s: solid density (unit-specific particle density).

- **Method B**: In boreholes where core samples were not collected, but neutron porosity petrophysical data exist and are within the range of expected values, Equation 6-4 (BSC 2004 [DIRS 169854], Equation 6-23) is used to calculate lithophysal porosity. In this case the smoothed neutron porosity data (BSC 2004 [DIRS 169854], Section 4.1.2) are used to calculate the volumetric water content, V_{wc}, of the composite rock. As in Method A, the unit-specific particle density (BSC 2004 [DIRS 169854], Table 5-4) and matrix water saturation of unity are applied (BSC 2006 [DIRS 178277], Figure 5).

$$\phi_L = 1 - \frac{\rho_b}{\rho_s} + \frac{V_{wc}\rho_w}{\rho_s} - \frac{V_{wc}}{S_w} \quad \text{(Eq. 6-4)}$$

- **Method C**: In boreholes where core samples were not collected and neutron porosity data are not available, Equation 6-3 is used to calculate lithophysal porosity. In such circumstances, matrix porosity, particle density, and water saturation are used in the calculation of lithophysal porosity as follow: matrix porosity equal to 0.10, particle density is obtained from the mean values in Figure 6-13 for the respective rock unit and water saturation equal to unity. The value of 0.10 for matrix porosity, which lies at near the lower end of the matrix porosity conditioning data (Figure 6-14), was chosen because it leads to somewhat larger calculated lithophysal porosity.

Of the three calculations, Method A is considered to be the most reliable as it uses direct measurements for all parameters affecting lithophysal porosity. Method B, which uses the same measurements as Method A except for the matrix density follows it. The matrix density is estimated from the neutron density data, as opposed to the more reliable estimate from core data used in Method A. Finally, Method C provides the least reliable estimates. Instead of using a value of the matrix porosity based on data, Method C uses 0.10. Method B was applied most often since most older boreholes were not cored, and Method C was applied the least since neutron porosity data are nearly as abundant as bulk density (BSC 2004 [DIRS 169854], Section 6.1.4).

In all three methods, the matrix continuum is water saturated. Setting S_w to unity may lead to smaller calculated matrix porosities; however, the calculated values of lithophysal porosity are not highly dependent on the values of matrix saturation. All three methods also use the mean values of particle density given in Figure 6-13. The narrowness of these histograms justifies the use of constant values (BSC 2004 [DIRS 169854], Section 6.1.4).

Histogram plots of calculated lithophysal porosity are depicted in Figure 6-15 for each of the four lithostratigraphic zones. Mean lithophysal porosity values of 0.1352, 0.0281, 0.0931, and 0.0322 were obtained for the Tptpul, Tptpmn, Tptpll, and Tptpln, respectively. Given the number and spatial distribution of boreholes used in the construction of these plots, they reflect the spatial variability of lithophysal porosity across the entire repository region. For a number of boreholes (e.g., data for borehole USW G-3 are illustrated in Figure 6-16), negative values of lithophysal porosity are calculated over some intervals. This is the result of the possible measurement errors associated with the petrophysical measurements and the analytical methods applied to calculate lithophysal porosity. These nonphysical negative values are treated as zeros in the construction of the lithophysal porosity distributions. This can be verified by examining

the minimum values of lithophysal porosity tabulated in Figure 6-15 (BSC 2004 [DIRS 169854], Section 6.1.4).

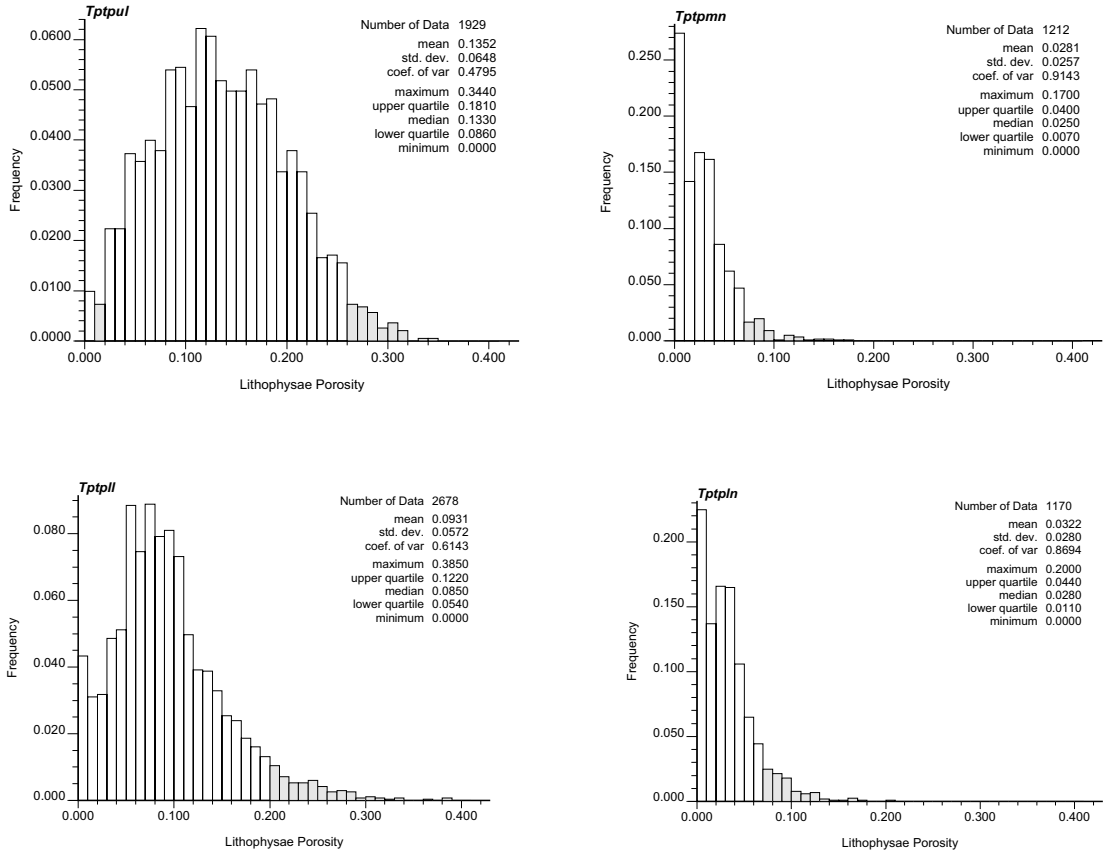

Source: BSC 2006 [DIRS 178277], Figure 2

Figure 6-15. Histogram of Lithophysal Porosity for the RHH Lithostratigraphic Zones

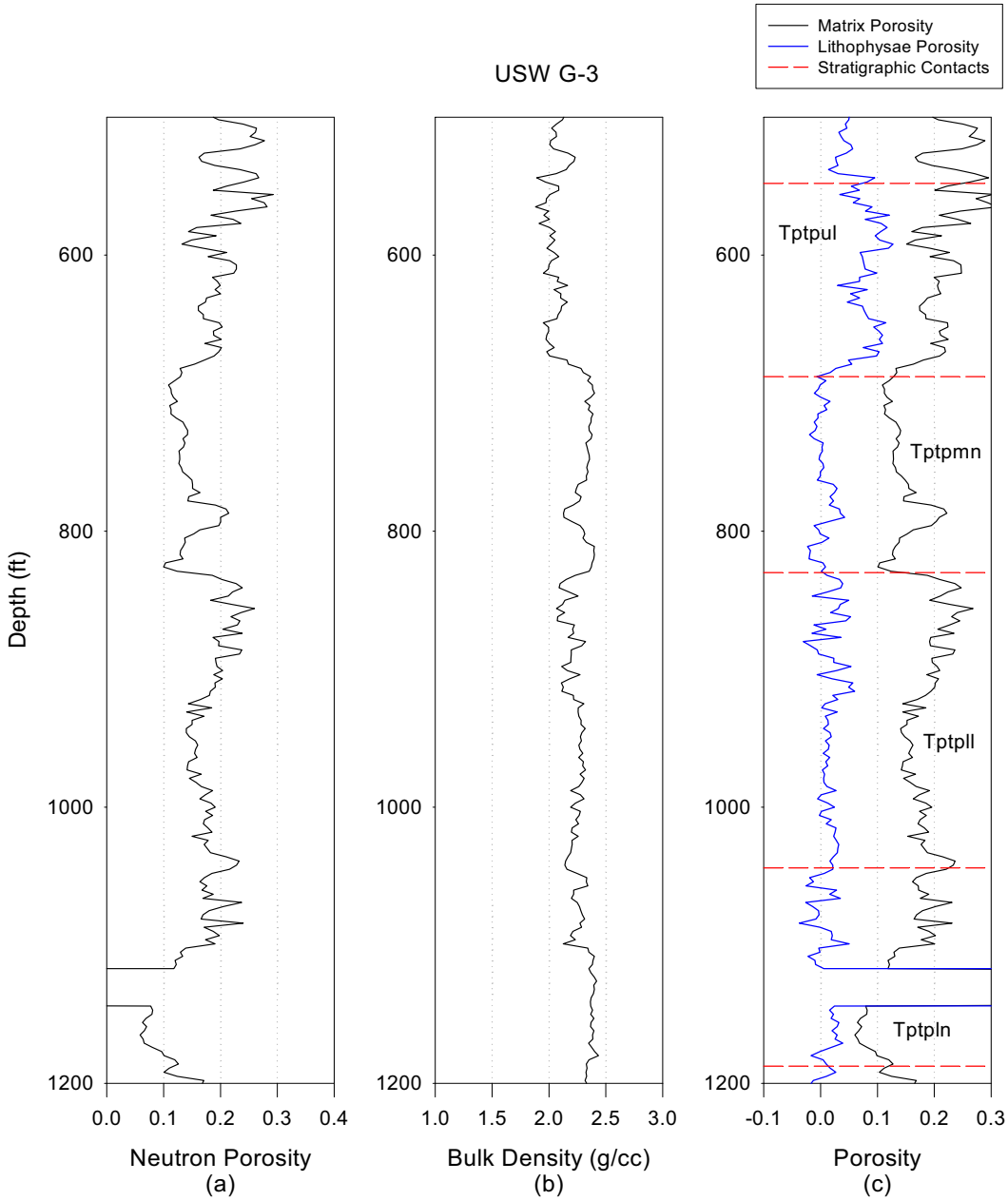

Source: BSC 2004 [DIRS 169854], Figure B-3.

Figure 6-16. Petrophysical Data for Borehole USW G-3

6.4.1.2.3 Total Porosity

The total porosity of a specimen is either calculated by saturating the specimen and determining what volume of the sample is occupied by water, by drying the samples and using the dry bulk and average grain densities, or by an approximation method using a point count of the exterior of the specimen in combination with the porosity of the components encountered.

In a homogeneous rock mass, core analyses can be used to determine the porosity of the rock. In the lithophysae-bearing rock, the lithophysal cavities are not adequately sampled and accounted for, so the estimation of total porosity from core analyses is not reliable.

The total porosity of a specimen is size dependant. Small samples cannot capture lithophysae in their entirety. Figure 6-17 is a photograph of the Tptpll zone at the right tunnel wall between stations 14+93 and 14+96 in the ECRB Cross-Drift. The one-meter high by three-meter long section of wall was analyzed for the abundance and location of lithophysae and altered material. The lithophysae (voids) are outlined in red, spot material (solid) is outlined in lavender, rim material is outlined in green, and clasts are outlined in yellow. This panel map and accompanying information is available in DTN: GS021008314224.002 [DIRS 161910]. The ability to capture a representative specimen of the rock mass is impractical as the specimen must be of several lithophysae in diameter, or in the order of several meters. Bulk rock consists of lithophysae, vapor phase altered material, cracks (healed), and matrix material. The largest specimens mechanically tested in the laboratory were 290 mm cylindrical cores obtained from the lithophysal zones, and the smallest specimens mechanically tested were 25.4 mm in diameter.

Figure 6-18 is the same panel map as shown in Figure 6-17 with six randomly located sets of specimen outlines. The rectangles at each of the six locations indicate the outline of theoretical core specimens with length to diameter ratios of 2:1. The outlines are of vertical cores with diameters of 25.4 mm, 50.8 mm, 82 mm, 127 mm, 228 mm, 267 mm, and 290 mm with corresponding lengths of twice the diameter of the specimen. The geometric centers of each set of concentric rings are common. The total porosity of a specimen is dependant on the volume that is sampled, and this is best illustrated in Figure 6-19, which is the same panel map in Figures 6-17 and 6-18 with the photograph removed and the theoretical specimens outlined. Figure 6-19 is an illustration of the difficulty in obtaining specimens that are representative of the bulk rock. Of the six sets of theoretical specimens, four of the six 25.4 mm specimens are composed entirely of matrix material (second, fourth, fifth, and sixth from the left); one is primarily lithophysae (furthest left) and one primarily of spot material (third from left). The porosity of the recoverable material would be representative of matrix material.

The specimen primarily composed of lithophysae (first from left) would be unrecoverable from the borehole intact and, therefore, would be unavailable for testing. The four specimens that are composed entirely of matrix material are from a lithophysal zone, but contain no lithophysae, therefore are comparable to specimens recovered from nonlithophysal zones. Because of their size, it is difficult to capture lithophysae having an impact on total porosity in small specimens, in particular 25.4 mm, 50.8 mm, and even 82 mm diameter specimens.

The first set of theoretical specimens (farthest to the left) most likely would not be recoverable as the lateral dimension of the large lithophysae located in the center of the specimen would make

recovery difficult. Recovery of specimens depends on the dimensions and location of the sample in relation to the lithophysae. Further sampling by large diameter core drilling is deemed impractical and it is concluded that full-scale in situ testing of tunnel performance would be necessary for characterization of these zones.

One important distinction between matrix and lithophysal porosity is that the two properties are defined with respect to different reference volumes. Consequently, these properties cannot be added directly, and care must be exercised when applying the geostatistical results. This difference in definition is required because core measurements do not account for the volume of lithophysae and, hence, are not based on the total volume. Instead, matrix porosity is measured and, therefore, defined as the volume fraction of small-scale void space with respect to the matrix volume, V_m, where the matrix volume is simply the total volume, V_t, less the lithophysae volume, V_L (BSC 2004 [DIRS 169854], Section 6.1.5):

$$V_m = V_t - V_L \quad \text{(Eq. 6-5)}$$

This same definition of matrix porosity is used in the derivation of Equation 6-2, so it is appropriate to combine the petrophysically derived values of matrix porosity with the laboratory measured values into a composite data set.

Using the matrix porosity (ϕ_m) and lithophysal porosity (ϕ_L) definitions employed in this report, the total porosity (ϕ_T) is given by the following equation (BSC 2006 [DIRS 178277], Figure 5).

$$\phi_T = \phi_L + \phi_m(1 - \phi_L) \quad \text{(Eq. 6-6)}$$

Source: DTN: GS021008314224.002 [DIRS 161910].

Figure 6-17. Panel Map Photograph and Stenciled Lithophysae and Vapor Phase Altered Material at Station 14+93 through Station 1 4+96 Right Wall, Tptpll Zone

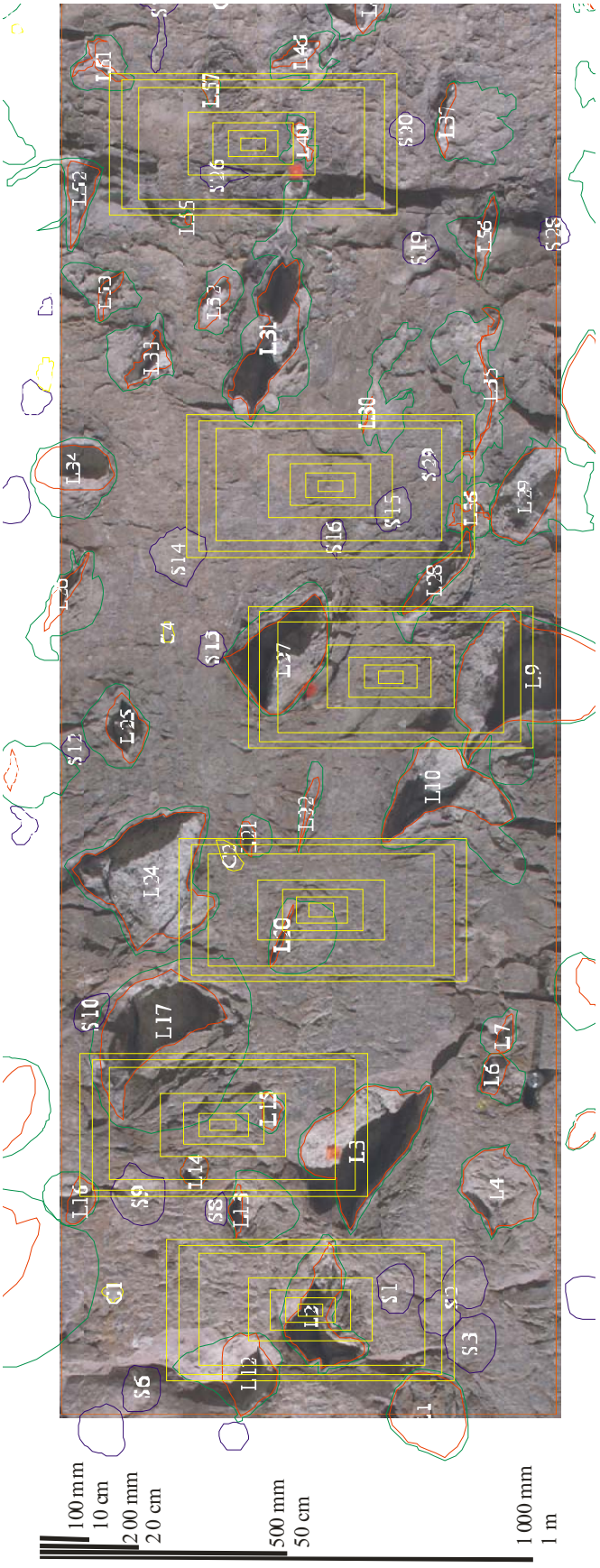

Source: Adapted from DTN: GS021008314224.002 [DIRS 161910].

Figure 6-18. Panel Map of Lithophysal Zone Tptpll at Station 14+93 through Station 14+96 Right Wall and Randomly Located Specimen Outlines

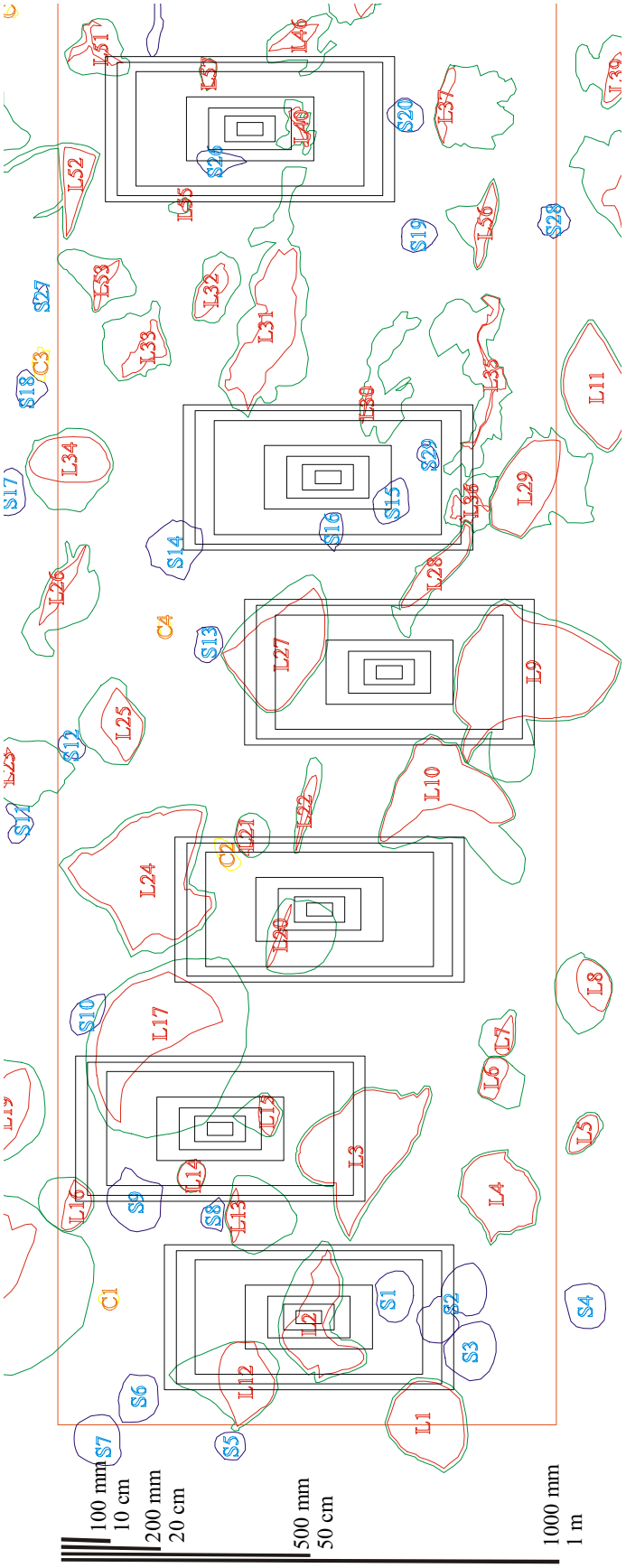

Source: Adapted from DTN: GS021008314224.002 [DIRS 161910].

Figure 6-19. Panel Map of Station 14+93 through 14+96 Right Wall Including Outline of Lithophysae and Randomly Selected Specimen Outlines

6.4.2 Mechanical Properties of the Intact Rock

A comprehensive series of mechanical property measurements has been conducted on specimens prepared from NRG, SD, Underground Exploratory (UE), USW-G drillholes, ESF, and ECRB Cross-Drift drilling operations, and from surface locations (i.e., Busted Butte and Fran Ridge area). Mechanical property measurements on tuff from Yucca Mountain include elastic constants, strength, and deformation characteristics. Measurements began in the late 1970s and are continuing. One objective of these measurements was to determine the baseline properties for each rock unit.

Properties of rocks are determined using specimen sizes ranging from microscopic mineral crystals to large volumes of rock mass, where features such as fractures may impact rock behavior such that it may no longer be treated as a uniform rock type. For practical reasons, small rock samples can be obtained and prepared for testing much easier than large-size specimens. General mechanical properties of intact rock, in most cases, provide a common basis for comparison of samples of different sizes. However, the data user should consider any additional factors and testing methods that may contribute to the specific behavior of rock at various sample sizes and testing conditions.

The purpose of baseline measurements was to study the vertical and lateral variability of bulk and mechanical properties of rock at Yucca Mountain. Boyd et al. (1995 [DIRS 120650], pp. 511 to 516) noted there was little lateral variability among the NRG boreholes along the axis of the North Ramp as determined from the NRG borehole series; however, there was significant vertical variability due to large differences in lithology and smaller differences in smaller scale fabric and pore structure characteristics.

This section provides a summary of the intact rock mechanical properties of the lithostratigraphic zones at Yucca Mountain. For statistical analysis of the intact rock mechanical data, it is assumed that the intact rock mechanical property has a normal distribution and it is, therefore, appropriate to use an arithmetic mean and standard deviation (Assumption 5.1.2). The detailed analyses of intact rock mechanical properties, including statistical analyses, are presented in *Intact Rock Mechanical Properties of Yucca Mountain Stratigraphic Units* (BSC 2005 [DIRS 176611]).

6.4.2.1 Strength Properties

Strength properties of the intact rock specimens obtained from core specimens were determined under a variety of environmental and physical conditions. Specimens were tested under both unconfined and confined axial compression as well as in indirect tension using the Brazilian method.

6.4.2.1.1 Unconfined/Uniaxial Compressive Strength

Table 6-8 presents the mean and standard deviation of the compressive strength for lithostratigraphic zones tested under all different testing or environmental conditions. The majority of specimens were 50.8 mm in diameter and tested saturated, under ambient temperature conditions, with an L:D ratio near 2:1 and at a strain rate of 10^{-5} s^{-1}. Several test procedures were used by the various laboratories that included ASTM D 2938-95, *Standard Test*

Method for Unconfined Compressive Strength of Intact Rock Core Specimens [DIRS 165094], and the International Society of Rock Mechanics (ISRM) procedure, *Suggested Methods for Determining the Uniaxial Compressive Strength and Deformability of Rock Materials* (Bieniawski et al. 1981 [DIRS 150684]). The test results from UCS tests exhibited considerable variability among lithostratigraphic zones as well as different testing conditions.

The UCS for baseline testing conditions (Code 231221) are summarized in Table 6-9 and illustrated in Figure 6-20. The table and figure show that the UCS values are variable among the lithostratigraphic zones.

UCS test results depend on the degree of welding, porosity, and fabric of the rock specimen. In general, welded tuff exhibited higher strength than nonwelded tuff with the exception of the TSw3 unit and measured 119.23, 8.59, 62.21, 153.92, 16.40, and 23.23 MPa for the TCw, PTn, TSw1, TSw2, TSw3, and CHn units, respectively (Table 6-9). Within the welded units, the variations in strength are related to the presence and size of lithophysae and vapor-phase altered zones (CRWMS M&O 1997 [DIRS 103564], p. 5-102). The *Yucca Mountain Site Geotechnical Report* (CRWMS M&O 1997 [DIRS 103564]) also reports that very little volumetric strain is measured in the welded tuffs as compared to other crystalline rocks. This behavior suggests that axial cracks extend without interacting with other cracks until failure is imminent (CRWMS M&O 1997 [DIRS 103564], p. 5-102). Similar effects have also been reported by others (Brace et al. 1966 [DIRS 101990]; Scholz 1968 [DIRS 104568]).

Table 6-9 also shows that the crystal-rich zones (Tpcrn, Tptrv3, Tptrn, and Tptrl) and vitric subzones (Tpcpv1, Tpcpv2, Tptrv3, and Tptpv3) have generally lower strength ranging from 4.3 MPa in the Tptrv3 subzone to 62 MPa in the Tptrn zone and generally below 30 MPa. In contrast, the crystal-poor zones in the Tiva Canyon Tuff (Tpcpmn, Tpcpll, and Tpcpln) and Topopah Spring tuff (Tptpmn, Tptpll, and Tptpln), except in the upper lithophysal zones (Tpcpul and Tptpul), have higher strength ranging from 123.0 to 186.7 MPa. The Tpcpul and Tptpul zones have relatively lower strength with a mean UCS of 62.1 and 65.2 MPa, respectively.

Figure 6-20 shows a similar pattern in strength between Tiva Canyon Tuff (Tpcrn, Tpcpul, Tpcpmn, Tpcpll, and Tpcpln) and Topopah Spring tuff (Tptrn, Tptrl, Tptrf, Tptpul, Tptpmn, Tptpll, and Tptpln). The mean UCS values in the Tiva Canyon Tuff range from 36 MPa at the Tpcrn zone to 186.7 MPa at the Tpcpll zone and the mean UCS values in Topopah Spring tuff range from 26.7 MPa at the Tptrl zone to 164.6 MPa at the Tptpmn zone. The UCS data are considered sufficient to make a bounded estimate for lithostratigraphic zones within the Tiva Canyon and Topopah Spring tuffs.

The mean UCS for the RHH Tptpul, Tptpmn, Tptpll, and Tptpln zones are 65.21, 164.58, 123.01, and 155.51 MPa, respectively (Table 6-9). It should be noted that the mean UCS for the lithophysal zones, Tptpul and Tptpll, is not considered to be representative of actual in situ rock strength since the tested samples are relatively small (38 to 70 mm) and are not representative of actual in situ porosity.

Table 6-8. Summary of UCS Test Results

TM Unit	Litho-stratigraphic Zone	Testing Group[a]	Number of Tests	Compressive Strength (MPa)[b, c]			
				Mean	Standard Deviation	Min.	Max.
UO	Tmr	231221	5	7.60	7.48	1.80	20.30
	Tpki	231221	7	5.94	2.72	1.10	9.80
TCw	Tpcrn	221221	3	100.30	31.19	64.40	120.70
		231221	18	36.02	32.98	10.40	132.90
	Tpcpul	221221	3	92.10	22.51	66.70	109.60
		221321	1	65.60	NA	65.60	65.60
		231221	5	62.14	26.54	32.50	85.50
	Tpcpmn	221221	3	232.13	38.65	198.60	274.40
		221321	1	128.90	NA	128.90	128.90
		231221	8	167.19	64.12	71.90	244.00
	Tpcpll	131221	4	311.55	20.05	284.20	332.40
		231221	5	186.74	112.86	75.40	313.60
	Tpcpln	221231	1	364.00	NA	364.00	364.00
		231221	20	172.33	58.09	78.20	278.40
PTn	Tpcpv2	231221	4	28.18	23.60	11.30	61.80
	Tpcpv1	231221	4	5.05	1.41	3.90	6.90
	Tpbt4	221221	1	3.50	NA	3.50	3.50
		221231	1	7.03	NA	7.03	7.03
		231221	1	1.20	NA	1.20	1.20
	Tpy	231221	5	19.30	6.99	7.80	26.20
	Tpbt3	221221	2	5.10	1.13	4.30	5.90
		231221	2	1.80	1.41	0.80	2.80
	Tpp	221221	2	3.70	0.57	3.30	4.10
		231221	10	3.19	2.45	1.30	9.40
	Tpbt2	221221	3	3.20	1.42	2.10	4.80
		231221	6	2.92	2.30	0.80	6.40
	Tptrv3	231221	2	4.25	2.19	2.70	5.80
TSw1	Tptrn	131221	10	103.68	36.02	62.60	162.00
		221221	5	63.34	36.60	26.50	114.30
		231221	53	61.98	31.06	25.70	148.40
	Tptrl	231221	3	26.73	9.25	17.40	35.90
	Tptf	131211	2	116.00	1.41	115.00	117.00
		131221	5	176.80	37.57	130.00	220.00
		231221	1	157.00	NA	157.00	157.00
	Tptpul	221221	2	47.50	14.42	37.30	57.70
		231221	8	65.21	44.40	15.70	149.40
		312111	3	30.47	9.47	19.60	37.00
		312221	1	17.70	NA	17.70	17.70
		321111	3	24.03	8.66	16.50	33.50
		321211	8	28.65	12.04	13.50	53.00
		321221	1	19.40	NA	19.40	19.40
TSw1	Tptpul	331211	4	18.75	15.10	9.40	41.30

Table 6-8. Summary of UCS Test Results (Continued)

TM Unit	Litho-stratigraphic Zone	Testing Group[a]	Number of Tests	Compressive Strength (MPa)[b, c]			
				Mean	Standard Deviation	Min.	Max.
TSw1	Tptpul	331221	11	16.12	4.73	10.30	27.80
TSw2	Tptpmn	111321	30	146.46	57.33	31.90	236.00
		131211	2	236.60	9.19	230.10	243.10
		131221	30	222.70	42.42	113.30	326.10
		131231	3	294.10	21.70	280.10	319.10
		211211	4	150.88	50.18	78.10	185.50
		211221	4	122.58	35.32	87.00	166.10
		212211	9	105.67	34.54	45.00	152.00
		212221	2	90.50	26.16	72.00	109.00
		212231	2	101.50	102.53	29.00	174.00
		221221	16	176.35	65.82	71.30	324.10
		221231	1	138.00	NA	138.00	138.00
		221321	36	139.58	58.07	34.30	245.70
		231211	10	103.65	32.07	45.30	149.00
		231221	42	164.58	65.62	38.40	288.90
		231231	4	113.20	42.86	68.10	169.00
		232211	11	196.79	25.85	148.30	229.50
		232221	4	117.38	20.67	89.40	135.80
		321221	1	159.60	NA	159.60	159.60
		331221	22	105.94	31.11	58.86	170.80
	Tptpll	121221	16	194.69	37.99	110.90	261.70
		131211	2	130.60	10.61	123.10	138.10
		131221	30	112.99	51.38	3.00	187.10
		211221	7	175.93	19.38	152.20	205.20
		212221	6	213.18	11.75	200.30	226.30
		221221	59	153.12	40.06	50.90	246.60
		231221	15	123.01	47.57	31.60	179.10
		312111	2	31.65	0.78	31.10	32.20
		312221	5	122.72	75.98	28.30	196.10
		321211	7	34.57	17.39	13.30	67.40
		321221	25	121.24	38.69	28.10	180.00
		331211	1	15.70	NA	15.70	15.70
		331221	1	38.00	NA	38.00	38.00
		421221	5	60.70	24.80	27.00	92.20
	Tptpln	131211	3	126.13	70.97	45.00	176.70
		131221	10	104.40	37.77	31.10	152.10
		131231	4	149.58	11.03	133.90	157.30
		221221	2	171.55	1.91	170.20	172.90
		221231	1	166.00	NA	166.00	166.00
		231221	10	155.51	30.35	82.90	192.90
TSw3	Tptpv3	221221	2	45.80	5.66	41.80	49.80
		231221	1	16.40	NA	16.40	16.40

Table 6-8. Summary of UCS Test Results (Continued)

TM Unit	Litho-stratigraphic Zone	Testing Group[a]	Number of Tests	Compressive Strength (MPa)[b, c]			
				Mean	Standard Deviation	Min.	Max.
CHn	Tptpv2	131221	2	91.65	1.63	90.50	92.80
		221221	1	90.20	NA	90.20	90.20
	Tptpv1	131211	2	10.10	2.83	8.10	12.10
		131221	5	12.90	4.76	6.10	19.10
		131231	3	12.10	3.61	8.10	15.10
	Tpbt1	131211	3	27.67	0.58	27.00	28.00
		131221	4	27.25	6.02	22.00	35.00
		231221	1	20.50	NA	20.50	20.50
	Tac	121221	2	36.95	5.87	32.80	41.10
		131211	2	20.80	1.13	20.00	21.60
		131221	34	27.46	8.87	14.30	53.10
		131231	2	24.15	0.92	23.50	24.80
		221231	2	44.25	4.88	40.80	47.70
		231221	2	24.60	2.69	22.70	26.50
	Tacbt	131221	8	35.04	20.45	14.90	70.70

Sources: DTNs: MO0311RCKPRPCS.003 [DIRS 166073]; SN0208L0207502.001 [DIRS 161871]; SN0211L0207502.002 [DIRS 161872]; SN0302L0207502.003 [DIRS 165014]; SN0305L0207502.004 [DIRS 165013]; SN0306L0207502.008 [DIRS 165015]; SNL02030193001.001 [DIRS 120572]; SN0505L0212303.005 [DIRS 174956].

[a] Testing group designation numbers represent parameters in the following order: size, saturation, temperature, L/D ratio, strain rate, and confining pressure as shown on Table 6-3. For example, group category 121212 (Table 6-3) represents a specimen less than 38 mm in diameter, ambient in saturation, at room temperature, with an L/D ratio of 1.8 to 2.2, strain rate smaller than 0.5×10^{-5} per second, and confining pressure of approximately 5 MPa.

[b] Data below Calico Hills Formation are not included.

[c] The spreadsheet containing the statistical analysis of UCS is presented in Appendix H (see *Worksheet_Static Data.xls*).

Max. = maximum; Min. = minimum; NA = not available; TM = thermal-mechanical.

Table 6-9. Summary of UCS for Base Case Testing Conditions

TM Unit	Lithostrati-graphic Zone	Number of Tests	UCS (MPa)				Note
			Mean	Standard Deviation*	Min	Max	
UO	Tmr	5	7.60	7.48	1.80	20.30	Rainer Mesa tuff
	Tpki	7	5.94	2.72	1.10	9.80	Tuff Unit "X" - Informal
	Overall UO	12	6.63	5.01	1.10	20.30	
TCw	Tpcrn	18	36.02	32.98	10.40	132.90	Crystal-rich, non-lithophysal zone
	Tpcpul	5	62.14	26.54	32.50	85.50	Crystal-poor, Upper lithophysal zone
	Tpcpmn	8	167.19	64.12	71.90	244.00	Crystal-poor, middle non- lithophysal zone
	Tpcpll	5	186.74	112.86	75.40	313.60	Crystal-poor, lower lithophysal zone
	Tpcpln	20	172.33	58.09	78.20	278.40	Crystal-poor, lower non-lithophysal zone
	Overall TCw	56	119.23	85.67	10.40	313.60	
PTn	Tpcpv2	4	28.18	23.60	11.30	61.80	Crystal-poor, vitric zone, Tiva Canyon tuff
	Tpcpv1	4	5.05	1.41	3.90	6.90	Crystal-poor, vitric zone, Tiva Canyon tuff
	Tpbt4	1	1.20	NA	1.20	1.20	Crystal-poor, Pre-Tiva Canyon bedded tuff
	Tpy	5	19.30	6.99	7.80	26.20	Crystal-poor, Yucca Mountain tuff
	Tpbt3	2	1.80	1.41	0.80	2.80	Crystal-poor, Pre-Yucca Mountain tuff
	Tpp	10	3.19	2.45	1.30	9.40	Pah Canyon tuff
	Tpbt2	6	2.92	2.30	0.80	6.40	Pre-Pah Canyon bedded tuff
	Tptrv3	2	4.25	2.19	2.70	5.80	Crystal-rich, vitric zone, Topopah Spring tuff
	Overall PTn	34	8.59	12.04	0.80	61.80	
TSw1	Tptrn	53	61.98	31.06	25.70	148.40	Crystal-rich, nonlithophysal zone
	Tptrl	3	26.73	9.25	17.40	35.90	Crystal-rich, lithophysal zone
	Tptf	1	157.00	NA	157.0	157.00	
	Tptpul	8	65.21	44.40	15.70	149.40	Crystal-poor, upper lithophysal zone
	Overall TSw1	65	62.21	34.68	15.70	157.00	
TSw2	Tptpmn	42	164.58	65.62	38.40	288.90	Crystal-poor, middle non- lithophysal zone
	Tptpll	15	123.01	47.57	31.60	179.10	Crystal-poor, lower lithophysal zone
	Tptpln	10	155.51	30.35	82.90	192.90	Crystal-poor, lower non-lithophysal zone
	Overall TSw2	67	153.92	59.75	31.60	288.90	
TSw3	Tptpv3	1	16.40	NA	16.40	16.40	Crystal-poor, vitric zone
CHn	Tpbt1	1	20.50	NA	20.50	20.50	Pre-Tonopah Spring bedded tuff
	Tac	2	24.60	2.69	22.70	26.50	Calico Hill Formation
	Overall CHn	3	23.23	3.04	20.50	26.50	

Sources: DTNs: MO0311RCKPRPCS.003 [DIRS 166073]; SN0208L0207502.001 [DIRS 161871]; SN0211L0207502.002 [DIRS 161872]; SN0302L0207502.003 [DIRS 165014]; SN0305L0207502.004 [DIRS 165013]; SN0306L0207502.008 [DIRS 165015]; SNL02030193001.001 [DIRS 120572].

NOTE: It should be noted that the UCS for Tptpul, and Tptpll may not be an accurate representative since these UCS values are based on small size specimens and may not be indicative of in situ conditions.

The spreadsheet containing the statistical analysis of UCS is presented in Appendix H (see *Worksheet_Static Data.xls*).

Max. = maximum; Min. = minimum; NA = not available; TM = thermal-mechanical.

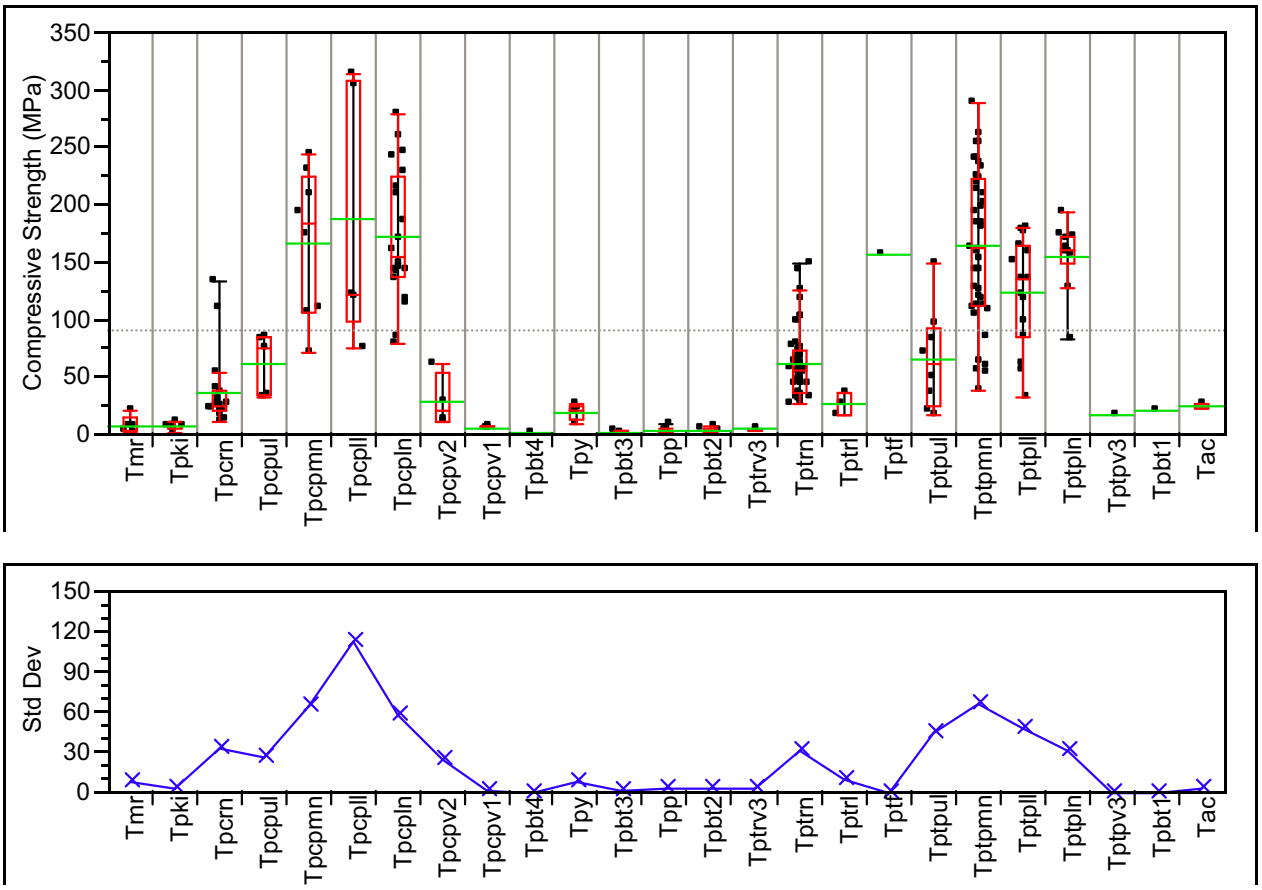

Sources: DTNs: MO0311RCKPRPCS.003 [DIRS 166073]; SN0208L0207502.001 [DIRS 161871]; SN0211L0207502.002 [DIRS 161872]; SN0302L0207502.003 [DIRS 165014]; SN0305L0207502.004 [DIRS 165013]; SN0306L0207502.008 [DIRS 165015]; SNL02030193001.001 [DIRS 120572].

Legends (in color):

Black: Jittered data point with range bar

Red: Box plot of quartiles include minimum, 25th percentile, median, 75th percentile, and maximum value Green: Mean value of each zone

Blue: Standard deviation

Figure 6-20. UCS by Lithostratigraphic Zone for Base Case Testing Conditions

As stated earlier, mechanical properties of intact rock change in response to variation in physical and environmental test conditions. The effects of test conditions, such as specimen size, saturation, temperature, and strain rate on UCS, are detailed in a calculation of *Intact Rock Mechanical Properties of Yucca Mountain Stratigraphic Units* (BSC 2005 [DIRS 176611], Section 6.3.2.2). Table 6-10 summarizes the results of the analysis of the effect of laboratory testing conditions on UCS.

Table 6-10. Summary of the Effect of Physical and Environmental Conditions on Compressive Strength

TM Units	Litho-stratigraphic Zone	Laboratory Test Conditions				
		Size	Saturation	Temperature	Strain Rate	Confining Pressure
TCw	Tpcrn	NA	Decreases with increasing saturation	NA	NA	NA
	Tpcpul	NA	Decreases with increasing saturation	NA	NA	NA
	Tpcpmn	NA	Decreases with increasing saturation	NA	NA	NA
	Tpcpll	NA	NA	NA	NA	NA
	Tpcpln	NA	NA	NA	NA	Increases with increasing confining pressure
TSw1	Tptrn	NA	No clear trend with saturation level	NA	NA	Increases with increasing confining pressure
	Tptpul	Decreases with increasing sample size	No clear trend with saturation level	NA	NA	Increases with increasing confining pressure
TSw2	Tptpmn	Decreases with increasing sample size	No clear trend with saturation level	Decreases with increasing temperature	No clear trend with strain rate	No clear trend with confining pressure
	Tptpll	Decreases with increasing sample size	Decreases with increasing saturation	NA	NA	NA
	Tptpln	NA	Decreases with increasing saturation	NA	NA	Increases with increasing confining pressure

NOTES: The relationships indicated in the table are based on qualitative comparison of means.

NA = not analyzed (due to limited number of tests); TM = thermal-mechanical.

UCS is plotted as a function of depth for selected SD and NRG boreholes in Figures 6-21 to 6-24 to examine the lateral variability of the strength for selected Yucca Mountain thermal-mechanical units. Some lateral correlation of the strength in thermal-mechanical units among the boreholes are observed from the figures that follow:

- TCw unit: NRG-2 and NRG-7a (Figure 6-21)
- PTn Unit: NRG-7a, NRG-4, and SD-9 (Figure 6-22)
- TSw1 unit: NRG-6, NRG-7a, NRG-4, and SD-9 (Figure 6-23)
- TSw2 unit: NRG-5, NRG-6, NRG-7a, and SD-9 (Figure 6-24).

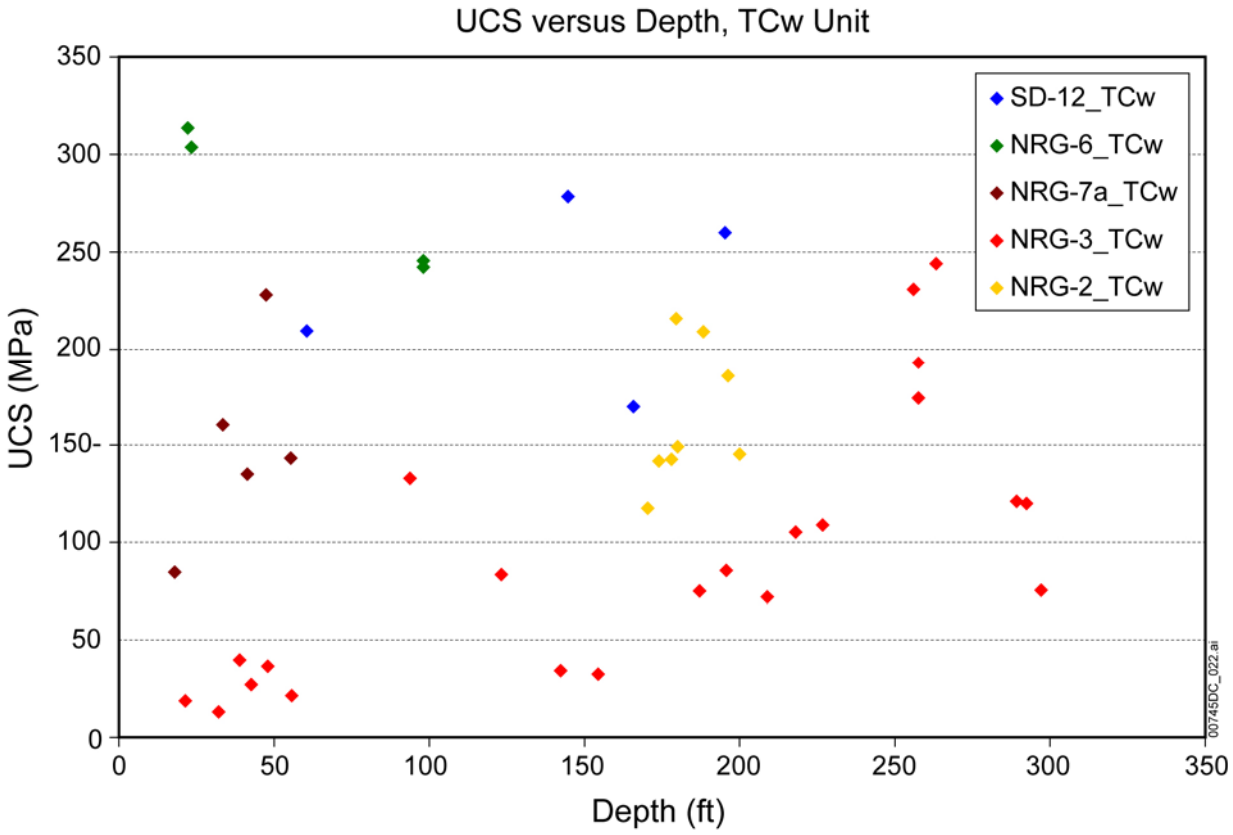

Sources: DTNs: MO0311RCKPRPCS.003 [DIRS 166073]; SNL02030193001.001 [DIRS 120572].

Figure 6-21. UCS versus Depth for SD and NRG Boreholes for TCw Unit

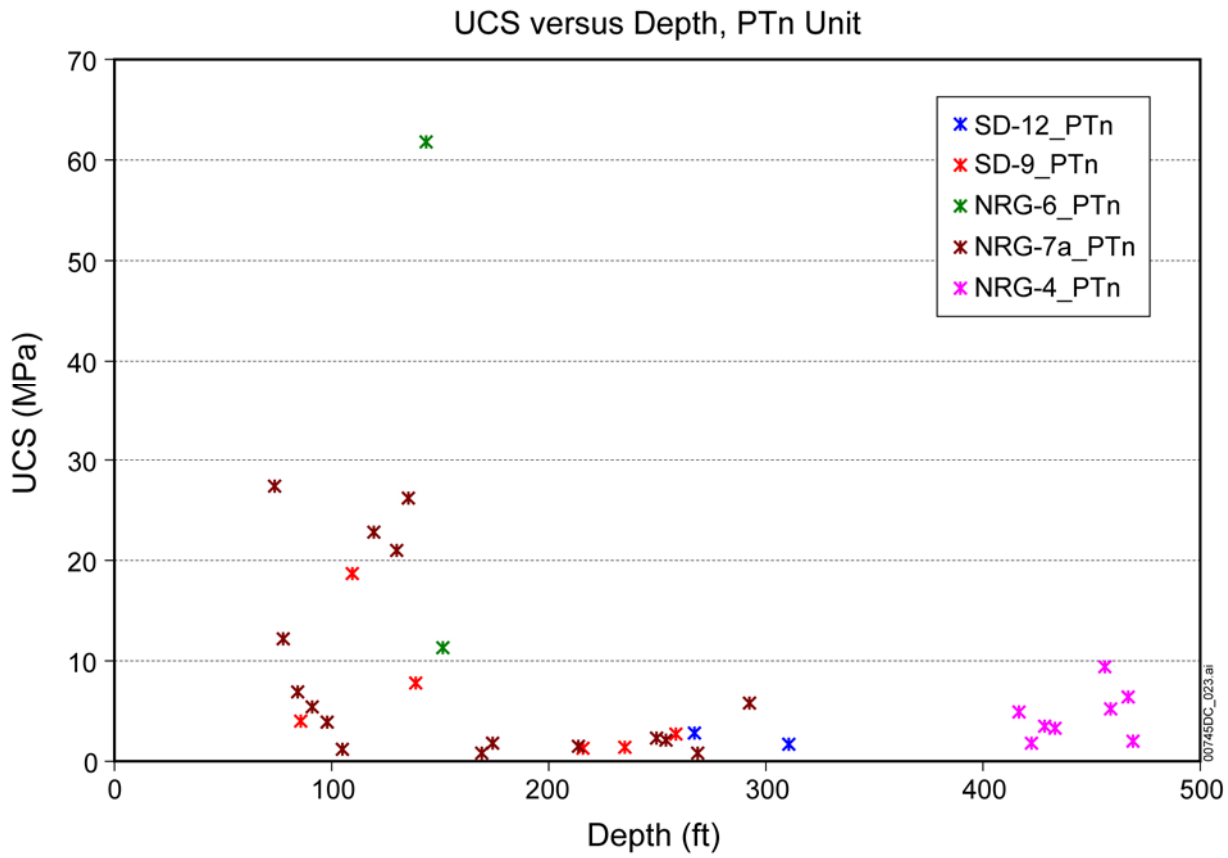

Sources: DTNs: MO0311RCKPRPCS.003 [DIRS 166073]; SNL02030193001.001 [DIRS 120572].

Figure 6-22. UCS versus Depth for SD and NRG Boreholes for PTn Unit

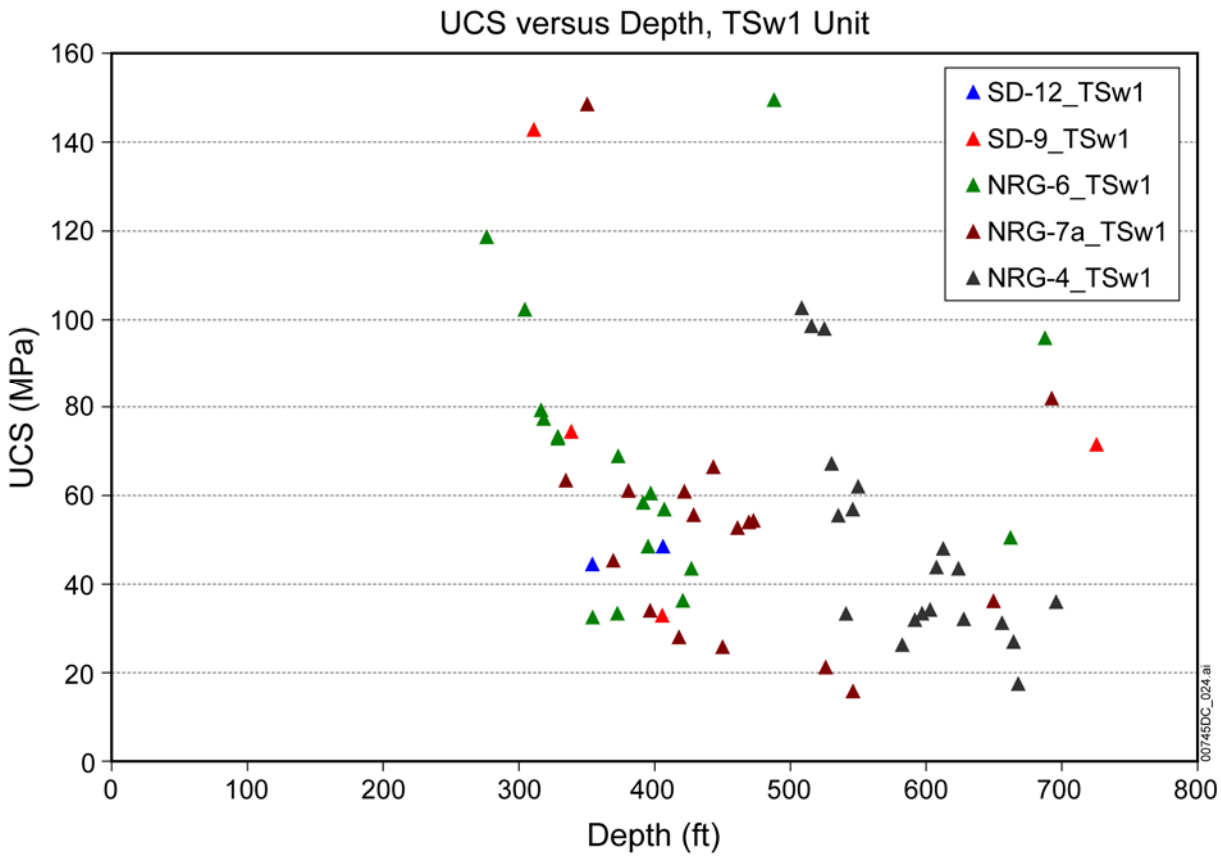

Sources: DTNs: MO0311RCKPRPCS.003 [DIRS 166073]; SNL02030193001.001 [DIRS 120572].

Figure 6-23. UCS versus Depth for SD and NRG Boreholes for TSw1 Unit

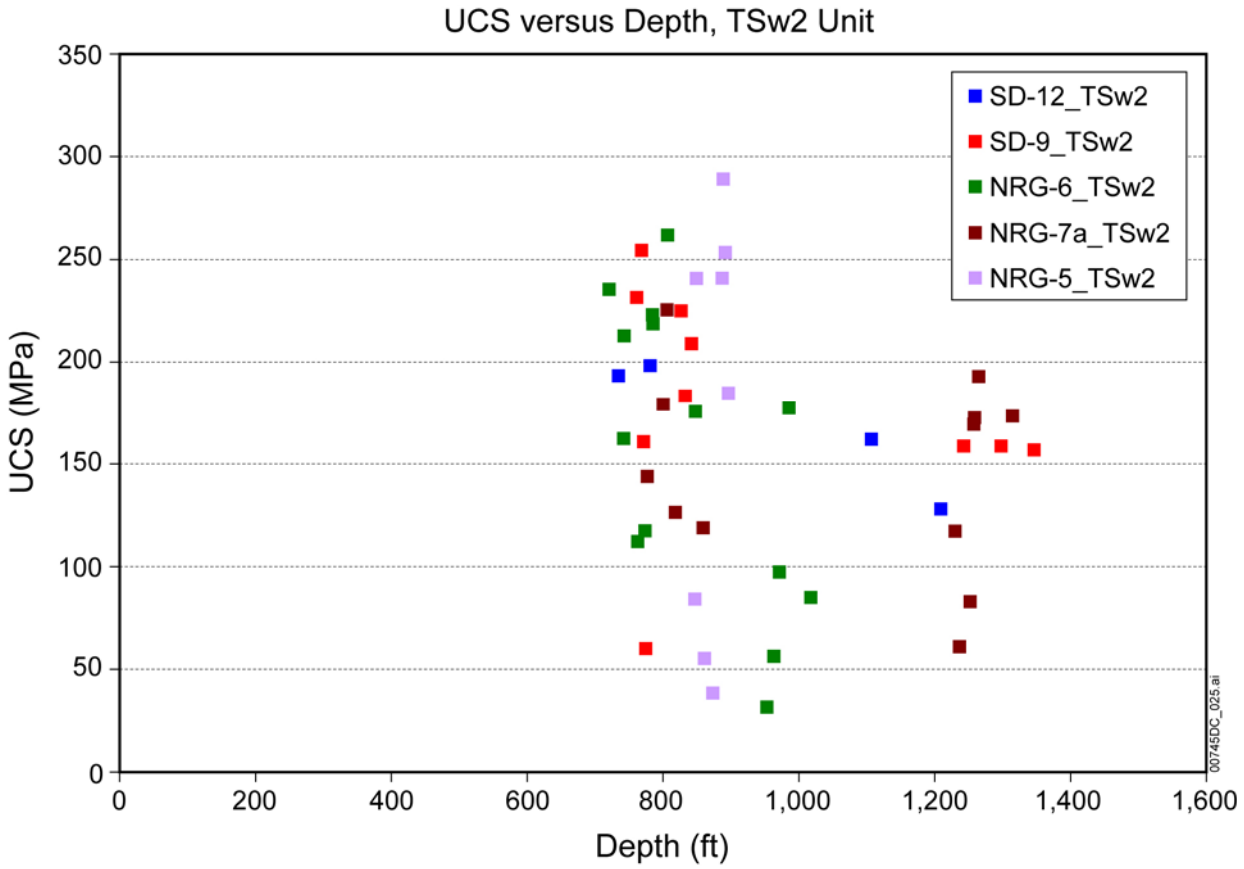

Sources: DTNs: MO0311RCKPRPCS.003 [DIRS 166073]; SNL02030193001.001 [DIRS 120572].

Figure 6-24. UCS versus Depth for SD and NRG Boreholes for TSw2 Unit

Figures 6-25 to 6-28 illustrate UCS from selected SD and NRG boreholes as a function of depth for the four RHH lithostratigraphic zones. Similar lateral continuity is observed among the boreholes of SD-9, NRG-6, NRG-7a, and NRG-5 in the Tptpmn zone (Figure 6-26) and boreholes of SD-9 and SD-12 for the Tptpln zone (Figure 6-27). No distinct lateral continuity of UCS is observed in the Tptpul and Tptpll zones (Figures 6-25 and 6-28).

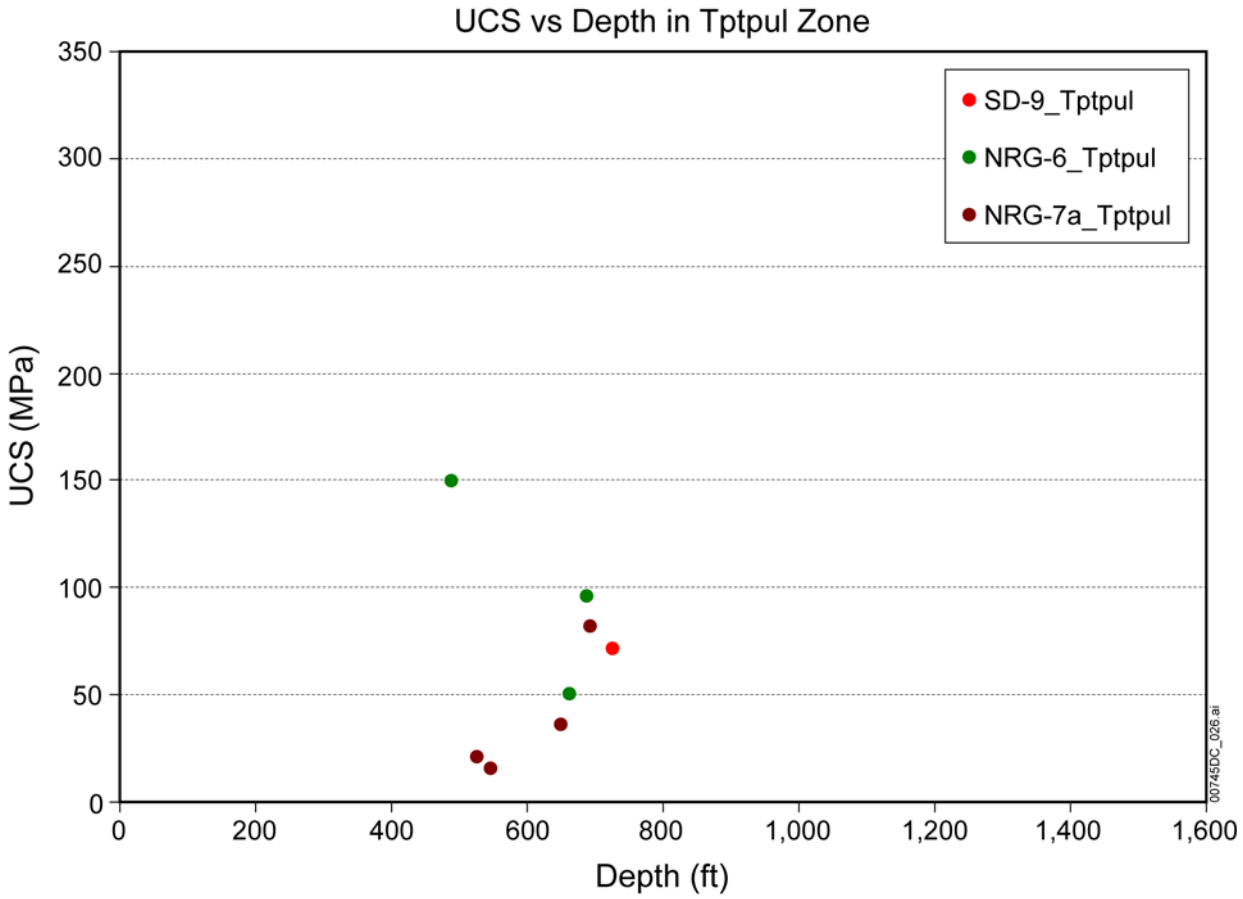

Sources: DTNs: MO0311RCKPRPCS.003 [DIRS 166073]; SNL02030193001.001 [DIRS 120572].

Figure 6-25. UCS versus Depth for SD and NRG Boreholes for Tptpul Zone

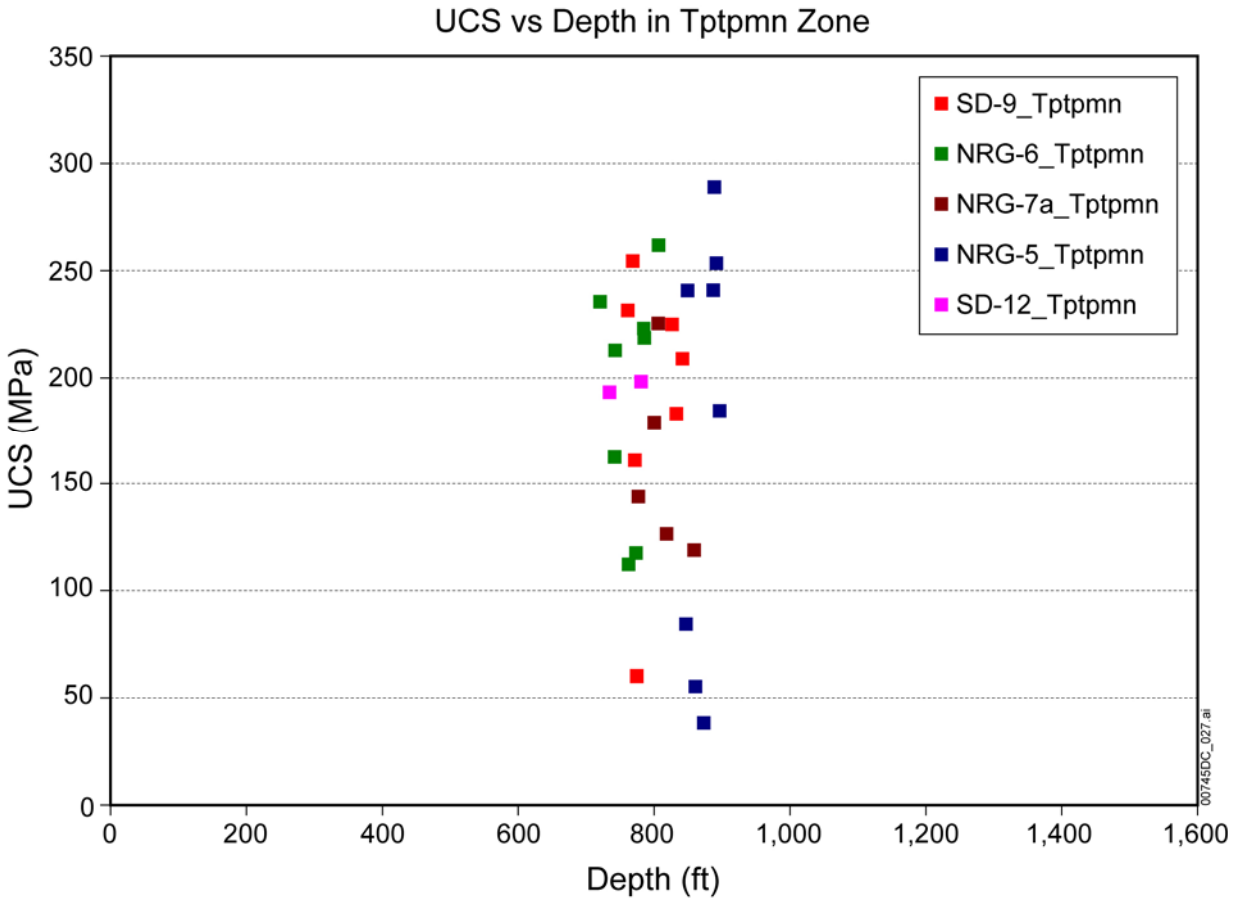

Sources: DTNs: MO0311RCKPRPCS.003 [DIRS 166073]; SNL02030193001.001 [DIRS 120572].

Figure 6-26. UCS versus Depth for SD and NRG Boreholes for Tptpmn Zone

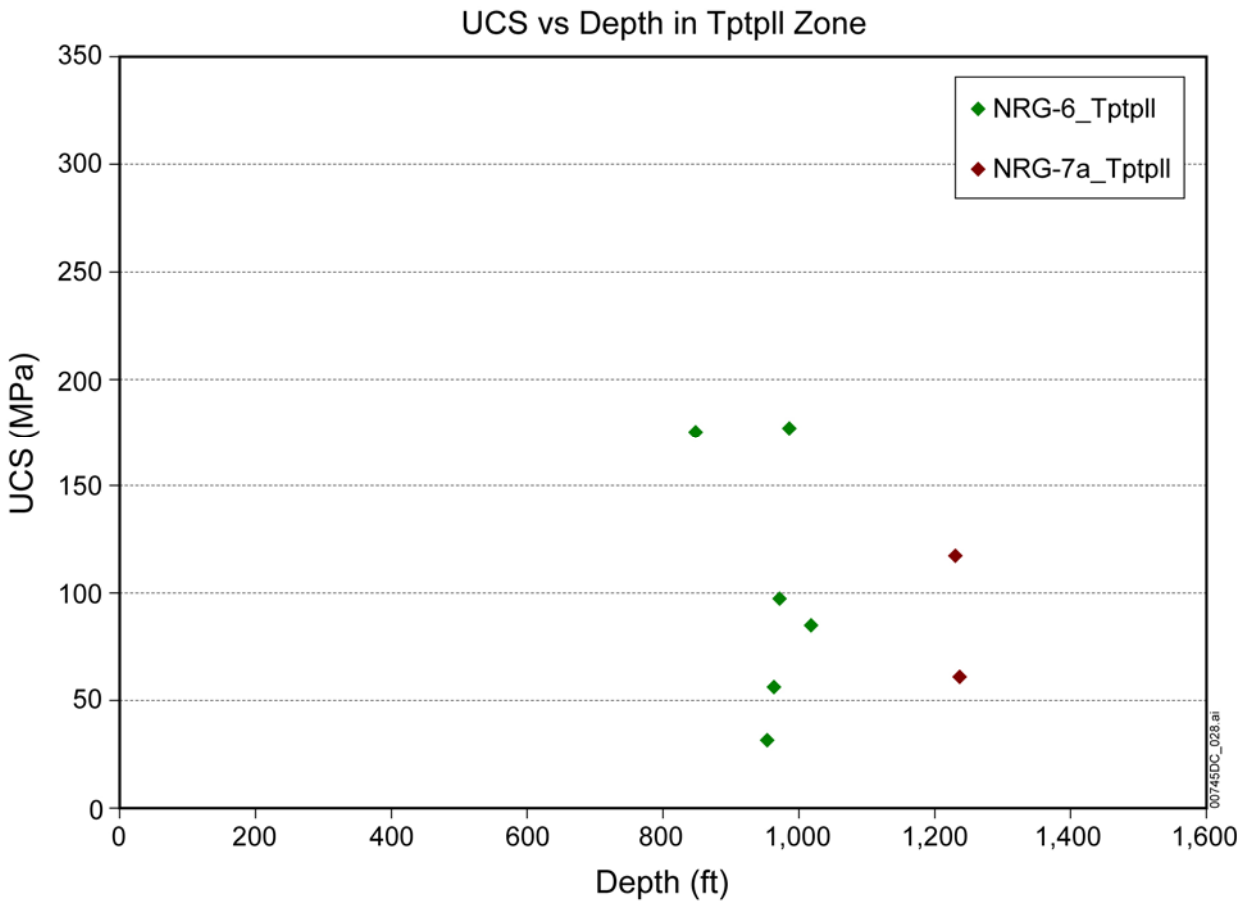

Sources: DTNs: MO0311RCKPRPCS.003 [DIRS 166073]; SNL02030193001.001 [DIRS 120572].

Figure 6-27. UCS versus Depth for SD and NRG Boreholes for Tptpll Zone

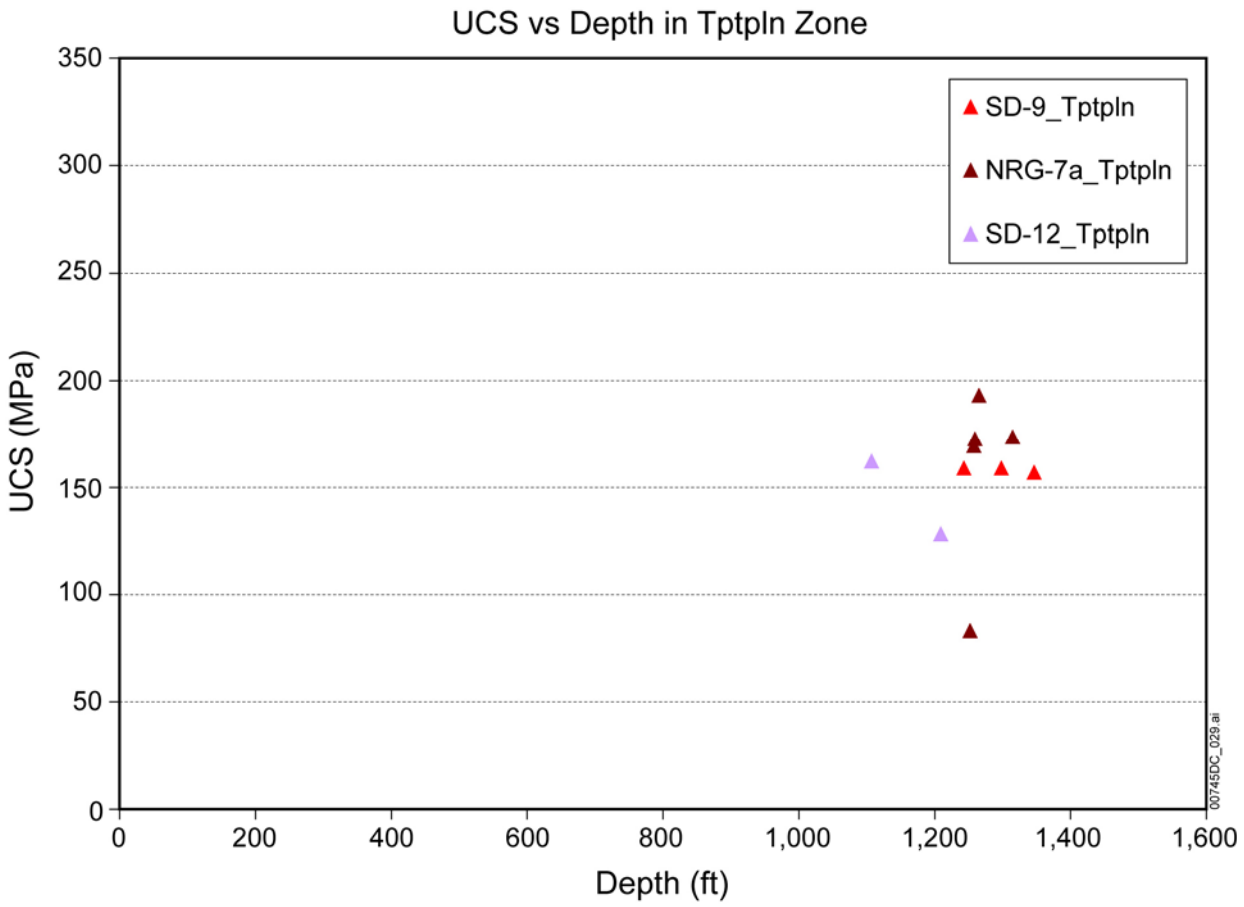

Sources: DTNs: MO0311RCKPRPCS.003 [DIRS 166073]; SNL02030193001.001 [DIRS 120572].

Figure 6-28. UCS versus Depth for SD and NRG Boreholes for Tptpln Zone

6.4.2.1.2 Triaxial/Confined Compressive Strength

Confined compression testing was performed on a relatively limited number of specimens. The confined compression tests were performed on specimens either 50.8 mm or 25.4 mm in diameter under varying temperature, saturation, and strain rate. A summary of the confined compressive strength test results is shown in Table 6-11. UCS results presented in Table 6-9 are also used in the plots of this section to enhance the plot of the Mohr-Coulomb failure envelope.

Table 6-11. Summary of Confined Compressive Strength Test Results

TM Unit	Lithostrati-graphic Zone	Testing Group[a]	Number of Tests	Compressive Strength (MPa)[b, c]			
				Mean	Standard Deviation	Min.	Max.
TCw	Tpcpul	221233	1	170.30	NA	170.30	170.30
		221234	1	227.60	NA	227.60	227.60
		221334	1	253.80	NA	253.80	253.80
	Tpcpmn	131222	4	227.38	68.25	158.20	295.90
		131223	4	327.35	34.01	291.40	369.00
		221233	1	206.90	NA	206.90	206.90

Table 6-11. Summary of Confined Compressive Strength Test Results (Continued)

TM Unit	Lithostrati-graphic Zone	Testing Group[a]	Number of Tests	Compressive Strength (MPa)[b, c]			
				Mean	Standard Deviation	Min.	Max.
TCw	Tpcpmn	221234	2	333.05	141.35	233.10	433.00
		231222	2	319.25	99.35	249.00	389.50
		231223	1	245.50	NA	245.50	245.50
	Tpcpll	131222	4	372.65	43.77	307.10	396.80
		131223	4	408.75	44.61	343.40	439.70
		231222	1	125.30	NA	125.30	125.30
		231223	1	157.90	NA	157.90	157.90
	Tpcpln	221233	1	406.00	NA	406.00	406.00
		221234	1	895.00	NA	895.00	895.00
		222234	1	125.70	NA	125.70	125.70
		231222	3	260.53	100.43	144.70	323.30
		231223	4	290.98	143.00	152.20	418.20
PTn	Tpcpv2	231223	1	71.40	NA	71.40	71.40
	Tpbt3	231222	1	13.30	NA	13.30	13.30
	Tpp	231223	1	17.30	NA	17.30	17.30
TSw1	Tptrn	131222	13	86.40	32.06	39.60	163.90
		131223	11	132.61	50.42	30.10	208.30
		231222	8	92.39	15.56	70.50	116.10
		231223	8	117.63	50.62	60.40	228.50
	Tptrl	231222	1	67.10	NA	67.10	67.10
	Tptpul	231222	2	94.40	24.75	76.90	111.90
		231223	1	227.90	NA	227.90	227.90
TSw2	Tptpmn	131222	6	220.30	81.58	92.00	322.30
		131223	6	325.90	48.54	235.50	370.00
		211222	3	196.40	32.99	160.40	225.20
		211223	3	235.10	68.81	192.80	314.50
		212223	3	196.33	64.53	122.00	238.00
		222234	1	153.70	NA	153.70	153.70
		231222	5	227.78	67.95	174.00	335.70
		231223	14	169.00	55.61	49.70	282.80
		231224	5	214.54	39.73	176.30	272.40
		232212	6	253.55	49.09	207.30	339.20
		232213	5	253.86	50.36	205.80	329.40
		232222	3	121.10	59.27	52.90	160.20
	Tptpll	131222	3	138.83	76.32	77.50	224.30
		131223	3	164.43	80.94	107.00	257.00
		231223	1	216.90	NA	216.90	216.90
	Tptpln	221233	1	422.00	NA	422.00	422.00
		221234	1	638.00	NA	638.00	638.00
		231222	3	216.43	64.00	152.60	280.60
		231223	3	265.60	21.65	246.10	288.90
		232213	1	274.50	NA	274.50	274.50

Table 6-11. Summary of Confined Compressive Strength Test Results (Continued)

TM Unit	Lithostrati-graphic Zone	Testing Group[a]	Number of Tests	Compressive Strength (MPa)[b, c]			
				Mean	Standard Deviation	Min.	Max.
TSw3	Tptpv3	131223	4	55.00	19.03	37.00	78.00
		231222	1	52.20	NA	52.20	52.20
		231223	1	80.00	NA	80.00	80.00
CHn	Tptpv1	131222	2	28.00	8.49	22.00	34.00
		131223	2	34.00	11.31	26.00	42.00
	Tac	121223	2	69.45	2.62	67.60	71.30
		131223	8	37.71	4.91	28.90	45.70
		131224	6	50.88	7.62	37.10	56.20
		221234	3	74.87	24.93	46.10	90.30

Sources: DTNs: MO0311RCKPRPCS.003 [DIRS 166073]; SN0208L0207502.001 [DIRS 161871]; SN0211L0207502.002 [DIRS 161872]; SN0302L0207502.003 [DIRS 165014]; SN0305L0207502.004 [DIRS 165013]; SN0306L0207502.008 [DIRS 165015]; SNL02030193001.001 [DIRS 120572].

[a] Testing group designation numbers represent parameter codes in the following order: size, saturation, temperature, L:D ratio, strain rate, and confining pressure as shown on Table 6-3. For example, group category 121212 (Table 6-3) represents the specimen less than 38 mm in diameter, ambient in saturation, room temperature, L:D ratio of 1.8 to 2.2, strain rate smaller than 0.5×10^{-5} per second, and confining pressure of approximately 5 MPa.

[b] Data below Calico Hills formation are not included.

[c] The spreadsheet containing the statistical analysis of confined compressive strength is presented in Appendix H (see *Worksheet_Static Data.xls*).

Max. = maximum; Min. = minimum; NA = not available; TM = thermal-mechanical.

Effects of Pressure: Under the range of anticipated repository conditions (i.e., saturation, temperature, pressure), the welded tuff exhibits brittle rock behavior. Therefore, the effect of confining pressure on strength for the Yucca Mountain Tuff conforms to specific parameters in the Mohr-Coulomb criterion, rock cohesion, and angle of internal friction.

Several studies were conducted to examine the effect of confining pressure on strength (Olsson and Jones 1980 [DIRS 102940]; Price et al. 1982 [DIRS 106603]; Martin et al. 1997 [DIRS 101432]). Olsson and Jones (1980 [DIRS 102940]) tested several samples from five units within Yucca Mountain, with a few specimens tested at elevated confining stresses mostly up to 20 MPa. The cohesions and internal friction angles calculated from the data (tests were conducted on room-dry samples at ambient temperature and a strain rate of about 10^{-4} s^{-1}) range from 12.1 MPa to 32.2 MPa and 25° to 68°, respectively.

In *Petrologic and Mechanical Properties of Outcrop Samples of the Welded, Devitrified Topopah Spring Member of the Paintbrush Tuff* (Price et al. 1987 [DIRS 100173]), three sets of test data allowed for the calculation of Mohr-Coulomb parameters:

- Dry samples at ambient temperature, a strain rate of 10^{-5} s^{-1}, and confining pressures of 0 MPa to 10 MPa

- Saturated samples tested at ambient temperature, a strain rate of 10^{-5} s^{-1}, and confining pressures of 0 MPa to 10 MPa
- Saturated samples tested at 150°C, a strain rate of 10^{-5} s^{-1}, and confining pressures of 0 MPa to 5 MPa.

The resulting cohesions are 18.8 MPa, 41.7 MPa, and 21.3 MPa, and the angles of internal friction are 57°, 31°, and 50°, respectively. Furthermore, Martin et al. (1997 [DIRS 101432]) tested some drillhole samples from the Tptpmn zone. The experiments were all conducted on saturated samples and at room temperature with confining pressures varying from 0 MPa to 10 MPa. The average strength values at 10 MPa pressure are more than double the strength of similar specimens tested under ambient pressure.

Figure 6-29 is a plot of σ_1 (axial stress or major principal stress) versus σ_3 (confining pressure or minor principal stress) for specimens from the RHH zone tested under baseline conditions (testing category 231221). The plot indicates that the average strength values increase with the increase in confining pressure for the Tptpul, Tptpll, and Tptpln zones; however, no distinct changes are observed for the Tptpmn zone.

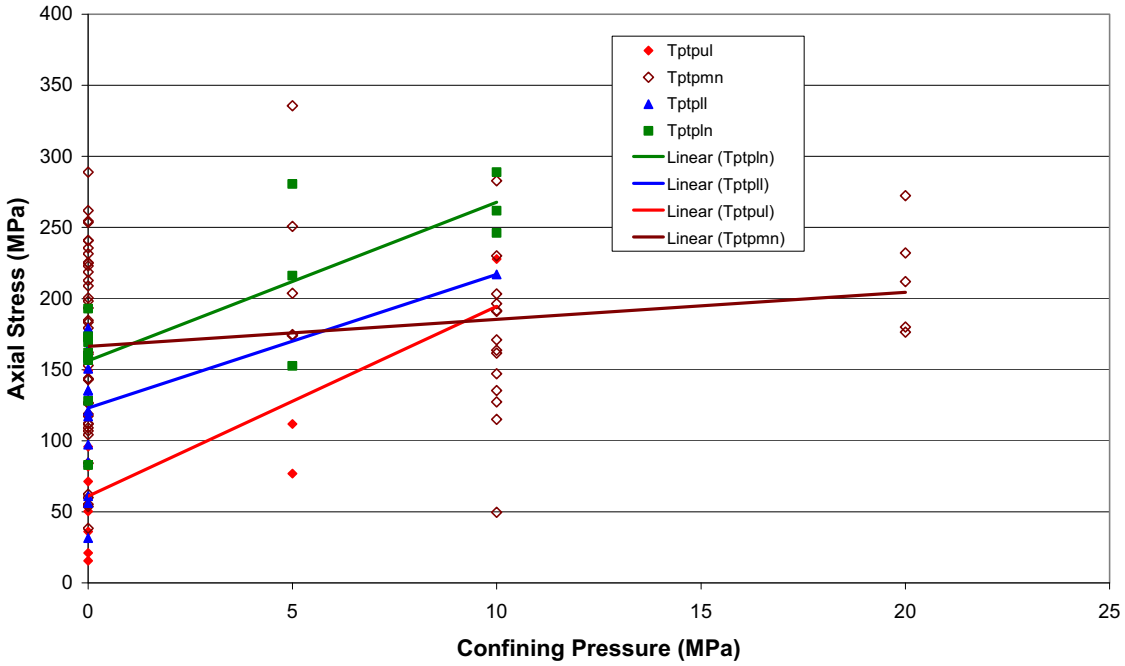

Source: DTN: MO0311RCKPRPCS.003 [DIRS 166073].

Figure 6-29. Axial Stress versus Confining Pressure for the RHH Zones—Base Case

Figure 6-30 is a plot of σ_1 versus σ_3 for specimens from rock units above the RHH zone, tested under baseline conditions, and indicates similar results for all units above the RHH zone.

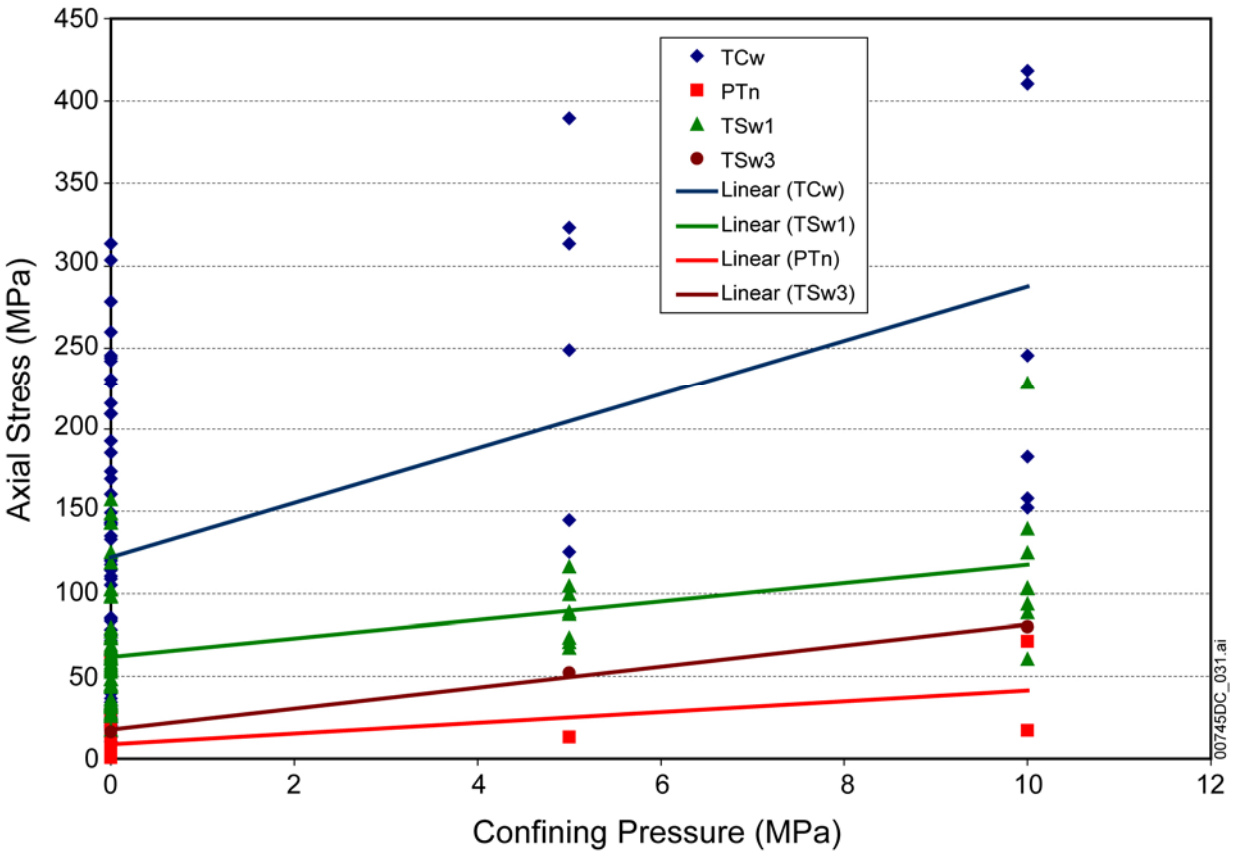

Source: DTN: MO0311RCKPRPCS.003 [DIRS 166073].

Figure 6-30. Axial Stress versus Confining Pressure Plot for Non-RHH Zone at Baseline Testing Conditions

Effects of Saturation: In general, the degree of saturation under the undrained testing condition is expected to have a greater effect on the confined compressive strength than under the drained testing condition. However, the available data do not indicate that saturation has any significant effect on the strength of the specimen. Figure 6-31 plots triaxial compressive strength test results for Tptpmn specimens at various saturation levels.

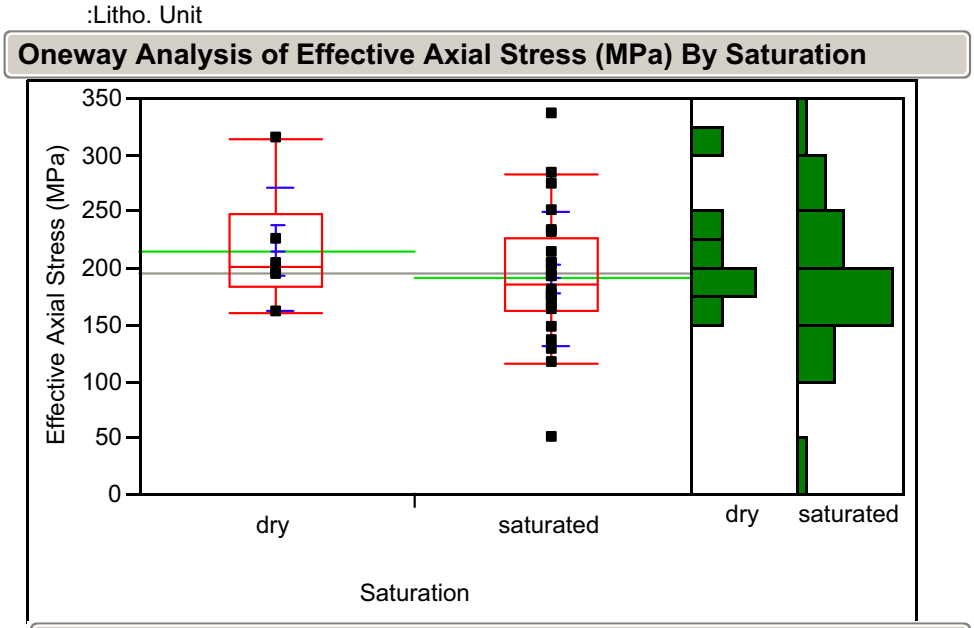

Means and Std Deviations

Level	Number	Mean	Std Dev	Std Err Mean	Lower 99%	Upper 99%
dry	6	215.750	52.7141	21.520	128.98	302.52
saturated	24	190.733	59.4503	12.135	156.67	224.80

Source: DTN: MO0311RCKPRPCS.003 [DIRS 166073].

NOTE: See Table 6-3 for Saturation Category.

Figure 6-31. Compressive Stress Plot for 50.8 mm Dry, Various Level of Saturation, Tptpmn Zone Specimens

Effects of Temperature: Figure 6-32 plots the compressive strength versus temperature for the Tptpmn and Tptpln rock samples tested under triaxial compressive loading conditions and indicates that temperature has little effect on the strength of the specimens. In other words, the temperature effect is well within the range of data expected at ambient conditions. Such a behavior is expected of the Tptpll and Tptpul rock samples too because of close resemblance in terms of matrix materials between nonlithophysal and lithophysal rock units. Furthermore, the temperature range to which the rock surrounding emplacement drifts will be exposed is rather low in comparison with the temperature ranges reportedly used to test rocks for temperature dependency.

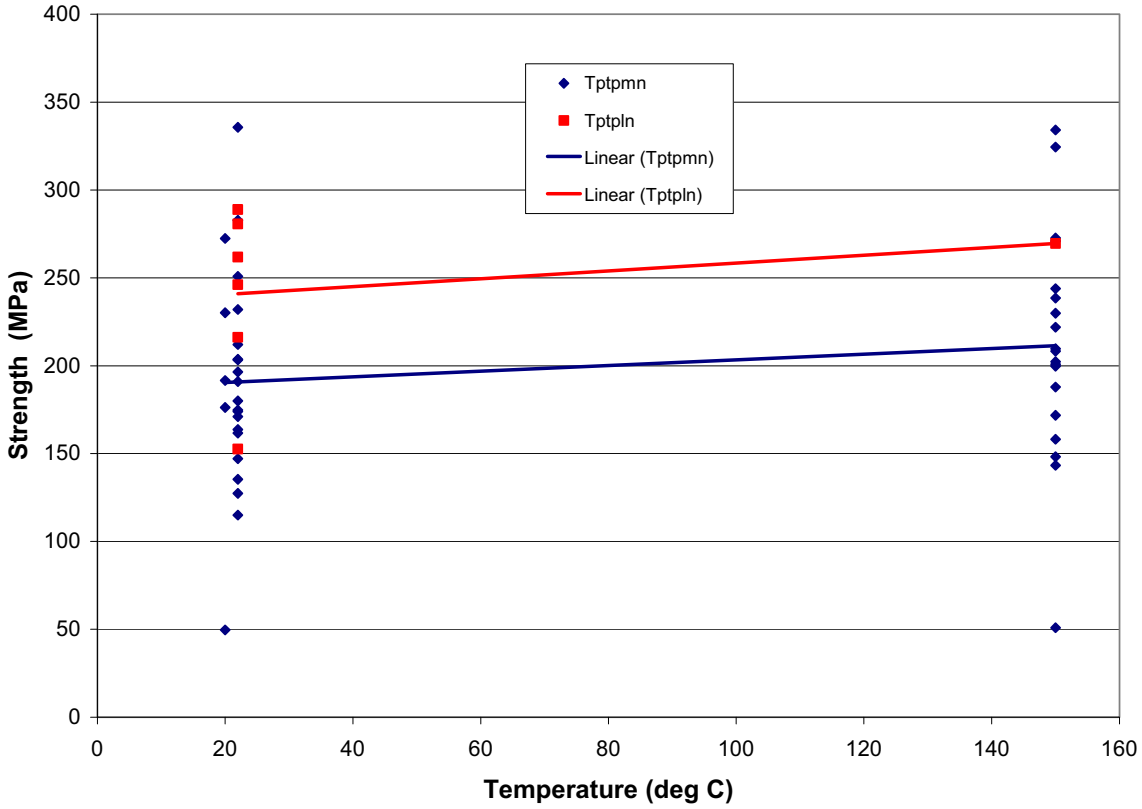

Source: DTN: MO0311RCKPRPCS.003 [DIRS 166073].

Figure 6-32. Confined Compressive Strength versus Temperature for Tptpmn and Tptpln Zones

6.4.2.1.3 Intact Rock Tensile Strength

Indirect tensile strength was obtained using the procedures outlined in ASTM D 3967-86, *Standard Test Method for Splitting Tensile Strength of Intact Rock Core Specimens* [DIRS 161616], and ASTM D 3967-92, *Standard Test Method for Splitting Tensile Strength of Intact Rock Core Specimens* [DIRS 161498], on samples recovered from surface boreholes USW-NRG-6, USW-NRG-7a, and UE-25-NRG#5. The Brazilian test (ASTM D 3967-92) is easier to perform and less expensive than direct-pull tensile testing and is an accepted standard (Mellor and Hawkes 1971 [DIRS 161566]).

Typical samples were 50.8 mm in diameter and 38.6 mm long and were tested at room temperature, saturated, and at a strain rate of 10^{-5} s^{-1}. A summary of results is shown in Table 6-12. Total porosity was determined prior to testing.

The effects of testing conditions on tensile strength were not considered as most samples were tested in category 231121 and a small number were tested in category 221121, in accordance with Table 6-3.

Table 6-12. Summary of Indirect Tensile Strength Results

TM Unit	Lithostratigraphic Zone	Testing Group	Number of Tests	Tensile Strength (MPa)			
				Mean	Standard Deviation	Min.	Max.
UO	Tmr	231121	3	1.23	1.27	0.40	2.70
	Tpki	231121	6	0.70	0.24	0.40	1.00
TCw	Tpcrn	231121	24	7.14	3.52	2.60	13.44
	Tpcpul	231121	23	9.99	1.67	6.23	13.58
	Tpcpmn	231121	16	14.52	3.88	5.30	19.08
	Tpcpll	231121	3	12.20	4.39	7.40	16.00
	Tpcpln	231121	19	10.89	1.73	8.20	13.40
PTn	Tpcpv2	231121	4	3.18	1.91	1.20	5.10
	Tpcpv1	231121	1	0.50	NA	0.50	0.50
	Tpy	231121	1	3.00	NA	3.00	3.00
	Tpbt3	221121	1	0.30	NA	0.30	0.30
	Tpp	221121	1	0.40	NA	0.40	0.40
		231121	12	0.16	0.18	0.02	0.70
	Tpbt2	221121	2	0.25	0.07	0.20	0.30
		231121	3	0.33	0.40	0.10	0.80
TSw1	Tptrn	221121	1	8.40	NA	8.40	8.40
		231121	52	5.43	2.07	1.60	10.50
	Tptrl	231121	7	4.81	1.36	3.40	7.30
	Tptpul	231121	19	5.57	3.10	1.90	12.90
TSw2	Tptpmn	231121	14	10.88	4.02	4.30	16.80
	Tptpll	231121	24	8.33	2.93	3.20	14.30
	Tptpln	231121	13	7.92	2.55	4.80	13.70
TSw3	Tptpv3	231121	3	3.97	0.32	3.60	4.20

Source: DTN: MO0401DQRIRPTS.003 [DIRS 168905], Table S04013_001.

The spreadsheet containing the statistical analysis of indirect Tensile strength is presented in Appendix H (see *Worksheet_Indirect Tensile Strength.xls)*.

Max. = maximum; Min. = minimum; NA = not available; TM = thermal-mechanical.

6.4.2.1.4 Mohr-Coulomb Strength Parameters

The Mohr-Coulomb strength parameters were estimated using the uniaxial and triaxial compressive strength test data. The triaxial data includes sets of confining pressure data paired with the corresponding axial stress at failure. Due to the limited numbers of triaxial test data, all test data of size category 1 and 2 (less than 70 mm, see Table 6-3) were used for estimating the Mohr-Coulomb strength parameters.

The Mohr-Coulomb strength parameters summarized in Table 6-13 are based on intact rock laboratory testing data, and the procedures for estimating the Mohr-Coulomb strength parameters, friction angle (ϕ), and cohesion (c) are documented in *Intact Rock Mechanical Properties of Yucca Mountain Stratigraphic Units* (BSC 2005 [DIRS 176611], Section 6.3.2.3).

Table 6-13. Summary of Friction Angle and Cohesion for Lithostratigraphic Zones

Lithostrati-graphic Zone	Mean Friction Angle (degree)	Friction Range (± 1 Standard Deviation) (degree)	Mean Cohesion (MPa)	Cohesion Range (± 1 Standard Deviation), (MPa)
Tpcpul	42	37-45	15.1	3.0-35.9
Tpcpmn	37	14-46	53.1	55.4-60.1
Tpcpll	58	55-59	35.6	22.5-49.2
Tpcpln[1]	61	47-66	22.8	23.1-25.5
Tptrn	44	39-49	14.4	8.6-17.8
Tptpul[2]	59	54-67	8.4	3.5-7.7
Tptpul[2]	45	18-55	12.6	3.5-26.8
Tptpmn[3]	34	15-42	50.7	49.2-57.3
Tptpll	45	37-52	24.0	14.1-26.8
Tptpln[4]	63	60-65	15.8	11.4-19.7
Tptpv3	36	32-44	5.5	2.5-7.1
Tptpv1	22	11-28	4.5	3.9-5.7
Tac	16	0-26	10.2	9.1-11.2

Sources: DTNs: MO0311RCKPRPCS.003 [DIRS 166073]; SN0208L0207502.001 [DIRS 161871]; SN0211L0207502.002 [DIRS 161872]; SN0302L0207502.003 [DIRS 165014]; SN0305L0207502.004 [DIRS 165013]; SN0306L0207502.008 [DIRS 165015]; SNL02030193001.001 [DIRS 120572].

NOTES: [1] Excluded 2 compressive strength data at confining pressure category 4 for the Tpcpln zone due to the wide spread of compressive strength data (895 and 126 MPa) at this category. The compressive strength of 895 MPa is too high and deemed anomalous.

[2] Estimated values of c and ϕ were used with and without category 3 confining pressure for the Tptpul zone since only one test was conducted.

[3] Excluded the compressive strength data, under category 4 (20 MPa or higher) since there are no significant changes compared to category 3.

[4] Excluded one test data in this confining pressure category due to high compressive strength (greater than 600 MPa).

[5] The worksheet of Mohr-Coulomb Strength analysis is presented in Appendix H (see *Worksheet_ Mohr-Coulomb Parameters.xls*).

6.4.2.2 Elastic Properties

The two elastic constants that are routinely determined from measurements are Young's modulus and Poisson's ratio. These properties are discussed in terms of their variability with changes in the physical characteristics and environmental conditions discussed earlier.

Intact rock elastic properties have been collected from core samples from surface and subsurface drilling efforts since the late 1970s and include data from drilling operations in the ESF and ECRB Cross-Drift. The samples tested range in diameter from 25.4 mm (1 in.) to 290 mm (11.4 in.).

6.4.2.2.1 Young's Modulus

Young's modulus is generally calculated from axial stress and axial strain between 10% and 50% of the ultimate strength. Investigators have utilized various methods of calculating the elastic modulus. The method of calculating Young's modulus is presented in ASTM D 3148-96, *Standard Test Method for Elastic Moduli of Intact Rock Core Specimens in Uniaxial Compression* [DIRS 145397].

Table 6-14 presents the mean and standard deviation of Young's modulus for lithostratigraphic zones tested, without regard for test methods or environmental conditions. It was apparent that Young's modulus for base case testing conditions is summarized in Table 6-15 and illustrated in Figure 6-33. The table and figure indicate that the mean Young's modulus varies significantly between lithostratigraphic zones with a range of 0.2 to 54.7 GPa in the Tpbt4 and Tptf zones, respectively.

Similar to the strength, Young's modulus depends on the degree of welding. Nonwelded tuff is weak and exhibits low Young's moduli (PTn and CHn), as compared to welded tuffs (TCw, TSw1, TSw2, and TSw3). The calculated Young's modulus for UO, TCw, PTn, TSw1, TSw2, TSw3, and CHn are 3.6, 27.3, 2.5, 20.9, 32.7, 25.2, and 5.6 GPa, respectively.

Figure 6-33 illustrates that the Young's moduli in the Topopah Spring tuff (Tptpul, Tptpmn, Tptpll, and Tptpln) are similar to those of the Tiva Canyon Tuff (Tpcpul, Tpcpmn, Tpcpll, and Tpcpln). In general, the upper crystal-rich zones (Tpcrn, Tptrv3, Tptrn, and Tptrl) and vitric zones (Tpcpv1, Tpcpv2, Tptrv3, and Tptpv3) have relatively low Young's moduli ranging from 1 GPa in the Tptrv3 subzone to 25.2 GPa in the Tptpv3 subzone and are generally below 15 GPa. In contrast, the crystal-poor zones in the Tiva Canyon Tuff (Tpcpul, Tpcpmn, Tpcpll, and Tpcpln) and Topopah Spring tuff (Tptpul, Tptpmn, Tptpll, and Tptpln) have higher Young's moduli from 20.4 to 37.8 GPa with most values above 30 GPa. These differences can be attributed to variations in the degree of crystallization (vitric vs. nonvitric). Other contributions to the Young's modulus include fracturing, porosity, and presence of lithophysae.

The mean Young's moduli for the Tptpul, Tptpmn, Tptpll, and Tptpln zones of the RHH zone are 20.4, 32.5, 30.0, and 37.8 GPa, respectively.

Table 6-14. Summary of Static Young's Modulus Test Results

TM Unit	Lithostratigraphic Zone	Testing Group[a]	Number of Tests	Static Young's Modulus (GPa)[b,c]			
				Mean	Standard Deviation	Min.	Max.
UO	Tmr	231221	5	3.36	2.69	0.70	7.20
	Tpki	231221	7	3.77	1.54	0.70	5.10
TCw	Tpcrn	221221	3	23.83	2.09	21.58	25.71
		231221	17	15.16	8.39	6.50	38.20
	Tpcpul	221221	3	26.24	3.84	22.61	30.26
		221321	1	23.16	NA	23.16	23.16
		231221	5	23.72	6.89	14.80	29.60
	Tpcpmn	131222	4	35.08	5.52	27.00	39.40
		131223	4	37.68	1.12	36.80	39.30
		221221	2	35.40	4.24	32.40	38.40
		221321	1	28.88	NA	28.88	28.88
		231221	8	35.81	7.35	20.00	41.40
		231222	2	35.40	10.61	27.90	42.90
		231223	1	27.40	NA	27.40	27.40
	Tpcpll	131221	4	36.93	0.46	36.40	37.40
		131222	4	36.73	0.50	36.30	37.40
		131223	4	37.23	1.25	35.60	38.30
		231221	5	32.82	5.65	24.60	39.00
		231222	1	24.40	NA	24.40	24.40
		231223	1	22.30	NA	22.30	22.30
	Tpcpln	221231	1	57.50	NA	57.50	57.50
		221233	1	43.90	NA	43.90	43.90
		221234	1	58.30	NA	58.30	58.30
		231221	20	33.84	6.05	21.40	40.10
		231222	3	32.73	8.56	23.00	39.10
		231223	4	37.68	14.45	18.80	54.00
PTn	Tpcpv2	231221	4	7.63	5.32	2.10	14.80
		231223	1	24.00	NA	24.00	24.00
	Tpcpv1	231221	4	2.53	1.67	0.30	3.90
	Tpbt4	221221	1	2.90	NA	2.90	2.90
		221231	1	0.41	NA	0.41	0.41
		231221	1	0.20	NA	0.20	0.20
	Tpy	231221	5	5.24	3.05	2.30	9.20
	Tpbt3	221221	2	1.80	0.85	1.20	2.40
		231221	2	1.30	1.56	0.20	2.40
	Tpp	221221	2	1.05	0.35	0.80	1.30
		231221	10	0.98	0.66	0.30	2.10
	Tpbt2	221221	3	0.90	0.53	0.50	1.50
		231221	6	0.67	0.68	0.01	1.70
	Tptrv3	231221	2	0.99	1.29	0.07	1.90
TSw1	Tptrn	131221	10	28.22	9.08	17.60	43.50
		131222	13	19.80	4.77	12.30	28.70

Table 6-14. Summary of Static Young's Modulus Test Results (Continued)

TM Unit	Lithostratigraphic Zone	Testing Group[a]	Number of Tests	Static Young's Modulus (GPa)[b,c]			
				Mean	Standard Deviation	Min.	Max.
TSw1	Tptrn	131223	11	22.58	5.83	8.40	29.40
		221221	5	21.32	5.98	14.80	28.30
		231221	53	20.95	9.66	9.20	59.90
		231222	8	22.36	5.16	14.00	29.00
		231223	8	19.65	8.19	2.00	28.40
	Tptrl	231221	3	9.13	2.38	6.40	10.70
		231222	1	14.40	NA	14.40	14.40
	Tptf	131211	2	42.00	0.14	41.90	42.10
		131221	5	48.84	11.58	38.60	68.30
		231221	1	54.70	NA	54.70	54.70
	Tptpul	221221	2	19.70	1.98	18.30	21.10
		231221	8	20.41	9.16	6.00	33.30
		231222	2	25.10	10.32	17.80	32.40
		231223	1	22.30	NA	22.30	22.30
		312111	3	10.30	3.22	7.30	13.70
		312221	1	6.70	NA	6.70	6.70
		321111	3	15.93	4.15	12.40	20.50
		321211	8	13.10	4.46	5.80	19.50
		321221	1	7.30	NA	7.30	7.30
		331211	4	8.30	4.92	5.00	15.60
		331221	11	14.72	3.89	7.20	21.50
TSw2	Tptpmn	111321	30	24.02	4.13	6.80	27.80
		131211	2	35.55	2.76	33.60	37.50
		131221	30	34.90	5.58	28.10	47.30
		131222	6	37.40	3.85	34.00	43.60
		131223	6	34.23	2.17	32.00	38.00
		131231	3	36.60	2.31	34.00	38.40
		211211	4	37.98	4.48	32.10	42.20
		211221	4	40.55	5.01	33.70	45.70
		211222	3	37.43	3.52	33.70	40.70
		211223	3	35.57	4.53	32.80	40.80
		212211	9	50.72	38.23	33.10	152.40
		212221	2	37.60	0.14	37.50	37.70
		212223	3	36.43	1.59	34.60	37.50
		212231	2	26.10	17.11	14.00	38.20
		221221	16	36.76	3.48	28.90	43.10
		221231	1	40.40	NA	40.40	40.40
		221321	36	32.08	3.74	20.10	37.00
		222234	1	23.90	NA	23.90	23.90
		231211	10	36.35	5.19	26.10	44.50
		231221	41	32.53	6.74	13.40	45.70
		231222	5	35.56	1.40	33.90	37.10

Table 6-14. Summary of Static Young's Modulus Test Results (Continued)

TM Unit	Lithostratigraphic Zone	Testing Group[a]	Number of Tests	Static Young's Modulus (GPa)[b,c]			
				Mean	Standard Deviation	Min.	Max.
TSw2	Tptpmn	231223	13	29.65	4.69	21.40	35.20
		231224	5	28.09	4.80	19.80	31.50
		231231	4	32.53	4.12	26.90	36.80
		232211	11	35.74	4.45	29.60	42.20
		232212	6	30.83	4.57	22.30	35.00
		232213	5	31.50	3.02	27.70	34.60
		232221	4	30.98	2.21	28.00	32.70
		232222	3	28.60	10.96	16.00	35.90
		321221	1	32.40	NA	32.40	32.40
		331221	22	38.26	5.66	25.30	46.00
	Tptpll	121221	16	32.26	2.91	26.00	38.10
		131211	2	27.40	7.64	22.00	32.80
		131221	28	28.20	7.63	2.44	38.10
		131222	3	26.00	8.55	19.20	35.60
		131223	3	24.13	9.39	14.10	32.70
		211221	7	36.09	2.22	32.70	38.40
		212221	6	37.13	1.42	35.30	39.40
		221221	59	34.52	3.75	24.50	41.30
		231221	15	29.97	6.43	16.90	37.60
		231223	1	29.60	NA	29.60	29.60
		312111	2	6.80	0.42	6.50	7.10
		312221	5	28.96	14.08	7.10	40.50
		321211	7	11.81	5.11	5.00	21.00
		321221	25	33.65	8.13	9.60	41.60
		331211	1	5.30	NA	5.30	5.30
		331221	1	10.90	NA	10.90	10.90
		421221	5	31.60	5.43	25.30	37.50
	Tptpln	131211	3	33.00	9.17	22.90	40.80
		131221	10	29.72	7.25	16.60	36.30
		131231	4	32.75	5.02	27.70	37.50
		221221	2	35.05	0.92	34.40	35.70
		221231	1	61.80	NA	61.80	61.80
		221233	1	73.00	NA	73.00	73.00
		221234	1	59.90	NA	59.90	59.90
		231221	10	37.78	4.53	30.40	44.40
		231222	3	34.27	3.00	30.80	36.10
		231223	3	35.50	3.59	32.90	39.60
		232213	1	43.90	NA	43.90	43.90
TSw3	Tptpv3	221221	2	34.25	3.32	31.90	36.60
		231221	1	25.20	NA	25.20	25.20
		231222	1	54.20	NA	54.20	54.20
		231223	1	32.90	NA	32.90	32.90

Table 6-14. Summary of Static Young's Modulus Test Results (Continued)

TM Unit	Lithostratigraphic Zone	Testing Group[a]	Number of Tests	Static Young's Modulus (GPa)[b,c]			
				Mean	Standard Deviation	Min.	Max.
CHn	Tptpv2	131221	2	16.45	0.49	16.10	16.80
		221221	1	16.70	NA	16.70	16.70
	Tptpv1	131211	2	2.26	1.20	1.41	3.10
		131221	5	2.40	0.79	1.53	3.70
		131222	2	3.39	0.41	3.10	3.68
		131223	2	3.75	0.86	3.14	4.35
		131231	3	2.70	0.84	1.76	3.37
	Tpbt1	131211	3	12.17	1.76	11.10	14.20
		131221	4	9.25	2.32	6.30	11.20
		231221	1	3.90	NA	3.90	3.90
	Tac	121221	2	7.31	1.15	6.50	8.12
		121223	2	7.27	0.10	7.20	7.34
		131211	2	7.45	0.59	7.03	7.86
		131221	33	7.07	2.13	3.51	12.80
		131223	8	6.76	1.56	4.28	8.90
		131224	6	7.42	2.13	3.92	9.72
		131231	2	5.43	0.03	5.41	5.45
		221231	2	13.16	1.22	12.29	14.02
		221234	3	8.69	0.81	7.99	9.57
		231221	2	6.50	0.57	6.10	6.90
	Tacbt	131221	8	8	6.92	2.52	12.70

Sources: DTNs: MO0402DQRIRPPR.003 [DIRS 168901]; SN0208L0207502.001 [DIRS 161871]; SN0211L0207502.002 [DIRS 161872]; SN0302L0207502.003 [DIRS 165014]; SN0305L0207502.004 [DIRS 165013]; SN0306L0207502.008 [DIRS 165015]; SN0505L0212303.005 [DIRS 174956]

NOTES: [a] Testing group designation numbers represent parameters in the following order: size, saturation, temperature, L:D ratio, strain rate, and confining pressure as shown on Table 6-3. For example, group category 121212 (Table 6-3) represents a specimen less than 38 mm in diameter, ambient in saturation, at room temperature, with L:D ratio of 1.8 to 2.2, strain rate smaller than 0.5×10^{-5} per second, and confining pressure of approximately 5 MPa.

[b] Data below Calico Hills formation are not included.

[c] The spreadsheet containing the statistical analysis of Young's modulus is presented in Appendix H (see *Worksheet_Static Data.xls*).

Max. = maximum; Min. = minimum; NA = not available; TM = thermal-mechanical.

Table 6-15. Summary of Static Young's Modulus by Thermal-Mechanical and Lithostratigraphic Zone—Base Case

TM Unit	Lithostrati-graphic Zone	Static Young's Modulus (GPa)					Note
		Number of Tests	Mean	Standard Deviation	Min	Max	
UO	Tmr	5	3.36	2.69	0.70	7.20	Rainer Mesa Tuff
	Tpki	7	3.77	1.54	0.70	5.10	Tuff Unit "X"—Informal
	Overall	12	3.60	1.99	0.70	7.20	
TCw	Tpcrn	17	15.16	8.39	6.50	38.20	Crystal-rich, non-lithophysal zone
	Tpcpul	5	23.72	6.89	14.80	29.60	Crystal-poor, Upper lithophysal zone
	Tpcpmn	8	35.81	7.35	20.00	41.40	Crystal-poor, middle non- lithophysal zone
	Tpcpll	5	32.82	5.65	24.60	39.00	Crystal-poor, lower lithophysal zone
	Tpcpln	20	33.84	6.05	21.40	40.10	Crystal-poor, lower non-lithophysal zone
	Overall	55	27.34	11.11	6.50	41.40	
PTn	Tpcpv2	4	7.63	5.32	2.10	14.80	Crystal-poor, vitric zone, Tiva Canyon Tuff
	Tpcpv1	4	2.53	1.67	0.30	3.90	Crystal-poor, vitric zone, Tiva Canyon Tuff
	Tpbt4	1	0.20	NA	0.20	0.20	Crystal-poor, Pre-Tiva Canyon bedded tuff
	Tpy	5	5.24	3.05	2.30	9.20	Crystal-poor, Yucca Mountain Tuff
	Tpbt3	2	1.30	1.56	0.20	2.40	Crystal-poor, Pre-Yucca Mountain tuff
	Tpp	10	0.98	0.66	0.30	2.10	Pah Canyon Tuff
	Tpbt2	6	0.67	0.68	0.01	1.70	Pre-Pah Canyon bedded tuff
	Tptrv3	2	0.99	1.29	0.07	1.90	Crystal-rich, vitric zone, Topopah Spring tuff
	Overall	34	2.51	3.21	0.01	14.80	
TSw1	Tptrn	53	20.95	9.66	9.20	59.90	Crystal-rich, nonlithophysal zone
	Tptrl	3	9.13	2.38	6.40	10.70	Crystal-rich, lithophysal zone
	Tptf	1	54.70	NA	54.70	54.70	
	Tptpul	8	20.41	9.16	6.00	33.30	Crystal-poor, upper lithophysal zone
	Overall	65	20.86	10.46	6.00	59.90	
TSw2	Tptpmn	41	32.53	6.74	13.40	45.70	Crystal-poor, middle non- lithophysal zone
	Tptpll	15	29.97	6.43	16.90	37.60	Crystal-poor, lower lithophysal zone
	Tptpln	10	37.78	4.53	30.40	44.40	Crystal-poor, lower non-lithophysal zone
	Overall	66	32.74	6.74	13.40	45.70	
TSw3	Tptpv3	1	25.20	NA	25.20	25.20	Crystal-poor, vitric zone
CHn	Tpbt1	1	3.90	NA	3.90	3.90	Pre-Tonopah Spring bedded tuff
	Tac	2	6.50	0.57	6.10	6.90	Calico Hill Formation
	Overall	3	5.63	1.55	3.90	6.90	

Sources: DTNs: MO0402DQRIRPPR.003 [DIRS 168901]; SN0208L0207502.001 [DIRS 161871]; SN0211L0207502.002 [DIRS 161872]; SN0302L0207502.003 [DIRS 165014]; SN0305L0207502.004 [DIRS 165013]; SN0306L0207502.008 [DIRS 165015].

The spreadsheet containing the statistical analysis of Young's modulus is presented in Appendix H (see *Worksheet_Static Data.xls*).

Max = maximum; Min = minimum; NA = not available; TM = thermal-mechanical.

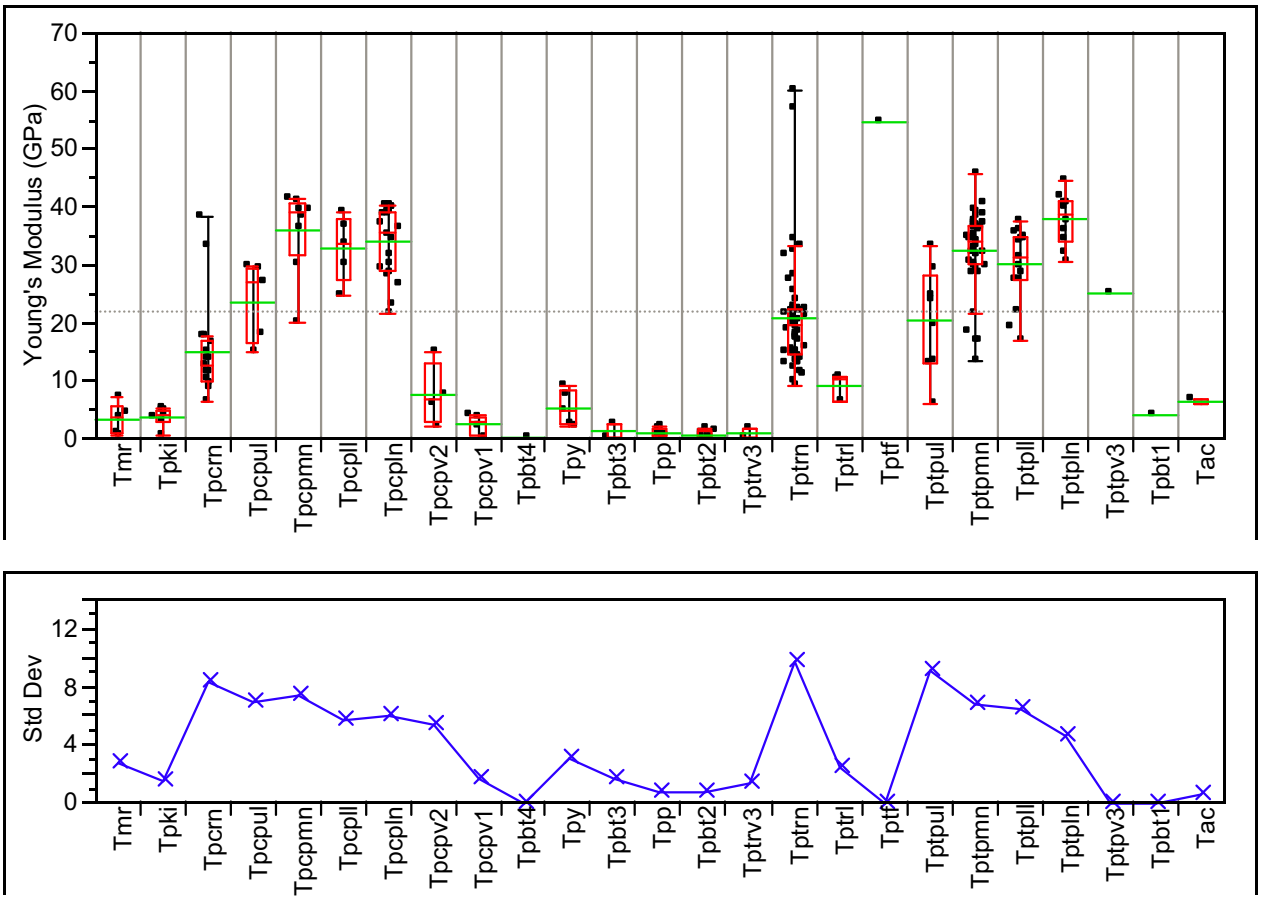

Sources: DTNs: MO0402DQRIRPPR.003 [DIRS 168901]; SN0208L0207502.001 [DIRS 161871]; SN0211L0207502.002 [DIRS 161872]; SN0302L0207502.003 [DIRS 165014]; SN0305L0207502.004 [DIRS 165013]; SN0306L0207502.008 [DIRS 165015].

Legends (in color):

Black: Jittered data point with range bar

Red: Box plot of quartiles include minimum, 25th percentile, median, 75th percentile, and maximum value

Green: Mean value of each zone

Blue: Standard deviation

Figure 6-33. Summary of Static Young's Modulus by Lithostratigraphic Zone for Base Case Testing Conditions

The effects of test conditions on Young's modulus are detailed in *Intact Rock Mechanical Properties of Yucca Mountain Stratigraphic Units* (BSC 2005 [DIRS 176611], Section 6.3.2.2). Table 6-16 summarizes the results of the effect of different laboratory testing conditions on Young's modulus.

Table 6-16. Results of the Effect of Different Laboratory Conditions on Young's Modulus

TM Units	Lithostrati-graphic Zone	Laboratory Test Conditions				
		Size	Saturation	Temperature	Strain Rate	Confining Pressure
TCw	Tpcrn	NA	Decreases with increasing saturation	NA	NA	NA
	Tpcpul	NA	Decreases with increasing saturation	NA	NA	NA
	Tpcpmn	NA	No clear trend with saturation level	NA	NA	NA
	Tpcpll	NA	NA	NA	NA	NA
	Tpcpln	NA	NA	NA	NA	No clear trend with confining pressure
TSw1	Tptrn	NA	No clear trend with saturation level	NA	NA	No clear trend with confining pressure
	Tptpul	Decreases with increasing sample size	No clear trend with saturation level	NA	NA	No clear trend with confining pressure
TSw2	Tptpmn	No clear trend with sample size	Decreases with increasing saturation	Decreases with increasing temperature	Decreases with increasing strain rate	No clear trend with confining pressure
	Tptpll	No clear trend with sample size	Decreases with increasing saturation	NA	NA	NA
	Tptpln	NA	No clear trend with saturation level	NA	NA	No clear trend with confining pressure

NOTES: The relationships indicated in the table are based on qualitative comparison of means.

NA = not analyzed (due to limited number of tests); TM = thermal-mechanical.

Dynamic Young's modulus was measured on specimens of 25 mm or less in diameter, air-dried (ambient) saturation, and at room temperature. Dynamic elastic properties of the rock samples were computed from the measured wave velocities and estimated bulk densities with the assumption that the sample is isotropic (Assumption 5.1.3).

A summary of the dynamic Young's moduli from dynamic testing by group category is presented in Table 6-17. The dynamic Young's modulus values are typically higher in most of the lithostratigraphic zones with the exception of the TCw unit. The dynamic elastic data are presented in this document for comparison purposes. Therefore, no further statistical analysis for the dynamic elastic data are performed.

Table 6-17. Summary of Dynamic Young's Modulus Test Results

TM Unit	Litho-stratigraphic Zone	Testing Group[a]	Number of Tests	Dynamic Young's Modulus (GPa)[b]			
				Mean	Standard Deviation	Min.	Max.
TCw	Tpcrn	2212N1	4	20.94	1.92	18.62	22.75
		2213N1	2	18.42	0.69	17.93	18.9
		6 (All Tpcrn)		20.1	2.00	17.93	22.75
	Tpcpul	2212N1	10	22.05	2.28	16.62	25.65
		2213N1	4	24.32	1.02	23.3	25.72
		14 (All Tpcpul)		22.7	2.23	16.62	25.72
	Tpcpmn	1213N1	1	35.7	NA	35.7	35.7
		2212N1	10	31.65	5.31	19.51	37.16
		2213N1	8	33.34	3.39	29.85	39.1
		19 (All Tpcpmn)		32.6	4.46	19.51	39.1
	Tpcpll	1213N1	4	33.55	11.73	22	44.2
		1213N2	5	41.1	7.41	32.1	47.3
		9 (All Tpcpll)		37.74	9.74	22	47.3
	Tpcpln	1213N1	6	42.05	2.68	38.5	43.9
		1213N2	9	43.29	2.95	39.3	46.6
		15 (All Tpcpln)		42.79	2.81	38.5	46.6
	63 (All TCw)			32.37	9.35	16.62	47.3
PTn	Tpcpv1	1213N1	1	6.8	NA	6.8	6.8
	Tpbt4	1213N1	4	2.96	0.19	2.79	3.13
		1213N2	6	3.27	0.33	2.91	3.67
		10 (All Tpbt4)		3.147	0.32	2.79	3.67
	Tpy	1213N1	2	5.98	0.03	5.96	6
		1213N2	3	6.29	0.08	6.21	6.37
		5 (All Tpy)		6.17	0.18	5.96	6.37
	Tpbt3	1213N1	2	6.35	0.02	6.33	6.36
		1213N2	3	7.98	0.59	7.33	8.49
		5 (All Tpbt3)		7.33	0.99	6.33	8.49
	Tpbt2	1211N1	2	2.27	0.01	2.26	2.28
		1211N2	3	3.12	0.45	2.67	3.56
		1213N1	2	3.69	0	3.69	3.69
		1213N2	3	3.87	0.06	3.82	3.93
		10 (All Tpbt2)		3.29	0.66	2.26	3.93
	31 (All PTn)			4.47	1.83	2.26	8.49
TSw1	Tptrn	1212N1	2	24.15	0.07	24.1	24.2
		1212N2	3	28.77	1.56	27.1	30.2
		1213N1	8	21.45	2.85	17.3	24.8
		1213N2	12	24.54	2.22	21	28.9
		2213N1	4	11.03	0.62	10.5	11.9
		29 (All Tptrn)		22.23	5.42	10.5	30.2
	Tptpul	1211N1	2	27.1	0.14	27	27.2
		1211N2	3	28.43	0.55	27.9	29
		1212N1	4	37.68	2.03	35.6	39.7

Table 6-17. Summary of Dynamic Young's Modulus Test Results (Continued)

TM Unit	Litho-stratigraphic Zone	Testing Group[a]	Number of Tests	Dynamic Young's Modulus (GPa)[b]			
				Mean	Standard Deviation	Min.	Max.
TSw1	Tptpul	1212N2	6	39.98	1.70	37.2	42
		1213N1	6	25.77	4.96	20.8	31.9
		1213N2	9	28.36	5.93	21.9	37.1
		30 (All Tptpul)		31.33	6.87	20.8	42
	59 (All TSw1)			26.86	7.67	10.5	42
TSw2	Tptpmn	1111N1	2	47.31	4.09	44.42	50.2
		1213N1	12	38.76	2.12	35.8	42.4
		1213N2	6	42.07	1.79	40.1	44.1
		1312N1	30	39.35	1.55	36.2	42.6
		1313N1	8	38.14	2.25	35.7	40.6
		2112N1	5	42.86	1.47	40.83	44.25
		2213N1	5	38.34	0.11	38.2	38.5
		2312N1	6	42.89	2.54	38.52	45.34
		2313N1	5	36.14	0.11	36	36.3
		79 (All Tptpmn)		39.77	2.76	35.7	50.2
	Tptpll	1211N1	2	33.6	0	33.6	33.6
		1211N2	3	35.63	0.70	34.9	36.3
		1212N1	2	34.5	0.14	34.4	34.6
		1212N2	3	37.53	1.12	36.3	38.5
		1213N1	6	33.03	3.30	28.7	35.7
		1213N2	9	34.66	3.87	29.1	38
		25 (All Tptpll)		34.63	3.05	28.7	38.5
	Tptpln	1213N1	8	41.08	0.84	39.9	42.2
		1213N2	12	42.02	0.76	40.8	43.3
		20 (All Tptpln)		41.64	0.90	39.9	43.3
	124 (All TSw2)			39.04	3.49	28.7	50.2
TSw3	Tptpv3	1213N1	2	53.6	0.42	53.3	53.9
		1213N2	3	57.83	0.31	57.5	58.1
	5 (All Tptpv3 and TSw3)			56.14	2.34	53.3	58.1
CHn	Tptpv1	1211N1	2	18.95	0.07	18.9	19
		1211N2	3	20.23	0.60	19.6	20.8
		5 (All Tptpv1)		19.72	0.82	18.9	20.8
	Tac	1211N1	2	14.55	0.07	14.5	14.6
		1211N2	3	18.27	1.62	16.8	20
		1212N1	4	14.78	0.33	14.4	15.1
		1212N2	6	16.5	1.07	15.1	18
		1213N1	8	14.19	3.57	11.2	19.4
		1213N2	12	15.59	3.34	12.3	20.9
		2213N1	3	15.8	0	15.8	15.8
		38 (All Tac)		15.53	2.70	11.2	20.9
	Tacbt	1213N1	2	18.9	0.28	18.7	19.1

Table 6-17. Summary of Dynamic Young's Modulus Test Results (Continued)

TM Unit	Litho-stratigraphic Zone	Testing Group[a]	Number of Tests	Dynamic Young's Modulus (GPa)[b]			
				Mean	Standard Deviation	Min.	Max.
CHn	Tacbt	1213N2	3	21.37	0.65	20.7	22
		5 (All Tacbt)		20.38	1.43	18.7	22
	48 (All CHn)			16.47	3.07	11.2	22

Source: DTN: MO0402DQRIRPPR.003 [DIRS 168901].

NOTES: [a] Testing group displays in following order: size (diameter), saturation, temperature, L/D ratio, strain rate and confining pressure as shown on Table 6-3.

[b] The spreadsheet containing the statistical analysis of dynamic Young's modulus is presented in Appendix H (see *Worksheet_Dynamic Data.xls*).

Max. = maximum; Min. = minimum; N (in the testing group) = not available; TM = thermal-mechanical.

6.4.2.2.2 Poisson's Ratio

Poisson's ratio was determined using linear-variable differential transformers (LVDTs) to physically measure the lateral displacement of the specimen or by measuring a change in volume of the fluid in the triaxial cell of a confined compression experiment.

Table 6-18 presents the mean and standard deviation of the Poisson's ratio for lithostratigraphic zones tested under all different testing or environmental conditions. The magnitude of Poisson's ratio depends on physical and environmental conditions, which are discussed below.

The results of static Poisson's ratio tests for base case testing conditions are summarized in Table 6-19 and illustrated in Figure 6-34. The table and figure show that the Poisson's ratio values differ among the lithostratigraphic zones. In the PTn unit, the crystal-poor, vitric subzone Tcpcv1 and Tcpcv2 have low Poisson's ratio with a mean of 0.10. However, the crystal-poor vitric subzone Tptpv3 has a higher Poisson's ratio of 0.39.

The mean Poisson's ratio for the Tptpul, Tptpmn, Tptpll, and Tptpln zones of the RHH zone are 0.25, 0.19, 0.22, and 0.22, respectively.

Table 6-18. Summary of Static Poisson's Ratio Test Results

TM Unit	Litho-stratigraphic Zone	Testing Group[a]	Number of Tests	Static Poisson's Ratio[b]			
				Mean[b]	Standard Deviation	Min.	Max.
UO	Tmr	231221	5	0.03	0.03	0.01	0.07
	Tpki	231221	7	0.19	0.14	0.05	0.48
TCw	Tpcrn	221221	3	0.16	0.02	0.15	0.18
		231221	17	0.20	0.03	0.15	0.29
	Tpcpul	221221	3	0.17	0.02	0.15	0.19
		221321	1	0.15	NA	0.15	0.15
		231221	5	0.19	0.02	0.15	0.2
	Tpcpmn	131222	4	0.24	0.04	0.2	0.29
		131223	4	0.20	0.01	0.19	0.21
		221221	2	0.18	0.00	0.18	0.18
		221321	1	0.17	NA	0.17	0.17
		231221	7	0.20	0.02	0.17	0.22
		231222	2	0.16	0.04	0.13	0.19
		231223	1	0.12	NA	0.12	0.12
	Tpcpll	131221	4	0.21	0.01	0.2	0.22
		131222	4	0.21	0.01	0.2	0.22
		131223	4	0.21	0.01	0.2	0.23
		231221	5	0.24	0.04	0.22	0.32
		231222	1	0.07	NA	0.07	0.07
		231223	1	0.10	NA	0.1	0.1
	Tpcpln	221231	1	0.31	NA	0.31	0.31
		221233	1	0.30	NA	0.3	0.3
		221234	1	0.22	NA	0.22	0.22
		231221	20	0.21	0.02	0.17	0.25
		231222	3	0.19	0.03	0.16	0.21
		231223	4	0.22	0.04	0.17	0.26
PTn	Tpcpv2	231221	4	0.10	0.03	0.06	0.13
		231223	1	0.19	NA	0.19	0.19
	Tpcpv1	231221	4	0.10	0.08	0.03	0.21
	Tpbt4	221221	1	0.16	NA	0.16	0.16
		221231	1	0.28	NA	0.28	0.28
		231221	1	0.17	NA	0.17	0.17
	Tpy	231221	5	0.16	0.01	0.15	0.17
	Tpbt3	221221	2	0.17	0.06	0.12	0.21
		231221	1	0.28	NA	0.28	0.28
	Tpp	221221	2	0.29	0.08	0.23	0.34
		231221	9	0.26	0.09	0.09	0.39
	Tpbt2	221221	3	0.25	0.03	0.23	0.29
		231221	6	0.21	0.10	0.13	0.4
	Tptrv3	231221	2	0.23	0.11	0.15	0.3
TSw1	Tptrn	131221	10	0.20	0.05	0.13	0.27
		131222	12	0.21	0.08	0.13	0.45
		131223	11	0.22	0.06	0.15	0.34
		221221	4	0.25	0.04	0.21	0.3
		231221	53	0.25	0.06	0.14	0.43
		231222	8	0.20	0.03	0.14	0.24
		231223	8	0.20	0.08	0.02	0.33
	Tptrl	231221	2	0.30	0.02	0.28	0.31

Table 6-18. Summary of Static Poisson's Ratio Test Results (Continued)

TM Unit	Litho-stratigraphic Zone	Testing Group[a]	Number of Tests	Static Poisson's Ratio[b]			
				Mean[b]	Standard Deviation	Min.	Max.
TSw1	Tptrl	231222	1	0.28	NA	0.28	0.28
	Tptf	131211	2	0.26	0.00	0.26	0.26
		131221	4	0.24	0.05	0.19	0.3
		231221	1	0.34	NA	0.34	0.34
	Tptpul	231221	8	0.25	0.13	0.09	0.46
		231222	2	0.31	0.16	0.19	0.42
		231223	1	0.11	NA	0.11	0.11
		321111	1	0.21	NA	0.21	0.21
		321211	4	0.26	0.13	0.14	0.39
		331211	3	0.17	0.12	0.03	0.25
		331221	10	0.16	0.03	0.13	0.21
TSw2	Tptpmn	131211	2	0.16	0.06	0.11	0.2
		131221	30	0.21	0.03	0.14	0.29
		131222	6	0.21	0.05	0.16	0.3
		131223	6	0.23	0.02	0.19	0.25
		131231	3	0.27	0.02	0.25	0.29
		211211	4	0.17	0.03	0.12	0.2
		211221	4	0.23	0.07	0.18	0.32
		211222	3	0.19	0.02	0.17	0.21
		211223	3	0.20	0.03	0.18	0.24
		212211	9	0.12	0.09	0.04	0.33
		212221	2	0.14	0.02	0.12	0.15
		212223	3	0.14	0.02	0.13	0.16
		212231	2	0.26	0.16	0.15	0.37
		221221	16	0.20	0.04	0.17	0.34
		221231	1	0.22	NA	0.22	0.22
		221321	36	0.18	0.04	0.12	0.39
		222234	1	0.15	NA	0.15	0.15
		231211	9	0.15	0.07	0.01	0.23
		231221	41	0.19	0.04	0.07	0.3
		231222	5	0.21	0.01	0.2	0.21
		231223	13	0.19	0.06	0.11	0.33
		231224	5	0.18	0.03	0.15	0.21
		231231	4	0.20	0.02	0.18	0.23
		232211	11	0.20	005	0.15	0.3
		232212	6	0.21	0.04	0.15	0.26
		232213	5	0.20	0.02	0.17	0.22
		321221	1	0.17	NA	0.17	0.17
		331221	20	0.22	0.03	0.17	0.27
	Tptpll	121221	16	0.17	0.02	0.12	0.20
		131211	2	0.16	0.06	0.11	0.2
		131221	24	0.21	0.06	0.11	0.36
		131222	3	0.25	0.10	0.14	0.32
		131223	3	0.26	0.05	0.21	0.3
		211221	7	0.17	0.01	0.16	0.19
		221221	57	0.19	0.02	0.14	0.23
		231221	15	0.22	0.07	0.11	0.4
		231223	1	0.20	NA	0.20	0.2
		312221	4	0.19	0.11	0.10	0.35
		321211	3	0.25	0.08	0.20	0.34

Table 6-18. Summary of Static Poisson's Ratio Test Results (Continued)

TM Unit	Litho-stratigraphic Zone	Testing Group[a]	Number of Tests	Static Poisson's Ratio[b]			
				Mean[b]	Standard Deviation	Min.	Max.
TSw2	Tptpll	321221	24	0.19	0.04	0.10	0.32
	Tptpln	131211	3	0.24	0.03	0.21	0.27
		131221	10	0.22	0.04	0.18	0.30
		131231	2	0.28	0.04	0.25	0.31
		221221	2	0.22	0.02	0.20	0.23
		221231	1	0.30	NA	0.30	0.30
		221233	1	0.23	NA	0.23	0.23
		221234	1	0.21	NA	0.21	0.21
		231221	10	0.22	0.04	0.14	0.28
		231222	3	0.24	0.03	0.22	0.28
		231223	3	0.23	0.03	0.21	0.26
		232214	1	0.12	NA	0.12	0.12
TSw3	Tptpv3	221221	1	0.18	NA	0.18	0.18
		231221	1	0.39	NA	0.39	0.39
		231222	1	0.17	NA	0.17	0.17
		231223	1	0.17	NA	0.17	0.17
CHn	Tptpv2	131221	2	0.20	0.02	0.18	0.21
		221221	1	0.22	NA	0.22	0.22
	Tptpv1	131211	2	0.17	0.00	0.17	0.17
		131221	5	0.18	0.03	0.14	0.21
		131222	2	0.21	0.01	0.20	0.21
		131223	2	0.30	0.00	0.30	0.30
		131231	3	0.18	0.07	0.12	0.26
	Tpbt1	131211	2	0.11	0.01	0.10	0.11
		131221	4	0.20	0.07	0.10	0.24
		231221	1	0.11	NA	0.11	0.11
	Tac	121221	2	0.30	0.01	0.29	0.31
		121223	2	0.28	0.01	0.27	0.28
		131211	2	0.22	0.01	0.21	0.22
		131221	24	0.16	0.08	0.07	0.36
		131223	6	0.31	0.05	0.22	0.36
		131224	4	0.26	0.13	0.17	0.45
		131231	1	0.33	NA	0.33	0.33
		221231	2	0.17	0.04	0.14	0.20
		221234	3	0.25	0.03	0.22	0.27
		231221	2	0.20	0.16	0.09	0.31
	Tacbt	131221	8	0.25	0.09	0.14	0.37

Sources: DTNs: MO0402DQRIRPPR.003 [DIRS 168901]; SN0208L0207502.001 [DIRS 161871]; SN0211L0207502.002 [DIRS 161872]; SN0302L0207502.003 [DIRS 165014]; SN0305L0207502.004 [DIRS 165013]; SN0306L0207502.008 [DIRS 165015]; SN0505L0212303.005 [DIRS 174956].

[a] Testing group designation numbers represent parameters in the following order: size, saturation, temperature, L:D ratio, strain rate, and confining pressure as shown on Table 6-3. For example, group category 121212 represents a specimen less than 38 mm in diameter, ambient in saturation, at room temperature, with L:D ratio of 1.8 to 2.2, strain rate smaller than $0.5 \times 10{-}5$ s-1, and confining pressure of approximately 5 MPa.

[b] Data below Calico Hills formation are not included.

[c] The spreadsheet containing the statistical analysis of Poisson's ratio is presented in Appendix H (see *Worksheet_Static Data.xls)*.

Max. = maximum; Min. = minimum; NA = not available; TM = thermal-mechanical.

Table 6-19. Summary of Static Poisson's Ratio for Baseline Case Testing Conditions

TM Unit	Litho-stratigraphic Zone	Number of Tests	Mean	Standard Deviation	Min	Max	Note
UO	Tmr	5	0.03	0.03	0.01	0.07	Rainer Mesa Tuff
	Tpki	7	0.19	0.14	0.05	0.48	Tuff Unit "X"—Informal
	Overall	12	0.12	0.13	0.01	0.48	
TCw	Tpcrn	17	0.20	0.03	0.15	0.29	Crystal-rich, non-lithophysal zone
	Tpcpul	5	0.19	0.02	0.15	0.20	Crystal-poor, Upper lithophysal zone
	Tpcpmn	7	0.20	0.02	0.17	0.22	Crystal-poor, middle non- lithophysal zone
	Tpcpll	5	0.24	0.04	0.22	0.32	Crystal-poor, lower lithophysal zone
	Tpcpln	20	0.21	0.02	0.17	0.25	Crystal-poor, lower non-lithophysal zone
	Overall	54	0.21	0.03	0.15	0.32	
PTn	Tpcpv2	4	0.10	0.03	0.06	0.13	Crystal-poor, vitric zone, Tiva Canyon Tuff
	Tpcpv1	4	0.10	0.08	0.03	0.21	Crystal-poor, vitric zone, Tiva Canyon Tuff
	Tpbt4	1	0.17	NA	0.17	0.17	Crystal-poor, Pre-Tiva Canyon bedded tuff
	Tpy	5	0.16	0.01	0.15	0.17	Crystal-poor, Yucca Mountain Tuff
	Tpbt3	1	0.28	NA	0.28	0.28	Crystal-poor, Pre-Yucca Mountain tuff
	Tpp	9	0.26	0.09	0.09	0.39	Pah Canyon Tuff
	Tpbt2	6	0.21	0.10	0.13	0.40	Pre-Pah Canyon bedded tuff
	Tptrv3	2	0.23	0.11	0.15	0.30	Crystal-rich, vitric zone, Topopah Spring tuff
	Overall	32	0.19	0.09	0.03	0.40	
TSw1	Tptrn	53	0.25	0.06	0.14	0.43	Crystal-rich, nonlithophysal zone
	Tptrl	2	0.30	0.02	0.28	0.31	Crystal-rich, lithophysal zone
	Tptf	1	0.34	NA	0.34	0.34	
	Tptpul	8	0.25	0.13	0.09	0.46	Crystal-poor, upper lithophysal zone
	Overall	64	0.25	0.07	0.09	0.46	
TSw2	Tptpmn	41	0.19	0.04	0.07	0.30	Crystal-poor, middle non- lithophysal zone
	Tptpll	15	0.22	0.07	0.11	0.40	Crystal-poor, lower lithophysal zone
	Tptpln	10	0.22	0.04	0.14	0.28	Crystal-poor, lower non-lithophysal zone
	Overall	66	0.20	0.05	0.07	0.40	
TSw3	Tptpv3	1	0.39	NA	0.39	0.39	Crystal-poor, vitric zone
CHn	Tpbt1	1	0.11	NA	0.11	0.11	Pre-Tonopah Spring bedded tuff
	Tac	2	0.20	0.16	0.09	0.31	Calico Hill Formation
	Overall	3	0.17	0.12	0.09	0.31	

Sources: DTNs: MO0402DQRIRPPR.003 [DIRS 168901]; SN0208L0207502.001 [DIRS 161871]; SN0211L0207502.002 [DIRS 161872]; SN0302L0207502.003 [DIRS 165014]; SN0305L0207502.004 [DIRS 165013]; SN0306L0207502.008 [DIRS 165015].

NOTE: The spreadsheet containing the statistical analysis of Poisson's ratio is presented in Appendix H (see *Worksheet_Static Data.xls*).

Max = maximum; Min = minimum; NA = not available; TM = thermal-mechanical.

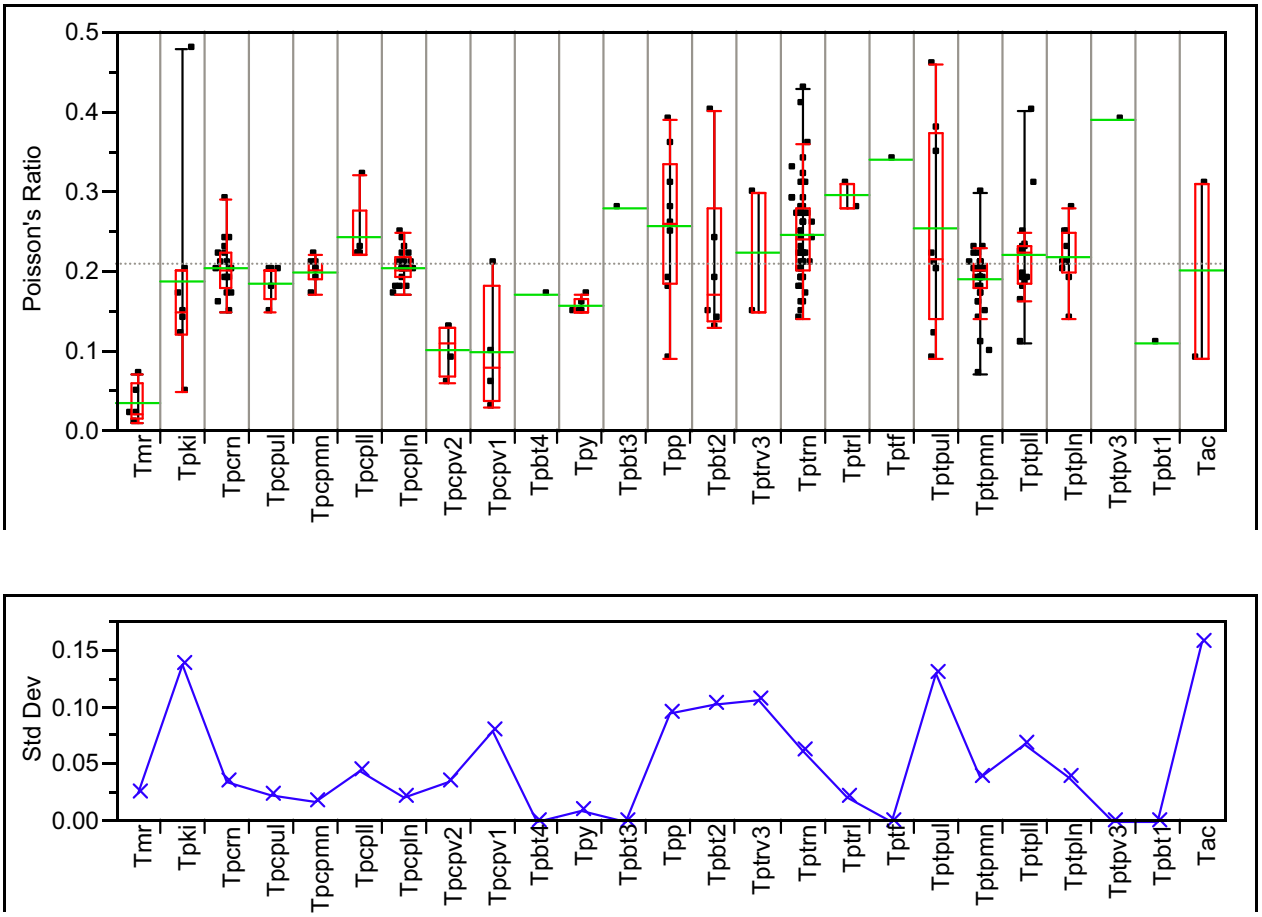

Sources: DTNs: MO0402DQRIRPPR.003 [DIRS 168901]; SN0208L0207502.001 [DIRS 161871]; SN0211L0207502.002 [DIRS 161872]; SN0302L0207502.003 [DIRS 165014]; SN0305L0207502.004 [DIRS 165013]; SN0306L0207502.008 [DIRS 165015].

Legends (in color):

Black: Jittered data point with range bar

Red: Box plot of quartiles include minimum, 25th percentile, median, 75th percentile, and maximum value

Green: Mean value of each zone

Blue: Standard deviation

Figure 6-34. Summary of Static Poisson's Ratio by Lithostratigraphic Zone for Baseline Case Testing Conditions

The effects of test conditions on Poisson's ratio are detailed in *Intact Rock Mechanical Properties of Yucca Mountain Stratigraphic Units* (BSC 2005 [DIRS 176611], Section 6.3.2.2). Table 6-20 summarizes the results of the effect of different laboratory testing conditions on static Poisson's ratio.

Table 6-20. Results of the Effect of Different Laboratory Conditions on Poisson's Ratio

TM Units	Lithostrati-graphic Zone	Laboratory Test Conditions				
		Size	Saturation	Temperature	Strain Rate	Confining Pressure
TCw	Tpcrn	NA	Increases with increasing saturation	NA	NA	NA
	Tpcpul	NA	Increases with increasing saturation	NA	NA	NA
	Tpcpmn	NA	Increases with increasing saturation	NA	NA	NA
	Tpcpll	NA	NA	NA	NA	NA
	Tpcpln	NA	NA	NA	NA	No clear trend with confining pressure
TSw1	Tptrn	NA	No clear trend with saturation level	NA	NA	Decreases with increasing confining pressure
	Tptpul	Decreases with increasing sample size	NA	NA	NA	No clear trend with confining pressure
TSw2	Tptpmn	No clear trend with sample size	Decrease with increasing saturation	NA	Increases with increasing strain rate	No clear trend with confining pressure
	Tptpll	NA	Increases with increasing saturation	NA	NA	NA
	Tptpln	NA	No clear trend with saturation level	NA	NA	No clear trend with confining pressure

NOTE: The relationships indicated in the table are based on a qualitative comparison of means.

NA = not analyzed (due to limited number of tests); TM = thermal-mechanical.

A summary of the dynamic Poisson's ratio from dynamic testing, by testing group, is presented in Table 6-21. As stated earlier (Section 6.4.2.2.1), dynamic elastic properties of the rock samples were computed from the measured wave velocities and estimated bulk densities, with the assumption that the sample is isotropic (Assumption 5.1.3). Most dynamic measurements were conducted on specimens with diameter 25 mm or less, air dried (ambient), and in saturated conditions. Comparing these dynamic elasticity data to static data presented in Table 6-18 (using similar test conditions), the dynamic Poisson's ratio values are generally low with the exception of the TCw unit. The dynamic elastic data are presented in this document for comparison purposes. Therefore, no further statistical analysis for the dynamic elastic data are performed.

Table 6-21. Summary of Dynamic Poisson's Ratio Test Results

TM Unit	Lithostratigraphic Zone	Testing Group[a]	Number of Tests	Dynamic Poisson's Ratio[b]			
				Mean	Standard Deviation	Min.	Max.
TCw	Tpcrn	2212N1	4	0.34	0.02	0.32	0.36
		2213N1	2	0.35	0	0.35	0.35
		6 (All Tpcrn)		0.34	0.01	0.32	0.36
	Tpcpul	2212N1	10	0.33	0.03	0.3	0.38
		2213N1	4	0.28	0.01	0.27	0.3

Table 6-21. Summary of Dynamic Poisson's Ratio Test Results (Continued)

TM Unit	Lithostratigraphic Zone	Testing Group[a]	Number of Tests	Dynamic Poisson's Ratio[b]			
				Mean	Standard Deviation	Min.	Max.
TCw	Tpcpul	14 (All Tpcpul)		0.32	0.03	0.27	0.38
	Tpcpmn	2212N1	10	0.30	0.03	0.27	0.35
		2213N1	4	0.27	0.02	0.24	0.28
		14 (All Tpcpmn)		0.29	0.03	0.24	0.35
	Tpcpll	1213N1	2	0.06	0.02	0.05	0.073
		1213N2	5	0.12	0.03	0.08	0.16
		7 (All Tpcpll)		0.10	0.04	0.05	0.16
	Tpcpln	1213N1	6	0.14	0.01	0.13	0.15
	Tpcpln	1213N2	9	0.15	0.02	0.12	0.17
		15 (All Tpcpln)		0.14	0.02	0.12	0.17
	56 (All TCw)			0.24	0.09	0.05	0.38
PTn	Tpbt4	1213N1	4	0.09	0.07	0.02	0.15
		1213N2	6	0.19	0.04	0.12	0.24
		10 (All Tpbt4)		0.15	0.08	0.02	0.24
	Tpy	1213N1	2	0.15	0.00	0.15	0.15
		1213N2	3	0.20	0.01	0.19	0.20
		5 (All Tpy)		0.18	0.03	0.15	20
	Tpbt3	1213N1	2	0.18	0.00	0.18	0.19
		1213N2	3	0.22	0.02	0.20	0.24
		5 (Tpbt3)		0.21	0.03	0.18	0.24
	Tpbt2	1211N1	2	0.09	0.00	0.09	0.09
		1211N2	3	0.23	0.02	0.21	0.25
		1213N1	2	0.30	0.00	0.30	0.30
		1213N2	3	0.36	0.02	0.35	0.38
		10 (All Tpbt2)		0.26	0.10	0.09	0.38
	30 (All PTn)			0.20	0.09	0.02	0.38
TSw1	Tptrn	1212N1	2	0.14	0.00	0.14	0.14
		1212N2	3	0.19	0.01	0.18	0.19
		1213N1	8	0.18	0.03	0.12	0.21
		1213N2	12	0.18	0.03	0.12	0.21
		25 (All Tptrn)		0.18	0.03	0.12	0.21
	Tptpul	1211N1	2	0.10	0.01	0.09	0.11
		1211N2	3	0.13	0.02	0.11	0.14
		1212N1	4	0.04	0.04	0	0.09
		1212N2	3	0.09	0.02	0.06	0.10
		1213N1	6	0.16	0.04	0.10	0.2
		1213N2	9	0.15	0.05	0.07	0.19
		27 (All Tptpul)		0.12	0.06	0	0.2
	52 (All TSw1)			0.15	0.05	0	0.22
TSw2	Tptpmn	1111N1	3	0.22	0.02	0.21	0.24
		1213N1	4	0.12	0.01	0.11	0.43
		1213N2	6	0.14	0.01	0.13	0.15
		1312N1	30	0.22	0.02	0.18	0.25

Table 6-21. Summary of Dynamic Poisson's Ratio Test Results (Continued)

TM Unit	Lithostratigraphic Zone	Testing Group[a]	Number of Tests	Dynamic Poisson's Ratio[b]			
				Mean	Standard Deviation	Min.	Max.
TSw2	Tptpmn	2112N1	5	0.21	0.01	0.2	0.22
		2312N1	6	0.24	0.02	0.23	0.28
	54 (All Tptpmn)			0.20	0.04	0.11	0.28
	Tptpll	1211N1	2	0.04	0.01	0.03	0.04
		1211N2	3	0.06	0.04	0.01	0.08
		1212N1	2	0.02	0.00	0.02	0.02
		1212N2	3	0.09	0.03	0.06	0.11
		1213N1	6	0.15	0.04	0.11	0.20
		1213N2	9	0.15	0.03	0.12	0.20
		25 (All Tptpll)	0.11	0.06	0.01	0.2	
	Tptpln	1213N1	8	0.14	0.01	0.13	0.16
		1213N2	12	0.15	0.01	0.14	0.17
		20 (All Tptpln)		0.15	0.01	0.13	0.17
	99 (All TSw2)			0.17	0.06	0.01	0.28
TSw3	Tptpv3	1213N1	2	0.19	0.01	0.18	0.2
		1213N2	3	0.15	0.02	0.13	0.16
	5 (All Tptpv3 and TSw3)			0.17	0.02	0.13	0.2
CHn	Tptpv1	1211N1	2	0.07	0.00	0.07	0.07
		1211N2	3	0.02	0.02	0.01	0.04
		5 (All Tptpv1)		0.04	0.03	0.01	0.07
	Tac	1211N1	2	0.14	0.01	0.13	0.14
		1211N2	3	0.18	0.01	0.17	0.2
		1212N1	4	0.15	0.04	0.11	0.19
		1212N2	6	0.15	0.02	0.12	0.18
		1213N1	8	0.12	0.03	0.09	0.18
		1213N2	12	0.14	0.03	0.08	0.17
		35 (All Tac)		0.14	0.03	0.08	0.2
	Tacbt	1213N1	2	0.06	0.03	0.04	0.08
		1213N2	3	0.13	0.02	0.11	0.15
		5 (All Tacbt)		0.10	0.04	0.04	0.15
	45 (All CHn)			0.13	0.05	0.08	0.2

Source: DTN: MO0402DQRIRPPR.003 [DIRS 168901].

NOTES: [a] The group category displays in the following order: size (diameter), saturation, temperature, L:D ratio, strain rate, and confining pressure as shown on Table 6-3.

[b] The spreadsheet containing the statistical analysis of dynamic Poisson's ratio is presented in Appendix H (see *Worksheet_Dynamic Data.xls*).

L/D = length to diameter; Max. = maximum; Min. = minimum; N (in the testing group) = not available; TM = thermal-mechanical.

6.4.2.3 Relationship of Young's Modulus versus UCS

The relationship of Young's modulus to the UCS for the RHH zones is plotted in Figures 6-35 through 6-38. The data show a linear relationship in most cases except for the small core samples tested in dry to ambient saturation for nonlithophysal zones (Tptpmn and Tptpln). Data also show that the large core samples tested under saturated conditions form lower bound strength for the Tptpul and Tptpmn zones.

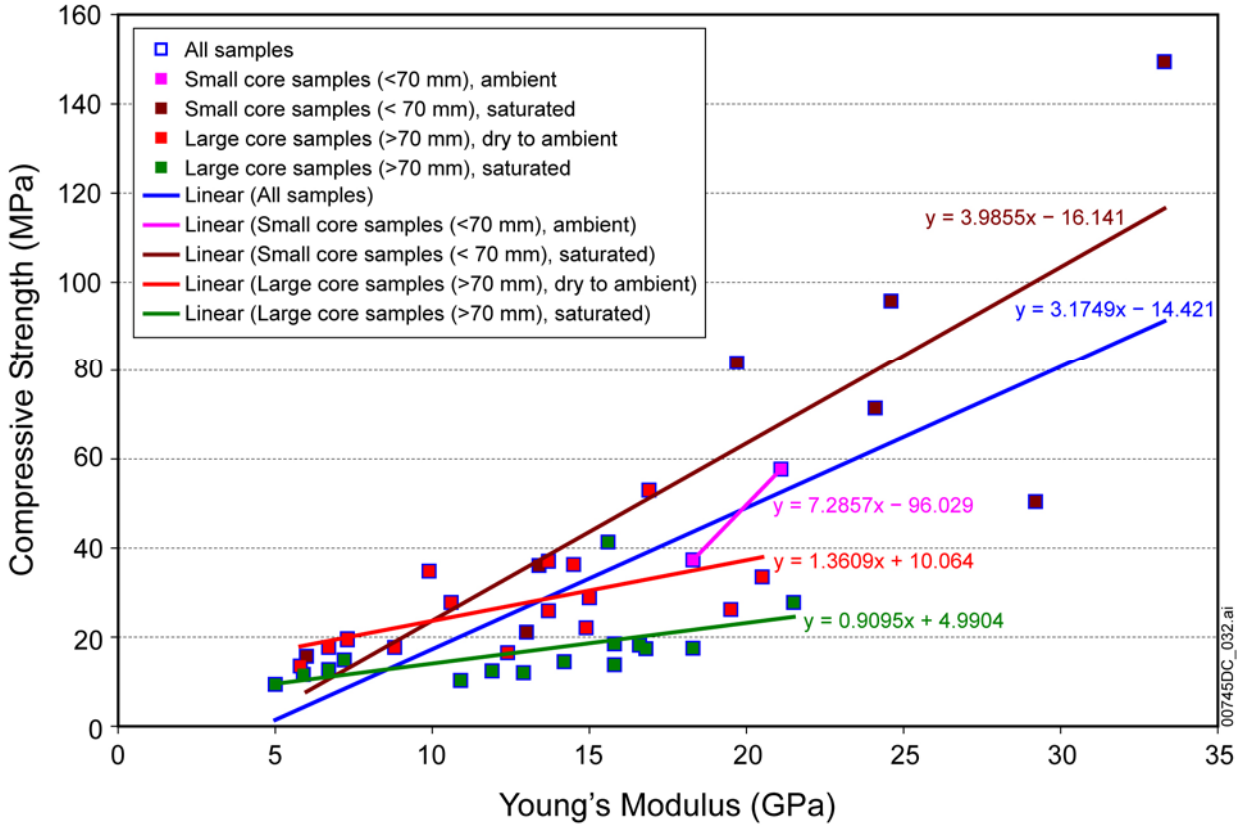

Sources: DTNs: MO0311RCKPRPCS.003 [DIRS 166073]; MO0402DQRIRPPR.003 [DIRS 168901]; SN0208L0207502.001 [DIRS 161871]; SN0211L0207502.002 [DIRS 161872]; SN0302L0207502.003 [DIRS 165014]; SN0305L0207502.004 [DIRS 165013]; SN0306L0207502.008 [DIRS 165015]; SNL02030193001.001 [DIRS 120572].

Figure 6-35. UCS versus Young's Modulus in Tptpul Zone

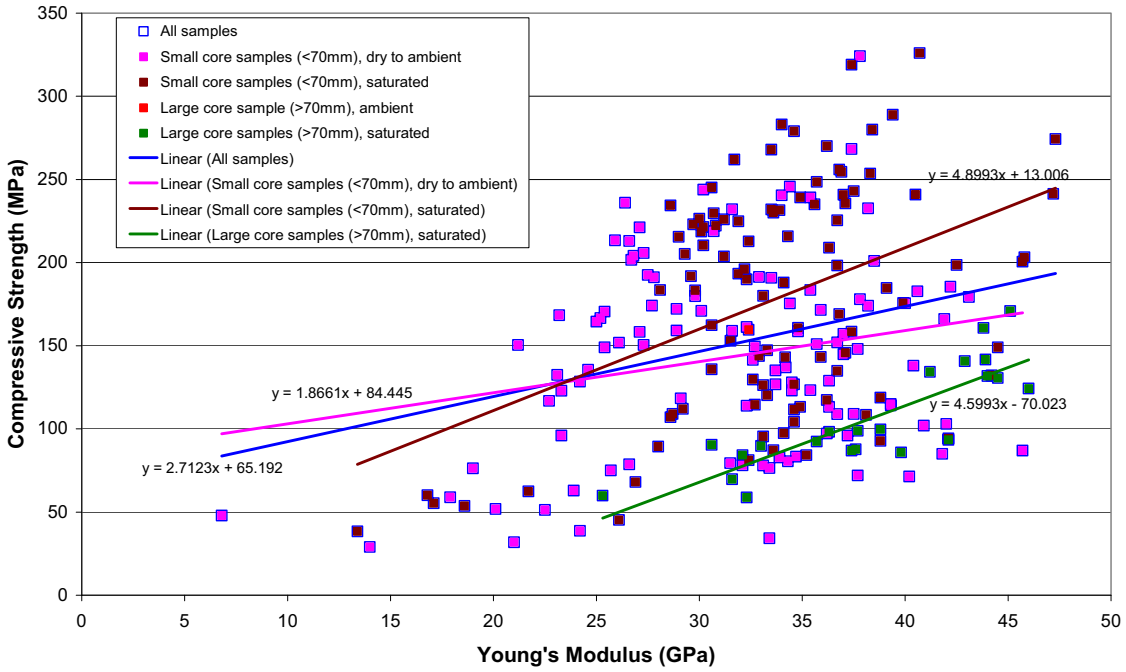

Sources: DTNs: MO0311RCKPRPCS.003 [DIRS 166073]; MO0402DQRIRPPR.003 [DIRS 168901]; SN0208L0207502.001 [DIRS 161871]; SN0211L0207502.002 [DIRS 161872]; SN0302L0207502.003 [DIRS 165014]; SN0305L0207502.004 [DIRS 165013]; SN0306L0207502.008 [DIRS 165015]; SNL02030193001.001 [DIRS 120572].

Figure 6-36. UCS versus Young's Modulus in Tptpmn Zone

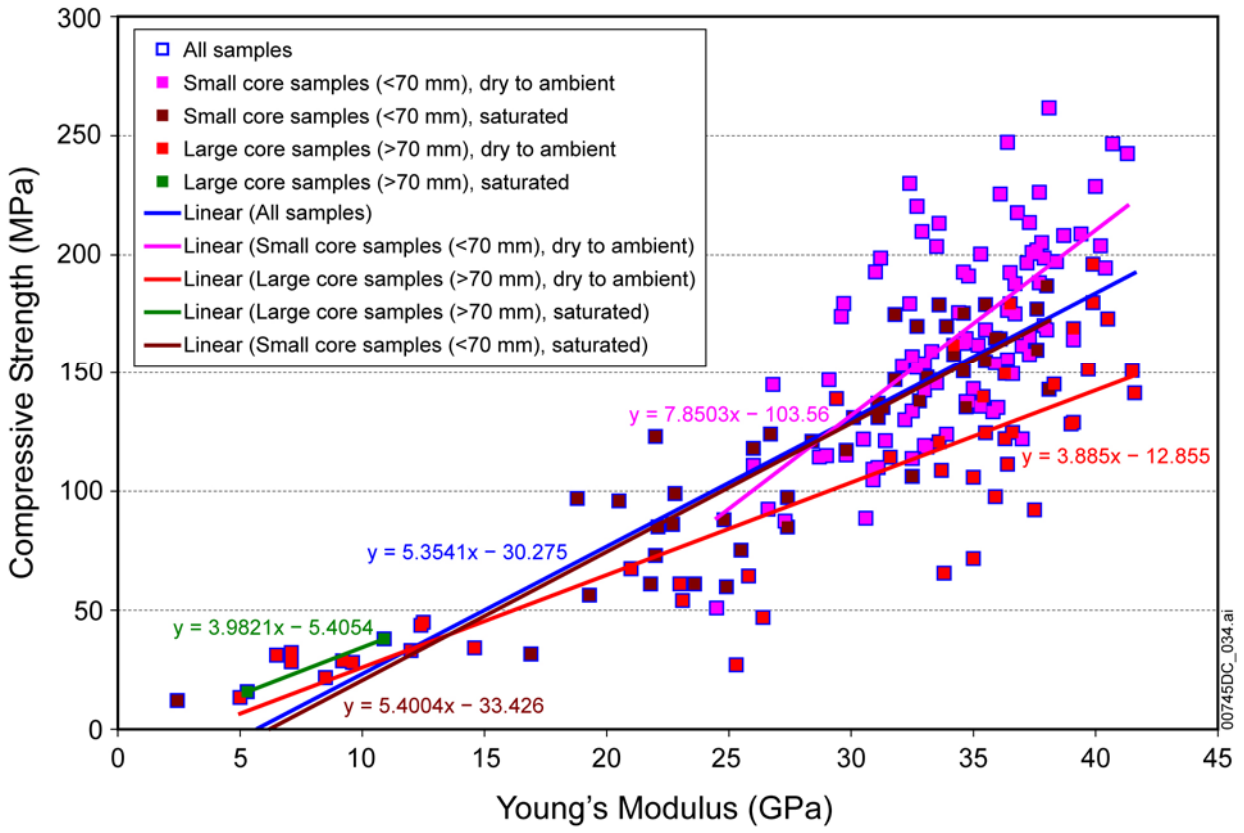

Sources: DTNs: MO0311RCKPRPCS.003 [DIRS 166073]; MO0402DQRIRPPR.003 [DIRS 168901]; SN0208L0207502.001 [DIRS 161871]; SN0211L0207502.002 [DIRS 161872]; SN0302L0207502.003 [DIRS 165014]; SN0305L0207502.004 [DIRS 165013]; SN0306L0207502.008 [DIRS 165015]; SNL02030193001.001 [DIRS 120572].

Figure 6-37. UCS versus Young's Modulus in Tptpll Zone

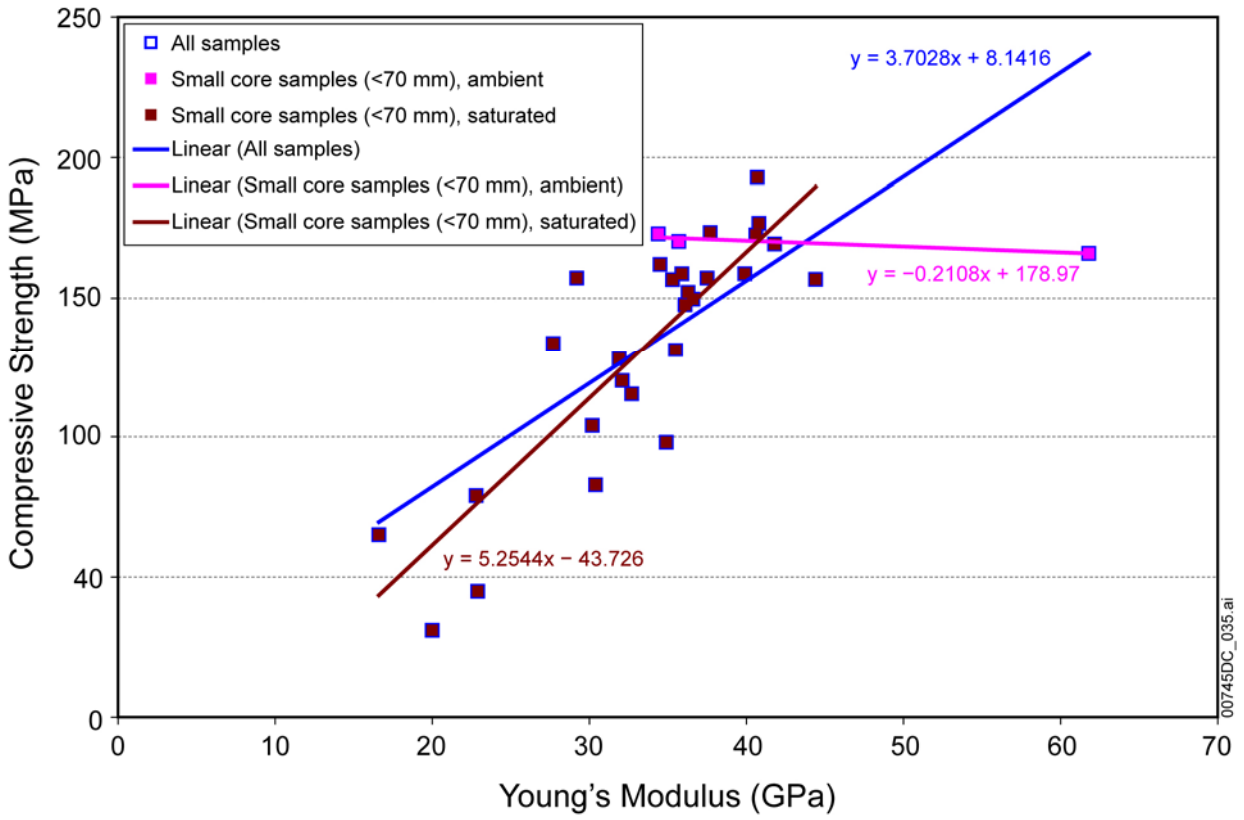

Sources: DTNs: MO0311RCKPRPCS.003 [DIRS 166073]; MO0402DQRIRPPR.003 [DIRS 168901]; SN0208L0207502.001 [DIRS 161871]; SN0211L0207502.002 [DIRS 161872]; SN0302L0207502.003 [DIRS 165014]; SN0305L0207502.004 [DIRS 165013]; SN0306L0207502.008 [DIRS 165015]; SNL02030193001.001 [DIRS 120572].

Figure 6-38. UCS versus Young's Modulus in Tptpln Zone

6.4.2.4 Analysis of Time-Dependent Behavior of Tuff

This section provides the impact of time-dependent behavior of Yucca Mountain Tuff. The stage for discussion of time dependent behavior is set by providing background information about testing methods and terminology related to this area. Further, this section summarizes the framework of the methodology applied and provides a summary of laboratory testing to assess the time-dependent performance of the rock mass.

6.4.2.4.1 Background on Time Dependent Characteristics of Brittle Rocks

One of the characteristics of brittle rocks is that at temperatures well below the melting point, a rock subjected to a constant load exhibits a continuous increase in strain with time. This time-dependent deformation is termed creep. Studies on creep indicate that the observed strain depends upon the applied stress, temperature, partial pressure of water, and confining pressure (e.g., Martin 1972 [DIRS 169721]). Moreover, the same mechanism responsible for the strain of brittle rocks in constant strain-rate tests is also operative in creep. That is, cracking, both along grain boundaries and through individual grains, produces the observed strain (e.g., Brace et al. 1966 [DIRS 101990]). Above approximately one half to two-thirds of the compressive strength,

the dominant mode of deformation for brittle rocks is the opening and growth of cracks parallel to the major principal stress direction or axial orientation in uniaxial compression. It is typically considered that the strain rate of hard rocks in creep is related to the time-dependent growth of these cracks.

Verification of the relationship between time-dependent crack growth and creep strain rate in brittle rock is performed through laboratory testing. Experimental results indicate that stable time-dependent crack growth at a constant compressive load or at a constant stress intensity factor occurs in quartz and glass in the presence of water vapor. Moreover, the rate of crack growth depends on the applied stress, the temperature, and the partial pressure of water in the atmosphere surrounding the crack. The relative weakening of quartz or silicate glass, reflected by an increase in the rate of crack growth with an increase in any of the three variables, is consistent with the general theory of stress corrosion in silicates proposed by Charles (1959 [DIRS 170308]). Charles postulated that the velocity of a slowly propagating crack with a high tensile stress at the crack tip is proportional to the rate of the hydration reaction at the crack tip. The following equation (Martin 1972 [DIRS 169721]) quantifies the general relationship for environment-sensitive crack growth.

$$\nu = \nu_0 \beta P^n \exp\left(\frac{\Delta F - V^* \sigma}{RT} + \frac{\gamma V_m}{\rho RT}\right) \quad \text{(Eq. 6-7)}$$

where,

ν is the rate of crack growth
ν_0 is the initial flaw size
P is the partial pressure of water
ΔF is the activation energy for the process
T is temperature
R is the universal gas constant
V^* is the activation volume
σ is stress
γ is the surface energy of the solid
V_m is the molar volume of the solid
ρ is the radius of curvature of the crack tip
β and n are constants.

If the partial pressure of water, temperature, and applied stress are constant, a constant crack propagation velocity will be observed. When any one of the thermodynamic variables is increased, the crack velocity increases. This expression has been verified with experimental studies (Wiederhorn 1968 [DIRS 170309]; Martin 1972 [DIRS 169721]; Scholz 1972 [DIRS 169724]).

The validation of Equation 6-7 is extremely important. First, the validation establishes a rate-dependent process for the propagation of cracks in quartz and silicate glass. If the same behavior is observed in rocks, then it implies that time can be scaled from very short times to extremely long times in the absence of other competing mechanisms. Specifically, if moisture-assisted stable crack growth is the primary mechanism of creep in brittle rocks, measurements made at

laboratory scales of up to 10^6 seconds can be extrapolated to much longer time scales on the order of 10^{11} to 10^{14} seconds. Presently there are no other independent data that suggest other competing mechanisms for time dependent deformation in brittle rocks at temperatures below 300°C. Based on these results and verifications by other experimenters, there is confidence that Equation 6-7 satisfactorily represents the behavior of the rate of crack growth at the crack tip for brittle silicate materials at temperatures below 300°C.

Next, the behavior of brittle rocks can be examined during creep and compared to the observations of stable, time-dependent crack growth gained from tests on quartz and glass. A creep test is conducted by rapid application of uniaxial or triaxial load to a rock sample to a given differential stress, followed by holding the load constant while monitoring the longitudinal and lateral strains.

The time-dependent deformation is commonly presented in a form of a creep curve. This curve is used to display the material capability to accumulate strain or deformation over time. Figure 6-39 shows the stress path (top) and corresponding response of the material, and creep curve (bottom). As shown in Figure 6-39, a creep curve includes several material response phases. The Phase 0 (line OA) shows the deformation that the tested material undergoes upon applying the load. Since the load is applied rapidly in a single step, this initial response does not include the time factor. The corresponding Phase 0 material response is also termed time-independent or instantaneous deformation. The following three time-dependent phases include Phase 1 (line AB)—the primary or transient creep; Phase 2 (line BC)—secondary or steady state creep; and Phase 3 (line CD)—the tertiary or accelerating creep.

In brittle materials, each subsequent loading phase causes an increase in a number of cracks developing within the material resulting in volume increase, also termed dilation. This volume increase can be used as a measure of damage the specimen sustained under a particular loading condition. The creep curve serves as a record of the magnitude of material damage under a given stress level.

During time-dependent phases 1, 2, and 3 encompassing the primary, secondary, and tertiary creep, material deformation increases. From the rock mechanics design point of view, it is desirable that Phase 2, which represents steady-state material deformation, be as long as possible. The tertiary creep (Phase 3) indicates the stage of material performance where the unstable crack propagation eventually leads to failure. Creep tests can be performed as single or multiple step tests.

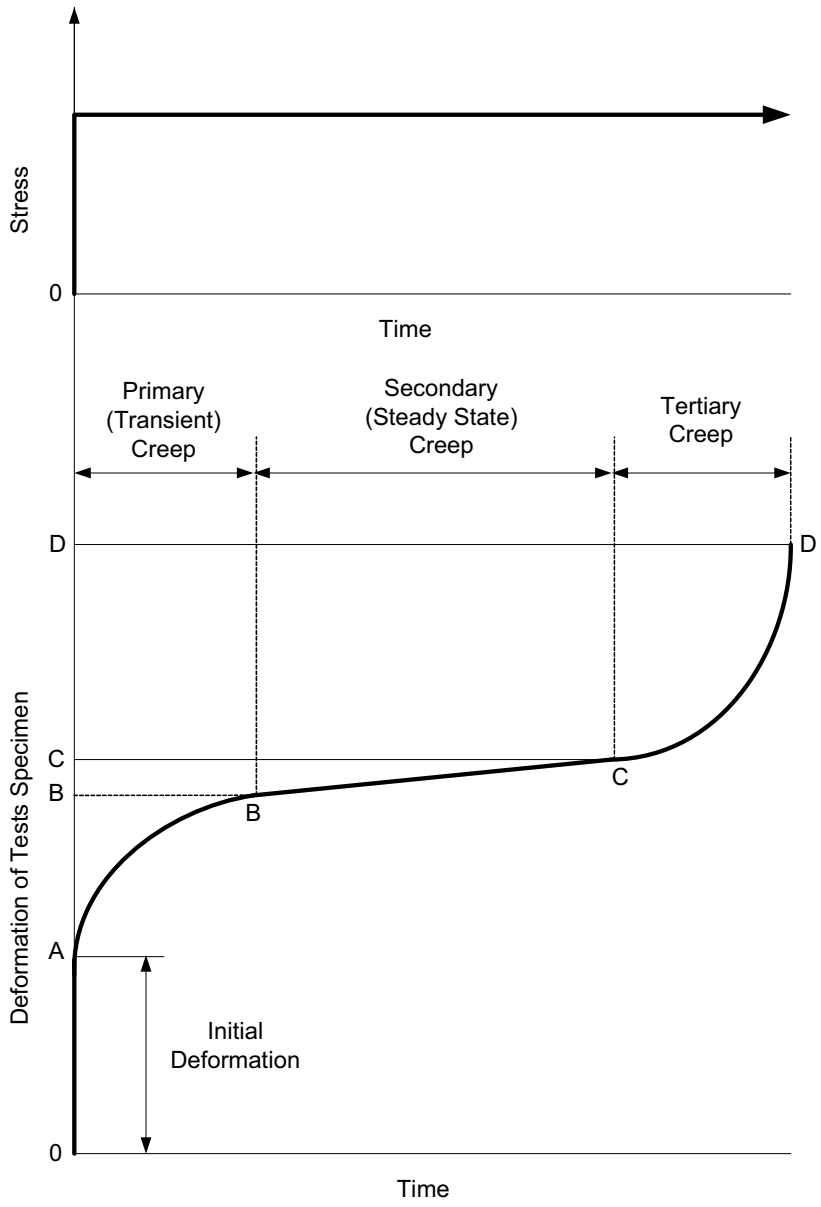

Figure 6-39. Example of a Typical Creep Curve

A typical example of the creep curve experimentally determined for Topopah Spring tuff displaying all three stages of time-dependent behavior is shown Figure 6-40.

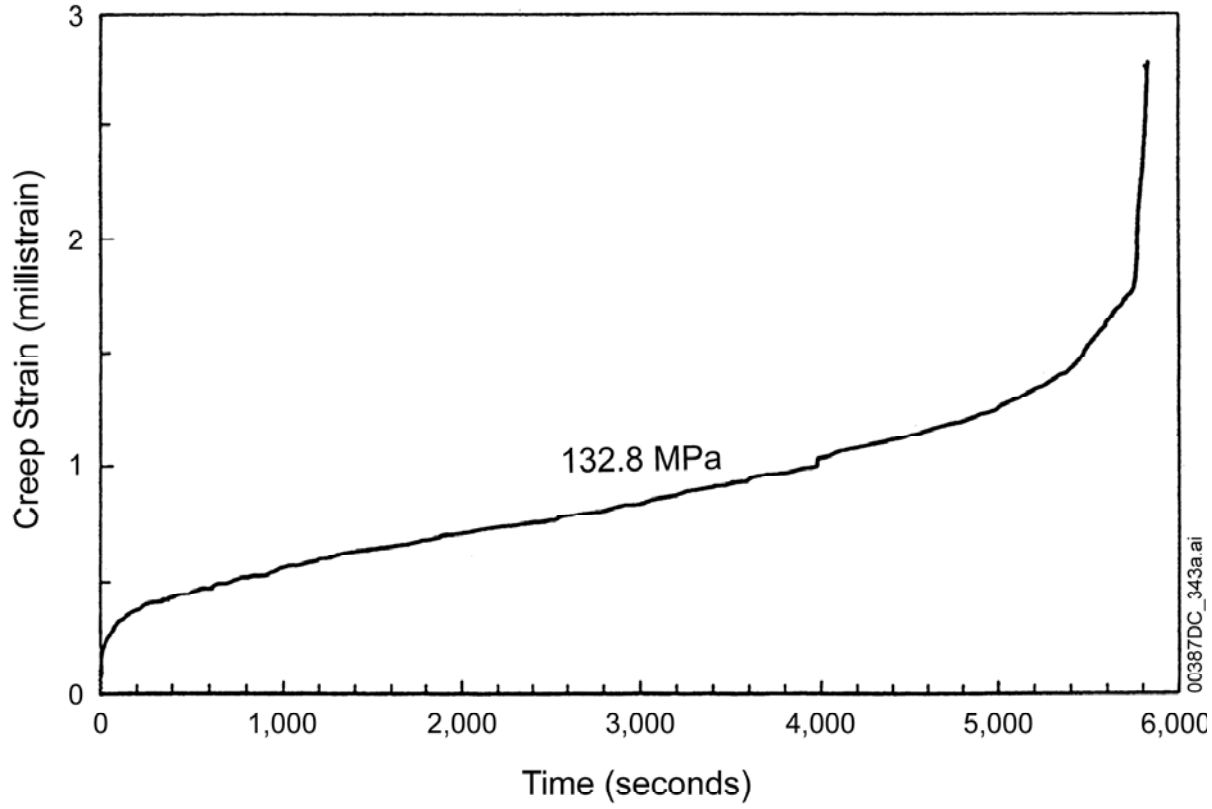

Source: Martin et al. 1997 [DIRS 165960], Figure 4.

NOTE: Specimen failed at tertiary creep phase.

Figure 6-40. Example of Creep Strain Plotted as a Function of Time for a Static Fatigue Test Conducted on a Sample of Topopah Spring Tuff at a Constant Differential Stress of 132.8 MPa, a Confining Pressure of 5.0 MPa, a Pore Pressure of 1 MPa, and a Temperature of 150°C

Although present in all rock types in its more visible/measurable form, creep is common in some low-to-moderate strength rock materials, such as rock salt and marble. The simple crystalline lattice of salt facilitates the phenomena involving deformation through sliding along planes of the crystalline lattice, also known as intercrystalline glide, crystal twinning, and progression of the intergranular microfracturing. In the brittle, hard rock materials displaying elastic properties within a wide range of stresses, such as tuff, these typical creep mechanisms may not be evident, and investigations of factors contributing to the time-dependent deformation leads to interpreting the data on welded tuff as consistent with the stress corrosion cracking (SCC) mechanism (Martin et al. 1995 [DIRS 100159], p. 20).

Creep tests are commonly performed at a number of stress levels and often at different temperatures. The tests are long and require substantial hardware base working in closely controlled environment. The resulting stress and temperature dependent creep rates allow for the development of constitutive relationships, which in a concise form of mathematical expression describe the response of rock material to stress and/or temperature and degree of saturation. These mathematical formulations can then be incorporated into computer codes to facilitate numerical analyses of structures developed within a particular rock material. The ability of the tested material to deform under stress remains central to the successful testing of the

time-dependent behavior of rocks. The tested material capable of displaying the time-dependent behavior over a wide range of stresses can be described more easily. However, other techniques (e.g., static fatigue tests) are considered more appropriate for rock materials displaying brittle-type behavior.

Transient creep has been reported for a variety of rock types over a wide range of temperatures and pressures. The strain in this region decelerates rapidly and is often reported as proportional to the logarithm of time. Moreover, both the lateral and longitudinal strains exhibit this logarithmic time dependence.

At low stresses, transient creep may account for the observed strain. However, at high stresses, secondary creep is often observed. Generally, in secondary creep, often called steady-state creep, the strain is proportional to time. The total strain caused by both primary and secondary creep is often represented by an equation of the form (Martin et al. 1995 [DIRS 100159], Equation 2).

$$\varepsilon = A + B \log t + Ct \qquad \text{(Eq. 6-8)}$$

where, ε is strain, t is time, and A, B, and C are constants.

If secondary creep is allowed to continue, eventually the strain rate increases (tertiary creep) and the rock fails. The three stages of creep have been observed in granite, quartzite, and tuff (Martin 1972 [DIRS 169721]; Martin et al. 1997 [DIRS 165960]). A typical creep curve for a specimen of welded tuff from the middle nonlithophysal unit of the Topopah Spring (Tptpmn) is shown in Figure 6-40. There the three stages of creep are clearly evident.

Stable crack growth in quartz reported by Martin (1972 [DIRS 169721]) and Martin and Durham (1975 [DIRS 170301]) illustrated specific characteristics that are related to creep deformation. In these studies, the specimens were loaded to a fixed compressive stress and the growth of a crack parallel to the applied load was observed. Each specimen was tested in a controlled environment and the change in crack length was noted as a function of time. A typical data set obtained on a single specimen of quartz tested at a temperature of 241°C and a partial pressure of water of 4.5×10^{-2} kPa is shown in Figure 6-41. The test specimen geometry is shown in the upper left portion of the graph. At a stress of 66 MPa, the change in crack length with time is very similar to that observed in the creep of brittle crystalline rock. The crack exhibits an initial period of rapidly decelerating growth followed by a quasi-linear or secondary segment. After 6.3×10^4 seconds, the stress was increased to 74 MPa. Immediately, the rate of crack growth increased. The same characteristics observed at the lower stress were exhibited for the 74 MPa segment. There was a strong transient followed by a secondary or quasi-linear crack growth segment. At approximately 8×10^4 seconds, the stress was increased to 83 MPa. The rate of crack growth increased dramatically, and the experiment was terminated when the crack length reached 3.7 mm. These data are consistent with Equation 6-7; that is, the rate of crack growth increased with increasing stress and nearly vanishes at low stresses. Additional experiments showed that increasing either the partial pressure of water surrounding the crack or the temperature also results in an increase in the rate of crack growth.

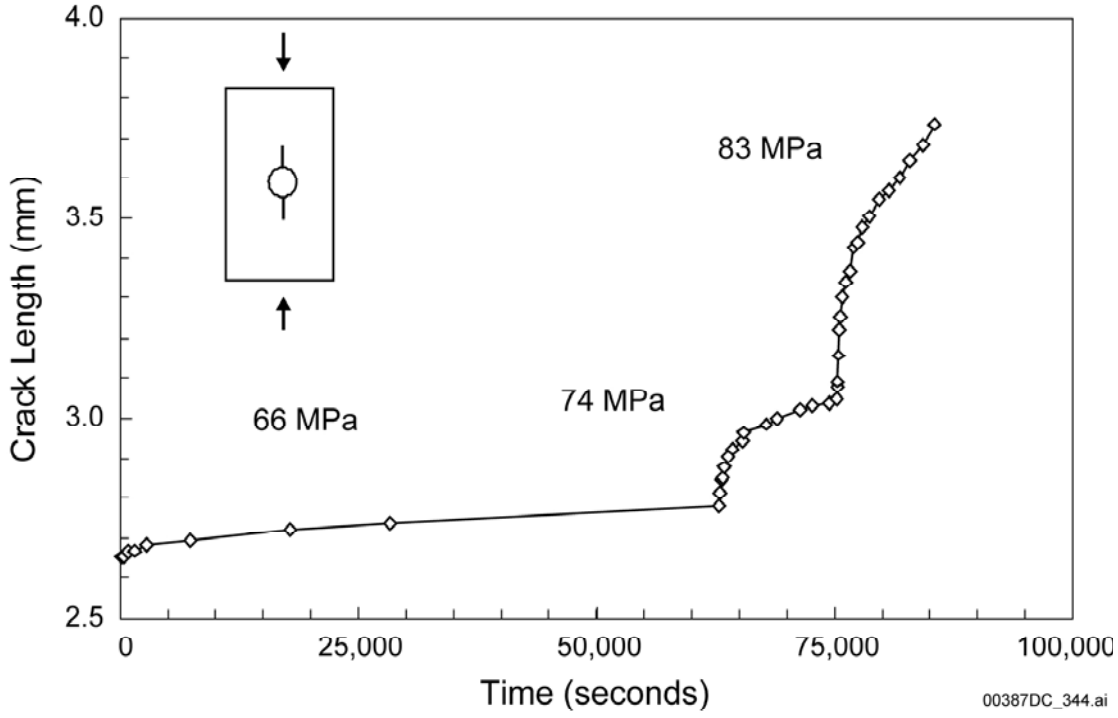

Source: Martin 1972 [DIRS 169721].

NOTE: The experiment was conducted at 241°C and a partial pressure of water of 4.05×10^{-2} kPa.

Figure 6-41. Crack Length as a Function of Time for an Axial Crack Growth Experiment in Single Crystal Quartz

The above discussion points out that creep experiments with complex, silicate rocks display the same basic time-dependent response as demonstrated by crack-growth studies in single crystals of quartz and glass. From a practical standpoint, it is advantageous to define the ultimate time-to-failure in terms of the stress, temperature, and partial pressure of water, rather than in terms of crack growth. Time-to-failure is typically defined using the creep test to determine the static fatigue of a material. Static fatigue refers to the failure time of a rock or single crystal at constant stress, temperature, confining pressure, and partial pressure of water without regard to the strain history. Scholz (1972 [DIRS 169724]) conducted a series of static fatigue tests in compression on single crystal quartz. He observed that the mean time to failure, $\langle t \rangle$, depended on the partial pressure of water (P), stress (σ), activation energy (ΔF), and temperature (T) according to:

$$\langle t \rangle = t_0 P^{-a} \exp\left(\frac{\Delta F}{RT} - K'^{\sigma}\right) \quad \text{(Eq. 6-9)}$$

where, a and K' are constants.

The foregoing discussion demonstrates that:

- The strength of brittle silicate rocks such as tuff is not a single-valued function of any parameter, but is a complex continuum that depends on the state of stress, saturation (pore pressure), temperature, and time (including strain rate).
- Studies of the basic growth of single fractures and the creep strain resulting from microcrack growth in complex silicate rocks demonstrate that the same basic stress corrosion mechanism is responsible for time-dependent crack growth and the ultimate time-to-failure of the material.
- The stress corrosion mechanism gives rise to a logarithmic relationship of time-to-failure as a function of the state of stress, temperature, and pore pressure.
- As a result of the basic understanding of the static fatigue mechanism in brittle rocks, it is possible to extrapolate long-term failure response from relatively short-term static fatigue experiments in the laboratory.

Since the effects of time-dependent fracture development on the weakening of tuff and its impact on drift degradation may be important in the postclosure repository environment, creep experiments on tuff samples have been conducted to determine its static fatigue response under the appropriate environmental conditions.

6.4.2.4.2 Static Fatigue Testing to Define Time-Dependent Behavior of Welded Tuff

A test called static fatigue test is performed in the absence of a permanent volume change displayed by a typical nonwelded tuff. The test is similar to a conventional creep test; however, it is carried out at higher stress levels, such that both measurable strain can be generated and material failure can occur within a reasonable time period. The concept of static fatigue tests performed at high stress levels, and eventually terminating in failure at some later time during the test, is the basis for attempting to estimate the time-to-failure of tuff. Subsequently, the time-to-failure obtained from these static fatigue tests provides the base for the development of the constitutive material simulation needed to extrapolate its response to stress over a much longer timeframe. Then, this material simulation can be used to incorporate this stress/deformation/time relationship into the effective design tool, by providing basis for estimating the duration of the time interval, during which the underground rock structure remains stable. The static fatigue test was adopted as a test providing potential for acquiring the time-dependent data for Yucca Mountain Tuff.

Stress Corrosion Cracking

Information related to tests performed on tuff provided in the following subsections indicates that the most likely driving mechanism behind the time dependent tuff behavior is SCC. In material science, SCC is a type of intergranular corrosion that occurs at the grain boundaries under tensile stress (Potyondy 2003 [DIRS 165550], Section 1.1). SCC occurs in susceptible materials when these materials are exposed to a specific chemical environment and the material is under tensile stress condition. In addition, SCC appears to be relatively independent of general uniform corrosion processes common in metals. In certain metals the general corrosion can be almost nonexistent, while stress cracking can still occur. In rocks

subjected to this chemical environment a defect initially present then grows as the material grains separate under stress, and the process continues. In very extreme cases, the time required for this cracking to occur is only a matter of minutes.

In volcanic tuff, stress corrosion is believed to contribute to the propagation of cracks within the stressed rock volume and its effects are recorded as a time-dependent deformation. Water appears to be the chemical agent necessary to enhance this process. Water-saturated tuff samples usually display lower strength and a more pronounced time-dependent deformation.

The most effective means of preventing SCC are: (a) proper design, involving the reduction of stress level; (b) removing critical environmental contributors, such as water and oxygen; and (c) avoiding creating areas where these corrosion-enhancing agents might become concentrated.

The damage process in the dry rock occurs through the propagation of cracks under high tensile stresses and represents the major factor in the progressive damage of rock structure. Underground workings subjected to elevated temperature generated by the emplaced waste are likely to behave as dry rock.

The typical way to define the time-dependent strength of rock is to establish the time required for failure of heated, saturated rock samples that are subjected to an applied constant axial stress. Creep test experiments are conducted to determine the static fatigue strength of the rock associated with tertiary creep rupture. These tests, typically conducted in uniaxial or triaxial compression, involve rapidly increasing the applied axial stress to a given percentage of the estimated compressive strength of the same size rock samples. The stress is then held constant until the sample spontaneously fails due to time-dependent rupture. A plot of the logarithm of the time-to-failure versus the ratio of the applied stress to the unconfined compressive strength is developed. The plot is typically linear, reflecting the basic mechanisms of stress corrosion as described above. Rock samples subjected to stress levels that are small in comparison to the compressive strength (i.e., below about 50% to 60%) result in excessively long times to failure and cannot be tested practically in the lab due to the long test duration. However, these loading conditions are not of interest for drift stability in the postclosure time frame of hundreds to thousands of years. The loading conditions of interest to time-dependent degradation at Yucca Mountain are those in which the applied stresses from in situ and thermal loading in the drift wall periphery are a high percentage of the rock strength (e.g., greater than approximately 60% to 70%). Here, the time to failure may result in significant degradation in hundreds to thousands of years. In this case, relatively short-term laboratory experiments (on the order of days to weeks) can supply time constants capable of describing the stress corrosion process.

6.4.2.4.3 Summary of Tests on Time Dependent Behavior of Nonlithophysal Units of Yucca Mountain Tuff

Over the past two decades, a number of testing programs have been undertaken with the purpose of characterizing the time-dependent properties of tuff. During that time, the Yucca Mountain Project has evolved from the first stage of providing an overall site characterization for the site suitability to house the nuclear waste repository through the subsequent stages of more detailed focus on providing particular rock property and other site-related data. The initial time-dependent rock property data for tuff were obtained from the Bullfrog Member of the

Crater Flat Group, borehole UE25A #1 (Senseny and Parrish 1981 [DIRS 163415]). Figure 6-42 shows the creep test sample locations. Locations of the sites, from which the rock samples for the various studies of Yucca Mountain welded tuff were obtained, are also shown in red and are referenced in the following sections.

In the Yucca Mountain Project, the total number of tests that have been performed to obtain the time dependent characteristics of tuff is rather limited. A summary of all relevant tests in this area was considered important, even though some tests were performed at the time before the project-wide QA program was implemented. Some tests, in addition to the details pertaining to the time-dependent test data, also include details pertaining to other tests associated with the particular testing program. These details are also included for the sake of completeness. The summaries of each testing program undertaken to obtain the time dependent tuff data are presented in the following sections.

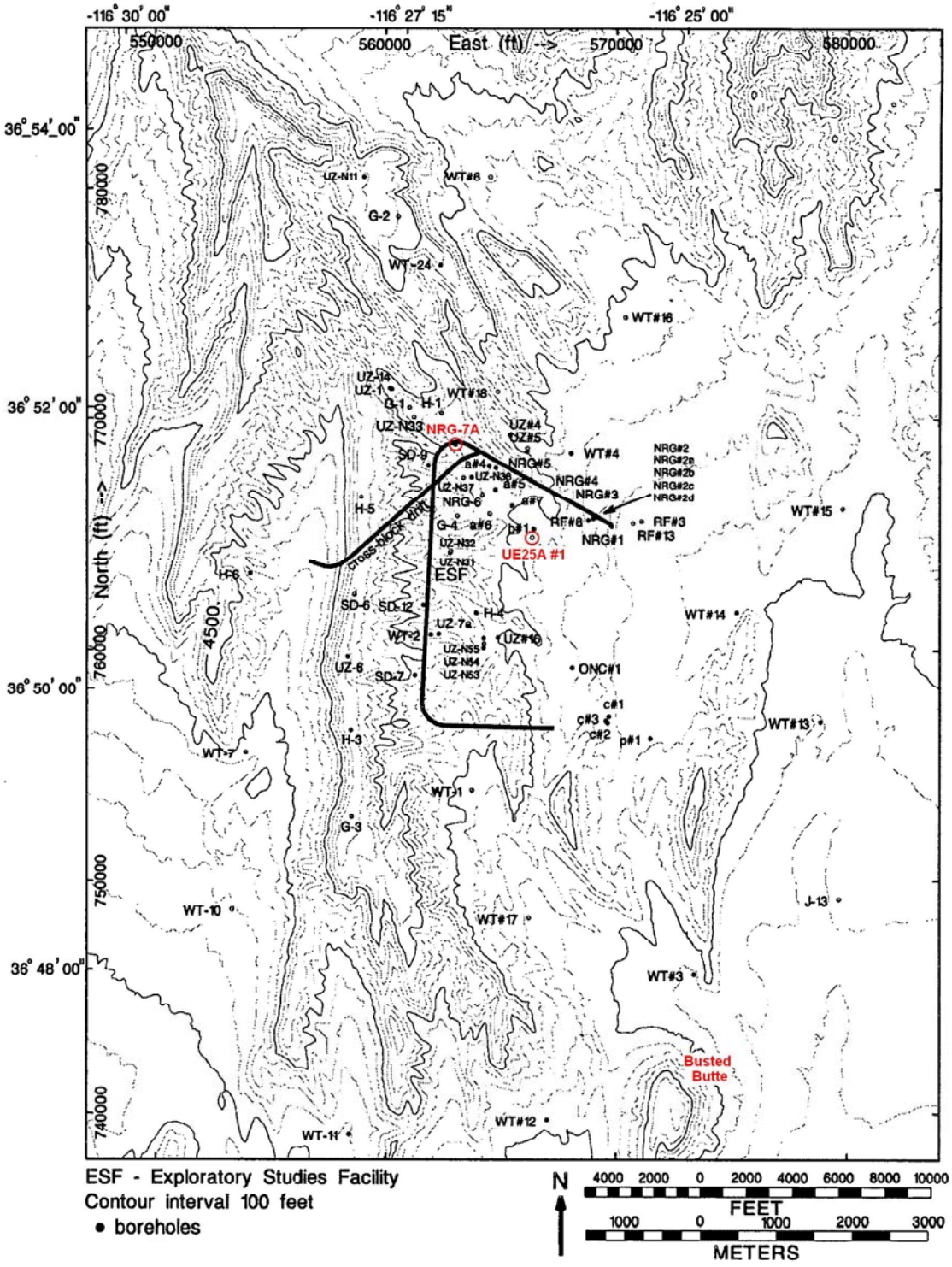

Source: Modified from BSC 2004 [DIRS 170029], Figure 6-1.

Figure 6-42. Creep Test Sample Locations (in Red)

Creep Tests on Bullfrog Member of the Crater Flat Group Tuff (1981)

Early creep tests on tuff were performed in 1981 on specimens of welded tuff with about 20% porosity from the Bullfrog Member of the Crater Flat group tuff from Yucca Mountain (Senseny and Parrish 1981 [DIRS 163415]). Prior to performing creep tests, the three UCS tests were completed resulting in UCS values equal to 48, 54, and 78 MPa. The average Young's modulus was determined to be equal to 15 GPa. Three creep tests were performed on dry specimens at confining pressures of 0.7 MPa and 3.5 MPa and at axial stress difference equal to 85% and 100% of the UCS. One test was performed on saturated (wet) specimens. Table 6-22 provides a list of parameters for each test carried out in this investigation.

Table 6-22. Laboratory Experiments in Support of the Tuff Mine Design Study

Test No.	Confining Pressure (MPa/psi)	Wet/Dry	Pore Pressure (MPa/psi)	Axial Stress Difference (% of Uniaxial) Dry Strength	Temperature (°C)	Duration (Days)
1*	0	Dry	0	100	100	0.5
2*	0	Dry	0	100	100	0.5
3*	0	Dry	0	100	100	0.5
4	0.69/100	Dry	0	85	100	34.0
5	3.45/500	Dry	0	100	100	26.0
6	3.45/500	Dry	0	100	100	34.0
7	1.38/200	Wet	0.69/100	60	100	21.0

* Tests performed to determine uniaxial compressive strength.

Source: Senseny and Parrish 1981 [DIRS 163415], Table 1.

Figure 6-43 (a) through (d) shows a series of four strain-time curves obtained from creep tests. Tests 5 and 6 listed in Table 6-22 (Figure 6-43 plots (b) and (c)) were performed under identical conditions; however, the recorded strains differ by a factor of two. For the duration of these tests all creep was transient and the creep rate decreased continuously with time. The results also show oscillations in the strain-time curves apparently resulting from fluctuations in the confining pressure (Senseny and Parrish 1981 [DIRS 163415], p. 11).

The creep data were fit to a commonly used creep law in the following form (Senseny and Parrish 1981 [DIRS 163415], p. 11):

$$\varepsilon = kt^n \qquad \text{(Eq. 6-10)}$$

where, ε is axial creep strain, t is time since the start of creep, and k and n are experimentally determined constants.

The test data indicate that saturated specimens creep faster than the dry specimens. The report by Senseny and Parrish (1981 [DIRS 163415]) includes a discussion about microscopic analyses of test specimens. These were performed on thin sections prepared from undeformed and deformed tuff. Here, attempt was made to identify any potential mechanisms that contributed to specimen creep and failure. It was observed that, for the test durations of about twenty-five days, no intercrystalline fractures or deformation mechanisms were observed. It was concluded

that some other mechanisms must be associated with the observed creep strain (Senseny and Parrish 1981 [DIRS 163415], p. 14). However, no lateral strains were measured during these tests. As a result, specimen volume change or dilation was not computed.

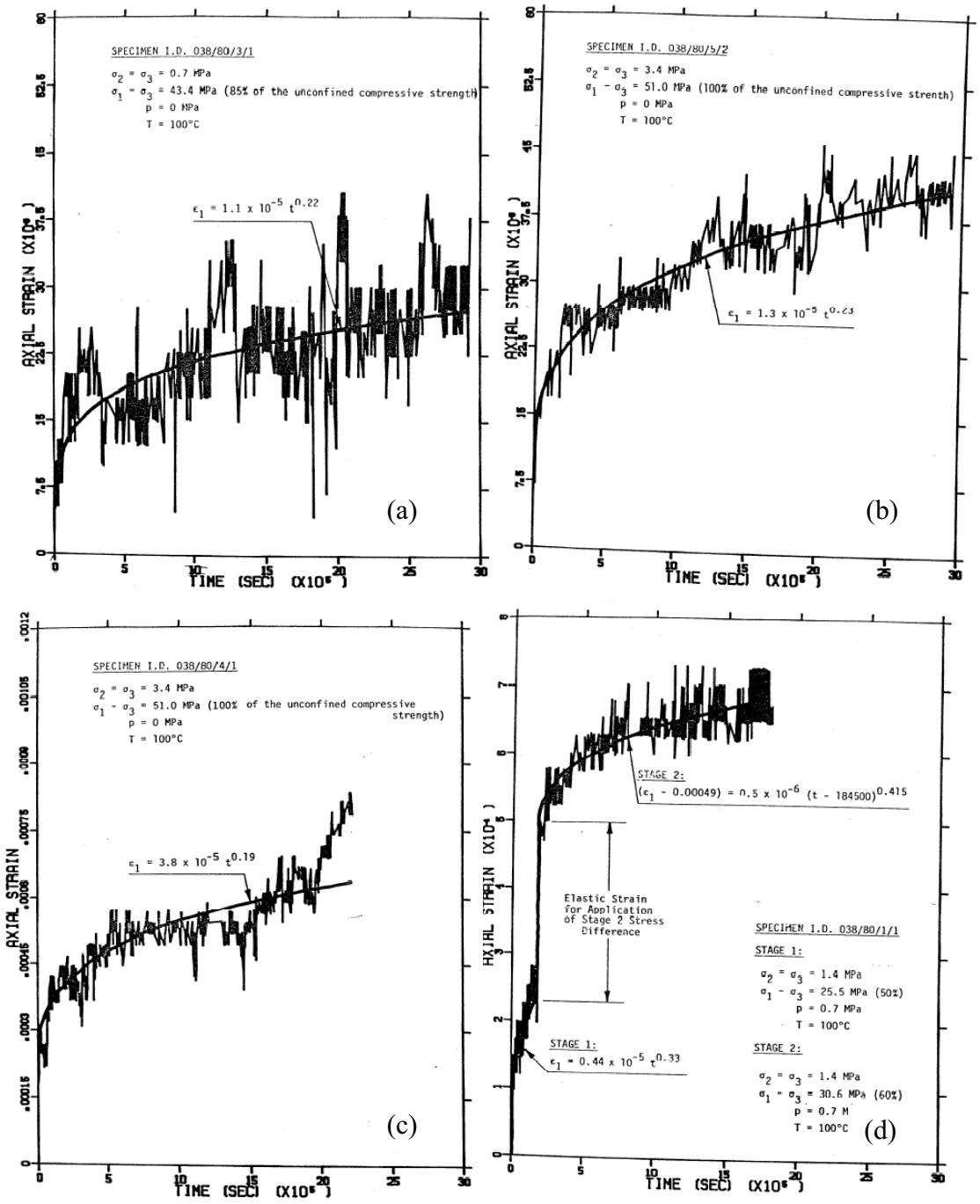

Source: Senseny and Parrish 1981 [DIRS 163415], Figures 3.1 to 3.4.

Figure 6-43. Initial Creep Tests on Bullfrog Tuff – Crater Flat Group

Creep in Topopah Spring Member Welded Tuff from Busted Butte (1995)

Martin et al. (1995 [DIRS 100159]) reported the results of the time-dependent properties of nonlithophysal welded tuff. During this test program a series of creep tests were performed on welded tuff. Figures 6-44 to 6-47 show four sets of plots, including: (a) histories of the differential axial stress, and (b) plots of differential axial stress versus volumetric strain. This method of presentation was selected to illustrate the fact that welded tuff displays elastic behavior over an unusually wide stress range. This behavior is characterized by almost ideal elastic volumetric response, especially at high stress levels approaching failure. The volumetric strain remains linear, consistently, regardless of stress path.

The welded tuff response to unloading shown in Figure 6-44 does not display typical hysteresis that could be used as a common indicator of crack development and propagation within the specimen volume. Martin et al. (1995 [DIRS 100159], pp. 9 and 10) indicate that "The implication is that the interaction of a large number of microcracks that produce a nonlinear increase in the radial strain normal to the loading axis, above approximately half of the compressive stress, is not operative in welded tuff." They also observed that "In most cases, the rock fails catastrophically through a series of extension fractures, often propagating through the ends of the specimen." This leads them to further observe that "… tuff exhibits a behavior that is somewhat different from other low porosity crystalline rocks, it is possible that the creep strains at a constant stress, observed in previous studies in crystalline rock may not be as pronounced in tuff, while the time to failure may still depend on temperature, stress, and water saturation." These observations are consistent with the results reported by Price (1986 [DIRS 106589], p. 7) and Martin et al. (1993 [DIRS 164770], p. 6) where investigations were focused on the impact of specimen size, strain rate and sample inhomogeneity on the mechanical behavior of welded tuff.

In general, Martin et al. (1995 [DIRS 100159], p. 20) concludes that: "The data on welded tuff are consistent with a SCC mechanism for the deformation and failure. These results suggest that the strength and creep deformation of tuff should be studied as a function of temperature, saturation, and applied load."

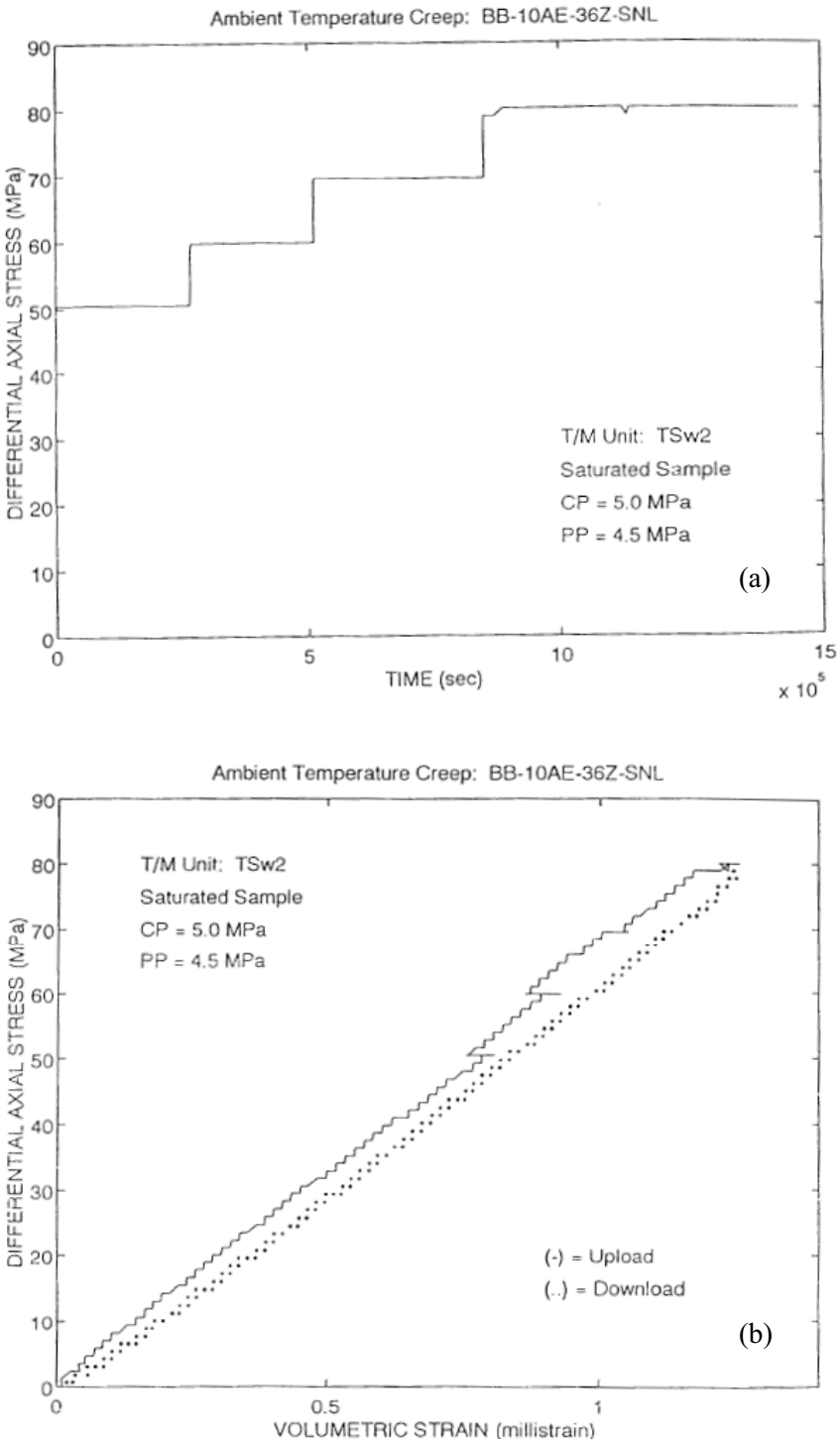

Source: Martin et al. 1995 [DIRS 100159], Figures 8a and 8e.

NOTES: CP=confining pressure, PP=pore pressure.

Figure 6-44. (a) Differential Axial Stress versus Time and (b) versus Volumetric Strain on Specimen BB-10AE-36Z-SNL at Ambient Temperature

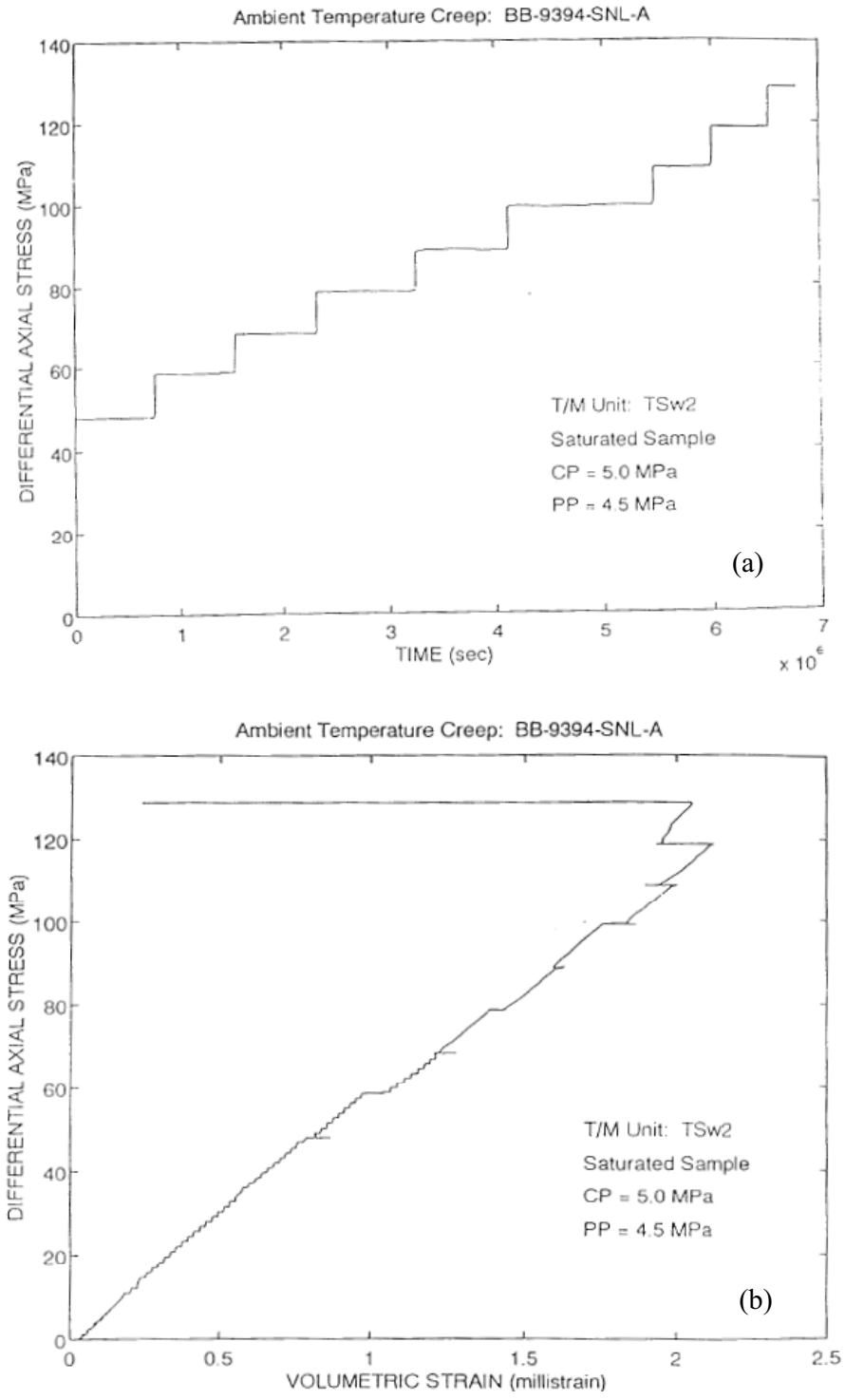

Source: Martin et al. 1995 [DIRS 100159], Figures 9a and 9f.

NOTES: CP=confining pressure, PP=pore pressure.

Figure 6-45. Plots of (a) Differential Axial Stress versus Time and (b) versus Volumetric Strain on Specimen BB-9394-SNL-A at Ambient Temperature

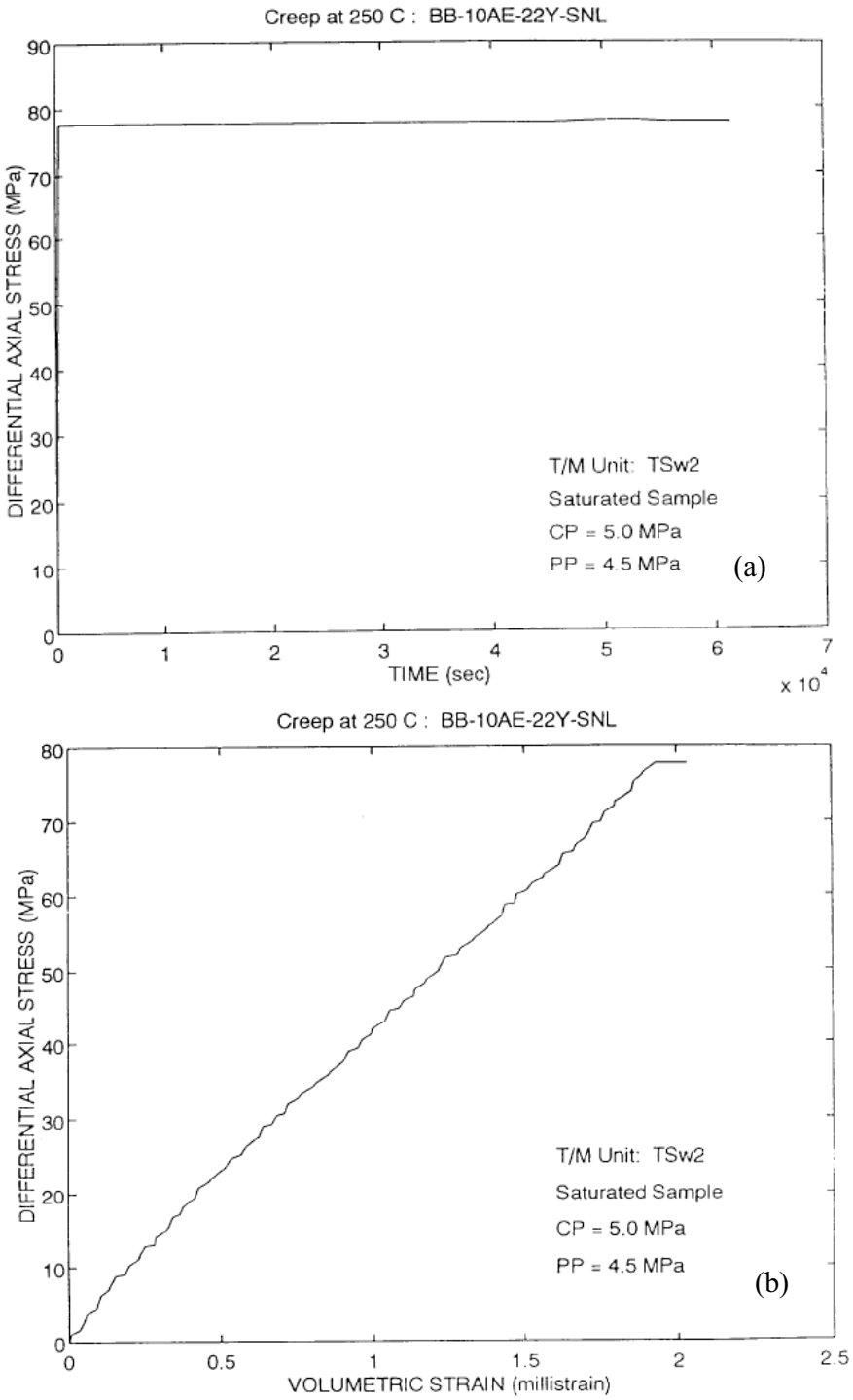

Source: Martin et al. 1995 [DIRS 100159], Figures 10a and 10f.

NOTES: CP=confining pressure, PP=pore pressure.

Figure 6-46. (a) Differential Axial Stress versus Time and (b) versus Volumetric Strain on Specimen BB-10AE-22Y-SNL at 250°C

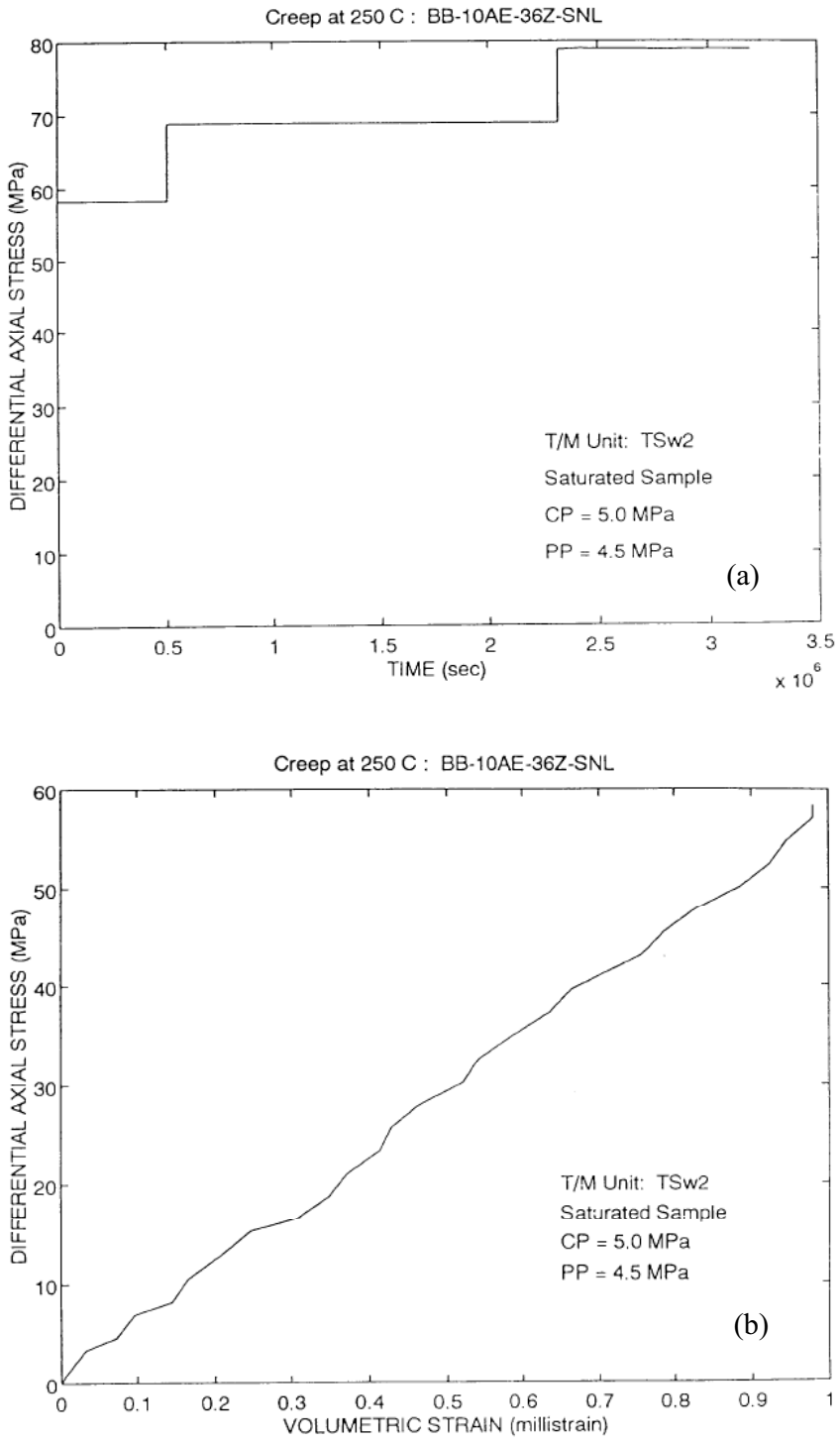

Source: Martin et al. 1995 [DIRS 100159], Figures 11a and 11e.

NOTES: CP=confining pressure, PP=pore pressure.

Figure 6-47. (a) Differential Axial Stress versus Time and (b) versus Volumetric Strain on Specimen BB-10AE-36Z-SNL at 250°C

Creep Tests on Paintbrush Welded Tuff from Borehole USW NRG-7/7A (1997)

A series of triaxial static fatigue experiments were conducted on heated and saturated nonlithophysal cores from the Tptpmn in 1997 (Martin et al. 1997 [DIRS 148875]). Triaxial experiments on 50.8 mm diameter cores with a confining pressure of 5 MPa and pore water pressure of 4.5 MPa were conducted so that pore water of the saturated samples would remain in a liquid state as the temperatures were increased over boiling (125°C and 150°C). The resulting effective stress (the confining pressure minus the pore water pressure) was approximately 0.5 MPa, or essentially a state of uniaxial compression. This procedure was used to ensure a conservative state in which saturated samples were maintained at postclosure rock temperatures. Figure 6-48 shows a typical specimen ready for testing.

Figure 6-48. Triaxial Static Fatigue Experimental Setup and Posttest Sample for Heated, Saturated, 50.8 mm Diameter Samples of Tptpmn

In this study reported by Martin et al. (1997 [DIRS 148875]), a suite of tests, including density, porosity, sonic velocity, and time-dependent characteristics of welded tuff, were performed on cores recovered from the USW NRG-7/7A. Seven specimens were prepared to perform creep tests. Table 6-23 provides a summary of all tests performed on each tuff specimen prepared for this study. As listed in this table, creep tests were performed under an elevated temperature of 225ºC and confining pressure of 10 MPa. The magnitude of the axial differential stress ranged from 40 MPa to 132 MPa. Only axial strain was monitored during these tests. Figure 6-49 shows a summary of creep curves obtained for the seven creep tests performed during this testing program. The axial differential stress for each test is shown next to each creep curve.

As discussed by Martin et al. (1997 [DIRS 148875], Section 4.0), the data obtained from the seven creep tests shows some consistent features, namely:

1) The time-dependent strain increases with increasing differential axial stress. At 40 MPa, no perceptible time-dependent strain accumulation is observed. This observation is significant as it provides evidence that even at this relatively high stress level no creep strain can be observed.

2) The data indicate that even at much higher stress levels the strain rate is decreasing. This observation is consistent with simulations for creep in brittle silicate rocks based on SCC.

3) The mechanism of deformation and fracture in brittle rocks is characterized (Martin et al. 1997 [DIRS 148875], p. 40) by the initiation and propagation of axial cracks and the strength is dependent on the water concentration around the specimen. They also express the opinion that it is likely that the mechanism of creep is in some way related to moisture-assisted crack growth (SCC).

While rocks such as natural salt exhibit substantial deformations even at low-to-moderate stress levels, brittle rocks show extremely small strains at failure even at elevated temperatures. Typically, creep experiments carried out on rocks displaying plastic behavior are performed with the purpose of determining the total strain as a function of time for a given stress level. Strains at failure displayed by the brittle rocks are usually small (generally less than 0.5%) and may vary even by as much as a factor of two. This makes any attempts to estimate the time-to-failure difficult. For this reason, brittle rocks are often tested by means of performing static fatigue tests where the objective is to determine the time-to-failure for the given rock material. In these tests, time-to-failure is plotted as a function of the applied stress. Using this method, an estimate of the long-term strength of brittle rocks can be achieved without specific reference to the associated strain (Martin et al. 1997 [DIRS 148875], pp. 41 and 42).

Table 6-23. Data and Summary of Tests Performed on Specimens Obtained from USW NRG-7/7A Borehole

Specimen Number	1	2	3	4	5	6	7
Depth, ft	776.6	807.6	808.3	858.4	1264.5	1281.4	1400.5
Thermal-Mechanical Unit	TSw2	TSw2	TSw2	TSw2	TSw2	TSw2	TSw2
Lithostratigraphic Unit	Tptpmn	Tptpmn	Tptpmn	Tptpmn	Tptpln	Tptpln	Tptpln
Data Test Initiated	3/28/1995	3/28/1995	2/17/1995	3/28/1995	9/30/1993	9/30/1993	9/30/1993
As Tested Bulk density (g/cc)	2.249	2.273	2.292	2.307	2.295	2.295	2.295
Average Grain Density (g/cc)	2.536	2.534	2.526	2.526	2.591	2.592	2.515
Porosity (%)	11.3	10.3	9.2	8.7	11.4	11.5	8.8
P Velocity (km/s)	4.357	4.426	4.455	4.488	4.064	4.431	NA
S1 Velocity (km/s)	2.774	2.775	2.8	2.816	2.563	NA	NA
S2 Velocity (km/s)	2.73	2.712	2.848	2.769	2.51	NA	NA
Radial P Velocity (km/s)	4.388	4.418	4.471	4.465	NA	4.618	NA
Radial S Velocity (km/s)	2.808	2.836	2.824	2.847	2.703	2.815	NA
Temperature (deg C)	225	225	225	225	225	225	225
Confining Pressure (MPa)	10	10	10	10	10	10	10
Stress Difference (MPa)	70	40	129	100	98	132	131
Creep Strain (x10-3)	2.34	1.08	3.02	2.69	3.01	3.7	3.47
Strain at Termination (x10-3)	2.52	1.16	3.06	2.88	3.25	4.04	3.84
Duration of Test (Days)	43.5	43.5	68.3	43.5	29.5	29.5	29.5
Duration of Test, (x105) seconds	3.76	3.76	5.9	3.76	2.55	2.55	2.55

Sources: Martin et al. 1997 [DIRS 148875], p. 24, Table 1; SNL02071596001.001 [DIRS 162205].

NOTES: Sample IDs are shortened from the NRG-7/7A-depth-SNLBOREHOLE
Nominal sample dimensions: 101.6 mm (length). 50.80 mm (diameter)

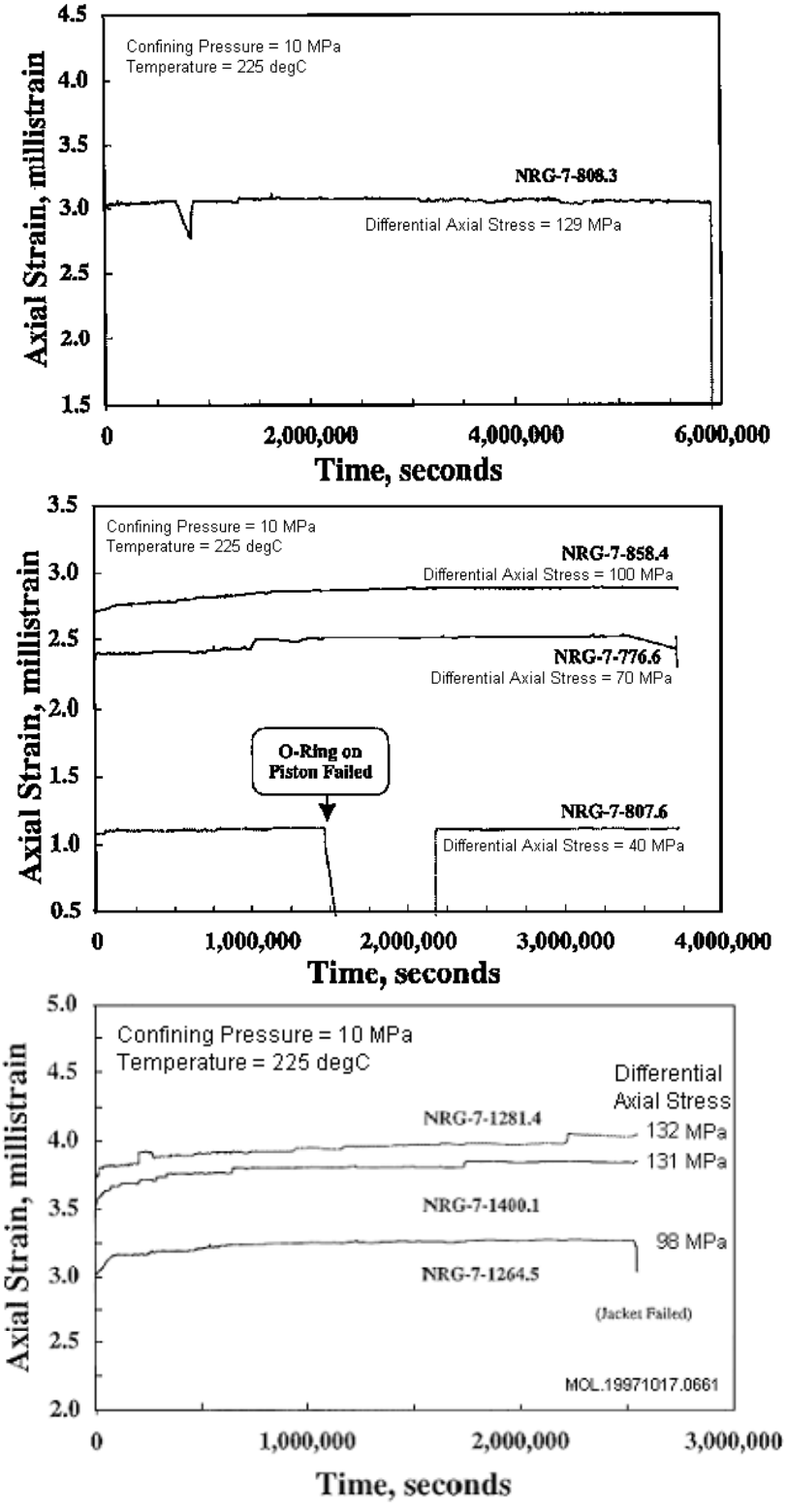

Source: Martin et al. 1997 [DIRS 148875], Figures 8, 11, and 14.

Figure 6-49. Axial Strain versus Time for Seven Specimens of Topopah Spring Welded Tuff TSw2, Tested at a Confining Pressure of 10 MPa and a Temperature of 225 ºC

Creep Tests on Welded Tuff from ESF Heated Drift Locations (2004 to 2005)

This section summarizes the results from the most recent tests on time-dependent behavior of welded tuff by New England Research Inc. The tests were performed on specimens obtained from the ESF at the heated drift (HD) location. The tests in this series were reported in two groups. The first group includes tests performed during the period January 02, 2004, to February 25, 2005 (DTN: SN0406L0212303.002 [DIRS 170289]).

Included in the first group are the results from 21 tests on welded tuff. Six tests were performed at the constant strain rate to determine the ultimate compressive strength for this group of specimens. The remaining 15 tests were creep/static fatigue type tests, which were carried out saturated, under the elevated temperature of 125ºC, confining pressure of 5 MPa, and pore pressure of 4.5 MPa (this pressure is maintained to prevent water from boiling out). The parameters determined from this test series include porosity, Poisson's ratio, Young's modulus, saturated bulk density, dry bulk density, axial strain at failure, time to failure, creep test duration, and creep test axial strain. The results obtained from creep tests are summarized in Table 6-24.

The second group includes the results obtained from an additional 17 creep tests on welded tuff from the same locations as indicated above. This group is further subdivided into two subsets. The first subset (10 specimens) contains the results of creep experiments that ended with specimen failure. The second subset (7 specimens) includes results from creep tests that were terminated without specimen failure. This second group includes tests performed during the period July 12, 2004, to October 27, 2004 (DTN: SN0505L0212303.004 [DIRS 174955]).

The two subsets of creep results that end with and without failure are presented in Tables 6-25 and 6-26. Figure 6-50 shows the plot of all 2004 New England Research test data. It is apparent that for the lower stress range the time to failure is larger than that for the higher stress range.

Table 6-24. Results of the First Group of Tests on Time-Dependent Behavior of Welded Tuff, January 02, 2004 to February 25, 2005.

Time Dependent Testing at New England Research Inc.
Summary Table
DTN: SN0406L0212303.002
Test Conditions: Confining Pressure = 5.0 MPa / Pore Pressure = 4.5 MPa / all at Temperature = 125 °C
Test Type: Time Dependent / Creep

Test Inventory Number	Test Completion Date	Sample ID	SMF Sample ID	Length	Diameter	Dry Bulk Density	Saturated Bulk Density	Porosity via Grain Density	Predicted Strength via Porosity	Applied Creep Differential Stress	Creep Stress as Percent of Predicted Strength	Time to Failure	Axial Strain at Failure	Moduli via Constant Strain Rate Preload/Unload	
														Young's Modulus	Poisson's Ratio
			SPC#	(in)	(in)	(g/cm3)	(g/cm3)	(%)	(MPa)	(MPa)	(%)	(seconds)	(millistrain)	(GPa)	
1	1/7/2004	ESF-HD-WH-38-16.2-A	01025487	3.995	1.998	2.28	2.37	9.39	208	180	86	17,016	8.4	33.6	0.26
2	1/15/2004	ESF-HD-WH-38-28.0-A	01025488	4.004	1.998	2.29	2.37	9.49	205	180	88	10,111	7.7	33.4	0.21
3	1/21/2004	ESF-HD-WH-39-8.2-A	01025491	3.998	1.998	2.26	2.35	10.90	158	144	91	6,611	8.0	30.5	0.21
4	1/28/2004	ESF-HD-WH-39-26.1-A	01025493	3.995	1.999	2.29	2.38	9.33	210	194	92	50,433	8.0	34.9	0.27
5	1/23/2004	ESF-HD-WH-40-0.0-A	01025494	4.000	1.999	2.26	2.36	10.29	178	170	95	17	7.1	28.4	0.42
6	1/28/2004	ESF-HD-WH-40-7.4-A	01025496	4.000	2.000	2.24	2.34	11.17	149	137	92	72	8.6	27.2	0.15
7	2/1/2004	ESF-HD-WH-40-8.0-A	01025497	3.997	1.999	2.28	2.36	9.81	194	165	85	173,690	9.6	32.2	0.05
8	1/30/2004	ESF-HD-WH-40-10.6-B	01025499	3.999	2.000	2.29	2.37	9.41	207	191	92	2,057	9.5	32.8	0.30
9	2/4/2004	ESF-HD-WH-40-17.6-A	01025501	3.999	1.999	2.29	2.37	9.52	204	173	85	34,849	7.4	34.3	0.27
10	2/6/2004	ESF-HD-WH-40-19.8-A	01025502	4.002	2.000	2.27	2.36	10.31	178	143	80	1,408	8.3	30.2	0.13
11	2/11/2004	ESF-HD-WH-40-32.8-A	01025505	3.996	2.000	2.29	2.37	9.44	207	166	80	18,944	8.6	36.0	0.27
12	2/15/2004	ESF-HD-WH-44-0.6-A	01025506	4.002	2.000	2.26	2.35	10.40	175	140	80	197,851	7.0	32.2	
13	2/17/2004	ESF-HD-WH-44-3.0-A	01025507	4.001	2.000	2.27	2.36	10.19	182	146	80	***2,621***	4.7	33.2	0.20
14	2/18/2004	ESF-HD-WH-44-17.9-A	01025509	3.995	2.000	2.26	2.36	10.05	186	140	75	***208***	6.9	30.2	
15	2/25/2004	ESF-HD-WH-48-6.0-A	01025518	4.000	2.000	2.25	2.35	10.86	160	120	75	***18,032***	4.7	29.4	

NOTES: ESF-HD-WH-44-3.0-A and -17.9-A failed along pre-existing fractures and the times to failure are considered to be invalid.
Load Cell failed during testing of ESF-HD-WH-48-6.0-A, so time to failure is not valid.
The blanks in the Poisson's ratio column indicate invalid results.

Source: DTN: SN0406L0212303.002 [DIRS 170289].

Table 6-25. Results of the Second Group of Creep Tests that Ended *With Failure*, July 12, 2004 to October 27, 2004

Time Dependent Testing at New England Research Inc.
Summary Table A

DTN: SN0505L0212303.004

Test Conditions: Confining Pressure = 5.0 MPa / Pore Pressure = 4.5 MPa / Temperature = 125 °C

									Creep Experiments Ended With Failure				Moduli via Constant Strain Rate Portion Only	
Test Inventory Number	SMF Sample ID	Sample ID	Length (mm)	Diameter (mm)	Dry Bulk Density (g/cm^3)	Saturated Bulk Density (g/cm^3)	Porosity via Grain Density (%)	Predicted[+] Strength via Porosity (MPa)	Applied Constant Differential Stress (MPa)	Constant Stress as Percent of Predicted Strength (%)	Time to Failure (seconds)	Axial Strain at Failure (millistrain)	Young's Modulus (GPa)	Poisson's Ratio
1	01025485	ESF-HD-WH-38-13.1-C-1	101.7	50.83	2.285	2.370	8.72	230	173	75	47,430	8.29	33.5	0.27
2	01025486	ESF-HD-WH-38-14.9-C-1*	101.6	50.83	2.277	2.366	9.39	208					33.0	0.20
3	01025492	ESF-HD-WH-39-9.0-C-1*	101.6	50.83	2.277	2.366	9.91	191					33.1	0.26
4	01025495	ESF-HD-WH-40-0.8-A*	101.7	50.80	2.265	2.360	10.11	184					31.7	0.18
5	01025498	ESF-HD-WH-40-10.0-A	101.7	50.80	2.269	2.363	9.91	191	153	80	1,454	8.00	31.3	0.19
6	01025504	ESF-HD-WH-40-31.9-C-1	101.6	50.80	2.279	2.369	9.54	203	162	80	75,842	11.06	34.0	0.22
7	01025505	ESF-HD-WH-40-32.8-C-1*	101.7	50.80	2.297	2.381	8.96	222					33.7	0.00
8	01025512	ESF-HD-WH-44-34.0-A	101.5	50.77	2.287	2.371	8.78	228	182	80	209,620	8.32	32.3	0.36
9	01025512	ESF-HD-WH-44-34.0-B	101.6	50.75	2.283	2.365	8.92	224	179	80	360,532	8.33	34.9	0.31
10	01025513	ESF-HD-WH-44-34.7-A	101.5	50.80	2.283	2.365	8.67	232	186	80	15,644	8.09	35.4	0.17
11	01025514	ESF-HD-WH-44-35.4-A	101.5	50.77	2.276	2.366	9.30	211	168	100**	2	7.57	31.7	0.29
12	01025514	ESF-HD-WH-44-35.4-B	101.5	50.77	2.273	2.363	9.40	208	167	80	537	7.92	30.0	0.08
13	01025515	ESF-HD-WH-45-23.8-A*	101.6	50.80	2.290	2.374	9.23	213					35.2	0.23
14	01025521	ESF-HD-WH-48-33.9-A*	101.6	50.80	2.295	2.374	9.16	216					33.2	0.05
15	01025522	ESF-HD-WH-49-9.4-B	101.6	50.80	2.274	2.360	9.81	194	150	77	11,739	9.09	29.5	0.26
16	01025523	ESF-HD-WH-49-13.1-A*	101.6	50.77	2.223	2.330	12.42	108					26.3	0.28
17	01025524	ESF-HD-WH-49-14.9-A	101.6	50.80	2.265	2.359	9.71	198	158	80	5,653	8.90	30.5	0.01

*: Specimen did not fail during constant stress portion of test. Loaded to failure post-creep at constant strain rate.
**: Sample failed immediately after completion of loading, so applied load considered to be equal to actual strength.
[+]: Predicted Strength = (-33 X Porosity) + 518

Source: DTN: SN0505L0212303.004 [DIRS 174955].

Table 6-26. Results of the Second Group of Creep Tests that Ended *Without Failure*, July 12, 2004 to October 27, 2004

Time Dependent Testing at New England Research Inc.
Summary Table B
DTN: SN0505L0212303.004
Test Conditions: Confining Pressure = 5.0 MPa / Pore Pressure = 4.5 MPa / Temperature = 125 °C

									Creep Experiments Ended Without Failure					Moduli via Constant Strain Rate Portion Only	
Test Inventory Number	SMF Sample ID	Sample ID	Length	Diameter	Dry Bulk Density	Saturated Bulk Density	Porosity via Grain Density	Predicted[+] Strength via Porosity	Actual Strength Determined Post-Constant Stress	Applied Constant Differential Stress	Constant Stress as Percent of Actual Strength	Creep Test Duration	Creep Test Axial Strain	Young's Modulus	Poisson's Ratio
			(mm)	(mm)	(g/cm^3)	(g/cm^3)	(%)	(MPa)	(MPa)	(MPa)	(%)	(seconds)	(millistrain)	(GPa)	
1	01025485	ESF-HD-WH-38-13.1-C-1	101.7	50.83	2.285	2.370	8.72	230						33.5	0.27
2	01025486	ESF-HD-WH-38-14.9-C-1	101.6	50.83	2.277	2.366	9.39	208	186	156	84	2,501,287	6.33	33.0	0.20
3	01025492	ESF-HD-WH-39-9.0-C-1*	101.6	50.83	2.277	2.366	9.91	191	213	144	68	3,550,003	5.38	33.1	0.26
4	01025495	ESF-HD-WH-40-0.8-A*	101.7	50.80	2.265	2.360	10.11	184	207	138	67	777,870	4.90	31.7	0.18
5	01025498	ESF-HD-WH-40-10.0-A	101.7	50.80	2.269	2.363	9.91	191						31.3	0.19
6	01025504	ESF-HD-WH-40-31.9-C-1	101.6	50.80	2.279	2.369	9.54	203						34.0	0.22
7	01025505	ESF-HD-WH-40-32.8-C-1	101.7	50.80	2.297	2.381	8.96	222	254	167	66	2,657,141	5.68	33.7	0.00
8	01025512	ESF-HD-WH-44-34.0-A	101.5	50.77	2.287	2.371	8.78	228						32.3	0.36
9	01025512	ESF-HD-WH-44-34.0-B	101.6	50.75	2.283	2.365	8.92	224						34.9	0.31
10	01025513	ESF-HD-WH-44-34.7-A	101.5	50.80	2.283	2.365	8.67	232						35.4	0.17
11	01025514	ESF-HD-WH-44-35.4-A	101.5	50.77	2.276	2.366	9.30	211						31.7	0.29
12	01025514	ESF-HD-WH-44-35.4-B	101.5	50.77	2.273	2.363	9.40	208						30.0	0.08
13	01025515	ESF-HD-WH-45-23.8-A*	101.6	50.80	2.290	2.374	9.23	213	209	160	77	6,002,150	7.19	35.2	0.23
14	01025521	ESF-HD-WH-48-33.9-A*	101.6	50.80	2.295	2.374	9.16	216	250	160	64	3,594,292	6.72	33.2	0.05
15	01025522	ESF-HD-WH-49-9.4-B	101.6	50.80	2.274	2.360	9.81	194						29.5	0.26
16	01025523	ESF-HD-WH-49-13.1-A*	101.6	50.77	2.223	2.330	12.42	108	152	86	57	1,793,813	3.65	26.3	0.28
17	01025524	ESF-HD-WH-49-14.9-A	101.6	50.80	2.265	2.359	9.71	198						30.5	0.01

*: Specimen did not fail during constant stress portion of test. Loaded to failure post-creep at constant strain rate.
**: Sample failed immediately after completion of loading, so applied load considered to be equal to actual strength.
[+]: Predicted Strength = (-33 X Porosity) + 518

Source: DTN: SN0505L0212303.004 [DIRS 174955].

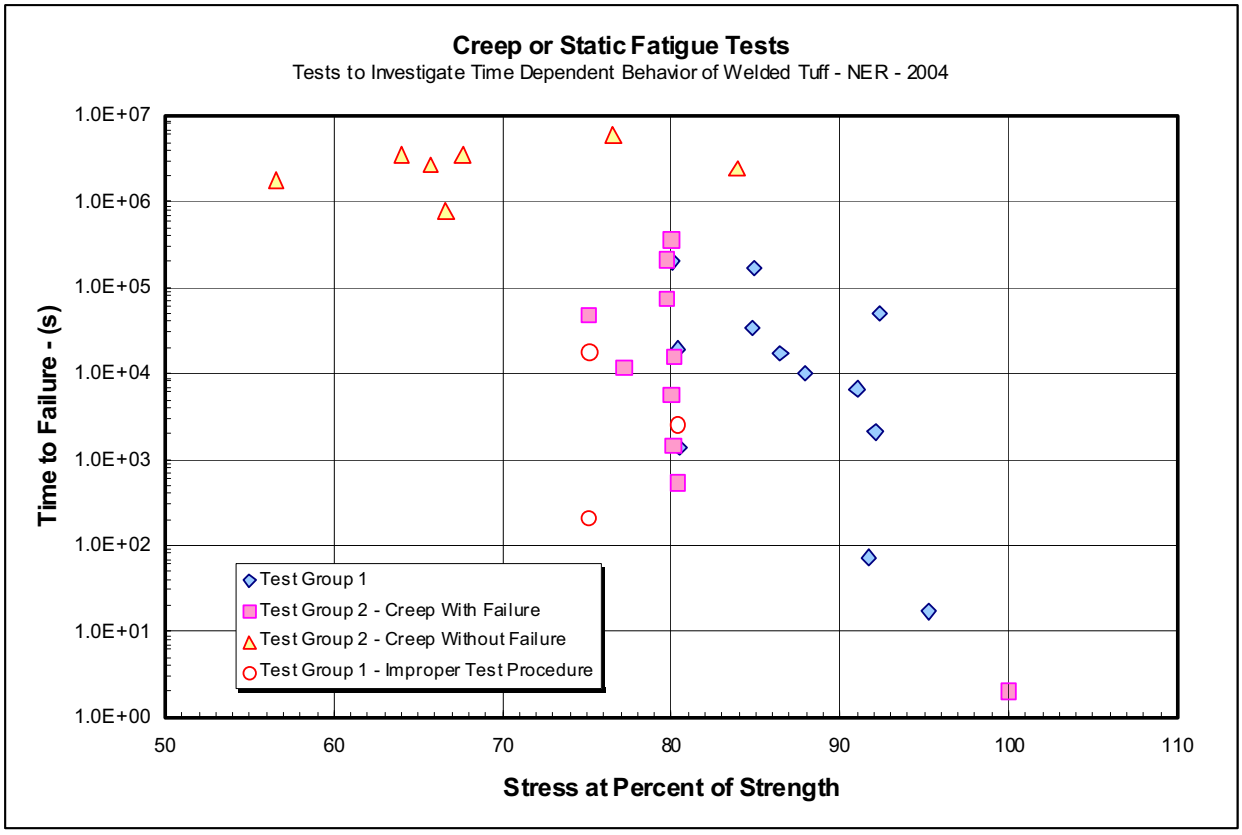

Sources: DTN: SN0406L0212303.002 [DIRS 170289]; SN0505L0212303.004 [DIRS 174955].

Figure 6-50. A Plot of Time to Failure as a Function of Stress Normalized by the Predicted Compressive Strength of the Intact Welded Tuff

Comparison of Static Fatigue Test Results on Granite and Tuff

The results of the earlier testing on nonlithophysal cores of Tptpmn (Martin et al. 1997 [DIRS 148875]) and the first group of tests performed during the period January 02, 2004 to February 25, 2004 (DTN: SN0406L0212303.002 [DIRS 170289]), as well as those from similar testing of Lac du Bonnet granite performed for the Canadian high-level radioactive waste program (Schmidtke and Lajtai 1985 [DIRS 164774]; Lau et al. 2000 [DIRS 164769]) are given in Figure 6-51. Granite results are included as a means of comparing the effects of rock type and for demonstrating the similarity in the general nature of the time-to-failure data for different rock types. Scatter in the data is due to sample inhomogeneity, as well as the fact that the driving stress ratio (the horizontal axis) uses an estimated value for the unconfined compressive strength (adjusted for sample porosity) for normalizing the applied stress level.

Since there is significant variability in the unconfined compressive strength of each sample, the scatter in the resulting plot of time-to-failure versus driving stress ratio is expected. As seen in Figure 6-51, the welded tuff has a slower static fatigue failure time than granite, as evidenced by the steeper slope of the linear fit to the data. This slower time-to-failure is presumably a result of the relatively homogeneous, fine-grained, high silica content nature of the tuff, as opposed to the heterogeneous nature of the grain structure of granite.

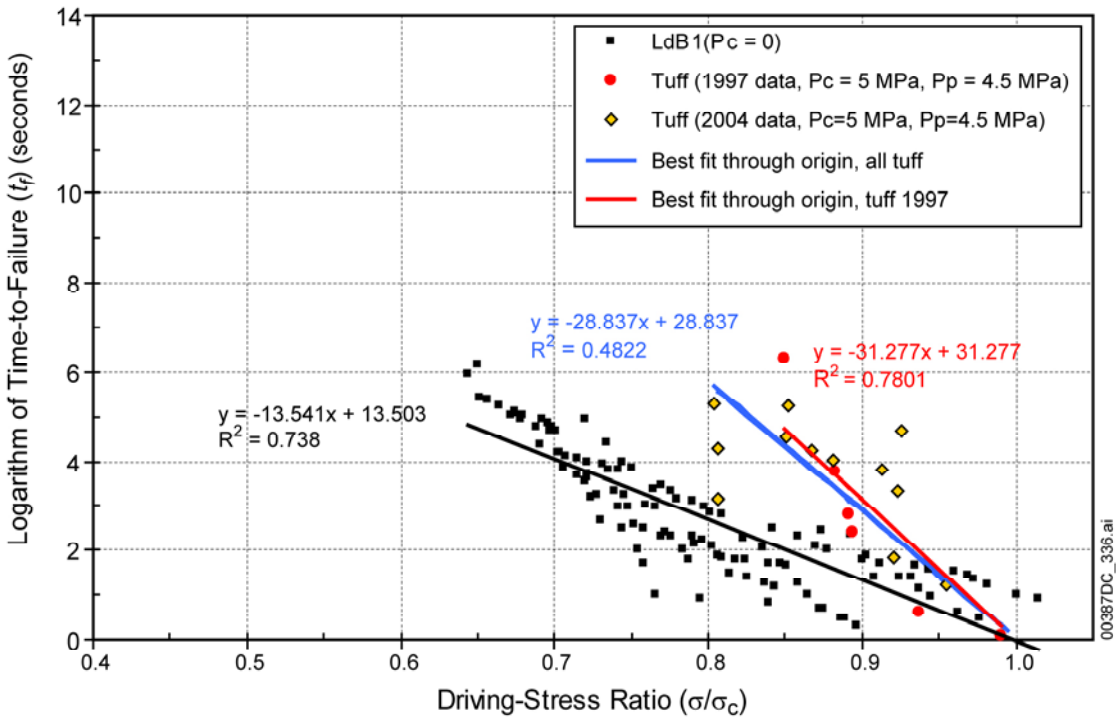

Source: BSC 2006 [DIRS 178277], Figure 1.

NOTES: Tests of Lac du Bonnet granite were conducted at 25°C. The driving stress ratio is defined as the ratio of applied constant test stress to the estimated unconfined compressive strength. 1997 tuff tests were conducted at 150°C, 2004 tuff tests were conducted at 125°C. LdB = Lac du Bonnet. Linear fits to 1997 Lac du Bonnet only and 1997 and 2004 tuff tests are shown. Samples that did not fail are also shown but not used in developing linear fits to data.

Figure 6-51. Example of Static-Fatigue Data and Time-To-Failure Estimates for Unconfined and Triaxial Compression of Heated, Saturated Welded Tuff and Lac du Bonnet Granite

Linear fits to the unconfined compression data of Lac du Bonnet granite and to the tuff 1997 data only and to the welded tuff data (including both 1997 and 2004 data) and the fits to both sets of welded tuff data are given. After these analyses were completed, the additional 2004 data were collected. The linear fits to the data sets show the general consistency of the overall slope of the fits, although there is considerably more scatter in the 2004 test results. Due to data uncertainty, a lower bound for the slope of the time-to-failure curve based on the Lac du Bonnet data, was also used in numerical simulation estimates. The static fatigue testing was performed on saturated tuff cores at elevated temperature, ensuring that the impact of water on time-dependent yielding was accounted for in the estimation of time-dependent effects on drift stability.

Creep of Artificial Joint (1995)

The time-dependent performance of the rock mass depends on the creep of both intact rock and rock joints. Olsson (1995 [DIRS 168736]) reports a simple creep test on an artificial joint. The joint was introduced into otherwise intact specimen prepared from rock samples obtained from Busted Butte, Topopah Spring Member of the Paintbrush Tuff. The specimen was assembled in the triaxial vessel and subjected to the stepwise increasing axial stress, while the confining pressure was kept constant at 10 MPa level.

Figure 6-52 shows the history of the shear stress normalized by the normal stress (τ/σ) and the corresponding slip history. Olsson (1995 [DIRS 168736]) observed that the majority of shear stress steps were accompanied by both immediate slip and transient slip. No steady state creep was observed. He also suggested that these observations imply that, under similar conditions, a smooth natural joint would probably not exhibit steady state, or for that matter, accelerating tertiary creep. According to Olsson (1995 [DIRS 168736], p. 7) it may also be expected that creep slip of a rough, interlocked natural fracture would be very unlikely.

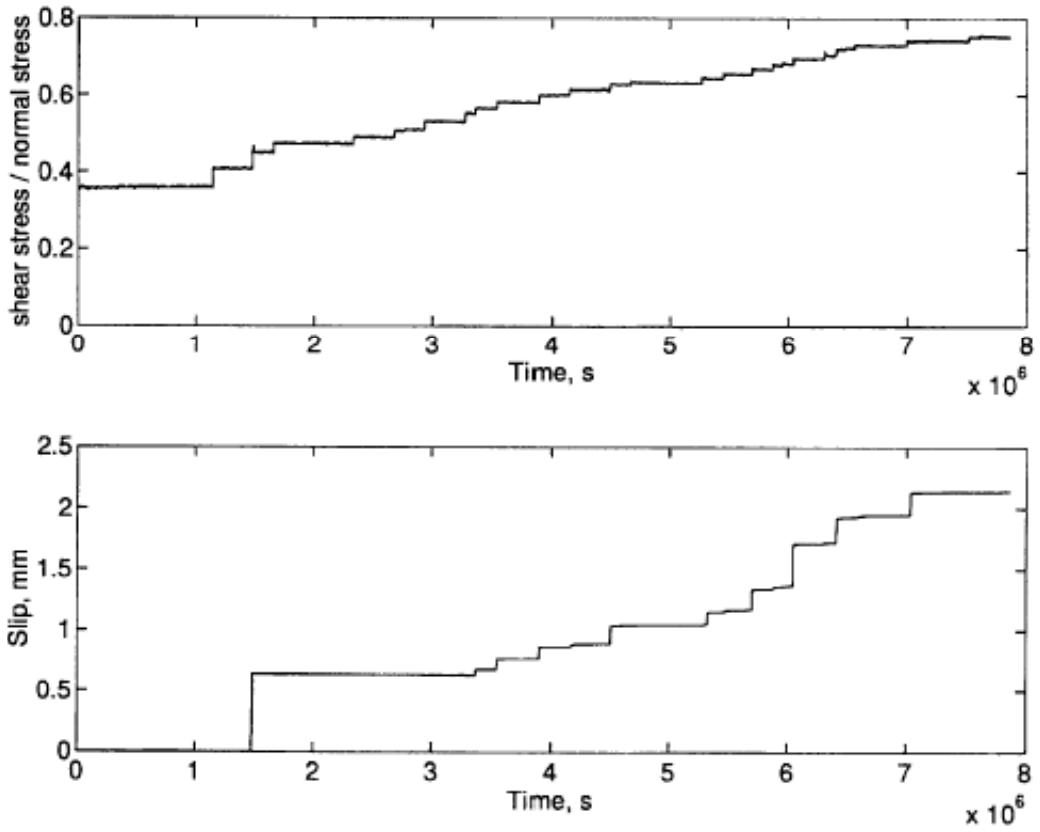

Source: Olsson 1995 [DIRS 168736], Figure 2.

NOTES: The top shows the applied stress in terms of shear stress divided by normal stress (τ/σ). The lower graph shows the resulting slip history.

Figure 6-52. Overall Test History for Creep Test on Artificial Sawcut Joint

Creep Tests – Summary

Observations related to the results of creep tests are summarized as follows:

1) The creep tests performed on Yucca Mountain Tuff indicate that tuff behaves much like a brittle hard rock in response to stress and temperature.

2) Tuff remains elastic over a wide range of stresses and often fails without prior "warning" displayed by other rock types in a form of increasing volumetric strain.

3) Strains accumulated during the series of tests designed to investigate the time-dependent behavior of the tuff, lead to the conclusion that tuff material behavior is consistent with simulations for creep in brittle silicate rocks based on SCC.

4) Presence of moisture results in higher creep rates than those observed for dry specimens.

5) The time-to-failure increases for the lower stress range.

6) The artificial joint displays similar behavior, where under confinement, slip occurs in response to the increasing axial stress, however, no long-term strain accumulation was observed.

In general, this type of rock behavior suggests that conventional creep tests performed routinely to determine rock time-dependent characteristics are not practical. Instead, static fatigue tests, which are performed at high stress levels relative to the uniaxial compressive strength are considered more appropriate, leading to determination of the time-to-failure, the parameter applicable in design of underground structures.

6.4.2.5 Corroborative Data

This section presents the corroborative data obtained from tests performed by organizations outside of the Project, such as University and Community College System of Nevada (UCCSN), and NRC. The purpose of presenting these data is from a corroborative viewpoint to compare or reinforce conclusions derived from the data gathered within a full QA-controlled domain. Only the static properties of intact tuff rocks for the planned RHH, i.e., Tptpul, Tptpmn, Tptpll, and the Tptpln zones, with focus on the Tptpmn and Tptpll zones, which are the primary rock units for waste emplacement, are included in this section.

6.4.2.5.1 Physical Properties

Table 6-27 presents dry bulk density results of RHH tuff rocks from 6-in cubic specimens. The average dry bulk density values for Tptpul, Tptpmn, and Tptpll zones are 1.88, 2.16, and 2.26 kg/m^3, respectively. The data presented in Table 6-28 include dry bulk density values from a number of cylindrical specimens from the Tptpmn zone. The average dry bulk density values range from 2.25 to 2.32 kg/m^3.

Tables 6-29 through 6-31 show the bulk density results of Tptpul, Tptpmn, and Tptpll zones. The saturation conditions of the specimens were not identified. The average bulk density values for these zones are 1.92 to 2.0, 2.22 to 2.31, and 2.07 to 2.19 kg/m^3, respectively. For the Tptpln zone, there is only one sample in this test conditions with a bulk density of 2.25 kg/m^3 (not shown in tables). It is noted that the average bulk density results for this test condition, i.e., saturation condition not identified, are generally similar to those tested for dry samples. Comparing these results with those presented in Table 6-6, it is observed that the results from the corroborative tests are slightly higher i.e., approximately 2% to 8% than those from the qualified sources. However, the trend is similar (i.e., the nonlithophysal units (Tptpmn and Tptpln) have the higher densities whereas the lithophysal units (Tptpul and Tptpll) have the lower values).

Table 6-27. Summary of Dry Bulk Density Results

Litho-stratigraphic Zone	Count	Dry Bulk Density (kg/m^3)						
		Mean	St. Dev.	St. Error	Median	Minimum	Maximum	Range
Tptpul	8	1.88	0.15	0.05	1.84	1.72	2.13	0.41
Tptpmn	5	2.16	0.06	0.03	2.15	2.09	2.23	0.14
Tptpll	2	2.26	0.01	0.00	2.26	2.25	2.26	0.01

Source: DTN: MO0302UCC027BA.006 [DIRS 177311].

NOTE: The density in this table is based on 6 in. cubic specimens.

Table 6-28. Summary of Dry Bulk Density Results—Tptpmn

Testing Group	Count	Dry Bulk Density (kg/m^3)						
		Mean	St. Dev.	St. Error	Median	Minimum	Maximum	Range
211111	1	2.29	N/A	N/A	2.29	2.29	2.29	0.00
211121	1	2.30	N/A	N/A	2.30	2.30	2.30	0.00
211131	1	2.28	N/A	N/A	2.28	2.28	2.28	0.00
2111X1	1	2.29	N/A	N/A	2.29	2.29	2.29	0.00
211211	14	2.28	0.03	0.01	2.29	2.23	2.33	0.10
211214	1	2.32	N/A	N/A	2.32	2.32	2.32	0.00
211221	8	2.28	0.02	0.01	2.28	2.24	2.31	0.06
211231	6	2.29	0.02	0.01	2.30	2.27	2.31	0.04
2112X1	1	2.32	N/A	N/A	2.32	2.32	2.32	0.00
211311	22	2.28	0.02	0.00	2.29	2.24	2.32	0.08
211321	25	2.26	0.06	0.01	2.28	1.99	2.31	0.32
211331	9	2.28	0.04	0.01	2.28	2.21	2.36	0.15
2113X1	3	2.25	0.04	0.02	2.23	2.22	2.30	0.08

Source: DTN: MO0311UCC018LM.001 [DIRS 177313].

NOTES: Designation of testing group is based on Table 6-3.

X in testing group denotes testing condition is not known.

Table 6-29. Summary of Bulk Density Results- Tptpul

Testing Group	Count	Bulk Density (kg/m^3)						
		Mean	St. Dev.	St. Error	Median	Minimum	Maximum	Range
2X1141	6	2.00	0.13	0.05	2.02	1.76	2.14	0.38
2X1241	6	1.92	0.07	0.03	1.92	1.82	2.02	0.20

Source: DTN: MO0311UCC018LM.001 [DIRS 177313].

NOTES: Designation of testing group is based on Table 6-3.

X in testing group denotes testing condition is not known.

Table 6-30. Summary of Bulk Density Results- Tptpmn

Testing Group	Count	Bulk Density (kg/m^3)						
		Mean	St. Dev.	St. Error	Median	Minimum	Maximum	Range
2X1111	1	2.29	N/A	N/A	2.29	2.29	2.29	0.00
2X1221	1	2.22	N/A	N/A	2.22	2.22	2.22	0.00
2X1321	1	2.25	N/A	N/A	2.25	2.25	2.25	0.00
2X1331	1	2.31	N/A	N/A	2.31	2.31	2.31	0.00

Source: DTN: MO0311UCC018LM.001 [DIRS 177313].

NOTES: Designation of testing group is based on Table 6-3.

X in testing group denotes testing condition is not known.

Table 6-31. Summary of Bulk Density Results- Tptpll

Testing Group	Count	Bulk Density (kg/m^3)						
		Mean	St. Dev.	St. Error	Median	Minimum	Maximum	Range
2X1141	1	2.18	N/A	N/A	2.18	2.18	2.18	0.00
2X1241	3	2.19	0.09	0.05	2.21	2.10	2.27	0.17
2X1341	1	2.07	N/A	N/A	2.07	2.07	2.07	0.00

Source: DTN: MO0311UCC018LM.001 [DIRS 177313].

NOTES: Designation of testing group is based on Table 6-3.

X in testing group denotes testing condition is not known.

Table 6-32 summarizes the matrix porosity data based on fifty-one cylindrical specimens. It should be noted that the porosity data presented in this table are measured by different investigators and estimated by different methods. The average matrix porosity values for the Tptpul, Tptpmn, Tptpll, and Tptpln zones are 17.61%, 12.13%, 11.76%, and 10.53%, respectively. Comparing these results with those presented in Figure 6-14, the corroborative data generally comparable to the qualified data presented in Section 6.4.1.

The values of total porosity are presented in Table 6-33 for the RHH zones. The Tptpul zone has the highest values whereas the values for the Tptpll zone are a little lower than those of the Tptpmn zone. The Tptpln zone has the lowest porosity. The reason for the porosity value of the Tptpll zone being lower than that of the Tptpmn zone is probably due to the fact that the lower lithophysal zone, such as the Tptpll, usually contains larger but fewer lithophysaes than the upper lithophysal zone, such as the Tptpul. Due to the limited number of specimens, i.e., two, the specimens for the Tptpll zone may not represent the larger lithophysae and result in smaller porosity value.

Figure 6-53 shows the relationship between total porosity and unconfined compressive strength based on the results of uniaxial compression tests on 6-in cubical specimens. This figure generally indicates that the compressive strength decreases with porosity. The middle nonlithophysal tuff, i.e., Tptpmn zone, has the highest compressive strength and lowest porosity whereas the upper lithophysal tuff, i.e., Tptpul zone, has the lowest compressive strength and highest porosity.

Table 6-32. Summary of Matrix Porosity Results

Litho-stratigraphic Zone	Count	Matrix Porosity (%)						
		Mean	St. Dev.	St. Error	Median	Minimum	Maximum	Range
Tptpul	10	17.61	4.24	1.34	17.65	12.40	28.00	15.60
Tptpmn	11	12.13	2.90	0.87	11.30	7.50	18.00	10.50
Tptpll	22	11.76	2.85	0.61	11.20	6.00	16.00	10.00
Tptpln	8	10.53	1.55	0.55	11.00	8.03	12.00	3.97

Source: Tien et al. 1985 [DIRS 102096].

Table 6-33. Summary of Total Porosity Results

Litho-stratigraphic Zone	Count	Porosity (%) (for ambient condition)						
		Mean	St. Dev.	St. Error	Median	Minimum	Maximum	Range
Tptpul	8	26.54	3.93	1.39	27.40	20.30	31.60	11.30
Tptpmn	5	13.72	2.43	1.09	13.90	11.20	16.30	5.10
Tptpll	2	13.35	0.07	0.05	13.35	13.30	13.40	0.10

Source: DTN: MO0302UCC027BA.006 [DIRS 177311].

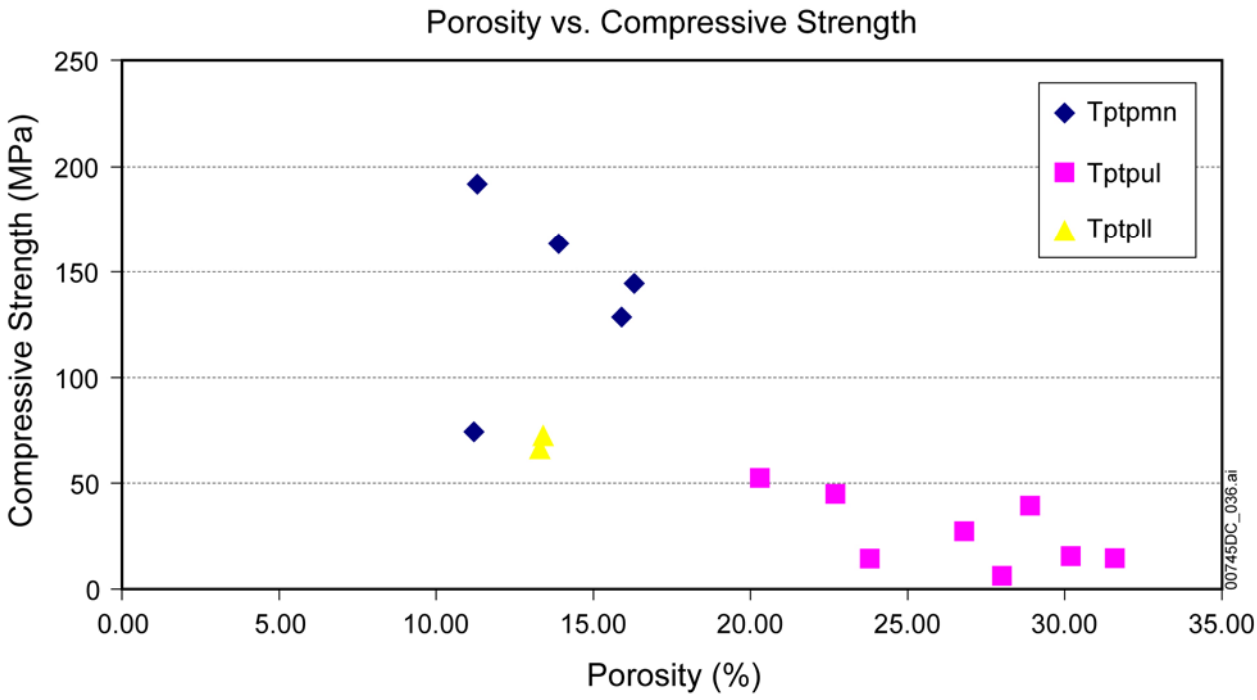

Source: DTN: MO0302UCC027BA.006 [DIRS 177311].

Figure 6-53. Porosity vs. Unconfined Compressive Strength

6.4.2.5.2 Strength Properties

6.4.2.5.2.1 Unconfined Compressive Strength

Tables 6-34 through 6-36 summarize the unconfined compressive strength results for a number of cylindrical specimens for the Tptpul, Tptpmn, and Tptpll zones (DTN: MO0311UCC018LM.001 [DIRS 177313]). The majority of data came from the Tptpmn zone with the remaining data for the other zones. The average unconfined compressive strength values for the Tptpul, Tptpmn, Tptpll, and Tptpln zones are 23.82 to 42.64, 121.69 to 263.06, 44.02 to 83.88, and 92.94 MPa, respectively. In comparison with the data shown in Table 6-8 where the average unconfined compressive strengths for these four zones are 16.12 to 65.21, 90.50 to 294.10, 15.70 to 213.18, and 104.40 to 171.55 MPa, respectively, the results are comparable.

Table 6-37 shows the unconfined compressive strength results for a number of 6-in cubical specimens for Tptpul, Tptpmn, and Tptpll zones (DTN: MO0302UCC027BA.006 [DIRS 177311]). The average unconfined compressive strength values for the Tptpul, Tptpmn, and Tptpll zones are 26.78, 140.55, and 69.20 MPa, respectively. These results are much higher UCS values when compare to those from larger cylindrical specimens of qualified sources (Table 6-8, code 331221).

Table 6-38 summarizes the unconfined compressive strength results from creep tests on cylindrical specimens (DTN: MO0311UCC018LM.003 [DIRS 177314]). The average unconfined compressive strength values for the Tptpmn, Tptpll, and Tptpln zones are 151.84, 103.53, and 143.93 MPa, respectively. Noted that the results for the Tptpll and Tptpln zones are only from one specimen each, which do not have any statistically significant value. The results of creep testing on the Tptpmn rock samples are comparable to those from short-term compression tests, indicating the insignificance of creep effect on nonlithophysal rock strength. Because of close resemblance in terms of matrix materials between nonlithophysal and lithophysal rock units, creep effect is not anticipated to be significant for the lithophysal rock either.

Table 6-34. Summary of Unconfined Compressive Strength Results—Tptpul

Code	Count	Unconfined Compressive Strength (MPa)						
		Mean	St. Dev.	St. Error	Median	Minimum	Maximum	Range
2X11X1	6	42.64	19.25	7.86	40.38	18.89	75.70	56.81
2X12X1	6	23.82	8.40	3.43	25.74	12.01	33.03	21.02

Source: DTN: MO0311UCC018LM.001 [DIRS 177313].

NOTE: X in testing group denotes testing condition is not known.

Table 6-35. Summary of Unconfined Compressive Strength Results—Tptpmn

Code	Count	Unconfined Compressive Strength (MPa)						
		Mean	St. Dev.	St. Error	Median	Minimum	Maximum	Range
211111	2	232.06	12.67	8.96	232.06	223.10	241.02	17.92
211121	1	261.63	N/A	N/A	261.63	261.63	261.63	0.00
211131	1	198.70	N/A	N/A	198.70	198.70	198.70	0.00
211141	1	133.55	N/A	N/A	133.55	133.55	133.55	0.00
211211	15	209.19	51.82	13.38	215.07	101.80	296.47	194.67
211214	1	264.26	N/A	N/A	264.26	264.26	264.26	0.00
211221	9	170.13	51.96	17.32	155.73	98.35	269.62	171.27
211231	6	249.27	31.44	12.83	256.57	209.32	285.88	76.56
211241	1	263.06	N/A	N/A	263.06	263.06	263.06	0.00
211311	23	172.48	49.01	10.22	173.21	91.07	275.22	184.15
211321	24	196.45	51.73	10.56	203.19	108.79	291.64	182.85
211331	10	188.52	41.60	13.15	205.18	107.78	228.02	120.24
211341	3	153.68	44.77	25.85	140.49	116.99	203.57	86.58
2x1111	1	241.02	N/A	N/A	241.02	241.02	241.02	0.00
2x1221	1	142.70	N/A	N/A	142.70	142.70	142.70	0.00
2x1321	1	121.69	N/A	N/A	121.69	121.69	121.69	0.00
2x1331	1	210.88	N/A	N/A	210.88	210.88	210.88	0.00

Source: DTN: MO0311UCC018LM.001 [DIRS 177313].

NOTE: X in testing group denotes testing condition is not known.

Table 6-36. Summary of Unconfined Compressive Strength Results—Tptpll

Code	Count	Unconfined Compressive Strength (MPa)						
		Mean	St. Dev.	St. Error	Median	Minimum	Maximum	Range
211341	1	80.53	N/A	N/A	80.53	80.53	80.53	0.00
2x1141	1	57.11	N/A	N/A	57.11	57.11	57.11	0.00
2x1241	3	83.88	22.06	12.74	94.31	58.54	98.80	40.26
2x1341	1	44.02	N/A	N/A	44.02	44.02	44.02	0.00

Source: DTN: MO0311UCC018LM.001 [DIRS 177313].

NOTE: X in testing group denotes testing condition is not known.

Table 6-37. Summary of Unconfined Compressive Strength Results

Lithostratigraphic Zone	Count	Compressive Strength (MPa) (for ambient condition)						
		Mean	St. Dev.	St. Error	Median	Minimum	Maximum	Range
Tptpul	8	26.78	16.92	5.98	21.39	6.13	52.46	46.33
Tptpmn	5	140.55	43.83	19.60	144.46	74.40	191.83	117.43
Tptpll	2	69.20	4.41	3.12	69.20	66.08	72.31	6.23

Source: DTN: MO0302UCC027BA.006 [DIRS 177311].

Table 6-38. Summary of Unconfined Compressive Strength Results – Creep Test

Lithostratigraphic Zone	Count	Compressive Strength (MPa) (for oven dry data)						
		Mean	St. Dev.	St. Error	Median	Minimum	Maximum	Range
Tptpmn	11	151.84	46.63	14.06	168.77	89.65	200.79	111.14
Tptpll	1	103.53	N/A	N/A	103.53	103.53	103.53	0.00
Tptpln	1	143.93	N/A	N/A	143.93	143.93	143.93	0.00

Source: DTN: MO0311UCC018LM.003 [DIRS 177314].

6.4.2.5.2.2 Intact Rock Tensile Strength

Indirect tensile strength data for 157 intact rock specimens were obtained from boreholes in ESF HD, ESF main drift niches, UE-25 UZ#16, and USW UZ-14 (DTN: MO0311UCC018LM.002 [DIRS 177315]). All data from the ESF drifts/niches, i.e., 154 data are in the Tptpmn zone whereas the remaining 3 data were from the Tptpll zone. All samples were 2.4 in. in diameter except 11 specimens from the ESF main drift niches, which were 1.8 in diameter, with thicknesses ranging from 0.6 to 1.5 in. A summary of test results is shown in Table 6-39. The distribution of indirect tensile strengths for all the specimens from the Tptpmn zone is shown in Figure 6-54.

It should be noted that the indirect tensile strengths presented in this section are obtained from Brazilian tensile strength tests, which is the most commonly used method. The test methods are standard and are described by Mellor and Hawkes (1971 [DIRS 161566]) or in ASTM D 3967-95a, *Standard Test Method for Splitting Tensile Strength of Intact Rock Core Specimens* [DIRS 108612]. The test specimens were oven dried and the tests were performed in ambient temperature condition.

As it is shown in Table 6-39, the average indirect tensile strength for the Tptpmn and Tptpll zones are 15.82 and 8.5 MPa, respectively. Figure 6-54 shows the frequency histogram of indirect tensile strengths for the Tptpmn zone. As can be seen in the figure, the majority of the data falls into the 15 to 20 MPa range. Based on Table 6-13, the average indirect tensile strength of qualified data for the Tptpmn and Tptpll zones are 10.88 and 8.33 MPa, respectively indicating the corroborative data to be lower by 40% for Tptpmn and 1% for Tptpll. It should be noted that the indirect tensile strength presented in Table 6-13 are based on saturated specimens. The difference may be due to the difference in saturation condition. However, since there are many factors to be considered, such as saturation, temperature, sample size, L:D ratio, number of samples, no conclusions can be made on the relationship between the saturated samples and oven dry samples.

Table 6-39. Summary of Indirect Tensile Strength Results (Oven Dry Data)

Lithostratigraphic Zone	Count	Tensile Strength (MPa) (for oven dry data)						
		Mean	St. Dev.	St. Error	Median	Minimum	Maximum	Range
Tptpmn	154	15.82	3.75	0.30	16.06	4.51	26.62	22.12
Tptpll	3	8.50	1.63	0.94	8.50	6.87	10.13	3.26

Source: DTN: MO0311UCC018LM.002 [DIRS 177315].

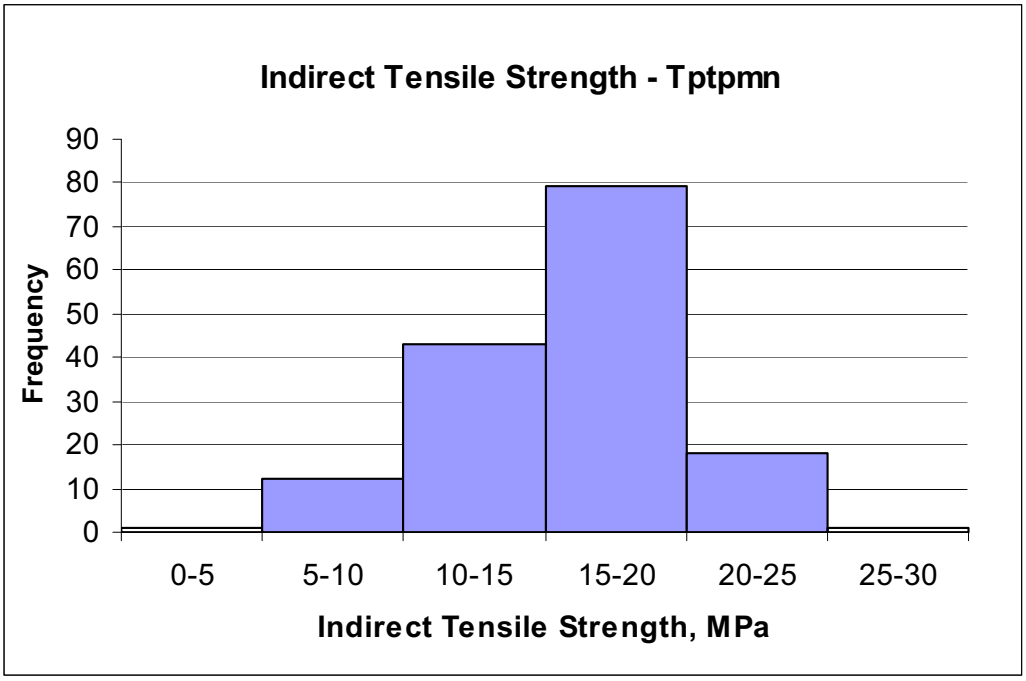

Source: DTN: MO0311UCC018LM.002 [DIRS 177315].

Figure 6-54. Distribution of Indirect Tensile Strength

6.4.2.5.3 Elastic Properties

Elastic property data presented in this section come from different studies performed by several laboratories (DTNs: MO0311UCC018LM.001 [DIRS 177313]; MO0302UCC027BA.006 [DIRS 177311]; MO0311UCC018LM.003 [DIRS 177314]).

6.4.2.5.3.1 Intact Rock Young's Modulus

Tables 6-40 and 6-41 summarize the Young's modulus results for a number of cylindrical specimens for the Tptpmn and Tptpll zones (DTN: MO0311UCC018LM.001 [DIRS 177313]). The majority of data came from the Tptpmn zone with the remaining data originating from the other zones. The average Young's modulus values for the Tptpul, Tptpmn, Tptpll, and Tptpln zones are 27.97, 29.57 to 41.62, 20.91 to 46.90, and 22.77 GPa, respectively (note that data for the Tptpul and Tptpln are not shown in tables since there is only one data point for each of these units from this source). In comparison with the qualified data presented in Table 6-15 the corroborative data are generally comparable to the Tptpmn and Tptpll zones and a slightly higher for the Tptpul and Tptpln zones. Since there is only one data point for each of those two zones, no conclusions can be made due to the lack of representative data.

Table 6-42 shows the Young's modulus results for a number of 6-in cubical specimens for the Tptpul, Tptpmn, and Tptpll zones (DTN: MO0302UCC027BA.006 [DIRS 177311]). The average Young's modulus values for the Tptpul, Tptpmn, and Tptpll zones are 4.16, 14.15, and 8.54 GPa, respectively. These results are smaller than those from lower cylindrical specimens.

It is not certain whether this difference is due to the specimen size and/or shape effect due to the small number of tested specimens.

Table 6-43 summarizes the Young's modulus results from creep tests on cylindrical specimens (DTN: MO0311UCC018LM.003 [DIRS 177314]). The average Young's modulus values for the Tptpmn, Tptpll, and Tptpln zones are 38.14, 42.18, and 41.40 GPa, respectively. In general, the results of Young's modulus from the creep tests are comparable to those from short-term compression tests. It should be noted that the Young's modulus values of Tptpll and Tptpln zones (Table 6-43) are only from one sample each, which cannot be considered as representative.

Table 6-40. Summary of Young's Modulus Results—Tptpmn

Code	Count	Young's Modulus (GPa)						
		Mean	St. Dev.	St. Error	Median	Minimum	Maximum	Range
211111	2	35.10	0.69	0.48	35.10	34.61	35.58	0.97
211121	1	36.18	N/A	N/A	36.18	36.18	36.18	0.00
211131	1	41.62	N/A	N/A	41.62	41.62	41.62	0.00
211141	1	29.57	N/A	N/A	29.57	29.57	29.57	0.00
211211	15	33.15	3.05	0.79	34.35	28.24	37.12	8.88
211214	1	35.91	N/A	N/A	35.91	35.91	35.91	0.00
211221	9	34.20	7.13	2.38	34.15	22.17	46.46	24.29
211231	6	37.10	3.14	1.28	35.92	35.06	43.22	8.16
211241	1	34.10	N/A	N/A	34.10	34.10	34.10	0.00
211311	23	35.85	3.96	0.83	35.42	28.15	46.55	18.40
211321	24	35.67	2.19	0.45	35.65	31.09	41.73	10.64
211331	10	36.65	1.85	0.58	36.44	33.85	39.36	5.51
211341	3	31.76	0.98	0.57	31.98	30.68	32.61	1.93
2x1111	1	35.58	N/A	N/A	35.58	35.58	35.58	0.00
2x1221	1	34.15	N/A	N/A	34.15	34.15	34.15	0.00
2x1321	1	35.94	N/A	N/A	35.94	35.94	35.94	0.00
2x1331	1	39.28	N/A	N/A	39.28	39.28	39.28	0.00

Source: DTN: MO0311UCC018LM.001 [DIRS 177313].

NOTE: X in testing group denotes testing condition is not known.

Table 6-41. Summary of Young's Modulus Results—Tptpll

Code	Count	Yung's Modulus (GPa)						
		Mean	St. Dev.	St. Error	Median	Minimum	Maximum	Range
211341	1	46.90	N/A	N/A	46.90	46.90	46.90	0.00
2x1241	1	25.73	N/A	N/A	25.73	25.73	25.73	0.00
2x1341	1	20.91	N/A	N/A	20.91	20.91	20.91	0.00

Source: DTN: MO0311UCC018LM.001 [DIRS 177313].

NOTE: X in testing group denotes testing condition is not known.

Table 6-42. Summary of Young's Modulus Results

Lithostratigraphic Zone	Count	Young's Modulus (GPa) (for ambient condition)						
		Mean	St. Dev.	St. Error	Median	Minimum	Maximum	Range
Tptpul	8	4.16	2.48	0.88	4.07	0.95	8.58	7.63
Tptpmn	5	14.15	3.47	1.55	13.78	10.94	19.07	8.13
Tptpll	2	8.54	1.41	0.99	8.54	7.54	9.53	1.99

Source: DTN: MO0302UCC027BA.006 [DIRS 177311].

Table 6-43. Summary of Young's Modulus Results – Creep Test

Lithostratigraphic Zone	Count	Young's Modulus (GPa) (for oven dry data)						
		Mean	St. Dev.	St. Error	Median	Minimum	Maximum	Range
Tptpmn	11	38.14	4.64	1.40	36.67	32.58	45.73	13.15
Tptpll	1	42.18	N/A	N/A	42.18	42.18	42.18	0.00
Tptpln	1	41.40	N/A	N/A	41.40	41.40	41.40	0.00

Source: DTN: MO0311UCC018LM.003 [DIRS 177314].

6.4.2.5.3.2 Intact Rock Poisson's Ratio

Tables 6-44 through 6-46 summarize the Poisson's ratio results for a number of cylindrical specimens for the Tptpul, Tptpmn and Tptpll zones (DTN: MO0311UCC018LM.001 [DIRS 177313]). The majority of data came from the Tptpmn zone with the remaining data originating from the other zones. The average Poisson's ratio values for the Tptpul, Tptpmn, Tptpll, and Tptpln zones are 0.19, 0.11 to 0.19, 0.13 to 0.24, and 0.13, respectively (data for the Tptpln zone is not shown in tables since there is only one data point from the source). For comparison with the qualified data presented in Table 6-19, the corroborative data are generally comparable for all zones.

Table 6-47 summarizes the Poisson's ratio results from creep tests on cylindrical specimens (DTN: MO0311UCC018LM.003 [DIRS 177314]). The average Poisson's ratio values for the Tptpmn, Tptpll, and Tptpln zones are 0.17, 0.22 and 0.20, respectively. In general, the results of Poisson's ratio from the creep tests are comparable to those from short-term compression tests and fall into the same range of values from those in Tables 6-24 through 6-26.

Table 6-44. Summary of Poisson's Ratio—Tptpul

Code	Count	Poisson's Ratio						
		Mean	St. Dev.	St. Error	Median	Minimum	Maximum	Range
2x11x1	3	0.19	0.05	0.03	0.20	0.14	0.24	0.10

Source: DTN: MO0311UCC018LM.001 [DIRS 177313].

NOTE: X in testing group denotes testing condition is not known.

Table 6-45. Summary of Poisson's Ratio—Tptpmn

Code	Count	Poisson's Ratio						
		Mean	St. Dev.	St. Error	Median	Minimum	Maximum	Range
211111	1	0.19	N/A	N/A	0.19	0.19	0.19	0.00
211121	1	0.18	N/A	N/A	0.18	0.18	0.18	0.00
211131	1	0.17	N/A	N/A	0.17	0.17	0.17	0.00
2111x1	1	0.18	N/A	N/A	0.18	0.18	0.18	0.00
211211	10	0.16	0.03	0.01	0.16	0.12	0.20	0.08
211214	1	0.15	N/A	N/A	0.15	0.15	0.15	0.00
211221	8	0.19	0.03	0.01	0.18	0.15	0.25	0.10
211231	6	0.15	0.02	0.01	0.15	0.12	0.17	0.05
211311	17	0.16	0.04	0.01	0.16	0.11	0.23	0.12
211321	22	0.17	0.03	0.01	0.17	0.12	0.22	0.10
211331	10	0.16	0.02	0.01	0.16	0.13	0.20	0.07
2113x1	3	0.16	0.01	0.00	0.16	0.15	0.16	0.01
2x1111	1	0.19	N/A	N/A	0.19	0.19	0.19	0.00
2x1221	1	0.16	N/A	N/A	0.16	0.16	0.16	0.00
2x1321	1	0.11	N/A	N/A	0.11	0.11	0.11	0.00
2x1331	1	0.16	N/A	N/A	0.16	0.16	0.16	0.00

Source: DTN: MO0311UCC018LM.001 [DIRS 177313].

Table 6-46. Summary of Poisson's Ratio—Tptpll

Code	Count	Poisson's Ratio						
		Mean	St. Dev.	St. Error	Median	Minimum	Maximum	Range
2113x1	1	0.24	N/A	N/A	0.24	0.24	0.24	0.00
2x12x1	1	0.13	N/A	N/A	0.13	0.13	0.13	0.00
2413x1	1	0.22	N/A	N/A	0.22	0.22	0.22	0.00

Source: DTN: MO0311UCC018LM.001 [DIRS 177313].

NOTE: X in testing group denotes testing condition is not known.

Table 6-47. Summary of Poisson's Ratio

Lithostratigraphic Zone	Count	Poisson's Ratio (for oven dry data)						
		Mean	St. Dev.	St. Error	Median	Minimum	Maximum	Range
Tptpmn	11	0.17	0.02	0.01	0.17	0.13	0.20	0.07
Tptpll	1	0.22	N/A	N/A	0.22	0.22	0.22	0.00
Tptpln	1	0.20	N/A	N/A	0.20	0.20	0.20	0.00

Source: DTN: MO0311UCC018LM.003 [DIRS 177314].

6.4.2.6 Discussion

The analysis of intact rock mechanical properties data are summarized in Tables 6-8, 6-9, 6-12, 6-14, 6-15, 6-17 through 6-19 and 6-21.

In addition, the effects of physical and environment conditions on intact rock mechanical properties were analyzed. To examine the variations in testing or environmental conditions a code system has been introduced as shown on Table 6-3. A testing code combination of 231221 is set for baseline conditions and the effect of changes in strength and elastic properties are summarized in Tables 6-9, 6-15, and 6-19.

The intact rock properties summarized in this section are used for the estimation of rock mass properties (Section 6.4.4). The intact rock properties data summarized in this section are considered suitable for the intended uses: supporting the subsurface design, developing the preclosure safety analysis, and assessing the postclosure performance of the repository (e.g., drift degradation and simulation of rockfall impacts on engineered barrier system components). However, the results of intact rock mechanical properties data presented in this document have limitations as described in Section 1.4. Therefore, the user should be aware of these limitations prior to using these intact rock mechanical data.

The corroborative data for planned RHH zones, i.e., Tptpul, Tptpmn, Tptpll, and the Tptpln zones, with focus on Tptpmn and Tptpll zones, are examined. In general, the physical, strength, and elastic properties from the corroborative data are comparable to the corresponding qualified data. Some difference in average and range data exists for certain types of data. However, the difference is mainly caused by limited number of data, different test laboratories, different test methods and specimen conditions, as well as different environmental conditions.

6.4.3 Mechanical Properties of Rock Joints/Fractures

The characterization of mechanical properties of rock fractures has direct relevance to repository design and the pre- and post-closure performance assessments. Characteristics of fractures are an important component of input to the major rock mass classification systems and tunnel rockfall analysis. The fracture behaviors considered in this report encompass fracture strength (cohesion, friction angle), dilation, and fracture stiffness (normal and shear stiffness). This section summarizes the methods and results of rock fracture characterization used by the YMP.

6.4.3.1 Experimental Methods

Two types of shear testing techniques have been used to investigate site-specific Yucca Mountain natural fractures. SNL conducted rotary shear tests on fracture samples mostly from vertical boreholes drilled in the 1990s and the USBR performed direct shear tests on samples taken from horizontal drill holes in the ECRB Cross-Drift in the early 2000s. These tests of rock fractures are mainly from the RHH lithostratigraphic zones with additional rotary shear tests on zones outside of the RHH and are described in this section.

Shear strength values may be determined at peak, ultimate, or residual strength values. “Peak” refers to the maximum shear stress, “ultimate” refers to the steady-state shear stress reached with continued shearing, and “residual” refers to the lower-bound shear strength when damage has removed all asperities. These terms are defined more completely below.

6.4.3.1.1 Rotary Shear Tests

SNL performed rotary shear tests on 22 samples with natural fractures from the RHH zones and from samples taken from drill holes USW-NRG-6, USW-NRG-7, USW-SD-7, USW-SD-9, USW-SD-12, and ESF-TMA-MPBX-3. Six samples were from lithophysal rock (one Tptpul and five Tptpll) and 16 were from nonlithophysal rock units (nine Tptpmn and seven Tptpln). All samples were taken from intact core pieces, the largest of which was approximately 76 mm (3 in.) in diameter, so larger scale roughness and any effects of lithophysae were not represented in these tests. All of the lithophysal rock tests were performed at room temperature. Eight of the nonlithophysal samples were tested at room temperature while the other eight were tested at 175°C. The data for the 22 tests are reported in the following DTNs: SNL02112293001.001 [DIRS 161629], SNL02112293001.003 [DIRS 108412], SNL02112293001.005 [DIRS 108413], SNL02112293001.006 [DIRS 159992], and SNL02112293001.007 [DIRS 108414].

SNL also performed rotary shear tests on 20 samples with natural fractures from non-RHH zones and taken from drill holes USW-NRG-4, USW-NRG-6, USW-NRG-7, and USW-SD-9. These data are reported in the following DTNs: SNL02112293001.001 [DIRS 161629], SNL02112293001.002 [DIRS 108411], SNL02112293001.003 [DIRS 108412], SNL02112293001.005 [DIRS 108413], and SNL02112293001.007 [DIRS 108414].

No physical descriptions were given of the fractures and no pictures were taken, so it is not possible to identify the type of fracture (e.g., vapor phase partings (VPP)). It may be possible to examine the photos of the cores to get an idea of the fracture type. Only some samples have a profile height plot provided. Also, no description was provided about infilling materials or mineralization on the fracture and the damaged material created by shearing.

Profilometer measurements were taken but the reported fractal surface roughness values are not helpful in making geomechanical classifications for tunnel design. The precondition to use fractal dimensions in characterizing roughness is that the topographical patterns of the fracture surface were considered to be self-affine, i.e. that the topographical patterns of rock joints are the same at all scales (the rule of self-similarity). However, this conflicts with the observed scale-dependency of the fracture surface roughness. Moreover, although the same fractal roughness parameters were measured for equivalent fracture morphologies, these same fractures have different physical properties. This may result from the randomness of the asperity distributions and the uncertainties inherent in asperity measurements. Preliminary efforts to correlate reported fractal roughness parameters to joint roughness coefficient (JRC) values have not been successful.

The rotary testing did not follow a published procedure, however the testing was based on a proposed ASTM procedure for rotary shear testing, and source SNL reports describe the procedure. In the rotary shear tests, the specimens were composed of two, short, hollow tubes surrounding the sample, divided at mid-height by the fracture. Samples were prepared by subcoring perpendicular to the fracture. Outer specimen diameters ranged from 44.2-75.9 mm (1.74-2.99 in.), but twenty specimens were about 44.3 mm in diameter. Inner specimen diameters ranged from 19.5-41.3 mm (0.77-1.63 in.), but most were about 19.6 mm. Considering the typical dimensions, the fracture area tested was generally about 1240 mm^2

(1.9 in^2). Test specimens were potted into metal specimen holders with gypsum-based hydraulic cement. The metal specimen holders were then bolted into the load-frame.

Stress was applied normal to the fracture while the change in fracture aperture was measured with LVDTs. One normal loading and unloading cycle was performed up to the pre-selected normal stress to obtain normal stiffness values and help mate the fracture before the sample was sheared.

The shear test was carried out by applying torque to the top sample in order to measure the shear stiffness and resulting sliding on the interface. All samples were sheared at constant normal stress in the air-dry condition with prevailing laboratory relative humidity of approximately 20% (Olsson and Brown 1997 [DIRS 106453], p. 14). Further testing details may be obtained from Olsson (1987 [DIRS 102935]). For each test, plots were provided showing normal stress vs. joint closure, shear stress vs. corrected shear displacement and dilation vs. corrected shear displacement. Friction angles were not determined for individual fracture surfaces as shear tests were performed at only one normal stress on each fracture. Olsson and Brown (1997 [DIRS 106453], p. 10) concluded it would be inappropriate to run multiple tests on the same fracture at incrementally increased normal stresses because the shear strength of these fractures is a strong function of plastic strain history (asperity damage).

The general literature specifically describing rotary shear tests on rock samples is sparse. One difficulty with this type of test equipment is that a gradient of shear stress and displacement exists across the sample during shearing. For the typical Yucca Mountain specimens tested, the rate of rotary shear displacement at the outer diameter is more than twice that of the inner diameter, implying that peak strength and peak dilation will occur at the outer part of the specimen first. While this makes estimation of specimen peak strength and dilation values difficult, the determination of ultimate shear strength in rotary devices can be reliable.

6.4.3.1.2 Direct Shear Tests

The USBR performed direct shear tests on five samples with natural fractures from nonlithophysal rock (Tptpmn) taken from drill holes in the ECRB Cross-Drift near Station 12+50. All of the shear tests were apparently performed at ambient conditions (room temperature and air-dry). The data for the 5 tests are reported in GS031083114222.002 [DIRS 177299]. No documentation is currently available describing the testing equipment that was used.

The fractures were identified by type (3 VPP and 2 cooling joints were tested) and digital images were taken of the fracture surfaces before and after testing. The JRC values were determined for each fracture before testing and roughness profiles were sketched both before and after shear testing. No discussion was given about whether vapor-phase crystals or minerals were present on the fracture and the damaged material created by shearing was neither analyzed nor retained.

YMP-USGS Technical Procedure YMP-USGS-GP-56, R0, *Method for Performing Laboratory Direct Shear Strength Tests on Rock Specimens Under Constant Normal Force with Allowance for Elevated Temperature* [DIRS 165435], was used to conduct the tests. Samples were prepared from the as-received core and encapsulated into the circular direct shear rings. Specimens were

generally irregularly shaped with shearing lengths with the range of 142 to 246 mm (5.6 to 9.7 in.). Top and bottom samples were roughly the same size.

A small normal load was applied to the fracture to help seat the sample. Then the load was continuously increased up to the pre-selected normal stress but the measurements of normal fracture displacement were not recorded. As a result, no normal stiffness parameters could be determined from these fractures.

Direct shear tests were conducted by applying shear load to the top fracture sample. Shear displacement measurements were made on the sample itself to minimize machine dependent displacement. All samples were sheared at constant normal stress to some distance beyond the peak shear value, but in general, the direct shear tests were not sheared sufficiently to obtain ultimate shear stress values. In particular, some tests on fractures were experiencing positive dilation and increasing shear stress when shearing was stopped. Ultimate shear stress is defined as the maximum stress reached after continued shearing under a constant normal stress when both shear strength and dilation angle no longer increase.

Next the sample was opened, blown free of damaged material and then repositioned back to the zero start position ready for shearing under a higher normal load increment. Each fracture sample was tested at four normal stresses in the following sequence: 1, 4, 7 and 1 MPa. The final Slide 4 test at 1 MPa represented a measure of degraded strength. Nominal shear area corrections were made as part of the normal and shear stress calculations. Friction angles were determined for individual joint surfaces between successive shear tests on the same joint.

Direct shear test equipment may not create a uniform normal stress distribution across the fracture surface during shearing. If the line of action of the applied shear force does not coincide with the average fracture plane, a moment may be created in loading the top moving sample that often produces higher normal and shear stresses on the front half of the shearing specimen. The effect of this is often evident in the increased damage found on the front half of the fracture surfaces. The Yucca Mountain direct shear specimens have not been examined for this effect and stresses were calculated using the total “apparent” interface contact area determined before testing.

6.4.3.2 Fracture Strength Behavior

Cohesion, c, and friction angle, ϕ, are measured to determine the behavior of Yucca Mountain rock fractures. The linear Coulomb law is used for simulation of shear strength by fitting the failure data to a straight line in a shear stress versus normal stress plot. Shear tests on an individual fracture includes one or more pairs of normal stress and peak or ultimate shear stress values. For example, using the following equation, the peak strength cohesion and friction angle parameters can be determined by plotting and making a linear fit of data pairs from one or more fractures:

$$\tau_p = \sigma \tan\phi_j + c_j \qquad \text{(Eq. 6-11)}$$

where, τ_p = peak shear stress (MPa)
ϕ_j = fracture friction angle
σ = normal stress (MPa)
c_j = fracture cohesion (MPa).

Experimental shear stress-shear displacement curves are generally of two types, characterized by an increase to a peak stress, $\tau_{p,}$ which may or may not be followed by a descent to an ultimate strength value, τ_r. The first type typically has a relatively rapid rise to a peak value, followed by an irregular decrease to an ultimate value. For the other type, the increase in shear stress is more gradual up to a poorly defined peak stress value. Residual strength is the frictional shear strength of smooth rock surfaces after all asperities have been removed through damage corresponding to a specific normal stress; residual strength has no cohesive strength component.

6.4.3.2.1 Rotary Shear Test Results

The fracture strength parameters determined from the rotary shear tests are reported in Table 6-48. Figures 6-55 and 6-56 illustrate plots of normal stress versus peak shear stress and residual shear stress, respectively. It should be noted that individual fractures are tested at only one normal stress. Multiple testing of the same fracture under increasing normal stresses was not done so that virgin peak strengths could be determined.

In the reported results it is considered that the specimen peak shear strength and dilation angle are the respective highest values measured. Because of the gradient problem in rotary tests mentioned earlier, these values might be biased in underrepresenting the actual values.

Table 6-48. Summary Statistics of Fracture Strength Using Rotary Shear

Lithostratigraphic Zone	Temp. (°C)	Count	Peak Cohesion (MPa)	Peak Friction Angle (deg)	Peak CC*
Tpcpll	Room	1	NA	46	NA
Tpcpln	Room	1	NA	46	NA
Tptrn	Room	13	1.75	37	0.84
Tptrl	Room	1	NA	55	NA
Tptpul	Room	1	NA	NA	NA
Tptpmn	Room	3	0**	51	0.97
Tptpmn	175	6	1.87	40	1.0
Tptpll	Room	5	1.30	40	0.93
Tptpln	Room	5	1.61	35	0.87
Tptpln	175	2	0.72	48	1.0
Tac	Room	4	1.69	38	0.83

Sources: DTNs: SNL02112293001.001 [DIRS 161629]; SNL02112293001.002 [DIRS 108411]; SNL02112293001.003 [DIRS 108412]; SNL02112293001.005 [DIRS 108413]; SNL02112293001.006 [DIRS 159992]; SNL02112293001.007 [DIRS 108414].

NOTE: CC* refers to the correlation coefficient of a linear fit through the data.

** Value set to zero when the linear fit appears negative value.

For the rotary tests, the dilation angle is the arctangent of the instantaneous slope of the dilation versus shear displacement curve, and the value reported is the dilation angle at peak stress. Estimates of peak shear strength and thus peak dilation angle appear to have been chosen somewhat arbitrarily, in part due to the smoothly increasing shear stresses.

Statistics on fracture dilation data are provided in Table 6-49. The large range in values illustrates the reason why the fractures should have been classified by fracture type. From the reported tests, no conclusion can be drawn as to the effect of temperature on dilation angle (Figure 6-57).

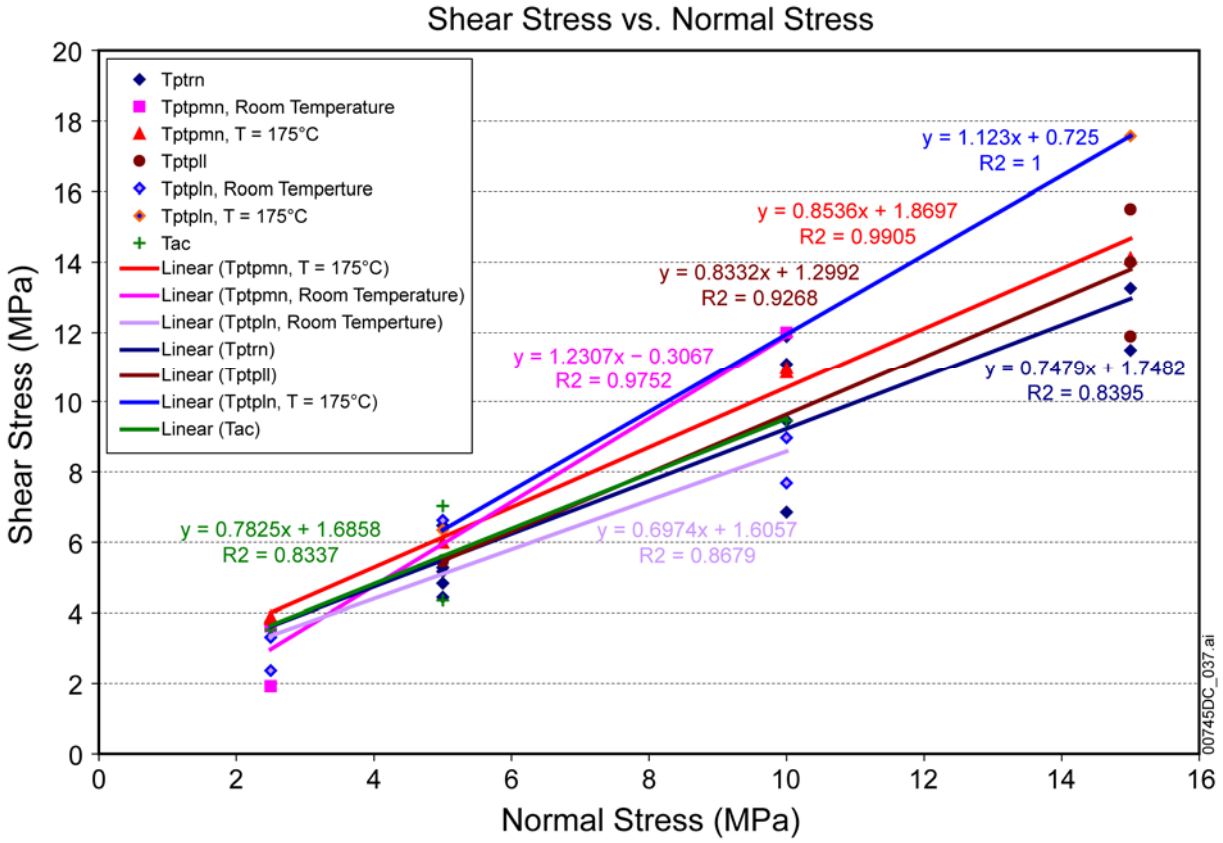

Sources: DTNs: SNL02112293001.001 [DIRS 161629]; SNL02112293001.002 [DIRS 108411]; SNL02112293001.003 [DIRS 108412]; SNL02112293001.005 [DIRS 108413]; SNL02112293001.006 [DIRS 159992]; SNL02112293001.007 [DIRS 108414].

Figure 6-55 Peak Shear Stress Versus Normal Stress from Rotary Shear Tests of Rock Fractures at High and Low Temperature

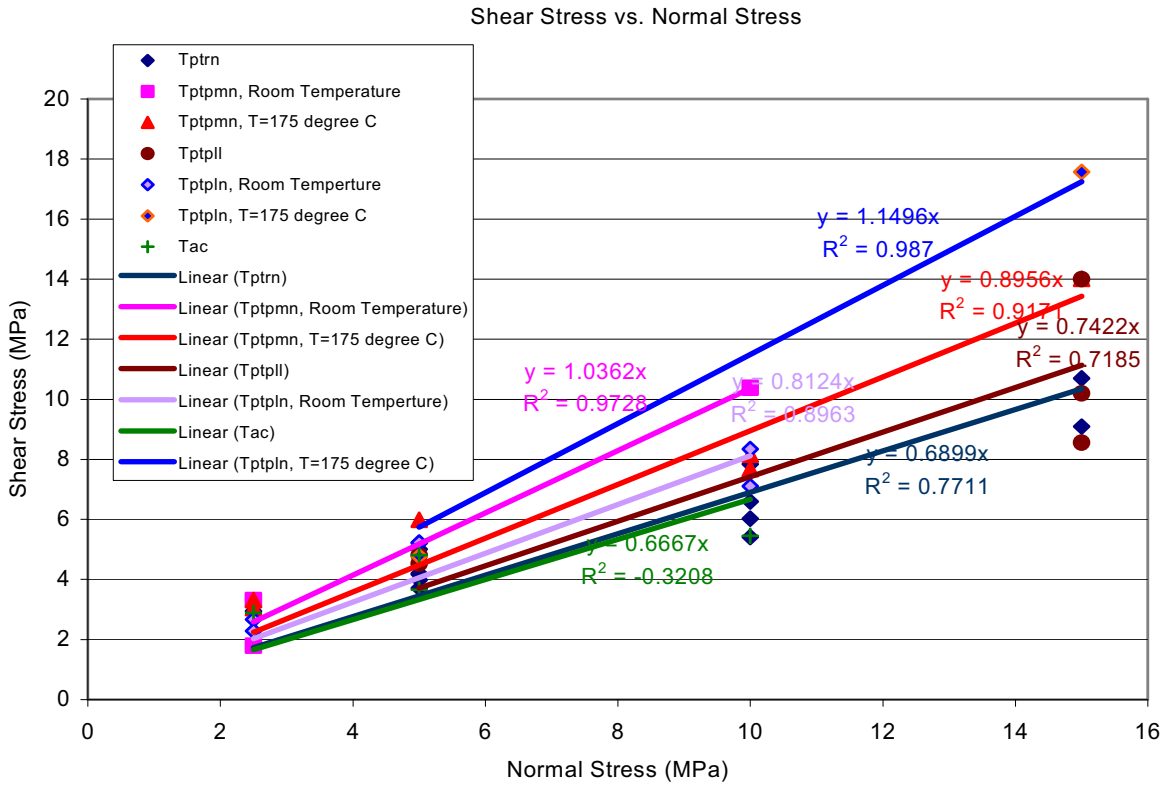

Sources: DTNs: SNL02112293001.001 [DIRS 161629]; SNL02112293001.002 [DIRS 108411]; SNL02112293001.003 [DIRS 108412]; SNL02112293001.005 [DIRS 108413]; SNL02112293001.006 [DIRS 159992]; SNL02112293001.007 [DIRS 108414].

Figure 6-56. Residual Shear Stress Versus Normal Stress from Rotary Shear Tests of Rock Fractures at High and Low Temperature

Table 6-49. Summary Statistics of the Rotary Test Peak Dilation Angle

Litho-stratigraphic Zone	Temp.	Count	Mean (deg)	Std Error	Std Dev	Dev/ Mean	Median (deg)	Minimum (deg)	Maximum (deg)
Tpcpll	Room	1	10.22	NA	NA	NA	10.22	10.22	10.22
Tpcpln	Room	1	7.35	NA	NA	NA	7.35	7.35	7.35
Tptrn	Room	12	7.21	1.52	5.27	0.73	6.38	1.19	16.02
Tptrl	Room	1	11.05	NA	NA	NA	11.05	11.05	11.05
Tptpul	Room	1	8.95	NA	NA	NA	8.95	8.95	8.95
Tptpmn	Room	3	11.00	5.05	8.74	0.79	14.20	1.11	17.7
Tptpmn	175°C	6	13.68	3.79	9.29	0.68	15.65	0	24.5
Tptpll	Room	5	14.33	4.27	9.55	0.67	15.70	1.23	27.2
Tptpln	Room	5	17.82	4.21	9.42	0.53	15.10	8.48	33.4
Tptpln	175°C	2	14.80	3.50	4.95	0.33	14.80	11.3	18.3
Tac	Room	4	14.04	4.27	8.54	0.61	13.50	4.44	24.7

Sources: DTNs: SNL02112293001.001 [DIRS 161629]; SNL02112293001.002 [DIRS 108411]; SNL02112293001.003 [DIRS 108412]; SNL02112293001.005 [DIRS 108413]; SNL02112293001.006 [DIRS 159992]; SNL02112293001.007 [DIRS 108414].

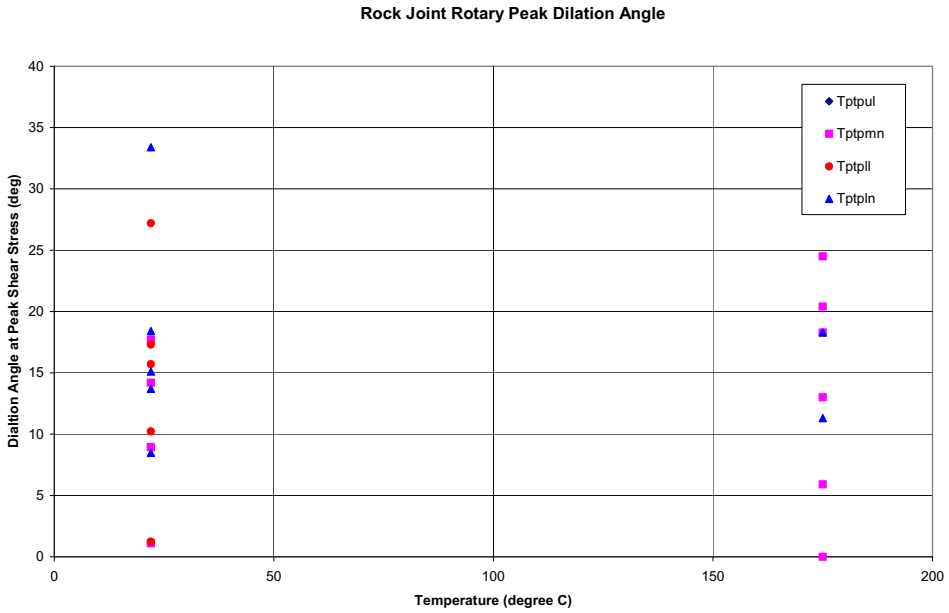

Sources: DTNs: SNL02112293001.001 [DIRS 161629]; SNL02112293001.003 [DIRS 108412]; SNL02112293001.005 [DIRS 108413]; SNL02112293001.006 [DIRS 159992]; SNL02112293001.007 [DIRS 108414].

Figure 6-57. Dilation Angles Obtained from Rotary Shear Tests of Rock Fractures at High and Low Temperature

6.4.3.2.2 Direct Shear Test Results

A summary of the direct shear tests performed on fracture surfaces from the Tptpmn zone is presented in Table 6-50. Table 6-52 illustrates that cooling fractures have lower cohesion, lower peak friction angle and much lower peak dilation angle than the VPP fractures. It is not known if this summary of results is representative of the underlying population of fracture behavior by fracture type. More testing on these fracture types as well as improved test methods would be helpful to confirm these results.

Table 6-50. Summary Statistics of Fracture Peak Strength from Direct Shear Tests

Direct Shear Rock Peak Cohesion (MPa):									
Joint	Zone	Count	Mean	Std Error	Std Dev	Dev/Mean	Median	Minimum	Maximum
Cooling	Tptpmn	2	0.032	0.044	0.063	1.97	0.032	-0.013	0.076
VPP	Tptpmn	3	0.74	0.05	0.09	0.12	0.72	0.66	0.84

Direct Shear Rock Peak Friction Angle (deg):									
Joint	Zone	Count	Mean	Std Error	Std Dev	Dev/Mean	Median	Minimum	Maximum
Cooling	Tptpmn	2	33.4	0.3	0.4	0.01	33.4	33.1	33.7
VPP	Tptpmn	3	44.0	1.1	1.9	0.04	44.5	41.9	45.7

Direct Shear Rock Joint Dilation Angle (deg) at Peak Stress									
Joint	Zone	Count	Mean	Std Error	Std Dev	Dev/Mean	Median	Minimum	Maximum
Cooling	Tptpmn	2	1.6	2.55	3.61	2.33	1.6	-1.0	4.1
VPP	Tptpmn	3	14.0	1.22	2.12	0.15	13.7	12.1	16.3

Source: DTN: GS031083114222.002 [DIRS 177299].

The fracture surface was to some degree mechanically degraded due to the three previous shear tests repeated on the same fracture surface at increasing normal loads. The subsequent slide 4 of each direct shear test series, which repeated shearing at the initial normal load, gave an indication of degraded shear strength. The final normal stress and shear stress measured in Slide 4 for each fracture was used to determine the degraded friction angle values.

The degraded shear results are shown in Table 6-51. The peak and degraded friction angles are approximately the same for the smooth subvertical cooling fracture. The degraded friction angle for VPP fractures was slightly higher than the peak value. Since all the Slide 4 final test values were still dilating when the test was stopped, the cohesion values are not zero and degraded values are not representative of ultimate stress values. To determine a lower bound for fracture ultimate strength, it may be useful to cut some rock samples in half and test the "fractures" by direct shear at several normal loads.

Table 6-51. Summary Statistics of Fracture Degraded Strength from Direct Shear Tests

Direct Shear Rock Degraded Friction Angle (deg):									
Joint	Zone	Count	Mean	Std Error	Std Dev	Dev/Mean	Median	Minimum	Maximum
Cooling	Tptpmn	2	33.4	1.9	2.7	0.08	33.4	31.5	35.3
VPP	Tptpmn	3	46.9	1.7	3.0	0.06	46.5	44.1	50.0

Source: DTN: GS031083114222.002 [DIRS 177299].

6.4.3.2.3 Empirical Estimate of Peak Dilation Angle of Fractures

Barton (Duan 2003 [DIRS 163586], Sections 2.2 and 4.2 to 4.4) used the following empirical equation to estimate peak dilation angles, ψ_{peak}, for some Yucca Mountain joint sets:

$$\psi_{peak} = \frac{1}{2} JRC \log\left(\frac{JCS}{\sigma_n}\right) \quad \text{(Eq. 6-12)}$$

where

JRC = joint roughness coefficient
JCS = joint wall normal strength (MPa)
σ_n = normal stress (MPa).

Barton estimated a range of lab scale JRC values for joint sets (Table 6-52) by making JRC measurements from roughness traces of the rotary shear and direct shear laboratory fractures, making field JRC measurements of fractures in the ESF, and attempting to correlate JRC values to USBR R1 to R6 field roughness statistics. Adopting a "common" value of joint wall normal strength of 100 MPa and a normal stress range of 4 to 8 MPa, Barton then derived the following range of peak dilation angles shown in Table 6-52. More details are documented in *An Application of Rock Mass Characterization and Rock Joint Empirical Models at Yucca Mountain, to Assist in the Disposal Tunnel Design Studies* (Duan 2003 [DIRS 163586], Sections 2.2 and 4.2 to 4.4).

Table 6-52. Estimate of Peak Dilation Angles for RHH Fracture Sets

For nonlithophysal rock:	JRC range	Peak Dilation Angle Range (deg)
Cooling Joint Sets 1 and 4	2 – 4	1.4 – 2.2
Cooling Joint Set 2	4 – 8	2.8 – 4.4
VPP Joint Set 3	12 –16	8.4 – 8.8
For lithophysal rock:		
Lithophysal Fractures	12 – 20	8.4 – 11.0

Source: Duan 2003 [DIRS 163586], Section 4.4.

6.4.3.3 Fracture Normal and Shear Stiffness

Normal stiffness is the slope of the normal stress versus normal displacement curve, and typically is highly nonlinear. The corresponding normal stiffness curve is concave upward with loading. Ideally, normal stiffness should be determined after multiple loading-unloading cycles to remove the hysteresis effect (especially the large plastic displacement of the first cycle). With repeated normal loading cycles the normal stiffness value typically increases and the fracture surfaces are better mated.

Shear stiffness is the slope of the shear stress versus shear displacement curve in the elastic region. In the pre-peak loading range the stiffness behavior is nonlinear with a convex downward shape, but usually the initial part of the loading curve is more or less linear. Shear stiffness plots that exhibit a continually changing slope are typically the result of an error of including plastic deformation as part of the curve. This unwanted deformation may be caused by damage to asperities, slip, shear within fracture fill material or other non-elastic machine or joint deformations.

6.4.3.3.1 Rotary Shear Test Results

Normal stiffness was estimated using the instantaneous slope (tangent value) at 5 MPa and a summary of results is shown in Table 6-53. The stiffness values were read from the instantaneous slope of the "normal stress-closure curves" plotted in the original SNL Report for each test. Only the first normal compression loading cycle was provided in the SNL rotary

results; the unloading curve and second loading cycle data were not retained. This was unfortunate since the first normal loading curve is considered not to be representative of the undisturbed behavior (Bandis et al. 1983 [DIRS 100003]). As a result, the tangent value was adopted instead of a secant value since a stiffer value was desired to best represent the non-hysteresis normal stiffness value. This tangent value will still likely underestimate the non-hysteresis stiffness response.

The normal stiffness values for the Yucca Mountain fractures under rotary shear increased with increasing normal stress as is typical for discontinuities of any type. A wide variation in values was reported from fracture to fracture, and in the six samples tested for lithophysal rock there was an order of magnitude difference in reported values. However, it appears that higher temperatures may result in slightly lower normal stiffness values (Figure 6-58).

Table 6-53. Summary Statistics of the RHH Fracture Normal Stiffness by Rotary Shear

Rotary Rock Joint Tangent Normal Stiffness at 5 MPa (MPa/mm):									
Zone	Temp.	Count	Mean	Std Error	Std Dev	Dev/Mean	Median	Minimum	Maximum
Tptpul/ll	Room	6	268	149	365	1.36	115	65	1000
Tptpmn/ln	Room	4	94	11	22	0.23	98	65	115
Tptpmn/ln	175 deg C	6	74	12	29	0.39	83	35	110

Sources: DTNs: SNL02112293001.001 [DIRS 161629]; SNL02112293001.003 [DIRS 108412]; SNL02112293001.005 [DIRS 108413]; SNL02112293001.006 [DIRS 159992]; SNL02112293001.007 [DIRS 108414].

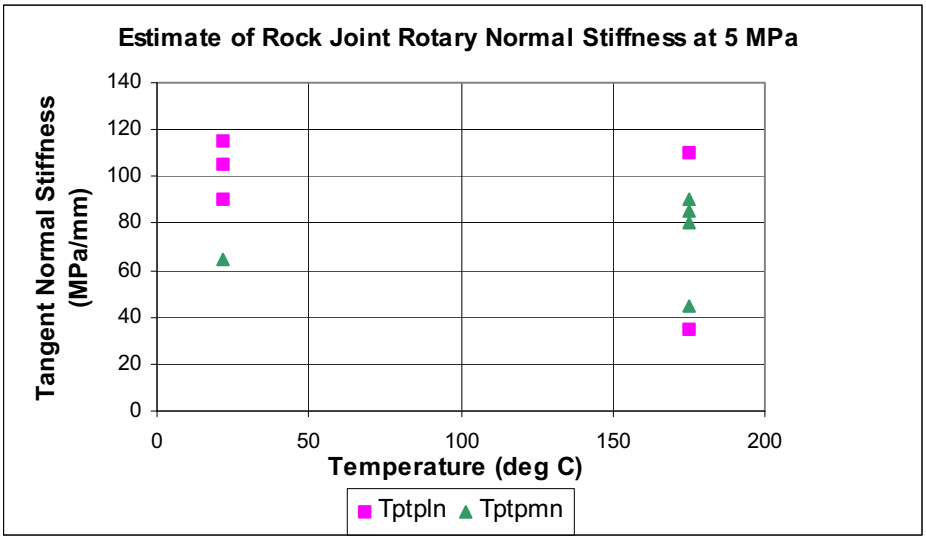

Sources: DTNs: SNL02112293001.001 [DIRS 161629]; SNL02112293001.003 [DIRS 108412]; SNL02112293001.005 [DIRS 108413]; SNL02112293001.006 [DIRS 159992]; SNL02112293001.007 [DIRS 108414].

Figure 6-58. Normal Stiffness Estimate at 5 MPa for RHH Rotary Fracture Tests

Shear stiffness was estimated from the most linear early portion of the experimental curve in the pre-peak strength region of the curve. The stiffness values were read from the instantaneous slope of the shear stress-slip curves plotted in the original SNL Report for each test. The initial

portions of these curves were used because in torsional tests the outer portions of the rock tend to reach peak strength first, obscuring any slip and local peak-softening behavior. As a result rotary tests typically produce a more gradual shear-stress shear-displacement curve than one would obtain in a direct shear test of the same rock fracture. These results are summarized in Table 6-54.

Based on the limited number of test data, it appears that higher temperatures may result in average lower shear stiffness values (Figure 6-59). One reason increased temperature tests may give smaller normal and shear stiffness values is that thermal stresses may act to increase roughness between asperities.

Table 6-54. Summary Statistics of the RHH Fracture Shear Stiffness by Rotary Shear

Rotary Rock Joint Maximum Tangent Shear Stiffness (MPa/mm):									
Zone	Temp.	Count	Mean	Std Error	Std Dev	Dev/Mean	Median	Minimum	Maximum
Tptpul/ll	Room	6	168	54	132	0.79	160	30	400
Tptpmn/ln	Room	8	97	19	55	0.57	108	23	180
Tptpmn/ln	175 deg C	8	56	14	39	0.70	38	18	115

Sources: DTNs: SNL02112293001.001 [DIRS 161629]; SNL02112293001.003 [DIRS 108412]; SNL02112293001.005 [DIRS 108413]; SNL02112293001.006 [DIRS 159992]; SNL02112293001.007 [DIRS 108414].

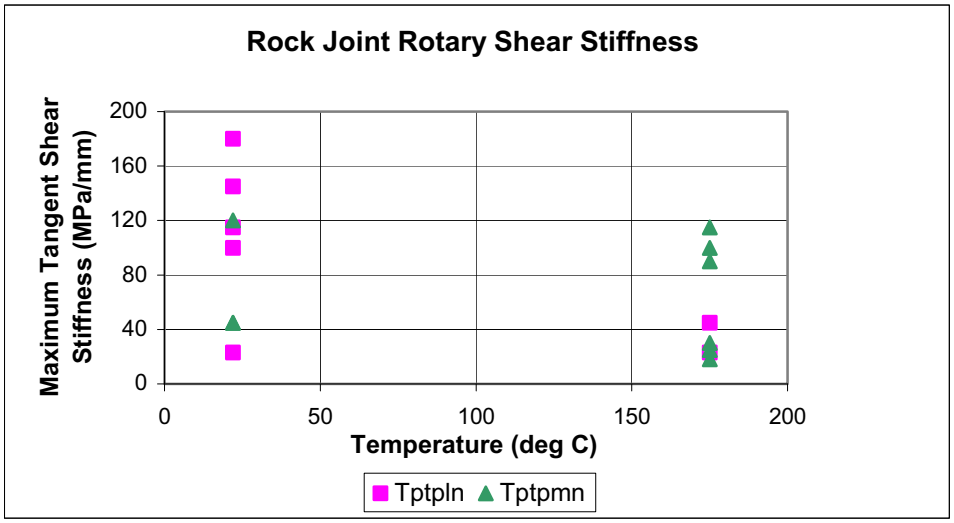

Sources: DTNs: SNL02112293001.001 [DIRS 161629]; SNL02112293001.003 [DIRS 108412]; SNL02112293001.005 [DIRS 108413]; SNL02112293001.006 ([DIRS 159992]; SNL02112293001.007 [DIRS 108414].

Figure 6-59. Shear Stiffness of RHH from Rotary Fracture Tests

6.4.3.3.2 Direct Shear Test Results

No normal loading data were provided by USBR/USGS for the direct shear tests, so no normal stiffness tests can be reported. Some basic information is missing from the source DTN: GS031083114222.002 [DIRS 177299] that describes these test results.

No unloading data were provided for the direct shear tests so the loading shear displacement values could not be corrected by the shear plastic displacement values to estimate elastic shear displacements. As a result, only the total displacements were used to calculate shear stiffness, which will give smaller than expected stiffness values. Since the rotary shear tests were properly corrected and the rotary samples were much smaller in size, the values cannot be directly compared. In all cases, the direct shear stiffness values were estimated from the first shear test performed on each fracture specimen (Slide 1), each having an applied normal stress of 1.0 MPa. The results of the five tests are summarized in Table 6-55.

Table 6-55. Summary Statistics of the RHH Fracture Shear Stiffness by Direct Shear

Direct Shear Stiffness (MPa/mm):									
Joint	**Zone**	**Count**	**Mean**	**Std Error**	**Std Dev**	**Dev/Mean**	**Median**	**Minimum**	**Maximum**
Cooling	Tptpmn	2	11.00	4.00	5.66	0.51	11.00	7.00	15.00
VPP	Tptpmn	3	13.33	3.53	6.11	0.46	12.00	8.00	20.00

Source: DTN: GS031083114222.002 [DIRS 177299].

6.4.3.3.3 Empirical Estimate of Fracture Stiffness Data

Barton in *An Application of Rock Mass Characterization and Rock Joint Empirical Models at Yucca Mountain, to Assist in the Disposal Tunnel Design Studies* (Duan 2003 [DIRS 163586], Sections 5.2 to 5.4 and Tables 5-2 and 5-3) used the Barton-Bandis joint model (Barton 1982 [DIRS 166166]; Barton et al. 1985 [DIRS 100005]; Barton and Bandis 1990 [DIRS 166167]) to predict normal and shear stiffness ranges for Yucca Mountain fractures in the RHH. For estimation of normal and shear stiffness ranges, Barton adopted the previous JRC estimates at normal compressive rock strength of 150 MPa, a joint wall normal strength value of 100 MPa, a rock block size of 0.25 m and a residual fracture shear strength of 30 degrees. Using a reference normal stress of 10 MPa, the stiffness ranges at the fifth normal loading/unloading cycle are shown in Table 6-56 (Duan 2003 [DIRS 163586], Sections 5.2 to 5.4 and Tables 5-2 and 5-3).

Table 6-56. Estimate of Normal and Shear Stiffness at 10 MPa for Fracture Sets

	JRC range	**Normal Stiffness (MPa/mm)**	**Shear Stiffness (MPa/mm)**
For nonlithophysal Rock:			
Cooling Joint Sets 1 and 4	2 – 4	1360 – 1750	2.5 – 2.2
Cooling Joint Set 2	4 – 8	1750 – 1240	2.2 – 1.9
VPP Joint Set 3	12 –16	870 – 720	1.8
For lithophysal Rock:			
Lithophysal Fractures	12 – 20	870 – 710	1.8 – 1.7

Source: Duan 2003 [DIRS 163586], Sections 5.2 to 5.4, Tables 5-2 and 5-3.

6.4.3.4 Field Measurements of the Rock Mass Discontinuities

6.4.3.4.1 Fracturing

The discussion of fracturing presented in this section is based on *Drift Degradation Analysis* (BSC 2004 [DIRS 166107], Section 6.1.4) developed using information presented by Mongano et al. 1999 [DIRS 149850]. Full periphery geologic mapping and detailed line surveys (consisting of a description of orientation, trace length, small and large scale roughness, and end terminations for fractures with trace lengths of greater than or equal to 1 m) were performed in the drifts. The database consists of over 35,000 entries and is recorded on CAD drawings as well as spreadsheets. There are, in general, four sets of fractures in the Tptpmn with the characteristics identified in Table 6-57.

The fractures have relatively short continuous trace lengths (Figure 6-60), with ends often terminating either against other fractures or in solid rock, leaving a solid rock "bridge" between joint tracks. Full periphery geologic maps that logged the fracture traces with lengths greater than 1 m were created behind the TBM as the ESF main loop and the ECRB Cross-Drift were driven. A typical full periphery geologic fracture map is shown in Figure 6-61. Figure 6-62 provides a photograph typical of the wall of the ECRB Cross-Drift within the Tptpmn, and shows the discontinuous nature of the fractures in each joint set. The fracture traces were painted during the detailed line mapping (Figure 6-62). Each fracture termination was logged as being against another fracture, within solid rock, or continuous. The photo shows the common occurrence of fractures that terminate in solid rock (T-junctions) as opposed to continuous structures (arrowheads). The sub-vertical fractures, in particular, often have curved surfaces with large-amplitude (dozens of centimeters) asperities and wavelength of meters. Fractures sometimes terminate in solid rock with discontinuous interconnection to adjacent joint tracks (i.e., a rock "bridge") or terminate against other joints.

Table 6-57. General Characteristics of Fracture Sets in the Middle Nonlithophysal Unit

Set	Mean Azimuth/Dip	Median Spacing (m)	Median Trace Length (m)	Comment
1	120/84	0.48	3.3	Rough to smooth, planar
2	215/88	1.08	2.8	Smooth but curved
3	302/38	3.40	3.7	Random fractures with generally flat to moderate dip
4	329/14	2.46	3.5	Vapor-phase partings, rough, cohesive with coating minerals, planar

Source: Median spacing and trace length are from tunnel mapping data (DTNs for tunnel mapping include: GS960908314224.020 [DIRS 106059]; GS000608314224.006 [DIRS 152572]; GS960908314224.015 [DIRS 108372]; GS960908314224.016 [DIRS 108373]; GS971108314224.025 [DIRS 106025]; GS960708314224.008 [DIRS 105617]; GS000608314224.004 [DIRS 152573]; GS960708314224.010 [DIRS 106031]; GS960908314224.014 [DIRS 106033]; GS970208314224.003 [DIRS 106048]; GS970808314224.010 [DIRS 106050]; and GS971108314224.028 [DIRS 106047]).

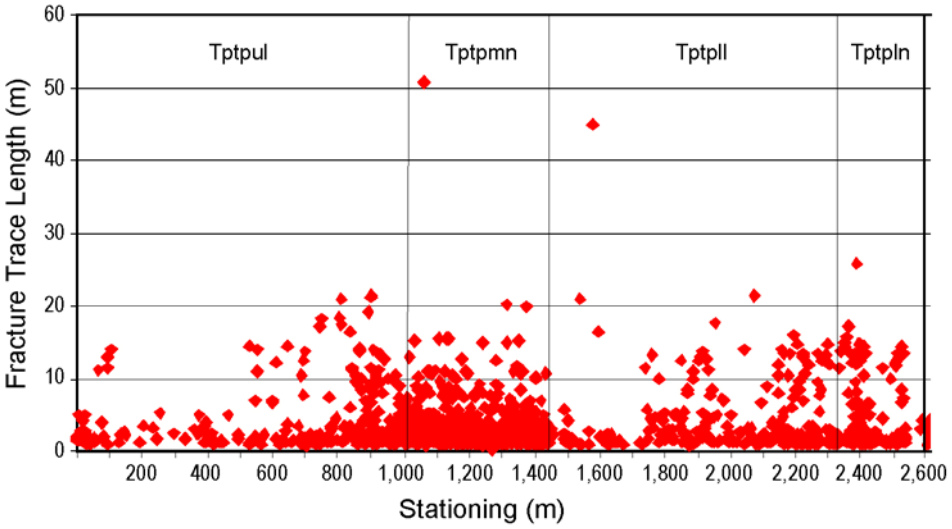

Source: Mongano et al. 1999 [DIRS 149850], Figure 14.

Figure 6-60. Fracture Trace Length from Detailed Line Surveys as a Function of Stationing Along the ECRB Cross-Drift

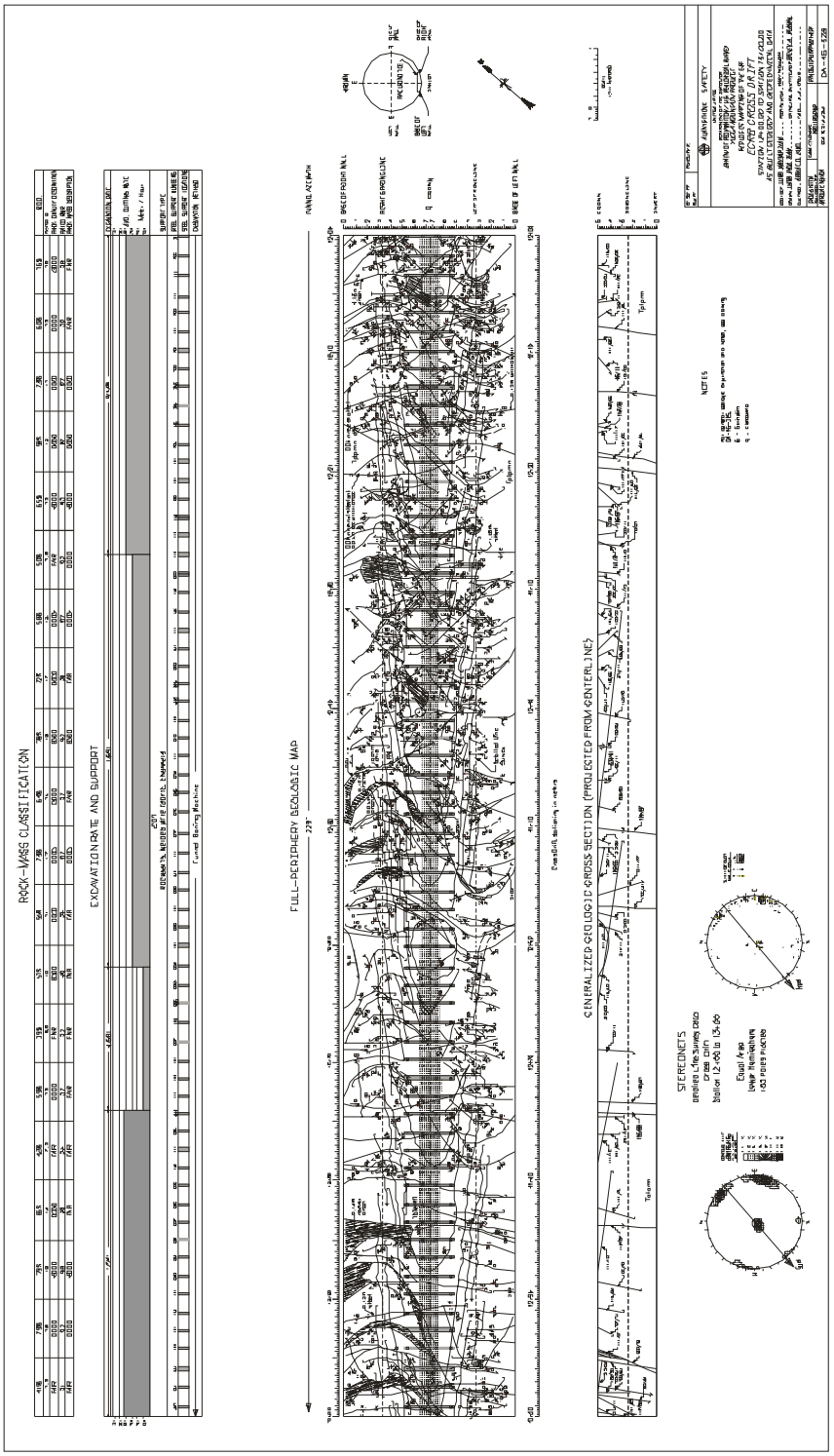

Source: DTN: GS990408314224.004 [DIRS 108405].

NOTE: The purpose of this figure is to illustrate the geologic structure contained on a full periphery geologic map. The annotated information on this figure is not intended to be legible. An enlarged, legible map is available through the source DTN.

Figure 6-61. Illustrative Example of a Full Periphery Geologic Map from the ESF, Tptpmn

Source: BSC 2004 [DIRS 166107], Figure 6-8.

NOTE: T-junctions on fractures indicate terminations; arrowheads show continuous features.

Figure 6-62. Fractures in Wall of the ECRB Cross-Drift in the Tptpmn

The sub-horizontal vapor-phase partings (Figure 6-63) are relatively continuous structures seen throughout the Tptpmn. These continuous, but anastomosing fractures are sub-parallel to the dip of the rock unit, and are filled with concentrations of vapor-phase minerals (primarily tridymite and cristobalite). The surfaces are rough on a small scale and, as a result of the mineral filling, they have cohesion (unlike the sub-vertical fractures).

The nature of the fracture geometry is extremely important to estimates of the stability of the rock mass, particularly under seismic shaking, as well as to estimates of the support function and level of required ground support. Most rock mass classification schemes are based on experience of rock masses with continuous joint sets that create regular, blocky masses (e.g., Hoek 2000 [DIRS 160705]). In the Tptpmn, the relatively short trace lengths and non-persistent joints create relatively few kinematically removable blocks. This sparseness is evidenced by the fact that only a very small number of rock blocks have actually been removed in the ECRB Cross-Drift. Those blocks removed actually occurred under the action of the tunnel boring machine or were scaled out of the back and walls.

Short-length fractures (less than 1-m trace length), coupled with the lithophysae, are the most important features that govern stability in the Tptpll because they impact the rock mass strength as described in *Drift Degradation Analysi*s (BSC 2004 [DIRS 166107], Appendix E, Section E4). Whereas the Tptpul tends to have some small-scale fractures in the matrix-groundmass between lithophysae, and a few that intersect lithophysae (Figure 6-64a), the Tptpll has abundant fractures. Figure 6-64b, from the upper portion of the Tptpll, shows the intensive fracturing of the matrix-groundmass between lithophysae, several “circum-lithophysal” fractures (fractures that formed around or parallel to the margins of lithophysae), and very few fractures that actually

intersect the lithophysae. The fractures, which exist throughout the Tptpll, have a primary vertical orientation, and have lateral spacing of a few centimeters.

Small-scale fracture traverses in the Tptpll confirm the close spacing and short trace lengths of fractures in this zone. The intensity and short trace lengths of fractures in this zone create a texture that severely limits the potential block size in this zone. By comparing the detailed line survey (fracture greater than 1m) and the small-scale surveys, this intensity is clearly due to small-scale fractures (less than 1m trace length). The detailed line survey sampled almost 880 m of tunnel in the ECRB Cross-Drift. There are 300 fractures recorded over this run of tunnel that have a trace length greater than 1 m. The small-scale survey in the Tptpll can be combined into 18 m of horizontal sampling. There are 376 fractures recorded over this 18 m of sampling.

In some cases, it is difficult to distinguish whether these fractures have been disturbed by mining or induced by in situ stresses, or whether they are newly created by mining along a weakness fabric in the rock. However, it is clear that the middle portion of the Tptpll has a ubiquitous fracture fabric that is most evident when large diameter core is removed from boreholes (BSC 2004 [DIRS 166107], Figure 7-1a). The core, although competent, has numerous fractured surfaces that break into small blocks when stressed. Lithophysae and occasional horizontal fractures tend to create blocks with dimensions on the order of about 10 cm or less on a side. Thin section analyses of the fracturing in the Tptpll and the Tptpmn show rims on many of the fracture surfaces within the rock mass away from the tunnel wall, indicating there are numerous natural fractures (i.e., not mining-induced) and were formed during the cooling process (Buesch 2003 [DIRS 163729]).

Source: BSC 2004 [DIRS 166107], Figure 6-9.

Figure 6-63. Low-Angle Vapor-Phase Partings in Nonlithophysal Units in the ESF

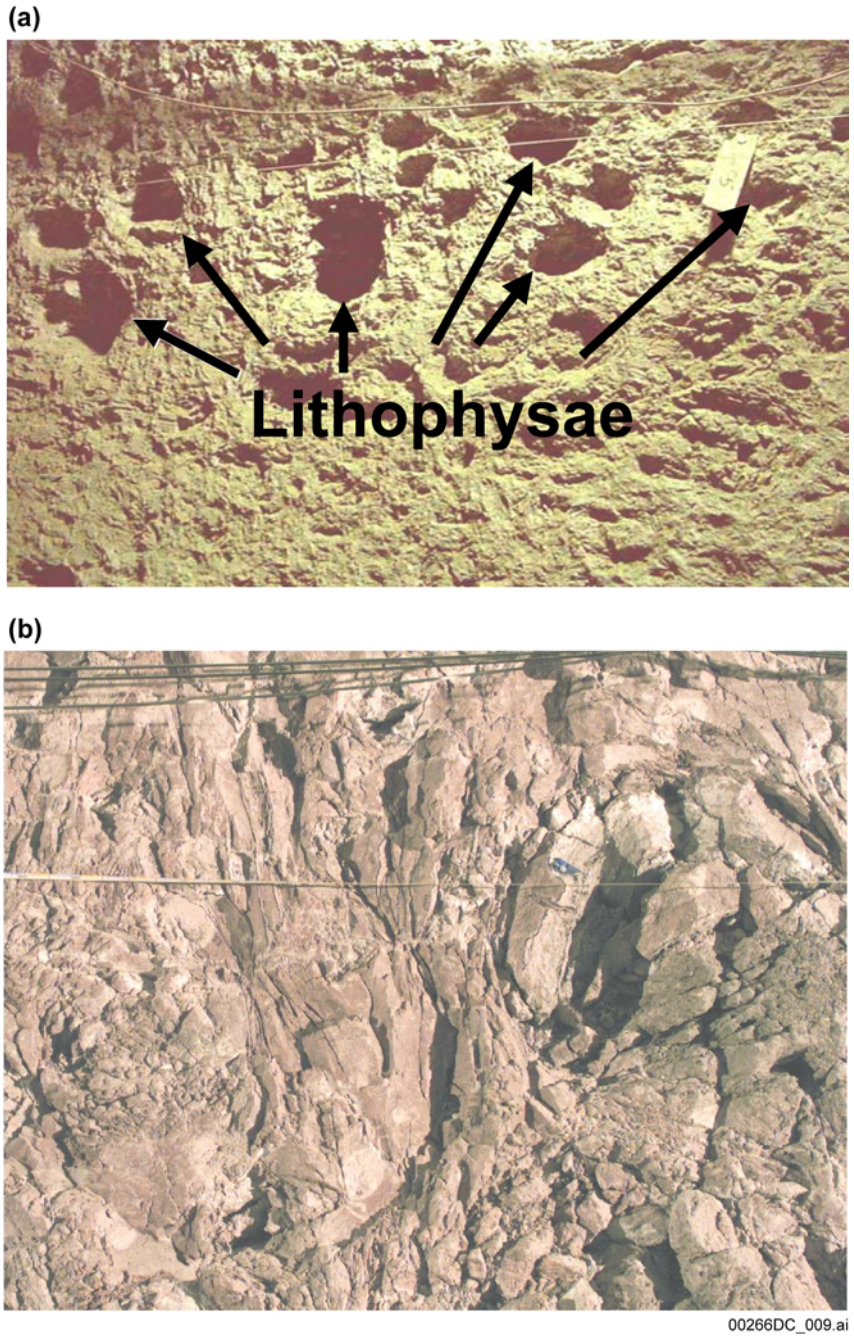

Source: BSC 2004 [DIRS 166107], Figure 6-10.

NOTE: The Tptpul (a) is characterized by a relatively few fractures in the matrix-groundmass between lithophysae whereas the Tptpll (b) has abundant, natural, short-length fractures in the matrix-groundmass, some of which intersect or connect lithophysae. Spacing of the fractures in the Tptpll is generally less than 5 cm.

Figure 6-64. Comparison of Lithophysae and Fracturing in the Tptpul and Tptpll

6.4.3.4.2 Lithophysae

Although the character of the lithophysae varies between the Tptpul and Tptpll as shown in Figure 6-64, the mineralogy of the matrix material within both of these units is generally the

same as in the nonlithophysal units, based on the rock unit descriptions provided by Mongano et al. (1999 [DIRS 149850]).

Compositionally and mineralogically the rocks in lithophysal and nonlithophysal zones are similar, but there can be variations in the amounts of quartz, cristobalite, and tridymite; however, the main difference is in the abundance of lithophysae and features formed by crystallization in the presence of the vapor phase (rims, spots, etc.). The upper and lower lithophysal zones share many characteristics, but there are also numerous distinctions (Mongano et al. 1999 [DIRS 149850]), and these general characteristics are as follows.

The lithophysae in the Tptpul:

- Tend to be smaller (roughly 1 to 10 cm in diameter) compared to the Tptpll
- Are more uniform in size and distribution within the unit compared to the Tptpll
- Vary in infilling and rim thicknesses
- Have a volume percentage that varies consistently with stratigraphic position
- Are stratigraphically predictable.

The lithophysae in the Tptpll:

- Are highly variable in size, from less than 1 cm to 1.8 m in size
- Have shapes that are highly variable and are described as simple (elliptical cross-sections and spherical to ellipsoidal shapes), irregular, cuspate, merged (two or more lithophysae joined into one large one), and extension-crack lithophysae
- Have infilling and rim thickness that vary greatly with vertical and horizontal spacing
- Have volume percentages that vary consistently with stratigraphic position
- Are stratigraphically predictable.

With the large amount of the repository located in the lower lithophysal zone, a detailed study of the lithostratigraphic features in the lower lithophysal zone exposed in the ECRB Cross-Drift has been completed (DTNs: GS021008314224.002 [DIRS 161910] and GS040608314224.001 [DIRS 171367]). The data package documents the distributions of size, shape, and abundance of lithophysal cavities, rims, spots, and lithic clasts, and these data can be displayed and analyzed as local variations, along the tunnel (a critical type of variation), and as values for the total zone. A detailed description of lithophysal abundance and lithophysal characteristics is provided in *Drift Degradation Analysi*s (BSC 2004 [DIRS 166107], Appendix O).

In addition to the along-the-tunnel variation in the abundance of features such as lithophysae, there are variations in the sizes, shapes, and distances between features. These types of variations are most easily observed with panel map data (Figure 6-65). Locations of the panel maps were positioned to capture representative variations in the rocks along the tunnel. Additional details on the development of these panel maps are provided in BSC 2004 [DIRS 166107], Appendix O.

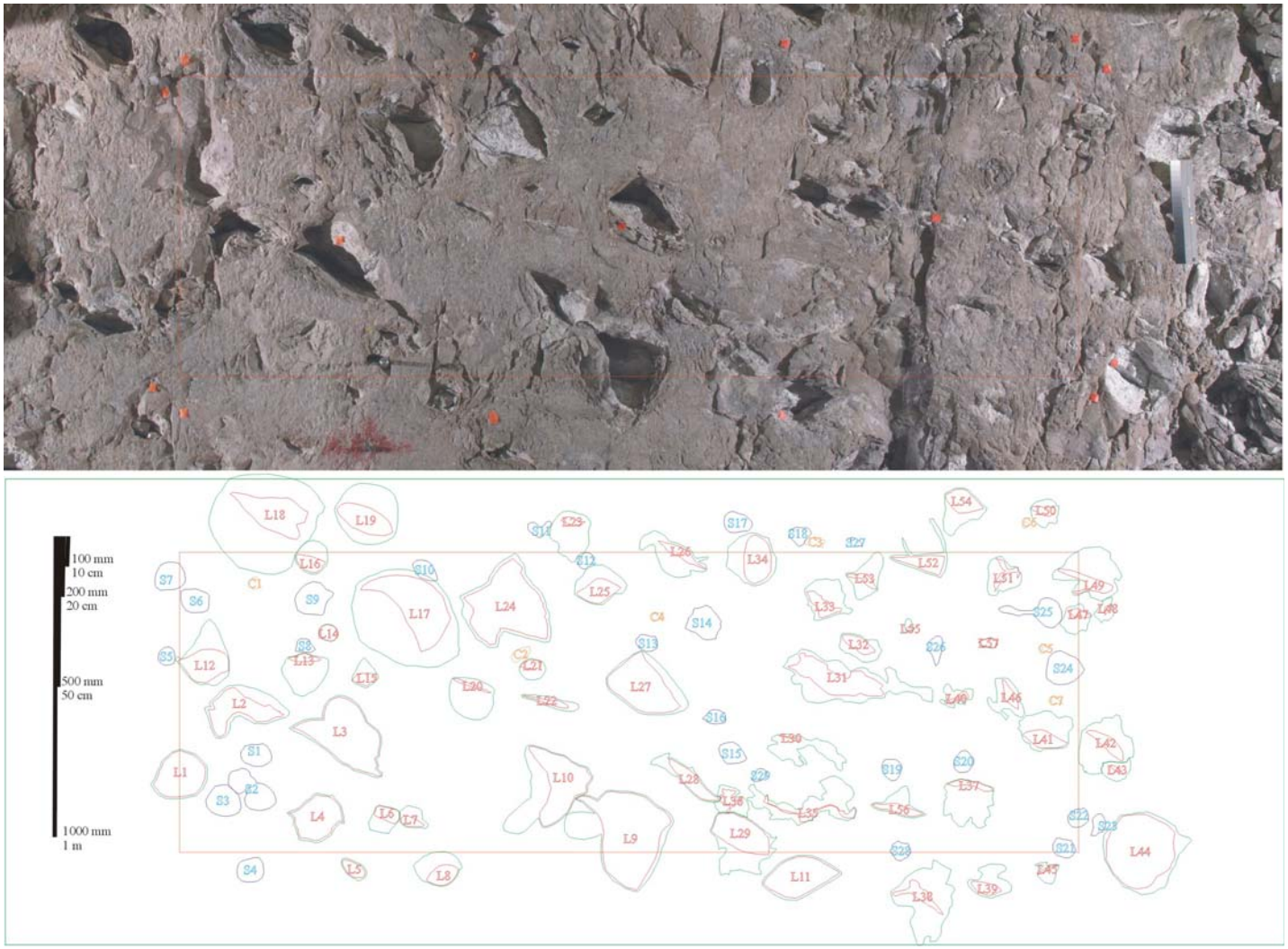

Source: BSC 2006 [DIRS 166107], Figure 6-11.

NOTE: Lithophysae have red “L” identifiers with cavities outlined in red and rims in green. Spots have blue “S” identifiers with cyan outlines. Lithic clasts have orange “C” identifiers with gold outlines.

Figure 6-65. Lithophysae, Spots, and Clasts of Tptpll in Panel Map 1493 Located on the Right Rib from Stations 14+93 to 14+96

Using the approach described in Appendix O of BSC 2004 [DIRS 166107], the total porosity of the component features of the lithophysal rock mass (i.e., the porosity of the lithophysal cavities, rims, and spots) has been calculated. The porosity variation along the ECRB Cross-Drift is shown in Figure 6-66, with total porosity typically ranging from 20 to 35 percent.

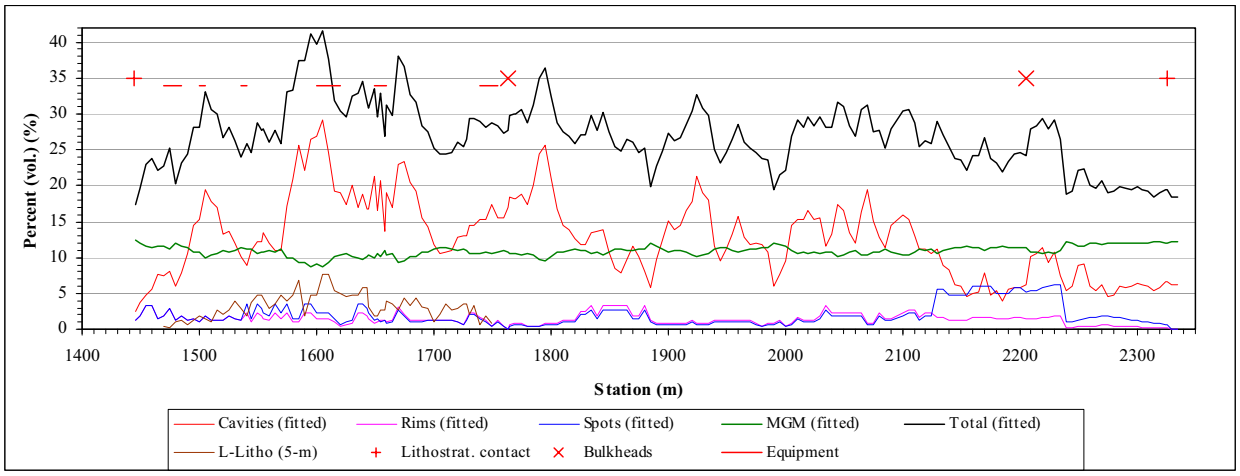

a. Porosity Along the Tunnel Displayed in Five Components (Excluding the 5-m Averaged Large-Lithophysae).

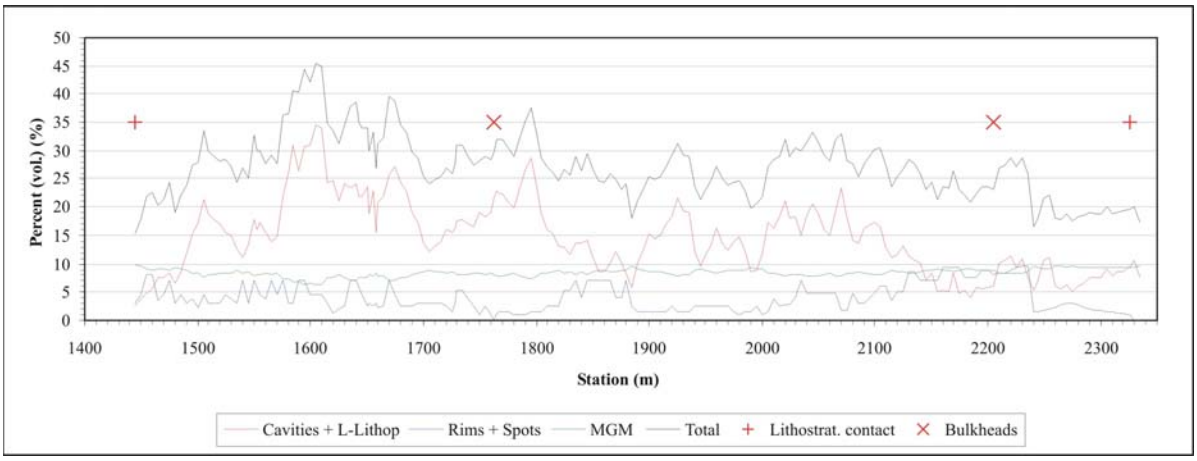

b. Porosity Along the Tunnel Displayed in Three Components (Lithophysal Cavities and Large-Lithophysae Inventory are Combined, and Rims and Spots are Combined).

NOTE: Source file provided in DTN: MO0408MWDDDMIO.002 [DIRS 171483], file *Drift Deg AMR AF T-A-P Fit V1.xls*.

Source: BSC 2006 [DIRS 178277], Figure 6.

Figure 6-66. Calculated Porosity of Lithophysal Cavities, Rims, Spots, Matrix-Groundmass, and the Total Porosity in the Tptpll Exposed Along the ECRB Cross-Drift

6.4.4 Mechanical Properties of Rock Mass

Design and evaluation of the repository performance requires that a range of intact rock and rock mass properties characterizing all major lithostratigraphic units within the footprint of the future repository be available to the designer of underground excavations.

The laboratory data are sufficient to characterize the properties of an undisturbed rock material. The detailed analysis of all available laboratory data for the lithostratigraphic units encountered within the repository footprint are analyzed and presented in *Intact Rock Mechanical Properties of Yucca Mountain Stratigraphic Units* (BSC 2005 [DIRS 176611]). However, the design of underground and surface structures within rock formations requires input parameters characterizing behavior of the rock mass. The laboratory data form a base from which the development of the rock mass parameters can be initiated.

To date, work performed on development of rock mass properties was focused mainly on rock strata at the RHH, which comprises four distinct lithostratigraphic zones (Section 6.1.3.2). These four units were further assigned to two groups, each representing two different rock mass characteristics, namely (1) the Tptpmn and Tptpln zones representing nonlithophysal units and (2) the Tptpul and Tptpll zones representing lithophysal units.

In the current analysis it was considered important that the rock mass characterization should include not only RHH strata but also all other strata overlaying the repository. In this analysis a standard methodology employing rock mass classifications used in tunneling and mining industries was applied consistently to obtain the rock mass parameters for all strata at and above the RHH.

The development of rock mass parameters was performed based on laboratory test data obtained for typical, approximately 50 mm, diameter rock specimens saturated and tested at room/ambient temperature and rock mass classification methods common in the mining and tunneling industries. Tunnel mapping data were used also to define a range of rock mass properties necessary to establish bounds required in the design of underground excavations. All these data are analyzed under a single form of Hoek-Brown failure criterion, utilizing the calculation technique described in this section.

The uniformity of presentation was considered useful for the design as it provides one document where properties for all significant rock strata units can be examined relative to each other. Their location in a stratigraphic column can be used for comparisons among various units and as a decision tool as to the future data needs and potential contractual areas of focus.

Williams (2004 [DIRS 176606], pp. 3-2 and 3-3) stated that for lithophysal rocks a definition of the material properties and mechanical constitutive simulation requires a somewhat different approach. In general, the concern was expressed that the use of common empirical techniques for estimating rock mass properties is not particularly applicable to these rock masses since there is little available experience in excavating and assessing the performance of similar rock types.

Due to the presence of the lithophysal cavities, the rock mass properties are both porosity- and size-dependent. In other words, the properties of the material are a function of the size of the sample being tested, and the size, shape and volume of lithophysal cavities that the sample contains. In effect, an approach involving the use of data from tests on large (10 in. diameter) specimens and porosity as a surrogate parameter, supplemented by an extensive use of advanced numerical simulation was developed to characterize these units (Williams 2004 [DIRS 176606], p. 3-3). The development and detailed analysis of the geotechnical parameters for lithophysal

strata encountered at the repository host horizon are documented in *Lithophysal Rock Mass Mechanical Properties of the Repository Host Horizon* (BSC 2004 [DIRS 172334]).

The experience gained during construction of the ESF and ECRB tunnels and other underground excavations indicates that, with the exception of lithophysal units at the RHH, rock mass properties for all other strata can be adequately determined using a standard approach common in tunneling and mining industries. In the current section, the development of rock mass properties is discussed in terms of two approaches: (1) a common methodology applied to all strata and (2) an alternative methodology applied to the lithophysal units at RHH only. The development of the rock mass strength properties based on the RMR methodology commonly used in tunneling and mining industries and in this report applied for all rock mass units is presented in Section 6.4.4.2, and the development of the alternative methodology for deriving rock mass strength parameters specifically for lithophysal units at RHH is presented in Section 6.4.4.3.

The results of analyses for all rock strata and the results for lithophysal rocks mass obtained using the alternative approach, including the common problem in the area of rock mechanics dealing with size effect and its consequences expressed in terms of the strength of rock mass as a function of specimen size, are presented in Section 6.4.4.5. Section 6.4.4.6 describes the limitations associated with rock mass parameter determinations.

Parameters Required for Rock Mass Characterization

To perform even the most fundamental rock mechanics calculations and estimates for underground excavation performance, it is necessary to determine a number of parameters that collectively form a basis for derivation of parameters characterizing the rock mass. The mechanical properties and geotechnical characteristics of rock mass that need to be determined are as follows:

Mechanical Properties of Rock Mass

- Tensile strength properties, (T_o), developed from tensile tests
- Compressive strength properties to describe the failure criteria, typically cohesion *(C)* and friction angle (ϕ), developed from uniaxial and triaxial tests
- Elastic moduli, specifically modulus of deformability (E) and Poisson's ratio (ν).

Geotechnical Characterization

- Rock mass classification using methods employing Q, RMR, and Geologic Strength Index (GSI) indices.

Other parameters such as mechanical properties of joints and thermal-mechanical properties of rock are also required for rock mass characterization. The mechanical properties of joints and thermal-mechanical properties of rock are addressed in Sections 6.4.3 and 6.5, respectively.

6.4.4.1 Elastic Properties of Rock Mass

Young's modulus or modulus of deformability and Poisson's Ratio are required to establish basic stress-strain relationships for a particular rock type. In the design of underground structures it is customary to consider the value of Poisson's ratio for rock mass being equal to that of intact rock. The value of Young's modulus or elastic modulus for intact rock is generally higher than that for the rock mass. The magnitude of Young's modulus for the rock mass is affected by factors including the presence of discontinuities, material anisotropy, moisture content, and stress level. It is common to refer to the elastic modulus of intact rock as Young's modulus and the elastic modulus of rock mass as a modulus of deformability.

6.4.4.2 General Methodology for All Rock Strata

Laboratory test results and the field mapping, with the accompanying observations and geological descriptions of rock strata, are the two sources of data used in the current analysis for developing the rock mass properties for the rock strata.

Figure 6-67 illustrates the approach taken to develop the nonlithophysal rock mass thermal-mechanical constitutive simulations and properties for design and performance assessment studies. In the current study this approach was adopted to characterize all strata. The details pertaining to the development of this approach and the methodology for characterizing specifically lithophysal units at the RHH are discussed in Board (2003 [DIRS 165036], Section 5.2.3) and Williams (2004 [DIRS 176606], Section 3.2). The results from laboratory testing of small cores from boreholes drilled from the surface (diameter of 50 mm) and of large cores from drilling within the ESF and ECRB Cross-Drift and Busted Butte (diameter of 305 mm and 267 mm), as well as field geotechnical characterization, form the basis for initial mechanical property estimates and rock mass simulation definition. Results of additional efforts extended to better characterize lithophysal units at the RHH are presented in Section 6.4.4.4.2.

More specialized calculations (e.g., rockfall analyses) require that the rock mass be simulated as a discontinuum material with explicitly defined fractures. Therefore, detailed statistical descriptions of the rock mass fracturing and fracture properties are required for direct input to three-dimensional numerical simulation. The FRACMAN program (FRACMAN V.2.512, STN: 10114-2.511-00 [DIRS 160577]) is used for the fracture geometric simulation and field estimates, and direct shear testing of large joints in the laboratory is used for estimating joint surface properties.

The following subsections describe the methodologies used for developing the rock mass parameters for all rock units.

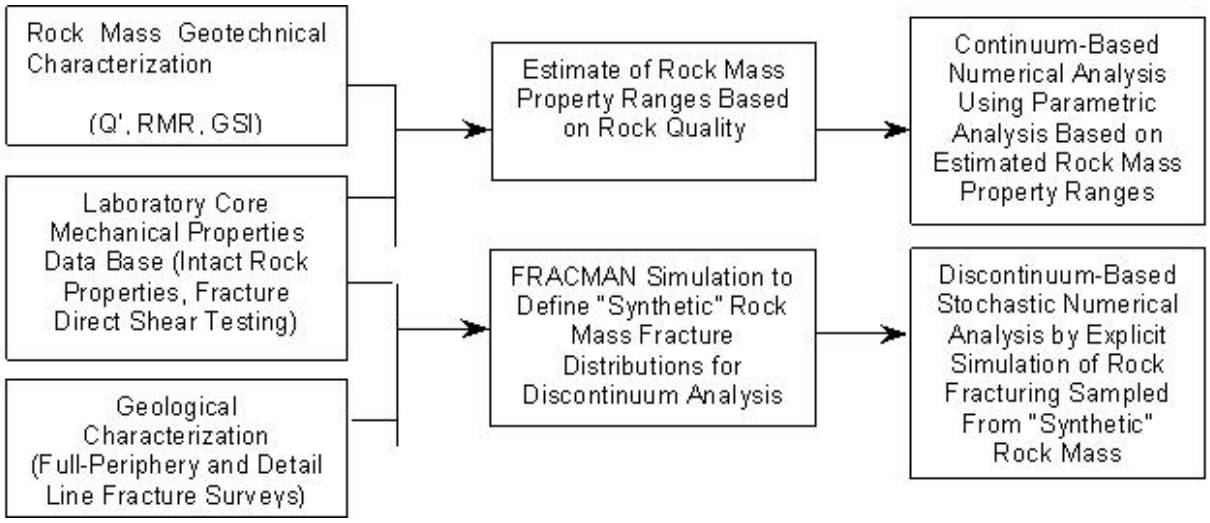

Source: Williams 2004 [DIRS 176606], p. 3-2.

Figure 6-67. Development Strategy for Rock Properties Database and Simulation Strategy for Nonlithophysal Rocks

6.4.4.2.1 Hoek-Brown Failure Criterion

As indicated in Section 6.4.2.1.5, the Hoek-Brown failure criterion for rock masses is widely accepted in the field of rock mechanics and has been applied in a large number of projects around the world. The paper *Hoek-Brown Failure Criterion – 2002 Edition* (Hoek et al. 2002 [DIRS 162204]) discusses the development and applicability of this criterion for estimating parameters of rock mass. Below, quoted directly from this paper, are a procedure and all relevant equations required for deriving rock mass parameters. An associated Windows program called RocLab has been developed based on the generalized Hoek-Brown failure criterion (Hoek et al. 2002 [DIRS 162204]) to provide a convenient means of solving and plotting the equations presented in the paper and has been used in current analyses to calculate properties of the rock mass.

The generalized Hoek-Brown criterion is defined by equation:

$$\sigma_1' = \sigma_3' + \sigma_{ci}\left(m_b \frac{\sigma_3'}{\sigma_{ci}} + s\right)^a \qquad \text{(Eq. 6-13)}$$

where,

a empirical curve fitting exponent characteristic for a particular rock type
σ_1' major effective principal stresses at failure
σ_3' minor effective principal stresses at failure
σ_{ci} uniaxial compressive strength of the intact rock material, and
m_b empirical curve fitting parameter, a reduced value of the intact rock material constant m_i and is given by

$$m_b = m_i \exp\left(\frac{GSI - 100}{28 - 14D}\right) \quad \text{(Eq. 6-14)}$$

And s is material constant for the rock mass and expressed as:

$$s = \exp\left(\frac{GSI - 100}{9 - 3D}\right) \quad \text{(Eq. 6-15)}$$

The value of α is defined by the following relationship:

$$a = \frac{1}{2} + \frac{1}{6}\left(e^{\frac{-GSI}{15}} - e^{\frac{-20}{3}}\right) \quad \text{(Eq. 6-16)}$$

D is a factor, which depends upon the degree of disturbance to which the rock mass has been subjected by blast damage and stress relaxation. D=0 for mechanically excavated openings and D=1.0 for heavily disturbed/damaged ground. D is taken to be in the range of 0 to 1.

The uniaxial compressive strength of the rock mass is obtained by setting $\sigma_3' = 0$ in Equation 6-13, resulting in:

$$\sigma_c = \sigma_{ci} s^a \quad \text{(Eq. 6-17)}$$

The tensile strength in Equation 6-18 is obtained by setting σ_1' to $\sigma_1' = \sigma_3' = \sigma_t$ and substituting in Equation 6-13:

$$\sigma_t = -\frac{s\sigma_{ci}}{m_b} \quad \text{(Eq. 6-18)}$$

Normal and shear stresses are related to principal stresses by the equations according to the following expression:

$$\sigma_n' = \frac{\sigma_1' + \sigma_3'}{2} - \frac{\sigma_1' - \sigma_3'}{2} \cdot \frac{\frac{d\sigma_1'}{d\sigma_3'} - 1}{\frac{d\sigma_1'}{d\sigma_3'} + 1} \quad \text{(Eq. 6-19)}$$

$$\tau = \left(\sigma_1' - \sigma_3'\right) \frac{\sqrt{\frac{d\sigma_1'}{d\sigma_3'}}}{\frac{d\sigma_1'}{d\sigma_3'} + 1} \quad \text{(Eq. 6-20)}$$

where:

$$\frac{d\sigma_1^{'}}{d\sigma_3^{'}} = 1 + am_b\left(\frac{m_b\sigma_3^{'}}{\sigma_{ci}} + s\right)^{a-1} \qquad \text{(Eq. 6-21)}$$

A method for determining the parameters of the Hoek-Brown Failure Criterion envelope is implemented in RocLab. In this analysis, the method was further checked by implementing equations 6-13 and 6-19 through 6-21 into the Excel spreadsheets as shown in Appendix G. The results of calculations using by RocLab and from equations implemented in Excel spreadsheet are compared side by side and are identical. Therefore, the use of RocLab is appropriate for calculating the Hoek-Brown Failure Criterion parameters.

Modulus of Deformation

The rock mass modulus of deformation is given by:

$$E_m(GPa) = \left(1 - \frac{D}{2}\right)\sqrt{\frac{\sigma_{ci}}{100}} \cdot 10^{\left(\frac{GSI-10}{40}\right)} \qquad \text{(Eq. 6-22)}$$

Note that the factor D was included to account for the effects of blast damage and stress relaxation. In mechanically excavated tunnels, disturbance of the surrounding rock mass is minimal and the value of D is taken to be equal to 0.

The equivalent Mohr Coulomb strength properties, i.e., internal friction angle (ϕ') and cohesion (c'), can be derived by fitting an average linear relationship to the curve generated by solving Equation 6-13 for a given value of the minimum principal stress ($\sigma_3^{'}$):

$$\varphi^{'} = a\sin\left[\frac{6am_b\left(s + m_b\sigma_{3n}^{'}\right)^{a-1}}{2(1+a)(2+a) + 6am_b\left(s + m_b\sigma_{3n}^{'}\right)^{a-1}}\right] \qquad \text{(Eq. 6-23)}$$

$$c^{'} = \frac{\sigma_{ci}\left[(1+2a)s + (1-a)m_b\sigma_{3n}^{'}\right](s + m_b\sigma_{3n}^{'})^{a-1}}{(1+a)(2+a)\sqrt{1 + \left(6am_b(s + m_b\sigma_{3n}^{'})^{a-1}\right)/\left((1+a)(2+a)\right)}} \qquad \text{(Eq. 6-24)}$$

where $\sigma'_{3n} = \dfrac{\sigma_{3\max}^{'}}{\sigma_{ci}}$

It should be noted that the value of $\sigma_{3\max}^{'}$, the upper limit of confining stress, over which the relationship between the Hoek-Brown and the Mohr Coulomb criteria is considered, has to be determined for each individual case.

The equivalent Mohr-Coulomb criteria plot in terms of the major and minor principal stresses is defined by:

$$\sigma_1^{'} = \frac{2c^{'}\cos\varphi'}{1-\sin\varphi^{'}} + \frac{1+\sin\varphi^{'}}{1-\sin\varphi^{'}}\sigma_3^{'} \qquad \text{(Eq. 6-25)}$$

The global rock mass strength proposed by Hoek-Brown as shown in Equation 6-27 can be estimated from the Mohr-Coulomb strength criterion:

$$\sigma_{cm}^{'} = \frac{2c^{'}\cos\varphi'}{1-\sin\varphi^{'}} \qquad \text{(Eq. 6-26)}$$

with c' and ϕ' determined for the stress range $\sigma_t < \sigma_3^{'} < \sigma_{ci}/4$, giving:

$$\sigma_{cm}^{'} = \sigma_{ci}\frac{(m_b + 4s - a(m_b - 8s))(m_b/4 + s)^{a-1}}{2(1+a)(2+a)} \qquad \text{(Eq. 6-27)}$$

Determination of σ'$_{3max}$

Case 1 – Deep Tunnels (Depth > 3D)

$$\frac{\sigma_{3\max}^{'}}{\sigma_{cm}^{'}} = 0.47\left(\frac{\sigma_{cm}^{'}}{\gamma H}\right)^{-0.94} \qquad \text{(Eq. 6-28)}$$

where, σ'_{cm}: rock mass strength as defined in Equation 6-27
γ: unit weight of the rock mass
H: depth of the tunnel below surface.

Note: Where the horizontal stress is higher than γH, use the horizontal stress value.

Case 2 – Shallow Tunnels (Depth < 3D)

Use Equation 6-28 for all underground excavations that are surrounded by a zone of failure that does not extend to the surface. Do not use Equation 6-28 for cases involving block caving.

6.4.4.2.2 Utilization of Mapping Data

In addition to the laboratory testing program, during tunnel construction, each section of the tunnel was carefully mapped providing additional field-based mapping data. Evidence gathered during the tunnel construction and resulting RMR, GSI, and Q index data are very valuable as they provide an estimate of tunnel performance under the real in situ conditions. The rock mass quality data presented in the tunnel mapping records provides a systematic assessment of rock mass properties for all rock units encountered at Yucca Mountain.

The laboratory data provide input for calculating the uniaxial compressive strength of intact rock for each rock unit. This strength data and the tunnel mapping data are the parameters required to calculate the RMR values and the resulting GSI index. Together they constitute input to the calculation to determine Hoek-Brown criterion constants for the rock mass and other rock mass parameters.

6.4.4.2.3 Rock Mass Classifications

The process of establishing a set of parameters characterizing the geotechnical quality of the rock mass is based on a number of input parameters, which are obtained from laboratory tests and field measurements. Sets of these parameters attempt to capture both parameters characterizing rock material and parameters characterizing rock mass structure and alteration. For engineers, rock mass classifications provide a means of assessing the quality of rock mass and/or to anticipate performance of the rock mass at a particular location.

There are two commonly used rock mass classifications that are designed to systematically assess the intact rock and the rock mass structure: (1) the RMR system (Bieniawski 1989 [DIRS 101715]) and (2) Q system (Barton et al. 1974 [DIRS 101541]; Barton 2002 [DIRS 160379]).

The RMR system has been used in mapping of the rock formations encountered in the ESF and ECRB Cross Drift excavations, and has been applied to calculate rock mass strength for the Yucca Mountain strata. Moreover, as illustrated in Barton 1988 ([DIRS 146587], Page 62), the RMR assessment of rock mass quality is more conservative than one resulting from estimates using the Q system. Therefore, in this document the RMR rock mass classification system is selected to assess the rock mass strength. Tables 6-58 through 6-60 illustrate the type of input parameters used in determining the RMR for each mapped tunnel section. More detailed discussion of these parameters is given in BSC 2004 ([DIRS 176608], Section 7.2.3). The report *Rock Mass Quality Ratings and Classifications of the Combined ESF, Heated Drift and ECRB Cross Drift* (BSC 2004 DIRS 176608]) summarizes RMR data obtained from the detailed geological field mapping performed during the ESF and ECRB Cross Drift excavation.

The rock mass property data reported in this section were obtained using the Hoek-Brown failure criterion (Hoek et al., 2002 [DIRS 162204]). Historically, the development of this criterion was at some stage tied closely to the 1976 or 1989 versions of the RMR system (Bieniawski 1976 [DIRS 101694]; Bieniawski 1989 [DIRS 101715]). The GSI, suggested by Hoek and Brown (1997 [DIRS 170501]), is used in derivation of Hoek-Brown failure criteria parameters. The GSI values were determined according to the guidance provided in Hoek and Brown 1997 ([DIRS 170501], p. 1172) and are equal to:

$$GSI = (RMR'_{(89)} - 5) \quad \text{(Eq. 6-29)}$$

Where, $RMR'_{(89)}$ are the RMR values as obtained by using the above stated procedure.

In fact, the GSI index, which constitutes an inherent part of the criterion, can be obtained either by using appropriate charts or, with the exception of poor quality rock, can be based on the RMR value (Equation 6-29).

Here, the GSI Index values were obtained using RMR values from the full periphery tunnel mapping data (BSC 2004 [DIRS 176608], Table 1). These values were used as one of two major sources of input for obtaining estimates of rock mass properties for all strata units. Once determined, the values of GSI including the corresponding UCS values and other required input parameters are used to obtain the values of Hoek-Brown parameters for the rock mass according to equations presented in Section 6.4.4.2.1.

The RMR or indexing systems are typically used for the description of rock mass quality in moderately strong to strong rock, in which the primary size effect occurs due to the presence of discontinuities in rock mass. At Yucca Mountain, the volcanic tuff occurs in a number of lithostratigraphic units, which, although chemically and mineralogically similar, are structurally different. The lithophysal units containing voids of varying shapes and dimensions distributed within the rock mass are the features that contribute to the increased total porosity, resulting in a size effect with an associated decrease in rock strength and an increase in specimen dimensions.

Therefore, the rock mass classification system is used for all Yucca Mountain rock units. The results of additional work performed to develop an alternative methodology to enhance understanding of lithophysal rock behavior and to provide estimates of strength properties of the lithophysae rich Tptpul and Tptpll RHH units are presented in Section 6.4.4.3. The results of both approaches are compared and presented in Section 6.4.4.5.

Table 6-58. Rock Mass Rating System

Parameter	Range of Values						
1. Strength of Intact Rock Material—C							
Point-Load Strength Index (MPa)	> 10	4 – 10	2 – 4	1 – 2	For this low range-uniaxial compressive test is preferred		
Uniaxial Compressive Strength (MPa)	> 250	100 – 250	50 – 100	25 – 50	5 – 25	1 – 5	< 1
Rating C	15	12	7	4	2	1	0
2. Drill Core Quality—RQD							
RQD	90% – 100%	75% – 90%	50% – 75%	25% – 50%	< 25%		
Rating RQD	20	17	13	8	3		
3. Spacing of Discontinuities—Js							
Js	> 2 m	600 – 2000 mm	200 – 600 mm	60 – 200mm	< 60 mm		
Rating Js	20	15	10	8	5		
4. Condition of Discontinuities –Jcd							
See Table 9b for Guidelines for Classification of Individual Discontinuity Conditions	Very rough surfaces Not continuous No separation Unweathered wall rock	Slightly rough surfaces Separation < 1mm Slightly weathered walls	Slightly rough surfaces Separation < 1 mm Highly weathered walls	Slickensided surfaces or Gouge < 5 mm thick or Separation 1 – 5 mm Continuous	Soft gouge > 5 mm thick or Separation > 5 mm Continuous		
Rating Jcd	30	25	20	10	0		
5. Groundwater—JwR							
Inflow per 10 m tunnel length (L/min)	None	< 10	10 – 25	25 – 125	> 125		
Joint water pressure/ Major principal σ	0	0 – 0.1	0.1 – 0.2	0.2 – 0.5	> 0.5		
General Conditions	Completely dry	Damp	Wet	Dripping	Flowing		
Rating JwR	15	10	7	4	0		
6. Rating Adjustment for Discontinuity Orientations—AJO							
Strike and Dip Orientations See Table 9c for Effect of Discontinuity Strike and Dip Orientation in Tunneling	Very Favorable	Favorable	Fair	Unfavorable	Very Unfavorable		
Rating AJO for Tunnels and Mines	0	-2	-5	-10	-12		

Source: Bieniawski 1989 [DIRS 101715], pp. 54 and 59.

Table 6-59. Guidelines for Classification of Discontinuity Conditions

Guidelines for Classification of Discontinuity Conditions, Jcd					
Discontinuity Length (persistence), CDl	< 1 m	1 – 3 m	3 – 10 m	10 – 20 m	> 20 m
Rating	6	4	2	1	0
Separation (aperture), CDs	None	< 0.1 mm	0.1 – 1.0 mm	1 – 5 mm	> 5 mm
Rating	6	5	4	1	0
Roughness, CDr	Very rough	Rough	Slightly rough	Smooth	Slickensided
Rating	6	5	3	1	0
Infilling (gouge), CDf	None	Hard Filling < 5 mm	Hard Filling > 5 mm	Soft Filling < 5 mm	Soft Filling > 5 mm
Rating	6	4	2	2	0
Weathering, CDw	Unweathered	Slightly weathered	Moderately weathered	Highly weathered	Decomposed
Rating	6	5	3	1	0

Source: Bieniawski 1989 [DIRS 101715], p. 54.

NOTE: The Discontinuity Condition, Jcd, is defined as:
Jcd = CDl + CDs + CDr + CDf + CDw
Where, CDl: Joint condition length
CDs: Joint condition separation
CDr: Joint condition roughness
CDf: Joint condition filling
CDw: Joint condition weathering

Table 6-60. Effect of Discontinuity Strike and Dip Orientation in Tunneling

Strike perpendicular to tunnel axis		Strike parallel to tunnel axis		Irrespective of strike
Drive with dip—Dip 45 – 90°	Drive with dip—Dip 20 – 45°	Dip 45 – 90°	Dip 20 – 45°	Dip 0 – 20°
Very favorable	Favorable	Very unfavorable	Fair	Fair
Drive against dip—Dip 45 – 90°	Drive against dip—Dip 20 – 45°			
Fair	Unfavorable			

Source: Bieniawski 1989 [DIRS 101715], p. 59.

NOTE: Modified from Wickham et al. (1972 [DIRS 146617]).

The RQD index is one of the primary rating parameters in RMR rock mass classification system. It was introduced as a quantitative measure of rock quality (Deere and Deere 1988 [DIRS 146611], pp. 91 to 101). The RQD is calculated as follows:

$$RQD\ (\%) = [\Sigma\ \text{Length of Core longer than 10 cm / Length of Core Run, (Typ. 5 m)}] \times 100 \quad \text{(Eq. 6-30)}$$

Lengths of intact rock adjacent to the DLS tape are estimated or calculated as the percentage of core pieces 10 cm or longer which would be recovered in an imaginary horizontal drill hole along the rib of the excavation. The fundamental approach for the RQD calculation is that the length of the rock between recorded fractures is an intact rock. Apparent man-made or mechanical fractures are excluded. The total length of intact rock pieces longer than 10 cm is determined from the fracture spacing. Table 6-61 shows the qualitative description of RQD ranges.

To provide another orientation/perspective and thus eliminate any bias from a strictly horizontal RQD line, a second, vertical RQD (VRQD) calculation was performed in the ECRB Cross Drift between the 5-m intervals. The VRQD lines are 2 m in length, and are taken at the midpoint of a given 5-m interval, about every 40 m in tunnel stationing.

Table 6-61. RQD vs. Qualitative Rock Description

RQD Ranges (%)	Rock Quality Description
< 25	Very Poor
25-50	Poor
51-75	Fair
76-90	Good
91-100	Excellent

Source: Deere and Deere 1988 [DIRS 146611], p. 93.

Lithophysae encountered while drilling core samples (mostly in the ECRB Cross-Drift) can produce little or no core recovery. This procedure of accounting for lithophysal cavities reduces the computed RQD and provides conservatism for the rock mass Q and RMR values. For this reason, the base case of rock mass classification is used with lithophysae being included in the calculation of RQD and the associated value of the GSI.

6.4.4.2.4 Statistical Analysis

The Microsoft Excel 2000 spreadsheet software was used for editing and formatting input data files and to perform simple statistical analyses including calculation of averages and standard deviations for particular data sets. Where warranted, the Excel spreadsheet data was used as input to the Level 2 computer software JMP Version 5, Release 5.1 (JMP 2002 [DIRS 171549]) to perform additional statistical analyses.

6.4.4.2.5 Analysis of Rock Strength Using RocLab

As discussed in the previous section, two sources of input were used to obtain estimates of the representative properties of rock mass. The first source is based on laboratory data available for a particular lithostratigraphic unit. The second source is based on tunnel mapping data performed in a tunnel section excavated in the same unit. By utilizing RocLab (Hoek et al. 2002 [DIRS 162204]) as a calculation tool, it uses data originating from two different sources to obtain an assessment of the properties of rock mass.

The first data source utilizes the intact rock properties as input to RocLab® rock mass properties calculator (Hoek et al. 2002 [DIRS 162204]). The second input data source is the RMR data available from the full periphery tunnel mapping performed in the Yucca Mountain tunnels and expressed in terms of GSI values.

As shown in Figure 6-68, the RocLab® tool can be used to present both input data (insert) and results of calculations shown both in numerical and graphical forms. As depicted in the left upper corner of Figure 6-68, the results will depend on the intact rock strength laboratory data, sigci (σ_{ci}) as well as on the values of GSI that represent the type of the rock mass quality of the tunnel surface, mi (or m_i) that reflects the quality of the lab test data, and the value of D that is used to estimate the impact of the excavation technique used to construct the tunnel.

When laboratory strength data are used as input, the values of σ_{ci} and m_i are calculated, D is typically equal to zero since the tunnel is excavated using the least disturbing mechanical

method, and GSI must be determined from the field mapping and observations. The GSI magnitude reflects the engineer's familiarity with the rock mass being analyzed. The magnitudes of GSIs provide an assessment of the overall quality of ground conditions encountered along the tunnel alignment. They provide a measure of the response of a particular rock mass surrounding the tunnel developed using a particular excavation method to stresses encountered along the tunnel. The GSI can be used as a starting point when information about the future excavation is limited. It can also be used to assess the rock mass behavior for a particular range of GSI values available from the field measurements and observations. This range can be used as a measure of assessing uncertainty associated with parameters estimates characterizing each rock strata.

In the process of calculating rock mass parameters, both the results of tunnel mapping to determine the GSI index and the intact rock mass strength are used as input. In general, the RocLab serves as a tool, through which the data originating from these two sources (laboratory and field) are merged to establish parameter values suitable for characterizing a range of rock mass conditions encountered at the site, further organized, and presented as rock mass categories.

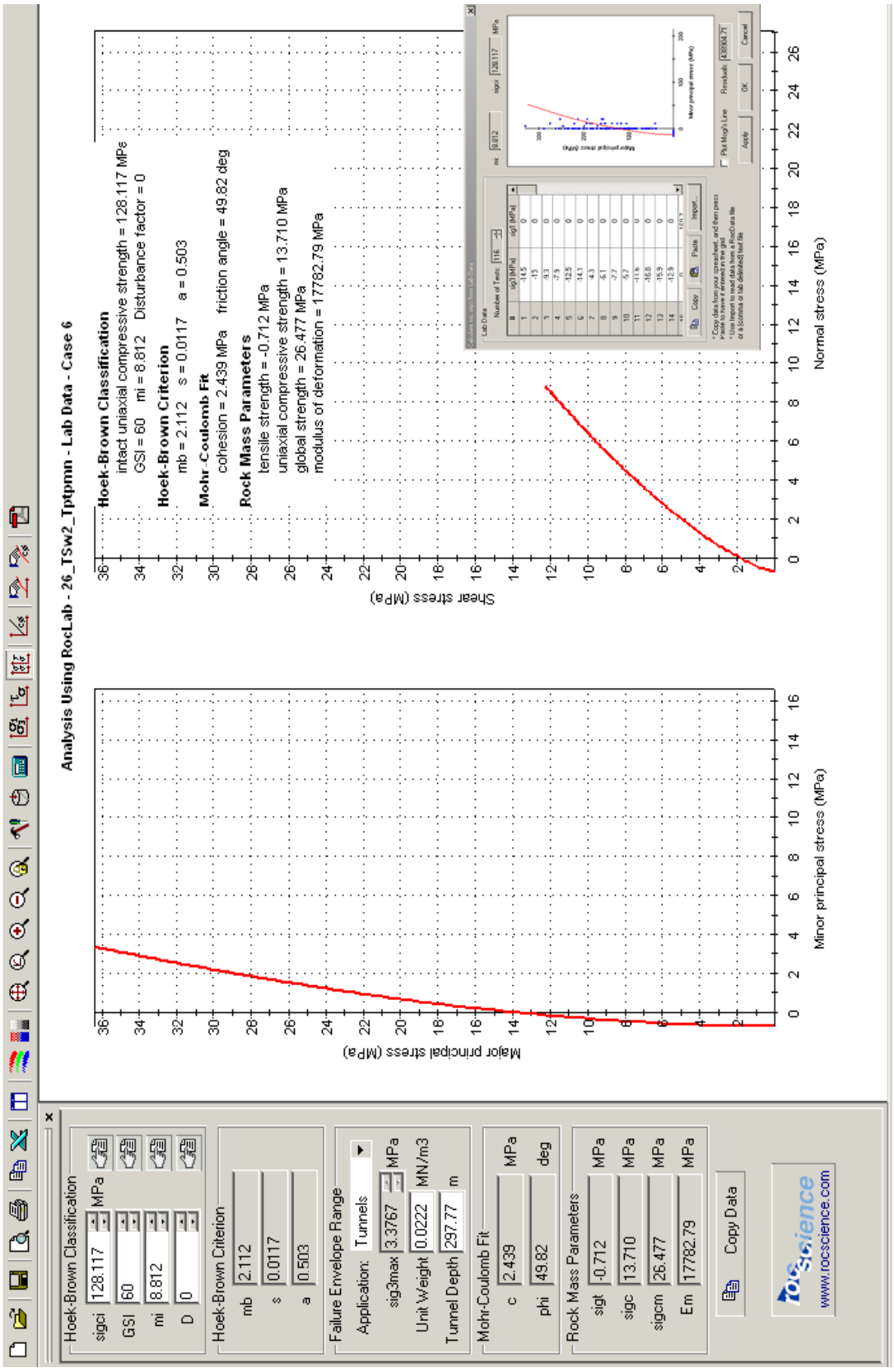

Figure 6-68. Typical RocLab Summary Page Showing Various Inputs and Results of Calculations Including Both Intact Rock and Rock Mass Properties

6.4.4.3 Methodology for Lithophysal Rock Strata at RHH

Prior to 2001, mechanical properties of the Topopah Spring Tuff were estimated as being homogeneous thermal-mechanical units that combined vitric, lithophysal, and nonlithophysal rocks. Rock mass properties were developed for these thermal-mechanical units using the traditional empirical approaches. Subsequently, it was recognized that (1) most of the repository will reside in lithophysal rock, (2) the mechanical rock behavior of lithophysal rock is different from that of nonlithophysal rock, and (3) the traditional methods of empirical classification of rock mass may not be applicable to lithophysal rock. As a result, YMP issued *Resolution Strategy for Geomechanically-Related Repository Design and Thermal-Mechanical Effects (RDTME)* (Board 2003 [DIRS 165036], Sections 5.2.3 and 6) and presented a new, alternative approach for the lithophysal rocks that involved new mechanical testing to better characterize lithophysal rock in the laboratory and in the field (Board 2003 [DIRS 165036], Sections 6.3.2 and 6.7).

Figure 6-69 illustrates the approach used to estimate the mechanical properties for the lithophysal rock masses at RHH. The approach relies on indirect estimation of the ranges of mechanical properties using correlations between porosity and rock mechanical behavior linked to field measured variations of rock porosity. The validation activities required for building more confidence in the predicted results are described in this section. The approach involves the steps described as follows:

- An initial set of base-case strength and modulus values, termed lithophysal rock mass categories, are developed from laboratory and field testing results with upper and lower strength bounds that span the entire range of lithophysal porosity conditions measured in the host rock.

- To supplement the laboratory data and improve understanding of the mechanical response of lithophysal rock, two discontinuum numerical simulations, PFC and UDEC, are used to conduct numerical biaxial experiments on simulated lithophysal rock specimens. The results of the numerical investigation are used to update the estimated upper and lower rock mass property bounds for the respective lithophysal rock mass categories that were initially established based on the laboratory and field-testing of the rock.

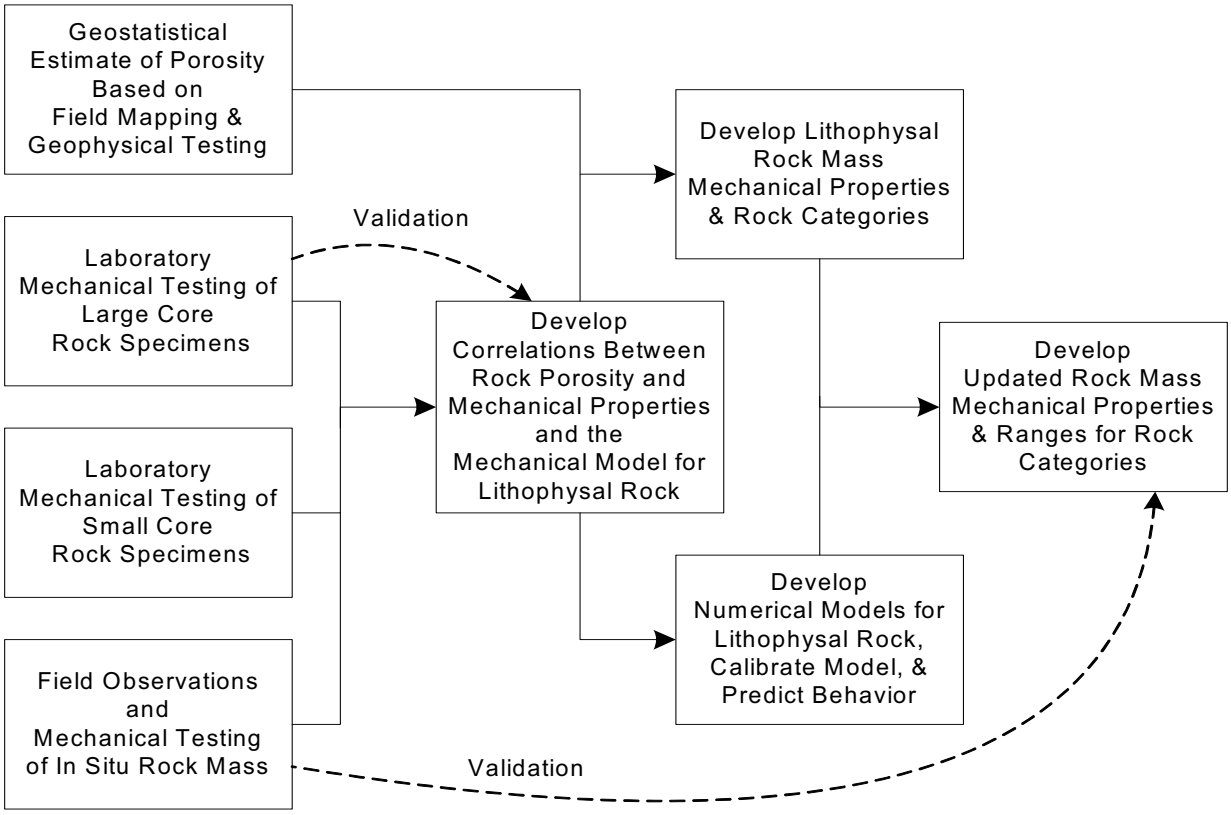

Source: BSC 2004 [DIRS 172334], Figure 1-5.

Figure 6-69. Strategy for Developing Rock Mass Mechanical Properties and Rock Classification Categories for Lithophysal Rock

The lithophysal rock mass mechanical property estimates developed with this method represent reasonable parameter values, especially considering the uncertainties assigned to these estimates. However, the developed properties are based on assumptions listed in Section 5.2.

Presented in Section 6.4.4.4 are the rock mass properties obtained using this alternative methodology along with the properties for the same lithophysal strata calculated utilizing a conventional approach and the discussion.

6.4.4.4 Determination of Rock Mass Mechanical Properties

Prior to performing more detailed analyses, it was considered important to provide an account of all tests performed on intact rock considering the origin of test specimens and the number and the type of tests performed for each lithostratigraphic unit. As shown in Table 6-62, the total number of specimens tested is equal to 1,208. This number includes both uniaxial tensile strength tests and tests performed under compressive loading conditions.

The test specimens were obtained either from drill cores or rock samples recovered from 42 locations as shown in Table 6-5 and Figure 6-11. A relatively large sample population originates from Busted Butte (245 specimens) and from borehole USW G-1 (121 specimens). Figure 6-12 shows the planar view of specimen locations relative to the ESF main loop tunnel. The majority of sampling points originated from borings located in the vicinity of the North Ramp.

6.4.4.4.1 Rock Mass Mechanical Properties for Strata at and Above the RHH

A summary of results of all available and qualified laboratory tests and associated statistical parameters are listed in Table 6-62. A summary of tests performed for each lithostratigraphic unit is presented in Appendix B. Test summaries displayed in Table 6-62 show all laboratory test groups and test conditions under which the specimens were tested. Listed in the table are test codes and test conditions defined by the test temperature, saturation, and magnitudes of confining pressure and the axial stress at failure. The last three columns provide an account of the number of tests and test groups for each lithostratigraphic zone and the number of test groups within each thermal-mechanical unit.

Among the tests carried out under a variety of test conditions, only the baseline condition tests were selected to calculate the rock mass strength parameters. The baseline tests are those carried out on approximately 50 mm diameter specimens tested under tensile and compressive loading conditions and tested fully saturated under room or ambient temperature (Test group code 231221). There are a few exceptions to this baseline rule when 50 mm diameter specimen data are lacking. The data selected for calculations of rock mass strength properties are listed in Table 6-63. Listed in this table are the average values of parameters used as input in the development of rock mass properties.

The detailed account of all intact rock strength and laboratory test data available for the Yucca Mountain Project are summarized in *Intact Rock Mechanical Properties of Yucca Mountain Stratigraphic Units* (BSC 2005 [DIRS 176611]). A summary of laboratory strength properties, Young's modulus, and Poisson's ratio data are summarized in Appendix A). The data provided in the Appendix A also includes information about the tests group code and associated statistics.

Table 6-62. Summary of Laboratory Test Conditions and Test Data for All Static Laboratory Tests

GFM2000[a] Layer	Test Group Number	No. of Tests	Testing Group	Minimum Depth (ft)	Maximum Depth (ft)	Specimen Diameter – D (mm)	Test Temp. Condition or Temp. (°C)	Spec. Saturation	Average Effective Confining Pressure, (MPa)	Effective Confining Pressure,Std. Dev. (MPa)	Average Effective Axial Stress (MPa)	Effective Axial Stress, Std. Dev. (MPa)	Average Young's Modulus (GPa)	Young's Modulus Std. Dev. (GPa)	Average Poisson's Ratio	Poisson's Ratio Std. Dev.	No. of Tests for Each Litho Zone	No. of Test Groups for Each Litho Zone	No. of Test Groups for Each TM Unit
02_UO_Tmr	Group 1	5	231221	2.7	87.6	50.8	22	Saturated	0	0	7.60	7.48	3.36	2.69	0.03	0.03			
02_UO_Tmr	Group 2	3	231121			51.6	Ambient	Saturated	-1.23	1.27	0.00						8	2	
03_UO_Tpki	Group 1	7	231221	90.0	145.3	50.8	22	Saturated	0	0	5.94	2.72	3.77	1.54	0.19	0.14			
03_UO_Tpki	Group 2	6	231121			51.6	Ambient	Saturated	-0.70	0.24	0.00						13	2	4
04_TCw_Tpcrn	Group 1	18	231221	21.4	254.5	50.8	22	Saturated	0	0	36.02	32.98	15.16	8.39	0.20	0.03			
04_TCw_Tpcrn	Group 2	3	221221	9.5	30.6	61.1	22	Ambient	0	0	100.30	31.19	23.83	2.09	0.16	0.02			
04_TCw_Tpcrn	Group 3	24	231121			51.6	Ambient	Saturated	-7.14	3.52	0.00						45	3	
07_TCw_Tpcpul	Group 1	5	231221	123.2	195.7	50.8	22	Saturated	0	0	62.14	26.54	23.72	6.89	0.19	0.02			
07_TCw_Tpcpul	Group 2	3	221221	38.0	115.1	61.2	22	Ambient	0	0	92.10	22.51	26.24	3.84	0.17	0.02			
07_TCw_Tpcpul	Group 3	1	221233	80.8	89.5	61.2	22	Ambient	13.80		170.30								
07_TCw_Tpcpul	Group 4	1	221234	85.9	97.8	61.1	22	Ambient	27.60		227.60								
07_TCw_Tpcpul	Group 5	1	221321	89.5	97.8	61.2	22	Ambient	0.00		65.60		23.16		0.15				
07_TCw_Tpcpul	Group 6	1	221334	80.8	89.5	61.2	22	Ambient	41.40		253.80								
07_TCw_Tpcpul	Group 7	23	231121			61.2	Ambient	Saturated	-9.99	1.67	0.00						35	7	
08_TCw_Tpcpmn	Group 1	4	131222	263.3	265.7	25.4	22	Saturated	5	0	227.38	68.25	35.08	5.52	0.24	0.04			
08_TCw_Tpcpmn	Group 2	4	131223	263.3	265.7	25.4	22	Saturated	10	0	327.35	34.01	37.68	1.12	0.20	0.01			
08_TCw_Tpcpmn	Group 3	3	221221	123.8	144.4	61.2	22	Ambient	0	0	232.13	38.65	35.40	4.24	0.18	0.00			
08_TCw_Tpcpmn	Group 4	1	221233	136.8	144.4	61.1	22	Ambient	13.80		206.90								
08_TCw_Tpcpmn	Group 5	2	221234	136.8	144.4	61.2	22	Ambient	34.5	9.758	333.05	141.35							
08_TCw_Tpcpmn	Group 6	1	221321	123.8	130.1	61.2	22	Ambient	0.00		128.90		28.88		0.17				
08_TCw_Tpcpmn	Group 7	8	231221	60.5	263.3	50.8	22	Saturated	0	0	167.19	64.12	35.81	7.35	0.20	0.02			
08_TCw_Tpcpmn	Group 8	2	231222	16.1	80.0	50.8	22	Saturated	5	0	319.25	99.35	35.40	10.61	0.16	0.04			
08_TCw_Tpcpmn	Group 9	1	231223	32.0	32.0	50.8	22	Saturated	10.00		245.50		27.40		0.12				
08_TCw_Tpcpmn	Group 10	16	231121			51.6	Ambient	Saturated	14.52	3.88	0.00						42	10	
09_TCw_Tpcpll	Group 1	4	131221	22.2	22.2	25.4	22	Saturated	0	0	311.55	20.05	36.93	0.46	0.21	0.01			
09_TCw_Tpcpll	Group 2	4	131222	22.2	22.2	25.4	22	Saturated	5	0	372.65	43.77	36.73	0.50	0.21	0.01			
09_TCw_Tpcpll	Group 3	4	131223	22.2	22.2	25.4	22	Saturated	10	0	408.75	44.61	37.23	1.25	0.21	0.01			
09_TCw_Tpcpll	Group 4	5	231221	22.2	297.1	50.8	22	Saturated	0	0	186.74	112.86	32.82	5.65	0.24	0.04			
09_TCw_Tpcpll	Group 5	1	231222	5.7	5.7	50.8	22	Saturated	5.00		125.30		24.40		0.07				
09_TCw_Tpcpll	Group 6	1	231223	46.4	46.4	50.8	22	Saturated	10.00		157.90		22.30		0.10				
09_TCw_Tpcpll	Group 7	3	231121			51.6	Ambient	Saturated	-12.2	4.39	0.00						22	7	
10_TCw_Tpcpln	Group 1	1	221231	87.6	87.6	56	22	Ambient	0.00		364.00		57.50		0.31				

Table 6-62. Summary of Laboratory Test Conditions and Test Data for All Static Laboratory Tests (Continued)

GFM2000[a] Layer	Test Group Number	No. of Tests	Testing Group	Minimum Depth (ft)	Maximum Depth (ft)	Specimen Diameter – D (mm)	Test Temp. Condition or Temp. (°C)	Spec. Saturation	Average Effective Confining Pressure, (MPa)	Effective Confining Pressure,Std. Dev. (MPa)	Average Effective Axial Stress (MPa)	Effective Axial Stress, Std. Dev. (MPa)	Average Young's Modulus (GPa)	Young's Modulus Std. Dev. (GPa)	Average Poisson's Ratio	Poisson's Ratio Std. Dev.	No. of Tests for Each Litho Zone	No. of Test Groups for Each Litho Zone	No. of Test Groups for Each TM Unit
10_TCw_Tpcpln	Group 2	1	221233	87.6	87.6	56	22	Ambient	10.00		406.00		43.90		0.30				
10_TCw_Tpcpln	Group 3	1	221234	87.6	87.6	56	22	Ambient	20.00		895.00		58.30		0.22				
10_TCw_Tpcpln	Group 4	1	222234	185.0	185.0	56	200	Ambient	20.70		125.70								
10_TCw_Tpcpln	Group 5	20	231221	18.0	200.0	50.8	22	Saturated	0	0	172.33	58.09	33.84	6.05	0.21	0.02			
10_TCw_Tpcpln	Group 6	3	231222	156.0	202.9	50.8	22	Saturated	5	0	260.53	100.43	32.73	8.56	0.19	0.03			
10_TCw_Tpcpln	Group 7	4	231223	122.7	176.1	50.8	22	Saturated	10	0	290.98	143.00	37.68	14.45	0.22	0.04			
10_TCw_Tpcpln	Group 8	19	231121			51.6	Ambient	Saturated	10.89	1.73	0.00						50	8	
12_TCw_Tpcpv2	Group 1	4	231221	73.7	151.2	50.8	22	Saturated	0	0	28.18	23.60	7.63	5.32	0.10	0.03			
12_TCw_Tpcpv2	Group 2	1	231223	250.0	250.0	50.8	22	Saturated	10		71.40		24.00		0.19				
12_TCw_Tpcpv2	Group 3	4	231121			51.6	Ambient	Saturated	-3.18	1.91	0.00						9	3	38
13_PTn_Tpcpv1	Group 1	4	231221	84.4	91.0	50.8	22	Saturated	0	0	5.05	1.41	2.53	1.67	0.10	0.08			
13_PTn_Tpcpv1	Group 2	1	231121			51.6	Ambient	Saturated	-0.50		0.00						5	2	
14_PTn_Tpbt4	Group 1	2	221231	161.4	212.7	56	22	Ambient	0	0	5.27	2.50	1.66	1.76	0.22	0.08			
14_PTn_Tpbt4	Group 2	1	231221	105.0	105.0	50.8	22	Saturated	0.00		1.20		0.20		0.17		3	2	
15_PTn_Tpy	Group 1	5	231221	109.5	138.7	50.8	22	Saturated	0	0	19.30	6.99	5.24	3.05	0.16	0.01			
15_PTn_Tpy	Group 2	1	231121			51.6	Ambient	Saturated	-3.00		0.00						6	2	
16_PTn_Tpbt3	Group 1	2	221221	169.5	174.0	50.8	22	Ambient	0	0	5.10	1.13	1.80	0.85	0.17	0.06			
16_PTn_Tpbt3	Group 2	2	231221	169.1	267.1	50.8	22	Saturated	0	0	1.80	1.41	1.30	1.56	0.28				
16_PTn_Tpbt3	Group 3	1	231222	276.9	276.9	50.8	22	Saturated	5.00		13.30								
16_PTn_Tpbt3	Group 4	1	221121			51.6	Ambient	Room Dry	-0.30		0.00						6	4	
17_PTn_Tpp	Group 1	2	221221	182.2	187.0	50.8	22	Ambient	0	0	3.70	0.57	1.05	0.35	0.29	0.08			
17_PTn_Tpp	Group 2	10	231221	174.1	456.0	50.8	22	Saturated	0	0	3.19	2.45	0.98	0.66	0.26	0.09			
17_PTn_Tpp	Group 3	1	231223	282.5	282.5	50.8	22	Saturated	10.00		17.30								
17_PTn_Tpp	Group 4	1	221121			51.6	Ambient	Room Dry	-0.40		0.00								
17_PTn_Tpp	Group 5	12	231121			51.6	Ambient	Saturated	-0.16	0.18	0.00						26	5	
18_PTn_Tpbt2	Group 1	3	221221	222.0	241.4	50.8	22	Ambient	0	0	3.20	1.42	0.90	0.53	0.25	0.03			
18_PTn_Tpbt2	Group 2	6	231221	235.0	469.0	50.8	22	Saturated	0	0	2.92	2.30	0.67	0.68	0.21	0.10			
18_PTn_Tpbt2	Group 3	2	221121			51.6	Ambient	Room Dry	-0.25	0.07	0.00								
18_PTn_Tpbt2	Group 4	3	231121			51.6	Ambient	Saturated	-0.33	0.40	0.00						14	4	
19_PTn_Tptrv3	Group 1	2	231221	258.5	292.4	50.8	22	Saturated	0	0	4.25	2.19	0.99	1.29	0.23	0.11	2	1	20
22_TSw1_Tptrn	Group 1	10	131221	344.4	818.4	25.4	22	Saturated	0	0	103.68	36.02	28.22	9.08	0.20	0.05			

Table 6-62. Summary of Laboratory Test Conditions and Test Data for All Static Laboratory Tests (Continued)

GFM2000[a] Layer	Test Group Number	No. of Tests	Testing Group	Minimum Depth (ft)	Maximum Depth (ft)	Specimen Diameter – D (mm)	Test Temp. Condition or Temp. (°C)	Spec. Saturation	Average Effective Confining Pressure, (MPa)	Effective Confining Pressure,Std. Dev. (MPa)	Average Effective Axial Stress (MPa)	Effective Axial Stress, Std. Dev. (MPa)	Average Young's Modulus (GPa)	Young's Modulus Std. Dev. (GPa)	Average Poisson's Ratio	Poisson's Ratio Std. Dev.	No. of Tests for Each Litho Zone	No. of Test Groups for Each Litho Zone	No. of Test Groups for Each TM Unit
22_TSw1_Tptrn	Group 2	13	131222	344.4	527.0	25.4	22	Saturated	5	0	86.40	32.06	19.80	4.77	0.21	0.08			
22_TSw1_Tptrn	Group 3	11	131223	344.4	527.0	25.4	22	Saturated	10	0	132.61	50.42	22.58	5.83	0.22	0.06			
22_TSw1_Tptrn	Group 4	5	221221	484.7	528.4	57.2	22	Ambient	0	0	63.34	36.60	21.32	5.98	0.25	0.04			
22_TSw1_Tptrn	Group 5	53	231221	276.2	797.0	50.93	22	Saturated	0	0	61.98	31.06	20.95	9.66	0.25	0.06			
22_TSw1_Tptrn	Group 6	8	231222	326.0	454.6	50.8	22	Saturated	5	0	92.39	15.56	22.36	5.16	0.20	0.03			
22_TSw1_Tptrn	Group 7	8	231223	290.5	470.2	50.8	22	Saturated	10	0	117.63	50.62	19.65	8.19	0.20	0.08			
22_TSw1_Tptrn	Group 8	1	221121			51.6	Ambient	Room Dry	-8.40		0.00								
22_TSw1_Tptrn	Group 9	52	231121			51.6	Ambient	Saturated	-5.43	2.07	0.00						161	9	
23_TSw1_Tptrl	Group 1	3	231221	664.4	695.8	50.8	22	Saturated	0	0	26.73	9.25	9.13	2.38	0.30	0.02			
23_TSw1_Tptrl	Group 2	1	231222	483.3	483.3	50.8	22	Saturated	5		67.10		14.40		0.28				
23_TSw1_Tptrl	Group 3	7	231121			51.6	Ambient	Saturated	-4.81	1.36	0.00						11	3	
24_TSw1_Tptf	Group 1	2	131211	948.4	948.4	25.3	22	Saturated	0	0	116.00	1.41	42.00	0.14	0.26	0.00			
24_TSw1_Tptf	Group 2	5	131221	948.4	969.0	25.3	22	Saturated	0	0	176.80	37.57	48.84	11.58	0.24	0.05			
25_TSw1_Tptpul	Group 1	2	221221	633.9	634.4	57.23	22	Ambient	0	0	47.50	14.42	19.70	1.98					
25_TSw1_Tptpul	Group 2	8	231221	488.0	725.6	50.8	22	Saturated	0	0	65.21	44.40	20.41	9.16	0.25	0.13			
25_TSw1_Tptpul	Group 3	2	231222	671.4	717.7	50.8	22	Saturated	5	0	94.40	24.75	25.10	10.32	0.31	0.16			
25_TSw1_Tptpul	Group 4	1	231223	672.0	672.0	50.8	22	Saturated	10		227.90		22.30		0.11				
25_TSw1_Tptpul	Group 5	3	312111			289	**200**	Dry	0	0	30.47	9.47	10.30	3.22					
25_TSw1_Tptpul	Group 6	1	312221			146.5	**200**	Dry	0		17.70		6.70						
25_TSw1_Tptpul	Group 7	3	321111			289	24	Ambient	0	0	24.03	8.66	15.93	4.15	0.21				
25_TSw1_Tptpul	Group 8	8	321211			289	24	Ambient	0	0	28.65	12.04	13.10	4.46	0.26	0.13			
25_TSw1_Tptpul	Group 9	1	321221			146.8	24	Ambient	0		19.40		7.30						
25_TSw1_Tptpul	Group 10	4	331211			288	24	Saturated	0	0	18.75	15.10	8.30	4.92	0.17	0.12			
25_TSw1_Tptpul	Group 11	11	331221			266.7	24	Saturated	0	0	16.12	4.73	14.72	3.89	0.16	0.03			
25_TSw1_Tptpul	Group 12	19	231121			51.6	Ambient	Saturated	-5.57	3.10	0.00						63	12	27
26_TSw2_Tptpmn	Group 1	30	111321			25.4	22	Dry	0	0	146.46	57.33	24.02	4.13					
26_TSw2_Tptpmn	Group 2	2	131211	742.8	742.8	25.32	22	Saturated	0.1	0	236.60	9.19	35.55	2.76	0.16	0.06			
26_TSw2_Tptpmn	Group 3	30	131221	686.6	865.4	25.4	22	Saturated	0.03	0.05	222.70	42.42	34.90	5.58	0.21	0.03			
26_TSw2_Tptpmn	Group 4	6	131222	686.6	865.4	25.4	22	Saturated	5	0	220.30	81.58	37.40	3.85	0.21	0.05			
26_TSw2_Tptpmn	Group 5	6	131223	686.6	865.4	25.4	22	Saturated	10	0	325.90	48.54	34.23	2.17	0.23	0.02			
26_TSw2_Tptpmn	Group 6	3	131231	742.8	742.8	25.32	22	Saturated	0.1	0	294.10	21.70	36.60	2.31	0.27	0.02			

Table 6-62. Summary of Laboratory Test Conditions and Test Data for All Static Laboratory Tests (Continued)

GFM2000[a] Layer	Test Group Number	No. of Tests	Testing Group	Minimum Depth (ft)	Maximum Depth (ft)	Specimen Diameter – D (mm)	Test Temp. Condition or Temp. (°C)	Spec. Saturation	Average Effective Confining Pressure, (MPa)	Effective Confining Pressure,Std. Dev. (MPa)	Average Effective Axial Stress (MPa)	Effective Axial Stress, Std. Dev. (MPa)	Average Young's Modulus (GPa)	Young's Modulus Std. Dev. (GPa)	Average Poisson's Ratio	Poisson's Ratio Std. Dev.	No. of Tests for Each Litho Zone	No. of Test Groups for Each Litho Zone	No. of Test Groups for Each TM Unit
26_TSw2_Tptpmn	Group 7	4	211211			50.8	22	Dry	0	0	150.88	50.18	37.98	4.48	0.17	0.03			
26_TSw2_Tptpmn	Group 8	4	211221			50.8	22	Dry	0	0	122.58	35.32	40.55	5.01	0.23	0.07			
26_TSw2_Tptpmn	Group 9	3	211222			50.8	22	Dry	5	0	196.40	32.99	37.43	3.52	0.19	0.02			
26_TSw2_Tptpmn	Group 10	3	211223			50.8	22	Dry	10	0	235.10	68.81	35.57	4.53	0.20	0.03			
26_TSw2_Tptpmn	Group 11	9	212211			50.9	150	Dry	0	0	105.67	34.54	50.72	38.23	0.12	0.09			
26_TSw2_Tptpmn	Group 12	2	212221			50.8	150	Dry	0	0	90.50	26.16	37.60	0.14	0.14	0.02			
26_TSw2_Tptpmn	Group 13	3	212223			50.8	150	Dry	10	0	196.33	64.53	36.43	1.59	0.14	0.02			
26_TSw2_Tptpmn	Group 14	2	212231			50.8	150	Dry	0	0	101.50	102.53	26.10	17.11	0.26	0.16			
26_TSw2_Tptpmn	Group 15	16	221221			38.1	22	Ambient	0	0	176.35	65.82	36.76	3.48	0.20	0.04			
26_TSw2_Tptpmn	Group 16	1	221231	723.0	723.0	56	22	Ambient	0		138.00		40.40		0.22				
26_TSw2_Tptpmn	Group 17	36	221321			41.9	22	Ambient	0	0	139.58	58.07	32.08	3.74	0.18	0.04			
26_TSw2_Tptpmn	Group 18	1	222234	739.0	739.0	56	**200**	Ambient	20.7		153.70		23.90		0.15				
26_TSw2_Tptpmn	Group 19	10	231211			50.8	22	Saturated	0	0	103.65	32.07	36.35	5.19	0.15	0.07			
26_TSw2_Tptpmn	Group 20	42	231221	720.7	896.5	50.8	22	Saturated	0	0	164.58	65.62	32.53	6.74	0.19	0.04			
26_TSw2_Tptpmn	Group 21	5	231222	745.6	861.7	50.8	22	Saturated	5	0	227.78	67.95	35.56	1.40	0.21	0.01			
26_TSw2_Tptpmn	Group 22	14	231223	762.6	827.4	50.8	22	Saturated	10	0	169.00	55.61	29.65	4.69	0.19	0.06			
26_TSw2_Tptpmn	Group 23	5	231224			50.8	22	Saturated	20	0	214.54	39.73	28.09	4.80	0.18	0.03			
26_TSw2_Tptpmn	Group 24	4	231231			50.8	22	Saturated	0	0	113.20	42.86	32.53	4.12	0.20	0.02			
26_TSw2_Tptpmn	Group 25	11	232211	764.8	842.1	50.8	150	Saturated	0.73	0.26	196.79	25.85	35.74	4.45	0.20	0.05			
26_TSw2_Tptpmn	Group 26	6	232212	764.8	842.1	50.8	150	Saturated	5	0	253.55	49.09	30.83	4.57	0.21	0.04			
26_TSw2_Tptpmn	Group 27	5	232213	766.0	836.3	50.8	150	Saturated	10	0	253.86	50.36	31.50	3.02	0.20	0.02			
26_TSw2_Tptpmn	Group 28	4	232221			50.8	150	Saturated	0	0	117.38	20.67	30.98	2.21					
26_TSw2_Tptpmn	Group 29	3	232222			50.8	150	Saturated	5	0	121.10	59.27	28.60	10.96					
26_TSw2_Tptpmn	Group 30	1	321221			145.5	24	Ambient	0		159.60		32.40		0.17				
26_TSw2_Tptpmn	Group 31	22	331221			228.6	22	Saturated	0	0	105.94	31.11	38.26	5.66	0.22	0.03			
26_TSw2_Tptpmn	Group 32	14	231121			51.6	Ambient	Saturated	-10.88	4.02	0.00						307	32	
27_TSw2_Tptpll	Group 1	16	121221			26.25	25	Ambient	0	0	194.69	37.99	32.26	2.91	0.17	0.02			
27_TSw2_Tptpll	Group 2	2	131211	1002.4	1002.4	25.32	22	Saturated	0.1	0	130.60	10.61	27.40	7.64	0.16	0.06			
27_TSw2_Tptpll	Group 3	30	131221	910.7	1587.8	26.1	22	Saturated	0.1	0.050	112.99	51.38	28.20	7.63	0.21	0.06			
27_TSw2_Tptpll	Group 4	3	131222	1154.9	1179.6	26.1	22	Saturated	5	0	138.83	76.32	26.00	8.55	0.25	0.10			
27_TSw2_Tptpll	Group 5	3	131223	965.2	1189.0	26.1	22	Saturated	10	0	164.43	80.94	24.13	9.39	0.26	0.05			

Table 6-62. Summary of Laboratory Test Conditions and Test Data for All Static Laboratory Tests (Continued)

GFM2000[a] Layer	Test Group Number	No. of Tests	Testing Group	Minimum Depth (ft)	Maximum Depth (ft)	Specimen Diameter – D (mm)	Test Temp. Condition or Temp. (°C)	Spec. Saturation	Average Effective Confining Pressure, (MPa)	Effective Confining Pressure,Std. Dev. (MPa)	Average Effective Axial Stress (MPa)	Effective Axial Stress, Std. Dev. (MPa)	Average Young's Modulus (GPa)	Young's Modulus Std. Dev. (GPa)	Average Poisson's Ratio	Poisson's Ratio Std. Dev.	No. of Tests for Each Litho Zone	No. of Test Groups for Each Litho Zone	No. of Test Groups for Each TM Unit
27_TSw2_Tptpll	Group 6	7	211221			51.05	25	Dry	0	0	175.93	19.38	36.09	2.22	0.17	0.01			
27_TSw2_Tptpll	Group 7	6	212221			51.05	200	Dry	0	0	213.18	11.75	37.13	1.42					
27_TSw2_Tptpll	Group 8	59	221221	853.4	874.6	51.07	25	Ambient	0	0	153.12	40.06	34.52	3.75	0.19	0.02			
27_TSw2_Tptpll	Group 9	15	231221	848.0	1236.7	51.05	25	Saturated	0	0	123.01	47.57	29.97	6.43	0.22	0.07			
27_TSw2_Tptpll	Group 10	1	231223	977.8	977.8	50.8	22	Saturated	10		216.90		29.60		0.20				
27_TSw2_Tptpll	Group 11	2	312111			289	200	Dry	0	0	31.65	0.78	6.80	0.42					
27_TSw2_Tptpll	Group 12	5	312221			146.9	200	Dry	0	0	122.72	75.98	28.96	14.08	0.19	0.11			
27_TSw2_Tptpll	Group 13	7	321211			288	24	Ambient	0	0	34.57	17.39	11.81	5.11	0.25	0.08			
27_TSw2_Tptpll	Group 14	25	321221			120.70	25	Ambient	0	0	121.24	38.69	33.65	8.13	0.19	0.04			
27_TSw2_Tptpll	Group 15	1	331211			288	24	Saturated	0		15.70		5.30						
27_TSw2_Tptpll	Group 16	1	331221			146.9	24	Saturated	0		38.00		10.90						
27_TSw2_Tptpll	Group 17	5	421221			245	25	Ambient	0	0	60.70	24.80	31.60	5.43					
27_TSw2_Tptpll	Group 18	24	231121			51.6	Ambient	Saturated	-8.33	2.93	0.00						212	18	
28_TSw2_Tptpln	Group 1	3	131211	1218.2	1279.5	26.1	22	Saturated	0.1	0	126.13	70.97	33.00	9.17	0.24	0.03			
28_TSw2_Tptpln	Group 2	10	131221	1050.4	1307.2	25.35	22	Saturated	0.050	0.053	104.40	37.77	29.72	7.25	0.22	0.04			
28_TSw2_Tptpln	Group 3	4	131231	1222.1	1262.4	26.1	22	Saturated	0.1	0	149.58	11.03	32.75	5.02	0.28	0.04			
28_TSw2_Tptpln	Group 4	2	221221	1067.8	1067.8	57.18	22	Ambient	0	0	171.55	1.91	35.05	0.92	0.22	0.02			
28_TSw2_Tptpln	Group 5	1	221231	1250.0	1250.0	56	22	Ambient	0		166.00		61.80		0.30				
28_TSw2_Tptpln	Group 6	1	221233	1250.0	1250.0	56	22	Ambient	10		422.00		73.00		0.23				
28_TSw2_Tptpln	Group 7	1	221234	1250.0	1250.0	56	22	Ambient	20		638.00		59.90		0.21				
28_TSw2_Tptpln	Group 11	1	232213	1325.4	1325.4	50.8	150	Saturated	10		274.50		43.90		0.12				
28_TSw2_Tptpln	Group 12	13	231121			51.6	Ambient	Saturated	-7.92	2.55	0.00						52	12	62
28_TSw2_Tptpln	Group 8	10	231221	1107.1	1346.5	50.8	22	Saturated	0	0	155.51	30.35	37.78	4.53	0.22	0.04			
28_TSw2_Tptpln	Group 9	3	231222	1073.3	1399.1	50.8	22	Saturated	5	0	216.43	64.00	34.27	3.00	0.24	0.03			
28_TSw2_Tptpln	Group 10	3	231223	1077.1	1400.5	50.8	22	Saturated	10	0	265.60	21.65	35.50	3.59	0.23	0.03			
29_TSw3_Tptpv3	Group 1	4	131223	1646.8	1659.2	25.3	22	Saturated	10	0	55.00	19.03							
29_TSw3_Tptpv3	Group 2	2	221221	1195.1	1197.5	57.15	22	Ambient	0	0	45.80	5.66	34.25	3.32	0.18				
29_TSw3_Tptpv3	Group 3	1	231221	1299.9	1299.9	50.8	22	Saturated	0		16.40		25.20		0.39				
29_TSw3_Tptpv3	Group 4	1	231222	1279.7	1279.7	50.8	22	Saturated	5		52.20		54.20		0.17				
29_TSw3_Tptpv3	Group 5	1	231223	1284.2	1284.2	50.8	22	Saturated	10		80.00		32.90		0.17				
29_TSw3_Tptpv3	Group 6	3	231121	29.0		51.62	Ambient	Saturated	-3.97	0.32	0.00						12	6	6

Table 6-62. Summary of Laboratory Test Conditions and Test Data for All Static Laboratory Tests (Continued)

GFM2000[a] Layer	Test Group Number	No. of Tests	Testing Group	Minimum Depth (ft)	Maximum Depth (ft)	Specimen Diameter – D (mm)	Test Temp. Condition or Temp. (°C)	Spec. Saturation	Average Effective Confining Pressure, (MPa)	Effective Confining Pressure,Std. Dev. (MPa)	Average Effective Axial Stress (MPa)	Effective Axial Stress, Std. Dev. (MPa)	Average Young's Modulus (GPa)	Young's Modulus Std. Dev. (GPa)	Average Poisson's Ratio	Poisson's Ratio Std. Dev.	No. of Tests for Each Litho Zone	No. of Test Groups for Each Litho Zone	No. of Test Groups for Each TM Unit
30_CHn1_Tptpv2	Group 1	2	131221	1280.6	1280.6	25.35	22	Saturated	0	0	91.65	1.63	16.45	0.49	0.20	0.02			
30_CHn1_Tptpv2	Group 2	1	221221	1280.6	1280.6	57.15	22	Ambient	0		90.20		16.70		0.22		3	2	
31_CHn1_Tptpv1	Group 1	2	131211	1369.1	1369.1	25.27	22	Saturated	0.1	0	10.10	2.83	2.26	1.20	0.17	0.00			
31_CHn1_Tptpv1	Group 2	5	131221	1369.1	1400.6	25.32	22	Saturated	0.1	0.00	12.90	4.76	2.40	0.79	0.18	0.03			
31_CHn1_Tptpv1	Group 3	2	131222	1400.6	1400.6	25.32	22	Saturated	5	0	28.00	8.49	3.39	0.41	0.21	0.01			
31_CHn1_Tptpv1	Group 4	2	131223	1400.6	1400.6	25.32	22	Saturated	10	0	34.00	11.31	3.75	0.86	0.30	0.00			
31_CHn1_Tptpv1	Group 5	3	131231	1369.1	1369.1	25.30	22	Saturated	0.1	0	12.10	3.61	2.70	0.84	0.18	0.07	14	5	
32_CHn1_Tpbt1	Group 1	3	131211	1748.0	1748.0	25.3	22	Saturated	0	0	27.67	0.58	12.17	1.76	0.11	0.01			
32_CHn1_Tpbt1	Group 2	4	131221	1748.0	1748.0	25.3	22	Saturated	0	0	27.25	6.02	9.25	2.32	0.20	0.07			
32_CHn1_Tpbt1	Group 3	1	231221	1477.2	1477.2	50.8	22	Saturated	0		20.50		3.90		0.11		8	3	
33_CHn1_Tac	Group 1	2	121221	1665.5	1665.5	25.4	22	Ambient	0.1	0	36.95	5.87	7.31	1.15	0.30	0.01			
33_CHn1_Tac	Group 2	2	121223	1665.5	1665.5	25.4	22	Ambient	10	0	69.45	2.62	7.27	0.10	0.28	0.01			
33_CHn1_Tac	Group 3	2	131211	1668.1	1668.1	25.4	22	Saturated	0.1	0.0	20.80	1.13	7.45	0.59	0.22	0.01			
33_CHn1_Tac	Group 4	34	131221	1441.9	1719.8	25.4	23	Saturated	0.05	0.05	27.46	8.87	7.07	2.13	0.16	0.08			
33_CHn1_Tac	Group 5	8	131223	1487.4	1668.1	25.4	22	Saturated	10	0	37.71	4.91	6.76	1.56	0.31	0.05			
33_CHn1_Tac	Group 6	6	131224	1487.4	1665.5	25.4	22	Saturated	20	0	50.88	7.62	7.42	2.13	0.26	0.13			
33_CHn1_Tac	Group 7	2	131231	1668.1	1668.1	25.4	22	Saturated	0.1	0	24.15	0.92	5.43	0.03	0.33				
33_CHn1_Tac	Group 8	2	221231	1692.0	1490.0	56	22	Ambient	0	0	44.25	4.88	13.16	1.22	0.17	0.04			
33_CHn1_Tac	Group 9	3	221234	1605.0	1662.0	56	22	Ambient	20.23	0.40	74.87	24.93	8.69	0.81	0.25	0.03			
33_CHn1_Tac	Group 10	2	231221	1499.9	1560.8	50.8	22	Saturated	0	0	24.60	2.69	6.50	0.57	0.20	0.16	63	10	
34_CHn1_Tacbt	Group 1	8	131221	1741.8	1784.8	25.4	23	Saturated	0.050	0.053	35.04	20.45	6.92	4.13	0.25	0.09	8	1	21
TOTAL																	1208	178	178

Sources: DTNs: MO0311RCKPRPCS.003 [DIRS 166073]; MO0402DQRIRPPR.003 [DIRS 168901]; SN0208L0207502.001 [DIRS 161871]; SN0211L0207502.002 [DIRS 161872]; SN0302L0207502.003 [DIRS 165014]; SN0305L0207502.004 [DIRS 165013]; SN0306L0207502.008 [DIRS 165015]; SNL02030193001.001 [DIRS 120572]; MO0401DQRIRPTS.003 [DIRS 168905]; SN0505L0212303.005 [DIRS 174956].

[a]BSC 2003 [DIRS 165802].

NOTE: Negative numbers indicate the tensile strength data.

Spec. = specimen; Std. Dev. = standard deviation; Temp. = temperature.

Table 6-63. Summary of the Average Laboratory Test Data for Use in RocLab Calculation

GFM 000[a] Layer	Test Group Number	Test Type	No. of Tests in Each Lithostratigraphic .Zone	Test Code	Max. Depth in ESF (m)	Specimen Diameter, D (mm)	Specimen Temp. Condition or Temp. (deg. C)	Specimen Saturation	Effective Confining Pressure, σ_3' (MPa)[b]	Effective Confining Pressure, Std. Dev. (MPa)	Effective Axial Stress, σ_1' (MPa)	Effective Axial Stress, Std. Dev. (MPa)	Young's Modulus, E (GPa)	Young's Modulus Std. Dev. (GPa)	Poisson's Ratio, ν	Poisson's Ratio Std. Dev.	Notes
1	2	3	4	5	6	7	8	9	10	11	12	13	14	15	16	17	18
02_UO_Tmr	Group 1	U	5	231221	28.2	50.8	22	Saturated	0	0	7.60	7.48	3.36	2.69	0.03	0.03	
02_UO_Tmr	Group 2	T	3	231121		51.6	Ambient	Saturated	-1.23	1.27	0.00						
03_UO_Tpki	Group 1	U	7	231221	28.2	50.8	22	Saturated	0	0	5.94	2.72	3.77	1.54	0.19	0.14	
03_UO_Tpki	Group 2	T	6	231121		51.6	Ambient	Saturated	-0.70	0.24	0.00						
04_TCw_Tpcrn	Group 1	U	18	231221	31.8	50.8	22	Saturated	0	0	36.02	32.98	15.16	8.39	0.20	0.03	
04_TCw_Tpcrn	Group 3	T	24	231121		51.6	Ambient	Saturated	-7.14	3.52	0.00						
07_TCw_Tpcpul	Group 1	U	5	231221	48.7	50.8	22	Saturated	0	0	62.14	26.54	23.72	6.89	0.19	0.02	
07_TCw_Tpcpul	Group 7	T	23	231121		61.2	Ambient	Saturated	-9.99	1.67	0.00						
08_TCw_Tpcpmn	Group 7	U	8	231221	55.8	50.8	22	Saturated	0	0	167.19	64.12	35.81	7.35	0.20	0.02	
08_TCw_Tpcpmn	Group 8	5	2	231222		50.8	22	Saturated	5	0	319.25	99.35	35.40	10.61	0.16	0.04	
08_TCw_Tpcpmn	Group 9	10	1	231223		50.8	22	Saturated	10		245.50		27.40		0.12		
08_TCw_Tpcpmn	Group 10	T	16	231121		51.6	Ambient	Saturated	-14.52	3.88	0.00						
09_TCw_Tpcpll	Group 4	U	5	231221	65.0	50.8	22	Saturated	0	0	186.74	112.86	32.82	5.65	0.24	0.04	
09_TCw_Tpcpll	Group 5	5	1	231222		50.8	22	Saturated	5		125.30		24.40		0.07		
09_TCw_Tpcpll	Group 6	10	1	231223		50.8	22	Saturated	10		157.90		22.30		0.10		
09_TCw_Tpcpll	Group 7	T	3	231121		51.6	Ambient	Saturated	-12.2	4.39	0.00						
10_TCw_Tpcpln	Group 5	U	20	231221	103.8	50.8	22	Saturated	0	0	172.33	58.09	33.84	6.05	0.21	0.02	
10_TCw_Tpcpln	Group 6	5	3	231222		50.8	22	Saturated	5	0	260.53	100.43	32.73	8.56	0.19	0.03	
10_TCw_Tpcpln	Group 7	10	4	231223		50.8	22	Saturated	10	0	290.98	143.00	37.68	14.45	0.22	0.04	
10_TCw_Tpcpln	Group 8	T	19	231121		51.6	Ambient	Saturated	-10.89	1.73	0.00						
12_TCw_Tpcpv2	Group 1	U	4	231221	104.7	50.8	22	Saturated	0	0	28.18	23.60	7.63	5.32	0.10	0.03	
12_TCw_Tpcpv2	Group 2	10	1	231223		50.8	22	Saturated	10		71.40		24.00		0.19		
12_TCw_Tpcpv2	Group 3	T	4	231121		51.6	Ambient	Saturated	-3.18	1.91	0.00						
13_PTn_Tpcpv1	Group 1	U	4	231221	105.6	50.8	22	Saturated	0	0	5.05	1.41	2.53	1.67	0.10	0.08	
13_PTn_Tpcpv1	Group 2	T	1	231121		51.6	Ambient	Saturated	-0.50		0.00						
14_PTn_Tpbt4	Group 2	U	1	231221	112.0	50.8	22	Saturated	0		1.20		0.20		0.17		c
15_PTn_Tpy	Group 1	U	5	231221	118.5	50.8	22	Saturated	0	0	19.30	6.99	5.24	3.05	0.16	0.01	
15_PTn_Tpy	Group 2	T	1	231121		51.6	Ambient	Saturated	-3.00		0.00						
16_PTn_Tpbt3	Group 2	U	2	231221	124.9	50.8	22	Saturated	0	0	1.80	1.41	1.30	1.56	0.28		
16_PTn_Tpbt3	Group 3	5	1	231222		50.8	22	Saturated	5		13.30						
17_PTn_Tpp	Group 2	U	10	231221	130.0	50.8	22	Saturated	0	0	3.19	2.45	0.98	0.66	0.26	0.09	
17_PTn_Tpp	Group 3	10	1	231223		50.8	22	Saturated	10		17.30						
17_PTn_Tpp	Group 5	T	12	231121		51.6	Ambient	Saturated	-0.16	0.18	0.00						
18_PTn_Tpbt2	Group 2	U	6	231221	138.9	50.8	22	Saturated	0	0	2.92	2.30	0.67	0.68	0.21	0.10	
18_PTn_Tpbt2	Group 4	T	3	231121		51.6	Ambient	Saturated	-0.33	0.40	0.00						
19_PTn_Tptrv3	Group 1	U	2	231221	139.2	50.8	22	Saturated	0	0	4.25	2.19	0.99	1.29	0.23	0.11	
22_TSw1_Tptrn	Group 5	U	53	231221	200.4	50.9	22	Saturated	0	0	61.98	31.06	20.95	9.66	0.25	0.06	
22_TSw1_Tptrn	Group 6	5	8	231222		50.8	22	Saturated	5	0	92.39	15.56	22.36	5.16	0.20	0.03	

Table 6-63. Summary of the Average Laboratory Test Data for Use in RocLab Calculation (Continued)

GFM 000[a] Layer	Test Group Number	Test Type	No. of Tests in Each Lithostratigraphic Zone	Test Code	Max. Depth in ESF (m)	Specimen Diameter, D (mm)	Specimen Temp. Condition or Temp. (deg. C)	Specimen Saturation	Effective Confining Pressure, σ_3' (MPa)[b]	Effective Confining Pressure, Std. Dev. (MPa)	Effective Axial Stress, σ_1' (MPa)	Effective Axial Stress, Std. Dev. (MPa)	Young's Modulus, E (GPa)	Young's Modulus Std. Dev. (GPa)	Poisson's Ratio, v	Poisson's Ratio Std. Dev.	Notes
1	2	3	4	5	6	7	8	9	10	11	12	13	14	15	16	17	18
22_TSw1_Tptrn	Group 7	10	8	231223		50.8	22	Saturated	10	0	117.63	50.62	19.65	8.19	0.20	0.08	
22_TSw1_Tptrn	Group 9	T	52	231121		51.6	Ambient	Saturated	-5.43	2.07	0.00						
23_TSw1_Tptrl	Group 1	U	3	231221	184.6	50.8	22	Saturated	0	0	26.73	9.25	9.13	2.38	0.30	0.02	
23_TSw1_Tptrl	Group 2	5	1	231222		50.8	22	Saturated	5		67.10		14.40		0.28		
23_TSw1_Tptrl	Group 3	T	7	231121		51.6	Ambient	Saturated	-4.81	1.36	0.00						
24_TSw1_Tptf	Group 3	U	1	231221	241.4	50.9	22	Saturated	0		157.00		54.70		0.34		c, e
25_TSw1_Tptpul	Group 2	U	8	231221	298.0	50.8	22	Saturated	0	0	65.21	44.40	20.41	9.16	0.25	0.13	
25_TSw1_Tptpul	Group 3	5	2	231222		50.8	22	Saturated	5	0	94.40	24.75	25.10	10.32	0.31	0.16	
25_TSw1_Tptpul	Group 4	10	1	231223		50.8	22	Saturated	10		227.90		22.30		0.11		
25_TSw1_Tptpul	Group 12	T	19	231121		51.6	Ambient	Saturated	-5.57	3.10	0.00						
26_TSw2_Tptpmn	Group 19	U	10	231211	297.8	50.8	22	Saturated	0	0	103.65	32.07	36.35	5.19	0.15	0.07	
26_TSw2_Tptpmn	Group 20	U	42	231221		50.8	22	Saturated	0	0	164.58	65.62	32.53	6.74	0.19	0.04	
26_TSw2_Tptpmn	Group 21	5	5	231222		50.8	22	Saturated	5	0	227.78	67.95	35.56	1.40	0.21	0.01	
26_TSw2_Tptpmn	Group 22	10	14	231223		50.8	22	Saturated	10	0	169.00	55.61	29.65	4.69	0.19	0.06	
26_TSw2_Tptpmn	Group 23	20	5	231224		50.8	22	Saturated	20	0	214.54	39.73	28.09	4.80	0.18	0.03	
26_TSw2_Tptpmn	Group 24	U	4	231231		50.8	22	Saturated	0	0	113.20	42.86	32.53	4.12	0.20	0.02	
26_TSw2_Tptpmn	Group 32	T	14	231121		51.6	Ambient	Saturated	-10.88	4.02	0.00						
27_TSw2_Tptpll	Group 9	U	15	231221	362.6	51.1	25	Saturated	0	0	123.01	47.57	29.97	6.43	0.22	0.07	
27_TSw2_Tptpll	Group 10	10	1	231223		50.8	22	Saturated	10		216.90		29.60		0.20		
27_TSw2_Tptpll	Group 18	T	24	231121		51.6	Ambient	Saturated	-8.33	2.93	0.00						
28_TSw2_Tptpln	Group 8	U	10	231221	259.5	50.8	22	Saturated	0	0	155.51	30.35	37.78	4.53	0.22	0.04	
28_TSw2_Tptpln	Group 9	5	3	231222		50.8	22	Saturated	5	0	216.43	64.00	34.27	3.00	0.24	0.03	
28_TSw2_Tptpln	Group 10	10	3	231223		50.8	22	Saturated	10	0	265.60	21.65	35.50	3.59	0.23	0.03	
28_TSw2_Tptpln	Group 12	T	13	231121		51.6	Ambient	Saturated	-7.92	2.55	0.00						
29_TSw3_Tptpv3	Group 3	U	1	231221		50.8	22	Saturated	0		16.40		25.20		0.39		e
29_TSw3_Tptpv3	Group 4	5	1	231222		50.8	22	Saturated	5		52.20		54.20		0.17		
29_TSw3_Tptpv3	Group 5	10	1	231223		50.8	22	Saturated	10		80.00		32.90		0.17		
29_TSw3_Tptpv3	Group 6	T	3	231121		51.6	Ambient	Saturated	-3.97	0.32	0.00						
30_CHn1_Tptpv2	Group 1	U	2	131221		25.4	22	Saturated	0	0	91.65	1.63	16.45	0.49	0.20	0.02	d
30_CHn1_Tptpv2	Group 2	U	1	221221		57.2	22	ambient	0		90.20		16.70		0.22		
31_CHn1_Tptpv1	Group 1	U	2	131211		25.3	22	Saturated	0.1	0	10.10	2.83	2.26	1.20	0.17	0.00	d
31_CHn1_Tptpv1	Group 2	U	5	131221		25.3	22	Saturated	0.1	0	12.90	4.76	2.40	0.79	0.18	0.03	d
31_CHn1_Tptpv1	Group 3	5	2	131222		25.3	22	Saturated	5	0	28.00	8.49	3.39	0.41	0.21	0.01	d
31_CHn1_Tptpv1	Group 4	10	2	131223		25.3	22	Saturated	10	0	34.00	11.31	3.75	0.86	0.30	0.00	d
31_CHn1_Tptpv1	Group 5	U	3	131231		25.3	22	Saturated	0.1	0	12.10	3.61	2.70	0.84	0.18	0.07	d
32_CHn1_Tpbt1	Group 1	U	3	131211		25.3	22	Saturated	0	0	27.67	0.58	12.17	1.76	0.11	0.01	d

Table 6-63. Summary of the Average Laboratory Test Data for Use in RocLab Calculation (Continued)

GFM 000[a] Layer	Test Group Number	Test Type	No. of Tests in Each Lithostratigraphic Zone	Test Code	Max. Depth in ESF (m)	Specimen Diameter, D (mm)	Specimen Temp. Condition or Temp. (deg. C)	Specimen Saturation	Effective Confining Pressure, σ_3' (MPa)[b]	Effective Confining Pressure, Std. Dev. (MPa)	Effective Axial Stress, σ_1' (MPa)	Effective Axial Stress, Std. Dev. (MPa)	Young's Modulus, E (GPa)	Young's Modulus Std. Dev. (GPa)	Poisson's Ratio, v	Poisson's Ratio Std. Dev.	Notes
1	2	3	4	5	6	7	8	9	10	11	12	13	14	15	16	17	18
32_CHn1_Tpbt1	Group 2	U	4	131221		25.3	22	Saturated	0	0	27.25	6.02	9.25	2.32	0.20	0.07	d
32_CHn1_Tpbt1	Group 3	U	1	231221		50.8	22	Saturated	0		20.50		3.90		0.11		d, e
33_CHn1_Tac	Group 1	U	2	121221		25.4	22	ambient	0.1	0	36.95	5.87	7.31	1.15	0.30	0.01	d
33_CHn1_Tac	Group 2	10	2	121223		25.4	22	ambient	10	0	69.45	2.62	7.27	0.10	0.28	0.01	d
33_CHn1_Tac	Group 3	U	2	131211		25.4	22	Saturated	0.1	0.0	20.80	1.13	7.45	0.59	0.22	0.01	d
33_CHn1_Tac	Group 4	U	34	131221		25.4	23	Saturated	0.05	0.05	27.46	8.87	7.07	2.13	0.16	0.08	d
33_CHn1_Tac	Group 5	10	8	131223		25.4	22	Saturated	10	0	37.71	4.91	6.76	1.56	0.31	0.05	d
33_CHn1_Tac	Group 6	20	6	131224		25.4	22	Saturated	20	0	50.88	7.62	7.42	2.13	0.26	0.13	d
33_CHn1_Tac	Group 7	U	2	131231		25.4	22	Saturated	0.1	0	24.15	0.92	5.43	0.03	0.33		d
33_CHn1_Tac	Group 8	U	2	221231		56.0	22	ambient	0	0	44.25	4.88	13.16	1.22	0.17	0.04	
33_CHn1_Tac	Group 9	20	3	221234		56.0	22	ambient	20.23	0.40	74.87	24.93	8.69	0.81	0.25	0.03	
33_CHn1_Tac	Group 10	U	2	231221		50.8	22	Saturated	0	0	24.60	2.69	6.50	0.57	0.20	0.16	
34_CHn1_Tacbt	Group 1	U	8	131221		25.4	23	Saturated	0.050	0.053	35.04	20.45	6.92	4.13	0.25	0.09	d

Sources: MO0311RCKPRPCS.003 [DIRS 166073], MO0402DQRIRPPR.003 [DIR S 168901], SN0208L0207502.001 [DIRS 161871], SN0211L0207502.002 [DIRS 161872], SN0302L0207502.003 [DIRS 165014], SN0305L0207502.004 [DIRS 165013], SN0306L0207502.008 [DIRS 165015], SNL02030193001.001 [DIRS 120572], MO0401DQRIRPTS.003 [DIRS 168905], and SN0505L0212303.005 [DIRS 174956].

NOTES: [a] BSC 2003 [DIRS 165802]
[b] Negative values in Column 10 indicate indirect tensile strength data
[c] No Indirect tensile strength data available.
[d] Data available for small specimens (25.4 mm diameter only)
[e] Only one specimen 50.8 mm diameter available.

Legend for Column 3:

U: Uniaxial compressive strength
T: Indirect tensile strength
5: Confining pressure of 5 MPa
10: Confining pressure of 10 MPa
20: Confining pressure of 20 MPa

6.4.4.4.1.1 Visual Presentation of Test Data Population

The average values of parameters used for calculating rock mass strength parameters represent a variety of data sets of different populations. A better understanding of these data populations can be accomplished by presenting a standardized portion of data arranged in vertical order corresponding to their natural occurrence in the field (e.g., such as used in design of a typical shaft). Figure 6-70, included for information only, provides a visual summary of the laboratory data for a hypothetical shaft, for which lithostratigraphic sequence and strata thicknesses were calculated as averages for the entire area of the repository using Vulcan representation of the GFM2000 (BSC 2003 [DIRS 165802]). For clarity, only the major rock units are labeled.

Figure 6-70 shows an average lithostratigraphic unit stratum thickness and a population of data representing each unit. The standardized test data are all of the same test type, and each represents uniaxial compressive strength of a 50 mm diameter specimen of saturated rock material tested under room temperature. Shown in this figure are the relative magnitudes and a number of tests available for each lithostratigraphic unit, as well as a range of uniaxial compressive strength values as available for each lithostratigraphic unit.

It is apparent that the strength of strata varies considerably especially between the major thermal-mechanical units, with the PTn strata being the weakest among all. Further analysis indicates that testing procedures that require specimens to be tested under saturated conditions may cause an overly conservative assessment of the compressive strength especially for the weaker strata.

It should also be noted that the RHH strata, which hosts the repository emplacement drifts operating under extreme temperature and stress conditions, must be investigated and documented much more thoroughly than other overlaying strata.

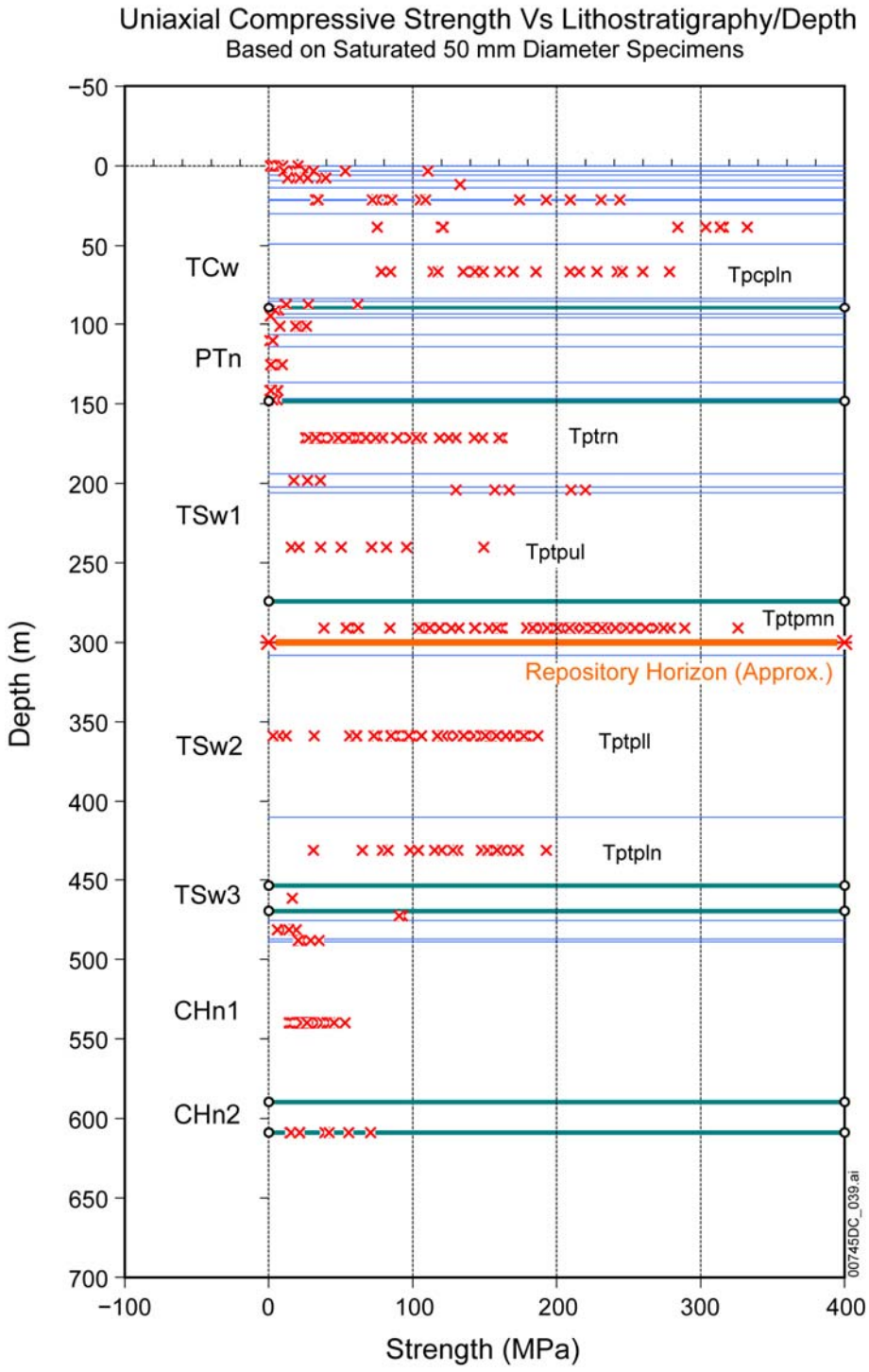

Sources: DTNs: MO0311RCKPRPCS.003 [DIRS 166073]; SN0208L0207502.001 [DIRS 161871]; SN0211L0207502.002 [DIRS 161872]; SN0302L0207502.003 [DIRS 165014]; SN0305L0207502.004 [DIRS 165013]; SN0306L0207502.008 [DIRS 165015]; SNL02030193001.001 [DIRS 120572].

NOTE: Thicker lines delineate the major thermal-mechanical units.

Figure 6-70. Vertical Distribution of Uniaxial Compressive Strength Tests Results for 50 mm Saturated Specimens Tested Under Room Temperature Condition as Available for Distinct Lithostratigraphic Zones

6.4.4.4.1.2 Rock Mass Mechanical Property Development

In Situ Stress

In situ stress data were determined by hydraulic fracturing in a borehole ESF-AOD-HDFR#1 located in the Tptpmn unit in the Thermal Test Facility in the ESF (DTN: SNF37100195002.001 [DIRS 131356]). The in situ stress measurements included a series of five hydraulic fracturing tests, resulting in an estimate of the state of stress in the ESF as follows:

σ_h = 1.7 (±0.1) MPa acting in the N75°W (± 14°)
σ_H = 2.9 (±0.4) MPa acting in the N15°E (± 14°)

The magnitude of vertical stress was estimated based on the depth of cover in the Thermal Test Facility at the test borehole location using dry bulk density data (CRWMS M&O 1997 [DIRS 147458], Table 4 and pp. 15, 19, and 20) to be equal to:

σ_V = 4.7 MPa

The measured stress regime reveals that the horizontal stresses are only moderately differential, but are both smaller than the vertical stress. The stress regime corresponds to the locally predominant normal faulting, and is in accord with the average normal fault strike direction.

Stresses Around the ESF Tunnel Due to Overburden

The ESF tunnel mapping data represents the second source of data used for determining properties of rock mass. The ESF Main loop includes the North and South Ramps and main drift at varying depths. The ramps penetrate all lithostratigraphic units and the repository horizon section, which contains the RHH units. Depending on the rock mass strength, the rock mass quality and the resulting ratings of rock mass encountered in the ESF tunnel are affected by the in situ stress level, which depends on the tunnel depth. The assessment of the lithostatic stress level at each ESF tunnel location is therefore required to provide a proper reference in evaluating the performance of the rock strata in situ in response to the tunnel excavation. Figure 6-71 displays the ESF tunnel elevation and surface elevation changes along the tunnel alignment. The thickness of the overburden above the tunnel alignment is shown in Figure 6-72. The magnitude of the vertical stress at each tunnel location can easily be calculated by using an average density of the overlaying strata.

The rock mass response at each location is affected by the tunnel diameter, magnitude of the vertical stress and Poisson's ratio. It is apparent that the same quality rock as affected by the magnitude of stress and the resulting RMR can be substantially different at different depths.

It should be noted that at the unlined tunnel circumference the state of stress is practically uniaxial because of the lack of confinement. At the tunnel surface only the tangential stresses exist and the value of the confining radial stress is equal to zero. The results of the tunnel mapping must be examined with reference to the magnitude of stress at the tunnel circumference. The maximum compressive stress values calculated at the tunnel springline can be applied as a benchmark for comparing the value of uniaxial compressive strength of intact rock and rock mass to the magnitude of stress at the same location.

Figure 6-73 illustrates a typical case of stress distribution calculated at the tunnel circumference using a closed-form solution (Poulos and Davis 1991 [DIRS 157885], pp. 232 to 235), for the tunnel excavated in the 25_TSw1_Tptpul lithostratigraphic unit. As shown in this figure, the stress magnitude at the tunnel springline is represented by three plane strain cases; Case I represents the lithostatic stress, where the vertical and horizontal stresses are equal, Case II represents the plane strain case for a wide range of depths, and Case III represents state of stress that might occur at shallow depths, and/or near-vertical free surfaces. As shown, Case III results in the largest compressive stress at the tunnel springline. The magnitude of this stress and the overburden stress calculated at the deepest location of each lithostratigraphic unit are calculated for the length of the ESF tunnel and is summarized in Table 6-64. It should be noted that Case III was used for conservative viewpoint since it generates the maximum compressive stress. Also included in Table 6-64 are the average values of Young's modulus and Poisson's ratio for each unit encountered along the ESF tunnel.

The inherent variability of the rock material makes the values of rock mass parameters dependent on the rock mass sampling location. As shown in Figure 6-74, it is apparent that the tangent line 1 drawn to the Hoek-Brown envelope at the contact with circle 1 representing the uniaxial compressive strength test (center Ou) and the second tangent line drawn to the envelope at the point of contact with the circle representing the triaxial test (Center Ot), result in two different estimates of cohesion (c) and internal friction angle (ϕ). It is essential therefore, that to obtain estimates of these two parameters for the uniaxial stress tests that the comparison of tunnel stresses and rock mass strength be made for the same stress condition.

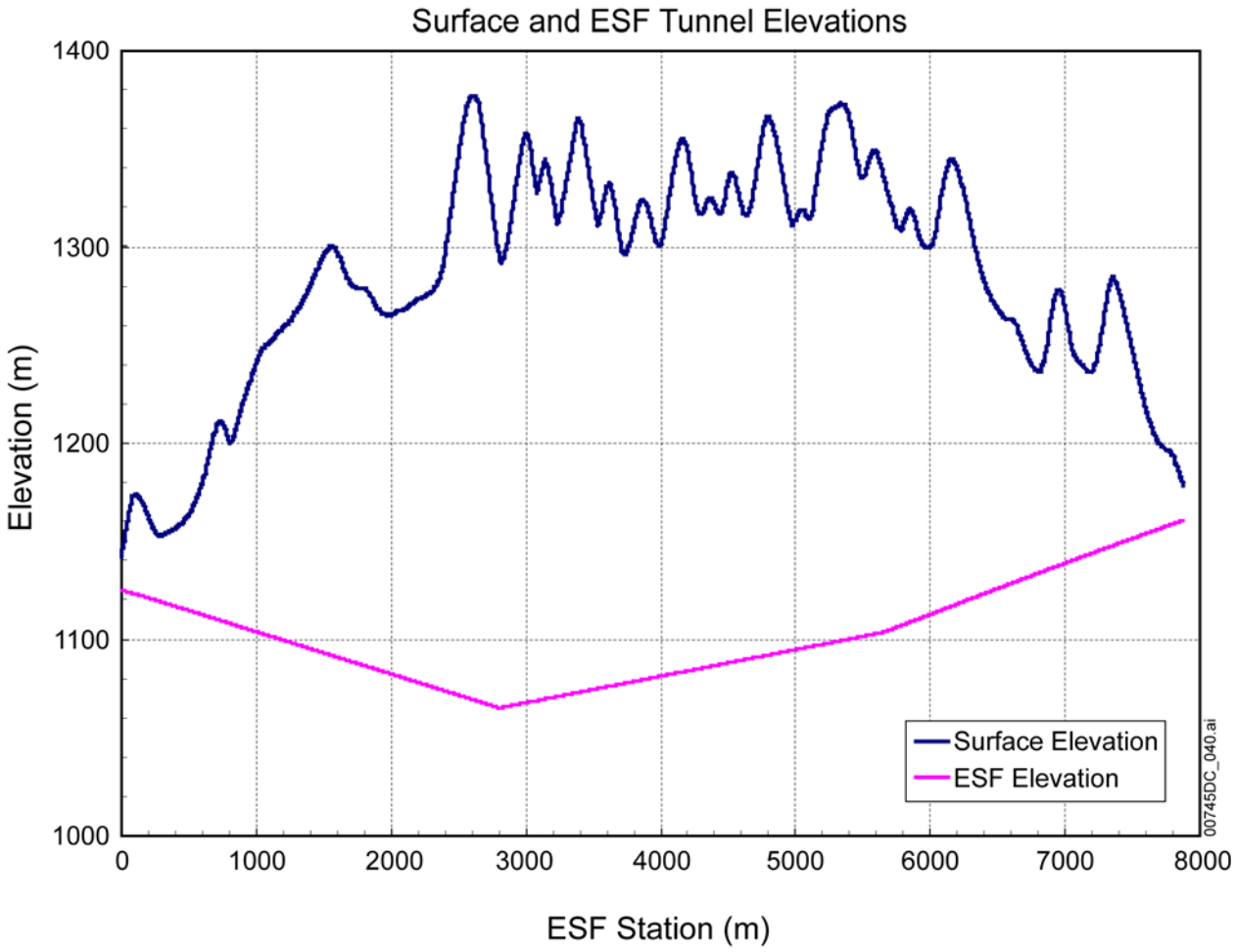

Source: DTN: MO0309MWDVCNGR.001 [DIRS 166600].

NOTE: Data File: *Surface and ESF Centerline Elevations - 101606.xls* (see Appendix H)

Figure 6-71. ESF Tunnel Showing Both ESF Centerline and Surface Elevations Along the Alignment

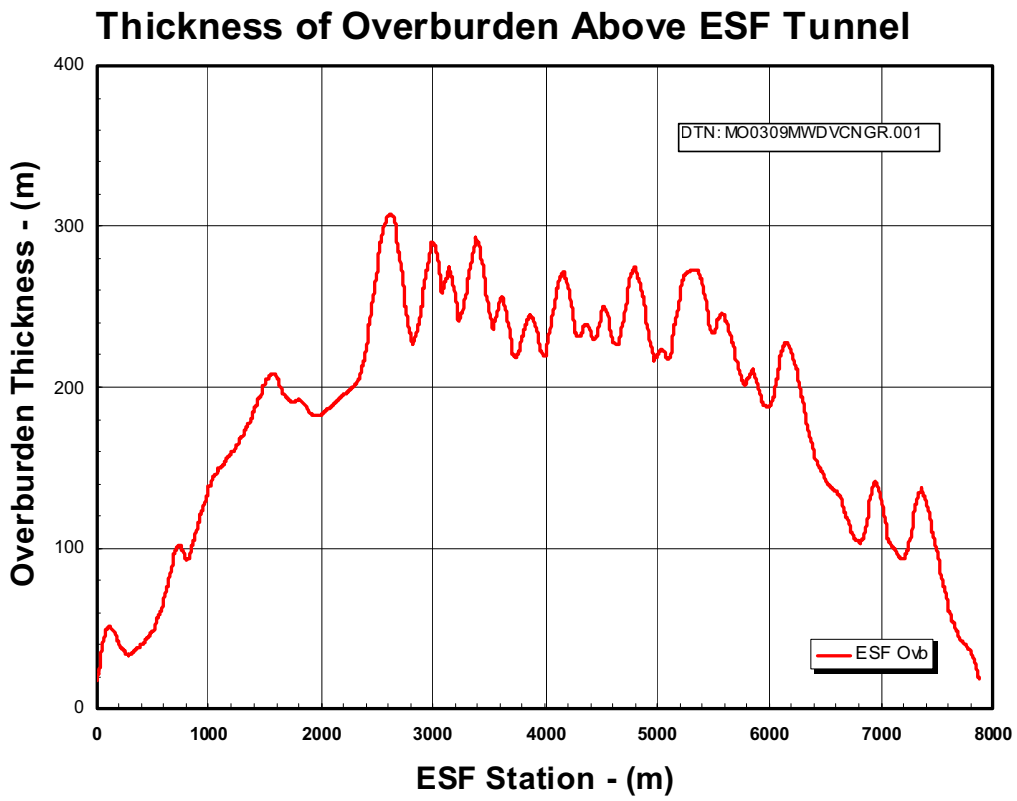

Source: DTN: MO0309MWDVCNGR.001 [DIRS 166600].

NOTE: Data File: *Surface and ESF Centerline Elevations - 101606.xls* (see Appendix H)

Figure 6-72. Overburden Thickness Above the ESF Tunnel

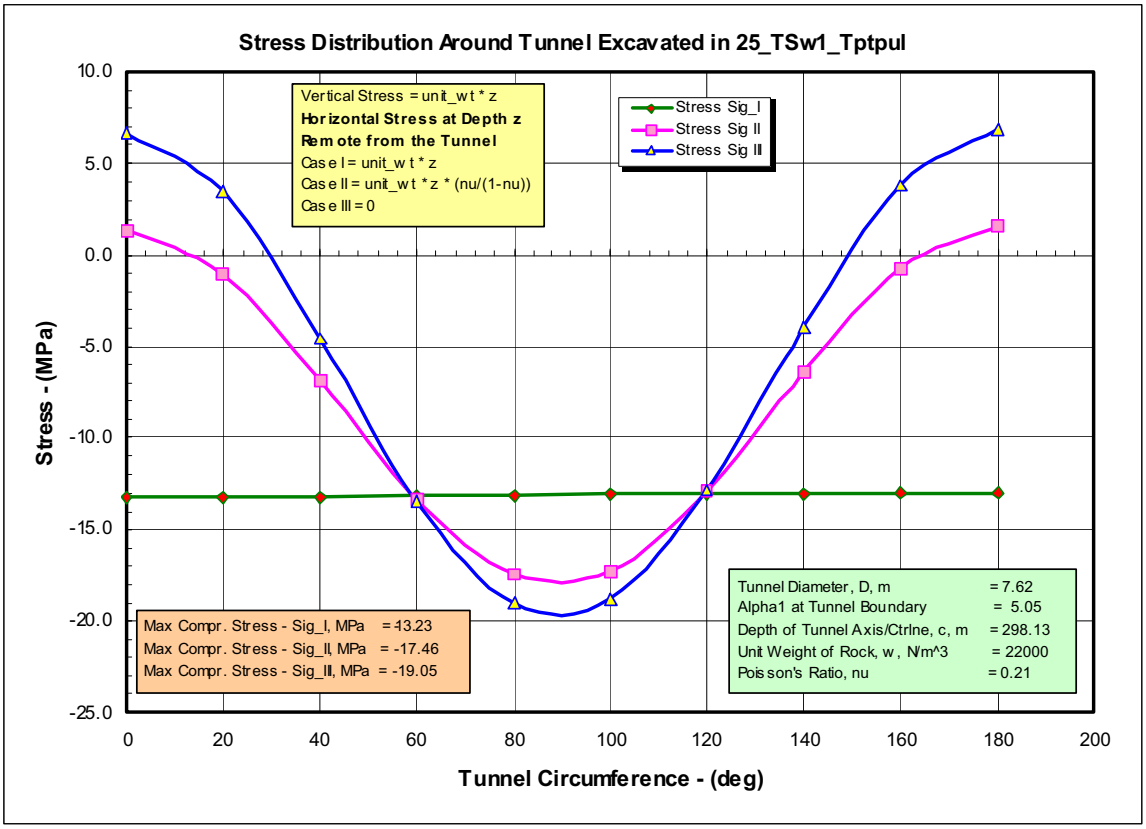

Source: Poulos and Davis 1991 [DIRS 157885], pp. 232 to 235.

NOTES: (1) Data File: *Sig_V and Stress Around Tunnel - 101606.xls* (see Appendix H)

(2) Tension considered positive

(3) Unit weight of rock based on conservative average value

(4) Negative stress indicate in compression

(5) Figure 6-73 presented here as illustration purpose and is based on values presented in green shade box.

Figure 6-73. A Typical Example of Stress Distribution Calculated Using Closed Form Solution Around ESF Tunnel at Particular Location

Table 6-64. Lithostratigraphy and Calculated Maximum Compressive Stress at Tunnel Springline for Each Lithostratigraphic Zone in the ESF Tunnel Using Closed Form Solution

TM	Combined Code	Max. Depth in ESF Tunnel (m)	Max Overburden Stress (MPa)	Average Young's Modulus (GPa)	Young's Modulus, St. Dev.	Average Poisson's Ratio	Poisson's Ratio, St. Dev.	Maximum Compressive Stress Around Tunnel (MPa)		
								Sig I	Sig II	Sig III
UO	02_UO_Tmr	28.16	0.62	3.40	2.70	0.20		1.35	1.73	1.89
	03_TCw_Tpki	28.16	0.62	3.77	1.54	0.19	0.14	1.35	1.74	1.89
TCw	04_TCw_Tpcrn	31.82	0.70	16.46	8.35	0.20	0.04	1.51	1.95	2.13
	05_TCw_Tpcrn2	34.03	0.75							
	06_TCw_Tpcrn1	41.36	0.91							
	07_TCw_Tpcpul	48.69	1.07	24.50	5.40	0.18	0.02	2.26	2.98	3.22
	08_TCw_Tpcpmn	55.79	1.23	35.62	5.90	0.20	0.04	2.57	3.36	3.67
	09_TCw_Tpcpll	65.01	1.43	34.44	4.98	0.21	0.05	2.97	3.88	4.26
	10_TCw_Tpcpln	103.76	2.28	36.18	9.52	0.21	0.03	4.68	6.14	6.72
	11_TCw_Tpcpv3	104.24	2.29							
	12_TCw_Tpcpv2	104.72	2.30	10.90	8.70	0.10	0.00	4.73	6.55	6.79
PTn	13_PTn_Tpcpv1	105.64	2.32	2.53	1.67	0.10	0.08	4.76	6.60	6.85
	14_PTn_Tpbt4	112.00	2.46	1.17	1.50	0.20	0.07	5.04	6.67	7.24
	15_PTn_Tpy	118.50	2.61	5.24	3.05	0.16	0.01	5.33	7.19	7.65
	16_PTn_Tpbt3	124.95	2.75	1.55	1.06	0.20	0.08	5.61	7.42	8.06
	17_PTn_Tpp	129.95	2.86	0.99	0.61	0.26	0.09	5.83	7.44	8.37
	18_PTn_Tpbt2	138.87	3.06	0.75	0.61	0.22	0.09	6.22	8.15	8.94
	19_PTn_Tptrv3	139.19	3.06	0.99	1.29	0.23	0.11	6.24	8.12	8.96
	20_PTn_Tptrv2	138.55	3.05							
TSw1	21_TSw1_Tptrv1	149.65	3.29							
	22_TSw1_Tptrn	200.40	4.41	21.68	8.40	0.23	0.06	8.93	11.65	12.86
	23_TSw1_Tptrl	184.62	4.06	10.45	3.27	0.29	0.02	8.23	10.34	11.85
	24_TSw1_Tptf	241.40	5.31	47.86	9.69	0.26	0.05	10.73	13.76	15.46
	25_TSw1_Tptpul	298.00	6.56	15.18	6.92	0.21	0.11	13.23	17.46	19.05
TSw2	26_TSw2_Tptpmn	297.77	6.55	33.04	6.34	0.19	0.05	13.22	17.66	19.03
	27_TSw2_Tptpll	362.56	7.98	30.96	8.32	0.19	0.05	16.09	21.47	23.15
	28_TSw2_Tptpln	259.52	5.71	36.49	10.40	0.23	0.04	11.53	15.03	16.59

Sources: DTNs: MO0402DQRIRPPR.003 [DIRS 168901]; SN0208L0207502.001 [DIRS 161871]; SN0211L0207502.002 [DIRS 161872]; SN0302L0207502.003 [DIRS 165014]; SN0305L0207502.004 [DIRS 165013]; SN0306L0207502.008 [DIRS 165015]; SN0505L0212303.005 [DIRS 174956]; MO0309MWDVCNGR.001 [DIRS 166600].

NOTES: 1. Overburden Stress values calculated for the deepest tunnel location in a particular unit.

2. Average Overburden Unit Weight = 22,000 N/m^3 used for all units, calculated from average bulk density data for all units (DTN: SNL02030193001.027 [DIRS 108410]) equal to (2.22 g/cm^3 × 1 × 106 cm^3/m^3 / 1000 g/kg × 10 m/s^2).

St. Dev. = standard deviation; TM = thermal-mechanical.

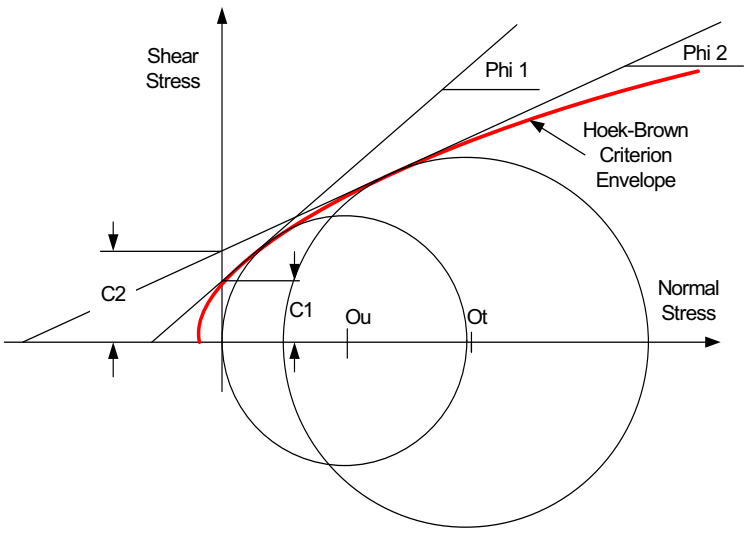

Figure 6-74. Hoek-Brown Strength Envelope and Tangent Lines Showing Dependence of Cohesion (c) and Internal Friction Angle (ϕ) on Stress Combinations.

6.4.4.4.1.3 Rock Mass Parameters Calculation Using Laboratory Data

Calculations of rock mass parameters using laboratory data also require that the rock mass quality be assessed in terms of RMR at specific locations in the tunnel. This is accomplished by using laboratory data in two different applications: (1) Types of laboratory tests and data populations available for each test type that are used to obtain a standardized (i.e., obtained for specific size specimens tested under particular test conditions) average compressive strength and associated statistics; this data is used as one of the required rock mass classification system input parameters, and (2) The data required for defining the Hoek-Brown criterion is based on tensile, uniaxial and triaxial laboratory test results.

The populations of each test type may vary considerably. Each test type is treated as an entity and carries with it its statistics, distributions, ranges, etc. Differences in populations of each test may cause that the overall Hoek-Brown criterion, which is used to integrate all test types for a particular material in a unique envelope, may result in more than one envelope fitting the data. For example, the uniaxial strength results for tests carried out on 1, 2, 5, or 12 in. diameter specimens will each contain its distinct population although all were obtained from the same test type. The integrating envelope for the rock type displaying strong size effect will be different depending whether all uniaxial tests for all specimen diameters are included or if only test results for a particular specimen diameter were selected.

Custom matching the RocLab® software (Hoek et al. 2002 [DIRS 162204]) calculations with a particular tunnel location requires that GSI values be provided for all individual lithostratigraphic units penetrated by the tunnel. In the process of determining these values, one of the input parameters is the uniaxial compressive strength of the intact rock. In this case caution must be exercised in determining which uniaxial compressive test results are appropriate. The use of results obtained from the specimen of a standard size is of primary importance for types of rocks displaying strong size effect, such as lithophysal units.

The uniaxial tensile strength and uniaxial compressive strength tests are easiest to perform and are most common among a variety of tests that can be performed on rock samples in the laboratory. In effect, the data sets from these test types are also most populous. Caution also must be exercised when interpreting the data that contain test results from a number of test groups of widely varying populations, as the tests containing more data will cause statistical bias and may distort the resulting overall material simulation.

It should also be noted, that while input to the calculation of GSI values includes uniaxial compressive strength only, the input to RocLab includes both uniaxial and triaxial test results. The uniaxial compressive test data alone can be represented by their basic statistics including average and standard deviation. In RocLab the uniaxial compressive strength of intact rock is obtained as one of the calculated parameters and is generally different than the value used as input to the GSI calculation. The latter is obtained as an intercept of the Hoek-Brown envelope with the σ_1 coordinate plotted in the σ_1 versus σ_3 coordinate system.

Table 6-63 contains a summary of all potentially applicable data sets for use in RocLab calculation. With few exceptions, assembled in this list are the average data for all tests groups performed on approximately 50 mm diameter specimens and tested fully saturated under room temperature. As indicated in Table 6-63, an exception to this rule was applied to the CHn units where 25.4- mm diameter specimen data were used because these were the only data available. Table 6-63 also includes uniaxial compressive strength test results obtained for large-diameter specimens and strata at the RHH. Each lithostratigraphic unit is represented by test data containing average values from uniaxial compressive strength, triaxial compressive strength and indirect tensile strength tests. It can be noted that each lithostratigraphic unit is represented by different numbers of input data of testing group ranging from one to eight, Tptpmn zone being the most extensively tested unit.

The RocLab® rock mass strength parameter calculator treats each data point as equal. In effect, as discussed earlier in this section, different populations in the individual test groups may result in a statistically biased material simulation fit. Numerous tests were performed to identify the impact of input supplied either as individual test results or as aggregate, average test data. It was determined that using the average data for each test group limits the impact of such different test data populations.

Each data set was used in an identical calculation sequence. As a minimum, at least two data sets including uniaxial compressive strength and indirect tensile strength data were required. It is clear that some lithostratigraphic units do not have sufficient number of specimens to be used for determination of the mechanical properties of rock mass. As a result, an engineering judgment is exercised to determine if the strength of units represented by an insufficient test data population can be extrapolated from adjacent units, for example, using density as an indicator of similarity between adjacent strata.

6.4.4.4.1.4 Tunnel Mapping and Rock Mass Characterization

During the development of the ESF underground excavations, detailed geological mapping was performed as a routine activity. As a result of the mapping, a set of detailed drawings summarizing as-built geological and geotechnical information was generated. This section

provides details and a summary pertaining to three major tunnels that were mapped as the tunnel construction progressed. The USBR performed geotechnical characterization of the rock mass in the ESF, HD, and ECRB Cross Drift tunnels and presented its results in the following reports: Beason et al. (1996 [DIRS 101191]), Barr et al. (1996 [DIRS 100029]), Albin et al. (1997 [DIRS 101367]), Eatman et al. (1997 [DIRS 157677]), Mongano et al. (1999 [DIRS 149850]), and *Rock Mass Quality Ratings and Classifications of the Combined ESF, Heated Drift and ECRB Cross Drift* (BSC 2004 [DIRS 176608]). Geologic site characterization activities by the USBR for the geotechnical characterization of rock mass included:

- Full-Periphery Geologic Mapping
- Detailed Line Surveys
- Stereophotographic Coverage
- Rock Sampling.

This report utilizes only full-periphery geotechnical mapping and rock sampling to develop the rock mass properties. Following is a brief summary of information related to activities associated with tunnel mapping and underground excavations. The details associated with mapping and geotechnical characterization of the YMP underground excavations are presented in *Rock Mass Quality Ratings and Classifications of the Combined ESF, Heated Drift and ECRB Cross Drift* (BSC 2004 [DIRS 176608]).

Full-Periphery Geologic Mapping

Geologic mapping in the ESF, HD and ECRB tunnels includes lithostratigraphic and structural features on 1:125 scale drawings. These maps were developed in the full-periphery style in which the tunnels were "unrolled" to produce a flat map of the tunnel periphery. Structural discontinuities with trace length longer than 1 m and lithostratigraphic contacts were recorded

Detailed Line Surveys

Detailed line surveys were conducted either along the right wall, 1 to 1.5 m below the springline (for the ESF and HD tunnels) or along the left wall, approximately at the springline (ECRB tunnel) on the tunnel wall. A metric measuring tape was affixed to the wall and discontinuities with trace lengths longer than 30 cm were reported on the survey. Discontinuities that intersect the walls within 30 cm above and below the tape were also documented. Typical detailed line survey data include location (station), orientation, discontinuity type, trace length, height and width of discontinuity plane, terminations, aperture, roughness, and infilling type and thickness.

6.4.4.4.1.4.1 ESF and HD

The ESF consists of a series of underground excavations designed to investigate the subsurface geology and hydrology of Yucca Mountain. Figure 6-75 shows a plan view of the ESF. The ESF tunnel excavation progressed starting with the North Ramp at the North Portal. The North Ramp is approximately 2,800 m long with a bearing of 299 degrees and a decline of 2.1%. The North Ramp provides access to the Main Drift, a north-south access excavation 3,131 m long, with a bearing of 183 degrees, which provides access to the rock units at the RHH level. The South Ramp, which provides a southern access to the repository horizon, is approximately

1,942 m long. The North Ramp, Main Drift, and the South Ramp form a continuous loop between the North Portal and the South Portal.

Except for the starter tunnel, the ESF was excavated with a 7.62 m TBM. The TBM was a fully shielded machine. A 45 m long section of the TBM trailing gear was constructed to provide space for geologic mapping activities. The starter tunnel opening is a 60 m long, 10 m high, horseshoe-shaped tunnel excavated by drill and blast methods. A number of alcoves also were excavated by drill and blast methods. In addition, a 5.5 m diameter HD, approximately 60 m long, with a bearing of 288 degrees and zero grade was excavated by the drill and blast method.

The lithostratigraphic units encountered during the ESF and HD excavations included the Tiva Canyon Tuff (Tpc), Pre-Tiva Canyon Bedded Tuff (Tpbt4), Yucca Mountain Tuff (Tpy), Pre-Yucca Mountain Bedded Tuff (Tpbt3), Pah Canyon Tuff (Tpp), Pre-Pah Canyon Bedded Tuff (Tpbt2), and Topopah Spring Tuff (Tpt). Detailed descriptions of lithostratigraphic units encountered during the ESF and HD excavation are presented in Beason et al. (1996 [DIRS 101191]), Barr et al. (1996 [DIRS 100029]), Albin et al. (1997 [DIRS 101367]), Eatman et al. (1997 [DIRS 157677]), and *Rock Mass Quality Ratings and Classifications of the Combined ESF, Heated Drift and ECRB Cross Drift* (BSC 2004 [DIRS 176608]). All lithologic descriptions are based on exposures on the mapping of tunnel walls.

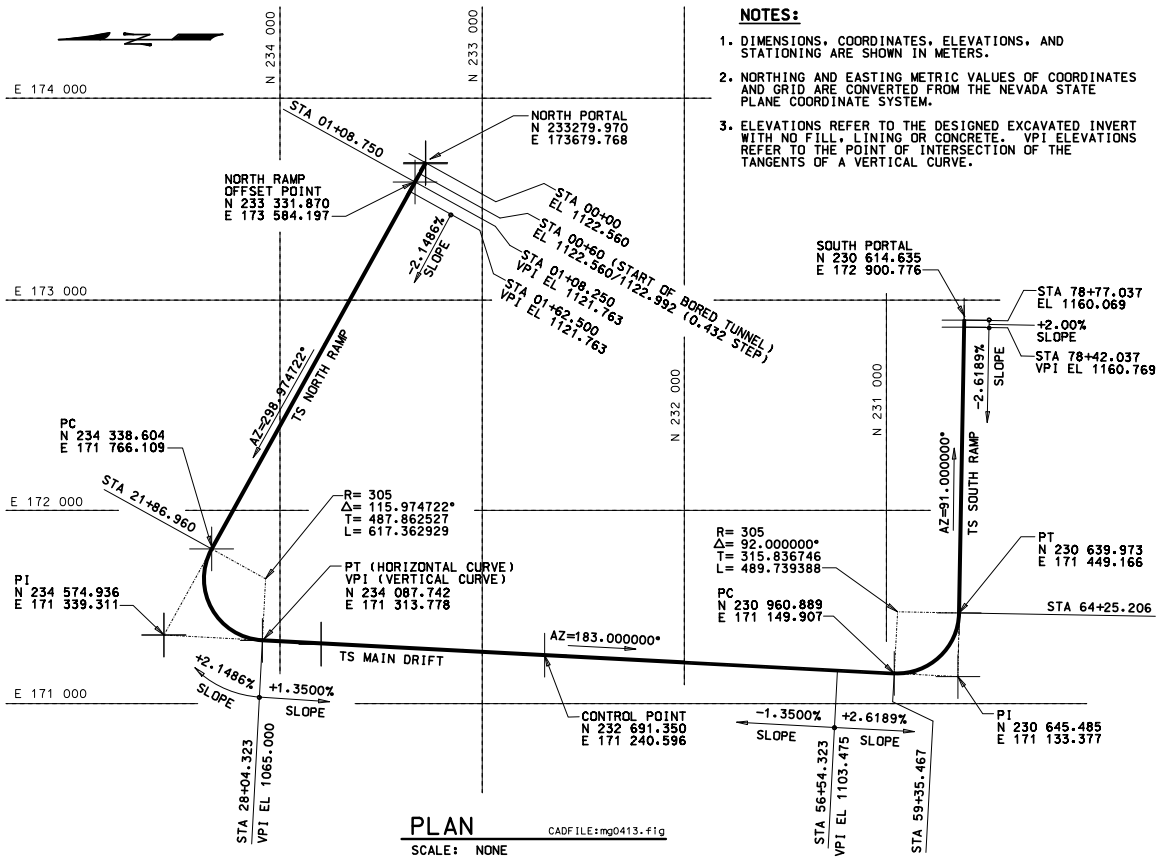

Source: BSC 2003 [DIRS 165572], Figure 3.

Figure 6-75. ESF Plan View

6.4.4.4.1.4.2 Enhanced Characterization of the Repository Block Cross-Drift

The ECRB Cross-Drift is a 2.8 km long, and 5.0 m diameter tunnel. It was constructed to extend underground access to the Solitario Canyon Fault Zone (SCFZ) and to the lithostratigraphic units within the RHH, which had limited exposure in the ESF (Mongano et al. 1999 [DIRS 149850], p. 3). It varies in orientation and gradient so that it passes over the ESF Main Drift and intersects the SCFZ at approximately 90 degrees.

Figure 6-76 shows a plan view of the ECRB Cross-Drift. The ECRB Cross-Drift starter tunnel, approximately 26.4 m long and 10.5 m high and wide, begins in the North Ramp of the ESF at station 19+92 and follows initially a bearing of 254 degrees and an incline of 0.5%. It was excavated by drill and blast methods. In plan view, the ECRB Cross-Drift is roughly s-shaped with two broad curves (305 m radius) near the beginning and the end. Except in the starter tunnel, the ECRB Cross-Drift was excavated with a 5 m TBM. The TBM was a conventional open-beam machine. A 70 m long platform, moving independently of the TBM, was constructed to provide space for geologic mapping activities.

The ECRB Cross-Drift is excavated entirely within the Topopah Spring Tuff, starting in the Tptpul lithostratigraphic unit and proceeding down section through the entire length of the excavation. The ECRB Cross-Drift does not penetrate the main trace of the SCFZ. The lithostratigraphic contacts in the ECRB Cross-Drift are presented in Table 6-65. Descriptions of lithostratigraphic units encountered in the ECRB Cross-Drift are presented in Mongano et al. (1999 [DIRS 149850]).

Table 6-65. Lithostratigraphic Contacts in the ECRB Cross-Drift

Contact	Station (m)	Orientation (Strike/Dip)	Comments
Tptpul-Tptpmn	10+15	286/09	–
Tptpmn-Tptpll	14+44	270/07	–
Tptpll-Tptpln	23+26	252/06	–
Tptpln-Tptpul	25+85	NA	Contact is the SCFZ
Tptpul-Tptpll	26+57.5	NA	Contact is an unknown fault

Source: Mongano el al. 1999 [DIRS 149850], Table 1.

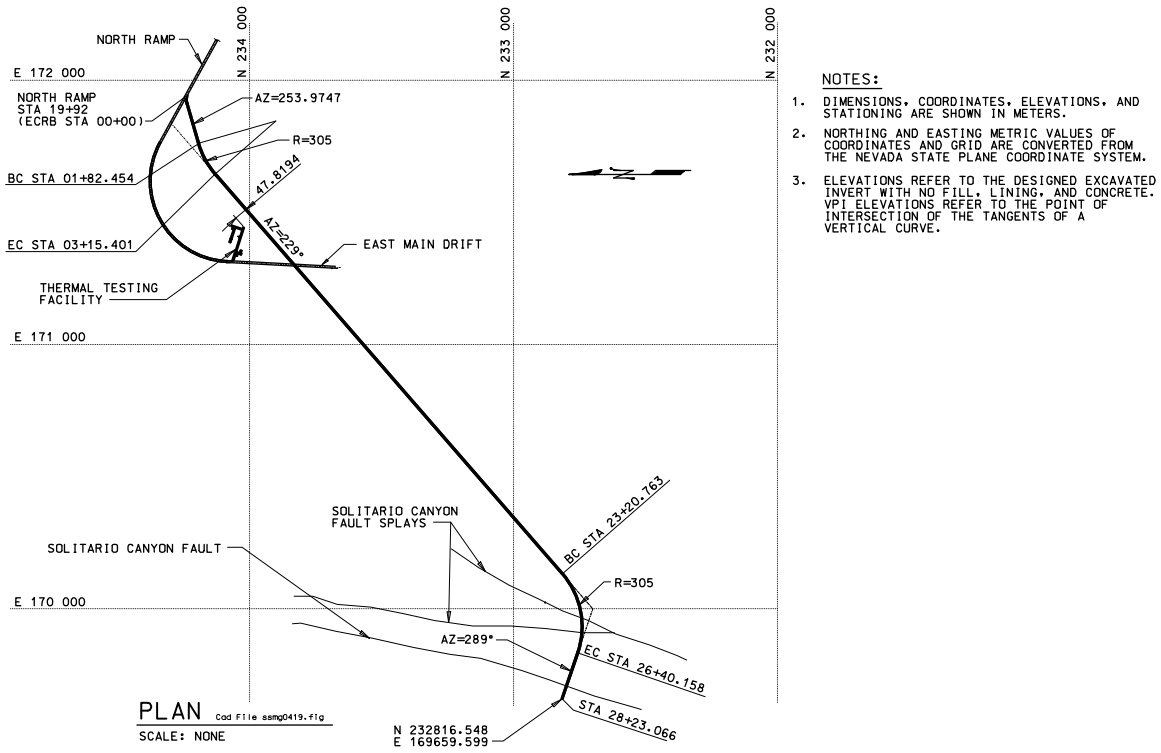

Source: BSC 2003 [DIRS 165572], Figure 4.

Figure 6-76. ECRB Cross-Drift Plan View

6.4.4.4.1.5 Use of Tunnel Mapping Results as Input to Rock Mass Strength Assessment

The RMR is expressed in terms of the GSI Index as a result of tunnel mapping. A GSI value is based on RMR (Equation 6-29), which is determined using rock mass characteristic parameters listed in Appendix D. The input value of the uniaxial compressive strength in this report was used as a standardized measure of tests performed on saturated, 50.8 mm diameter specimens tested under uniaxial loading conditions at room/ambient temperature. A specific UCS value was assigned to represent strength of rock encountered along each 5 m tunnel section and used to classify as one of the lithostratigraphic units. A detailed account of rock mass characterization parameters and the resulting rock mass classification are provided in Appendix D. Table 6-66 provides a summary of the rock mass characterization parameters for the ESF, ECRB Cross-Drift, and HD tunnel sections intercepting various lithostratigraphic units.

The data from Appendix D is further refined by extracting GSI values along the documented portion of the tunnel located within each distinct lithostratigraphic unit. These extracted data sets, which represent rock mass properties of a particular lithostratigraphic unit sampled at several sections of tunnels, are grouped and then sorted according to the GSI values and presented in Appendix F. These values are presented as a cumulative frequency distribution plots of the GSI index corresponding to five rock mass categories.

The procedure to obtain representative GSI values can be described as a succession of the following steps:

(1) The rock mass is characterized within a range of five rock mass categories, with the category 1 representing the lowest ranking. The categories are established by the GSI values corresponding to 5%, 20%, 40%, 70%, and 90% of GSI cumulative frequency of occurrence cutoffs. The applied range of cutoff values follows the pattern established in *Confirmation of Empirical Design Methodologies* (CRWMS M&O 1997 [DIRS 100930], Section 7.4.1.3, p. 43);

(2) Extract the tunnel mapping data sets for each distinct lithostratigraphic unit and combine them on a spreadsheet;

(3) For each lithostratigraphic unit sort the data according to the increasing value of GSI for that unit;

(4) Generate a plot showing the cumulative frequency of GSI occurrence (expressed as a percentage of the given GSI number count to the total count of all GSI numbers recorded along all mapped tunnel sections excavated in a particular lithostratigraphic unit) to the total count of GSI-rated tunnel sections in that unit. It should be noted, that the total number of GSI-rated 5 m sections vary depending on the tunnel section length excavated through the individual unit. The cumulative GSI frequency of occurrence curve is better documented (smoother) for the rock strata through which longer tunnel sections are excavated as they contain more mapped and rated 5 m tunnel intervals. The cumulative GSI curves shown in Appendix E are constructed from data sets ranging from few to several hundred;

(5) Manually fit a smooth "S-type" curve representing a normal distribution to the data. Strata containing larger GSI populations clearly point to the normal distribution being a reasonable representation of a typical GSI frequency of occurrence data population;

(6) On a vertical GSI percentage of the frequency of occurrence and for each of the GSI values corresponding to the rock mass categories cutoffs (i.e., 5%, 20%…) draw a horizontal line until it crosses the "S-type" distribution curve; and

(7) For each of the intersecting points find on the horizontal coordinate the value of a corresponding GSI number. A set of five GSI numbers represents the range of rock mass quality encountered along all tunnel sections excavated through a particular lithostratigraphic unit.

Figure 6-77 shows a typical plot of cumulative frequency distribution for GSI index values obtained from the ESF, ECRB Cross-Drift, and HD tunnel mapping data in the 03_UO_Tpki zone. The GSI frequency of occurrence, which synthesizes tunnel mapping data, is plotted in blue. By applying a dashed red curve these data are smoothed. This smoothed curve, approximately represents a normal distribution of the GSI index values. Pencil lines intersecting this red line depict a procedure applied to obtain the five GSI numbers representing cumulative frequencies of 5%, 20%, 40%, 70%, and 90% that correspond to rock mass categories 1 to 5. In

addition, as shown later in Table 6-76, the sixth set representing rock mass strength parameters and an average GSI value for each unit was also calculated.

The five GSI index values plus average value for each rock mass category obtained using the procedure described above along with the laboratory strength data are then used as input to RocLab. As a result, for each lithostratigraphic unit, for which the required input is available, RocLab is used to obtain six sets of parameters characterizing the strength of rock mass for that unit.

Table 6-67 presents a summary of RMR and resulting GSI index values for each lithostratigraphic unit as determined using the procedure describe above. This summary is based on calculations including all RMR-based mapping data as they were entered into the Project records during tunnel construction. In total, field data from 10,370 m of tunnel length with identified lithostratigraphy and some 165 m of additional tunnel length, where detailed lithostratigraphy was not identified for construction-related reasons, were used. The GSI data values shown in Table 6-67 represent a range of rock mass conditions as encountered in each lithostratigraphic unit, and determined using a sum of exposures within that unit in the Yucca Mountain tunnels. Each tunnel section is sampled along the 5 m intervals, of which length were judged reasonable considering compatibility of mapping activities and required level of mapping data details, with the rate of tunnel advance, dimensions of the mapping platforms adjacent to the advancing TBM, and personnel safety concerns. A set of parameters determined for each tunnel sampling section can be conceptualized as an equivalent to a typical data point. Consequently, longer tunnel sections excavated within a particular unit yield databases with larger data populations, for which more meaningful statistical analyses can be carried out. The longest portion of the ESF tunnel was excavated in Tptpmn unit. Consequently, this unit represents by the largest, filed-derived data population.

As evident in Table 6-67, data populations resulting from the tunnel mapping for individual lithostratigraphic units vary. Not all units listed in the full lithostratigraphic sequence shown in Table 6-2 are present in the tunnel. The units in the tunnel are represented by one or more intervals of varying length and resulting different number of 5 m rated intervals or data sets. Units occurring both in the North and South ramps provide a basis for estimation of spatial distribution of individual lithostratigraphic units within the repository block. Similar data obtained from the ESF Main Loop tunnel at the RHH provide large data population and displays consistency that allows for the development of numerical rock mass simulation that reflect response of the real rock mass more closely.

It should be noted that intuitively one would expect that the rock strata with higher UCS would also be characterized by high values of GSI. However, as shown in Table 6-67, strong rock strata at RHH have GSI numbers lower than those of weak Tpki rock unit. It is apparent that GSI numbers characterizing rock mass performance are affected by additional factors, such as depth and associated in situ stresses, and the method of excavation. Orientation of tunnel with respect to orientation of joints may cause the rock mass at the same depth to display behavior in one tunnel direction different than in the other direction.

All populations of GSI estimates listed in Table 6-67 are visualized in Figure 6-78, which shows GSI data for the five rock mass categories and each thermal-mechanical unit mapped along the

combined tunnel length in that unit. Included in this plot are GSI estimates for both nonlithophysal and lithophysal units. Shown in Figure 6-79 is a plot summarizing estimates of RMR at the RHH for non-lithophysal units only.

For all lithostratigraphic units the extreme GSI values equal to 32 and 85 for the lowest and highest value, respectively. In general, they reflect the condition of the rock mass along the mapped tunnel as representative of fair to good quality rock. Along with the laboratory data, these GSI values are used as input to RocLab to determine the range of rock mass parameters for each unit, for which both data sets are available. Along with the laboratory test data, the GSI values constitute the second key input into the RocLab required for determining the strength parameters of rock mass.

The integration of laboratory data and tunnel mapping data into one system for evaluating strength characteristics of rock mass must always be performed considering the quality of laboratory data and their statistical representativeness (see Section 6.4.4.4.1.2).

Table 6-66. Summary of Tunnel Mapping Data and Rock Mass Ratings Along ESF, ECRB Cross-Drift, and Heated Drift

General Location	Litho stratigraphy	Location and Mapped Distance (m)				Input Data		Depth (m)		GSI	
	Lithostratigraphic Unit Number	Begin Station	End Station	Tunnel Segment Length	Lithostratigraphic Segment—Total	RQD	Mean Intact UCS, σ_{ci} (MPa)	Depth of Tunnel—Min, H_{min}	Depth of Tunnel—Max, H_{max}	GSI_min	GSI_max
ESF	03_UO_Tpki	02+66	03+35	69	69	95	5.94	25.42	28.16	49	84
ESF	04_TCw_Tpcrn	03+55	03+90	35	35	100	36.02	29.88	31.82	61	84
ESF	05_TCw_Tpcrn2	03+90	04+30	40	40	92	36.02	32.06	34.03	61	79
ESF	06_TCw_Tpcrn1	04+30	04+40	10	10	59	36.02	34.47	34.91	43	61
ESF	07_TCw_Tpcpul	00+60	01+00	40		99	62.14	35.32	42.02	49	70
ESF	07_TCw_Tpcpul	04+40	05+50	110		10	62.14	35.35	48.69	37	78
ESF	07_TCw_Tpcpul	78+40	78+75	35	185	69	62.14	5.58	17.99	59	72
ESF	08_TCw_Tpcpmn	01+00	01+88	88		92	167.19	34.99	42.51	55	87
ESF	08_TCw_Tpcpmn	05+50	05+85	35		84	167.19	49.47	55.79	45	74
ESF	08_TCw_Tpcpmn	76+05	78+40	235	358	75	167.19	19.09	52.91	52	79
ESF	09_TCw_Tpcpll	01+93	01+98	10		10	186.74	33.71	34.19	64	68
ESF	09_TCw_Tpcpll	05+85	06+20	35	45	54	186.74	56.72	65.01	54	82
ESF	10_TCw_Tpcpln	06+20	07+75	155		95	172.33	66.61	90.34	38	82
ESF	10_TCw_Tpcpln	67+30	67+60	30		76	172.33	98.93	103.76	71	82
ESF	10_TCw_Tpcpln	67+65	67+85	20		81	172.33	97.90	98.05	56	76
ESF	10_TCw_Tpcpln	75+15	76+05	90	295	87	172.33	54.40	81.76	57	76
ESF	12_PTn_Tpcpv2	07+75	07+90	15		97	28.18	89.64	90.13	66	68
ESF	12_PTn_Tpcpv2	75+10	75+15	5		77	28.18	83.60	83.60	56	56
ESF	12_PTn_Tpcpv2	67+25	67+30	5		92	28.18	104.72	104.72	66	66
ESF	12_PTn_Tpcpv2	67+60	67+65	5	30	92	28.18	98.10	98.10	64	64
ESF	13_PTn_Tpcpv1	07+90	08+70	80		100	5.05	87.65	97.82	64	79
ESF	13_PTn_Tpcpv1	66+97	67+25	28		100	5.05	105.64	105.64	69	69
ESF	13_PTn_Tpcpv1	75+05	75+10	5	113	90	5.05	0.00	0.00	NA	NA

Table 6-66. Summary of Tunnel Mapping Data and Rock Mass Ratings Along ESF, ECRB Cross-Drift, and Heated Drift (Continued)

General Location	Litho stratigraphy	Location and Mapped Distance (m)				Input Data		Depth (m)		GSI	
	Lithostratigraphic Unit Number	Begin Station	End Station	Tunnel Segment Length	Lithostratigraphic Segment—Total	RQD	Mean Intact UCS, σ_{ci} (MPa)	Depth of Tunnel—Min, H_{min}	Depth of Tunnel—Max, H_{max}	GSI_min	GSI_max
ESF	14_PTn_Tpbt4	74+95	75+05	10	10	99	1.20	0.00	0.00	NA	NA
ESF	16_PTn_Tpbt3	08+70	08+95	25	25	NA	1.80	124.93	124.95	79	79
ESF	17_PTn_Tpp	08+95	10+20	125	125	100	3.19	125.48	129.95	67	79
ESF	18_PTn_Tpbt2	10+20	10+50	30		100	2.92	131.44	138.87	69	79
ESF	18_PTn_Tpbt2	70+25	70+55	30		NA	2.92	0.00	0.00	NA	NA
ESF	18_PTn_Tpbt2	74+50	74+75	25	85	NA	2.92	0.00	0.00	NA	NA
ESF	19_PTn_Tptrv3	10+50	10+60	10		98	4.25	138.87	139.19	67	69
ESF	19_PTn_Tptrv3	66+45	66+50	5	15	NA	4.25	0.00	0.00	NA	NAS
ESF	20_PTn_Tptrv2	10+60	10+75	15		68	7.60	137.90	138.55	50	61
ESF	20_PTn_Tptrv2	66+40	66+45	5		96	7.60	121.64	121.64	75	75
ESF	20_PTn_Tptrv2	70+00	70+25	20	40	99	7.60	121.54	121.54	68	68
ESF	21_TSw1_Tptrv1	10+75	11+80	105		15	64.90	136.94	149.65	25	74
ESF	21_TSw1_Tptrv1	66+35	66+40	5		95	64.90	122.44	130.67	48	74
ESF	21_TSw1_Tptrv1	69+95	70+00	5	115	59	64.90	122.61	122.61	58	58
ESF	22_TSw1_Tptrn	11+80	17+10	530		39	61.98	147.11	200.40	45	81
ESF	22_TSw1_Tptrn	65+10	65+25	15		89	61.98	131.54	133.21	63	68
ESF	22_TSw1_Tptrn	65+30	66+35	105		95	61.98	NA	NA	NA	NA
ESF	22_TSw1_Tptrn	67+85	67+90	5		42	61.98	97.59	97.59	34	34
ESF	22_TSw1_Tptrn	68+90	69+95	105		82	61.98	116.88	116.88	46	46
ESF	22_TSw1_Tptrn	73+45	74+40	95	855	76	61.98	109.78	129.71	53	75
ESF	23_TSw1_Tptrl	17+10	17+95	85		37	26.73	183.44	184.62	39	66
ESF	23_TSw1_Tptrl	64+60	65+10	50		92	26.73	134.38	142.14	42	61
ESF	23_TSw1_Tptrl	65+25	65+30	5		60	26.73	131.11	131.11	56	56
ESF	23_TSw1_Tptrl	68+50	68+90	40		87	26.73	105.38	115.49	43	67
ESF	23_TSw1_Tptrl	73+05	73+45	40	220	90	26.73	118.55	124.76	53	62
ESF	25_TSw1_Tptpul	17+95	27+10	915		62	65.21	173.73	298.18	22	80
ESF	25_TSw1_Tptpul	63+10	63+25	15		43	65.21	174.96	178.59	48	61
ESF	25_TSw1_Tptpul	63+30	64+60	130		48	65.21	142.64	171.93	40	70
ESF	25_TSw1_Tptpul	67+90	68+50	60		77	65.21	95.15	103.93	41	54
ESF	25_TSw1_Tptpul	71+70	73+05	135		49	65.21	86.30	116.30	38	63
CD	25_TSw1_Tptpul	0	1015	1015		44	65.21	174.72	252.20	45	80
CD	25_TSw1_Tptpul	25+85	2665	80	2350	28	65.21	180.55	188.30	51	69
ESF	26_TSw2_Tptpmn	27+10	57+25	3015		37	164.58	206.06	282.25	41	82
ESF	26_TSw2_Tptpmn	59+45	63+10	365		47	164.58	179.17	219.14	47	74
ESF	26_TSw2_Tptpmn	63+25	63+30	5		28	164.58	173.44	173.44	51	51
ESF	26_TSw2_Tptpmn	70+55	71+70	115		60	164.58	87.15	98.72	51	68
CD	26_TSw2_Tptpmn	1015	1440	425		89	164.58	239.50	297.77	48	77
HD	26_TSw2_Tptpmn	0	60	60	3985	54	164.58	232.74	236.61	61	78
ESF	27_TSw2_Tptpll	57+25	59+45	220		58	123.01	187.15	204.45	46	70
CD	27_TSw2_Tptpll	1440	2325	885	1105	33	123.01	260.35	362.56	51	75

Table 6-66. Summary of Tunnel Mapping Data and Rock Mass Ratings Along ESF, ECRB Cross-Drift, and Heated Drift (Continued)

General Location	Litho stratigraphy	Location and Mapped Distance (m)				Input Data		Depth (m)		GSI	
	Lithostratigraphic Unit Number	Begin Station	End Station	Tunnel Segment Length	Lithostratigraphic Segment—Total	RQD	Mean Intact UCS, σ_{ci} (MPa)	Depth of Tunnel—Min, H_{min}	Depth of Tunnel—Max, H_{max}	GSI_min	GSI_max
CD	28_TSw2_Tptpln	2325	2585	260	260	NA	155.51	188.95	259.52	53	76
				Total:	10370						
ESF	Not Identified	01+98	02+66	68		NA	7.60	27.13	27.13	0	0
ESF	Not Identified	03+35	03+45	10		100	7.14	28.49	28.82	54	84
ESF	Not Identified	03+45	03+55	10		100	36.02	29.15	29.48	69	69
ESF	Not Identified	66+50	66+97	47		NA	7.60	0.00	0.00	NA	NA
ESF	Not Identified	74+40	74+50	10		NA	64.90	0.00	0.00	NA	NA
ESF	Not Identified	74+75	74+95	20	20	NA	7.60	0.00	0.00	NA	NA

Sources: DTNs: GS950508314224.003 [DIRS 107488]; GS000608314224.005 [DIRS 166002]; GS960408314224.001 [DIRS 168135]; GS960408314224.003 [DIRS 168136]; GS960708314224.009 [DIRS 168137]; GS000608314224.006 [DIRS 152572]; GS960908314224.015 [DIRS 108372]; GS960908314224.016 [DIRS 108373]; GS960908314224.017 [DIRS 108376]; GS970108314224.002 [DIRS 107490]; GS970208314224.004 [DIRS 107492]; GS970808314224.009 [DIRS 107494]; GS970808314224.011 [DIRS 107495]; GS970808314224.013 [DIRS 107497]; GS990408314224.003 [DIRS 108404]; GS990408314224.004 [DIRS 108405]; GS990408314224.005 [DIRS 108408]; GS990408314224.006 [DIRS 108409]; GS970608314224.007 [DIRS 158430].

NOTE: The Starter Tunnel Section 00+00 to 00+60 not included as it was excavated using drill and blast technology, different than in the major portions of the tunnels.

NA or blank in the cell represent the data is not available.

CD = ECRB Cross-Drift.

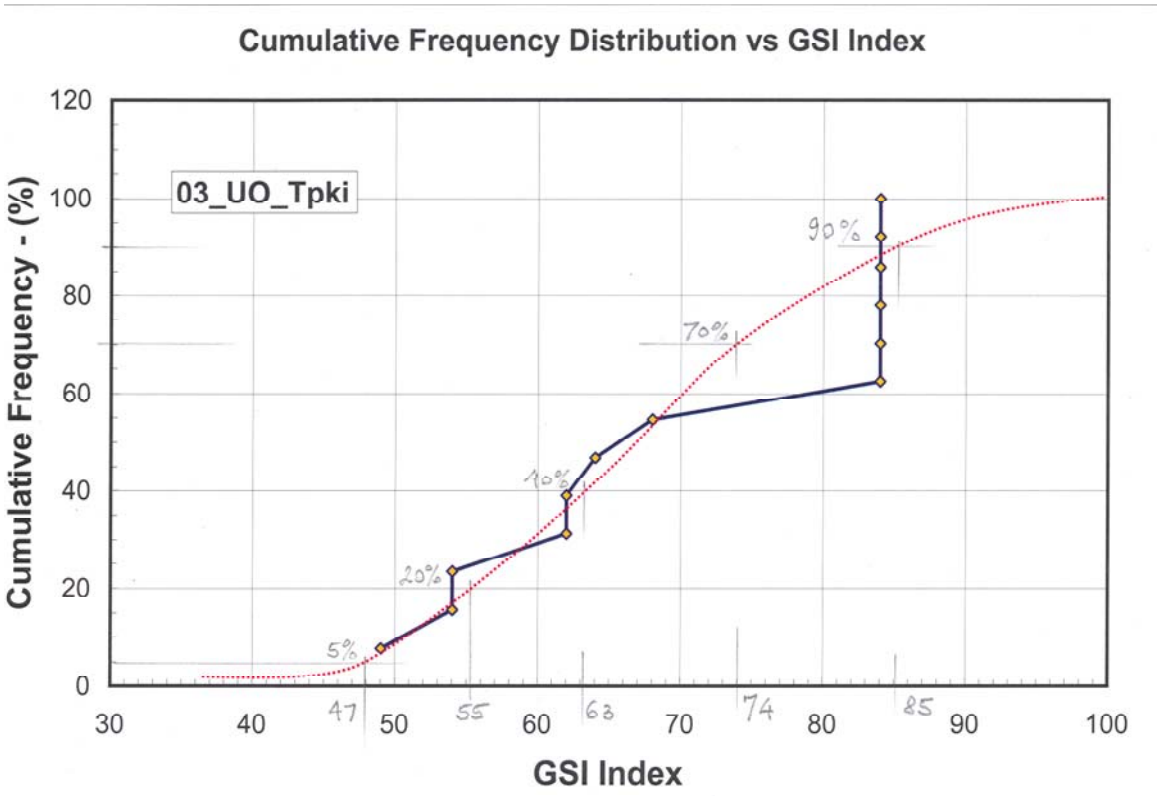

Sources: DTNs: GS950508314224.003 [DIRS 107488]; GS000608314224.005 [DIRS 166002]; GS960408314224.001 [DIRS 168135]; GS960408314224.003 [DIRS 168136]; GS960708314224.009 [DIRS 168137]; GS000608314224.006 [DIRS 152572]; GS960908314224.015 [DIRS 108372]; GS960908314224.016 [DIRS 108373]; GS960908314224.017 [DIRS 108376]; GS970108314224.002 [DIRS 107490]; GS970208314224.004 [DIRS 107492]; GS970808314224.009 [DIRS 107494]; GS970808314224.011 [DIRS 107495]; GS970808314224.013 [DIRS 107497]; GS990408314224.003 [DIRS 108404]; GS990408314224.004 [DIRS 108405]; GS990408314224.005 [DIRS 108408]; GS990408314224.006 [DIRS 108409]; GS970608314224.007 [DIRS 158430].

NOTE: Displayed are data in the 03_UO_Tpki Unit. Intersecting Pencil Lines Depict Procedure Applied to Obtain GSI Numbers Representing Cumulative Frequencies of GSI at 5, 20, 40, 70, and 90% for Estimating the Corresponding Rock Mass Categories 1 to 5

Figure 6-77. A Typical Plot of Cumulative Frequency Distribution for GSI Index Values Obtained from ESF, ECRB Cross-Drift, and HD Tunnel Mapping Data

Table 6-67. Summary of Rated Tunnel Sections Expressed in Terms of RMR and GSI Values

Lithostratigraphic Unit Number	Average Saturated Bulk Density (g/cm3)	Maximum Depth in Tunnels (m)	Rated Tunnel Section – Total (m)	Average RMR' = (RQD Index+C+Js+Jcd+JwR)	RMR' Std Dev	Average Geological Strength Index = (RMR'-5)	Average Geological Strength Index Std Dev	Number of Rated Tunnel Sections	Rock Mass Rating—GSI				
									Rock Mass Cat_1—GSI—5 (%)	Rock Mass Cat_2—GSI—20 (%)	Rock Mass Cat_3—GSI—40 (%)	Rock Mass Cat_4—GSI—70 (%)	Rock Mass Cat_5—GSI—90 (%)
1	2		3	4	5	6	7	8	9	10	11	12	13
02_UO_Tmr	1.75	28.16	0	NA	NA	NA	NA	0	47	55	63	74	85
03_UO_Tpki	1.66	28.16	69	76	14	71	14	13	47	55	63	74	85
04_TCw_Tpcrn	2.12	31.82	35	77	9	72	9	7	56	62	67	73	80
05_TCw_Tpcrn2	NA	34.03	40	72	11	67	11	10	45	56	63	72	77
06_TCw_Tpcrn1	NA	41.36	10	72	11	67	11	0	45	56	63	72	77
07_TCw_Tpcpul	2.23	48.69	185	66	10	61	10	37	40	53	60	67	73
08_TCw_Tpcpmn	2.36	55.79	358	71	8	66	8	71	50	59	63	69	77
09_TCw_Tpcpll	2.38	65.01	45	77	10	72	10	9	47	63	70	77	81
10_TCw_Tpcpln	2.36	103.76	295	76	9	71	9	57	54	65	70	75	81
11_TCw_Tpcpv3	2.40	104.24	0	NA	NA	NA	NA	0	NA	NA	NA	NA	NA
12_PTn_Tpcpv2	1.96	104.72	30	70	4	65	4	6	51	60	64	66	69
13_PTn_Tpcpv1	1.81	105.64	113	75	5	70	5	17	62	65	67	71	77
14_PTn_Tpbt4	1.72	112.00	10	NA	NA	NA	NA	0	NA	NA	NA	NA	NA
15_PTn_Tpy	1.86	118.50	0	NA	NA	NA	NA	0	NA	NA	NA	NA	NA
16_PTn_Tpbt3	1.66	124.94	25	84	0	79	0	2	NA	NA	NA	NA	NA
17_PTn_Tpp	1.63	129.95	125	80	6	75	6	4	59	66	71	76	81
18_PTn_Tpbt2	1.73	138.87	85	78	5	73	5	5	63	67	69	74	78
19_PTn_Tptrv3	NA	139.19	15	73	1	68	1	2	60	64	66	68	70
20_PTn_Tptrv2	NA	138.55	40	67	10	62	10	5	41	50	56	64	72
21_TSw1_Tptrv1	2.46	149.65	115	60	12	55	12	16	32	46	52	60	69
22_TSw1_Tptrn	2.31	200.40	855	70	7	76	2	169	50	60	65	69	74
23_TSw1_Tptrl	2.26	184.62	220	61	7	56	7	44	42	50	55	59	64
24_TSw1_Tpf	NA	241.40	0	NA	NA	NA	NA	0	NA	NA	NA	NA	NA
25_TSw1_Tptpul	2.27	298.00	2350	62	9	57	9	465	42	50	55	61	69
26_TSw2_Tptpmn	2.36	297.77	3985	69	7	64	7	788	51	59	62	68	72

Table 6-67. Summary of Rated Tunnel Sections Expressed in Terms of RMR and GSI Values (Continued)

Lithostratigraphic Unit Number	Average Saturated Bulk Density (g/cm3)	Maximum Depth in Tunnels (m)	Rated Tunnel Section – Total (m)	Average RMR' = (RQD Index+C+Js+Jcd+JwR)	RMR' Std Dev	Average Geological Strength Index = (RMR'-5)	Average Geological Strength Index Std Dev	Number of Rated Tunnel Sections	Rock Mass Rating—GSI				
									Rock Mass Cat_1—GSI—5 (%)	Rock Mass Cat_2—GSI—20 (%)	Rock Mass Cat_3—GSI—40 (%)	Rock Mass Cat_4—GSI—70 (%)	Rock Mass Cat_5—GSI—90 (%)
27_TSw2_Tptpll	2.36	362.56	1105	66	5	61	5	214	52	56	59	63	68
28_TSw2_Tptpln	2.41	259.52	260	71	5	66	5	43	57	61	64	69	72

Sources: DTNs: GS950508314224.003 [DIRS 107488]; GS000608314224.005 [DIRS 166002]; GS960408314224.001 [DIRS 168135]; GS960408314224.003 [DIRS 168136]; GS960708314224.009 [DIRS 168137]; GS000608314224.006 [DIRS 152572]; GS960908314224.015 [DIRS 108372]; GS960908314224.016 [DIRS 108373]; GS960908314224.017 [DIRS 108376]; GS970108314224.002 [DIRS 107490]; GS970208314224.004 [DIRS 107492]; GS970808314224.009 [DIRS 107494]; GS970808314224.011 [DIRS 107495]; GS970808314224.013 [DIRS 107497]; GS990408314224.003 [DIRS 108404]; GS990408314224.004 [DIRS 108405]; GS990408314224.005 [DIRS 108408]; GS990408314224.006 [DIRS 108409]; GS970608314224.007 [DIRS 158430].

NOTES: 1 Source for density data: SNL02030193001.027 [DIRS 108410], See source below for others.

2 Minimum and maximum GSI values are higher and lower, respectively, than recorded in tunnel because data in the table originates from plotted distribution curves within 5% to 90% frequency distribution interval.

3 For 02_UO_Tmr values of GSIs (shown in green) are taken the same as for 03_UO_Tpki Unit

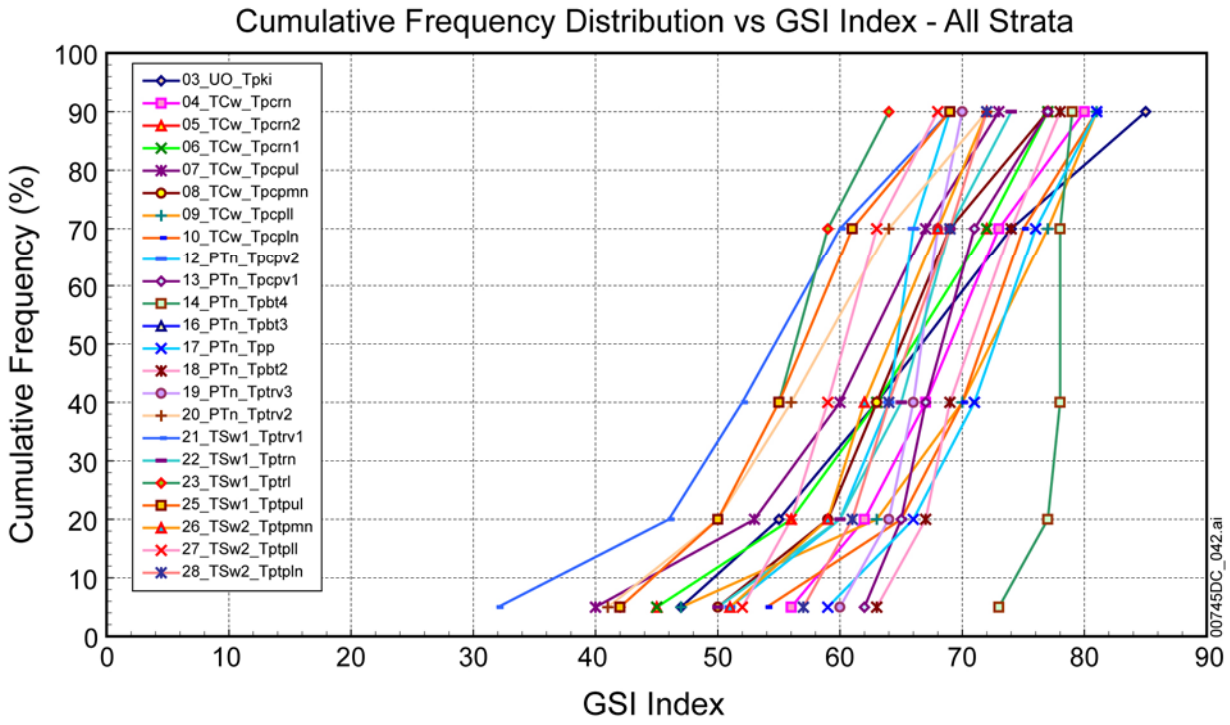

Sources: DTNs: GS950508314224.003 [DIRS 107488]; GS000608314224.005 [DIRS 166002]; GS960408314224.001 [DIRS 168135]; GS960408314224.003 [DIRS 168136]; GS960708314224.009 [DIRS 168137]; GS000608314224.006 [DIRS 152572]; GS960908314224.015 [DIRS 108372]; GS960908314224.016 [DIRS 108373]; GS960908314224.017 [DIRS 108376]; GS970108314224.002 [DIRS 107490]; GS970208314224.004 [DIRS 107492]; GS970808314224.009 [DIRS 107494]; GS970808314224.011 [DIRS 107495]; GS970808314224.013 [DIRS 107497]; GS990408314224.003 [DIRS 108404]; GS990408314224.004 [DIRS 108405]; GS990408314224.005 [DIRS 108408]; GS990408314224.006 [DIRS 108409]; GS970608314224.007 [DIRS 158430].

NOTE: Tptpul and Tptpll zones included for information only.

Figure 6-78. Cumulative Frequency Distribution for GSI in All Lithostratigraphic Zones Encountered and Documented in Yucca Mountain Subsurface Excavations During Tunnel Mapping

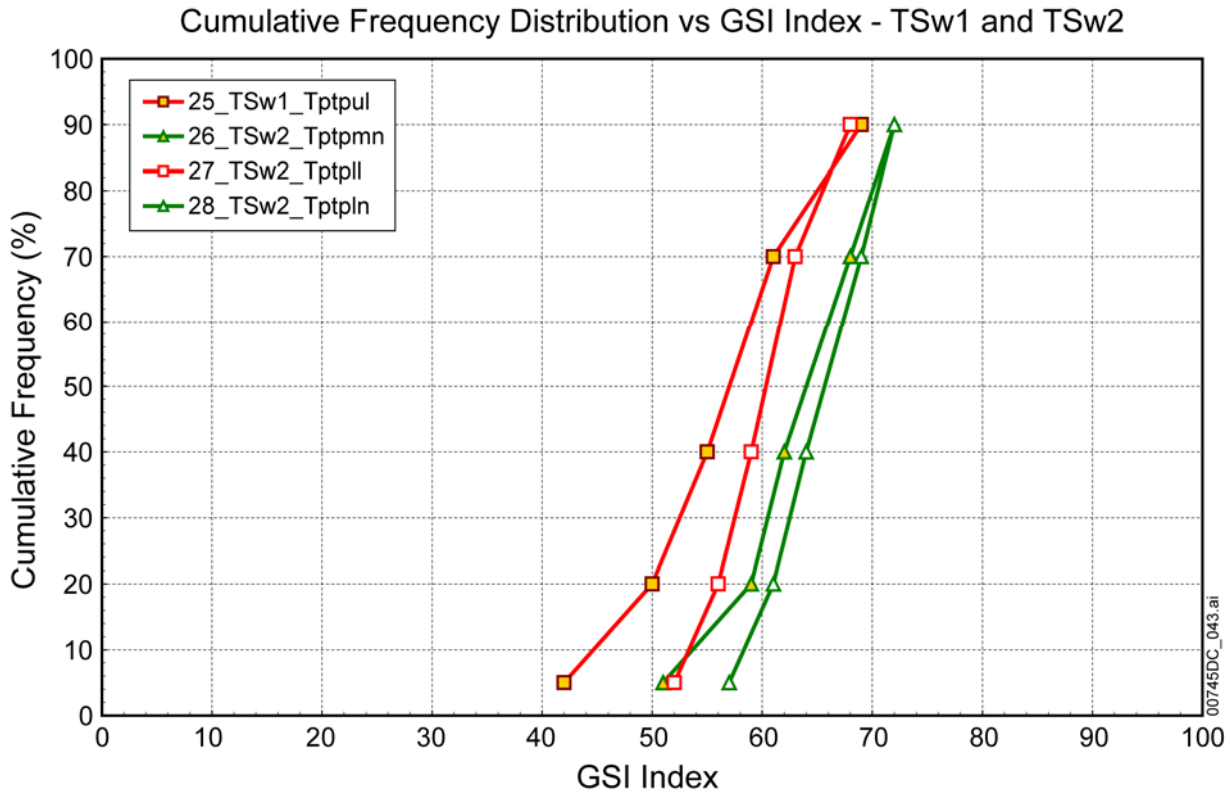

Sources: DTNs: GS950508314224.003 [DIRS 107488]; GS000608314224.005 [DIRS 166002]; GS960408314224.001 [DIRS 168135]; GS960408314224.003 [DIRS 168136]; GS960708314224.009 [DIRS 168137]; GS000608314224.006 [DIRS 152572]; GS960908314224.015 [DIRS 108372]; GS960908314224.016 [DIRS 108373]; GS960908314224.017 [DIRS 108376]; GS970108314224.002 [DIRS 107490]; GS970208314224.004 [DIRS 107492]; GS970808314224.009 [DIRS 107494]; GS970808314224.011 [DIRS 107495]; GS970808314224.013 [DIRS 107497]; GS990408314224.003 [DIRS 108404]; GS990408314224.004 [DIRS 108405]; GS990408314224.005 [DIRS 108408]; GS990408314224.006 [DIRS 108409]; GS970608314224.007 [DIRS 158430].

Figure 6-79. Cumulative Frequency Distribution for GSI in Nonlithophysal of Lithostratigraphic Zones Encountered and Documented in Yucca Mountain Subsurface Excavations at the RHH

6.4.4.4.1.6 Rock Mass Categories and Data Uncertainty

The classification of rock mass quality into five rock mass categories was introduced to provide the designer with a range of geotechnical parameters that would cover the most extreme rock mass behavior encountered in the Yucca Mountain tunnels and other underground excavations. The lower category indicates rock mass with lower strength and lower values of the modulus of deformability. This categorization of rock mass quality imposes a limit as to the range of values used to characterize each unit.

As shown in Figure 6-78, the average tunnel conditions among all units are represented by the rock mass categories ranging from 2 to 4. The GSI values estimated between 20% and 70% of the cumulative frequency of occurrence as determined from the entire population of mapping data falls in the range between 45 and 75, approximately. The corresponding RMR values ranging from 40 to 70 indicate rock mass quality being *fair* to *good*. It should be noted that on

the average in the tunnel even the poorest rock conditions recorded still show at least a fair quality rock rating in all lithostratigraphic units encountered.

At the RHH, the GSI range for lithophysal units is slightly lower than similar range for the nonlithophysal strata. The GSI values characterizing the Tptpul unit are the lowest among all units and range from 50 to 61 (for the 20% to 70% frequency range), with the corresponding RMR values ranging from 45 to 56, which indicates rock mass class rated as fair. On the other end, the Tptpln unit is characterized by the highest rock mass ranking and GSI values for the rock mass category 2 to 4 range from 61 to 69 with the corresponding RMR values in the range of 56 to 64, or rock mass quality rated as fair to good.

In effect, the field-mapping based classification of rock mass indicates fair-to-good rock mass that is evident for all strata. It does not categorize rock conditions worse or better that potentially could also be encountered in the tunnels. The rock mass of low quality category 1, and the high rock mass category 5, together represent a relatively small fraction of the overall rock mass quality representation. Each must be treated differently as the potential problems and the associated significance are different as well. Each extreme case must be interpreted within a framework of evidence obtained during detailed mapping in the tunnel under locally existing in situ loading and environmental conditions.

In general, the range of rock mass quality documented in the tunnels in all lithostratigraphic units provides the evidence that an assessment of the rock mass performance, regardless of individual rock unit, is indicative of generally *fair-to-good* rock strata.

The rock mass quality estimates presented in this section are based on a standard mining and tunneling practice. As discussed earlier in Section 6.4.4, there is a concern that this methodology may not be appropriate for assessing the properties of lithophysae-rich rock mass. This concern was mainly related to the ability of providing a reasonable estimate of RQD value, one of the key input parameters required to assess the rock mass quality. To resolve this issue, especially for the lithophysal units at the RHH, an alternative methodology was developed. In the following section, the lithophysal rock mass parameters are assessed using this alternative approach, where a combination of tests results on large-core specimens and numerical simulation of synthetic specimens are used to obtain the estimates of the lithophysal rock mass properties.

6.4.4.4.2 Rock Mass Properties for Lithophysal Strata at the RHH

The analyses of the rock mass mechanical properties for lithophysal rock units at the RHH include the following:

- Use of lithophysal porosity as a surrogate property and the plausible conceptual simulation of lithophysal rock
- Characterization of lithophysal host rock porosity
- Analysis of the lithophysal rock mechanical behavior and properties based on laboratory testing
- Mechanical property bounding analysis and rock mass categories

- Numerical simulation of lithophysal rock
- Evaluation of the mechanical property bounding analyses based on the numerical simulation
- Confirmation of the Lithophysal Rock Mechanical Simulation and Property Bounds.

Details of lithophysal rock mass mechanical property analysis are presented in *Lithophysal Rock Mass Mechanical Properties of the Repository Host Horizon* (BSC 2004 [DIRS 172334], Section 6) and summarized in the following sections.

6.4.4.4.2.1 Use of Lithophysal Porosity as a Surrogate Property and the Plausible Conceptual Simulations of Lithophysal Rock

The approach of using lithophysal porosity as a surrogate property involves estimating lithophysal rock mass properties based on incorporating site-specific laboratory and field testing, in particular the correlation between rock mechanical properties and specimen lithophysal porosity, supplemented by numerical simulation of lithophysal rock. As a result, tests of large-diameter core (up to 0.3 m diameter) and in situ compression tests (slot tests up to 1.1 m across) have been conducted and analyzed on lithophysal rock in the Tptpul and Tptpll zones. Additionally, the Tptpll portion of the ECRB Cross-Drift has been systematically measured by a number of different methods to identify lithophysal rock characteristics (abundance, shape, and size variability), and it would be useful to similarly measure and study portions of the Tptpul zone in the ECRB Cross-Drift as well. The measured abundance of lithophysae was used to produce a simulation of the spatial variation of lithophysal porosity in the repository area (BSC 2004 [DIRS 172334], Appendix A). Lastly, two- and three-dimensional numerical simulation of larger-scale samples (1 m scale) with realistic lithophysal voids have been carried out using the PFC and UDEC discontinuum programs. These numerical simulations have been utilized to further develop the stress-strain response of lithophysal rocks and to confirm rock parameter ranges necessary to extrapolate the possible behavior and material properties of lithophysal bulk rock.

6.4.4.4.2.2 Characterization of the Lithophysal Host Rock Porosity

A detailed study of the lithophysal features in the Tptpll from geologic data collected in the ESF and ECRB Cross-Drift (DTNs: GS021008314224.002 [DIRS 161910]; GS040608314224.001 [DIRS 171367]) is described in the *Subsurface Geotechnical Parameters Report* (BSC 2003 [DIRS 166660], Attachment VII).

The abundance of lithophysal features is measured using a variety of one and two-dimensional mapping techniques. Figure 6-80 shows the variation in abundance of lithophysal cavities and other features along the ECRB Cross-Drift. Figure 6-81 shows histograms of the acquired and corrected tape traverse data based on 5 m increment measurements and averaging over 15 m. In comparing the plots, averaging the data has the expected consequence of reducing the scatter in the data and pulling inward the tails of the data distribution. The 15 m adjusted tape traverse data was next fitted to the more accurate angular traverse and panel map measurements of lithophysae abundance, and a new estimate of the variation of lithophysal cavities was made

(BSC 2004 [DIRS 172334], Appendix B: Drift Deg AMR AF T-A-P Fit_V1_DBR.xls). A histogram of this fitted cavity data and the fitted data including the 5 m averaged large-lithophysal inventory is shown in Figure 6-82. Table 6-68 lists the summary statistics for these various descriptions of lithophysal porosity, and a summary of panel map lithophysae.

The scale effect is illustrated by examining smaller portions of panel maps. Out of the 18 panel maps, the largest lithophysal porosity for the 1×3 m panel area was 19% (BSC 2003 [DIRS 166660], Attachment VII, Table VII-3). After each panel map was sliced into 1×1 m squares, some of the squares were determined to have a lithophysal porosity approaching 30% (BSC 2004 [DIRS 172334], Appendix B: *LithophysalRockRanges_Calc.xls*, worksheet 'PFC').

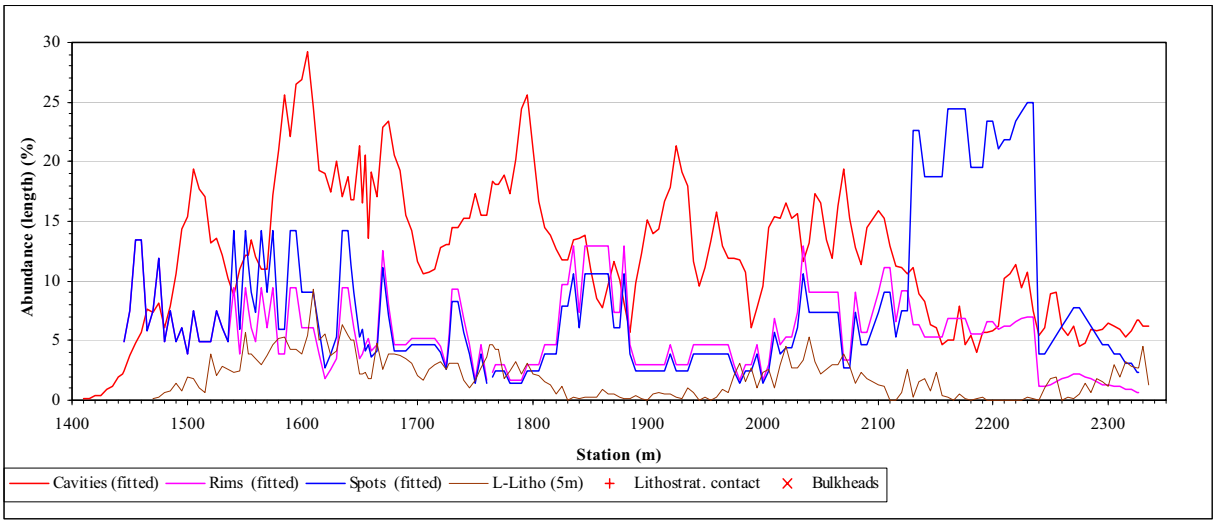

(a) Abundance curves of "fitted" lithophysal cavities, rims, spots, and the 5 m averaged large-lithophysal inventory along the ECRB Cross-Drift. "Fitted" data refers to the process of combining panel map, tape, and angular traverse abundance data to obtain the best overall estimates of component abundance.

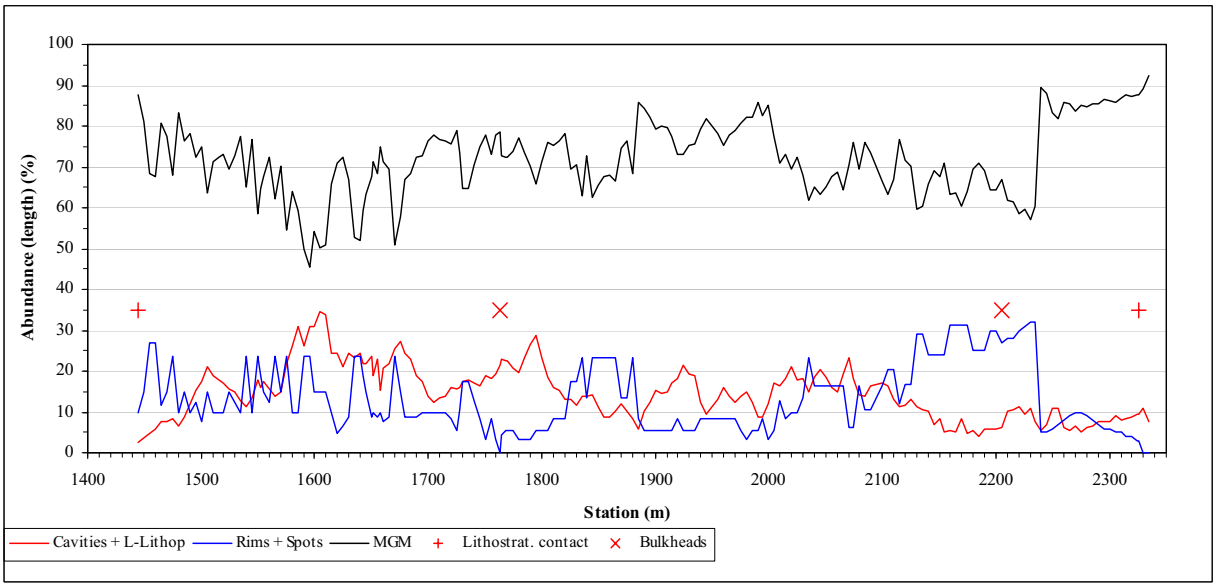

(b) Abundance curves for a three-component rock material simulation (matrix groundmass, "fitted" lithophysal cavities plus the 5 m large-lithophysal inventory, and rims plus spots) along the ECRB Cross-Drift. The combination of "fitted" lithophysal cavities and the large-lithophysal inventory is considered to represent the best estimate of lithophysal cavity abundance.

Source: BSC 2004 [DIRS 172334], Appendix B: *Drift Deg AMR AF T-A-P Fit_V1_DBR.xls*, worksheet *Length - Fit and Stats*.

Figure 6-80. Abundance Curves of Lithophysal Rock Cavities, Rims, Spots, and Matrix-Groundmass in the Tptpll Exposed along the ECRB Cross-Drift

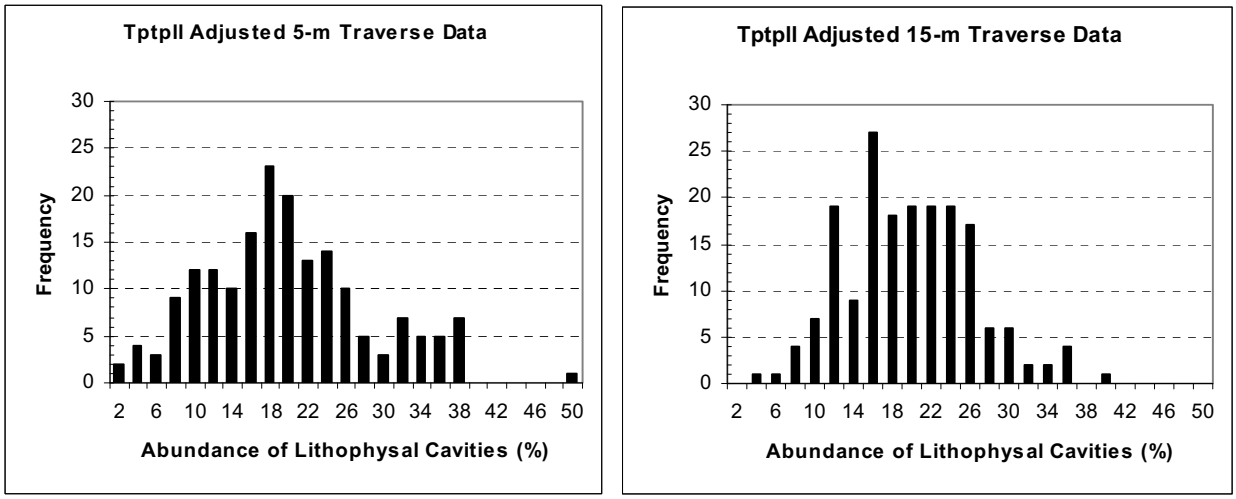

Source: BSC 2004 [DIRS 172334], Appendix B: *Drift Deg AMR AF T-A-P Fit_V1_DBR.xls*, worksheet 'T-A-P Cav Fit, cells O213 and AF213'.

NOTE: Lithophysal porosity data are from ECRB Cross-Drift station 14+44 to 23+26, which includes the entire thickness of the Tptpll lithostratigraphic rock unit.

Figure 6-81. Histograms of Lithophysal Porosity for the Tptpll in the ECRB Cross-Drift Based on 5 m and 15 m Adjusted Tape Traverse Data

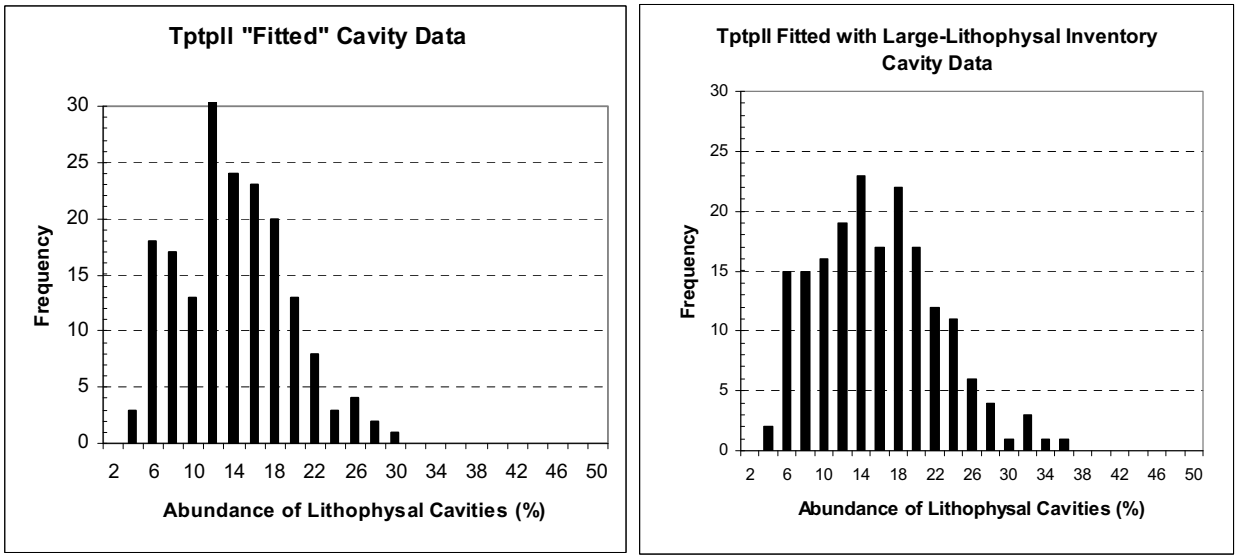

Source: BSC 2004 [DIRS 172334], Appendix B: *Drift Deg AMR AF T-A-P Fit_V1_DBR.xls*, worksheet 'Length – Fit and Stats, cells M216 and AX230'.

NOTE: Lithophysal porosity data are from ECRB Cross-Drift station 14+44 to 23+26, which includes the entire thickness of the Tptpll lithostratigraphic rock unit.

Figure 6-82. Histograms of Lithophysal Porosity for the Tptpll in the ECRB Cross-Drift Based on Tape Traverse Fitted Cavity Data and Angular Traverse Data

Table 6-68. Descriptive Statistics of Tptpll Lithophysal Porosity Data

Type of Measurement	Count	Mean ± 1 SE	Mean ± 1 SE Percentage	Mean± 1 SD	Mean ± 1 SD Percentage	Median	Minimum	Maximum	Range
5m Tape Trav	181	19 ± 1	19 ± 5%	19 ± 9	19 ± 50%	17.8	1.2	48.4	47.2
15m Tape Trav	181	19 ± 1	19 ± 5%	19 ± 7	19 ± 39%	18.2	3.3	39.0	35.7
Fitted Cavities	180	13 ± 1	13 ± 8%	13 ± 5	13 ± 40%	12.9	2.2	29.2	27.0
Fitted Cav+LL	185	15 ± 1	15 ± 7%	15 ± 7	15 ± 49%	14.5	2.5	34.6	32.1
Angular Trav	22	15 ± 2	15 ± 13%	15 ± 8	15 ± 54%	14.8	2.2	30.7	28.5
Panel Maps	18	13 ± 1	13 ± 8%	13 ± 5	13 ± 36%	13.4	5.3	19.0	13.7

Sources: BSC 2003 [DIRS 166660], Attachment VII, Table VII-10; BSC 2004 [DIRS 172334], Appendix B: *Drift Deg AMR AF T-A-P Fit_V1_DBR.xls*, worksheet 'Length – Fit and Stats, cells J244 to Z251'.

NOTES: (1) LL stands for the 5 m averaged large-lithophysae inventory.

(2) SE stands for the standard error rounded to nearest positive whole number.

(3) SD stands for standard deviation (including the uncertainty in the standard deviation).

(4) Lithophysal porosities in the table are reported as percent by volume.

(5) Since the field measurement uncertainty ranges from about 5% to 10% or higher (BSC 2004 [DIRS 172334], Section 6.2.1.1), one significant digit will be used to represent porosity uncertainty.

6.4.4.4.2.3 Mechanical Properties of Lithophysal Rock Based on Laboratory Testing

The bulk of the historical testing program, including characterization of the Topopah Spring Tuff, consisted of compressive and tensile strength tests on small diameter (25 to 50 mm (1 to 2 in.)) rock cores. These data are described in the *Subsurface Geotechnical Parameters Report* (BSC 2003 [DIRS 166660]) and *Intact Rock Mechanical Properties of Yucca Mountain Stratigraphic Units* (BSC 2005 [DIRS 176611]) and additional analyses of these data are presented in *Lithophysal Rock Mass Mechanical Properties of the Repository Host Horizon* (BSC 2004 [DIRS 172334], Section 6.3.1).

As discussed above, the small diameter cores (about 50 mm or 2 in. diameter and less) may not accurately reflect the true strength or elastic properties of the lithophysal rock since the diameter precludes a reasonable sampling of the lithophysal voids. Therefore, to estimate ranges of lithophysal rock strength and elastic modulus, greater reliance is placed on measurements from large-diameter core samples that contain multiple lithophysal cavities within a given sample.

The results of compressive strength testing on 290 mm (11.5 in.) diameter samples from the Tptpul and Tptpll from the ESF main loop and ECRB Cross Drift and 267 mm (10.5 in.) diameter samples from the Tptpul at Busted Butte form the basis for the development of mechanical property ranges. The laboratory data from these tests are provided in Table 6-69.

Figure 6-83 plots the UCS and Young's modulus as functions of approximate lithophysal porosity for the 267 mm (10.5 in.) and 290 mm (11.5 in.) diameter samples of the Tptpll and Tptpul. Although significant scatter exists in the data, a best-fit exponential function has been superimposed on the data for both room dry and saturated sample conditions. These data show little impact of saturation level on Young's Modulus, but results in a general reduction in UCS with the saturated samples tending to form a lower bound to the room dry strengths. A mean strength of 17.8 MPa and a mean modulus of 12.2 GPa were calculated based on large-diameter

samples (BSC 2004 [DIRS 172334], Appendix B: *LithophysalRockRanges_Calc.xls*, worksheet 'histograms').

Figure 6-84 plots the relationship between the UCS and Young's modulus by core saturation level. These data show that a reasonably linear relationship exists between these mechanical properties, which was the case also for the small-diameter core data (BSC 2004 [DIRS 172334], Figures 6.3-3 and 6.3-4). As seen in this plot, the saturated samples tend to form a lower bound to the room dry strengths. On the average, small-diameter core UCS values are slightly higher than large-diameter core UCS values for corresponding Young's moduli less than 25 GPa (BSC 2004 [DIRS 172334], Figure 6.3-4).

Figures 6-85 and 6-86 show plots of the UCS versus Young's modulus for medium to large-sized (both room dry and saturated samples) and small and large-sized (only saturated samples) Topopah Spring Tuff specimens, respectively, and indicate a significant sample-size effect on mechanical rock properties. A study by Price (2004 [DIRS 170894]) indicated similar results with the slight drop in strength observed between small-diameter core specimens (from drill holes) and large-diameter core specimens (from ESF and ECRB Cross-Drift tunnel wall borings) sampled from Topopah Spring Tuff near the repository rock.

Table 6-69. Mechanical Test Results of Lithophysal Tuff from 267 and 290 mm-Diameter Samples

Test ID	Lithostratigraphic Unit	L/D Ratio	Saturation	Temperature (°C)	Uniaxial Strength (MPa)	Young's Modulus (GPa)	Poisson's Ratio	Estimated Lithophysal Porosity	Estimated Total Porosity	DTN
YMPLL49A	Tptpll	1.1 : 1	Dry	195	32.2	7.1	—	11.7	23.6	SN0211L0207502.002* [DIRS 161872]
YMPLL43A	Tptpll	1.1 : 1	Dry	200	31.1	6.5	—	20.3	29.2	SN0211L0207502.002* [DIRS 161872]
YMPLL23A	Tptpll	1.8 : 1	Room Dry	24	28.7	9.2	—	19.2	30.6	SN0211L0207502.002* [DIRS 161872]
YMPLL24A	Tptpll	1.8 : 1	Room Dry	24	13.3	5.0	—	22.2	32.4	SN0211L0207502.002* [DIRS 161872]
YMPLL46A	Tptpll	1.8 : 1	Room Dry	24	21.7	8.5	—	28.4	37.4	SN0211L0207502.002* [DIRS 161872]
YMPLL87A	Tptpll	1.9 : 1	Saturated	24	15.7	5.3	—	14.5	25.7	SN0211L0207502.002* [DIRS 161872]
YMPUL59B	Tptpul	1.2 : 1	Dry	190	19.6	7.3	—	39.4	56.8	SN0208L0207502.001* [DIRS 161871]
YMPUL67A	Tptpul	1.3 : 1	Dry	190	34.8	9.9	—	6.2	25.3	SN0208L0207502.001* [DIRS 161871]
YMPUL62B	Tptpul	1.0 : 1	Dry	200	37.0	13.7	—	19.3	42.8	SN0208L0207502.001* [DIRS 161871]
YMPUL50A	Tptpul	1.5 : 1	Room Dry	24	22.1	14.9	0.21	28.5	40.9	SN0211L0207502.002* [DIRS 161872]
YMPUL59A	Tptpul	2.0 : 1	Room Dry	24	13.5	5.8	0.39	30.3	51.7	SN0208L0207502.001* [DIRS 161871]

Table 6-69. Mechanical Test Results of Lithophysal Tuff from 267 and 290 mm-Diameter Samples (Continued)

Test ID	Lithostratigraphic Unit	L/D Ratio	Saturation	Temperature (°C)	Uniaxial Strength (MPa)	Young's Modulus (GPa)	Poisson's Ratio	Estimated Lithophysal Porosity	Estimated Total Porosity	DTN
YMPUL61A	Tptpul	1.9 : 1	Room Dry	24	17.7	8.8	—	23.9	38.2	SN0208L0207502.001* [DIRS 161871]
YMPUL62A	Tptpul	1.8 : 1	Room Dry	24	25.9	13.7	—	12.7	32.2	SN0208L0207502.001* [DIRS 161871]
YMPUL64A	Tptpul	1.7 : 1	Room Dry	24	33.5	20.5	—	12.8	31.0	SN0208L0207502.001* [DIRS 161871]
YMPUL65A	Tptpul	2.0 : 1	Room Dry	24	26.2	19.5	—	11.9	25.6	SN0208L0207502.001* [DIRS 161871]
YMPUL66A	Tptpul	1.7 : 1	Room Dry	24	16.5	12.4	—	16.7	31.0	SN0208L0207502.001* [DIRS 161871]
YMPUL60A	Tptpul	1.8 : 1	Saturated	24	12.7	6.7	—	18.6	38.7	SN0208L0207502.001* [DIRS 161871]
YMPUL63A	Tptpul	1.9 : 1	Saturated	24	9.4	5.0	0.24	20.0	38.7	SN0208L0207502.001* [DIRS 161871]
YMPUL68A	Tptpul	2.1 : 1	Saturated	24	11.6	5.9	0.03	25.8	39.3	SN0208L0207502.001* [DIRS 161871]
1B	Tptpul	2.0 : 1	Saturated	22	14.5	14.2	0.14	17.3	32.7	MO0311RCKPRPCS.003 [DIRS 166073]
1D	Tptpul	2.0 : 1	Saturated	22	10.3	10.9	0.14	22.2	33.3	MO0311RCKPRPCS.003 [DIRS 166073]
2A	Tptpul	2.0 : 1	Saturated	22	12.4	11.9	0.16	14.1	30.9	MO0311RCKPRPCS.003 [DIRS 166073]
3A	Tptpul	2.0 : 1	Saturated	22	12.0	12.9	0.14	14.0	40.0	MO0311RCKPRPCS.003 [DIRS 166073]
8A	Tptpul	2.0 : 1	Saturated	22	18.2	16.6	0.14	13.5	38.2	MO0311RCKPRPCS.003 [DIRS 166073]
8B	Tptpul	2.0 : 1	Saturated	22	17.4	16.8	0.18	14.2	32.0	MO0311RCKPRPCS.003 [DIRS 166073]
8C	Tptpul	2.0 : 1	Saturated	22	18.5	15.8	0.13	17.9	34.4	MO0311RCKPRPCS.003 [DIRS 166073]
8D	Tptpul	2.0 : 1	Saturated	22	17.5	18.3	0.13	21.4	37.9	MO0311RCKPRPCS.003 [DIRS 166073]
8E	Tptpul	2.0 : 1	Saturated	22	13.8	15.8	0.21	19.3	35.5	MO0311RCKPRPCS.003 [DIRS 166073]
8F	Tptpul	2.0 : 1	Saturated	22	27.8	21.5	0.21	12.6	37.2	MO0311RCKPRPCS.003 [DIRS 166073]

NOTES: 1. DTNs are also listed in Table 4-2.

2. For DTNs listed above and marked with an (*), the estimate of lithophysal porosity is given in DTN: SN0305L0207502.005 [DIRS 163373] as volume fraction of lithophysae, and the estimate of total porosity is given in DTN: SN0305L0207502.006 [DIRS 165747].

3. The associated qualified DTN of compressive strength values is MO0311RCKPRPCS.003 [DIRS 166073] and qualified DTN of Young's Modulus values is MO0402DQRIRPPR.003 [DIRS168901].

4. Not all DTNs above are used in Section 6. Excluded are test results conducted at high temperatures (greater than 100 °C) and specimen results where the length to diameter (L/D) ratio is 1.5 or less.

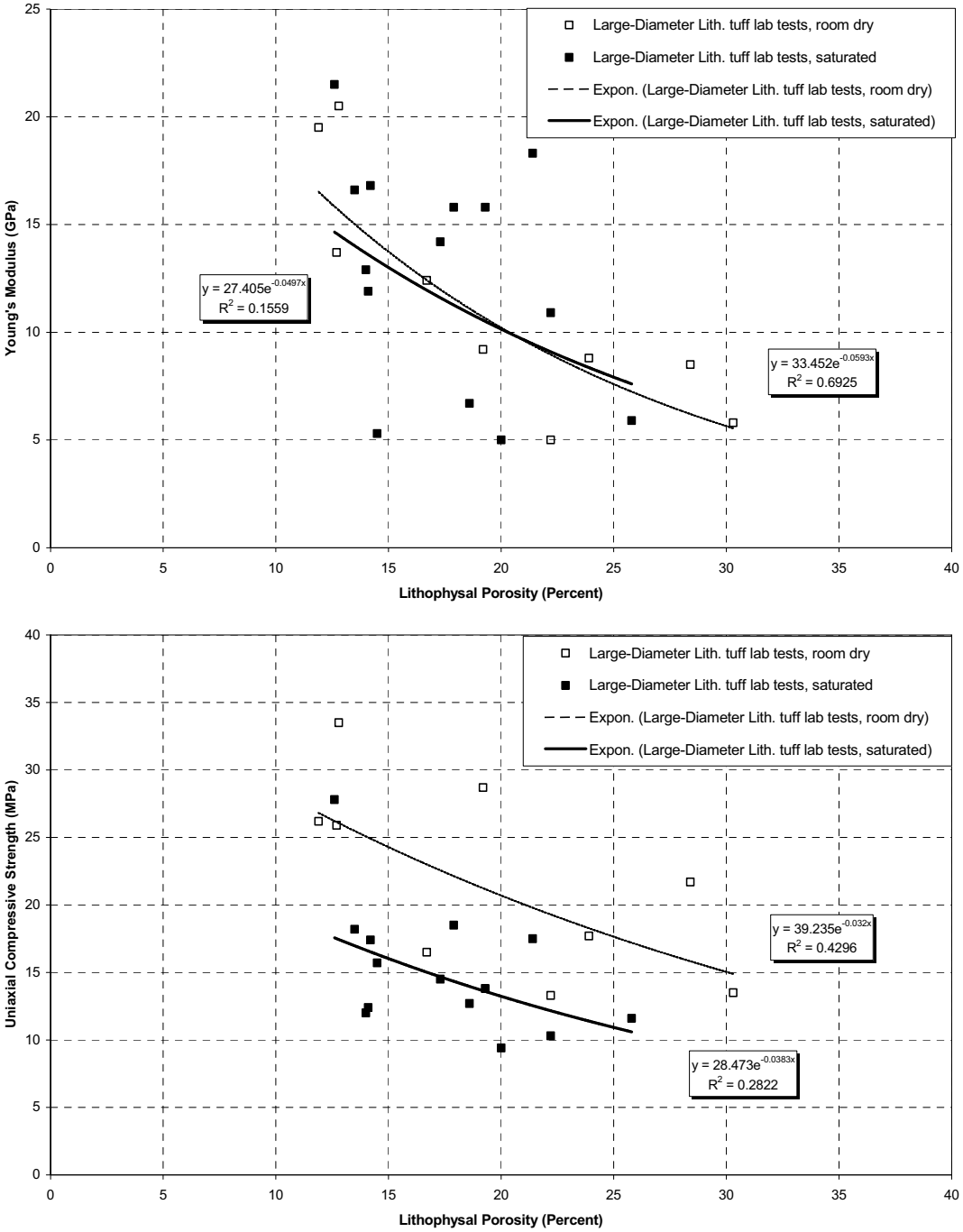

Source: BSC 2004 [DIRS 172334], Appendix B: *LithophysalRockRanges_Calc.xls*, worksheets 'LC E-por and LC q-por'.

Figure 6-83. Variation in Young's Modulus (top) and Uniaxial Compressive Strength (bottom) as a Function of the Lithophysal Void Porosity for 10.5 and 11.5 in. Diameter Cores from the Tptpul and Tptpll Units

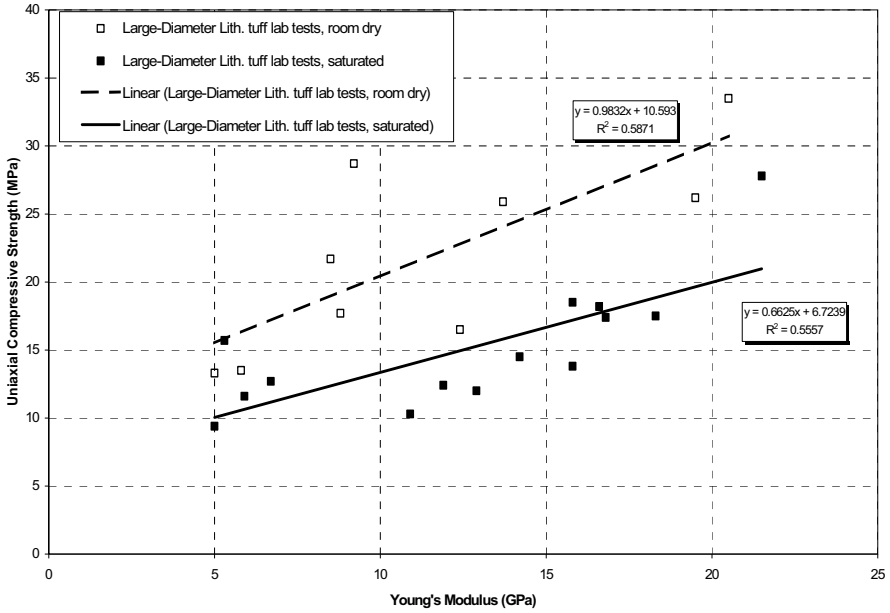

Source: BSC 2004 [DIRS 172334], Appendix B: *LithophysalRockRanges_Calc.xls*, worksheet 'LC q-E'.

Figure 6-84. Uniaxial Compressive Strength as a Function of Young's Modulus and Saturation Level for 10.5 and 11.5 in. Diameter Cores from the Tptpul and Tptpll Units

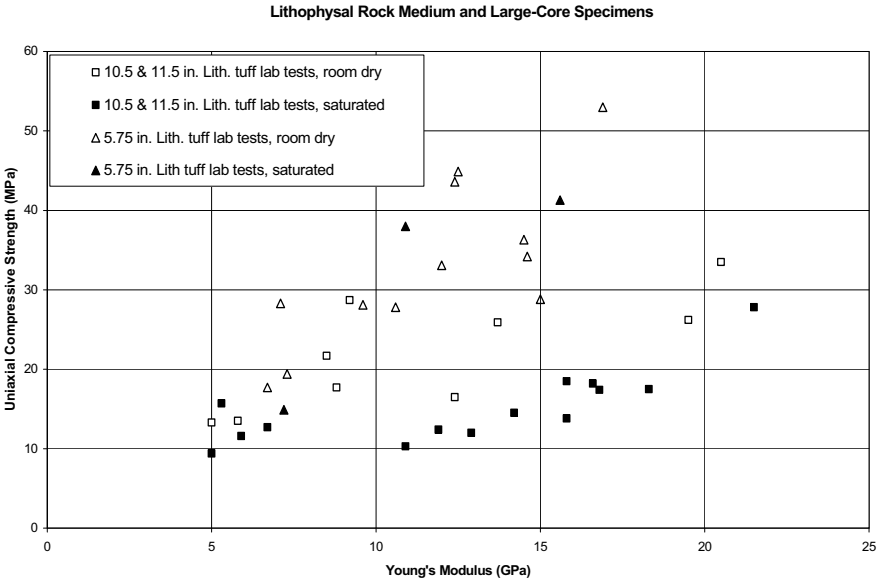

Source: BSC 2004 [DIRS 172334], Appendix B: *LithophysalRockRanges_Calc.xls*, worksheet '6-in cores'.

Figure 6-85. Results of Intact Uniaxial Compressive Strength to Young's Modulus for Medium and Large-Core Specimens of Lithophysal Rock

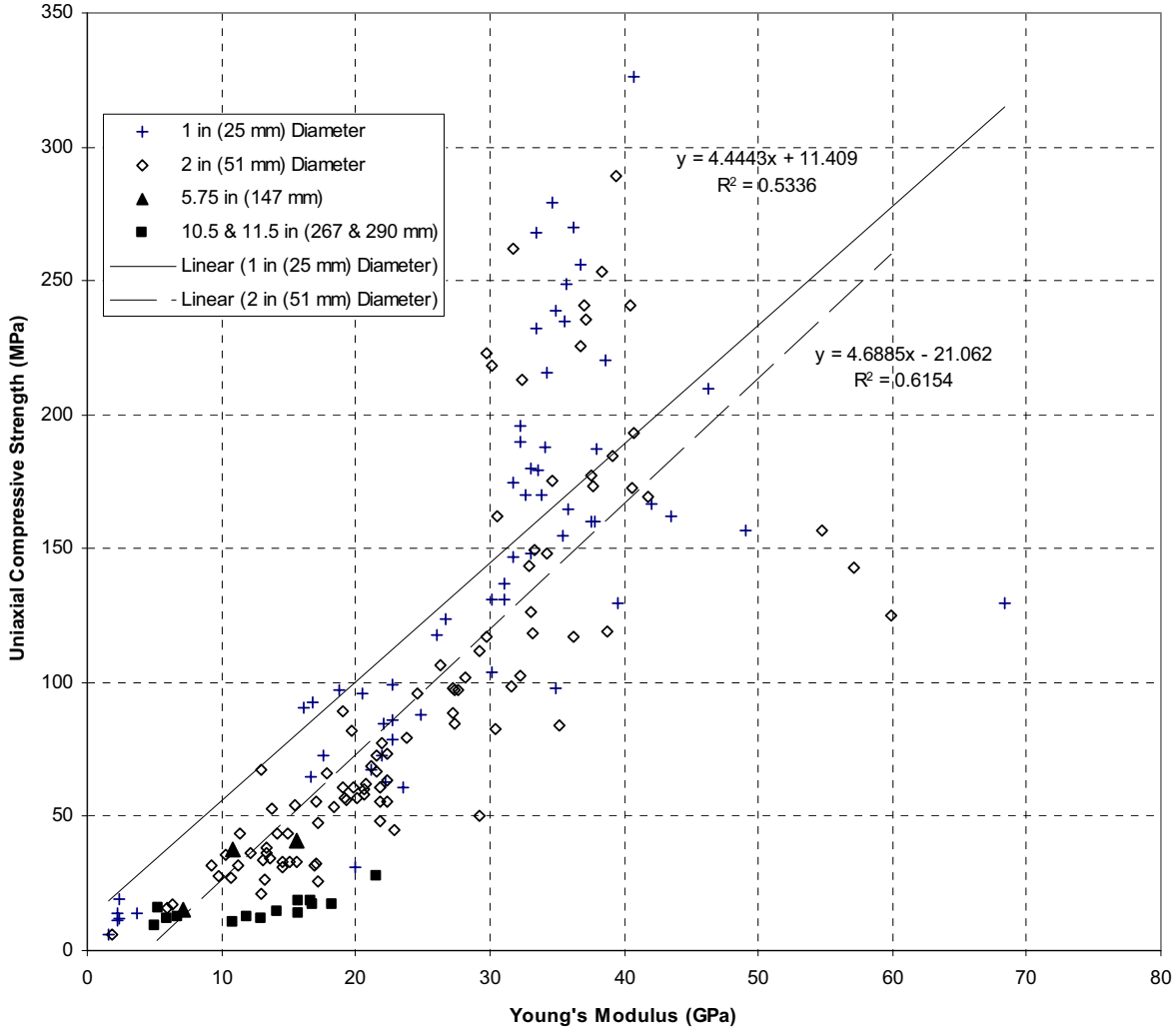

Source: BSC 2004 [DIRS 172334], Appendix B: *Compressive and Porosity Data REV00B_PorosityOnly_Tpt.xls*, worksheet 'Plots'.

NOTES: (1) From the best fit lines to the 25 mm and 51 mm diameter test data shows that for the same Young's modulus the 25 mm diameter samples are on the average about 25 MPa stronger.

(2) The 147 mm diameter test data plots near the 51 mm data, but at greatly reduced strength and modulus levels.

(3) The large-core data (267 and 290 mm diameter) has the least strength of all sample sizes for similar Young's modulus values.

Figure 6-86. Results of Intact Uniaxial Compressive Strength to Young's Modulus for Saturated Small and Large-Core Specimens of Topopah Spring Lithophysal Rock

A number of detailed geological studies have been conducted at the Yucca Mountain site to define the basic mineralogy of the rocks, and the petrologic and geochemical processes that occurred during the formation of the Topopah Spring Tuff, and that have continued over time. From the standpoint of potential geochemical alteration of the rock by water, these studies show the following (BSC 2004 [DIRS 170003], Table 6.2; BSC 2004 [DIRS 166107], Section 6.3.1.5; BSC 2005 [DIRS 170137], Section A1.1.1.2):

- The Topopah Spring Tuff is largely composed of fine-grained feldspars and silicate-based rocks that formed during the cooling of the rock mass shortly after deposition. Clay-forming minerals were typically not formed during the petrogenesis of the repository host horizon.

- Clay is not common in the crystallized rocks of the repository host horizon, nor is clay a volumetrically significant fracture-coating material.

- It is not likely that, even over the postclosure period, mineral alteration will occur to form clay in any significant amount in repository rocks and fractures due to the lack of suitable environmental conditions.

Actual testing of welded Topopah Spring Tuff specimens (50.8 mm diameter) up to elevated temperatures of 200˚C indicates a slight to marginal decrease in Young's modulus (BSC 2003 [DIRS 166660], p. 8-64 and Figure 8-14) and inconclusive results for uniaxial compressive strength (BSC 2003 [DIRS 166660], p. 8-93 and Figures 8-25 and 8-26).

6.4.4.4.2.4 Development of Lithophysal Rock Mass Categories and Bounds

6.4.4.4.2.4.1 Rock Mass Categories Based on Laboratory Testing

Figure 6-87 plots the relationship between the UCS and Young's modulus values of the 290 mm (11.5 in.) diameter samples. Since a relatively linear relationship exists between the UCS and Young's modulus and both of these key parameters are dependent on the volume percentage of lithophysal porosity (BSC 2004 [DIRS 172334], Section 6.3), the best-fit line in Figure 6-87 is defined as the theoretical base-case relationship. The base-case line is subdivided into five rock mass categories based on UCS values starting at 10 MPa (weakest rock) and ending at 30 MPa (strongest rock), in increments of 5 MPa. The Young's Modules corresponding to the selected UCS values (10, 15, 20, 25, and 30 MPa) are 1.9, 6.4, 10.8, 15.3, and 19.7 GPa, respectively. For each lithophysal rock mass category there corresponds an estimated uniform distribution of Young's modulus and trapezoidal (upper to lower bound) distribution of uniaxial compressive strength.

Figure 6-88 plots the relationship of Young's modulus and lithophysal porosity based on laboratory test data that shows how the lithophysal porosity ranges were developed for the five lithophysal rock mass categories. The results obtained are summarized in Table 6-70 for the five rock mass categories proposed.

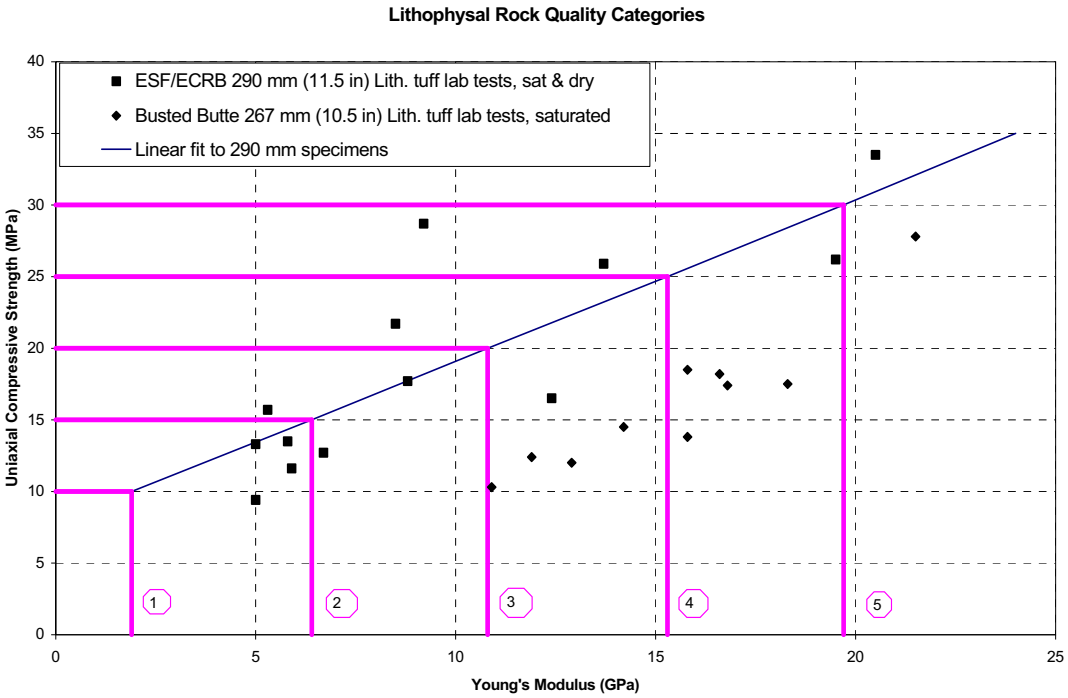

Sources: BSC 2004 [DIRS 172334], Appendix B: *LithophysalRockRanges_Calc.xls*, worksheet 'Categories'; DTNs: SN0208L0207502.001 [DIRS 161871]; SN0211L0207502.002 [DIRS 161872]; SN0305L0207502.005 [DIRS 163373]; SN0305L0207502.006 [DIRS 165747]; MO0311RCKPRPCS.003 [DIRS 166073]; MO0402DQRIRPPR.003 [DIRS 168901].

NOTES: Plot of large-diameter test results of Tptpll and Tptpul specimens from the ESF and ECRB Cross-Drift. Linear Relationship given is of Uniaxial Compressive Strength to Young's Modulus for 290 mm (11.5 in.) diameter core samples. See Table 6-70 for numerical values associated with proposed rock mass categories.

Figure 6-87. Proposed Rock Mass Categories Based on Unconfined Compressive Strength as a Function of Young's Modulus Based on Large-Core Tests of Lithophysal Rock

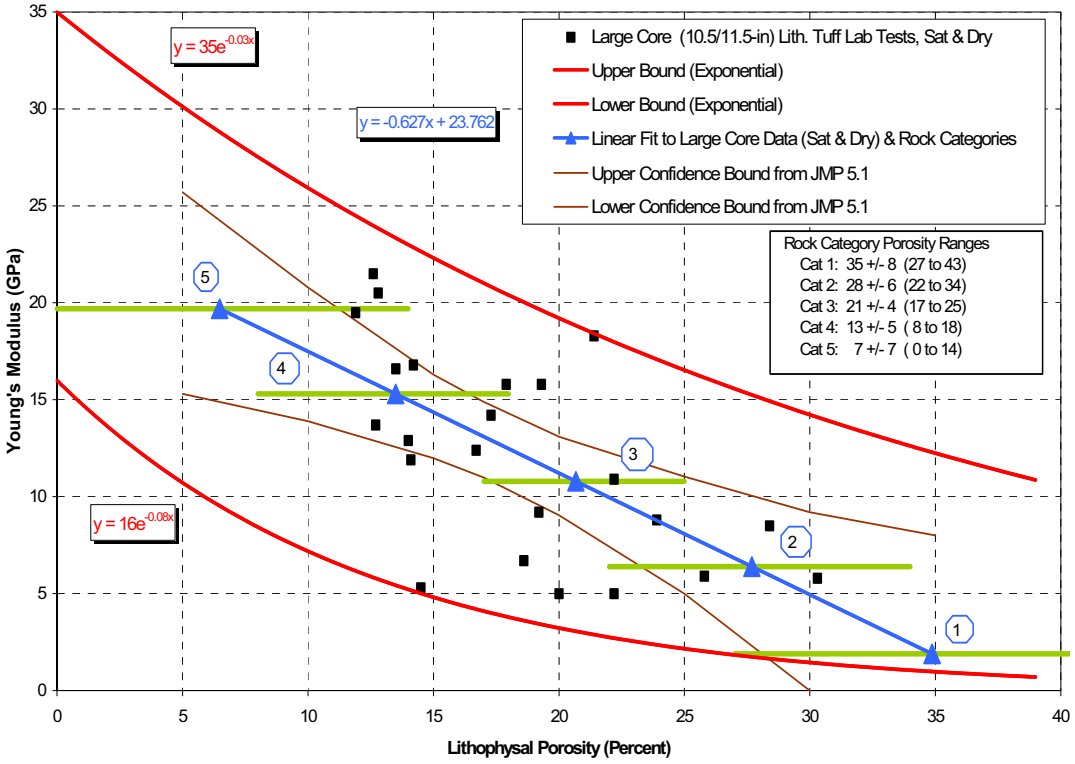

Source: BSC 2004 [DIRS 172334], Appendix B: *LithophysalRockRanges_Calc.xls*, worksheet 'LC E-por (Range)'.

NOTES First a linear fit was made to the 267 and 290 mm (10.5 and 11.5 in.) diameter large-core test data, both under dry and saturated conditions (blue line). Second, the large-core data was placed in the statistical software JMP® 5.1 and analyzed to obtain 95% confidence intervals around the linear fit line (brown lines, Appendix B, JMP® file *LargeCoreLithophysalData.JMP*). Third, uncertainty ranges of lithophysal porosity for each of the rock mass categories was subjectively determined (green lines). More details of this process are provided in Appendix B: Microsoft Excel® file *LithophysalRockRanges_Calc.xls*, worksheet 'Fits'.

Figure 6-88. Development of the Lithophysal Porosity Ranges that Correspond to Each of the Lithophysal Rock Mass Categories

Table 6-70. Estimated Mechanical Properties Developed from ESF and ECRB Cross-Drift Large-Core Testing

Rock Mass Category	Base-Case Uniaxial Compressive Strength (MPa)	Base-Case Estimated Young's Modulus[a] (GPa)	Approximate Lithophysal Porosity From Laboratory Tests[b] (%)	Lithophysal Porosity Ranges for Rock Mass Categories[c] (%)
1	10	1.9	35 +/- 8	greater than 30
2	15	6.4	28 +/- 6	25-30
3	20	10.8	21 +/- 4	15-25
4	25	15.3	13 +/- 5	10-15
5	30	19.7	7 +/- 7	less than 10

Sources: DTNs: SN0208L0207502.001 [DIRS 161871]; SN0211L0207502.002 [DIRS 161872]; SN0305L0207502.005 [DIRS 163373]; SN0305L0207502.006 [DIRS 165747]; MO0311RCKPRPCS.003 [DIRS 166073].

NOTES: See BSC 2004 [DIRS 172334], Appendix B: *LithophysalRockRanges_Calc.xls*, for further explanation and supporting calculations.

[a] Young's Modulus estimated from linear fit to 290 mm (11.5 in.) diameter core data in Figure 6-87.

[b] Estimated from correlation of Young's modulus to lithophysal porosity in Figure 6-88.

[c] For convenience the lithophysal porosity ranges (column five) will be used based on an approximate correlation with the laboratory lithophysal porosity determinations (column four).

6.4.4.4.2.4.2 Field Distribution of Lithophysal Porosity for Rock Mass Categories

The histogram given in Figure 6-89 shows the abundance (frequency) of lithophysal porosity in the ECRB Cross-Drift from stations 14+44 to 23+26 (essentially from the top to the bottom of the Tptpll). This plot subdivides the abundance of lithophysal porosity into the 5% intervals that roughly correspond to lithophysal porosity ranges for the rock mass categories given in Table 6-70. The lowest quality categories (1 and 2) represent the rock mass with 20% or greater lithophysal porosity, and make up approximately 20% of the repository host rock. Category 1, which represents the lowest quality and highest porosity rock, makes up less than 10% of the rock mass and represents localized conditions of high porosity rock found primarily near the top of the Tptpll, observed along ECRB Cross-Drift stations 15+50 to 16+00. Rock mass categories 3, 4, and 5 consist of higher geomechanical quality rock and are representative of approximately 80% of the lithophysal rock mass.

6.4.4.4.2.5 Numerical Simulation of Lithophysal Rock

Numerical simulation was performed to supplement the existing intact rock property database and to confirm the mechanical property estimates of lithophysal rock. The PFC and UDEC codes were used to examine the basic mechanisms of how lithophysae affect the failure characteristics and moduli of the Tptpul and Tptpll rock. The details of the numerical simulation are presented in *Lithophysal Rock Mass Mechanical Properties of the Repository Host Horizon* (BSC 2004 [DIRS 172334], Section 6.5). This section provides the summary of the numerical simulation analysis.

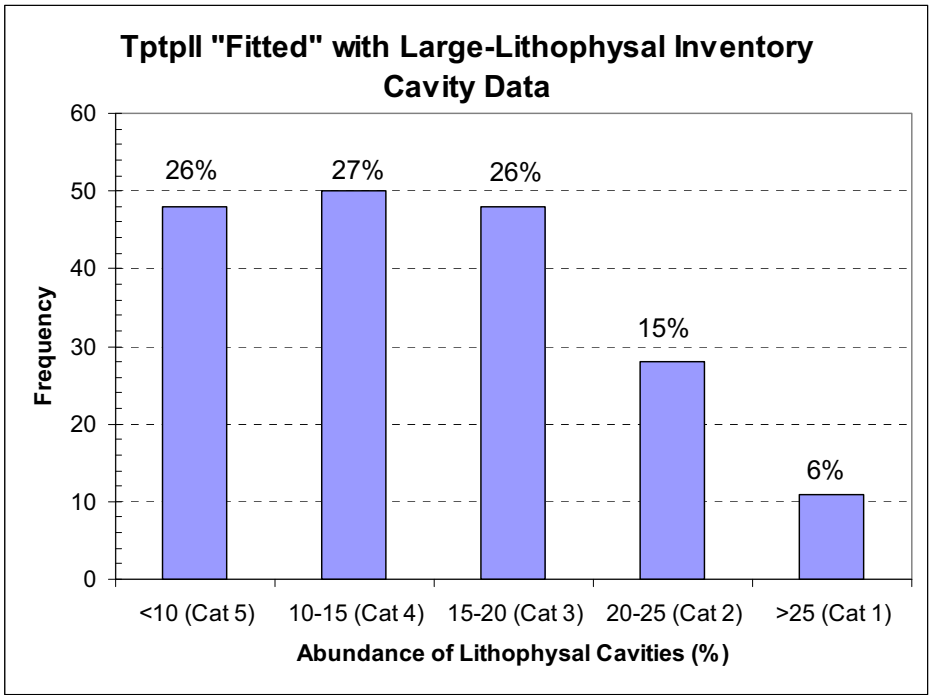

Source: BSC 2004 [DIRS 172334], Appendix B: *Drift Deg AMR AF T-A-P Fit_V1_DBR.xls*, worksheet 'Length – Fit and Stats, cell AF268'.

NOTE: The percent value given above each histogram bar represents the percent of measured Tptpll rock corresponding to each rock mass quality category (Cat). Lithophysal porosity data are from ECRB Cross-Drift stations 14+44 to 23+26, which includes the entire thickness of the Tptpll lithostratigraphic rock unit.

Figure 6-89. Distribution of Lithophysal Porosity and Estimated Rock Mass Categories for the Tptpll Zone in the Enhanced Characterization of the Repository Block Cross-Drift

6.4.4.4.2.5.1 Computational Simulations Adopted

The physics-based discontinuum numerical simulation programs, PFC2D (V.2.0, STN: 10828-2.0-01 [DIRS 169930]), PFC3D (V.2.0, STN: 10830-2.0-01 [DIRS 169931]), and UDEC, are used as numerical "laboratories" to simulate and test the basic deformation and failure response mechanisms of lithophysal tuff. These programs were chosen due to their ability to simulate the physics of deformation and fracture of a bonded granular matrix that contains void space of varying shape, size and porosity. Details of both PFC and UDEC simulation calibrations are addressed in *Lithophysal Rock Mass Mechanical Properties of the Repository Host Horizon* (BSC 2004 [DIRS 172334], Section 6.5.3). Figures 6-90 to 6-95 show the PFC and UDEC simulation results as they compare to measured rock physical and mechanical properties of the lithophysal tuff.

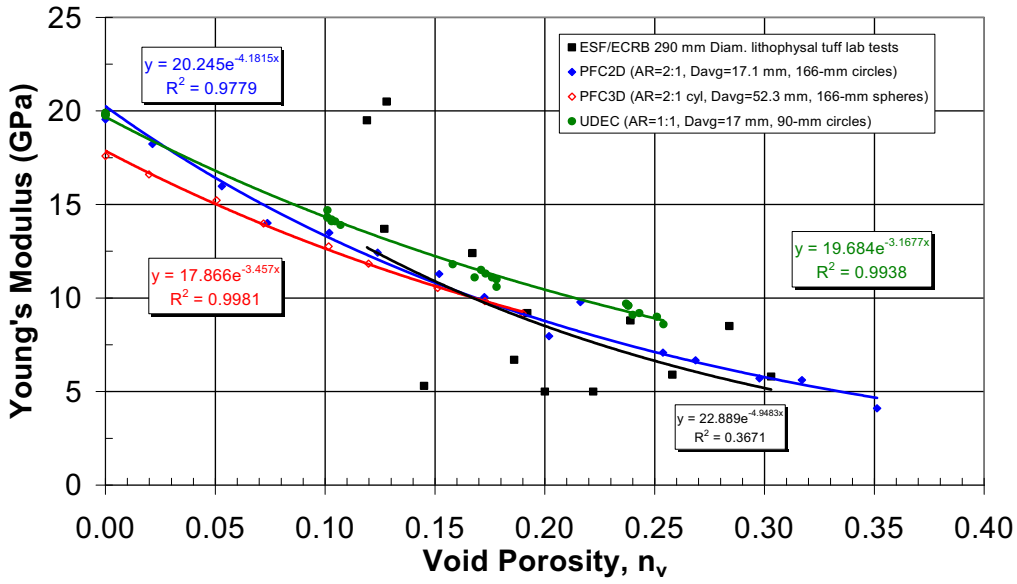

Source: BSC 2004 [DIRS 172334], Appendix B: *PFC&UDEC_Plots.xls*, worksheet 'mpl-E(bf4)'.

Figure 6-90. Young's Modulus (E) vs. Void Porosity (n_v) for Lithophysal Tuff and Simulations of Randomly Distributed Circular and Spherical Voids

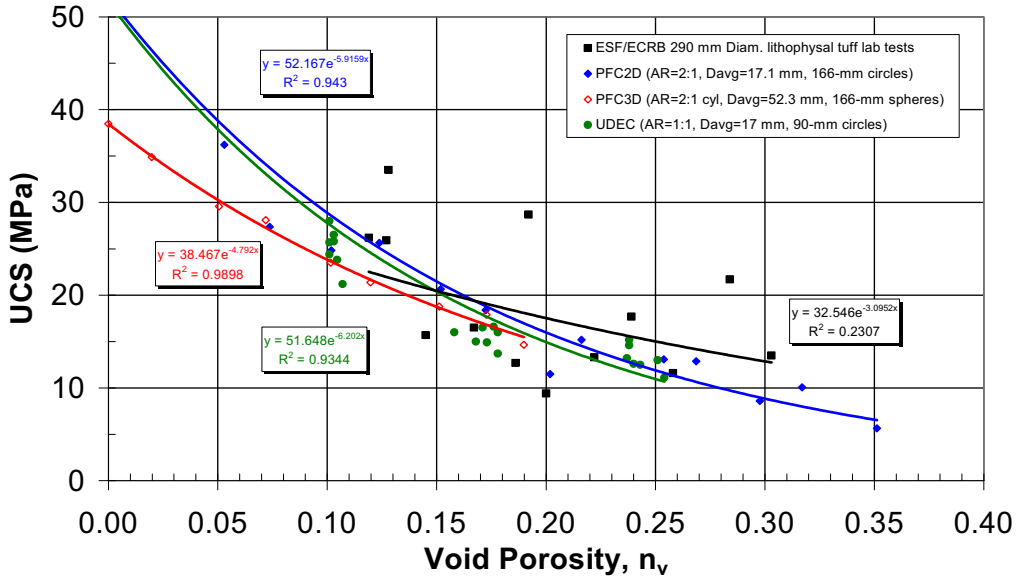

Source: BSC 2004 [DIRS 172334], Appendix B: *PFC&UDEC_Plots.xls*, worksheet 'mpl-qu(bf4)'.

Figure 6-91. Uniaxial Compressive Strength vs. Void Porosity for Lithophysal Tuff and Simulations of Randomly Distributed Circular and Spherical Voids

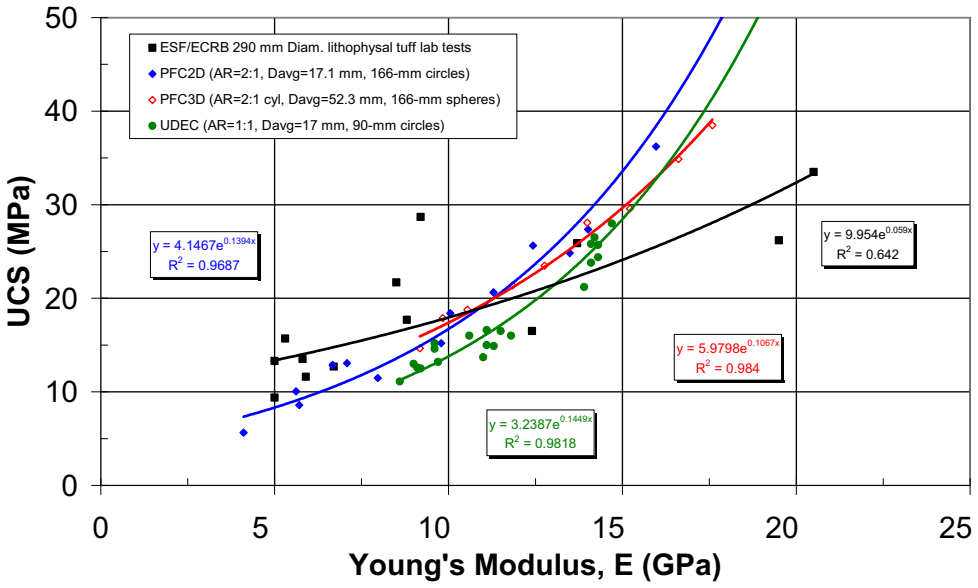

Source: BSC 2004 [DIRS 172334], Appendix B: *PFC&UDEC_Plots.xls*, worksheet 'mpl-que(bf4)'.

Figure 6-92. Young's Modulus (E) vs. UCS for Lithophysal Tuff and Simulations of Randomly Distributed Circular and Spherical Voids

6.4.4.4.2.5.2 Confined Biaxial Behavior of Synthetic Lithophysal Material

A series of uniaxial (extension and compression) and biaxial compression, as well as extensional experiments was conducted on the simulated samples, with circular lithophysal voids added randomly to create porosities of 10.3%, 17.8%, and 23.8%. Figures 6-93 to 6-96 show samples of the stress strain curves predicted by the simulations for each of the nominal lithophysal porosity groups.

The numerical results of the calculated properties from the uniaxial and biaxial tests on simulated lithophysal specimens are presented in Table 6-71 with a summary presented in Table 6-72.

The following general observations can be made from the numerical tests:

- Reduction of peak compressive strength with increased lithophysal porosity
- Reduction of Young's modulus with increased lithophysal porosity
- Less brittle postpeak response, leading to elastic-plastic response for the higher confining pressures, and
- Reduction in tensile strength with increased lithophysal porosity.

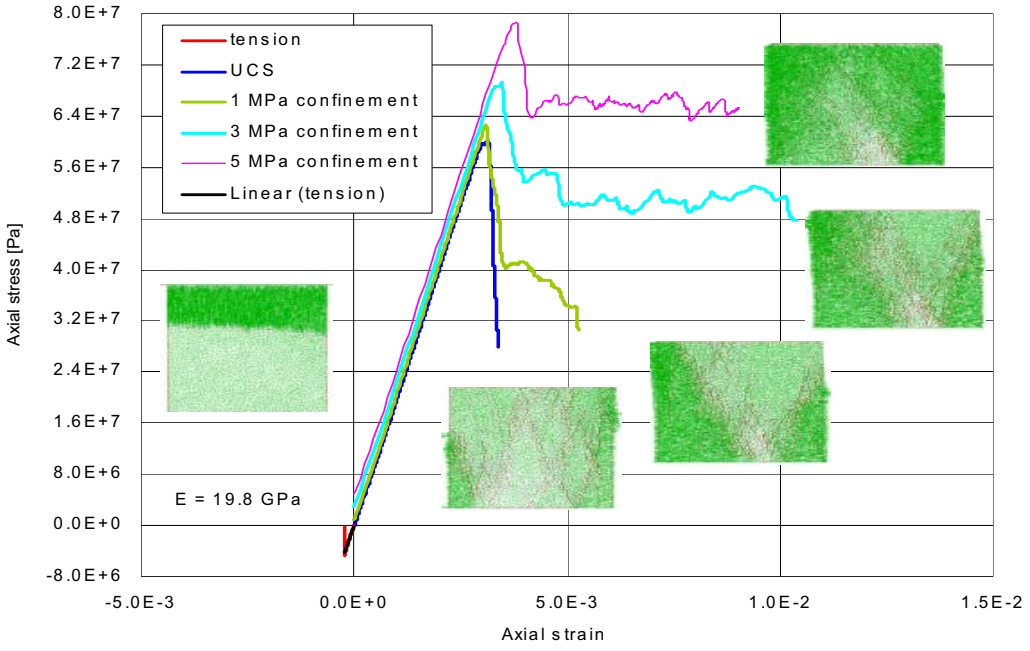

Source: BSC 2003 [DIRS 166660], Section 9.2.3, p. 9-33, Figure 9-30.

Figure 6-93. Stress-Strain Response and Failure Mechanisms for Lithophysal Porosity of 0.0%

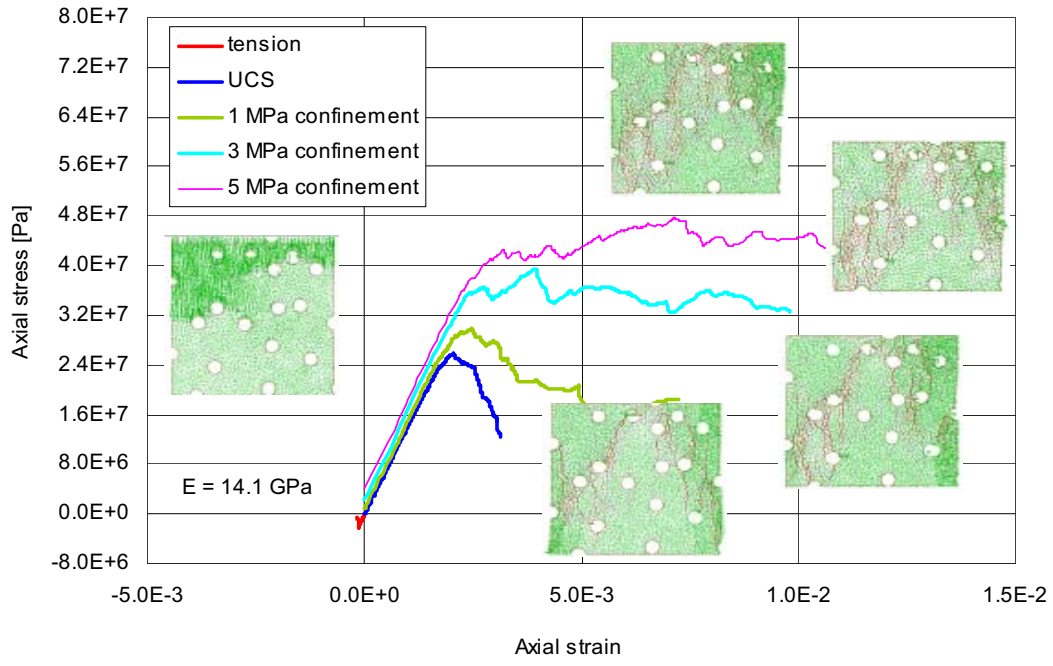

Source: BSC 2003 [DIRS 166660], Section 9.2.3, p. 9-37, Figure 9-33.

Figure 6-94. Stress-Strain Response and Failure Mechanisms for Lithophysal Porosity of 10.3%

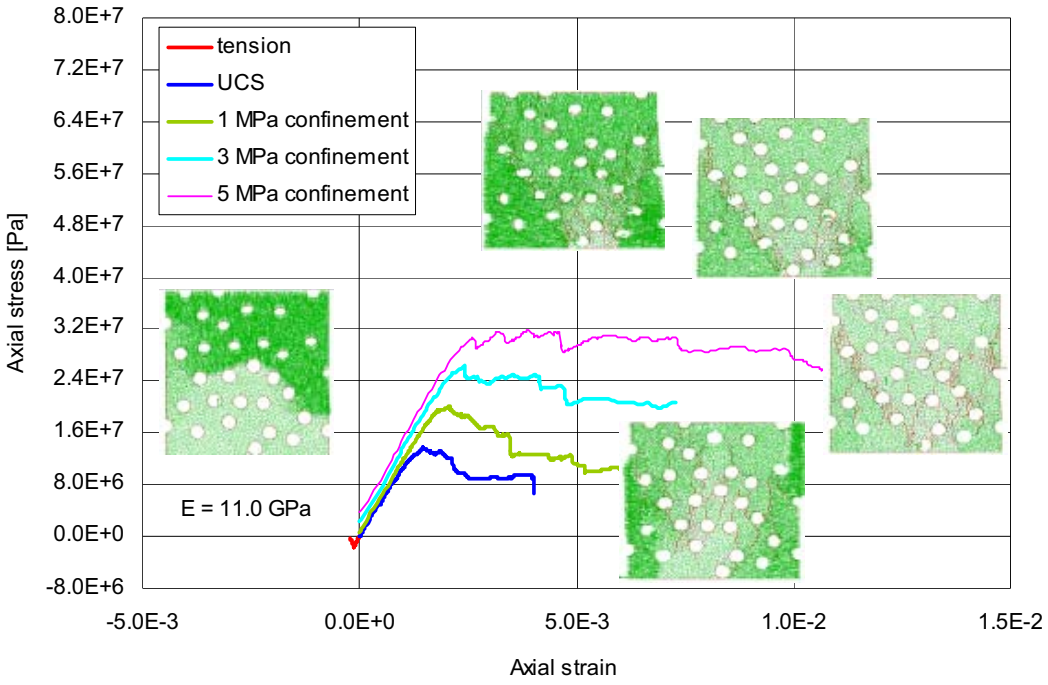

Source: BSC 2003 [DIRS 166660], Section 9.2.3, p. 9-37, Figure 9-34.

Figure 6-95. Stress-Strain Response and Failure Mechanisms for Lithophysal Porosity of 17.8%

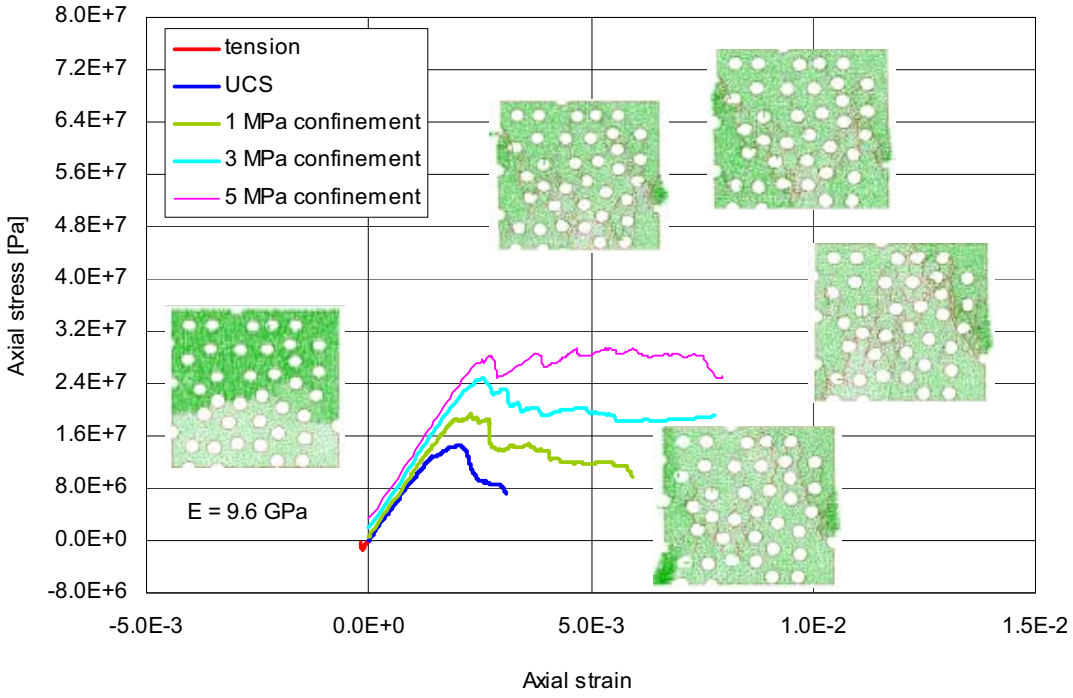

Source: BSC 2003 [DIRS 166660], Section 9.2.3, p. 9-38, Figure 9-35.

Figure 6-96. Stress-Strain Response and Failure Mechanisms for Lithophysal Porosity of 23.8%

Table 6-71. Physical Property Results from UDEC Numerical Simulation on Simulated Lithophysal Tuff

Lithophysal Porosity	Elasticity		Tensile Strength (MPa)	Compressive Strengths				Dilation			Mohr-Coulomb Strength Parameters		Hoek Brown Strength Parameters	
				Confining Pressure (MPa)				Confining Pressure (MPa)						
	E (GPa)	ν		0	1	3	5	1	3	5	φ	c (MPa)	σ_{ci} (MPa)	m_i
0.000	19.8	0.16	4.66	60.1	62.7	69.3	78.7	48°	39°	35°	35°	15.6	59.1	6.2
0.000	19.9	0.16	4.86	59.7	63.4	71.9	78.1	55°	40°	34°	35°	15.4	59.7	6.1
0.000	19.8	0.17	3.91	58.7	62.5	70.5	78.4	49°	42°	36°	37°	14.8	58.4	6.7
0.000	19.8	0.16	4.52	59.9	64.2	72.2	79.0	52°	44°	37°	36°	15.3	60.1	6.3
0.000	19.8	0.16	4.26	55.1	60.1	69.2	76.5	45°	38°	32°	38°	13.3	55.4	7.5
0.103	14.1	0.19	2.11	25.8	30.0	39.5	47.8	42°	32°	27°	39°	6.1	25.2	9.4
0.101	14.3	0.19	1.96	24.4	29.1	33.3	39.8	35°	30°	14°	29°	7.1	24.9	4.6
0.101	14.7	0.18	2.17	28.0	33.0	40.0	48.0	37°	29°	22°	36°	7.1	28.1	7.4
0.101	14.3	0.22	2.16	25.7	32.5	41.4	47.0	38°	30°	29°	38°	6.3	27.0	8.1
0.105	14.1	0.17	2.09	23.8	28.7	34.7	42.3	40°	32°	28°	34°	6.3	23.9	6.7
0.107	13.9	0.18	1.95	21.2	27.0	35.5	40.0	39°	32°	29°	39°	5.0	21.2	9.9
0.103	14.2	0.19	2.09	26.5	29.9	37.0	46.0	37°	38°	25°	36°	6.7	25.6	7.6
0.178	11.0	0.20	1.70	13.7	20.1	26.4	32.0	40°	30°	25°	34°	3.7	15.0	6.9
0.176	11.1	0.19	1.84	16.6	22.6	29.8	35.0	39°	28°	26°	35°	4.4	17.7	7.0
0.171	11.5	0.19	1.74	16.5	22.2	28.9	32.1	35°	29°	25°	31°	4.7	18.1	5.1
0.158	11.8	0.18	1.89	16.0	23.0	31.3	38.7	39°	27°	22°	39°	3.8	16.8	10.3
0.168	11.1	0.19	1.72	15.0	21.4	26.7	31.2	36°	25°	21°	31°	4.3	16.6	5.2
0.173	11.3	0.18	1.62	14.9	20.5	28.5	35.7	34°	27°	21°	37°	3.7	15.1	9.5
0.178	10.6	0.23	1.65	16.0	21.1	28.1	34.6	35°	26°	27°	35°	4.2	16.3	7.4
0.238	9.6	0.21	1.52	14.6	19.4	25.0	29.4	35°	29°	23°	29°	4.3	15.5	4.8
0.254	8.6	0.19	1.46	11.1	15.9	20.9	24.6	35°	19°	13°	27°	3.4	12.2	4.2
0.237	9.7	0.17	1.62	13.2	17.8	24.1	29.0	32°	19°	15°	31°	3.7	13.8	5.8
0.251	9.0	0.18	1.52	13.0	17.0	24.7	29.3	37°	24°	18°	32°	3.6	13.3	6.5
0.240	9.1	0.20	1.55	12.6	17.1	21.7	27.7	30°	27°	18°	29°	3.7	13.0	5.2
0.243	9.2	0.19	1.53	12.5	18.5	23.0	28.0	37°	27°	21°	29°	3.7	13.9	4.9
0.238	9.6	0.19	1.55	15.2	20.0	25.5	28.7	34°	21°	15°	27°	4.7	16.4	3.9

Source: BSC 2004 [DIRS172334], Appendix B: summary2_newest.xls, Worksheet “UDEC”.

Table 6-72. Summary of Average Compressive Strength, Young's Modulus, Mohr-Coulomb, and Hoek-Brown Failure Law Parameters Derived from UDEC Simulations

Lithophysal Porosity (%)	UCS (MPa)	Young's Modulus (GPa)	Friction Angle (degree)	Cohesion (MPa)	Tensile Strength (MPa)	Hoek Brown σ_{ci} (MPa)	Hoek Brown m_i
0	58.7	19.8	36	14.9	4.4	58.5	6.6
10	25.1	14.2	36	6.4	2.1	25.1	7.7
17	15.5	11.2	35	4.1	1.7	16.5	7.3
24	13.2	9.3	29	3.9	1.5	14.0	5.0

Source: BSC 2003 [DIRS 166660], Section 9.2.4, p. 9-42, Table 9-3.

The relationships of uniaxial compressive strength and Young's modulus to lithophysal porosity based on numerical simulation are shown in Figures 6-97 and 6-98, respectively, indicating good agreement with laboratory compressive strength tests on large diameter (0.27 to 0.29 m/10.5 to 11.5 in.) cores samples of lithophysal tuff. The correlation of uniaxial compressive strength and Young's modulus from the numerical simulation and laboratory measurements is shown in Figure 6-99. The UDEC results, as shown, are in good agreement with the PFC simulations but give higher uniaxial compressive strength values than the laboratory test data, especially when the void porosity is low (Young's modulus greater than 15 GPa). This is because the UDEC simulation was calibrated for the 0% porosity case with a uniaxial compressive strength of 60 MPa and a Young's modulus of 20 GPa. A recalibration of the UDEC simulation may allow a better fit to the laboratory UCS versus Young's modulus data, but the resulting fits to plots of laboratory UCS and Young's modulus with lithophysal porosity may worsen.

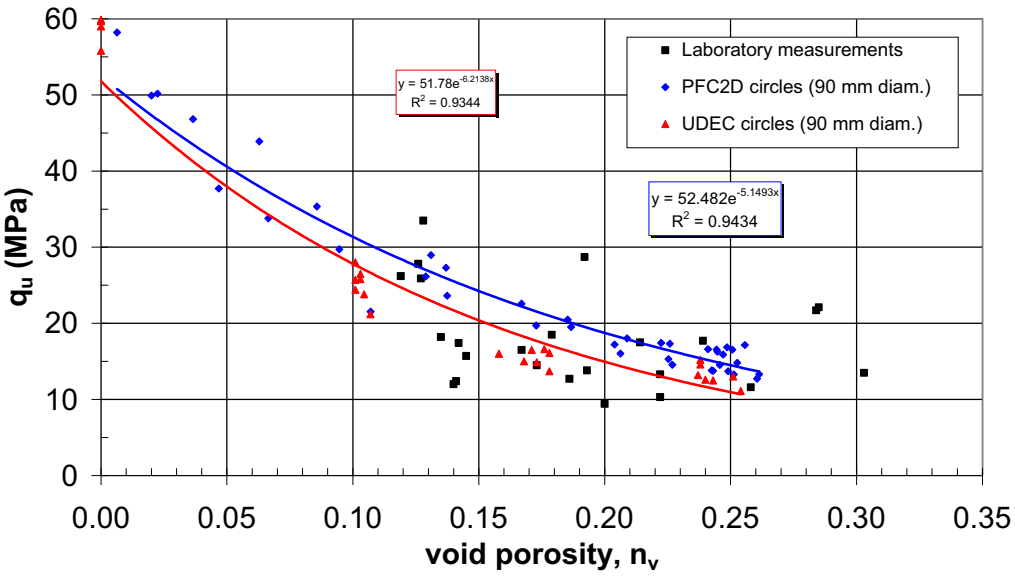

Source: BSC 2003 [DIRS 166660], Section 9.2.3, p. 9-39, Figure 9-36.

Figure 6-97. Comparison of UDEC Simulations of Lithophysal Porosity Effects on Uniaxial Compressive Strength (q_u) to Laboratory Measurements on Large Samples and to PFC Simulations

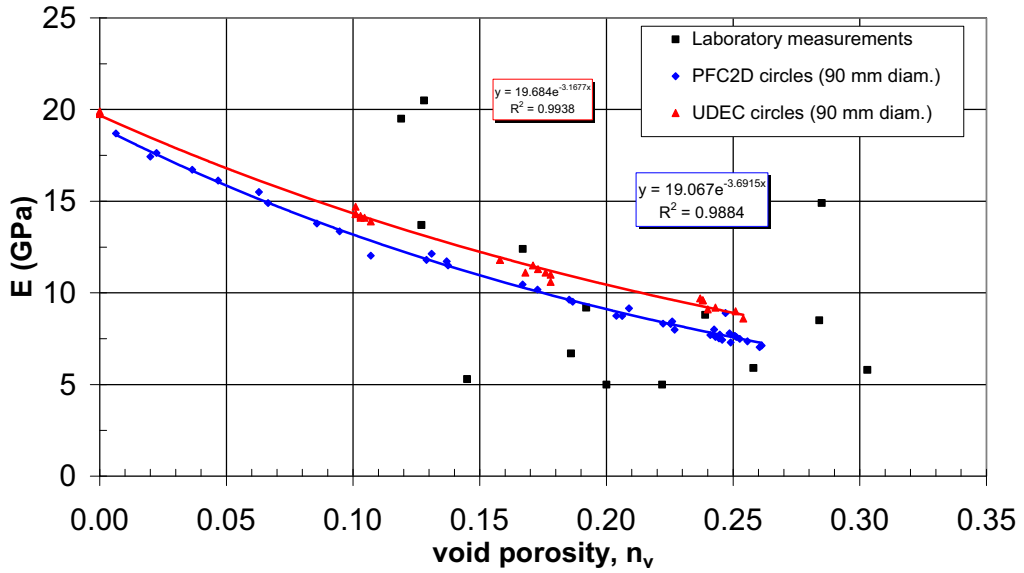

Source: BSC 2003 [DIRS 166660], Section 9.2.3, p. 9-39, Figure 9-37.

Figure 6-98. Comparison of UDEC Simulations of Lithophysal Porosity Effects on Young's Modulus (E) to Laboratory Measurements on Large Samples and to PFC Simulations

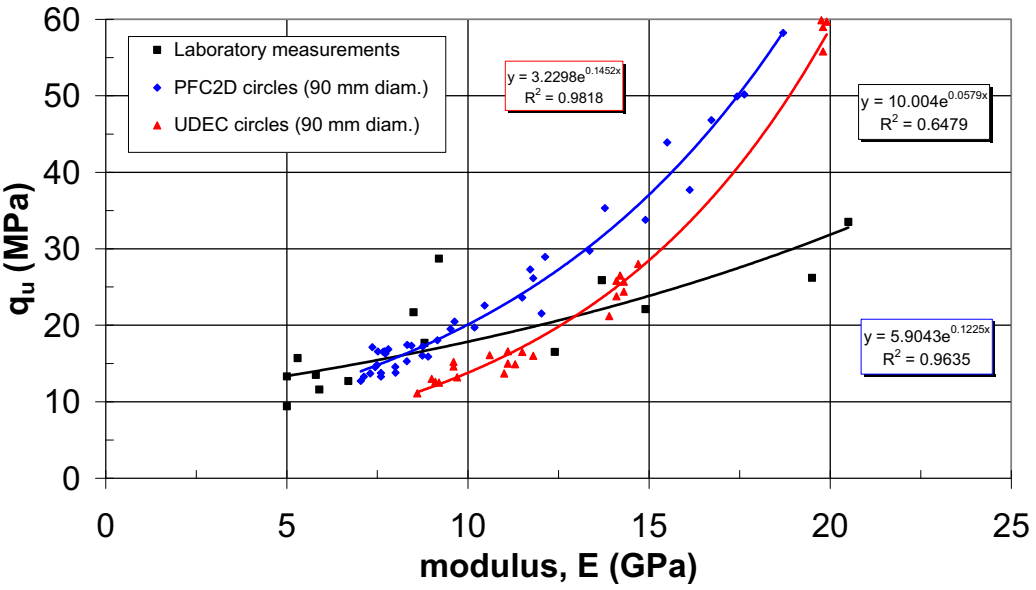

Source: BSC 2003 [DIRS 166660], Section 9.2.3, p. 9-40, Figure 9-38.

Figure 6-99. Comparison of UDEC Simulations of Uniaxial Compressive Strength (qu) vs. Young's Modulus (E) to Laboratory Measurements on Large Samples and to PFC Simulations

6.4.4.4.2.5.3 Estimation of Linear and Nonlinear Failure Envelopes

Figure 6-100 shows the failure stress values plotted in principal stress space with the respective Hoek-Brown envelopes fitted to the results (Hoek 2000 [DIRS 160705], p. 179). In each case,

multiple simulations were made for each confining stress level in which different random distributions of *UDEC* block structures and void placements were used. The Mohr-Coulomb and Hoek-Brown strength parameters derived from the envelope fits to this data are given in Table 6-73.

As seen in Figure 6-100 the primary effect of increasing lithophysal porosity is a significant reduction in the compressive and tensile strength components, with minor strength reduction when the lithophysal porosity is raised above 17.8%. The value of cohesion behaves in a similar way. There is little apparent impact of lithophysal porosity on peak friction angle until porosity exceeds 20%.

The values of UDEC simulated friction angle and cohesion presented in Table 6-73 are compared to the results from laboratory triaxial tests on small (51 mm and less) diameter rock specimens presented in Table 6-13. The laboratory values are indicative of a stronger strength envelope than the simulated rock strength envelope using the 0% lithophysal porosity case (values of 36 degrees and 14.9 MPa), which is expected since small laboratory specimens are biased toward nonlithophysal rock samples (BSC 2004 [DIRS 172334], Section 6.3.1).

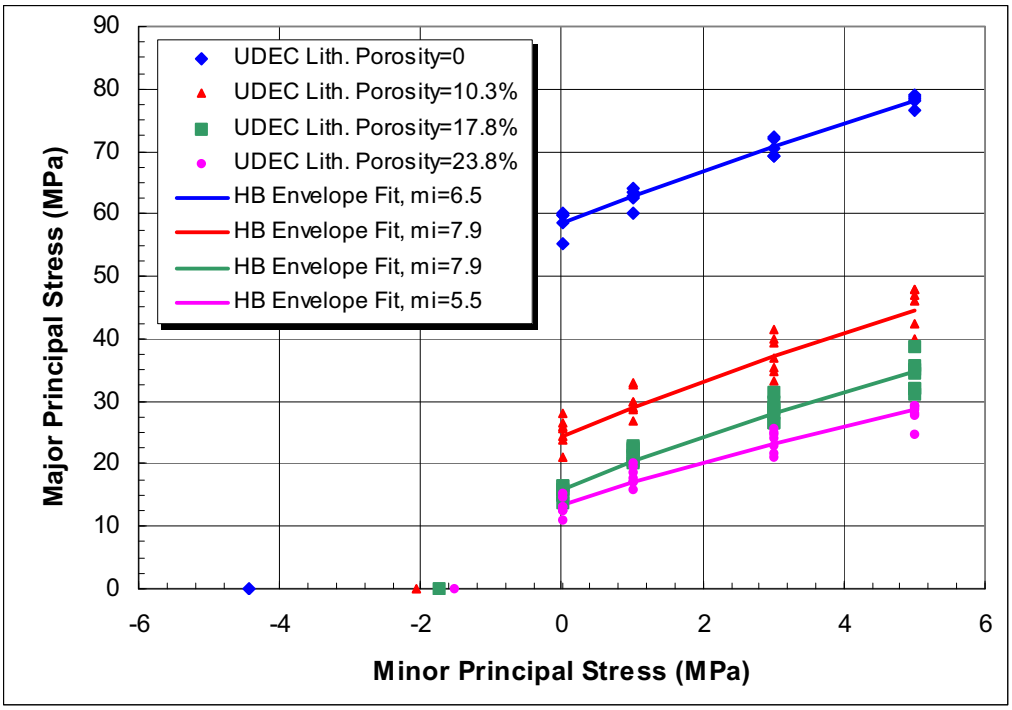

Source: BSC 2003 [DIRS 166660], Section 9.2.4, p. 9-41, Figure 9-40.

Figure 6-100. Major Principal Stress Versus Minor Principal Stress from UDEC Simulations as well as Hoek-Brown Non-Linear Failure Envelope Fits for Various Lithophysal Porosities

Table 6-73. Average UCS, Young's Modulus, Mohr-Coulomb (Linear) Parameters, and Hoek-Brown (Nonlinear) Parameters from UDEC Biaxial Test Simulations of Lithophysal Tuff

Lithophysal Porosity (%)	Estimated UCS (MPa)	Estimated Young's Modulus (GPa)	Estimated Friction Angle (deg)	Estimated Cohesion (MPa)	Estimated Hoek-Brown UCS (MPa)	Estimated Hoek-Brown mi
0	58.7	19.8	36	14.9	58.5	6.6
10	25.1	14.2	36	6.4	25.1	7.7
17	15.5	11.2	35	4.1	16.5	7.3
24	13.2	9.3	29	3.9	14.0	5.0

Source: BSC 2003 [DIRS 166660], p. 9-42, Table 9-3.

6.4.4.4.2.5.4 Limitations and Uncertainty Analysis of the Numerical Simulation

The following limitations are inherent in the PFC simulation study and are summarized and described as follows:

- Both the panel maps and the PFC2D analyses are two-dimensional slices, whereas the true lithophysal geometries are three-dimensional.
- The void geometries from the panel maps (on the scale of a meter) may not be representative of the laboratory specimens (on the scale of a foot).
- The PFC material does not contain fractures already present in the matrix material of some of the lithophysal tuff.
- The effects of rims, spots and lithic clasts on the material properties are not accounted for directly by the PFC simulation, because it only provides a base material to which voids can be added.

The following uncertainties and limitations are inherent in the UDEC simulation study.

- The effect of lithophysal cavity shape and size on lithophysal rock properties has not been addressed in this study. In this study, the shape of cavity is circular and the size is fixed at 0.09 m. In reality, both the shape and the size vary with location.
- The UDEC analyses are two-dimensional, whereas the true lithophysal cavities are three-dimensional.
- The effect of specimen size on lithophysal rock properties has not been addressed in this study.
- Preexisting fractures in the matrix material of lithophysal rock are not accounted for directly by the UDEC simulation.

- Comparisons of the UDEC simulations are made to actual large-core laboratory tests under uniaxial compressive loading conditions only.

- The UDEC study uses the average large-core laboratory values of Young's modulus and uniaxial compressive strength to calibrate the UDEC base-case simulations and does not account for the effect of variations across lithophysal rock mass categories or rock condition.

6.4.4.4.2.5.5 Summary and Conclusions Relative to Lithophysal Rock Behavior

The simulation results showed good agreement with laboratory data (Figures 6-90 to 6-92). Results indicated that the primary strength-decreasing effect of the lithophysae is due to initiation and propagation of tensile splitting between lithophysae under compressive load. As porosity increases, the spacing between lithophysae decreases, and rock acquires a greater propensity for tensile splitting at the lower applied stresses.

Variability in the rock response and size effect appear to be a function primarily of the distribution of the lithophysae (i.e., percentage porosity and how evenly distributed it is through the rock mass), and, to a lesser extent, the deviation of the shape of true voids from circular voids. The property scatter apparent at given values of lithophysal porosity reduces significantly when the data are plotted in terms of uniaxial compressive strength versus Young's modulus, suggesting that this correlation is independent of void geometry. Approximately 80 simulated uniaxial compression tests of actual lithophysae distributions were simulated, and the results in terms of UCS and Young's Modulus as functions of the lithophysal porosity and UCS versus Young's Modulus were discussed in *Lithophysal Rock Mass Mechanical Properties of the Repository Host Horizon* (BSC 2004 [DIRS 172334], Section 6.5.5).

Standard forms of yield conditions for rock masses – Mohr-Coulomb and Hoek-Brown – were fit to the laboratory and simulation extrapolation data, and their standard strength parameters were determined. The best-fit Hoek-Brown envelopes for the UDEC lithophysal rock simulations yield strength envelopes that are weaker than those derived from laboratory tests on Topopah Spring small-diameter lithophysal rock specimens. Again, this is likely an artifact of the bias against rims, spots, and fractures in actual small-diameter specimens.

The conclusions drawn from the PFC and UDEC simulations are that this approach provides a viable methodology for simulating the mechanical response of lithophysal welded tuff to stressing, and that this tool can be used to study variability in material response in addition to laboratory and field testing. These numerical results are added to the bounding analyses in the next section.

6.4.4.4.2.6 Numerical Mechanical Property Bounding Analysis

The numerical results are compared to the 267 and 290 mm (10.5 and 11.5 in.) diameter laboratory data in this section to see how well the numerically derived test results fit the rock mass categories derived from large-core laboratory test data and bounding estimates.

Figures 6-101 to 6-103 present the PFC and UDEC simulated uniaxial compression test results superimposed on the laboratory UCS versus Young's Modulus and bounding estimates. As can be seen, the upper and lower bounds encompass the laboratory and numerical data with the exception of the highest values of numerically predicted uniaxial compressive strength and Young's modulus as shown in Figure 6-103.

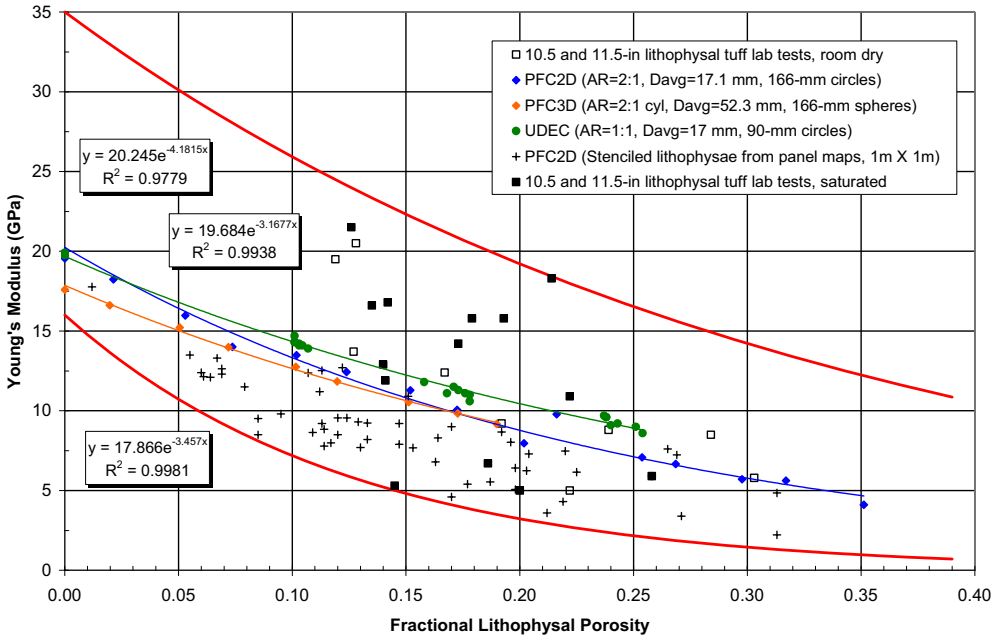

Source: BSC 2004 [DIRS 172334], Appendix B: LithophysalRockRanges_Calc.xls, Worksheet E-por.

Figure 6-101. Upper and Lower Bounds of the Young's Modulus versus Lithophysal Porosity Relationship for 10.5 and 11.5-in Diameter Cores and Simulated Numerical Test Results

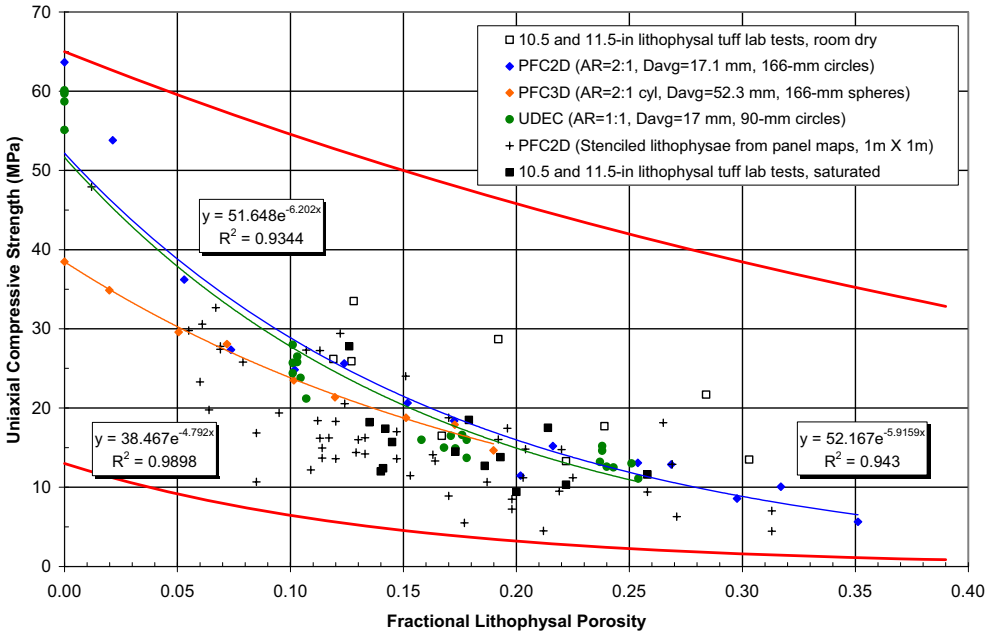

Source: BSC 2004 [DIRS 172334], Appendix B: LithophysalRockRanges_Calc.xls, Worksheet q-por.

Figure 6-102. Upper and Lower Bounds of the Uniaxial Compressive Strength versus Lithophysal Porosity Relationship for 10.5 and 11.5-in Diameter Cores and Simulated Numerical Test Results

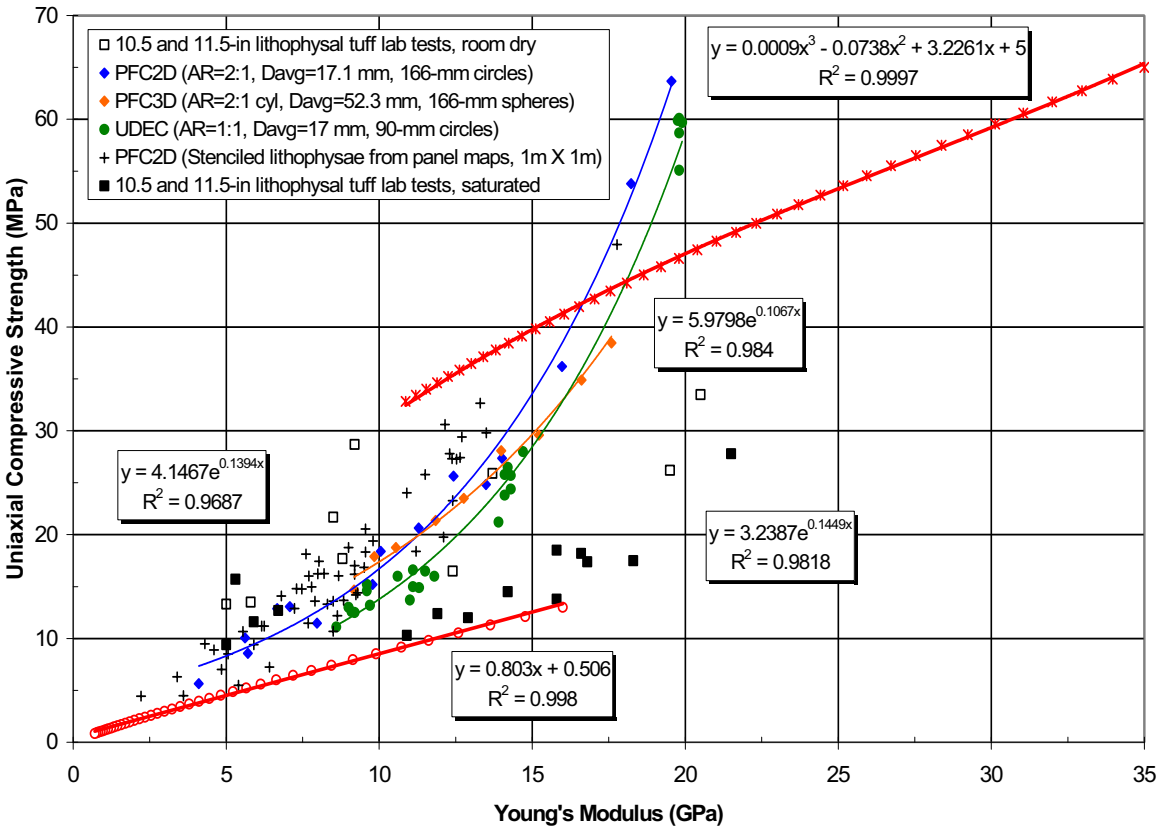

Source: BSC 2004 [DIRS 172334], Appendix B: LithophysalRockRanges_Calc.xls, Worksheet q-E".

NOTE: The plotted points making up the upper and lower bounds are from the estimated exponential equations. The solid lines are polynomial best-fit lines constructed for ease of extrapolation using the standard "Add Trendline" function of Microsoft Excel. The extrapolated polynomial upper and lower bounds are plotted subsequently in Figures 6-112 and 6-113.

Figure 6-103. Upper and Lower Bounds of the Uniaxial Compressive Strength versus Young's Modulus Relationship for 10.5 and 11.5-in Diameter Cores and Simulated Numerical Test Results

Figure 6-104 illustrates a simplified version of Figure 6-103, where the polynomial upper and lower bounds have been plotted for the full range of depicted properties. Since no laboratory large core data is available below a Young's Modulus of 5 GPa, the lines representing the bounding values are dashed. Some of the PFC simulations of the ECRB Cross-Drift panel-map specimens plot within the dashed low modulus and low strength range in Figure 6-104, which also shows that the low Young's modulus and uniaxial compressive strength results of available small-diameter core tests of Topopah Spring Tuff (BSC 2004 [DIRS 172334], Figure 6.3-4) largely plot within the dashed bounds range. It is seen that the uniaxial compressive strength of saturated specimens generally forms the lower bound of the laboratory data range, with a minimum strength value of approximately 10 MPa.

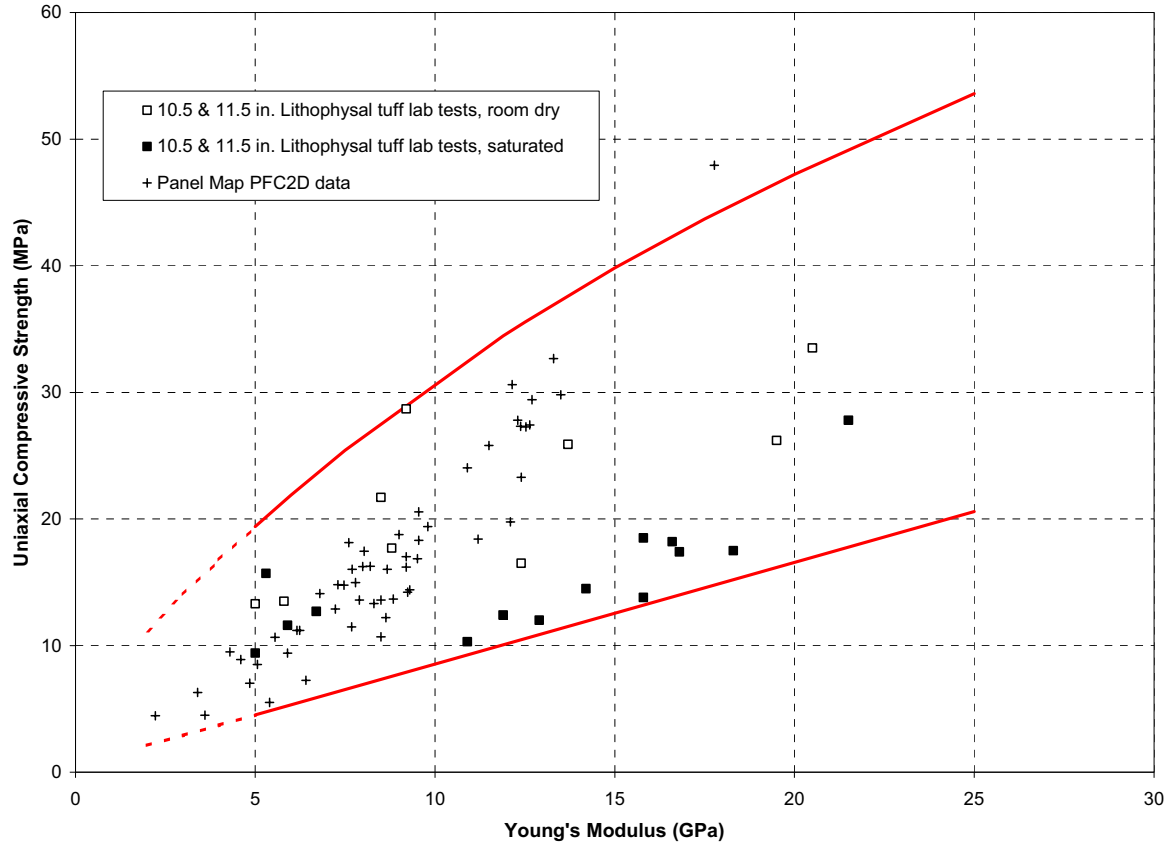

Source: BSC 2004 [DIRS 172334], Appendix B: *LithophysalRockRanges_Calc.xls*, worksheet 'Bounds'.

NOTES: The upper and lower bounds that are shown as das hed lines represent bounds that are outside the range of measured values. Some of the PFC simulations of the ECRB Cross-Drift panel map specimens plot within this range.

Figure 6-104. Upper and Lower Bounds of the Uniaxial Compressive Strength versus Young's Modulus Relationship with Large-Core Laboratory and PFC Panel Map Lithophysae Shape Study Results

In Figure 6-105, the base-case rock mass property categories are superimposed to Figure 6-104, illustrating the estimated upper and lower bounding values of UCS associated with each value of the base-case Young's modulus (Table 6-74). The linear line of base-case Young's modulus and uniaxial compressive strength pair are also added to the diagram and compared with the nonlinear line (blue) forming the means between the upper and lower bounds. Figure 6-105 shows that the base-case line and the means lines are close to one another, however, the trend of the bounds is to converge toward the origin. This convergence of the nonlinear bounds at the origin is more realistic than the base-case rock mechanical property prediction, which yields a positive uniaxial compressive strength of about 8 MPa for a Young's modulus of zero.

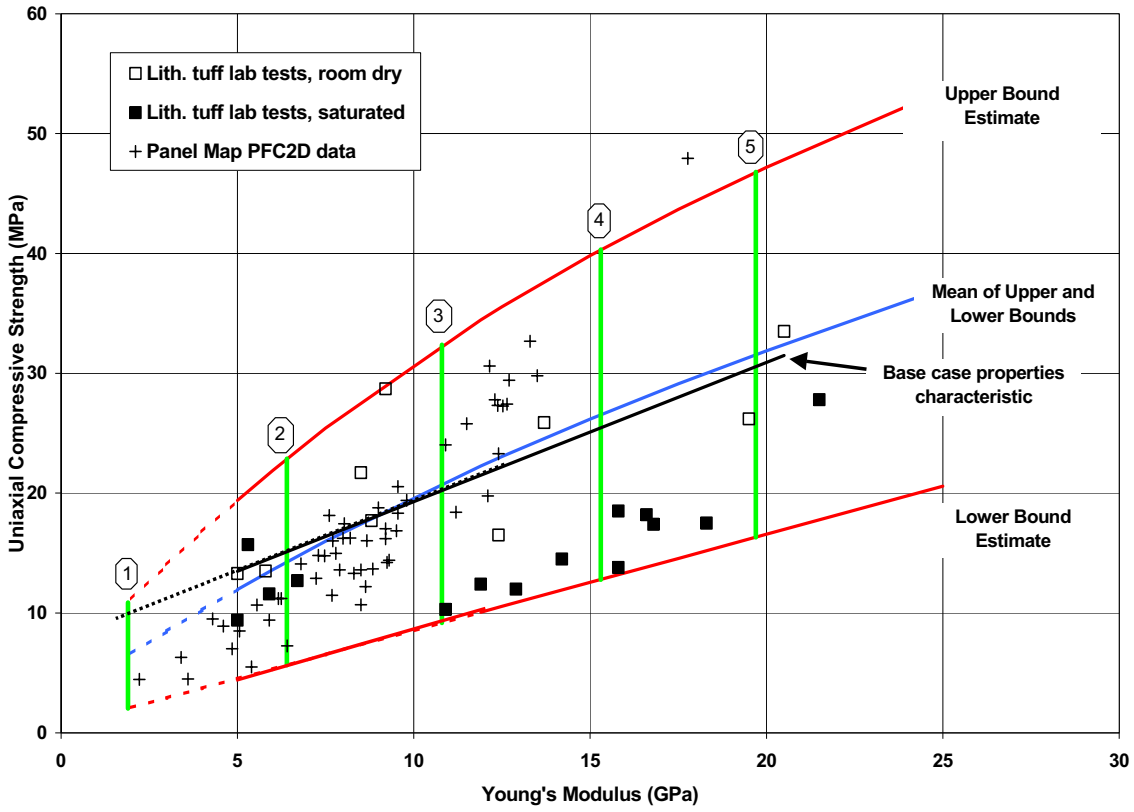

Source: Modified from *Lithophysal Rock Mass Mechanical Properties of the Repository Host Horizon* (BSC 2004 [DIRS 172334], Appendix B: *LithophysalRockRanges_Calc.xls*, worksheet 'Bounds (cat)').

Figure 6-105. Uniaxial Compressive Strength vs. Young's Modulus Showing Approximate UCS Upper and Lower Bounds

Table 6-74. Base Case, Upper and Lower Bound Strength Values for the Five Lithophysal Rock Mass Categories

Rock Mass Category	Uniaxial Compressive Strength (MPa)			Estimated Young's Modulus (GPa)	Lithophysal Porosity Ranges for Rock Mass Categories (%)
	Base Case	Lower Bound	Upper Bound		
1	10	2.0	10.9	1.9	greater than 30
2	15	5.6	22.9	6.4	25-30
3	20	9.2	32.4	10.8	15-25
4	25	12.8	40.3	15.3	10-15
5	30	16.3	46.8	19.7	less than 10

NOTE: Modified from Table 6-70 with information from Figure 6-105.

To simulate the expected behavior of tuff at the drift scale for each of the lithophysal rock mass categories of rock, the analyses were carried out with the UDEC program and involved examination of stability of the emplacement drifts under in situ and thermal loading for the lower bound values for all categories. The simulation results showed that UCS values less than

approximately 10 MPa result in predicted extensive sidewall failure of emplacement tunnels under in situ stresses only (Figure 6-106). This is obviously not observed in the ECRB Cross-Drift or ESF where tunnels are in stable and excellent condition with minimal ground support in the crown and generally no ground support in the sidewalls. Consequently the upper and lower bounds for the various lithophysal rock mass categories with the 10 MPa strength cutoff are summarized in Table 6-75.

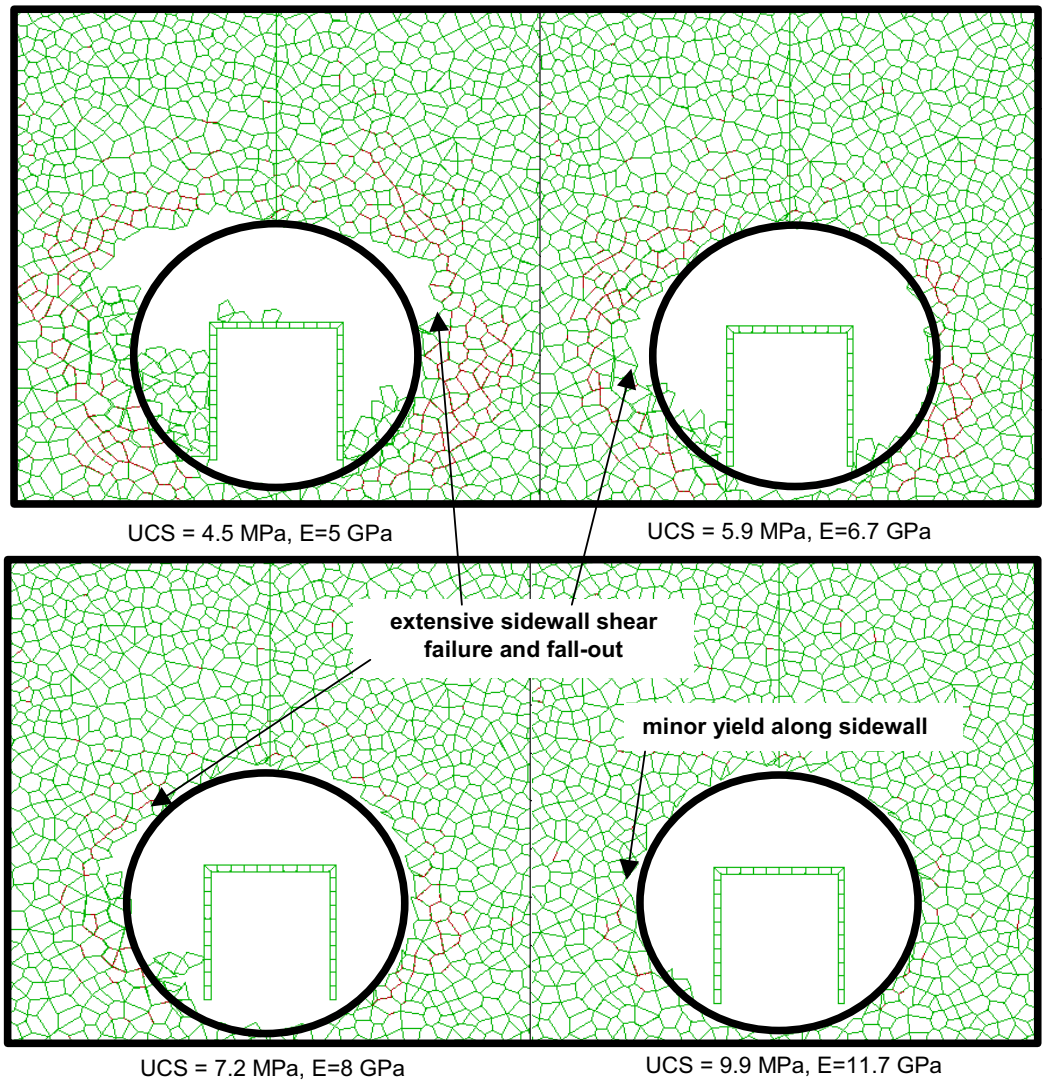

Source: BSC 2004 [DIRS 166107], Appendix E, p. E-36, Figure E-14.

NOTES: The lower bound properties line is shown in Figure 6-105. Drift exhibits extensive sidewall failure under in situ load only for UCS values less than approximately 10 MPa. This behavior is not observed in the ESF or ECRB Cross-Drift and so lower bound properties (UCS less than approx. 10 MPa) underpredict the actual in situ strength values.

Figure 6-106. UDEC Emplacement Drift Stability Analysis under In Situ Loading for Combinations of UCS and Young's Modulus along the Lower Bound Properties Line

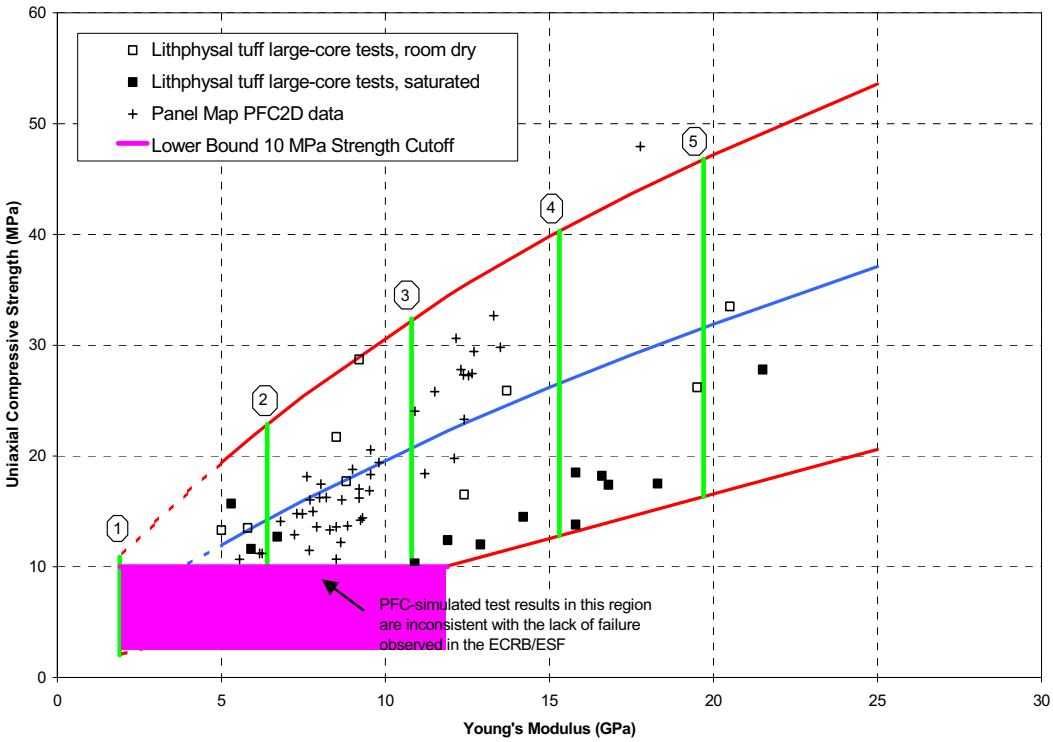

Source: BSC 2004 [DIRS 172334], Appendix B: *LithophysalRockRanges_Calc.xls*, worksheet 'Bounds (cutoff)'.

NOTES: Base-case average properties defined for each category are the mean and upper and lower bounds of each range. Category 1 is highest porosity, lowest quality rock, and category 5 is lowest porosity, highest quality rock. The strength cutoff applies for a homogeneous rock mass and is based on numerical UDEC simulations at drift scale.

Figure 6-107. Uniaxial Compressive Strength vs. Young's Modulus Showing Approximate Upper and Lower Bounds with 10 MPa Strength Cutoff

Table 6-75. Base Case, Upper and Lower Bound Strength Values for the Five Lithophysal Rock Mass Categories with 10 MPa Strength Cutoff

Rock Mass Category	Uniaxial Compressive Strength (MPa)			Estimated Young's Modulus (GPa)	Lithophysal Porosity Ranges for Rock Mass Categories (%)
	Base Case	Lower Bound	Upper Bound		
1	10	10	10.9	1.9	greater than 30
2	15	10	22.9	6.4	25-30
3	20	10	32.4	10.8	15-25
4	25	12.8	40.3	15.3	10-15
5	30	16.3	46.8	19.7	less than 10

Source: Modified from Table 6-74 with information from Figure 6-107.

The impact of spatial variability of porosity on the lower bound and mean rock mass properties was carried out using the calibrated UDEC Voronoi drift scale model in *Drift Degradation Analysis* (BSC 2004 [DIRS 166107], Appendix E, Section E4.1.4.2). The purpose of the analyses was to determine the rock mass stress-strain response for an inhomogeneous rock mass

composed of spatially varying lithophysal porosity, and thus spatially varying rock mass UCS and Young's Modulus.

The UDEC numerical uniaxial compression tests of drift scale samples typically show that the samples fail as expected in an axial splitting mode (Figure 6-108). Two sets of numerical tests were carried out, the first using base-case mechanical properties and the second using lower bound properties. The results of these simulated compression tests are plotted in Figure 6-109 in terms of the relationship of UCS and Young's Modulus. Several conclusions from this work can be made, including:

1. The variability in porosity distribution inherent in the samples results in UCS values that roughly equal or exceed 10 MPa. As seen in Figure 6-109 the spatial variability in rock mass compressive strength results in sample strengths that are grouped nearest rock mass category 4, which correspond to an average porosity of 10% to 15% (Table 6-74). It is difficult, considering variable rock mass porosity, to produce average rock mass strength values that are at the low end of the category range. This agrees with observations in the ESF main loop and ECRB Cross-Drift of stable, lightly supported excavations in the lithophysal zones that show little or no signs of instability.

2. The distribution of sample UCS and Young's moduli for both the base case and lower bound properties naturally fall within the range of lithophysal rock mass categories 3 to 4. This is in agreement with the in situ distribution of lithophysal porosities (Section 6.4.4.4.2.2 and Figure 6-89) that show the most common values lie in the Category 3 to 4 ranges. This confirms the consideration that the typical rock mass properties for the lithophysal zones lie in the Category 3 to 4 ranges, and that the occurrence of Category 1 or 2 rocks is typically as localized regions of high porosity, potentially accompanied by large lithophysae.

3. The results verify that the consideration of homogenous rock mass properties used in the base-case lithophysal rock mass categories is conservative in nature.

The details of numerical analysis and the conclusions are documented in *Drift Degradation Analysis* (BSC 2004 [DIRS 166107], Appendix E, Section E4.1.4.2). Based on these calculations, the range of lithophysal rock mass properties are considered to have a lower-bound strength of 10 MPa, with the lower bound following the saturated rock strength estimate for strengths greater than 10 MPa.

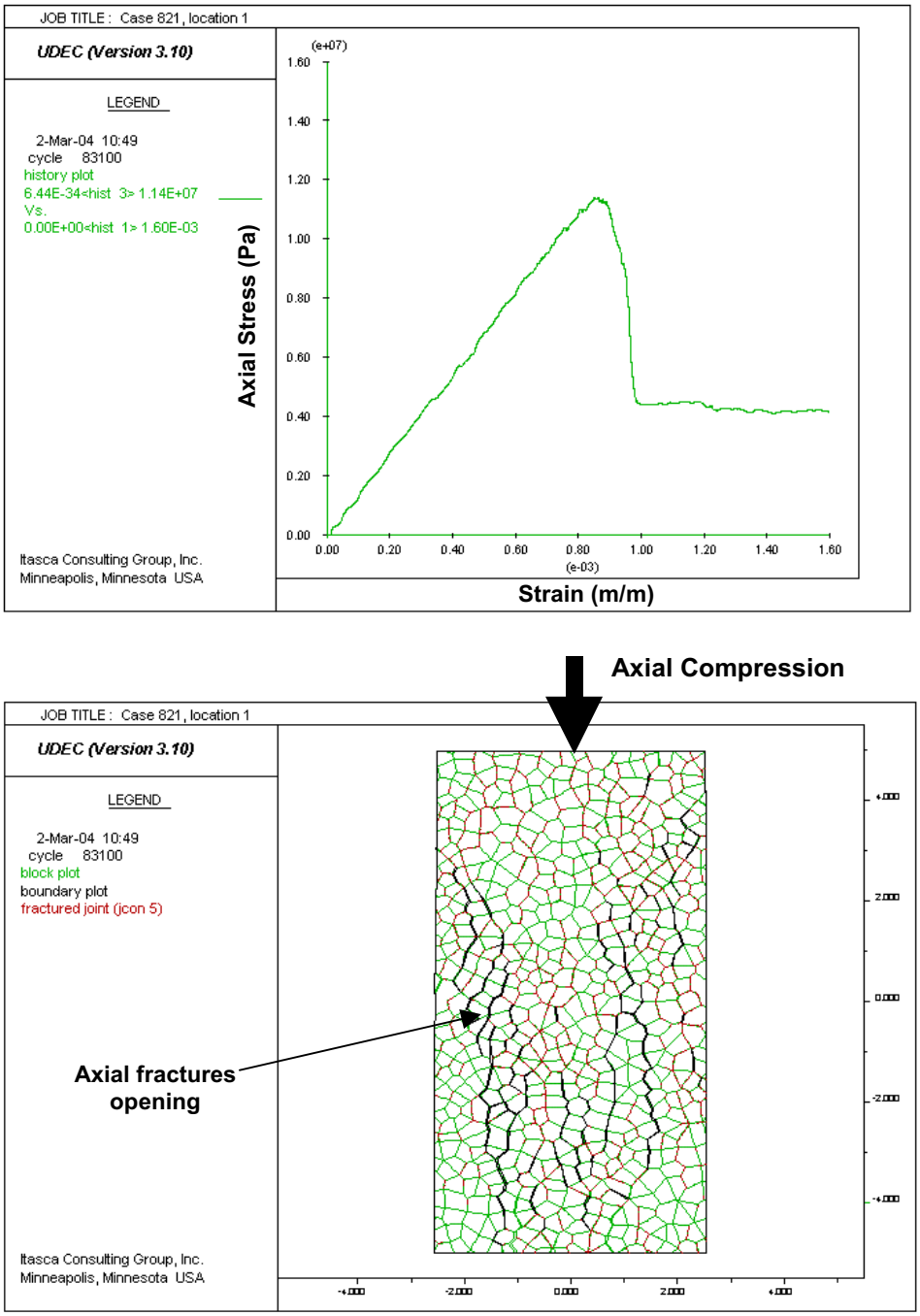

Source: BSC 2004 [DIRS 166107], Appendix E, p. E-41, Figure E-17.

NOTES: Estimated modulus and peak strength are determined from stress-strain curve. Sample fails in axial splitting mode as seen by black, axially oriented macro-fractures. Red block contacts indicate yield in either tension or shear.

Figure 6-108. Example of Uniaxial Compressive Strength Test Results on 10 × 5 m Rock Mass Sample Containing Spatially Variable Lithophysal Porosity

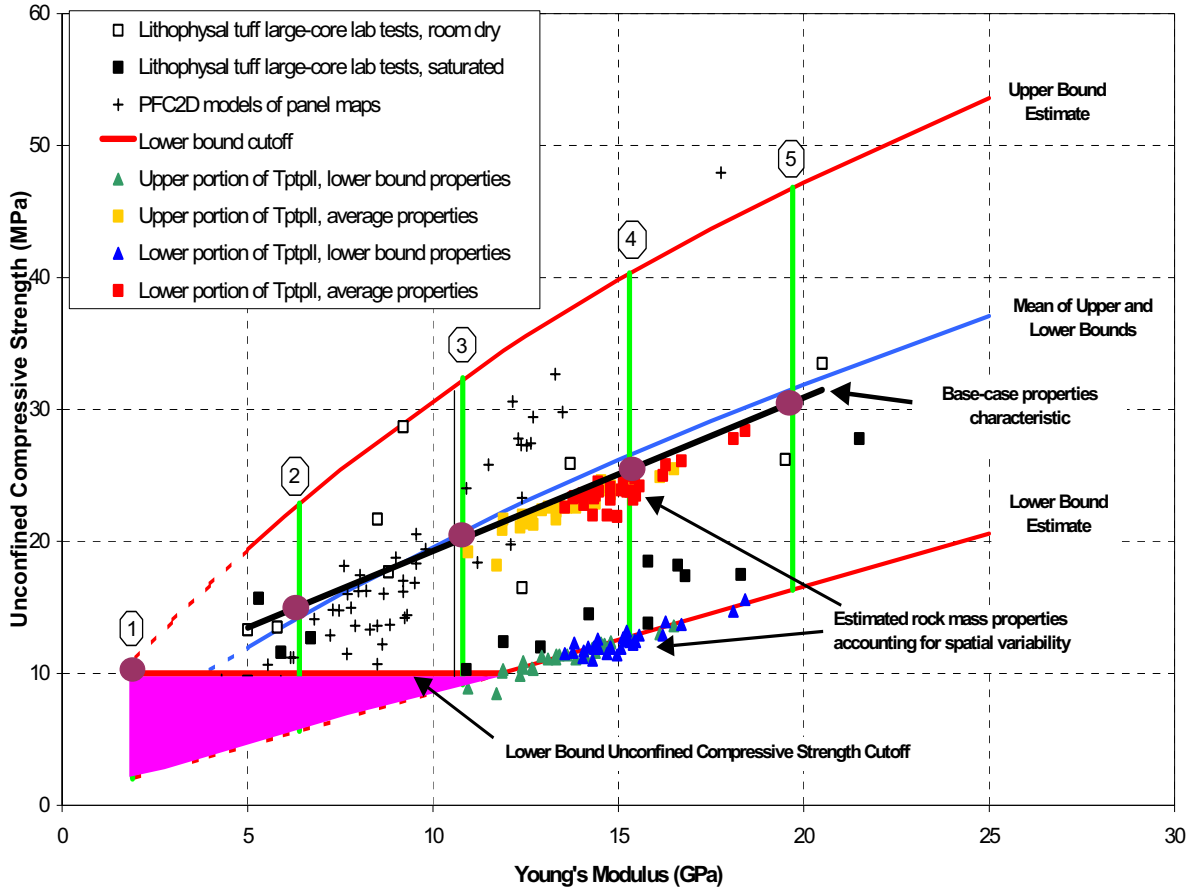

Source: BSC 2004 [DIRS 172334], Appendix B: *LithophysalRockRanges_Calc.xls*, worksheet 'Bounds (NLS)'.

NOTES: Base-case average properties defined for each category are the mean and upper and lower bounds of each range. Category 1 is highest porosity, lowest quality rock, and category 5 is lowest porosity, highest quality rock.

Figure 6-109. Lithophysal Rock Strength and Modulus Range Divided into Five Rock Mass Categories Covering the Large-Diameter Core Laboratory Testing and PFC Lithophysal Shape Extrapolation Studies

6.4.4.4.2.7 Analysis of Lithophysal Rock Mass Strength

The combined uncertainty and spatial variation of Young's modulus and uniaxial compressive strength for lithophysal rock of the Topopah Spring Tuff has been estimated using Yucca Mountain laboratory and field data, and calibrated numerical simulation of simulated lithophysal rock. This combined uncertainty and spatial variation of lithophysal rock mass mechanical properties are high due to the limited amount of site-specific test data available. To suitably account for this large variability, the range of rock properties has been subdivided into five rock mass categories that cover the entire range of expected deformability and strength. For each lithophysal rock mass category there corresponds an approximate range of lithophysal porosity, an estimated value of Young's modulus, and a bounded range of uniaxial compressive strength. These calculated rock mass properties are reasonable compared to the inputs used, and are

realistically bounded. Additional numerical simulation, field observations, and in situ field-testing provide confidence in the estimated uncertainty and spatial variation of the parameters. The lithophysal rock mass properties documented in this report are suitable for their intended use in engineering design, preclosure safety analysis, and postclosure performance assessment, according to the guidelines provided in the following paragraphs.

The mechanical behavior of lithophysal rock is found to strongly depend on rock porosity based on laboratory and numerical testing. A two-component conceptual simulation of lithophysal rock is adopted, consisting of rock matrix material and lithophysal cavities, and is used to determine the laboratory correlations between the mechanical parameters (Young's modulus and uniaxial compressive strength) and lithophysal porosity. Estimates of the uncertainty and spatial variability of lithophysal porosity at the repository scale are developed from field measurements and assumptions of stratiform geometry of rock zones (Tptpul and Tptpll) listed in Section 5.2. The expected ranges of in situ mechanical properties for lithophysal rock are predicted using the characterized lithophysal porosity as a surrogate property.

For convenience, five lithophysal rock mass categories are established with category 1 rock being mechanically weak (associated with high lithophysal porosity) and category 5 rock being relatively stiff and strong (associated with low lithophysal porosity). About 80% of the repository rock is estimated to be of higher geomechanical quality (rock mass categories 3 and higher). The lower-quality rock categories 1 and 2 have a range of lithophysal porosity that are observed to occur in approximately 20% (6% for category 1 rock alone) of the measured sample of repository lithophysal rock. These areas of high porosity are observed to occur at approximately the meter scale, creating only localized pockets of mechanical weakness. In situ compressive tests of lithophysal rock mass at the meter scale resulted in properties near the predicted lower bound of rock mass category 1; the low values are considered to be a consequence of excavation-related damage in the immediate sidewall of the tunnels. Accordingly, these field test results are considered to be unrepresentative of the rock mass in the confined state away from the tunnel excavation disturbed zone. Numerical simulations of lithophysal tuff at the drift scale coupled with underground observations were used to establish and confirm a lower bound strength cutoff for category 1 to 3 rock masses.

The PFC and UDEC computer programs were calibrated to reproduce the basic compressive strength and elastic moduli as functions of lithophysal porosity as well as to provide a basic understanding of the mechanisms of deformation and yielding in this material. The introduction of voids within rock produces a distinctly different mechanical failure mechanism from that found in nonlithophysal rock. It was found that the primary strength-decreasing effect of the lithophysae is due to the formation of tensile splitting between neighboring lithophysae under uniaxial compressive load. Numerical simulation of tuff with no voids exhibits brittle behavior, but increasing lithophysal porosity results in an increasingly ductile post–peak response. This predicted failure mechanism and deformation response are consistent with observations of lithophysal rock fracturing observed in laboratory testing and in the excavations. The transition from using circles to more realistic lithophysal shapes and void distributions results in greater variability in test results (particularly at low porosities) and a lower estimate of mean uniaxial compressive strength and Young's modulus. The variability is largely a function of the distribution of solid matrix length between lithophysae. The numerical simulations of laboratory uniaxial compressive strength tests were used to extrapolate the mechanical properties for

lithophysal rock masses over the range of in situ conditions determined from the detailed field study of lithophysae in Tptpll rock. These generated data provide a more detailed estimate of the range of variability of the properties. Constitutive simulation of yielding for rock, Mohr-Coulomb and Hoek-Brown, were fit to the laboratory and simulation extrapolation data, and their strength parameters were determined. The PFC and UDEC simulation approaches provide a viable methodology for simulating the mechanical response of welded lithophysal tuff to stressing and this tool is useful in studying the variability of material responses in addition to laboratory and field testing.

Proper use of the rock mass category data from this document depends on a suitable choice of representative range of lithophysal porosity for the rock under consideration. This requires that an appropriate value or range of lithophysal porosity be selected, the corresponding rock mass category be identified (Table 6-75), and the entire range of mechanical properties associated with that rock mass category be considered. Use of only the baseline mean values of rock category mechanical properties will not reflect the spatial heterogeneity or range of parameters estimated in this document. Adopting a more realistic variation of lithophysal porosity at the meter to 5 m scale (e.g., the simulation in *Lithophysal Rock Mass Mechanical Properties of the Repository Host Horizon* (BSC 2004 [DIRS 172334], Appendix A)) may require employing the bounding range data from multiple rock mass categories without using the limiting 10 MPa strength cutoff value for category 1 to 3 rock (Table 6-74). The confirmation activities of Section 6.4.4.4.2.8 further illustrate the proper use of rock mass category data presented in this document.

These estimates of mechanical rock parameters are not applicable to nonlithophysal rock mass, except for lithophysal subzones, since nonlithophysal rock typically has higher stiffness and compressive strength than those of lithophysal rock mass category 5. The reported mechanical parameters and rock behavior described as there being no effects of geochemical alterations to the rock that might significantly alter geomechanical rock mass properties. The property estimates of this document reflect the best current understanding of lithophysal rock behavior based on laboratory tests, field data, and numerical simulation.

Since the mechanical parameters estimated in this document are inputs to subsurface design, preclosure safety analysis, and postclosure performance assessment, these geotechnical parameters are potential candidates for performance confirmation. Furthermore, the relationship between porosity and mechanical behavior could be better understood by additional numerical simulation of lithophysal rock to address the limitations stated in Section 6.4.4.4.2.5.4

6.4.4.4.2.8 Confirmation of the Lithophysal Rock Mechanical Simulation and Property Bounds

This section describes the activities conducted to validate the mechanical behavioral simulation of lithophysal rock and the estimated range of properties associated with the assigned rock mass categories. The validation activities consist of:

- Comparison of the numerical mechanical material failure mechanisms in lithophysal rock to observations in laboratory specimens.

- Comparison of the prediction of drift scale fracturing in the Tptpll at the ECRB Cross-Drift depth to observations of tunnel sidewall fracturing in the ECRB Cross-Drift

- Comparison of the rock mass property ranges to preliminary results from in situ slot tests.

The details of the validation comparisons are given in *Drift Degradation Analysis* (BSC 2004 [DIRS 166107], Sections 7.6.5.1 and 7.6.5.2) and demonstrate the following:

- The mechanical simulation, implemented within the UDEC program has been calibrated against laboratory compressive strength tests to reproduce the basic deformability and strength properties of the lithophysal rock. To account for variability introduced by lithophysal porosity, lithophysal rock mass categories are used that cover the entire deformability and strength ranges. The base simulation was calibrated to reproduce both the mean Young's modulus and uniaxial compressive strength for each of these categories. The calibrated simulation is capable of reproducing the basic axial splitting fracturing and failure mode of lithophysal samples observed in laboratory uniaxial compression, while reproducing the proper compressive strength and elastic moduli.

- The calibrated simulation was applied to several boundary value problems to demonstrate reasonable ability to predict failure mode and failure extent observed in the field. The simulation was applied to represent tunnel response of the ECRB Cross-Drift at various depths. Sidewall springline fracturing and yield occur in the simulation for the lower end of the calibrated strength range for depths of around 300 to 350 m. The simulation predicts sidewall fracturing, parallel to the tunnel surface, developing at the springline region and extending less than 1 m into the sidewall. This agrees qualitatively to observations of springline fracturing in boreholes and alcoves observed in the lower lithophysal (Tptpll) exposures in the ECRB Cross-Drift and ESF main loop. Observations show that wall-parallel fractures in the springline extend approximately 0.5 m in depth. For the Tptpul, the UDEC simulation predict that minimal fracturing should be present, and underground observations confirm this prediction. Although Tptpul rock is of the same general strength range as Tptpll rock, the shallower depth of burial results in stresses insufficient to fail the Tptpul rock mass.

- The simulation shows minimal fracturing for rock with lithophysal rock mass categories 2 or higher at the current time. This is consistent with the typical condition within the ESF and ECRB Cross-Drift, which shows no observation of sidewall yield. This observation is also consistent with the general lithophysal porosity determined from the detailed study of Tptpll rock along the ECRB Cross-Drift (Figure 6-89), showing that approximately 80% of the Tptpll rock is indicative of a rock mass category of 3 or higher, with about 94% of the rock classified as Category 2 and greater. In other words, the small number of observations of sidewall spalling is consistent with the relatively infrequent occurrence of rock mass classified as category 1 or 2.

- The results of in situ field compressive tests (slot tests) of approximately 1 m size rock blocks resulted in values of Young's modulus and compressive strength that were within the predicted range of properties but near the lower bound of category 1 lithophysal rock mass. The values of Young's modulus and strength are low since the skin of rock surrounding the tunnels, particularly at the sidewalls, is likely in a damaged state due to excavation-induced stress and excavation effects induced by the TBM.

6.4.4.4.3 Discussion of Critical Specimen Size

As discussed briefly in Section 6.4.4.4.1.3, the problem of size or scale effect must be resolved by establishing a relationship between the strength of a small laboratory specimen and strength of rock mass. The approach applied in the current case involves defining the so-called critical specimen size. The critical size is understood as a specimen of a size, such that its strength is equal to the strength of the rock mass.

The task of defining the critical specimen size (for cylindrical specimens) requires strength data on specimens of various sizes. A data summary presented in Table 6-62 shows that only data for three lithostratigraphic zones at the RHH contains data on various specimen diameters. In this section, the data from RHH units only were used in an attempt to obtain the diameter of the critical size specimen. For these units the two groups are analyzed, one group contains the laboratory test data for the saturated tests only and the second group including all available uniaxial strength tests for a particular RHH unit. In Figures 6-110 to 6-112, each shows the power fit to these two data sets.

Not included in this figure series are the Tptpln data, of which population does not include tests on specimens of larger diameter. The regression line fitted to the combined population of Tptpmn and Tptpln showed no significant difference when compared to the regression line used to fit the larger and more complete Tptpmn test population. Figure 6-113 shows the plots of power fit curves for the RHH units (i.e., Tptpul, Tptpmn, and Tptpll specimen data extended to the specimen size equal to 3 m). The regression curves for these 3 m diameter specimens are considered a reasonable approximation of the size representing the rock mass and the estimate of rock mass strength based on the laboratory data available.

It should be noted that between two lithophysal units the strength of the Tptpul is lower than the strength of Tptpll. The strength of the Tptpmn unit is higher than the strength of either of lithophysal units.

It is apparent that that in Tptpmn unit, the intact rock strength appears to stabilize for a specimen diameter equal to approximately one (1.0) m. It also appears that the results from tests on large specimens for lithophysal strata provide data that are indicative of the lower bound strength of the rock mass. The Tptpul data on large specimens also shows strength somewhat lower than the stress level calculated to exist in the field. Although this conservatively calculated stress is shown for the relative comparison only it provides an indication that the strength of rock mass calculated from laboratory test data is lower than the strength displayed in the existing, stable, and only moderately supported ESF tunnel.

An attempt of explaining this apparent discrepancy can be made by considering the laboratory testing procedure. According to this procedure the majority of Yucca Mountain tests were performed on fully saturated rock specimens as shown in *Lithophysal Rock Mass Mechanical Properties of the Repository Host Horizon* (BSC 2004 [DIRS 172334], Figure 6.3-9). It common knowledge that the degree of saturation may have potentially significant impact on test results by lowering the strength of the rock tested. By comparing this laboratory and field evidence it is clear that tests on fully saturated large specimens result in very conservative estimate of the rock strength. These data can be used as an indication of the lower bound of uniaxial compressive strength for the Tptpul unit and the in situ strength of Tptpul rock is higher.

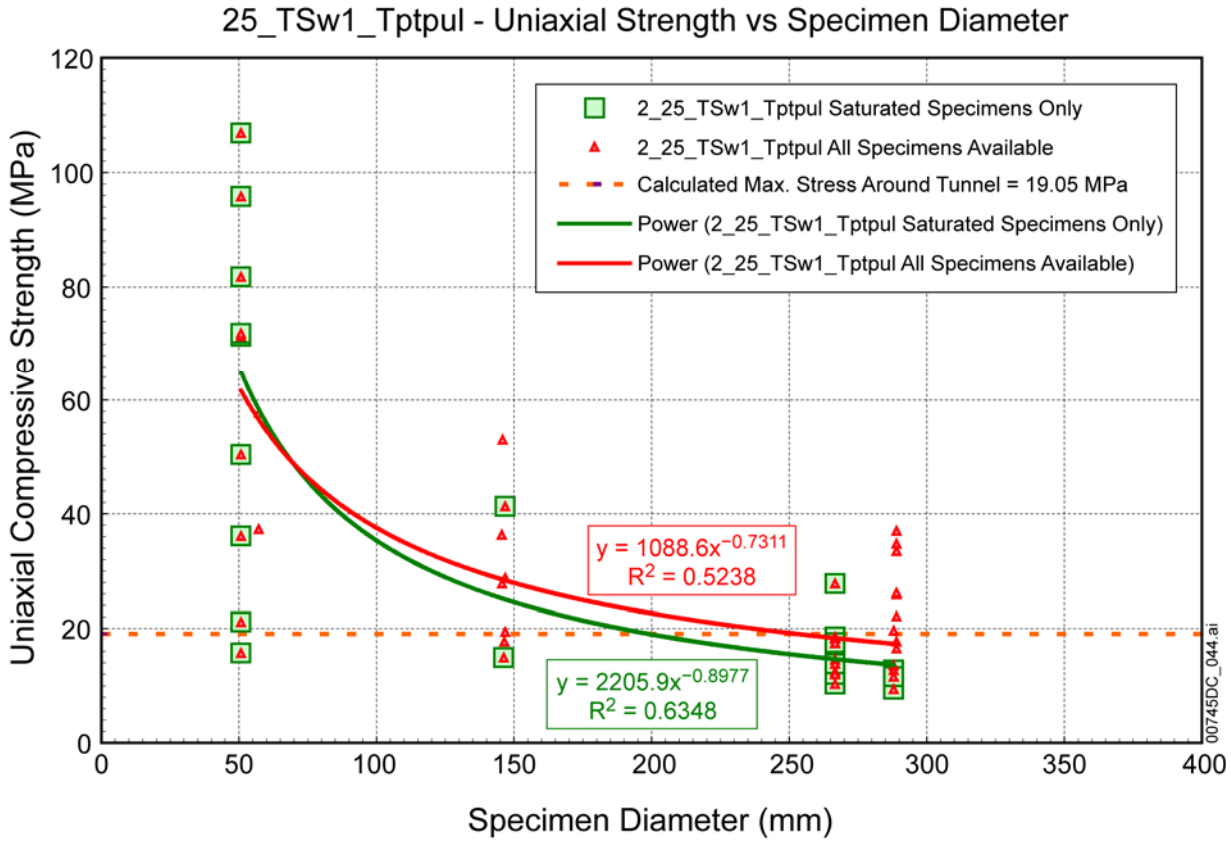

Sources: DTNs: MO0311RCKPRPCS.003 [DIRS 166073]; SN0208L0207502.001 [DIRS 161871]; SN0211L0207502.002 [DIRS 161872]; SN0302L0207502.003 [DIRS 165014]; SN0305L0207502.004 [DIRS 165013]; SN0306L0207502.008 [DIRS 165015]; SNL02030193001.001 [DIRS 120572]; SN0505L0212303.005 [DIRS 174956].

NOTES: The maximum stress calculated around the tunnel is used for information only. It is provided as a conservative estimate for comparing relative strength of the rock mass and stresses surrounding the tunnel.

Figure 6-110. Power Regression Fit to Uniaxial Strength Versus Specimen Diameter for the 25_TSw1_Tptpul Zone and Two Sets of Data: (1) Including All Data Sets Available, and (2) Including Average Values for Each Specimen Diameter

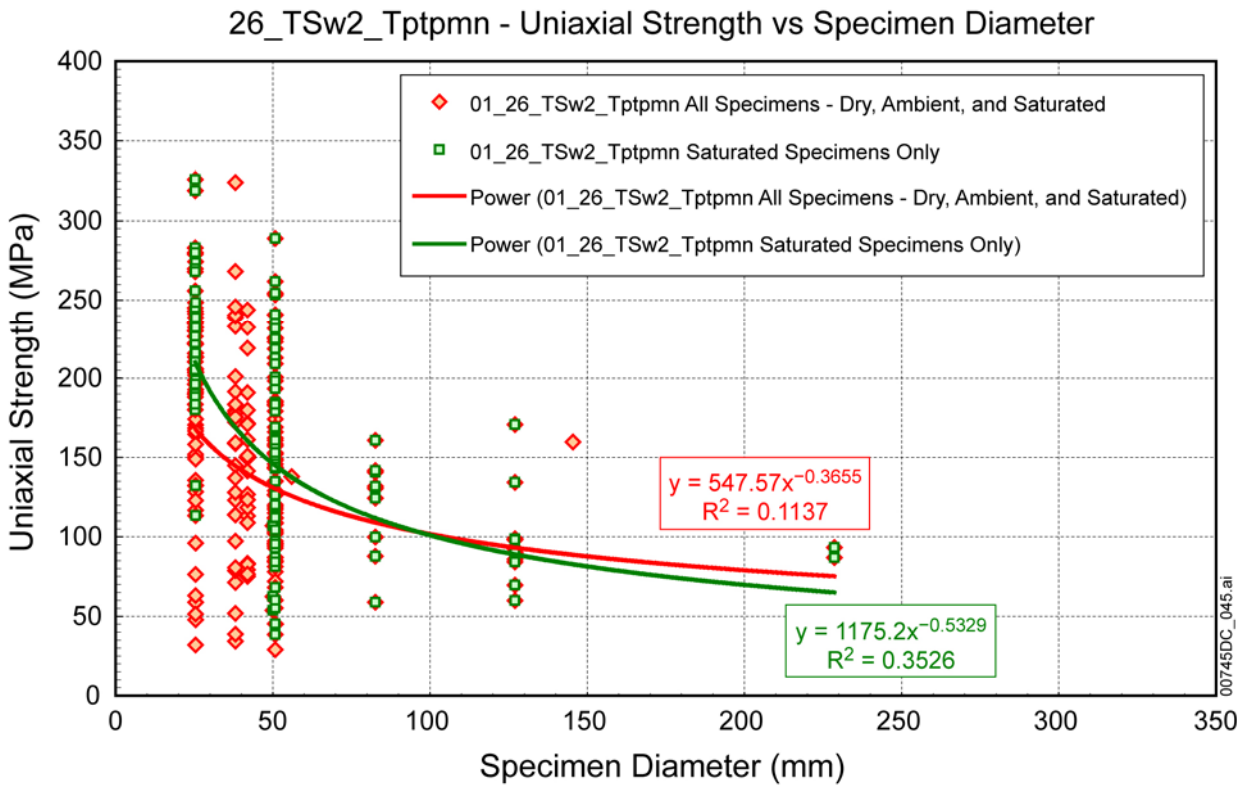

Sources: DTNs: MO0311RCKPRPCS.003 [DIRS 166073]; SN0208L0207502.001 [DIRS 161871]; SN0211L0207502.002 [DIRS 161872]; SN0302L0207502.003 [DIRS 165014]; SN0305L0207502.004 [DIRS 165013]; SN0306L0207502.008 [DIRS 165015]; SNL02030193001.001 [DIRS 120572]; SN0505L0212303.005 [DIRS 174956].

NOTES: The maximum stress calculated around the tunnel is used for information only. It is provided as a conservative estimate for comparing relative strength of the rock mass and stresses surrounding the tunnel.

Figure 6-111. Power Regression Fit to Uniaxial Strength Versus Specimen Diameter for 26_TSw2_Tptpmn Zone and Two Sets of Data: (1) Including All Data Sets Available, and (2) Including Average Values for Each Specimen Diameter

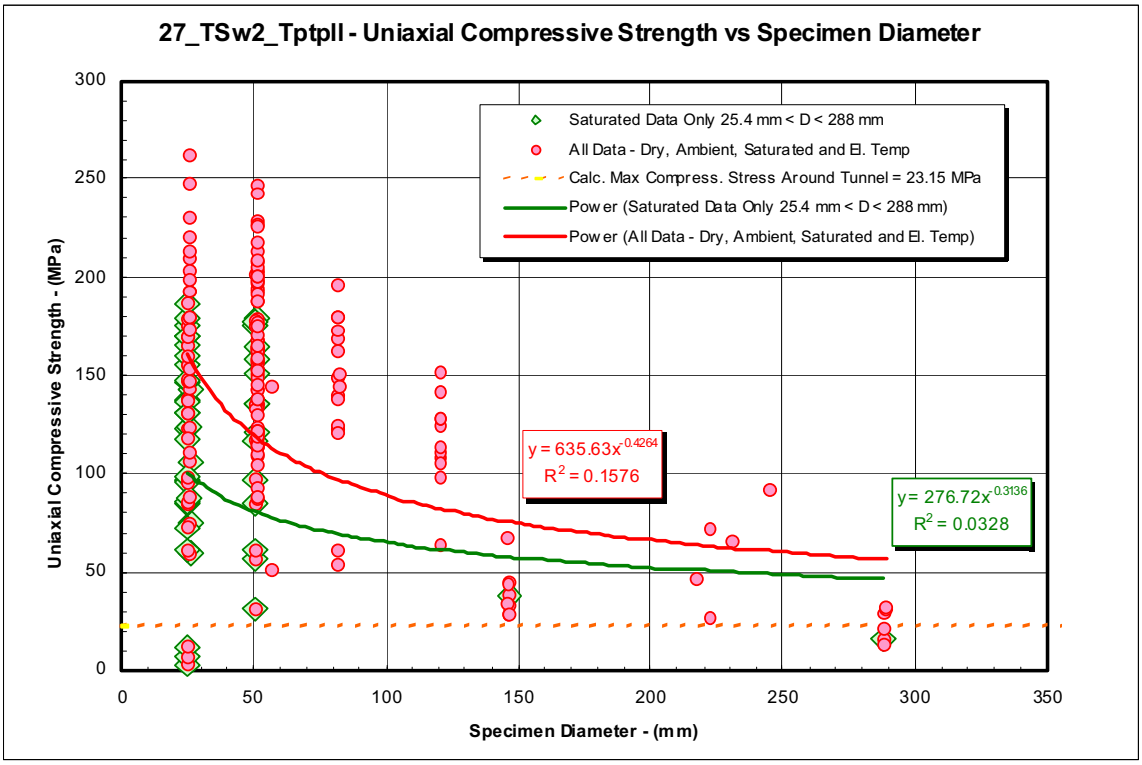

Sources: DTNs: MO0311RCKPRPCS.003 [DIRS 166073]; SN0208L0207502.001 [DIRS 161871]; SN0211L0207502.002 [DIRS 161872]; SN0302L0207502.003 [DIRS 165014]; SN0305L0207502.004 [DIRS 165013]; SN0306L0207502.008 [DIRS 165015]; SNL02030193001.001 [DIRS 120572]; SN0505L0212303.005 [DIRS 174956].

NOTES: The maximum stress calculated around the tunnel is used for information only. It is provided as a conservative estimate for comparing relative strength of the rock mass and stresses surrounding the tunnel.

Figure 6-112. Power Regression Fit to Uniaxial Compressive Strength Versus Specimen Diameter for the 27_TSw2_Tptpll Zone and Two Sets of Data: (1) Including All Data Sets Available, and (2) Including Average Values for Each Specimen Diameter

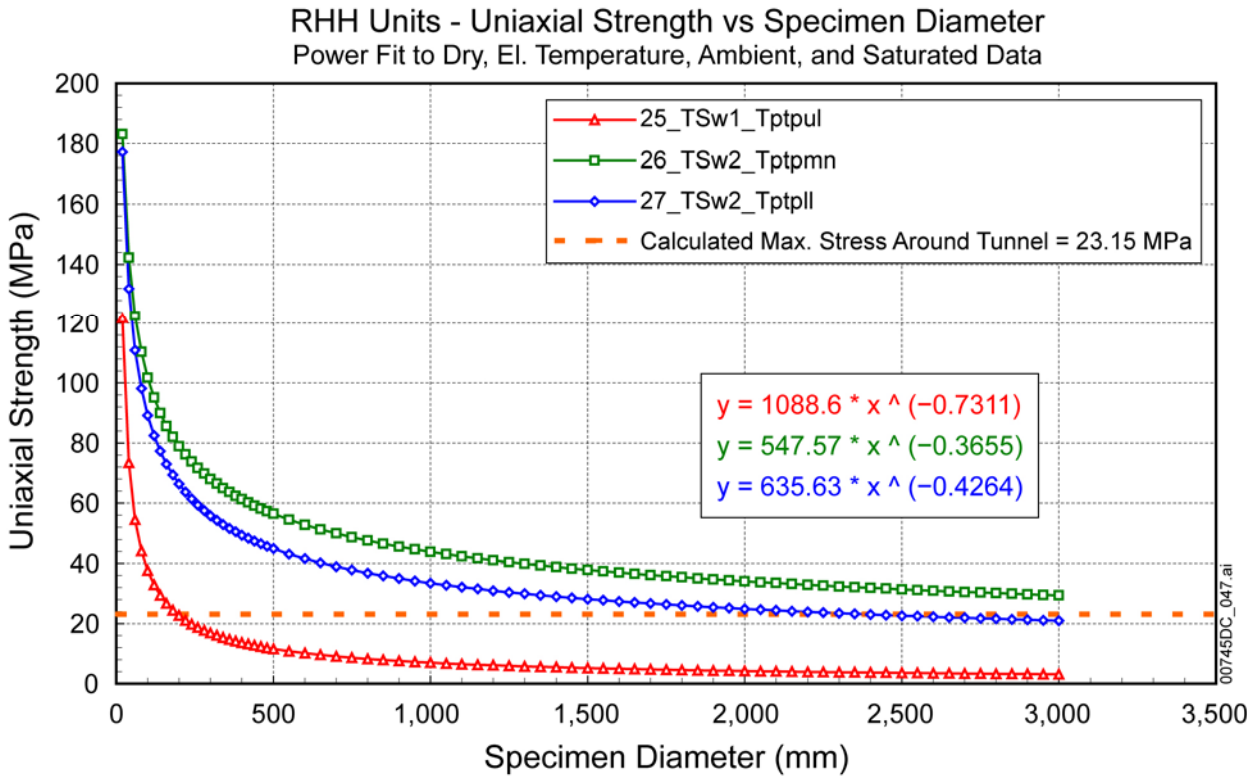

Sources: DTNs: MO0311RCKPRPCS.003 [DIRS 166073]; SN0208L0207502.001 [DIRS 161871]; SN0211L0207502.002 [DIRS 161872]; SN0302L0207502.003 [DIRS 165014]; SN0305L0207502.004 [DIRS 165013]; SN0306L0207502.008 [DIRS 165015]; SNL02030193001.001 [DIRS 120572]; SN0505L0212303.005 [DIRS 174956].

NOTES: The maximum stress calculated around the tunnel is used for information only. It is provided as a conservative estimate for comparing relative strength of the rock mass and stresses surrounding the tunnel.

Figure 6-113. Power Regression Fit to Uniaxial Compressive Strength Versus Specimen Diameter for All Four RHH Zones. Fit to Zones 26 and 28 Represented by a Single (Red) Line

It is intuitive to expect that the strength of a fractured rock mass is always lower than the strength of a small, intact specimen prepared from an undisturbed portion of the rock material from which the rock mass is composed. Rock shows a pronounced size effect as a result of the presence of discontinuities and other defects (Hoek and Brown 1988 [DIRS 106158], p. 36, Figure 1). The number of discontinuities increases with increasing specimen size, resulting in a reduction of strength in moving from the small, intact, sample to the rock mass scale (Figure 6-114). The size effect is demonstrated by the plot given in Figure 6-115, which shows the decrease in the uniaxial compressive strength of the rock sample as a function of sample diameter. This figure shows the robustness of the size effect for many different rock types. The size effect in reduction of rock strength from intact to in situ scale is automatically accounted for in the Hoek-Brown methodology proposed in this report based on the use of rock mass quality ratings, determined through geotechnical mapping, and resulting in derivation of failure criteria parameters.

To verify to what extent and which strata follow this robust trend the RHH strata were plotted along with the digitized "template curve" shown in Figure 6-115. Figures 6-116 to 6-118 show the size effect for the Tptpul, Tptpmn, and Tptpll zones, respectively along with the template curve.

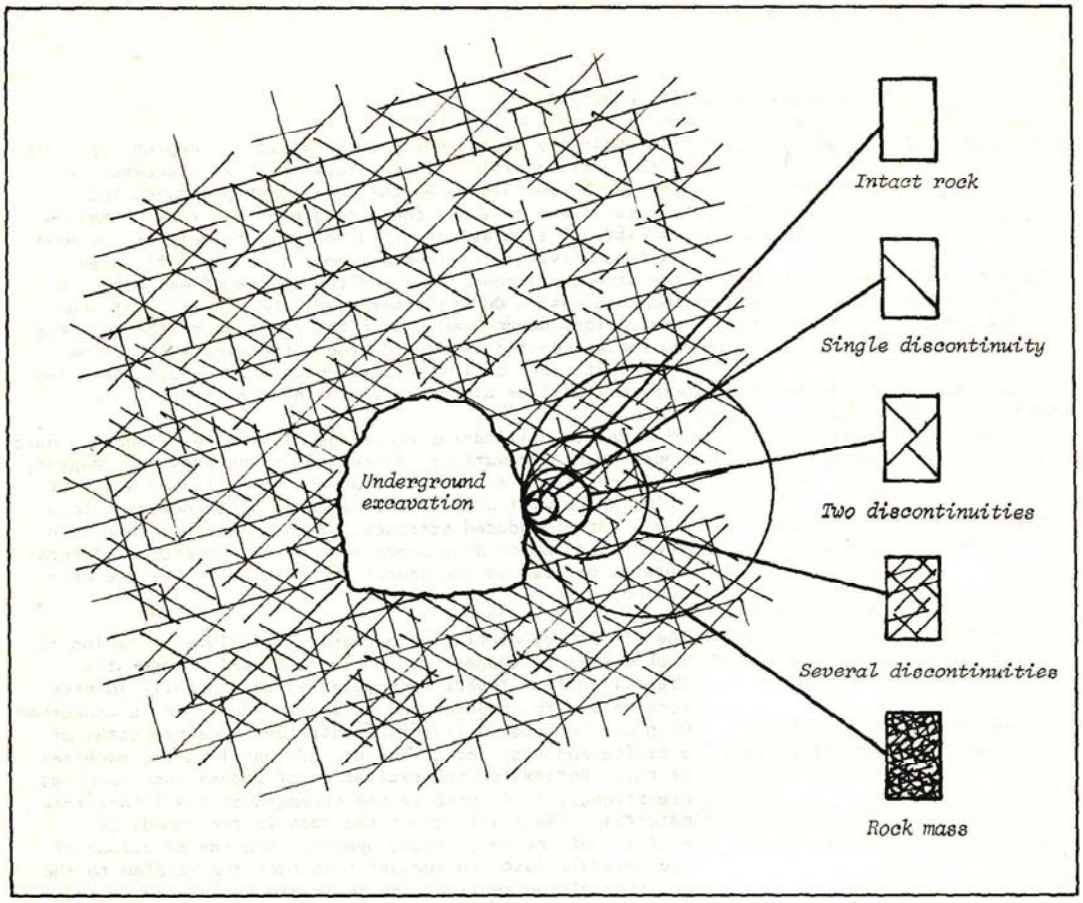

Source: Hoek and Brown 1988 [DIRS 106158], p. 36, Figure 1.

Figure 6-114. Diagram Showing the Transition from Intact Rock to a Heavily Jointed Rock Mass with Increasing Sample Size

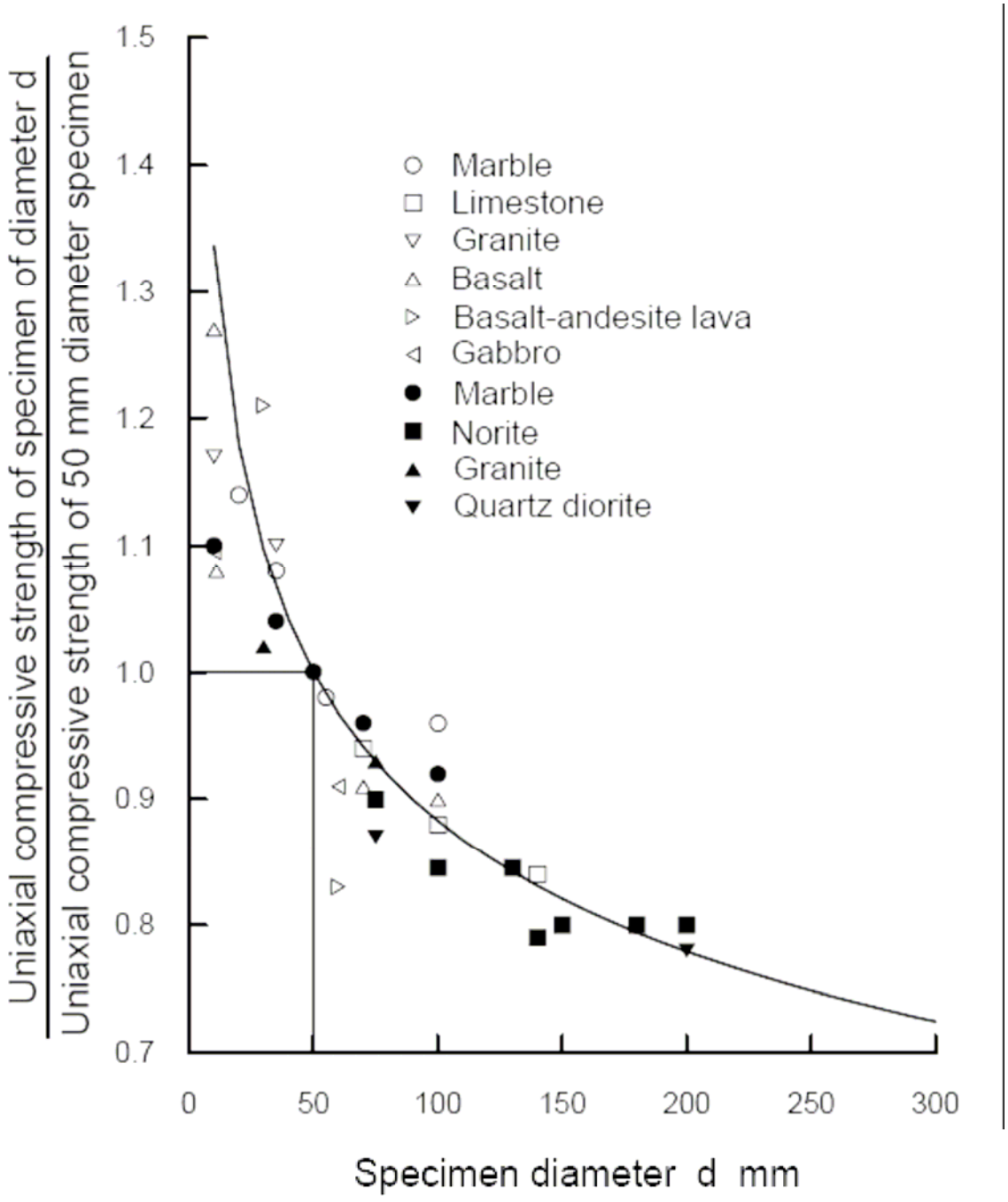

Source: Hoek 2000 [DIRS 160705].

Figure 6-115. Impact of Specimen Diameter on the Uniaxial Compressive Strength of Rock

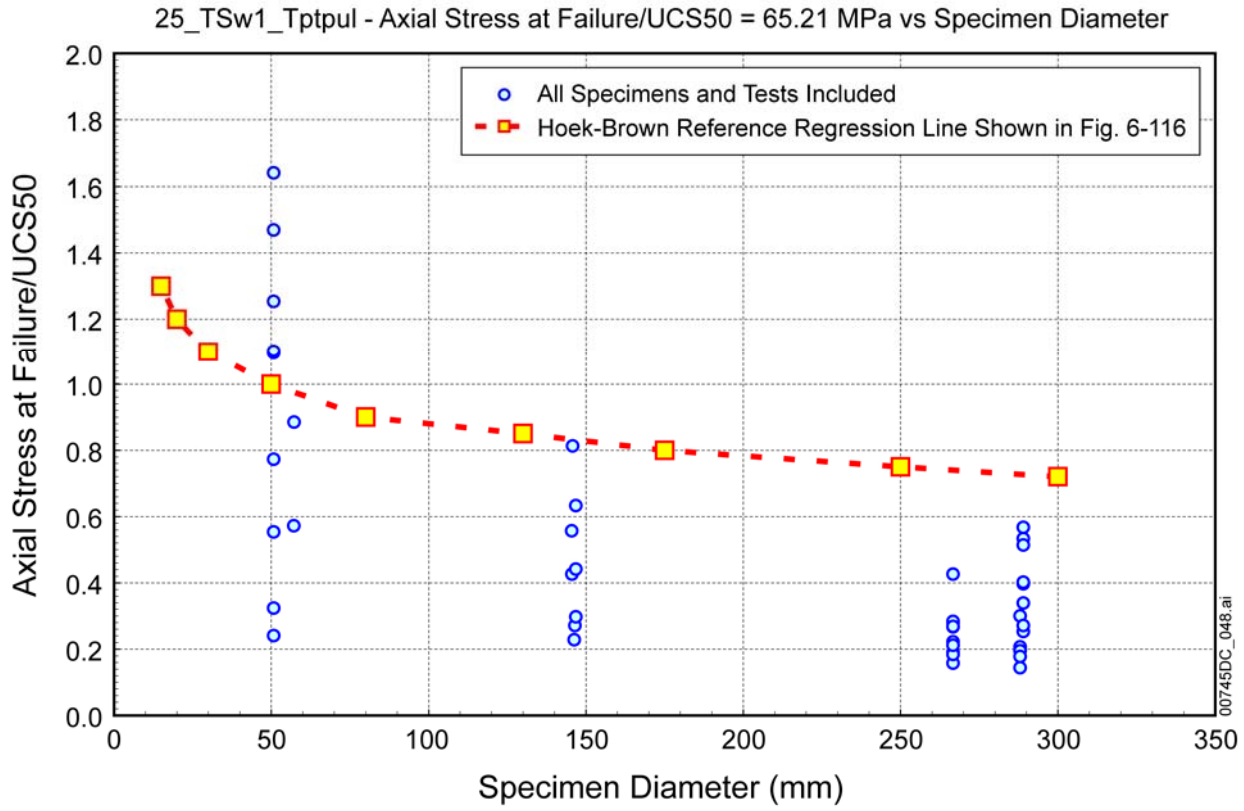

Sources: DTNs: MO0311RCKPRPCS.003 [DIRS 166073]; SN0208L0207502.001 [DIRS 161871]; SN0211L0207502.002 [DIRS 161872]; SN0302L0207502.003 [DIRS 165014]; SN0305L0207502.004 [DIRS 165013]; SN0306L0207502.008 [DIRS 165015]; SNL02030193001.001 [DIRS 120572]; SN0505L0212303.005 [DIRS 174956].

NOTE: UCS50 = 65.21 MPa is the average value from uniaxial tests on Tptpul 50 mm nominal diameter specimens tested saturated under room temperature conditions.

Figure 6-116. Unit 25_TSw1_Tptpul—Axial Stress at Failure Normalized by the Average Strength of 50 mm Diameter Specimen Versus Specimen Diameter

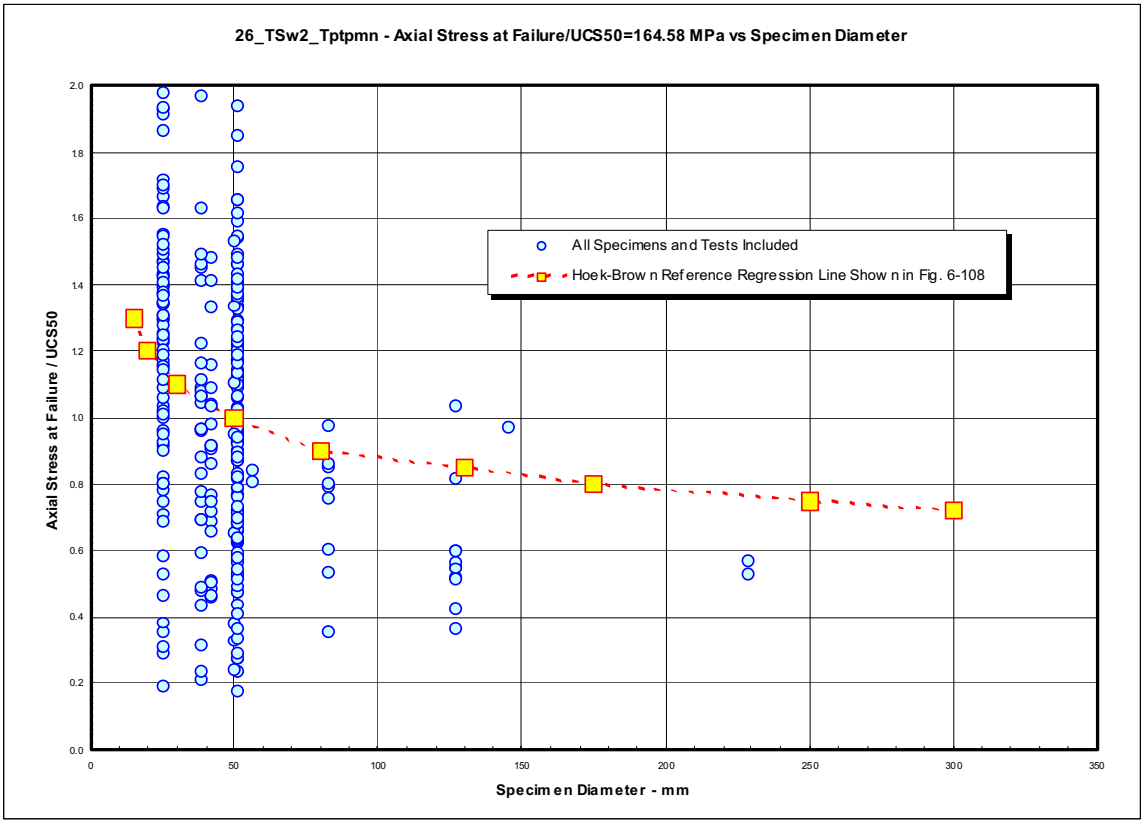

Sources: DTNs: MO0311RCKPRPCS.003 [DIRS 166073]; SN0208L0207502.001 [DIRS 161871]; SN0211L0207502.002 [DIRS 161872]; SN0302L0207502.003 [DIRS 165014]; SN0305L0207502.004 [DIRS 165013]; SN0306L0207502.008 [DIRS 165015]; SNL02030193001.001 [DIRS 120572]; SN0505L0212303.005 [DIRS 174956].

NOTE: UCS50 = 164.58 MPa is the average value from uniaxial tests on Tptpmn 50 mm nominal diameter specimens tested saturated under room temperature conditions.

Figure 6-117. Unit 26_TSw2_Tptpmn—Axial Stress at Failure Normalized by the Average Strength of 50 mm Diameter Specimen Versus Specimen Diameter

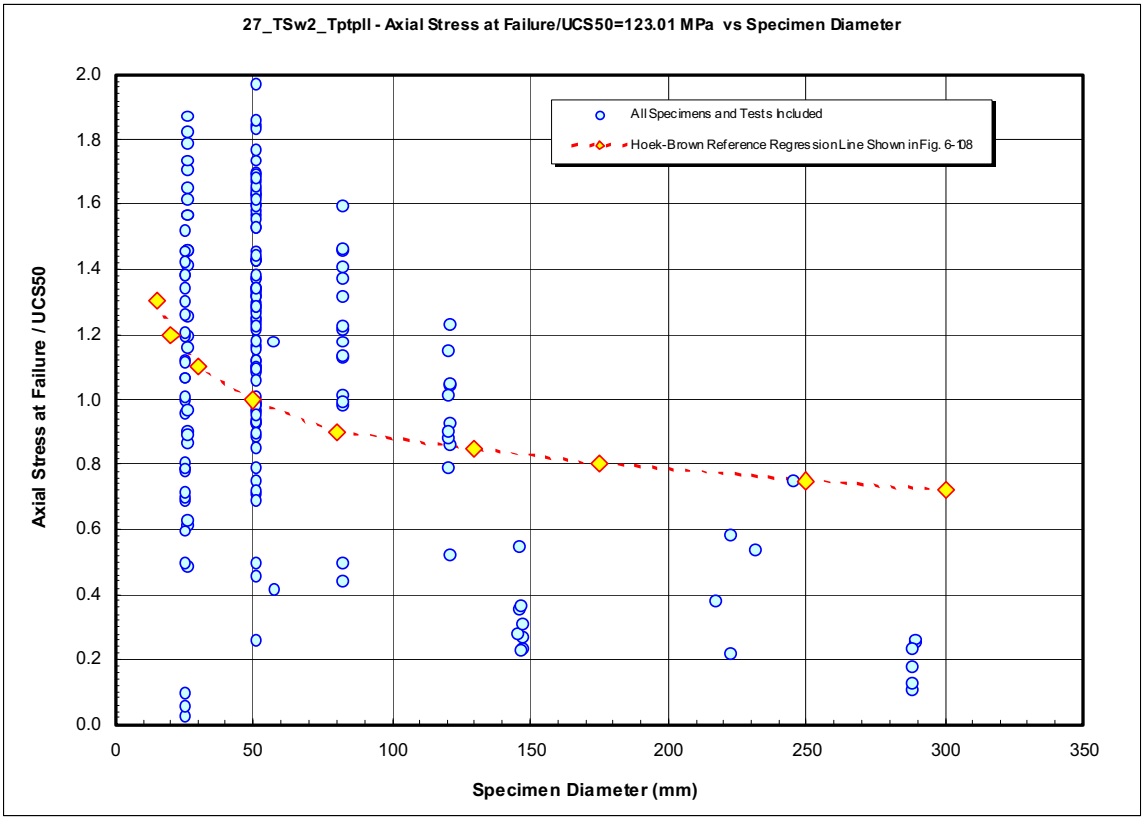

Sources: DTNs: MO0311RCKPRPCS.003 [DIRS 166073]; SN0208L0207502.001 [DIRS 161871]; SN0211L0207502.002 [DIRS 161872]; SN0302L0207502.003 [DIRS 165014]; SN0305L0207502.004 [DIRS 165013]; SN0306L0207502.008 [DIRS 165015]; SNL02030193001.001 [DIRS 120572]; SN0505L0212303.005 [DIRS 174956].

NOTE: UCS50 = 164.58 MPa is the average value from uniaxial tests on Tptpll 50 mm nominal diameter specimens tested saturated under room temperature conditions.

Figure 6-118. Unit 27_TSw2_Tptpll—Axial Stress at Failure Normalized by the Average Strength of 50 mm Diameter Specimen Versus Specimen Diameter

6.4.4.5 Summary of Rock Mass Mechanical Properties

6.4.4.5.1 Mechanical Properties of Rock Mass—General

The properties of rock mass strength were estimated using two approaches. The first approach was based on applying common mining and tunneling industry methodology of estimating RMR for all lithostratigraphic units available and calculating the GSI as a measure of rock mass quality. The GSI values obtained for each unit, and the corresponding values of uniaxial compressive strength obtained from laboratory tests, were used as input into the RocLab® software to calculate the properties of rock mass using the procedure outlined in Section 6.4.4.2. The second approach applied to the lithophysal units at the RHH was based on applying testing a numerically modeled combination of a large-scale field testing, laboratory testing of large core diameter specimens, constructing a computer-generated rock specimen and subjecting it to a variety of tests to determine the impact of varying input parameters range. In this second

approach, the porosity was used as a surrogate parameter to derive the strength and elastic properties of the lithophysal units.

The rock mass parameter values resulting from applying the first approach were used as a benchmark for relative comparisons of rock mass strength characteristics among various lithostratigraphic units and in the case of lithophysal units at the RHH, for comparisons with parameters calculated using an alternative approach.

Historically, the most detailed analyses on the YMP were carried out on strata and structures located within the RHH. Therefore, the results of the analyses are arranged in two groups. The first group presents the results for the entire sequence of lithostratigraphic units at and above the RHH as calculated using conventional RMR-based methodology and RocLab® software. The second group presents data for the rock units at the RHH. Here the rock mass data for nonlithophysal units at the RHH calculated using conventional method are presented along with the rock mass properties calculated using an alternative methodology involving porosity as a common thread property to which rock mass strength properties are related.

To facilitate their future use, the rock mass properties are presented in two tables. Table 6-76 contains the rock mass property data for the entire range of lithostratigraphic units at and above the RHH and Table 6-77 contains the rock mass properties for the lithostratigraphic units within the RHH. The top portion of the Table 6-77 contains the rock mass properties data summary for the nonlithophysal units calculated using both RocLab® and the results for lithophysal rock mass strength obtained using the alternative rock mass parameters calculation method.

The following sections present the results of rock mass strength parameters calculations.

Table 6-76. Summary of Rock Mass Parameters for Rock Strata Calculated Using RocLab

Thermal Mechanical and Lithostratigraphic Designation	Rock Mass Cat.	Hoek-Brown Classification				Hoek-Brown Criterion			Mohr-Coulomb Fit		Rock Mass Parameters				
		σ_{ci} MPa	GSI	m_i	D	m_b	s	a	C, MPa	ϕ, degrees	σ_t, MPa	σ_c, MPa	σ_{cm}', MPa	Em, GPa	Avg Poisson's Ratio
02_UO_Tmr		7.60	65.0	6.02	0	1.724	0.020	0.502	0.44	30.43	-0.09	1.08	1.54	6.54	0.03
02_UO_Tmr	1	7.60	47	6.02	0	0.906	0.003	0.507	0.31	25.46	-0.02	0.38	0.98	2.32	
02_UO_Tmr	2	7.60	55	6.02	0	1.206	0.007	0.504	0.36	27.69	-0.04	0.61	1.18	3.68	
02_UO_Tmr	3	7.60	63	6.02	0	1.605	0.016	0.502	0.42	29.89	-0.08	0.96	1.45	5.83	
02_UO_Tmr	4	7.60	74	6.02	0	2.377	0.056	0.501	0.56	32.77	-0.18	1.79	2.05	10.98	
02_UO_Tmr	5	7.60	85	6.02	0	3.521	0.189	0.500	0.83	35.22	-0.41	3.30	3.20	20.67	
03_UO_Tpki		5.94	65.0	8.37	0	2.397	0.020	0.502	0.37	33.32	-0.05	0.84	1.36	5.78	0.19
03_UO_Tpki	1	5.94	47	8.37	0	1.261	0.003	0.507	0.27	28.14	-0.01	0.30	0.89	2.05	
03_UO_Tpki	2	5.94	55	8.37	0	1.677	0.007	0.504	0.31	30.46	-0.02	0.48	1.07	3.25	
03_UO_Tpki	3	5.94	63	8.37	0	2.232	0.016	0.502	0.35	32.76	-0.04	0.75	1.29	5.15	
03_UO_Tpki	4	5.94	74	8.37	0	3.306	0.056	0.501	0.45	35.80	-0.10	1.40	1.76	9.70	
03_UO_Tpki	5	5.94	85	8.37	0	4.897	0.189	0.500	0.64	38.49	-0.23	2.58	2.64	18.28	
04_TCw_Tpcrn		36.02	68.0	4.85	0	1.546	0.029	0.502	2.17	29.32	-0.67	6.05	7.43	16.92	0.20
04_TCw_Tpcrn	1	36.02	56	4.85	0	1.007	0.008	0.504	1.63	26.18	-0.27	3.07	5.24	8.48	
04_TCw_Tpcrn	2	36.02	62	4.85	0	1.248	0.015	0.502	1.86	27.78	-0.42	4.32	6.17	11.97	
04_TCw_Tpcrn	3	36.02	67	4.85	0	1.492	0.026	0.502	2.11	29.07	-0.62	5.72	7.19	15.97	
04_TCw_Tpcrn	4	36.02	73	4.85	0	1.848	0.050	0.501	2.53	30.55	-0.97	8.01	8.85	22.56	
04_TCw_Tpcrn	5	36.02	80	4.85	0	2.373	0.108	0.501	3.25	32.09	-1.65	11.84	11.76	33.75	

Table 6-76. Summary of Rock Mass Parameters for Rock Strata Calculated Using RocLab (Continued)

Thermal Mechanical and Lithostratigraphic Designation	Rock Mass Cat.	Hoek-Brown Classification				Hoek-Brown Criterion			Mohr-Coulomb Fit		Rock Mass Parameters				
		σ_{ci} MPa	GSI	m_i	D	m_b	s	a	C, MPa	ϕ, degrees	σ_t, MPa	σ_c, MPa	σ_{cm}', MPa	Em, GPa	Avg Poisson's Ratio
07_TCw_Tpcpul		62.14	59.0	6.06	0	1.401	0.011	0.503	3.16	28.86	-0.47	6.28	10.70	13.23	0.19
07_TCw_Tpcpul	1	62.14	40	6.06	0	0.711	0.001	0.511	2.22	23.56	-0.11	2.05	6.79	4.43	
07_TCw_Tpcpul	2	62.14	53	6.06	0	1.131	0.005	0.505	2.81	27.19	-0.30	4.45	9.22	9.37	
07_TCw_Tpcpul	3	62.14	60	6.06	0	1.452	0.012	0.503	3.23	29.13	-0.50	6.65	10.98	14.02	
07_TCw_Tpcpul	4	62.14	67	6.06	0	1.864	0.026	0.502	3.78	31.03	-0.85	9.87	13.36	20.97	
07_TCw_Tpcpul	5	62.14	73	6.06	0	2.310	0.050	0.501	4.44	32.59	-1.34	13.82	16.20	29.63	
08_TCw_Tpcpm		207.81	64.0	14.24	0	3.938	0.018	0.502	14.28	37.72	-0.97	27.89	58.18	22.39	0.20
08_TCw_Tpcpm	1	207.81	50	14.24	0	2.388	0.004	0.506	11.52	33.55	-0.34	12.52	42.92	10.00	
08_TCw_Tpcpm	2	207.81	59	14.24	0	3.294	0.011	0.503	13.19	36.24	-0.66	21.01	52.02	16.79	
08_TCw_Tpcpm	3	207.81	63	14.24	0	3.800	0.016	0.502	14.04	37.43	-0.90	26.35	56.87	21.13	
08_TCw_Tpcpm	4	207.81	69	14.24	0	4.708	0.032	0.501	15.56	39.18	-1.41	36.94	65.51	29.85	
08_TCw_Tpcpm	5	207.81	77	14.24	0	6.265	0.078	0.501	18.27	41.44	-2.58	57.79	80.99	47.32	
09_TCw_Tpcpll		125.31	68.0	10.13	0	3.230	0.029	0.502	8.57	35.86	-1.11	21.06	33.53	28.18	0.24
09_TCw_Tpcpll	1	125.31	47	10.13	0	1.526	0.003	0.507	5.97	29.74	-0.23	6.33	20.58	8.41	
09_TCw_Tpcpll	2	125.31	63	10.13	0	2.702	0.016	0.502	7.79	34.43	-0.76	15.89	29.55	21.13	
09_TCw_Tpcpll	3	125.31	70	10.13	0	3.469	0.036	0.501	8.93	36.43	-1.29	23.56	35.39	31.62	
09_TCw_Tpcpll	4	125.31	77	10.13	0	4.454	0.078	0.501	10.54	38.34	-2.18	34.85	43.53	47.32	
09_TCw_Tpcpll	5	125.31	81	10.13	0	5.138	0.121	0.501	11.78	39.37	-2.95	43.56	49.81	59.57	
10_TCw_Tpcpln		198.87	69.0	18.21	0	6.019	0.032	0.501	15.73	41.34	-1.05	35.35	69.59	29.85	0.21
10_TCw_Tpcpln	1	198.87	54	18.21	0	3.523	0.006	0.504	12.56	36.89	-0.34	15.10	50.27	12.59	
10_TCw_Tpcpln	2	198.87	65	18.21	0	5.218	0.020	0.502	14.76	40.17	-0.78	28.23	63.54	23.71	
10_TCw_Tpcpln	3	198.87	70	18.21	0	6.238	0.036	0.501	16.00	41.63	-1.14	37.39	71.25	31.62	
10_TCw_Tpcpln	4	198.87	75	18.21	0	7.458	0.062	0.501	17.49	43.06	-1.66	49.46	80.59	42.17	
10_TCw_Tpcpln	5	198.87	81	18.21	0	9.240	0.121	0.501	19.81	44.71	-2.61	69.13	94.96	59.57	
12_PTn_Tpcpv2		29.87	62.0	9.30	0	2.393	0.015	0.502	1.79	33.39	-0.18	3.58	6.63	10.91	0.10
12_PTn_Tpcpv2	1	29.87	51	9.30	0	1.615	0.004	0.505	1.48	30.19	-0.08	1.91	5.14	5.79	
12_PTn_Tpcpv2	2	29.87	60	9.30	0	2.228	0.012	0.503	1.72	32.81	-0.16	3.20	6.32	9.72	
12_PTn_Tpcpv2	3	29.87	64	9.30	0	2.570	0.018	0.502	1.85	33.97	-0.21	4.01	6.97	12.24	
12_PTn_Tpcpv2	4	29.87	66	9.30	0	2.760	0.023	0.502	1.93	34.54	-0.25	4.49	7.33	13.73	
12_PTn_Tpcpv2	5	29.87	69	9.30	0	3.072	0.032	0.501	2.05	35.38	-0.31	5.31	7.94	16.32	
13_PTn_Tpcpv1		5.05	68.0	10.00	0	3.189	0.029	0.502	0.34	35.75	-0.05	0.85	1.34	6.33	0.10
13_PTn_Tpcpv1	1	5.05	62	10.00	0	2.574	0.015	0.502	0.31	34.03	-0.03	0.61	1.16	4.48	
13_PTn_Tpcpv1	2	5.05	65	10.00	0	2.865	0.020	0.502	0.32	34.90	-0.04	0.72	1.24	5.33	
13_PTn_Tpcpv1	3	5.05	67	10.00	0	3.077	0.026	0.502	0.34	35.47	-0.04	0.80	1.31	5.98	
13_PTn_Tpcpv1	4	5.05	71	10.00	0	3.550	0.040	0.501	0.37	36.59	-0.06	1.00	1.46	7.53	
13_PTn_Tpcpv1	5	5.05	77	10.00	0	4.398	0.078	0.501	0.42	38.22	-0.09	1.40	1.75	10.63	
17_PTn_Tpp		1.68	71.0	3.10	0	1.100	0.040	0.501	0.11	26.07	-0.06	0.33	0.35	4.34	0.26
17_PTn_Tpp	1	1.68	59	3.10	0	0.717	0.011	0.503	0.07	23.35	-0.02	0.17	0.22	2.17	
17_PTn_Tpp	2	1.68	66	3.10	0	0.920	0.023	0.502	0.09	24.99	-0.04	0.25	0.28	3.25	
17_PTn_Tpp	3	1.68	71	3.10	0	1.100	0.040	0.501	0.11	26.07	-0.06	0.33	0.35	4.34	
17_PTn_Tpp	4	1.68	76	3.10	0	1.315	0.069	0.501	0.13	27.04	-0.09	0.44	0.43	5.79	
17_PTn_Tpp	5	1.68	81	3.10	0	1.572	0.121	0.501	0.16	27.86	-0.13	0.58	0.55	7.72	
18_PTn_Tpbt2		2.92	70.0	8.74	0	2.992	0.036	0.501	0.20	35.10	-0.03	0.55	0.78	5.40	0.21
18_PTn_Tpbt2	1	2.92	63	8.74	0	2.330	0.016	0.502	0.18	33.13	-0.02	0.37	0.65	3.61	
18_PTn_Tpbt2	2	2.92	67	8.74	0	2.688	0.026	0.502	0.19	34.27	-0.03	0.46	0.72	4.55	
18_PTn_Tpbt2	3	2.92	69	8.74	0	2.887	0.032	0.501	0.20	34.83	-0.03	0.52	0.76	5.10	
18_PTn_Tpbt2	4	2.92	74	8.74	0	3.451	0.056	0.501	0.22	36.19	-0.05	0.69	0.88	6.80	
18_PTn_Tpbt2	5	2.92	78	8.74	0	3.981	0.087	0.501	0.25	37.23	-0.06	0.86	1.00	8.56	
22_TSw1_Tptrn		63.37	64.0	11.59	0	3.203	0.018	0.502	4.14	35.90	-0.36	8.50	16.22	17.82	0.25
22_TSw1_Tptrn	1	63.37	50	11.59	0	1.943	0.004	0.506	3.30	31.77	-0.13	3.82	11.85	7.96	

Table 6-76. Summary of Rock Mass Parameters for Rock Strata Calculated Using RocLab (Continued)

Thermal Mechanical and Lithostratigraphic Designation	Rock Mass Cat.	Hoek-Brown Classification				Hoek-Brown Criterion			Mohr-Coulomb Fit		Rock Mass Parameters				
		σ_{ci} MPa	GSI	m_i	D	m_b	s	a	C, MPa	ϕ, degrees	σ_t, MPa	σ_c, MPa	σ_{cm}', MPa	Em, GPa	Avg Poisson's Ratio
22_TSw1_Tptrn	2	63.37	60	11.59	0	2.777	0.012	0.503	3.87	34.73	-0.27	6.78	14.77	14.16	
22_TSw1_Tptrn	3	63.37	65	11.59	0	3.320	0.020	0.502	4.21	36.19	-0.39	9.00	16.61	18.88	
22_TSw1_Tptrn	4	63.37	69	11.59	0	3.830	0.032	0.501	4.54	37.35	-0.53	11.27	18.36	23.77	
22_TSw1_Tptrn	5	63.37	74	11.59	0	4.578	0.056	0.501	5.05	38.75	-0.77	14.90	21.04	31.69	
23_TSw1_Tptrl		38.06	54.0	7.82	0	1.512	0.006	0.504	1.89	29.60	-0.15	2.89	6.48	7.77	0.30
23_TSw1_Tptrl	1	38.06	42	7.82	0	0.985	0.002	0.510	1.54	26.14	-0.06	1.42	4.93	3.89	
23_TSw1_Tptrl	2	38.06	50	7.82	0	1.311	0.004	0.506	1.76	28.45	-0.11	2.29	5.91	6.17	
23_TSw1_Tptrl	3	38.06	55	7.82	0	1.567	0.007	0.504	1.92	29.88	-0.16	3.06	6.63	8.23	
23_TSw1_Tptrl	4	38.06	59	7.82	0	1.808	0.011	0.503	2.06	31.03	-0.22	3.85	7.29	10.36	
23_TSw1_Tptrl	5	38.06	64	7.82	0	2.161	0.018	0.502	2.27	32.45	-0.32	5.11	8.27	13.81	
Rock Mass Strength Properties for the Repository Host Horizon (RHH) Strata															
25_TSw1_Tptpul		97.13	55.0	17.41	0	3.489	0.007	0.504	6.14	36.79	-0.19	7.81	24.53	13.14	0.25
25_TSw1_Tptpul	1	97.13	42	17.41	0	2.193	0.002	0.510	5.09	32.87	-0.07	3.63	18.68	6.22	
25_TSw1_Tptpul	2	97.13	50	17.41	0	2.918	0.004	0.506	5.72	35.29	-0.13	5.85	22.11	9.86	
25_TSw1_Tptpul	3	97.13	55	17.41	0	3.489	0.007	0.504	6.14	36.79	-0.19	7.81	24.53	13.14	
25_TSw1_Tptpul	4	97.13	61	17.41	0	4.323	0.013	0.503	6.70	38.59	-0.29	11.00	27.85	18.56	
25_TSw1_Tptpul	5	97.13	69	17.41	0	5.752	0.032	0.501	7.60	40.95	-0.54	17.27	33.33	29.42	
26_TSw2_Tptpmn		136.36	62.0	12.39	0	3.189	0.015	0.502	8.75	35.91	-0.63	16.34	34.28	19.95	0.19
26_TSw2_Tptpmn	1	136.36	51	12.39	0	2.153	0.004	0.505	7.36	32.64	-0.27	8.71	26.90	10.59	
26_TSw2_Tptpmn	2	136.36	59	12.39	0	2.865	0.011	0.503	8.33	35.02	-0.50	13.79	32.02	16.79	
26_TSw2_Tptpmn	3	136.36	62	12.39	0	3.189	0.015	0.502	8.75	35.91	-0.63	16.34	34.28	19.95	
26_TSw2_Tptpmn	4	136.36	68	12.39	0	3.951	0.029	0.502	9.73	37.65	-0.99	22.92	39.57	28.18	
26_TSw2_Tptpmn	5	136.36	72	12.39	0	4.557	0.045	0.501	10.52	38.79	-1.33	28.68	43.90	35.48	
27_TSw2_Tptpll		129.79	60.0	15.52	0	3.720	0.012	0.503	8.56	37.29	-0.41	13.89	34.55	17.78	0.22
27_TSw2_Tptpll	1	129.79	52	15.52	0	2.795	0.005	0.505	7.60	34.89	-0.22	8.78	29.14	11.22	
27_TSw2_Tptpll	2	129.79	56	15.52	0	3.224	0.008	0.504	8.06	36.09	-0.30	11.06	31.71	14.13	
27_TSw2_Tptpll	3	129.79	59	15.52	0	3.589	0.011	0.503	8.43	36.99	-0.38	13.12	33.81	16.79	
27_TSw2_Tptpll	4	129.79	63	15.52	0	4.140	0.016	0.502	8.97	38.18	-0.51	16.46	36.91	21.13	
27_TSw2_Tptpll	5	129.79	68	15.52	0	4.950	0.029	0.502	9.73	39.65	-0.75	21.81	41.41	28.18	
28_TSw2_Tptpln		165.59	65.0	20.86	0	5.977	0.020	0.502	12.72	41.36	-0.57	23.51	56.27	23.71	0.22
28_TSw2_Tptpln	1	165.59	57	20.86	0	4.492	0.008	0.504	11.34	38.98	-0.31	14.94	47.53	14.96	
28_TSw2_Tptpln	2	165.59	61	20.86	0	5.182	0.013	0.503	12.00	40.17	-0.42	18.75	51.66	18.84	

Table 6-76. Summary of Rock Mass Parameters for Rock Strata Calculated Using RocLab (Continued)

Thermal Mechanical and Lithostratigraphic Designation	Rock Mass Cat.	Hoek-Brown Classification				Hoek-Brown Criterion			Mohr-Coulomb Fit		Rock Mass Parameters				
		σ_{ci} MPa	GSI	m_i	D	m_b	s	a	C, MPa	ϕ, degrees	σ_t, MPa	σ_c, MPa	σ_{cm}', MPa	Em, GPa	Avg Poisson's Ratio
28_TSw2_Tptpln	3	165.59	64	20.86	0	5.768	0.018	0.502	12.53	41.06	-0.53	22.22	55.07	22.39	
28_TSw2_Tptpln	4	165.59	69	20.86	0	6.895	0.032	0.501	13.52	42.53	-0.77	29.44	61.49	29.85	
28_TSw2_Tptpln	5	165.59	72	20.86	0	7.675	0.045	0.501	14.20	43.39	-0.96	34.82	65.92	35.48	

Sources: Mapping and GSI data from DTNs: GS950508314224.003 [DIRS 107488]; GS000608314224.005 [DIRS 166002]; GS960408314224.001 [DIRS 168135]; GS960408314224.003 [DIRS 168136]; GS960708314224.009 [DIRS 168137]; GS000608314224.006 [DIRS 152572]; GS960908314224.015 [DIRS 108372]; GS960908314224.016 [DIRS 108373]; GS960908314224.017 [DIRS 108376]; GS970108314224.002 [DIRS 107490]; GS970208314224.004 [DIRS 107492]; GS970808314224.009 [DIRS 107494]; GS970808314224.011 [DIRS 107495]; GS970808314224.013 [DIRS 107497]; GS990408314224.003 [DIRS 108404]; GS990408314224.004 [DIRS 108405]; GS990408314224.005 [DIRS 108408]; GS990408314224.006 [DIRS 108409]; GS970608314224.007 [DIRS 158430].

Intact rock strength data are from DTNs: MO0311RCKPRPCS.003 [DIRS 166073]; MO0402DQRIRPPR.003 [DIRS 168901]; SN0208L0207502.001 [DIRS 161871]; SN0211L0207502.002 [DIRS 161872]; SN0302L0207502.003 [DIRS 165014]; SN0305L0207502.004 [DIRS 165013]; SN0306L0207502.008 [DIRS 165015]; SNL02030193001.001 [DIRS 120572]; SN0505L0212303.005 [DIRS 174956]; MO0401DQRIRPTS.003 [DIRS 168905].

NOTES:
1. Provided in this table are values of GENERAL rock mass strength data obtained using values of average parameters for individual lithostratigraphic units (Also see File in Appendix H: *Rock Mass Strength Parameters - All_Plus Porosity_Based Dat.xls*).
2. GSI values correspond to 5%, 20%, 40%, 70%, and 90% of cumulative frequency of occurrence in the tunnels.
3. Green values represent an average GSI for a particular lithostratigraphic unit.
4. Poisson's ratio taken as equal to the intact rock (see Appendix C).
5. Rock mass properties calculated using porosity as a surrogate parameter to develop the lithophysal rock mass strength properties.

AVG = average; Cat. = category.

Table 6-77. Summary of Rock Mass Parameters for Rock Strata at RHH Calculated Using RocLab for Nonlithophysal Units and Alternative Method for Lithophysal Units

Thermal Mechanical and Lithostratigraphic Designation	Rock Mass Cat.	Hoek-Brown Classification				Hoek-Brown Criterion			Mohr-Coulomb Fit		Rock Mass Parameters				
		σ_{ci} MPa	GSI	mi	D	mb	s	a	C, MPa	ϕ degrees	σ_t, MPa	σ_c, MPa	σ_{cm}', MPa	Em, GPa	Avg Poiss. Ratio
Rock Mass Strength Properties for Nonlithophysal Rock Strata Units at the RHH Calculated Using RocLab															
Data Based on Average Saturated 50 mm Diameter Specimens Only															
26_TSw2_Tptpmn		136.36	62	12.39	0	3.189	0.015	0.502	8.75	35.91	-0.63	16.34	34.28	19.95	0.19
26_TSw2_Tptpmn	1	136.36	51	12.39	0	2.153	0.004	0.505	7.36	32.64	-0.27	8.71	26.90	10.59	
26_TSw2_Tptpmn	2	136.36	59	12.39	0	2.865	0.011	0.503	8.33	35.02	-0.50	13.79	32.02	16.79	
26_TSw2_Tptpmn	3	136.36	62	12.39	0	3.189	0.015	0.502	8.75	35.91	-0.63	16.34	34.28	19.95	
26_TSw2_Tptpmn	4	136.36	68	12.39	0	3.951	0.029	0.502	9.73	37.65	-0.99	22.92	39.57	28.18	
26_TSw2_Tptpmn	5	136.36	72	12.39	0	4.557	0.045	0.501	10.52	38.79	-1.33	28.68	43.90	35.48	
28_TSw2_Tptpln		165.59	65	20.86	0	5.977	0.020	0.502	12.72	41.36	0.57	23.51	56.27	23.71	0.22
28_TSw2_Tptpln	1	165.59	57	20.86	0	4.492	0.008	0.504	11.34	38.98	0.31	14.94	47.53	14.96	
28_TSw2_Tptpln	2	165.59	61	20.86	0	5.182	0.013	0.503	12.00	40.17	0.42	18.75	51.66	18.84	
28_TSw2_Tptpln	3	165.59	64	20.86	0	5.768	0.018	0.502	12.53	41.06	0.53	22.22	55.07	22.39	
28_TSw2_Tptpln	4	165.59	69	20.86	0	6.895	0.032	0.501	13.52	42.53	0.77	29.44	61.49	29.85	
28_TSw2_Tptpln	5	165.59	72	20.86	0	7.675	0.045	0.501	14.20	43.39	0.96	34.82	65.92	35.48	
Rock Mass Strength Properties for Lithophysal Rock Strata Units at the RHH Calculated Using Alternative Approach[5]															
		UDEC Calcs							UDEC Derived	UDEC Derived					Slot Test [6]
Lithophysal Rock Porosity—0%		**58.70**		**6.60**					**14.90**	**36.00**			**58.50**	**19.80**	
Lithophysal Rock and Rock Mass		13.20		5.00					3.90	29.00			14.00	9.30	Tptpul 0.20
Source: BSC 2004 [DIRS 172334], p. 6-92, Table 6.5-5		15.50		7.30					4.10	35.00			16.50	11.20	
		25.10		7.70					6.40	36.00			25.10	14.20	Tptpll 0.20 to 0.33
Lithophysal Rock Mass Categories	1												10.00	1.90	
	2												15.00	6.40	
Source: BSC 2004 [DIRS 172334], p. 6-105, Table 6.6-2	3												20.00	10.80	
	4												25.00	15.30	
	5												30.00	19.70	

Sources: Mapping and GSI data from DTNs: GS950508314224.003 [DIRS 107488]; GS000608314224.005 [DIRS 166002]; GS960408314224.001 [DIRS 168135]; GS960408314224.003 [DIRS 168136]; GS960708314224.009 [DIRS 168137]; GS000608314224.006 [DIRS 152572]; GS960908314224.015 [DIRS 108372]; GS960908314224.016 [DIRS 108373]; GS960908314224.017 [DIRS 108376]; GS970108314224.002 [DIRS 107490]; GS970208314224.004 [DIRS 107492]; GS970808314224.009 [DIRS 107494]; GS970808314224.011 [DIRS 107495]; GS970808314224.013 [DIRS 107497]; GS990408314224.003 [DIRS 108404]; GS990408314224.004 [DIRS 108405]; GS990408314224.005 [DIRS 108408]; GS990408314224.006 [DIRS 108409]; GS970608314224.007 [DIRS 158430].

Intact rock strength data are from DTNs: MO0311RCKPRPCS.003 [DIRS 166073]; MO0402DQRIRPPR.003 [DIRS 168901]; SN0208L0207502.001 [DIRS 161871]; SN0211L0207502.002 [DIRS 161872]; SN0302L0207502.003 [DIRS 165014]; SN0305L0207502.004 [DIRS 165013]; SN0306L0207502.008 [DIRS 165015]; SNL02030193001.001 [DIRS 120572]; SN0505L0212303.005 [DIRS 174956]; MO0401DQRIRPTS.003 [DIRS 168905].

NOTES:
1. Provided in this table are values of GENERAL rock mass strength data obtained using values of average parameters for individual lithostratigraphic units (Also see file in Appendix H: *Rock Mass Strength Parameters - All_Plus Porosity_Based Dat.xls*).
2. GSI values correspond to 5%, 20%, 40%, 70%, and 90% of cumulative frequency of occurrence in the tunnels.
3. Green GSI values represent an average for a particular lithostratigraphic unit.
4. Poisson's ratio taken as equal to the intact rock (see Appendix C).
5. Rock mass properties calculated using porosity as a surrogate parameter to develop the lithophysal rock mass strength properties.
6. Poisson's ratio data source: BSC 2004 [DIRS 172334], p. 6-127, Table 6.7-2.

6.4.4.5.2 Results of Calculations of Rock Mass Strength At and Above RHH

Full periphery tunnel mapping data gathered during tunnel construction for every 5 m tunnel segments and average values of uniaxial compressive strength representative of the rock occurring within each segment are used to calculate RMR and GSI values for Yucca Mountain tunnels. A range of GSI values sorted in an increasing order and a sum of cumulative value of GSI occurrence is plotted as a function of GSI value. A GSI frequency of occurrence curve is divided into five intervals and corresponding GSI values are determined, each representing one of the five categories of rock mass quality, where the category 1 represents the rock mass of the lowest strength whereas the category 5 represents the rock mass of the highest strength.

The range of rock mass quality values expressed in terms of GSI magnitude is used to delineate the bounds of rock mass behavior under in situ conditions and the rock quality is estimated in terms of five rock mass categories. The GSI values listed in Table 6-67 representing each of the five rock mass categories and average values of tensile and compressive strength tests carried out at standardized test conditions are used as input to the RocLab® software to calculate properties of the rock mass. The procedure for calculating the properties of rock mass using RocLab® software is identical for all lithostratigraphic units encountered and documented within the Yucca Mountain rock mass. The laboratory test data listed in Table 6-63 are entered into the RocLab® calculator along with values of GSI, each representing one of the rock mass categories listed in Table 6-67. The RocLab® software provides instant results in terms of rock mass parameters values. This process is repeated for all five rock mass categories and one additional case representing the average GSI value.

In fact, for each parameter, a set of five GSI values that represents a range of this rock mass parameter can collectively capture the rock mass variability within a particular unit of rock strata. This parameter range provides a basis for investigating the impact of the parameter value variability on the strength of rock mass and consequences of parameter change on the stability of structures excavated within a particular unit of rock strata.

The rock mass properties summarized in Table 6-76 represent a spectrum of rock mass types. The UCS of intact rock listed in the second column can be used as an indicator of rock mass strength. It indicates that among the same thermal-mechanical unit a range of rock strength can span up to two orders of magnitude. For example, the weakest among the strata are the PTn units, where the average UCS values range from 1.68 to 10 MPa. The corresponding RMR-based GSI values indicate the rock mass quality is in the range of fair to good.

Closed form solutions allow for calculating the magnitude of in situ stresses around underground excavations, while tunnel inspections may be able to make possible observing any unusual rock mass response. Calculations of stresses around the tunnel using a closed form formulation and comparisons of these stresses to the strength of rock mass at a particular depth serves as a "reality check" for the calculated values of rock mass strength.

Fracturing of the rock mass surrounding the tunnel causes stress redistribution around the tunnel until a new state of equilibrium is attained. Field evidence indicates that this initial stress redistribution resulted in the tunnel attaining a stable condition. This observation is indirectly confirmed by the fact that the tunnel section excavated through this weak rock remains stable,

even though it is supported only by the light ground support system. This system consisting of wire mesh, steel channels, and rockbolts, was installed during tunnel construction some 12 years ago, and unchanged since, and appears to perform its function well. Along these tunnel sections the rock appears to be stable, and to date, periodic tunnel inspections have not identified any observable evidence of rock deterioration or time-related damage.

The stable tunnel conditions suggest that the laboratory tests performed on fully saturated intact rock material might have been carried out under test conditions more severe than those encountered in the field (e.g., full saturation of specimens prior to testing, resulting in overly conservative estimates of rock mass strength). However, existing fractures testify to the fact that in situ stress and rock mass strength for a number of units are very close. Practically, this can be interpreted that although performance of the openings within various rock strata under static loading conditions is satisfactory, the same openings may display more extensive damage when subjected to seismic and thermal loading conditions.

Using available laboratory and field data and observations, rock mass parameters are developed based on information that integrates the laboratory and field measurements and observations. For the lithophysal units at RHH the effort of defining rock mass parameters extends one step further. Here the rock porosity is used as a surrogate parameter and rock mass properties are estimated using porosity as a common thread for determining the range of rock mass strength properties characterizing lithophysal units. Computer software, calibrated using the laboratory data, is used to further confirm the validity of the approach adopted in the calculations performed utilizing this alternative methodology.

The results of rock mass property calculations for the strata above the RHH are summarized in Table 6-76, which presents the rock mass strength parameters calculated using the RocLab® methodology only. Within the Table 6-76 content, the sequential numbering of strata is interrupted and some units are not included. This is because in this table the rock mass parameters are provided only for the strata for which required input, in terms of laboratory test data and GSI values derived from the tunnel mapping, was available.

Each set of data contains a set of parameters that characterize a range of rock mass properties, which can be used to describe the rock mass behavior in terms of the Hoek-Brown Classification, Hoek-Brown Criterion, Mohr-Coulomb Criterion, or simply in terms of familiar parameters including rock mass tensile and compressive strengths, modulus of elasticity and Poisson's ratio. It should be noted that Poisson's ratio for rock mass is typically taken to be the same as Poisson's ratio for intact rock.

Table 6-76 presents a summary of rock mass property data sets, each calculated for all five and one average rock mass quality categories. Listed in this table are parameters characterizing strata for which a minimum of sets with the required input parameters were available, as well as parameters characterizing rock strata at the RHH. It should be noted that a set of parameters characterizing Tptpul and Tptpll units is included in Table 6-76 for information only. A set of parameters characterizing rock mass for units at the RHH is included in Table 6-77. Included in this table are the properties of rock mass for nonlithophysal units Tptpmn and Tptpln extracted from the preceding Table 6-76 in addition to values of lithophysal rock mass parameters common for both the Tptpul and Tptpll units.

Traditionally, rock mass data analyses have concluded by assigning calculated rock mass properties as representative of one of the major thermal-mechanical units, i.e., UO, TCw, PTn, TSw1, and TSw2. When applying this traditional approach, properties of individual lithostratigraphic units are combined and their average values are used to represent properties of rock mass of the entire unit. In this report, this traditional methodology is refined, by treating each lithostratigraphic unit as an entity, hence providing more detailed account of properties characterizing individual rock strata. The results of rock mass calculations presented in Tables 6-76 and 6-77 provide the most complete set of rock mass properties to date. This detailed information allows for making more informed decisions in situations where the design of a structure excavated in a particular stratum can be optimized by utilizing the customized set of rock mass properties characterizing that particular rock mass unit only.

As a result, presentation of rock mass data in a form shown in Tables 6-76 and 6-77 allows for consistent and traceable selection of rock mass parameter values.

6.4.4.5.3 Results of Calculations of Rock Mass Strength At RHH

Rock stratum at the RHH is composed of four lithostratigraphic units: Tptpul, Tptpmn, Tptpll, and Tptpln, in descending order. As summarized in the preceding section, the properties of nonlithophysal rock mass are characterized by applying common mining and tunneling methodology. The methodology of determining properties of the lithophysal rock mass is based on using porosity as a common parameter in calculating strength and elastic moduli and by using laboratory, field data and observation, and state-of-the art software to establish, calibrate, and verify properties of the lithophysal rock mass.

Table 6-77 provides the summary of results of rock mass strength calculations using these two approaches. The data at the top tier portion of the table contains the RocLab®-calculated rock mass parameters for nonlithophysal units (Tptpmn and Tptpln) extracted from Table 6-76. The lower tier portion of Table 6-77 contains rock mass parameters calculated for the lithophysal units using an alternative approach. The values of rock mass parameters representing the lithophysal Tptpul and Tptpll units are listed in one group, as the methodology and data analysis discussed in Section 6.4.4.4.2.4 treats both units as belonging to and representing one lithophysal rock type.

The lithophysal rock mass data is presented in two subgroups. The upper subgroup contains the data derived from testing a computer-generated 1 m square synthetic specimen with properties that represent those of lithophysae-free intact rock material. By matching the results of this synthetic specimen with the performance of a real rock in the laboratory, the properties of this computer-generated rock are matched to replicate the performance of a real rock both in terms of strength and deformational characteristics. The subsequent specimen testing involves adding the voids that introduce porosities in the range similar to those encountered in the real rock. The computer-generated results are used to determine Mohr-Coulomb fit parameters c and ϕ. These results are also compared to results obtained from the large specimens tested in the laboratory and in the field to confirm and to verify that results obtained from computer calculations are reasonable in comparison to the real rock material.

Using large-core test data, the strength and modulus of elasticity of the lithophysal rock are established as functions of porosity and then the values of rock strength and elastic modulus corresponding to identical values of porosity are plotted together. Five rock mass categories are assigned to the arbitrarily selected values of rock mass strength from 10 to 30 MPa, and the corresponding elastic moduli are selected using the regression line as a function describing the relationship between these two parameters. Additional data analysis is performed to establish an upper and lower bound of lithophysal porosity associated with each rock mass category.

Two subgroups of parameters shown in the lower tier portion of Table 6-77, collectively characterize lithophysal rock mass strength and Young's modulus corresponding to one of the five rock mass categories. As a result, parameters derived for the lithophysal rock mass can be compared to those obtained using conventional method based on RMR techniques and field observations. The data summarized in Table 6-77 can be used in the design of excavations at the RHH and establishes a benchmark for the future refinements of rock mass strength of these rock units as more data become available.

6.4.4.6 Limitations and Uncertainties

The rock mass strength parameter estimates developed in this section are considered to represent reasonable values for the rock units at Yucca Mountain; however, these estimates may be affected by several uncertainties related to assumptions listed in Section 5.2, the input data and their interpretation. Discussed in Sections 6.4.4.6.1.1 to 6.4.4.6.1.5 are limitations and uncertainties that could potentially affect the results of this document.

6.4.4.6.1.1 Number and Representativeness of Specimens Tested

Typically, statistical samples for each type of test should include at least six specimens. On the other hand, Yucca Mountain stratigraphy includes a number of strata for which properties vary in magnitude and spatial distribution. In addition, specimen sizes range from 25.4 mm (1 in.) to 300 mm (12 in.) in diameter. These specimens with different diameter are also tested at various levels of saturation, ranging from fully saturated to room-dry to dry conditions. Some data sets include a substantial number of tests of similar type, while other test types are represented by a few tests. While the availability of various tests allows for a wide range of studies and comparisons, the limited number of test results indicates a need of specific test condition for rock mass characterization and requires more careful data interpretation. The differences from having a representative number of tests available in some strata and not in others cause some uncertainty in data interpretation.

6.4.4.6.1.2 Location of Intact Rock Samples

The rock samples from cores retrieved during exploratory drillings from different boreholes and varying depths were selected for testing at various times during the Site Characterization phase of the YMP. It is commonly known that rock properties obtained from the same geological unit may vary considerably even within short vertical distance. In the process of characterizing each lithostratigraphic zone, some zones were tested more extensively than other. This lack of standardized number of specimens for each test type results in higher uncertainty for units from which only few specimens were tested.

This source of uncertainty may result in a high degree of uncertainty in estimating rock strength. The consequence of varying degree of details associated with the extent of the testing program must be considered in the context of the future data uses. For example, insufficient characterization of a particular rock unit will have a much different implication if the data is used for the design of a tunnel or a shaft that penetrates that unit.

6.4.4.6.1.3 Time of Laboratory Tests

The results of laboratory tests are the resultant of a number of factors that contribute to the final value of rock strength and its elastic moduli. Factors such as the initial specimen weakening due to drilling, retrieval and storage, transportation, loss of moisture over storage time, and further weakening by re-exposing the specimen to water during saturation prior to testing may impact the results of tests. It is natural to expect that the most impacted are the rock samples obtained from the weakest units of rock strata. Although the method of specimen handling is usually uniform in any particular exploratory drilling program, the effect on specimens from rock strata displaying higher strength is much less severe than that for specimens obtained from the lower strength units. Consequently the uncertainty associated with time in characterizing these week units is of the largest consequence.

6.4.4.6.1.4 Testing Technique and Loading Procedure

Although the laboratory testing procedures for compressive strength tests are standardized, a potential source of uncertainty may originate from the capacity of the machine used for testing. While it is desirable for using machine of large capacity to test stronger rocks, it may pose a problem of accuracy for test results for specimens from weak strata units. For these weak units, the testing that occurs at the low end of the load range for a particular machine may result in a less precise determination of their strength. During a typical uniaxial compressive loading test, the test specimen rests on lower loading platen, which is slowly brought in contact with the upper platen until a small preload is applied. Depending on the machine capacity, this small preload may range from tens to hundreds of pounds. While for high-strength rock specimens this preload is rather small compared to the ultimate load at failure, the same load applied to the low strength specimens can be a significant proportion of the ultimate load at failure. Therefore, the uncertainty of test results measured from large-capacity test machine is greater for weaker rock types.

6.4.4.6.1.5 Impact of Lithophysal Voids on Test Results

In general, the rock strata at RHH of Yucca Mountain can be categorized into lithophysal or nonlithophysal units. This simple distinction is made between relatively common massive and/or fractured units and somewhat less common lithophysae-containing strata. The need to characterize this lithophysal rock brings into consideration both sampling and testing procedures. Since laboratory tests provide one of the major inputs into rock mass characterization, the attributes of sampling and resulting specimen size and shape are one of the major sources of uncertainty. Typically it is required that a specimen size is at least 10 times of grain size. Considering that the lithophysae is a constituent feature of the specimen and an average diameter of lithophysae is equal to 2 in., and if the thickness of the bridge connecting them is 1 in., then the minimum specimen diameter must be equal to 30 in. (0.76 m) approximately. The largest

specimens tested in the lithophysal zones are about a 12 in. (0.30 m) in diameter. In addition, the test on void-containing rock is not a subject of standardization, and impacts of voids on the distribution of stress within the specimen have not been studied adequately. These issues are all potential sources of uncertainty.

6.5 THERMAL PROPERTIES OF LITHOSTRATIGRAPHIC ROCK UNITS

6.5.1 Introduction

A distinctive feature of the nuclear waste repository design is to assess the performance of the repository subjected to a large amount of heat load generated by waste packages emplaced in emplacement drifts. The heat transport comprises the processes of heat transfer, fluid migration, phase changes, and volumetric changes. These processes are directly related to intact rock and rock mass thermal properties such as thermal conductivity, heat capacity, and thermal expansion.

Use of laboratory and field measurements to determine thermal properties of the Yucca Mountain Tuff has been a significant part of the YMP Site Characterization efforts due to the performance and design issues (DOE 1988 [DIRS 100282], Section 8.3.1.15). These measurements are crucial in providing not only the site-specific values of thermal properties but also the information of spatial variability, and their dependencies on temperature, porosity and/or fracture, and moisture content among other parameters and conditions.

These testing efforts have also assisted in development of theoretical simulations that describe a spatial correlation of thermal properties and a correlation between rock mass thermal properties, intact rock thermal properties, and other rock properties such as porosity and moisture content. Use of theoretical simulations to estimate rock mass thermal properties, for example thermal conductivity, is an important alternative to the field measurements when such measurements are either unfeasible or unavailable.

The data collected through March 2006 cover a number of lithostratigraphic zones of the Yucca Mountain Tuff. The majority of the data are for the RHH rock units including the Tptpul, Tptpmn, Tptpll and Tptpln zones. These four zones can be grouped into the lithophysal (Tptpul and Tptpll) and nonlithophysal (Tptpmn and Tptpln) rocks based on their dominant features of lithophysal voids and fractures, respectively. The dominant features of lithophysal rocks are the presence of large-scale air-filled voids, while those of nonlithophysal rocks are fractures.

Numerous laboratory tests using small specimens containing few voids and/or fractures show that intact rock thermal characteristics of these two types of rocks are similar (CRWMS M&O 1997 [DIRS 103564], Tables 5-11, 5-13, 5-15, and 5-16), indicating that similar methods may be used for acquiring intact rock thermal properties. However, rock mass characteristics of these rocks are quite different due to their different dominant features, large-scale lithophysae, or fractures. These impacting factors will be reflected in the difference in their rock mass thermal properties, suggesting the use of different methods of acquiring rock mass thermal properties for the lithophysal rocks versus those methods used for the nonlithophysal rocks.

In addition, theoretical simulations were performed to aid in describing the correlation between intact rock and rock mass thermal properties and the spatial variations.

6.5.1.1 Factors Impacting Thermal Rock Properties

Many parameters and conditions such as temperature, porosity, discontinuities, moisture content, specimen size or scale effect, mineral content, and loading condition may affect thermal properties. A brief discussion regarding the dependencies of thermal properties on these factors is provided below.

Temperature. Thermal properties of intact rock and rock mass are highly temperature dependent. This dependency is primarily related to mineralogical phase changes, liquid phase changes, and volumetric changes when the rocks experience variations in temperature. This may also include the effect of heating and cooling cycles because rock may behave differently during a heating phase than during a cooling phase. Heat and resulting changes in temperature due to waste emplacement play an important role in the physical processes in the rock mass surrounding the emplacement drifts. Understanding of the temperature effect on thermal properties has been an essential part of the investigation within the scope of YMP site characterization activities.

Porosity—A large number of voids exist in the Yucca Mountain Tuff. Most of these voids are air-filled and some of them, called lithophysae, are of large scale. Porosity, a measure of volumetric fraction of void space, in the lithophysal rock may be as high as 40% (BSC 2004 [DIRS 169854], Figure 6-5). Since the thermal energy transport rate and expansion are different in solid than in air, the porosity including both matrix and lithophysae will affect the effective thermal properties of rock mass, especially the lithophysal rock. According to the subsurface layout for the license application, about 81% of the emplacement drifts will be excavated in the Tptpll zone (BSC 2003 [DIRS 165572], Table II-2).

Discontinuities—Concerning effects of discontinuities (i.e., fractures and joints) are the effects of porosity on thermal properties when discontinuities are not completely closed, and when mineral deposits fill the opening. For instance, the sub-horizontal fractures of Tptpmn are filled with concentrations of vapor-phase minerals, primarily tridymite and cristobalite (Mongano et al. 1999 [DIRS 149850]), which have quite different thermal behaviors from the Tptpmn matrix material. However, if the discontinuities are completely closed and enclose no filling minerals, they may have insignificant effect on thermal energy transport and expansion.

Moisture Content—Moisture content contained in voids, measured in terms of degree of saturation, may also affect the effective thermal energy transport rate and expansion. This effect is sometime reflected in the dependency of thermal properties on temperature because pore water will experience phase changes at the boiling temperature, followed by a dry out in the rock. For instance, a dry rock has a lower thermal conductivity compared to a saturated or partially saturated rock since the air thermal conductivity is much lower than that of water.

Specimen Size or Scale Effect—The size dependency of thermal properties reflects the effect of heterogeneity or discontinuities in rock. With increasing size of rock specimens, the degree of heterogeneity or discontinuities increases as well and so does the effect on thermal properties. Investigation of the size effect may lead to an improved understanding of the effect of porosity or fracture on the rock mass effective thermal properties.

Mineral Content—The effect of mineralogy on thermal properties is related to phase change of minerals incorporated with temperature variation. For instance, the presence of certain minerals such as tridymite and cristobalite in welded tuffs instigates their phase changes at a certain "transition temperature" of approximately 175°C to 225°C (Brodsky et al. 1997 [DIRS 100653], Section 4.2.2.2). The phase changes of tridymite and cristobalite induce significant increase of thermal expansion coefficient among the welded tuffs. The effect of mineralogy on thermal properties could be considered a part of the temperature dependency on thermal properties.

Loading Condition—By definition, thermal properties are measured under stress-free conditions. However, in field thermal-mechanical measurements, rock mass is subjected to in situ confining stresses. Achieving a stress-free condition in the field test is hardly feasible, and in situ stress free thermal-mechanical data is not available in most field tests. The in situ stresses usually cause rock to deform, which in turn results in a reduction in fracture apertures or porosity, and are expected to mainly affect the thermal properties. Investigation of the loading condition effects should lead to an improved understanding of the effect of confining stresses on the rock mass thermal properties.

6.5.1.2 Addressing Uncertainties and Limitations

Uncertainties of a thermal property arise due to a lack of knowledge and understanding of the unique system where values of the property were obtained. Limitations of the thermal property are directly associated to the uncertainties of the property. Ideally, the limitations of the thermal property could be addressed and quantified by identifying the degree of the uncertainties.

Primary uncertainties of the rock thermal properties are originate from the factors affecting the rock thermal properties, based on degree of impact of the individual parameters and conditions. The factors impacting the rock thermal properties are associated with heterogeneity of a geologic rock mass and create significant variance of the thermal properties. Addressing uncertainties should consider both the impacting factors and the variance in the rock mass.

Uncertainties in laboratory measurements of thermal properties are relatively small since the measurements are conducted in a small rock sample under a controlled environment. Uncertainties related to the laboratory measurements are somewhat systematic and small compared to the field measurements. Errors in the laboratory measurements of thermal conductivity are often caused from equipment calibration, variations of test environment, and inconsistent operation of equipment. Since laboratory measurements of thermal conductivity were conducted under a controlled environmental condition, and equipment used was calibrated and operated to the requirements specified by test procedures or manufacturers, the uncertainties associated with measurements are relatively insignificant.

Uncertainties in field measurements are relatively high, since the impacting factors of the thermal properties and the heterogeneity of a rock mass directly impact the measured value. The impacting factors and the heterogeneity of a rock mass should be considered carefully in measuring the field values. One of the significant limitations of field measurements is feasibility of the field tests. In many geological materials, the field measurement is not feasible or very limited to the scale of the field test.

Analytical estimation of the rock mass thermal properties usually yields different uncertainties from those of field measurements. Estimated thermal properties are usually based on the geostatistically simulated rock properties. There is some degree of uncertainty in the determination of these properties because their simulations are conditioned to the measured data. For example, use of the well-log petrophysical measurements of bulk density and neutron porosity or those from the ECRB mapping may yield different estimates of the lithophysal porosity. These differences will consequently be carried over in the prediction of rock mass thermal conductivity. Since the physical system of porous media like the lithophysal and nonlithophysal rocks may or may not be accurately represented by the developed simulation, estimated rock mass thermal properties are often limited to upper and lower bounds, such as the dry and fully saturated wet conditions, which may not cover the range of application. Any errors in laboratory or field measurements of rock properties that are used in the estimates of rock mass thermal conductivity will also contribute to the uncertainty.

6.5.2 Thermal Properties for Intact Rock

6.5.2.1 Thermal Conductivity

A significant number of laboratory thermal conductivity tests using small specimens taken from the Yucca Mountain Tuff have been performed since the late 1990s under a fully qualified QA program (Brodsky et al. 1997 [DIRS 100653], p. ii). The majority of the tests were conducted by SNL and specimens were taken from various boreholes including UE25 NRG-4, UE25 NRG-5, USW NRG-6, USW NRG-7/7A, USW SD-7, USW SD-9, and USW SD-12 (BSC 2004 [DIRS 169854], Figure 4-1). Additional intact rock thermal conductivity tests were conducted on Tptpmn specimens taken from the SHT block and the DST area (BSC 2004 [DIRS 169900], Sections 6.2.1.3 and 6.3.1.3; DTNs: SNL22080196001.001 [DIRS 109722]; SNL22100196001.006 [DIRS 158213]; SN0203L2210196.007 [DIRS 158322]).

Supplementary tests of the intact rock thermal conductivity were performed on Tptpll specimens from various locations including the ECRB Cross-Drift thermal test hole cores. The supplementary tests were a part of the field thermal-testing program in the ECRB Cross-Drift and examined effects of temperature, saturation, and artificial porosity on the intact rock thermal conductivity. Details of the intact rock thermal conductivity data were presented in DTN: SN0209L01A1202.001 [DIRS 163601].

The laboratory thermal conductivity measurements obtained by SNL were conducted using a guarded heat flow meter following the SNL technical procedure TP-202, Revision 01, *Measurement of Thermal Conductivity of Geologic Specimens Using the Guarded Heat-Flow Meter Method* [DIRS 108553]. The specimens were either air dry, oven dry, vacuum saturated, or partially saturated. Tests were conducted over a temperature range of 30°C to 300°C (Brodsky et al. 1997 [DIRS 100653], Abstract). The laboratory thermal conductivity was calculated using Equation 6-31 (Holman 1997 [DIRS 101978], Equation 1-1).

$$\frac{\Delta Q}{\Delta t} = -kA\frac{\Delta T}{\Delta x} \qquad \text{(Eq. 6-31)}$$

where $\Delta Q/\Delta t$ is the heat transfer rate, $\Delta T/\Delta x$ is the temperature gradient in the direction of the heat flow, A is the cross-sectional area, and k is the thermal conductivity of the material.

Detailed descriptions of the intact rock thermal conductivity measurements and data were presented in Brodsky et al. (1997 [DIRS 100653], Sections 3.1 and 4.1) and *Yucca Mountain Site Geotechnical Report* (CRWMS M&O 1997 [DIRS 103564], Section 5.2.1).

6.5.2.1.1 Summary of Intact Rock Thermal Conductivity

A summary of the intact rock thermal conductivity measurements for the oven-dried specimens is presented in Table 6-78, while Table 6-79 shows the intact rock thermal conductivities of the saturated specimens. The intact thermal conductivity of the two main repository zones, Tptpmn and Tptpll, are provided in Figure 6-119, which exhibits only minor differences in their mean intact dry and wet thermal conductivities. The intact dry thermal conductivity with 95% confidence intervals substantiates minor differences (Figure 6-120), while Figure 6-121 displays some differences in the 95% confidence intervals between their intact wet thermal conductivities. In spite of the 95% confidence interval differences in the wet thermal conductivities, the intact thermal conductivities of the Tptpmn and Tptpll could be interpreted as very similar.

Table 6-78. Intact Rock Thermal Conductivity of Oven-Dried Specimens

Stratigraphic Unit	Intact Rock Thermal Conductivity (W/m-K), Oven-Dried							
	°C	30-50	50-70	~110	~150	~200	~250	~290
Crystal-Rich Tiva/Post-Tiva Canyon Tuff (Tpcr)	Count	12	6	12	12	12	12	9
	Mean+1 SD	1.14+0.35	1.22+0.38	1.50+0.18	1.54+0.19	1.53+0.18	1.53+0.17	1.55+0.14
	Mean+1 SD%	1.14+30.6%	1.22+31.2%	1.50+12.3%	1.54+12.2%	1.53+12.0%	1.53+11.4%	1.55+9.1%
	Mean+1 SE	1.14+0.10	1.22+0.16	1.50+0.05	1.54+0.05	1.53+0.05	1.53+0.05	1.55+0.05
	Mean+1 SE%	1.14+8.8%	1.22+12.7%	1.50+3.6%	1.54+3.5%	1.53+3.5%	1.53+3.3%	1.55+3.0%
	Median	1.12	1.18	1.52	1.555	1.545	1.54	1.56
	Minimum	0.73	0.81	1.16	1.18	1.18	1.19	1.21
	Maximum	1.70	1.73	1.79	1.82	1.81	1.8	1.69
Tpcpv2	Count	3	2	2	2	2	2	1
	Mean+1 SD	0.57+0.02	0.60+0.01	0.75+0.01	0.79+0.01	0.81+0.01	0.83+0.00	0.85+n/a
	Mean+1 SD%	0.57+2.7%	0.60+1.2%	0.75+0.9%	0.79+1.8%	0.81+1.7%	0.83+0.0%	0.85+n/a
	Mean+1 SE	0.57+0.01	0.60+0.00	0.75+0.01	0.79+0.01	0.81+0.01	0.83+0.00	0.85+n/a
	Mean+1 SE%	0.57+1.5%	0.60+0.8%	0.75+0.7%	0.79+1.3%	0.81+1.2%	0.83+0.0%	0.85+n/a
	Median	0.57	0.595	0.745	0.79	0.81	0.83	0.85
	Minimum	0.56	0.59	0.74	0.78	0.8	0.83	0.85
	Maximum	0.59	0.6	0.75	0.8	0.82	0.83	0.85
Tpcpv1	Count	5	3	4	4	4	4	3
	Mean+1 SD	0.42+0.01	0.44+0.02	0.43+0.00	0.46+0.00	0.48+0.01	0.49+0.00	0.51+0.01
	Mean+1 SD%	0.42+3.1%	0.44+3.4%	0.43+1.2%	0.46+1.1%	0.48+2.1%	0.49+1.0%	0.51+1.1%
	Mean+1 SE	0.42+0.01	0.44+0.01	0.43+0.00	0.46+0.00	0.48+0.00	0.49+0.00	0.51+0.00
	Mean+1 SE%	0.42+1.4%	0.44+2.0%	0.43+0.6%	0.46+0.5%	0.48+1.1%	0.49+0.5%	0.51+0.7%
	Median	0.42	0.44	0.43	0.46	0.47	0.49	0.51
	Minimum	0.41	0.43	0.43	0.46	0.47	0.49	0.5
	Maximum	0.44	0.46	0.44	0.47	0.49	0.5	0.51
Tpbt4	Count	2	3	2	2	2	2	1
	Mean+1 SD	0.34+0.00	0.35+0.01	0.32+0.00	0.33+0.00	0.35+0.00	0.36+0.00	0.37+n/a

Table 6-78. Intact Rock Thermal Conductivity of Oven-Dried Specimens (Continued)

Stratigraphic Unit	Intact Rock Thermal Conductivity (W/m-K), Oven-Dried							
	°C	30-50	50-70	~110	~150	~200	~250	~290
Tpbt4	Mean+1 SD%	0.34+0.0%	0.35+1.6%	0.32+0.0%	0.33+0.0%	0.35+0.0%	0.36+0.0%	0.37+n/a
	Mean+1 SE	0.34+0.00	0.35+0.00	0.32+0.00	0.33+0.00	0.35+0.00	0.36+0.00	0.37+n/a
	Mean+1 SE%	0.34+0.0%	0.35+0.9%	0.32+0.0%	0.33+0.0%	0.35+0.0%	0.36+0.0%	0.37+n/a
	Median	0.34	0.35	0.32	0.33	0.35	0.36	0.37
	Minimum	0.34	0.35	0.32	0.33	0.35	0.36	0.37
	Maximum	0.34	0.36	0.32	0.33	0.35	0.36	0.37
Yucca Mountain Tuff (Tpy)	Count	3	2	2	2	2	2	1
	Mean+1 SD	0.39+0.02	0.42+0.01	0.44+0.02	0.47+0.02	0.48+0.02	0.49+0.02	0.48+n/a
	Mean+1 SD%	0.39+3.9%	0.42+1.7%	0.44+4.9%	0.47+4.6%	0.48+4.5%	0.49+4.4%	0.48+n/a
	Mean+1 SE	0.39+0.01	0.42+0.00	0.44+0.02	0.47+0.02	0.48+0.02	0.49+0.02	0.48+n/a
	Mean+1 SE%	0.39+2.2%	0.42+1.2%	0.44+3.4%	0.47+3.2%	0.48+3.2%	0.49+3.1%	0.48+n/a
	Median	0.39	0.415	0.435	0.465	0.475	0.485	0.48
	Minimum	0.38	0.41	0.42	0.45	0.46	0.47	0.48
	Maximum	0.41	0.42	0.45	0.48	0.49	0.5	0.48
Pah Canyon (Tpp)	Count	10	8	8	8	8	8	5
	Mean+1 SD	0.34+0.04	0.32+0.08	0.33+0.02	0.35+0.02	0.37+0.02	0.38+0.02	0.38+0.02
	Mean+1 SD%	0.34+12.2%	0.32+25.4%	0.33+6.4%	0.35+6.2%	0.37+5.5%	0.38+5.3%	0.38+5.8%
	Mean+1 SE	0.34+0.01	0.32+0.03	0.33+0.01	0.35+0.01	0.37+0.01	0.38+0.01	0.38+0.01
	Mean+1 SE%	0.34+3.9%	0.32+9.0%	0.33+2.3%	0.35+2.2%	0.37+1.9%	0.38+1.9%	0.38+2.6%
	Median	0.35	0.355	0.33	0.35	0.36	0.37	0.36
	Minimum	0.23	0.18	0.31	0.33	0.34	0.35	0.36
	Maximum	0.37	0.38	0.36	0.39	0.39	0.4	0.4
Tpbt2	Count	4	4	4	4	4	4	3
	Mean+1 SD	0.28+0.10	0.33+0.11	0.30+0.06	0.32+0.06	0.33+0.06	0.34+0.06	0.33+0.06
	Mean+1 SD%	0.28+35.8%	0.33+33.8%	0.30+20.3%	0.32+19.1%	0.33+17.9%	0.34+17.3%	0.33+16.9%
	Mean+1 SE	0.28+0.05	0.33+0.06	0.30+0.03	0.32+0.03	0.33+0.03	0.34+0.03	0.33+0.03
	Mean+1 SE%	0.28+17.9%	0.33+16.9%	0.30+10.1%	0.32+9.6%	0.33+8.9%	0.34+8.7%	0.33+9.7%
	Median	0.28	0.38	0.305	0.32	0.325	0.335	0.3
	Minimum	0.18	0.16	0.24	0.26	0.27	0.28	0.29
	Maximum	0.36	0.38	0.36	0.37	0.38	0.39	0.39
Tptrn	Count	27	20	29	29	29	29	20
	Mean+1 SD	0.95+0.29	0.94+0.28	1.14+0.13	1.18+0.13	1.18+0.13	1.17+0.12	1.17+0.11
	Mean+1 SD%	0.95+30.0%	0.94+29.6%	1.14+11.0%	1.18+11.0%	1.18+10.7%	1.17+10.1%	1.17+9.5%
	Mean+1 SE	0.95+0.05	0.94+0.06	1.14+0.02	1.18+0.02	1.18+0.02	1.17+0.02	1.17+0.02
	Mean+1 SE%	0.95+5.8%	0.94+6.6%	1.14+2.0%	1.18+2.0%	1.18+2.0%	1.17+1.9%	1.17+2.1%
	Median	0.82	0.815	1.16	1.2	1.2	1.17	1.17
	Minimum	0.55	0.62	0.89	0.92	0.93	0.95	0.97
	Maximum	1.49	1.54	1.36	1.39	1.4	1.4	1.41
Tptrl	Count	1	2	1	1	1	1	1
	Mean+1 SD	1.20+n/a	1.23+0.01	1.29+n/a	1.33+n/a	1.34+n/a	1.31+n/a	1.26+n/a
	Mean+1 SD%	1.20+n/a	1.23+1.1%	1.29+n/a	1.33+n/a	1.34+n/a	1.31+n/a	1.26+n/a
	Mean+1 SE	1.20+n/a	1.23+0.01	1.29+n/a	1.33+n/a	1.34+n/a	1.31+n/a	1.26+n/a
	Mean+1 SE%	1.20+n/a	1.23+0.8%	1.29+n/a	1.33+n/a	1.34+n/a	1.31+n/a	1.26+n/a
	Median	1.2	1.23	1.29	1.33	1.34	1.31	1.26
	Minimum	1.2	1.22	1.29	1.33	1.34	1.31	1.26

Table 6-78. Intact Rock Thermal Conductivity of Oven-Dried Specimens (Continued)

Stratigraphic Unit	Intact Rock Thermal Conductivity (W/m-K), Oven-Dried							
	°C	30-50	50-70	~110	~150	~200	~250	~290
Tptrl	Maximum	1.2	1.24	1.29	1.33	1.34	1.31	1.26
Tptpul	Count	1	2	3	3	3	3	2
	Mean+1 SD	1.08+n/a	1.08+0.01	1.23+0.27	1.25+0.27	1.26+0.26	1.25+0.25	1.16+0.29
	Mean+1 SD%	1.08+n/a	1.08+1.3%	1.23+22.4%	1.25+21.7%	1.26+20.2%	1.25+19.7%	1.16+25.1%
	Mean+1 SE	1.08+n/a	1.08+0.01	1.23+0.16	1.25+0.16	1.26+0.15	1.25+0.14	1.16+0.21
	Mean+1 SE%	1.08+n/a	1.08+0.9%	1.23+12.9%	1.25+12.5%	1.26+11.7%	1.25+11.4%	1.16+17.7%
	Median	1.08	1.08	1.37	1.39	1.38	1.37	1.155
	Minimum	1.08	1.07	0.91	0.94	0.97	0.97	0.95
	Maximum	1.08	1.09	1.4	1.43	1.44	1.42	1.36
Tptpmn	Count	67	66	66	65	66	32	20
	Mean+1 SD	1.49+0.37	1.59+0.33	1.57+0.26	1.60+0.25	1.60+0.25	1.52+0.25	1.52+0.22
	Mean+1 SD%	1.49+24.6%	1.59+20.7%	1.57+16.5%	1.60+15.9%	1.60+15.4%	1.52+16.4%	1.52+14.7%
	Mean+1 SE	1.49+0.04	1.59+0.04	1.57+0.03	1.60+0.03	1.60+0.03	1.52+0.04	1.52+0.05
	Mean+1 SE%	1.49+3.0%	1.59+2.5%	1.57+2.0%	1.60+2.0%	1.60+1.9%	1.52+2.9%	1.52+3.3%
	Median	1.57	1.6	1.65	1.68	1.68	1.615	1.57
	Minimum	0.14	0.18	0.23	0.29	0.37	0.83	0.85
	Maximum	2.2	2.25	1.91	1.85	1.82	1.81	1.76
Tptpll	Count	44	79	42	42	42	4	3
	Mean+1 SD	1.71+0.27	1.73+0.26	1.71+0.24	1.71+0.21	1.69+0.21	1.54+0.03	1.49+0.05
	Mean+1 SD%	1.71+15.9%	1.73+14.9%	1.71+13.7%	1.71+12.4%	1.69+12.1%	1.54+2.0%	1.49+3.4%
	Mean+1 SE	1.71+0.04	1.73+0.03	1.71+0.04	1.71+0.03	1.69+0.03	1.54+0.02	1.49+0.03
	Mean+1 SE%	1.71+2.4%	1.73+1.7%	1.71+2.1%	1.71+1.9%	1.69+1.9%	1.54+1.0%	1.49+1.9%
	Median	1.8	1.8	1.8	1.8	1.8	1.535	1.5
	Minimum	0.9	0.9	0.9	1	1	1.5	1.44
	Maximum	2.1	2.1	2	1.9	1.9	1.57	1.54
Calico	Count	6	6	6	6	6	n/a	n/a
	Mean+1 SD	0.47+0.03	0.52+0.03	0.57+0.03	0.60+0.03	0.64+0.03	n/a	n/a
	Mean+1 SD%	0.47+6.8%	0.52+5.3%	0.57+5.3%	0.60+5.0%	0.64+4.9%	n/a	n/a
	Mean+1 SE	0.47+0.01	0.52+0.01	0.57+0.01	0.60+0.01	0.64+0.01	n/a	n/a
	Mean+1 SE%	0.47+2.8%	0.52+2.2%	0.57+2.2%	0.60+2.0%	0.64+2.0%	n/a	n/a
	Median	0.47	0.515	0.57	0.6	0.65	n/a	n/a
	Minimum	0.43	0.49	0.53	0.56	0.59	n/a	n/a
	Maximum	0.52	0.56	0.61	0.64	0.67	n/a	n/a

Sources: DTNs: SNL01A05059301.005 [DIRS 109002]; SNL22100196001.002 [DIRS 153138]; SNL22080196001.001 [DIRS 109722]; SN0209L01A1202.001 [DIRS 163601].

NOTE: Stratigraphic units were obtained by comparing the samples to unit contacts in DTN: MO0004QGFMPICK.000 [DIRS 152554].

Data below the Calico unit are not included in this table.

Table 6-79. Intact Rock Thermal Conductivity of Saturated Specimens

Stratigraphic Unit	Intact Rock Thermal Conductivity (W/m-K), Saturated			
	°C	~30	~50	~70
Crystal-Rich Tiva/Post-Tiva Canyon Tuff (Tpcr)	Count	6	6	6
	Mean+1 SD	1.79+0.08	1.96+0.09	1.92+0.12
	Mean+1 SD%	1.79+4.2%	1.96+4.8%	1.92+6.0%
	Mean+1 SE	1.79+0.03	1.96+0.04	1.92+0.05
	Mean+1 SE%	1.79+1.7%	1.96+2.0%	1.92+2.5%
	Minimum	1.66	1.81	1.71
	Maximum	1.89	2.04	2.04
Tpcpv2	Count	2	2	1
	Mean+1 SD	1.03+0.00	1.13+0.01	1.20+n/a
	Mean+1 SD%	1.03+0.0%	1.13+0.6%	1.20+n/a
	Mean+1 SE	1.03+0.00	1.13+0.00	1.20+n/a
	Mean+1 SE%	1.03+0.0%	1.13+0.4%	1.20+n/a
	Minimum	1.03	1.12	1.20
	Maximum	1.03	1.13	1.20
Tpcpv1	Count	3	3	2
	Mean+1 SD	0.83+0.06	0.92+0.05	1.03+0.02
	Mean+1 SD%	0.83+7.3%	0.92+5.2%	1.03+2.1%
	Mean+1 SE	0.83+0.04	0.92+0.03	1.03+0.02
	Mean+1 SE%	0.83+4.2%	0.92+3.0%	1.03+1.5%
	Minimum	0.79	0.88	1.01
	Maximum	0.90	0.97	1.04
Tpbt4	Count	2	2	1
	Mean+1 SD	0.79+0.02	0.87+0.01	0.95+n/a
	Mean+1 SD%	0.79+2.7%	0.87+1.6%	0.95+n/a
	Mean+1 SE	0.79+0.02	0.87+0.01	0.95+n/a
	Mean+1 SE%	0.79+1.9%	0.87+1.1%	0.95+n/a
	Minimum	0.77	0.86	0.95
	Maximum	0.80	0.88	0.95
Yucca Mountain Tuff (Tpy)	Count	2	2	1
	Mean+1 SD	0.91+0.00	0.99+0.01	1.04+n/a
	Mean+1 SD%	0.91+0.0%	0.99+0.7%	1.04+n/a
	Mean+1 SE	0.91+0.00	0.99+0.00	1.04+n/a
	Mean+1 SE%	0.91+0.0%	0.99+0.5%	1.04+n/a
	Minimum	0.91	0.98	1.04
	Maximum	0.91	0.99	1.04
Pah Canyon (Tpp)	Count	3	3	2
	Mean+1 SD	0.76+0.05	0.83+0.09	0.89+0.13
	Mean+1 SD%	0.76+6.5%	0.83+11.4%	0.89+15.2%
	Mean+1 SE	0.76+0.03	0.83+0.05	0.89+0.09
	Mean+1 SE%	0.76+3.8%	0.83+6.6%	0.89+10.7%
	Minimum	0.70	0.72	0.79
	Maximum	0.79	0.90	0.98

Table 6-79 Intact Rock Thermal Conductivity of Saturated Specimens (Continued)

Stratigraphic Unit	Intact Rock Thermal Conductivity (W/m-K), Saturated			
	°C	~30	~50	~70
Tpbt2	Count	2	2	2
	Mean+1 SD	0.80+0.25	0.80+0.18	0.86+0.18
	Mean+1 SD%	0.80+31.1%	0.80+22.2%	0.86+20.7%
	Mean+1 SE	0.80+0.18	0.80+0.13	0.86+0.13
	Mean+1 SE%	0.80+22.0%	0.80+15.7%	0.86+14.6%
	Minimum	0.62	0.67	0.73
	Maximum	0.97	0.92	0.98
Tptrv2	Count	2	2	1
	Mean+1 SD	0.98+0.01	1.05+0.00	1.13+n/a
	Mean+1 SD%	0.98+0.7%	1.05+0.0%	1.13+n/a
	Mean+1 SE	0.98+0.01	1.05+0.00	1.13+n/a
	Mean+1 SE%	0.98+0.5%	1.05+0.0%	1.13+n/a
	Minimum	0.97	1.05	1.13
	Maximum	0.98	1.05	1.13
Tptrn	Count	12	12	11
	Mean+1 SD	1.55+0.15	1.63+0.10	1.66+0.10
	Mean+1 SD%	1.55+9.5%	1.63+6.1%	1.66+6.2%
	Mean+1 SE	1.55+0.04	1.63+0.03	1.66+0.03
	Mean+1 SE%	1.55+2.8%	1.63+1.8%	1.66+1.9%
	Minimum	1.34	1.45	1.49
	Maximum	1.76	1.80	1.82
Tptrl	Count	1	1	1
	Mean	1.64	1.69	1.7
Tptpul	Count	2	2	2
	Mean+1 SD	2.07+0.14	2.04+0.12	1.99+0.08
	Mean+1 SD%	2.07+6.8%	2.04+5.9%	1.99+3.9%
	Mean+1 SE	2.07+0.10	2.04+0.09	1.99+0.06
	Mean+1 SE%	2.07+4.8%	2.04+4.2%	1.99+2.8%
	Minimum	1.97	1.95	1.93
	Maximum	2.17	2.12	2.04
Tptpmn	Count	35	35	35
	Mean+1 SD	2.20+0.35	2.19+0.32	2.14+0.31
	Mean+1 SD%	2.20+15.9%	2.19+14.4%	2.14+14.2%
	Mean+1 SE	2.20+0.06	2.19+0.05	2.14+0.05
	Mean+1 SE%	2.20+2.7%	2.19+2.4%	2.14+2.4%
	Minimum	1.56	1.65	1.66
	Maximum	3.57	3.36	3.09

Table 6-79 Intact Rock Thermal Conductivity of Saturated Specimens (Continued)

Stratigraphic Unit	Intact Rock Thermal Conductivity (W/m-K), Saturated			
	°C	~30	~50	~70
Tptpll	Count	41	41	41
	Mean+1 SD	2.14+0.17	2.13+0.15	2.11+0.14
	Mean+1 SD%	2.14+7.9%	2.13+7.2%	2.11+6.8%
	Mean+1 SE	2.14+0.03	2.13+0.02	2.11+0.02
	Mean+1 SE%	2.14+1.2%	2.13+1.1%	2.11+1.1%
	Minimum	1.80	1.80	1.80
	Maximum	2.50	2.40	2.40

Sources: DTNs: SNL01A05059301.005 [DIRS 109002]; SN0203L2210196.007 [DIRS 158322]; SN0209L01A1202.001 [DIRS 163601].

NOTE: Stratigraphic units were obtained by comparing the samples to unit contacts in DTN: MO0004QGFMPICK.000 [DIRS 152554].

Data below Tptpll unit are not included in this table.

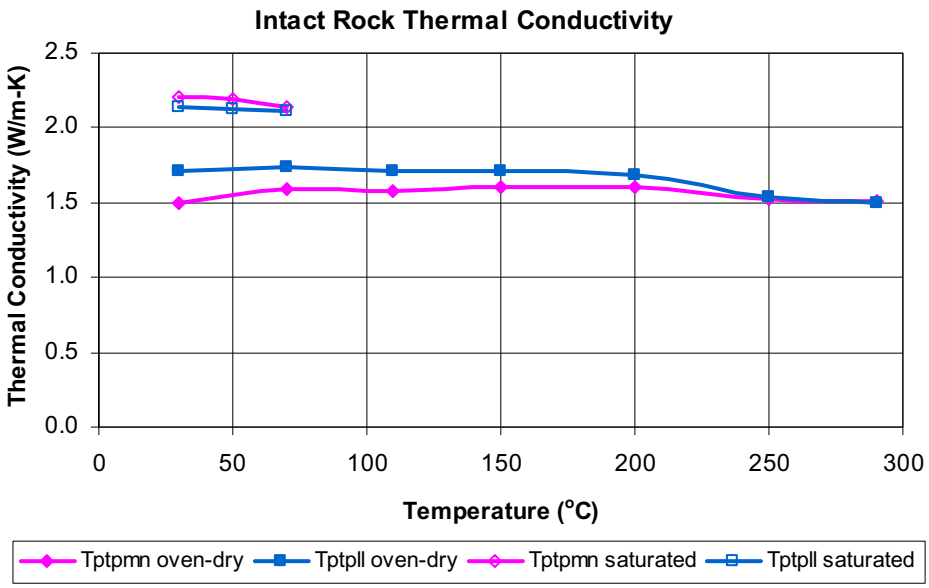

Sources: DTNs: SNL01A05059301.005 [DIRS 109002]; SNL22100196001.002 [DIRS 153138]; SN0203L2210196.007 [DIRS 158322]; SN0209L01A1202.001 [DIRS 163601]; SNL22080196001.001 [DIRS 109722].

Figure 6-119. Intact Dry and Wet Thermal Conductivity of Tptpmn and Tptpll Zones

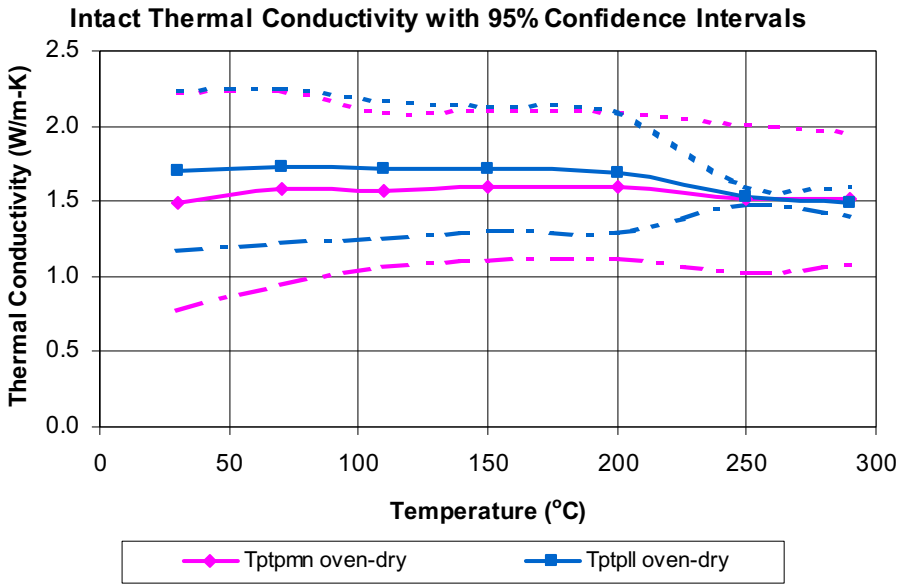

Sources: DTNs: SNL01A05059301.005 [DIRS 109002]; SNL22100196001.002 [DIRS 153138]; SN0203L2210196.007 [DIRS 158322]; SN0209L01A1202.001 [DIRS 163601]; SNL22080196001.001 [DIRS 109722].

Figure 6-120. Intact Dry Thermal Conductivity of Tptpmn and Tptpll Zones with 95% Confidence Intervals (1.96 Times of the Standard Deviations)

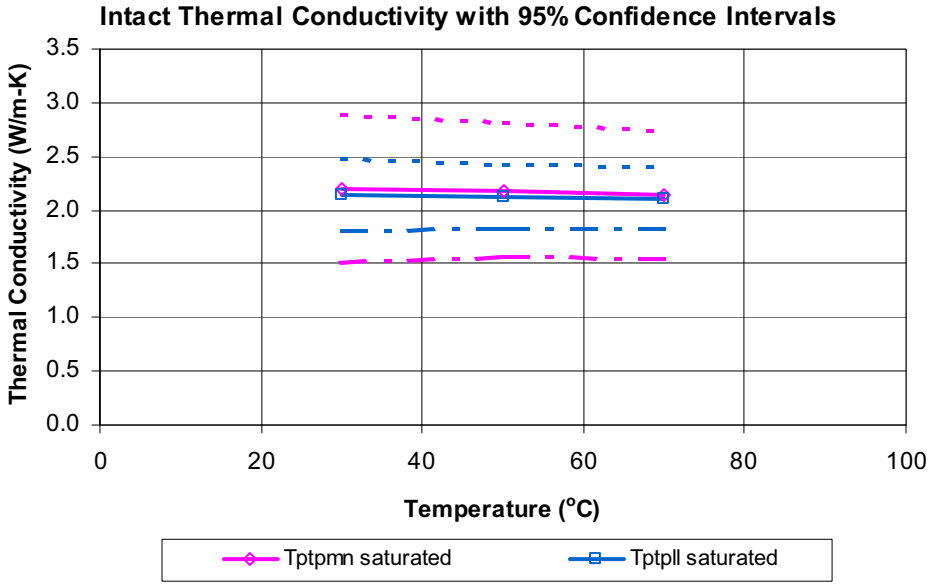

Sources: DTNs: SNL01A05059301.005 [DIRS 109002]; SNL22100196001.002 [DIRS 153138]; SN0203L2210196.007 [DIRS 158322]; SN0209L01A1202.001 [DIRS 163601]; SNL22080196001.001 [DIRS 109722].

Figure 6-121. Intact Wet Thermal Conductivity of Tptpmn and Tptpll Zones with 95 % Confidence Intervals (1.96 Times of the Standard Deviations)

The sensitivity of intact rock thermal conductivity to temperature, porosity, moisture content, and specimen size has been evaluated based on these laboratory tests. The evaluation was carried out by comparing the results of tests on specimens at these different conditions. Measured data presented in most test reports and the TDMS are grouped according to either the thermal-mechanical or lithostratigraphic zone for each saturation state or specimen size. For each rock zone, saturation state, or specimen size, the data are presented as a function of temperature. Statistical analyses of the data within each group have been limited to the information of mean and standard deviation about the mean. The evaluation could provide valuable information regarding the uncertainties and limitations of the intact rock thermal conductivity data.

Effect of Temperature—Intact rock thermal conductivity for oven-dried specimens either increases or remains constant with increasing temperature (Brodsky et al. 1997 [DIRS 100653], Section 4.1; CRWMS M&O 1997 [DIRS 103564], Section 5.2.1). Dry thermal conductivity of Tptpll specimen NRG-6-987 is presented in Figure 6-122. The thermal conductivity of the oven-dried sample increases with increasing temperature up to 160ºC and decreases slightly with temperatures beyond 160ºC. Decreases in thermal conductivity with increasing temperature as observed in saturated specimens are attributed to dehydration (Figures 6-119 and 6-120). Increases in thermal conductivity observed for temperatures up to 160°C for oven-dried specimens might be associated with the vaporization of remaining water. Thermal conductivity increases with temperature for plagioclase and glasses; however, it decreases with temperature for quartz (Lappin 1980 [DIRS 102973], Figure 3). Overall, if constant moisture content is maintained during a test, the effect of temperature on intact rock thermal conductivity may be insignificant. This was observed in over hundreds of tests using specimens taken from both the lithophysal and nonlithophysal rocks (Brodsky et al. 1997 [DIRS 100653], Section 4.1; BSC 2004 [DIRS 169900], Sections 6.2.1.3 and 6.3.1.3; DTN: SN0209L01A1202.001 [DIRS 163601]). Table 6-80 presents averaged values of the oven-dried samples and saturated thermal conductivity of the Tptpmn zone from data in Tables 6-78 and 6-79.

Effect of Porosity—Investigations on the effect of porosity on thermal conductivity have been performed on the lithophysal rock. In addition to the previous borehole specimen data (DTN: SNL01A05059301.005 [DIRS 109002]), more tests have been conducted on the Tptpll core specimens obtained from the ECRB. The measurements data indicate that intact rock thermal conductivity decreases with increasing natural or matrix porosity for both saturated and oven-dried specimens, as shown in Figure 6-123 (DTN: SN0209L01A1202.001 [DIRS 163601], Tables 6, 7, 8, and 9).

The effects of porosity on thermal conductivity of the Tptpll rock were further investigated by artificial porosity tests on the oven-dried specimens that were drilled to add up to 9% additional artificial porosity (DTN: SN0209L01A1202.001 [DIRS 163601], Tables 10 and 11). The artificial porosity results indicate that thermal conductivity decreases between 0.5 to 0.65 W/m·K per 10% increases in porosity over a limited range of porosity.

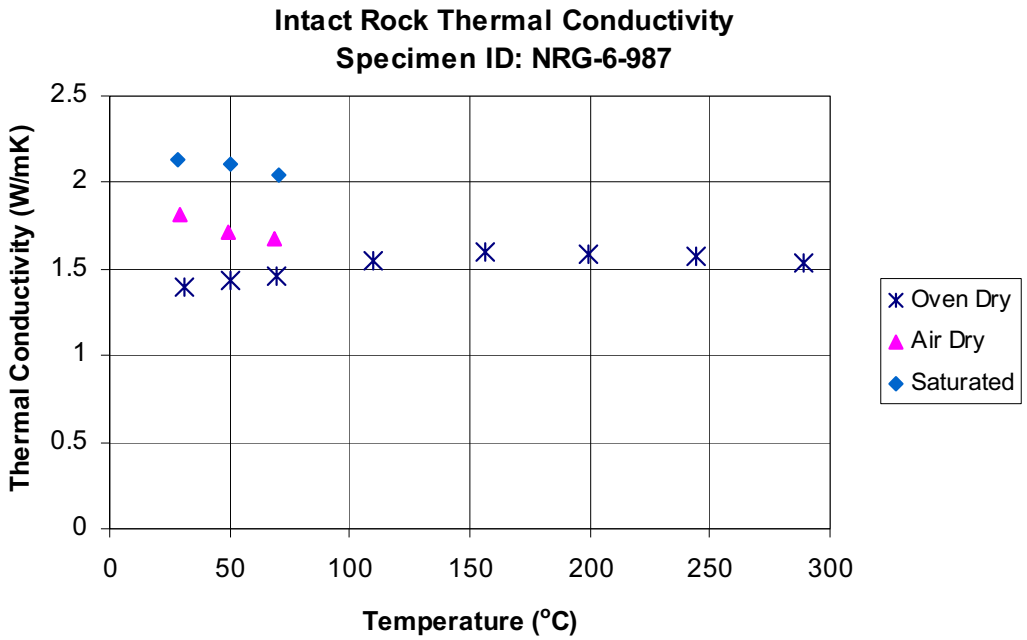

Source: DTN: SNL01A05059301.005 [DIRS 109002].

Figure 6-122. Thermal Conductivity for Tptpll Specimens NGR-6-987.0-SNL-A (Saturated) and NGR-6-987.0-SNL-B (Air and Oven Dried)

Table 6-80. Thermal Conductivities for Oven-Dried and Saturated Specimens from Tptpmn for Repository Zones

Intact Rock Thermal Conductivity (W/mk); Oven Dried							
°C	30-50	50-70	~110	~150	~200	~250	~290
Count	67	66	66	65	66	32	20
Mean+1 SD	1.49+0.37	1.59+0.33	1.57+0.26	1.60+0.25	1.60+0.25	1.52+0.25	1.52+0.22
Mean+1 SD%	1.49+24.6%	1.59+20.7%	1.57+16.5%	1.60+15.9%	1.60+15.4%	1.52+16.4%	1.52+14.7%
Mean+1 SE	1.49+0.04	1.59+0.04	1.57+0.03	1.60+0.03	1.60+0.03	1.52+0.04	1.52+0.05
Mean+1 SE%	1.49+3.0%	1.59+2.5%	1.57+2.0%	1.60+2.0%	1.60+1.9%	1.52+2.9%	1.52+3.3%
Median	1.57	1.60	1.65	1.68	1.68	1.62	1.57
Minimum	0.14	0.18	0.23	0.29	0.37	0.83	0.85
Maximum	2.20	2.25	1.91	1.85	1.82	1.81	1.76
Intact Rock Thermal Conductivity (W/mk); Saturated							
°C	~30	~50	~70	NA	NA	NA	NA
Count	35	35	35	NA	NA	NA	NA
Mean+1 SD	2.20+0.35	2.19+0.32	2.14+0.31	NA	NA	NA	NA
Mean+1 SD%	2.20+15.9%	2.19+14.4%	2.14+14.2%	NA	NA	NA	NA
Mean+1 SE	2.20+0.06	2.19+0.05	2.14+0.05	NA	NA	NA	NA
Mean+1 SE%	2.20+2.7%	2.19+2.4%	2.14+2.4%	NA	NA	NA	NA
Median	2.14	2.13	2.11	NA	NA	NA	NA
Minimum	1.56	1.65	1.66	NA	NA	NA	NA
Maximum	3.57	3.36	3.09	NA	NA	NA	NA

Sources: DTNs: SNL01A05059301.005 [DIRS 109002]; SNL22100196001.002 [DIRS 153138]; SN0203L2210196.007 [DIRS 158322]; SN0209L01A1202.001 [DIRS 163601]; SNL22080196001.001 [DIRS 109722].

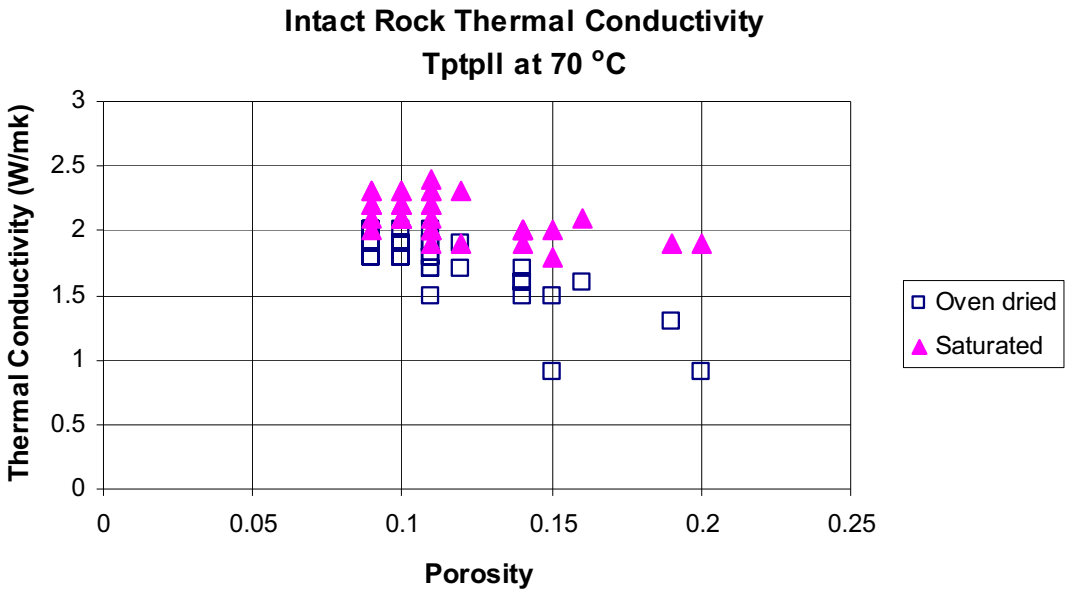

Source: DTN: SN0209L01A1202.001 [DIRS 163601].

Figure 6-123. Porosity versus Thermal Conductivity for Tptpll Specimens (Saturated and Oven Dried)

Effect of Moisture Content—The effect of moisture content, measured in terms of degree of saturation, on the intact rock thermal conductivity was studied extensively based on laboratory tests using specimens from various lithostratigraphic zones (Brodsky et al. 1997 [DIRS 100653], Section 4.1; BSC 2004 [DIRS 169900], Sections 6.2.1.3 and 6.3.1.3; DTN: SNL22100196001.006 [DIRS 158213]).

The results indicate that thermal conductivity measured on saturated specimens is higher than that measured on dried specimens. For instance, the average thermal conductivity for the saturated specimens from the Tptpmn rock is about 2.14 W/m·K at a temperature of 70°C in Table 6-80, while it is about 1.59 W/m·K for the oven-dried specimens. The impact of the saturation on the intact rock thermal conductivity is presented in Figure 6-124. The figure shows that thermal conductivity increases almost linearly with increasing saturation. Therefore, the thermal conductivity increase could be anticipated as linear with the saturation increase.

Effect of Specimen Size—The diameter of most specimens used in laboratory thermal conductivity measurements is 50.8 mm (Brodsky et al. 1997 [DIRS 100653], Table 2-1; BSC 2004 [DIRS 169900], Section 6.3.1.3; DTN: SN0209L01A1202.001 [DIRS 163601]). To investigate the effect of specimen size on thermal conductivity, laboratory tests on thermal conductivity of the Tptpll rock were also conducted on specimens with a diameter of 38.1 mm (DTN: SN0209L01A1202.001 [DIRS 163601]). The results indicate that the thermal conductivity values for the smaller specimens appear to be slightly higher than those for the larger specimens (Table 6-81). However, it is difficult to conclude that the two different specimen diameters produced a systematic difference in thermal conductivity since the effect of porosity was not included in this comparison between diameters of 50.8 and 38.1 mm specimens.

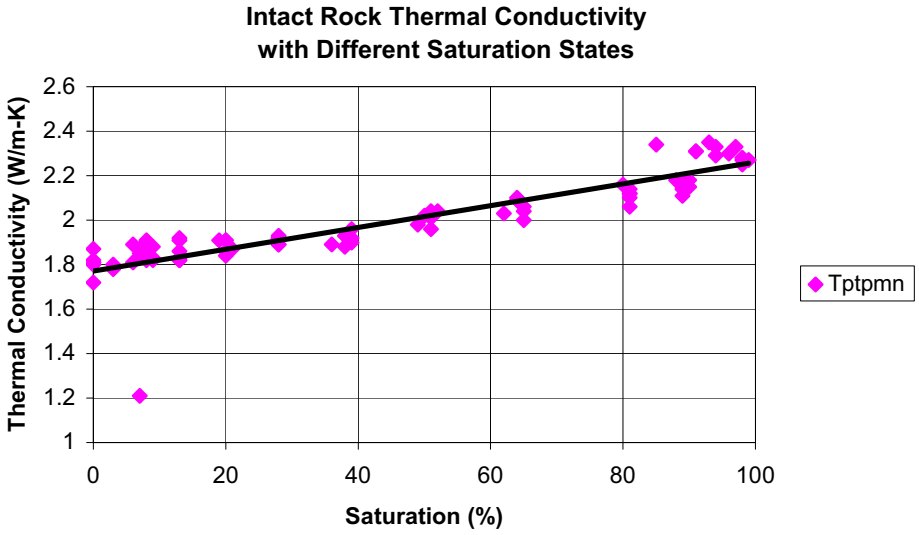

Source: DTN: SNL22100196001.006 [DIRS 158213].

Figure 6-124. Saturation versus Thermal Conductivity from Tptpmn Specimens

Table 6-81. Thermal Conductivities from 38.1 mm and 50.8 mm Diameter Specimens of Tptpll

Intact Rock Thermal Conductivity (W/m-K) of Tptpll at 70 °C				
	38.1 mm Diameter		50.8 mm Diameter	
	Oven Dried	Saturated	Oven Dried	Saturated
N	20	20	18	18
Mean	1.83	2.20	1.64	2.02
Std. Dev.	0.18	0.13	0.29	0.11

Source: DTN: SN0209L01A1202.001 [DIRS 163601].

Effect of Mineral Content—As discussed in Section 6.5.1.1, the effect of mineralogy on thermal properties could be considered a part of the temperature dependency on thermal properties.

Effect of Loading Condition—By definition, the intact rock thermal conductivity is measured under stress-free conditions. Therefore, the impact of the loading condition is not investigated.

6.5.2.2 Heat Capacity

Heat capacity of a material (C_p, J/kg•K) is defined as the amount of energy required to raise the temperature of a unit mass of the substance by one degree (Nimick and Connolly 1991 [DIRS 100690], p. 5). For solid materials, heat capacity is virtually independent of changes in pressure, but it is strongly dependent on temperature. To determine the intact rock heat capacity, a number of laboratory tests using small specimens taken from the Yucca Mountain Tuff have been performed since the late 1990s under a fully qualified QA program (Brodsky et al. 1997 [DIRS 100653], p. ii). The specimens were taken from boreholes UE25 NRG-4 and UE25 NRG-5 (BSC 2004 [DIRS 169854], Figure 4-1).

Laboratory measurements for heat capacity of rock specimens were conducted using an adiabatic pulse calorimeter following the SNL technical procedure, TP-204, *Measurement of Specific Heat of Geologic Samples by Adiabatic Pulse Calorimetry* [DIRS 108538]. The specimens were right circular cylinders approximately 57 mm in length and 51 mm in diameter (Brodsky et al. 1997 [DIRS 100653], Table 2-1), and were tested in the air-dried saturation status. The measurements were conducted at atmospheric pressure and over a temperature range of 25°C to 300°C with 5°C intervals. The equation used to calculate the heat capacity at constant pressure follows (Brodsky et al. 1997 [DIRS 100653], p. 20):

$$C_p = \frac{1}{m}\frac{\Delta Q}{\Delta T} \qquad \text{(Eq. 6-32)}$$

where m is the mass of the specimen (kg), ΔQ is the increment of heat added to the specimen (J), and ΔT is the change of specimen temperature (K).

6.5.2.2.1 Summary of Intact Rock Heat Capacity

The laboratory-measured heat capacities are presented in Tables 6-82 and 6-83, measured from three Tptrn specimens of borehole UE25 NRG-4 and seven Tptpmn specimens of borehole UE25 NRG-5, respectively (DTN: SNL01C12159302.002 [DIRS 148289]). Their mean values with one standard deviation (plus and minus) are also presented in Figures 6-125 and 6-126. The mean heat capacity values for the Tptpmn are slightly higher than those for the Tptrn. The values of the standard deviation and standard error for the Tptpmn are also slightly higher than those for the Tptrn, especially when temperatures are over 150°C. Uncertainty for the mean and standard deviation values presented in the referenced tables and figures may be relatively high because of the limited specimen numbers. This is confirmed by the relatively high standard error values compared to the standard deviation values in Tables 6-82 and 6-83. However, those specimens showing consistent values of the laboratory-measured heat capacity are indicated by the small standard deviations (Figures 6-125 and 6-126).

Table 6-82. Laboratory-Measured Heat Capacity from Three Specimens of UE25 NRG-4 (Tptrn)

Temperature (°C)	Count	Mean±1 SD (J/g-K)	Mean±1 SD% (J/g-K)	Mean±1 SE (J/g-K)	Mean±1 SE% (J/g-K)	Median (J/g-K)	Minimum (J/g-K)	Maximum (J/g-K)
25	3	0.75±0.02	0.75±1.7%	0.75±0.01	0.75±1.0%	0.74	0.74	0.77
30	3	0.76±0.02	0.76±1.7%	0.76±0.01	0.76±1.0%	0.75	0.75	0.78
35	3	0.77±0.02	0.77±1.7%	0.77±0.01	0.77±1.0%	0.76	0.76	0.79
40	3	0.78±0.02	0.78±2.1%	0.78±0.01	0.78±1.2%	0.77	0.76	0.80
45	3	0.79±0.02	0.79±2.1%	0.79±0.01	0.79±1.2%	0.78	0.77	0.81
50	3	0.80±0.02	0.80±2.1%	0.80±0.01	0.80±1.2%	0.79	0.78	0.82
55	3	0.81±0.02	0.81±2.1%	0.81±0.01	0.81±1.2%	0.80	0.79	0.83
60	3	0.82±0.02	0.82±2.1%	0.82±0.01	0.82±1.2%	0.81	0.80	0.84
65	3	0.83±0.02	0.83±2.1%	0.83±0.01	0.83±1.2%	0.82	0.81	0.85
70	3	0.84±0.02	0.84±2.1%	0.84±0.01	0.84±1.2%	0.83	0.82	0.86
75	3	0.85±0.02	0.85±1.5%	0.85±0.01	0.85±0.9%	0.85	0.84	0.87
80	3	0.86±0.02	0.86±1.5%	0.86±0.01	0.86±0.9%	0.86	0.85	0.88
85	3	0.87±0.02	0.87±1.5%	0.87±0.01	0.87±0.9%	0.87	0.86	0.89

Table 6-82. Laboratory-Measured Heat Capacity from Three Specimens of UE25 NRG-4 (Tptrn) (Continued)

Temperature (°C)	Count	Mean±1 SD (J/g-K)	Mean±1 SD% (J/g-K)	Mean±1 SE (J/g-K)	Mean±1 SE% (J/g-K)	Median (J/g-K)	Minimum (J/g-K)	Maximum (J/g-K)
90	3	0.89±0.02	0.89±2.1%	0.89±0.01	0.89±1.2%	0.88	0.87	0.91
95	3	0.90±0.02	0.90±2.1%	0.90±0.01	0.90±1.2%	0.89	0.88	0.92
100	3	0.91±0.02	0.91±2.1%	0.91±0.01	0.91±1.2%	0.90	0.89	0.93
105	3	0.92±0.02	0.92±1.7%	0.92±0.01	0.92±1.0%	0.91	0.91	0.94
110	3	0.93±0.02	0.93±1.7%	0.93±0.01	0.93±1.0%	0.92	0.92	0.95
115	3	0.94±0.02	0.94±1.7%	0.94±0.01	0.94±1.0%	0.93	0.93	0.96
120	3	0.95±0.02	0.95±1.5%	0.95±0.01	0.95±0.9%	0.95	0.94	0.97
125	3	0.96±0.02	0.96±1.5%	0.96±0.01	0.96±0.9%	0.96	0.95	0.98
130	3	0.97±0.02	0.97±2.1%	0.97±0.01	0.97±1.2%	0.98	0.95	0.99
135	3	0.98±0.02	0.98±2.1%	0.98±0.01	0.98±1.2%	0.99	0.96	1.00
140	3	1.00±0.02	1.00±2.3%	1.00±0.01	1.00±1.3%	1.01	0.97	1.01
145	3	1.00±0.03	1.00±2.9%	1.00±0.02	1.00±1.7%	1.02	0.97	1.02
150	3	1.01±0.04	1.01±3.8%	1.01±0.02	1.01±2.2%	1.03	0.97	1.04
155	3	1.02±0.04	1.02±4.0%	1.02±0.02	1.02±2.3%	1.03	0.98	1.06
160	3	1.02±0.04	1.02±3.5%	1.02±0.02	1.02±2.0%	1.02	0.98	1.05
165	3	1.02±0.04	1.02±3.5%	1.02±0.02	1.02±2.0%	1.02	0.98	1.05
170	3	1.01±0.03	1.01±3.0%	1.01±0.02	1.01±1.7%	1.01	0.98	1.04
175	3	1.01±0.03	1.01±2.5%	1.01±0.01	1.01±1.5%	1.01	0.98	1.03
180	3	1.01±0.03	1.01±2.5%	1.01±0.01	1.01±1.5%	1.01	0.98	1.03
185	3	1.00±0.02	1.00±2.0%	1.00±0.01	1.00±1.2%	1.00	0.98	1.02
190	3	1.00±0.02	1.00±2.0%	1.00±0.01	1.00±1.2%	1.00	0.98	1.02
195	3	0.99±0.02	0.99±1.5%	0.99±0.01	0.99±0.9%	0.99	0.98	1.01
200	3	0.99±0.02	0.99±1.5%	0.99±0.01	0.99±0.9%	0.99	0.98	1.01
205	3	0.99±0.01	0.99±1.0%	0.99±0.01	0.99±0.6%	0.99	0.98	1.00
210	3	0.99±0.01	0.99±1.2%	0.99±0.01	0.99±0.7%	0.98	0.98	1.00
215	3	0.99±0.01	0.99±1.2%	0.99±0.01	0.99±0.7%	0.98	0.98	1.00
220	3	0.98±0.01	0.98±0.6%	0.98±0.00	0.98±0.3%	0.98	0.98	0.99
225	3	0.98±0.01	0.98±1.2%	0.98±0.01	0.98±0.7%	0.97	0.97	0.99
230	3	0.98±0.01	0.98±1.2%	0.98±0.01	0.98±0.7%	0.97	0.97	0.99
235	3	0.97±0.01	0.97±0.6%	0.97±0.00	0.97±0.3%	0.97	0.97	0.98
240	3	0.97±0.01	0.97±1.0%	0.97±0.01	0.97±0.6%	0.97	0.96	0.98
245	3	0.97±0.01	0.97±1.0%	0.97±0.01	0.97±0.6%	0.97	0.96	0.98
250	3	0.97±0.01	0.97±1.0%	0.97±0.01	0.97±0.6%	0.97	0.96	0.98
255	3	0.97±0.01	0.97±1.0%	0.97±0.01	0.97±0.6%	0.97	0.96	0.98
260	3	0.96±0.01	0.96±1.2%	0.96±0.01	0.96±0.7%	0.97	0.95	0.97
265	3	0.96±0.01	0.96±1.2%	0.96±0.01	0.96±0.7%	0.97	0.95	0.97
270	3	0.96±0.01	0.96±1.2%	0.96±0.01	0.96±0.7%	0.97	0.95	0.97
275	3	0.96±0.01	0.96±1.2%	0.96±0.01	0.96±0.7%	0.97	0.95	0.97
280	3	0.96±0.01	0.96±1.2%	0.96±0.01	0.96±0.7%	0.97	0.95	0.97

Table 6-82. Laboratory-Measured Heat Capacity from Three Specimens of UE25 NRG-4 (Tptrn) (Continued)

Temperature (°C)	Count	Mean±1 SD (J/g-K)	Mean±1 SD% (J/g-K)	Mean±1 SE (J/g-K)	Mean±1 SE% (J/g-K)	Median (J/g-K)	Minimum (J/g-K)	Maximum (J/g-K)
285	3	0.96±0.02	0.96±1.7%	0.96±0.01	0.96±1.0%	0.97	0.94	0.97
290	3	0.96±0.02	0.96±1.7%	0.96±0.01	0.96±1.0%	0.97	0.94	0.97
295	3	0.96±0.02	0.96±1.7%	0.96±0.01	0.96±1.0%	0.97	0.94	0.97
300	3	0.96±0.02	0.96±1.7%	0.96±0.01	0.96±1.0%	0.97	0.94	0.97

Source: DTN: SNL01C12159302.002 [DIRS 148289].

NOTE: SD represents the standard deviation, while SE represents the standard error.

Table 6-83. Laboratory-Measured Heat Capacity from Seven Specimens of UE25 NRG-5 (Tptpmn)

Temperature (°C)	Count	Mean±1 SD (J/g-K)	Mean±1 SD% (J/g-K)	Mean±1 SE (J/g-K)	Mean±1 SE% (J/g-K)	Median (J/g-K)	Minimum (J/g-K)	Maximum (J/g-K)
25	7	0.80±0.03	0.80±2.7%	0.80±0.01	0.80±1.0%	0.79	0.76	0.83
30	7	0.80±0.03	0.80±2.5%	0.80±0.01	0.80±1.0%	0.80	0.77	0.84
35	7	0.81±0.02	0.81±2.3%	0.81±0.01	0.81±0.9%	0.80	0.78	0.84
40	7	0.82±0.03	0.82±2.5%	0.82±0.01	0.82±0.9%	0.81	0.79	0.85
45	7	0.82±0.02	0.82±2.5%	0.82±0.01	0.82±0.9%	0.82	0.79	0.86
50	7	0.83±0.02	0.83±2.5%	0.83±0.01	0.83±0.9%	0.83	0.80	0.87
55	7	0.84±0.02	0.84±2.3%	0.84±0.01	0.84±0.9%	0.84	0.82	0.88
60	7	0.85±0.02	0.85±2.4%	0.85±0.01	0.85±0.9%	0.85	0.83	0.89
65	7	0.87±0.02	0.87±2.3%	0.87±0.01	0.87±0.9%	0.86	0.84	0.90
70	7	0.88±0.02	0.88±2.5%	0.88±0.01	0.88±0.9%	0.88	0.85	0.91
75	7	0.89±0.02	0.89±2.3%	0.89±0.01	0.89±0.9%	0.89	0.86	0.92
80	7	0.90±0.02	0.90±2.4%	0.90±0.01	0.90±0.9%	0.91	0.87	0.93
85	7	0.92±0.02	0.92±2.1%	0.92±0.01	0.92±0.8%	0.92	0.89	0.95
90	7	0.93±0.02	0.93±2.4%	0.93±0.01	0.93±0.9%	0.94	0.90	0.96
95	7	0.95±0.02	0.95±2.2%	0.95±0.01	0.95±0.8%	0.95	0.91	0.97
100	7	0.96±0.02	0.96±2.3%	0.96±0.01	0.96±0.9%	0.97	0.92	0.98
105	7	0.98±0.02	0.98±2.1%	0.98±0.01	0.98±0.8%	0.99	0.94	1.00
110	7	0.99±0.02	0.99±2.2%	0.99±0.01	0.99±0.8%	1.00	0.95	1.01
115	7	1.01±0.02	1.01±2.4%	1.01±0.01	1.01±0.9%	1.02	0.96	1.03
120	7	1.02±0.02	1.02±2.2%	1.02±0.01	1.02±0.8%	1.03	0.98	1.04
125	7	1.03±0.02	1.03±2.3%	1.03±0.01	1.03±0.9%	1.05	0.99	1.05
130	7	1.05±0.03	1.05±2.6%	1.05±0.01	1.05±1.0%	1.06	1.00	1.07
135	7	1.06±0.02	1.06±2.1%	1.06±0.01	1.06±0.8%	1.07	1.02	1.08
140	7	1.07±0.02	1.07±2.2%	1.07±0.01	1.07±0.8%	1.07	1.03	1.09
145	7	1.08±0.02	1.08±2.0%	1.08±0.01	1.08±0.7%	1.08	1.05	1.10
150	7	1.09±0.02	1.09±2.3%	1.09±0.01	1.09±0.9%	1.08	1.06	1.12
155	7	1.10±0.03	1.10±3.2%	1.10±0.01	1.10±1.2%	1.09	1.05	1.13
160	7	1.09±0.04	1.09±4.0%	1.09±0.02	1.09±1.5%	1.07	1.05	1.14
165	7	1.09±0.05	1.09±4.8%	1.09±0.02	1.09±1.8%	1.06	1.05	1.16

Table 6-83. Laboratory-Measured Heat Capacity from Seven Specimens of UE25 NRG-5 (Tptpmn) (Continued)

Temperature (°C)	Count	Mean±1 SD (J/g-K)	Mean±1 SD% (J/g-K)	Mean±1 SE (J/g-K)	Mean±1 SE% (J/g-K)	Median (J/g-K)	Minimum (J/g-K)	Maximum (J/g-K)
170	7	1.09±0.05	1.09±5.1%	1.09±0.02	1.09±1.9%	1.06	1.04	1.15
175	7	1.08±0.04	1.08±4.4%	1.08±0.02	1.08±1.7%	1.06	1.03	1.13
180	7	1.08±0.04	1.08±4.2%	1.08±0.02	1.08±1.6%	1.06	1.03	1.13
185	7	1.07±0.04	1.07±4.1%	1.07±0.02	1.07±1.5%	1.06	1.02	1.13
190	7	1.07±0.04	1.07±4.0%	1.07±0.02	1.07±1.5%	1.06	1.02	1.12
195	7	1.07±0.04	1.07±3.9%	1.07±0.01	1.07±1.5%	1.06	1.02	1.12
200	7	1.07±0.04	1.07±4.0%	1.07±0.02	1.07±1.5%	1.06	1.02	1.12
205	7	1.07±0.04	1.07±3.9%	1.07±0.01	1.07±1.5%	1.06	1.02	1.12
210	7	1.06±0.04	1.06±3.7%	1.06±0.01	1.06±1.4%	1.06	1.02	1.11
215	7	1.06±0.04	1.06±3.9%	1.06±0.01	1.06±1.5%	1.06	1.02	1.11
220	7	1.06±0.04	1.06±4.1%	1.06±0.02	1.06±1.5%	1.06	1.02	1.12
225	7	1.06±0.04	1.06±4.3%	1.06±0.02	1.06±1.6%	1.06	1.01	1.12
230	7	1.06±0.04	1.06±4.4%	1.06±0.02	1.06±1.6%	1.06	1.01	1.12
235	7	1.06±0.05	1.06±4.7%	1.06±0.02	1.06±1.8%	1.06	1.01	1.13
240	7	1.06±0.05	1.06±4.7%	1.06±0.02	1.06±1.8%	1.06	1.01	1.13
245	7	1.06±0.05	1.06±4.9%	1.06±0.02	1.06±1.8%	1.06	1.00	1.13
250	7	1.06±0.05	1.06±5.0%	1.06±0.02	1.06±1.9%	1.06	1.00	1.13
255	7	1.06±0.05	1.06±5.2%	1.06±0.02	1.06±2.0%	1.06	0.99	1.13
260	7	1.06±0.05	1.06±5.4%	1.06±0.02	1.06±2.1%	1.06	0.99	1.14
265	7	1.06±0.06	1.06±5.8%	1.06±0.02	1.06±2.2%	1.06	0.98	1.14
270	7	1.06±0.06	1.06±5.8%	1.06±0.02	1.06±2.2%	1.06	0.98	1.14
275	7	1.06±0.06	1.06±6.3%	1.06±0.02	1.06±2.4%	1.06	0.97	1.15
280	7	1.07±0.06	1.07±6.3%	1.07±0.02	1.07±2.4%	1.07	0.97	1.15
285	7	1.06±0.07	1.06±6.9%	1.06±0.03	1.06±2.6%	1.07	0.96	1.16
290	7	1.07±0.07	1.07±7.1%	1.07±0.03	1.07±2.7%	1.08	0.96	1.17
295	7	1.07±0.08	1.07±7.6%	1.07±0.03	1.07±2.9%	1.08	0.96	1.19
300	7	1.08±0.08	1.08±8.1%	1.08±0.03	1.08±3.1%	1.09	0.96	1.21

Source: DTN: SNL01C12159302.002 [DIRS 148289].

NOTE: SD represents the standard deviation, while SE represents the standard error.

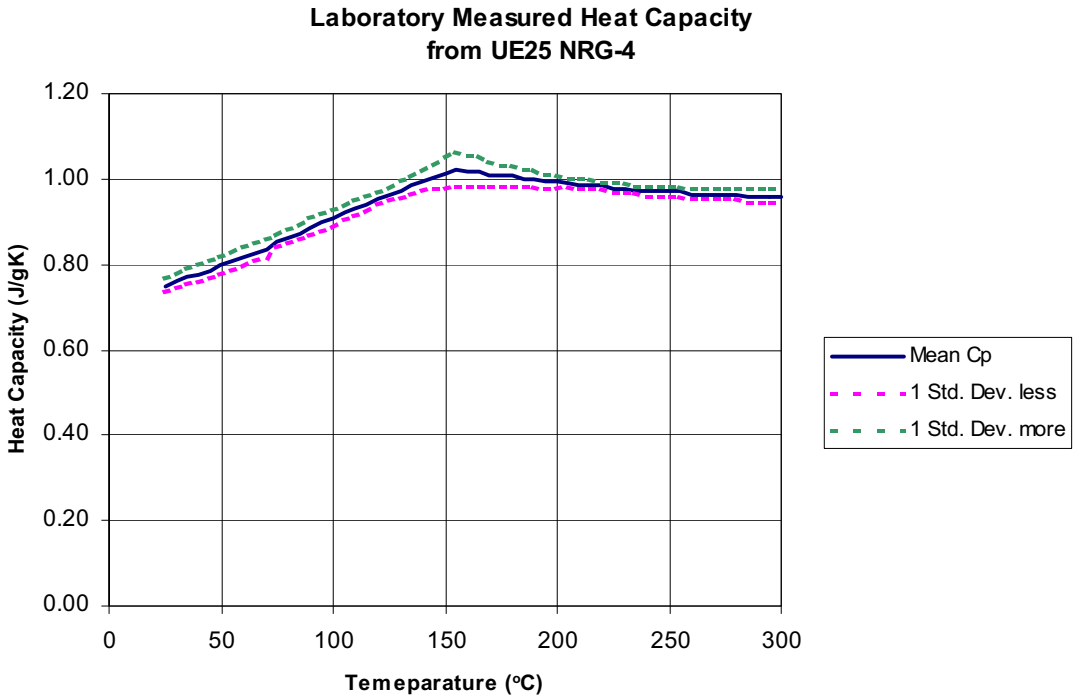

Source: DTN: SNL01C12159302.002 [DIRS 148289].

Figure 6-125. Laboratory-Measured Heat Capacity from Three Specimens of UE25 NRG-4 (Tptrn)

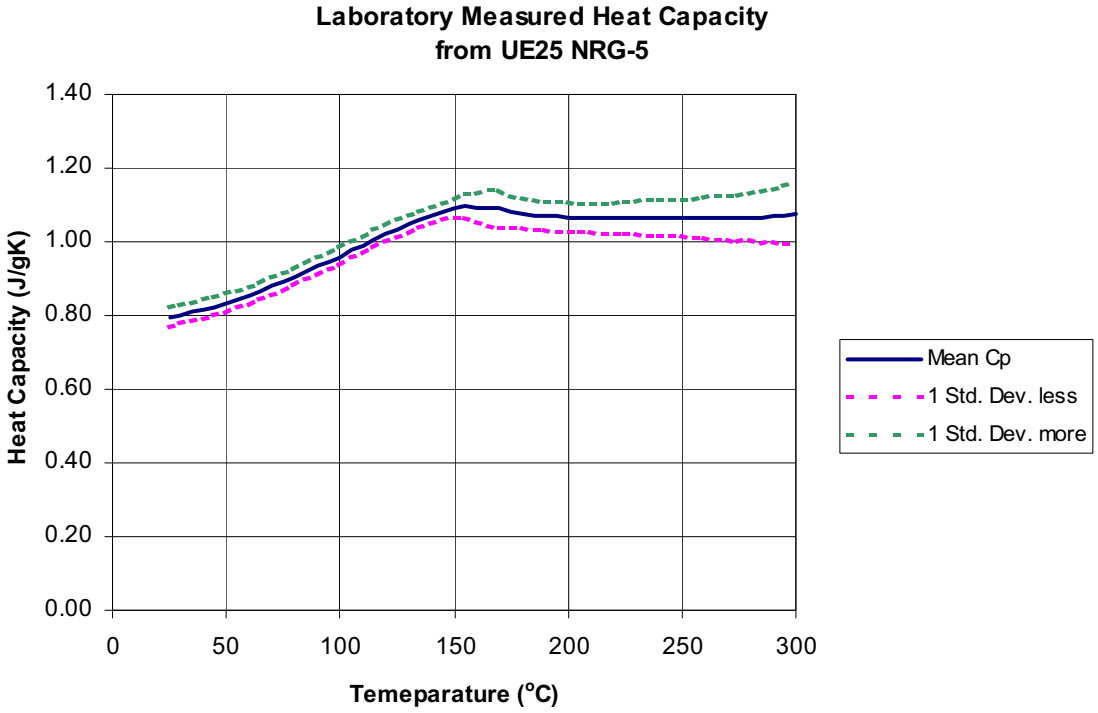

Source: DTN: SNL01C12159302.002 [DIRS 148289].

Figure 6-126. Laboratory-Measured Heat Capacity from Seven Specimens of UE25 NRG-5 (Tptpmn)

Uncertainties of the intact rock heat capacity are instigated from the factors impacting the heat capacity, based on sensitivity of the impact from the individual factors. The sensitivity of intact rock heat capacity to the impacting factors has been evaluated based on these laboratory tests. The evaluation is provided in the following:

Effect of Temperature—Intact rock heat capacity for the air-dried specimens from boreholes UE25 NRG-4 and UE25 NRG-5 increases with increasing temperature up to 160°C in Figures 6-125 and 6-126. Slight decrease in the heat capacity with increasing temperature is observed at temperatures over 160°C and becomes stable at higher temperature (Figures 6-125 and 6-126). The change of heat capacity value is probably due to the phase change of tridymite since phase changes of a mineral absorb heat and raise the heat capacity value (Brodsky et al. 1997 [DIRS 100653], Section 4.3.1).

Effect of Porosity—Effect of porosity on the intact rock heat capacity has been investigated, and it is incorporated with matrix porosity data from DTN: SNL01A05059301.007 [DIRS 108980]. The heat capacity values of three specimens from borehole UE25 NRG-4 with various matrix porosities are presented in Figure 6-127. The figure shows that the higher porosity specimens have slightly lower values of heat capacity. However, the effect of porosity is very minor considering that the higher porosity specimen has almost twice the matrix porosity value (i.e., 0.24 instead of 0.13). Therefore, the effect of matrix porosity on the intact rock heat capacity is considered minor compared to the effect of temperature. However, since the number of

specimens is very limited, the investigation for the effect of porosity on the intact rock heat capacity has relatively higher uncertainty.

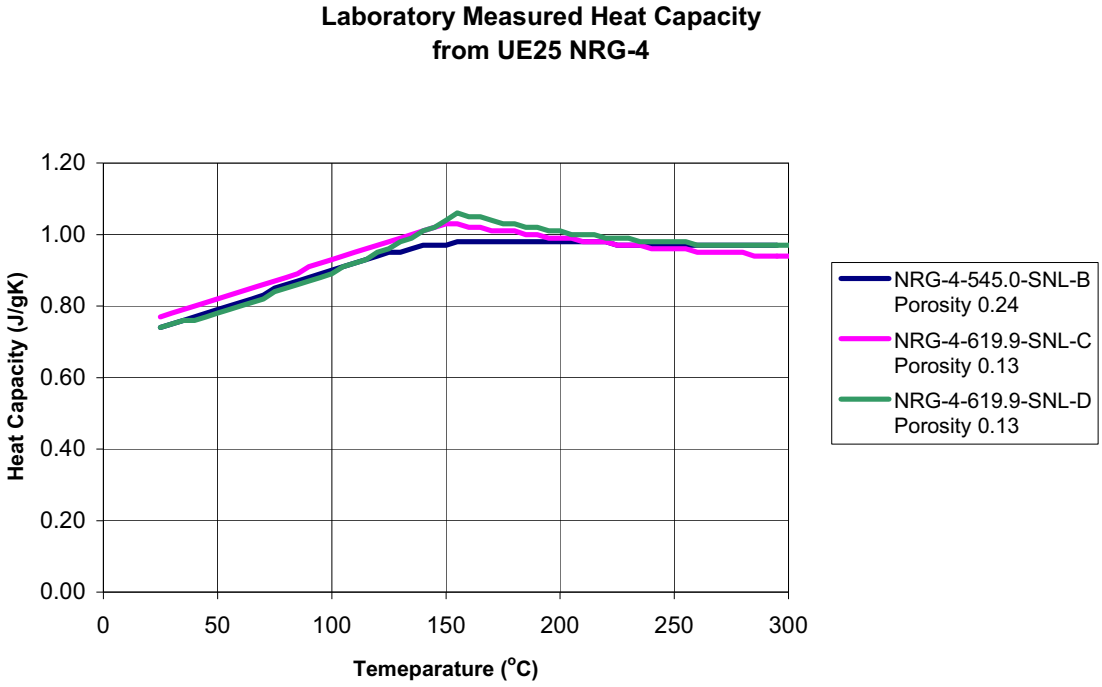

Sources: DTNs: SNL01C12159302.002 [DIRS 148289]; SNL01A05059301.007 [DIRS 108980].

Figure 6-127. Heat Capacity from Borehole UE25 NRG-4 (Tptrn zone) Specimens with Different Matrix Porosity

Effect of Moisture Content—Effect of moisture content, measured in terms of degree of saturation, on the intact rock thermal conductivity was not investigated. However, the effect of moisture content may be considered in rock mass or analytical estimation of the heat capacity.

Effect of Specimen Size—Effect of the specimen size for the intact rock heat capacity was not investigated since it is assumed that the scale of the specimens is small enough to exclude all the heterogeneity and discontinuity that affect the heat capacity (Assumption 5.4.2).

Effect of Mineral Content—As discussed in Section 6.5.1.1, the effect of mineralogy on thermal properties could be considered a part of the temperature dependency on thermal properties.

Effect of Loading Condition—Since heat capacity for a solid material is virtually independent of changes in pressure (BSC 2004 [DIRS 170003], Section 6), the measurement of the intact rock heat capacity does not consider the effect of loading condition whether in situ or induced.

6.5.2.3 Coefficient of Thermal Expansion (CTE)

A number of laboratory thermal expansion tests using small specimens taken from the Yucca Mountain Tuff have been conducted since the late 1990s. These rock specimens were taken from NRG boreholes (DTN: SNL01B05059301.006 [DIRS 129168]), Alcoves 5 and 7, and SD boreholes (DTN: SNL22100196001.002 [DIRS 153138]), the SHT block and the DST area (DTNs: SNL22080196001.001 [DIRS 109722]; SNL22080196001.003 [DIRS 119042]; SN0203L2210196.007 [DIRS 158322]).

The laboratory thermal expansion tests were conducted at ambient pressure over a temperature range of 25°C to over 325°C. Temperature was increased and decreased at a rate of less than 1°C per minute. Test specimens used in the laboratory thermal expansion measurements at ambient pressure were right circular cylinders, and the size of most rock specimens was typically 25.4 mm in diameter and 50.8 mm in length (Brodsky et al. 1997 [DIRS 100653], Table 2-1; CRWMS M&O 1999 [DIRS 129261], Table 6-3; CRWMS M&O 1997 [DIRS 101539], Table 3-2). The laboratory thermal expansion measurements were made using a push rod dilatometer (Brodsky et al. 1997 [DIRS 100653], Section 3.2; CRWMS M&O 1999 [DIRS 129261], Section 6.2.2.2; CRWMS M&O 1997 [DIRS 101539], Section 3.3.2). Moisture contents were either air dried (as received), oven dried, or vacuum saturated. Specimens under saturated conditions were tested up to 100°C. The tests were conducted in accordance with the SNL procedure TP-203, Revision 01, *Measurement of Thermal Expansion of Geologic Supplies Using a Push Rod Dilatometer* [DIRS 145491].

CTE under confining stresses was also measured in laboratory tests using the specimens taken from borehole USW SD-12. The tests were conducted at confining pressures of 1, 5, 10, 20, and 30 MPa over a temperature range of 25°C to 250°C. The specimens were heated and cooled at a nominal rate of 0.319°C per minute in a drained condition (Martin et al. 1997 [DIRS 104758], Section 2.3). The test specimens used in the laboratory thermal expansion measurements under confining stresses were right circular cylinders, and the size of most rock specimens was typically 50.8 mm in diameter and 101.6 mm in length (Martin et al. 1997 [DIRS 104758], Section 2.0). The test procedure adheres to the requirements of ASTM D 4535-85, *Standard Test Method for Measurement of Thermal Expansion of Rock Using a Dilatometer* [DIRS 118930].

The CTE is defined as the ratio of the change in length of a line segment in a specimen per unit of temperature change to its length at a reference temperature. The mean CTE is the linear thermal expansion per unit change in temperature and is calculated as follows (Brodsky et al. 1997 [DIRS 100653], Equation 3-10a):

$$\alpha_m = \frac{L_2 - L_1}{L_0 (T_2 - T_1)} \qquad \text{(Eq. 6-33)}$$

where α_m is the mean CTE between two temperatures, T_1 and T_2; L_0 is the sample length at reference temperature; L_1 is the sample displacement at temperature T_1; and L_2 is the sample displacement at temperature T_2. Temperatures and displacements of rock specimens were measured throughout a heating and cooling cycle.

The mean CTE was then calculated using Equation 6-33 in 25°C intervals from data obtained at the endpoints of the interval. Because data are not always collected at exact 25°C intervals, a linear least squares fit may be used to calculate the specimen lengths L_1 and L_2 at temperatures T_1 and T_2, respectively (Brodsky et al. 1997 [DIRS 100653], Section 3.2.3; CRWMS M&O 1997 [DIRS 101539], Section 3.3.2).

Equation 6-33 applies only to the linear change in specimen length caused by change in temperature. For specimens with a high degree of temperature dependency, the temperature interval should be kept small to calculate the mean CTE accurately. Otherwise, the instantaneous CTE, α_T, should be calculated. The instantaneous CTE is the slope of the linear thermal expansion curve at a temperature T defined as (Brodsky et al. 1997 [DIRS 100653], Equation 3-11):

$$\alpha_T = \frac{1}{L_0}\frac{dL}{dT} \qquad \text{(Eq. 6-34)}$$

It should be noted that the actual measurements of the instantaneous CTE were conducted on a small window of temperature (5°C); therefore, the measurements of the instantaneous CTE are not truly instantaneous (Brodsky et al. 1997 [DIRS 100653], Section 3.2.3; CRWMS M&O 1997 [DIRS 101539], Section 3.3.2).

6.5.2.3.1 Measurements of Intact Rock Thermal Expansion Coefficient

Statistical summary of the CTE of air-dried specimens from heating cycles is presented in Table 6-84. The CTE measurements of air-dried specimens are the most abundant and were conducted for the most various stratigraphic units. The differences of CTE measurements between the air-dried, oven-dried, and saturated specimens of the Tptpmn and Tptpll zones are presented in Figure 6-128. The intact rock CTE of Tptpmn indicates that conditions of water content do not have a significant impact on the values of intact CTE (Figure 6-128a). Decrease of the CTE values with increase in the water content (i.e., from oven dried to saturated) in the 75°C to 100°C temperature range is observed. The observation suggests the effect of phase change of pore water, but the change is insignificant compared to the increase of the CTE values with increase in temperature. The effect of the specimen condition is not apparent for the Tptpll zone (Figure 6-128b). This may be partially due to the relatively small numbers of the Tptpll specimens compared to the number of Tptpmn specimens (Table 6-84). The independency of saturation state for the welded specimens is also discussed in Brodsky et al. (1997 [DIRS 100653], Section 4.2.2.1). Based on that observation, the air-dried CTE measurements could be used for representing the values of the intact rock CTE.

The intact air-dried CTE values with 95% confidence intervals (1.96 times the standard deviations) for Tptpmn and the Tptpll are presented in Figure 6-129. Both the CTE values for the Tptpmn and the Tptpll show a steep increase of the CTE values at the "transition temperature" of approximately 175°C to 225°C, in which the presence of certain minerals such as tridymite and cristobalite instigate their phase changes. The phase changes of tridymite and cristobalite induce significant increase of CTE among welded tuffs (Brodsky et al. 1997 [DIRS 100653], Section 4.2.2.2). Figure 6-129 shows substantial differences between the CTE

values for the Tptpmn and the Tptpll zones after the transition temperature of 200°C. The difference might be from variation in tridymite and cristobalite contents. However, since the observed mineral abundance of the two zones is similar (BSC 2004 [DIRS 170003], Table 6-2), the source of the substantial difference is not clear. Source of the decrease of CTE measurement values over the temperature range of 300°C to 325°C is also uncertain. However, completion of the phase change may cause the decrease of the measurement values.

Table 6-84. Intact Rock Coefficients of Thermal Expansion of Air-Dried Specimens

Stratigraphic Units	Intact Rock Coefficient of Thermal Expansion (10^{-6}/°C), Air-Dried												
	Temperature °C	25-5	50-75	75-100	100-125	125-150	150-175	175-200	200-225	225-250	250-275	275-300	300-325
Crystal-Rich Tiva/Post-Tiva Canyon Tuff (Tpcr)	Count	12	12	12	6	6	6	6	6	6	6	6	NA
	Mean+1 SD	6.96+1.78	7.67+1.17	9.50+1.11	10.15+0.87	12.03+1.24	13.83+1.49	16.14+1.95	18.92+1.85	21.75+1.38	37.55+13.85	48.84+18.34	NA
	Mean+1 SD%	6.96+25.5%	7.67+15.2%	9.50+11.7%	10.15+8.6%	12.03+10.3%	13.83+10.8%	16.14+12.1%	18.92+9.8%	21.75+6.4%	37.55+36.9%	48.84+37.5%	NA
	Mean+1 SE	6.96+0.51	7.67+0.34	9.50+0.32	10.15+0.36	12.03+0.51	13.83+0.61	16.14+0.80	18.92+0.75	21.75+0.56	37.55+5.65	48.84+7.49	NA
	Mean+1 SE%	6.96+7.4%	7.67+4.4%	9.50+3.4%	10.15+3.5%	12.03+4.2%	13.83+4.4%	16.14+4.9%	18.92+4.0%	21.75+2.6%	37.55+15.1%	48.84+15.3%	NA
	Median	7.53	7.985	9.55	10.335	12.055	14.04	16.55	19.265	21.94	34.535	44.01	NA
	Minimum	2.71	5.16	7.84	8.81	10.28	11.82	13.31	15.95	19.5	25.22	33.16	NA
	Maximum	9.1	8.81	11.55	11.31	13.94	15.62	18.4	21.11	23.79	62.82	81.37	NA
Tpcpv2	Count	2	2	2	1	2	2	2	NA	NA	NA	NA	NA
	Mean+1 SD	6.90+0.32	6.06+0.92	4.91+0.89	7.45+n/a	8.94+0.57	6.60+1.29	1.57+2.06	NA	NA	NA	NA	NA
	Mean+1 SD%	6.90+4.6%	6.06+15.2%	4.91+18.1%	7.45+n/a	8.94+6.3%	6.60+19.5%	1.57+131.5%	NA	NA	NA	NA	NA
	Mean+1 SE	6.90+0.23	6.06+0.65	4.91+0.63	7.45+n/a	8.94+0.40	6.60+0.91	1.57+1.46	NA	NA	NA	NA	NA
	Mean+1 SE%	6.90+3.3%	6.06+10.7%	4.91+12.8%	7.45+n/a	8.94+4.5%	6.60+13.8%	1.57+93.0%	NA	NA	NA	NA	NA
	Median	6.895	6.06	4.91	7.45	8.94	6.6	1.57	NA	NA	NA	NA	NA
	Minimum	6.67	5.41	4.28	7.45	8.54	5.69	0.11	NA	NA	NA	NA	NA
	Maximum	7.12	6.71	5.54	7.45	9.34	7.51	3.03	NA	NA	NA	NA	NA
Tpcpv1	Count	4	4	3	2	2	2	2	2	2	2	1	NA
	Mean+1 SD	4.72+0.58	3.43+1.03	3.12+1.89	4.39+1.31	6.27+0.58	5.80+0.22	5.75+0.23	5.66+0.23	5.10+0.79	3.82+0.74	1.71+n/a	NA
	Mean+1 SD%	4.72+12.2%	3.43+30.2%	3.12+60.5%	4.39+29.8%	6.27+9.2%	5.80+3.8%	5.75+4.1%	5.66+4.0%	5.10+15.5%	3.82+19.5%	1.71+n/a	NA
	Mean+1 SE	4.72+0.29	3.43+0.52	3.12+1.09	4.39+0.93	6.27+0.41	5.80+0.15	5.75+0.17	5.66+0.16	5.10+0.56	3.82+0.53	1.71+n/a	NA
	Mean+1 SE%	4.72+6.1%	3.43+15.1%	3.12+34.9%	4.39+21.1%	6.27+6.5%	5.80+2.7%	5.75+2.9%	5.66+2.8%	5.10+11.0%	3.82+13.8%	1.71+n/a	NA
	Median	4.65	3.915	3.93	4.385	6.27	5.795	5.745	5.66	5.1	3.815	1.71	NA
	Minimum	4.08	1.88	0.96	3.46	5.86	5.64	5.58	5.5	4.54	3.29	1.71	NA
	Maximum	5.48	4.01	4.46	5.31	6.68	5.95	5.91	5.82	5.66	4.34	1.71	NA
Tpbt4	Count	2	2	0	1	2	2	2	2	2	2	2	NA
	Mean+1 SD	4.20+0.35	2.11+0.78	NA	5.31+n/a	5.53+0.06	4.67+0.25	5.80+0.60	6.30+0.13	6.70+0.18	5.82+0.35	3.03+1.75	NA
	Mean+1 SD%	4.20+8.4%	2.11+36.9%	NA	5.31+n/a	5.53+1.0%	4.67+5.5%	5.80+10.4%	6.30+2.1%	6.70+2.6%	5.82+6.1%	3.03+57.7%	NA
	Mean+1 SE	4.20+0.25	2.11+0.55	NA	5.31+n/a	5.53+0.04	4.67+0.18	5.80+0.42	6.30+0.10	6.70+0.13	5.82+0.25	3.03+1.24	NA
	Mean+1 SE%	4.20+6.0%	2.11+26.1%	NA	5.31+n/a	5.53+0.7%	4.67+3.9%	5.80+7.3%	6.30+1.5%	6.70+1.9%	5.82+4.3%	3.03+40.8%	NA
	Median	4.2	2.11	NA	5.31	5.53	4.67	5.795	6.295	6.695	5.82	3.025	NA
	Minimum	3.95	1.56	NA	5.31	5.49	4.49	5.37	6.2	6.57	5.57	1.79	NA
	Maximum	4.45	2.66	NA	5.31	5.57	4.85	6.22	6.39	6.82	6.07	4.26	NA

Table 6-84 Intact Rock Coefficients of Thermal Expansion of Air-Dried Specimens (Continued)

Stratigraphic Units	Intact Rock Coefficient of Thermal Expansion (10^{-6}/°C), Air-Dried												
	Temperature °C	**25-5**	**50-75**	**75-100**	**100-125**	**125-150**	**150-175**	**175-200**	**200-225**	**225-250**	**250-275**	**275-300**	**300-325**
Yucca Mountain Tuff (Tpy)	Count	4	4	4	4	4	4	4	2	2	2	2	NA
	Mean+1 SD	4.73+0.56	4.87+0.30	5.33+0.34	4.77+2.48	6.41+0.29	5.88+0.46	4.09+2.24	5.97+0.25	5.47+0.54	3.92+0.70	1.24+0.93	NA
	Mean+1 SD%	4.73+11.9%	4.87+6.1%	5.33+6.4%	4.77+51.9%	6.41+4.5%	5.88+7.9%	4.09+54.7%	5.97+4.3%	5.47+10.0%	3.92+17.9%	1.24+75.3%	NA
	Mean+1 SE	4.73+0.28	4.87+0.15	5.33+0.17	4.77+1.24	6.41+0.14	5.88+0.23	4.09+1.12	5.97+0.18	5.47+0.38	3.92+0.50	1.24+0.66	NA
	Mean+1 SE%	4.73+6.0%	4.87+3.1%	5.33+3.2%	4.77+26.0%	6.41+2.3%	5.88+3.9%	4.09+27.4%	5.97+3.0%	5.47+7.0%	3.92+12.6%	1.24+53.2%	NA
	Median	4.71	4.895	5.295	5.73	6.41	5.845	4.435	5.97	5.465	3.915	1.24	NA
	Minimum	4.12	4.52	4.94	1.11	6.11	5.46	1.2	5.79	5.08	3.42	0.58	NA
	Maximum	5.39	5.18	5.77	6.49	6.72	6.38	6.28	6.15	5.85	4.41	1.9	NA
Pah Canyon (Tpp)	Count	8	7	6	3	6	6	2	2	2	2	2	NA
	Mean+1 SD	4.22+0.75	2.84+0.59	3.14+0.56	6.32+0.49	5.72+0.90	3.72+1.00	3.73+0.59	4.46+0.10	4.10+0.51	3.31+1.20	1.02+1.00	NA
	Mean+1 SD%	4.22+17.7%	2.84+20.8%	3.14+17.8%	6.32+7.7%	5.72+15.7%	3.72+27.0%	3.73+15.9%	4.46+2.2%	4.10+12.4%	3.31+36.2%	1.02+98.2%	NA
	Mean+1 SE	4.22+0.26	2.84+0.22	3.14+0.23	6.32+0.28	5.72+0.37	3.72+0.41	3.73+0.42	4.46+0.07	4.10+0.36	3.31+0.85	1.02+0.71	NA
	Mean+1 SE%	4.22+6.3%	2.84+7.9%	3.14+7.3%	6.32+4.4%	5.72+6.4%	3.72+11.0%	3.73+11.3%	4.46+1.6%	4.10+8.8%	3.31+25.6%	1.02+69.5%	NA
	Median	4.225	2.85	3.275	6.31	5.935	3.675	3.73	4.46	4.1	3.305	1.015	NA
	Minimum	2.82	2	2.45	5.84	4.03	2.62	3.31	4.39	3.74	2.46	0.31	NA
	Maximum	5.56	3.71	3.99	6.81	6.52	4.95	4.15	4.53	4.46	4.15	1.72	NA
Tptrv2	Count	2	2	2	2	2	2	2	1	NA	NA	NA	NA
	Mean+1 SD	5.76+0.94	6.11+0.18	6.56+0.10	4.22+3.62	8.07+0.35	8.05+0.30	5.67+1.35	2.65+n/a	NA	NA	NA	NA
	Mean+1 SD%	5.76+16.3%	6.11+2.9%	6.56+1.5%	4.22+85.8%	8.07+4.3%	8.05+3.7%	5.67+23.8%	2.65+n/a	NA	NA	NA	NA
	Mean+1 SE	5.76+0.67	6.11+0.13	6.56+0.07	4.22+2.56	8.07+0.24	8.05+0.21	5.67+0.96	2.65+n/a	NA	NA	NA	NA
	Mean+1 SE%	5.76+11.6%	6.11+2.0%	6.56+1.1%	4.22+60.7%	8.07+3.0%	8.05+2.6%	5.67+16.9%	2.65+n/a	NA	NA	NA	NA
	Median	5.755	6.105	6.56	4.22	8.065	8.05	5.665	2.65	NA	NA	NA	NA
	Minimum	5.09	5.98	6.49	1.66	7.82	7.84	4.71	2.65	NA	NA	NA	NA
	Maximum	6.42	6.23	6.63	6.78	8.31	8.26	6.62	2.65	NA	NA	NA	NA
Tptrn	Count	28	28	28	18	18	18	18	18	18	18	18	NA
	Mean+1 SD	6.52+1.05	7.02+0.87	7.90+0.91	8.30+1.01	9.90+1.78	16.30+5.97	20.83+10.26	25.04+14.75	27.58+12.50	30.80+10.09	33.22+9.43	NA
	Mean+1 SD%	6.52+16.2%	7.02+12.4%	7.90+11.5%	8.30+12.2%	9.90+17.9%	16.30+36.6%	20.83+49.2%	25.04+58.9%	27.58+45.3%	30.80+32.7%	33.22+28.4%	NA
	Mean+1 SE	6.52+0.20	7.02+0.16	7.90+0.17	8.30+0.24	9.90+0.42	16.30+1.41	20.83+2.42	25.04+3.48	27.58+2.95	30.80+2.38	33.22+2.22	NA
	Mean+1 SE%	6.52+3.1%	7.02+2.3%	7.90+2.2%	8.30+2.9%	9.90+4.2%	16.30+8.6%	20.83+11.6%	25.04+13.9%	27.58+10.7%	30.80+7.7%	33.22+6.7%	NA
	Median	6.435	7.07	7.99	8.37	9.895	13.545	15.815	20.125	24.22	31.41	37.22	NA
	Minimum	4.13	5.26	6.26	6.73	7.05	10.19	12.32	13.59	14.84	16.92	16.88	NA
	Maximum	8.47	8.44	9.68	10.78	14.44	29.96	43.22	62.11	56.39	49.02	44.23	NA

Table 6-84 Intact Rock Coefficients of Thermal Expansion of Air-Dried Specimens (Continued)

Stratigraphic Units	Intact Rock Coefficient of Thermal Expansion (10^{-6}/°C), Air-Dried												
	Temperature °C	25-5	50-75	75-100	100-125	125-150	150-175	175-200	200-225	225-250	250-275	275-300	300-325
Tptrl	Count	4	4	4	4	4	4	4	4	4	4	4	NA
	Mean+1 SD	7.76+1.07	8.21+1.05	9.13+0.94	10.31+1.35	11.89+1.98	23.82+6.33	33.69+11.21	39.90+11.50	37.59+7.42	38.82+7.95	39.95+4.13	NA
	Mean+1 SD%	7.76+13.7%	8.21+12.8%	9.13+10.3%	10.31+13.1%	11.89+16.6%	23.82+26.6%	33.69+33.3%	39.90+28.8%	37.59+19.7%	38.82+20.5%	39.95+10.3%	NA
	Mean+1 SE	7.76+0.53	8.21+0.52	9.13+0.47	10.31+0.68	11.89+0.99	23.82+3.16	33.69+5.61	39.90+5.75	37.59+3.71	38.82+3.98	39.95+2.07	NA
	Mean+1 SE%	7.76+6.9%	8.21+6.4%	9.13+5.1%	10.31+6.6%	11.89+8.3%	23.82+13.3%	33.69+16.6%	39.90+14.4%	37.59+9.9%	38.82+10.2%	39.95+5.2%	NA
	Median	7.63	8.19	9.2	10.17	11.645	23.37	32.24	39.995	36.7	38.49	39.565	NA
	Minimum	6.6	7.28	8.08	8.91	9.92	16.61	23.67	28.82	31.22	31.52	35.57	NA
	Maximum	9.16	9.17	10.03	11.97	14.33	31.92	46.6	50.78	45.75	46.78	45.09	NA
Tptpul	Count	12	12	12	12	12	12	12	12	12	12	12	NA
	Mean+1 SD	7.78+0.62	8.21+0.48	9.00+0.68	9.62+0.53	10.81+0.83	14.94+4.44	23.36+7.77	31.07+10.97	33.71+9.76	42.41+20.22	45.98+16.80	NA
	Mean+1 SD%	7.78+8.0%	8.21+5.9%	9.00+7.5%	9.62+5.5%	10.81+7.7%	14.94+29.7%	23.36+33.3%	31.07+35.3%	33.71+29.0%	42.41+47.7%	45.98+36.5%	NA
	Mean+1 SE	7.78+0.18	8.21+0.14	9.00+0.20	9.62+0.15	10.81+0.24	14.94+1.28	23.36+2.24	31.07+3.17	33.71+2.82	42.41+5.84	45.98+4.85	NA
	Mean+1 SE%	7.78+2.3%	8.21+1.7%	9.00+2.2%	9.62+1.6%	10.81+2.2%	14.94+8.6%	23.36+9.6%	31.07+10.2%	33.71+8.4%	42.41+13.8%	45.98+10.5%	NA
	Median	7.77	8.445	9.025	9.62	10.72	13.015	22.755	29.1	35.025	36.67	39.43	NA
	Minimum	6.7	7.26	7.78	8.58	9.45	10.7	11.97	13.42	15.51	18.41	25.17	NA
	Maximum	8.74	8.72	10.07	10.35	12.73	25.83	35.88	49.03	50.46	84.01	75.58	NA
Tptpmn	Count	71	71	71	71	71	71	71	65	65	65	65	28
	Mean+1 SD	8.06+0.73	9.00+0.82	9.11+0.56	9.77+0.57	10.46+0.74	11.42+0.89	12.94+1.68	16.55+3.43	21.87+4.80	33.56+9.28	49.17+11.24	43.34+13.29
	Mean+1 SD%	8.06+9.1%	9.00+9.1%	9.11+6.1%	9.77+5.8%	10.46+7.0%	11.42+7.8%	12.94+13.0%	16.55+20.7%	21.87+21.9%	33.56+27.7%	49.17+22.9%	43.34+30.7%
	Mean+1 SE	8.06+0.09	9.00+0.10	9.11+0.07	9.77+0.07	10.46+0.09	11.42+0.11	12.94+0.20	16.55+0.43	21.87+0.60	33.56+1.15	49.17+1.39	43.34+2.51
	Mean+1 SE%	8.06+1.1%	9.00+1.1%	9.11+0.7%	9.77+0.7%	10.46+0.8%	11.42+0.9%	12.94+1.5%	16.55+2.6%	21.87+2.7%	33.56+3.4%	49.17+2.8%	43.34+5.8%
	Median	8.09	8.81	9	9.6	10.35	11.33	12.51	15.87	21.5	31.66	47.56	40.2
	Minimum	6.03	6.47	7.4	8.66	8.99	9.16	10.74	10.93	12.58	11.97	29.53	27.2
	Maximum	9.58	11	10.63	11.2	12.3	13.3	20.5	28.1	35	57.9	81.4	73
TptpII	Count	10	10	10	10	10	6	6	6	6	6	6	NA
	Mean+1 SD	7.71+0.69	8.51+0.38	8.84+0.56	9.09+0.51	9.88+0.57	10.82+0.87	12.96+2.57	15.06+3.06	17.77+3.16	21.77+3.41	28.51+4.58	NA
	Mean+1 SD%	7.71+8.9%	8.51+4.4%	8.84+6.3%	9.09+5.6%	9.88+5.7%	10.82+8.1%	12.96+19.8%	15.06+20.3%	17.77+17.8%	21.77+15.7%	28.51+16.1%	NA
	Mean+1 SE	7.71+0.22	8.51+0.12	8.84+0.18	9.09+0.16	9.88+0.18	10.82+0.36	12.96+1.05	15.06+1.25	17.77+1.29	21.77+1.39	28.51+1.87	NA
	Mean+1 SE%	7.71+2.8%	8.51+1.4%	8.84+2.0%	9.09+1.8%	9.88+1.8%	10.82+3.3%	12.96+8.1%	15.06+8.3%	17.77+7.3%	21.77+6.4%	28.51+6.6%	NA
	Median	7.555	8.555	8.955	9.02	9.925	10.685	11.875	13.635	17.105	21.18	27.79	NA
	Minimum	6.9	7.89	8.11	8.35	9.15	9.83	10.7	12.13	14.42	17.59	22.76	NA
	Maximum	9.02	9.06	9.65	9.86	10.75	11.92	17.5	19.62	22.1	27.04	35.63	NA

Table 6-84 Intact Rock Coefficients of Thermal Expansion of Air-Dried Specimens (Continued)

Stratigraphic Units	Intact Rock Coefficient of Thermal Expansion (10^{-6}/°C), Air-Dried												
	Temperature °C	**25-5**	**50-75**	**75-100**	**100-125**	**125-150**	**150-175**	**175-200**	**200-225**	**225-250**	**250-275**	**275-300**	**300-325**
TptpIn	Count	10	10	10	10	10	10	10	10	10	10	10	NA
	Mean+1 SD	7.18+1.31	8.19+0.68	8.97+0.79	9.74+1.26	10.69+2.19	11.33+2.62	12.22+2.07	12.95+1.56	14.27+1.46	15.48+2.51	18.62+4.91	NA
	Mean+1 SD%	7.18+18.2%	8.19+8.3%	8.97+8.8%	9.74+12.9%	10.69+20.4%	11.33+23.1%	12.22+17.0%	12.95+12.1%	14.27+10.3%	15.48+16.2%	18.62+26.4%	NA
	Mean+1 SE	7.18+0.41	8.19+0.22	8.97+0.25	9.74+0.40	10.69+0.69	11.33+0.83	12.22+0.66	12.95+0.49	14.27+0.46	15.48+0.79	18.62+1.55	NA
	Mean+1 SE%	7.18+5.7%	8.19+2.6%	8.97+2.8%	9.74+4.1%	10.69+6.5%	11.33+7.3%	12.22+5.4%	12.95+3.8%	14.27+3.2%	15.48+5.1%	18.62+8.3%	NA
	Median	7.345	8.095	8.745	9.235	9.835	10.285	11.2	12.46	13.98	14.715	17.905	NA
	Minimum	4.32	7.38	8.01	8.85	9.05	9.17	10.47	11.51	12.45	12.13	11.5	NA
	Maximum	8.97	9.48	10.53	12.57	15.06	16.45	16.06	16.01	17.15	19.74	26.16	NA
Calico	Count	8	8	8	8	7	8	8	8	6	5	4	4
	Mean+1 SD	5.75+1.20	6.36+1.11	5.14+1.47	3.64+1.76	4.53+1.51	4.50+2.27	4.78+1.91	4.53+2.40	5.12+2.84	5.26+2.34	5.13+2.42	2.50+2.48
	Mean+1 SD%	5.75+20.9%	6.36+17.4%	5.14+28.5%	3.64+48.5%	4.53+33.4%	4.50+50.4%	4.78+40.1%	4.53+52.9%	5.12+55.5%	5.26+44.4%	5.13+47.1%	2.50+99.2%
	Mean+1 SE	5.75+0.42	6.36+0.39	5.14+0.52	3.64+0.62	4.53+0.57	4.50+0.80	4.78+0.68	4.53+0.85	5.12+1.16	5.26+1.04	5.13+1.21	2.50+1.24
	Mean+1 SE%	5.75+7.4%	6.36+6.2%	5.14+10.1%	3.64+17.1%	4.53+12.6%	4.50+17.8%	4.78+14.2%	4.53+18.7%	5.12+22.7%	5.26+19.9%	5.13+23.6%	2.50+49.6%
	Median	5.8	6.15	5.6	4.1	4.9	5.05	4.85	4.35	5.85	5.8	4.45	1.4
	Minimum	4	4.6	2.5	1.1	2.4	0.3	1.8	1.9	0.2	2	3	1
	Maximum	7.8	8	6.9	6	6.8	7.4	7.5	8.3	8.6	8.3	8.6	6.2

Sources: DTNs: SNL01B05059301.006 [DIRS 129168]; SNL22100196001.002 [DIRS 153138]; SNL22080196001.003 [DIRS 119042]; SNL22080196001.001 [DIRS 109722].

NOTE: Data below the Calico unit are not included in this table.

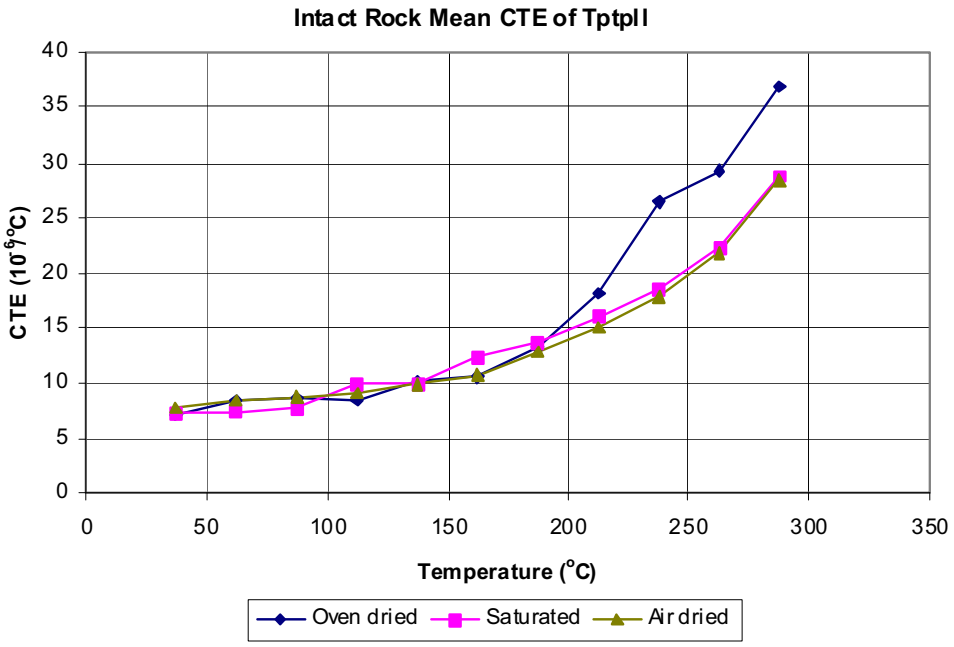

a)

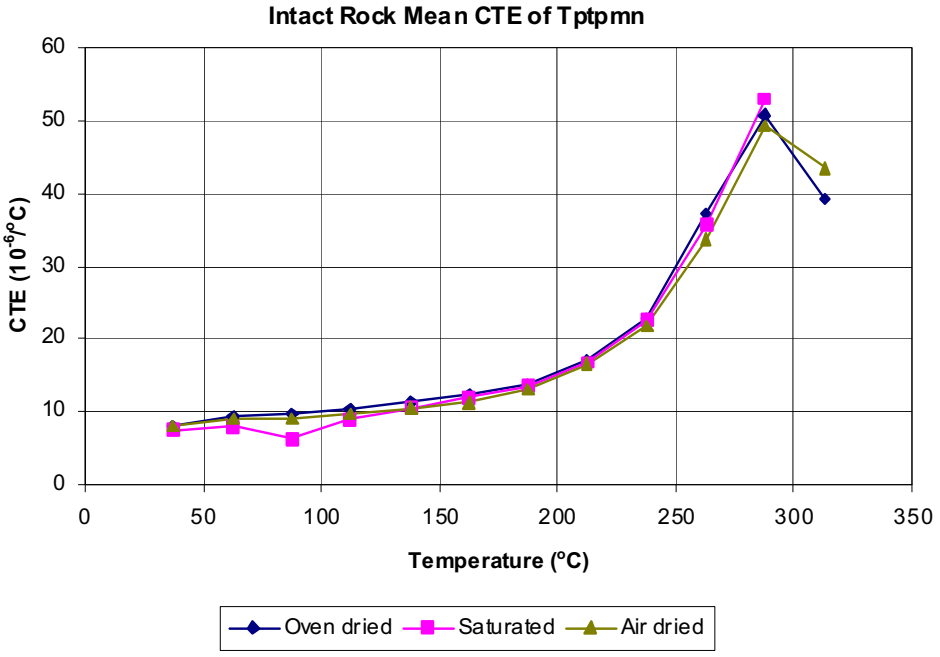

b)

Sources: DTNs: SNL01B05059301.006 [DIRS 129168]; SNL22100196001.002 [DIRS 153138]; SNL22080196001.003 [DIRS 119042]; SNL22080196001.001 [DIRS 109722].

Figure 6-128. Intact Rock Mean CTE Measured from Oven-Dried, Saturated, and Air-Dried Specimens of a) Tptpmn and b) Tptpll Zones

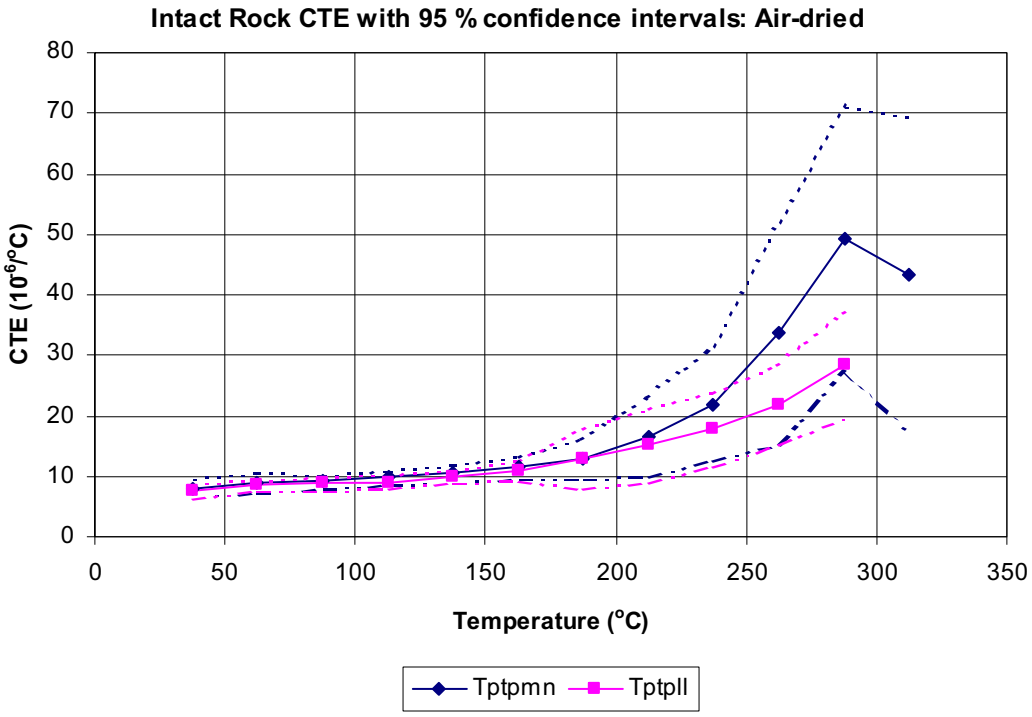

Sources: DTNs: SNL01B05059301.006 [DIRS 129168]; SNL22100196001.002 [DIRS 153138]; SNL22080196001.003 [DIRS 119042]; SNL22080196001.001 [DIRS 109722].

Figure 6-129. Intact Air-Dried CTE of Tptpmn and Tptpll Zones with 95% Confidence Intervals (1.96 Times the Standard Deviations)

Sensitivity of intact rock CTE to temperature, thermal cycles, moisture content, specimen size, and confining stress has been evaluated based on laboratory tests. The evaluation on the effects of the impacting factors was carried out by comparing results from the laboratory tests at different testing conditions.

Effect of Temperature—Intact rock CTE is highly temperature dependent and increases with increasing temperatures (Brodsky et al. 1997 [DIRS 100653], Section 4.2.1). This can be observed in the CTE values from the Tptpmn and Tptpll zone specimens, as shown in Figure 6-129. Over a temperature range from 150°C to 200°C, the CTE values start to increase more steeply, which is believed to be associated with mineral phase changes occurring in Yucca Mountain welded tuff. Both the CTE values for the Tptpmn and the Tptpll zones show steep increase of the CTE values at the transition temperature of approximately 175°C to 225°C due to the presence of tridymite and cristobalite (Brodsky et al. 1997 [DIRS 100653], Section 4.2.2.2). The phase changes of tridymite and cristobalite induce a significant increase in CTE values among the welded tuffs. It is also observed that the CTE values for the Tptpmn specimens are greater than those for the Tptpll, especially when temperatures exceed 200°C. The temperature dependency of CTE was also observed on both wet (saturated) and dry (oven-dried) specimens (Figure 6-128).

Effect of Thermal Cycles—The laboratory CTE measurements were made on both thermal heating and cooling cycles (Brodsky et al. 1997 [DIRS 100653], Section 4.2.1; CRWMS M&O 1997 [DIRS 101539], Section 3.4.2). The impact on the first and subsequent thermal cycles are small in spite of permanent strains that accumulated during the first thermal cycle, and the intact rock CTE are reproducible from cycle to cycle (CRWMS M&O 1997 [DIRS 101539], Section 3.4.2 and Appendix B). The observation is confirmed in the CTE measurements for the Tptpmn specimens from the SHT and the DST areas (Tables 6-85 and 6-86). The CTE for the Tptpmn zone from the heating and cooling phases is presented in Figure 6-130. The CTE from the cooling phase has larger values than the CTE from the heating phase except in the high temperature regime over 250°C. The difference in the CTE in the cooling phase may be from the different path of phase change of tridymite and cristobalite, or it could be from slower recovery of pore space in the specimens.

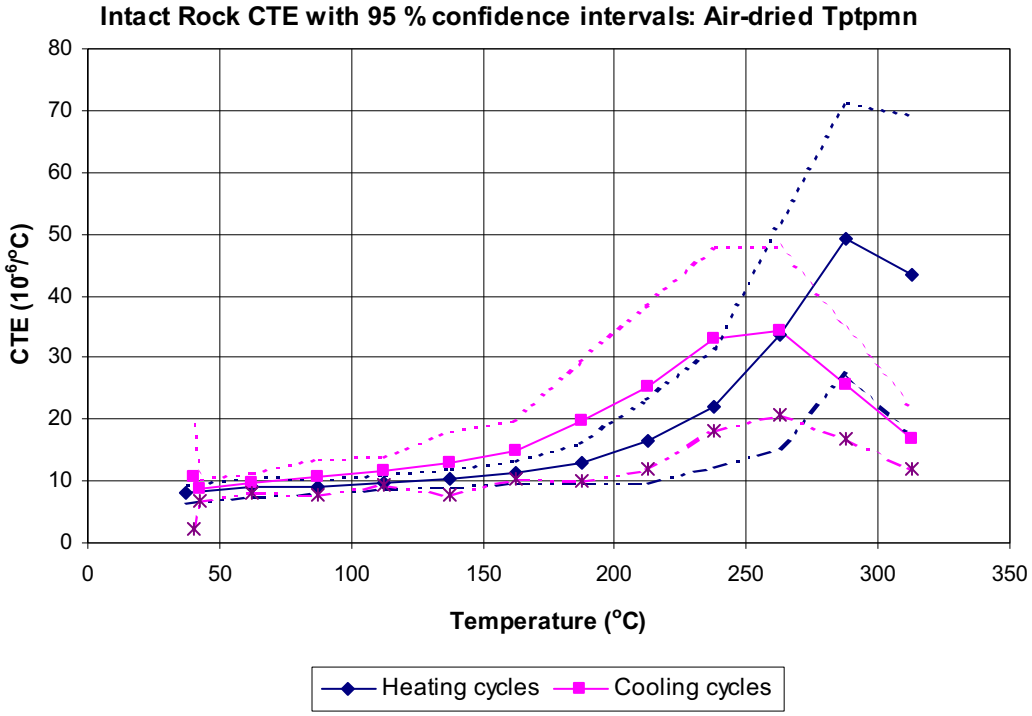

Sources: DTNs: SNL01B05059301.006 [DIRS 129168]; SNL22100196001.002 [DIRS 153138]; SNL22080196001.003 [DIRS 119042]; SNL22080196001.001 [DIRS 109722].

Figure 6-130. Intact Air-Dried CTE for the Tptpmn Zone with 95% Confidence Intervals (1.96 Times the Standard Deviations) from Heating and Cooling Phases

Table 6-85. Intact CTE measurements of Tptpmn Specimens from the SHT during Thermal Cycles

Mean CTE on the First Heating Cycle (10^{-6}/c)												
Temperature	**25-50 °C**	**50-75 °C**	**75-100 °C**	**100-125 °C**	**125-150 °C**	**150-175 °C**	**175-200 °C**	**200-225 °C**	**225-250 °C**	**250-275 °C**	**275-300 °C**	**300-325 °C**
N	14	14	14	14	14	14	14	14	14	14	14	14
Mean	8.63	9.87	8.95	9.64	10.62	11.77	12.34	15.37	21.89	33.56	57.06	54.88
Std. Deviation	0.46	0.65	0.55	0.60	0.62	0.72	0.97	1.66	5.47	8.58	12.03	8.49
Mean CTE on the First Cooling Cycle (10^{-6}/c)												
Temperature	300-325 °C	275-300 °C	275-250 °C	225-250 °C	200-225 °C	175-200 °C	150-175 °C	125-150 °C	100-125 °C	75-100 °C	50-75 °C	30-50 °C
N	14	14	14	14	14	14	14	14	14	14	14	14
Mean	16.55	28.52	38.83	36.47	28.54	21.19	15.57	12.92	11.95	10.95	10.11	10.43
Std. Deviation	2.55	3.86	5.32	8.94	11.86	5.86	2.28	0.99	0.68	1.30	0.54	2.87
Mean CTE on the Second Heating Cycle (10^{-6}/c)												
Temperature	25-50 °C	50-75 °C	75-100 °C	100-125 °C	125-150 °C	150-175 °C	175-200 °C	200-225 °C	225-250 °C	250-275 °C	275-300 °C	300-325 °C
N	14	14	14	14	14	14	14	14	14	14	14	14
Mean	8.53	9.67	9.01	10.21	11.13	12.23	14.10	19.08	25.17	43.56	49.64	31.80
Std. Deviation	0.41	0.56	0.55	0.34	0.39	0.61	2.09	3.25	4.17	9.33	8.15	2.83
Mean CTE on the Second Cooling Cycle (10^{-6}/c)												
Temperature	300-325 °C	275-300 °C	275-250 °C	225-250 °C	200-225 °C	175-200 °C	150-175 °C	125-150 °C	100-125 °C	75-100 °C	50-75 °C	30-50 °C
N	14	14	14	14	14	14	14	14	14	14	14	14
Mean	17.38	28.64	39.99	38.36	26.02	20.00	15.16	13.69	11.81	11.13	10.13	10.84
Std. Deviation	2.57	3.65	4.63	7.23	3.36	3.89	2.10	5.42	1.49	2.87	1.42	5.42

Source: DTN: SNL22080196001.003 [DIRS 119042].

NOTE: Air dried.

Table 6-86. Intact CTE Measurements of Tptpmn Specimens from the DST[a] during Thermal Cycles

Mean CTE on the First Heating Cycle (10^{-6}/°C)												
Temperature	**25~50 °C**	**50~75 °C**	**75~100 °C**	**100~125 °C**	**125~150 °C**	**150~175 °C**	**175~200 °C**	**200~225 °C**	**225~250 °C**	**250~275 °C**	**275~300 °C**	**300~325 °C**
N	17	17	17	17	17	17	17	17	17	17	17	13
Mean	7.34	8.99	9.73	10.22	10.91	12.20	14.74	22.31	27.34	33.88	54.13	52.28
Std. Dev.	0.57	0.47	0.54	0.58	0.79	1.04	4.79	18.09	15.70	6.94	12.18	13.42
Mean CTE on the First Cooling Cycle (10-6/oC)												
Temperature	300~325 °C	275~300 °C	250~275 °C	225~250 °C	200~225 °C	175~200 °C	150~175 °C	125~150 °C	100~125 °C	75~100 °C	50~75 °C	30~50 °C
N	13	17	17	17	17	17	17	17	17	17	16	15
Mean	15.74	24.07	35.63	36.01	26.50	24.19	18.30	14.14	12.36	11.05	10.24	9.67
Std. Dev.	1.88	5.70	8.39	8.32	4.69	9.82	7.37	2.61	1.76	0.84	1.24	0.66
Mean CTE on the Second Heating Cycle (10-6/oC)												
Temperature	25~50 °C	50~75 °C	75~100 °C	100~125 °C	125~150 °C	150~175 °C	175~200 °C	200~225 °C	225~250 °C	250~275 °C	275~300 °C	300~325 °C
N	17	17	17	17	17	17	17	17	17	17	17	13
Mean	7.22	8.87	9.63	10.24	11.28	13.22	19.37	22.66	24.82	37.84	46.78	34.46
Std. Dev.	0.76	0.59	0.54	0.61	0.98	2.98	14.97	10.66	5.47	9.52	11.63	10.17
Mean CTE on the Second Heating Cycle (10-6/°C)												
Temperature	300~325 °C	275~300 °C	250~275 °C	225~250 °C	200~225 °C	175~200 °C	150~175 °C	125~150 °C	100~125 °C	75~100 °C	50~75 °C	30~50 °C
N	13	17	17	17	17	17	17	17	17	17	17	17
Mean	16.50	26.48	37.06	36.39	26.44	23.64	17.46	13.75	12.01	11.36	10.16	9.81
Std. Dev.	1.06	2.32	4.00	3.77	2.14	4.50	2.92	0.99	0.56	0.87	0.31	0.33

Source: DTN: SN0203L2210196.007 [DIRS 158322].

NOTES: Air dried. Lithostratigraphic zone is Tptpmn except for HDFR1-97.9, which may be from Tptpll.

Effect of Porosity—Effect of porosity on the intact rock CTE has been investigated, and it is incorporated with matrix porosity data from DTN: SNL01A05059301.007 [DIRS 108980]. The CTE of the six specimens of UE25 NRG-5 with matrix porosity are presented in Figure 6-131. The figure does not show any significant correlation between porosity and CTE for either the temperature ranges of 150°C to175°C and 175°C to 200°C. Therefore, the effect of matrix porosity on the intact rock CTE may be considered minor compared to the effect of temperature. However, since the number of specimens is very limited, the investigation for the effect of porosity on the intact rock CTE has relatively higher uncertainty.

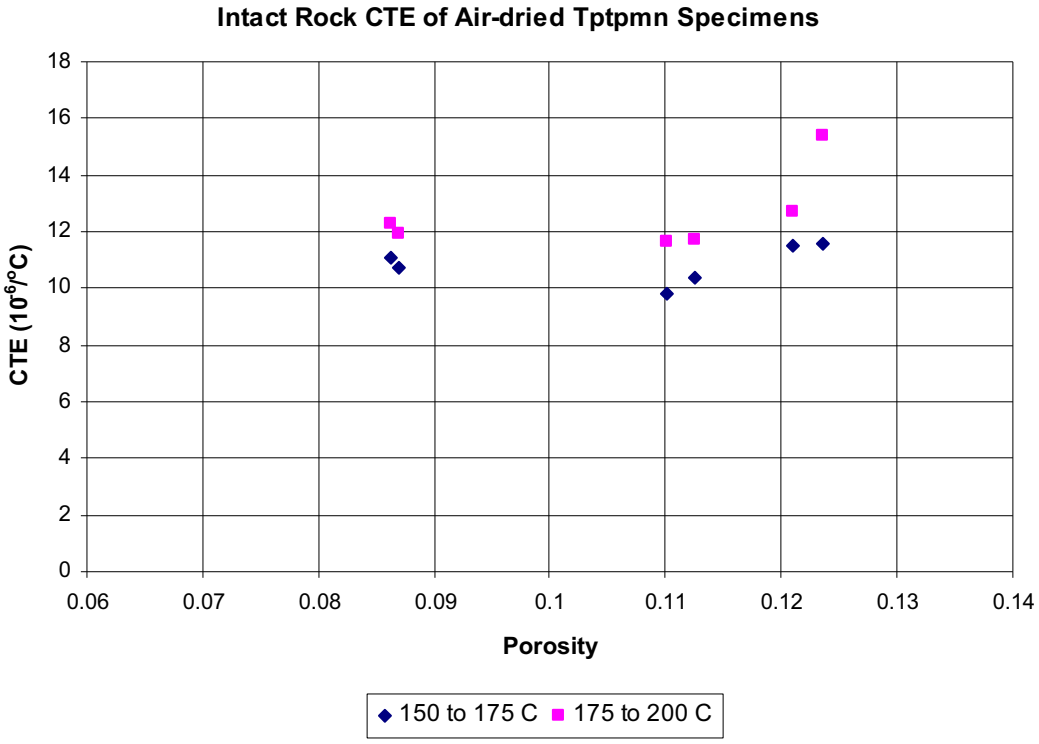

Sources: DTNs: SNL01B05059301.006 [DIRS 129168]; SNL01A05059301.007 [DIRS 108980].

Figure 6-131. Intact Rock CTE from Borehole UE25 NRG-5 (Tptpmn) Specimens with Different Matrix Porosity

Effect of Moisture Content—The effect of moisture content on intact rock CTE was investigated through laboratory CTE measurements using air- or oven-dried and vacuum-saturated specimens. The independency of the saturation state for the welded specimens is discussed in Brodsky et al. (1997 [DIRS 100653], Section 4.2.2.1). The laboratory CTE measurements indicate that the moisture content of specimens has insignificant effect on the CTEs, especially at temperatures below 200°C. The differences of CTE measurements between the air-dried, oven-dried, and saturated specimens of the Tptpmn and Tptpll zones are presented in Figure 6-128. The intact rock CTE for the Tptpmn zone indicates that the conditions of water contents do not have a significant impact on the values of CTE (Figure 6-128a). Decrease of CTE with increase in the water content in the 75°C to 100°C temperature range suggests the

effect of phase change of pore water, but the change is small compared to the increase in the CTE values with increasing temperature. The effect of the moisture is insignificant for the Tptpll zone (Figure 6-128b).

Effect of Specimen Size—Most of laboratory thermal expansion measurements were made on small specimens with a nominal diameter of 25.4 mm or 1 in. (Brodsky et al. 1997 [DIRS 100653], Table 2-1; CRWMS M&O 1997 [DIRS 101539], Table 3-2). Since the Yucca Mountain Tuff contains features such as lithophysae and fractures, the effect of these features on CTE depends upon the size of specimens tested. This effect was investigated for Tptpll rock unit by comparing the CTE values obtained from tests on small 1-in (25.4 mm) specimens to those on large 12-in (30.5 cm) specimens (DTNs: SN0208L01B8102.001 [DIRS 165211]; SN0211L01B8102.002 [DIRS 165218]). Comparison of the results is shown in Figure 6-132. The CTE values from the smaller specimens are generally greater than those from the larger specimens, indicating that portion of the space occupied by air in larger specimens is "absorbed" by expanding rock matrix during heating, resulting in a lower CTE. The difference in CTE between two sizes of specimens is diminishing as temperature increases, which may be a result of voids or fractures closing because of the increase in temperature.

Effect of Mineral Content—As discussed in Section 6.5.1.1, the effect of mineralogy on thermal properties could be considered a part of the temperature dependency on thermal properties.

Effect of Loading Condition—Most of the laboratory thermal expansion measurements were made at ambient atmospheric pressure. By definition, CTE is measured at a stress-free condition. This can be achieved in a laboratory test; however, in a drift-scale field thermal expansion measurement, a stress-free condition is difficult to achieve. Adjustment of field measurements for confining stresses is a complex issue as it requires an accurate determination of the magnitude of stresses at the location where the thermal expansion is measured. Sometimes the stress conditions are unknown. Additionally, some mineralogical phase changes are not only temperature dependent but also pressure sensitive. For these reasons, the effect of confining stress on CTE was assessed in laboratory tests using the specimens taken from borehole USW SD-12, covering the rock units of the Tptpmn, Tptpll, and Tptpln zones (Martin et al. 1997 [DIRS 104758], Sections 3 and 4). Tests were conducted at a confining stress ranging from 1 to 30 MPa. At each confining stress, several thermal cycles were performed up to a temperature of about 250°C.

The CTE measurements for the Tptpmn zone under different confining stresses are presented in Figure 6-133. It appears that at low temperature, the CTE values at high confining stresses are slightly higher than those at higher confining stress, while at higher temperature the CTE values at high confining stresses are lower than those at higher confining stress. Overall, the CTE measurements are not very sensitive to the confining stress, compared to the effect of temperature (Martin et al. 1997 [DIRS 104758], Sections 3 and 4).

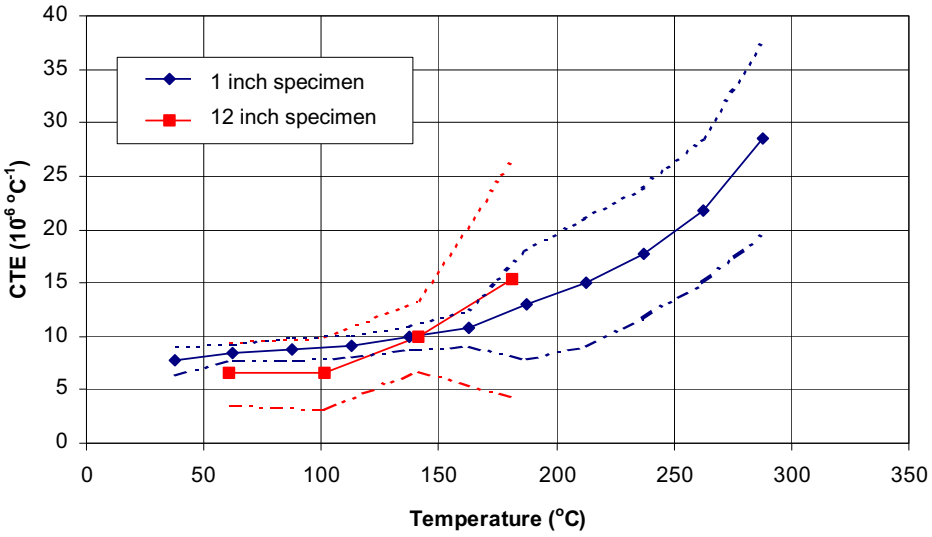

Sources: DTNs: SNL01B05059301.006 [DIRS 129168]; SNL22100196001.002 [DIRS 153138]; SNL22080196001.003 [DIRS 119042]; SNL22080196001.001 [DIRS 109722]; SN0208L01B8102.001 [DIRS 165211]; SN0211L01B8102.002 [DIRS 165218].

Figure 6-132. CTEs Measurements with 95% Confidence Intervals (1.96 Times the Standard Deviations) on 1-in (25.4 mm) and 12-in (30.5 cm) Specimens from the Tptpll Zone

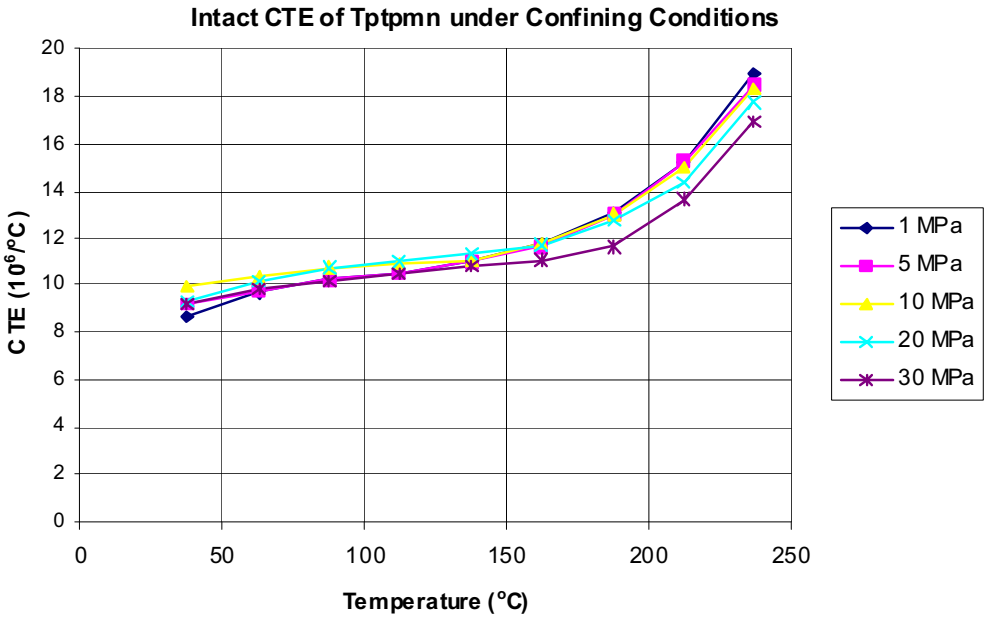

Source: DTN: SNL01B02019501.001 [DIRS 177308].

Figure 6-133. Intact CTE of Tptpmn Zone under Different Confining Stresses from Heating Phase

6.5.3 Thermal Properties for Rock Mass

6.5.3.1 Thermal Conductivity

Significant efforts have been made to develop some correlations between intact rock matrix thermal conductivity, porosity of both matrix and lithophysae, and rock mass thermal conductivity. These efforts included developing theoretical approaches and conducting field experimental tests. Determination of rock mass thermal conductivity is more difficult than that of intact rock because of the scale requirement in a test. It is difficult to conduct laboratory testing using a specimen with a size at drift scale. Field measurements are usually used and require more effort and resources. To compensate for the lack of field measurements, use of either laboratory measurements with large specimens or analytical calculations based on the correlation between intact rock thermal conductivity, rock mass thermal conductivity, and key controlling factors such as porosity may serve as alternatives to estimating the rock mass thermal conductivity.

Field measurements are considered the most effective and valuable methods to determine rock mass thermal conductivity. The measurements can be made using a thermal probe consisting of a heat source and several temperature sensors. During measurements, a certain amount of heat is transferred to the rock, and temperature differences caused by the heat are measured.

6.5.3.1.1 Field Measurements of Rock Mass Thermal Conductivity

Two major field tests to measure the rock mass thermal conductivity include the DST and the In Situ Measurements of Thermal Conductivity in the ECRB Cross-Drift. The DST measurements are made on the Tptpmn rock, while the ECRB Cross-Drift measurements are made on the Tptpll rock.

The DST is conducted in a block of rock of approximately 60 m wide, 50 m deep, and 50 m high. The test includes 9 floor/canister heaters in a 5 m diameter drift and 50 wing heaters installed in horizontal boreholes drilled perpendicular to the drift into the rock (BSC 2004 [DIRS 169900], Figure 6.3-2). The DST lasted about 8 years with 4 years of heating and four years of cooling. The maximum drift wall temperature at the end of the heating phase was about 200°C. For measurements of the rock mass thermal conductivity, five locations were selected based on the competency of the wall rock, including minimal fracturing, sufficient separation from rock bolts installed, and similarity of density. The testing boreholes were drilled in random directions to average the effects of unseen physical phenomena (e.g., faulting, stress relief). The temperatures during the heating phase in these boreholes were measured using the Rapid Estimation of thermal conductivity ($\boldsymbol{k}$) and thermal diffusivity (α, Alpha) with a REKA probe developed at the University of Nevada, Reno, and they were used to determine the rock mass thermal conductivity (BSC 2004 [DIRS 169900], Section 6.3.1.4; CRWMS M&O 1997 [DIRS 101539], Section 10.2). The REKA probe used a two-dimensional optimization procedure based on the least-squares-fit of the simulated temperature field to the measured temperature field (CRWMS M&O 1997 [DIRS 101539], Section 10.2) to evaluate the best prediction for thermal conductivity and thermal diffusivity.

Rock mass thermal conductivities of the Tptpmn zone measured at the DST during the preheating phase are presented in Table 6-87, while field thermal conductivity measurements during the heating phase are shown in Figure 6-134 and Table 6-88. The thermal conductivity values are generally lower than those observed in the laboratory measurements on the saturated specimens from the same rock unit, but are higher than those for the oven-dried specimens (Tables 6-78 and 6-79). However, the field thermal conductivity values obtained from the field measurements normally fall within the same range as those from the laboratory measurements (Figures 6-120 and 6-121), indicating that the effects of the heterogeneity and discontinuities in the Tptpmn on thermal conductivity are not as significant as anticipated.

Table 6-87. In Situ Field Rock Thermal Conductivity at DST During the Preheating Phase

REKA Probe Location	No Background Temperature Correction		With Background Temperature Correction	
	Thermal Conductivity (W/m-K)	Error of Fit [a] (°C)	Thermal Conductivity (W/m-K)	Error of Fit [a] (°C)
1	1.69	0.033	1.72	0.015
2	1.95	0.037	1.92	0.010
3	1.86	0.024	1.89	0.018
4	1.88	0.039	1.93	0.015
5	1.70	0.025	1.76	0.025
Average	1.82		1.84	

Source: CRWMS M&O 1997 [DIRS 101539], Tables 10-1 and 10-2.

NOTE: [a] Error of fit is the root mean square between the simulated and measured temperature fields, all having 35 readings with time and 6 readings along the length of the Sierra Science REKA probe.

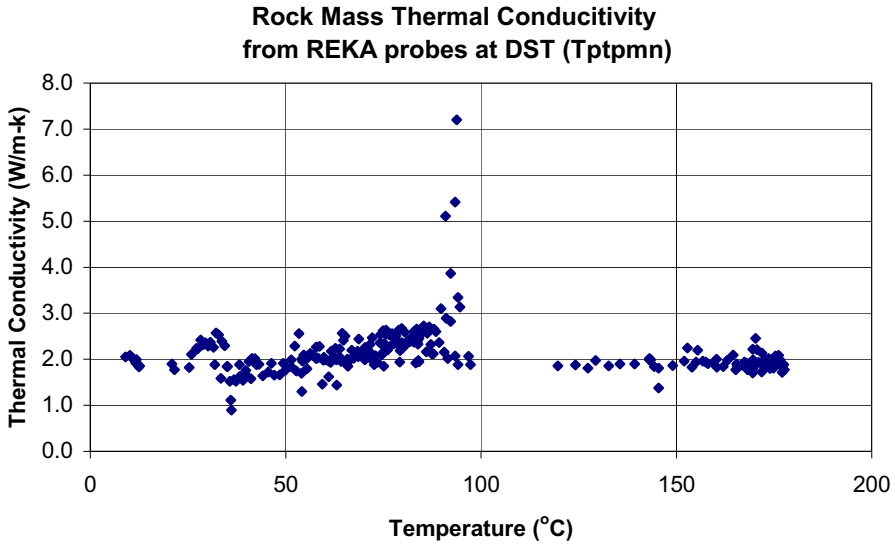

Sources: DTNs: UN0106SPA013GD.004 [DIRS 159116]; UN0201SPA013GD.007 [DIRS 159119].

Figure 6-134. In situ Field Rock Thermal Conductivity at DST During the Heating Phase

Table 6-88. In Situ Field Rock Thermal Conductivity at the DST During the Heating Phase

Field Rock Thermal Conductivity (W/m-K)						
Temperature	**20~35 °C**	**35~50 °C**	**50~70 °C**	**70~90 °C**	**90~100 °C**	**120~180 °C**
Count	14	21	33	55	9	76
Mean+1 SD	2.28+0.23	1.65+0.26	2.05+0.31	2.44+0.21	3.98+1.63	1.92+0.14
Mean+1 SD%	2.28+10.3%	1.65+16.1%	2.05+15.3%	2.44+8.4%	3.98+40.9%	1.92+7.3%
Mean+1 SE	2.28+0.06	1.65+0.06	2.05+0.05	2.44+0.03	3.98+0.54	1.92+0.02
Mean+1 SE%	2.28+2.7%	1.65+3.5%	2.05+2.7%	2.44+1.1%	3.98+13.6%	1.92+0.8%
Median	2.30	1.65	2.08	2.45	3.34	1.91
Minimum	1.58	0.90	1.30	1.89	2.02	1.38
Maximum	2.57	2.02	2.57	3.10	7.20	2.45

Sources: DTNs: UN0106SPA013GD.004 [DIRS 159116]; UN0201SPA013GD.007 [DIRS 159119].

The field measurements of rock mass thermal conductivity in the ECRB Cross-Drift consisted of three tests. The first test involved a single heater and single instrumentation borehole (two-hole test in Table 6-89, DTN: SN0206F3504502.012 [DIRS 159145]). The heater was 5 m long and was inset approximately 3 m from the ECRB drift wall. The second borehole, perpendicular to the first and about 12 cm above it, contained 30 thermocouples. The second test comprised an array of three heaters and three instrumentation boreholes and sampled a much larger test volume (six-hole test in Table 6-89, DTN: SN0208F3504502.019 [DIRS 161883]). The other dimensions were similar to the first test. The third test used a single heater but had instrumentation holes both above and below the heater to measure any effect of convection on temperature distribution (three-hole test in Table 6-89, DTN: SN0206F3504502.013 [DIRS 159146]). Other dimensions were also similar to the first test. Details on the configurations of these three field tests are provided in *Field Measurements of Thermal Conductivity in the Topopah Spring Lower Lithophysal Unit (Tptpll)* (Kalia 2001 [DIRS 165092], Section 2). The rock mass thermal conductivity was determined by a "back calculation" method based on a relationship for heat conduction in a heated sphere (Carslaw and Jaeger 1959 [DIRS 100968], Equation 4). In this method, predicted temperatures are calculated using initial guesses for thermal conductivity and diffusivity. The measured and predicted temperatures are compared, and the error is taken as the sum of the squares of the differences between measured and predicted values. The values of thermal conductivity and diffusivity are adjusted until the error is within the specified criterion.

The results of three field tests of rock mass thermal conductivity are presented in Table 6-89. The mean values ranged from 1.73 to 2.18 W/m-K. Similar to what was indicated in the field measurements of the DST for the Tptpmn rock (Tables 6-87 and 6-88), the in situ field measurement values are placed between the saturated and oven-dried values (Tables 6-78 and 6-79). The in situ field measurement values are also within the same range as those observed in the laboratory measurements on specimens in Figures 6-120 and 6-121. The observation from the field measurements may indicate that the effects of the heterogeneity and discontinuities on thermal conductivity are not as significant.

Table 6-89. Rock Mass Thermal Conductivity Values from ECRB Cross-Drift Thermal K Tests

ECRB Cross-Drift Thermal K Test 1 (Two-Hole Test)[1]	ECRB Cross-Drift Thermal K Test 2 (Six-Hole Test)[2]		ECRB Cross-Drift Thermal K Test 3 (Three-Hole Test)[3]	
Thermal conductivity (W/m-K)	Borehole	Thermal conductivity (W/m-K)	Borehole	Thermal conductivity (W/m-K)
1.75[a] or 1.74[b]	TMK6	2.18	TMK10	1.73
	TMK7	2.09	TMK11	1.76
	TMK8	2.03		
Average: 1.92 W/m-K				

Sources: [1]DTN: SN0206F3504502.012 [DIRS 159145].

[2]DTN: SN0208F3504502.019 [DIRS 161883].

[3]DTN: SN0206F3504502.013 [DIRS 159146].

[a] A single value of each thermal property was calculated using all the data shown in DTN: SN0206F3504502.011 [DIRS 165270].

[b] A single value of each thermal property was calculated using the data shown in DTN: SN0206F3504502.011 [DIRS 165270] from an elapsed time of 2.665 days through 28.63 days. The earlier data were scattered.

Effect of Temperature—The temperature impact on the field-measured thermal conductivity is apparent in the DST REKA measurements during the heating phase (Figure 6-134) and Table 6-88). As temperature increases from ambient temperature, the field measured thermal conductivity increases gradually. When the temperature approaches the boiling temperature of water, the thermal conductivity values increase sharply (Figure 6-134) and reach a peak of 7.2 W/m-K. After the boiling point is passed, thermal conductivity becomes temperature independent and maintains a low value around 1.9 W/m-K. The increase in thermal conductivities for temperature increases around the boiling point are rather similar to the laboratory thermal conductivity values from the oven-dried specimens (Table 6-78), which suggests that the same mechanisms increasing the oven-dried thermal conductivity are dominant for the field thermal conductivity. While the sharp increase of the field thermal conductivity values near the boiling point is not clearly explained, the post-boiling thermal conductivity that has relatively low values is obvious because of water content removal.

Effect of Porosity—Investigation on the effect of porosity should be considered in the field measurements at the ECRB since the DST REKA measurements represent a relatively small volume of rock mass (Assumption 5.4.2). The ECRB field thermal conductivity values (Table 6-89), which are associated with the bulk porosity that includes lithophysae and fractures, are between the saturated and oven-dried laboratory intact values (Tables 6-78 and 6-79) and are within the same range as the laboratory measurements (Figures 6-120 and 6-121). Therefore, the effects of the rock mass bulk porosity on thermal conductivity are not clear in the field measurements.

Effect of Moisture Content—The effect of moisture content, measured in terms of degree of saturation, is not obvious for the DST field thermal conductivity measurements during the preheating (Table 6-87) and the ECRB field thermal conductivity measurements (Table 6-89). Ambient saturation is estimated as 93% in the SHT, with a range from 81% to 99% (BSC 2004 [DIRS 169900], Table 6.2.2.5-2); therefore, the field thermal conductivity values are equivalent

to those between saturated and oven-dried intact values (Tables 6-78 and 6-79). However, the degree of impact of moisture content on thermal conductivity may not be quantified because the bulk porosity also contributes to the field thermal conductivity.

The effect of moisture content on thermal conductivity is apparent in the post-boiling field measurements at the DST during the heating phase (Figure 6-134). The relatively low and temperature independent values of the field thermal conductivity beyond the boiling point suggest virtual removal of moisture content. The *Thermal Testing Measurements Report* (BSC 2004 [DIRS 169900], Figure 6.3.2.3-2) supports this observation. The DST field measurements for temperatures below the boiling point don't show any distinctive correlation with the moisture content.

Scale Effect—Scale effect for the field thermal conductivity was not investigated since it is assumed that the scale of the field thermal conductivity measurements is sufficient enough to correspond to a representative volume of the unit of interest that contains all the heterogeneity or discontinuities that affect thermal conductivity (Assumption 5.4.2).

Effect of Mineral Content—As discussed in Section 6.5.1.1, the effect of mineralogy on thermal properties could be considered a part of the temperature dependency on thermal properties.

Effect of Loading Condition—Thermally induced stress during the heating phase of the DST field measurements is estimated quite high compared to the in situ stress. However, the DST field thermal conductivity values show a clear temperature independency for the post-boiling measurements (Figure 6-134). Therefore, the effect of the additional load induced by the temperature increase appears to be very minor, and the impact of loading condition is considered insignificant.

6.5.3.1.2 Analytical Estimation of Thermal Conductivity

Various analytical approaches have been developed for estimating the effective value of rock mass thermal conductivity, taking into account the effects of matrix, fracture, and lithophysal porosity (Kaviany 1991 [DIRS 148383]). Most of the approaches are capable of assessing the effective thermal conductivity of two-phase media (e.g., solid and fluid) using deterministic approaches idealizing microstructures of the media as spheres, disks, thin crack, and so on. The effective-medium approximation may not accurately predict the microstructure-sensitive conductivity of most real two-phase media because of its simple microstructures. Therefore, Torquato (1987 [DIRS 165105]) discussed statistical approaches by defining the upper and lower bounds of the effective thermal properties in order to deal with the limitation of the effective-medium approximation.

A comprehensive study for the rock mass thermal conductivity based on the three-dimensional cubic simulation (Hsu et al. 1995 [DIRS 158073]) and the parallel simulation (Torquato 1987 [DIRS 165105]) is presented in *Thermal Conductivity of the Potential Repository Horizon* (BSC 2004 [DIRS 169854], Section 6.1.7). Primary focus of the investigations was to assess spatial variability and uncertainty of the rock mass thermal conductivity. In the study (BSC 2004 [DIRS 169854]), the rock mass is conceptualized as a porous medium composed of matrix and

lithophysae, air-filled large-scale voids found to varying degrees in both lithophysal and nonlithophysal rocks. The matrix component was represented as solid minerals and their associated intergranular pore space. The matrix thermal conductivity was expressed as a function of the matrix porosity, the thermal conductivity of saturating fluid, the thermal conductivity of solid minerals, and the geometry and connectivity of the solid. The thermal conductivity of the saturating fluid is treated as constant, but the remaining simulation parameters are available from measurements of core samples or borehole petrophysical logs and are treated statically as spatially unconditional random functions.

The geostatistical method known as sequential Gaussian simulation (BSC 2004 [DIRS 169854], Section 6.1.3) was used to develop spatially independent realizations of these uncertain properties. The available measurements from core samples and borehole petrophysical logs are used to derive simulations of spatial continuity and to condition the three-dimensional geostatistical simulations. These three-dimensional property sets then serve as inputs to the matrix thermal conductivity simulation, yielding three-dimensional geostatistically-based realizations of the matrix thermal conductivity. Detailed description of the analytical approach for the matrix thermal conductivity based on the simulation by Hsu et al. (1995 [DIRS 158073]) and on the sequential Gaussian simulation is provided in *Thermal Conductivity of the Potential Repository Horizon* (BSC 2004 [DIRS 169854], Section 6.1.7).

The spatial variability and uncertainty of the bulk thermal conductivity is addressed in a similar manner. To estimate the bulk thermal conductivity, the parallel simulation is selected to incorporate the effects of lithophysal porosity on the composite bulk thermal conductivity. The lithophysal porosity is calculated from measurements of core samples or borehole petrophysical logs and is treated statically as a spatially unconditional random function (BSC 2004 [DIRS 169854], Section 6.1.4). The bulk thermal conductivity is calculated by considering that the matrix and lithophysae act in parallel with respect to energy transport. Applying Fourier's equation of heat conduction to a parallel system with Assumption 5.4.1 yields the following relation (Hadley 1986 [DIRS 153165], p. 914, Equation 18):

$$k_b = \phi_L k_a + (1 - \phi_L) k_m \qquad \text{(Eq. 6-35)}$$

where k_b and k_m are the rock mass and matrix thermal conductivity, respectively; ϕ_L is the lithophysal porosity; and k_a is the thermal conductivity of air.

Note that the volume average simulation expressed in Equation 6-35 represents a physical system of a series of parallel solid plates sandwiched by pore space and gives a higher bound estimate of the effective rock mass thermal conductivity since the system represented is the most efficient configuration of solid and pore space. To get a lower bound estimate for the rock mass thermal conductivity, other simulations, such as the simulation developed by Torquato (1987 [DIRS 165105]) or a simulation for a physical system of solid and pore space in series, may be used (BSC 2004 [DIRS 169854], Section 6.1.8). Details of the analytical estimation for the bulk thermal conductivity are provided in *Thermal Conductivity of the Potential Repository Horizon* (BSC 2004 [DIRS 169854], Section 6.1.8).

6.5.3.1.2.1 Estimation of Effective Thermal Conductivity

Estimated spatial variation and uncertainty of the rock mass thermal conductivity of four lithostratigraphic zones, Tptpul, Tptpmn, Tptpll, and Tptpln, are presented in *Thermal Conductivity of the Potential Repository Horizon* (BSC 2004 [DIRS 169854], Section 6.2). The spatial variability and uncertainty of the bulk thermal conductivity is characterized using 50 stochastic realizations using the described analytical approach. Summary of statistics (i.e., mean and standard deviation) are presented in Table 6-90, extracted from *Thermal Conductivity of the Potential Repository Horizon* (BSC 2004 [DIRS 169854], Table 6-6). The mean values are averaged values of all the 50 geostatistical realizations, while the standard deviation values are averaged from standard deviation values of realizations 15, 30, and 45. The standard deviation represents a statistical measure of the spatial variability and uncertainty for the repository stratigraphic units. Realizations 15, 30, and 45 are chosen simply because they are multiples of the number 15. However, statistical characteristics are quite similar to each other and indistinguishable from the other realizations (BSC 2004 [DIRS 169854], Sections 6.2.3 and 6.2.4). Therefore, the average standard deviation from realizations 15, 30, and 45 is presumed to be representative of the spatial variability and uncertainty for all the realizations.

The results indicated that rock mass thermal conductivity is substantially less in the lithophysal rock than in the nonlithophysal rock, confirming the expected influence of lithophysae on thermal conductivity (Table 6-90). The mean values of dry bulk thermal conductivity vary from 1.18 to 1.28 W/m·K for the lithophysal rock and from 1.42 to 1.49 W/m·K for the nonlithophysal rock, while the mean values of wet bulk thermal conductivity range from 1.77 to 1.89 W/m·K for the lithophysal rock and from 2.07 to 2.13 W/m·K for the nonlithophysal rock. The standard deviations of these means are about 0.25 W/m·K, with a slightly higher value for the nonlithophysal rock than for the lithophysal rock, which contradicts what would be expected due to the high variation of the lithophysal porosity (BSC 2004 [DIRS 169854], Table 6-6). This may be due to the fact that uncertainty in the matrix thermal conductivity instead of the lithophysal porosity plays an important role in the uncertainty estimate of the bulk thermal conductivity (BSC 2004 [DIRS 169854], Section 6.2.1).

Statistical summary of the rock matrix thermal conductivity is also presented in Table 6-90 (BSC 2004 [DIRS 169854], Table 6-6). The matrix thermal conductivity of the lithophysal zones is slightly lower than that of the nonlithophysal zones, due to the slightly higher matrix porosity associated with the vapor phase alteration in the lithophysal rock (BSC 2004 [DIRS 169854], Section 6.1.5). Detailed statistics of the thermal conductivity for the repository units are presented in *Thermal Conductivity of the Potential Repository Horizon* (BSC 2004 [DIRS 169854], Figures 6-31 to 6-54).

Estimations of thermal conductivity for the nonrepository units are presented in *Thermal Conductivity of Non-Repository Lithostratigraphic Layers* (BSC 2004 [DIRS 170033]). The analytical estimation of the thermal conductivity is conducted in a similar manner in *Thermal Conductivity of the Potential Repository Horizon* (BSC 2004 [DIRS 169854]), except that no stochastic realization is conducted. Therefore, a standard deviation of the thermal conductivity represents simply a variation of the mean value of the estimated thermal conductivity and not a statistical measure of the spatial variability and uncertainty for the nonrepository stratigraphic units.

Among the nonrepository stratigraphic units, only the Tiva Canyon Tuff has lithophysal porosity based on observations from Rautman and Engstrom (1996 [DIRS 100693], Appendix B). However, the formation is exposed at the surface and eroded. Because of the near-surface effects, the thermal properties of the Tiva Canyon Tuff have been altered, and the impact of the alteration may have more significant impact on the thermal conductivity than the lithophysal porosity. Based on this observation, the effect of lithophysal porosity on the rock mass thermal conductivity is not considered in the estimation (BSC 2004 [DIRS 170033], Section 1).

Table 6-91 shows a statistical summary of the thermal conductivity for the nonrepository units extracted from *Thermal Conductivity of Non-Repository Lithostratigraphic Layers* (BSC 2004 [DIRS 170033], Table 6-13). Since the lithophysal porosity is not accounted for in the calculation of the bulk thermal conductivity, the bulk thermal conductivity in Table 6-91 is the same as the matrix thermal conductivity. Details of the thermal conductivity for the nonrepository units are presented in *Thermal Conductivity of Non-Repository Lithostratigraphic Layers* (BSC 2004 [DIRS 170033], Section 6.6).

The analytical approach on the rock thermal conductivity was validated using data from various measurements including from laboratory and field (BSC 2004 [DIRS 169854], Section 7; BSC 2004 [DIRS 170033], Section 7). The validation was performed by comparing the estimated values with the measured ones on rock matrix thermal conductivity and rock mass thermal conductivity. The results indicate that the spatially independent realizations of rock matrix and mass thermal conductivity are valid and appropriate for their intended use.

Table 6-90. Rock Mass Thermal Conductivity for Repository Stratigraphic Units

Stratigraphic	Dry Bulk Thermal Conductivity (W/m-K)		Wet Bulk Thermal Conductivity (W/m-K)		Dry Matrix Thermal Conductivity (W/m-K)		Wet Matrix Thermal Conductivity (W/m-K)	
Unit	Mean	Std. Dev.	Mean	Std. Dev.	Mean	Std. Dev.	Mean	Std. Dev.
Tptpul	1.18E+00	2.44E-01	1.77E+00	2.47E-01	1.35E+00	2.64E-01	2.02E+00	2.48E-01
Tptpmn	1.42E+00	2.65E-01	2.07E+00	2.52E-01	1.46E+00	2.69E-01	2.13E+00	2.52E-01
Tptpll	1.28E+00	2.51E-01	1.89E+00	2.48E-01	1.40E+00	2.64E-01	2.07E+00	2.46E-01
Tptpln	1.49E+00	2.84E-01	2.13E+00	2.68E-01	1.54E+00	2.91E-01	2.20E+00	2.76E-01

Source: DTN: SN0404T0503102.011 [DIRS 169129].

NOTE: Standard deviation is calculated by averaging the standard deviations from realizations 15, 30, and 45. The standard deviation is a measure of the spatial variability of the data over the entire simulation region and should not be confused with the uncertainty in the mean values given in the table.

Table 6-91. Rock Mass Thermal Conductivity for Nonrepository Stratigraphic Units

Stratigraphic Unit	# of Points	Dry Bulk Thermal Conductivity (W/m-K)		Wet Bulk Thermal Conductivity (W/m-K)	
		Mean	Std. Div.	Mean	Std. Div.
Crystal-Rich Tiva/Post-Tiva	17	1.30E+00	2.31E-01	1.81E+00	1.95E-01
Tpcp	17	1.30E+00	2.31E-01	1.81E+00	1.95E-01
TpcLD	17	1.30E+00	2.31E-01	1.81E+00	1.95E-01
Tpcpv3	2	6.88E-01	2.29E-01	7.96E-01	2.51E-01
Tpcpv2	9	4.90E-01	1.58E-01	1.06E+00	1.46E-01
Tpcpv1	9	4.90E-01	1.58E-01	1.06E+00	1.46E-01
Tpbt4	9	4.90E-01	1.58E-01	1.06E+00	1.46E-01
Yucca	9	4.90E-01	1.58E-01	1.06E+00	1.46E-01
Tpbt3_dc	9	4.90E-01	1.58E-01	1.06E+00	1.46E-01
Pah	9	4.90E-01	1.58E-01	1.06E+00	1.46E-01
Tpbt2	9	4.90E-01	1.58E-01	1.06E+00	1.46E-01
Tptrv3	9	4.90E-01	1.58E-01	1.06E+00	1.46E-01
Tptrv2	9	4.90E-01	1.58E-01	1.06E+00	1.46E-01
Tptrv1	2	6.88E-01	2.29E-01	7.96E-01	2.51E-01
Tptrn	17	1.30E+00	2.31E-01	1.81E+00	1.95E-01
Tptrl	17	1.30E+00	2.31E-01	1.81E+00	1.95E-01
Tptf	17	1.30E+00	2.31E-01	1.81E+00	1.95E-01
Tptpv3	2	6.88E-01	2.29E-01	7.96E-01	2.51E-01
Tptpv2	9	4.90E-01	1.58E-01	1.06E+00	1.46E-01
Tptpv1	9	4.90E-01	1.58E-01	1.06E+00	1.46E-01
Tpbt1	9	4.90E-01	1.58E-01	1.06E+00	1.46E-01
Calico	5	5.95E-01	1.12E-01	1.26E+00	1.41E-01

Source: DTN: SN0303T0503102.008 [DIRS 162401].

NOTE: Data below the Calico unit are not presented in this table.

6.5.3.2 Rock Mass Heat Capacity

Rock mass heat capacity is the effective value of heat capacity that accounts for the effect of heterogeneity and discontinuity (i.e., solids, voids, and water content that exist in the voids). To determine the rock mass heat capacity, the in situ field tests were performed in the ECRB Cross-Drift. The field measurements of rock mass heat capacity in the ECRB Cross-Drift consisted of three tests. Section 6.5.3.1.1 provides a description of the ECRB tests.

6.5.3.2.1 Field Measurements of Rock Mass Heat Capacity

The summary of three field measurements of rock mass heat capacity in the ECRB Cross-Drift are presented in Table 6-92 as volumetric heat capacity (i.e., heat capacity multiplied by density [$=\cdot\rho\ C_p$]. The volumetric heat capacity of the Tptpll rock was calculated using the temperature measurements from the two-hole, six-hole, and three-hole tests in the ECRB Cross-Drift (DTNs: SN0206F3504502.012 [DIRS 159145], SN0208F3504502.019 [DIRS 161883], and SN0206F3504502.013 [DIRS 159146], respectively).

Table 6-92. Summary of Volumetric Heat Capacity for ECRB Cross-Drift Thermal K Tests 1, 2,and 3

ECRB Cross-Drift Thermal K Test 1 (Two-Hole Test)[1]	ECRB Cross-Drift Thermal K Test 2 (Six-Hole Test)[2]		ECRB Cross-Drift Thermal K Test 3 (Three-Hole Test)[3]	
Volumetric Heat Capacity (J/m^3K)	Borehole	Volumetric Heat Capacity (J/m^3K)	Borehole	Volumetric Heat Capacity (J/m^3K)
2.13E+06[a] or 2.15E+06[b]	TMK6	1.97E+06	TMK10	1.96E+06
	TMK7	1.95E+06	TMK11	2.01E+06
	TMK8	2.30E+06		
Average: 2.06E+06 J/m^3K.				

Sources: [1] DTN: SN0206F3504502.012 [DIRS 159145].
[2] DTN: SN0208F3504502.019 [DIRS 161883].
[3] DTN: SN0206F3504502.013 [DIRS 159146].

[a] A single value of each thermal property was calculated using all the data.

[b] A single value of each thermal property was calculated using the data shown from an elapsed time of 2.665 days through 28.63 days. The earlier data were scattered.

The mean values of rock mass volumetric heat capacity range from 1.96×10^6 to 2.30×10^6 $J/m^3 \cdot K$ and are averaged to 2.06×10^6 $J/m^3 \cdot K$. Using bulk density of the Tptpll rock as 1979 kg/m^3 (DTN: SN0404T0503102.011 [DIRS 169129]), the averaged rock mass heat capacity is 1039 J/kg-K (1.039 J/g-k). The field measurement value is within the range of the laboratory measurement on Tptpmn specimens (Figure 6-126). The Tptpmn intact rock heat capacity value could be presumed as that of Tptpll intact rock heat capacity since mineral compositions between the Tptpmn and Tptpll zones are very similar (BSC 2004 [DIRS 170003], Table 6-2). The field measurements may indicate that the effects of the heterogeneity and discontinuities on the heat capacity are not as significant as anticipated.

6.5.3.2.2 Analytical Estimation of Heat Capacity

Heat capacity values for the repository horizon and surrounding stratigraphic units are estimated using an analytical method. Based on the available essential input data (i.e., mineral abundance, mineral heat capacity, rock matrix property, lithophysal porosity, lithostratigraphic contacts, and physical properties of water), the mineral summation method is selected as the analytical technique. This technique is used for estimating the heat capacity values of the repository and nonrepository units in *Heat Capacity Analysis Report* (BSC 2004 [DIRS 170003], Section 6.1) and are summarized in this section.

First, the mineral summation method is used to estimate rock grain heat capacity, which is defined as the heat capacity of the rock grain, and does not consider the effect of water in the rock pores. The mineral summation method is based on Kopp's law (Nimick and Connolly 1991 [DIRS 100690], p. 6):

$$C_{p,g} = \sum_{j=1}^{j=n} x_j C_{p\,j} \qquad \text{(Eq. 6-36)}$$

where x_j is the abundance (weight fraction) of mineral j, C_{pj} is the heat capacity of mineral j, n is the number of mineral components, and $C_{p,g}$ is the effective heat capacity of rock grain.

Berryman (1995 [DIRS 159696], p. 219) has shown that a temperature-dependent correction to Kopp's law is small at temperatures lower than 500ºC. Since the temperature range of interest is below 500ºC, the use of Kopp's law is deemed to be appropriate.

To determine the rock grain heat capacity, three temperature ranges of 25°C to 94°C, 95°C to 114°C, and 115°C to 325°C are established from the temperature range of interest, 25°C to 325°C, which correspond to the preboiling, transboiling, and postboiling regimes (BSC 2004 [DIRS 170003], Section 6). The rock grain heat capacity is weighted–averaged over each temperature range.

The mineral abundance data are provided in the *Mineralogic Model (MM3.0) Report* (BSC 2004 [DIRS 170031]). The input abundance data were averaged for each layer and used in determining the rock grain heat capacity. The only exceptions are the heat capacity values of the Calico Hills Formation and adjacent layers since the layers of the Calico Hills and the adjacent bedded tuff layers exhibit a bimodal composition and are characterized as either vitric or zeolitic (BSC 2004 [DIRS 170003], Section 6.3).

Statistical measures to estimate the mean and standard deviation of the rock grain heat capacity are developed following the principles outlined in Bulmer (1979 [DIRS 111961], pp. 71 to 73). The mean and standard deviation values calculated are the result of propagating uncertainties in the mineral abundance and mineral heat capacity through Kopp's law (Equation 6-36). If the expected value of $C_{p,g}$ over a specified temperature range and an expected value of x_j were denoted as $E\left[C_{p,g}\right]$ and $E\left[x_j\right]$, the expected value of the rock grain heat capacity could be expressed in terms of the expected mineral abundance and the expected weight fraction (BSC 2004 [DIRS 170003], Equation 6-12):

$$E\left[C_{p,g}\right] = \sum_{j=1}^{j=n} E\left[x_j\right] \cdot E\left[C_{pj}\right] \qquad \text{(Eq. 6-37)}$$

Similarly, the standard deviation of $C_{p,g}$, denoted as $\sigma\left[C_{p,g}\right]$, can be written as (BSC 2004 [DIRS 170003], Equation 6-17):

$$\sigma\left[C_{p,g}\right] = \sqrt{\sum_{j=1}^{j=n} \left(\left(E\left[C_{pj}\right] \cdot \sigma\left[x_j\right]\right)^2 + \left(E\left[x_j\right] \cdot \sigma\left[C_{pj}\right]\right)^2 \right)} \qquad \text{(Eq. 6-38)}$$

After the rock grain heat capacity has been determined, heat capacity of the rock mass is estimated for the three temperature ranges: 25°C to 94°C (preboiling), 95°C to 114°C (transboiling), and 115°C to 325°C (postboiling). For temperatures below boiling (the pre-boiling regime), Nimick and Connolly (1991 [DIRS 100690], p. 31, Equations 9 and 10) presented equations for estimating the thermal capacitance and the heat capacity of the rock mass:

$$(\rho C_p)_{rm} = \rho_g(1-\phi_m)(1-\phi_L)C_{p,g} + \rho_w (1-\phi_L)\, \phi_m S_w C_{p,w} + \rho_a[\phi_L + (1-\phi_L)\, \phi_m(1-S_w)]C_{p,a}$$

$$\approx \rho_g(1-\phi_m)(1-\phi_L)C_{p,g} + \rho_w(1-\phi_L)\phi_m S_w C_{p,w} \qquad \text{(Eq. 6-39)}$$

$$C_{p,rm} = \frac{(\rho C_p)_{rm}}{\rho_{rm}} \approx \frac{(\rho C_p)_{rm}}{\rho_g (1-\phi_L)(1-\phi_m) + (1-\phi_L)\phi_m S_w \rho_w} \quad \text{(Eq. 6-40)}$$

where $(\rho\, C_p)_{rm}$ is the thermal capacitance of the rock mass, J/m^3-K
$C_{p,rm}$ is the heat capacity of the rock mass, J/kg•K
ϕ_m is matrix porosity, m^3/m^3
ϕ_L is the volume fraction of lithophysal cavities, m^3/m^3
$C_{p,g}$ is the rock grain heat capacity, J/kg•K
S_w is the degree of matrix saturation, m^3/m^3
$C_{p,w}$ and $C_{p,a}$ are the heat capacity of water and air, respectively, J/kg•K
ρ_g is the rock grain density, kg/m^3
ρ_w and ρ_a are the densities of water and air, respectively, kg/m^3

The simplification of Equations 6-39 and 6-40 is based on the fact that the air density is negligible relative to the other terms (e.g., gain density and water density) due to the extremely low density of air. Substituting Equation 6-39 into Equation 6-40 yields (BSC 2004 [DIRS 170003], Equation 6-21):

$$C_{p,rm} = \frac{\rho_g (1-\phi_m) C_{p,g} + \rho_w \phi_m S_w C_{p,g}}{\rho_g (1-\phi_m) + \phi_m S_w \rho_w} \quad \text{(Eq. 6-41)}$$

As can be seen from Equation 6-41, the rock mass heat capacity is independent of the lithophysal porosity and is identical to the rock matrix heat capacity. Averaged values of rock matrix properties including grain density, matrix porosity, and matrix water saturation are used (BSC 2004 [DIRS 170003], Table 6-8).

Following the preboiling phase, water content in pore space starts to boil at 95°C. In the transboiling regime, 95°C to 114°C (Nimick and Connolly 1991 [DIRS 100690], Section 3.4), additional energy required for vaporizing the pore water can be accounted for in the rock mass heat capacity. In the transboiling phase, the water saturation is assumed to decrease linearly from its initial value to zero over the 19°C temperature range (Assumption 5.4.5). The linear variation of the matrix saturation, S_w, is expressed by:

$$S_w = S_{wo}\,(20.376316 - 0.05263T) \quad \text{(Eq. 6-42)}$$

where S_{wo} is the initial water saturation and T is the absolute temperature (BSC 2004 [DIRS 170003], Equation 6-22).

The temperature of 105°C is selected and used to calculate the saturation because 105°C is the approximate midpoint or average temperature for the transboiling regime. During the trans-boiling phase, a correction is added to the calculation of the rock mass heat capacity, which accounts for the "heat capacity of boiling" (BSC 2004 [DIRS 170003], Equation 6-23):

$$C_{p,rm} = \left(C_{p,rm}\right)_{T=105} + \frac{\rho_w (1-\phi_l)\phi_m S_w}{\rho_{rm}} \left[\frac{H_{fg}}{\Delta T}\right] \quad \text{(Eq. 6-43)}$$

Similar to the preboiling phase, the rock mass heat capacity for the transboiling phase is also independent of the lithophysal porosity.

For temperatures above 114°C, the water has completely boiled (BSC 2004 [DIRS 169900], Figure 6.3.2.3-2). Therefore, the matrix saturation is zero, $S_w = 0$. In this case, Equation 6-39 reduces to:

$$(\rho C_p)_{rm} = \rho_g(1-\phi_m)(1-\phi_L)C_{p,g} \quad \text{(Eq. 6-44)}$$

Substituting Equation 6-44 into Equation 6-40 gives the result that the rock mass heat capacity is equal to the rock grain heat capacity (BSC 2004 [DIRS 170003], Equation 6-26), which is also independent of the lithophysal porosity.

$$C_{p,rm} = \frac{(\rho C_p)_{rm}}{\rho_g(1-\phi_L)(1-\phi_m)} = C_{p,g} \quad \text{(Eq. 6-45)}$$

The analytical estimation of the rock grain and mass heat capacity using the mineral summation method (Nimick and Connolly 1991 [DIRS 100690], p. 6) has probably the most complete results, including all the repository and nonrepository layers. Based on mineral abundance and matrix porosities, the analytical estimation of the rock grain heat capacity is provided in Table 6-93. The standard deviation of the rock grain heat capacity values incorporates uncertainties of the mineral abundance and mineral heat capacity, including spatial variation.

6.5.3.2.2.1 Estimation of Heat Capacity

The summary of rock grain heat capacities is presented in Table 6-93 (BSC 2004 [DIRS 169900], Tables 6-6 and 6-7; DTN: SN0307T0510902.003 [DIRS 164196]). The rock grain heat capacity may be intended to be used in simulations and analyses that explicitly account for the thermodynamic effects of water within the rock porosity, while rock mass heat capacity is intended to be used in the simulations and analyses that do not explicitly account for these thermodynamic effects, particularly boiling.

Table 6-93. Rock Grain Heat Capacities for Lithostratigraphic Units

Mineralogic Unit	Avg. Rock Grain Heat Capacity for T = 25-325°C J/g K	Std Dev of Rock Grain Heat Capacity T = 25-325°C J/g K	Avg. Rock Grain Heat Capacity for T = 25-94°C J/g K	Std Dev of Rock Grain Heat Capacity T = 25-94°C J/g K	Avg. Rock Grain Heat Capacity for T = 95-114°C J/g K	Std Dev of Rock Grain Heat Capacity T = 95-114°C J/g K	Avg. Rock Grain Heat Capacity for T = 115-325°C J/g K	Std Dev of Rock Grain Heat Capacity T = 115-325°C J/g K
Tpc_un	0.93	0.11	0.79	0.08	0.87	0.08	0.99	0.10
Tpcpv3-Tpcpv2	0.95	0.11	0.83	0.09	0.90	0.09	1.00	0.10
PTn	0.96	0.23	0.84	0.20	0.90	0.22	1.00	0.24
Tptrv1	0.95	0.10	0.84	0.08	0.90	0.08	0.99	0.10
Tptrn-Tptrl-Tptf	0.93	0.13	0.78	0.10	0.87	0.10	0.99	0.12
Tptpul	0.93	0.12	0.78	0.09	0.87	0.09	0.99	0.11
Tptpmn	0.93	0.14	0.78	0.11	0.87	0.11	0.99	0.13
Tptpll	0.93	0.13	0.78	0.10	0.87	0.10	0.99	0.12
Tptpln	0.93	0.10	0.78	0.07	0.87	0.07	0.99	0.09
Tptpv3	0.98	0.24	0.86	0.21	0.93	0.23	1.02	0.25
Tptpv2	0.98	0.19	0.86	0.16	0.93	0.17	1.02	0.19
Tptpv1-Tpbt1	1.08	0.42	0.95	0.37	1.02	0.40	1.12	0.43
Tac4	1.07	0.42	0.93	0.38	1.01	0.40	1.12	0.44
Tac3	1.07	0.38	0.93	0.33	1.01	0.36	1.12	0.39
Tac2	1.07	0.36	0.94	0.32	1.01	0.34	1.12	0.38
Tac1	1.07	0.35	0.94	0.31	1.01	0.33	1.12	0.37
Tacbt	1.02	0.24	0.88	0.21	0.95	0.22	1.07	0.25
Vitric								
Tptpv2	0.96	0.15	0.84	0.12	0.90	0.13	1.00	0.15
Tptpv1-Tpbt1	0.96	0.12	0.84	0.09	0.90	0.10	1.00	0.11
Tac4	0.96	0.10	0.83	0.08	0.90	0.08	1.00	0.09
Tac3	0.96	0.13	0.84	0.11	0.91	0.11	1.01	0.13
Tac2	0.96	0.13	0.84	0.11	0.91	0.11	1.01	0.13
Tac1	0.97	0.11	0.85	0.09	0.91	0.10	1.01	0.11
Tacbt	0.97	0.10	0.84	0.08	0.91	0.08	1.01	0.09
Zeolitic								
Tptpv2	1.02	0.13	0.90	0.11	0.96	0.11	1.06	0.13
Tptpv1-Tpbt1	1.12	0.21	0.99	0.18	1.06	0.19	1.17	0.21
Tac4	1.11	0.25	0.97	0.22	1.05	0.24	1.16	0.26
Tac3	1.10	0.22	0.96	0.19	1.04	0.20	1.15	0.23
Tac2	1.10	0.20	0.97	0.18	1.04	0.19	1.16	0.21
Tac1	1.10	0.20	0.96	0.17	1.04	0.18	1.15	0.20
Tacbt	1.03	0.17	0.89	0.15	0.97	0.16	1.09	0.17

Source: DTN: SN0307T0510902.003 [DIRS 164196].

NOTE: Data below Tacbt1 unit are not presented in this Table.

The rock mass heat capacities are also determined for the three temperature intervals (i.e., 25–94°C, 95–114°C, and 115–325°C) and are presented in Table 6-94 (BSC 2004 [DIRS 169900], Table 6-9; DTN: SN0307T0510902.003 [DIRS 164196]). The values of the rock mass heat capacity given in Table 6-94 are only valid up to two significant figures because of the uncertainty associated with the nature of the averaged input data (i.e., mineral abundance, mineral heat capacities, rock matrix properties, lithophysal porosity, lithostratigraphic contacts, and physical properties of water) (Section 6.5.3.2.2). The standard deviation for each simulation layer has been assigned a value of approximately 30% of the average value. The 30% of the average is selected as the uncertainty associated with the rock mass heat capacity values and is based on the standard deviations calculated for the rock grain heat capacity. The influence of the other properties' uncertainty (i.e., porosity, density, and saturation) have not been accounted for explicitly in the rock mass heat capacity values given in Table 6-94.

Table 6-94. Rock Mass Heat Capacities for Lithostratigraphic Units

Mineralogic Unit	Average Rock Mass Heat Capacity T=25–94°C J/kg K*	Standard Deviation of Rock Mass Heat Capacity T=25–94°C J/kg K	Average Rock Mass Heat Capacity T=95–114°C J/kg K*	Standard Deviation of Rock Mass Heat Capacity T=95–114°C J/kg K	Average Rock Mass Heat Capacity T=115–325°C J/kg K*	Standard Deviation of Rock Mass Heat Capacity T=115–325°C J/kg K
Tpc_un	9.1E+02	3.E+02	3.0E+03	9.E+02	9.9E+02	3.E+02
Tpcpv3-Tpcpv2	1.2E+03	4.E+02	8.4E+03	2.E+03	1.0E+03	3.E+02
PTn	1.3E+03	4.E+02	9.1E+03	3.E+03	1.0E+03	3.E+02
Tptrv1	8.9E+02	3.E+02	1.8E+03	5.E+02	9.9E+02	3.E+02
Tptrn-Tptrl-Tptf	8.9E+02	3.E+02	2.7E+03	8.E+02	9.9E+02	3.E+02
Tptpul	9.4E+02	3.E+02	3.6E+03	1.E+03	9.9E+02	3.E+02
Tptpmn	9.1E+02	3.E+02	3.0E+03	9.E+02	9.9E+02	3.E+02
Tptpll	9.3E+02	3.E+02	3.3E+03	1.E+03	9.9E+02	3.E+02
Tptpln	9.0E+02	3.E+02	2.8E+03	8.E+02	9.9E+02	3.E+02
Tptpv3	9.1E+02	3.E+02	1.7E+03	5.E+02	1.0E+03	3.E+02
Tptpv2	1.1E+03	3.E+02	5.1E+03	1.E+03	1.0E+03	3.E+02
Tptpv1-Tpbt1	1.2E+03	4.E+02	6.4E+03	2.E+03	1.1E+03	3.E+02
Tac4	1.4E+03	4.E+02	9.8E+03	3.E+03	1.1E+03	3.E+02
Tac3	1.4E+03	4.E+02	9.8E+03	3.E+03	1.1E+03	3.E+02
Tac2	1.4E+03	4.E+02	9.8E+03	3.E+03	1.1E+03	3.E+02
Tac1	1.4E+03	4.E+02	9.8E+03	3.E+03	1.1E+03	3.E+02
Tacbt	1.2E+03	4.E+02	7.6E+03	2.E+03	1.1E+03	3.E+02
Vitric						
Tptpv2	1.1E+03	3.E+02	5.1E+03	1.E+03	1.0E+03	3.E+02
Tptpv1-Tpbt1	1.0E+03	3.E+02	4.3E+03	1.E+03	1.0E+03	3.E+02
Tac4	1.3E+03	4.E+02	8.5E+03	2.E+03	1.0E+03	3.E+02
Tac3	1.3E+03	4.E+02	8.5E+03	2.E+03	1.0E+03	3.E+02
Tac2	1.3E+03	4.E+02	8.5E+03	2.E+03	1.0E+03	3.E+02
Tac1	1.3E+03	4.E+02	8.5E+03	2.E+03	1.0E+03	3.E+02
Tacbt	1.6E+03	5.E+02	1.5E+04	4.E+03	1.0E+03	3.E+02

Table 6-94. Rock Mass Heat Capacities for Lithostratigraphic Units (Continued)

Mineralogic Unit	Average Rock Mass Heat Capacity T=25–94°C J/kg K*	Standard Deviation of Rock Mass Heat Capacity T=25–94°C J/kg K	Average Rock Mass Heat Capacity T=95–114°C J/kg K*	Standard Deviation of Rock Mass Heat Capacity T=95–114°C J/kg K	Average Rock Mass Heat Capacity T=115–325°C J/kg K*	Standard Deviation of Rock Mass Heat Capacity T=115–325°C J/kg K
Zeolitic						
Tptpv2	1.1E+03	3.E+02	3.9E+03	1.E+03	1.1E+03	3.E+02
Tptpv1-Tpbt1	1.4E+03	4.E+02	8.8E+03	3.E+03	1.2E+03	4.E+02
Tac4	1.4E+03	4.E+02	9.7E+03	3.E+03	1.2E+03	4.E+02
Tac3	1.4E+03	4.E+02	9.6E+03	3.E+03	1.2E+03	3.E+02
Tac2	1.4E+03	4.E+02	9.6E+03	3.E+03	1.2E+03	3.E+02
Tac1	1.4E+03	4.E+02	9.6E+03	3.E+03	1.2E+03	3.E+02
Tacbt	1.3E+03	4.E+02	7.5E+03	2.E+03	1.1E+03	3.E+02

Source: DTN: SN0307T0510902.003 [DIRS 164196].

NOTE: Data below Tacbt1 unit are not presented in this table.

6.5.3.3 Rock Mass Coefficient of Thermal Expansion

Field measurements are conducted on heat-induced in situ displacements at different temperatures. These displacements are then used to calculate rock mass dimension changes and thermal expansion at the corresponding temperature. Measurements of rock displacements are usually made by multi-point borehole extensometer (MPBX), while those of rock temperatures are made by thermal probes. In order to evaluate the effects of porosity, fractures, moisture contents, and confining stresses, mapping voids or fractures of the measuring boreholes and measuring in situ moisture contents and confining stresses are considered necessary.

6.5.3.3.1 Field Measurements of Rock Mass Thermal Expansion Coefficient

There are no field thermal expansion measurements available in the Tptpll rock unit. The best data available on rock mass thermal expansion for this rock unit are those from laboratory thermal expansion measurements on specimens with a nominal diameter of 12 in. (DTNs: SN0208L01B8102.001 [DIRS 165211]; SN0211L01B8102.002 [DIRS 165218]). The CTE values from the 12-in specimens are generally lower than those from the smaller specimens, indicating that portions of the space occupied by air in larger specimens is "absorbed" by expanding rock matrix during heating, resulting in a lower CTE (Figure 6-132). The difference in the CTE values between the specimens diminishes as temperature increases, which may be a result of voids or fractures closing with the increase of temperature. However, no definite conclusion can be drawn in terms of the effects of scaling and lithophysal cavities or fractures on rock mass thermal expansion since the 12-in. specimens could not represent the rock mass of Tptpll zones due to the presence of large lithophysae. The results may still help to shed some light on the understanding of this effect. A comprehensive knowledge of the effect of lithophysal cavities on rock mass thermal expansion may be acquired by conducting additional laboratory tests with specimens of various sizes or via field measurements.

6.6 SITE-SPECIFIC FIELD TESTING

6.6.1 General

Laboratory tests are essential in obtaining the basic rock parameter data in a standardized form that makes rock properties of various stratigraphic units comparable with each other. However, the question remains: How do these laboratory test results relate to the field conditions? A satisfactory answer to this question can only be obtained by identifying appropriate scaling relationships. These will assist in calibrating the associated numerical simulations such, that their performance reflects the performance of the full-sized excavations or other underground structures.

Field tests play a key role in confirming the range and validity of laboratory-generated results. Because of the size and characteristics of field specimens, however, the standardized procedures cannot always be completely followed. Test logistics in a confined underground environment are more complex than those encountered in a typical laboratory environment, and the number of tests is usually limited because the time involved in preparation and the cost of each is substantial. Although attempts are made to ensure the proper performance of test equipment, the rate of equipment failure in these tests is relatively high. Test data often require substantial effort to analyze and reduce to meaningful results. Frequently, attempts are made to salvage results obtained from only partially completed tests due to equipment malfunction. These technical, equipment-related difficulties are magnified by the unique and often complex responses of in situ rock to testing.

On the Yucca Mountain Project, the lithophysae-containing lithostratigraphic units pose especially difficult challenges to researchers. The presence of voids often makes the standardized field-testing approaches inadequate because the location and size of the voids are difficult to predict. Moreover, their presence causes distortions of otherwise uniform load and stress distributions, thus making the results of field testing difficult to interpret.

As pointed out in *Resolution Strategy for Geomechanically-Related Repository Design and Thermal-Mechanical Effects (RDTME)* (Board 2003 [DIRS 165036], Section 2.2.1), in situ mechanical and thermal testing and confirmation of parameters required to replicate behavior of lithophysal rocks is necessary to determine the size effect (i.e., porosity and fracture) on rock mass constitutive behavior. These tests are to be used further for validation of the numerical simulations at increasing size scales. It is anticipated that, as a result of these field-testing activities, it will be possible to develop a numerical material representation that can be used with confidence for extrapolating the mechanical response of lithophysal rocks. The ongoing field tests are natural extensions of the testing experience and needs identified as a result of the past in situ tests. A brief account of these past field activities is provided with appropriate references to the original data sources published in appropriate project reports.

Although very important, field tests are not the only sources of information about rock performance. Other field activities providing valuable information about the rock involve mapping of the exposed excavation walls, in situ deformation measurements, steel set load measurements, and observations of the performance of rock and ground support elements applied to maintain safety and stability of existing excavations. Data originating from all available

sources are analyzed because each approach offers a unique methodology of evaluating and quantifying performance of lithostratigraphic rock units and engineering components used in ground control.

This section provides a summary of tests and other field activities performed to enhance engineers' understanding of rock mass behavior and in situ performance of ground control hardware installed to maintain the safety and stability of underground excavations.

6.6.2 Single Heater Test

The SHT is the first of the in situ thermal tests conducted as a part of Yucca Mountain site characterization activities. The overall objective of the SHT was to gain an understanding of the coupled thermal, mechanical, hydrological, and chemical processes that are anticipated to occur in the local rock mass in the repository as a result of heat from radioactive decay of the emplaced waste.

The SHT was performed not only to characterize the thermal and mechanical response of the rock strata but also as a pilot test necessary to gain experience in the following areas: (1) selection of the type of instrumentation installed, (2) development of procedures for instrument calibration and installation, and (3) verification of the long-term stability and performance of the instrumentation installed.

The heating and cooling of the test block was carried out between August 1996 and January 1998. The test results encompass a wide range of findings associated with rock performance, instrumentation stability and accuracy, and suggestions regarding improvements of data accuracy in similar future tests.

The details associated with the SHT are provided in *Single Heater Test Final Report* (CRWMS M&O 1999 [DIRS 129261], Section 3).

6.6.3 Drift Scale Test

The DST is an integral part of the Yucca Mountain Site Characterization program. The DST is a full-scale in situ thermal test with the purpose of developing a better understanding of thermal, mechanical, hydrological, and chemical processes, as well as the interaction between those processes taking place in the rock mass adjoining the subsurface facility of the nuclear waste repository at Yucca Mountain. Another purpose for the test is to obtain information about the performance of the metal components of the container cylinder shells and the ground support elements. Another important aspect covers the comparison of performance of the two tunnel sections, one equipped with the concrete liner and the other supported with the very basic ground support system, including wire mesh and friction-type rockbolts.

The heated drift of the DST is 5 m in diameter, 47.5 m in length, and nominally isolated from the access drift by an insulated bulkhead. Heaters within the heated drift supplied about 184 kW of power at the beginning of the test and about 155 kW of power at later test stages. Data were collected from approximately 3,800 sensors once per hour, and additional measurements were taken at less frequent intervals using a variety of sensors and techniques.

Heaters in the heated drift were turned on December 3, 1997 and turned off on January 14, 2002. It took four years before the rock surrounding the drift cooled down enough from the test temperature level on the order of 200ºC, such that reentry into the drift on April 3, 2006 was possible.

Inspection of the drift in the spring of 2006 revealed the following:

- The two ground support systems, including the friction-type expandable rockbolts and cast-in-place concrete liner installed in the HD, performed very well.
- The concrete liner displayed no signs of stress-related effects, and the shrinkage fractures commonly occurring during the concrete curing stage displayed no indication of movement or temperature-related deterioration.
- In the HD section supported by rockbolts and wire mesh, some small, localized in the tunnel crown rock failures were evident. These caused some sagging of the mesh stretched between the adjacent rockbolts. However, the sagging was very localized and the mesh stretching was not excessive.
- Thin rock flakes, ranging in thickness from very thin to less than approximately 2 in., were formed in the roof parallel to the tunnel wall surface.
- The rock flaking resulted in the formation of small, thin rock chips that were able to pass through the 3 × 3 in. wire mesh grid and precipitated to the floor of the drift.

In general, the HD excavated in the Tptpmn unit performed as expected. Preparation of reports containing results of inspections, analyses of measurements, and posttest evaluations are currently underway.

More details pertaining to the test and various resulting analyses are presented in Williams (2001 [DIRS 160809]).

6.6.4 Rock Mass Mechanical Field Tests

The presence of multiple joint sets in the Tptpmn and Tptpln zones and the presence of significant lithophysae and fracture networks in the Tptpul and Tptpll units preclude obtaining representative rock mass properties from laboratory-sized specimens. Empirical techniques for obtaining rock mass properties from intact laboratory test data and field mapping information have also been judged to have an inadequate basis for application to lithophysal rock. Because of these limitations, in situ measurements on a scale as large as practicable were designed to attempt to measure rock mass mechanical behavior in both lithophysal and nonlithophysal rock units. Heuze states that field moduli generally appear to be between 20% and 60% of laboratory measured moduli, and field strength values are generally several times smaller than laboratory values (Heuze 1980 [DIRS 166174], p. 167).

6.6.4.1 Borehole Jack Tests

A suite of borehole jack tests was performed as part of the SHT in an alcove excavated off the ESF. The purpose of the NX-borehole jack tests, also known as Goodman jack or hard-rock

jack, was to obtain an in situ estimate of elastic modulus of deformation under ambient and hot rock conditions for the Topopah Spring middle nonlithophysal tuff (Tptpmn). Testing details and results are presented in DTN: SNF35110695001.010 [DIRS 158300] and the *Single Heater Test Final Report* (CRWMS M&O 1999 [DIRS 129261], Section 9.2).

A single borehole (ESF-TMA-BJ-1) was drilled roughly horizontal and perpendicular to the SHT heater borehole for operation of the borehole jack. The borehole was collared in the observation drift and extended towards the heater. Once the heater was energized, a decreasing temperature gradient existed from the end of the borehole towards the collar. The nonpermanent jack was periodically inserted into the borehole and pressurized at borehole distances (from the collar) of 2.0, 3.0, 4.0, 4.51, and 6.2 m, although not all locations were tested on each of the test dates. Tests were conducted on August 26, 1996 (before heater startup); October 10, 1996; November 26, 1996; March 18, 1997; October 23, 1997; and January 29,1998. No additional boreholes were tested, so no spatial variation or anisotropy of the rock modulus was determined.

The cylindrical jack consists of two 20.3-cm long (8-in. long) platens, which apply a unidirectional load to a nominal 7.62-cm (3-in.) diameter borehole wall. The platens pressurize 90 degrees of the borehole wall on opposite sides. Deformation was measured by an LVDT at each end of the loading platens, and jack pressure was applied using an Enerpak hand pump, typically in 3.44 MPa (500 psi) increments.

The borehole jack tests were based on the procedures of standard ASTM D 4971-89 [DIRS 101786] with minor exceptions. The jack was inserted into the borehole and the platens slowly expanded until the pressure just began to rise. This represented the values of "zero" displacement and pressure. The jack pressure was then increased in increments to the desired maximum pressure and then decreased in similar increments. The calculated minimum pressure to achieve "full platen contact" based on the approximate borehole diameter (7.57 to 7.90 cm) was about 21 MPa (3000 psi). Only data above a jack pressure of about 21 MPa were used to calculate the rock mass modulus. For the tests conducted on August 26, 1996, the maximum pressure applied to the rock by the jack was limited to about 34.5 MPa. For all subsequent tests, the maximum pressure employed was about 55.2 MPa.

The historical use of the borehole jack has shown that corrections must be taken into consideration for the mismatch between borehole and platen radii, longitudinal bending of the platens, and tensile cracking of the intact rock or opening of existing fractures. These corrections are discussed in ASTM D 4971-89 [DIRS 101786], as well as in Heuze and Amadei (1985 [DIRS 101598]). Corrections were applied in the results that followed. For analyzing the test data, the rock was considered to be linearly elastic, isotropic, and homogeneous. The rock Poisson's ratio is estimated for the modulus calculation.

The results from the borehole jack tests show that most of the estimated in situ rock modulus values range from about 6 to 12 GPa, as shown in Table 6-95. Generally, the lower temperatures are reported near the collar and typically increase with distance from the collar. The borehole jack results do not show a clear correlation between modulus value and rock temperature. The increase in modulus after heating may be consistent with the closing of fractures due to thermal expansion. The mean estimated rock mass modulus was about 8.4 GPa for all borehole locations at ambient rock temperature (Table 6-96).

Table 6-95. Estimated In Situ Rock Modulus in Borehole ESF-TMA-BJ-1 Using Borehole Jack

Date	Distance from Collar (m)				
	2.0	3.0	4.0	4.51	6.2
	In Situ Rock Elastic Modulus, GPa (Temp °C)				
08/26/96	6.9 (25)	3.71 (25)	no test	no test	no test
10/10/96	10.3 (27.5)	10.3 (27.7)	8.3 (30.2)	6.0 (34)	no test
11/26/96	Discarded	10.2 (35.9)	*5.71 (46.4)*	*5.01 (55.4)*	8.4 (141.8)
03/18/97	Discarded	6.3 (41)	*10.3 (52)*	*5.7 (58.7)*	22.8 (143.1)
10/23/97 1st	no test	no test	6.28 (ambient)	discarded	8.28 (ambient)
10/23/97 2nd	no test	no test	8.98 (ambient)	7.1 (ambient)	10.0 (ambient)
01/29/98 1st	5.47 (ambient)	9.67 (ambient)	8.28 (ambient)	7.6 (ambient)	not calculated
01/29/98 2nd	no test	no test	no test	no test	11.72 (ambient)
01/29/98 3rd	no test	no test	no test	no test	11.72 (ambient)

Sources: DTN: SNF35110695001.010 [DIRS 158300]; CRWMS M&O 1999 [DIRS 129261], Table 9-6.

NOTES: Estimated moduli presented in italics are based on field data for which the difference between the two borehole jack LVDT readings slightly exceeded the limits set in ASTM D 4971-89 [DIRS 101786]. Discarded results were for data that far exceeded ASTM D 4971-89 limits. These values should not be used in calculations requiring rock mass modulus and are not used in the Table 6-96 summary.

Table 6-96. Summary of Ambient In Situ Rock Modulus (Borehole ESF-TMA-BJ-1)

In Situ Rock Elastic Modulus (GPa) in Borehole ESF-TMA-BJ-1at 25°C and Ambient Temperature									
Unit	Condition	Count	Mean	Std Error	Std Dev	Dev/Mean	Median	Minimum	Maximum
Tptpmn	Ambient	15	8.42	0.59	2.29	0.27	8.28	3.7	11.7

Source: DTN: SNF35110695001.010 [DIRS 158300].

The estimated volume of rock mass (Heuze 1980 [DIRS 166174], Table 1) involved in an NX-NB borehole jack test is about 0.13 m^3 (4.6 ft^3). Since this is not large enough to incorporate discontinuities on the drift scale, properly conducted borehole jack tests in better rock may overestimate actual rock mass modulus values. On the other hand, fracturing around the tested borehole was reported, and these nearby fractures could have resulted in lower modulus values estimated from the test.

6.6.4.2 Plate Loading Test

The purpose of plate load testing in the Topopah Spring middle nonlithophysal tuff (Tptpmn) was to measure the in situ deformation characteristics of the rock mass under ambient and elevated temperature conditions, as part of the DST. The DST is a large-scale long-term in situ field thermal-mechanical study being undertaken in Alcove 5 of the ESF. The plate load test was designed to mechanically load the rock horizontally using large square-shaped flatjacks that press against both ribs of a narrow niche constructed perpendicular to the access drift of the heated drift (Sobolik and George 2001 [DIRS 165420], p. 25). The niche where the plate load test was conducted was located 5 m outside the heated drift bulkhead in the Tptpmn rock unit. The niche was mined using drill and blast techniques to roughly 2.5 m wide with a nominally flat floor (Sobolik and George 2001 [DIRS 165420], p. 25). Plate load tests were conducted by incremental and cyclic loading over a prescribed range and by monitoring rock displacement and

applied pressure histories. These results were then used to determine the in situ rock mass modulus, as well as the unloading and reloading moduli of the rock mass.

A decision was made to determine the thermal-mechanical properties of the niche rock before, during, and after significant thermal strains were developed in the rock because the rock mass modulus was thought to be temperature dependent. The DST heating of the drift began December 3, 1997 and, as a result, the rock on the western side of the plate load test experienced thermal expansion, increasing the horizontal stress in the immediate rock area. It was expected that the thermal expansion would cause closure of rock fractures and increase the rock stiffness (i.e., higher rock mass modulus). The rock on the eastern or ambient side of the plate load test was also expected to experience some elevated temperatures and increased stresses, but to a lesser degree than the heated side. Analysis of these tests would allow measurement of in situ mechanical rock properties and a comparison of the influence of heating on these same properties.

The DST plate load tests were conducted first in May and June of 1998, several months after the drift began to be heated; in October 2000 after the drift had experienced heating for almost three years; and finally in April 2003 after the rock had experienced significant cool down (heating was turned off January 14, 2002). The two plate load tests conducted in 1998 were loaded to maximum bearing pressures of 6.4 and then 11.9 MPa but were made with a defective reaction frame. Additionally, the flatjacks experienced premature failures, making the results unreliable (Sobolik and George 2001 [DIRS 165420], p. 31). Design changes were made for the October 2000 test, and these changes produced much better results. Preliminary calculation and testing details of the 2000 tests are presented in DTNs: SN0011F3912298.022 [DIRS 158392] and SN0011F3912298.023 [DIRS 158399] and documented in Sobolik and George (2001 [DIRS 165420], pp. 33 to 42). A third set of loading cycles was performed in April 2003 after approximately 18 months of cooling had occurred in the heated drift (DTNs: SN0306F3912298.048 [DIRS 165416]; SN0310F3912298.054 [DIRS 168527]).

The plate loading tests were designed based on the International Society of Rock Mechanics (ISRM) test standard, *Suggested Methods for Determining In Situ Deformability of Rock* (Brown 1981 [DIRS 102003], pp. 141 to 160), ASTM D 4394-84, *Standard Test Method for Determining the In Situ Modulus of Deformation of Rock Mass Using the Rigid Plate Loading Method* [DIRS 149445], and ASTM D 4395-84, *Standard Test Method for Determining the In Situ Modulus of Deformation of Rock Mass Using the Flexible Plate Loading Method* [DIRS 160054]. The plate-loading test conducted as part of the DST differed somewhat from the standard techniques, although the differences were considered appropriate by the investigators (Sobolik and George 2001 [DIRS 165420], p. 25).

During the test, both sides of the niche were loaded simultaneously and reacted in opposite directions against a central reaction frame. The reaction frame was sandwiched on both sides by a flatjack and a bearing plate. The reaction frame consisted of 0.914-m-square (36-in.-square) aluminum plates that were oriented vertically and stacked horizontally across the 2.5 m wide test niche near the springline. Sandia National Laboratories (SNL) designed the flatjacks, which had unpressurized dimensions of nominally 0.813 × 0.813 m (32 × 32 in.) with the corners rounded to an 8.0 cm (3 in.) radius and a maximum jack pressure design of 55.2 MPa (8000 psi). Each flatjack was placed between the aluminum reaction frame and a single steel 2.5 cm (1 in.) thick

and 91.4 cm (36 in.) square. This bearing platen was located adjacent to a 10.1-cm-thick (4-in.-thick) grout pad cast directly on a hand-smoothed rock bearing surface; therefore, uniform bearing pressure from the flatjack through the grout to the smoothed rock can be applied. The estimated volume of rock mass (Heuze 1980 [DIRS 166174], Table 1) involved in a 91-cm-diameter (36-in.-diameter) plate-bearing test is about 26 m^3 (910 ft^3) (Sobolik and George 2001 [DIRS 165420], pp. 25 to 28).

Instrumentation consisted of pressure transducers, MPBX with C-ring or Snap-ring Geokon anchors, and type-K thermocouples. Instrumentation was installed in two boreholes, one extending into the ambient temperature rock and the other into the elevated temperature rock. Three anchors were used per borehole and were connected to LVDTs via Invar connecting rods to measure displacement. MPBX anchor locations in the borehole on the ambient rock side were 2.70 m (deep), 1.31 m (middle) and 0.87 m (shallow). MPBX anchor locations on the heated rock side were 3.21 m (deep), 1.54 m (mid) and 0.86 m (shallow). The thermocouples were attached to the connecting rods. Displacement measurements taken during the tests were not corrected for rod thermal expansion because during the short loading and unloading periods, the rods and measurement transducers were being considered to remain at a constant temperature (Sobolik et al. 1998 [DIRS 162049], p. 84; Sobolik et al. 1999 [DIRS 163202], p. 89; Sobolik and George 2001 [DIRS 165420], pp. 28 to 30).

A simplified "first-order" analysis approach (Sobolik and George 2001 [DIRS 165420], p. 34) was used to calculate the in situ rock deformation modulus (rock mass modulus), E. This equation is commonly used in foundation engineering to estimate the deflection of a footing pressed onto the surface of a semi-infinite isotropic elastic medium (Bowles 1982 [DIRS 168880], pp. 183 to 185). This is a slightly different equation than those suggested in ASTM D 4394-84 [DIRS 149445] or ASTM D 4395-84 [DIRS 160054]:

$$E = \frac{I_w \, P \, B \left(1 - \nu^2\right)}{\delta}, \qquad \text{(Eq. 6-46)}$$

where: E = deformation modulus of the isotropic, homogeneous, elastic rock

I_w = a constant dependent on the shape and stiffness of the loading platens (for square platens: 0.82 for a rigid plate and 1.12 for the center of a flexible plate)

P = bearing pressure applied to the rock mass

B = dimension of the bearing platens (0.914 m, the width of the metal platens)

ν = Poisson's ratio

δ = displacement of the rock due to the applied load

Equation 6-46 is valid for displacements of the bearing plate at its center, but actual plate movements are not available. The best estimate of the plate movement at its center is the MPBX displacement relative to the deepest available anchor, since the deepest anchor measurement represents the total displacement over the largest volume of rock. Calculating moduli at individual anchor locations may result in different moduli because of rock heterogeneities and the variation of rock stress with depth.

Also, the pressure required for plots and subsequent analyses is the pressure, P, applied to the surface of the rock, and not the pressure measured in the flatjacks:

$$P = \textit{flatjack pressure} * \textit{flatjack contact area} / \textit{bearing plate area} \quad \text{(Eq. 6-47)}$$

The flatjack contact area must be measured in the field after each test because the flatjacks are flexible and they deform under their internal pressure. For the 1998 tests the flatjack loading surface dimensions were measured to be about 78 cm x 78 cm. For both the 2000 and 2003 tests, the dimensions used in the above calculation of E were 79.4 cm x 79.4 cm. The bearing plate area for all tests was 91.4 cm x 91.4 cm.

Tables 6-97 and 6-98 present some of the 2000 and 2003 plate load test results, respectively. However, the accuracy of the Equation 6-46 "simplified approach" needs further evaluation, and the reported results "should be considered preliminary" (DTN: SN0011F3912298.023 [DIRS 158399]; Sobolik and George 2001 [DIRS 165420], p. 41). These test-related issues require that these results be used with caution. For the 2000 test, the calculated maximum applied bearing pressure was 31.75 MPa with no sign of rock failure in the pressure versus displacement plots. For the 2003 test, the calculated maximum applied bearing pressure was 31.27 MPa, again with no sign of rock failure in the pressure versus displacement plots. The hot rock, deep-anchor displacement transducer failed, so no values are reported.

In both the 2000 and 2003 tests, the modulus measured on the hot side of the plate load test was generally more than twice that of the ambient temperature side. The principal investigators attribute this to both the difference in the original condition of the rock and the cumulative effects of the entire length of the Heated Drift expanding towards the test niche. They state that the moduli on the hot and ambient sides of the tests are not functions of temperature and, accordingly, temperatures are not used in the calculation of the moduli. For completeness, the 2000 test temperature of the ambient rock at the deep anchor position was measured to be 34.5ºC and for the "hot" rock, 58.6ºC at the medium anchor position (DTN: SN0011F3912298.023 [DIRS 158399]; Sobolik and George 2001 [DIRS 165420], p. 15). For the 2003 test, the temperatures of the ambient rock at the deep anchor position and the hot rock are not yet available.

To cover the estimated range of in situ stresses from 5 to 10 MPa, a calculation was made to estimate rock mass modulus, E, at a bearing pressure of 5 MPa. First, anchor displacement was estimated from the initial loading curves on the "average bearing pressure vs. displacement" plots of the respective DTNs (DTNs: SN0011F3912298.023 [DIRS 158399]; SN0310F3912298.054 [DIRS 168527]). Next, this value of displacement was entered into Equation 6-46 to estimate the rock mass modulus, E, treating rock to be isotropic, homogeneous, and elastic. For both the 2000 and 2003 calculation, Poisson's ratio was used as 0.20, and the *Iw* value was 1.05.

Table 6-97. October 2000 Plate Load Test Results

Bearing Pressure		Ambient 2.7 m			Ambient 1.31 m			Ambient 0.87 m			Hot 1.54 m			Hot 0.86 m		
P1 (MPa)	P2 (MPa)	D1 (mm)	D2 (mm)	E (GPa)	D1 (mm)	D2 (mm)	E (GPa)	D1 (mm)	D2 (mm)	E (GPa)	D1 (mm)	D2 (mm)	E (GPa)	D1 (mm)	D2 (mm)	E (GPa)
0.00	10.00	0.00	0.53	17.4	0.00	0.43	21.4	0.00	0.43	21.4	0.00	0.23	40.1	0.00	0.16	57.6
0.00	20.00	0.00	1.00	18.4	0.00	0.87	21.2	0.00	0.76	24.2	0.00	0.42	43.9	0.00	0.29	63.5
0.00	30.00	0.00	1.56	17.7	0.00	1.38	20.0	0.00	1.13	24.5	0.00	0.63	43.9	0.00	0.49	56.4
0.00	31.75	0.00	1.69	17.3	0.00	1.49	19.6	0.00	1.21	24.2	0.00	0.68	43.0	0.00	0.55	53.2
2.64	5.02	0.23	0.32	24.4	0.20	0.24	54.8	0.20	0.27	31.3	0.09	0.14	43.9	0.07	0.10	73.1
5.38	10.55	0.43	0.56	36.6	0.38	0.46	59.5	0.36	0.45	52.9	0.16	0.24	59.5	0.12	0.17	95.3
7.89	15.90	0.62	0.81	38.8	0.55	0.69	52.7	0.49	0.63	52.7	0.21	0.34	56.8	0.15	0.23	92.2
10.50	20.98	0.83	1.07	40.2	0.73	0.93	48.3	0.64	0.80	60.3	0.28	0.44	60.3	0.22	0.32	96.6
13.27	26.16	1.07	1.36	41.0	0.95	1.19	49.5	0.79	0.99	59.4	0.34	0.53	62.5	0.28	0.40	99.0

Source: DTN: SN0011F3912298.023 [DIRS 158399].

NOTES: $E=(P2-P1)*b*(1-n^2)Iw/(D2-D1)$

where E is the Young's Modulus in GPa

b = 914 mm (width of the square plate)

D1 and D2 = displacement range in mm used to calculate E

n = 0.2 (Poisson's ratio) (George et al. 1999 [DIRS 160044])

Iw = 1.05 (influence factor, which is intermediate between 0.82 for a rigid plate and 1.12 for a flexible plate)

P1 or P2 bearing pressure = (average pressure in the flat jack)*contact area / bearing plate area

where contact area = $(794\ mm)^2$ and bearing plate area = $(914\ mm)^2$

E in the shaded area represents Elastic (Young's) Modulus obtained from the slope of the unloading and reloading curves.

Table 6-98. April 2003 Plate Load Test Results

Bearing Pressure (MPa)		Ambient, 2.7 m			Ambient, 1.31 m			Ambient, 0.87 m			Hot, 1.54 m			Hot, 0.86 m		
P1	P2	D1 (mm)	D2 (mm)	E (GPa)	D1 (mm)	D2 (mm)	E (GPa)	D1 (mm)	D2 (mm)	E (GPa)	D1 (mm)	D2 (mm)	E (GPa)	D1 (mm)	D2 (mm)	E (GPa)
0.00	10.00	0.00	0.45	20.6	0.00	0.56	16.4	0.00	0.46	20.2	0.00	0.21	44.8	0.00	0.15	61.1
0.00	20.00	0.00	0.77	23.8	0.00	1.00	18.4	0.00	0.87	21.3	0.00	0.42	44.4	0.00	0.30	61.3
0.00	30.00	0.00	1.06	26.0	0.00	1.40	19.7	0.00	1.26	21.9	0.00	0.63	44.0	0.00	0.45	61.7
0.00	31.27	0.00	1.10	26.3	0.00	1.45	19.9	0.00	1.31	22.1	0.00	0.65	44.4	0.00	0.46	62.7
2.74	5.31	0.18	0.25	30.6	0.21	0.31	24.7	0.19	0.24	54.1	0.06	0.10	55.1	0.05	0.08	80.5
5.38	10.54	0.35	0.47	39.6	0.43	0.59	29.5	0.39	0.48	49.3	0.13	0.22	54.5	0.11	0.17	77.2
7.93	15.80	0.50	0.65	49.0	0.61	0.82	35.0	0.56	0.70	51.4	0.21	0.33	59.4	0.16	0.24	90.4
10.48	21.01	0.62	0.81	52.0	0.78	1.04	37.1	0.71	0.91	49.2	0.28	0.44	59.4	0.21	0.32	89.1
13.14	26.23	0.75	0.95	60.8	0.96	1.25	41.0	0.88	1.11	51.3	0.36	0.55	62.1	0.27	0.40	92.1

Source: DTN: SN0310F3912298.054 [DIRS 168527].

NOTES: $E=(P2-P1)*b*(1-n^2)Iw/(D2-D1)$

where E is the Young's Modulus in GPa

b = 914 mm (width of the square plate)

D1 and D2 = displacement range in mm used to calculate E

n = 0.2 (Poisson's ratio) (George et al. 1999 [DIRS 160044])

Iw=1.05 (influence factor which is intermediate between 0.82 for a rigid plate and 1.12 for a flexible plate)

E in the shaded area represents Elastic (Young's) Modulus obtained from the slope of the unloading and reloading curves.

P1 or P2 bearing pressure = (average pressure in the flat jack)*contact area / bearing plate area

where contact area = $(794\ mm)^2$ and bearing plate area=$(914\ mm)^2$

Following are some common observations that apply to both the 2000 and 2003 plate loading tests:

- In general the initial loading and unloading/reloading portions of the average pressure vs. displacement plots were quite linear.
- From the plots and tables given in the developed DTNs, it is evident that the unloading/reloading moduli mostly increase with pressure.
- The total displacement measured was 2 to 3 times greater in ambient rock than in heated rock.

The ambient rock has a relatively larger hysteresis loop during overall loading and unloading, compared to the heated rock.

6.6.4.3 In Situ Slot Tests

The purpose of the pressurized slot testing program was to perform field tests on meter scale blocks of lithophysal rock in order to determine bulk thermal-mechanical rock properties

(i.e., elastic rock mass modulus, compressive strength, and thermal expansion coefficient) over a range of temperature and rock conditions (BSC 2002 [DIRS 165421]).

The test plan consisted of:

1. Estimating the in situ stress acting normal to the slots
2. Performing loading and unloading cycles of pressure-deformation history to estimate rock mass deformation moduli
3. Estimating rock failure stress at various locations
4. Estimating the tendon rock mass strength
5. Holding at maximum pressure to determine time-dependent effects on rock properties
6. Estimating rock mass thermal expansion
7. Discussing the influence of temperature on the thermal-mechanical properties
8. Conducting a field posttest analysis of the tested rock.

Three-dimensional numerical simulations are required for both test design and posttest analyses of the results because of all the complexities involved. The final analyses and report have not yet been issued.

Slot Test 1

Slot test 1 was conducted in a highly fractured Tptpll rock mass near the contact between the bottom of the Tptpmn and the top of the Tptpll at Station 57+77 in the South Ramp. This test was conducted on May 8, 2002, in the ESF right rib. The test configuration consisted of two vertical slots oriented normal to the rib of the tunnel, nominally 4 cm in width, an average of 120 cm high, and an average of 1.8 m deep, which resulted in a nominal slot area of 2.2 m^2. The nominal distance between the slots (tendon length) was 1.2 m. A 30.5 cm borehole, approximately 1.5 m deep, oriented in a horizontal plane and extending into the wall, perpendicular to the rib, was located between the slots about mid-height. Prior to test initiation, the rock was visibly fractured, and three sections of the borehole had undergone rockfall. The lithophysal porosity at the location of slot test 1 was estimated to be 12%, based on visual surveys of the rib surface, video surveys of one slot, and video surveys of the central borehole. The total porosity was estimated to be 24% (DTN: SN0301F4102102.008 [DIRS 165431]). This area was targeted to assess the expected lowest strength and shear modulus (lower bound) data representing the lowest quality lithophysal rock visible in the ESF.

The test was initiated by raising the pressure in the jacks to approximately 2.4 MPa during the first 50 minutes and holding this pressure for about 20 minutes. Starting at a pressure of approximately 2.1 MPa, significant scaling of the rock in the borehole and on the drift wall surrounding the borehole began, and inelastic behavior was noted. The pressure was subsequently dropped to approximately 1.5 MPa, and then raised again over the next 40 minutes up to approximately 6.07 MPa, when multiple fractures formed in the rock tendon parallel to the free face, indicating possible rock failure in biaxial compression around the hole. At about the same pressure, there were clear indicators that the load platens were punching into the slot faces,

also indicating a crushing failure of the rock behind the platens. Scaling, audible reports, and some significant fracturing events continued periodically, up to the maximum pressure. Substantial spalling was noted in the central borehole; rubble was about fist size. The pressure was then dropped back to approximately 4.2 MPa, increased to approximately 5 MPa and held for 5 minutes, then raised again to approximately 5.8 MPa at which point the rock offered no further resistance. The test was terminated after about 2.5 hours total.

A visual observation was made to ascertain the failure mode. It was determined that failure was induced near the top of the right platen. Instead of failing the rock tendon, the platen pressed into the adjacent rock mass through a series of preexisting but previously discontinuous fractures leading from the top of the right slot up to about 1 m above the left slot (Howard et al. 2003 [DIRS 166047], p. 377). Displacement from one central borehole gage showed a significant inelastic displacement as the flatjacks approached the maximum load, so the rock tendon was likely failed to some degree.

Displacement-pressure data up to the initial 2.1-MPa point were used to determine a rock mass Poisson's ratio and modulus value. The Kirsch solution yielded elastic estimates of 0.48 GPa for Young's Modulus and 0.2 for Poisson's ratio. In the finite element analysis, estimates of the deformation modulus to be between 0.50 and 0.55 GPa. The more conservative value of 0.50 GPa was selected as the rock mass modulus. The peak flatjack pressure was 6.1 MPa.

Slot Test 2

Slot test 2 was conducted in a more competent zone of Tptpul rock with fewer fractures and lithophysae on the right rib of the ESF at Station 63+83. This ESF location was selected to represent the upper bound of rock behavior in an area composed of relatively higher quality rock that also lacked the pervasive fracturing of the Tptpll zone. The test, conducted first at ambient temperatures and later at high temperatures, was performed from October 15 through October 30, 2002.

The orientation of the slots and borehole were similar to slot test 1. The slots cut into the rib for slot test 2 were nominally 4 cm wide, 2.0 m deep and 1.7 m high, which resulted in a nominal slot area of 3.4 m^2. After the slots were cut, the vertical borehole gages in the center borehole closed by approximately 2 mm. A 30.5 cm borehole, approximately 1.8 m deep, oriented in a horizontal plane and extending into the wall, perpendicular to the rib, was located between the slots about mid-height. A total of six heater holes 4 cm in diameter and 122 cm deep were drilled above and below the test tendon, and rod heaters were installed for the high-temperature test (Howard et al. 2003 [DIRS 166047], p. 377). The lithophysal porosity at the location of slot test 2 was estimated to be 13% based on a visual survey of the rib, and video surveys of both slots and the central borehole; the total porosity was estimated to be 24% (DTN: SN0302F4102102.010 [DIRS 165436]).

For the first test, performed October 15, 2002, a single measurement session was conducted at ambient temperature. The second test was performed on October 30, 2002 and represented loading of a heated rock mass. The center borehole was video taped during the pressurization cycles to observe the borehole response to rock mass failure. Any rubble dislodged as the result

of spalling within the center borehole was collected, characterized in terms of particle size, and quantified.

The ambient temperature test was conducted by raising the jack pressure to approximately 0.5 MPa, holding 5 minutes, then lowering the pressure to approximately 0.1 MPa. The second loading cycle increased the pressure up to approximately 1.8 MPa, was held for about 20 minutes then pressure was reduced to approximately 1.5 MPa and held for about 5 minutes. The third loading cycle raised the pressure to approximately 3.45 MPa, where it was held for about 20 minutes. The pressure was subsequently dropped to approximately 1.8 MPa, held for 5 minutes, and then lowered to zero. The slots responded elastically during this ambient temperature test phase. No significant scaling of the rock in the borehole or on the drift wall was observed.

The Kirsch solution was applied to the ambient results and produced a Young's modulus estimate of 2.0 GPa and Poisson's ratio of 0.20 for the initial loading. In the finite element analysis for the ambient test, estimates of the deformation modulus were determined to be in the range of 2.0 to 3.0 GPa and 0.20 for Poisson's ratio. The value of 3.0 GPa was selected as the rock mass modulus.

Following completion of the ambient test, the heaters were turned on and kept on for more than two weeks to raise the rock tendon to about 90ºC. During the heating cycle, borehole deformations of approximately 3 mm were recorded. Visual examination of the center borehole after the thermal test revealed two axial fractures that ran the length of the borehole. These fractures were the result of an apparent compressive failure of the rock under thermal load. The failure was attributed to: (1) the concentration of the vertical stress at the borehole springline due to creation of the tunnel and the borehole, (2) removal of the confining horizontal stress due to slot cutting, and (3) thermal stress in the vertical direction concentrated on the borehole wall. It was considered likely that the combination of (1) and (2) created a stress condition close to the failure stress near the springline of the borehole. Finally, the addition of thermal stress (3) exceeded the rock strength and created the axial spalling (Howard et al. 2003 [DIRS 166047], pp. 378 and 379).

After the tendon temperature had stabilized to around 90ºC, the heated pressurization test was initiated. Pressure in both jacks was increased (and unloaded) in four cycles to values of 1.7, 3.4, 6.9, and 10.3 MPa over about 1 hour, then held at 10.3 MPa for about 75 minutes. During loading, audible reports were heard, and minor spalling was recorded on video cameras located in the center borehole (Howard et al. 2003 [DIRS 166047], p. 379). Slot data indicated that compressive failure of the rock surrounding the left slot began at approximately 4 MPa. A significant failure of the rock to the right of the right slot occurred at a flatjack pressure of approximately 8 MPa. Creep closure of about 6 mm was recorded in the center borehole, and about 3.5 mm of creep deformation was recorded in the right slot during the hold period at 10.3 MPa, indicating that failure was beginning to occur. The pressure was then unloaded to approximately 7.8 MPa and then increased to 10.7 MPa when a "loud report and a small cloud of dust" was noted coming from an approximately 2 m high wedge block that failed in the rib to the right of the right slot. The pressure could be raised no higher, and after unloading, a surveillance revealed that the right platen of the right jack was impacted into the right side of the slot about 1 cm. Also, newly opened fractures were evident, most having an orientation parallel in both

strike and dip to preexisting fractures that transect the ESF (Howard et al. 2003 [DIRS 166047], p. 379).

Finite element simulations for the heated test produced estimates of deformation modulus to be in the range from 1.0 to 2.0 GPa and 0.20 for Poisson's ratio. The average value of 1.5 GPa was selected as the most appropriate rock mass modulus for average rock temperatures of about 90°C. One unloading curve slope corresponded to a reported Young's modulus of about 4 GPa. This measured reduction in modulus after heating is significant in that it indicates that the rock mass was damaged by thermal stresses, thus reducing the rock modulus. This is corroborated by the observation of fracturing in the central borehole as a result of elevated thermal stresses.

Slot Test 3

Slot test 3 was located at Station 21+25 of the ECRB in an area selected to have the most representative geomechanical properties of lithophysal (Tptpll) rock mass. However, once the slots were cut many noticeable fractures and numerous lithophysae were discovered. To avoid the vertical stress concentration present at the springline of the rib, the location of the slot test was moved to the floor of the tunnel. Otherwise, the test setup was the same as the previous slot tests, except that the central borehole had a vertical orientation. A 30.5 cm borehole was drilled approximately 1.8 m deep into the floor. The slots cut into the floor were nominally 4 cm wide, 1.4 m deep, and 1.7 m long, which resulted in a nominal slot area of 2.4 m^2. The lithophysal porosity at the location of slot test 3 was estimated to be 8% based on a visual survey of the rib, video surveys of both slots, and video surveys of the central borehole. The total porosity was estimated to be 22% (DTN: SN0303F4102102.012 [DIRS 165440]).

This test was conducted on December 10, 2002. Pressure in both jacks was increased, held for about 20 minutes, and then unloaded in four cycles to values of approximately 0.8, 1.7, 3.3, and 5.0 MPa. Around 0.7 MPa, 0.4 to 0.5 mm slip displacement was registered in all the borehole and rib gages, likely on a fracture traversing near the borehole. When the flatjack pressure was increased to approximately 5 MPa, visible signs of compression failure were evident in the borehole collar and the drift invert surrounding the borehole. There was significant fracturing and vertical movement of rock on the floor as well as substantial rockfall into the borehole. The slot and tendon measurement data clearly show this failure. Analysis of the data appears to indicate that the rock near the left rib behaved inelastically from the outset of the test. The pressure could not be maintained at 5 MPa. The pressure was then reduced to approximately 3.9 MPa, held for 5 minutes, then increased up to 6.8 MPa, which was the maximum pressure that could be applied. Above 5 MPa significant and continuous displacements were measured in borehole gages, the tendon displacements, and the left slot. The right slot data was not provided in the DTN.

The Kirsch solution was applied and produced a Young's modulus estimate of 0.7 GPa and Poisson's ratio of 0.33 for the initial loading. In finite element analysis, an estimate of the deformation modulus were determined to be about 1.0 GPa and 0.33 for Poisson's ratio. The value of 1.0 GPa was adopted as the preliminary rock mass modulus.

Slot Tests—Summary

A total of three pressurized slot tests have been conducted in both the Tptpul and Tptpll lithophysal rock units. Two tests were carried out in the rib of the ESF, a 7.6 m diameter bored tunnel, and one test was conducted in the floor of the ECRB (Figure 6-135) a 5.0 m diameter bored tunnel. Slot tests 1 and 3 were carried out under ambient temperature conditions. Slot test 2 involved testing at ambient conditions (about 25°C) and at elevated rock temperature conditions (about 90°C). Preliminary results are summarized in Table 6-99.

A central borehole, 0.305 m in diameter and 1.5 to 1.8 m deep, was drilled into the rock to be tested and instrumented prior to creation of the slots. The slots were cut vertically into the ESF rib (tests 1 and 2) or into the floor perpendicular to the ECRB tunnel (test 3) using a custom rock saw. The nominal distance between the slots (tendon length) for all tests was 1.2 m. Each test employed two hydraulically inflated flatjacks measuring 0.81 x 0.81 m (0.66 m^2) sandwiched between 0.91 x 0.91 m (0.83 m^2) aluminum bearing plates, the flatjack and bearing plate assembly having a nominal width of 3.80 cm. The jacks and plates were located within the two parallel slots. The pressurization sequence used was adapted based on ASTM D 4394-84, *Standard Test Method for Determining the In Situ Modulus of Deformation of Rock Mass Using the Rigid Plate Loading Method* [DIRS 149445]. The flatjack pressure was increased, with two or more unloading/reloading cycles, until gross failure of the rock occurred. Measurements of rock mass deformation were made in the borehole, on the rib surfaces, and around the edges of the platens as a function of jack pressure and time.

Figure 6-136 shows flatjack pressure versus instrumentation hole diametral deformation for the tests. The loading results show a typical elastic-plastic response, in which a linear loading slope is followed by yield and plastic deformation. Yielding of the rock was typically in shear, emanating from the central borehole, and resulting in rockfall in the form of small rock particles in the central borehole during yield. The results, summarized in Table 6-99, show that the rock mass has deformation modulus and strength that lie at the lower end of the design range, but that are consistent with the same general relationship of strength to modulus. The low values of modulus indicate that the skin of rock surrounding the tunnels, particularly at the sidewalls, is likely in a pre-yielded state due to mining induced stress.

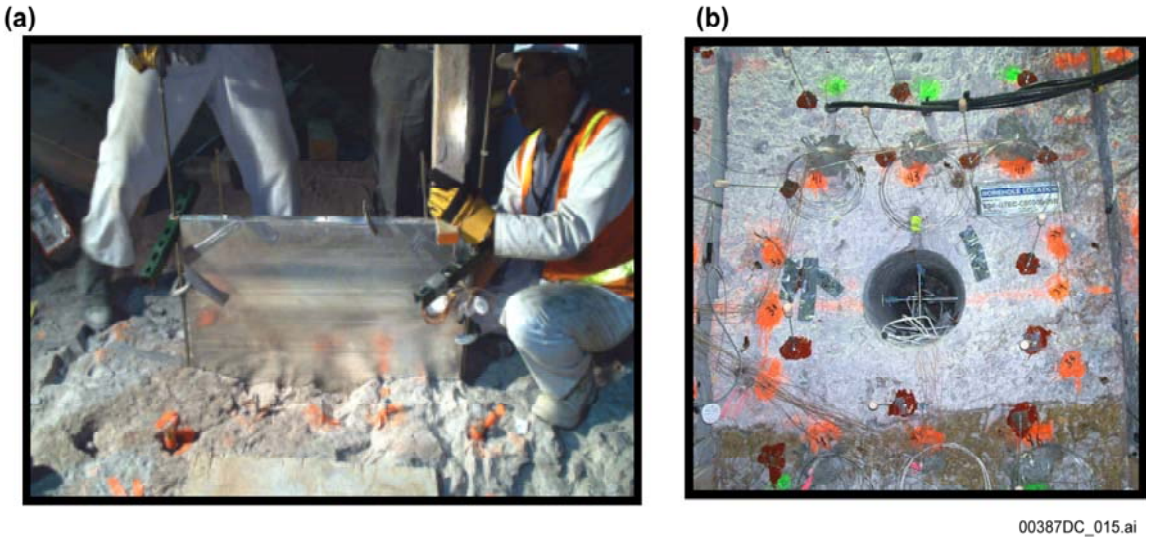

Figure 6-135. Photographs of (a) Preparation of Slot Test 3 in the Floor of the Enhanced Characterization of the Repository Block, Tptpll Unit, Lowering of Flatjack into Place in Sawcut Slot and (b) Slot Test 2 Showing Central Instrumentation Hole and Parallel Slots

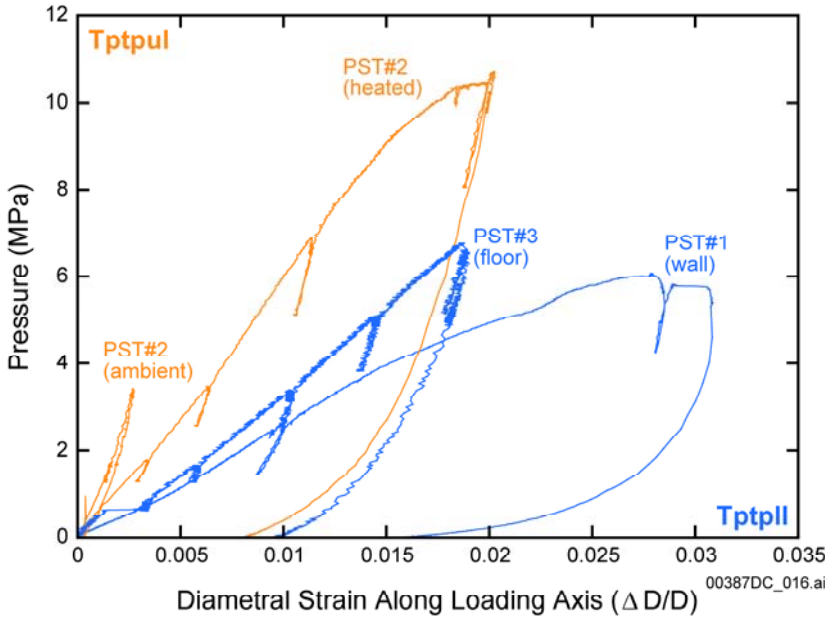

Sources: DTNs: SN0207F4102102.001 [DIRS 165429]; SN0208F4102102.002 [DIRS 161874]; SN0212F4102102.003 [DIRS 165432]; SN0212F4102102.004 [DIRS 161875].

Figure 6-136. Composite of Flatjack Pressure versus Central Hole Diametral Strain for the Three Pressurized Slot Tests

The Young's modulus and Poisson's ratio of the rock were analytically estimated using two different methods. A closed-form solution for horizontal stress change applied near an underground borehole, the Kirsch solution, was used to make initial estimates of rock mass elastic constants. Then the Kirsch solution estimates were used to derive the final estimates of elastic properties by trying to match the actual pressure and deformation history. In situ stresses

were estimated to be 4.3 MPa in the vertical direction; 3.0 MPa horizontally parallel to the ESF main drift; and 2.0 MPa horizontally perpendicular to the ESF main drift. For slot tests 1 and 2, the test configuration consisted of two vertical slots oriented normal to the rib of the ESF tunnel (normal to maximum horizontal in situ stress). For slot test 3, the slots were oriented approximately 52º from the principal stress orientations. However, locally near the rib of the tunnel, these stresses are altered as a result of the stress redistribution around the tunnel.

Table 6-99. Rock Mass Mechanical Properties from In Situ Slot Tests

Slot Test	UNIT	Temp. (°C)	Poisson' s Ratio	$E_{initial}$ (GPa)	E_{reload} (GPa)	Slot Area (m^2)	Tendon Length (m)	Peak Flatjack Pressure (MPa)	Estimated Lithophysal/ Total Rock Porosity (%)	Compressive Strength (MPa)
1	Tptpll	25	0.20	0.5	NA	2.2	1.2	6.1	12/24	6
2	Tptpul	25	0.20	3.0	NA	3.4	1.2	3.4	13/24	NA
2	Tptpul	90	0.20	1.5	4	3.4	1.2	10.7	13/24	11[a]
3	Tptpll	25	0.33	1.0	NA	2.4	1.2	6.8	8/22	7[a]

Sources: DTNs: SN0207F4102102.001 [DIRS 165429]; SN0208F4102102.002 [DIRS 161874]; SN0212F4102102.003 [DIRS 165432]; SN0212F4102102.004 [DIRS 161875].

NOTES: PST#1 in poorest quality Tptpll, PST#2 in good quality Tptpul and PST#3 in typical repository Tptpll. Strength here is the peak flatjack pressure at yield.
[a] Results do not account for presence of central hole in failure load.

Source DTNs for each slot test are presented in Table 6-100. Some further details concerning slot tests 1 and 2 can be found in Howard et al. (2003 [DIRS 166047]). The feature abundance DTNs include the necessary estimated lithophysal and total porosity information. These DTNs also include what information is available regarding mapped fractures.

Table 6-100. Source DTN Data for the In Situ Slot Tests

Slot Test #	Data Type	DTNs
1	Slot Test Results	SN0207F4102102.001 [DIRS 165429]; SN0208F4102102.002 [DIRS 161874]
	Feature Abundances	SN0301F4102102.007 [DIRS 165430]; SN0301F4102102.008 [DIRS 165431]
2	Slot Test Results	SN0212F4102102.003 [DIRS 165432]; SN0212F4102102.004 [DIRS 161875]
	Feature Abundances	SN0302F4102102.009 [DIRS 165433]; SN0302F4102102.010 [DIRS 165436]
3	Slot Test Results	SN0212F4102102.003 [DIRS 165432]; SN0212F4102102.004 [DIRS 161875]
	Feature Abundances	SN0303F4102102.011 [DIRS 165439]; SN0303F4102102.012 [DIRS 165440]

Site-specific geotechnical characterization was conducted at each slot test location. The entire surface of one side of one slot at each test and the 0.305 m central borehole were video recorded. The video was then mapped onto digital images, which were then used to quantify lithophysal and other feature abundances and to determine the nature and interconnectivity of the visible fracture network (Howard et al. 2003 [DIRS 166047], p. 377).

Uncertainties Impacting Slot Test Results

A number of uncertainties impact the reported slot test results:

- No failure stress was reported, only maximum flatjack pressure. Since the flatjack bearing plate area was about 25% larger than the flatjack contact area, the plate bearing stress was smaller than the recorded flatjack pressure. Furthermore, the applied load acted over an even larger bulk rock cross-sectional area within the tendon, suggesting the likely tendon rock mass failure stress was smaller than the bearing plate pressure. Additionally, the multiaxial failure stress should be adjusted lower still to compensate for confining stresses existing in the rock, since uniaxial rock mass strength is desired.

- The tested rock in situ stress conditions have been changed due to tunnel excavation and excavation of the central borehole and slots. In fact, for the two tests conducted in the tunnel ribs, the rock tendon was likely prestressed vertically to a significant percentage of the failure stress. Also, stress concentration in the rock around the large central borehole produced large stress gradients in the rock tendon, thus making it difficult to estimate a uniaxial rock mass strength. Posttest numerical analysis will attempt to back out a failure envelope for each slot test, based on locations within the tendon where failure was observed.

- For slot tests 1 and 2, the in situ stresses were dominated by the vertical stress (resulting from the stress concentration near the tunnel wall) after the slots reduced the horizontal stress to close to zero. During testing, the increasing horizontal stress created a biaxial stress condition, with failure occurring by fracturing parallel to the free face. Slot test 3, located in the floor, eliminated the in situ vertical stress and resulted in a test where the stress state in the tendon and stress paths to failure were better known.

- The rock mass modulus values reported were estimated from the initial loading data, which most closely correspond to deformation from near-field damaged rock caused by tunnel construction and heating. Modulus values from the stiffer unload/reload data, which may more closely represent rock deformation away from the tunnel face, were not reported.

6.6.5 ESF Ground Support Confirmation

Completion of the ESF main loop tunnel represented a major YMP milestone and set a natural stage for the assessment of the new data acquired from the ESF tunnel. The evaluation of their impact (if any) on the methodology followed, initially, when the rock property data were limited. A series of reports was prepared with the overall objective of evaluating design methodology, assumptions made prior to construction, and verification of these assumptions after the tunnel construction was completed. *ESF Ground Support Confirmation* (CRWMS M&O 1998 [DIRS 124140]) summarizes evaluation of the ground control measures introduced in the ESF tunnel during construction.

The purpose of that report (CRWMS M&O 1998 [DIRS 124140]) was confirmation of geotechnical parameters used in rock support design. The range of the rock mass property values

used in the design of the ESF ground support system was originally based on NRG borehole data. Scanline data, full peripheral mapping, tunnel convergence measurements, and ground support instrumentation provided a substantial volume of data and information that were used to confirm key ESF design parameters and, hence, the original basis for design. The acquired data and information also served to confirm the empirical and analytical design methodologies used in the design of the ESF ground support systems.

The specific objectives for this analysis included the following:

- Assembly of a list of design parameters to facilitate a comparison of the initial core-based ESF design parameters to geomechanics parameters acquired from scanline and full-peripheral field mapping
- Identification of significant differences between the original core-based parameters and the field-based parameters from tunnel mapping
- Revisitation of the original ESF ground support design analysis using field-based rock mass and joint properties from tunnel mapping as key design inputs
- Comparison of predicted displacements and ground support loads with the actual in situ performance using both tunnel mapping and construction monitoring data and information
- Demonstration of the adequacy of ESF design simulation and ground support performance in the ESF
- Comparison of the installed support in the ESF to the recommended support based on the guidelines in the ESF ground support design analysis and on the field mapping rock mass quality data
- Assessment of the adequacy of the installed support relative to the mapped ground conditions.

The results from this analysis may serve as a base for establishing a procedure leading to verification of ground support performance during construction and operation of emplacement drifts. Those results may also provide a baseline for planned inspection and maintenance during the operations and maintenance phase of future repository operations. Additionally, the results from this activity may support Repository Design data and information needs.

The confirmation process presented in this study can be used to identify any significant variance between the actual and predicted performance of the installed ground support system. These data and information can be incorporated into the performance confirmation baseline and may serve as the technical basis for assessments of the future repository, including periodic inspection and maintenance of the facility openings and ground support.

6.6.6 ESF Deformation Monitoring

During ESF construction, efforts were made to obtain information pertaining to the magnitude of deformation occurring as a result of tunnel excavation. The analysis of tunnel deformation data was presented in *Deformation Monitoring Analysis* (CRWMS M&O 1998 [DIRS 131317]). The report presents an analysis of tunnel deformation in the ESF based on convergence monitoring data. Displacement data from 94 tape extensometer stations and 18 borehole extensometer stations along the ESF main loop (i.e., the North Ramp, main drift, and South Ramp) were evaluated as part of this analysis. A semiempirical convergence solution was applied to interpret the convergence measurements to estimate ground behavior prior to installation of the convergence monitoring station and to predict long-term tunnel displacement. An analytical solution that relates convergence to elastic modulus was applied to estimate rock mass modulus.

The specific objectives for this analysis included the following:

- Correlation of tunnel convergence rates and magnitudes as a function of the thermal mechanical unit and the associated rock mass properties
- Confirmation of the design assumption(s) that limited displacements (50% to 60% of the total displacement) will occur prior to ground support installation
- Direction of a regression analysis of displacement data to address future potential displacement anomalies.
- Prediction of long-term tunnel displacement and convergence rates
- Comparison of tunnel closure rates and closure rates in the ESF to the DOE Site Characterization Plan tentative goals
- Assessment of long-term tunnel stability, based on predicted long-term tunnel displacement and convergence rates.

The results from this analysis may assist in the ground support selection process and may provide a baseline for planning inspections and maintenance during the operations and maintenance phase of future repository operations. The results from this activity are also available to support Repository Design data and information needs.

It should be noted that the instrumentation data from monitoring in the ESF tunnel were obtained under ambient conditions. The predictions of long-term tunnel displacement based on the ESF monitored data are, therefore, not directly applicable to those underground openings that will be subjected to thermal loads.

6.6.7 Steel Sets Monitoring

Steel sets were placed in the ESF as ground support for the tunnel. The *ESF Design Confirmation Steel Set Loads Analysis* (CRWMS M&O 1998 [DIRS 141028]) provides an assessment of the data collected from the field measurements. Deformations of the rock mass over time would be reflected by changes of loading (and strains) in the steel sets. The analysis is

developed using mainly the steel set strain gage data, in order to assess the rock loads acting on individual sets. The analysis takes into account the geological factors, such as depth of tunnel section, and the influence of jacking loads used during installation on the development of postinstallation loads.

In total, forty steel sets were instrumented with strain gages with the purpose of monitoring the steel set performance over time. Some sets were instrumented before jacking and some after jacking load was applied. The purpose of monitoring the steel set was to see if the rock mass, which was initially relaxed around the excavated opening, would undergo further deformation as time progressed. The data from four sets were not available, and so the analysis was based on the remaining 36 data sets; however, the data for one of the 36 sets was found to be unreliable.

The loads estimated for steel sets in *ESF Ground Support Design Analysis* (CRWMS M&O 1995 [DIRS 101427]) were used as input to a structural analysis (CRWMS M&O 1996 [DIRS 158154]), the objective of which was to provide a basis for the calculations associated with the sizing of steel sets and components of the installation setup that were needed to assemble and install the steel sets in the tunnel. Instrumented steel sets were to provide the data for an in situ verification of the steel set performance.

ESF Design Confirmation Steel Set Loads Analysis (CRWMS M&O 1998 [DIRS 141028]) included both evaluation of stresses measured in the steel and numerical simulations. Numerical simulations were used as a tool, facilitating replication of the loading pattern imposed on the typical steel set during installation. Since the results of the measurements indicated relatively minor stress changes in steel sets over time, it was reasonable to consider that steel set stresses were developed mainly as a result of the initial jacking load used to expand the set in place. The factor of safety calculated for each instrumented set was used as a measure of the load imposed on the set.

Figure 6-137 displays the minimum factors of safety obtained for all instrumented steel sets. The results obtained for a group of steel sets instrumented before jacking are considered a better indicator of the magnitude of total loads imposed upon each instrumented set. Analysis of measurements and numerical simulations results revealed that the maximum stresses were generated by the bending moment imposed during installation.

The field-obtained set of steel set stress measurements for steel set 261, shown in Figure 6-138, indicates that maximum stresses induced in the steel set by jacking are about 10% of the design installation stress. The load increases slightly with time.

Steel Sets Monitoring—Summary

The steel set monitoring program provides several important benefits:

1. Steel sets performance reflects the performance of the real rock strata in which they are installed and, as such, provides a direct link to the properties of the intact rock and a means of verification of the theoretical and empirical methods used determine the performance of the rock mass.
2. The data allow for the development of the long-term strategy for measurements planned for the performance confirmation program, considering locations of the future monitoring stations.
3. The data reflect the potential accuracy of measurements and provide input for the future estimates of portions of the uncertainty that must be attributed to the seasonal changes of temperature.
4. The data provide evidence necessary for estimating the type of instrumentation needed, along with the long-term stability of that instrumentation.

In general, the data obtained from steel sets at the repository horizon indicate that no significant measurable stress buildup was observed following the steel set installation. Minor stress increases were recorded in the steel sets installed in the softer PTn/TSw1 units.

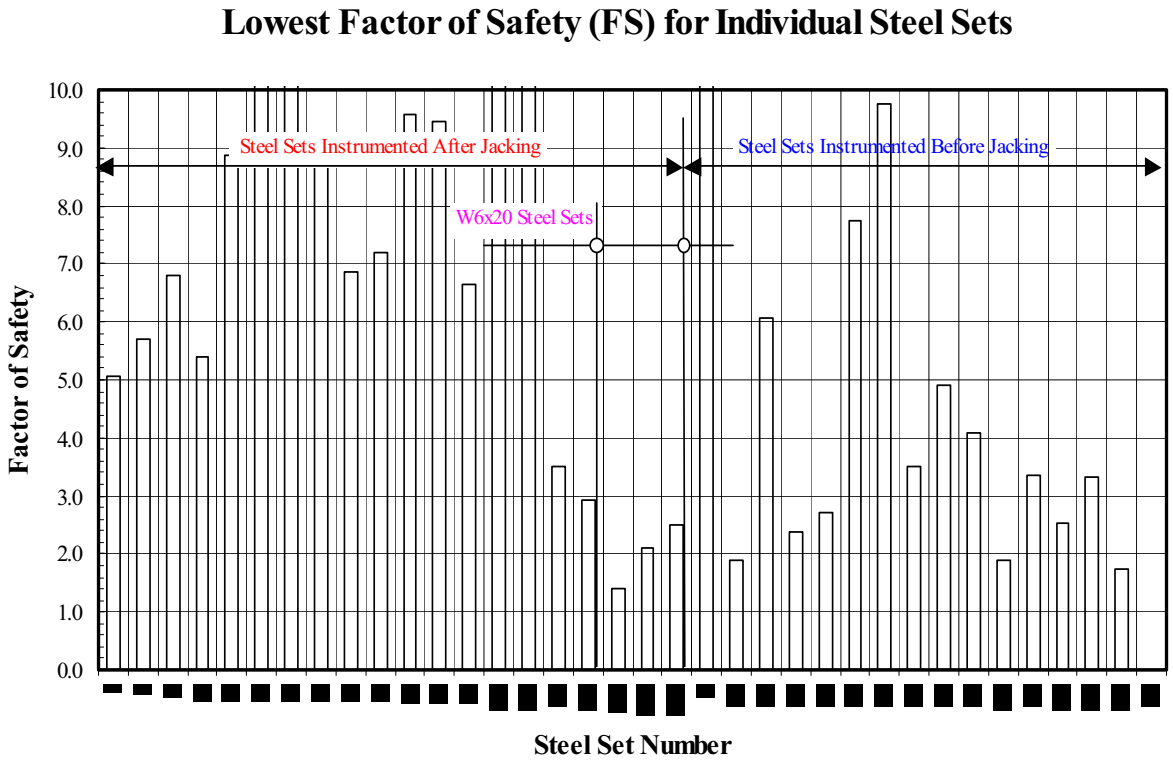

Source: CRWMS M&O 1998 [DIRS 141028], p. 124, Figure 50.

NOTES: Steel sets are W8 x 31, except as indicated. Steel Set 731 data was determined to be unreliable.

Figure 6-137. Factor of Safety under Combined Loading Conditions for Instrumented Steel Sets

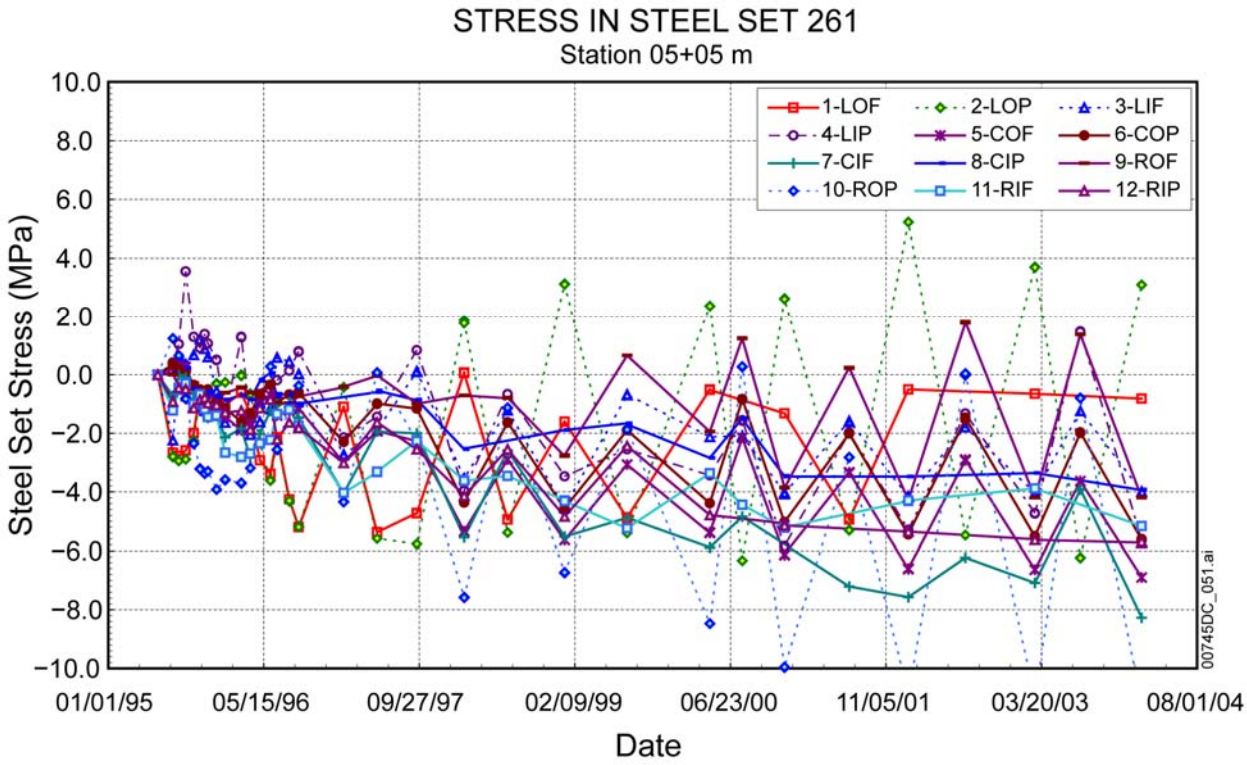

Source: DTN: SN0405F3312393.015 [DIRS 177261].

NOTES: Positive values indicate compression. For details pertaining to the legend and associated nomenclature see CRWMS M&O (1998 [DIRS 141028]).

Figure 6-138. Typical Stress Data Obtained from the Field Measurements for Steel Set 244

6.7 DATA APPRAISAL

6.7.1 Introduction

The purpose of this report was collecting and analyzing data for use in the thermal-mechanical analysis of rock and design of the repository. The data originates from many sources, such as laboratory testing, field testing, field observations, and numerical simulation. The analysis and design process involves the use of these data for many different calculations and analyses performed by different data users. Often a single user or product requires the use of a number of rock parameters in a variety of combinations.

A rock parameter summary of data seldom results in defining a singular value that represents a particular parameter. Most frequently, assigning a value for a parameter requires defining a bounded range or distribution that a parameter may use. Under certain circumstances, the use of a particular distribution or a range with upper and lower bounds may result in a design application being acceptable or deficient. By defining a parameter range or distribution that incorporates uncertainty, the user becomes aware of the imprecision inherent in the data. The resulting uncertainty associated with each rock parameter can also be manifested as part of the measure of design reliability or uncertainty associated with derived parameters. The analyst or designer also needs to know how each parameter summary has been determined and how

particular rock conditions (e.g., temperature, saturation, porosity) will affect a parameter range or distribution.

Ultimately, two questions must be answered that are related to the project evaluation of data adequacy: Are the parameter summaries proposed based on solid premises? Are the parameter summaries adequate for each application and product in which they will be used? The evaluation of each of the subsurface geotechnical parameters for their adequacy in license application products involves a number of issues. In this section an attempt is made to discuss approaches for uncertainty as it relates to the geotechnical data, the spatial variation of parameters, and the conditions under which the data can be declared adequate.

6.7.2 Data Representativeness from a Regulatory Perspective

Data appraisal at the current project stage was performed to assess the adequacy of the data to support the license application process. The data were assessed using an engineering approach. The major emphasis was placed on verifying the quality and completeness of the data available, as well as identifying potential gaps in the data that would require immediate, extensive remediation measures, whether in terms of additional laboratory tests or field work. Potential areas of concern are associated with fulfilling the need for data completeness. Other concerns are related to the meaningful interpretation of data and the subsequent use of those data in the design. Future characterization activities will lead to the acquisition of additional geotechnical data and the further development of alternative numerical approaches to enhance the understanding of the rock mass performance. This overall data appraisal is further discussed in terms of license application and post-license application project phases.

The license application project phase includes the current period where evidence contained in license application documents is presented for a review and thorough evaluation by a number of reviewers representing all parties involved in any and all aspects of the future repository design. The site characterization activities contributed to a body of knowledge about mechanical and thermal properties of intact rock and rock mass that are targeted as a host of the future repository. The body of evidence characterizing the nonlithophysal TSw2 units is adequate to support the preliminary design associated with the license application. Work on the development of additional details characterizing behavior and performance of lithophysal zones is continuing, and new approaches designed to better characterize these units are being used successfully.

The post-license application project phase extends in time and includes the repository design, construction and operation until closure. The major source of data complementing the existing rock property database will be obtained from the detailed record keeping required at every stage of repository development and operation. Routine inspections of the existing drifts, both those containing the nuclear waste and those under development, will provide an increasing bulk of evidence associated with the performance of subsurface structures. Performance Confirmation activities and periodical assessments will aid in maintaining the focus on continuing comparisons and the evaluation of the subsurface facility performance. These activities will result in an increasing body of evidence regarding lithostratigraphic rock unit performance, reducing uncertainty in data and increasing confidence in the implemented design.

6.7.2.1 Methodology of Characterizing Uncertainty and Spatial Variation

Uncertainty in technical data parameters arises from measurement error, limited data, spatial variability, or imperfect knowledge. For parameters that are based on data that are measured directly and at the appropriate scale, the uncertainty treatment could include discussions of random and systematic measurement errors, accuracy, precision, statistical significance and related issues. Parameters with extensive data sets will have uncertainty distributions that are largely statistically defined. On the other hand, for cases of limited field or laboratory data sets, the uncertainty distribution will be based more heavily on experience and judgment, commensurate with the extent of knowledge concerning the parameter. Due to limited data, unique geology, and the complexity of rock behavior, the characterization of rock parameter uncertainty normally requires professional judgment to quantify a measure of belief in rock parameter distributions and ranges. Both approaches must complement each other: Statistical approaches apply best to uncertainties in data and degree-of-belief (judgment) to uncertainties in knowledge.

Derived or developed rock parameters use some analytical or interpretive process to arrive at their final determined values. This process may involve conceptual simulations, calculation using other parameters, or scaling to appropriate dimensions. Each of these methods of approaching the problem has an associated signature of uncertainty that needs to be characterized and propagated through the development of the parameter.

Previous to the current effort, and as part of the Total System Performance Assessment, the DOE, and the NRC developed five Total System Performance Assessment and Integration KTI agreements, which in part, related to parameter uncertainty (NRC 2002 [DIRS 159538], Appendix A, pp. A-34 and A-35: TSPAI 3.38, 3.39, 3.40, 3.41, 4.01). These agreements were concerned with the development, implementation, and documentation of written guidance to provide for a systematic approach to developing and documenting simulation parameter uncertainty and related concerns. Subsequently, the following documents have been issued by the DOE and the TSPA organization: *Uncertainty Analyses and Strategy* (Williams 2001 [DIRS 157389]), *Guidelines for Developing and Documenting Alternative Conceptual Models, Model Abstractions, and Parameter Uncertainty in the Total System Performance Assessment for the License Application* (BSC 2002 [DIRS 158794]), *Total System Performance Assessment - License Application Methods and Approach* (BSC 2002 [DIRS 160146]), and *Scientific Processes Guidelines Manual* (BSC 2002 [DIRS 160313], Appendix A).

The referenced reports are relevant yet were not directly concerned with characterizing the uncertainty and variability of acquired geotechnical parameters. As a result, additional guidance will be prepared, based on the previously agreed upon uncertainty terminology and approaches, to describe the uncertainties associated with gathering data from the field and laboratory. In particular, an approach for determining uncertainty will be outlined to balance mathematical probability and statistics with professional judgment. A major objective of developing the new written guidance is to ensure a repeatable and complete yet simplified characterization of the uncertainties in data parameters.

6.7.2.2 Simulation Choices Affecting the Uncertainty of Spatial Variation

Spatial variation of the subsurface rock parameters occurs largely as a result of the natural variation of geology. As such, it is fundamentally random or aleatoric uncertainty since the variability of the parameter population is dependent upon chance occurrences of geologic processes and features such as lithophysae. However, the current knowledge of site-specific geology from limited measurements and from the physical rock behavior in terms of field or laboratory testing might not be sufficient to accurately bracket the aleatoric uncertainty. Accordingly, there is a judgment aspect of the total spatial uncertainty that varies according to the dimensions of the rock unit to be simulated and other available knowledge. Consequently, the current scientific activities of fracture characterization, lithophysae characterization, and laboratory testing will lead to better characterization of the aleatoric uncertainty.

The first level at which spatial variation is addressed is in the choice of rock formation or lithostratigraphic zone or subzone chosen by the designer or analyst for simulation purposes. Every rock unit currently simulated by mechanical and thermal simulator is idealized to be isotropic (i.e., no directional variation of property from a point) and homogeneous (i.e., no spatial variation vertically or horizontally within the rock unit).

For the isotropic and homogeneous rock parameter, aleatoric and epistemic uncertainty is used in developing the probabilistic distribution for the rock parameter. For example, if the rock parameter exhibits known anisotropic behavior or is known to vary horizontally or vertically at some scale by applying a variogram or other approach, then the magnitude of this effect is incorporated into the spatial uncertainty part of the parameter distribution.

The simulator may be able to reduce uncertainties by choosing to simulate a more “refined” geologic zone (e.g., the choice to simulate lithostratigraphic zones or subzones instead of an entire geologic formation) or by excluding an unrepresentative area. Obviously, with such a simulation change, the degree of heterogeneity would be reduced, which should result in a decrease of spatial uncertainty. For example, this is the case when the intensely fractured zone of the ESF is excluded in characterizing fractures of the Tptpmn zone. If and when more “coarse” geologic units are simulated, it is the responsibility of the simulator to aggregate properly the uncertainties involved with combining the lithostratigraphic zones.

6.7.2.3 Geostatistical Simulation of Spatial Variability Using Porosity as a Surrogate

The philosophy and general approach of using porosity as part of a geostatistical method to characterize spatial heterogeneity and uncertainty of other rock parameters is discussed in the *Rock Properties Model Analysis Model Report* (BSC 2002 [DIRS 159530]). Key parts of this report that summarize the approach follow (BSC 2004 [DIRS 170031], Sections 5.1 and 6.3):

Simulation Approach—A fundamental principle involved in the numerical representation of real-world physical processes is that the relevant material properties of the simulated domain must be known at all positions within that domain. However, in contrast to this requirement for an “exhaustive” spatial description, the process of describing or characterizing a site invariably consists of collecting observations of properties or state variables at a limited number of locations, the exact positions of which are frequently determined by less-than-optimal external

factors. This is particularly true for the 3-D characterization of a geologic site, such as Yucca Mountain. Because descriptive characterization is limited both by access (particularly to the subsurface) and by the availability of resources, that description is necessarily incomplete. Therefore, the exhaustive description of a geologic site for purposes of numerical simulation requires the prior basis of some type of conceptual simulation for the site, which is then implemented to assign the necessary properties and other variables at every relevant point in space (BSC 2004 [DIRS 170031], Section 6.3.1).

A more realistic conceptual simulation of rock than the isotropic, homogeneous simulation is one that makes use of the known vertical and lateral heterogeneity within geologic layers. Knowledge of property values at one location imposes limits on the values of those properties likely to exist at "nearby" locations. Therefore, an alternative conceptual simulation of "filling-in" a geologic framework with values randomly assigned from some inferred univariate distribution without regard for other nearby values (spatial correlation) is an unnecessary oversimplification (and potentially an unwarranted distortion) of the real world (BSC 2004 [DIRS 170031], Section 6.3.1.1).

Heterogeneity versus Uncertainty—In contrast to heterogeneity, which is an objective feature of the real world, uncertainty is a knowledge-based concept. Distinguishing properly between uncertainty (as a state of imperfect information resulting from less-than-complete observation and scientific judgment) and spatial heterogeneity (as a state of being, unaffected by the availability or lack of information) becomes critically important in the application of predictive engineering methods to the geologic environment. Incomplete information must be accounted for in predictive simulation, as must the effects of material properties that are different in different locations. A key attribute, therefore, of the rock properties simulation activities, has been the description and quantification of the effects of geologic uncertainty on the physical description of the Yucca Mountain site (BSC 2004 [DIRS 170031], Section 6.3.1.2).

Geostatistical Methods—Geostatistical methods in general are one of a variety of methods for distributing isolated measurements of different attributes in space, and thus for simulation of spatial heterogeneity. A fundamental principle underlying all geostatistical techniques is the quantification and use of some measure of spatial correlation, which may be defined informally as the degree to which samples "close" to one another resemble each other more than do samples "far" away from each other, where "close" and "far" are defined from the data values. These measures of spatial correlation are usually simplified to be statistically homogeneous properties of the rock unit simulated, and they are used in addition to any geologic heterogeneous trends discovered in the measured data. Furthermore, unlike many other methods for predicting the material property attributes of a large volume of material from direct observation of a relatively minuscule fraction of that volume, geostatistical methods offer a quantitative and more-or-less rigorous approach to the issues of knowledge-based uncertainty discussed earlier (BSC 2004 [DIRS 170031], Section 6.3.1.3).

Within the purview of geostatistical methods are two broad classes of algorithms for predicting attributes at unsampled locations constrained by some limited set of actual measurements: estimation and simulation. Geostatistical *estimation* is focused on the prediction of the attribute values most likely to be encountered at a given spatial position and may be thought of as simulation of the expected value of a variable of interest. Geostatistical estimation is most

frequently described using the term, *kriging*, and it is simply a weighted-average *interpolation* method using some *neighborhood* of nearby relevant data. a common thread connecting all estimation methodologies (including nongeostatistical ones) is that they are interpolation techniques directed toward producing a simulation in which the estimated values grade progressively and generally smoothly away from the data locations and away from one another (BSC 2004 [DIRS 170031], Section 6.3.1.3).

The other broad class of geostatistical methods comprises a variety of *simulation* algorithms. In contrast with estimation, geostatistical simulation places principal emphasis on reproducing the input data values and the overall statistical character (including the spatial correlation characteristics) exhibited by the data ensemble, the total collection of input values. Simulations produced by geostatistical simulation typically do not grade smoothly between measured data values, but rather are more highly variable at the same time that they represent the broad heterogeneity structure of the measurements. These techniques are conceptually equivalent to the Monte Carlo simulation process frequently employed in engineering analyses. In common with other Monte Carlo simulation approaches, the emphasis is less on the specific predicted values, which are in effect simply the products of a random number generator with certain "desirable" properties, and much more on evaluation of the space of uncertainty associated with some performance measure computed to represent the behavior of the simulated system (BSC 2004 [DIRS 170031], Section 6.3.1.3).

For the project geostatistical approach, selected major lithostratigraphic horizons are used as the constraining (framework) boundaries for a statistically based description of the measured rock material properties that have been sampled within those boundaries. First, the individual measured values of a material property are combined with the overall statistical character of the complete data set (the data *ensemble*) and with the spatial correlation patterns exhibited by the data to produce replicate "exhaustive" simulations showing the distribution of that material property in space. Each replicate simulation reproduces the measured data at the data locations, and the overall variability of all the values in the simulation reproduces the histogram of the measurements. Additionally, the spatial correlation structure of the simulation, evaluated as a whole, approximates the spatial correlation among the input measurements (BSC 2004 [DIRS 170031], Section 6.3.1.4).

Porosity as a Surrogate—The rock property simulation approach involves the use of porosity as a surrogate for the spatial variability of other, "secondary" material properties that are typically of greater interest in performance simulation than porosity itself, but which are almost universally undersampled at Yucca Mountain. This concept of using the more abundant porosity data as a surrogate for other properties is not a new YMP approach. Some rock parameters that have been proposed for use with the porosity as a surrogate approach include rock mass hydraulic conductivity, Young's modulus, and compressive strength (BSC 2004 [DIRS 170031], Section 5.1).

Using porosity as a surrogate for various other parameters is supported by consideration of the physics involved in the site-specific rock units being simulated. For example, for a given rock type, increasing the volume of pore space must decrease the bulk density of the rock mass. The part of the rock that "isn't there" is available to hold fluids, but it contributes nothing to the total mass contained within a unit volume: the definition of bulk density. Again for a given rock type,

the conduction of heat energy through the material is directly related to the density (or, inversely to the pore space) of the material. All else being equal, a higher porosity–lower density tuff will conduct heat less readily, leading to a lower thermal conductivity value. Note here that it is the total amount of void space in a rock that affects thermal conductivity, not simply the amount of pore space that is conducting water within the unsaturated zone. This fact has important implications in simulation of whole-rock thermal conductivity in the presence of large-diameter (up to 1 m) lithophysal cavities (BSC 2004 [DIRS 170031], Section 5.1).

The concept of porosity as a surrogate is based on empirically observed correlations of porosity with undersampled secondary properties. A consequence of undersampling is that the spatial variability of the undersampled variable cannot be described confidently on a stand-alone basis, much less with the joint spatial continuity patterns of two (or more) variables be reproduced simultaneously. It is important to understand that simulation of the spatial distribution of several material properties without considering the intervariable correlations can lead to highly unrealistic input to physical-process simulation codes, which in turn can lead to highly unreasonable estimates of performance parameters. Simply sampling randomly from separate (univariate) probability density functions may easily produce such unphysical combinations as a low porosity–high thermal conductivity–high hydraulic conductivity tuff. The severity of neglecting cross-variable correlations in simulation spatially variable domains increases as physical-process simulation attempts to capture multiple coupled processes (BSC 2004 [DIRS 170031], Section 5.1).

6.7.3 Data Uncertainty and Adequacy

The extent to which geotechnical parameters, based on measurements from a finite set of samples, can be used to characterize in situ conditions of lithostratigraphic units at Yucca Mountain is affected by uncertainties associated with the available data and in the parameters used to characterize the units. The uncertainty and variability in the data, and therefore, the determination of geotechnical parameters are due, in part, to the natural variability and heterogeneity in subsurface geologic conditions. For example, uncertainty is affected by natural variations in geotechnical parameters within and between the lithostratigraphic units, including the precise nature and extent of the fracture network and presence, size, and extent of lithophysae, as well as other naturally occurring variations in the rock mass. Additional uncertainty can be introduced through the selection of sampling and testing methodologies, time dependencies, and up-scaling effects. Uncertainty in data produces corresponding uncertainty in the description of resulting geotechnical models and processes.

Due to the naturally occurring spatial variation in the thickness and extent of the lithostratigraphic units at Yucca Mountain and the accessibility of units to sampling, the number of samples available to characterize various units can vary significantly. As a result, quantification of uncertainties presents challenges specific to the lithostratigraphic unit and the representative sample population. Therefore, the sample size, as well as natural and introduced uncertainties, contributes to the overall assessment of data and parameter uncertainties derived to characterize each lithostratigraphic unit.

When using geotechnical parameters derived from relatively small sample specimens to describe the strength of the rock mass with associated voids, fractures, and all other natural variabilities,

scaling effects must be considered. Even the relatively populous data set available for lithostratigraphic units of the repository host rock must be treated with caution while this relationship between size and scale is being defined. The presence and size of lithophysal voids, which can exceed sample size within the rock mass, presents a unique challenge when up-scaling parameter assessments derived from the sample scale. Since the effects of these large voids can not be directly assessed due to sample size limitations, computer simulations are used to assess the nature and mechanisms impacting the strength and performance of the rock mass and associated uncertainties. Computer simulation can be used to assess the impact of parameters spanning the range of uncertainty by examining a variety of hypothetical scenarios.

The design of underground excavations may also require consideration of time-dependent effects on the rock mass and ground support materials that result from environmental parameters, e.g., ground saturation, variable temperature, ground chemistry, and seismic ground motion input. The time factor included in an analysis and associated time-dependent properties of rock introduce additional variables that will contribute to the overall uncertainty characterizing the final design product.

The consequence of the representativeness of the data must be judged in the context of the potential contribution from the uncertainties on the intended use in subsurface design products, e.g., tunnels, shafts, or other subsurface openings. In effect, the user of geotechnical data and rock parameters presented in this analysis is advised to exercise caution while using any and all data presented herein. The details pertaining to each data set should be consulted to verify the potential ranges of each parameter considering the number of tests, test attributes and the purpose of the particular calculations or analysis. Throughout this analysis, wherever appropriate, potential types of uncertainties and identification of their sources is provided to benefit subsequent quantification by the users of this data.

6.7.3.1 Engineering Perspective

6.7.3.1.1 General

The long-term site characterization activities designed to provide the evidence needed to assess the Yucca Mountain Site suitability for housing the future nuclear waste repository reached the important milestone. The rock property data gathered in the past are being assessed for their adequacy in the process of applying for the license to design and construct the repository. The data are assessed from the perspective of the underground design engineer, considering rock property data needs within the timeframe encompassing license application and post-license application design stages.

The role of the design engineer for the subsurface facility at Yucca Mountain is to develop a design that is safe to construct and that fulfills its functional requirements over the required time period. The design must encompass three phases associated with the facility development: (1) the construction phase, (2) the repository operations phase until closure of the facility, and (3) the phase extending through the postclosure time period. The result of this report is to provide the designer with rock parameters and sources of information needed to accomplish not only the basic design task but to assist in making a reasonable prediction of the future performance of this underground facility.

In the following parts of this section, data variability and data adequacy are addressed, considering the needs of the design engineer. A discussion is presented that summarizes salient aspects of lithostratigraphic rock unit sampling and testing. Where appropriate, limitations encountered in the data acquisition process are discussed, and methods for the subsequent data enhancement are presented.

6.7.3.1.2 Terminology

Scientific adequacy is related to using the data in the process of developing a sufficiently detailed understanding of natural phenomena, along with satisfactory characterization of the associated behaviors. The data gathering process is conducted utilizing certain rules and procedures that allow for the separation of other factors that may affect the quality, representativeness, and validity of data. Assisting in this process is the availability of standards that prescribe in detail methods of sample and specimen preparation, testing conditions, form of data reporting, and methods of data interpretation.

Adherence to standards provides the basis for communication among those involved in testing similar materials. It sets the basis for comparing results for similar conditions. These tasks of testing can be simplified if the material studied is uniform in its physical properties (e.g., density and mineralogical composition) and testing conditions involve a simple testing procedure (e.g., uniaxial compressive loading condition).

Examples of common questions related to testing are (1) how many specimens must be tested to obtain a representative range of the parameter value; (2) what consequences might be expected if the test conditions are changed or modified; (3) will the test results be different if specimens are tested at dimensions other than those actually tested; and (4) if the testing procedure is not followed in its entirety, are the test results still useable? These, and a range of similar questions are commonly asked because the person examining/auditing the data wants to develop an opinion, not only about the quality of data itself, but also about the many other issues seemingly unrelated to the process of data acquisition.

This interrogative process has a common agenda: The results should allow a person not involved in the original data acquisition and processing to understand how the specimens were acquired; what testing conditions were used; if the data interpretation followed the established guidelines; and, as a consequence, whether the results from test(s) can be used within a range of conditions or bounds replicated in the test. The process also often involves undocumented comparisons, where by using personal experience as a supplement, one makes an attempt to benchmark the data obtained from the current tests against other data obtained elsewhere for a material displaying similar characteristics. The net result is the development of a certain level of confidence needed to apply the data for specific purposes.

The acquired and developed data presented in *Yucca Mountain Site Geotechnical Report* (CRWMS M&O 1997 [DIRS 103564]) and the new data summarized in this report reflect both the enhancement to the previously available data and an evolution of the Yucca Mountain Project understanding of the importance of data in supporting various design and performance confirmation activities.

6.7.3.1.3 Scientific and Engineering Adequacy

Scientific adequacy is related to the scientific task of sufficiently understanding natural phenomena along with satisfactory characterization of the associated behaviors. On the other hand, engineers design and build projects using whatever information is available, whether the data are considered scientifically adequate or not. Thus, engineering adequacy is concerned with gathering the available relevant data and then supplementing it with sufficient knowledge and judgment to safely build the project at hand. Both types of adequacy are intricately tied to uncertainty. Science has been traditionally dominated by statistically defined uncertainties, while engineering has been dominated by degree-of-belief uncertainties that are usually estimated as a first approximation by applying a suitable factor of safety. As a result, statements of adequacy for either scientific or engineering purposes cannot be considered complete until the significant uncertainties are identified and quantified.

As has been discussed earlier in this report, uncertainty treatments for many of the geotechnical parameters have not been finalized. As a result, the following discussion should be understood to be a preliminary approach to defining uncertainty and engineering adequacy. It represents the current best engineering judgment for license application needs.

6.7.3.1.4 Rock Property Data Sampling – A Perspective

Although site characterization activities date back more than two decades, for a number of years it was considered that those activities would be successful if sufficient information were obtained for the mid-tertiary volcanic rocks at the Yucca Mountain site represented by the sequence of major thermal-mechanical units. Rocks of the Paintbrush Group were represented as seven thermal-mechanical units (Ortiz et al. 1985 [DIRS 101280]): UO, TCw, PTn, TSw1, TSw2, TSw3, and CHn (Table 6-2).

The construction of the ESF main loop tunnel and subsequent excavation of the ECRB Cross-Drift provided a direct access to the most important lithostratigraphic rock units at the repository level. The detailed tunnel mapping, field observations and in situ measurements performed in both tunnels during construction provided evidence that the TSw2 unit targeted for locating nuclear waste emplacement drifts in the future repository required more detailed characterization. This new realization required more detailed testing to be performed on four distinct zones within TSw2. Counted from the top, these zones are identified as: Tptpul, Tptpmn, Tptpll, and Tptpln.

6.7.3.1.5 Rock Coring and Limitations of Applicability

A large part of this report reflects the realization that much more detailed data are required in order to simulate and characterize behavior of several lithostratigraphic zones (Tptpul, Tptpmn, Tptpll, and Tptpln) within the proposed repository horizon that were previously treated as mostly one large and thermo-mechanically uniform unit (TSw2 with a small part of TSw1). The latest (2002) rock sampling exploratory activities were directed at obtaining a sufficient number of larger diameter lithophysal rock samples that would be considered more representative of the larger intact rock behavior of lithophysal rock, along with fracture samples of nonlithophysal rock to characterize mechanical fracture properties.

A typical process of rock characterization begins with obtaining a minimal number of rock samples with a sufficient distribution and quantity to allow an engineer to produce a rough picture of the rock behavior and properties. Subsequently, additional sampling and testing, according to engineering judgment, fill in the picture more completely. These specimens, tested within a range of pre-defined conditions, would yield information needed to characterize the simulated lithostratigraphic rock units. The sampling process usually consists of the simple task of selecting portions of diamond-drilled sections of core obtained from the exploratory drillings.

The associated geological core log allows for making this selection within the zone of interest. This process is routinely completed without major problems, provided that core has been obtained from the lithostratigraphic layer of interest. The diameter of a typical core falls within the range of 2 in. to 4 in.

Among the four repository horizon lithostratigraphic zones (Tptpul, Tptpmn, Tptpll, and Tptpln), different structural features characterize the two nonlithophysal and two lithophysal zones. The nonlithophysal rock mass is composed of a relatively strong welded tuff containing sets of discontinuities. The discontinuities are identified within the nonlithophysal zone by mapping, and are characterized by their own set of parameters. It is the abundance and geometry of these discontinuities that significantly influence the overall performance of the nonlithophysal rock zones. In contrast, the behavior of the lithophysal rock zones is most strongly influenced by the presence, shape, dimensions, and distribution of the lithophysal voids existing within the rock mass.

The coring of nonlithophysal rock zones typically resulted in abundant cores of intact rock that were easily tested in the laboratory. On the other hand, coring in lithophysal rock zones was a much more difficult process. The lithophysae encountered during drilling, having dimensions of centimeters or larger, typically caused a total loss of a core when using 5 cm (2 in.) barrels and resulted in essentially no cores containing representative lithophysae. Coring of larger diameter boreholes up to 30 cm (12 in.) has resulted in limited core recovery, including some lithophysae. However, the remaining rock core within the drill barrel was often disturbed and fractured to the extent that only a small number of intact rock cores were obtained for testing.

This core loss within the lithophysal zones represents only one aspect of rock characterization. Another related issue concerns locating the retrieved core sections within the lithostratigraphic rock unit. Initially, the core logging procedure implemented at the time of core retrieval, did not consider lithophysal voids to be important elements of site characterization. As a consequence, a section of the core missing due to the presence of lithophysae was reported as zero recovery in the original core log. It was only realized later that this fact constitutes a valuable piece of information helpful in better characterizing the lithophysal zones of the TSw2.

The common core logging procedure concentrates on characterizing the rock sample retrieved from the borehole. In the context of the void-containing strata, it is the void size and distribution that becomes the major characterizing parameter. A small-diameter rock sample is not capable of containing larger lithophysae and, thus, the recovered intact rock cores do not provide representative information about the lithophysal rock unit as a whole. Consequently, the solid rock material retrieved and tested from the lithophysal zones provides an important but incomplete basis for rock mass characterization. The solid portion of the rock is referred to as

rock matrix, and matrix properties are important in the overall task of characterizing the performance of the void-containing lithostratigraphic rock unit.

To obtain more representative lithophysal rock samples, a large core sampling technique was applied, as mentioned above, in which a number of 30-cm-diameter (12-in.-diameter) boreholes were drilled in the ESF and ECRB tunnels. The results of drilling proved that even 30-cm-diameter boreholes were too small to obtain a representative lithophysae-containing rock volume suitable for test specimen preparation and testing. In particular, the presence of voids within a tested sample made it difficult to conduct a basic uniaxial compressive strength test according to test standards. The nonstandard result was caused by stress redistribution around lithophysal cavities and within the specimen, which produced stress conditions in the rock sample that were not uniaxial, making the test results difficult to interpret. Furthermore, understanding the development of fractures within the void-containing specimen during testing becomes an important issue.

6.7.3.1.6 Reducing Uncertainty and Establishing Adequacy for Mechanical Parameters of Lithophysal Rock

From the foregoing discussion it is apparent that the uniqueness of lithophysal rock poses formidable challenges to obtaining data directly by the process of testing larger rock specimens. Sampling logistics are difficult to manage, and applicable testing standards are inadequate when dealing with lithophysal rock. As a result of this and of having no available laboratory tests of rock containing lithophysae, at the time, the uncertainty associated with mechanical lithophysal rock parameters was high. The project recognized this fact and outlined a general approach in *Resolution Strategy for Geomechanically-Related Repository Design and Thermal-Mechanical Effects (RDTME)* (Board 2003 [DIRS 165036]) to reduce this uncertainty. The approach is summarized in Section 6.4.4.4.2.

On the other hand, field observations provide evidence about rock performance under ambient and elevated temperature conditions. This, coupled with new laboratory testing, field testing, and numerical testing of lithophysal rock has reduced the uncertainty associated with lithophysal rock parameters. Because the assessment of uncertainty is a required part of the assessment of data adequacy, there is a clear need to assess uncertainty based on all the available sources of information. Since the rock parameters are used as inputs to rock fall and ground support design, scoping analyses can be utilized to determine whether the current level of uncertainty of a given rock parameter is adequate.

The approach to reduce uncertainty in order to obtain adequate lithophysal rock data for the license application has been largely successful. The methodology targeted obtaining missing pieces of rock property characterization information prior to developing a more routine method of quantifying data uncertainty or establishing a basis for declaring data as adequate. In defining this methodology, a path was established based on performing a limited number of laboratory tests on lithophysal rock samples. Numerical simulation techniques could then be used to extrapolate the intact rock characteristics into the rock mass characteristics associated with the volume, geometry, and distribution of lithophysae.

Over the last two years, substantial progress was made in the area of testing lithophysal rock in the laboratory and field, as well as in the area of employing numerical techniques to focus investigative efforts on analyzing these rock characteristics. The major steps applied using this approach are summarized as follows:

- Obtain an applicable summary of rock property data based on laboratory tests performed on small (1 to 4 in.) specimens (BSC 2004 [DIRS 172334], Figures 6.3-1, 6.3-3, and 6.3-4).

- Supplement this initial, relatively well-documented rock property database with the results obtained from the laboratory tests on large core specimens containing some lithophysae (BSC 2004 [DIRS 172334], Figures 6.3-14, 6.3-15, 6.3-16, and 6.3-17).

- Utilizing the PFC, develop a numerical simulation of lithophysal rock capable of reproducing general lithophysal rock behavior. This simulation includes testing numerical specimens sufficiently large to simulate behavior of small portions of the rock mass equivalent to large-scale specimens (1 m × 1 m × 1 m).

- Utilizing the laboratory-obtained data, calibrate the PFC numerical simulation so that its performance matches the behavior of intact rock material (i.e., with no lithophysal cavities). As part of the calibration exercise, a series of typical triaxial tests is conducted on the synthetic rock specimens and analyzed.

- Within the volume of large numerical specimens, introduce different lithophysal shapes including circles, triangles and stars, and examine their impact on the process of rock fracturing and overall response to various stress regimes.

- Vary the "synthetic" lithophysal porosity to examine the impact of increased porosity on rock performance (BSC 2004 [DIRS 172334], Figures 6.5-12, 6.5-13, and 6.5-14).

- Obtain field pictures of the real lithophysae (BSC 2004 [DIRS 172334], Figures 6.5-23 and 6.5-24) and stencil their location within bounds of the synthetic, large-scale specimens (1 m × 1 m × 1 m) (BSC 2004 [DIRS 172334], Figure 6.5-25).

- Perform PFC analyses using numerical specimens containing this actual map of lithophysal voids, and compare the results with the performance of previously developed circular-shaped synthetic specimens (BSC 2004 [DIRS 172334], Figures 6.5-28, 6.5-29, and 6.5-30).

- Select and use a different numerical simulation tool (UDEC was adopted) to develop a parallel discontinuous synthetic rock simulation.

- Calibrate the UDEC simulation performance to the same laboratory data used to calibrate the PFC simulation. Again, perform a series of typical triaxial tests on a synthetic solid rock numerical specimen.

- Develop plots showing the relationship between lithophysal rock properties in terms of the numerically derived UCS and Young's modulus (E) as a function of the effective specimen porosity, including uncertainty bounds (Figures 6-101 through 6-104). Also develop a plot showing the relationship between UCS versus E (Figure 6-105).

- Develop a summary of all lithophysal rock data including laboratory, field, and numerical results, and recommend the ranges of UCS and E parameters that can be reasonably assigned for the entire population of data (Tables 6-70 through 6-74). Produce UCS versus porosity, E versus porosity and UCS versus E plots that are based on the data summary, and verify that all sources of data are appropriately illustrated in the plots (Figures 6-97, 6-98, and 6-99).

- Assign intervals corresponding to a convenient number of rock mass categories to use in rockfall analysis and ground support design (Table 6-75).

- Conduct scoping analyses using the referenced rock mass categories for rock fall and ground support design (BSC 2004 [DIRS 166107]).

This approach, summarized in Figure 6-139, has significantly reduced the level of uncertainty surrounding the mechanical rock parameters of lithophysal rock. In general this effort provides a base for the future procedure needed to develop a consistent methodology of assessing and quantifying data uncertainties. It provides a tool that could be used to assign confidence levels for various aspects of underground design.

The robustness of this approach provides a strong foundation for making reasonable assessments of the impact of various factors that may affect the performance of the lithophysae-containing rock. In the context of this analysis, the conventional testing techniques combined with the alternative numerical simulation approaches provide evidence that the existing data are likely adequate for license application. Although it is understood that this combined approach will have to be finished, documented, and supplemented by future testing and field data, the current scoping analyses provide convincing evidence that it is unlikely that future results would invalidate or run contrary to preliminary adequacy conclusions formulated at this stage.

6.7.3.2 Data Adequacy from a Design Perspective

The issue of data adequacy must be addressed considering the end use of data. The use of data invariably leads to the attempt to define in simple terms, whether the data are sufficient to allow engineers to design safe structures with a specified safety range or whether science simulation data inputs result in a calculation of dose that is within required limits.

In engineering design, the typical approach to solving such a problem emphasizes the use of conservative design assumptions. In structural engineering design terms, conservative assumption may indicate that structural members were sized with a capacity exceeding that required by the worst combination of loading conditions possible. The properties of structural members are usually well defined. Changes in loading applied to the structure, such as thermal or seismic loads, can generally be handled in a straightforward manner.

In underground design, this issue is somewhat less clear. The definition of stability may consider different forms, depending whether one attempts to define the overall stability as satisfactory or treat the localized poor roof conditions as unacceptable. Furthermore, the rock material itself poses a different set of challenges. Behavior of rock subjected to the local stress conditions may satisfy performance requirements until heat-induced stresses or seismic event-generated stresses are imposed, creating complex conditions that are difficult to analyze.

6.7.3.2.1 Spatial and Temporal Variability

Section 6.4.2 includes a number of plots that are used to provide a visual, concise summary of all intact rock mechanical tests performed within the outlined bounds of the future repository. It is clear that attempts were made to obtain rock samples over as large an area as possible. The excavation of both the ESF tunnel (TBM excavation began in 1994) and the ECRB Cross-Drift (TBM excavation started in 1997) made access to the rock interior possible. It also allowed for the continuous observation of rock features over relatively long distances of the tunnel, cutting down through the four lithostratigraphic zones in the proximity of the proposed repository emplacement area. Additional exploratory information is also available from boreholes and extensive field mapping efforts undertaken prior to, during, and after tunnel construction. This tunnel mapping is enhanced through peripheral mapping of outcrops and provides a corroborative body of field data. Investigations of the mechanics of volcano eruption provide insight into the sequence of deposition, thickness regularity, uniformity of composition, and areal extent of each stratigraphic layer at the Yucca Mountain site. Results from geological mapping activities indicate that the Yucca Mountain volcanic tuff deposits can be characterized as massive, uniform, flat-bedded deposits. Results of detailed geological mapping serve as corroborative evidence required to provide reasonable evidence that data obtained from the limited number of boreholes is, in fact, representative of properties at a particular horizon and throughout the entire area of interest.

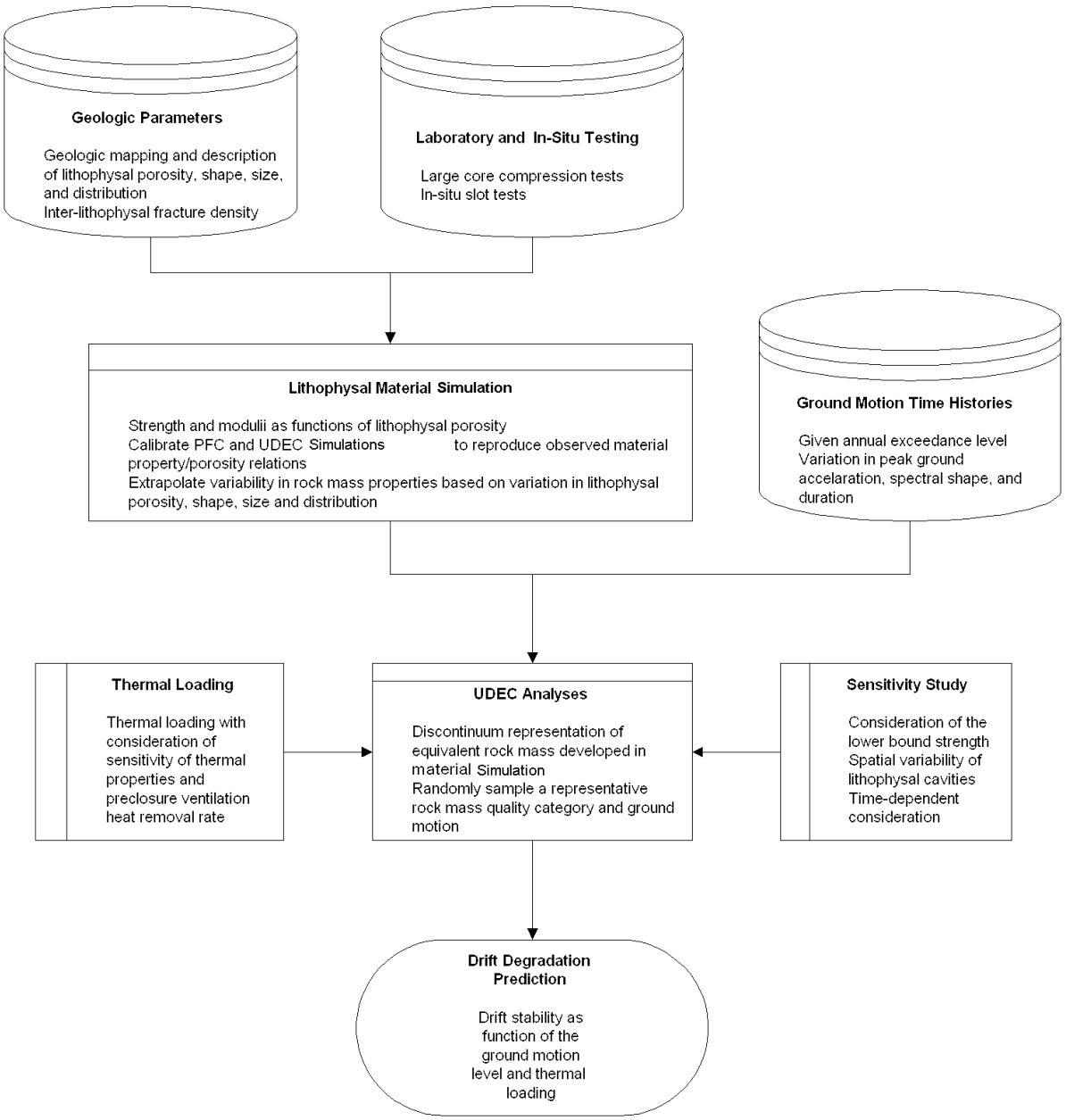

Figure 6-139. Approach of Engineering Analyses for Lithophysal Rock

The data variability must consider the evolution of rock properties with time. Presence of moisture and elevated temperature may not only contribute to deteriorating properties of rock, but it may also diminish the effectiveness of ground control components through potentially accelerated corrosion. The DST provides evidence of tunnel performance under elevated temperature. Both the concrete-lined portion of the tunnel and the portion including only modest ground reinforcement measures appear to perform well under these adverse temperature conditions. While this evidence is limited to several years only, the maximum test temperature maintained in this tunnel was approximately 200ºC (BSC 2003 [DIRS 166296], Section 6.3.1.1 and Figure 6.3.1.1-1), which is much higher than the currently planned emplacement drift temperatures.

6.7.3.2.2 Data Adequacy Evaluation for Groups of Lithostratigraphic Rock Unit Parameters

This section provides an account of groups of lithostratigraphic rock unit parameters from the perspective of their adequacy for the license application.

6.7.3.2.2.1 Adequacy of Physical Properties

Porosity—Partial and preliminary statistical summaries of porosity features from measured ECRB Cross-Drift data are available. These preliminary results are considered adequate for the current drift degradation analysis and preliminary ground support design work. Currently, lithophysal or total rock porosity estimates are considered adequate to use for project work; the impact of the weaker rim and spot material can be simulated because matrix-groundmass will need to be further explored. One condition that has been discovered is that the geophysics-derived porosity estimates for lithophysal rock are not representative of the bulk rock; much of the lithophysal contributions to bulk density were systematically edited out in order to obtain estimates of the rock matrix density or porosity for comparison with laboratory-determined estimates of rock core material.

6.7.3.2.2.2 Adequacy of Thermal Properties

Thermal Conductivity—A large number of laboratory thermal conductivity tests have been conducted on small specimens from lithophysal and nonlithophysal zones. Considering the number of specimens tested, the available data have been deemed sufficient for the intact rock thermal conductivity of these units. On the other hand, the laboratory measurements provide an upper bound of the effective rock mass thermal conductivity, which is the ultimate interest of investigation. It is not appropriate to use the laboratory-measured thermal conductivity in the prediction of repository performance. Therefore, no further laboratory tests on small specimens are necessary.

The field-measured data for rock mass or effective thermal conductivity are limited. Uncertainties associated with field measurements are usually high because of some unknown and uncontrollable field conditions. Assessment of spatial variations and uncertainty of rock mass thermal conductivity using these limited data require the use of the assumptions listed in Section 5.4. To reduce the uncertainties associated with the rock mass thermal conductivity and build a high confidence in the collected data, additional field thermal conductivity measurements are needed, particularly in lithophysal rock. Estimated rock mass thermal conductivity is only for the dry and fully saturated wet conditions, which may not cover all application needs.

The use of analytical simulations is an effective means of supplementing field measurements in the estimation of the rock mass thermal conductivity. With this approach, a comprehensive study on the effect of porosity and other rock properties can be conducted. The analytical simulations are validated as being satisfactory using the existing field data, and additional field tests may not be required. These analytical simulation results, in combination with the results of laboratory and field measurements of thermal conductivity, are adequate for the current drift degradation analysis, as well as preliminary ground support design work.

Heat Capacity—A limited number of laboratory heat capacity measurements have been conducted on small specimens from Tptrn and Tptpmn zones. Since the zones for which specimens were attained are localized in the nonlithophysal zones and the number of specimens tested is limited, uncertainties associated with the laboratory measurements for the repository units are considered high. To reduce the uncertainties associated with the intact rock heat capacity and build higher confidence in the collected data, additional laboratory heat capacity measurements are needed, particularly in lithophysal rock.

The field-measured data are also limited in terms of rock mass heat capacity. Uncertainties associated with field measurements of the rock mass heat capacity are relatively high. These uncertainties are associated with unknown and uncontrollable field variations. In order to reduce the uncertainties associated with the rock mass heat capacity, additional field heat capacity measurements appear to be needed, particularly in lithophysal rock.

The use of analytical simulations provides an effective means of supplementing the laboratory and field measurements of the intact and rock mass thermal conductivity, especially when the measurement data have high uncertainties. The analytical simulations based on the mineral summation method are available to estimate the intact rock (i.e., rock grain) heat capacity. Since the analytical simulations are based on mineralogy of the rock units measured from numerous boreholes, uncertainties associated with the analytical simulations for intact rock heat capacity are considered well defined (i.e., associated uncertainty is low). The rock mass heat capacity of each unit is also estimated from the intact rock heat capacity, using the various analytical simulations. With these approaches, a comprehensive study on the effect of porosity and other rock properties can be conducted. The approach for validating the analytical simulations of intact and rock mass thermal behavior compares analytical results with the existing laboratory and field data. These analytical simulation results are considered adequate for the current drift degradation analysis and preliminary ground support design work.

Coefficient of Thermal Expansion (CTE)—Laboratory thermal expansion measurements have been made on small specimens taken from Tptpmn and Tptpll rock units. Judging by the number of specimens tested, it is considered that the available data are sufficient for the intact rock CTEs of these units. The uncertainties associated with the measurements are considered low. Therefore, no further laboratory tests on small specimens for these rock units are necessary.

The only available field data for the rock mass CTE are from the DST for the Tptpmn zone. Laboratory measurements using large specimens from the Tptpll zone are also limited. As indicated earlier, the rock mass CTEs contain much higher uncertainties than those for the intact rock. To reduce the uncertainties associated with the rock mass CTEs, additional field thermal expansion measurements appear to be needed. The intact rock CTEs provide an upper bound for the rock mass CTEs. Use of a higher CTE will tend to overpredict thermally induced rock deformation and associated thermal stresses. This issue is being more closely examined and verified through ongoing scoping analyses. Overall, using the intact rock values as bounding estimates of Tptpmn rock mass thermal expansion is considered to be conservative and adequate for the current drift degradation analysis and preliminary ground support design work. Whether or not there is a need to conduct field measurements, to develop an analytical approach, or to conduct numerical experiments to determine the rock mass CTEs for the Tptpll zone will be determined using the results from the ongoing scoping analyses.

6.7.3.2.2.3 Adequacy of Mechanical Properties

A large number of laboratory tests designed to determine the mechanical properties of lithostratigraphic rock units have been performed over the years. The majority of those were completed on nonlithophysal zones. The recent interest in lithophysae-containing lithostratigraphic zones of the repository host horizon caused attempts to characterize lithophysal stratigraphic units in more detail. During the rock sampling and testing effort using large 30 cm (12 in.) coring techniques, it became apparent that core yield from the lithophysal zones is relatively low. Furthermore, application of the traditional testing techniques used to determine even a simple uniaxial strength of lithophysal rock has encountered difficulties due to the relatively large size of voids in comparison to the specimen diameter.

Alternative numerical methods have been applied to develop a better understanding of lithophysal rock response to stress. These methods hold the promise of providing the means of more thorough characterization of lithophysal lithostratigraphic rock units where other methods are insufficient.

A comprehensive strategy for developing estimates of rock-mass properties and material models for lithophysal rocks is presented in *Resolution Strategy for Geomechanically Related Repository Design and Thermal-Mechanical Effects (RDTME)* [DIRS 165036]. The strategy does not rely on rock-mass classification methods for empirically deriving the rock-mass mechanical properties for the lithophysal rock. Instead, the approach for determining the effects of lithophysae involves:

1. Conducting a detailed site-specific geologic description of the lithophysal rock mass in the ESF and ECRB Cross-Drift.
2. Testing of large-diameter core in the laboratory and in situ slot testing to establish properties of rock material as functions of specimen size and lithophysal porosity for a limited data set.
3. Calibrating the PFC (i.e., collectively, the PFC2D (V.2.0, STN: 10828-2.0-00 [DIRS 161950]; V.2.0, STN: 10828-2.0-01 [DIRS 169930]), PFC3D (V.2.0, STN: 10830-2.0-00 [DIRS 160612]; V.2.0, STN: 10830-2.0-01 [DIRS 169931]), UDEC (V.3.1 Sub-Release 3.10.109, STN: 10173-3.1-00 [DIRS 161949]) discontinuum numerical models of unfractured lithophysal rock to provide a mechanics-based predictive tool of lithophysal behavior.
4. Utilizing the models to extrapolate rock-mass mechanical behavior to a wide range of rock-mass lithophysal conditions, including the size, shape, porosity, and distribution of lithophysae to establish their impact on variability of the rock-mass properties.
5. Developing bounding rock-mass mechanical properties ranges based on the laboratory testing, numerical extrapolation, and examination of the spatial variability of lithophysal porosity.

The development and technical basis for the above strategy is documented in *Lithophysal Rock Mass Mechanical Properties of the Repository Host Horizon* (BSC 2004) [DIRS 172334] and the *SGPR Rev A* (BSC 2003 [DIRS 166660). The results from these assessments are implemented in design calculations and sensitivity analyses presented in detail in *Drift Degradation Analysis*

(BSC 2004 [DIRS 166107]) and *Evaluation of Emplacement Drift Stability for KTI Resolutions* (BSC 2004 [DIRS 168889]).

The uncertainty in terms of standard deviation and standard error of parameter values varies because nonlithophysal rock layers are characterized more extensively than lithophysal zones. Computer simulation involving sensitivity analyses is designed to examine the interaction of various parameters and provide a more objective means of assessment about what is considered "conservative" and "satisfactory" and under what circumstances. By incorporating the statistical variability of lithostratigraphic rock unit parameters under a range of underground operating conditions, a body of evidence was developed, which lessens dependence on the accuracy of experimentally determined values of parameters. Examining how the performance of underground excavations varies over the range of input rock parameter values and loading conditions leads to a better understanding of the importance of various parameters. This enhanced engineering judgment can then be applied to the issues of the characterization adequacy of parameters and reduction of uncertainties in design.

In general, due to random size, shape, and spatial distribution of lithophysae in the volume of lithophysal rock mass, it is impractical, if not impossible, to obtain representative mechanical properties by carrying exhaustive physical tests on the lithophysal rock. Therefore, the data adequacy is further justified using the evidence from tunnel mapping (see Table 6-66) and field observation of the existing tunnel performance. Documented in this table are the two tunnel sections excavated in Tptpll totaling 1105 m. The section excavated in the ESF is equal to 220 m, and the section excavated in the ECRB Cross-Drift is equal to 885 m. For both rated tunnel sections the GSI determined using the RMR indicate the rock mass quality in the range of fair to good condition. Furthermore, these tunnel sections although supported with relatively light ground support system, do not display any observable deterioration in the last 10 years approximately. This observed opening stability provides evidence that the actual rock mass strength is at least equal to and likely greater than the rock mass strength calculated.

It is recognized that the current type of analyses are based on the base case approach, whereby the rock response to various loads is examined without considering the benefits of ground control measures and maintenance. These two design elements are within the realm of engineering domain and must be considered, especially for the preclosure period of repository operation.

6.7.3.2.2.4 Adequacy of Mechanical Fracture Properties

The performance of nonlithophysal zones is related to the presence of joints within the rock mass. To date, testing activities leading to a better characterization of joints have been performed on a very limited scale. The level of uncertainty in the area of defining joint parameters is relatively high. The issue of joint characterization in the context of currently increasing interest in lithophysal zones is somewhat more complex.

While the characterization of joints occurring in nonlithophysal strata is a relatively straightforward task, characterizing a smaller and more intricate jointing pattern that contributes to the behavior of lithophysal rock units requires a new and non-standard approach. Extensive numerical analyses of drift degradation patterns related to the impact of jointing on drift stability (BSC 2004 [DIRS 166107]) have been performed over the past several years. The results indicate that, even under the most severe loading combinations, the drifts remain stable with relatively few blocks separated from the otherwise stable rock.

The preliminary statistical summaries of joint sets from measured ESF and ECRB Cross-Drift data are available. These preliminary results are adequate for the current drift degradation analysis and preliminary ground support design work. Geostatistical analysis of the fractures has been carried out as a part of the FRACMAN simulation of fractures. The approach for integrating FRACMAN and other analytical codes into engineering analyses of the nonlithophysal rock is illustrated in Figure 6-140.

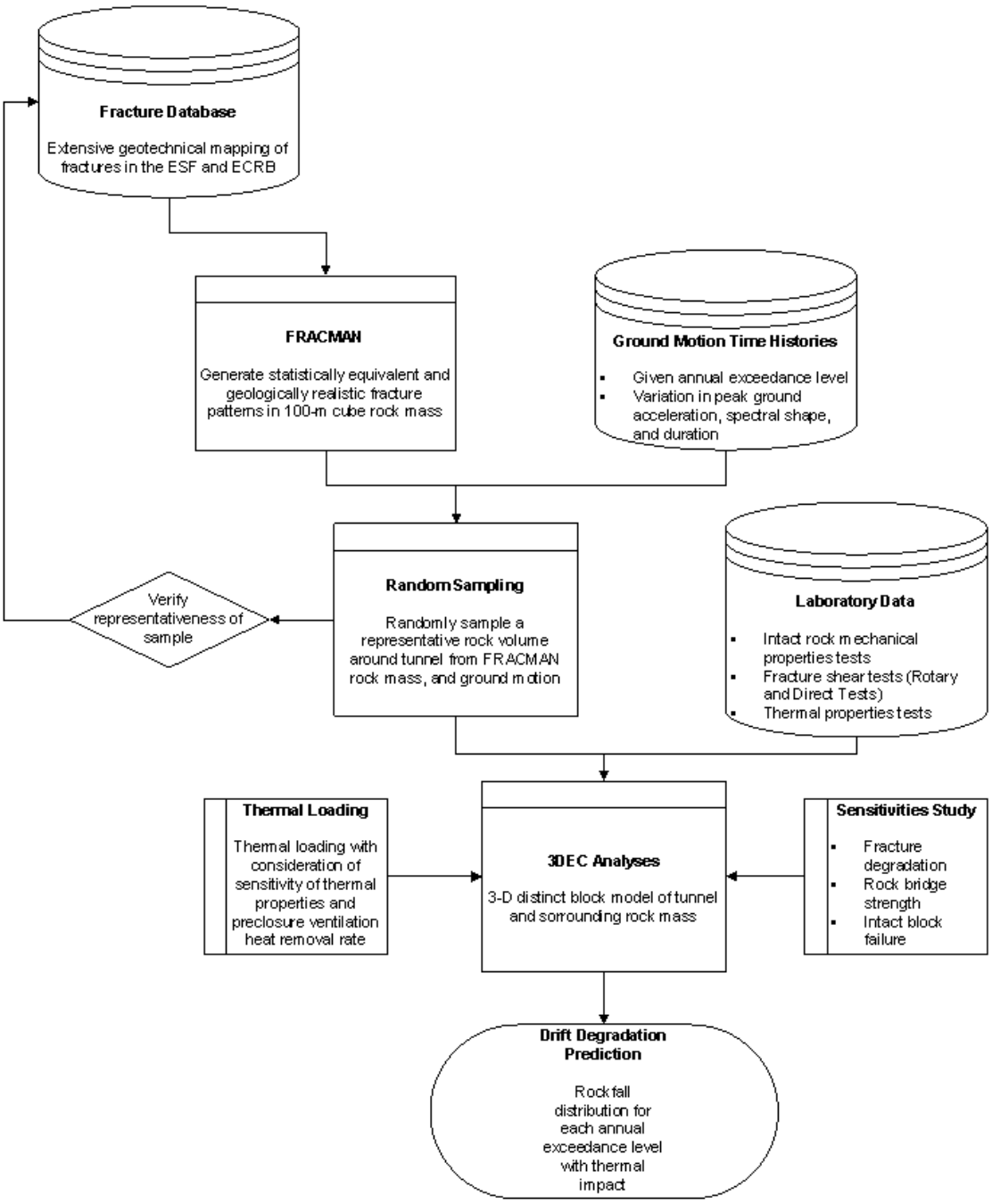

Figure 6-140. Approaches of Engineering Analyses for Nonlithophysal Rock

6.7.4 Further Data Enhancements

As the site activities progress, the amount of supplementary data will increase as well. This process will continue during the entire operational period of the repository. The additional sources of data and confidence building activities follow:

- As new tunnel sections and niches are constructed in the future, additional data will be collected and analyzed in comparison to the existing understanding.

- In the context of lithostratigraphic rock unit variability, the tunnel excavation itself becomes the best possible probe because the areas of extrapolated rock parameters are revealed, and the tunnel diameter is large in comparison to void dimensions. The tunnel mapping process provides a detailed observation of the features of interest in the rock mass.

- The tunnel excavation provides the direct evidence regarding the feasibility of tunnel construction.

- The overall tunnel stability with relatively minor ground control or roof support measures provides reassuring evidence that maintaining the tunnel in a stable and functional state over extended time periods should be achievable.

- Numerical simulation involving bounding analyses provides an assessment of extreme cases related to the rock parameters and data quality. Results of these analyses will assist designers in evaluating "what if" scenarios and the consequences of adopting less or more conservative rock parameter data under a particular set of circumstances.

7. CONCLUSIONS

Currently, the YMP is focused on finalizing the license application and continuing to work toward accomplishing design, construction, and operations goals. Geotechnical data plays a key role in design and the license application.

The SGPR REV 00A (BSC 2003 [DIRS 166660]) focused on the repository host horizon and presents the results of (1) laboratory and field tests, (2) empirical determination and approximation of mechanical properties of the rock mass, and (3) calibration and justification of numerical simulation approaches used over the course of the Yucca Mountain Site Characterization Program.

The overall intent of this SGPR REV 00 is to provide a single source document for all geotechnical rock parameters to be used in design. It takes the initial simple data compilation a step further by providing the designer not only intact rock behavior and parameter-related data but rock mass properties as well. Collectively these components serve to form the basis for a better understanding of rock properties, and consequently, facilitate the correct use of these properties in various areas of design and analysis.

Analyses and discussions in this document are presented in sufficient detail to allow the design engineer to use the data with confidence in the design of subsurface structures. In contrast to man-made materials such as concrete and steel commonly used in civil construction projects, rock at the YMP site presents substantial challenges in predicting its performance under uncertain loading conditions, complex material behaviors, and complicated rock fracture and porosity feature geometries. Successful design of underground structures requires appropriate and satisfactory conceptual simulations, sufficient understanding of rock behavior, and adequate characterization of the associated mechanical and thermal simulation parameters. In particular, limited data, uncertainties associated with in situ loading conditions, conceptual simulation, rock behavior, and the process of determining site-specific rock parameters are the most challenging issues. These issues were addressed by bounding values of rock mass parameters considering the data scatter, numerical simulations of large size specimens with properties representing expected range and examining the impact of specimen size. In addition, the field mapping data and an on-going field monitoring, in combination with closed form solution, are used to provide assessment and verification of the range of rock mass parameters values determined in this analysis.

Furthermore, emplacement drifts as part of the upper natural barrier are classified as ITS and important to waste isolation. Non-emplacement openings such as the north portal and north ramp, the access main, and turnouts, that will be used as routes for the subsurface waste transport and emplacement vehicle, are also classified as ITS. Design parameters such as rock properties and drift layout dimensions are used as input for predicting rockfalls in these ITS underground openings. Predicted rockfalls have been analyzed and determined not capable of breaching a waste package upon impact. A thorough understanding of thermo-mechanical properties and behaviors of the rock mass surrounding these openings, essential to rockfall analysis, is presented in this report. In addition, data results presented in this report serve as necessary baseline information for postclosure performance assessment.

7.1 GENERAL

This section includes a brief description of how SGPR REV 00, as a deliverable to DOE, meets acceptance criteria outlined as part of the work scope and a roadmap for addressing and meeting the YMRP (NRC 2003 [DIRS 163274]) expectations as mentioned in the TWP (BSC 2006 [DIRS 178063]) and detailed in Section 4.3.3.2 of SGPR REV 00. A status summary of Geotechnical Data Issue Resolutions is provided with the reconciliation of future work scope as outlined in the SGPR REV 00A (BSC 2003 [DIRS 166660]). A summary of Geotechnical Parameters for license application is provided in Section 7.2.2 of SGPR REV 00. Section 7.3 in SGPR REV 00 discusses general suggestions and recommendations. Section 7.4 in SGPR REV 00 outlines the planned future work on the SGPR. Section 7.5 in SGPR REV 00 presents geotechnical data recommendations and planned future work and discussed TDMS data issues, data uncertainty, time-dependent behavior of rock and recommended future improvements in computer simulations of rock behavior by using the recent developments in computer technology and software.

7.1.1 A Roadmap towards Meeting the Deliverable's Acceptance Criteria

As a deliverable to DOE, this SGPR REV 00 has covered the specific items to meet the acceptance criteria outline in the TWP prepared in accordance with LP-2.29Q-BSC. Table 7.1 provides a roadmap on where and how these acceptance criteria are addressed.

7.1.2 A Roadmap Addressing YMRP Expectations on Geotechnical Data

Section 4.3.3.2 of SGPR REV 00 lists a number of relevant YMRP Review Methods and Acceptance Criteria (NRC 2003 [DIRS 163274]) to be met in support of the development of the Safety Analysis Report for license application in the areas of rock mass characterization, site-specific geotechnical data, repository drift and shaft stability, ground support design, and rockfall prediction. Table 7-2 provides a road map on how and where these YMRP aspects are addressed in SGPR REV 00.

Table 7-1. Meeting the Deliverable's Acceptance Criteria

Acceptance Criteria as Defined per Deliverable Definition Sheet	SGPR	
	Section No.	Remark
Provide an executive summary of the thermal-mechanical properties (based on measured and derived data) of both the intact rock and rock mass for the repository footprint. The data set will serve as a unified data source for subsurface design	Executive Summary	The Executive Summary provides a summary of the thermal-mechanical properties (based on measured and derived data) of both the intact rock and rock mass for the repository footprint. The data set serves as a unified data source for subsurface design
Provide technical information to respond to the Nuclear Regulatory Commission (NRC)'s comments related to closure of technical agreements 3.04, 3.05, and 3.07 on RDTME KTIs (Note: specific follow-up actions stated in a letter from NRC to DOE, dated January 11, 2005. The letter is entitled "Pre-Licensing Evaluation of Agreements in 'Technical Basis Document Number 4, Mechanical Degradation and Seismic Effects' and Three Other Associated Agreements" (Kokajko 2005 [DIRS 176613]))	6.1, 6.3.4, 6.4.2, 6.4.4.3, 6.4.4.4.2, 6.6, 6.7, and 7	Noted sections provide technical information to respond to the Nuclear Regulatory Commission (NRC)'s comments related to closure of technical agreements 3.04, 3.05, and 3.07 on RDTME KTIs (Note: specific follow-up actions stated in a letter from NRC to DOE, dated January 11, 2005. The letter is entitled "Pre-Licensing Evaluation of Agreements in 'Technical Basis Document Number 4, Mechanical Degradation and Seismic Effects' and Three Other Associated Agreements" (Kokajko 2005 [DIRS 176613]))
Resolve valid geotechnical data issues and deficiencies identified in 1) Section 11.2 of the *Subsurface Geotechnical Parameters Report*, Revision 00A (BSC 2003 [DIRS 166660]), and 2) documented as CRs (particularly CR 6288)	7.3	Section 7.3 provides the basis for the resolution of valid geotechnical data issues and deficiencies identified in 1) Section 11.2 of the *Subsurface Geotechnical Parameters Report*, Revision 00A (BSC 2003 [DIRS 166660]), and 2) documented as condition reports (particularly, Condition Report (CR) 6288)
Support issuing new Data Tracking Numbers (DTNs) needed to streamline a complex system of existing geotechnical data sources, for examples, some existing DTNs are inconsistent, overlapping and lacking correlation among data entries	6.4, Attachments	Section 6.4 and associated attachments discuss the issuance of new Data Tracking Numbers (DTNs) needed to streamline a complex system of existing geotechnical data sources, for examples, some existing DTNs are inconsistent, overlapping and lacking correlation among data entries

Table 7-2. Assessment of Relevant YMRP Review Methods and Acceptance Criteria

YMRP			SGPR	
Section No.	**Review Method No.**	**Acceptance Criteria No.**	**Section No.**	**Remark**
1.5.2	2	NA	6.1	A focused description of geology, geologic features, and principal rock units is provided.
1.5.3	NA	1 and 2		
2.1.1.1.2	5	NA	6.1, 6.2 and 6.3	Topical discussions are provided regarding site geology, in situ and laboratory tests, and groundwater conditions.
2.1.1.1.3	NA	5 and 8		
2.1.1.5.1.2	2	NA	6.4	Site-specific geotechnical data are presented and discussed.
2.1.1.7.2.3.II	5	NA	6.4, 6.5, and 6.7	Topical evaluations and discussions are provided regarding site-specific mechanical properties, thermal properties, and their spatial and temporal variations.
2.1.1.7.3.3.II	NA	1, 4 and 5		
2.2.1.3.1.1	Areas of Review		6.7 and 7	Focused discussions on data availability, adequacy, and uncertainty are presented.
2.2.1.3.1.2	2 and 3	NA		
2.2.1.3.2.1	Areas of Review			
2.2.1.3.2.2	2 and 3	NA		
2.2.1.3.2.3	NA	2 and 3		
2.4.1	Areas of Review		6.2.6 and 7	Performance confirmation aspects on geotechnical data and design parameters are presented.
2.4.2	1	2		

NA = not applicable.

7.1.3 Geotechnical Data Issue Resolution Status

7.1.3.1 General

During the preparation of the SGPR REV 00A and during the subsequent revision of this document, a number of data-related issues and concerns and numerous suggestions for data enhancement in terms of data transparency, adequacy and traceability were identified. Proposed data enhancement products and tasks identified during the preparation of the SGPR REV 00A were summarized in SGPR REV 00A (BSC 2003 [DIRS 166660], Tables 11-1 and 11-2). Subsequently, additional data-related concerns were identified through the Employee Concerns Program (ECP). To facilitate further discussion, all issues and concerns are treated as issues. In total, 63 issues (issues and concerns) have been identified for further evaluation (Fray 2005 [DIRS 176612]).

Issues identified encompass a range of topics related directly and indirectly to geotechnical data. Issues requiring timely attention are addressed in this report. Others have been deferred pending the decision of management, considering present and future Project priorities. Geotechnical data typically involves interaction between professionals representing several disciplines, e.g., geologists, laboratory testing specialists, designers of underground structures, who provide their professional services and opinions in their particular area of expertise. Addressing these issues required a forum of professionals representing not only technical expertise, but management and various Project organizations as well. In general, it is also worth noting that the perceived needs for a specific data or analysis are often subjective and require frequent re-evaluation, justification and planning.

7.1.3.2 Process of Issue Resolution

The process of issue resolution focused on systematically documenting geotechnical data issues, their evaluation and resolution. The process was initiated by assembling the issues on a spreadsheet, issue by issue, and providing a complete history for each issue including its status. The "issue spreadsheet" contained the following columns:

1) Item/issue assignment

2) Item/issue origin

3) Problem description as stated by the originator,

4) Problem evaluation and identification of the other related issues

5) Recommended actions and paths forward, and

6) Issue Status as decided by consensus of all parties involved.

For planning and logistics purposes, each geotechnical data issue was assigned to one of the four categories:

1) Geotechnical data-related Condition Reports (CRs).

2) Subsurface Engineering's Geotechnical Group data activities for enhancing transparency, traceability and qualification, addressing data uncertainty, and updating reports.

3) Project and programmatic issues, relating to YMP management, culture and planning, which were identified during the course of performing geotechnical data activities.

4) No action items, consisting of those items already addressed adequately and those that do not need to be addressed because of their lack of relevancy in terms of resolving the geotechnical data issues already identified in other categories.

The chronological order, in which each issue was identified, is described in *Geotechnical Data Issues and Concerns – An Overview* by Fei Duan (Fray 2005 [DIRS 176612]).

The process of issue resolution included all parties involved in data preparation, the end users of data, as well as representatives of YMP management, the DOE, the Employee Concerns Program, and Information Technology (IT) specialists. The process has evolved through several stages including issue identification, assessment and resolution. In total there were five meetings that took place from March 3 to December 8, 2005, during which issues were defined and with the exception of those listed below, each issue was thoroughly evaluated and resolved.

Initial meetings, which took place on March 3 and March 10, 2005, defined an initial set of 33 issues. A set of 25 items was assembled from work performed while preparing the SGPR REV 00. In addition, 5 items were defined in SGPR REV 00A (BSC 2003 [DIRS 166660], Tables 11-1 and 11-2). In October 2005 one additional CR, CR 6623 identified a typographical error in the geotechnical database. In total, 64 issues were identified and subjected to the process of evaluation and resolution.

During three meetings held on (1) June 21, 2005 (Rusinko 2005 [DIRS 176610]), (2) September 15, 2005 (Fray 2005 [DIRS 176612]), and (3) December 8, 2005, (Johnson 2006 [DIRS 178329]) groups of related issues were evaluated and resolved. The final account of issues and their status is provided in Johnson 2006 ([DIRS 178329], enclosure).

7.1.3.3 Scope of Issue Resolution

Issues identified while working with the data, in large part reflect essential designer needs for basic physical and strength characteristics of the rock strata. Science attention is focused on other data, e.g., those required to explain interaction of water at elevated temperature and chemistry of rock and various materials, components of engineering barriers. Here, no attempt was made to extend data requirements beyond those deemed necessary for the subsurface design and design support for License Application.

It should be noted that among issues identified, none was classified as critical to the licensing process. The majority of issues, especially those in the CR category have been resolved and closed. CR 6623 and CR 6288, related to geotechnical data integrity and transparency, are discussed below in greater detail. A number of issues are either in progress or deferred until a later date. Among them, six of these issues, related directly to the geotechnical data, are also discussed below in this section.

7.1.4 A Summary of Geotechnical Data Issue Resolution Status

7.1.4.1 Resolution of CRs

A group of four CRs (5219, 5281, 5282, and 6288) was submitted to assure the data integrity. CR 5219 pertained to the problem of numerical TDMS data occurring in worksheet files as characters, rather than numerical values. This issue, which affected data in many project products was resolved on the project level. The project issued a Lesson Learned OCRWM-LL-2005-070 on 5/18/05. In effect, Excel spreadsheets in TDMS were required to be checked. CRs 5281 and 5282 were related to the verification of the origin of samples obtained from the strata outcrops. CR 5281 was closed based on the verification of correct sample block locations. CR 5282 addressed the discrepancy between geologic mapping and GFM-defined units related to mapping performed at Busted Butte located several miles from the future repository. Here the discrepancy was found to be of no consequence to the underground design and the issue was closed. In addition, CR 6623, pertaining to a typographic error identified in the rock property data, was initiated on 10/18/2005.

Details of CR 6623 and CR 6288 resolution and a summary of the status of issues related to geotechnical data that were categorized as "in progress" and scope of work defined for this SGPR REV 00 are discussed below.

Resolution of CR 6623—Correct the Modulus Value in TDMS

CR 6623 was resolved by correcting the typographic error that expressed Young's modulus as 23 MPa, rather than 123 MPA. The action included the initiation of the required impact review action notice (IRAN), correction of the data, submittal of the data to TDMS, processing the data, and submitting the record package to supplement the source document. The error was corrected and the CR was closed on 11/28/2005. The details associated with this CR resolution are documented in Corrective Action Program records.

Resolution of CR 6288—Verification of TDMS Data

CR 6288 identified the need to check and verify all TDMS entries pertaining to geotechnical data. Resolution of this issue was considered essential to assuring the integrity and transparency of geotechnical data included in this SGPR REV 00. The TDMS is designed as a storage of data and data-related documentation. The system, does not provide a means to verify if a particular data search yields the complete list of data entries being investigated. In effect, to do a comprehensive data compilation and verification of data completeness for evaluation and analysis with the TDMS is very difficult and time-consuming.

The solution to this TDMS problem was resolved by carrying out two major tasks. The first task determined if all relevant geotechnical data residing in the TDMS were properly identified and included in this SGPR REV 00. The second task performed an independent check of the data used in current analysis, identified errors, and provided an assessment of the number and the type errors encountered.

The first task of DTNs identification was designed as a five-stage process. During stage 1 a large spreadsheet developed by the BSC Geotechnical Group containing all available data was assembled and broken down into DTNs containing the source data files. This data was already manually checked to assure that all items were traceable to the source data. Stage 2 included six steps that resulted in filtering the relevant 60 DTNs from the total number of 11050 DTNs (as of March 7, 2006) listed in TDMS. During stage 3 DTNs identified through the independent data search were compared with DTNs used by the Geotechnical Group to assemble the master spreadsheet containing all data. Stage 4 contains a breakdown of DTNs resulting from a new TDMS search using a different set of keywords than those applied in stage 2. Although this search yielded some 656 DTNs, checking revealed that none of them contained new geotechnical data.

During stage 5, a master list of DTNs resulting from an independent database search yielded one additional DTN containing new data submitted to TDMS after the initial Master List was prepared.

The second major task included the development and application of a methodology for error identification and evaluation. The approach was based on applying a method commonly accepted in industry practice as a means of determining the size of the test data sample. In effect, among 41,781 pieces of geotechnical data record gathered in the master tables, a total of 10,328 pieces were considered to be affecting critical data. By using this method, a sampling size of 315 data records was randomly selected for an accuracy recheck.

The recheck found four (4) data records in error. Considering the acceptance criteria established in the method used, for the given sampling size and specified quality level, the critical affecting data set was found acceptable. The CR 6288 action plan called for a systematic recheck of data entries. The recheck carried out met the criteria established and described in detail in the CR 6288 resolution. As a result, CR 6288 was considered as resolved and was closed on 8/18/2006.

7.1.4.2 Status of Geotechnical Data Issues

The Geotechnical Data Issues Meeting held on December 8, 2005 resulted in closing of all but 6 geotechnical data-related issues classified as “in progress.” Only issues pertaining to the scope of work addressed by this SGPR REV 00 are included in this Section and are listed in Table 7-3. Following is an account of active issues, while more details can be found in Johnson (2006 [DIRS 178329], Meeting Minutes). The comments presented below reflect the designer perspective on the information needs in the context of subsurface design and the support of design for license application.

Table 7-3 In Progress Items Associated with the Scope of Work for SGPR REV 00

Problem Description	Problem Evaluation	SGPR Section Addressing this Issue
1) G-1. Lack of sufficient uncertainty guidance for developing basic site-specific data.	G-1. Statistical procedures and evaluation of data uncertainty have varied on the project and in the industry (e.g., range, standard deviation, histograms, distribution tests, standard error, confidence limits, adequate number of tests, coefficient of variation, reliability, etc.).	Data uncertainty should be tied to the problem or application at hand. This task is beyond the scope of work for this SGPR REV 00. See also Section 7.2.1.
2) G-3. Should a significant effort be extended to attempt to reconcile differences in lithophysal porosity values obtained from boreholes (i.e., geophysical and video logs) and tunnel measurements?	G-3. The bounding analyses that have been performed for design and performance assessment assume a *very large* range of material properties covering entire range of the measured data.	In general, for design purposes the detailed knowledge of porosity distribution is not required. Porosity is discussed in Section 6.4.1.2.
3) G-6. Do we have plans to update any of our products based on additional porosity data?	G-6. Porosity values used in current TSPA analyses bound the measured values. It is impractical and unnecessary to know porosity at a specific location with greater accuracy.	Porosity data characterizing mainly RHH units are presented in Section 6.4.1.2.
4) G-8. How representative are all our estimates of mechanical and thermal rock parameters to those of the actual repository block?	G-8. The issue here is how effectively we deal with spatial variability in data. The data we have now are considered to be adequate for us to move the design forward.	The issue of data representativeness is discussed throughout this Report and in particular in Section 6.4.4.6.1.1 discussion on representativeness of specimens tested, Section 6.7.2 data representativeness from the regulatory perspective.
5) G-19. Need to enhance defensibility (transparency and traceability) on both lithophysal and nonlithophysal rock properties	G-19. Problem confirmed.	Development of rock mass parameters for both lithophysal and nonlithophysal units is presented in Section 6.4.4. Tables 6-76 and 6-77 contain a list of both lithophysal rock and nonlithophysal rock mass parameters.
6) G-23. Correction of source Data and TDMS Problems	G-23. ATDT is a document management system and not a database system. It cannot be queried consistently or reliably, nor will it function as a database for the large amount of new geotechnical data to be collected during construction and operation. Existing problems include difficult data traceability, inconsistent terminology, duplication of data, and non-standard data reporting.	See earlier discussion in Section 7.1.4 for details associated with the resolution of CR 6288. Work on searchable database has been initiated and examples of potential implementation prepared.

Source: Johnson 2006 [DIRS 178329].

NOTE: The Item number shown in the Problem Description column indicates item number provided in the source document.

7.2 DATA SUMMARY AND STATUS

7.2.1 Accomplishment of the SGPR Work Scope

The SGPR REV 00 has accomplished the central task of updating and improving the subsurface geotechnical design parameters to better support the license application. Part of the work scope for the SGPR REV 00 addressed and refocused the remaining subtasks as discussed, recommended, and detailed in the SGPR REV 00A (BSC 2003 [DIRS 166660], Section 11.2). This section provides a brief summary of status on how these remaining subtasks are being carried out. Provided in Table 7-4 is a list of items originating from the *Subsurface Geotechnical Parameters Report*, Revision 00A.

Table 7-4. A Summary of Status of SGPR Work Scope Recommended in SGPR REV 00A

Primary Tasks Recommended	SGPR Section	Remark
1. Collect all relevant existing subsurface geotechnical data from the TDMS needed to summarize the identified rock parameters. Status: Collection of data through March 2006 is completed. All relevant data tracking numbers were examined for consistency of information and for accuracy. Whenever inconsistencies were found, condition reports were submitted to the Corrective Action Program, and corresponding corrections were made to data entries under those DTNs. Systematic rechecks and representative sampling tests were performed to verify data accuracy and information correctness. Additional corroborative data generated outside of the Project were reviewed and are discussed in Section 6.4.2.5.	Attachment A. Also see CR 6288 closure for further information.	Task completed
2. Perform evaluation of the TDMS data according to significant rock material conditions (e.g., porosity, temperature, saturated or dry, fracture set) and method of testing Status: Data obtained from TDMS sources, representing different testing methods, test specimen dimensions, and rock material conditions were extracted, grouped according to the testing procedure and analyzed in a consistent manner	Attachment A. Also see CR 6288 closure for further information.	Task completed
3. Perform calculations and analyses of the TDMS acquired data to determine the required developed rock parameters, using Yucca Mountain Project–approved software and procedures. Status: Derived data calculations and analyses are completed. The SGPR REV 00 addresses the topic in detail. In Addition, one individual calculation was specifically done to determine the mechanical properties for the lithophysal rock mass.	6.4.4	Task completed
4. Perform the appropriate statistical data analyses of the acquired and developed parameter database. Status: The SGPR REV 00 includes statistical summaries for all parameters, when sufficient data are available.	6.4.2	Task completed
5. Provide comprehensive reference tables of intact rock mechanical parameters by combining all the qualified and analyzed test data. Status: A master table in Microsoft Excel format is provided. The table contains qualified data only.	Attachment A	Task completed
6. Describe and demonstrate the range of applicability of preliminary, alternative numerical modeling techniques, which when used in combination	6.4.4	Subtask 6a was completed by producing a calculation used as input by this SGPR REV 00.

Table 7-4. A Status of SGPR Work Scope Recommended in SGPR Rev. 00A (Continued)

Primary Tasks Recommended	SGPR Section	Remark
with limited data, enhance engineers' understanding of rock behavior, processes, and descriptions. **6a**. Modeling of Lithophysal Rock Mechanical Behavior Using PFC and UDEC **6b**. Modeling of Time Degradation of Rock Properties Using PFC		Subtask 6b belongs to Drift Degradation Analysis work scope that remains in SNL domain.
7. Develop a statistical and judgment-based approach for assessment of data uncertainty, variability, and representativeness that will be used to produce recommended statistical values, ranges, and distributions for subsurface rock parameters. Create Parameter Summary Sheets and DTNs for all parameters. **7a**. *Uncertainty Analysis Guide* **7b**. Geostatistical simulation of the spatial variation of fracture geometry using FracMAN **7c**. Geostatistical simulation of the spatial variation of lithophysae **7d**. Assign Uncertainty information to all parameters Status: This task was closely evaluated with the recognition that there are a large number of data users that can approach data assessment and data application in a quite diverse way. It is a project level task and was considered to be beyond the planned scope of work	N/A	All subtasks identified here are either to enhance general parameter acceptance or to minimize data uncertainty. They are evaluated to be project considerations, and were not planned to be part of this SGPR, REV 00, work scope.
8. Provide a definition and assessment of data adequacy for all license application products using subsurface geotechnical parameters.	N/A	Task deleted. Data adequacy depends on the data application and is addressed in the volume of the report on the case-by-case basis..
9. Propose additional work needed for LA submittal and any remaining issues needed to close KTI RDTME 3.04	N/A	This primary task was identified in preparation for requests for additional information from NRC towards closing RDTME KTI 3.04. These subtasks are either to help determine site-specific rock properties and their variations, or to enhance general parameter acceptance, or to minimize data uncertainty.
9a. Technical Review of all relevant TDMS: • physical and mechanical data TDMS summary of above data	Appendices A and B	Data reviewed and included in this SGPR Rev 00.

Table 7-4. A Status of SGPR Work Scope Recommended in SGPR Rev. 00A (Continued)

Primary Tasks Recommended	SGPR Section	Remark
9b. Place technically reviewed data in project GIS relational database	N/A	Demonstration Geotechnical Parameters Database developed and recommended for inclusion in the forthcoming annual planned activity for completion prior to LA application
9c. Do Calculation/Analysis of October 2002 Barton Report	N/A	Task not required for LA – will be addressed in detailed design.
9d. Produce Rock Mass Characterization of Lithophysal Rock Using Empirical Methods	Section 6.4.4.4.2	Task Completed.
9e. Reanalysis of geophysical- derived density and porosity data to account properly for lithophysae	N/A	Task not required for LA – will be addressed in detailed design.
9f. Map lithophysae in a number of additional boreholes and correlate data with geophysical-derived data	N/A	Task not required for LA – will be addressed in detailed design.
9g. Conduct more triaxial tests on nonlithophysal rock	N/A	Task not required for LA – will be addressed in detailed design.
9h. Conduct more UCS tests on large sample-size lithophysal rock and properly quantified lithophysal porosity before each test	N/A	Task not required for LA – will be addressed in detailed design.
9i. Direct shear tests (peak, residual, normal stiffness) on rock fractures by joint set	N/A	Task not required for LA – will be addressed in detailed design.
9j. Plate-loading test analysis and report	N/A	Task not required for LA – will be addressed in detailed design.
9k. Slot test analysis and report for the 3 slot tests	N/A	Task not required for LA – will be addressed in detailed design.
9l. Additional large-scale in situ field testing	N/A	Task not required for LA – will be addressed in detailed design.
9m. Large-scale in situ fracture roughness measurements	N/A	Task not required for LA – will be addressed in detailed design.
9n. Index testing on spot and rim material, lab testing on disturbed samples	N/A	Task not required for LA – will be addressed in detailed design.
9o. Limited index testing along the tunnels (Schmidt hammer, geophysical, dilatometer, other?)	N/A	Task not required for LA – will be addressed in detailed design.
9p. Develop rock mass parameters for the intensively fractured zone	N/A	Task not required for LA – will be addressed in detailed design.
9q. Perform a qualified site-specific Q vs. RMR correlation for use in rock mass calculations	N/A	Task not required for LA – will be addressed in detailed design.
9r. Quantify and evaluate effect of tunnel size on rock mass characterization data sets	N/A	Task not required for LA – will be addressed in detailed design.
9s. Numerical predictive modeling of site-specific lab/field tests for validation of lithophysal modeling (in update of Modeling of Lithophysal Rock	N/A	Task not required for LA – will be addressed in detailed design.

Table 7-4. A Status of SGPR Work Scope Recommended in SGPR Rev. 00A (Continued)

Primary Tasks Recommended	SGPR Section	Remark
Mechanical Behavior report)		
9t. Analysis of ESF/ECRB tunnel deformation monitoring, steel sets monitoring, ESF ground Support confirmation, Tunnel Boring Machine pressure and mining rate data, Drift Scale Test, and any other construction records to augment site-specific rock mass mechanical data	N/A	Task not required for LA – will be addressed in detailed design.
9u. Digitally map the ESF and ECRB tunnels	N/A	Task not required for LA – will be addressed in detailed design.
9v. Identify key geotechnical and design parameters that will be part of the performance confirmation program	N/A	Task not required for LA – will be addressed in detailed design. Future scope to be determined in coordination with the PC Organization.
9w. Continued revisions of SGPR and associated DTNs	N/A	Task not required for LA. The need for the subsequent SGPR revisions will be dictated by the detailed design.

7.2.2 Summary of Geotechnical Parameters for License Application

This Section summarizes work accomplished since the issuance of SGPR REV 00A (BSC 2003 [DIRS 166660]). It includes details on intact rock data enhancements and rock mass data developed in calculations utilizing laboratory data.

The work performed during preparation of the SGPR REV 00A (BSC 2003 [DIRS 166660]), concentrated mainly on issues related to data transparency and the integrity of data sources. The urgency of work on completing Revision 3 of *Drift Degradation Analysis* (BSC 2004 [DIRS 166107]) dictated the priority of work performed on the SGPR at that time. In effect the focus of SGPR REV 00A was mainly on the four rock strata units at the RHH, i.e., the Tptpul, Tptpmn, Tptpll, and Tptpln. While the intact rock data provide the basis for the analysis of underground structures, rock mass data is also required not only for the RHH units but for overlaying strata as well. The SGPR REV 00A reported on initial steps taken to address this issue or rock mass properties.

In general, two types of rock are encountered at Yucca Mountain, non-lithophysal, a strong rock displaying characteristics of a typical discontinuum, and lithophysal, more massive and described better in terms of continuum rock mass. While rock mass parameters for the nonlithophysal rock strata could be developed using the conventional rock mass rating approach, the behavior of the massive, lithophysal units required a more complex methodology involving a combination of laboratory and field testing, and the use of advanced numerical modeling to aid describing its behavior.

The SGPR REV 00A (BSC 2003 [DIRS 166660]) provided the first summary of the complex procedure required to obtain properties of lithophysal rock strata units. This methodology warranted a somewhat specialized treatment. A separate report, *Lithophysal Rock Mass Mechanical Properties of the Repository Host Horizon* (BSC 2004 [DIRS 172334]), was developed, where the entire approach is discussed in detail.

Laboratory data provide the basis for analyses covering both pre- and postclosure. To facilitate streamlining information already presented in SGPR REV 00A (BSC 2003 [DIRS 166660]), intact rock strength properties data were reanalyzed within the scope of a separate report, *Intact Rock Mechanical Properties of Yucca Mountain Stratigraphic Units* (BSC 2005 [DIRS 176611]). Section 6.4.2 presents a summary of intact rock property data. A summary of this data and basic statistics are presented in Tables 6-8 through 6-21.

Section 6.4.2.4 was added to summarize the time-dependent behavior of tuff was added. The data includes the latest results on tuff creep obtained between January 02, 2004 and February 25, 2005. The data presented in this Section will be used to address the impact of time-dependent behavior on drift degradation, dealing with a set of issues related to postclosure behavior of tuff.

A significant portion of the intact rock and rock mass density and porosity data in 2005–2006 time period were unavailable for analysis within the scope of this Report because they were reevaluated in the context of on-going seepage analysis. As a result relatively small amount of new information on dry bulk density and matrix porosity pertaining mainly to the RHH units is included in Section 6.4.1.

Properties of fractures are important while treating the rock mass as a discontinuum. A comprehensive report on fracture mapping and fracture properties is in process. In effect, fracture property data included in Section 6.4.3 present no new information on fracture properties.

Section 6.4.4 contains information on the development of the properties of rock mass. The Section includes two parts. The first part contains new information on the development of rock mass properties including all lithostratigraphic units at and above the RHH. The second part contains the summary of the approach used to develop properties of the lithophysal rock mass at the RHH only. A large portion of information has been presented already in *Subsurface Geotechnical Parameters Report*, Revision 00A (BSC 2003 [DIRS 166660]). Additional effort was expended to enhance this information through the use of an alternative approach to characterizing lithophysal rock mass behavior. This work is described in great detail in a separate report, *Lithophysal Rock Mass Mechanical Properties of the Repository Host Horizon* (BSC 2004 [DIRS 172334]). A summary of work presented in that report is given in Section 6.4.4.4.2.

The initial scope of work to develop rock mass parameters for the nonlithophysal rock only using conventional rock mass rating approach was extended to include entire sequence of Yucca Mountain rock units from the surface to the RHH. This decision was dictated by the need of developing one methodology that would serve as a benchmark for all units. It was also dictated by the practical need to tie the laboratory and numerical analyses to the readily verifiable field evidence—the existing system of underground openings (ESF, ECRB and ancillary openings) and observation of their performance. It was apparent that this "reality check" is beneficial for reconciling results generated while applying different approaches.

It is worth noting that during the development of the benchmark case including properties of all rock strata for which input data information is considered as a minimum available, both laboratory and field mapping data were used as a base for the development of rock mass properties. A "reality check" was performed to verify the reasonableness of rock mass properties obtained from closed-form calculations. This task was accomplished by comparing the rock mass strength data to the maximum stress level calculated at a particular location in the tunnel, considering the composite average density and varying topography above the tunnel at that location. This check revealed that in some cases overly conservative test conditions adopted in the laboratory resulted in low estimates of rock mass strength.

The calculated rock mass parameters were further evaluated in terms of specimen size. This was possible for RHH units because strength data from specimens of various diameters were available for these units only. The estimates of a minimum or critical specimen size and associated rock mass strength were used to compare the relative magnitudes of the maximum calculated stress at the tunnel wall and the rock mass strength. The strength of Tptpul was found to display the lowest strength among all RHH units. RHH units strength properties were further checked against a typical normalized strength versus specimen diameter displayed by the most common hard rocks (Figures 6-116 to 6-118). It was found that the lithophysal unit's behavior departs significantly from the trend characterizing typical hard rocks strength. The normalized strength versus specimen diameter for nonlithophysal Tptpmn unit was in relatively good agreement with the trend displayed by other typical hard rocks. The rock mass strength data for

all rock units are summarized in Table 6-76. In Table 6-77, the rock mass properties presented for nonlithophysal units were determined based on the conventional rock mass rating technique while the lithophysal rock mass strength was based on using the alternative method employing a combination of laboratory and field measurements and numerical simulations are presented.

In effect, the design engineer is presented with qualified data and their sources needed to pursue design activities whether treating rock mass as a continuum or discontinuum. From the engineering design perspective, the parameters presented in this report are considered adequate and are sufficient for subsurface design in support of the License Application.

INTENTIONALLY LEFT BLANK

8. INPUTS AND REFERENCES

8.1 DOCUMENT CITED

101367 Albin, A.L.; Singleton, W.L.; Moyer, T.C.; Lee, A.C.; Lung, R.C.; Eatman, G.L.W.; and Barr, D.L. 1997. *Geology of the Main Drift - Station 28+00 to 55+00, Exploratory Studies Facility, Yucca Mountain Project, Yucca Mountain, Nevada.* Milestone SPG42AM3. Denver, Colorado: Bureau of Reclamation and U.S. Geological Survey. ACC: MOL.19970625.0096.

101423 Arnold, B.W.; Altman, S.J.; Robey, T.H.; Barnard, R.W.; and Brown, T.J. 1995. *Unsaturated-Zone Fast-Path Flow Calculations for Yucca Mountain Groundwater Travel Time Analyses (GWTT-94).* SAND95-0857. Albuquerque, New Mexico: Sandia National Laboratories. ACC: MOL.19960327.0336.

100003 Bandis, S.C.; Lumsden, A.C.; and Barton, N.R. 1983. "Fundamentals of Rock Joint Deformation." *International Journal of Rock Mechanics and Mining Science & Geomechanics Abstracts, 20,* (6), 249-268. [New York, New York]: Pergamon Press. TIC: 224201.

100029 Barr, D.L.; Moyer, T.C.; Singleton, W.L.; Albin, A.L.; Lung, R.C.; Lee, A.C.; Beason, S.C.; and Eatman, G.L.W. 1996. *Geology of the North Ramp — Stations 4+00 to 28+00, Exploratory Studies Facility, Yucca Mountain Project, Yucca Mountain, Nevada.* Denver, Colorado: U.S. Geological Survey. ACC: MOL.19970106.0496.

166166 Barton, N. 1982. *Modelling Rock Joint Behavior from In Situ Block Tests: Implications for Nuclear Waste Repository Design.* ONWI-308. Columbus, Ohio: U.S. Department of Energy, Office of Nuclear Waste Isolation, Battelle Memorial Institute. ACC: HQS.19880517.2252.

146587 Barton, N. 1988. "Rock Mass Classification and Tunnel Reinforcement Selection Using the Q-System." *Rock Classification Systems for Engineering Purposes.* Kirkaldie, L., ed. ASTM STP 984. Pages 59-84. Philadelphia, Pennsylvania: American Society for Testing and Materials. TIC: 216484.

160379 Barton, N. 2002. "Some New Q-Value Correlations to Assist in Site Characterisation and Tunnel Design." *International Journal of Rock Mechanics & Mining Sciences, 39,* (2), 185-216. New York, New York: Elsevier. TIC: 252648.

166167 Barton, N. and Bandis, S. 1990. "Review of Predictive Capacities of JRC-JCS Model in Engineering Practice." *Rock Joints, Proceedings of the International Symposium on Rock Joints, Loen, Norway, 4-6 June 1990.* Barton, N. and Stephansson, O., eds. Pages 603-610. Brookfield, Vermont: A.A. Balkema. TIC: 103532.

101541 Barton, N.; Lien, R.; and Lunde, J. 1974. "Engineering Classification of Rock Masses for the Design of Tunnel Support." *Rock Mechanics, 6,* (4), 189-236. New York, New York: Springer-Verlag. TIC: 219995.

100005 Barton, N.R.; Bandis, S.; and Bakhtar, K. 1985. "Strength, Deformation, and Conductivity Coupling of Rock Joints." *International Journal of Rock Mechanics and Mining Science & Geomechanics Abstracts, 22,* (3), 121-140. New York, New York: Pergamon Press. TIC: 217135.

101191 Beason, S.C.; Turlington, G.A.; Lung, R.C.; Eatman, G.L.W.; Ryter, D.; and Barr, D.L. 1996. *Geology of the North Ramp - Station 0+60 to 4+00, Exploratory Studies Facility, Yucca Mountain Project, Yucca Mountain, Nevada.* Denver, Colorado: U.S. Geological Survey. ACC: MOL.19970106.0449.

159696 Berryman, James G. 1995. "Mixture Theories for Rock Properties." *AGU Reference Shelf 3, Rock Physics and Phase Relations A Handbook of Physical Constants.* Ahrens, T.J. Pages 205-228. [Washington, D.C.]: American Geophysical Union. TIC: 239165.

101694 Bieniawski, Z.T. 1976. "Rock Mass Classification in Rock Engineering." *Exploration for Rock Engineering, Proceedings, Symposium on Exploration for Rock Engineering, Johannesburg, 1-5 November 1-5 1976. 1,* 97-106. Rotterdam, The Netherlands: A.A. Balkema. TIC: 226223.

101715 Bieniawski, Z.T. 1989. *Engineering Rock Mass Classifications.* New York, New York: John Wiley & Sons. TIC: 226350.

150684 Bieniawski, Z.T.; Franklin, J.A.; Bernede, M.J.; Duffaut, P.; Rummel, F.; Horibe, T.; Broch, E.; Rodrigues, E.; Van Heerden, W.L.; Vogler, U.W.; Hansagi, I.; Szlavin, J.; Brady, B.T.; Deere, D.U.; Hawkes, I.; and Milovanovic, D. 1981. "Suggested Methods for Determining the Uniaxial Compressive Strength and Deformability of Rock Materials." *Rock Characterization Testing & Monitoring, ISRM Suggested Methods.* Brown, E.T., ed. New York, New York: Pergamon Press. TIC: 209865.

165036 Board, M. 2003. *Resolution Strategy for Geomechanically-Related Repository Design and Thermal-Mechanical Effects (RDTME).* REV 00. Las Vegas, Nevada: Bechtel SAIC Company. ACC: MOL.20030708.0153.

168880 Bowles, J.E. 1982. *Foundation Analysis and Design.* 3rd Edition. Pages 100, 134, 135, 183, 184, and 185. New York, New York: McGraw-Hill. TIC: 240874.

120650 Boyd, P.J.; Martin, R.J., III; and Price, R.H. 1995. "Variability of the Physical Properties of Tuff at Yucca Mountain, NV." *Rock Mechanics, Proceedings of the 35th U.S. Symposium, University of Nevada, Reno, 5-7 June 1995.* Daemen, J.J.K. and Schultz, R.A., eds. Pages 511-516. Brookfield, Vermont: A.A. Balkema. TIC: 225160.

101491 Boyd, P.J.; Price, R.H.; Martin, R.J.; and Noel, J.S. 1996. *Bulk and Mechanical Properties of the Paintbrush Tuff Recovered from Boreholes UE25 NRG-2, 2A, 2B, and 3: Data Report.* SAND94-1902. Albuquerque, New Mexico: Sandia National Laboratories. ACC: MOL.19970102.0002.

101492 Boyd, P.J.; Price, R.H.; Noel, J.S.; and Martin, R.J. 1996. *Bulk and Mechanical Properties of the Paintbrush Tuff Recovered from Boreholes UE25 NRG-4 and -5: Data Report.* SAND94-2138. Albuquerque, New Mexico: Sandia National Laboratories. ACC: MOL.19970102.0004.

101990 Brace, W.F.; Paulding, B.W., Jr.; and Scholz, C.H. 1966. "Dilatancy in the Fracture of Crystalline Rocks." *Journal of Geophysical Research, 71,* (16), 3939-3953. Washington, D.C.: American Geophysical Union. TIC: 226778.

101493 Brechtel, C.E.; Lin, M.; Martin, E.; and Kessel, D.S. 1995. *Geotechnical Characterization of the North Ramp of the Exploratory Studies Facility.* SAND95-0488/1 and 2. Two volumes. Albuquerque, New Mexico: Sandia National Laboratories. ACC: MOL.19950502.0004; MOL.19950502.0005.

100653 Brodsky, N.S.; Riggins, M.; Connolly, J.; and Ricci, P. 1997. *Thermal Expansion, Thermal Conductivity, and Heat Capacity Measurements for Boreholes UE25 NRG-4, UE25 NRG-5, USW NRG-6, and USW NRG-7/7A.* SAND95-1955. Albuquerque, New Mexico: Sandia National Laboratories. ACC: MOL.19980311.0316.

102003 Brown, E.T., ed. 1981. *Rock Characterization Testing & Monitoring, ISRM Suggested Methods.* New York, New York: Pergamon Press. TIC: 209865.

178063 BSC (Bechtel SAIC Company) 2006. *Technical Work Plan for Subsurface Geotechnical Parameters Report.* TWP-SSD-GE-000001 REV 00. Las Vegas, Nevada: Bechtel SAIC Company. ACC: DOC.20061004.0001.

158794 BSC (Bechtel SAIC Company) 2002. *Guidelines for Developing and Documenting Alternative Conceptual Models, Model Abstractions, and Parameter Uncertainty in the Total System Performance Assessment for the License Application.* TDR-WIS-PA-000008 REV 00 ICN 01. Las Vegas, Nevada: Bechtel SAIC Company. ACC: MOL.20020904.0002.

160313 BSC (Bechtel SAIC Company) 2002. *Scientific Processes Guidelines Manual.* MIS-WIS-MD-000001 REV 01. Las Vegas, Nevada: Bechtel SAIC Company. ACC: MOL.20020923.0176.

165421 BSC (Bechtel SAIC Company) 2002. *Test Plan for: Rock Modulus Testing.* SITP-02-SSD-001 REV 00. Las Vegas, Nevada: Bechtel SAIC Company. ACC: MOL.20020225.0260.

165802 BSC (Bechtel SAIC Company) 2003. *GFM2000 Representation in the VULCAN Software System.* 800-00C-TU00-00100-000-00A. Las Vegas, Nevada: Bechtel SAIC Company. ACC: ENG.20030922.0005.

164670 BSC (Bechtel SAIC Company) 2003. *Heat Capacity and Thermal Expansion Coefficients Analysis Report.* ANL-NBS-GS-000013 REV 00. Las Vegas, Nevada: Bechtel SAIC Company. ACC: DOC.20030820.0002.

166183 BSC (Bechtel SAIC Company) 2003. *Scoping Analysis on Sensitivity and Uncertainty of Emplacement Drift Stability.* 800-K0C-TEG0-00600-000-000. Las Vegas, Nevada: Bechtel SAIC Company. ACC: ENG.20031125.0002.

166660 BSC (Bechtel SAIC Company) 2003. *Subsurface Geotechnical Parameters Report.* 800-K0C-WIS0-00400-000-00A. Las Vegas, Nevada: Bechtel SAIC Company. ACC: ENG.20040108.0001; ENG.20050816.0020.

166296 BSC (Bechtel SAIC Company) 2003. *Total System Performance Assessment-License Application Methods and Approach.* TDR-WIS-PA-000006 REV 00 ICN 01. Las Vegas, Nevada: Bechtel SAIC Company. ACC: DOC.20031215.0001.

165572 BSC (Bechtel SAIC Company) 2003. *Underground Layout Configuration.* 800-P0C-MGR0-00100-000-00E. Las Vegas, Nevada: Bechtel SAIC Company. ACC: ENG.20031002.0007; ENG.20050817.0005.

166107 BSC (Bechtel SAIC Company) 2004. *Drift Degradation Analysis.* ANL-EBS-MD-000027 REV 03. Las Vegas, Nevada: Bechtel SAIC Company. ACC: DOC.20040915.0010; DOC.20050419.0001; DOC.20051130.0002.

168889 BSC (Bechtel SAIC Company) 2004. *Evaluation of Emplacement Drift Stability for KTI Resolutions.* 800-KMC-SSE0-00200-000-00A. Las Vegas, Nevada: Bechtel SAIC Company. ACC: ENG.20040520.0001; ENG.20050816.0023.

170029 BSC (Bechtel SAIC Company) 2004. *Geologic Framework Model (GFM2000).* MDL-NBS-GS-000002 REV 02. Las Vegas, Nevada: Bechtel SAIC Company. ACC: DOC.20040827.0008.

170003 BSC (Bechtel SAIC Company) 2004. *Heat Capacity Analysis Report.* ANL-NBS-GS-000013 REV 01. Las Vegas, Nevada: Bechtel SAIC Company. ACC: DOC.20041101.0003.

172334 BSC (Bechtel SAIC Company) 2004. *Lithophysal Rock Mass Mechanical Properties of the Repository Host Horizon.* 800-K0C-SS00-00200-000-00A. Las Vegas, Nevada: Bechtel SAIC Company. ACC: ENG.20041111.0001.

170031 BSC (Bechtel SAIC Company) 2004. *Mineralogic Model (MM3.0) Report.* MDL-NBS-GS-000003 REV 01. Las Vegas, Nevada: Bechtel SAIC Company. ACC: DOC.20040908.0006.

176608 BSC (Bechtel SAIC Company) 2004. *Rock Mass Quality Ratings and Classifications of the Combined ESF, Heated Drift and ECRB Cross Drift.* 800-K0C-SS00-00700-000-00A. Las Vegas, Nevada: Bechtel SAIC Company. ACC: ENG.20040901.0031.

170033 BSC (Bechtel SAIC Company) 2004. *Thermal Conductivity of Non-Repository Lithostratigraphic Layers.* MDL-NBS-GS-000006 REV 01. Las Vegas, Nevada: Bechtel SAIC Company. ACC: DOC.20041022.0004.

169854 BSC (Bechtel SAIC Company) 2004. *Thermal Conductivity of the Potential Repository Horizon.* MDL-NBS-GS-000005 REV 01. Las Vegas, Nevada: Bechtel SAIC Company. ACC: DOC.20040928.0006.

169900 BSC (Bechtel SAIC Company) 2004. *Thermal Testing Measurements Report.* TDR-MGR-HS-000002 REV 00. Las Vegas, Nevada: Bechtel SAIC Company. ACC: DOC.20040928.0005.

169734 BSC (Bechtel SAIC Company) 2004. *Yucca Mountain Site Description.* TDR-CRW-GS-000001 REV 02 ICN 01. Two volumes. Las Vegas, Nevada: Bechtel SAIC Company. ACC: DOC.20040504.0008.

176611 BSC (Bechtel SAIC Company) 2005. *Intact Rock Mechanical Properties of Yucca Mountain Stratigraphic Units.* 800-K0C-SS00-00800-000-00A. Las Vegas, Nevada: Bechtel SAIC Company. ACC: ENG.20051108.0007.

170137 BSC (Bechtel SAIC Company) 2005. *Peak Ground Velocities for Seismic Events at Yucca Mountain, Nevada.* ANL-MGR-GS-000004 REV 00. Las Vegas, Nevada: Bechtel SAIC Company. ACC: DOC.20050223.0002; DOC.20050725.0002.

175539 BSC (Bechtel SAIC Company) 2005. *Q-List.* 000-30R-MGR0-00500-000-003. Las Vegas, Nevada: Bechtel SAIC Company. ACC: ENG.20050929.0008.

178277 BSC (Bechtel SAIC Company) 2006. *IED Geotechnical and Thermal Parameters II.* 800-IED-MGR0-00402-000-00A. Las Vegas, Nevada: Bechtel SAIC Company. ACC: ENG.20070108.0001

178308 BSC (Bechtel SAIC Company) 2006. *Project Design Criteria Document.* 000-3DR-MGR0-00100-000-006. Las Vegas, Nevada: Bechtel SAIC Company. ACC: ENG.20061201.0005

177655 BSC (Bechtel SAIC Company) 2006. *Quality Management Directive.* QA-DIR-10, Rev. 0. Las Vegas, Nevada: Bechtel SAIC Company. ACC: DOC.20060906.0001.

163729 Buesch, D. 2003. "Fractures in Thin Sections with Rims as Cooling Joints in Tptpmn and Tptpll for AMR." E-mail from D. Buesch to D. Kicker, June 2, 2003. ACC: MOL.20030610.0067.

162271 Buesch, D. 2003. "Hydrogeologic Properties of Features in Crystallized Topopah Spring Tuff." E-mail from D. Buesch to D. Kicker and D. Rigby, March 10, 2003, with attachment. ACC: MOL.20030314.0188.

101433 Buesch, D.C. and Spengler, R.W. 1998. "Character of the Middle Nonlithophysal Zone of the Topopah Spring Tuff at Yucca Mountain." *High-Level Radioactive Waste Management, Proceedings of the Eighth International Conference, Las Vegas, Nevada, May 11-14, 1998.* Pages 16-23. La Grange Park, Illinois: American Nuclear Society. TIC: 237082.

100106 Buesch, D.C.; Spengler, R.W.; Moyer, T.C.; and Geslin, J.K. 1996. *Proposed Stratigraphic Nomenclature and Macroscopic Identification of Lithostratigraphic Units of the Paintbrush Group Exposed at Yucca Mountain, Nevada.* Open-File Report 94-469. Denver, Colorado: U.S. Geological Survey. ACC: MOL.19970205.0061.

111961 Bulmer, M.G. 1979. *Principles of Statistics.* 3rd Edition. New York, New York: Dover. TIC: 245835.

104639 Byers, F.M., Jr.; Carr, W.J.; Orkild, P.P.; Quinlivan, W.D.; and Sargent, K.A. 1976. *Volcanic Suites and Related Cauldrons of Timber Mountain-Oasis Valley Caldera Complex, Southern Nevada.* Professional Paper 919. Washington, D.C.: U.S. Geological Survey. TIC: 201146.

100968 Carslaw, H.S. and Jaeger, J.C. 1959. *Conduction of Heat in Solids.* 2nd Edition. Oxford, Great Britain: Oxford University Press. TIC: 206085.

170308 Charles, R.J. 1959. "The Strength of Silicate Glasses and Some Crystalline Oxides." *Fracture, Proceedings of an International Conference on the Atomic Mechanisms of Fracture held in Swampscott, Massachusetts, April 12-16, 1959.* Averback, B.L.; Felbeck, D.K.; Hahn, G.T.; and Thomas, D.A., eds. Pages 225-249. New York, New York: John Wiley & Sons. TIC: 236240.

101427 CRWMS M&O 1995. *ESF Ground Support Design Analysis.* BABEE0000-01717-0200-00002 REV 00. Las Vegas, Nevada: CRWMS M&O. ACC: MOL.19960409.0355.

158154 CRWMS M&O 1996. *ESF Ground Support - Structural Steel Analysis.* BABEE0000-01717-0200-00003 REV 02. Las Vegas, Nevada: CRWMS M&O. ACC: MOL.19961114.0137.

111105 CRWMS M&O 1996. *Yucca Mountain Site Geotechnical Report.* BAAA00000-01717-4600-00065 REV 00. Las Vegas, Nevada: CRWMS M&O. ACC: MOL.19970425.0062.

101539 CRWMS M&O 1997. *Ambient Characterization of the Drift Scale Test Block.* BADD00000-01717-5705-00001 REV 01. Las Vegas, Nevada: CRWMS M&O. ACC: MOL.19980416.0689.

100930 CRWMS M&O 1997. *Confirmation of Empirical Design Methodologies.* BABEE0000-01717-5705-00002 REV 00. Las Vegas, Nevada: CRWMS M&O. ACC: MOL.19980219.0104.

147458 CRWMS M&O 1997. *Data Transmittal Package (DTP) for "Hydraulic Fracturing Stress Measurements in Test Hole: ESF-AOD-HDFR#1, Thermal Test Facility, Exploratory Studies Facility at Yucca Mountain.* DTN: SNF37100195002.001, TDIF 305878. Las Vegas, Nevada: CRWMS M&O. ACC: MOL.19970717.0005; MOL.19970717.0006; MOL.19970717.0007; MOL.19970717.0008.

100223 CRWMS M&O 1997. *Determination of Available Volume for Repository Siting.* BCA000000-01717-0200-00007 REV 00. Las Vegas, Nevada: CRWMS M&O. ACC: MOL.19971009.0699.

103564 CRWMS M&O 1997. *Yucca Mountain Site Geotechnical Report.* B00000000-01717-5705-00043 REV 01. Two volumes. Las Vegas, Nevada: CRWMS M&O. ACC: MOL.19971017.0736; MOL.19971017.0737.

131317 CRWMS M&O 1998. *Deformation Monitoring Analysis.* BABEE0000-01717-5705-00005 REV 00. Las Vegas, Nevada: CRWMS M&O. ACC: MOL.19981014.0002.

141028 CRWMS M&O 1998. *ESF Design Confirmation Steel Set Loads Analysis.* BABEE0000-01717-5705-00006 REV 00. Las Vegas, Nevada: CRWMS M&O. ACC: MOL.19981014.0001.

124140 CRWMS M&O 1998. *ESF Ground Support Confirmation.* BABEE0000-01717-5705-00003 REV 00. Las Vegas, Nevada: CRWMS M&O. ACC: MOL.19980727.0308.

102679 CRWMS M&O 1998. *Geology of the Exploratory Studies Facility Topopah Spring Loop.* BAB000000-01717-0200-00002 REV 01. Las Vegas, Nevada: CRWMS M&O. ACC: MOL.19980415.0283.

129261 CRWMS M&O 1999. *Single Heater Test Final Report.* BAB000000-01717-5700-00005 REV 00 ICN 1. Las Vegas, Nevada: CRWMS M&O. ACC: MOL.20000103.0634.

107475 CRWMS M&O 1999. *Stratigraphy of Shaft Sites.* Design Input Transmittal SSR-NEP-99209.T. Las Vegas, Nevada: CRWMS M&O. ACC: MOL.19990521.0143.

146611 Deere, D.U. and Deere, D.W. 1988. "The Rock Quality Designation (RQD) Index in Practice." *Rock Classification Systems for Engineering Purposes.* Kirkaldie, L., ed. ASTM STP 984. Pages 91-101. Philadelphia, Pennsylvania: American Society for Testing and Materials. TIC: 216484.

177092 DOE (U.S. Department of Energy) 2006. *Quality Assurance Requirements and Description.* DOE/RW-0333P, Rev. 18. Washington, D.C.: U.S. Department of Energy, Office of Civilian Radioactive Waste Management. ACC: DOC.20060602.0001.

100282 DOE (U.S. Department of Energy) 1988. *Site Characterization Plan Yucca Mountain Site, Nevada Research and Development Area, Nevada.* DOE/RW-0199. Nine volumes. Washington, D.C.: U.S. Department of Energy, Office of Civilian Radioactive Waste Management. ACC: HQO.19881201.0002.

163586 Duan, F. 2003. "A White Paper by Nick Barton." E-mail from F. Duan to D. Kicker, May 28, 2003, with attachment. ACC: MOL.20030603.0132; MOL.20030219.0058.

157677 Eatman, G.L.W.; Singleton, W.L.; Moyer, T.C.; Barr, D.L.; Albin, A.L.; Lung, R.C.; and Beason, S.C. 1997. *Geology of the South Ramp - Station 55+00 to 78+77, Exploratory Studies Facility, Yucca Mountain Project, Yucca Mountain, Nevada.* Denver, Colorado: U.S. Department of Energy. ACC: MOL.19980127.0396.

176612 Fray, R.E. 2005. "Contract No. DE-AC28-01RW12101 - Minutes of September 15, 2005 Geotechnical Data Issues and Concerns Meeting." Letter from R.E. Fray (BSC) to Distribution, October 6, 2005, BLG:REF:lm-1004056921, with enclosures. ACC: MOL.20051118.0072.

160044 George, J.T.; Finley, R.E.; and Riggins, M. 1999. "Conduct of Plate Loading Tests at Yucca Mountain, Nevada." *Rock Mechanics for Industry, Proceedings of the 37th U.S. Symposium, Vail, Colorado, USA, 6-9 June, 1999.* Amadei, B.; Kranz, R.L.; Scott, G.A.; and Smeallie, P.H.; eds. *2,* 721-727. Brookfield, Vermont: A.A. Balkema. TIC: 245246.

103330 Geslin, J.K.; Moyer, T.C.; and Buesch, D.C. 1995. *Summary of Lithologic Logging of New and Existing Boreholes at Yucca Mountain, Nevada, August 1993 to February 1994.* Open-File Report 94-342. Denver, Colorado: U.S. Geological Survey. ACC: MOL.19940810.0011.

153165 Hadley, G.R. 1986. "Thermal Conductivity of Packed Metal Powders." *International Journal of Heat and Mass Transfer, 29,* (6), 909-920. [New York, New York]: Pergamon Journals. TIC: 249320.

166174 Heuze, F.E. 1980. "Scale Effects in the Determination of Rock Mass Strength and Deformability." *Rock Mechanics, 12,* (3-4), 167-192. [New York, New York]: Springer-Verlag. TIC: 218372.

101598 Heuze, F.E. and Amadei, B. 1985. "The NX-Borehole Jack: A Lesson In Trials and Errors." *International Journal of Rock Mechanics, Mining Sciences & Geomechanics Abstracts, 22,* (2), 105-112. New York, New York: Pergamon Press. TIC: 218975.

160705 Hoek, E. 2000. *[Practical] Rock Engineering, [2000 Edition].* Toronto, Ontario, Canada: RocScience. TIC: 253544.

106158 Hoek, E. and Brown, E.T. 1988. "The Hoek-Brown Failure Criterion - A 1988 Update." *Proceedings of the 15th Canadian Rock Mechanics Symposium, Toronto, Canada, October 1988.* Pages 31-38. Toronto, Canada: University of Toronto Press. TIC: 240286.

170501 Hoek, E. and Brown, E.T. 1997. "Practical Estimates of Rock Mass Strength." *International Journal of Rock Mechanics and Mining Science & Geomechanics Abstracts, 34,* (8), 1165-1186. [Oxford], England: Pergamon. TIC: 256245.

162204 Hoek, E.; Carranza-Torres, C.; and Corkum, B. 2002. "Hoek-Brown Failure Criterion – 2002 Edition." [5th North American Rock Mechanics Symposium and 17th Tunnelling Association of Canada Conference: NARMS-TAC 2002, July 7-10, University of Toronto.] Toronto, Ontario, Canada: Rocscience. Accessed March 17, 2003. TIC: 253954. URL: http://www.rocscience.com/Anon/ResearchPapers/NARMS.pdf

101978 Holman, J.P. 1997. *Heat Transfer.* 8th Edition. New York, New York: McGraw-Hill. TIC: 239954.

166047 Howard, C.L.; Schuhen, M.D.; George, J.T.; Lee, M.Y.; Taylor, R.S.; and Bronowski, D.R. 2003. "Rock-Mass Deformation Modulus Testing of Lithophysal Stratigraphic Units at the Yucca Mountain Project." *Soil and Rock America 2003, 12th Panamerican Conference on Soil Mechanics and Geotechnical Engineering, 39th U.S. Rock Mechanics Symposium, June 22-26, 2003, Cambridge, Massachusetts, USA.* Culligan, P.J.; Einstein, H.H.; and Whittle, A.J., eds. *1,* 375-380. Essen, Germany: Verlag Glückauf GmbH. TIC: 255152.

158073 Hsu, C.T.; Cheng, P.; and Wong, K.W. 1995. "A Lumped-Parameter Model for Stagnant Thermal Conductivity of Spatially Periodic Porous Media." *Journal of Heat Transfer, 117,* (2), 264-269. New York, New York: American Society of Mechanical Engineers. TIC: 252402.

160331 Itasca Consulting Group [2002]. *Itasca Software–Cutting Edge Tools for Computational Mechanics.* Minneapolis, Minnesota: Itasca Consulting Group. TIC: 252592.

171549 JMP 2002. *The Statistical Discovery Software.* Multivolume set. Cary, North Carolina: SAS Institute. TIC: 256485.

178329 Johnson, M.L. 2006. "Contract No. DE-AC28-01RW12101 - Minutes of December 8, 2005 Geotechnical Data Issues and Concerns Meeting". Letter from M.L. Johnson (BSC) to Distribution, November 2, 2006, MJM:LM-1101069808, with enclosure. ACC: CCU.20061102.0006.

165092 Kalia, H. 2001. "Description of the Field Measurements of Thermal Conductivity in the Topopah Spring Lower Lithophysal Unit (Tptpll)." Memorandum from H. Kalia (BSC) to Distribution, July 23, 2001, PROJ.07/01.045, with enclosure. ACC: MOL.20010822.0260.

148383 Kaviany, M. 1991. *Principles of Heat Transfer in Porous Media.* New York, New York: Springer-Verlag. TIC: 240655.

176613 Kokajko, L.E. 2005. "Pre-Licensing Evaluation of Agreements in 'Technical Basis Document Number 4, Mechanical Degradation and Seismic Effects' and Three Other Associated Agreements." Letter from L.E. Kokajko (NRC) to J.D. Ziegler (DOE/ORD), January 11, 2005, 0119054487, with enclosure. ACC: MOL.20050214.0005.

102973 Lappin, A.R. 1980. *Thermal Conductivity of Silicic Tuffs: Predictive Formalism and Comparison with Preliminary Experimental Results.* SAND80-0769. Albuquerque, New Mexico: Sandia National Laboratories. ACC: NNA.19890327.0052.

164769 Lau, J.S.O.; Gorski, B.; Conlon, B.; and Anderson, T. 2000. *Long-Term Loading Tests on Saturated Granite and Granodiorite.* Report No. 06819-REP-01300-10016 R00. Toronto, Ontario, Canada: Ontario Power Generation, Nuclear Waste Management Division. TIC: 254970.

169721 Martin, R.J., III 1972. "Time-Dependent Crack Growth in Quartz and its Application to the Creep of Rocks." *Journal of Geophysical Research, 77,* (8), 1406-1419. [Washington, D.C.]: American Geophysical Union. TIC: 224770.

170301 Martin, R.J., III and Durham, W.B. 1975. "Mechanisms of Crack Growth in Quartz." *Journal of Geophysical Research, 80,* (35), 4837-4844. Washington, D.C.: American Geophysical Union. TIC: 224771.

160028 Martin, R.J., III; Price, R.H.; Boyd, P.J.; and Haupt, R.W. 1992. *Anisotropy of the Topopah Spring Member Tuff.* SAND91-0894. Albuquerque, New Mexico: Sandia National Laboratories. ACC: NNA.19920522.0041.

164770 Martin, R.J., III; Price, R.H.; Boyd, P.J.; and Noel, J.S. 1993. "The Influence of Strain Rate and Sample Inhomogeneity on the Moduli and Strength of Welded Tuff." *International Journal of Rock Mechanics and Mining Science & Geomechanics Abstracts, 30,* (7), 1507–1510. [New York, New York]: Pergamon. TIC: 254873.

100159 Martin, R.J., III; Price, R.H.; Boyd, P.J.; and Noel, J.S. 1995. *Creep in Topopah Spring Member Welded Tuff.* SAND94-2585. Albuquerque, New Mexico: Sandia National Laboratories. ACC: MOL.19950502.0006.

165960 Martin, R.J.; Noel, J.S.; Boyd, P.J.; and Price, R.H. 1997. "Creep and Static Fatigue of Welded Tuff from Yucca Mountain, Nevada." *International Journal of Rock Mechanics and Mining Sciences, 34,* (3-4), Paper No. 190. [New York, New York]: Pergamon. TIC: 255298.

148875 Martin, R.J.; Noel, J.S.; Boyd, P.J.; and Price, R.H. 1997. *Creep Properties of the Paintbrush Tuff Recovered from Borehole USW NRG-7/7A: Data Report.* SAND95-1759. Albuquerque, New Mexico: Sandia National Laboratories. ACC: MOL.19971017.0661.

101432 Martin, R.J.; Noel, J.S.; Boyd, P.J.; and Price, R.H. 1997. *The Effects of Confining Pressure on the Strength and Elastic Properties of the Paintbrush Tuff Recovered from Boreholes USW NRG-6 and USW NRG-7/7A: Data Report.* SAND95-1887. Albuquerque, New Mexico: Sandia National Laboratories. ACC: MOL.19971017.0662.

104758 Martin, R.J.; Noel, J.S.; Boyd, P.J.; Riggins, M.; and Price, R.H. 1997. *Thermal Expansion of the Paintbrush Tuff Recovered from Borehole USW SD-12 at Pressures 30 MPa: Data Report.* SAND95-1904. Albuquerque, New Mexico: Sandia National Laboratories. ACC: MOL.19971017.0680.

104760 Martin, R.J.; Price, R.H.; Boyd, P.J.; and Noel, J.S. 1994. *Bulk and Mechanical Properties of the Paintbrush Tuff Recovered from Borehole USW NRG-6: Data Report.* SAND93-4020. Albuquerque, New Mexico: Sandia National Laboratories. ACC: MOL.19940811.0001.

104761 Martin, R.J.; Price, R.H.; Boyd, P.J.; and Noel, J.S. 1995. *Bulk and Mechanical Properties of the Paintbrush Tuff Recovered from Borehole USW NRG-7/7A: Data Report.* SAND94-1996. Albuquerque, New Mexico: Sandia National Laboratories. ACC: MOL.19950316.0087.

161566 Mellor, M. and Hawkes, I. 1971. "Measurement of Tensile Strength by Diametral Compression of Discs and Annuli." *Engineering Geology, 5,* 173-225. Amsterdam, The Netherlands: Elsevier. TIC: 253847.

149850 Mongano, G.S.; Singleton, W.L.; Moyer, T.C.; Beason, S.C.; Eatman, G.L.W.; Albin, A.L.; and Lung, R.C. 1999. *Geology of the ECRB Cross Drift - Exploratory Studies Facility, Yucca Mountain Project, Yucca Mountain, Nevada.* [Deliverable SPG42GM3]. Denver, Colorado: U.S. Geological Survey. ACC: MOL.20000324.0614.

103777 Moyer, T.C.; Geslin, J.K.; and Buesch, D.C. 1995. *Summary of Lithologic Logging of New and Existing Boreholes at Yucca Mountain, Nevada, July 1994 to November 1994.* Open-File Report 95-102. Denver, Colorado: U.S. Geological Survey. TIC: 224224.

106399 Munsell Color Company 1994. *Munsell Soil Color Charts.* 1994 Revised Edition. New Windsor, New York: GretagMacbeth. TIC: 238646.

100690 Nimick, F.B. and Connolly, J.R. 1991. *Calculation of Heat Capacities for Tuffaceous Units from the Unsaturated Zone at Yucca Mountain, Nevada.* SAND88-3050. Albuquerque, New Mexico: Sandia National Laboratories. ACC: NNA.19910308.0017.

105195 Nimick, F.B.; Price, R.H.; Van Buskirk, R.G.; and Goodell, J.R. 1985. *Uniaxial and Triaxial Compression Test Series on Topopah Spring Tuff from USW G-4, Yucca Mountain, Nevada.* SAND84-1101. Albuquerque, New Mexico: Sandia National Laboratories. ACC: MOL.19980602.0332.

159538 NRC (U.S. Nuclear Regulatory Commission) 2002. *Integrated Issue Resolution Status Report.* NUREG-1762. Washington, D.C.: U.S. Nuclear Regulatory Commission, Office of Nuclear Material Safety and Safeguards. TIC: 253064.

163274 NRC (U.S. Nuclear Regulatory Commission) 2003. *Yucca Mountain Review Plan, Final Report.* NUREG-1804, Rev. 2. Washington, D.C.: U.S. Nuclear Regulatory Commission, Office of Nuclear Material Safety and Safeguards. TIC: 254568.

102935 Olsson, W.A. 1987. *Rock Joint Compliance Studies.* SAND86-0177. Albuquerque, New Mexico: Sandia National Laboratories. ACC: NNA.19870511.0131.

168736 Olsson, W.A. 1995. *Creep of an Artificial Joint in Tuff under Static Triaxial Stress States.* SAND95-1769 [ABSTRACT]. Albuquerque, New Mexico: Sandia National Laboratories. ACC: MOL.19970806.0300.

106453 Olsson, W.A. and Brown, S.R. 1997. *Mechanical Properties of Fractures from Drillholes UE25-NRG-4, USW-NRG-6, USW-NRG-7, USW-SD-9 at Yucca Mountain, Nevada.* SAND95-1736. Albuquerque, New Mexico: Sandia National Laboratories. ACC: MOL.19970224.0064.

102940 Olsson, W.A. and Jones, A.K. 1980. *Rock Mechanics Properties of Volcanic Tuffs from the Nevada Test Site.* SAND80-1453. Albuquerque, New Mexico: Sandia National Laboratories. ACC: NNA.19870406.0497.

101280 Ortiz, T.S.; Williams, R.L.; Nimick, F.B.; Whittet, B.C.; and South, D.L. 1985. *A Three-Dimensional Model of Reference Thermal/Mechanical and Hydrological Stratigraphy at Yucca Mountain, Southern Nevada.* SAND84-1076. Albuquerque, New Mexico: Sandia National Laboratories. ACC: MOL.19980602.0331.

165550 Potyondy, D.O. 2003. "PFC Stress Corrosion Model." Annex 11.4 of *Seismic Validation of 3-D Thermo-Mechanical Models for the Prediction of the Rock Damage Around Radioactive Spent Fuel Waste.* Project No. FIKW-2001-00200. Liverpool, England: University of Liverpool. TIC: 254978.

157885 Poulos, H.G. and Davis, E.H. 1991. *Elastic Solutions for Soil and Rock Mechanics.* Series in Soil Engineering. Lambe, T.W., and Whitman, R.V., eds. New York, New York: Center for Geotechnical Research. TIC: 252578.

106589 Price, R.H. 1986. *Effects of Sample Size on the Mechanical Behavior of Topopah Spring Tuff.* SAND85-0709. Albuquerque, New Mexico: Sandia National Laboratories. ACC: NNA.19891106.0125.

160023 Price, R.H. 1993. "Strength-Size-Porosity Empirical Model for Yucca Mountain Tuff." *EOS, Transactions (Supplement), 74,* (43), 571. Washington, D.C.: American Geophysical Union. TIC: 210057.

170894 Price, R.H. 2004. *The Mechanical Properties of Lithophysal Tuff: Laboratory Experiments.* TDR-EBS-MD-000027 REV 00. Las Vegas, Nevada: Bechtel SAIC Company. ACC: DOC.20040506.0001.

106590 Price, R.H. and Bauer, S.J. 1985. "Analysis of the Elastic and Strength Properties of Yucca Mountain Tuff, Nevada." *Research & Engineering Applications in Rock Masses, Proceedings of the 26th U.S. Symposium on Rock Mechanics, Rapid City, South Dakota, June 26-28, 1985.* Ashworth, E., ed. Pages 89-96. Boston, [Massachusetts]: A.A. Balkema. TIC: 218790.

161289 Price, R.H.; Boyd, P.J.; Martin, R.J.; Haupt, R.W.; and Noel, J.S. 1991. "Mechanical Anisotropy of the Yucca Mountain Tuffs." *High Level Radioactive Waste Management, Proceedings of the Second Annual International Conference, Las Vegas, Nevada, April 28-May 3, 1991. 1,* 268-271. La Grange Park, Illinois: American Nuclear Society. TIC: 204272.

100173 Price, R.H.; Connolly, J.R.; and Keil, K. 1987. *Petrologic and Mechanical Properties of Outcrop Samples of the Welded, Devitrified Topopah Spring Member of the Paintbrush Tuff.* SAND86-1131. Albuquerque, New Mexico: Sandia National Laboratories. ACC: NNA.19870601.0013.

106603 Price, R.H.; Nimick, K.G.; and Zirzow, J.A. 1982. *Uniaxial and Triaxial Compression Test Series on Topopah Spring Tuff.* SAND82-1723. Albuquerque, New Mexico: Sandia National Laboratories. ACC: NNA.19870406.0063.

106604 Price, R.H.; Spence, S.J.; and Jones, A.K. 1984. *Uniaxial Compression Test Series on Topopah Spring Tuff from USW GU-3, Yucca Mountain, Southern Nevada.* SAND83-1646. Albuquerque, New Mexico: Sandia National Laboratories. ACC: NNA.19870406.0252.

100693 Rautman, C.A. and Engstrom, D.A. 1996. *Geology of the USW SD-7 Drill Hole, Yucca Mountain, Nevada (Final Draft).* SAND96-1474. Albuquerque, New Mexico: Sandia National Laboratories. ACC: MOL.19971218.0440.

176610 Rusinko, B.E. 2005. "Contract No. DE-AC28-01RW12101 - Minutes of June 21, 2005 Geotechnical Data Issues and Concerns Meeting." Letter from B.E. Rusinko (BSC) to Distribution, August 23, 2005, PJB:BER:LM-0726056197, with enclosure. ACC: MOL.20050906.0347.

100075 Sawyer, D.A.; Fleck, R.J.; Lanphere, M.A.; Warren, R.G.; Broxton, D.E.; and Hudson, M.R. 1994. "Episodic Caldera Volcanism in the Miocene Southwestern Nevada Volcanic Field: Revised Stratigraphic Framework, {superscript 40}Ar/{superscript 39}Ar Geochronology, and Implications for Magmatism and Extension." *Geological Society of America Bulletin, 106,* (10), 1304-1318. Boulder, Colorado: Geological Society of America. TIC: 222523.

104580 Sawyer, D.A.; Wahl, R.R.; Cole, J.C.; Minor, S.A.; Laczniak, R.J.; Warren, R.G.; Engle, C.M.; and Vega, R.G. 1995. *Preliminary Digital Geological Map Database of the Nevada Test Site Area, Nevada.* Open-File Report 95-0567. Denver, Colorado: U.S. Geological Survey. TIC: 232986.

164774 Schmidtke, R.H. and Lajtai, E.Z. 1985. "The Long-Term Strength of Lac du Bonnet Granite." *International Journal of Rock Mechanics and Mining Science & Geomechanics Abstracts, 22,* (6), 461-465. [New York, New York]: Pergamon. TIC: 254874.

104568 Scholz, C.H. 1968. "Microfracturing and the Inelastic Deformation of Rock in Compression." *Journal of Geophysical Research, 73,* 1417-1432. Washington, D.C.: American Geophysical Union. TIC: 234866.

169724 Scholz, C.H. 1972. "Static Fatigue of Quartz." *Journal of Geophysical Research, 77,* (11), 2104-2114. [Washington, D.C.]: American Geophysical Union. TIC: 224772.

107248 Schuraytz, B.C.; Vogel, T.A.; and Younker, L.W. 1989. "Evidence for Dynamic Withdrawal from a Layered Magma Body: The Topopah Spring Tuff, Southwestern Nevada." *Journal of Geophysical Research, 94,* (B5), 5925-5942. Washington, D.C.: American Geophysical Union. TIC: 225936.

163415 Senseny, P.E. and Parrish, D.K. 1981. *Creep Experiments on Welded Tuff from the Bullfrog Member of the Crater Flat Tuff, Nevada Test Site.* Topical Report RSI-0136. Rapid City, South Dakota: RE/SPEC. ACC: NNA.19940608.0307.

165420 Sobolik, S.R. and George, J.T. 2001. Drift Scale Test: Determination of the In Situ Rock Mass Modulus in the DST Plate Loading Test Niche. SN-SNL-SCI-021-V1 and V2. ACC: MOL.20010605.0094.

163202 Sobolik, S.R.; Finley, R.E.; and Ballard, S. 1999. "Thermal-Mechanical Measurements in the Drift Scale Test, Yucca Mountain, Nevada." *Rock Mechanics for Industry, Proceedings of the 37th U.S. Rock Mechanics Symposium, Vail, Colorado, USA, 6-9 June, 1999.* Amadei, B.; Kranz, R.L.; Scott, G.A.; and Smeallie, P.H., eds. *2,* 735-742. Brookfield, Vermont: A.A. Balkema. TIC: 245246.

162049 Sobolik, S.R.; Finley, R.E.; and Ballard, S. 1998. "Post-Test Comparison of Thermal-Mechanical Measurements vs. Analyses for the In-Situ Single Heater Test, Yucca Mountain, Nevada." *International Journal of Rock Mechanics and Mining Sciences, 35,* (4-5), 649. New York, New York: Pergamon. TIC: 253944.

102096 Tien, P-L.; Updegraff, C.D.; Wahi, K.K.; Siegel, M.D.; and Guzowski, R.V. 1985. *Repository Site Data Report for Unsaturated Tuff, Yucca Mountain, Nevada.* NUREG/CR-4110. Washington, D.C.: U.S. Nuclear Regulatory Commission. ACC: HQS.19880517.1853.

165105 Torquato, S. 1987. "Thermal Conductivity of Disordered Heterogeneous Media from the Microstructure." *Reviews in Chemical Engineering, 4,* (3-4), 151-204. [London, England]: Freund Publishing House. TIC: 249565.

146617 Wickham, G.E.; Tiedemann, H.R.; and Skinner, E.H. 1972. "Support Determinations Based on Geologic Predictions." *Proceedings: North American Rapid Excavation and Tunneling Conference, Chicago, Illinois, June 5-7, 1972.* 43-64. New York, New York: American Institute of Mining, Metallurgical, and Petroleum Engineers. TIC: 226274.

170309 Wiederhorn, S.M. 1968. "Moisture Assisted Crack Growth in Ceramics." *International Journal of Fracture Mechanics, 4,* (2), 171-177. Groningen, The Netherlands: Wolters–Noordhoff Publishing. TIC: 256161.

160809 Williams, N.H. 2001. "Contract #: DE-AC08-01RW12101--Thermal Test Progress Report #7." Letter from N.H. Williams (BSC) to S.P. Mellington (DOE/YMSCO), November 9, 2001, NHW:TJV:bm-1025010261, with enclosure. ACC: MOL.20011207.0060.

176606 Williams, N.H. 2004. "Contract No. DE-AC28-01RW12101 – Transmittal of Report Technical Basis Document No. 4: Mechanical Degradation and Seismic Effects Addressing Fourteen Key Technical Issue (KTI) Agreements Related Repository Design and Thermal-Mechanical Effects." Letter from N.H. Williams (BSC) to J.D. Ziegler (DOE/ORD), June 11, 2004, RK:mm - 0610041943, with enclosure. ACC: MOL.20040812.0085.

157389 Williams, N.H. 2001. "Contract No. DE-AC08-01RW12101 – Uncertainty Analyses and Strategy Letter Report, REV 00, Activity #SA011481M4." Letter from N.H. Williams (BSC) to S.J. Brocoum (DOE/YMSCO), November 19, 2001, JM:cs-1116010483, with enclosure. ACC: MOL.20020109.0064.

8.2 CODES, STANDARDS, REGULATIONS, AND PROCEDURES

176544 10 CFR 63. 2006. Energy: Disposal of High-Level Radioactive Wastes in a Geologic Repository at Yucca Mountain, Nevada. Internet Accessible.

175755 40 CFR 197. 2005. Protection of Environment: Public Health and Environmental Radiation Protection Standards for Yucca Mountain, Nevada. ACC: MOL.20051121.0084.

165094 ASTM D 2938-95. 1995. *Standard Test Method for Unconfined Compressive Strength of Intact Rock Core Specimens.* West Conshohocken, Pennsylvania: American Society for Testing and Materials. TIC: 242992.

145397 ASTM D 3148-96. 1997. *Standard Test Method for Elastic Moduli of Intact Rock Core Specimens in Uniaxial Compression.* West Conshohocken, Pennsylvania: American Society for Testing and Materials. TIC: 247128.

161616 ASTM D 3967-86. 1986. *Standard Test Method for Splitting Tensile Strength of Intact Rock Core Specimens.* Philadelphia, Pennsylvania: American Society for Testing and Materials. TIC: 231530.

161498 ASTM D 3967-92 (Reapproved 1992). *Standard Test Method for Splitting Tensile Strength of Intact Rock Core Specimens.* Philadelphia, Pennsylvania: American Society for Testing and Materials. TIC: 104130.

108612 ASTM D 3967-95. 1995. *Standard Test Method for Splitting Tensile Strength of Intact Rock Core Specimens.* West Conshohocken, Pennsylvania: American Society for Testing and Materials. TIC: 247125.

149445 ASTM D 4394-84. 1985. *Standard Test Method for Determining the In Situ Modulus of Deformation of Rock Mass Using the Rigid Plate Loading Method.* Philadelphia, Pennsylvania: American Society for Testing and Materials. TIC: 231530.

160054 ASTM D 4395-84. 1985. *Standard Test Method for Determining the In Situ Modulus of Deformation of Rock Mass Using the Flexible Plate Loading Method.* Philadelphia, Pennsylvania: American Society for Testing and Materials. TIC: 231530.

118930 ASTM D 4535-85. 1985. *Standard Test Methods for Measurement of Thermal Expansion of Rock Using a Dilatometer.* Philadelphia, Pennsylvania: American Society for Testing and Materials. TIC: 236774.

101786 ASTM D 4971-89. 1989. *Standard Test Method for Determining the In Situ Modulus of Deformation of Rock Using the Diametrically Loaded 76-mm (3-in.) Borehole Jack.* Philadelphia, Pennsylvania: American Society for Testing and Materials. TIC: 245311.

103817 Atomic Energy Act of 1954. 42 U.S.C. 2011 et seq. ACC: MOL.20050511.0158

105989 Energy Policy Act of 1992. 42 U.S.C. 13201 et seq. Internet Accessible.

100017 Energy Policy Act of 1992. Public Law No. 102-486, 106 Stat. 2776. TIC: 233191.

152452 Energy Reorganization Act of 1974. 42 U.S.C. 5801 et seq. Internet Accessible.

100014 Nuclear Waste Policy Act of 1982. Public Law No. 97-425, 96 Stat. 2201. ACC: HQS.19880517.0905.

100016 Nuclear Waste Policy Amendments Act of 1987. Public Law No. 100-203, 101 Stat. 1330. TIC: 223717.

108553 TP-202, Rev. 01. *Measurement of Thermal Conductivity of Geologic Specimens Using the Guarded Heat-Flow Meter Method.* Albuquerque, New Mexico: Sandia National Laboratories. ACC: MOL.19981103.0396.

145491 TP-203, Rev. 01. *Measurement of Thermal Expansion of Geologic Supplies Using a Push Rod Dilatometer.* Albuquerque, New Mexico: Sandia National Laboratories. ACC: MOL.19971121.0264.

108538 TP-204, Rev. 00. *Measurement of Specific Heat of Geologic Samples by Adiabatic Pulse Calorimetry.* Albuquerque, New Mexico: Sandia National Laboratories. ACC: MOL.19981103.0401.

165435 YMP-USGS-GP-56, R0. *Method for Performing Laboratory Direct Shear Strength Tests on Rock Specimens Under Constant Normal Force with Allowance for Elevated Temperature.* Denver, Colorado: U.S. Geological Survey. ACC: MOL.20020930.0328.

AP-3.12Q, Rev. 2, ICN 1. *Design Calculations and Analyses.* Washington, D.C.: U.S. Department of Energy, Office of Civilian Radioactive Waste Management. ACC: DOC.20030827.0013.

EG-PRO-3DP-G04T-00905. *Determination of Quality Levels*.

LP-2.29Q-BSC. *Planning for Scientific Activities.*

LP-SIII.9Q-BSC. *Scientific Analyses.*

LS-PRO-0203. *Q-List and Classification of Structures, Systems, and Components.*

PA-PRO-0301, *Managing Technical Product Inputs*.

PA-PRO-0601, *Document Review*.

IT-PRO-0011. *Software Management*.

8.3 SOURCE DATA, LISTED BY DATA TRACKING NUMBERS

152573 GS000608314224.004. Provisional Results: Geotechnical Data for Station 35+00 to Station 40+00, Main Drift of the ESF. Submittal date: 06/20/2000.

166002 GS000608314224.005. Provisional Results: Geotechnical Data - Full Periphery Maps for the North Ramp of the Exploratory Studies Facility, Stations 4+00 to 8+00. Submittal date: 06/28/2000.

152572 GS000608314224.006. Provisional Results: Geotechnical Data for Station 26+00 to 30+00, North Ramp and Main Drift of the ESF, Full-Periphery Geotechnical Maps (Drawings OA-46-222 through OA-46-226) and Rock Mass Quality Ratings Report. Submittal date: 06/28/2000.

161910 GS021008314224.002. Lithophysal Data Study from the Tptpll in the ECRB from Stations 14+44 to 23+26. Submittal date: 01/28/2003.

177299 GS031083114222.002. Direct Shear Data from Selected Samples of the Topopah Spring Tuff. Submittal date: 06/02/2004.

171367 GS040608314224.001. Large-Lithophysal Inventory Data from the Tptpll and Tptpln in the ECRB from Stations 14+44 to 25+35. Submittal date: 08/19/2004.

107488 GS950508314224.003. Provisional Results: Geotechnical Data - Full Periphery Map Data from North Ramp of the Exploratory Studies Facility, Stations 0+60 to 4+00. Submittal date: 05/24/1995.

168135 GS960408314224.001. Provisional Results: Geotechnical Data – Full Periphery Geotechnical Maps of the North Ramp, Exploratory Studies Facility, Station 8+00 to 10+00, Plots OA-46-201, -202, -203; Geotechnical Report – Rock Mass Quality Ratings. Submittal date: 06/24/1996.

168136 GS960408314224.003. Provisional Results: Geotechnical Data – Full-Periphery Geotechnical Maps (Drawing OA-46-204 through -212) and Rock Mass Quality Ratings from North Ramp of the Exploratory Studies Facility, Stations 10+00 to 18+00. Submittal date: 08/29/1996.

105617 GS960708314224.008. Provisional Results: Geotechnical Data for Station 30 + 00 to Station 35 + 00, Main Drift of the ESF. Submittal date: 08/05/1996.

168137 GS960708314224.009. Provisional Results: Geotechnical Data for Station 18+00 to 26+00, North Ramp of the ESF, Full-Periphery Geotechnical Maps and Rock Mass Quality Ratings Report. Submittal date: 09/09/1996.

106031 GS960708314224.010. Provisional Results: Geotechnical Data for Station 40+00 to Station 45+00, Main Drift of the ESF. Submittal date: 08/05/1996.

106033 GS960908314224.014. Provisional Results - ESF Main Drift, Station 50+00 to Station 55+00. Submittal date: 09/09/1996.

108372 GS960908314224.015. Provisional Results: Geotechnical Data for Stations 30+00 to 40+00, Main Drift of the ESF, Full-Periphery Geotechnical Maps and Rock Mass Quality Ratings Report. Submittal date: 09/09/1996.

108373 GS960908314224.016. Provisional Results: Geotechnical Data for Station 40+00 to 50+00, Main Drift of the ESF, Full-Periphery Geotechnical Maps and Rock Mass Quality Ratings Report. Submittal date: 09/09/1996.

108376 GS960908314224.017. Provisional Results: Geotechnical Data for Stations 50+00 to 55+00, Main Drift of the ESF, Full-Periphery Geotechnical Maps and Rock Mass Quality Ratings Report. Submittal date: 09/09/1996.

106059 GS960908314224.020. Analysis Report: Geology of the North Ramp - Stations 4+00 to 28+00 and Data: Detailed Line Survey and Full-Periphery Geotechnical Map - Alcoves 3 (UPCA) and 4 (LPCA), and Comparative Geologic Cross Section - Stations 0+60 to 28+00. Submittal date: 09/09/1996.

107490 GS970108314224.002. Geotechnical Data for Station 55+00 to Station 60+00, Main Drift of the ESF, Full Periphery Geotechnical Maps. Submittal date: 01/31/1997.

106048 GS970208314224.003. Geotechnical Data for Station 60+00 to Station 65+00, South Ramp of the ESF. Submittal date: 02/12/1997.

107492 GS970208314224.004. Geotechnical Data for Station 60+00 to Station 65+00, South Ramp of the ESF. Submittal date: 02/12/1997.

158430 GS970608314224.007. Provisional Results: Geotechnical Data for the Exploratory Studies Facility, Main Drift, Alcove 5 (DWFA): Heated Drift and Cross Drift Full Periphery Geotechnical Map (Drawing OA-46-300) and Rock Mass Quality Ratings Report. Submittal date: 06/24/1997.

107494 GS970808314224.009. Provisional Results: Geotechnical Data for Station 65+00 to Station 70+00, South Ramp of the ESF; Full-Periphery Geotechnical Maps (Drawings 0A-46-269 through 0A-46-274) and Rock Mass Quality Ratings Report. Submittal date: 08/18/1997.

106050 GS970808314224.010. Provisional Results: Geotechnical Data for Station 70+00 to Station 75+00, South Ramp of the ESF. Submittal date: 08/25/1997.

107495 GS970808314224.011. Provisional Results: Geotechnical Data for Station 70+00 to Station 75+00, South Ramp of the ESF. Submittal date: 08/25/1997.

107497 GS970808314224.013. Provisional Results: Geotechnical Data for Station 75+00 to Station 78+77, South Ramp of the ESF. Submittal date: 08/25/1997.

106025 GS971108314224.025. Revision 1 of Detailed Line Survey Data, Station 26+00 to Station 30+00, North Ramp and Main Drift, Exploratory Studies Facility. Submittal date: 12/03/1997.

106047 GS971108314224.028. Revision 1 of Detailed Line Survey Data, Station 55+00 to Station 60+00, Main Drift and South Ramp, Exploratory Studies Facility. Submittal date: 12/03/1997.

107024 GS980608314221.002. Revised Bedrock Geologic Map of the Yucca Mountain Area, Nye County, Nevada. Submittal date: 06/09/1998.

106748 GS980808312242.014. Physical Properties of Borehole Core Samples and Water Potential Measurements Using the Filter Paper Technique for Borehole Samples from USW SD-6. Submittal date: 08/11/1998.

108404 GS990408314224.003. Full-Periphery Geologic Maps for Station -0+10 to 10+00, ECRB Cross Drift. Submittal date: 09/09/1999.

108405 GS990408314224.004. Full-Periphery Geologic Maps for Station 10+00 to 15+00, ECRB Cross Drift. Submittal date: 09/09/1999.

108408 GS990408314224.005. Full-Periphery Geologic Maps for Station 15+00 to 20+00, ECRB Cross Drift. Submittal date: 09/09/1999.

108409 GS990408314224.006. Full-Periphery Geologic Maps for Station 20+00 to 26+81, ECRB Cross Drift. Submittal date: 09/09/1999.

152554 MO0004QGFMPICK.000. Lithostratigraphic Contacts from MO9811MWDGFM03.000 to be Qualified Under the Data Qualification Plan, TDP-NBS-GS-000001. Submittal date: 04/04/2000.

155229 MO0010CPORGLOG.002. Calculated Porosity from Geophysical Logs Data from "Old 40" Boreholes. Submittal date: 10/16/2000.

155959 MO0010CPORGLOG.003. Calculated Porosity Values at Depth Derived from Qualified Geophysical Log Data from Modern Boreholes. Submittal date: 10/16/2000.

155989 MO0109HYMXPROP.001. Matrix Hydrologic Properties Data. Submittal date: 09/17/2001.

177311 MO0302UCC027BA.006. Stress and Modulus for Plaster and Tuff. Submittal date: 02/19/2003.

166600 MO0309MWDVCNGR.001. Data Files for GFM2000 Representation in the VULCAN Software System. Submittal date: 09/25/2003.

166073 MO0311RCKPRPCS.003. Intact Rock Properties Data on Uniaxial and Triaxial Compressive Strength. Submittal date: 11/04/2003.

177313 MO0311UCC018LM.001. Uniaxial Compression Tests Results. Submittal date: 11/19/2003.

177315 MO0311UCC018LM.002. Brazilian Tensile Strength Rock Tests Analysis Results. Submittal date: 11/19/2003.

177314 MO0311UCC018LM.003. Results from Creep Tests on Rock Specimens. Submittal date: 11/19/2003.

168905 MO0401DQRIRPTS.003. Data Summary for Intact Rock Properties Data on Tensile Strength. Submittal date: 01/07/2004.

168901 MO0402DQRIRPPR.003. Intact Rock Properties Data on Poisson's Ratio and Young's Modulus. Submittal date: 02/19/2004.

171483 MO0408MWDDDMIO.002. Drift Degradation Model Inputs and Outputs. Submittal date: 08/31/2004.

103801 MO9510RIB00002.004. RIB Item: Stratigraphic Characteristics: Geologic/Lithologic Stratigraphy. Submittal date: 06/26/1996.

158392 SN0011F3912298.022. Plate-Loading Measured Displacement and Test Pressure Data (with Results from 10/16/2000 through 10/17/2000). Submittal date: 11/30/2000.

158399 SN0011F3912298.023. Plate-Loading Rock Mass Modulus Data (with Results from 10/16/2000 through 10/17/2000). Submittal date: 11/30/2000.

158322 SN0203L2210196.007. Thermal Expansion and Thermal Conductivity of Test Specimens from the Drift Scale Test Area of the Exploratory Studies Facility at Yucca Mountain, Nevada. VA Supporting Data. Submittal date: 03/06/2002.

165270 SN0206F3504502.011. Revised Data for Changes in Temperature at Each Thermocouple Location for ECRB Thermal K Test 1 (Two-Hole Test). Submittal date: 06/07/2002.

159145 SN0206F3504502.012. Revised Thermal Conductivity, Volumetric Heat Capacity and Thermal Diffusivity Data for ECRB Thermal K Test 1 (Two-Hole Test). Submittal date: 06/07/2002.

159146 SN0206F3504502.013. Revised Thermal Conductivity, Volumetric Heat Capacity and Thermal Diffusivity Data for ECRB Thermal K Test 3 (Three-Hole Test, with Results from 1/22/2002 through 4/9/2002). Submittal date: 06/07/2002.

165429 SN0207F4102102.001. Rock Modulus Slot Test #1, Location 57+70 in the ESF. Submittal date: 07/22/2002.

161883 SN0208F3504502.019. Thermal Conductivity, Volumetric Heat Capacity and Thermal Diffusivity Data for ECRB Thermal K Test 2 (Six-Hole Test). Submittal date: 08/30/2002.

161874 SN0208F4102102.002. Rock Mass Mechanical Properties, Slot Test #1, Location 57+77 in the ESF. Submittal date: 08/27/2002.

165211 SN0208L01B8102.001. Thermal Expansion Properties of Lithophysal Tuff, Batch #1 (Test Dates: August 3, 2002 through August 16, 2002). Submittal date: 08/28/2002.

161871 SN0208L0207502.001. Mechanical Properties of Lithophysal Tuff, Batch #1 (Test Dates: July 31, 2002 through August 16, 2002). Submittal date: 08/20/2002.

163601 SN0209L01A1202.001. Thermal Conductivity Laboratory Data (Including Densities and Porosities) Generated in FY02 on the Topopah Springs Lower Lithophysal (Tptpll) Lithostratigraphic Unit. Submittal date: 09/23/2002.

165218 SN0211L01B8102.002. Thermal Expansion Properties of Lithophysal Tuff, Batch #2 (Test Dates: October 20, 2002 through October 25, 2002). Submittal date: 11/13/2002.

161872 SN0211L0207502.002. Mechanical Properties of Lithophysal Tuff, Batch #2 (Test Dates: October 22, 2002 through October 25, 2002). Submittal date: 11/13/2002.

165432 SN0212F4102102.003. Rock Modulus Slot Test #2, Location 63+83 in the ESF. Submittal date: 12/04/2002.

161875 SN0212F4102102.004. Rock Mass Mechanical Properties, Slot Test #2, Location 63+83 in the ESF. Submittal date: 12/17/2002.

165430 SN0301F4102102.007. Abundance of Lithophysal Features at Slot Test #1, Location 57+77 in the ESF. Submittal date: 01/23/2003.

165431 SN0301F4102102.008. Lithophysal Porosity Summary Report for Slot Test #1, Location 57+77 in the ESF. Submittal date: 01/23/2003.

165433 SN0302F4102102.009. Abundance of Lithophysal Features at Slot Test #2, Location 63+83 in the ESF. Submittal date: 02/14/2003.

165436 SN0302F4102102.010. Lithophysal Porosity Summary Report for Slot Test #2, Location 63+83 in the ESF. Submittal date: 02/14/2003.

165014 SN0302L0207502.003. Mechanical Properties of Lithophysal Tuff, Room Temperature Batch #4, Set 1 (Test Dates: 01/21/03 through 01/23/03). Submittal date: 02/25/2003.

165439 SN0303F4102102.011. Abundance of Lithophysal Features at Slot Test #3, Location 21+25 in the ECRB. Submittal date: 03/12/2003.

165440 SN0303F4102102.012. Lithophysal Porosity Summary Report for Slot Test #3, Location 21+25 in the ECRB. Submittal date: 03/12/2003.

162401 SN0303T0503102.008. Revised Thermal Conductivity of the Non-Repository Layers of Yucca Mountain. Submittal date: 03/19/2003.

165013 SN0305L0207502.004. Mechanical Properties of Lithophysal Tuff, Batch #4, Set 2 (Test Dates: March 5, 2003 through March 13, 2003). Submittal date: 05/01/2003.

163373 SN0305L0207502.005. Material Abundances from Point Counts on Laboratory Mechanical Property Specimens for Batch #1 and Batch #2. Submittal date: 05/20/2003.

165747 SN0305L0207502.006. Porosity of Laboratory Mechanical Properties Test Specimens for Batch #1 and Batch #2. Submittal date: 05/20/2003.

165416 SN0306F3912298.048. Plate-Loading Measured Displacement and Test Pressure Data for 2003 (with Results from 4/30/2003). Submittal date: 06/25/2003.

165015 SN0306L0207502.008. Revised Mechanical Properties of Welded Tuff from the Lower Lithophysal Zone of the Topopah Spring Tuff, Batch #3 (Test Dates: March 6, 2003 through April 18, 2003). Submittal date: 06/20/2003.

164196 SN0307T0510902.003. Updated Heat Capacity of Yucca Mountain Stratigraphic Units. Submittal date: 07/15/2003.

168527 SN0310F3912298.054. Updated Plate-Loading Rock Mass Modulus Data for 2003. Submittal date: 10/27/2003.

169129 SN0404T0503102.011. Thermal Conductivity of the Potential Repository Horizon Rev 3. Submittal date: 04/27/2004.

177261 SN0405F3312393.015. Tunnel Convergence and MPBX Data (with Results from 7/3/1999 through 2/5/2004). Submittal date: 04/14/2005.

170289 SN0406L0212303.002. Static Fatigue Data from New England Research (NER) (Test Dates: 1/2/2004 through 2/25/2004). Submittal date: 06/08/2004.

174955 SN0505L0212303.004. Time to Failure Data from Static Fatigue Experiments on Welded Tuff (Test Dates: 7/12/2004 - 10/27/2004). Submittal date: 05/05/2005.

174956 SN0505L0212303.005. The Strengths of Welded Tuffs Determined in Constant Strain Rate Experiments (Test Dates: 11/12/2003 - 11/21/2003). Submittal date: 05/05/2005.

158300 SNF35110695001.010. Goodman Jack Measurements in the Single Heater Test Block. Submittal date: 05/25/1999.

131356 SNF37100195002.001. Hydraulic Fracturing Stress Measurements in Test Hole: ESF-AOD-HDFR1, Thermal Test Facility, Exploratory Studies Facility at Yucca Mountain. Submittal date: 12/18/1996.

109002 SNL01A05059301.005. Laboratory Thermal Conductivity Data for Boreholes UE25 NRG-4, NRG-5; USW NRG-6 and NRG-7/7A. Submittal date: 02/07/1996.

108980 SNL01A05059301.007. Calculated Porosities for Thermal Conductivity Specimens from Boreholes UE25 NRG-4, UE25 NRG-5, USW NRG-6, and USW NRG-7/7a. Submittal date: 10/14/1998.

177308 SNL01B02019501.001. Thermal Expansion of the Paintbrush Tuff Recovered from Borehole USW SD-12 at Pressures to 30 MPA: Data Report. Submittal date: 10/10/1997.

129168 SNL01B05059301.006. Laboratory Thermal Expansion Data for Boreholes UE25 NRG-4, NRG-5; USW NRG-6 and NRG-7/7A. Submittal date: 02/07/1996.

148289 SNL01C12159302.002. Laboratory Measurements of Heat Capacity/Thermal Capacitance, for Boreholes UE25 NRG-4 and NRG-5. Submittal date: 02/07/1996.

120572 SNL02030193001.001. Mechanical Properties Data for Drillhole USW NRG-6 Samples from Depth 22.2 ft. to 328.7 ft. Submittal date: 05/17/1993.

108410 SNL02030193001.027. Summary of Bulk Property Measurements Including Saturated Bulk Density for NRG-2, NRG-2A, NRG-2B, NRG-3, NRG-4, NRG-5, NRG-6, NRG-7/7A, SD-9, and SD-12. Submittal date: 08/14/1996.

162205 SNL02071596001.001. Creep Properties of the Paintbrush Tuff Recovered From Borehole USW NGR-7/7A: Data Report. Submittal date: 10/01/1997.

161629 SNL02112293001.001. Results from Shear Stress Experiments on Natural Fractures on Samples from NRG-4 and NRG-6 Drillholes. Submittal date: 08/18/1994.

108411 SNL02112293001.002. Results from Shear Stress Experiments on Natural Fractures from NRG-7. Submittal date: 03/10/1995.

108412 SNL02112293001.003. Results from Shear Stress Experiments on Natural Fractures from NRG-4 & NRG-6. Submittal date: 03/13/1995.

108413 SNL02112293001.005. Mechanical Properties of Fractures in Specimens from Drillhole USW SD-9. Submittal date: 07/15/1996.

159992 SNL02112293001.006. Mechanical Properties of Fractures in Specimens from Drillhole USW SD-7 and ESF-TMA-MPBX-3 at Elevated Temperature. Submittal date: 07/30/1996.

108414 SNL02112293001.007. Mechanical Properties of Fractures in Specimens from Drillholes USW NRG-7/7A and USW SD-12. Submittal date: 08/08/1996.

109722 SNL22080196001.001. Thermal Properties of Test Specimens from the Single Heater Test Area in the Thermal Testing Facility at Yucca Mountain, Nevada. Submittal date: 08/15/1996.

119042 SNL22080196001.003. Posttest Laboratory Thermal and Mechanical Characterization for Single Heater Test (SHT) Block. Submittal date: 08/26/1998.

153138 SNL22100196001.002. Laboratory Measurements of Thermal Expansion and Thermal Conductivity for Test Specimens from Alcove 5 and 7 and from SD Drill Holes of the Exploratory Studies Facility at Yucca Mountain, Nevada. Submittal date: 08/25/97.

158213 SNL22100196001.006. Laboratory Measurements of Thermal Conductivity as a Function of Saturation State for Welded and Nonwelded Tuff Specimens. Submittal date: 06/08/1998.

159116 UN0106SPA013GD.004. Drift Scale Thermal Test (DST) REKA Probe Developed Data for Thermal Conductivity and Diffusivity for the Period 05/01/1998 to 04/30/2001 (Heated Measurements for Boreholes 151, 152, and 153). Submittal date: 06/28/2001.

159119 UN0201SPA013GD.007. DST REKA Probe Developed Data for Thermal Conductivity and Diffusivity for the Period 05/01/2001 to 12/31/2001 (Heated Measurements for Boreholes 151 and 152). Submittal date: 01/07/2002.

8.4 SOFTWARE CODES

160577 FRACMAN V. 2.512. 1999. WINDOWS NT. STN: 10114-2.511-00.

161950 PFC2D V. 2.0. 2002. WINDOWS 2000/NT 4.0. STN: 10828-2.0-00.

169930 PFC2D V. 2.0. 2004. WINDOWS 2000. STN: 10828-2.0-01.

160612 PFC3D V. 2.0. 2002. WINDOWS 2000/NT 4.0. STN: 10830-2.0-00.

169931 PFC3D V. 2.0. 2004. WINDOWS 2000. STN: 10830-2.0-01.

177556 RocLab V1.020. 2005. Microsoft Windows. NA.

161949 UDEC V. 3.1 Sub-Release 3.10.109. 2002. WINDOWS 2000/NT 4.0. STN: 10173-3.1-00.

INTENTIONALLY LEFT BLANK

APPENDIX A
INTACT ROCK MECHANICAL PROPERTIES DATA

Table A-1 Intact Rock Mechanical Properties Data - Strength and Elastic Properties Data

Axial Stress, σ_1 (MPa)	Axial Stress, effective σ_1' (MPa)	Confining Pressure (MPa) σ_3	Pore Pressure (MPa)	Confining Pressure, Effective (MPa), σ_3'	Differential Strength, (MPa) $\sigma_1 - \sigma_3$	Young's Modulus (GPa)	Poisson's Ratio	TM Unit	Litho-stratigraphic Unit	General Location	Sample Location	Specimen Number	Depth (ft)	Specimen Diameter (mm)	Specimen Length (mm)	Specimen Saturation	Specimen Temperature (deg. C)	l/d Ratio	Strain Rate (1/s)	Specimen Orientation (degree)	Test Standard	Laboratory	Failure Strain (millistrain)	Rock Property	Source DTN	Notes
89.4	87.4	2	2	0	89.4	28		TSw2	Tptpmn	Busted Butte	Busted Butte	10AE48Y		50.8	101.60	saturated	150	2.0	1.00E-05			SNL	4.9	Uniaxial compressive strength	MO0311RCKPRPCS.003, MO0402DQRIRPPR.003	Undrained test w/ pore pressure of 2 MPa.
135.8	133.8	2	2	0	135.8	30.6		TSw2	Tptpmn	Busted Butte	Busted Butte	10AE3W		50.8	101.60	saturated	150	2.0	1.00E-05			SNL	5.7	Uniaxial compressive strength	MO0311RCKPRPCS.003, MO0402DQRIRPPR.003	Undrained test w/ pore pressure of 2 MPa.
129.7	127.7	2	2	0	129.7	32.6		TSw2	Tptpmn	Busted Butte	Busted Butte	10AE29W		50.8	101.60	saturated	150	2.0	1.00E-05			SNL	5.3	Uniaxial compressive strength	MO0311RCKPRPCS.003, MO0402DQRIRPPR.003	Undrained test w/ pore pressure of 2 MPa.
114.6	112.6	2	2	0	114.6	32.7		TSw2	Tptpmn	Busted Butte	Busted Butte	10AE41Z		50.8	101.60	saturated	150	2.0	1.00E-05			SNL	5.5	Uniaxial compressive strength	MO0311RCKPRPCS.003, MO0402DQRIRPPR.003	Undrained test w/ pore pressure of 2 MPa.
60.4	60.4	0	0	0	60.4	11.7	0.1	CFUn	Tcbbt	ESF/ECRB/Borehole	USW G-1	794.9	2607.9	25.4		saturated	23	2.0	1.00E-05			Terra Tek	5.1	Uniaxial compressive strength	MO0311RCKPRPCS.003, MO0402DQRIRPPR.003	Drained test.
72.7	72.7	0	0	0	72.7	17.2	0.16	CFUn	Tcbbt	ESF/ECRB/Borehole	USW G-1	794.9	2607.9	25.4		saturated	23	2.0	1.00E-05			Terra Tek	4.9	Uniaxial compressive strength	MO0311RCKPRPCS.003, MO0402DQRIRPPR.003	Drained test.
67.1	67.1	0	0	0	67.1	11.6	0.17	CFUn	Tcblv	ESF/ECRB/Borehole	USW G-1	787.9	2584.9	25.4		saturated	23	2.0	1.00E-05			Terra Tek	6.4	Uniaxial compressive strength	MO0311RCKPRPCS.003, MO0402DQRIRPPR.003	Drained test.
73.9	73.9	0	0	0	73.9	12.5	0.13	CFUn	Tcblv	ESF/ECRB/Borehole	USW G-1	787.9	2584.9	25.4		saturated	23	2.0	1.00E-05			Terra Tek	6.9	Uniaxial compressive strength	MO0311RCKPRPCS.003, MO0402DQRIRPPR.003	Drained test.
101	101	0	0	0	101	20.6	0.12	CFUn	Tcblv	ESF/ECRB/Borehole	USW G-1	781.2	2563.0	25.4		saturated	23	2.0	1.00E-05			Terra Tek	5.2	Uniaxial compressive strength	MO0311RCKPRPCS.003, MO0402DQRIRPPR.003	Drained test.
104	104	0	0	0	104	22.7	0.19	CFUn	Tcblv	ESF/ECRB/Borehole	USW G-1	781.2	2563.0	25.4		saturated	23	2.0	1.00E-05			Terra Tek	5.5	Uniaxial compressive strength	MO0311RCKPRPCS.003, MO0402DQRIRPPR.003	Drained test.
54	54	0	0	0	54	6.37	0.05	CFUn	Tcbm	ESF/ECRB/Borehole	UE-25 a #1	2452	2452.0	56	L:D = 2:1	ambient	22	2.0	1.00E-04			SNL		Uniaxial compressive strength	MO0311RCKPRPCS.003, MO0402DQRIRPPR.003	Drained test.
37.2	37.2	0	0	0	37.2	3.82	0.12	CFUn	Tcbm	ESF/ECRB/Borehole	USW G-1	752.2	2467.8	25.4		saturated	23	2.0	1.00E-05			Terra Tek	7.4	Uniaxial compressive strength	MO0311RCKPRPCS.003, MO0402DQRIRPPR.003	Drained test.
45.2	45.2	0	0	0	45.2	6.56	0.12	CFUn	Tcbm	ESF/ECRB/Borehole	USW G-1	752.2	2467.8	25.4		saturated	23	2.0	1.00E-05			Terra Tek	6.0	Uniaxial compressive strength	MO0311RCKPRPCS.003, MO0402DQRIRPPR.003	Drained test.
38.3	38.3	0	0	0	38.3	12		CFUn	Tcbm	ESF/ECRB/Borehole	USW G-1	757.8	2486.2	25.4		saturated	23	2.0	1.00E-05			Terra Tek	3.6	Uniaxial compressive strength	MO0311RCKPRPCS.003, MO0402DQRIRPPR.003	Drained test.
46	46	0	0	0	46	13.1	0.09	CFUn	Tcbm	ESF/ECRB/Borehole	USW G-1	757.8	2486.2	25.4		saturated	23	2.0	1.00E-05			Terra Tek	5.1	Uniaxial compressive strength	MO0311RCKPRPCS.003, MO0402DQRIRPPR.003	Drained test.
47	47	0	0	0	47	13.7	0.11	CFUn	Tcbm	ESF/ECRB/Borehole	USW G-1	757.8	2486.2	25.4		saturated	23	2.0	1.00E-05			Terra Tek	5.2	Uniaxial compressive strength	MO0311RCKPRPCS.003, MO0402DQRIRPPR.003	Drained test.
117	117	0	0	0	117	14	0.09	CFUn	Tcbm	ESF/ECRB/Borehole	USW G-1	773.5	2537.7	25.4		saturated	23	2.0	1.00E-05			Terra Tek	7.5	Uniaxial compressive strength	MO0311RCKPRPCS.003, MO0402DQRIRPPR.003	Drained test.
59	59	0	0	0	59	14.6	0.14	CFUn	Tcbm	ESF/ECRB/Borehole	USW G-1	757.8	2486.2	25.4		saturated	23	2.0	1.00E-05			Terra Tek	5.8	Uniaxial compressive strength	MO0311RCKPRPCS.003, MO0402DQRIRPPR.003	Drained test.
58	58	0	0	0	58	15.1		CFUn	Tcbm	ESF/ECRB/Borehole	USW G-1	762.4	2501.3	25.4		saturated	23	2.0	1.00E-05			Terra Tek	4.1	Uniaxial compressive strength	MO0311RCKPRPCS.003, MO0402DQRIRPPR.003	Drained test.
58	58	0	0	0	58	15.8	0.13	CFUn	Tcbm	ESF/ECRB/Borehole	USW G-1	762.4	2501.3	25.4		saturated	23	2.0	1.00E-05			Terra Tek	4.7	Uniaxial compressive strength	MO0311RCKPRPCS.003, MO0402DQRIRPPR.003	Drained test.
49.9	49.9	0	0	0	49.9	15.8		CFUn	Tcbm	ESF/ECRB/Borehole	USW G-1	757.8	2486.2	25.4		saturated	23	2.0	1.00E-05			Terra Tek	4.0	Uniaxial compressive strength	MO0311RCKPRPCS.003, MO0402DQRIRPPR.003	Drained test.
59	59	0	0	0	59	16.4	0.11	CFUn	Tcbm	ESF/ECRB/Borehole	USW G-1	762.4	2501.3	25.4		saturated	23	2.0	1.00E-05			Terra Tek	4.8	Uniaxial compressive strength	MO0311RCKPRPCS.003, MO0402DQRIRPPR.003	Drained test.
59	59	0	0	0	59	17.2	0.14	CFUn	Tcbm	ESF/ECRB/Borehole	USW G-1	762.4	2501.3	25.4		saturated	23	2.0	1.00E-05			Terra Tek	4.5	Uniaxial compressive strength	MO0311RCKPRPCS.003, MO0402DQRIRPPR.003	Drained test.
72.9	72.9	0	0	0	72.9	17.2		CFUn	Tcbm	ESF/ECRB/Borehole	USW G-1	762.4	2501.3	25.4		saturated	23	2.0	1.00E-05			Terra Tek	4.9	Uniaxial compressive strength	MO0311RCKPRPCS.003, MO0402DQRIRPPR.003	Drained test.
60.1	60.1	0	0	0	60.1	18.2		CFUn	Tcbm	ESF/ECRB/Borehole	USW G-1	757.8	2486.2	25.4		saturated	23	2.0	1.00E-05			Terra Tek	4.0	Uniaxial compressive strength	MO0311RCKPRPCS.003, MO0402DQRIRPPR.003	Drained test.
73.2	73.2	0	0	0	73.2	20.8		CFUn	Tcbm	ESF/ECRB/Borehole	USW G-1	762.4	2501.3	25.4		saturated	23	2.0	1.00E-05			Terra Tek	4.0	Uniaxial compressive strength	MO0311RCKPRPCS.003, MO0402DQRIRPPR.003	Drained test.
23.6	23.6	0	0	0	23.6	2.64	0.13	CFUn	Tcbuc	ESF/ECRB/Borehole	USW G-1	740.3	2428.8	25.4		saturated	23	2.0	1.00E-05			Terra Tek	6.9	Uniaxial compressive strength	MO0311RCKPRPCS.003, MO0402DQRIRPPR.003	Drained test.
29.2	29.2	0	0	0	29.2	3.18	0.13	CFUn	Tcbuc	ESF/ECRB/Borehole	USW G-1	740.3	2428.8	25.4		saturated	23	2.0	1.00E-05			Terra Tek	6.7	Uniaxial compressive strength	MO0311RCKPRPCS.003, MO0402DQRIRPPR.003	Drained test.
26.4	26.4	0	0	0	26.4	3.24	0.13	CFUn	Tcbuc	ESF/ECRB/Borehole	USW G-1	740.3	2428.8	25.4		saturated	23	2.0	1.00E-05			Terra Tek	6.6	Uniaxial compressive strength	MO0311RCKPRPCS.003, MO0402DQRIRPPR.003	Drained test.
27	27	0	0	0	27	7.74	0.11	CFUn	Tcbuc	ESF/ECRB/Borehole	USW G-1	733.4	2406.1	25.4		saturated	23	2.0	1.00E-05			Terra Tek	5.0	Uniaxial compressive strength	MO0311RCKPRPCS.003, MO0402DQRIRPPR.003	Drained test.
30.4	30.4	0	0	0	30.4	8.1		CFUn	Tcbuc	ESF/ECRB/Borehole	USW G-1	736	2414.7	25.4		saturated	23	2.0	1.00E-05			Terra Tek	3.8	Uniaxial compressive strength	MO0311RCKPRPCS.003, MO0402DQRIRPPR.003	Drained test.
29.2	29.2	0	0	0	29.2	8.38	0.14	CFUn	Tcbuc	ESF/ECRB/Borehole	USW G-1	721.4	2366.8	25.4		saturated	23	2.0	1.00E-05			Terra Tek	5.0	Uniaxial compressive strength	MO0311RCKPRPCS.003, MO0402DQRIRPPR.003	Drained test.
29	29	0	0	0	29	8.67	0.16	CFUn	Tcbuc	ESF/ECRB/Borehole	USW G-1	736	2414.7	25.4		saturated	23	2.0	1.00E-05			Terra Tek	5.3	Uniaxial compressive strength	MO0311RCKPRPCS.003, MO0402DQRIRPPR.003	Drained test.
32	32	0	0	0	32	8.89	0.13	CFUn	Tcbuc	ESF/ECRB/Borehole	USW G-1	733.4	2406.1	25.4		saturated	23	2.0	1.00E-05			Terra Tek	5.3	Uniaxial compressive strength	MO0311RCKPRPCS.003, MO0402DQRIRPPR.003	Drained test.
35	35	0	0	0	35	9.2	0.12	CFUn	Tcbuc	ESF/ECRB/Borehole	USW G-1	736	2414.7	25.4		saturated	23	2.0	1.00E-05			Terra Tek	6.0	Uniaxial compressive strength	MO0311RCKPRPCS.003, MO0402DQRIRPPR.003	Drained test.
36	36	0	0	0	36	9.26	0.13	CFUn	Tcbuc	ESF/ECRB/Borehole	USW G-1	736	2414.7	25.4		saturated	23	2.0	1.00E-05			Terra Tek	6.0	Uniaxial compressive strength	MO0311RCKPRPCS.003, MO0402DQRIRPPR.003	Drained test.
35.8	35.8	0	0	0	35.8	9.73		CFUn	Tcbuc	ESF/ECRB/Borehole	USW G-1	733.4	2406.1	25.4		saturated	23	2.0	1.00E-05			Terra Tek	3.9	Uniaxial compressive strength	MO0311RCKPRPCS.003, MO0402DQRIRPPR.003	Drained test.
34.7	34.7	0	0	0	34.7	9.82		CFUn	Tcbuc	ESF/ECRB/Borehole	USW G-1	733.4	2406.1	25.4		saturated	23	2.0	1.00E-05			Terra Tek	4.1	Uniaxial compressive strength	MO0311RCKPRPCS.003, MO0402DQRIRPPR.003	Drained test.
36	36	0	0	0	36	10		CFUn	Tcbuc	ESF/ECRB/Borehole	USW G-1	736	2414.7	25.4		saturated	23	2.0	1.00E-05			Terra Tek	4.0	Uniaxial compressive strength	MO0311RCKPRPCS.003, MO0402DQRIRPPR.003	Drained test.
38	38	0	0	0	38	10.2		CFUn	Tcbuc	ESF/ECRB/Borehole	USW G-1	736	2414.7	25.4		saturated	23	2.0	1.00E-05			Terra Tek	4.2	Uniaxial compressive strength	MO0311RCKPRPCS.003, MO0402DQRIRPPR.003	Drained test.
19.1	19.1	0	0	0	19.1	2.72	0.03	CFUn	Tcbuv	ESF/ECRB/Borehole	USW G-1	693.7	2275.9	25.4		saturated	23	2.0	1.00E-05			Terra Tek	5.4	Uniaxial compressive strength	MO0311RCKPRPCS.003, MO0402DQRIRPPR.003	Drained test.
17.9	17.9	0	0	0	17.9	2.76	0.08	CFUn	Tcbuv	ESF/ECRB/Borehole	USW G-1	680.3	2231.9	25.4		saturated	23	2.0	1.00E-05			Terra Tek	5.2	Uniaxial compressive strength	MO0311RCKPRPCS.003, MO0402DQRIRPPR.003	Drained test.
30.4	30.4	0	0	0	30.4	3.73	0.04	CFUn	Tcbuv	ESF/ECRB/Borehole	USW G-1	693.7	2275.9	25.4		saturated	23	2.0	1.00E-05			Terra Tek	5.8	Uniaxial compressive strength	MO0311RCKPRPCS.003, MO0402DQRIRPPR.003	Drained test.
29.9	29.9	0	0	0	29.9	5.76	0.07	CFUn	Tcbuv	ESF/ECRB/Borehole	USW G-1	693.7	2275.9	25.4		saturated	23	2.0	1.00E-05			Terra Tek	4.6	Uniaxial compressive strength	MO0311RCKPRPCS.003, MO0402DQRIRPPR.003	Drained test.
23.7	23.7	0	0	0	23.7	6.24	0.06	CFUn	Tcbuv	ESF/ECRB/Borehole	USW G-1	689.1	2260.8	25.4		saturated	23	2.0	1.00E-05			Terra Tek	4.0	Uniaxial compressive strength	MO0311RCKPRPCS.003, MO0402DQRIRPPR.003	Drained test.
24.1	24.1	0	0	0	24.1	8.17	0.18	CFUn	Tcbuv	ESF/ECRB/Borehole	USW G-1	704.7	2312.0	25.4		saturated	23	2.0	1.00E-05			Terra Tek	3.4	Uniaxial compressive strength	MO0311RCKPRPCS.003, MO0402DQRIRPPR.003	Drained test.
32.7	32.7	0	0	0	32.7	9.56	0.09	CFUn	Tcbuv	ESF/ECRB/Borehole	USW G-1	704.7	2312.0	25.4		saturated	23	2.0	1.00E-05			Terra Tek	3.5	Uniaxial compressive strength	MO0311RCKPRPCS.003, MO0402DQRIRPPR.003	Drained test.
11.7	11.7	0	0	0	11.7	3.14	0.09	CFUn	Tcpbt	ESF/ECRB/Borehole	USW G-1	604.9	1984.6	25.4		saturated	23	2.0	1.00E-05			Terra Tek	3.5	Uniaxial compressive strength	MO0311RCKPRPCS.003, MO0402DQRIRPPR.003	Drained test.
13.6	13.6	0	0	0	13.6	3.21	0.05	CFUn	Tcpbt	ESF/ECRB/Borehole	USW G-1	604.9	1984.6	25.4		saturated	23	2.0	1.00E-05			Terra Tek	4.0	Uniaxial compressive strength	MO0311RCKPRPCS.003, MO0402DQRIRPPR.003	Drained test.
14.7	14.7	0	0	0	14.7	4.91	0.43	CFUn	Tcpbt	ESF/ECRB/Borehole	USW G-1	604.9	1984.6	25.4		saturated	23	2.0	1.00E-05			Terra Tek	3.6	Uniaxial compressive strength	MO0311RCKPRPCS.003, MO0402DQRIRPPR.003	Drained test.
13.5	13.5	0	0	0	13.5	5.25	0.39	CFUn	Tcpbt	ESF/ECRB/Borehole	USW G-1	604.9	1984.6	25.4		saturated	23	2.0	1.00E-05			Terra Tek	3.0	Uniaxial compressive strength	MO0311RCKPRPCS.003, MO0402DQRIRPPR.003	Drained test.
47.5	47.5	0	0	0	47.5	8.58	0.11	CFUn	Tcpbt	ESF/ECRB/Borehole	USW G-1	661.4	2169.9	25.4		saturated	23	2.0	1.00E-05			Terra Tek	4.6	Uniaxial compressive strength	MO0311RCKPRPCS.003, MO0402DQRIRPPR.003	Drained test.
42.3	42.3	0	0	0	42.3	8.67	0.11	CFUn	Tcpbt	ESF/ECRB/Borehole	USW G-1	661.4	2169.9	25.4		saturated	23	2.0	1.00E-05			Terra Tek	4.6	Uniaxial compressive strength	MO0311RCKPRPCS.003, MO0402DQRIRPPR.003	Drained test.
130	130	0		0	130	47.9	0.3	CFUn	Tcplc	ESF/ECRB/Borehole	UE-25 a #1	2014	2014.0	56	L:D = 2:1	ambient	22	2.0	1.00E-04			SNL		Uniaxial compressive strength	MO0311RCKPRPCS.003, MO0402DQRIRPPR.003	L:D = 2:1 or greater; Specimen diameter: 64, 48
32.2	32.2	0		0	32.2	7.84	0.18	CFUn	Tcplv	ESF/ECRB/Borehole	UE 25A#1	2039	2039.0	56	L:D = 2:1	ambient	22	2.0	1.00E-04			SANDIA		Uniaxial compressive strength	MO0311RCKPRPCS.003, MO0402DQRIRPPR.003	L:D = 2:1 or greater; Specimen diameter: 64, 48
84.2	84.2	0	0	0	84.2	10.1	0.07	CFUn	Tctlc	ESF/ECRB/Borehole	USW G-1	913.4	2996.7	25.4		saturated	23	2.0	1.00E-05			Terra Tek	6.3	Uniaxial compressive strength	MO0311RCKPRPCS.003, MO0402DQRIRPPR.003	Drained test.
40.9	40.9	0		0	40.9	18.9		CFUn	Tctlc	ESF/ECRB/Borehole	USW G-1	G12996.9 SLD	2996.9	25.3	51	saturated	22	2.0	1.00E-05			Terra Tek	2.9	Uniaxial compressive strength	MO0311RCKPRPCS.003, MO0402DQRIRPPR.003	

Table A-1 Intact Rock Mechanical Properties Data - Strength and Elastic Properties Data

Axial Stress, σ_1 (MPa)	Axial Stress, effective σ_1' (MPa)	Confining Pressure (MPa) σ_3	Pore Pressure (MPa)	Confining Pressure, Effective (MPa), σ_3'	Differential Strength, (MPa) $\sigma_1'-\sigma_3'$	Young's Modulus (GPa)	Poisson's Ratio	TM Unit	Litho-stratigraphic Unit	General Location	Sample Location	Specimen Number	Depth (ft)	Specimen Diameter (mm)	Specimen Length (mm)	Specimen Saturation	Specimen Temperature (deg. C)	l/d Ratio	Strain Rate (1/s)	Specimen Orientation (degree)	Test Standard	Laboratory	Failure Strain (millistrain)	Rock Property	Source DTN	Notes
90.7	90.7	0	0	0	90.7	21.8	0.24	CFUn	Tctlc	ESF/ECRB/Borehole	USW G-1	913.4	2996.7	25.4		saturated	23	2.0	1.00E-05			Terra Tek	3.9	Uniaxial compressive strength	MO0311RCKPRPCS.003, MO0402DQRIRPPR.003	Drained test.
67.6	67.6	0		0	67.6	22.5	0.23	CFUn	Tctlc	ESF/ECRB/Borehole	USW G-1	G12996.9 SLB	2996.9	25.3	51	saturated	22	2.0	1.00E-05			Terra Tek	3.7	Uniaxial compressive strength	MO0311RCKPRPCS.003, MO0402DQRIRPPR.003	
32.2	32.2	0	0	0	32.2	2.61	0.07	CFUn	Tctlv	ESF/ECRB/Borehole	USW G-1	975.4	3200.1	25.4		saturated	23	2.0	1.00E-05			Terra Tek	7.8	Uniaxial compressive strength	MO0311RCKPRPCS.003, MO0402DQRIRPPR.003	Drained test.
26.1	26.1	0	0	0	26.1	4.9	0.15	CFUn	Tctlv	ESF/ECRB/Borehole	USW G-1	1066.3	3498.3	25.4		saturated	23	2.0	1.00E-05			Terra Tek	4.6	Uniaxial compressive strength	MO0311RCKPRPCS.003, MO0402DQRIRPPR.003	Drained test.
24.4	24.4	0		0	24.4	5.17		CFUn	Tctlv	ESF/ECRB/Borehole	USW G-1	G13202.7 SLG	3202.7	25.3	51	saturated	22	2.0	1.00E-02			SNL	5.0	Uniaxial compressive strength	MO0311RCKPRPCS.003, MO0402DQRIRPPR.003	
17.4	17.4	0		0	17.4	5.47		CFUn	Tctlv	ESF/ECRB/Borehole	USW G-1	G13498.4 SLD	3498.4	25.3	51	saturated	22	2.0	1.00E-05			SNL	3.1	Uniaxial compressive strength	MO0311RCKPRPCS.003, MO0402DQRIRPPR.003	
17.8	17.8	0		0	17.8	5.56	0.31	CFUn	Tctlv	ESF/ECRB/Borehole	USW G-1	G13498.4 SLB	3498.4	25.3	51	saturated	22	2.0	1.00E-05			SNL	3.5	Uniaxial compressive strength	MO0311RCKPRPCS.003, MO0402DQRIRPPR.003	
20.2	20.2	0		0	20.2	5.8	0.20	CFUn	Tctlv	ESF/ECRB/Borehole	USW G-1	G13102.3 SLD	3102.3	25.3	51	saturated	22	2.0	1.00E-05			SNL	4.2	Uniaxial compressive strength	MO0311RCKPRPCS.003, MO0402DQRIRPPR.003	
27.6	27.6	0	0	0	27.6	6.3	0.17	CFUn	Tctlv	ESF/ECRB/Borehole	USW G-1	1066.3	3498.3	25.4		saturated	23	2.0	1.00E-05			Terra Tek	4.1	Uniaxial compressive strength	MO0311RCKPRPCS.003, MO0402DQRIRPPR.003	Drained test.
25.3	25.3	0		0	25.3	6.42		CFUn	Tctlv	ESF/ECRB/Borehole	USW G-1	G13202.7 SLD	3202.7	25.3	51	saturated	22	2.0	1.00E-04			SNL	5.0	Uniaxial compressive strength	MO0311RCKPRPCS.003, MO0402DQRIRPPR.003	
31.1	31.1	0		0	31.1	6.63		CFUn	Tctlv	ESF/ECRB/Borehole	USW G-1	G13202.7 SLA	3202.7	25.3	51	saturated	22	2.0	1.00E-05			SNL	5.2	Uniaxial compressive strength	MO0311RCKPRPCS.003, MO0402DQRIRPPR.003	
29.9	29.9	0	0	0	29.9	6.66	0.23	CFUn	Tctlv	ESF/ECRB/Borehole	USW G-1	1037.9	3405.1	25.4		saturated	23	2.0	1.00E-05			Terra Tek	3.9	Uniaxial compressive strength	MO0311RCKPRPCS.003, MO0402DQRIRPPR.003	Drained test.
37.1	37.1	0	0	0	37.1	6.78	0.16	CFUn	Tctlv	ESF/ECRB/Borehole	USW G-1	945.6	3102.3	25.4		saturated	23	2.0	1.00E-05			Terra Tek	5.0	Uniaxial compressive strength	MO0311RCKPRPCS.003, MO0402DQRIRPPR.003	Drained test.
14.5	14.5	0		0	14.5	7.04	0.30	CFUn	Tctlv	ESF/ECRB/Borehole	USW G-1	G13202.7 SLI	3202.7	25.3	51	saturated	22	2.0	1.00E-06			SNL	3.1	Uniaxial compressive strength	MO0311RCKPRPCS.003, MO0402DQRIRPPR.003	
41.5	41.5	0	0	0	41.5	7.2	0.14	CFUn	Tctlv	ESF/ECRB/Borehole	USW G-1	945.6	3102.3	25.4		saturated	23	2.0	1.00E-05			Terra Tek	5.0	Uniaxial compressive strength	MO0311RCKPRPCS.003, MO0402DQRIRPPR.003	Drained test.
25.8	25.8	0		0	25.8	7.36		CFUn	Tctlv	ESF/ECRB/Borehole	USW G-1	G13200.2 SLD	3200.2	25.3	51	saturated	22	2.0	1.00E-05			SNL	4.8	Uniaxial compressive strength	MO0311RCKPRPCS.003, MO0402DQRIRPPR.003	
52.6	52.6	0	0	0	52.6	7.92	0.19	CFUn	Tctlv	ESF/ECRB/Borehole	USW G-1	975.4	3200.1	25.4		saturated	23	2.0	1.00E-05			Terra Tek	5.5	Uniaxial compressive strength	MO0311RCKPRPCS.003, MO0402DQRIRPPR.003	Drained test.
51.7	51.7	0	0	0	51.7	8.26	0.11	CFUn	Tctlv	ESF/ECRB/Borehole	USW G-1	1008.3	3308.0	25.4		saturated	23	2.0	1.00E-05			Terra Tek	5.7	Uniaxial compressive strength	MO0311RCKPRPCS.003, MO0402DQRIRPPR.003	Drained test.
26.5	26.5	0		0	26.5	8.26	0.14	CFUn	Tctlv	ESF/ECRB/Borehole	USW G-1	G13202.7 SLJ	3202.7	25.3	51	saturated	22	2.0	1.00E-06			SNL	5.0	Uniaxial compressive strength	MO0311RCKPRPCS.003, MO0402DQRIRPPR.003	
25.6	25.6	0		0	25.6	8.47	0.26	CFUn	Tctlv	ESF/ECRB/Borehole	USW G-1	G13308.0 SLB	3308.0	25.3	51	saturated	22	2.0	1.00E-05			SNL	3.3	Uniaxial compressive strength	MO0311RCKPRPCS.003, MO0402DQRIRPPR.003	
33	33	0		0	33	8.6	0.17	CFUn	Tctlv	ESF/ECRB/Borehole	USW G-1	G13200.2 SLB	3200.2	25.3	51	saturated	22	2.0	1.00E-05			SNL	4.7	Uniaxial compressive strength	MO0311RCKPRPCS.003, MO0402DQRIRPPR.003	
22.1	22.1	0		0	22.1	8.76		CFUn	Tctlv	ESF/ECRB/Borehole	USW G-1	G13202.7 SLE	3202.7	25.3	51	saturated	22	2.0	1.00E-04			SNL	3.2	Uniaxial compressive strength	MO0311RCKPRPCS.003, MO0402DQRIRPPR.003	
30	30	0		0	30.0	8.85	0.18	CFUn	Tctlv	ESF/ECRB/Borehole	USW G-1	G13405.2 SLB	3405.2	25.3	51	saturated	22	2.0	1.00E-05			SNL	3.5	Uniaxial compressive strength	MO0311RCKPRPCS.003, MO0402DQRIRPPR.003	
32.6	32.6	0		0	32.6	8.97	0.09	CFUn	Tctlv	ESF/ECRB/Borehole	USW G-1	G13202.7 SLF	3202.7	25.3	51	saturated	22	2.0	1.00E-04			SNL	4.4	Uniaxial compressive strength	MO0311RCKPRPCS.003, MO0402DQRIRPPR.003	
46.4	46.4	0	0	0	46.4	9.39	0.11	CFUn	Tctlv	ESF/ECRB/Borehole	USW G-1	1008.3	3308.0	25.4		saturated	23	2.0	1.00E-05			Terra Tek	5.1	Uniaxial compressive strength	MO0311RCKPRPCS.003, MO0402DQRIRPPR.003	Drained test.
41.2	41.2	0	0	0	41.2	9.95	0.29	CFUn	Tctlv	ESF/ECRB/Borehole	USW G-1	1037.9	3405.1	25.4		saturated	23	2.0	1.00E-05			Terra Tek	3.7	Uniaxial compressive strength	MO0311RCKPRPCS.003, MO0402DQRIRPPR.003	Drained test.
28.6	28.6	0		0	28.6	10.5	0.28	CFUn	Tctlv	ESF/ECRB/Borehole	USW G-1	G13030.9 SLD	3030.9	25.3	51	saturated	22	2.0	1.00E-05			SNL	4.6	Uniaxial compressive strength	MO0311RCKPRPCS.003, MO0402DQRIRPPR.003	
51.7	51.7	0	0	0	51.7	10.9	0.14	CFUn	Tctlv	ESF/ECRB/Borehole	USW G-1	923.8	3030.8	25.4		saturated	23	2.0	1.00E-05			Terra Tek	4.5	Uniaxial compressive strength	MO0311RCKPRPCS.003, MO0402DQRIRPPR.003	Drained test.
64.7	64.7	0	0	0	64.7	11.9	0.21	CFUn	Tctlv	ESF/ECRB/Borehole	USW G-1	923.8	3030.8	25.4		saturated	23	2.0	1.00E-05			Terra Tek	5.1	Uniaxial compressive strength	MO0311RCKPRPCS.003, MO0402DQRIRPPR.003	Drained test.
37.3	37.3	0		0	37.3	12.4	0.31	CFUn	Tctlv	ESF/ECRB/Borehole	USW G-1	G13405.2 SLD	3405.2	25.3	51	saturated	22	2.0	1.00E-05			SNL	3.4	Uniaxial compressive strength	MO0311RCKPRPCS.003, MO0402DQRIRPPR.003	
33.1	33.1	0		0	33.1	13.4		CFUn	Tctlv	ESF/ECRB/Borehole	USW G-1	G13030.9 SLB	3030.9	25.3	51	saturated	22	2.0	1.00E-02			SNL	3.7	Uniaxial compressive strength	MO0311RCKPRPCS.003, MO0402DQRIRPPR.003	
95.8	95.8	0	0	0	95.8	18.3	0.27	CFUn	Tctm	ESF/ECRB/Borehole	USW G-1	883	2896.9	25.4		saturated	23	2.0	1.00E-05			Terra Tek	5.0	Uniaxial compressive strength	MO0311RCKPRPCS.003, MO0402DQRIRPPR.003	Drained test.
69.2	69.2	0		0	69.2	19.9	0.24	CFUn	Tctm	ESF/ECRB/Borehole	USW G-1	G12897.0 SLD	2897.0	25.3	51	saturated	22	2.0	1.00E-05			SNL	4.6	Uniaxial compressive strength	MO0311RCKPRPCS.003, MO0402DQRIRPPR.003	
115	115	0	0	0	115	20	0.22	CFUn	Tctm	ESF/ECRB/Borehole	USW G-1	883	2896.9	25.4		saturated	23	2.0	1.00E-05			Terra Tek	5.5	Uniaxial compressive strength	MO0311RCKPRPCS.003, MO0402DQRIRPPR.003	Drained test.
68.1	68.1	0		0	68.1	21.3	0.27	CFUn	Tctm	ESF/ECRB/Borehole	USW G-1	G12897.0 SLB	2897.0	25.3	51	saturated	22	2.0	1.00E-05			SNL	4.3	Uniaxial compressive strength	MO0311RCKPRPCS.003, MO0402DQRIRPPR.003	
66.4	66.4	0	0	0	66.4	14.2	0.21	CFUn	Tduc	ESF/ECRB/Borehole	USW G-1	856.5	2810.0	25.4		saturated	23	2.0	1.00E-05			Terra Tek	4.2	Uniaxial compressive strength	MO0311RCKPRPCS.003, MO0402DQRIRPPR.003	Drained test.
46	46	0		0	46.0	14.2	0.31	CFUn	Tduc	ESF/ECRB/Borehole	USW G-1	G12810.0 SLD	2810.0	25.3	51	saturated	22	2.0	1.00E-05			SNL	4.3	Uniaxial compressive strength	MO0311RCKPRPCS.003, MO0402DQRIRPPR.003	
76.2	76.2	0	0	0	76.2	14.9	0.17	CFUn	Tduc	ESF/ECRB/Borehole	USW G-1	856.5	2810.0	25.4		saturated	23	2.0	1.00E-05			Terra Tek	3.9	Uniaxial compressive strength	MO0311RCKPRPCS.003, MO0402DQRIRPPR.003	Drained test.
42	42	0		0	42.0	15.2	0.38	CFUn	Tduc	ESF/ECRB/Borehole	USW G-1	G12810.0 SLB	2810.0	25.3	51	saturated	22	2.0	1.00E-05			SNL	3.6	Uniaxial compressive strength	MO0311RCKPRPCS.003, MO0402DQRIRPPR.003	
47	47	0	0	0	47.0	6.66	0.11	CFUn	Tduv	ESF/ECRB/Borehole	USW G-1	804.9	2640.7	25.4		saturated	23	2.0	1.00E-05			Terra Tek	6.9	Uniaxial compressive strength	MO0311RCKPRPCS.003, MO0402DQRIRPPR.003	Drained test.
45.2	45.2	0	0	0	45.2	6.99	0.12	CFUn	Tduv	ESF/ECRB/Borehole	USW G-1	804.9	2640.7	25.4		saturated	23	2.0	1.00E-05			Terra Tek	6.3	Uniaxial compressive strength	MO0311RCKPRPCS.003, MO0402DQRIRPPR.003	Drained test.
45.3	45.3	0	0	0	45.3	9.47	0.11	CFUn	Tduv	ESF/ECRB/Borehole	USW G-1	822.7	2699.1	25.4		saturated	23	2.0	1.00E-05			Terra Tek	5.0	Uniaxial compressive strength	MO0311RCKPRPCS.003, MO0402DQRIRPPR.003	Drained test.
63.9	63.9	0	0	0	63.9	10.9	0.11	CFUn	Tduv	ESF/ECRB/Borehole	USW G-1	822.7	2699.1	25.4		saturated	23	2.0	1.00E-05			Terra Tek	5.8	Uniaxial compressive strength	MO0311RCKPRPCS.003, MO0402DQRIRPPR.003	Drained test.
53.6	53.6	0		0	53.6	13.3	0.18	CFUn	Tduv	ESF/ECRB/Borehole	USW G-1	G12699.1 SLD	2699.1	25.3	51	saturated	23	2.0	1.00E-05			Terra Tek	5.1	Uniaxial compressive strength	MO0311RCKPRPCS.003, MO0402DQRIRPPR.003	
60.1	60.1	0		0	60.1	14.5	0.16	CFUn	Tduv	ESF/ECRB/Borehole	USW G-1	G12699.1 SLB	2699.1	25.3	51	saturated	23	2.0	1.00E-05			Terra Tek	4.6	Uniaxial compressive strength	MO0311RCKPRPCS.003, MO0402DQRIRPPR.003	
47.7	47.7	0		0	47.7	12.29	0.14	CHn	Tac	ESF/ECRB/Borehole	UE 25A#1	1490	1490.0	56	L:D = 2:1	ambient	22	2.0	1.00E-04			SANDIA		Uniaxial compressive strength	MO0311RCKPRPCS.003, MO0402DQRIRPPR.003	L:D = 2:1 or greater; Specimen diameter: 64, 48
40.8	40.8	0		0	40.8	14.02	0.20	CHn	Tac	ESF/ECRB/Borehole	UE 25A#1	1692	1692.0	56	L:D = 2:1	ambient	22	2.0	1.00E-04			SANDIA		Uniaxial compressive strength	MO0311RCKPRPCS.003, MO0402DQRIRPPR.003	L:D = 2:1 or greater; Specimen diameter: 64, 48
29.6	29.6	0	0	0	29.6	4.41	0.17	CHn	Tac	ESF/ECRB/Borehole	USW G-1	463.3	1520.0	25.4		saturated	23	2.0	1.00E-05			Terra Tek	6.0	Uniaxial compressive strength	MO0311RCKPRPCS.003, MO0402DQRIRPPR.003	Drained test.
23.2	23.2	0	0	0	23.2	5.45	0.09	CHn	Tac	ESF/ECRB/Borehole	USW G-1	453.4	1487.5	25.4		saturated	23	2.0	1.00E-05			Terra Tek	6.9	Uniaxial compressive strength	MO0311RCKPRPCS.003, MO0402DQRIRPPR.003	Drained test.
22.6	22.6	0	0	0	22.6	5.61	0.1	CHn	Tac	ESF/ECRB/Borehole	USW G-1	463.3	1520.0	25.4		saturated	23	2.0	1.00E-05			Terra Tek	6.0	Uniaxial compressive strength	MO0311RCKPRPCS.003, MO0402DQRIRPPR.003	Drained test.
24.3	24.3	0	0	0	24.3	6.03	0.09	CHn	Tac	ESF/ECRB/Borehole	USW G-1	439.5	1441.9	25.4		saturated	23	2.0	1.00E-05			Terra Tek	4.3	Uniaxial compressive strength	MO0311RCKPRPCS.003, MO0402DQRIRPPR.003	Drained test.
22.3	22.3	0	0	0	22.3	6.37	0.1	CHn	Tac	ESF/ECRB/Borehole	USW G-1	486.1	1594.8	25.4		saturated	23	2.0	1.00E-05			Terra Tek	4.3	Uniaxial compressive strength	MO0311RCKPRPCS.003, MO0402DQRIRPPR.003	Drained test.
23.7	23.7	0	0	0	23.7	6.39	0.18	CHn	Tac	ESF/ECRB/Borehole	USW G-1	507.6	1665.3	25.4		saturated	23	2.0	1.00E-05			Terra Tek	5.7	Uniaxial compressive strength	MO0311RCKPRPCS.003, MO0402DQRIRPPR.003	Drained test.
22.3	22.3	0	0	0	22.3	6.6	0.09	CHn	Tac	ESF/ECRB/Borehole	USW G-1	486.1	1594.8	25.4		saturated	23	2.0	1.00E-05			Terra Tek	4.2	Uniaxial compressive strength	MO0311RCKPRPCS.003, MO0402DQRIRPPR.003	Drained test.
23.7	23.7	0	0	0	23.7	6.81	0.21	CHn	Tac	ESF/ECRB/Borehole	USW G-1	524.2	1719.8	25.4		saturated	23	2.0	1.00E-05			Terra Tek	5.0	Uniaxial compressive strength	MO0311RCKPRPCS.003, MO0402DQRIRPPR.003	Drained test.
34.2	34.2	0	0	0	34.2	8.84	0.07	CHn	Tac	ESF/ECRB/Borehole	USW G-1	439.5	1441.9	25.4		saturated	23	2.0	1.00E-05			Terra Tek	5.6	Uniaxial compressive strength	MO0311RCKPRPCS.003, MO0402DQRIRPPR.003	Drained test.
40.6	40.6	0	0	0	40.6	9.12	0.07	CHn	Tac	ESF/ECRB/Borehole	USW G-1	472.6	1550.5	25.4		saturated	23	2.0	1.00E-05			Terra Tek	6.4	Uniaxial compressive strength	MO0311RCKPRPCS.003, MO0402DQRIRPPR.003	Drained test.

Table A-1 Intact Rock Mechanical Properties Data - Strength and Elastic Properties Data

Axial Stress, σ_1 (MPa)	Axial Stress, effective σ_1' (MPa)	Confining Pressure (MPa) σ_3	Pore Pressure (MPa)	Confining Pressure, Effective (MPa), σ_3'	Differential Strength, (MPa) σ_1-σ_3	Young's Modulus (GPa)	Poisson's Ratio	TM Unit	Litho-stratigraphic Unit	General Location	Sample Location	Specimen Number	Depth (ft)	Specimen Diameter (mm)	Specimen Length (mm)	Specimen Saturation	Specimen Temperature (deg. C)	l/d Ratio	Strain Rate (1/s)	Specimen Orientation (degree)	Test Standard	Laboratory	Failure Strain (millistrain)	Rock Property	Source DTN	Notes
26.6	26.6	0	0	0	26.6	9.41	0.1	CHn	Tac	ESF/ECRB/Borehole	USW G-1	492.9	1617.1	25.4		saturated	23	2.0	1.00E-05			Terra Tek	3.6	Uniaxial compressive strength	MO0311RCKPRPCS.003, MO0402DQRIRPPR.003	Drained test.
45.3	45.3	0	0	0	45.3	9.42	0.09	CHn	Tac	ESF/ECRB/Borehole	USW G-1	453.4	1487.5	25.4		saturated	23	2.0	1.00E-05			Terra Tek	6.2	Uniaxial compressive strength	MO0311RCKPRPCS.003, MO0402DQRIRPPR.003	Drained test.
34.6	34.6	0	0	0	34.6	9.52	0.1	CHn	Tac	ESF/ECRB/Borehole	USW G-1	524.2	1719.8	25.4		saturated	23	2.0	1.00E-05			Terra Tek	5.1	Uniaxial compressive strength	MO0311RCKPRPCS.003, MO0402DQRIRPPR.003	Drained test.
37.6	37.6	0	0	0	37.6	9.85	0.14	CHn	Tac	ESF/ECRB/Borehole	USW G-1	507.6	1665.3	25.4		saturated	23	2.0	1.00E-05			Terra Tek	4.7	Uniaxial compressive strength	MO0311RCKPRPCS.003, MO0402DQRIRPPR.003	Drained test.
42.7	42.7	0	0	0	42.7	11	0.1	CHn	Tac	ESF/ECRB/Borehole	USW G-1	492.9	1617.1	25.4		saturated	23	2.0	1.00E-05			Terra Tek	4.8	Uniaxial compressive strength	MO0311RCKPRPCS.003, MO0402DQRIRPPR.003	Drained test.
53.1	53.1	0	0	0	53.1	12.8	0.07	CHn	Tac	ESF/ECRB/Borehole	USW G-1	472.6	1550.5	25.4		saturated	23	2.0	1.00E-05			Terra Tek	7.0	Uniaxial compressive strength	MO0311RCKPRPCS.003, MO0402DQRIRPPR.003	Drained test.
22.7	22.7	0		0	22.7	6.1	0.31	CHn	Tac	ESF/ECRB/Borehole	USW SD-9	SD-9-1560.8-SNL-A	1560.8	50.8	101.6	saturated	22	2.0	1.00E-05			NER	4.13	Uniaxial compressive strength	MO0311RCKPRPCS.003, MO0402DQRIRPPR.003	
26.5	26.5	0		0	26.5	6.9	0.09	CHn	Tac	ESF/ECRB/Borehole	USW SD-9	SD-9-1499.9-SNL-A	1499.9	50.8	101.6	saturated	22	2.0	1.00E-05			NER	4.56	Uniaxial compressive strength	MO0311RCKPRPCS.003, MO0402DQRIRPPR.003	
20.8	20.8	0	0	0	20.8	4.05	0.21	CHn	Tacbt	ESF/ECRB/Borehole	USW G-1	544	1784.8	25.4		saturated	23	2.0	1.00E-05			Terra Tek	7.3	Uniaxial compressive strength	MO0311RCKPRPCS.003, MO0402DQRIRPPR.003	Drained test.
21.6	21.6	0	0	0	21.6	4.61	0.2	CHn	Tacbt	ESF/ECRB/Borehole	USW G-1	544	1784.8	25.4		saturated	23	2.0	1.00E-05			Terra Tek	6.4	Uniaxial compressive strength	MO0311RCKPRPCS.003, MO0402DQRIRPPR.003	Drained test.
55.5	55.5	0	0	0	55.5	12.4	0.14	CHn	Tacbt	ESF/ECRB/Borehole	USW G-1	530.9	1741.8	25.4		saturated	23	2.0	1.00E-05			Terra Tek	6.3	Uniaxial compressive strength	MO0311RCKPRPCS.003, MO0402DQRIRPPR.003	Drained test.
70.7	70.7	0	0	0	70.7	12.7	0.15	CHn	Tacbt	ESF/ECRB/Borehole	USW G-1	530.9	1741.8	25.4		saturated	23	2.0	1.00E-05			Terra Tek	7.1	Uniaxial compressive strength	MO0311RCKPRPCS.003, MO0402DQRIRPPR.003	Drained test.
22	22	0	0	0	22	6.3	0.24	CHn	Tpbt1	ESF/ECRB/Borehole	USW G-2	G2-1725.05-A	1725.1	25.3	50.8	saturated	22	2.0	1.00E-05			Terra Tek	3.9	Uniaxial compressive strength	MO0311RCKPRPCS.003, MO0402DQRIRPPR.003	Drained test.
29	29	0	0	0	29	8.5	0.1	CHn	Tpbt1	ESF/ECRB/Borehole	USW G-2	G2-1725.05-C	1725.1	25.3	50.9	saturated	22	2.0	1.00E-05			Terra Tek	4.0	Uniaxial compressive strength	MO0311RCKPRPCS.003, MO0402DQRIRPPR.003	Drained test.
23	23	0	0	0	23	11	0.22	CHn	Tpbt1	ESF/ECRB/Borehole	USW G-2	G2-1748.0-C	1748.0	25.3	50.9	saturated	22	2.0	1.00E-05			Terra Tek	3.4	Uniaxial compressive strength	MO0311RCKPRPCS.003, MO0402DQRIRPPR.003	Drained test.
28	28	0	0	0	28	11.1	0.11	CHn	Tpbt1	ESF/ECRB/Borehole	USW G-2	G2-1748.0-F	1748.0	25.3	50.8	saturated	22	2.0	1.00E-07			Terra Tek	4.3	Uniaxial compressive strength	MO0311RCKPRPCS.003, MO0402DQRIRPPR.003	Drained test.
35	35	0	0	0	35	11.2	0.23	CHn	Tpbt1	ESF/ECRB/Borehole	USW G-2	G2-1748.0-E	1748.0	25.3	50.8	saturated	22	2.0	1.00E-05			Terra Tek	3.5	Uniaxial compressive strength	MO0311RCKPRPCS.003, MO0402DQRIRPPR.003	Drained test.
27	27	0	0	0	27	11.2		CHn	Tpbt1	ESF/ECRB/Borehole	USW G-2	G2-1748.0-D	1748.0	25.3	50.9	saturated	22	2.0	1.00E-07			Terra Tek	3.2	Uniaxial compressive strength	MO0311RCKPRPCS.003, MO0402DQRIRPPR.003	Drained test.
28	28	0	0	0	28	14.2	0.1	CHn	Tpbt1	ESF/ECRB/Borehole	USW G-2	G2-1748.0-A	1748.0	25.3	50.8	saturated	22	2.0	1.00E-07			Terra Tek	2.5	Uniaxial compressive strength	MO0311RCKPRPCS.003, MO0402DQRIRPPR.003	Drained test.
20.5	20.5	0		0	20.5	3.9	0.11	CHn	Tpbt1	ESF/ECRB/Borehole	USW SD-9	SD-9-1477.2-SNL-B	1477.2	50.8	101.6	saturated	22	2.0	1.00E-05			NER	5.4	Uniaxial compressive strength	MO0311RCKPRPCS.003, MO0402DQRIRPPR.003	
90.5	90.5	0		0	90.5	16.1	0.21	CHn	Tptpv2	ESF/ECRB/Borehole	USW GU-3	GU-3 1280.6/3	1280.6	25.35	50.9	saturated	22	2.0	1.00E-05	90		SANDIA	6.39	Uniaxial compressive strength	MO0311RCKPRPCS.003, MO0402DQRIRPPR.003	
90.2	90.2	0		0	90.2	16.7	0.22	CHn	Tptpv2	ESF/ECRB/Borehole	USW GU-3	GU-3 1280.6/1	1280.6	57.15	114.4	ambient	22	2.0	1.00E-05	90		SANDIA	6.15	Uniaxial compressive strength	MO0311RCKPRPCS.003, MO0402DQRIRPPR.003	
92.8	92.8	0		0	92.8	16.8	0.18	CHn	Tptpv2	ESF/ECRB/Borehole	USW GU-3	GU-3 1280.6/2	1280.6	25.37	50.85	saturated	22	2.0	1.00E-05	90		SANDIA	5.75	Uniaxial compressive strength	MO0311RCKPRPCS.003, MO0402DQRIRPPR.003	
2	2	0		0	2	0.2	0.19	PTn	Tpbt2	ESF/ECRB/Borehole	UE-25 NRG#4	NRG-4-469.0-SNL-A	469.0	50.8	101.6	saturated	22	2.0	1.00E-05			NER	6.04	Uniaxial compressive strength	MO0311RCKPRPCS.003, MO0402DQRIRPPR.003	
5.2	5.2	0		0	5.2	0.8	0.15	PTn	Tpbt2	ESF/ECRB/Borehole	UE-25 NRG#4	NRG-4-458.7-SNL-A	458.7	50.8	101.6	saturated	22	2.0	1.00E-05			NER	6.66	Uniaxial compressive strength	MO0311RCKPRPCS.003, MO0402DQRIRPPR.003	
6.4	6.4	0		0	6.4	1.7	0.14	PTn	Tpbt2	ESF/ECRB/Borehole	UE-25 NRG#4	NRG-4-466.8-SNL-A	466.8	50.8	101.6	saturated	22	2.0	1.00E-05			NER	4.11	Uniaxial compressive strength	MO0311RCKPRPCS.003, MO0402DQRIRPPR.003	
0.8	0.8	0		0	0.8	0.1	0.13	PTn	Tpbt2	ESF/ECRB/Borehole	USW NRG-7a	NRG-7/7A-268.6-SNL-A	268.6	50.8	101.6	saturated	22	2.0	1.00E-05			NER	7.48	Uniaxial compressive strength	MO0311RCKPRPCS.003, MO0402DQRIRPPR.003	
1.7	1.7	0		0	1.7	1.2	0.40	PTn	Tpbt2	ESF/ECRB/Borehole	USW SD-12	SD-12-310.6-SNL-A	310.6	50.8	101.6	saturated	22	2.0	1.00E-05			NER	1.46	Uniaxial compressive strength	MO0311RCKPRPCS.003, MO0402DQRIRPPR.003	
1.4	1.4	0		0	1.4	0.01	0.24	PTn	Tpbt2	ESF/ECRB/Borehole	USW SD-9	SD-9-235.0-SNL-A	235.0	50.8	101.6	saturated	22	2.0	1.00E-05			NER	5.12	Uniaxial compressive strength	MO0311RCKPRPCS.003, MO0402DQRIRPPR.003	
2.1	2.1	0		0	2.10	0.5	0.29	PTn	Tpbt2	ESF/ECRB/Borehole	USW NRG-6	NRG-6-241.5-SNL-A	241.5	50.80	101.60	ambient	22	2.0	1.00E-05			NER	5.46	Uniaxial compressive strength	SNL02030193001.001, MO0402DQRIRPPR.003	
2.7	2.7	0		0	2.70	0.7	0.23	PTn	Tpbt2	ESF/ECRB/Borehole	USW NRG-6	NRG-6-227.9-SNL-A	227.9	50.80	101.60	ambient	22	2.0	1.00E-05			NER	4.95	Uniaxial compressive strength	SNL02030193001.001, MO0402DQRIRPPR.003	
4.8	4.8	0		0	4.8	1.5	0.23	PTn	Tpbt2	ESF/ECRB/Borehole	USW NRG-6	NRG-6-222.0-SNL-A	222.0	50.8	101.6	ambient	22	2.0	1.00E-05			NER	3.9	Uniaxial compressive strength	SNL02030193001.001, MO0402DQRIRPPR.003	
0.8	0.8	0		0	0.8	0.2	0.28	PTn	Tpbt3	ESF/ECRB/Borehole	USW NRG-7a	NRG-7/7A-169.1-SNL-A	169.1	50.8	101.6	saturated	22	2.0	1.00E-05			NER	4.94	Uniaxial compressive strength	MO0311RCKPRPCS.003, MO0402DQRIRPPR.003	
2.8	2.8	0		0	2.8	2.4		PTn	Tpbt3	ESF/ECRB/Borehole	USW SD-12	SD-12-267.1-SNL-A	267.1	50.8	101.6	saturated	22	2.0	1.00E-05			NER	1.09	Uniaxial compressive strength	MO0311RCKPRPCS.003, MO0402DQRIRPPR.003	
4.3	4.3	0		0	4.30	1.2	0.21	PTn	Tpbt3	ESF/ECRB/Borehole	USW NRG-6	NRG-6-174.0-SNL-A	174.0	50.8	101.6	ambient	22	2.0	1.00E-05			NER	4.43	Uniaxial compressive strength	SNL02030193001.001, MO0402DQRIRPPR.003	
5.9	5.9	0		0	5.9	2.4	0.12	PTn	Tpbt3	ESF/ECRB/Borehole	USW NRG-6	NRG-6-169.5-SNL-A	169.5	50.8	101.6	ambient	22	2.0	1.00E-05			NER	3.36	Uniaxial compressive strength	SNL02030193001.001, MO0402DQRIRPPR.003	
7.03	7.03	0		0	7.03	0.41	0.28	PTn	Tpbt4	ESF/ECRB/Borehole	UE-25 a #1	212.7	212.7	56	L:D = 2:1	ambient	22	2.0	1.00E-04			SNL		Uniaxial compressive strength	MO0311RCKPRPCS.003, MO0402DQRIRPPR.003	L:D = 2:1 or greater; Specimen diameter: 64, 48
1.2	1.2	0		0	1.2	0.2	0.17	PTn	Tpbt4	ESF/ECRB/Borehole	USW NRG-7a	NRG-7/7A-105.0-SNL-A	105.0	50.8	101.6	saturated	22	2.0	1.00E-05			NER	9.17	Uniaxial compressive strength	MO0311RCKPRPCS.003, MO0402DQRIRPPR.003	
3.5	3.5	0		0	3.50	2.9	0.16	PTn	Tpbt4	ESF/ECRB/Borehole	USW NRG-6	NRG-6-161.4-SNL-A	161.4	50.80	101.60	ambient	22	2.0	1.00E-05			NER	2.69	Uniaxial compressive strength	SNL02030193001.001, MO0402DQRIRPPR.003	
3.9	3.9	0		0	3.9	0.3	0.21	PTn	Tpcpv1	ESF/ECRB/Borehole	USW NRG-7a	NRG-7/7A-97.9-SNL-A	97.9	50.8	101.6	saturated	22	2.0	1.00E-05			NER	9.61	Uniaxial compressive strength	MO0311RCKPRPCS.003, MO0402DQRIRPPR.003	Failure strain underestimated. Displacement measurement devices (LVDTs) went off scale prior to failure.
6.9	6.9	0		0	6.9	3.7	0.10	PTn	Tpcpv1	ESF/ECRB/Borehole	USW NRG-7a	NRG-7/7A-84.4-SNL-A	84.4	50.8	101.6	saturated	22	2.0	1.00E-05			NER	2.56	Uniaxial compressive strength	MO0311RCKPRPCS.003, MO0402DQRIRPPR.003	
5.4	5.4	0		0	5.4	3.9	0.06	PTn	Tpcpv1	ESF/ECRB/Borehole	USW NRG-7a	NRG-7/7A-91.0-SNL-A	91.0	50.8	101.6	saturated	22	2.0	1.00E-05			NER	5.31	Uniaxial compressive strength	MO0311RCKPRPCS.003, MO0402DQRIRPPR.003	
4	4	0		0	4.0	2.2	0.03	PTn	Tpcpv1	ESF/ECRB/Borehole	USW SD-9	SD-9-85.8-SNL-A	85.8	50.8	101.6	saturated	22	2.0	1.00E-05			NER	2.81	Uniaxial compressive strength	MO0311RCKPRPCS.003, MO0402DQRIRPPR.003	
12.2	12.2	0		0	12.2	2.1	0.06	PTn	Tpcpv2	ESF/ECRB/Borehole	USW NRG-7a	NRG-7/7A-77.7-SNL-A	77.7	50.8	101.6	saturated	22	2.0	1.00E-05			NER	9.15	Uniaxial compressive strength	MO0311RCKPRPCS.003, MO0402DQRIRPPR.003	
27.4	27.4	0		0	27.4	7.7	0.09	PTn	Tpcpv2	ESF/ECRB/Borehole	USW NRG-7a	NRG-7/7A-73.7-SNL-A	73.7	50.8	101.6	saturated	22	2.0	1.00E-05			NER	4.99	Uniaxial compressive strength	MO0311RCKPRPCS.003, MO0402DQRIRPPR.003	
11.3	11.3	0		0	11.30	5.9	0.13	PTn	Tpcpv2	ESF/ECRB/Borehole	USW NRG-6	NRG-6-151.2-SNL-A	151.2	50.80	101.60	saturated	22	2.0	1.00E-05			NER	2.4	Uniaxial compressive strength	SNL02030193001.001, MO0402DQRIRPPR.003	
61.8	61.8	0		0	61.80	14.8	0.13	PTn	Tpcpv2	ESF/ECRB/Borehole	USW NRG-6	NRG-6-143.5-SNL-A	143.5	50.80	101.60	saturated	22	2.0	1.00E-05			NER	7.38	Uniaxial compressive strength	SNL02030193001.001, MO0402DQRIRPPR.003	
1.8	1.8	0		0	1.8	0.7		PTn	Tpp	ESF/ECRB/Borehole	UE-25 NRG#4	NRG-4-422.3-SNL-A	422.3	50.8	101.6	saturated	22	2.0	1.00E-05			NER	2.79	Uniaxial compressive strength	MO0311RCKPRPCS.003, MO0402DQRIRPPR.003	
3.3	3.3	0		0	3.3	0.8	0.36	PTn	Tpp	ESF/ECRB/Borehole	UE-25 NRG#4	NRG-4-433.2-SNL-A	433.2	50.8	101.6	saturated	22	2.0	1.00E-05			NER	3.82	Uniaxial compressive strength	MO0311RCKPRPCS.003, MO0402DQRIRPPR.003	
3.5	3.5	0		0	3.5	1.2	0.18	PTn	Tpp	ESF/ECRB/Borehole	UE-25 NRG#4	NRG-4-428.4-SNL-A	428.4	50.8	101.6	saturated	22	2.0	1.00E-05			NER	2.97	Uniaxial compressive strength	MO0311RCKPRPCS.003, MO0402DQRIRPPR.003	
4.9	4.9	0		0	4.9	1.9	0.28	PTn	Tpp	ESF/ECRB/Borehole	UE-25 NRG#4	NRG-4-416.6-SNL-A	416.6	50.8	101.6	saturated	22	2.0	1.00E-05			NER	3	Uniaxial compressive strength	MO0311RCKPRPCS.003, MO0402DQRIRPPR.003	
9.4	9.4	0		0	9.4	2.1	0.09	PTn	Tpp	ESF/ECRB/Borehole	UE-25 NRG#4	NRG-4-456.0-SNL-A	456.0	50.8	101.6	saturated	22	2.0	1.00E-05			NER	4.9	Uniaxial compressive strength	MO0311RCKPRPCS.003, MO0402DQRIRPPR.003	
1.8	1.8	0		0	1.8	0.3	0.19	PTn	Tpp	ESF/ECRB/Borehole	USW NRG-7a	NRG-7/7A-174.1-SNL-A	174.1	50.8	101.6	saturated	22	2.0	1.00E-05			NER	6.32	Uniaxial compressive strength	MO0311RCKPRPCS.003, MO0402DQRIRPPR.003	
1.5	1.5	0		0	1.5	0.3	0.25	PTn	Tpp	ESF/ECRB/Borehole	USW NRG-7a	NRG-7/7A-213.6-SNL-A	213.6	50.8	101.6	saturated	22	2.0	1.00E-05			NER	5.24	Uniaxial compressive strength	MO0311RCKPRPCS.003, MO0402DQRIRPPR.003	
2.1	2.1	0		0	2.1	0.4	0.26	PTn	Tpp	ESF/ECRB/Borehole	USW NRG-7a	NRG-7/7A-254.0-SNL-A	254.0	50.8	101.6	saturated	22	2.0	1.00E-05			NER	4.78	Uniaxial compressive strength	MO0311RCKPRPCS.003, MO0402DQRIRPPR.003	
2.3	2.3	0		0	2.3	0.6	0.31	PTn	Tpp	ESF/ECRB/Borehole	USW NRG-7a	NRG-7/7A-249.7-SNL-A	249.7	50.8	101.6	saturated	22	2.0	1.00E-05			NER	4.64	Uniaxial compressive strength	MO0311RCKPRPCS.003, MO0402DQRIRPPR.003	
1.3	1.3	0		0	1.3	1.5	0.39	PTn	Tpp	ESF/ECRB/Borehole	USW SD-9	SD-9-215.7-SNL-A	215.7	50.8	101.6	saturated	22	2.0	1.00E-05			NER	3.73	Uniaxial compressive strength	MO0311RCKPRPCS.003, MO0402DQRIRPPR.003	

Table A-1 Intact Rock Mechanical Properties Data - Strength and Elastic Properties Data

Axial Stress, σ_1 (MPa)	Axial Stress, effective σ_1' (MPa)	Confining Pressure (MPa) σ_3	Pore Pressure (MPa)	Confining Pressure, Effective (MPa), σ_3'	Differential Strength, (MPa) $\sigma_1'-\sigma_3'$	Young's Modulus (GPa)	Poisson's Ratio	TM Unit	Litho-stratigraphic Unit	General Location	Sample Location	Specimen Number	Depth (ft)	Specimen Diameter (mm)	Specimen Length (mm)	Specimen Saturation	Specimen Temperature (deg. C)	l/d Ratio	Strain Rate (1/s)	Specimen Orientation (degree)	Test Standard	Laboratory	Failure Strain (millistrain)	Rock Property	Source DTN	Notes
3.3	3.3	0		0	3.30	0.8	0.23	PTn	Tpp	ESF/ECRB/Borehole	USW NRG-6	NRG-6-182.2-SNL-A	182.2	50.80	101.60	ambient	22	2.0	1.00E-05			NER	3.25	Uniaxial compressive strength	SNL02030193001.001, MO0402DQRIRPPR.003	
4.1	4.1	0		0	4.10	1.3	0.34	PTn	Tpp	ESF/ECRB/Borehole	USW NRG-6	NRG-6-187.0-SNL-A	187.0	50.80	101.60	ambient	22	2.0	1.00E-05			NER	3.94	Uniaxial compressive strength	SNL02030193001.001, MO0402DQRIRPPR.003	
5.8	5.8	0		0	5.8	1.9	0.30	PTn	Tptrv3	ESF/ECRB/Borehole	USW NRG-7a	NRG-7/7A-292.4-SNL-A	292.4	50.8	101.6	saturated	22	2.0	1.00E-05			NBR	3.03	Uniaxial compressive strength	MO0311RCKPRPCS.003, MO0402DQRIRPPR.003	
2.7	2.7	0		0	2.7	0.07	0.15	PTn	Tptrv3	ESF/ECRB/Borehole	USW SD-9	SD-9-258.5-SNL-A	258.5	50.8	101.6	saturated	22	2.0	1.00E-05			NBR	2.38	Uniaxial compressive strength	MO0311RCKPRPCS.003, MO0402DQRIRPPR.003	
21	21	0		0	21	2.3	0.17	PTn	Tpy	ESF/ECRB/Borehole	USW NRG-7a	NRG-7/7A-130.0-SNL-A	130.0	50.8	101.6	saturated	22	2.0	1.00E-05			NBR	9.37	Uniaxial compressive strength	MO0311RCKPRPCS.003, MO0402DQRIRPPR.003	
26.2	26.2	0		0	26.2	4.9	0.16	PTn	Tpy	ESF/ECRB/Borehole	USW NRG-7a	NRG-7/7A-135.3-SNL-A	135.3	50.8	101.6	saturated	22	2.0	1.00E-05			NBR	6.85	Uniaxial compressive strength	MO0311RCKPRPCS.003, MO0402DQRIRPPR.003	
22.8	22.8	0		0	22.8	9.2	0.15	PTn	Tpy	ESF/ECRB/Borehole	USW NRG-7a	NRG-7/7A-119.4-SNL-A	119.4	50.8	101.6	saturated	22	2.0	1.00E-05			NBR	2.78	Uniaxial compressive strength	MO0311RCKPRPCS.003, MO0402DQRIRPPR.003	
7.8	7.8	0		0	7.8	2.4	0.15	PTn	Tpy	ESF/ECRB/Borehole	USW SD-9	SD-9-138.7-SNL-A	138.7	50.8	101.6	saturated	22	2.0	1.00E-05			NBR	5.92	Uniaxial compressive strength	MO0311RCKPRPCS.003, MO0402DQRIRPPR.003	
18.7	18.7	0		0	18.7	7.4	0.15	PTn	Tpy	ESF/ECRB/Borehole	USW SD-9	SD-9-109.5-SNL-A	109.5	50.8	101.6	saturated	22	2.0	1.00E-05			NBR	3.25	Uniaxial compressive strength	MO0311RCKPRPCS.003, MO0402DQRIRPPR.003	
75.4	75.4	0		0	75.4	24.6	0.22	TCw	Tpcpll	ESF/ECRB/Borehole	UE-25 NRG #3	NRG-3-297.1-SNL-A	297.1	50.8	101.6	saturated	22	2.0	1.00E-05			NBR	4.74	Uniaxial compressive strength	MO0311RCKPRPCS.003, MO0402DQRIRPPR.003	
119.9	119.9	0		0	119.9	30.3	0.32	TCw	Tpcpll	ESF/ECRB/Borehole	UE-25 NRG #3	NRG-3-292.4-SNL-A	292.4	50.8	101.6	saturated	22	2.0	1.00E-05			NBR	4.92	Uniaxial compressive strength	MO0311RCKPRPCS.003, MO0402DQRIRPPR.003	
121.1	121.1	0		0	121.1	33.5	0.23	TCw	Tpcpll	ESF/ECRB/Borehole	UE-25 NRG #3	NRG-3-289.2-SNL-A	289.2	50.8	101.6	saturated	22	2.0	1.00E-05			NBR	3.39	Uniaxial compressive strength	MO0311RCKPRPCS.003, MO0402DQRIRPPR.003	
313.8	313.8	0		0	313.8	36.4	0.22	TCw	Tpcpll	ESF/ECRB/Borehole	USW NRG-6	NRG-6-222.2-SNL-L	222.2	25.4	50.8	saturated	22	2.0	1.00E-05			NBR	9.32	Uniaxial compressive strength	MO0311RCKPRPCS.003, MO0402DQRIRPPR.003	
332.4	332.4	0		0	332.4	36.7	0.22	TCw	Tpcpll	ESF/ECRB/Borehole	USW NRG-6	NRG-6-222.2-SNL-M	222.2	25.4	50.8	saturated	22	2.0	1.00E-05			NBR	9.75	Uniaxial compressive strength	MO0311RCKPRPCS.003, MO0402DQRIRPPR.003	
315.8	315.8	0		0	315.8	37.2	0.21	TCw	Tpcpll	ESF/ECRB/Borehole	USW NRG-6	NRG-6-222.2-SNL-J	222.2	25.4	50.8	saturated	22	2.0	1.00E-05			NER	9.24	Uniaxial compressive strength	MO0311RCKPRPCS.003, MO0402DQRIRPPR.003	
284.2	284.2	0		0	284.2	37.4	0.20	TCw	Tpcpll	ESF/ECRB/Borehole	USW NRG-6	NRG-6-222.2-SNL-K	222.2	25.4	50.8	saturated	22	2.0	1.00E-05			NER	8.55	Uniaxial compressive strength	MO0311RCKPRPCS.003, MO0402DQRIRPPR.003	
313.6	313.6	0		0	313.60	36.7	0.22	TCw	Tpcpll	ESF/ECRB/Borehole	USW NRG-6	NRG-6-222.2-SNL-A	222.2	50.8	101.6	saturated	22	2.0	1.00E-05			NER		Uniaxial compressive strength	SNL02030193001.001, MO0402DQRIRPPR.003	
303.7	303.7	0		0	303.7	39	0.22	TCw	Tpcpll	ESF/ECRB/Borehole	USW NRG-6	NRG-6-223.4-SNL-A	223.4	50.8	101.6	saturated	22	2.0	1.00E-05			NER	8.38	Uniaxial compressive strength	SNL02030193001.001, MO0402DQRIRPPR.003	
364	364	0		0	364	57.5	0.31	TCw	Tpcpln	ESF/ECRB/Borehole	UE-25 a #1	87.6	87.6	56	L:D = 2:1	ambient	22	2.0	1.00E-04			SNL		Uniaxial compressive strength	MO0311RCKPRPCS.003, MO0402DQRIRPPR.003	L:D = 2:1 or greater; Specimen diameter: 64, 48
185.6	185.6	0		0	185.6	36.5	0.22	TCw	Tpcpln	ESF/ECRB/Borehole	UE-25 NRG-2	NRG-2-196.2-SNL-A	196.2	50.80	101.60	saturated	22	2.0	1.00E-05			NER	5.28	Uniaxial compressive strength	MO0311RCKPRPCS.003, MO0402DQRIRPPR.003	
149.1	149.1	0		0	149.1	37.1	0.20	TCw	Tpcpln	ESF/ECRB/Borehole	UE-25 NRG-2	NRG-2-180.0-SNL-A	180.0	50.80	101.60	saturated	22	2.0	1.00E-05			NER	4.42	Uniaxial compressive strength	MO0311RCKPRPCS.003, MO0402DQRIRPPR.003	
141.8	141.8	0		0	141.8	38.7	0.20	TCw	Tpcpln	ESF/ECRB/Borehole	UE-25 NRG-2	NRG-2-174.0-SNL-A	174.0	50.80	101.60	saturated	22	2.0	1.00E-05			NER	3.82	Uniaxial compressive strength	MO0311RCKPRPCS.003, MO0402DQRIRPPR.003	
145.3	145.3	0		0	145.3	38.7	0.23	TCw	Tpcpln	ESF/ECRB/Borehole	UE-25 NRG-2	NRG-2-200.0-SNL-A	200.0	50.80	101.60	saturated	22	2.0	1.00E-05			NER	5.77	Uniaxial compressive strength	MO0311RCKPRPCS.003, MO0402DQRIRPPR.003	
142.7	142.7	0		0	142.7	39.8	0.20	TCw	Tpcpln	ESF/ECRB/Borehole	UE-25 NRG-2	NRG-2-178.0-SNL-A	178.0	50.80	101.60	saturated	22	2.0	1.00E-05			NER	3.74	Uniaxial compressive strength	MO0311RCKPRPCS.003, MO0402DQRIRPPR.003	
209.2	209.2	0		0	209.2	39.8	0.20	TCw	Tpcpln	ESF/ECRB/Borehole	UE-25 NRG-2	NRG-2-188.3-SNL-A	188.3	50.80	101.60	saturated	22	2.0	1.00E-05			NER	5.54	Uniaxial compressive strength	MO0311RCKPRPCS.003, MO0402DQRIRPPR.003	
117.5	117.5	0		0	117.5	40.1	0.19	TCw	Tpcpln	ESF/ECRB/Borehole	UE-25 NRG-2	NRG-2-170.4-SNL-A	170.4	50.80	101.60	saturated	22	2.0	1.00E-05			NER	4.54	Uniaxial compressive strength	MO0311RCKPRPCS.003, MO0402DQRIRPPR.003	
215.8	215.8	0		0	215.8	40.1	0.22	TCw	Tpcpln	ESF/ECRB/Borehole	UE-25 NRG-2	NRG-2-179.5-SNL-A	179.5	50.80	101.60	saturated	22	2.0	1.00E-05			NER	5.57	Uniaxial compressive strength	MO0311RCKPRPCS.003, MO0402DQRIRPPR.003	
143.3	143.3	0		0	143.3	21.4	0.20	TCw	Tpcpln	ESF/ECRB/Borehole	USW NRG-7a	NRG-7/7A-55.4-SNL-A	55.4	50.8	101.6	saturated	22	2.0	1.00E-05		ASTM D 3148-86 ISRM U	NBR	7.48	Uniaxial compressive strength	MO0311RCKPRPCS.003, MO0402DQRIRPPR.003	
228.1	228.1	0		0	228.1	28.1	0.20	TCw	Tpcpln	ESF/ECRB/Borehole	USW NRG-7a	NRG-7/7A-47.4-SNL-A	47.4	50.8	101.6	saturated	22	2.0	1.00E-05		ASTM D 3148-86 ISRM U	NBR	8.92	Uniaxial compressive strength	MO0311RCKPRPCS.003, MO0402DQRIRPPR.003	
84.6	84.6	0		0	84.6	28.7	0.18	TCw	Tpcpln	ESF/ECRB/Borehole	USW NRG-7a	NRG-7/7A-18.0-SNL-A	18.0	50.8	101.6	saturated	22	2.0	1.00E-05		ASTM D 3148-86 ISRM U	NBR	1.34	Uniaxial compressive strength	MO0311RCKPRPCS.003, MO0402DQRIRPPR.003	Failure strain not a valid value due to inaccurate displacement measurement as failure was approached.
135	135	0		0	135.0	31.5	0.18	TCw	Tpcpln	ESF/ECRB/Borehole	USW NRG-7a	NRG-7/7A-41.4-SNL-A	41.4	50.8	101.6	saturated	22	2.0	1.00E-05		ASTM D 3148-86 ISRM U	NBR	5.32	Uniaxial compressive strength	MO0311RCKPRPCS.003, MO0402DQRIRPPR.003	
160.4	160.4	0		0	160.4	35	0.21	TCw	Tpcpln	ESF/ECRB/Borehole	USW NRG-7a	NRG-7/7A-33.5-SNL-A	33.5	50.8	101.6	saturated	22	2.0	1.00E-05		ASTM D 3148-86 ISRM U	NBR	4.85	Uniaxial compressive strength	MO0311RCKPRPCS.003, MO0402DQRIRPPR.003	
169.8	169.8	0		0	169.8	34.3	0.17	TCw	Tpcpln	ESF/ECRB/Borehole	USW SD-12	SD-12-165.8-SNL-A	165.8	50.8	101.6	saturated	22	2.0	1.00E-05		ISRM T and ASTM D 2664-86	NBR	5.66	Uniaxial compressive strength	MO0311RCKPRPCS.003, MO0402DQRIRPPR.003	
278.4	278.4	0		0	278.4	39	0.18	TCw	Tpcpln	ESF/ECRB/Borehole	USW SD-12	SD-12-144.7-SNL-A	144.7	50.8	101.6	saturated	22	2.0	1.00E-05		ISRM T and ASTM D 2664-86	NBR	N/A	Uniaxial compressive strength	MO0311RCKPRPCS.003, MO0402DQRIRPPR.003	
259.9	259.9	0		0	259.9	39.1	0.21	TCw	Tpcpln	ESF/ECRB/Borehole	USW SD-12	SD-12-195.3-SNL-A	195.3	50.8	101.6	saturated	22	2.0	1.00E-05		ISRM T and ASTM D 2664-86	NBR	7.09	Uniaxial compressive strength	MO0311RCKPRPCS.003, MO0402DQRIRPPR.003	
78.2	78.2	0		0	78.2	23.1	0.21	TCw	Tpcpln	ESF/ECRB/Borehole	USW NRG-6	NRG-6-111.0-SNL-A	111.0	50.80	101.60	saturated	22	2.0	1.00E-05			NBR	3.6	Uniaxial compressive strength	SNL02030193001.001, MO0402DQRIRPPR.003	
114.1	114.1	0		0	114.1	26.5	0.21	TCw	Tpcpln	ESF/ECRB/Borehole	USW NRG-6	NRG-6-111.0-SNL-B	111.0	50.8	101.6	saturated	22	2.0	1.00E-05			NBR	5.03	Uniaxial compressive strength	SNL02030193001.001, MO0402DQRIRPPR.003	
242.2	242.2	0		0	242.2	29.2	0.25	TCw	Tpcpln	ESF/ECRB/Borehole	USW NRG-6	NRG-6-98.1-SNL-B	98.1	50.8	101.6	saturated	22	2.0	1.00E-05			NBR	8.72	Uniaxial compressive strength	SNL02030193001.001, MO0402DQRIRPPR.003	
245.6	245.6	0		0	245.6	30	0.24	TCw	Tpcpln	ESF/ECRB/Borehole	USW NRG-6	NRG-6-98.1-SNL-A	98.1	50.8	101.6	saturated	22	2.0	1.00E-05			NBR	8.58	Uniaxial compressive strength	SNL02030193001.001, MO0402DQRIRPPR.003	
274.4	274.4	0		0	274.4			TCw	Tpcpmn	ESF/ECRB/Borehole	UE-25 NRG-1	136.8-144.4FT.-04,-01	136.8-144.4	61.2	132.5	ambient	22	2.2	1.00E-05		ASTM D 2664-86	USBR	8	Uniaxial compressive strength	MO0311RCKPRPCS.003	
71.9	71.9	0		0	71.9	20	0.17	TCw	Tpcpmn	ESF/ECRB/Borehole	UE-25 NRG #3	NRG-3-208.9-SNL-A	208.9	50.80	101.60	saturated	22	2.0	1.00E-05			NBR	4.94	Uniaxial compressive strength	MO0311RCKPRPCS.003, MO0402DQRIRPPR.003	
108.9	108.9	0		0	108.9	30.1		TCw	Tpcpmn	ESF/ECRB/Borehole	UE-25 NRG #3	NRG-3-226.7-SNL-A	226.7	50.80	101.60	saturated	22	2.0	1.00E-05			NBR	4.48	Uniaxial compressive strength	MO0311RCKPRPCS.003, MO0402DQRIRPPR.003	
105.2	105.2	0		0	105.2	36.3	0.20	TCw	Tpcpmn	ESF/ECRB/Borehole	UE-25 NRG #3	NRG-3-218.0-SNL-A	218.0	50.80	101.60	saturated	22	2.0	1.00E-05			NBR	2.95	Uniaxial compressive strength	MO0311RCKPRPCS.003, MO0402DQRIRPPR.003	
174.3	174.3	0		0	174.3	38.4	0.19	TCw	Tpcpmn	ESF/ECRB/Borehole	UE-25 NRG #3	NRG-3-257.6-SNL-A	257.6	50.80	101.60	saturated	22	2.0	1.00E-05			NBR	4.88	Uniaxial compressive strength	MO0311RCKPRPCS.003, MO0402DQRIRPPR.003	
192.8	192.8	0		0	192.8	39.5	0.20	TCw	Tpcpmn	ESF/ECRB/Borehole	UE-25 NRG #3	NRG-3-257.6-SNL-B	257.6	50.80	101.60	saturated	22	2.0	1.00E-05			NBR	5.09	Uniaxial compressive strength	MO0311RCKPRPCS.003, MO0402DQRIRPPR.003	
244	244	0		0	244.0	39.6	0.22	TCw	Tpcpmn	ESF/ECRB/Borehole	UE-25 NRG #3	NRG-3-263.3-SNL-A	263.3	50.80	101.60	saturated	22	2.0	1.00E-05			NBR	6.71	Uniaxial compressive strength	MO0311RCKPRPCS.003, MO0402DQRIRPPR.003	
230.9	230.9	0		0	230.9	41.4	0.21	TCw	Tpcpmn	ESF/ECRB/Borehole	UE-25 NRG #3	NRG-3-256.0-SNL-A	256.0	50.80	101.60	saturated	22	2.0	1.00E-05			NBR		Uniaxial compressive strength	MO0311RCKPRPCS.003, MO0402DQRIRPPR.003	
128.9	128.9	0		0	128.9	28.88	0.17	TCw	Tpcpmn	ESF/ECRB/Borehole	UE-25 NRG-1	123.8-130.1FT.-02,-02	123.8-130.1	61.2	139.0	ambient	22	2.3	1.00E-05		ASTM D 3148-86	USBR	5.0	Uniaxial compressive strength	MO0311RCKPRPCS.003, MO0402DQRIRPPR.003	
223.4	223.4	0		0	223.4	32.4	0.18	TCw	Tpcpmn	ESF/ECRB/Borehole	UE-25 NRG-1	123.8-130.1FT.-05,-01	123.8-130.1	61.2	126.3	ambient	22	2.1	1.00E-05		ASTM D 3148-86	USBR	7.3	Uniaxial compressive strength	MO0311RCKPRPCS.003, MO0402DQRIRPPR.003	
198.6	198.6	0		0	198.6	38.4	0.18	TCw	Tpcpmn	ESF/ECRB/Borehole	UE-25 NRG-1	123.8-130.1FT.-01,-02	123.8-130.1	61.2	125.6	ambient	22	2.1	1.50E-05		ASTM D 3148-86	USBR	5.5	Uniaxial compressive strength	MO0311RCKPRPCS.003, MO0402DQRIRPPR.003	
209.5	209.5	0		0	209.5	41.2	0.21	TCw	Tpcpmn	ESF/ECRB/Borehole	USW SD-12	SD-12-60.5-SNL-A	60.5	50.8	101.6	saturated	22	2.0	1.00E-05			NER	5.3	Uniaxial compressive strength	MO0311RCKPRPCS.003, MO0402DQRIRPPR.003	
34.3	34.3	0		0	34.3	14.8	0.18	TCw	Tpcpul	ESF/ECRB/Borehole	UE-25 NRG #3	NRG-3-142.3-SNL-A	142.3	50.80	101.60	saturated	22	2.0	1.00E-05			NER	3.45	Uniaxial compressive strength	MO0311RCKPRPCS.003, MO0402DQRIRPPR.003	
32.5	32.5	0		0	32.5	17.9	0.15	TCw	Tpcpul	ESF/ECRB/Borehole	UE-25 NRG #3	NRG-3-154.4-SNL-A	154.4	50.80	101.60	saturated	22	2.0	1.00E-05			NER	2.42	Uniaxial compressive strength	MO0311RCKPRPCS.003, MO0402DQRIRPPR.003	
85.5	85.5	0		0	85.5	27	0.20	TCw	Tpcpul	ESF/ECRB/Borehole	UE-25 NRG #3	NRG-3-195.7-SNL-A	195.7	50.80	101.60	saturated	22	2.0	1.00E-05			NER	3.37	Uniaxial compressive strength	MO0311RCKPRPCS.003, MO0402DQRIRPPR.003	
75	75	0		0	75.0	29.3	0.20	TCw	Tpcpul	ESF/ECRB/Borehole	UE-25 NRG #3	NRG-3-187.1-SNL-A	187.1	50.80	101.60	saturated	22	2.0	1.00E-05			NER	2.60	Uniaxial compressive strength	MO0311RCKPRPCS.003, MO0402DQRIRPPR.003	
83.4	83.4	0		0	83.4	29.6	0.20	TCw	Tpcpul	ESF/ECRB/Borehole	UE-25 NRG #3	NRG-3-123.2-SNL-A	123.2	50.80	101.60	saturated	22	2.0	1.00E-05			NBR	3.30	Uniaxial compressive strength	MO0311RCKPRPCS.003, MO0402DQRIRPPR.003	
66.7	66.7	0		0	66.7	22.61	0.15	TCw	Tpcpul	ESF/ECRB/Borehole	UE-25 NRG-1	38.0-47.1FT.-01,-01	38.0-47.1	61.2	132.0	ambient	22	2.2	1.00E-05		ASTM D 3148-86	USBR	3.7	Uniaxial compressive strength	MO0311RCKPRPCS.003, MO0402DQRIRPPR.003	
65.6	65.6	0		0	65.6	23.16	0.15	TCw	Tpcpul	ESF/ECRB/Borehole	UE-25 NRG-1	89.5-97.8FT.-06,-01	89.5-97.8	61.2	139.0	ambient	22	2.3	1.00E-05		ASTM D 3148-86	USBR	3.2	Uniaxial compressive strength	MO0311RCKPRPCS.003, MO0402DQRIRPPR.003	

Table A-1 Intact Rock Mechanical Properties Data - Strength and Elastic Properties Data

Axial Stress, σ_1 (MPa)	Axial Stress, effective σ_1' (MPa)	Confining Pressure (MPa) σ_3	Pore Pressure (MPa)	Confining Pressure, Effective (MPa), σ_3'	Differential Strength, (MPa) σ_1'-σ_3'	Young's Modulus (GPa)	Poisson's Ratio	TM Unit	Litho-stratigraphic Unit	General Location	Sample Location	Specimen Number	Depth (ft)	Specimen Diameter (mm)	Specimen Length (mm)	Specimen Saturation	Specimen Temperature (deg. C)	l/d Ratio	Strain Rate (1/s)	Specimen Orientation (degree)	Test Standard	Laboratory	Failure Strain (millistrain)	Rock Property	Source DTN	Notes
100	100	0		0	100.0	25.85	0.19	TCw	Tpcpul	ESF/ECRB/Borehole	UE-25 NRG-1	89.5-97.8FT,-05,-01	89.5-97.8	61.2	111.4	ambient	22	1.8	2.00E-05		ASTM D 3148-86	USBR	4.3	Uniaxial compressive strength	MO0311RCKPRPCS.003, MO0402DQRIRPPR.003	
109.6	109.6	0		0	109.6	30.26	0.17	TCw	Tpcpul	ESF/ECRB/Borehole	UE-25 NRG-1	105.1-115.1FT,-01,-01	105.1-115.1	61.1	122.3	ambient	22	2.0	1.00E-05		ASTM D 3148-86	USBR	3.9	Uniaxial compressive strength	MO0311RCKPRPCS.003, MO0402DQRIRPPR.003	
10.4	10.4	0		0	10.4	6.5	0.16	TCw	Tpcm	ESF/ECRB/Borehole	UE-25 NRG #2a	NRG-2A-234.9-SNL-A	234.9	50.80	101.60	saturated	22	2.0	1.00E-05			NER	2.22	Uniaxial compressive strength	MO0311RCKPRPCS.003, MO0402DQRIRPPR.003	
17.5	17.5	0		0	17.5	8.9	0.20	TCw	Tpcm	ESF/ECRB/Borehole	UE-25 NRG #2a	NRG-2A-199.4-SNL-A	199.4	50.80	101.60	saturated	22	2.0	1.00E-05			NER	2.07	Uniaxial compressive strength	MO0311RCKPRPCS.003, MO0402DQRIRPPR.003	
19.9	19.9	0		0	19.9	9.7	0.24	TCw	Tpcm	ESF/ECRB/Borehole	UE-25 NRG #2a	NRG-2A-223.1-SNL-A	223.1	50.80	101.60	saturated	22	2.0	1.00E-05			NER	2.98	Uniaxial compressive strength	MO0311RCKPRPCS.003, MO0402DQRIRPPR.003	
20.2	20.2	0		0	20.2	10.3	0.29	TCw	Tpcm	ESF/ECRB/Borehole	UE-25 NRG #2a	NRG-2A-238.4-SNL-A	238.4	50.80	101.60	saturated	22	2.0	1.00E-05			NER	2.69	Uniaxial compressive strength	MO0311RCKPRPCS.003, MO0402DQRIRPPR.003	
23.6	23.6	0		0	23.6	11.4	0.19	TCw	Tpcm	ESF/ECRB/Borehole	UE-25 NRG #2a	NRG-2A-213.0-SNL-A	213.0	50.80	101.60	saturated	22	2.0	1.00E-05			NER	2.53	Uniaxial compressive strength	MO0311RCKPRPCS.003, MO0402DQRIRPPR.003	
22.2	22.2	0		0	22.2	11.5	0.19	TCw	Tpcm	ESF/ECRB/Borehole	UE-25 NRG #2a	NRG-2A-209.3-SNL-A	209.3	50.80	101.60	saturated	22	2.0	1.00E-05			NER	2.49	Uniaxial compressive strength	MO0311RCKPRPCS.003, MO0402DQRIRPPR.003	
24.5	24.5	0		0	24.5	11.5	0.24	TCw	Tpcm	ESF/ECRB/Borehole	UE-25 NRG #2a	NRG-2A-226.4-SNL-A	226.4	50.80	101.60	saturated	22	2.0	1.00E-05			NER	2.62	Uniaxial compressive strength	MO0311RCKPRPCS.003, MO0402DQRIRPPR.003	
31.1	31.1	0		0	31.1	13.8	0.17	TCw	Tpcm	ESF/ECRB/Borehole	UE-25 NRG #2a	NRG-2A-203.9-SNL-A	203.9	50.80	101.60	saturated	22	2.0	1.00E-05			NER	2.94	Uniaxial compressive strength	MO0311RCKPRPCS.003, MO0402DQRIRPPR.003	
25.5	25.5	0		0	25.5	13.8	0.21	TCw	Tpcm	ESF/ECRB/Borehole	UE-25 NRG #2a	NRG-2A-218.8-SNL-A	218.8	50.80	101.60	saturated	22	2.0	1.00E-05			NER	2.38	Uniaxial compressive strength	MO0311RCKPRPCS.003, MO0402DQRIRPPR.003	
53.2	53.2	0		0	53.2	17.5	0.22	TCw	Tpcm	ESF/ECRB/Borehole	UE-25 NRG #2a	NRG-2A-254.5-SNL-A	254.5	50.80	101.60	saturated	22	2.0	1.00E-05			NER	4.12	Uniaxial compressive strength	MO0311RCKPRPCS.003, MO0402DQRIRPPR.003	
110.6	110.6	0		0	110.6	38.2	0.23	TCw	Tpcm	ESF/ECRB/Borehole	UE-25 NRG #2a	NRG-2A-172.1-SNL-A	172.1	50.80	101.60	saturated	22	2.0	1.00E-05			NER	2.9	Uniaxial compressive strength	MO0311RCKPRPCS.003, MO0402DQRIRPPR.003	
13.1	13.1	0		0	13.1	9.7	0.21	TCw	Tpcm	ESF/ECRB/Borehole	UE-25 NRG #3	NRG-3-32.1-SNL-A	32.1	50.80	101.60	saturated	22	2.0	1.00E-05			NER	1.44	Uniaxial compressive strength	MO0311RCKPRPCS.003, MO0402DQRIRPPR.003	
27.1	27.1	0		0	27.1	12.6	0.15	TCw	Tpcm	ESF/ECRB/Borehole	UE-25 NRG #3	NRG-3-42.6-SNL-A	42.6	50.80	101.60	saturated	22	2.0	1.00E-05			NER	2.65	Uniaxial compressive strength	MO0311RCKPRPCS.003, MO0402DQRIRPPR.003	
36.6	36.6	0		0	36.6	15	0.19	TCw	Tpcm	ESF/ECRB/Borehole	UE-25 NRG #3	NRG-3-48.0-SNL-A	48.0	50.80	101.60	saturated	22	2.0	1.00E-05			NER	3.09	Uniaxial compressive strength	MO0311RCKPRPCS.003, MO0402DQRIRPPR.003	
21.5	21.5	0		0	21.5	16.4	0.17	TCw	Tpcm	ESF/ECRB/Borehole	UE-25 NRG #3	NRG-3-55.7-SNL-A	55.7	50.80	101.60	saturated	22	2.0	1.00E-05			NER	1.14	Uniaxial compressive strength	MO0311RCKPRPCS.003, MO0402DQRIRPPR.003	
39.7	39.7	0		0	39.7	17.6	0.20	TCw	Tpcm	ESF/ECRB/Borehole	UE-25 NRG #3	NRG-3-38.9-SNL-A	38.9	50.80	101.60	saturated	22	2.0	1.00E-05			NER	2.64	Uniaxial compressive strength	MO0311RCKPRPCS.003, MO0402DQRIRPPR.003	
132.9	132.9	0		0	132.9	33.4	0.22	TCw	Tpcm	ESF/ECRB/Borehole	UE-25 NRG #3	NRG-3-93.8-SNL-A	93.8	50.80	101.60	saturated	22	2.0	1.00E-05			NER	3.93	Uniaxial compressive strength	MO0311RCKPRPCS.003, MO0402DQRIRPPR.003	
18.8	18.8	0		0	18.8			TCw	Tpcrn	ESF/ECRB/Borehole	UE-25 NRG #3	NRG-3-21.4-SNL-A	21.4	50.80	101.60	saturated	22	2.0	1.00E-05			NER		Uniaxial compressive strength	MO0311RCKPRPCS.003, MO0402DQRIRPPR.003	
64.4	64.4	0		0	64.4	21.58	0.15	TCw	Tpcrn	ESF/ECRB/Borehole	UE-25 NRG-1	9.5-16.2FT,-01	9.5-16.2	61.1	134.7	ambient	22	2.2	1.00E-05		ASTM D 3148-86	USBR	3.3	Uniaxial compressive strength	MO0311RCKPRPCS.003, MO0402DQRIRPPR.003	
120.7	120.7	0		0	120.7	24.2	0.18	TCw	Tpcrn	ESF/ECRB/Borehole	UE-25 NRG-1	16.2-21.8FT,-03	16.2-21.8	61.3	124.9	ambient	22	2.0	1.50E-05		ASTM D 3148-86	USBR	5.4	Uniaxial compressive strength	MO0311RCKPRPCS.003, MO0402DQRIRPPR.003	
115.8	115.8	0		0	115.8	25.71	0.16	TCw	Tpcrn	ESF/ECRB/Borehole	UE-25 NRG-1	21.8-30.6FT,-01,03	21.8-30.6	61.3	124.7	ambient	22	2.0	1.50E-05		ASTM D 3148-86	USBR	4.8	Uniaxial compressive strength	MO0311RCKPRPCS.003, MO0402DQRIRPPR.003	
220	220	0	0	0	220	38.6	0.19	TSw1	Tptf	ESF/ECRB/Borehole	USW G-2	G2-949.6-C	949.6	25.3	50.7	saturated	22	2.0	1.00E-05			Terra Tek	6.2	Uniaxial compressive strength	MO0311RCKPRPCS.003, MO0402DQRIRPPR.003	Drained test.
115	115	0	0	0	115	41.9	0.26	TSw1	Tptf	ESF/ECRB/Borehole	USW G-2	G2-948.4-B	948.4	25.2	50.8	saturated	22	2.0	1.00E-07			Terra Tek	3.0	Uniaxial compressive strength	MO0311RCKPRPCS.003, MO0402DQRIRPPR.003	Drained test.
167	167	0	0	0	167	42	0.30	TSw1	Tptf	ESF/ECRB/Borehole	USW G-2	G2-948.4-A	948.4	25.3	50.8	saturated	22	2.0	1.00E-05			Terra Tek	4.6	Uniaxial compressive strength	MO0311RCKPRPCS.003, MO0402DQRIRPPR.003	Drained test.
117	117	0	0	0	117	42.1	0.26	TSw1	Tptf	ESF/ECRB/Borehole	USW G-2	G2-948.4-D	948.4	25.3	50.8	saturated	22	2.0	1.00E-07			Terra Tek	3.2	Uniaxial compressive strength	MO0311RCKPRPCS.003, MO0402DQRIRPPR.003	Drained test.
210	210	0	0	0	210	46.3	0.21	TSw1	Tptf	ESF/ECRB/Borehole	USW G-2	G2-969.0-B	969.0	25.3	50.8	saturated	22	2.0	1.00E-05			Terra Tek	4.8	Uniaxial compressive strength	MO0311RCKPRPCS.003, MO0402DQRIRPPR.003	Drained test.
157	157	0	0	0	157	49	0.26	TSw1	Tptf	ESF/ECRB/Borehole	USW G-2	G2-948.4-C	948.4	25.3	50.8	saturated	22	2.0	1.00E-05			Terra Tek	3.3	Uniaxial compressive strength	MO0311RCKPRPCS.003, MO0402DQRIRPPR.003	Drained test.
157	157	0	0	0	157	54.7	0.34	TSw1	Tptf	ESF/ECRB/Borehole	USW G-2	G2-969.0-D	969.0	50.9	101.7	saturated	22	2.0	1.00E-05			Terra Tek	3.1	Uniaxial compressive strength	MO0311RCKPRPCS.003, MO0402DQRIRPPR.003	Drained test.
130	130	0	0	0	130	68.3		TSw1	Tptf	ESF/ECRB/Borehole	USW G-2	G2-969.0-A	969.0	25.3	50.8	saturated	22	2.0	1.00E-05			Terra Tek	2.6	Uniaxial compressive strength	MO0311RCKPRPCS.003, MO0402DQRIRPPR.003	Drained test.
10.3	10.3	0		0	10.3	10.9	0.14	TSw1	Tptpul	Busted Butte	Busted Butte	1d		266.7	533.4	saturated	22	2.0	1.20E-05			SNL	1.01	Uniaxial compressive strength	MO0311RCKPRPCS.003, MO0402DQRIRPPR.003	
12.4	12.4	0		0	12.4	11.9	0.16	TSw1	Tptpul	Busted Butte	Busted Butte	2a		266.7	533.4	saturated	22	2.0	8.00E-06			SNL	1.20	Uniaxial compressive strength	MO0311RCKPRPCS.003, MO0402DQRIRPPR.003	
12	12	0		0	12.0	12.9	0.14	TSw1	Tptpul	Busted Butte	Busted Butte	3a		266.7	533.4	saturated	22	2.0	1.20E-05			SNL	1.09	Uniaxial compressive strength	MO0311RCKPRPCS.003, MO0402DQRIRPPR.003	
14.5	14.5	0		0	14.5	14.2	0.14	TSw1	Tptpul	Busted Butte	Busted Butte	1b		266.7	533.4	saturated	22	2.0	1.40E-05			SNL	1.09	Uniaxial compressive strength	MO0311RCKPRPCS.003, MO0402DQRIRPPR.003	
18.5	18.5	0		0	18.5	15.8	0.13	TSw1	Tptpul	Busted Butte	Busted Butte	8c		266.7	533.4	saturated	22	2.0	9.00E-06			SNL	1.29	Uniaxial compressive strength	MO0311RCKPRPCS.003, MO0402DQRIRPPR.003	
13.8	13.8	0		0	13.8	15.8	0.21	TSw1	Tptpul	Busted Butte	Busted Butte	8e		266.7	533.4	saturated	22	2.0	8.00E-06			SNL	1.16	Uniaxial compressive strength	MO0311RCKPRPCS.003, MO0402DQRIRPPR.003	
18.2	18.2	0		0	18.2	16.6	0.14	TSw1	Tptpul	Busted Butte	Busted Butte	8a		266.7	533.4	saturated	22	2.0	9.00E-06			SNL	1.35	Uniaxial compressive strength	MO0311RCKPRPCS.003, MO0402DQRIRPPR.003	
17.4	17.4	0		0	17.4	16.8	0.18	TSw1	Tptpul	Busted Butte	Busted Butte	8b		266.7	533.4	saturated	22	2.0	8.00E-06			SNL	1.49	Uniaxial compressive strength	MO0311RCKPRPCS.003, MO0402DQRIRPPR.003	
17.5	17.5	0		0	17.5	18.3	0.13	TSw1	Tptpul	Busted Butte	Busted Butte	8d		266.7	533.4	saturated	22	2.0	8.00E-06			SNL	1.10	Uniaxial compressive strength	MO0311RCKPRPCS.003, MO0402DQRIRPPR.003	
27.8	27.8	0		0	27.8	21.5	0.21	TSw1	Tptpul	Busted Butte	Busted Butte	8f		266.7	533.4	saturated	22	2.0	8.00E-06			SNL	1.53	Uniaxial compressive strength	MO0311RCKPRPCS.003, MO0402DQRIRPPR.003	
37.3	37.3	0		0	37.3	18.3		TSw1	Tptpul	ESF/ECRB/Borehole	USW GU-3	GU-3 633.9/1	633.9	57.15	114.40	ambient	22	2.0	1.00E-05	90		SNL	2.45	Uniaxial compressive strength	MO0311RCKPRPCS.003, MO0402DQRIRPPR.003	
57.7	57.7	0		0	57.7	21.1		TSw1	Tptpul	ESF/ECRB/Borehole	USW GU-3	GU-3 634.4/1	634.4	57.23	114.43	ambient	22	2.0	1.00E-05	90		SNL	2.93	Uniaxial compressive strength	MO0311RCKPRPCS.003, MO0402DQRIRPPR.003	
95.8	95.8	0		0	95.8	24.6	0.12	TSw1	Tptpul	ESF/ECRB/Borehole	USW NRG-6	NRG-6-687.5-SNL-A	687.5	50.80	101.60	saturated	22	2.0	1.00E-05		ASTM D-3148 and ISRM U	NER	4.37	Uniaxial compressive strength	MO0311RCKPRPCS.003, MO0402DQRIRPPR.003	
50.4	50.4	0		0	50.4	29.2	0.38	TSw1	Tptpul	ESF/ECRB/Borehole	USW NRG-6	NRG-6-662.2-SNL-A	662.2	50.80	101.60	saturated	22	2.0	1.00E-05		ASTM D-3148 and ISRM U	NER	2.79	Uniaxial compressive strength	MO0311RCKPRPCS.003, MO0402DQRIRPPR.003	
149.4	149.4	0		0	149.4	33.3	0.21	TSw1	Tptpul	ESF/ECRB/Borehole	USW NRG-6	NRG-6-488.0-SNL-A	488.0	50.80	101.60	saturated	22	2.0	1.00E-05		ASTM D-3148 and ISRM U	NER	8.76	Uniaxial compressive strength	MO0311RCKPRPCS.003, MO0402DQRIRPPR.003	
15.7	15.7	0		0	15.7	6	0.46	TSw1	Tptpul	ESF/ECRB/Borehole	USW NRG-7a	NRG-7/7A-546.2-SNL-A	546.2	50.8	101.6	saturated	22	2.0	1.00E-05		ASTM D 3148 & ISRM U	NER	3.79	Uniaxial compressive strength	MO0311RCKPRPCS.003, MO0402DQRIRPPR.003	
21.1	21.1	0		0	21.1	13	0.35	TSw1	Tptpul	ESF/ECRB/Borehole	USW NRG-7a	NRG-7/7A-525.9-SNL-A	525.9	50.8	101.6	saturated	22	2.0	1.00E-05		ASTM D 3148 & ISRM U	NER	1.27	Uniaxial compressive strength	MO0311RCKPRPCS.003, MO0402DQRIRPPR.003	
36.1	36.1	0		0	36.1	13.4	0.2	TSw1	Tptpul	ESF/ECRB/Borehole	USW NRG-7a	NRG-7/7A-649.6-SNL-A	649.6	50.8	101.6	saturated	22	2.0	1.00E-05		ASTM D 3148 & ISRM U	NER	3.18	Uniaxial compressive strength	MO0311RCKPRPCS.003, MO0402DQRIRPPR.003	
81.8	81.8	0		0	81.8	19.7	0.09	TSw1	Tptpul	ESF/ECRB/Borehole	USW NRG-7a	NRG-7/7A-692.5-SNL-A	692.5	50.8	101.6	saturated	22	2.0	1.00E-05		ASTM D 3148 & ISRM U	NER	6.42	Uniaxial compressive strength	MO0311RCKPRPCS.003, MO0402DQRIRPPR.003	
71.4	71.4	0		0	71.4	24.1	0.22	TSw1	Tptpul	ESF/ECRB/Borehole	USW SD-9	SD-9-725.6-SNL-A	725.6	50.8	101.6	saturated	22	2.0	1.00E-05		ISRM T and ASTM D 2664-86	NER	3.37	Uniaxial compressive strength	MO0311RCKPRPCS.003, MO0402DQRIRPPR.003	only uniaxial tested to date
13.5	13.5	0		0	13.5	5.8	0.39	TSw1	Tptpul	ESF/ECRB/Borehole	ESF 63+60.5	ESF-GTEC-C6500-01-0'-3.9'-01023259-SNL-A		288	591	ambient	24	2.0	3.00E-06			SANDIA	3.0	Uniaxial Compressive Strength	SN0208L0207502.001	
12.7	12.7	0		0	12.7	6.7		TSw1	Tptpul	ESF/ECRB/Borehole	ESF 63+60.5	ESF-GTEC-CS6500-01A 0'-2.4'-01023260-SNL-A		288	526	saturated	24	1.8	2.00E-06			SANDIA	2.7	Uniaxial Compressive Strength	SN0208L0207502.001	
19.6	19.6	0		0	19.6	7.3		TSw1	Tptpul	ESF/ECRB/Borehole	ESF 63+60.5	ESF-GTEC-C 6500-01-0'-3.9'-01023259-SNL-B		288	359	dry	190	1.2	2.00E-06			SANDIA	3.9	Uniaxial Compressive Strength	SN0208L0207502.001	
17.7	17.7	0		0	17.7	8.8		TSw1	Tptpul	ESF/ECRB/Borehole	ESF 63+60.5	ESF-GTEC-CS6500-01A 2.4'-5.2'-01023261-SNL-A		289	544	ambient	24	1.9	2.00E-06			SANDIA	2.8	Uniaxial Compressive Strength	SN0208L0207502.001	
37	37	0		0	37.0	13.7		TSw1	Tptpul	ESF/ECRB/Borehole	ESF 63+60.5	ESF-GTEC-CS6500-01A 5.2'-8.6'-01023262-SNL-B		289	289	dry	200	1.0	1.00E-06			SANDIA	3.9	Uniaxial Compressive Strength	SN0208L0207502.001	

Table A-1 Intact Rock Mechanical Properties Data - Strength and Elastic Properties Data

Axial Stress, σ_1 (MPa)	Axial Stress, effective σ_1' (MPa)	Confining Pressure (MPa) σ_3	Pore Pressure (MPa)	Confining Pressure, Effective (MPa), σ_3'	Differential Strength, (MPa) $\sigma_1 - \sigma_3$	Young's Modulus (GPa)	Poisson's Ratio	TM Unit	Litho-stratigraphic Unit	General Location	Sample Location	Specimen Number	Depth (ft)	Specimen Diameter (mm)	Specimen Length (mm)	Specimen Saturation	Specimen Temperature (deg. C)	l/d Ratio	Strain Rate (1/s)	Specimen Orientation (degree)	Test Standard	Laboratory	Failure Strain (millistrain)	Rock Property	Source DTN	Notes
25.9	25.9	0		0	25.9	13.7		TSw1	Tptpul	ESF/ECRB/Borehole	ESF 63+60.5	ESF-GTEC-CS6500-01A 5.2'-8.6'-01023262-SNL-A		289	509	ambient	24	1.8	1.00E-06			SANDIA	2.6	Uniaxial Compressive Strength	SN0208L0207502.001	
9.4	9.4	0		0	9.4	5	0.24	TSw1	Tptpul	ESF/ECRB/Borehole	ESF 63+68.8	ESF-GTEC-CS6500-02-4.0'-6.4'-01023263-SNL-A		288	545	saturated	24	1.9	3.00E-06			SANDIA	2.5	Uniaxial Compressive Strength	SN0208L0207502.001	
11.6	11.6	0		0	11.6	5.9	0.03	TSw1	Tptpul	ESF/ECRB/Borehole	ESF 63+69	ESF-GTEC-CS6500-06-3.3'-5.9'-01023268-SNL-A		288	595	saturated	24	2.1	3.00E-06			SANDIA	2.6	Uniaxial Compressive Strength	SN0208L0207502.001	
34.8	34.8	0		0	34.8	9.9		TSw1	Tptpul	ESF/ECRB/Borehole	ESF 63+85.9	ESF-GTEC-CS6500-05A 0'-2.0'-01023267-SNL-A		289	363	dry	190	1.3	2.00E-06			SANDIA	4.7	Uniaxial Compressive Strength	SN0208L0207502.001	
16.5	16.5	0		0	16.5	12.4		TSw1	Tptpul	ESF/ECRB/Borehole	ESF 63+96	ESF-GTEC-CS6500-04A 7.0'-9.1'-01023266-SNL-A		289	480	ambient	24	1.7	1.00E-06			SANDIA	1.8	Uniaxial Compressive Strength	SN0208L0207502.001	
26.2	26.2	0		0	26.2	19.5		TSw1	Tptpul	ESF/ECRB/Borehole	ESF 63+96	ESF-GTEC-CS6500-04A 4.4'-7.0'-01023265-SNL-A		289	580	ambient	24	2.0	1.00E-06			SANDIA	1.8	Uniaxial Compressive Strength	SN0208L0207502.001	
33.5	33.5	0		0	33.5	20.5		TSw1	Tptpul	ESF/ECRB/Borehole	ESF 63+96	ESF-GTEC-CS6500-04A 2.0'-4.4'-01023264-SNL-A		289	481	ambient	24	1.7	1.00E-06			SANDIA	2.0	Uniaxial Compressive Strength	SN0208L0207502.001	
22.1	22.1	0		0	22.1	14.9	0.21	TSw1	Tptpul	ESF/ECRB/Borehole	ESF 63+96	ESF-GTEC-CS6500-04a-0.0'-1.8'-01023450-SNL-A		289	430	ambient	24	1.5	6.00E-06			SANDIA	2.0	Uniaxial Compressive Strength	SN0211L0207502.002	
53	53	0		0	53.0	16.9	0.140	TSw1	Tptpul	ESF/ECRB/Borehole	ESF-GTEC-CS6350	ESF-GTEC-CS6350-03B 3.7'-4.9'-01023555-SNL		145.80	286.7	ambient	22	2.0	8.00E-06			SNL	4.60	Uniaxial compressive strength	SN0302L0207502.003	
27.8	27.8	0		0	27.8	10.6	0.350	TSw1	Tptpul	ESF/ECRB/Borehole	ESF-GTEC-CS6500	ESF-GTEC-CS6500-01-0.0'-1.0'-01023565-SNL		145.60	290.5	ambient	22	2.0	8.00E-06			SNL	3.20	Uniaxial compressive strength	SN0302L0207502.003	
36.3	36.3	0		0	36.3	14.5	0.140	TSw1	Tptpul	ESF/ECRB/Borehole	ESF-GTEC-CS6500	ESF-GTEC-CS6500-05-3.8'-5.0'-01023541-SNL		145.50	281.5	ambient	22	1.9	8.00E-06			SNL	3.20	Uniaxial compressive strength	SN0302L0207502.003	
28.8	28.8	0		0	28.8	15		TSw1	Tptpul	ESF/ECRB/Borehole	ESF-GTEC-CS6500	ESF-GTEC-CS6500-09-3.8'-4.4'-01023564-SNL		146.80	297.3	ambient	22	2.0	8.00E-06			SNL	2.30	Uniaxial compressive strength	SN0302L0207502.003	
41.3	41.3	0		0	41.3	15.6	0.250	TSw1	Tptpul	ESF/ECRB/Borehole	ESF-GTEC-CS6500	ESF-GTEC-CS6500-05A 4.8'-5.9'-01023563-SNL		146.80	288.2	saturated	22	2.0	8.00E-06			SNL	3.40	Uniaxial compressive strength	SN0302L0207502.003	
17.7	17.7	0		0	17.7	6.7		TSw1	Tptpul	ESF/ECRB/Borehole	ESF-GTEC-CS6500	ESF-GTEC-CS6500-07-0.2'-1.4'-01023675-SNL		146.5	301.8	dry	200	2.1	1.00E-05			SNL	4.4	Uniaxial compressive strength	SN0305L0207502.004	
14.9	14.9	0		0	14.9	7.2		TSw1	Tptpul	ESF/ECRB/Borehole	ESF-GTEC-CS6500	ESF-GTEC-CS6500-09-0.3'-1.5'-01023676-SNL		146.3	276.3	saturated	24	1.9	1.10E-05			SNL	3.4	Uniaxial compressive strength	SN0305L0207502.004	
19.4	19.4	0		0	19.4	7.3		TSw1	Tptpul	ESF/ECRB/Borehole	ESF-GTEC-CS6500	ESF-GTEC-CS6500-07A 0.2'-1.4'-01023677-SNL		146.8	279.6	ambient	24	1.9	1.00E-05			SNL	3.4	Uniaxial compressive strength	SN0305L0207502.004	
17.4	17.4	0		0	17.4	6.4	0.31	TSw1	Tptrl	ESF/ECRB/Borehole	UE-25 NRG#4	NRG-4-667.8-SNL-A	667.8	50.8	101.6	saturated	22	2.0	1.00E-05			NER	3.21	Uniaxial compressive strength	MO0311RCKPRPCS.003, MO0402DQRIRPPR.003	
35.9	35.9	0		0	35.9	10.3	0.28	TSw1	Tptrl	ESF/ECRB/Borehole	UE-25 NRG#4	NRG-4-695.8-SNL-A	695.8	50.8	101.6	saturated	22	2.0	1.00E-05			NER	4.12	Uniaxial compressive strength	MO0311RCKPRPCS.003, MO0402DQRIRPPR.003	
26.9	26.9	0		0	26.9	10.7		TSw1	Tptrl	ESF/ECRB/Borehole	UE-25 NRG#4	NRG-4-664.4-SNL-A	664.4	50.8	101.6	saturated	22	2.0	1.00E-05			NER	3.23	Uniaxial compressive strength	MO0311RCKPRPCS.003, MO0402DQRIRPPR.003	
31.8	31.8	0		0	31.8	9.2	0.26	TSw1	Tptrn	ESF/ECRB/Borehole	UE-25 NRG#4	NRG-4-591.7-SNL-A	591.7	50.8	101.6	saturated	22	2.0	1.00E-05			NER	4.50	Uniaxial compressive strength	MO0311RCKPRPCS.003, MO0402DQRIRPPR.003	
32	32	0		0	32.0	11.2	0.20	TSw1	Tptrn	ESF/ECRB/Borehole	UE-25 NRG#4	NRG-4-627.7-SNL-A	627.7	50.8	101.6	saturated	22	2.0	1.00E-05			NER	3.34	Uniaxial compressive strength	MO0311RCKPRPCS.003, MO0402DQRIRPPR.003	
43.7	43.7	0		0	43.7	11.4	0.27	TSw1	Tptrn	ESF/ECRB/Borehole	UE-25 NRG#4	NRG-4-607.6-SNL-A	607.6	50.8	101.6	saturated	22	2.0	1.00E-05			NER	5.07	Uniaxial compressive strength	MO0311RCKPRPCS.003, MO0402DQRIRPPR.003	
26.2	26.2	0		0	26.2	13.2	0.28	TSw1	Tptrn	ESF/ECRB/Borehole	UE-25 NRG#4	NRG-4-582.4-SNL-A	582.4	50.8	101.6	saturated	22	2.0	1.00E-05			NER	2.27	Uniaxial compressive strength	MO0311RCKPRPCS.003, MO0402DQRIRPPR.003	
34.1	34.1	0		0	34.1	13.6	0.27	TSw1	Tptrn	ESF/ECRB/Borehole	UE-25 NRG#4	NRG-4-602.9-SNL-A	602.9	50.8	101.6	saturated	22	2.0	1.00E-05			NER	3.41	Uniaxial compressive strength	MO0311RCKPRPCS.003, MO0402DQRIRPPR.003	
31.1	31.1	0		0	31.1	14.5	0.41	TSw1	Tptrn	ESF/ECRB/Borehole	UE-25 NRG#4	NRG-4-655.8-SNL-A	655.8	50.8	101.6	saturated	22	2.0	1.00E-05			NER	2.90	Uniaxial compressive strength	MO0311RCKPRPCS.003, MO0402DQRIRPPR.003	
33.2	33.2	0		0	33.2	14.6	0.34	TSw1	Tptrn	ESF/ECRB/Borehole	UE-25 NRG#4	NRG-4-541.0-SNL-A	541.0	50.8	101.6	saturated	22	2.0	1.00E-05			NER	2.50	Uniaxial compressive strength	MO0311RCKPRPCS.003, MO0402DQRIRPPR.003	
43.4	43.4	0		0	43.4	14.9	0.27	TSw1	Tptrn	ESF/ECRB/Borehole	UE-25 NRG#4	NRG-4-623.8-SNL-A	623.8	50.8	101.6	saturated	22	2.0	1.00E-05			NER	4.57	Uniaxial compressive strength	MO0311RCKPRPCS.003, MO0402DQRIRPPR.003	
33.3	33.3	0		0	33.3	15.6	0.29	TSw1	Tptrn	ESF/ECRB/Borehole	UE-25 NRG#4	NRG-4-597.0-SNL-A	597.0	50.8	101.6	saturated	22	2.0	1.00E-05			NER	2.41	Uniaxial compressive strength	MO0311RCKPRPCS.003, MO0402DQRIRPPR.003	
47.9	47.9	0		0	47.9	17.2	0.32	TSw1	Tptrn	ESF/ECRB/Borehole	UE-25 NRG#4	NRG-4-612.5-SNL-A	612.5	50.8	101.6	saturated	22	2.0	1.00E-05			NER	3.03	Uniaxial compressive strength	MO0311RCKPRPCS.003, MO0402DQRIRPPR.003	
56.8	56.8	0		0	56.8	19.2	0.26	TSw1	Tptrn	ESF/ECRB/Borehole	UE-25 NRG#4	NRG-4-546.0-SNL-A	546.0	50.8	101.6	saturated	22	2.0	1.00E-05			NER	3.4	Uniaxial compressive strength	MO0311RCKPRPCS.003, MO0402DQRIRPPR.003	
61.9	61.9	0		0	61.9	20.8	0.22	TSw1	Tptrn	ESF/ECRB/Borehole	UE-25 NRG#4	NRG-4-550.0-SNL-A	550.0	50.8	101.6	saturated	22	2.0	1.00E-05			NER	3.46	Uniaxial compressive strength	MO0311RCKPRPCS.003, MO0402DQRIRPPR.003	
67.1	67.1	0		0	67.1	21.6	0.20	TSw1	Tptrn	ESF/ECRB/Borehole	UE-25 NRG#4	NRG-4-630.4-SNL-A	530.4	50.8	101.6	saturated	22	2.0	1.00E-05			NER	3.37	Uniaxial compressive strength	MO0311RCKPRPCS.003, MO0402DQRIRPPR.003	
55.4	55.4	0		0	55.4	22.3	0.22	TSw1	Tptrn	ESF/ECRB/Borehole	UE-25 NRG#4	NRG-4-535.3-SNL-A	535.3	50.8	101.6	saturated	22	2.0	1.00E-05			NER	2.50	Uniaxial compressive strength	MO0311RCKPRPCS.003, MO0402DQRIRPPR.003	
97.9	97.9	0		0	97.9	27.3	0.21	TSw1	Tptrn	ESF/ECRB/Borehole	UE-25 NRG#4	NRG-4-525.0-SNL-A	525.0	50.8	101.6	saturated	22	2.0	1.00E-05			NER	3.96	Uniaxial compressive strength	MO0311RCKPRPCS.003, MO0402DQRIRPPR.003	
98.5	98.5	0		0	98.5	31.6	0.22	TSw1	Tptrn	ESF/ECRB/Borehole	UE-25 NRG#4	NRG-4-515.5-SNL-A	515.5	50.8	101.6	saturated	22	2.0	1.00E-05			NER	3.17	Uniaxial compressive strength	MO0311RCKPRPCS.003, MO0402DQRIRPPR.003	
102.6	102.6	0		0	102.6	32.3	0.22	TSw1	Tptrn	ESF/ECRB/Borehole	UE-25 NRG#4	NRG-4-508.4-SNL-A	508.4	50.8	101.6	saturated	22	2.0	1.00E-05			NER	3.43	Uniaxial compressive strength	MO0311RCKPRPCS.003, MO0402DQRIRPPR.003	
160	160	0	0	0	160	37.8	0.24	TSw1	Tptrn	ESF/ECRB/Borehole	USW G-2	G2-818.4-A	818.4	25.2	50.9	saturated	22	2.0	1.00E-05			Terra Tek	5.3	Uniaxial compressive strength	MO0311RCKPRPCS.003, MO0402DQRIRPPR.003	Drained test.
130	130	0	0	0	130	39.6	0.26	TSw1	Tptrn	ESF/ECRB/Borehole	USW G-2	G2-797.0-B	797.0	25.3	50.8	saturated	22	2.0	1.00E-05			Terra Tek	3.6	Uniaxial compressive strength	MO0311RCKPRPCS.003, MO0402DQRIRPPR.003	Drained test.
162	162	0	0	0	162	43.5	0.25	TSw1	Tptrn	ESF/ECRB/Borehole	USW G-2	G2-797.0-A	797.0	25.3	50.9	saturated	22	2.0	1.00E-05			Terra Tek	3.8	Uniaxial compressive strength	MO0311RCKPRPCS.003, MO0402DQRIRPPR.003	Drained test.
143	143	0	0	0	143	57.1	0.28	TSw1	Tptrn	ESF/ECRB/Borehole	USW G-2	G2-797.0-1	797.0	50.8	101.7	saturated	22	2.0	1.00E-05			Terra Tek	2.7	Uniaxial compressive strength	MO0311RCKPRPCS.003, MO0402DQRIRPPR.003	Drained test.
125	125	0	0	0	125	59.9	0.31	TSw1	Tptrn	ESF/ECRB/Borehole	USW G-2	G2-797.0-2	797.0	50.9	101.7	saturated	22	2.0	1.00E-05			Terra Tek	2.2	Uniaxial compressive strength	MO0311RCKPRPCS.003, MO0402DQRIRPPR.003	Drained test.
67.5	67.5	0		0	67.5	13	0.14	TSw1	Tptrn	ESF/ECRB/Borehole	USW GU-3	GU-3 519.4/1	519.4	50.93	101.57	saturated	22	2.0	1.00E-05	90		SANDIA	6.13	Uniaxial compressive strength	MO0311RCKPRPCS.003, MO0402DQRIRPPR.003	
30.5	30.5	0		0	30.5	14.8	0.21	TSw1	Tptrn	ESF/ECRB/Borehole	USW GU-3	GU-3 484.7/1	484.7	57.15	114.33	ambient	22	2.0	1.00E-05	90		SANDIA	2.78	Uniaxial compressive strength	MO0311RCKPRPCS.003, MO0402DQRIRPPR.003	
26.5	26.5	0		0	26.5	16.9	0.30	TSw1	Tptrn	ESF/ECRB/Borehole	USW GU-3	GU-3 484.7/2	484.7	57.1	114.4	ambient	22	2.0	1.00E-05	90		SANDIA	1.73	Uniaxial compressive strength	MO0311RCKPRPCS.003, MO0402DQRIRPPR.003	
72.8	72.8	0		0	72.8	17.6	0.19	TSw1	Tptrn	ESF/ECRB/Borehole	USW GU-3	GU-3 484.7/3	484.7	25.37	50.85	saturated	22	2.0	1.00E-05			SANDIA	4.27	Uniaxial compressive strength	MO0311RCKPRPCS.003, MO0402DQRIRPPR.003	
64	64	0		0	64.0	19.8		TSw1	Tptrn	ESF/ECRB/Borehole	USW GU-3	GU-3 528.4/1	528.4	57.10	114.40	ambient	22	2.0	1.00E-05	90		SANDIA	4.14	Uniaxial compressive strength	MO0311RCKPRPCS.003, MO0402DQRIRPPR.003	
67.7	67.7	0		0	67.7	21.2	0.13	TSw1	Tptrn	ESF/ECRB/Borehole	USW GU-3	GU-3 519.4/2	519.4	25.35	50.85	saturated	22	2.0	1.00E-05	90		SANDIA	3.72	Uniaxial compressive strength	MO0311RCKPRPCS.003, MO0402DQRIRPPR.003	
62.6	62.6	0		0	62.6	22.2	0.27	TSw1	Tptrn	ESF/ECRB/Borehole	USW GU-3	GU-3 519.4/3	519.4	25.35	50.85	saturated	22	2.0	1.00E-05	90		SANDIA	3.11	Uniaxial compressive strength	MO0311RCKPRPCS.003, MO0402DQRIRPPR.003	
81.4	81.4	0		0	81.4	26.8	0.26	TSw1	Tptrn	ESF/ECRB/Borehole	USW GU-3	GU-3 528.4/3	528.4	57.20	114.43	ambient	22	2.0	1.00E-05	90		SANDIA	3.45	Uniaxial compressive strength	MO0311RCKPRPCS.003, MO0402DQRIRPPR.003	
114.3	114.3	0		0	114.3	28.3	0.21	TSw1	Tptrn	ESF/ECRB/Borehole	USW GU-3	GU-3 528.4/2	528.4	57.18	114.43	ambient	22	2.0	1.00E-05	90		SANDIA	4.27	Uniaxial compressive strength	MO0311RCKPRPCS.003, MO0402DQRIRPPR.003	
36.2	36.2	0		0	36.2	12.2	0.33	TSw1	Tptrn	ESF/ECRB/Borehole	USW NRG-6	NRG-6-420.8-SNL-A	420.8	50.80	101.60	saturated	22	2.0	1.00E-05			NER	3.70	Uniaxial compressive strength	MO0311RCKPRPCS.003, MO0402DQRIRPPR.003	
43.4	43.4	0		0	43.4	14.2	0.19	TSw1	Tptrn	ESF/ECRB/Borehole	USW NRG-6	NRG-6-427.0-SNL-A	427.0	50.80	101.60	saturated	22	2.0	1.00E-05			NER	3.94	Uniaxial compressive strength	MO0311RCKPRPCS.003, MO0402DQRIRPPR.003	

Table A-1 Intact Rock Mechanical Properties Data - Strength and Elastic Properties Data

Axial Stress, σ_1 (MPa)	Axial Stress, effective σ_1' (MPa)	Confining Pressure (MPa) σ_3	Pore Pressure (MPa)	Confining Pressure, Effective (MPa), σ_3'	Differential Strength, (MPa) σ_1'-σ_3'	Young's Modulus (GPa)	Poisson's Ratio	TM Unit	Litho-stratigraphic Unit	General Location	Sample Location	Specimen Number	Depth (ft)	Specimen Diameter (mm)	Specimen Length (mm)	Specimen Saturation	Specimen Temperature (deg. C)	l/d Ratio	Strain Rate (1/s)	Specimen Orientation (degree)	Test Standard	Laboratory	Failure Strain (millistrain)	Rock Property	Source DTN	Notes
33.3	33.3	0		0	33.3	15.1	0.16	TSw1	Tptrn	ESF/ECRB/Borehole	USW NRG-6	NRG-6-372.6-SNL-A	372.6	50.80	101.60	saturated	22	2.0	1.00E-05			NER	2.72	Uniaxial compressive strength	MO0311RCKPRPCS.003, MO0402DQRIRPPR.003	
32.4	32.4	0		0	32.4	17	0.15	TSw1	Tptrn	ESF/ECRB/Borehole	USW NRG-6	NRG-6-354.4-SNL-A	354.4	50.80	101.60	saturated	22	2.0	1.00E-05			NER	3.51	Uniaxial compressive strength	MO0311RCKPRPCS.003, MO0402DQRIRPPR.003	
56.8	56.8	0		0	56.8	20.1	0.27	TSw1	Tptrn	ESF/ECRB/Borehole	USW NRG-6	NRG-6-407.2-SNL-A	407.2	50.80	101.60	saturated	22	2.0	1.00E-05			NER	3.12	Uniaxial compressive strength	MO0311RCKPRPCS.003, MO0402DQRIRPPR.003	
58.3	58.3	0		0	58.3	20.6	0.22	TSw1	Tptrn	ESF/ECRB/Borehole	USW NRG-6	NRG-6-391.6-SNL-A	391.6	50.80	101.60	saturated	22	2.0	1.00E-05			NER	3.34	Uniaxial compressive strength	MO0311RCKPRPCS.003, MO0402DQRIRPPR.003	
60.4	60.4	0		0	60.4	20.6	0.29	TSw1	Tptrn	ESF/ECRB/Borehole	USW NRG-6	NRG-6-397.0-SNL-A	397.0	50.80	101.60	saturated	22	2.0	1.00E-05			NER	4.27	Uniaxial compressive strength	MO0311RCKPRPCS.003, MO0402DQRIRPPR.003	
68.8	68.8	0		0	68.8	21.2	0.25	TSw1	Tptrn	ESF/ECRB/Borehole	USW NRG-6	NRG-6-373.1-SNL-A	373.1	50.80	101.60	saturated	22	2.0	1.00E-05			NER	3.79	Uniaxial compressive strength	MO0311RCKPRPCS.003, MO0402DQRIRPPR.003	
48.4	48.4	0		0	48.4	21.8	0.21	TSw1	Tptrn	ESF/ECRB/Borehole	USW NRG-6	NRG-6-395.2-SNL-A	395.2	50.80	101.60	saturated	22	2.0	1.00E-05			NER	2.54	Uniaxial compressive strength	MO0311RCKPRPCS.003, MO0402DQRIRPPR.003	
27.9	27.9	0		0	27.9	9.8	0.16	TSw1	Tptrn	ESF/ECRB/Borehole	USW NRG-7a	NRG-7/7A-417.9-SNL-A	417.9	50.8	101.6	saturated	22	2.0	1.00E-05			NER	4.75	Uniaxial compressive strength	MO0311RCKPRPCS.003, MO0402DQRIRPPR.003	
33.9	33.9	0		0	33.9	13.1	0.26	TSw1	Tptrn	ESF/ECRB/Borehole	USW NRG-7a	NRG-7/7A-396.6-SNL-A	396.6	50.8	101.6	saturated	22	2.0	1.00E-05			NER	2.98	Uniaxial compressive strength	MO0311RCKPRPCS.003, MO0402DQRIRPPR.003	
52.6	52.6	0		0	52.6	13.7	0.36	TSw1	Tptrn	ESF/ECRB/Borehole	USW NRG-7a	NRG-7/7A-461.0-SNL-A	461.0	50.8	101.6	saturated	22	2.0	1.00E-05			NER	5.05	Uniaxial compressive strength	MO0311RCKPRPCS.003, MO0402DQRIRPPR.003	
54.2	54.2	0		0	54.2	15.5	0.23	TSw1	Tptrn	ESF/ECRB/Borehole	USW NRG-7a	NRG-7/7A-472.9-SNL-A	472.9	50.8	101.6	saturated	22	2.0	1.00E-05			NER	4.20	Uniaxial compressive strength	MO0311RCKPRPCS.003, MO0402DQRIRPPR.003	
25.7	25.7	0		0	25.7	17.2	0.28	TSw1	Tptrn	ESF/ECRB/Borehole	USW NRG-7a	NRG-7/7A-450.1-SNL-A	450.1	50.8	101.6	saturated	22	2.0	1.00E-05			NER	1.55	Uniaxial compressive strength	MO0311RCKPRPCS.003, MO0402DQRIRPPR.003	
66.3	66.3	0		0	66.3	17.9	0.31	TSw1	Tptrn	ESF/ECRB/Borehole	USW NRG-7a	NRG-7/7A-443.2-SNL-A	443.2	50.8	101.6	saturated	22	2.0	1.00E-05			NER	4.95	Uniaxial compressive strength	MO0311RCKPRPCS.003, MO0402DQRIRPPR.003	
53.9	53.9	0		0	53.9	18.4	0.43	TSw1	Tptrn	ESF/ECRB/Borehole	USW NRG-7a	NRG-7/7A-469.4-SNL-A	469.4	50.8	101.6	saturated	22	2.0	1.00E-05			NER	3.63	Uniaxial compressive strength	MO0311RCKPRPCS.003, MO0402DQRIRPPR.003	
60.8	60.8	0		0	60.8	19	0.18	TSw1	Tptrn	ESF/ECRB/Borehole	USW NRG-7a	NRG-7/7A-422.0-SNL-A	422.0	50.8	101.6	saturated	22	2.0	1.00E-05			NER	4.09	Uniaxial compressive strength	MO0311RCKPRPCS.003, MO0402DQRIRPPR.003	
89.5	89.5	0		0	89.5	19.1	0.15	TSw1	Tptrn	ESF/ECRB/Borehole	USW NRG-7a	NRG-7/7A-344.4-SNL-J	344.4	25.4	50.8	saturated	22	2.0	1.00E-05			NER	5.68	Uniaxial compressive strength	MO0311RCKPRPCS.003, MO0402DQRIRPPR.003	
61	61	0		0	61.0	19.9	0.22	TSw1	Tptrn	ESF/ECRB/Borehole	USWNRG-7a	NRG-7/7A-380.8-SNL-A	380.8	50.8	101.6	saturated	22	2.0	1.00E-05			NER	3.98	Uniaxial compressive strength	MO0311RCKPRPCS.003, MO0402DQRIRPPR.003	
55.5	55.5	0		0	55.5	21.8	0.20	TSw1	Tptrn	ESF/ECRB/Borehole	USWNRG-7a	NRG-7/7A-428.7-SNL-A	428.7	50.8	101.6	saturated	22	2.0	1.00E-05			NER	2.68	Uniaxial compressive strength	MO0311RCKPRPCS.003, MO0402DQRIRPPR.003	
63.3	63.3	0		0	63.3	22.4	0.19	TSw1	Tptrn	ESF/ECRB/Borehole	USWNRG-7a	NRG-7/7A-334.5-SNL-A	334.5	50.8	101.6	saturated	22	2.0	1.00E-05			NER	3.32	Uniaxial compressive strength	MO0311RCKPRPCS.003, MO0402DQRIRPPR.003	
45.2	45.2	0		0	45.2	22.9	0.19	TSw1	Tptrn	ESF/ECRB/Borehole	USWNRG-7a	NRG-7/7A-369.5-SNL-A	369.5	50.8	101.6	saturated	22	2.0	1.00E-05			NER	2.40	Uniaxial compressive strength	MO0311RCKPRPCS.003, MO0402DQRIRPPR.003	
106.2	106.2	0		0	106.2	26.3	0.17	TSw1	Tptrn	ESF/ECRB/Borehole	USWNRG-7a	NRG-7/7A-344.4-SNL-I	344.4	25.4	50.8	saturated	22	2.0	1.00E-05			NER	4.46	Uniaxial compressive strength	MO0311RCKPRPCS.003, MO0402DQRIRPPR.003	
88.7	88.7	0		0	88.7	27.2	0.15	TSw1	Tptrn	ESF/ECRB/Borehole	USWNRG-7a	NRG-7/7A-344.4-SNL-L	344.4	25.4	50.8	saturated	22	2.0	1.00E-05			NER	3.50	Uniaxial compressive strength	MO0311RCKPRPCS.003, MO0402DQRIRPPR.003	
97.3	97.3	0		0	97.3	27.7	0.18	TSw1	Tptrn	ESF/ECRB/Borehole	USWNRG-7a	NRG-7/7A-344.4-SNL-K	344.4	25.4	50.8	saturated	22	2.0	1.00E-05			NER	3.53	Uniaxial compressive strength	MO0311RCKPRPCS.003, MO0402DQRIRPPR.003	
148.4	148.4	0		0	148.4	34.3	0.17	TSw1	Tptrn	ESF/ECRB/Borehole	USWNRG-7a	NRG-7/7A-350.3-SNL-A	350.3	50.8	101.6	saturated	22	2.0	1.00E-05			NER	4.72	Uniaxial compressive strength	MO0311RCKPRPCS.003, MO0402DQRIRPPR.003	
44.4	44.4	0		0	44.4	17.8	0.19	TSw1	Tptrn	ESF/ECRB/Borehole	USW SD-12	SD-12-354.1-SNL-A	354.1	50.8	101.6	saturated	22	2.0	1.00E-05			NER	1.95	Uniaxial compressive strength	MO0311RCKPRPCS.003, MO0402DQRIRPPR.003	
48.4	48.4	0		0	48.4	19.7	0.25	TSw1	Tptrn	ESF/ECRB/Borehole	USW SD-12	SD-12-406.1-SNL-A	406.1	50.8	101.6	saturated	22	2.0	1.00E-05			NER	3.94	Uniaxial compressive strength	MO0311RCKPRPCS.003, MO0402DQRIRPPR.003	
32.8	32.8	0		0	32.8	14.8	0.31	TSw1	Tptrn	ESF/ECRB/Borehole	USW SD-9	SD-9-405.6-SNL-A	405.6	50.8	101.6	saturated	22	2.0	1.00E-05			NER	2.67	Uniaxial compressive strength	MO0311RCKPRPCS.003, MO0402DQRIRPPR.003	
74.3	74.3	0		0	74.3	25.5	0.24	TSw1	Tptrn	ESF/ECRB/Borehole	USW SD-9	SD-9-338.6-SNL-A	338.6	50.8	101.6	saturated	22	2.0	1.00E-05			NER	3.27	Uniaxial compressive strength	MO0311RCKPRPCS.003, MO0402DQRIRPPR.003	
142.7	142.7	0		0	142.7	32.3	0.18	TSw1	Tptrn	ESF/ECRB/Borehole	USW SD-9	SD-9-311.1-SNL-A	311.1	50.8	101.6	saturated	22	2.0	1.00E-05			NER	4.85	Uniaxial compressive strength	MO0311RCKPRPCS.003, MO0402DQRIRPPR.003	
73.2	73.2	0		0	73.20	21.5	0.29	TSw1	Tptrn	ESF/ECRB/Borehole	USW NRG-6	NRG-6-328.7-SNL-A	328.7	50.80	101.60	saturated	22	2.0	1.00E-05			NER	3.92	Uniaxial compressive strength	SNL02030193001.001, MO0402DQRIRPPR.003	
79.2	79.2	0		0	79.20	22	0.26	TSw1	Tptrn	ESF/ECRB/Borehole	USW NRG-6	NRG-6-316.3-SNL-A	316.3	50.80	101.60	saturated	22	2.0	1.00E-05			NER	4.26	Uniaxial compressive strength	SNL02030193001.001, MO0402DQRIRPPR.003	
77.2	77.2	0		0	77.20	22.4	0.27	TSw1	Tptrn	ESF/ECRB/Borehole	USW NRG-6	NRG-6-318.2-SNL-A	318.2	50.80	101.60	saturated	22	2.0	1.00E-05			NER	4.4	Uniaxial compressive strength	SNL02030193001.001, MO0402DQRIRPPR.003	
72.8	72.8	0		0	72.80	23.8	0.24	TSw1	Tptrn	ESF/ECRB/Borehole	USW NRG-6	NRG-6-328.7-SNL-B	328.7	50.80	101.60	saturated	22	2.0	1.00E-05			NER	3.75	Uniaxial compressive strength	SNL02030193001.001, MO0402DQRIRPPR.003	
102.2	102.2	0		0	102.20	28.1	0.21	TSw1	Tptrn	ESF/ECRB/Borehole	USW NRG-6	NRG-6-304.4-SNL-A	304.4	50.80	101.60	saturated	22	2.0	1.00E-05			NER	4.08	Uniaxial compressive strength	SNL02030193001.001, MO0402DQRIRPPR.003	
118.6	118.6	0		0	118.60	33.2	0.21	TSw1	Tptrn	ESF/ECRB/Borehole	USW NRG-6	NRG-6-276.2-SNL-A	276.2	50.80	101.60	saturated	22	2.0	1.00E-05			NER	3.75	Uniaxial compressive strength	SNL02030193001.001, MO0402DQRIRPPR.003	
7	7	0		0	7			TSw2	Tptpll	ESF/ECRB/Borehole	USW G-2	G2-1297.6-B	1297.6	25.3	50.9	saturated	22	2.0	1.00E-05			Terra Tek	2.4	Uniaxial compressive strength	MO0311RCKPRPCS.003	Report indicates low strength due to unusual lithology of sample
3	3	0		0	3			TSw2	Tptpll	ESF/ECRB/Borehole	USW G-2	G2-1297.6-A	1297.6	25.2	50.8	saturated	22	2.0	1.00E-05			Terra Tek	1.4	Uniaxial compressive strength	MO0311RCKPRPCS.003	Report indicates low strength due to unusual lithology of sample
97	97	0		0	97	18.8	0.18	TSw2	Tptpll	ESF/ECRB/Borehole	USW G-2	G2-1579.1-C	1579.1	25.3	50.8	saturated	22	2.0	1.00E-05			Terra Tek	6.3	Uniaxial compressive strength	MO0311RCKPRPCS.003, MO0402DQRIRPPR.003	
96	96	0		0	96	20.5	0.19	TSw2	Tptpll	ESF/ECRB/Borehole	USW G-2	G2-1579.1-E	1579.1	25.3	50.8	saturated	22	2.0	1.00E-05			Terra Tek	5.8	Uniaxial compressive strength	MO0311RCKPRPCS.003, MO0402DQRIRPPR.003	
73	73	0		0	73	22	0.17	TSw2	Tptpll	ESF/ECRB/Borehole	USW G-2	G2-1561.3-C	1561.3	25.3	50.8	saturated	22	2.0	1.00E-05			Terra Tek	4.1	Uniaxial compressive strength	MO0311RCKPRPCS.003, MO0402DQRIRPPR.003	
85	85	0		0	85	22.1	0.11	TSw2	Tptpll	ESF/ECRB/Borehole	USW G-2	G2-1561.3-A	1561.3	25.3	50.8	saturated	22	2.0	1.00E-05			Terra Tek	4.7	Uniaxial compressive strength	MO0311RCKPRPCS.003, MO0402DQRIRPPR.003	
86	86	0		0	86	22.7		TSw2	Tptpll	ESF/ECRB/Borehole	USW G-2	G2-1561.3-D	1561.3	25.3	50.8	saturated	22	2.0	1.00E-05			Terra Tek	4.1	Uniaxial compressive strength	MO0311RCKPRPCS.003, MO0402DQRIRPPR.003	
61	61	0		0	61	23.6		TSw2	Tptpll	ESF/ECRB/Borehole	USW G-2	G2-1561.3-E	1561.3	25.3	50.8	saturated	22	2.0	1.00E-05			Terra Tek	3.7	Uniaxial compressive strength	MO0311RCKPRPCS.003, MO0402DQRIRPPR.003	
175	175	0		0	175	31.8	0.17	TSw2	Tptpll	ESF/ECRB/Borehole	USW G-2	G2-1579.1-D	1579.1	25.2	50.9	saturated	22	2.0	1.00E-05			Terra Tek	6.1	Uniaxial compressive strength	MO0311RCKPRPCS.003, MO0402DQRIRPPR.003	
170	170	0		0	170	33.9	0.17	TSw2	Tptpll	ESF/ECRB/Borehole	USW G-2	G2-1579.1-A	1579.1	25.3	50.8	saturated	22	2.0	1.00E-05			Terra Tek	5.6	Uniaxial compressive strength	MO0311RCKPRPCS.003, MO0402DQRIRPPR.003	
155	155	0		0	155	35.5	0.16	TSw2	Tptpll	ESF/ECRB/Borehole	USW G-2	G2-1587.8-D	1587.8	25.3	50.9	saturated	22	2.0	1.00E-05			Terra Tek	5.5	Uniaxial compressive strength	MO0311RCKPRPCS.003, MO0402DQRIRPPR.003	
165	165	0		0	165	35.9	0.2	TSw2	Tptpll	ESF/ECRB/Borehole	USW G-2	G2-1587.8-B	1587.8	25.3	50.8	saturated	22	2.0	1.00E-05			Terra Tek	6.1	Uniaxial compressive strength	MO0311RCKPRPCS.003, MO0402DQRIRPPR.003	
50.9	50.9	0		0	50.9	24.5		TSw2	Tptpll	ESF/ECRB/Borehole	USW GU-3	GU-3 874.6/1	874.6	57.18	114.40	ambient	22	2.0	1.00E-05	90		SNL	4.09	Uniaxial compressive strength	MO0311RCKPRPCS.003, MO0402DQRIRPPR.003	
144.9	144.9	0		0	144.9	26.8		TSw2	Tptpll	ESF/ECRB/Borehole	USW GU-3	GU-3 853.4/1	853.4	57.05	114.53	ambient	22	2.0	1.00E-05	90		SNL	5.79	Uniaxial compressive strength	MO0311RCKPRPCS.003, MO0402DQRIRPPR.003	
31.6	31.6	0		0	31.6	16.9	0.11	TSw2	Tptpll	ESF/ECRB/Borehole	USW NRG-6	NRG-6-953.2-SNL-A	953.2	50.80	101.60	saturated	22	2.0	1.00E-05		ASTM D-3148 and ISRM U	NER	4.56	Uniaxial compressive strength	MO0311RCKPRPCS.003, MO0402DQRIRPPR.003	
56.3	56.3	0		0	56.3	19.3	0.31	TSw2	Tptpll	ESF/ECRB/Borehole	USW NRG-6	NRG-6-963.3-SNL-A	963.3	50.80	101.60	saturated	22	2.0	1.00E-05		ASTM D-3148 and ISRM U	NER	3.86	Uniaxial compressive strength	MO0311RCKPRPCS.003, MO0402DQRIRPPR.003	
97.3	97.3	0		0	97.3	27.4	0.19	TSw2	Tptpll	ESF/ECRB/Borehole	USW NRG-6	NRG-6-971.4-SNL-A	971.4	50.80	101.60	saturated	22	2.0	1.00E-05		ASTM D-3148 and ISRM U	NER	4.48	Uniaxial compressive strength	MO0311RCKPRPCS.003, MO0402DQRIRPPR.003	
84.9	84.9	0		0	84.9	27.4	0.23	TSw2	Tptpll	ESF/ECRB/Borehole	USW NRG-6	NRG-6-1017.8-SNL-A	1017.8	50.80	101.60	saturated	22	2.0	1.00E-05		ASTM D-3148 and ISRM U	NER	3.29	Uniaxial compressive strength	MO0311RCKPRPCS.003, MO0402DQRIRPPR.003	
175.5	175.5	0		0	175.5	34.6	0.19	TSw2	Tptpll	ESF/ECRB/Borehole	USW NRG-6	NRG-6-848.0-SNL-A	848.0	50.80	101.60	saturated	22	2.0	1.00E-05		ASTM D-3148 and ISRM U	NER	5.52	Uniaxial compressive strength	MO0311RCKPRPCS.003, MO0402DQRIRPPR.003	
177.3	177.3	0		0	177.3	37.6	0.25	TSw2	Tptpll	ESF/ECRB/Borehole	USW NRG-6	NRG-6-985.7-SNL-A	985.7	50.80	101.60	saturated	22	2.0	1.00E-05		ASTM D-3148 and ISRM U	NER	4.96	Uniaxial compressive strength	MO0311RCKPRPCS.003, MO0402DQRIRPPR.003	
61	61	0		0	61.0	21.8	0.4	TSw2	Tptpll	ESF/ECRB/Borehole	USW NRG-7a	NRG-7/7A-1236.7-SNL-A	1236.7	50.8	101.6	saturated	22	2.0	1.00E-05		ASTM D-3148 & ISRM U	NER	3.66	Uniaxial compressive strength	MO0311RCKPRPCS.003, MO0402DQRIRPPR.003	
117.2	117.2	0		0	117.2	29.8	0.23	TSw2	Tptpll	ESF/ECRB/Borehole	USW NRG-7a	NRG-7/7A-1230.2-SNL-A	1230.2	50.8	101.6	saturated	22	2.0	1.00E-05		ASTM D-3148 & ISRM U	NER	3.79	Uniaxial compressive strength	MO0311RCKPRPCS.003, MO0402DQRIRPPR.003	
31.1	31.1	0		0	31.1	6.5		TSw2	Tptpll	ESF/ECRB/Borehole	ESF 19+22.2	ECRB-GTEC-CS1922-01 5.1'-6.8'-01023443-SNL-A		289	320	dry	200	1.1	7.00E-06			SANDIA	8.1	Uniaxial Compressive Strength	SN0211L0207502.002	

Table A-1 Intact Rock Mechanical Properties Data - Strength and Elastic Properties Data

Axial Stress, σ_1 (MPa)	Axial Stress, effective σ_1' (MPa)	Confining Pressure (MPa) σ_3	Pore Pressure (MPa)	Confining Pressure, Effective (MPa), σ_3'	Differential Strength, (MPa) $\sigma_1'-\sigma_3'$	Young's Modulus (GPa)	Poisson's Ratio	TM Unit	Litho-stratigraphic Unit	General Location	Sample Location	Specimen Number	Depth (ft)	Specimen Diameter (mm)	Specimen Length (mm)	Specimen Saturation	Specimen Temperature (deg. C)	l/d Ratio	Strain Rate (1/s)	Specimen Orientation (degree)	Test Standard	Laboratory	Failure Strain (millistrain)	Rock Property	Source DTN	Notes
21.7	21.7	0		0	21.7	8.5		TSw2	Tptpll	ESF/ECRB/Borehole	ESF 19+22.2	ECRB-GTEC-CS1922-01 8.7'-10.6'-01023446-SNL-A		288	508	ambient	24	1.8	7.00E-06			SANDIA	3.9	Uniaxial Compressive Strength	SN0211L0207502.002	
13.3	13.3	0		0	13.3	5		TSw2	Tptpll	ESF/ECRB/Borehole	ESF 19+28.7	ECRB-GTEC-CS1928-02 0.0'-2.5'-01023424-SNL-A		288	528	ambient	24	1.8	8.00E-06			SANDIA	4.0	Uniaxial Compressive Strength	SN0211L0207502.002	
15.7	15.7	0		0	15.7	5.3		TSw2	Tptpll	ESF/ECRB/Borehole	ESF 19+28.7	ECRB-GTEC-CS1928-01 4.6'-6.9'-01023387-SNL-A		288	552	saturated	24	1.9	8.00E-06			SANDIA	4.5	Uniaxial Compressive Strength	SN0211L0207502.002	
32.2	32.2	0		0	32.2	7.1		TSw2	Tptpll	ESF/ECRB/Borehole	ESF 19+28.7	ECRB-GTEC-CS1928-03 6.1'-7.7'-01023449-SNL-A		289	304	dry	195	1.1	7.00E-06			SANDIA	7.7	Uniaxial Compressive Strength	SN0211L0207502.002	
28.7	28.7	0		0	28.7	9.2		TSw2	Tptpll	ESF/ECRB/Borehole	ESF 19+28.7	ECRB-GTEC-CS1928-01-11.3'-13.7'-01023423-SNL-A		288	521	ambient	24	1.8	7.00E-06			SANDIA	4.6	Uniaxial Compressive Strength	SN0211L0207502.002	
43.6	43.6	0		0	43.6	12.4		TSw2	Tptpll	ESF/ECRB/Borehole	ESF-GTEC-CS1922	ECRB-GTEC-CS1922-02 7.1'-8.6'-01023447-SNL		146.20	291.2	ambient	22	2.0	8.00E-06			SNL	4.80	Uniaxial compressive strength	SN0302L0207502.003	
33.1	33.1	0		0	33.1	12	0.340	TSw2	Tptpll	ESF/ECRB/Borehole	ESF-GTEC-CS1928	ECRB-GTEC-CS1928-01 0.1'-1.2'-01023545-SNL		146.80	279.5	ambient	22	1.9	8.00E-06			SNL	3.50	Uniaxial compressive strength	SN0302L0207502.003	
34.2	34.2	0		0	34.2	14.6	0.2	TSw2	Tptpll	ESF/ECRB/Borehole	ESF-GTEC-CS2150	ECRB-GTEC-CS2150-02 3.7'-4.9'-01023543-SNL		145.70	278.8	ambient	22	1.9	8.00E-06			SNL	3.80	Uniaxial compressive strength	SN0302L0207502.003	
67.4	67.4	0		0	67.4	21	0.200	TSw2	Tptpll	ESF/ECRB/Borehole	ESF-GTEC-CS2150	ECRB-GTEC-CS2150-02 2.3'-3.4'-01023542-SNL		145.80	293.6	ambient	22	2.0	7.00E-06			SNL	4.00	Uniaxial compressive strength	SN0302L0207502.003	
44.9	44.9	0		0	44.9	12.5		TSw2	Tptpll	ESF/ECRB/Borehole	ESF-GTEC-CS1900	ESF-GTEC-CS1900-22A 3.3'-4.2'-01023674-SNL		146.6	267.8	ambient	24	1.8	9.00E-06			SNL	4.7	Uniaxial compressive strength	SN0305L0207502.004	
28.3	28.3	0		0	28.3	7.1		TSw2	Tptpll	ESF/ECRB/Borehole	ESF-GTEC-CS2200	ESF-GTEC-CS2200-12-3.7'-4.9'-01023673-SNL		146.9	287.5	dry	200	2.0	1.00E-05			SNL	5.6	Uniaxial compressive strength	SN0305L0207502.004	
28.1	28.1	0		0	28.1	9.6	0.32	TSw2	Tptpll	ESF/ECRB/Borehole	ESF-GTEC-CS2200	ESF-GTEC-CS2200-10-6.7'-8.0'-01023680-SNL		146.3	290.3	ambient	24	2.0	1.00E-05			SNL	3.7	Uniaxial compressive strength	SN0305L0207502.004	
38	38	0		0	38	10.9		TSw2	Tptpll	ESF/ECRB/Borehole	ESF-GTEC-CS2200	ESF-GTEC-CS2200-12-2.0'-3.1'-01023678-SNL		146.9	279.8	saturated	24	1.9	1.00E-05			SNL	4.9	Uniaxial compressive strength	SN0305L0207502.004	
61	61	0		0	61.0	23	0.165	TSw2	Tptpll	Busted Butte	Busted Butte	B1D2302Z		81.99	164.50	ambient	25	2.0	1.00E-05			SNL	4.79	Uniaxial compressive strength	SN0306L0207502.008	
54.1	54.1	0		0	54.1	23.1	0.348	TSw2	Tptpll	Busted Butte	Busted Butte	B1D2301Z		81.89	168.10	dry	200	2.1	1.00E-05			SNL	4.08	Uniaxial compressive strength	SN0306L0207502.008	
27	27	0		0	27.0	25.3		TSw2	Tptpll	Busted Butte	Busted Butte	B0CZ		Specimens were rectangular	410.1, 197.1, 197.6	ambient	25	2.1	7.00E-06			SNL	2.07	Uniaxial compressive strength	SN0306L0207502.008	Specimens were rectangular
64.4	64.4	0		0	64.4	25.8	0.098	TSw2	Tptpll	Busted Butte	Busted Butte	B1D2501Z		120.70	237.50	ambient	25	2.0	9.00E-06			SNL	3.45	Uniaxial compressive strength	SN0306L0207502.008	
110.9	110.9	0		0	110.9	26	0.115	TSw2	Tptpll	Busted Butte	Busted Butte	B1D2104Z		26.20	50.77	ambient	25	1.9	1.00E-05			SNL	5.11	Uniaxial compressive strength	SN0306L0207502.008	
47	47	0		0	47.0	26.4		TSw2	Tptpll	Busted Butte	Busted Butte	B1CZ		Specimens were rectangular	395.7, 197.0, 188.2	ambient	25	2.1	7.00E-06			SNL	2.62	Uniaxial compressive strength	SN0306L0207502.008	Specimens were rectangular
92.4	92.4	0		0	92.4	26.6	0.209	TSw2	Tptpll	Busted Butte	Busted Butte	B1D1202Z		51.03	101.60	ambient	25	2.0	1.00E-05			SNL	4.24	Uniaxial compressive strength	SN0306L0207502.008	
87.4	87.4	0		0	87.4	27.3	0.156	TSw2	Tptpll	Busted Butte	Busted Butte	B1D1203Y		51.04	98.81	ambient	25	1.9	1.00E-05			SNL	3.77	Uniaxial compressive strength	SN0306L0207502.008	
121	121	0		0	121.0	28.4	0.232	TSw2	Tptpll	Busted Butte	Busted Butte	B0E2204Z		51.00	101.60	saturated	25	2.0	1.00E-05			SNL	5.49	Uniaxial compressive strength	SN0306L0207502.008	
114.4	114.4	0		0	114.4	28.7	0.158	TSw2	Tptpll	Busted Butte	Busted Butte	B1D1201Z		51.05	101.60	ambient	25	2.0	1.00E-05			SNL	4.66	Uniaxial compressive strength	SN0306L0207502.008	
114.9	114.9	0		0	114.9	29	0.141	TSw2	Tptpll	Busted Butte	Busted Butte	B2F201X		50.94	101.20	ambient	25	2.0	1.00E-05			SNL	4.84	Uniaxial compressive strength	SN0306L0207502.008	
146.9	146.9	0		0	146.9	29.1	0.159	TSw2	Tptpll	Busted Butte	Busted Butte	B1D2103Z		26.20	50.86	ambient	25	1.9	1.00E-05			SNL	6.16	Uniaxial compressive strength	SN0306L0207502.008	
138.9	138.9	0		0	138.9	29.4	0.161	TSw2	Tptpll	Busted Butte	Busted Butte	B1B301Z		81.99	174.80	ambient	25	2.1	9.00E-06			SNL	5.02	Uniaxial compressive strength	SN0306L0207502.008	
174.1	174.1	0		0	174.1	29.6	0.170	TSw2	Tptpll	Busted Butte	Busted Butte	B1D2102Z		26.20	50.83	ambient	25	1.9	1.00E-05			SNL	6.82	Uniaxial compressive strength	SN0306L0207502.008	
179.6	179.6	0		0	179.6	29.7	0.163	TSw2	Tptpll	Busted Butte	Busted Butte	B1D2101Z		26.22	50.84	ambient	25	1.9	1.00E-05			SNL	7.32	Uniaxial compressive strength	SN0306L0207502.008	
115.2	115.2	0		0	115.2	29.8	0.169	TSw2	Tptpll	Busted Butte	Busted Butte	B1D2202Z		51.02	102.10	ambient	25	2.0	1.00E-05			SNL	4.63	Uniaxial compressive strength	SN0306L0207502.008	
121.9	121.9	0		0	121.9	30.5	0.159	TSw2	Tptpll	Busted Butte	Busted Butte	B1D2201Z		51.02	101.60	ambient	25	2.0	1.00E-05			SNL	4.71	Uniaxial compressive strength	SN0306L0207502.008	
88.6	88.6	0		0	88.6	30.6	0.210	TSw2	Tptpll	Busted Butte	Busted Butte	B3F2202Y		50.99	100.53	ambient	25	2.0	1.00E-05			SNL	3.66	Uniaxial compressive strength	SN0306L0207502.008	
104.8	104.8	0		0	104.8	30.9	0.163	TSw2	Tptpll	Busted Butte	Busted Butte	B3F2203X		50.98	102.20	ambient	25	2.0	1.00E-05			SNL	4.44	Uniaxial compressive strength	SN0306L0207502.008	
109.2	109.2	0		0	109.2	30.9	0.165	TSw2	Tptpll	Busted Butte	Busted Butte	B0E1203Y		51.00	101.50	ambient	25	2.0	9.00E-06			SNL	4.30	Uniaxial compressive strength	SN0306L0207502.008	
192.8	192.8	0		0	192.8	31	0.179	TSw2	Tptpll	Busted Butte	Busted Butte	B2F101Z		26.25	50.67	ambient	25	1.9	1.00E-05			SNL	7.36	Uniaxial compressive strength	SN0306L0207502.008	
109.9	109.9	0		0	109.9	31.1	0.155	TSw2	Tptpll	Busted Butte	Busted Butte	B1E201Z		51.06	101.50	ambient	25	2.0	1.00E-05			SNL	4.87	Uniaxial compressive strength	SN0306L0207502.008	
198.7	198.7	0		0	198.7	31.2	0.169	TSw2	Tptpll	Busted Butte	Busted Butte	B3A2101Z		26.20	51.03	ambient	25	1.9	1.00E-05			SNL	8.04	Uniaxial compressive strength	SN0306L0207502.008	
135.1	135.1	0		0	135.1	31.3	0.225	TSw2	Tptpll	Busted Butte	Busted Butte	B0H1207Z		51.04	97.93	saturated	25	1.9	9.00E-06			SNL	5.35	Uniaxial compressive strength	SN0306L0207502.008	
121.2	121.2	0		0	121.2	31.4	0.164	TSw2	Tptpll	Busted Butte	Busted Butte	B1D1201X		51.05	101.60	ambient	25	2.0	1.00E-05			SNL	4.65	Uniaxial compressive strength	SN0306L0207502.008	
114.3	114.3	0		0	114.3	31.6	0.159	TSw2	Tptpll	Busted Butte	Busted Butte	B1D2502Z		120.70	242.30	ambient	25	2.0	9.00E-06			SNL	4.12	Uniaxial compressive strength	SN0306L0207502.008	
153.2	153.2	0		0	153.2	32.1	0.186	TSw2	Tptpll	Busted Butte	Busted Butte	B1D2203Z		51.01	99.07	ambient	25	1.9	1.00E-05			SNL	5.54	Uniaxial compressive strength	SN0306L0207502.008	
130	130	0		0	130.0	32.2	0.205	TSw2	Tptpll	Busted Butte	Busted Butte	B3F2201Z		51.03	101.80	ambient	25	2.0	1.00E-05			SNL	4.60	Uniaxial compressive strength	SN0306L0207502.008	
179.5	179.5	0		0	179.5	32.4	0.162	TSw2	Tptpll	Busted Butte	Busted Butte	B2F103Z		26.24	50.69	ambient	25	1.9	1.00E-05			SNL	6.76	Uniaxial compressive strength	SN0306L0207502.008	
230	230	0		0	230.0	32.4	0.166	TSw2	Tptpll	Busted Butte	Busted Butte	B0E2101Z		26.12	50.76	ambient	25	1.9	1.00E-05			SNL	8.39	Uniaxial compressive strength	SN0306L0207502.008	
113.7	113.7	0		0	113.7	32.5	0.170	TSw2	Tptpll	Busted Butte	Busted Butte	B1D1201Y		51.05	100.30	ambient	25	2.0	9.00E-06			SNL	4.49	Uniaxial compressive strength	SN0306L0207502.008	
133.7	133.7	0		0	133.7	32.5	0.176	TSw2	Tptpll	Busted Butte	Busted Butte	B1B202Z		51.05	101.50	ambient	25	2.0	1.00E-05			SNL	4.54	Uniaxial compressive strength	SN0306L0207502.008	
157.2	157.2	0		0	157.2	32.5	0.185	TSw2	Tptpll	Busted Butte	Busted Butte	B1D1202Y		51.04	99.09	ambient	25	1.9	9.00E-06			SNL	5.51	Uniaxial compressive strength	SN0306L0207502.008	
152.2	152.2	0		0	152.2	32.7	0.169	TSw2	Tptpll	Busted Butte	Busted Butte	B0H1201Z		51.05	100.30	dry	25	2.0	1.00E-05			SNL	6.48	Uniaxial compressive strength	SN0306L0207502.008	
220.3	220.3	0		0	220.3	32.7	0.177	TSw2	Tptpll	Busted Butte	Busted Butte	B0E2104Z		26.14	51.10	ambient	25	2.0	1.00E-05			SNL	7.39	Uniaxial compressive strength	SN0306L0207502.008	
209.8	209.8	0		0	209.8	32.9	0.160	TSw2	Tptpll	Busted Butte	Busted Butte	B0E2102Z		26.09	50.76	ambient	25	1.9	1.00E-05			SNL	7.86	Uniaxial compressive strength	SN0306L0207502.008	
142.5	142.5	0		0	142.5	33	0.162	TSw2	Tptpll	Busted Butte	Busted Butte	B3D1201Z		51.06	101.50	ambient	25	2.0	1.00E-05			SNL	5.78	Uniaxial compressive strength	SN0306L0207502.008	
154.2	154.2	0		0	154.2	33	0.194	TSw2	Tptpll	Busted Butte	Busted Butte	B3A2103Z		26.24	50.97	ambient	25	1.9	1.00E-05			SNL	6.03	Uniaxial compressive strength	SN0306L0207502.008	
119.2	119.2	0		0	119.2	33	0.234	TSw2	Tptpll	Busted Butte	Busted Butte	B3A2201Z		51.00	101.60	ambient	25	2.0	1.00E-05			SNL	4.06	Uniaxial compressive strength	SN0306L0207502.008	
118.6	118.6	0		0	118.6	33.1	0.162	TSw2	Tptpll	Busted Butte	Busted Butte	B0H1202Z		51.03	100.38	ambient	25	2.0	9.00E-06			SNL	4.23	Uniaxial compressive strength	SN0306L0207502.008	
159.4	159.4	0		0	159.4	33.3	0.167	TSw2	Tptpll	Busted Butte	Busted Butte	B0H1205Z		51.05	99.11	dry	25	1.9	1.00E-05			SNL	5.67	Uniaxial compressive strength	SN0306L0207502.008	
203.5	203.5	0		0	203.5	33.5	0.201	TSw2	Tptpll	Busted Butte	Busted Butte	B0E2103Z		26.12	50.79	ambient	25	1.9	1.00E-05			SNL	8.06	Uniaxial compressive strength	SN0306L0207502.008	
145.6	145.6	0		0	145.6	33.5	0.203	TSw2	Tptpll	Busted Butte	Busted Butte	B3D2201Z		50.98	101.60	ambient	25	2.0	1.00E-05			SNL	4.91	Uniaxial compressive strength	SN0306L0207502.008	
120.8	120.8	0		0	120.8	33.6	0.166	TSw2	Tptpll	Busted Butte	Busted Butte	B2D1301Z		82.22	167.10	ambient	25	2.0	9.00E-06			SNL	4.08	Uniaxial compressive strength	SN0306L0207502.008	
213.2	213.2	0		0	213.2	33.6	0.184	TSw2	Tptpll	Busted Butte	Busted Butte	B2F104Z		26.23	50.70	ambient	25	1.9	1.00E-05			SNL	7.80	Uniaxial compressive strength	SN0306L0207502.008	
108.7	108.7	0		0	108.7	33.7	0.175	TSw2	Tptpll	Busted Butte	Busted Butte	B1B501Z		120.60	245.30	ambient	25	2.0	8.00E-06			SNL	3.70	Uniaxial compressive strength	SN0306L0207502.008	
65.6	65.6	0		0	65.6	33.8		TSw2	Tptpll	Busted Butte	Busted Butte	B0DZ		Specimens were rectangular	400.8, 213.2, 196.6	ambient	25	2.0	6.00E-06			SNL	2.60	Uniaxial compressive strength	SN0306L0207502.008	Specimens were rectangular
123.9	123.9	0		0	123.9	33.9	0.178	TSw2	Tptpll	Busted Butte	Busted Butte	B0E1201Z		51.03	101.55	ambient	25	2.0	9.00E-06			SNL	4.50	Uniaxial compressive strength	SN0306L0207502.008	
162	162	0		0	162.0	34.2	0.134	TSw2	Tptpll	Busted Butte	Busted Butte	B1D2301Z		81.94	164.40	dry	200	2.0	9.00E-06			SNL	5.67	Uniaxial compressive strength	SN0306L0207502.008	
158.1	158.1	0		0	158.1	34.2	0.195	TSw2	Tptpll	Busted Butte	Busted Butte	B0H1203Z		51.03	101.60	saturated	25	2.0	9.00E-06			SNL	5.23	Uniaxial compressive strength	SN0306L0207502.008	
175.8	175.8	0		0	175.8	34.4	0.190	TSw2	Tptpll	Busted Butte	Busted Butte	B1B201Z		51.07	101.60	ambient	25	2.0	9.00E-06			SNL	5.59	Uniaxial compressive strength	SN0306L0207502.008	
192.7	192.7	0		0	192.7	34.6	0.170	TSw2	Tptpll	Busted Butte	Busted Butte	B2F102Z		26.17	50.86	ambient	25	1.9	1.00E-05			SNL	6.79	Uniaxial compressive strength	SN0306L0207502.008	
162.8	162.8	0		0	162.8	34.6	0.179	TSw2	Tptpll	Busted Butte	Busted Butte	B0H1206Z		51.03	99.09	ambient	25	1.9	9.00E-06			SNL	5.81	Uniaxial compressive strength	SN0306L0207502.008	
150.7	150.7	0		0	150.7	34.6	0.225	TSw2	Tptpll	Busted Butte	Busted Butte	B0F1211Z		51.05	101.60	saturated	25	2.0	9.00E-06			SNL	4.98	Uniaxial compressive strength	SN0306L0207502.008	
135.4	135.4	0		0	135.4	34.7	0.162	TSw2	Tptpll	Busted Butte	Busted Butte	B0F1203Z		51.00	101.70	saturated	25	2.0	9.00E-06			SNL	4.72	Uniaxial compressive strength	SN0306L0207502.008	
163.6	163.6	0		0	163.6	34.7	0.170	TSw2	Tptpll	Busted Butte	Busted Butte	B0E2201Z		51.04	97.75	ambient	25	1.9	9.00E-06			SNL	5.46	Uniaxial compressive strength	SN0306L0207502.008	
164.9	164.9	0		0	164.9	34.7	0.184	TSw2	Tptpll	Busted Butte	Busted Butte	B1D1203X		51.05	101.60	ambient	25	2.0	9.00E-06			SNL	5.88	Uniaxial compressive strength	SN0306L0207502.008	
137.7	137.7	0		0	137.7	34.7	0.210	TSw2	Tptpll	Busted Butte	Busted Butte	B2D1201Z		51.04	101.00	ambient	25	2.0	1.00E-05			SNL	4.66	Uniaxial compressive strength	SN0306L0207502.008	
137.6	137.6	0		0	137.6	34.8	0.164	TSw2	Tptpll	Busted Butte	Busted Butte	B3F2201Y		50.99	99.77	ambient	25	2.0	1.00E-05			SNL	4.27	Uniaxial compressive strength	SN0306L0207502.008	
191.1	191.1	0		0	191.1	34.8	0.177	TSw2	Tptpll	Busted Butte	Busted Butte	B3F2202X		50.96	99.07	ambient	25	1.9	9.00E-06			SNL	6.15	Uniaxial compressive strength	SN0306L0207502.008	
143.2	143.2	0		0	143.2	35	0.177	TSw2	Tptpll	Busted Butte	Busted Butte	B1D1202X		51.05	99.08	ambient	25	1.9	9.00E-06			SNL	5.40	Uniaxial compressive strength	SN0306L0207502.008	
105.9	105.9	0		0	105.9	35	0.193	TSw2	Tptpll	Busted Butte	Busted Butte	B0E2502Z		120.70	246.10	ambient	25	2.0	8.00E-06			SNL	3.54	Uniaxial compressive strength	SN0306L0207502.008	
71.7	71.7	0		0	71.7	35		TSw2	Tptpll	Busted Butte	Busted Butte	B2CZ		Specimens were rectangular	399.7, 211.2, 204.3	ambient	25	1.9	6.00E-06			SNL	3.07	Uniaxial compressive strength	SN0306L0207502.008	Specimens were rectangular
162	162	0		0	162.0	35.2	0.190	TSw2	Tptpll	Busted Butte	Busted Butte	B3F2201X		50.99	102.00	ambient	25	2.0	9.00E-06			SNL	5.68	Uniaxial compressive strength	SN0306L0207502.008	
135.7	135.7	0		0	135.7	35.3	0.203	TSw2	Tptpll	Busted Butte	Busted Butte	B2B201Z		50.91	101.30	ambient	25	2.0	9.00E-06			SNL	4.60	Uniaxial compressive strength	SN0306L0207502.008	
200.3	200.3	0		0	200.3	35.3		TSw2	Tptpll	Busted Butte	Busted Butte	B0H1204Z		51.05	101.60	dry	200	2.0	9.00E-06			SNL	6.75	Uniaxial compressive strength	SN0306L0207502.008	
139.8	139.8	0		0	139.8	35.4	0.232	TSw2	Tptpll	Busted Butte	Busted Butte	B3A2301Z		81.89	166.20	ambient	25	2.0	9.00E-06			SNL	4.47	Uniaxial compressive strength	SN0306L0207502.008	
179.1	179.1	0		0	179.1	35.5	0.180	TSw2	Tptpll	Busted Butte	Busted Butte	B0F1207Z		51.03	101.60	saturated	25	2.0	9.00E-06			SNL	5.91	Uniaxial compressive strength	SN0306L0207502.008	
124.6	124.6	0		0	124.6	35.5	0.191	TSw2	Tptpll	Busted Butte	Busted Butte	B0F1302Z		81.94	168.80	ambient	25	2.1	9.00E-06			SNL	4.00	Uniaxial compressive strength	SN0306L0207502.008	
168.5	168.5	0		0	168.5	35.5	0.195	TSw2	Tptpll	Busted Butte	Busted Butte	B0F1206Z		51.00	100.44	ambient	25	2.0	9.00E-06			SNL	5.74	Uniaxial compressive strength	SN0306L0207502.008	
133.4	133.4	0		0	133.4	35.8	0.171	TSw2	Tptpll	Busted Butte	Busted Butte	B2B202Z		50.88	101.50	ambient	25	2.0	9.00E-06			SNL	4.25	Uniaxial compressive strength	SN0306L0207502.008	

Table A-1 Intact Rock Mechanical Properties Data - Strength and Elastic Properties Data

Axial Stress, σ_1 (MPa)	Axial Stress, effective σ_1' (MPa)	Confining Pressure (MPa) σ_3	Pore Pressure (MPa)	Confining Pressure, Effective (MPa), σ_3'	Differential Strength, (MPa) $\sigma_1' - \sigma_3'$	Young's Modulus (GPa)	Poisson's Ratio	TM Unit	Litho-stratigraphic Unit	General Location	Sample Location	Specimen Number	Depth (ft)	Specimen Diameter (mm)	Specimen Length (mm)	Specimen Saturation	Specimen Temperature (deg. C)	l/d Ratio	Strain Rate (1/s)	Specimen Orientation (degree)	Test Standard	Laboratory	Failure Strain (millistrain)	Rock Property	Source DTN	Notes
154	154	0		0	154.0	35.9	0.195	TSw2	Tptpll	Busted Butte	Busted Butte	B2D1202Z		51.03	101.30	ambient	25	2.0	9.00E-06			SNL	5.16	Uniaxial compressive strength	SN0306L0207502.008	
97.7	97.7	0		0	97.7	35.9	0.219	TSw2	Tptpll	Busted Butte	Busted Butte	B3A2501Z		120.60	247.90	ambient	25	2.1	9.00E-06			SNL	3.27	Uniaxial compressive strength	SN0306L0207502.008	
135.2	135.2	0		0	135.2	36	0.180	TSw2	Tptpll	Busted Butte	Busted Butte	B0E2206Z		51.03	101.57	ambient	25	2.0	9.00E-06			SNL	4.27	Uniaxial compressive strength	SN0306L0207502.008	
164.7	164.7	0		0	164.7	36.1	0.186	TSw2	Tptpll	Busted Butte	Busted Butte	B0F1213Z		51.05	101.60	saturated	25	2.0	9.00E-06			SNL	5.14	Uniaxial compressive strength	SN0306L0207502.008	
225.5	225.5	0		0	225.5	36.1		TSw2	Tptpll	Busted Butte	Busted Butte	B0H1209Z		51.04	102.90	dry	200	2.0	9.00E-06			SNL	6.95	Uniaxial compressive strength	SN0306L0207502.008	
122.1	122.1	0		0	122.1	36.3	0.196	TSw2	Tptpll	Busted Butte	Busted Butte	B3D2301Z		81.86	170.40	ambient	25	2.1	9.00E-06			SNL	3.98	Uniaxial compressive strength	SN0306L0207502.008	
149.6	149.6	0		0	149.6	36.3	0.201	TSw2	Tptpll	Busted Butte	Busted Butte	B0E2302Z		81.94	165.20	ambient	25	2.0	9.00E-06			SNL	5.01	Uniaxial compressive strength	SN0306L0207502.008	
155.9	155.9	0		0	155.9	36.4	0.168	TSw2	Tptpll	Busted Butte	Busted Butte	B2D2202Z		51.05	101.60	ambient	25	2.0	9.00E-06			SNL	4.71	Uniaxial compressive strength	SN0306L0207502.008	
176.7	176.7	0		0	176.7	36.4	0.173	TSw2	Tptpll	Busted Butte	Busted Butte	B0E2207Z		51.05	101.60	dry	200	2.0	9.00E-06			SNL	5.94	Uniaxial compressive strength	SN0306L0207502.008	
247.2	247.2	0		0	247.2	36.4	0.182	TSw2	Tptpll	Busted Butte	Busted Butte	B3A2104Z		26.25	50.85	ambient	25	1.9	1.00E-05			SNL	8.18	Uniaxial compressive strength	SN0306L0207502.008	
111.3	111.3	0		0	111.3	36.4	0.205	TSw2	Tptpll	Busted Butte	Busted Butte	B3A2502Z		120.60	248.20	ambient	25	2.1	8.00E-06			SNL	3.45	Uniaxial compressive strength	SN0306L0207502.008	
179.5	179.5	0		0	179.5	36.5	0.196	TSw2	Tptpll	Busted Butte	Busted Butte	B1B302Z		81.99	168.80	ambient	25	2.1	9.00E-06			SNL	5.43	Uniaxial compressive strength	SN0306L0207502.008	
192.6	192.6	0		0	192.6	36.5	0.201	TSw2	Tptpll	Busted Butte	Busted Butte	B0F1210Z		51.07	100.34	ambient	25	2.0	8.00E-06			SNL	5.81	Uniaxial compressive strength	SN0306L0207502.008	
149.5	149.5	0		0	149.5	36.6	0.184	TSw2	Tptpll	Busted Butte	Busted Butte	B0E1202Y		51.02	101.60	ambient	25	2.0	9.00E-06			SNL	4.64	Uniaxial compressive strength	SN0306L0207502.008	
124.7	124.7	0		0	124.7	36.6	0.193	TSw2	Tptpll	Busted Butte	Busted Butte	B2E2501Z		120.60	233.60	ambient	25	1.9	9.00E-06			SNL	3.80	Uniaxial compressive strength	SN0306L0207502.008	
175.2	175.2	0		0	175.2	36.7	0.161	TSw2	Tptpll	Busted Butte	Busted Butte	B0F1201Z		51.02	100.90	dry	25	2.0	9.00E-06			SNL	5.71	Uniaxial compressive strength	SN0306L0207502.008	
187.9	187.9	0		0	187.9	36.7	0.202	TSw2	Tptpll	Busted Butte	Busted Butte	B2B201X		50.97	101.20	ambient	25	2.0	9.00E-06			SNL	5.94	Uniaxial compressive strength	SN0306L0207502.008	
217.7	217.7	0		0	217.7	36.8		TSw2	Tptpll	Busted Butte	Busted Butte	B0F1204Z		51.00	101.10	dry	200	2.0	9.00E-06			SNL	6.78	Uniaxial compressive strength	SN0306L0207502.008	
122	122	0		0	122.0	37	0.180	TSw2	Tptpll	Busted Butte	Busted Butte	B3F2202Z		51.04	101.10	ambient	25	2.0	9.00E-06			SNL	3.65	Uniaxial compressive strength	SN0306L0207502.008	
161.7	161.7	0		0	161.7	37.0	0.193	TSw2	Tptpll	Busted Butte	Busted Butte	B0E2203Z		51.00	101.55	ambient	25	2.0	8.00E-06			SNL	4.77	Uniaxial compressive strength	SN0306L0207502.008	
196.6	196.6	0		0	196.6	37.2	0.197	TSw2	Tptpll	Busted Butte	Busted Butte	B2D2201Z		51.05	101.56	ambient	25	2.0	9.00E-06			SNL	5.99	Uniaxial compressive strength	SN0306L0207502.008	
158.1	158.1	0		0	158.1	37.3	0.166	TSw2	Tptpll	Busted Butte	Busted Butte	B3F1201Z		51.05	101.50	ambient	25	2.0	9.00E-06			SNL	4.79	Uniaxial compressive strength	SN0306L0207502.008	
165.6	165.6	0		0	165.6	37.3	0.177	TSw2	Tptpll	Busted Butte	Busted Butte	B0F1205Z		51.00	101.60	dry	25	2.0	9.00E-06			SNL	5.06	Uniaxial compressive strength	SN0306L0207502.008	
213.6	213.6	0		0	213.6	37.3	0.183	TSw2	Tptpll	Busted Butte	Busted Butte	B0F1202Z		51.00	100.32	ambient	25	2.0	8.00E-06			SNL	7.42	Uniaxial compressive strength	SN0306L0207502.008	
201	201	0		0	201.0	37.4	0.210	TSw2	Tptpll	Busted Butte	Busted Butte	B2A201Z		50.90	101.50	ambient	25	2.0	9.00E-06			SNL	5.95	Uniaxial compressive strength	SN0306L0207502.008	
200.5	200.5	0		0	200.5	37.5		TSw2	Tptpll	Busted Butte	Busted Butte	B0F1206Z		51.03	101.60	dry	200	2.0	9.00E-06			SNL	6.17	Uniaxial compressive strength	SN0306L0207502.008	
92.2	92.2	0		0	92.2	37.5		TSw2	Tptpll	Busted Butte	Busted Butte	B3CZ		Specimens were rectangular	421.1, 222.9, 212.0	ambient	25	1.9	6.00E-06			SNL	3.59	Uniaxial compressive strength	SN0306L0207502 .008	Specimens were rectangular
202.1	202.1	0		0	202.1	37.6	0.187	TSw2	Tptpll	Busted Butte	Busted Butte	B0E1203X		51.00	101.80	ambient	25	2.0	9.00E-06			SNL	5.77	Uniaxial compressive strength	SN0306L0207502.008	
188.3	188.3	0		0	188.3	37.7	0.190	TSw2	Tptpll	Busted Butte	Busted Butte	B3F2204Y		51.07	101.70	ambient	25	2.0	9.00E-06			SNL	5.77	Uniaxial compressive strength	SN0306L0207502.008	
226.3	226.3	0		0	226.3	37.7		TSw2	Tptpll	Busted Butte	Busted Butte	B0H1208Z		51.05	101.60	dry	200	2.0	9.00E-06			SNL	6.72	Uniaxial compressive strength	SN0306L0207502.008	
205.2	205.2	0		0	205.2	37.8	0.186	TSw2	Tptpll	Busted Butte	Busted Butte	B0E2202Z		51.03	97.94	dry	25	1.9	9.00E-06			SNL	6.02	Uniaxial compressive strength	SN0306L0207502.008	
170.3	170.3	0		0	170.3	37.9	0.200	TSw2	Tptpll	Busted Butte	Busted Butte	B3D2202Z		50.99	101.60	ambient	25	2.0	9.00E-06			SNL	4.99	Uniaxial compressive strength	SN0306L0207502.008	
198.7	198.7	0		0	198.7	37.9	0.207	TSw2	Tptpll	Busted Butte	Busted Butte	B2F202Y		50.97	101.80	ambient	25	2.0	9.00E-06			SNL	5.82	Uniaxial compressive strength	SN0306L0207502.008	
168.5	168.5	0		0	168.5	38	0.216	TSw2	Tptpll	Busted Butte	Busted Butte	B2F202X		50.97	101.30	ambient	25	2.0	9.00E-06			SNL	5.01	Uniaxial compressive strength	SN0306L0207502.008	
261.7	261.7	0		0	261.7	38.1	0.202	TSw2	Tptpll	Busted Butte	Busted Butte	B3A2102Z		26.21	49.57	ambient	25	1.9	1.00E-05			SNL	8.81	Uniaxial compressive strength	SN0306L0207502.008	
145	145	0		0	145.0	38.3	0.189	TSw2	Tptpll	Busted Butte	Busted Butte	B2B301Z		82.24	171.20	ambient	25	2.1	9.00E-06			SNL	4.24	Uniaxial compressive strength	SN0306L0207502.008	
197.2	197.2	0		0	197.2	38.4	0.191	TSw2	Tptpll	Busted Butte	Busted Butte	B0F1209Z		51.03	101.60	dry	25	2.0	9.00E-06			SNL	5.57	Uniaxial compressive strength	SN0306L0207502.008	
208.1	208.1	0		0	208.1	38.7	0.200	TSw2	Tptpll	Busted Butte	Busted Butte	B0E1201Y		51.00	101.55	ambient	25	2.0	9.00E-06			SNL	5.82	Uniaxial compressive strength	SN0306L0207502.008	
128.3	128.3	0		0	128.3	39	0.186	TSw2	Tptpll	Busted Butte	Busted Butte	B0F1101Z		120.70	241.60	ambient	25	2.0	8.00E-06			SNL	3.89	Uniaxial compressive strength	SN0306L0207502.008	
169	169	0		0	169.0	39.1	0.180	TSw2	Tptpll	Busted Butte	Busted Butte	B0F1301Z		81.92	166.40	ambient	25	2.0	9.00E-06			SNL	4.84	Uniaxial compressive strength	SN0306L0207502.008	
164.3	164.3	0		0	164.3	39.1	0.186	TSw2	Tptpll	Busted Butte	Busted Butte	B2D2203Z		51.05	101.60	ambient	25	2.0	9.00E-06			SNL	4.86	Uniaxial compressive strength	SN0306L0207502.008	
128.9	128.9	0		0	128.9	39.1	0.197	TSw2	Tptpll	Busted Butte	Busted Butte	B2D1501Z		120.70	243.80	ambient	25	2.0	8.00E-06			SNL	3.65	Uniaxial compressive strength	SN0306L0207502.008	
208.8	208.8	0		0	208.8	39.4		TSw2	Tptpll	Busted Butte	Busted Butte	B0E2206Z		51.04	101.80	dry	200	2.0	9.00E-06			SNL	6.51	Uniaxial compressive strength	SN0306L0207502.008	
151.3	151.3	0		0	151.3	39.7	0.209	TSw2	Tptpll	Busted Butte	Busted Butte	B0E2501Z		120.70	246.90	ambient	25	2.0	8.00E-06			SNL	4.37	Uniaxial compressive strength	SN0306L0207502.008	
196.1	196.1	0		0	196.1	39.9	0.097	TSw2	Tptpll	Busted Butte	Busted Butte	B2B302Z		81.89	167.89	dry	200	2.1	9.00E-06			SNL	5.90	Uniaxial compressive strength	SN0306L0207502.008	
180	180	0		0	180.0	39.9	0.201	TSw2	Tptpll	Busted Butte	Busted Butte	B3A2303Z		81.99	169.20	ambient	25	2.1	9.00E-06			SNL	4.98	Uniaxial compressive strength	SN0306L0207502.008	
228.7	228.7	0		0	228.7	40	0.200	TSw2	Tptpll	Busted Butte	Busted Butte	B3A2202Z		50.99	101.60	ambient	25	2.0	9.00E-06			SNL	6.18	Uniaxial compressive strength	SN0306L0207502.008	
203.8	203.8	0		0	203.8	40.2	0.191	TSw2	Tptpll	Busted Butte	Busted Butte	B2F201Y		50.97	101.30	ambient	25	2.0	9.00E-06			SNL	5.71	Uniaxial compressive strength	SN0306L0207502.008	
194.5	194.5	0		0	194.5	40.4	0.192	TSw2	Tptpll	Busted Butte	Busted Butte	B2D2201Y		51.04	101.50	ambient	25	2.0	9.00E-06			SNL	5.63	Uniaxial compressive strength	SN0306L0207502.008	
173.1	173.1	0		0	173.1	40.5	0.187	TSw2	Tptpll	Busted Butte	Busted Butte	B3A2302Z		81.89	166.80	dry	200	2.0	9.00E-06			SNL	4.92	Uniaxial compressive strength	SN0306L0207502.008	
246.6	246.6	0		0	246.6	40.7	0.199	TSw2	Tptpll	Busted Butte	Busted Butte	B0E1201X		51.00	101.55	ambient	25	2.0	9.00E-06			SNL	6.73	Uniaxial compressive strength	SN0306L0207502.008	
242.5	242.5	0		0	242.5	41.3	0.197	TSw2	Tptpll	Busted Butte	Busted Butte	B0E1202X		51.02	101.60	ambient	25	2.0	9.00E-06			SNL	6.49	Uniaxial compressive strength	SN0306L0207502.008	
150.8	150.8	0		0	150.8	41.5	0.190	TSw2	Tptpll	Busted Butte	Busted Butte	B2D1302Z		82.27	163.50	ambient	25	2.0	9.00E-06			SNL	4.40	Uniaxial compressive strength	SN0306L0207502.008	
141.3	141.3	0		0	141.3	41.6	0.216	TSw2	Tptpll	Busted Butte	Busted Butte	B3D2501Z		120.60	234.90	ambient	25	1.9	8.00E-06			SNL	3.60	Uniaxial compressive strength	SN0306L0207502.008	
166	166	0		0	166	61.8	0.3	TSw2	Tptpln	ESF/ECRB/Borehole	UE-25 a #1	1250	1250.0	56	L:D = 2:1 or greater	ambient	22	2.0	1.00E-04			SNL		Uniaxial compressive strength	MO0311RCKPRPCS.003, MO0402DQRIRPPR.003	
120.1	120.1	0		0	120.1	32.1	0.24	TSw2	Tptpln	ESF/ECRB/Borehole	USW GU-3	GU-3 1067.8/4	1067.8	25.35	50.88	saturated	22	2.0	1.00E-05	90		SNL	5.32	Uniaxial compressive strength	MO0311RCKPRPCS.003, MO0402DQRIRPPR.003	
115.3	115.3	0		0	115.3	32.7	0.24	TSw2	Tptpln	ESF/ECRB/Borehole	USW GU-3	GU-3 1067.8/3	1067.8	25.35	50.90	saturated	22	2.0	1.00E-05	90		SNL	4.46	Uniaxial compressive strength	MO0311RCKPRPCS.003, MO0402DQRIRPPR.003	
172.9	172.9	0		0	172.9	34.4	0.2	TSw2	Tptpln	ESF/ECRB/Borehole	USW GU-3	GU-3 1067.8/1	1067.8	57.18	114.40	ambient	22	2.0	1.00E-05	90		SNL	4.97	Uniaxial compressive strength	MO0311RCKPRPCS.003, MO0402DQRIRPPR.003	
131.3	131.3	0		0	131.3	35.5	0.18	TSw2	Tptpln	ESF/ECRB/Borehole	USW GU-3	GU-3 1050.4/1	1050.4	25.35	50.85	saturated	22	2.0	1.00E-05	90		SNL	4.17	Uniaxial compressive strength	MO0311RCKPRPCS.003, MO0402DQRIRPPR.003	
170.2	170.2	0		0	170.2	35.7	0.23	TSw2	Tptpln	ESF/ECRB/Borehole	USW GU-3	GU-3 1067.8/2	1067.8	57.18	114.40	ambient	22	2.0	1.00E-05	90		SNL	4.98	Uniaxial compressive strength	MO0311RCKPRPCS.003, MO0402DQRIRPPR.003	
147.7	147.7	0		0	147.7	36.1	0.19	TSw2	Tptpln	ESF/ECRB/Borehole	USW GU-3	GU-3 1050.4/2	1050.4	25.35	50.85	saturated	22	2.0	1.00E-05	90		SNL	4.56	Uniaxial compressive strength	MO0311RCKPRPCS.003, MO0402DQRIRPPR.003	
152.1	152.1	0		0	152.1	36.3	0.19	TSw2	Tptpln	ESF/ECRB/Borehole	USW GU-3	GU-3 1050.4/3	1050.4	25.35	50.85	saturated	22	2.0	1.00E-05	90		SNL	5.01	Uniaxial compressive strength	MO0311RCKPRPCS.003, MO0402DQRIRPPR.003	
82.9	82.9	0		0	82.9	30.4	0.14	TSw2	Tptpln	ESF/ECRB/Borehole	USW NRG-7a	NRG-7/7A-1252.3-SNL-A	1252.3	50.8	101.6	saturated	22	2.0	1.00E-05		ASTM D-3148 & ISRM U	NBR	4.21	Uniaxial compressive strength	MO0311RCKPRPCS.003, MO0402DQRIRPPR.003	
173.4	173.4	0		0	173.4	37.7	0.21	TSw2	Tptpln	ESF/ECRB/Borehole	USW NRG-7a	NRG-7/7A-1314.8-SNL-A	1314.8	50.8	101.6	saturated	22	2.0	1.00E-05		ASTM D-3148 & ISRM U	NBR	6.27	Uniaxial compressive strength	MO0311RCKPRPCS.003, MO0402DQRIRPPR.003	
172.5	172.5	0		0	172.5	40.6	0.21	TSw2	Tptpln	ESF/ECRB/Borehole	USW NRG-7a	NRG-7/7A-1259.1-SNL-A	1259.1	50.8	101.6	saturated	22	2.0	1.00E-05		ASTM D-3148 & ISRM U	NBR	4.44	Uniaxial compressive strength	MO0311RCKPRPCS.003, MO0402DQRIRPPR.003	
192.9	192.9	0		0	192.9	40.7	0.21	TSw2	Tptpln	ESF/ECRB/Borehole	USW NRG-7a	NRG-7/7A-1265.2-SNL-A	1265.2	50.8	101.6	saturated	22	2.0	1.00E-05		ASTM D-3148 & ISRM U	NBR	4.88	Uniaxial compressive strength	MO0311RCKPRPCS.003, MO0402DQRIRPPR.003	
169.3	169.3	0		0	169.3	41.8	0.2	TSw2	Tptpln	ESF/ECRB/Borehole	USW NRG-7a	NRG-7/7A-1257.8-SNL-A	1257.8	50.8	101.6	saturated	22	2.0	1.00E-05		ASTM D-3148 & ISRM U	NBR	4.32	Uniaxial compressive strength	MO0311RCKPRPCS.003, MO0402DQRIRPPR.003	
128	128	0		0	128	31.9	0.28	TSw2	Tptpln	ESF/ECRB/Borehole	USW SD-12	SD-12-1209.0-SNL-B	1209.0	50.8	101.6	saturated	22	2.0	1.00E-05		ISRM T and ASTM D 2664-86	NBR	4.55	Uniaxial compressive strength	MO0311RCKPRPCS.003, MO0402DQRIRPPR.003	
162	162	0		0	162	34.5	0.23	TSw2	Tptpln	ESF/ECRB/Borehole	USW SD-12	SD-12-1107.1-SNL-B	1107.1	50.8	101.6	saturated	22	2.0	1.00E-05		ISRM T and ASTM D 2664-86	NER	5.54	Uniaxial compressive strength	MO0311RCKPRPCS.003, MO0402DQRIRPPR.003	
158.7	158.7	0		0	158.7	35.9	0.19	TSw2	Tptpln	ESF/ECRB/Borehole	USW SD-9	SD-9-1243.0-SNL-A	1243.0	50.8	101.6	saturated	22	2.0	1.00E-05		ISRM T and ASTM D 2664-86	NBR	4.81	Uniaxial compressive strength	MO0311RCKPRPCS.003, MO0402DQRIRPPR.003	only uniaxial tested to date
158.7	158.7	0		0	158.7	39.9	0.25	TSw2	Tptpln	ESF/ECRB/Borehole	USW SD-9	SD-9-1298.0-SNL-A	1298.0	50.8	101.6	saturated	22	2.0	1.00E-05		ISRM T and ASTM D 2664-86	NBR	4.20	Uniaxial compressive strength	MO0311RCKPRPCS.003, MO0402DQRIRPPR.003	only uniaxial tested to date
156.7	156.7	0		0	156.7	44.4	0.25	TSw2	Tptpln	ESF/ECRB/Borehole	USW SD-9	SD-9-1346.5-SNL-A	1346.5	50.8	101.6	saturated	22	2.0	1.00E-05		ISRM T and ASTM D 2664-86	NBR	4.00	Uniaxial compressive strength	MO0311RCKPRPCS.003, MO0402DQRIRPPR.003	only uniaxial tested to date
179.2	179.2	0		0	179.2			TSw2	Tptpmn	ESF/ECRB/Borehole	USW NRG-7a	NRG-7/7A-800.2-SNL-A	800.2	50.8	101.6	saturated	22	2.0	1.00E-05		ASTM D 3148 & ISRM U	NBR	N/A	Uniaxial compressive strength	MO0311RCKPRPCS.003, MO0402DQRIRPPR.003	
29	29	0		0	29	14	0.37	TSw2	Tptpmn	Busted Butte	Busted Butte	BB-10-AE-34Y		50.8	101.60	dry	150	2.0	1.00E-03		RSI TP-04e	RE/SPEC	5.23	Uniaxial compressive strength	MO0311RCKPRPCS.003, MO0402DQRIRPPR.003	
53.7	53.7	0		0	53.7	18.6	0.07	TSw2	Tptpmn	Busted Butte	Busted Butte	10-AE-3Y		50	100	saturated	20	2.0	1.00E-05			RE/SPEC	3.3	Uniaxial compressive strength	MO0311RCKPRPCS.003, MO0402DQRIRPPR.003	
62.4	62.4	0		0	62.4	21.7	0.11	TSw2	Tptpmn	Busted Butte	Busted Butte	10-AE-8X		50	100	saturated	20	2.0	1.00E-05			RE/SPEC	3.68	Uniaxial compressive strength	MO0311RCKPRPCS.003, MO0402DQRIRPPR.003	
59.91	59.91	0		0	59.91	25.3		TSw2	Tptpmn	Busted Butte	Busted Butte	10A1		127.0	254.00	saturated	22	2.0	1.00E-05			SNL	2.7	Uniaxial compressive strength	MO0311RCKPRPCS.003, MO0402DQRIRPPR.003	
45.3	45.3	0		0	45.3	26.1		TSw2	Tptpmn	Busted Butte	Busted Butte	BB-10AE-49W-SNL		50.8	101.6	saturated	22	2.0	1.00E-09			NBR	4.91	Uniaxial compressive strength	MO0311RCKPRPCS.003, MO0402DQRIRPPR.003	CT scan showed a large lithophysal cavity, causing the low value
68.1	68.1	0	0	0	68.1	26.9	0.18	TSw2	Tptpmn	Busted Butte	Busted Butte	10AE52Z		50.8	101.6	saturated	22	2.0	1.00E-03			SNL	3.0	Uniaxial compressive strength	MO0311RCKPRPCS.003, MO0402DQRIRPPR.003	saturated, drained test
107	107	0		0	107.0	28.6	0.14	TSw2	Tptpmn	Busted Butte	Busted Butte	10-AE-6X		50	100	saturated	20	2.0	1.00E-05			RE/SPEC	4.17	Uniaxial compressive strength	MO0311RCKPRPCS.003, MO0402DQRIRPPR.003	
109	109	0	0	0	109	28.71	0.17	TSw2	Tptpmn	Busted Butte	Busted Butte	10/AE/2/Z		50.8	101.6	saturated	22	2.0	2.78E-05			Terra Tek	N/A	Uniaxial compressive strength	MO0311RCKPRPCS.003, MO0402DQRIRPPR.003	Samples are indicated as saturated and drained.
90.41	90.41	0		0	90.41	30.6	0.27	TSw2	Tptpmn	Busted Butte	Busted Butte	281		127.0	254.00	saturated	22	2.0	1.00E-05			SNL	3.6	Uniaxial compressive strength	MO0311RCKPRPCS.003, MO0402DQRIRPPR.003	
153	153	0	0	0	153	31.52	0.2	TSw2	Tptpmn	Busted Butte	Busted Butte	10/AE/9Z		50.8	101.6	saturated	22	2.0	1.39E-05			Terra Tek	N/A	Uniaxial compressive strength	MO0311RCKPRPCS.003, MO0402DQRIRPPR.003	Samples are indicated as saturated and drained.

Table A-1 Intact Rock Mechanical Properties Data - Strength and Elastic Properties Data

Axial Stress, σ_1 (MPa)	Axial Stress, effective σ_1' (MPa)	Confining Pressure (MPa) σ_3	Pore Pressure (MPa)	Confining Pressure, Effective (MPa), σ_3'	Differential Strength, (MPa) $\sigma_1 - \sigma_3$	Young's Modulus (GPa)	Poisson's Ratio	TM Unit	Litho-stratigraphic Unit	General Location	Sample Location	Specimen Number	Depth (ft)	Specimen Diameter (mm)	Specimen Length (mm)	Specimen Saturation	Specimen Temperature (deg. C)	l/d Ratio	Strain Rate (1/s)	Specimen Orientation (degree)	Test Standard	Laboratory	Failure Strain (millistrain)	Rock Property	Source DTN	Notes
69.67	69.67	0		0	69.67	31.6	0.17	TSw2	Tptpmn	Busted Butte	Busted Butte	10D2		127.0	254.00	saturated	22	2.0	1.00E-05			SNL	3.0	Uniaxial compressive strength	MO0311RCKPRPCS.003, MO0402DQRIRPPR.003	
78.1	78.1	0		0	78.1	32.1	0.12	TSw2	Tptpmn	Busted Butte	Busted Butte	10AE28X		50.8	101.6	dry	22	2.0	1.00E-07			SNL	2.8	Uniaxial compressive strength	MO0311RCKPRPCS.003, MO0402DQRIRPPR.003	Large Inhomogeneties in sample
84.25	84.25	0		0	84.25	32.1	0.18	TSw2	Tptpmn	Busted Butte	Busted Butte	10A2		127.0	254.00	saturated	22	2.0	1.00E-05			SNL	3.0	Uniaxial compressive strength	MO0311RCKPRPCS.003, MO0402DQRIRPPR.003	
58.86	58.86	0		0	58.86	32.3	0.21	TSw2	Tptpmn	Busted Butte	Busted Butte	27I		82.6	165.20	saturated	22	2.0	1.00E-05			SNL	3.9	Uniaxial compressive strength	MO0311RCKPRPCS.003, MO0402DQRIRPPR.003	
81.2	81.2	0		0	81.2	32.4	0.01	TSw2	Tptpmn	Busted Butte	Busted Butte	BB-10AE-5X-SNL		50.8	101.6	saturated	22	2.0	1.00E-09			NBR	2.91	Uniaxial compressive strength	MO0311RCKPRPCS.003, MO0402DQRIRPPR.003	Results are in SAND report and not in DTN.
89.77	89.77	0		0	89.77	33	0.22	TSw2	Tptpmn	Busted Butte	Busted Butte	10D1		127.0	254.00	saturated	22	2.0	1.00E-05			SNL	3.0	Uniaxial compressive strength	MO0311RCKPRPCS.003, MO0402DQRIRPPR.003	
78	78	0		0	78	33.1	0.05	TSw2	Tptpmn	Busted Butte	Busted Butte	BB-10-AE-45Y		50.8	101.60	dry	150	2.0	1.00E-08		RSI TP-04e	RE/SPEC	2.46	Uniaxial compressive strength	MO0311RCKPRPCS.003, MO0402DQRIRPPR.003	
95.5	95.5	0	0	0	95.5	33.1	0.23	TSw2	Tptpmn	Busted Butte	Busted Butte	10AE38X		50.8	101.6	saturated	22	2.0	1.00E-03			SNL	3.0	Uniaxial compressive strength	MO0311RCKPRPCS.003, MO0402DQRIRPPR.003	saturated, drained test
120.2	120.2	0	0	0	120.2	33.3	0.18	TSw2	Tptpmn	Busted Butte	Busted Butte	10AE23X		50.8	101.6	saturated	22	2.0	1.00E-03			SNL	3.8	Uniaxial compressive strength	MO0311RCKPRPCS.003, MO0402DQRIRPPR.003	saturated, drained test
87.2	87.2	0		0	87.2	33.6	0.12	TSw2	Tptpmn	Busted Butte	Busted Butte	BB-10AE-11Z-SNL		50.8	101.6	saturated	22	2.0	1.00E-09			NBR	2.77	Uniaxial compressive strength	MO0311RCKPRPCS.003, MO0402DQRIRPPR.003	
135.2	135.2	0		0	135.2	33.7	0.24	TSw2	Tptpmn	Busted Butte	Busted Butte	10AE34Z		50.8	101.6	dry	22	2.0	1.00E-05			SNL	5.3	Uniaxial compressive strength	MO0311RCKPRPCS.003, MO0402DQRIRPPR.003	
97.4	97.4	0		0	97.4	34.1	0.11	TSw2	Tptpmn	Busted Butte	Busted Butte	BB-10AE-11Y-SNL		50.8	101.6	saturated	22	2.0	1.00E-09			NBR	4.42	Uniaxial compressive strength	MO0311RCKPRPCS.003, MO0402DQRIRPPR.003	
143	143	0	0	0	143	34.17	0.18	TSw2	Tptpmn	Busted Butte	Busted Butte	10/AE/46/Z		50.8	101.8	saturated	22	2.0	2.64E-05			Terra Tek	N/A	Uniaxial compressive strength	MO0311RCKPRPCS.003, MO0402DQRIRPPR.003	Samples are indicated as saturated and drained.
104.3	104.3	0		0	104.3	34.6	0.2	TSw2	Tptpmn	Busted Butte	Busted Butte	28A2		50.8	101.6	saturated	22	2.0	1.00E-05			SNL	3.4	Uniaxial compressive strength	MO0311RCKPRPCS.003, MO0402DQRIRPPR.003	
111.7	111.7	0		0	111.7	34.6	0.21	TSw2	Tptpmn	Busted Butte	Busted Butte	26B1		50.8	101.6	saturated	22	2.0	1.00E-05			SNL	3.2	Uniaxial compressive strength	MO0311RCKPRPCS.003, MO0402DQRIRPPR.003	
126.8	126.8	0		0	126.8	34.6	0.21	TSw2	Tptpmn	Busted Butte	Busted Butte	10X12		50.8	101.6	saturated	22	2.0	1.00E-05			SNL	4.3	Uniaxial compressive strength	MO0311RCKPRPCS.003, MO0402DQRIRPPR.003	
113.3	113.3	0		0	113.3	34.9	0.21	TSw2	Tptpmn	Busted Butte	Busted Butte	13A2		25.4	50.8	saturated	22	2.0	1.00E-05			SNL	4.7	Uniaxial compressive strength	MO0311RCKPRPCS.003, MO0402DQRIRPPR.003	
92.4	92.4	0		0	92.40	35.7	0.18	TSw2	Tptpmn	Busted Butte	Busted Butte	10C1		127.0	254.00	saturated	22	2.0	1.00E-05			SNL	3.6	Uniaxial compressive strength	MO0311RCKPRPCS.003, MO0402DQRIRPPR.003	
143.2	143.2	0		0	143.2	35.9	0.2	TSw2	Tptpmn	Busted Butte	Busted Butte	10Y47		50.8	101.6	saturated	22	2.0	1.00E-05			SNL	4.3	Uniaxial compressive strength	MO0311RCKPRPCS.003, MO0402DQRIRPPR.003	
129	129	0		0	129	36.3	0.06	TSw2	Tptpmn	Busted Butte	Busted Butte	BB-10-AE-49X (Tuff/84/49X)		50.8	101.6	dry	150	2.0	1.00E-07		RSI TP-04e	RE/SPEC	3.78	Uniaxial compressive strength	MO0311RCKPRPCS.003, MO0402DQRIRPPR.003	
98.16	98.16	0		0	98.16	36.3	0.2	TSw2	Tptpmn	Busted Butte	Busted Butte	10C2		127.0	254.00	saturated	22	2.0	1.00E-05			SNL	3.5	Uniaxial compressive strength	MO0311RCKPRPCS.003, MO0402DQRIRPPR.003	
152	152	0		0	152	36.7	0.14	TSw2	Tptpmn	Busted Butte	Busted Butte	BB-10-AE-27Z (Tuff/84/27Z)		50.8	101.6	dry	150	2.0	1.00E-05		RSI TP-04e	RE/SPEC	4.23	Uniaxial compressive strength	MO0311RCKPRPCS.003, MO0402DQRIRPPR.003	
134.9	134.9	0	0	0	134.9	36.7	0.19	TSw2	Tptpmn	Busted Butte	Busted Butte	10AE53Z		50.8	101.6	saturated	22	2.0	1.00E-07			SNL	4.0	Uniaxial compressive strength	MO0311RCKPRPCS.003, MO0402DQRIRPPR.003	saturated, drained test
169	169	0	0	0	169	36.8	0.19	TSw2	Tptpmn	Busted Butte	Busted Butte	10AE24Y		50.8	101.6	saturated	22	2.0	1.00E-03			SNL	4.7	Uniaxial compressive strength	MO0311RCKPRPCS.003, MO0402DQRIRPPR.003	saturated, drained test
157.1	157.1	0		0	157.1	37	0.18	TSw2	Tptpmn	Busted Butte	Busted Butte	10AE30Z		50.8	101.6	dry	22	2.0	1.00E-07			SNL	4.6	Uniaxial compressive strength	MO0311RCKPRPCS.003, MO0402DQRIRPPR.003	
145.8	145.8	0	0	0	145.8	37.1	0.18	TSw2	Tptpmn	Busted Butte	Busted Butte	10AE4Y		50.8	101.6	saturated	22	2.0	1.00E-07			SNL	4.3	Uniaxial compressive strength	MO0311RCKPRPCS.003, MO0402DQRIRPPR.003	saturated, drained test
96	96	0		0	96	37.2	0.09	TSw2	Tptpmn	Busted Butte	Busted Butte	BB-10-AE-7W (Tuff/84/7W)		50.8	101.6	dry	150	2.0	1.00E-07		RSI TP-04e	RE/SPEC	2.71	Uniaxial compressive strength	MO0311RCKPRPCS.003, MO0402DQRIRPPR.003	
158.4	158.4	0		0	158.4	37.4	0.2	TSw2	Tptpmn	Busted Butte	Busted Butte	10Z15		50.8	101.6	saturated	22	2.0	1.00E-05			SNL	4.4	Uniaxial compressive strength	MO0311RCKPRPCS.003, MO0402DQRIRPPR.003	
86.92	86.92	0		0	86.92	37.4	0.22	TSw2	Tptpmn	Busted Butte	Busted Butte	222		228.6	457.20	saturated	22	2.0	1.00E-05			SNL	2.9	Uniaxial compressive strength	MO0311RCKPRPCS.003, MO0402DQRIRPPR.003	
109	109	0		0	109	37.5	0.15	TSw2	Tptpmn	Busted Butte	Busted Butte	BB-10-AE-28Y (Tuff/84/28Y)		50.8	101.6	dry	150	2.0	1.00E-05		RSI TP-04e	RE/SPEC	3.25	Uniaxial compressive strength	MO0311RCKPRPCS.003, MO0402DQRIRPPR.003	
87.69	87.69	0		0	87.69	37.6	0.22	TSw2	Tptpmn	Busted Butte	Busted Butte	11A2		82.6	165.20	saturated	22	2.0	1.00E-05			SNL	3.2	Uniaxial compressive strength	MO0311RCKPRPCS.003, MO0402DQRIRPPR.003	
72	72	0		0	72	37.7	0.12	TSw2	Tptpmn	Busted Butte	Busted Butte	BB-10-AE-53Y (Tuff/84/53Y)		50.8	101.6	dry	150	2.0	1.00E-05		RSI TP-04e	RE/SPEC	2.04	Uniaxial compressive strength	MO0311RCKPRPCS.003, MO0402DQRIRPPR.003	
148	148	0		0	148	37.7	0.13	TSw2	Tptpmn	Busted Butte	Busted Butte	BB-10-AE-32Y (Tuff/84/32Y)		50.8	101.6	dry	150	2.0	1.00E-07		RSI TP-04e	RE/SPEC	4.04	Uniaxial compressive strength	MO0311RCKPRPCS.003, MO0402DQRIRPPR.003	
98.81	98.81	0		0	98.81	37.7	0.21	TSw2	Tptpmn	Busted Butte	Busted Butte	282		127.0	254.00	saturated	22	2.0	1.00E-05			SNL	3.5	Uniaxial compressive strength	MO0311RCKPRPCS.003, MO0402DQRIRPPR.003	
108.5	108.5	0		0	108.5	38.1	0.16	TSw2	Tptpmn	Busted Butte	Busted Butte	BB-10AE-24Z-SNL		50.8	101.6	saturated	22	2.0	1.00E-09			NBR	3.04	Uniaxial compressive strength	MO0311RCKPRPCS.003, MO0402DQRIRPPR.003	
174	174	0		0	174	38.2	0.15	TSw2	Tptpmn	Busted Butte	Busted Butte	BB-10-AE-19Y		50.8	101.60	dry	150	2.0	1.00E-03		RSI TP-04e	RE/SPEC	4.75	Uniaxial compressive strength	MO0311RCKPRPCS.003, MO0402DQRIRPPR.003	
92.9	92.9	0		0	92.9	38.8	0.13	TSw2	Tptpmn	Busted Butte	Busted Butte	BB-10AE-6Y-SNL		50.8	101.6	saturated	22	2.0	1.00E-09			NBR	2.24	Uniaxial compressive strength	MO0311RCKPRPCS.003, MO0402DQRIRPPR.003	
99.76	99.76	0		0	99.76	38.8	0.19	TSw2	Tptpmn	Busted Butte	Busted Butte	10E4		82.6	165.20	saturated	22	2.0	1.00E-05			SNL	2.9	Uniaxial compressive strength	MO0311RCKPRPCS.003, MO0402DQRIRPPR.003	
115	115	0		0	115	39.3	0.1	TSw2	Tptpmn	Busted Butte	Busted Butte	BB-10-AE-13W		50.8	101.60	dry	150	2.0	1.00E-08		RSI TP-04e	RE/SPEC	3.07	Uniaxial compressive strength	MO0311RCKPRPCS.003, MO0402DQRIRPPR.003	
85.84	85.84	0		0	85.84	39.8	0.25	TSw2	Tptpmn	Busted Butte	Busted Butte	234		127.0	254.00	saturated	22	2.0	1.00E-05			SNL	2.5	Uniaxial compressive strength	MO0311RCKPRPCS.003, MO0402DQRIRPPR.003	
182.8	182.8	0		0	182.8	40.6	0.17	TSw2	Tptpmn	Busted Butte	Busted Butte	10AE40W		50.8	101.6	dry	22	2.0	1.00E-07			SNL	4.7	Uniaxial compressive strength	MO0311RCKPRPCS.003, MO0402DQRIRPPR.003	
102	102	0		0	102	40.9	0.18	TSw2	Tptpmn	Busted Butte	Busted Butte	10AE46W		50.8	101.6	dry	22	2.0	1.00E-05			SNL	2.6	Uniaxial compressive strength	MO0311RCKPRPCS.003, MO0402DQRIRPPR.003	
134.3	134.3	0		0	134.3	41.2		TSw2	Tptpmn	Busted Butte	Busted Butte	221		127.0	254.00	saturated	22	2.0	1.00E-05			SNL	3.6	Uniaxial compressive strength	MO0311RCKPRPCS.003, MO0402DQRIRPPR.003	
85	85	0		0	85	41.8	0.04	TSw2	Tptpmn	Busted Butte	Busted Butte	BB-10-AE-22X (Tuff/84/22X)		50.8	101.6	dry	150	2.0	1.00E-07		RSI TP-04e	RE/SPEC	2.03	Uniaxial compressive strength	MO0311RCKPRPCS.003, MO0402DQRIRPPR.003	
166.1	166.1	0		0	166.1	41.9	0.18	TSw2	Tptpmn	Busted Butte	Busted Butte	10AE24W		50.8	101.6	dry	22	2.0	1.00E-05			SNL	4.3	Uniaxial compressive strength	MO0311RCKPRPCS.003, MO0402DQRIRPPR.003	
103	103	0		0	103	42	0.11	TSw2	Tptpmn	Busted Butte	Busted Butte	BB-10-AE-34X		50.8	101.60	dry	150	2.0	1.00E-08		RSI TP-04e	RE/SPEC	2.63	Uniaxial compressive strength	MO0311RCKPRPCS.003, MO0402DQRIRPPR.003	
94.3	94.3	0	0	0	94.3	42.1	0.21	TSw2	Tptpmn	Busted Butte	Busted Butte	10AE25Y		50.8	101.6	saturated	22	2.0	1.00E-07			SNL	2.3	Uniaxial compressive strength	MO0311RCKPRPCS.003, MO0402DQRIRPPR.003	saturated, drained test
93.36	93.36	0		0	93.36	42.1	0.21	TSw2	Tptpmn	Busted Butte	Busted Butte	282		228.6	457.20	saturated	22	2.0	1.00E-05			SNL	2.4	Uniaxial compressive strength	MO0311RCKPRPCS.003, MO0402DQRIRPPR.003	
185.5	185.5	0		0	185.5	42.2	0.2	TSw2	Tptpmn	Busted Butte	Busted Butte	10AE33X		50.8	101.6	dry	22	2.0	1.00E-07			SNL	4.8	Uniaxial compressive strength	MO0311RCKPRPCS.003, MO0402DQRIRPPR.003	
198.6	198.6	0		0	198.6	42.5	0.14	TSw2	Tptpmn	Busted Butte	Busted Butte	26D1		25.4	50.8	saturated	22	2.0	1.00E-05			SNL	5.0	Uniaxial compressive strength	MO0311RCKPRPCS.003, MO0402DQRIRPPR.003	
140.7	140.7	0		0	140.7	42.9	0.23	TSw2	Tptpmn	Busted Butte	Busted Butte	231		82.6	165.20	saturated	22	2.0	1.00E-05			SNL	3.5	Uniaxial compressive strength	MO0311RCKPRPCS.003, MO0402DQRIRPPR.003	
160.7	160.7	0		0	160.7	43.8	0.22	TSw2	Tptpmn	Busted Butte	Busted Butte	211		82.6	165.20	saturated	22	2.0	1.00E-05			SNL	3.9	Uniaxial compressive strength	MO0311RCKPRPCS.003, MO0402DQRIRPPR.003	
141.7	141.7	0		0	141.7	43.9	0.23	TSw2	Tptpmn	Busted Butte	Busted Butte	10E3		82.6	165.20	saturated	22	2.0	1.00E-05			SNL	3.9	Uniaxial compressive strength	MO0311RCKPRPCS.003, MO0402DQRIRPPR.003	
131.8	131.8	0		0	131.8	44	0.22	TSw2	Tptpmn	Busted Butte	Busted Butte	11D1		82.6	165.20	saturated	22	2.0	1.00E-05			SNL	3.7	Uniaxial compressive strength	MO0311RCKPRPCS.003, MO0402DQRIRPPR.003	
132.2	132.2	0		0	132.2	44.2	0.21	TSw2	Tptpmn	Busted Butte	Busted Butte	12A3		25.4	50.8	saturated	22	2.0	1.00E-05			SNL	3.3	Uniaxial compressive strength	MO0311RCKPRPCS.003, MO0402DQRIRPPR.003	
149	149	0	0	0	149	44.5	0.23	TSw2	Tptpmn	Busted Butte	Busted Butte	10AE44X		50.8	101.6	saturated	22	2.0	1.00E-07			SNL	3.8	Uniaxial compressive strength	MO0311RCKPRPCS.003, MO0402DQRIRPPR.003	saturated, drained test
130.6	130.6	0		0	130.6	44.5	0.25	TSw2	Tptpmn	Busted Butte	Busted Butte	11A1		82.6	165.20	saturated	22	2.0	1.00E-05			SNL	3.3	Uniaxial compressive strength	MO0311RCKPRPCS.003, MO0402DQRIRPPR.003	

Table A-1 Intact Rock Mechanical Properties Data - Strength and Elastic Properties Data

Axial Stress, σ_1 (MPa)	Axial Stress, effective σ_1' (MPa)	Confining Pressure (MPa) σ_3	Pore Pressure (MPa)	Confining Pressure, Effective (MPa), σ_3'	Differential Strength, (MPa) $\sigma_1 - \sigma_3$	Young's Modulus (GPa)	Poisson's Ratio	TM Unit	Litho-stratigraphic Unit	General Location	Sample Location	Specimen Number	Depth (ft)	Specimen Diameter (mm)	Specimen Length (mm)	Specimen Saturation	Specimen Temperature (deg. C)	l/d Ratio	Strain Rate (1/s)	Specimen Orientation (degree)	Test Standard	Laboratory	Failure Strain (millistrain)	Rock Property	Source DTN	Notes
170.8	170.8	0		0	170.8	45.1	0.2	TSw2	Tptpmn	Busted Butte	Busted Butte	261		127.0	254.00	saturated	22	2.0	1.00E-05			SNL	4.1	Uniaxial compressive strength	MO0311RCKPRPCS.003, MO0402DQRIRPPR.003	
200.5	200.5	0		0	200.5	45.7	0.2	TSw2	Tptpmn	Busted Butte	Busted Butte	26A1		50.8	101.6	saturated	22	2.0	1.00E-05			SNL	4.8	Uniaxial compressive strength	MO0311RCKPRPCS.003, MO0402DQRIRPPR.003	
87	87	0		0	87	45.7	0.32	TSw2	Tptpmn	Busted Butte	Busted Butte	10AE41Y		50.8	101.6	dry	22	2.0	1.00E-05			SNL	2.7	Uniaxial compressive strength	MO0311RCKPRPCS.003, MO0402DQRIRPPR.003	Large Inhomogeneities in sample
203.2	203.2	0		0	203.2	45.8	0.22	TSw2	Tptpmn	Busted Butte	Busted Butte	12A2		25.4	50.8	saturated	22	2.0	1.00E-05			SNL	4.8	Uniaxial compressive strength	MO0311RCKPRPCS.003, MO0402DQRIRPPR.003	
124.3	124.3	0		0	124.3	46	0.24	TSw2	Tptpmn	Busted Butte	Busted Butte	11C1		82.6	165.20	saturated	22	2.0	1.00E-05			SNL	3.2	Uniaxial compressive strength	MO0311RCKPRPCS.003, MO0402DQRIRPPR.003	
241.3	241.3	0		0	241.3	47.2	0.19	TSw2	Tptpmn	Busted Butte	Busted Butte	26E1		25.4	50.8	saturated	22	2.0	1.00E-05			SNL	5.5	Uniaxial compressive strength	MO0311RCKPRPCS.003, MO0402DQRIRPPR.003	
274.3	274.3	0		0	274.3	47.3	0.19	TSw2	Tptpmn	Busted Butte	Busted Butte	26C1		25.4	50.8	saturated	22	2.0	1.00E-05			SNL	5.9	Uniaxial compressive strength	MO0311RCKPRPCS.003, MO0402DQRIRPPR.003	
45	45	0		0	45	152.4	0.33	TSw2	Tptpmn	Busted Butte	Busted Butte	BB-10-AE-41X		50.9	101.80	dry	150	2.0	1.00E-08		RSI TP-04e	RE/SPEC	0.3	Uniaxial compressive strength	MO0311RCKPRPCS.003, MO0402DQRIRPPR.003	
123.1	123.1	0		0	123.1	34.5	0.34	TSw2	Tptpmn	ESF/ECRB/Borehole	ESF-AOD-HDFR1-32.2-A	UCDST011		38.1	76.2	ambient	22	2.0	1.00E-05		SNL TP-219 & ASTM D2938-86	SNL	3.497	Uniaxial compressive strength	MO0311RCKPRPCS.003, MO0402DQRIRPPR.003	
175.6	175.6	0		0	175.6	40	0.19	TSw2	Tptpmn	ESF/ECRB/Borehole	ESF-AOD-HDFR1-48.7-A	UCDST012		38.1	76.2	ambient	22	2.0	1.00E-05		SNL TP-219 & ASTM D2938-86	SNL	3.668	Uniaxial compressive strength	MO0311RCKPRPCS.003, MO0402DQRIRPPR.003	
159	159	0		0	159.0	31.6	0.17	TSw2	Tptpmn	ESF/ECRB/Borehole	ESF-AOD-HDFR1-68.8-A	UCDST013		38.1	76.2	ambient	22	2.0	1.00E-05		SNL TP-219 & ASTM D2938-86	SNL	5.536	Uniaxial compressive strength	MO0311RCKPRPCS.003, MO0402DQRIRPPR.003	
268.3	268.3	0		0	268.3	37.4	0.2	TSw2	Tptpmn	ESF/ECRB/Borehole	ESF-AOD-HDFR1-8.6-A	UCDST010		38.1	76.2	ambient	22	2.0	1.00E-05		SNL TP-219 & ASTM D2938-86	SNL	7.966	Uniaxial compressive strength	MO0311RCKPRPCS.003, MO0402DQRIRPPR.003	
179.4	179.4	0		0	179.4	43.1	0.18	TSw2	Tptpmn	ESF/ECRB/Borehole	ESF-SDM-MPBX-1-1.0-A	UCDST017/UCDST001		38.1	76.2	ambient	22	2.0	1.00E-05		SNL TP-219 & ASTM D2938-86	SNL	3.582	Uniaxial compressive strength	MO0311RCKPRPCS.003, MO0402DQRIRPPR.003	sample UCDST001 retested. Original test not carried to failure.
201	201	0		0	201.0	38.5	0.21	TSw2	Tptpmn	ESF/ECRB/Borehole	ESF-SDM-MPBX-1-32.1-A	UCDST002		38.1	76.2	ambient	22	2.0	1.00E-05		SNL TP-219 & ASTM D2938-86	SNL	5.642	Uniaxial compressive strength	MO0311RCKPRPCS.003, MO0402DQRIRPPR.003	
232.6	232.6	0		0	232.6	38.2	0.19	TSw2	Tptpmn	ESF/ECRB/Borehole	ESF-SDM-MPBX-1-40.6-A	UCDST003		38.1	76.2	ambient	22	2.0	1.00E-05		SNL TP-219 & ASTM D2938-86	SNL	6.191	Uniaxial compressive strength	MO0311RCKPRPCS.003, MO0402DQRIRPPR.003	
114.1	114.1	0		0	114.1	39.3	0.19	TSw2	Tptpmn	ESF/ECRB/Borehole	ESF-SDM-MPBX-1-62.0-A	UCDST004		38.1	76.2	ambient	22	2.0	1.00E-05		SNL TP-219 & ASTM D2938-86	SNL	3.016	Uniaxial compressive strength	MO0311RCKPRPCS.003, MO0402DQRIRPPR.003	
97.2	97.2	0		0	97.2	36.2	0.22	TSw2	Tptpmn	ESF/ECRB/Borehole	ESF-SDM-MPBX-1-80.5-A	UCDST005		38.1	76.2	ambient	22	2.0	1.00E-05		SNL TP-219 & ASTM D2938-86	SNL	3.577	Uniaxial compressive strength	MO0311RCKPRPCS.003, MO0402DQRIRPPR.003	
178	178	0		0	178.0	37.8	0.2	TSw2	Tptpmn	ESF/ECRB/Borehole	ESF-SDM-MPBX-2-29.0-A	UCDST006		38.1	76.2	ambient	22	2.0	1.00E-05		SNL TP-219 & ASTM D2938-86	SNL	5.467	Uniaxial compressive strength	MO0311RCKPRPCS.003, MO0402DQRIRPPR.003	
128	128	0		0	128.0	34.5	0.19	TSw2	Tptpmn	ESF/ECRB/Borehole	ESF-SDM-MPBX-2-48.4-A	UCDST007		38.1	76.2	ambient	22	2.0	1.00E-05		SNL TP-219 & ASTM D2938-86	SNL	3.877	Uniaxial compressive strength	MO0311RCKPRPCS.003, MO0402DQRIRPPR.003	
71.3	71.3	0		0	71.3	40.2	0.17	TSw2	Tptpmn	ESF/ECRB/Borehole	ESF-SDM-MPBX-2-71.5-A	UCDST008		38.1	76.2	ambient	22	2.0	1.00E-05		SNL TP-219 & ASTM D2938-86	SNL	1.852	Uniaxial compressive strength	MO0311RCKPRPCS.003, MO0402DQRIRPPR.003	
324.1	324.1	0		0	324.1	37.8	0.19	TSw2	Tptpmn	ESF/ECRB/Borehole	ESF-SDM-MPBX-2-84.6-A	UCDST009		38.1	76.2	ambient	22	2.0	1.00E-05		SNL TP-219 & ASTM D2938-86	SNL	9.506	Uniaxial compressive strength	MO0311RCKPRPCS.003, MO0402DQRIRPPR.003	
172.2	172.2	0		0	172.2	28.9	0.18	TSw2	Tptpmn	ESF/ECRB/Borehole	ESF-SDM-MPBX-3-17.7-A	UCDST014		38.1	76.2	ambient	22	2.0	1.00E-05		SNL TP-219 & ASTM D2938-86	SNL	6.551	Uniaxial compressive strength	MO0311RCKPRPCS.003, MO0402DQRIRPPR.003	
158.6	158.6	0		0	158.6	34.8	0.22	TSw2	Tptpmn	ESF/ECRB/Borehole	ESF-SDM-MPBX-3-38.7-A	UCDST015		38.1	76.2	ambient	22	2.0	1.00E-05		SNL TP-219 & ASTM D2938-86	SNL	7.332	Uniaxial compressive strength	MO0311RCKPRPCS.003, MO0402DQRIRPPR.003	
239.1	239.1	0		0	239.1	35.4	0.18	TSw2	Tptpmn	ESF/ECRB/Borehole	ESF-SDM-MPBX-3-85.3-A	UCDST016		38.1	76.2	ambient	22	2.0	1.00E-05		SNL TP-219 & ASTM D2938-86	SNL	6.082	Uniaxial compressive strength	MO0311RCKPRPCS.003, MO0402DQRIRPPR.003	
149.5	149.5	0		0	149.5	32.7	0.16	TSw2	Tptpmn	ESF/ECRB/Borehole	ESF-TMA-BJ-1	ESF-TMA-BJ-1-17.5-A		41.9	101.6	ambient	22	2.4	1.00E-05		ASTM D 3148 and ISRM U	NBR	4.95	Uniaxial compressive strength	MO0311RCKPRPCS.003, MO0402DQRIRPPR.003	
190.8	190.8	0		0	190.8	33.5	0.15	TSw2	Tptpmn	ESF/ECRB/Borehole	ESF-TMA-BJ-1	ESF-TMA-BJ-1-16.9-A		41.9	101.6	ambient	22	2.4	1.00E-05		ASTM D 3148 and ISRM U	NBR	6.30	Uniaxial compressive strength	MO0311RCKPRPCS.003, MO0402DQRIRPPR.003	
171.5	171.5	0		0	171.5	35.9	0.18	TSw2	Tptpmn	ESF/ECRB/Borehole	ESF-TMA-BJ-1	ESF-TMA-BJ-1-0.0-C		41.9	101.6	ambient	22	2.4	1.00E-05		ASTM D 3148 and ISRM U	NBR	4.96	Uniaxial compressive strength	MO0311RCKPRPCS.003, MO0402DQRIRPPR.003	
113.2	113.2	0		0	113.2	36.3	0.16	TSw2	Tptpmn	ESF/ECRB/Borehole	ESF-TMA-BJ-1	ESF-TMA-BJ-1-1.0-C		41.9	101.6	ambient	22	2.4	1.00E-05		ASTM D 3148 and ISRM U	NBR	3.24	Uniaxial compressive strength	MO0311RCKPRPCS.003, MO0402DQRIRPPR.003	
118.4	118.4	0		0	118.4	29.1	0.15	TSw2	Tptpmn	ESF/ECRB/Borehole	ESF-TMA-H1	ESF-TMA-H1-10.0-A		41.9	101.6	ambient	22	2.4	1.00E-05		ASTM D 3148 and ISRM U	NBR	6.85	Uniaxial compressive strength	MO0311RCKPRPCS.003, MO0402DQRIRPPR.003	
171	171	0		0	171.0	30.1	0.16	TSw2	Tptpmn	ESF/ECRB/Borehole	ESF-TMA-H1	ESF-TMA-H1-19.9-D		41.9	101.6	ambient	22	2.4	1.00E-05		ASTM D 3148 and ISRM U	NBR	6.23	Uniaxial compressive strength	MO0311RCKPRPCS.003, MO0402DQRIRPPR.003	
79.4	79.4	0		0	79.4	31.5	0.16	TSw2	Tptpmn	ESF/ECRB/Borehole	ESF-TMA-H1	ESF-TMA-H1-0.6-D		41.9	101.6	ambient	22	2.4	1.00E-05		ASTM D 3148 and ISRM U	NBR	2.51	Uniaxial compressive strength	MO0311RCKPRPCS.003, MO0402DQRIRPPR.003	
75.1	75.1	0		0	75.1	25.7	0.18	TSw2	Tptpmn	ESF/ECRB/Borehole	ESF-TMA-MPBX-1	ESF-TMA-MPBX-1-7.8-C		41.9	101.6	ambient	22	2.4	1.00E-05		ASTM D 3148 and ISRM U	NBR	4.98	Uniaxial compressive strength	MO0311RCKPRPCS.003, MO0402DQRIRPPR.003	
161.2	161.2	0		0	161.2	32.3	0.19	TSw2	Tptpmn	ESF/ECRB/Borehole	ESF-TMA-MPBX-1	ESF-TMA-MPBX-1-6.0-D		41.9	101.6	ambient	22	2.4	1.00E-05		ASTM D 3148 and ISRM U	NER	6.18	Uniaxial compressive strength	MO0311RCKPRPCS.003, MO0402DQRIRPPR.003	
141.5	141.5	0		0	141.5	32.6	0.22	TSw2	Tptpmn	ESF/ECRB/Borehole	ESF-TMA-MPBX-1	ESF-TMA-MPBX-1-6.0-C		41.9	101.6	ambient	22	2.4	1.00E-05		ASTM D 3148 and ISRM U	NER	4.53	Uniaxial compressive strength	MO0311RCKPRPCS.003, MO0402DQRIRPPR.003	
243.8	243.8	0		0	243.8	30.2	0.16	TSw2	Tptpmn	ESF/ECRB/Borehole	ESF-TMA-MPBX-2	ESF-TMA-MPBX-2-8.6-G		41.9	101.6	ambient	22	2.4	1.00E-05		ASTM D 3148 and ISRM U	NER	9.07	Uniaxial compressive strength	MO0311RCKPRPCS.003, MO0402DQRIRPPR.003	
218.9	218.9	0		0	218.9	30.7	0.16	TSw2	Tptpmn	ESF/ECRB/Borehole	ESF-TMA-MPBX-2	ESF-TMA-MPBX-2-8.6-E		41.9	101.6	ambient	22	2.4	1.00E-05		ASTM D 3148 and ISRM U	NER	4.79	Uniaxial compressive strength	MO0311RCKPRPCS.003, MO0402DQRIRPPR.003	
232.1	232.1	0		0	232.1	31.6	0.17	TSw2	Tptpmn	ESF/ECRB/Borehole	ESF-TMA-MPBX-2	ESF-TMA-MPBX-2-8.6-F		41.9	101.6	ambient	22	2.4	1.00E-05		ASTM D 3148 and ISRM U	NER	8.22	Uniaxial compressive strength	MO0311RCKPRPCS.003, MO0402DQRIRPPR.003	
150.5	150.5	0		0	150.5	27.3	0.17	TSw2	Tptpmn	ESF/ECRB/Borehole	ESF-TMA-MPBX-3	ESF-TMA-MPBX-3-12.5-D		41.9	101.6	ambient	22	2.4	1.00E-05		ASTM D 3148 and ISRM U	NER	5.82	Uniaxial compressive strength	MO0311RCKPRPCS.003, MO0402DQRIRPPR.003	
179.8	179.8	0		0	179.8	29.8	0.15	TSw2	Tptpmn	ESF/ECRB/Borehole	ESF-TMA-MPBX-3	ESF-TMA-MPBX-3-12.5-C		41.9	101.6	ambient	22	2.4	1.00E-05		ASTM D 3148 and ISRM U	NER	8.32	Uniaxial compressive strength	MO0311RCKPRPCS.003, MO0402DQRIRPPR.003	
108.9	108.9	0		0	108.9	36.7	0.16	TSw2	Tptpmn	ESF/ECRB/Borehole	ESF-TMA-MPBX-3	ESF-TMA-MPBX-3-5.1-A		41.9	101.6	ambient	22	2.4	1.00E-05		ASTM D 3148 and ISRM U	NER	3.20	Uniaxial compressive strength	MO0311RCKPRPCS.003, MO0402DQRIRPPR.003	
76.5	76.5	0		0	76.5	33.4	0.17	TSw2	Tptpmn	ESF/ECRB/Borehole	ESF-TMA-MPBX-4	ESF-TMA-MPBX-4-5.0-C		41.9	101.6	ambient	22	2.4	1.00E-05		ASTM D 3148 and ISRM U	NER	2.15	Uniaxial compressive strength	MO0311RCKPRPCS.003, MO0402DQRIRPPR.003	
126.8	126.8	0		0	126.8	33.7	0.15	TSw2	Tptpmn	ESF/ECRB/Borehole	ESF-TMA-MPBX-4	ESF-TMA-MPBX-4-16.5-B		41.9	101.6	ambient	22	2.4	1.00E-05		ASTM D 3148 and ISRM U	NBR	5.54	Uniaxial compressive strength	MO0311RCKPRPCS.003, MO0402DQRIRPPR.003	
82.8	82.8	0		0	82.8	33.9	0.16	TSw2	Tptpmn	ESF/ECRB/Borehole	ESF-TMA-MPBX-4	ESF-TMA-MPBX-4-18.3-D		41.9	101.6	ambient	22	2.4	1.00E-05		ASTM D 3148 and ISRM U	NBR	2.78	Uniaxial compressive strength	MO0311RCKPRPCS.003, MO0402DQRIRPPR.003	
83.4	83.4	0		0	83.4	34.7	0.15	TSw2	Tptpmn	ESF/ECRB/Borehole	ESF-TMA-MPBX-4	ESF-TMA-MPBX-4-16.5-A		41.9	101.6	ambient	22	2.4	1.00E-05		ASTM D 3148 and ISRM U	NBR	3.94	Uniaxial compressive strength	MO0311RCKPRPCS.003, MO0402DQRIRPPR.003	
123.3	123.3	0		0	123.3	35.4	0.15	TSw2	Tptpmn	ESF/ECRB/Borehole	ESF-TMA-MPBX-4	ESF-TMA-MPBX-4-18.3-E		41.9	101.6	ambient	22	2.4	1.00E-05		ASTM D 3148 and ISRM U	NBR	3.62	Uniaxial compressive strength	MO0311RCKPRPCS.003, MO0402DQRIRPPR.003	
151	151	0		0	151.0	35.7	0.17	TSw2	Tptpmn	ESF/ECRB/Borehole	ESF-TMA-MPBX-4	ESF-TMA-MPBX-4-5.0-D		41.9	101.6	ambient	22	2.4	1.00E-05		ASTM D 3148 and ISRM U	NBR	4.47	Uniaxial compressive strength	MO0311RCKPRPCS.003, MO0402DQRIRPPR.003	
78.7	78.7	0		0	78.7	26.6	0.39	TSw2	Tptpmn	ESF/ECRB/Borehole	ESF-TMA-PTC-1	PTC1 12.5		38.1	95.3	ambient	22	2.5	1.00E-05			SNL	1.641	Uniaxial compressive strength	MO0311RCKPRPCS.003, MO0402DQRIRPPR.003	Tested @ ambient temp. after sample exposed to 2 heat/cool cycles betwn 25 & ~325C
159.2	159.2	0		0	159.2	28.9	0.18	TSw2	Tptpmn	ESF/ECRB/Borehole	ESF-TMA-PTC-1	PTC1-B 15.7		38.1	95.3	ambient	22	2.5	1.00E-05			SNL	5.614	Uniaxial compressive strength	MO0311RCKPRPCS.003, MO0402DQRIRPPR.003	Tested @ ambient temp. after sample exposed to 2 heat/cool cycles betwn 25 & ~325C
51.8	51.8	0		0	51.8	20.1	0.25	TSw2	Tptpmn	ESF/ECRB/Borehole	ESF-TMA-PTC-2	PTC2-B 10.8		38.1	95.3	ambient	22	2.5	1.00E-05			SNL	2.130	Uniaxial compressive strength	MO0311RCKPRPCS.003, MO0402DQRIRPPR.003	Tested @ ambient temp. after sample exposed to 2 heat/cool cycles betwn 25 & ~325C
113.9	113.9	0		0	113.9	32.3	0.17	TSw2	Tptpmn	ESF/ECRB/Borehole	ESF-TMA-PTC-4	PTC4-B 6.6		38.1	95.3	ambient	22	2.5	1.00E-05			SNL	3.637	Uniaxial compressive strength	MO0311RCKPRPCS.003, MO0402DQRIRPPR.003	Tested @ ambient temp. after sample exposed to 2 heat/cool cycles betwn 25 & ~325C
191.4	191.4	0		0	191.4	32.9	0.18	TSw2	Tptpmn	ESF/ECRB/Borehole	ESF-TMA-PTC-4	PTC4-B 26.0		38.1	95.3	ambient	22	2.5	1.00E-05			SNL	6.003	Uniaxial compressive strength	MO0311RCKPRPCS.003, MO0402DQRIRPPR.003	Tested @ ambient temp. after sample exposed to 2 heat/cool cycles betwn 25 & ~325C
34.3	34.3	0		0	34.3	33.4	0.17	TSw2	Tptpmn	ESF/ECRB/Borehole	ESF-TMA-PTC-4	PTC4-B 4.3		38.1	95.3	ambient	22	2.5	1.00E-05			SNL	1.138	Uniaxial compressive strength	MO0311RCKPRPCS.003, MO0402DQRIRPPR.003	Tested @ ambient temp. after sample exposed to 2 heat/cool cycles betwn 25 & ~325C
240.5	240.5	0		0	240.5	34	0.18	TSw2	Tptpmn	ESF/ECRB/Borehole	ESF-TMA-PTC-4	PTC4 17.4		38.1	95.3	ambient	22	2.5	1.00E-05			SNL	7.924	Uniaxial compressive strength	MO0311RCKPRPCS.003, MO0402DQRIRPPR.003	Tested @ ambient temp. after sample exposed to 2 heat/cool cycles betwn 25 & ~325C
175.4	175.4	0		0	175.4	34.4	0.19	TSw2	Tptpmn	ESF/ECRB/Borehole	ESF-TMA-PTC-4	PTC4-B 9.2		38.1	95.3	ambient	22	2.5	1.00E-05			SNL	5.274	Uniaxial compressive strength	MO0311RCKPRPCS.003, MO0402DQRIRPPR.003	Tested @ ambient temp. after sample exposed to 2 heat/cool cycles betwn 25 & ~325C
245.7	245.7	0		0	245.7	34.4	0.19	TSw2	Tptpmn	ESF/ECRB/Borehole	ESF-TMA-PTC-4	PTC4 20.9		38.1	95.3	ambient	22	2.5	1.00E-05			SNL	7.909	Uniaxial compressive strength	MO0311RCKPRPCS.003, MO0402DQRIRPPR.003	Tested @ ambient temp. after sample exposed to 2 heat/cool cycles betwn 25 & ~325C
144.9	144.9	0		0	144.9	37	0.26	TSw2	Tptpmn	ESF/ECRB/Borehole	ESF-TMA-PTC-4	PTC4 11.8		38.1	95.3	ambient	22	2.5	1.00E-05			SNL	8.941	Uniaxial compressive strength	MO0311RCKPRPCS.003, MO0402DQRIRPPR.003	Tested @ ambient temp. after sample exposed to 2 heat/cool cycles betwn 25 & ~325C
38.7	38.7	0		0	38.7	24.2	0.12	TSw2	Tptpmn	ESF/ECRB/Borehole	ESF-TMA-PTC-H-1	PTCH1 15.6		38.1	95.3	ambient	22	2.5	1.00E-05			SNL	2.316	Uniaxial compressive strength	MO0311RCKPRPCS.003, MO0402DQRIRPPR.003	Tested @ ambient temp. after sample exposed to 2 heat/cool cycles betwn 25 & ~325C

Table A-1 Intact Rock Mechanical Properties Data - Strength and Elastic Properties Data

Axial Stress, σ_1 (MPa)	Axial Stress, effective σ_1' (MPa)	Confining Pressure (MPa) σ_3	Pore Pressure (MPa)	Confining Pressure, Effective (MPa), σ_3'	Differential Strength, (MPa) $\sigma_1 - \sigma_3$	Young's Modulus (GPa)	Poisson's Ratio	TM Unit	Litho-stratigraphic Unit	General Location	Sample Location	Specimen Number	Depth (ft)	Specimen Diameter (mm)	Specimen Length (mm)	Specimen Saturation	Specimen Temperature (deg. C)	l/d Ratio	Strain Rate (1/s)	Specimen Orientation (degree)	Test Standard	Laboratory	Failure Strain (millistrain)	Rock Property	Source DTN	Notes
137	137	0		0	137.0	34.2	0.17	TSw2	Tptpmn	ESF/ECRB/Borehole	ESF-TMA-PTC-H-1	PTCH1 18.7		38.1	95.3	ambient	22	2.5	1.00E-05			SNL	4.349	Uniaxial compressive strength	MO0311RCKPRPCS.003, MO0402DQRIRPPR.003	Tested @ ambient temp. after sample exposed to 2 heat/cool cycles betwn 25 & ~325C
80.5	80.5	0		0	80.5	34.3	0.16	TSw2	Tptpmn	ESF/ECRB/Borehole	ESF-TMA-PTC-H-1	PTCH1 8.6		38.1	95.3	ambient	22	2.5	1.00E-05			SNL	2.629	Uniaxial compressive strength	MO0311RCKPRPCS.003, MO0402DQRIRPPR.003	Tested @ ambient temp. after sample exposed to 2 heat/cool cycles betwn 25 & ~325C
183.5	183.5	0		0	183.5	35.4	0.17	TSw2	Tptpmn	ESF/ECRB/Borehole	ESF-TMA-PTC-MPBX-1	PTC MPBX1-B 14.4		38.1	95.3	ambient	22	2.5	1.00E-05			SNL	5.806	Uniaxial compressive strength	MO0311RCKPRPCS.003, MO0402DQRIRPPR.003	Tested @ ambient temp. after sample exposed to 2 heat/cool cycles betwn 25 & ~325C
47.9	47.9	0		0	47.9	6.8		TSw2	Tptpmn	Fran Ridge	Fran Ridge	2		25.4	76.2	dry	22	3.0	1.00E-05		ASTM D-2938-86	LLNL	10.0	Uniaxial compressive strength	MO0311RCKPRPCS.003, MO0402DQRIRPPR.003	radiated
58.9	58.9	0		0	58.9	17.9		TSw2	Tptpmn	Fran Ridge	Fran Ridge	9		25.4	76.2	dry	22	3.0	1.00E-05		ASTM D-2938-86	LLNL	3.6	Uniaxial compressive strength	MO0311RCKPRPCS.003, MO0402DQRIRPPR.003	non-radiated
76.3	76.3	0		0	76.3	19		TSw2	Tptpmn	Fran Ridge	Fran Ridge	40		25.4	76.2	dry	22	3.0	1.00E-05		ASTM D-2938-86	LLNL	4.5	Uniaxial compressive strength	MO0311RCKPRPCS.003, MO0402DQRIRPPR.003	radiated
31.9	31.9	0		0	31.9	21		TSw2	Tptpmn	Fran Ridge	Fran Ridge	39		25.4	76.2	dry	22	3.0	1.00E-05		ASTM D-2938-86	LLNL	2.0	Uniaxial compressive strength	MO0311RCKPRPCS.003, MO0402DQRIRPPR.003	radiated
150.5	150.5	0		0	150.5	21.2		TSw2	Tptpmn	Fran Ridge	Fran Ridge	10		25.4	76.2	dry	22	3.0	1.00E-05		ASTM D-2938-86	LLNL	7.5	Uniaxial compressive strength	MO0311RCKPRPCS.003, MO0402DQRIRPPR.003	radiated
51.3	51.3	0		0	51.3	22.5		TSw2	Tptpmn	Fran Ridge	Fran Ridge	35		25.4	76.2	dry	22	3.0	1.00E-05		ASTM D-2938-86	LLNL	2.3	Uniaxial compressive strength	MO0311RCKPRPCS.003, MO0402DQRIRPPR.003	radiated
116.8	116.8	0		0	116.8	22.7		TSw2	Tptpmn	Fran Ridge	Fran Ridge	31		25.4	76.2	dry	22	3.0	1.00E-05		ASTM D-2938-86	LLNL	7.3	Uniaxial compressive strength	MO0311RCKPRPCS.003, MO0402DQRIRPPR.003	non-radiated
132.4	132.4	0		0	132.4	23.1		TSw2	Tptpmn	Fran Ridge	Fran Ridge	30		25.4	76.2	dry	22	3.0	1.00E-05		ASTM D-2938-86	LLNL	7.0	Uniaxial compressive strength	MO0311RCKPRPCS.003, MO0402DQRIRPPR.003	non-radiated
168.3	168.3	0		0	168.3	23.2		TSw2	Tptpmn	Fran Ridge	Fran Ridge	33		25.4	76.2	dry	22	3.0	1.00E-05		ASTM D-2938-86	LLNL	7.8	Uniaxial compressive strength	MO0311RCKPRPCS.003, MO0402DQRIRPPR.003	non-radiated
96	96	0		0	96.0	23.3		TSw2	Tptpmn	Fran Ridge	Fran Ridge	3		25.4	76.2	dry	22	3.0	1.00E-05		ASTM D-2938-86	LLNL	6.8	Uniaxial compressive strength	MO0311RCKPRPCS.003, MO0402DQRIRPPR.003	radiated
123	123	0		0	123.0	23.3		TSw2	Tptpmn	Fran Ridge	Fran Ridge	43		25.4	76.2	dry	22	3.0	1.00E-05		ASTM D-2938-86	LLNL	6.2	Uniaxial compressive strength	MO0311RCKPRPCS.003, MO0402DQRIRPPR.003	radiated. Typo on line 2 of SEP entry corrected.
63	63	0		0	63.0	23.9		TSw2	Tptpmn	Fran Ridge	Fran Ridge	37		25.4	76.2	dry	22	3.0	1.00E-05		ASTM D-2938-86	LLNL	3.5	Uniaxial compressive strength	MO0311RCKPRPCS.003, MO0402DQRIRPPR.003	radiated
128.4	128.4	0		0	128.4	24.2		TSw2	Tptpmn	Fran Ridge	Fran Ridge	26		25.4	76.2	dry	22	3.0	1.00E-05		ASTM D-2938-86	LLNL	7.3	Uniaxial compressive strength	MO0311RCKPRPCS.003, MO0402DQRIRPPR.003	non-radiated
135.6	135.6	0		0	135.6	24.6		TSw2	Tptpmn	Fran Ridge	Fran Ridge	4		25.4	76.2	dry	22	3.0	1.00E-05		ASTM D-2938-86	LLNL	7.5	Uniaxial compressive strength	MO0311RCKPRPCS.003, MO0402DQRIRPPR.003	non-radiated
164.5	164.5	0		0	164.5	25		TSw2	Tptpmn	Fran Ridge	Fran Ridge	12		25.4	76.2	dry	22	3.0	1.00E-05		ASTM D-2938-86	LLNL	8.0	Uniaxial compressive strength	MO0311RCKPRPCS.003, MO0402DQRIRPPR.003	non-radiated
166.6	166.6	0		0	166.6	25.2		TSw2	Tptpmn	Fran Ridge	Fran Ridge	41		25.4	76.2	dry	22	3.0	1.00E-05		ASTM D-2938-86	LLNL	7.8	Uniaxial compressive strength	MO0311RCKPRPCS.003, MO0402DQRIRPPR.003	non-radiated
149	149	0		0	149.0	25.4		TSw2	Tptpmn	Fran Ridge	Fran Ridge	25		25.4	76.2	dry	22	3.0	1.00E-05		ASTM D-2938-86	LLNL	7.4	Uniaxial compressive strength	MO0311RCKPRPCS.003, MO0402DQRIRPPR.003	non-radiated
170.5	170.5	0		0	170.5	25.4		TSw2	Tptpmn	Fran Ridge	Fran Ridge	1		25.4	76.2	dry	22	3.0	1.00E-05		ASTM D-2938-86	LLNL	8.0	Uniaxial compressive strength	MO0311RCKPRPCS.003, MO0402DQRIRPPR.003	non-radiated
213.4	213.4	0		0	213.4	25.9		TSw2	Tptpmn	Fran Ridge	Fran Ridge	28		25.4	76.2	dry	22	3.0	1.00E-05		ASTM D-2938-86	LLNL	8.7	Uniaxial compressive strength	MO0311RCKPRPCS.003, MO0402DQRIRPPR.003	radiated
151.9	151.9	0		0	151.9	26.1		TSw2	Tptpmn	Fran Ridge	Fran Ridge	16		25.4	76.2	dry	22	3.0	1.00E-05		ASTM D-2938-86	LLNL	6.9	Uniaxial compressive strength	MO0311RCKPRPCS.003, MO0402DQRIRPPR.003	radiated
236	236	0		0	236.0	26.4		TSw2	Tptpmn	Fran Ridge	Fran Ridge	22		25.4	76.2	dry	22	3.0	1.00E-05		ASTM D-2938-86	LLNL	9.6	Uniaxial compressive strength	MO0311RCKPRPCS.003, MO0402DQRIRPPR.003	radiated
213	213	0		0	213.0	26.6		TSw2	Tptpmn	Fran Ridge	Fran Ridge	32		25.4	76.2	dry	22	3.0	1.00E-05		ASTM D-2938-86	LLNL	8.9	Uniaxial compressive strength	MO0311RCKPRPCS.003, MO0402DQRIRPPR.003	radiated
201.6	201.6	0		0	201.6	26.7		TSw2	Tptpmn	Fran Ridge	Fran Ridge	14		25.4	76.2	dry	22	3.0	1.00E-05		ASTM D-2938-86	LLNL	8.7	Uniaxial compressive strength	MO0311RCKPRPCS.003, MO0402DQRIRPPR.003	non-radiated
204	204	0		0	204.0	26.8		TSw2	Tptpmn	Fran Ridge	Fran Ridge	6		25.4	76.2	dry	22	3.0	1.00E-05		ASTM D-2938-86	LLNL	7.9	Uniaxial compressive strength	MO0311RCKPRPCS.003, MO0402DQRIRPPR.003	radiated
158.3	158.3	0		0	158.3	27.1		TSw2	Tptpmn	Fran Ridge	Fran Ridge	20		25.4	76.2	dry	22	3.0	1.00E-05		ASTM D-2938-86	LLNL	7.3	Uniaxial compressive strength	MO0311RCKPRPCS.003, MO0402DQRIRPPR.003	non-radiated
221.2	221.2	0		0	221.2	27.1		TSw2	Tptpmn	Fran Ridge	Fran Ridge	8		25.4	76.2	dry	22	3.0	1.00E-05		ASTM D-2938-86	LLNL	8.9	Uniaxial compressive strength	MO0311RCKPRPCS.003, MO0402DQRIRPPR.003	radiated
205.8	205.8	0		0	205.8	27.3		TSw2	Tptpmn	Fran Ridge	Fran Ridge	15		25.4	76.2	dry	22	3.0	1.00E-05		ASTM D-2938-86	LLNL	8.6	Uniaxial compressive strength	MO0311RCKPRPCS.003, MO0402DQRIRPPR.003	radiated
192.6	192.6	0		0	192.6	27.5		TSw2	Tptpmn	Fran Ridge	Fran Ridge	11		25.4	76.2	dry	22	3.0	1.00E-05		ASTM D-2938-86	LLNL	7.8	Uniaxial compressive strength	MO0311RCKPRPCS.003, MO0402DQRIRPPR.003	non-radiated
174.1	174.1	0		0	174.1	27.7		TSw2	Tptpmn	Fran Ridge	Fran Ridge	44		25.4	76.2	dry	22	3.0	1.00E-05		ASTM D-2938-86	LLNL	7.8	Uniaxial compressive strength	MO0311RCKPRPCS.003, MO0402DQRIRPPR.003	non-radiated
191.1	191.1	0		0	191.1	27.8		TSw2	Tptpmn	Fran Ridge	Fran Ridge	7		25.4	76.2	dry	22	3.0	1.00E-05		ASTM D-2938-86	LLNL	7.0	Uniaxial compressive strength	MO0311RCKPRPCS.003, MO0402DQRIRPPR.003	non-radiated
138	138	0		0	138	40.4	0.22	TSw2	Tptpmn	ESF/ECRB/Borehole	UE-25 a #1	723	723.0	56	L:D = 2:1	ambient	22	2.0	1.00E-04			SNL		Uniaxial compressive strength	MO0311RCKPRPCS.003, MO0402DQRIRPPR.003	
38.4	38.4	0		0	38.4	13.4	0.3	TSw2	Tptpmn	ESF/ECRB/Borehole	UE-25 NRG #5	NRG-5-873.4-SNL-A	873.4	50.8	101.6	saturated	22	2.0	1.00E-05		ASTM D-3148 and ISRM U	NBR	4.64	Uniaxial compressive strength	MO0311RCKPRPCS.003, MO0402DQRIRPPR.003	
55.3	55.3	0		0	55.3	17.1	0.23	TSw2	Tptpmn	ESF/ECRB/Borehole	UE-25 NRG #5	NRG-5-861.2-SNL-A	861.2	50.8	101.6	saturated	22	2.0	1.00E-05		ASTM D-3148 and ISRM U	NBR	3.38	Uniaxial compressive strength	MO0311RCKPRPCS.003, MO0402DQRIRPPR.003	
84.2	84.2	0		0	84.2	35.2	0.21	TSw2	Tptpmn	ESF/ECRB/Borehole	UE-25 NRG #5	NRG-5-847.2-SNL-A	847.2	50.8	101.6	saturated	22	2.0	1.00E-05		ASTM D-3148 and ISRM U	NBR	2.58	Uniaxial compressive strength	MO0311RCKPRPCS.003, MO0402DQRIRPPR.003	
240.8	240.8	0		0	240.8	37	0.19	TSw2	Tptpmn	ESF/ECRB/Borehole	UE-25 NRG #5	NRG-5-849.4-SNL-A	849.4	50.8	101.6	saturated	22	2.0	1.00E-05		ASTM D-3148 and ISRM U	NBR	7.46	Uniaxial compressive strength	MO0311RCKPRPCS.003, MO0402DQRIRPPR.003	
253.5	253.5	0		0	253.5	38.3	0.15	TSw2	Tptpmn	ESF/ECRB/Borehole	UE-25 NRG #5	NRG-5-891.9-SNL-A	891.9	50.8	101.6	saturated	22	2.0	1.00E-05		ASTM D-3148 and ISRM U	NBR	7.30	Uniaxial compressive strength	MO0311RCKPRPCS.003, MO0402DQRIRPPR.003	
184.7	184.7	0		0	184.7	39.1	0.1	TSw2	Tptpmn	ESF/ECRB/Borehole	UE-25 NRG #5	NRG-5-896.5-SNL-A	896.5	50.8	101.6	saturated	22	2.0	1.00E-05		ASTM D-3148 and ISRM U	NBR	N/A	Uniaxial compressive strength	MO0311RCKPRPCS.003, MO0402DQRIRPPR.003	
288.9	288.9	0		0	288.9	39.4	0.19	TSw2	Tptpmn	ESF/ECRB/Borehole	UE-25 NRG #5	NRG-5-888.8-SNL-A	888.8	50.8	101.6	saturated	22	2.0	1.00E-05		ASTM D-3148 and ISRM U	NBR	8.11	Uniaxial compressive strength	MO0311RCKPRPCS.003, MO0402DQRIRPPR.003	
240.9	240.9	0		0	240.9	40.5	0.2	TSw2	Tptpmn	ESF/ECRB/Borehole	UE-25 NRG #5	NRG-5-887.2-SNL-A	887.2	50.8	101.6	saturated	22	2.0	1.00E-05		ASTM D-3148 and ISRM U	NBR	6.37	Uniaxial compressive strength	MO0311RCKPRPCS.003, MO0402DQRIRPPR.003	
183.5	183.5	0		0	183.5	28.1	0.16	TSw2	Tptpmn	ESF/ECRB/Borehole	USW GU-3	GU-3 760.9/4B	760.9	25.37	50.90	saturated	22	2.0	1.00E-05	0		SNL	7.24	Uniaxial compressive strength	MO0311RCKPRPCS.003, MO0402DQRIRPPR.003	
234.4	234.4	0		0	234.4	28.6	0.29	TSw2	Tptpmn	ESF/ECRB/Borehole	USW GU-3	GU-3 760.9/1B	760.9	25.35	50.90	saturated	22	2.0	1.00E-05	90		SNL	8.48	Uniaxial compressive strength	MO0311RCKPRPCS.003, MO0402DQRIRPPR.003	
215.5	215.5	0		0	215.5	29	0.22	TSw2	Tptpmn	ESF/ECRB/Borehole	USW GU-3	GU-3 760.9/2A	760.9	25.35	50.90	saturated	22	2.0	1.00E-05	0		SNL	8.01	Uniaxial compressive strength	MO0311RCKPRPCS.003, MO0402DQRIRPPR.003	
205.2	205.2	0		0	205.2	29.3	0.19	TSw2	Tptpmn	ESF/ECRB/Borehole	USW GU-3	GU-3 760.9/4A	760.9	25.37	50.88	saturated	22	2.0	1.00E-05	0		SNL	7.54	Uniaxial compressive strength	MO0311RCKPRPCS.003, MO0402DQRIRPPR.003	
226.4	226.4	0		0	226.4	30	0.21	TSw2	Tptpmn	ESF/ECRB/Borehole	USW GU-3	GU-3 760.9/5B	760.9	25.35	50.88	saturated	22	2.0	1.00E-05	90		SNL	8.41	Uniaxial compressive strength	MO0311RCKPRPCS.003, MO0402DQRIRPPR.003	
210.3	210.3	0		0	210.3	30.2	0.19	TSw2	Tptpmn	ESF/ECRB/Borehole	USW GU-3	GU-3 760.9/1A	760.9	25.35	50.90	saturated	22	2.0	1.00E-05	90		SNL	7.76	Uniaxial compressive strength	MO0311RCKPRPCS.003, MO0402DQRIRPPR.003	
221.4	221.4	0		0	221.4	30.2	0.22	TSw2	Tptpmn	ESF/ECRB/Borehole	USW GU-3	GU-3 760.9/2B	760.9	25.37	50.88	saturated	22	2.0	1.00E-05	0		SNL	8.04	Uniaxial compressive strength	MO0311RCKPRPCS.003, MO0402DQRIRPPR.003	
245.2	245.2	0		0	245.2	30.6	0.23	TSw2	Tptpmn	ESF/ECRB/Borehole	USW GU-3	GU-3 760.9/3A	760.9	25.35	50.83	saturated	22	2.0	1.00E-05	90		SNL	9.19	Uniaxial compressive strength	MO0311RCKPRPCS.003, MO0402DQRIRPPR.003	
229.7	229.7	0		0	229.7	30.7	0.22	TSw2	Tptpmn	ESF/ECRB/Borehole	USW GU-3	GU-3 760.9/5A	760.9	25.35	50.85	saturated	22	2.0	1.00E-05	90		SNL	8.57	Uniaxial compressive strength	MO0311RCKPRPCS.003, MO0402DQRIRPPR.003	
222.2	222.2	0		0	222.2	30.8	0.21	TSw2	Tptpmn	ESF/ECRB/Borehole	USW GU-3	GU-3 760.9/3B	760.9	25.37	50.88	saturated	22	2.0	1.00E-05	90		SNL	8.05	Uniaxial compressive strength	MO0311RCKPRPCS.003, MO0402DQRIRPPR.003	
112.1	112.1	0		0	112.1	29.2	0.18	TSw2	Tptpmn	ESF/ECRB/Borehole	USW NRG-6	NRG-6-762.9-SNL-A	762.9	50.80	101.60	saturated	22	2.0	1.00E-05		ASTM D-3148 and ISRM U	NER	4.85	Uniaxial compressive strength	MO0311RCKPRPCS.003, MO0402DQRIRPPR.003	
223	223	0		0	223.0	29.7	0.17	TSw2	Tptpmn	ESF/ECRB/Borehole	USW NRG-6	NRG-6-784.8-SNL-A	784.8	50.80	101.60	saturated	22	2.0	1.00E-05		ASTM D-3148 and ISRM U	NER	9.46	Uniaxial compressive strength	MO0311RCKPRPCS.003, MO0402DQRIRPPR.003	
218.6	218.6	0		0	218.6	30.1	0.16	TSw2	Tptpmn	ESF/ECRB/Borehole	USW NRG-6	NRG-6-785.6-SNL-A	785.6	50.80	101.60	saturated	22	2.0	1.00E-05		ASTM D-3148 and ISRM U	NER	7.94	Uniaxial compressive strength	MO0311RCKPRPCS.003, MO0402DQRIRPPR.003	
162.3	162.3	0		0	162.3	30.6	0.2	TSw2	Tptpmn	ESF/ECRB/Borehole	USW NRG-6	NRG-6-742.3-SNL-A	742.3	50.80	101.60	saturated	22	2.0	1.00E-05		ASTM D-3148 and ISRM U	NER	7.03	Uniaxial compressive strength	MO0311RCKPRPCS.003, MO0402DQRIRPPR.003	
261.9	261.9	0		0	261.9	31.7	0.16	TSw2	Tptpmn	ESF/ECRB/Borehole	USW NRG-6	NRG-6-806.8-SNL-A	806.8	50.80	101.60	saturated	22	2.0	1.00E-05		ASTM D-3148 and ISRM U	NER	8.05	Uniaxial compressive strength	MO0311RCKPRPCS.003, MO0402DQRIRPPR.003	

Table A-1 Intact Rock Mechanical Properties Data - Strength and Elastic Properties Data

Axial Stress, σ_1 (MPa)	Axial Stress, effective σ_1' (MPa)	Confining Pressure (MPa) σ_3	Pore Pressure (MPa)	Confining Pressure, Effective (MPa), σ_3'	Differential Strength, (MPa) $\sigma_1 - \sigma_3$	Young's Modulus (GPa)	Poisson's Ratio	TM Unit	Litho-stratigraphic Unit	General Location	Sample Location	Specimen Number	Depth (ft)	Specimen Diameter (mm)	Specimen Length (mm)	Specimen Saturation	Specimen Temperature (deg. C)	l/d Ratio	Strain Rate (1/s)	Specimen Orientation (degree)	Test Standard	Laboratory	Failure Strain (millistrain)	Rock Property	Source DTN	Notes
212.8	212.8	0		0	212.8	32.4	0.22	TSw2	Tptpmn	ESF/ECRB/Borehole	USW NRG-6	NRG-6-742.9-SNL-A	742.9	50.80	101.60	saturated	22	2.0	1.00E-05		ASTM D-3148 and ISRM U	NBR	7.37	Uniaxial compressive strength	MO0311RCKPRPCS.003, MO0402DQRIRPPR.003	
117.4	117.4	0		0	117.4	36.2	0.23	TSw2	Tptpmn	ESF/ECRB/Borehole	USW NRG-6	NRG-6-773.5-SNL-A	773.5	50.80	101.60	saturated	22	2.0	1.00E-05		ASTM D-3148 and ISRM U	NBR	2.90	Uniaxial compressive strength	MO0311RCKPRPCS.003, MO0402DQRIRPPR.003	
235.5	235.5	0		0	235.5	37.1	0.19	TSw2	Tptpmn	ESF/ECRB/Borehole	USW NRG-6	NRG-6-720.7-SNL-A	720.7	50.80	101.60	saturated	22	2.0	1.00E-05		ASTM D-3148 and ISRM U	NBR	6.82	Uniaxial compressive strength	MO0311RCKPRPCS.003, MO0402DQRIRPPR.003	
143.8	143.8	0		0	143.8	32.9	0.22	TSw2	Tptpmn	ESF/ECRB/Borehole	USW NRG-7a	NRG-7/7A-777.0-SNL-A	777.0	50.8	101.6	saturated	22	2.0	1.00E-05		ASTM D 3148 & ISRM U	NBR	4.87	Uniaxial compressive strength	MO0311RCKPRPCS.003, MO0402DQRIRPPR.003	
126.3	126.3	0		0	126.3	33.1	0.2	TSw2	Tptpmn	ESF/ECRB/Borehole	USW NRG-7a	NRG-7/7A-818.5-SNL-A	818.5	50.8	101.6	saturated	22	2.0	1.00E-05		ASTM D 3148 & ISRM U	NBR	5.18	Uniaxial compressive strength	MO0311RCKPRPCS.003, MO0402DQRIRPPR.003	
232	232	0		0	232.0	33.5	0.19	TSw2	Tptpmn	ESF/ECRB/Borehole	USW NRG-7a	NRG-7/7A-865.4-SNL-J	865.4	25.4	50.8	saturated	22	2.0	1.00E-05			NER	7.14	Uniaxial compressive strength	MO0311RCKPRPCS.003, MO0402DQRIRPPR.003	
215.8	215.8	0		0	215.8	34.3	0.2	TSw2	Tptpmn	ESF/ECRB/Borehole	USW NRG-7a	NRG-7/7A-865.4-SNL-I	865.4	25.4	50.8	saturated	22	2.0	1.00E-05			NER	6.67	Uniaxial compressive strength	MO0311RCKPRPCS.003, MO0402DQRIRPPR.003	
239.1	239.1	0		0	239.1	34.9	0.22	TSw2	Tptpmn	ESF/ECRB/Borehole	USW NRG-7a	NRG-7/7A-865.4-SNL-K	865.4	25.4	50.8	saturated	22	2.0	1.00E-05			NER	7.15	Uniaxial compressive strength	MO0311RCKPRPCS.003, MO0402DQRIRPPR.003	
248.5	248.5	0		0	248.5	35.7	0.21	TSw2	Tptpmn	ESF/ECRB/Borehole	USW NRG-7a	NRG-7/7A-865.4-SNL-L	865.4	25.4	50.8	saturated	22	2.0	1.00E-05			NBR	7.52	Uniaxial compressive strength	MO0311RCKPRPCS.003, MO0402DQRIRPPR.003	
225.4	225.4	0		0	225.4	36.7	0.19	TSw2	Tptpmn	ESF/ECRB/Borehole	USW NRG-7a	NRG-7/7A-806.3-SNL-A	806.3	50.8	101.6	saturated	22	2.0	1.00E-05		ASTM D 3148 & ISRM U	NBR	6.02	Uniaxial compressive strength	MO0311RCKPRPCS.003, MO0402DQRIRPPR.003	
118.8	118.8	0		0	118.8	38.8	0.2	TSw2	Tptpmn	ESF/ECRB/Borehole	USW NRG-7a	NRG-7/7A-859.2-SNL-A	859.2	50.8	101.6	saturated	22	2.0	1.00E-05		ASTM D 3148 & ISRM U	NBR	4.09	Uniaxial compressive strength	MO0311RCKPRPCS.003, MO0402DQRIRPPR.003	
193.3	193.3	0		0	193.3	31.9	0.18	TSw2	Tptpmn	ESF/ECRB/Borehole	USW SD-12	SD-12-734.7-SNL-B	734.7	50.8	101.6	saturated	22	2.0	1.00E-05		ISRM T and ASTM D 2664-86	NBR	6.56	Uniaxial compressive strength	MO0311RCKPRPCS.003, MO0402DQRIRPPR.003	
198.2	198.2	0		0	198.2	36.7	0.21	TSw2	Tptpmn	ESF/ECRB/Borehole	USW SD-12	SD-12-781.1-SNL-B	781.1	50.8	101.6	saturated	22	2.0	1.00E-05		ISRM T and ASTM D 2664-86	NBR	6.02	Uniaxial compressive strength	MO0311RCKPRPCS.003, MO0402DQRIRPPR.003	
60.1	60.1	0		0	60.1	16.8	0.19	TSw2	Tptpmn	ESF/ECRB/Borehole	USW SD-9	SD-9-774.6-SNL-B	774.6	50.8	101.6	saturated	22	2.0	1.00E-05		ISRM T and ASTM D 2664-86	NBR	5.36	Uniaxial compressive strength	MO0311RCKPRPCS.003, MO0402DQRIRPPR.003	only uniaxial tested to date
183.3	183.3	0		0	183.3	29.8	0.19	TSw2	Tptpmn	ESF/ECRB/Borehole	USW SD-9	SD-9-832.8-SNL-C	832.8	50.8	101.6	saturated	22	2.0	1.00E-05		ISRM T and ASTM D 2664-86	NBR	8.72	Uniaxial compressive strength	MO0311RCKPRPCS.003, MO0402DQRIRPPR.003	only uniaxial tested to date
224.9	224.9	0		0	224.9	31.9	0.21	TSw2	Tptpmn	ESF/ECRB/Borehole	USW SD-9	SD-9-826.7-SNL-A	826.7	50.8	101.6	saturated	22	2.0	1.00E-05		ISRM T and ASTM D 2664-86	NBR	7.02	Uniaxial compressive strength	MO0311RCKPRPCS.003, MO0402DQRIRPPR.003	only uniaxial tested to date
231.5	231.5	0		0	231.5	33.9	0.21	TSw2	Tptpmn	ESF/ECRB/Borehole	USW SD-9	SD-9-761.5-SNL-A	761.5	50.8	101.6	saturated	22	2.0	1.00E-05		ISRM T and ASTM D 2664-86	NBR	7.93	Uniaxial compressive strength	MO0311RCKPRPCS.003, MO0402DQRIRPPR.003	only uniaxial tested to date
160.8	160.8	0		0	160.8	34.8	0.19	TSw2	Tptpmn	ESF/ECRB/Borehole	USW SD-9	SD-9-771.7-SNL-A	771.7	50.8	101.6	saturated	22	2.0	1.00E-05		ISRM T and ASTM D 2664-86	NBR	5.13	Uniaxial compressive strength	MO0311RCKPRPCS.003, MO0402DQRIRPPR.003	only uniaxial tested to date
208.9	208.9	0		0	208.9	36.3	0.2	TSw2	Tptpmn	ESF/ECRB/Borehole	USW SD-9	SD-9-842.1-SNL-E-1	842.1	50.8	101.6	saturated	22	2.0	1.00E-05		ISRM T and ASTM D 2664-86	NBR	5.66	Uniaxial compressive strength	MO0311RCKPRPCS.003, MO0402DQRIRPPR.003	only uniaxial tested to date
254.5	254.5	0		0	254.5	36.9	0.2	TSw2	Tptpmn	ESF/ECRB/Borehole	USW SD-9	SD-9-768.7-SNL-A	768.7	50.8	101.6	saturated	22	2.0	1.00E-05		ISRM T and ASTM D 2664-86	NBR	7.73	Uniaxial compressive strength	MO0311RCKPRPCS.003, MO0402DQRIRPPR.003	only uniaxial tested to date
159.6	159.6	0		0	159.6	32.4	0.17	TSw2	Tptpmn	ESF/ECRB/Borehole	ESF-GTEC-CS1250	ESF-GTEC-CS1250-04C 0.0'-1.1'-01023710-SNL		145.5	291	ambient	24	2.0	8.00E-06			SNL	5.4	Uniaxial compressive strength	SN0305L0207502.004	
41.8	41.8	0		0	41.8	31.9	0.18	TSw3	Tptpv3	ESF/ECRB/Borehole	USW GU-3	GU-3 1197.5/1	1197.5	57.15	114.38	ambient	22	2.0	1.00E-05	90		SANDIA	1.91	Uniaxial compressive strength	MO0311RCKPRPCS.003, MO0402DQRIRPPR.003	
49.8	49.8	0		0	49.8	36.6		TSw3	Tptpv3	ESF/ECRB/Borehole	USW GU-3	GU-3 1195.1/1	1195.1	57.15	114.43	ambient	22	2.0	1.00E-05	90		SANDIA	2.22	Uniaxial compressive strength	MO0311RCKPRPCS.003, MO0402DQRIRPPR.003	
16.4	16.4	0		0	16.4	25.2	0.39	TSw3	Tptpv3	ESF/ECRB/Borehole	USW SD-12	SD-12-1299.9-SNL-A	1299.9	50.8	101.6	saturated	22	2.0	1.00E-05			NBR	1.18	Uniaxial compressive strength	MO0311RCKPRPCS.003, MO0402DQRIRPPR.003	
1.8	1.8	0		0	1.8	0.7	0.01	UO	Tmr	ESF/ECRB/Borehole	UE-25 NRG #2b	NRG-2B-87.6-SNL-A	87.6	50.8	101.6	saturated	22	2.0	1.00E-05			NBR	3.06	Uniaxial compressive strength	MO0311RCKPRPCS.003, MO0402DQRIRPPR.003	
2.4	2.4	0		0	2.4	0.9	0.02	UO	Tmr	ESF/ECRB/Borehole	UE-25 NRG #2b	NRG-2B-86.9-SNL-A	86.9	50.8	101.6	saturated	22	2.0	1.00E-05			NBR	3.60	Uniaxial compressive strength	MO0311RCKPRPCS.003, MO0402DQRIRPPR.003	
7	7	0		0	7.0	3.7	0.05	UO	Tmr	ESF/ECRB/Borehole	UE-25 NRG #2b	NRG-2B-42.3-SNL-A	42.3	50.8	101.6	saturated	22	2.0	1.00E-05			NBR	2.28	Uniaxial compressive strength	MO0311RCKPRPCS.003, MO0402DQRIRPPR.003	
6.5	6.5	0		0	6.5	4.3	0.02	UO	Tmr	ESF/ECRB/Borehole	UE-25 NRG #2b	NRG-2B-46.1-SNL-A	46.1	50.8	101.6	saturated	22	2.0	1.00E-05			NBR	1.83	Uniaxial compressive strength	MO0311RCKPRPCS.003, MO0402DQRIRPPR.003	
20.3	20.3	0		0	20.3	7.2	0.07	UO	Tmr	ESF/ECRB/Borehole	UE-25 NRG #2b	NRG-2B-2.7-SNL-A	2.7	50.8	101.6	saturated	22	2.0	1.00E-05			NBR	3.38	Uniaxial compressive strength	MO0311RCKPRPCS.003, MO0402DQRIRPPR.003	
1.1	1.1	0		0	1.1	0.7	0.48	UO	Tpki	ESF/ECRB/Borehole	UE-25 NRG #2a	NRG-2A-145.3-SNL-A	145.3	50.80	101.60	saturated	22	2.0	1.00E-05			NBR	2.67	Uniaxial compressive strength	MO0311RCKPRPCS.003, MO0402DQRIRPPR.003	
4.1	4.1	0		0	4.1	3.1	0.05	UO	Tpki	ESF/ECRB/Borehole	UE-25 NRG #2a	NRG-2A-90.0-SNL-A	90.0	50.80	101.60	saturated	22	2.0	1.00E-05			NBR	1.54	Uniaxial compressive strength	MO0311RCKPRPCS.003, MO0402DQRIRPPR.003	
6.5	6.5	0		0	6.5	3.7	0.20	UO	Tpki	ESF/ECRB/Borehole	UE-25 NRG #2a	NRG-2A-127.0-SNL-A	127.0	50.80	101.60	saturated	22	2.0	1.00E-05			NBR	2.26	Uniaxial compressive strength	MO0311RCKPRPCS.003, MO0402DQRIRPPR.003	
6.7	6.7	0		0	6.7	4	0.12	UO	Tpki	ESF/ECRB/Borehole	UE-25 NRG #2a	NRG-2A-98.4-SNL-A	98.4	50.80	101.60	saturated	22	2.0	1.00E-05			NBR	2.51	Uniaxial compressive strength	MO0311RCKPRPCS.003, MO0402DQRIRPPR.003	
7.2	7.2	0		0	7.2	4.9	0.14	UO	Tpki	ESF/ECRB/Borehole	UE-25 NRG #2a	NRG-2A-105.6-SNL-A	105.6	50.80	101.60	saturated	22	2.0	1.00E-05			NBR	1.92	Uniaxial compressive strength	MO0311RCKPRPCS.003, MO0402DQRIRPPR.003	
6.2	6.2	0		0	6.2	4.9	0.17	UO	Tpki	ESF/ECRB/Borehole	UE-25 NRG #2a	NRG-2A-96.0-SNL-A	96.0	50.80	101.60	saturated	22	2.0	1.00E-05			NBR	1.74	Uniaxial compressive strength	MO0311RCKPRPCS.003, MO0402DQRIRPPR.003	
9.8	9.8	0		0	9.8	5.1	0.15	UO	Tpki	ESF/ECRB/Borehole	UE-25 NRG #2a	NRG-2A-136.1-SNL-A	136.1	50.80	101.60	saturated	22	2.0	1.00E-05			NER	2.37	Uniaxial compressive strength	MO0311RCKPRPCS.003, MO0402DQRIRPPR.003	
73	73	0		0	73	21.4				G-Tunnel, Block 1	G-Tunnel, Block 1	208		25.3		saturated	22	2.0	1.00E-02			SANDIA		Uniaxial compressive strength	SNL02030180001.001, MO0402DQRIRPPR.003	
70	70	0		0	70	22.8				G-Tunnel, Block 1	G-Tunnel, Block 1	206		25.3		saturated	22	2.0	1.00E-02			SANDIA		Uniaxial compressive strength	SNL02030180001.001, MO0402DQRIRPPR.003	
114	114	0		0	114	22.8				G-Tunnel, Block 1	G-Tunnel, Block 1	211		25.3		saturated	22	2.0	1.00E-02			SANDIA		Uniaxial compressive strength	SNL02030180001.001, MO0402DQRIRPPR.003	
118	118	0		0	118	23.8				G-Tunnel, Block 1	G-Tunnel, Block 1	210		25.3		saturated	22	2.0	1.00E-02			SANDIA		Uniaxial compressive strength	SNL02030180001.001, MO0402DQRIRPPR.003	
102	102	0		0	102	24				G-Tunnel, Block 1	G-Tunnel, Block 1	202		25.3		saturated	22	2.0	1.00E-04			SANDIA		Uniaxial compressive strength	SNL02030180001.001, MO0402DQRIRPPR.003	
112	112	0		0	112	24.8				G-Tunnel, Block 1	G-Tunnel, Block 1	200		25.3		saturated	22	2.0	1.00E-04			SANDIA		Uniaxial compressive strength	SNL02030180001.001, MO0402DQRIRPPR.003	
122	122	0		0	122	25.3				G-Tunnel, Block 1	G-Tunnel, Block 1	201		25.3		saturated	22	2.0	1.00E-04			SANDIA		Uniaxial compressive strength	SNL02030180001.001, MO0402DQRIRPPR.003	
110	110	0		0	110	25.4				G-Tunnel, Block 1	G-Tunnel, Block 1	207		25.3		saturated	22	2.0	1.00E-06			SANDIA		Uniaxial compressive strength	SNL02030180001.001, MO0402DQRIRPPR.003	
175	175	0		0	175	25.9				G-Tunnel, Block 1	G-Tunnel, Block 1	105		25.3		dry	22	2.0	1.00E-02			SANDIA		Uniaxial compressive strength	SNL02030180001.001, MO0402DQRIRPPR.003	
81.1	81.1	0		0	81.1	25.9				G-Tunnel, Block 1	G-Tunnel, Block 1	204		25.3		saturated	22	2.0	1.00E-06			SANDIA		Uniaxial compressive strength	SNL02030180001.001, MO0402DQRIRPPR.003	
142	142	0		0	142	26.1				G-Tunnel, Block 1	G-Tunnel, Block 1	205		25.3		saturated	22	2.0	1.00E-02			SANDIA		Uniaxial compressive strength	SNL02030180001.001, MO0402DQRIRPPR.003	
160	160	0		0	160	26.2				G-Tunnel, Block 1	G-Tunnel, Block 1	100		25.3		dry	22	2.0	1.00E-04			SANDIA		Uniaxial compressive strength	SNL02030180001.001, MO0402DQRIRPPR.003	
91.8	91.8	0		0	92	26.8				G-Tunnel, Block 1	G-Tunnel, Block 1	212		25.3		saturated	22	2.0	1.00E-06			SANDIA		Uniaxial compressive strength	SNL02030180001.001, MO0402DQRIRPPR.003	
135	135	0		0	135	27.4				G-Tunnel, Block 1	G-Tunnel, Block 1	106		25.3		dry	22	2.0	1.00E-06			SANDIA		Uniaxial compressive strength	SNL02030180001.001, MO0402DQRIRPPR.003	
160	160	0		0	160	27.4				G-Tunnel, Block 1	G-Tunnel, Block 1	102		25.3		dry	22	2.0	1.00E-04			SANDIA		Uniaxial compressive strength	SNL02030180001.001, MO0402DQRIRPPR.003	
141	141	0		0	141	28.3				G-Tunnel, Block 1	G-Tunnel, Block 1	107		25.3		dry	22	2.0	1.00E-06			SANDIA		Uniaxial compressive strength	SNL02030180001.001, MO0402DQRIRPPR.003	
177	177	0		0	177	28.4				G-Tunnel, Block 1	G-Tunnel, Block 1	110		25.3		dry	22	2.0	1.00E-02			SANDIA		Uniaxial compressive strength	SNL02030180001.001, MO0402DQRIRPPR.003	
155	155	0		0	155	28.5				G-Tunnel, Block 1	G-Tunnel, Block 1	101		25.3		dry	22	2.0	1.00E-04			SANDIA		Uniaxial compressive strength	SNL02030180001.001, MO0402DQRIRPPR.003	
189	189	0		0	189	28.7				G-Tunnel, Block 1	G-Tunnel, Block 1	108		25.3		dry	22	2.0	1.00E-02			SANDIA		Uniaxial compressive strength	SNL02030180001.001, MO0402DQRIRPPR.003	
133.9	133.9	0		0	133.9	29.5				G-Tunnel, Block 1	G-Tunnel, Block 1	109		25.3		dry	22	2.0	1.00E-06			SANDIA		Uniaxial compressive strength	SNL02030180001.001, MO0402DQRIRPPR.003	
72	72	0.1		0.1	71.9	18.4	0.14	CFUn	Tcbbt	ESF/ECRB/Borehole	USW G-1	G126085B	2608.0	25.3	49.4-60.1	saturated	23	2.0	1.00E-05			SANDIA	4.5	Uniaxial compressive strength	MO0311RCKPRPCS.003, MO0402DQRIRPPR.003	

Table A-1 Intact Rock Mechanical Properties Data - Strength and Elastic Properties Data

Axial Stress, σ_1 (MPa)	Axial Stress, effective σ_1' (MPa)	Confining Pressure (MPa) σ_3	Pore Pressure (MPa)	Confining Pressure, Effective (MPa), σ_3'	Differential Strength, (MPa) $\sigma_1 - \sigma_3$	Young's Modulus (GPa)	Poisson's Ratio	TM Unit	Litho-stratigraphic Unit	General Location	Sample Location	Specimen Number	Depth (ft)	Specimen Diameter (mm)	Specimen Length (mm)	Specimen Saturation	Specimen Temperature (deg. C)	l/d Ratio	Strain Rate (1/s)	Specimen Orientation (degree)	Test Standard	Laboratory	Failure Strain (millistrain)	Rock Property	Source DTN	Notes
73.6	73.6	0.1		0.1	73.5	19.4	0.13	CFUn	Tcbbt	ESF/ECRB/Borehole	USW G-1	G126085D	2608.0	25.3	49.4-60.1	saturated	23	2.0	1.00E-05			SANDIA	4.7	Uniaxial compressive strength	MO0311RCKPRPCS.003, MO0402DQRIRPPR.003	
71.8	71.8	0.1		0.1	71.7	15.2	0.08	CFUn	Tcblv	ESF/ECRB/Borehole	USW G-1	G12585SB	2585.0	25.3	49.4-60.1	saturated	23	2.0	1.00E-05			SANDIA	5.1	Uniaxial compressive strength	MO0311RCKPRPCS.003, MO0402DQRIRPPR.003	
83.8	83.8	0.1		0.1	83.7	15.7	0.12	CFUn	Tcblv	ESF/ECRB/Borehole	USW G-1	G12585SD	2585.0	25.3	49.4-60.1	saturated	23	2.0	1.00E-05			SANDIA	5.8	Uniaxial compressive strength	MO0311RCKPRPCS.003, MO0402DQRIRPPR.003	
120.1	120.1	0.1		0.1	120	21.9	0.14	CFUn	Tcblv	ESF/ECRB/Borehole	USW G-1	G12563SB	2563.0	25.3	49.4-60.1	saturated	23	2.0	1.00E-05			SANDIA	5.8	Uniaxial compressive strength	MO0311RCKPRPCS.003, MO0402DQRIRPPR.003	
153.1	153.1	0.1		0.1	153	28.9	0.14	CFUn	Tcblv	ESF/ECRB/Borehole	USW G-1	G12563SD	2563.0	25.3	49.4-60.1	saturated	23	2.0	1.00E-05			SANDIA	5.4	Uniaxial compressive strength	MO0311RCKPRPCS.003, MO0402DQRIRPPR.003	
36.7	36.7	0.1		0.1	36.6			CFUn	Tcbm	ESF/ECRB/Borehole	USW G-1	G124689B	2468.0	25.3	49.4-60.1	saturated	23	2.0	1.00E-05			SNL		Uniaxial compressive strength	MO0311RCKPRPCS.003	Specimin length reported as 49.4- 60.1. 49.4 was used because it gives a LD ratio doser 2:1
46.4	46.4	0.1		0.1	46.3	12.6	0.14	CFUn	Tcbm	ESF/ECRB/Borehole	USW G-1	G12468SD	2468.0	25.3	49.4-60.1	saturated	23	2.0	1.00E-05			SNL	5.6	Uniaxial compressive strength	MO0311RCKPRPCS.003, MO0402DQRIRPPR.003	Specimin length reported as 49.4- 60.1. 49.4 was used because it gives a LD ratio doser 2:1
16.7	16.7	0.1		0.1	16.6	3.93	0.16	CFUn	Tcbuc	ESF/ECRB/Borehole	USW G-1	G12429SD	2429.0	25.3	49.4-60.1	saturated	23	2.0	1.00E-05			SANDIA	5.0	Uniaxial compressive strength	MO0311RCKPRPCS.003, MO0402DQRIRPPR.003	
29.1	29.1	0.1		0.1	29	8.01	0.16	CFUn	Tcbuc	ESF/ECRB/Borehole	USW G-1	G12429SF	2429.0	25.3	49.4-60.1	saturated	23	2.0	1.00E-05			SANDIA	5.2	Uniaxial compressive strength	MO0311RCKPRPCS.003, MO0402DQRIRPPR.003	
29.3	29.3	0.1		0.1	29.2	8.38	0.14	CFUn	Tcbuc	ESF/ECRB/Borehole	USW G-1	G12367SD	2367.0	25.3	49.4-60.1	saturated	23	2.0	1.00E-05			SANDIA	5.0	Uniaxial compressive strength	MO0311RCKPRPCS.003, MO0402DQRIRPPR.003	
30.7	30.7	0.1		0.1	30.6	8.71	0.11	CFUn	Tcbuc	ESF/ECRB/Borehole	USW G-1	G12429SB	2429.0	25.3	49.4-60.1	saturated	23	2.0	1.00E-05			SANDIA	5.5	Uniaxial compressive strength	MO0311RCKPRPCS.003, MO0402DQRIRPPR.003	
4.73	4.73	0.1		0.1	4.63	2.03		CFUn	Tcbuv	ESF/ECRB/Borehole	USW G-1	G12276SF	2276.0	25.3	49.4-60.1	saturated	23	2.0	1.00E-05			SANDIA	3.4	Uniaxial compressive strength	MO0311RCKPRPCS.003, MO0402DQRIRPPR.003	
19.4	19.4	0.1		0.1	19.3	5.34	0.12	CFUn	Tcbuv	ESF/ECRB/Borehole	USW G-1	G12232SB	2232.0	25.3	49.4-60.1	saturated	23	2.0	1.00E-05			SANDIA	4.5	Uniaxial compressive strength	MO0311RCKPRPCS.003, MO0402DQRIRPPR.003	
26.8	26.8	0.1		0.1	26.7	10.3	0.12	CFUn	Tcbuv	ESF/ECRB/Borehole	USW G-1	G12276SD	2276.0	25.3	49.4-60.1	saturated	23	2.0	1.00E-05			SANDIA	2.8	Uniaxial compressive strength	MO0311RCKPRPCS.003, MO0402DQRIRPPR.003	
41.7	41.7	0.1		0.1	41.6	15.8	0.11	CFUn	Tcbuv	ESF/ECRB/Borehole	USW G-1	G12312SD	2312.0	25.3	49.4-60.1	saturated	23	2.0	1.00E-05			SANDIA	3.4	Uniaxial compressive strength	MO0311RCKPRPCS.003, MO0402DQRIRPPR.003	
27.5	27.5	0.1		0.1	27.4	9.39		CFUn	Tqpbt	ESF/ECRB/Borehole	USW G-1	G12170SB	2170.0	25.3	49.4-60.1	saturated	23	2.0	1.00E-05			SANDIA	4.4	Uniaxial compressive strength	MO0311RCKPRPCS.003, MO0402DQRIRPPR.003	
47.2	47.2	0.1		0.1	47.1	11.5	0.11	CFUn	Tqpbt	ESF/ECRB/Borehole	USW G-1	G12170SD	2170.0	25.3	49.4-60.1	saturated	23	2.0	1.00E-05			SANDIA	4.9	Uniaxial compressive strength	MO0311RCKPRPCS.003, MO0402DQRIRPPR.003	
50.3	50.3	0.1		0.1	50.2	10.4	0.14	CFUn	Tcbuv	ESF/ECRB/Borehole	USW G-1	G12641SD	2641.0	25.3	49.4-60.1	saturated	23	2.0	1.00E-05			Terra Tek	5.7	Uniaxial compressive strength	MO0311RCKPRPCS.003, MO0402DQRIRPPR.003	
27.5	27.5	0.1	0	0.1	27.4			CHn	Tac	ESF/ECRB/Borehole	USW G-1	G11487.4 SL1	1487.4	25.4	50.0-51.3	saturated	22	2.0	1.00E-05			SNL		Uniaxial compressive strength	MO0311RCKPRPCS.003	Specimin length: 50.0 to 51.3, Specimin diameter: 25.4 to 25.5.Drained test.
14.3	14.3	0.1	0	0.1	14.2	3.51		CHn	Tac	ESF/ECRB/Borehole	USW G-1	G11594.8 SL13	1594.8	25.4	50.0-51.3	saturated	22	2.0	1.00E-05			SANDIA	4.1	Uniaxial compressive strength	MO0311RCKPRPCS.003, MO0402DQRIRPPR.003	Specimin length: 50.0 to 51.3, Specimin diameter: 25.4 to 25.5.Drained test.
15.4	15.4	0.1	0	0.1	15.3	4.23	0.19	CHn	Tac	ESF/ECRB/Borehole	USW G-1	G11594.8 SL14	1594.8	25.4	50.0-51.3	saturated	22	2.0	1.00E-05			SANDIA	4.2	Uniaxial compressive strength	MO0311RCKPRPCS.003, MO0402DQRIRPPR.003	Specimin length: 50.0 to 51.3, Specimin diameter: 25.4 to 25.5.Drained test.
23	23	0.1	0	0.1	22.9	4.87		CHn	Tac	ESF/ECRB/Borehole	USW G-1	G11487.4 SL2	1487.4	25.4	50.0-51.3	saturated	22	2.0	1.00E-05			SANDIA	5.8	Uniaxial compressive strength	MO0311RCKPRPCS.003, MO0402DQRIRPPR.003	Specimin length: 50.0 to 51.3, Specimin diameter: 25.4 to 25.5.Drained test.
16.8	16.8	0.1	0	0.1	16.7	4.92	0.18	CHn	Tac	ESF/ECRB/Borehole	USW G-1	G11668.1 SL25F	1668.1	25.4	50.0-51.3	saturated	22	2.0	1.00E-05			SANDIA	4.3	Uniaxial compressive strength	MO0311RCKPRPCS.003, MO0402DQRIRPPR.003	Specimin length: 50.0 to 51.3, Specimin diameter: 25.4 to 25.5.Drained test.
19	19	0.1	0	0.1	18.9	4.93		CHn	Tac	ESF/ECRB/Borehole	USW G-1	G11519.9 SL32	1519.9	25.4	50.0-51.3	saturated	22	2.0	1.00E-05			SANDIA	7.6	Uniaxial compressive strength	MO0311RCKPRPCS.003, MO0402DQRIRPPR.003	Specimin length: 50.0 to 51.3, Specimin diameter: 25.4 to 25.5.Drained test.
20.8	20.8	0.1	0	0.1	20.7	5.14		CHn	Tac	ESF/ECRB/Borehole	USW G-1	G11519.9 SL33	1519.9	25.4	50.0-51.3	saturated	22	2.0	1.00E-05			SANDIA	5.4	Uniaxial compressive strength	MO0311RCKPRPCS.003, MO0402DQRIRPPR.003	Specimin length: 50.0 to 51.3, Specimin diameter: 25.4 to 25.5.Drained test.
24.8	24.8	0.1	0	0.1	24.7	5.41	0.33	CHn	Tac	ESF/ECRB/Borehole	USW G-1	G1166 8.1 SL23A	1668.1	25.4	50.0-51.3	saturated	22	2.0	1.00E-03			SANDIA	6.1	Uniaxial compressive strength	MO0311RCKPRPCS.003, MO0402DQRIRPPR.003	Specimin length: 50.0 to 51.3, Specimin diameter: 25.4 to 25.5.Drained test.
23.5	23.5	0.1	0	0.1	23.4	5.45		CHn	Tac	ESF/ECRB/Borehole	USW G-1	G116 68.1 SL23B	1668.1	25.4	50.0-51.3	saturated	22	2.0	1.00E-03			SANDIA	5.8	Uniaxial compressive strength	MO0311RCKPRPCS.003, MO0402DQRIRPPR.003	Specimin length: 50.0 to 51.3, Specimin diameter: 25.4 to 25.5.Drained test.
22.1	22.1	0.1	0	0.1	22	5.79		CHn	Tac	ESF/ECRB/Borehole	USW G-1	G11442.0 SL31	1442.0	25.4	50.0-51.3	saturated	22	2.0	1.00E-05			SANDIA	4.3	Uniaxial compressive strength	MO0311RCKPRPCS.003, MO0402DQRIRPPR.003	Specimin length: 50.0 to 51.3, Specimin diameter: 25.4 to 25.5.Drained test.
20.2	20.2	0.1	0	0.1	20.1	5.83	0.29	CHn	Tac	ESF/ECRB/Borehole	USW G-1	G11719.7 SL17	1719.7	25.4	50.0-51.3	saturated	22	2.0	1.00E-05			SANDIA	4.3	Uniaxial compressive strength	MO0311RCKPRPCS.003, MO0402DQRIRPPR.003	Specimin length: 50.0 to 51.3, Specimin diameter: 25.4 to 25.5.Drained test.
25.5	25.5	0.1	0	0.1	25.4	6.15	0.36	CHn	Tac	ESF/ECRB/Borehole	USW G-1	G116 68.1 SL 25E	1668.1	25.4	50.0-51.3	saturated	22	2.0	1.00E-05			SANDIA	5.7	Uniaxial compressive strength	MO0311RCKPRPCS.003, MO0402DQRIRPPR.003	Specimin length: 50.0 to 51.3, Specimin diameter: 25.4 to 25.5.Drained test.
21.8	21.8	0.1	0	0.1	21.7	6.4		CHn	Tac	ESF/ECRB/Borehole	USW G-1	G11442.0 SL30	1442.0	25.4	50.0-51.3	saturated	22	2.0	1.00E-05			SANDIA	4.3	Uniaxial compressive strength	MO0311RCKPRPCS.003, MO0402DQRIRPPR.003	Specimin length: 50.0 to 51.3, Specimin diameter: 25.4 to 25.5.Drained test.
32.8	32.8	0.1	0	0.1	32.7	6.5	0.31	CHn	Tac	ESF/ECRB/Borehole	USW G-1	G11665.5 SL11A	1665.5	25.4	50.0-51.3	ambient	22	2.0	1.00E-05			SANDIA	5.4	Uniaxial compressive strength	MO0311RCKPRPCS.003, MO0402DQRIRPPR.003	Specimin length: 50.0 to 51.3, Specimin diameter: 25.4 to 25.5.Drained test.
26.3	26.3	0.1	0	0.1	26.2	6.86	0.18	CHn	Tac	ESF/ECRB/Borehole	USW G-1	G11665.5 SL7	1665.5	25.4	50.0-51.3	saturated	22	2.0	1.00E-05			SANDIA	5	Uniaxial compressive strength	MO0311RCKPRPCS.003, MO0402DQRIRPPR.003	Specimin length: 50.0 to 51.3, Specimin diameter: 25.4 to 25.5.Drained test.
20	20	0.1	0	0.1	19.9	7.03	0.22	CHn	Tac	ESF/ECRB/Borehole	USW G-1	G11668.1 SL26H	1668.1	25.4	50.0-51.3	saturated	22	2.0	1.00E-07			SANDIA	5.1	Uniaxial compressive strength	MO0311RCKPRPCS.003, MO0402DQRIRPPR.003	Specimin length: 50.0 to 51.3, Specimin diameter: 25.4 to 25.5.Drained test.
36	36	0.1	0	0.1	35.9	7.03		CHn	Tac	ESF/ECRB/Borehole	USW G-1	G11550.4 SL28	1550.4	25.4	50.0-51.3	saturated	22	2.0	1.00E-05			SANDIA	6.1	Uniaxial compressive strength	MO0311RCKPRPCS.003, MO0402DQRIRPPR.003	Specimin length: 50.0 to 51.3, Specimin diameter: 25.4 to 25.5.Drained test.
19.5	19.5	0.1	0	0.1	19.4	7.17	0.25	CHn	Tac	ESF/ECRB/Borehole	USW G-1	G11617.0 SL16	1617.0	25.4	50.0-51.3	saturated	22	2.0	1.00E-05			SANDIA	3.7	Uniaxial compressive strength	MO0311RCKPRPCS.003, MO0402DQRIRPPR.003	Specimin length: 50.0 to 51.3, Specimin diameter: 25.4 to 25.5.Drained test.
30.6	30.6	0.1	0	0.1	30.5	7.45		CHn	Tac	ESF/ECRB/Borehole	USW G-1	G11550.4 SL29	1550.4	25.4	50.0-51.3	saturated	22	2.0	1.00E-05			SANDIA	5.4	Uniaxial compressive strength	MO0311RCKPRPCS.003, MO0402DQRIRPPR.003	Specimin length: 50.0 to 51.3, Specimin diameter: 25.4 to 25.5.Drained test.
21.6	21.6	0.1	0	0.1	21.5	7.86	0.21	CHn	Tac	ESF/ECRB/Borehole	USW G-1	G11668.1 SL26G	1668.1	25.4	50.0-51.3	saturated	22	2.0	1.00E-07			SANDIA	5.5	Uniaxial compressive strength	MO0311RCKPRPCS.003, MO0402DQRIRPPR.003	Specimin length: 50.0 to 51.3, Specimin diameter: 25.4 to 25.5.Drained test.
26.6	26.6	0.1	0	0.1	26.5	7.86	0.26	CHn	Tac	ESF/ECRB/Borehole	USW G-1	G11617.0 SL15	1617.0	25.4	50.0-51.3	saturated	22	2.0	1.00E-05			SANDIA	4.3	Uniaxial compressive strength	MO0311RCKPRPCS.003, MO0402DQRIRPPR.003	Specimin length: 50.0 to 51.3, Specimin diameter: 25.4 to 25.5.Drained test.
27.5	27.5	0.1	0	0.1	27.4	7.93	0.30	CHn	Tac	ESF/ECRB/Borehole	USW G-1	G11719.7 SL18	1719.7	25.4	50.0-51.3	saturated	22	2.0	1.00E-05			SANDIA	4.1	Uniaxial compressive strength	MO0311RCKPRPCS.003, MO0402DQRIRPPR.003	Specimin length: 50.0 to 51.3, Specimin diameter: 25.4 to 25.5.Drained test.
41.1	41.1	0.1	0	0.1	41.0	8.12	0.29	CHn	Tac	ESF/ECRB/Borehole	USW G-1	G11665.5 SL11	1665.5	25.4	50.0-51.3	ambient	22	2.0	1.00E-05			SANDIA	5.8	Uniaxial compressive strength	MO0311RCKPRPCS.003, MO0402DQRIRPPR.003	Specimin length: 50.0 to 51.3, Specimin diameter: 25.4 to 25.5.Drained test.
34.2	34.2	0.1	0	0.1	34.1	9.52		CHn	Tac	ESF/ECRB/Borehole	USW G-1	G11665.5 SL8	1665.5	25.4	50.0-51.3	saturated	22	2.0	1.00E-05			SANDIA	4.2	Uniaxial compressive strength	MO0311RCKPRPCS.003, MO0402DQRIRPPR.003	Specimin length: 50.0 to 51.3, Specimin diameter: 25.4 to 25.5.Drained test.
14.9	14.9	0.1	0	0.1	14.8	2.52	0.37	CHn	Tacbt	ESF/ECRB/Borehole	USW G-1	G11784.8 SL20	1784.8	25.4	50.0-51.3	saturated	22	2.0	1.00E-05			SANDIA	7.5	Uniaxial compressive strength	MO0311RCKPRPCS.003, MO0402DQRIRPPR.003	Specimin length: 50.0 to 51.3, Specimin diameter: 25.4 to 25.5.Drained test.
15.5	15.5	0.1	0	0.1	15.4	2.55	0.34	CHn	Tacbt	ESF/ECRB/Borehole	USW G-1	G11784.8 SL19	1784.8	25.4	50.0-51.3	saturated	22	2.0	1.00E-05			SANDIA	7.9	Uniaxial compressive strength	MO0311RCKPRPCS.003, MO0402DQRIRPPR.003	Specimin length: 50.0 to 51.3, Specimin diameter: 25.4 to 25.5.Drained test.
42.1	42.1	0.1	0	0.1	42.0	8.14	0.32	CHn	Tacbt	ESF/ECRB/Borehole	USW G-1	G11741.8 SL22	1741.8	25.4	50.0-51.3	saturated	22	2.0	1.00E-05			SANDIA	7.1	Uniaxial compressive strength	MO0311RCKPRPCS.003, MO0402DQRIRPPR.003	Specimin length: 50.0 to 51.3, Specimin diameter: 25.4 to 25.5.Drained test.
39.2	39.2	0.1	0	0.1	39.1	8.41	0.27	CHn	Tacbt	ESF/ECRB/Borehole	USW G-1	G11741.8 SL21	1741.8	25.4	50.0-51.3	saturated	22	2.0	1.00E-05			SANDIA	8.7	Uniaxial compressive strength	MO0311RCKPRPCS.003, MO0402DQRIRPPR.003	Specimin length: 50.0 to 51.3, Specimin diameter: 25.4 to 25.5.Drained test.
8.1	8.1	0.1		0.1	8	1.41	0.17	CHn	Tptpv1	ESF/ECRB/Borehole	USW G-4	G4-1369.1-D	1369.1	25.27	50.83	saturated	22	2.0	1.00E-07			Terra Tek	5.5	Uniaxial compressive strength	MO0311RCKPRPCS.003, MO0402DQRIRPPR.003	
6.1	6.1	0.1		0.1	6	1.53	0.19	CHn	Tptpv1	ESF/ECRB/Borehole	USW G-4	G4-1369.1-G	1369.1	25.25	50.80	saturated	22	2.0	1.00E-05			Terra Tek	6.5	Uniaxial compressive strength	MO0311RCKPRPCS.003, MO0402DQRIRPPR.003	
8.1	8.1	0.1		0.1	8	1.76	0.16	CHn	Tptpv1	ESF/ECRB/Borehole	USW G-4	G4- 1369.1-B	1369.1	25.27	50.77	saturated	22	2.0	1.00E-03			Terra Tek	6.0	Uniaxial compressive strength	MO0311RCKPRPCS.003, MO0402DQRIRPPR.003	
11.1	11.1	0.1		0.1	11	2.21	0.21	CHn	Tptpv1	ESF/ECRB/Borehole	USW G-4	G4- 1369.1-E	1369.1	25.27	50.80	saturated	22	2.0	1.00E-05			Terra Tek	7.3	Uniaxial compressive strength	MO0311RCKPRPCS.003, MO0402DQRIRPPR.003	
14.1	14.1	0.1		0.1	14	2.25	0.18	CHn	Tptpv1	ESF/ECRB/Borehole	USW G-4	G4-1400.6-H	1400.6	25.32	50.85	saturated	22	2.0	1.00E-05			Terra Tek	6.1	Uniaxial compressive strength	MO0311RCKPRPCS.003, MO0402DQRIRPPR.003	
19.1	19.1	0.1		0.1	19	2.32	0.18	CHn	Tptpv1	ESF/ECRB/Borehole	USW G-4	G4- 1400.6-E	1400.6	25.30	50.83	saturated	22	2.0	1.00E-05			Terra Tek	7.2	Uniaxial compressive strength	MO0311RCKPRPCS.003, MO0402DQRIRPPR.003	
13.1	13.1	0.1		0.1	13	2.96	0.26	CHn	Tptpv1	ESF/ECRB/Borehole	USW G-4	G4- 1369.1-A	1369.1	25.27	50.83	saturated	22	2.0	1.00E-03			Terra Tek	7.0	Uniaxial compressive strength	MO0311RCKPRPCS.003, MO0402DQRIRPPR.003	
12.1	12.1	0.1		0.1	12	3.1	0.17	CHn	Tptpv1	ESF/ECRB/Borehole	USW G-4	G4- 1369.1-H	1369.1	25.27	50.80	saturated	22	2.0	1.00E-07			Terra Tek	6.3	Uniaxial compressive strength	MO0311RCKPRPCS.003, MO0402DQRIRPPR.003	
15.1	15.1	0.1		0.1	15	3.37	0.12	CHn	Tptpv1	ESF/ECRB/Borehole	USW G-4	G4- 1369.1-C	1369.1	25.30	50.77	saturated	22	2.0	1.00E-03			Terra Tek	6.8	Uniaxial compressive strength	MO0311RCKPRPCS.003, MO0402DQRIRPPR.003	
14.1	14.1	0.1		0.1	14	3.7	0.14	CHn	Tptpv1	ESF/ECRB/Borehole	USW G-4	G4-1369.1-F	1369.1	25.30	50.88	saturated	22	2.0	1.00E-05			Terra Tek	6.4	Uniaxial compressive strength	MO0311RCKPRPCS.003, MO0402DQRIRPPR.003	
59.9	59.9	0.1	0	0.1	59.8	24.9	0.15	TSw2	Tptpll	ESF/ECRB/Borehole	USW G-1	G1-1096.0 SL	1096.0	26.1	50.1 to 51.3	saturated	22	2.0	1.00E-05			SNL	3.4	Uniaxial compressive strength	MO0311RCKPRPCS.003, MO0402DQRIRPPR.003	Samples saturated and drained.
75.3	75.3	0.1	0	0.1	75.2	25.5	0.25	TSw2	Tptpll	ESF/ECRB/Borehole	USW G-1	G1-1021.8 SL	1021.8	26.1	50.1 to 51.3	saturated	22	2.0	1.00E-05			SNL	3.8	Uniaxial compressive strength	MO0311RCKPRPCS.003, MO0402DQRIRPPR.003	Samples saturated and drained.

Table A-1 Intact Rock Mechanical Properties Data - Strength and Elastic Properties Data

Axial Stress, σ_1 (MPa)	Axial Stress, effective σ_1' (MPa)	Confining Pressure (MPa) σ_3	Pore Pressure (MPa)	Confining Pressure, Effective (MPa), σ_3'	Differential Strength, (MPa) $\sigma_1 - \sigma_3$	Young's Modulus (GPa)	Poisson's Ratio	TM Unit	Litho-stratigraphic Unit	General Location	Sample Location	Specimen Number	Depth (ft)	Specimen Diameter (mm)	Specimen Length (mm)	Specimen Saturation	Specimen Temperature (deg. C)	l/d Ratio	Strain Rate (1/s)	Specimen Orientation (degree)	Test Standard	Laboratory	Failure Strain (millistrain)	Rock Property	Source DTN	Notes
106.3	106.3	0.1	0	0.1	106.2	32.5	0.33	TSw2	Tptpll	ESF/ECRB/Borehole	USW G-1	G1-1154.9 SLA	1154.9	26.1	50.1 to 51.3	saturated	22	2.0	1.00E-05			SNL	3.7	Uniaxial compressive strength	MO0311RCKPRPCS.003, MO0402DQRIRPPR.003	Samples saturated and drained.
142.9	142.9	0.1	0	0.1	142.8	38.1	0.32	TSw2	Tptpll	ESF/ECRB/Borehole	USW G-1	G1-1060.8 SL	1060.8	26.1	50.1 to 51.3	saturated	22	2.0	1.00E-05			SNL	5.0	Uniaxial compressive strength	MO0311RCKPRPCS.003, MO0402DQRIRPPR.003	Samples saturated and drained.
12.1	12.1	0.1		0.1	12	2.44		TSw2	Tptpll	ESF/ECRB/Borehole	USW G-4	G4-1065.8-A	1065.8	25.30	50.88	saturated	22	2.0	1.00E-05			Terra Tek	18.5	Uniaxial compressive strength	MO0311RCKPRPCS.003, MO0402DQRIRPPR.003	
123.1	123.1	0.1		0.1	123	22	0.11	TSw2	Tptpll	ESF/ECRB/Borehole	USW G-4	G4-1002.4-A	1002.4	25.32	50.88	saturated	22	2.0	1.00E-07			Terra Tek	4.4	Uniaxial compressive strength	MO0311RCKPRPCS.003, MO0402DQRIRPPR.003	
99.1	99.1	0.1		0.1	99	22.8	0.19	TSw2	Tptpll	ESF/ECRB/Borehole	USW G-4	G4-1001.9-A	1001.9	25.32	50.88	saturated	22	2.0	1.00E-05			Terra Tek	5.1	Uniaxial compressive strength	MO0311RCKPRPCS.003, MO0402DQRIRPPR.003	
88.1	88.1	0.1		0.1	88	24.8	0.15	TSw2	Tptpll	ESF/ECRB/Borehole	USW G-4	G4-911.3-B	911.3	25.35	49.91	saturated	22	2.0	1.00E-05			Terra Tek	4.8	Uniaxial compressive strength	MO0311RCKPRPCS.003, MO0402DQRIRPPR.003	
118.1	118.1	0.1		0.1	118	26	0.19	TSw2	Tptpll	ESF/ECRB/Borehole	USW G-4	G4-911.3-C	911.3	25.32	50.85	saturated	22	2.0	1.00E-05			Terra Tek	5.1	Uniaxial compressive strength	MO0311RCKPRPCS.003, MO0402DQRIRPPR.003	
124.1	124.1	0.1		0.1	124	26.7	0.21	TSw2	Tptpll	ESF/ECRB/Borehole	USW G-4	G4-1065.8-C	1065.8	25.35	50.90	saturated	22	2.0	1.00E-05			Terra Tek	4.3	Uniaxial compressive strength	MO0311RCKPRPCS.003, MO0402DQRIRPPR.003	
131.1	131.1	0.1		0.1	131	30.1	0.18	TSw2	Tptpll	ESF/ECRB/Borehole	USW G-4	G4-910.7-A	910.7	25.32	50.88	saturated	22	2.0	1.00E-05			Terra Tek	5.5	Uniaxial compressive strength	MO0311RCKPRPCS.003, MO0402DQRIRPPR.003	
131.1	131.1	0.1		0.1	131	31.1	0.18	TSw2	Tptpll	ESF/ECRB/Borehole	USW G-4	G4-965.2-D	965.2	25.32	50.80	saturated	22	2.0	1.00E-05			Terra Tek	4.4	Uniaxial compressive strength	MO0311RCKPRPCS.003, MO0402DQRIRPPR.003	
137.1	137.1	0.1		0.1	137	31.1		TSw2	Tptpll	ESF/ECRB/Borehole	USW G-4	G4-1002.4-C	1002.4	25.30	50.75	saturated	22	2.0	1.00E-05			SNL	4.5	Uniaxial compressive strength	MO0311RCKPRPCS.003, MO0402DQRIRPPR.003	
147.1	147.1	0.1		0.1	147	31.8	0.18	TSw2	Tptpll	ESF/ECRB/Borehole	USW G-4	G4-1001.9-C	1001.9	25.32	50.80	saturated	22	2.0	1.00E-05			Terra Tek	4.8	Uniaxial compressive strength	MO0311RCKPRPCS.003, MO0402DQRIRPPR.003	
170.1	170.1	0.1		0.1	170	32.7	0.2	TSw2	Tptpll	ESF/ECRB/Borehole	USW G-4	G4-1001.9-B	1001.9	25.32	50.85	saturated	22	2.0	1.00E-05			Terra Tek	N/A	Uniaxial compressive strength	MO0311RCKPRPCS.003, MO0402DQRIRPPR.003	
138.1	138.1	0.1		0.1	138	32.8	0.2	TSw2	Tptpll	ESF/ECRB/Borehole	USW G-4	G4-1002.4-D	1002.4	25.32	50.88	saturated	22	2.0	1.00E-07			Terra Tek	4.5	Uniaxial compressive strength	MO0311RCKPRPCS.003, MO0402DQRIRPPR.003	
148.1	148.1	0.1		0.1	148	33.1	0.19	TSw2	Tptpll	ESF/ECRB/Borehole	USW G-4	G4-965.2-H	965.2	25.32	50.88	saturated	22	2.0	1.00E-05			Terra Tek	6.0	Uniaxial compressive strength	MO0311RCKPRPCS.003, MO0402DQRIRPPR.003	
179.1	179.1	0.1		0.1	179	33.6	0.32	TSw2	Tptpll	ESF/ECRB/Borehole	USW G-4	G4-1002.4-B	1002.4	25.30	50.77	saturated	22	2.0	1.00E-05			SNL	5.6	Uniaxial compressive strength	MO0311RCKPRPCS.003, MO0402DQRIRPPR.003	
160.1	160.1	0.1		0.1	160	37.6	0.36	TSw2	Tptpll	ESF/ECRB/Borehole	USW G-4	G4-911.3-A	911.3	25.30	50.77	saturated	22	2.0	1.00E-05			SNL	4.8	Uniaxial compressive strength	MO0311RCKPRPCS.003, MO0402DQRIRPPR.003	
187.1	187.1	0.1		0.1	187	38	0.21	TSw2	Tptpll	ESF/ECRB/Borehole	USW G-4	G4-965.2-A	965.2	25.32	50.75	saturated	22	2.0	1.00E-05			Terra Tek	5.6	Uniaxial compressive strength	MO0311RCKPRPCS.003, MO0402DQRIRPPR.003	
45	45	0.1	0	0.1	44.9	22.9	0.27	TSw2	Tptpln	ESF/ECRB/Borehole	USW G-1	G1-1279.5 SL	1279.5	26.1	50.1 to 51.3	saturated	22	2.0	1.00E-06			SNL	4.1	Uniaxial compressive strength	MO0311RCKPRPCS.003, MO0402DQRIRPPR.003	Drained test.
133.9	133.9	0.1	0	0.1	133.8	27.7		TSw2	Tptpln	ESF/ECRB/Borehole	USW G-1	G1-1222.1 SLB	1222.1	26.1	50.1 to 51.3	saturated	22	2.0	1.00E-04			SNL	5.7	Uniaxial compressive strength	MO0311RCKPRPCS.003, MO0402DQRIRPPR.003	Drained test.
157.3	157.3	0.1	0	0.1	157.2	29.2	0.31	TSw2	Tptpln	ESF/ECRB/Borehole	USW G-1	G1-1222.1 SLA	1222.1	26.1	50.1 to 51.3	saturated	22	2.0	1.00E-02			SNL	4.8	Uniaxial compressive strength	MO0311RCKPRPCS.003, MO0402DQRIRPPR.003	Drained test.
156.7	156.7	0.1	0	0.1	156.6	35.3	0.21	TSw2	Tptpln	ESF/ECRB/Borehole	USW G-1	G1-1223.7 SLB	1223.7	26.1	50.1 to 51.3	saturated	22	2.0	1.00E-06			SNL	4.7	Uniaxial compressive strength	MO0311RCKPRPCS.003, MO0402DQRIRPPR.003	Drained test.
149.8	149.8	0.1	0	0.1	149.7	36.6		TSw2	Tptpln	ESF/ECRB/Borehole	USW G-1	G1-1262.4 SL	1262.4	26.1	50.1 to 51.3	saturated	22	2.0	1.00E-02			SNL	4.9	Uniaxial compressive strength	MO0311RCKPRPCS.003, MO0402DQRIRPPR.003	Drained test.
157.3	157.3	0.1	0	0.1	157.2	37.5	0.25	TSw2	Tptpln	ESF/ECRB/Borehole	USW G-1	G1-1223.7 SLA	1223.7	26.1	50.1 to 51.3	saturated	22	2.0	1.00E-04			SNL	4.50	Uniaxial compressive strength	MO0311RCKPRPCS.003, MO0402DQRIRPPR.003	Drained test.
176.7	176.7	0.1	0	0.1	176.6	40.8	0.25	TSw2	Tptpln	ESF/ECRB/Borehole	USW G-1	G1-1218.2 SL	1218.2	26.1	50.1 to 51.3	saturated	22	2.0	1.00E-06			SNL	5.1	Uniaxial compressive strength	MO0311RCKPRPCS.003, MO0402DQRIRPPR.003	Drained test.
65.1	65.1	0.1		0.1	65	16.6	0.24	TSw2	Tptpln	ESF/ECRB/Borehole	USW G-4	G4-1307.2-E	1307.2	25.27	50.72	saturated	22	2.0	1.00E-05			Terra Tek	7.2	Uniaxial compressive strength	MO0311RCKPRPCS.003, MO0402DQRIRPPR.003	
31.1	31.1	0.1		0.1	31	20	0.3	TSw2	Tptpln	ESF/ECRB/Borehole	USW G-4	G4-1307.2-D	1307.2	25.27	50.85	saturated	22	2.0	1.00E-05			Terra Tek	1.9	Uniaxial compressive strength	MO0311RCKPRPCS.003, MO0402DQRIRPPR.003	
79.1	79.1	0.1		0.1	79	22.8	0.2	TSw2	Tptpln	ESF/ECRB/Borehole	USW G-4	G4-1307.2-C	1307.2	25.27	50.88	saturated	22	2.0	1.00E-05			Terra Tek	3.3	Uniaxial compressive strength	MO0311RCKPRPCS.003, MO0402DQRIRPPR.003	
104.1	104.1	0.1		0.1	104	30.2	0.23	TSw2	Tptpln	ESF/ECRB/Borehole	USW G-4	G4-1307.2-A	1307.2	25.27	50.88	saturated	22	2.0	1.00E-05			Terra Tek	5.3	Uniaxial compressive strength	MO0311RCKPRPCS.003, MO0402DQRIRPPR.003	
98.1	98.1	0.1		0.1	98	34.9	0.2	TSw2	Tptpln	ESF/ECRB/Borehole	USW G-4	G4-1307.2-F	1307.2	25.27	50.88	saturated	22	2.0	1.00E-05			Terra Tek	3.3	Uniaxial compressive strength	MO0311RCKPRPCS.003, MO0402DQRIRPPR.003	
196.1	196.1	0.1		0.1	196	32.2	0.16	TSw2	Tptpmn	ESF/ECRB/Borehole	USW G-4	G4-748.6-A	748.6	25.35	50.88	saturated	22	2.0	1.00E-05			Terra Tek	6.6	Uniaxial compressive strength	MO0311RCKPRPCS.003, MO0402DQRIRPPR.003	
190.1	190.1	0.1		0.1	190	32.3	0.21	TSw2	Tptpmn	ESF/ECRB/Borehole	USW G-4	G4-748.6-B	748.6	25.32	50.85	saturated	22	2.0	1.00E-05			Terra Tek	7.0	Uniaxial compressive strength	MO0311RCKPRPCS.003, MO0402DQRIRPPR.003	
180.1	180.1	0.1		0.1	180	33.1	0.21	TSw2	Tptpmn	ESF/ECRB/Borehole	USW G-4	G4-686.6-G	686.6	25.30	50.85	saturated	22	2.0	1.00E-05			Terra Tek	6.4	Uniaxial compressive strength	MO0311RCKPRPCS.003, MO0402DQRIRPPR.003	
268.1	268.1	0.1		0.1	268	33.5	0.29	TSw2	Tptpmn	ESF/ECRB/Borehole	USW G-4	G4-749.0-A	749.0	25.30	50.77	saturated	22	2.0	1.00E-05			SNL	8.7	Uniaxial compressive strength	MO0311RCKPRPCS.003, MO0402DQRIRPPR.003	
230.1	230.1	0.1		0.1	230	33.6	0.11	TSw2	Tptpmn	ESF/ECRB/Borehole	USW G-4	G4-742.75-H	742.8	25.32	50.88	saturated	22	2.0	1.00E-07			Terra Tek	7.5	Uniaxial compressive strength	MO0311RCKPRPCS.003, MO0402DQRIRPPR.003	
283.1	283.1	0.1		0.1	283	34	0.28	TSw2	Tptpmn	ESF/ECRB/Borehole	USW G-4	G4-742.75-B	742.8	25.32	50.85	saturated	22	2.0	1.00E-03			Terra Tek	9.4	Uniaxial compressive strength	MO0311RCKPRPCS.003, MO0402DQRIRPPR.003	
188.1	188.1	0.1		0.1	188	34.1	0.27	TSw2	Tptpmn	ESF/ECRB/Borehole	USW G-4	G4-749.0-B	749.0	25.30	50.77	saturated	22	2.0	1.00E-05			SNL	6.7	Uniaxial compressive strength	MO0311RCKPRPCS.003, MO0402DQRIRPPR.003	
279.1	279.1	0.1		0.1	279	34.6	0.21	TSw2	Tptpmn	ESF/ECRB/Borehole	USW G-4	G4-742.75-G	742.8	25.32	50.88	saturated	22	2.0	1.00E-05			Terra Tek	9.3	Uniaxial compressive strength	MO0311RCKPRPCS.003, MO0402DQRIRPPR.003	
235.1	235.1	0.1		0.1	235	35.6	0.21	TSw2	Tptpmn	ESF/ECRB/Borehole	USW G-4	G4-742.75-E	742.8	25.32	50.88	saturated	22	2.0	1.00E-05			Terra Tek	7.2	Uniaxial compressive strength	MO0311RCKPRPCS.003, MO0402DQRIRPPR.003	
270.1	270.1	0.1		0.1	270	36.2	0.18	TSw2	Tptpmn	ESF/ECRB/Borehole	USW G-4	G4-686.6-A	686.6	25.32	50.88	saturated	22	2.0	1.00E-05			Terra Tek	8.7	Uniaxial compressive strength	MO0311RCKPRPCS.003, MO0402DQRIRPPR.003	
256.1	256.1	0.1		0.1	256	36.8	0.21	TSw2	Tptpmn	ESF/ECRB/Borehole	USW G-4	G4-742.75-F	742.8	25.32	50.85	saturated	22	2.0	1.00E-05			Terra Tek	8.3	Uniaxial compressive strength	MO0311RCKPRPCS.003, MO0402DQRIRPPR.003	
319.1	319.1	0.1		0.1	319	37.4	0.29	TSw2	Tptpmn	ESF/ECRB/Borehole	USW G-4	G4-742.75-A	742.8	25.32	50.83	saturated	22	2.0	1.00E-03			Terra Tek	9.5	Uniaxial compressive strength	MO0311RCKPRPCS.003, MO0402DQRIRPPR.003	
243.1	243.1	0.1		0.1	243	37.5	0.2	TSw2	Tptpmn	ESF/ECRB/Borehole	USW G-4	G4-742.75-D	742.8	25.32	50.88	saturated	22	2.0	1.00E-07			Terra Tek	6.9	Uniaxial compressive strength	MO0311RCKPRPCS.003, MO0402DQRIRPPR.003	
280.1	280.1	0.1		0.1	280	38.4	0.25	TSw2	Tptpmn	ESF/ECRB/Borehole	USW G-4	G4-742.75-C	742.8	25.32	50.88	saturated	22	2.0	1.00E-03			Terra Tek	8.9	Uniaxial compressive strength	MO0311RCKPRPCS.003, MO0402DQRIRPPR.003	
326.1	326.1	0.1		0.1	326	40.7	0.17	TSw2	Tptpmn	ESF/ECRB/Borehole	USW G-4	G4-686.6-D	686.6	25.32	50.88	saturated	22	2.0	1.00E-05			Terra Tek	10.0	Uniaxial compressive strength	MO0311RCKPRPCS.003, MO0402DQRIRPPR.003	
192.8	187.8	6	5	1	191.8	29.6	0.20	TSw2	Tptpmn	ESF/ECRB/Borehole	USW SD-9	SD-9-832.8-SNL-A	832.8	50.8	101.6	saturated	150	2.0	1.00E-06		ISRM T and ASTM D 2664-86	NER	8.06	Triaxial Data	MO0311RCKPRPCS.003, MO0402DQRIRPPR.003	Undrained test w/ constant Pore pressure of 5 MPa.
226.9	221.9	6	5	1	225.9	31.2	0.20	TSw2	Tptpmn	ESF/ECRB/Borehole	USW SD-9	SD-9-764.8-SNL-A	764.8	50.8	101.6	saturated	150	2.0	1.00E-06		ISRM T and ASTM D 2664-86	NER	N/A	Triaxial Data	MO0311RCKPRPCS.003, MO0402DQRIRPPR.003	Undrained test w/ constant Pore pressure of 5 MPa.
204.7	199.7	6	5	1	203.7	31.2	0.20	TSw2	Tptpmn	ESF/ECRB/Borehole	USW SD-9	SD-9-842.1-SNL-A	842.1	50.8	101.6	saturated	150	2.0	1.00E-06		ISRM T and ASTM D 2664-86	NER	9.03	Triaxial Data	MO0311RCKPRPCS.003, MO0402DQRIRPPR.003	Undrained test w/ constant Pore pressure of 5 MPa.
148.3	143.3	6	5	1	147.3	33.3	0.15	TSw2	Tptpmn	ESF/ECRB/Borehole	USW SD-9	SD-9-774.6-SNL-A	774.6	50.8	101.6	saturated	150	2.0	1.00E-06		ISRM T and ASTM D 2664-86	NER	7.04	Triaxial Data	MO0311RCKPRPCS.003, MO0402DQRIRPPR.003	Undrained test w/ constant Pore pressure of 5 MPa.
176.7	171.7	6	5	1	175.7	39.9	0.23	TSw2	Tptpmn	ESF/ECRB/Borehole	USW SD-9	SD-9-775.8-SNL-B	775.8	50.8	101.6	saturated	150	2.0	1.00E-06		ISRM T and ASTM D 2664-86	NER	6.61	Triaxial Data	MO0311RCKPRPCS.003, MO0402DQRIRPPR.003	Undrained test w/ constant Pore pressure of 5 MPa.
52.9	50.9	7	2	5	47.9	16		TSw2	Tptpmn	Busted Butte	Busted Butte	10AE34W		50.8	101.60	saturated	150	2.0	1.00E-05			SNL	6.4	Triaxial Data	MO0311RCKPRPCS.003, MO0402DQRIRPPR.003	Undrained test w/ pore pressure of 2 MPa.
160.2	158.2	7	2	5	155.2	33.9		TSw2	Tptpmn	Busted Butte	Busted Butte	10AE14W		50.8	101.60	saturated	150	2.0	1.00E-05			SNL	6.2	Triaxial Data	MO0311RCKPRPCS.003, MO0402DQRIRPPR.003	Undrained test w/ pore pressure of 2 MPa.
150.2	148.2	7	2	5	145.2	35.9		TSw2	Tptpmn	Busted Butte	Busted Butte	10AE35Y		50.8	101.60	saturated	150	2.0	1.00E-05			SNL	5.4	Triaxial Data	MO0311RCKPRPCS.003, MO0402DQRIRPPR.003	Undrained test w/ pore pressure of 2 MPa.
75	70	10	5	5	70	13.1		CFUn	Tcbm	ESF/ECRB/Borehole	USW G-1	7 758.9-759.2	2490-2491	25.4	50.8	saturated	200	2.0	1.00E-04			SNL		Triaxial data	MO0311RCKPRPCS.003, MO0402DQRIRPPR.003	Pore fluids pressure (MPa) = 5.
92	92	5	0	5	87	16.5		CFUn	Tcbm	ESF/ECRB/Borehole	USW G-1	3 758.9-759.2	2490-2491	25.4	50.8	dry	200	2.0	1.00E-04			SNL		Triaxial data	MO0311RCKPRPCS.003, MO0402DQRIRPPR.003	Drained test.
22	22	5	0	5	17	3.1	0.21	CHn	Tptpv1	ESF/ECRB/Borehole	USW G-4	G4-1400.6-C	1400.6	25.32	50.85	saturated	22	2.0	1.00E-05			Terra Tek	19.8	Triaxial data	MO0311RCKPRPCS.003, MO0402DQRIRPPR.003	Drained test.
34	34	5	0	5	29	3.68	0.2	CHn	Tptpv1	ESF/ECRB/Borehole	USW G-4	G4-1400.6-F	1400.6	25.32	50.83	saturated	22	2.0	1.00E-05			Terra Tek	12.0	Triaxial data	MO0311RCKPRPCS.003, MO0402DQRIRPPR.003	Drained test.

Table A-1 Intact Rock Mechanical Properties Data - Strength and Elastic Properties Data

Axial Stress, σ_1 (MPa)	Axial Stress, effective σ_1' (MPa)	Confining Pressure (MPa) σ_3	Pore Pressure (MPa)	Confining Pressure, Effective (MPa), σ_3'	Differential Strength, (MPa) $\sigma_1 - \sigma_3'$	Young's Modulus (GPa)	Poisson's Ratio	TM Unit	Litho-stratigraphic Unit	General Location	Sample Location	Specimen Number	Depth (ft)	Specimen Diameter (mm)	Specimen Length (mm)	Specimen Saturation	Specimen Temperature (deg. C)	l/d Ratio	Strain Rate (1/s)	Specimen Orientation (degree)	Test Standard	Laboratory	Failure Strain (millistrain)	Rock Property	Source DTN	Notes
13.3	13.3	5		5	8.3			PTn	Tpbt3	ESF/ECRB/Borehole	USW SD-12	SD-12-276.9-SNL-A	276.9	50.8	101.6	saturated	22	2.0	1.00E-05		ISRM T and ASTM D 2664-86	NBR	N/A	Triaxial data	MO0311RCKPRPCS.003	Drained/undrained status unknown.
125.3	125.3	5	0	5	120.3	24.4	0.07	TCw	Tpcpll	ESF/ECRB/Borehole	USW NRG-6	NRG-6-5.7-SNL-A	5.7	50.8	101.6	saturated	22	2.0	1.00E-05		ISRM T and ASTM D 2664	NBR	5.51	Triaxial data	MO0311RCKPRPCS.003, MO0402DQRIRPPR.003	Drained test.
307.1	307.1	5		5	302.1	36.3	0.20	TCw	Tpcpll	ESF/ECRB/Borehole	USW NRG-6	NRG-6-22.2-SNL-I	22.2	25.4	50.8	saturated	22	2.0	1.00E-05			NBR	8.7	Triaxial data	MO0311RCKPRPCS.003, MO0402DQRIRPPR.003	
395.5	395.5	5		5	390.5	36.4	0.22	TCw	Tpcpll	ESF/ECRB/Borehole	USW NRG-6	NRG-6-22.2-SNL-F	22.2	25.4	50.8	saturated	22	2.0	1.00E-05			NBR	12.28	Triaxial data	MO0311RCKPRPCS.003, MO0402DQRIRPPR.003	
396.8	396.8	5		5	391.8	36.8	0.21	TCw	Tpcpll	ESF/ECRB/Borehole	USW NRG-6	NRG-6-22.2-SNL-H	22.2	25.4	50.8	saturated	22	2.0	1.00E-05			NBR	12.36	Triaxial data	MO0311RCKPRPCS.003, MO0402DQRIRPPR.003	
391.2	391.2	5		5	386.2	37.4	0.22	TCw	Tpcpll	ESF/ECRB/Borehole	USW NRG-6	NRG-6-22.2-SNL-G	22.2	25.4	50.8	saturated	22	2.0	1.00E-05			NBR	11.67	Triaxial data	MO0311RCKPRPCS.003, MO0402DQRIRPPR.003	
144.7	144.7	5		5	139.7	23	0.16	TCw	Tpcpln	ESF/ECRB/Borehole	USW SD-12	SD-12-167.9-SNL-A	167.9	50.8	101.6	saturated	22	2.0	1.00E-05		ISRM T and ASTM D 2664-86	NBR	8.86	Triaxial data	MO0311RCKPRPCS.003, MO0402DQRIRPPR.003	Drained/undrained status unknown.
323.3	323.3	5		5	318.3	36.1	0.21	TCw	Tpcpln	ESF/ECRB/Borehole	USW SD-12	SD-12-202.9-SNL-A	202.9	50.8	101.6	saturated	22	2.0	1.00E-05		ISRM T and ASTM D 2664-86	NBR	9.2	Triaxial data	MO0311RCKPRPCS.003, MO0402DQRIRPPR.003	Drained/undrained status unknown.
313.6	313.6	5		5	308.6	39.1	0.21	TCw	Tpcpln	ESF/ECRB/Borehole	USW SD-12	SD-12-156.0-SNL-A	156.0	50.8	101.6	saturated	22	2.0	1.00E-05		ISRM T and ASTM D 2664-86	NBR	8.88	Triaxial data	MO0311RCKPRPCS.003, MO0402DQRIRPPR.003	Drained/undrained status unknown.
158.2	158.2	5		5	153.2	27	0.29	TCw	Tpcpmn	ESF/ECRB/Borehole	UE-25 NRG #3	NRG-3-263.3-SNL-E	263.3	25.4	50.8	saturated	22	2.0	1.00E-05			NBR	7.32	Triaxial data	MO0311RCKPRPCS.003, MO0402DQRIRPPR.003	Drained/undrained status unknown.
275.1	275.1	5		5	270.1	36.5	0.20	TCw	Tpcpmn	ESF/ECRB/Borehole	UE-25 NRG #3	NRG-3-265.7-SNL-D	265.7	25.4	50.8	saturated	22	2.0	1.00E-05			NBR	7.94	Triaxial data	MO0311RCKPRPCS.003, MO0402DQRIRPPR.003	Drained/undrained status unknown.
295.9	295.9	5		5	290.9	37.4	0.20	TCw	Tpcpmn	ESF/ECRB/Borehole	UE-25 NRG #3	NRG-3-265.7-SNL-B	265.7	25.4	50.8	saturated	22	2.0	1.00E-05			NBR	8.42	Triaxial data	MO0311RCKPRPCS.003, MO0402DQRIRPPR.003	Drained/undrained status unknown.
180.3	180.3	5		5	175.3	39.4	0.25	TCw	Tpcpmn	ESF/ECRB/Borehole	UE-25 NRG #3	NRG-3-265.7-SNL-F	265.7	25.4	50.8	saturated	22	2.0	1.00E-05			NBR	6.00	Triaxial data	MO0311RCKPRPCS.003, MO0402DQRIRPPR.003	Drained/undrained status unknown.
249	249	5		5	244.0	27.9	0.13	TCw	Tpcpmn	ESF/ECRB/Borehole	USW SD-12	SD-12-80.0-SNL-A	80.0	50.8	101.6	saturated	22	2.0	1.00E-05		ISRM T and ASTM D 2664-86	NBR	8.86	Triaxial data	MO0311RCKPRPCS.003, MO0402DQRIRPPR.003	Drained/undrained status unknown.
389.5	389.5	5		5	384.5	42.9	0.19	TCw	Tpcpmn	ESF/ECRB/Borehole	USW SD-12	SD-12-16.1-SNL-A	16.1	50.8	101.6	saturated	22	2.0	1.00E-05		ISRM T and ASTM D 2664-86	NBR	8.54	Triaxial data	MO0311RCKPRPCS.003, MO0402DQRIRPPR.003	Drained/undrained status unknown.
76.9	76.9	5	0	5	71.9	17.8	0.42	TSw1	Tptpul	ESF/ECRB/Borehole	USW NRG-7a	NRG-7/7A-717.7-SNL-A	717.7	50.8	101.6	saturated	22	2.0	1.00E-05		ISRM T and ASTM D 2664	NBR	5.99	Triaxial Data	MO0311RCKPRPCS.003, MO0402DQRIRPPR.003	Drained test.
111.9	111.9	5	0	5	106.9	32.4	0.19	TSw1	Tptpul	ESF/ECRB/Borehole	USW NRG-7a	NRG-7/7A-671.4-SNL-A	671.4	50.8	101.6	saturated	22	2.0	1.00E-05		ISRM T and ASTM D 2664	NBR	3.96	Triaxial Data	MO0311RCKPRPCS.003, MO0402DQRIRPPR.003	Drained test.
67.1	67.1	5	0	5	62.1	14.4	0.28	TSw1	Tptrl	ESF/ECRB/Borehole	USW NRG-7a	NRG-7/7A-483.3-SNL-A	483.3	50.8	101.6	saturated	22	2.0	1.00E-05		ISRM T and ASTM D 2664	NBR	5.95	Triaxial data	MO0311RCKPRPCS.003, MO0402DQRIRPPR.003	Drained test.
67.5	67.5	5		5	62.5	14.7	0.13	TSw1	Tptrn	ESF/ECRB/Borehole	UE-25 NRG #4	NRG-4-527.0-SNL-G	527.0	25.4	50.8	saturated	22	2.0	1.00E-05		ISRM T and ASTM D 2664-86	NBR	5.43	Triaxial data	MO0311RCKPRPCS.003, MO0402DQRIRPPR.003	Drained/undrained status unknown.
90	90	5		5	85.0	19.7	0.17	TSw1	Tptrn	ESF/ECRB/Borehole	UE-25 NRG #4	NRG-4-527.0-SNL-E	527.0	25.4	50.8	saturated	22	2.0	1.00E-05		ISRM T and ASTM D 2664-86	NBR	7.51	Triaxial data	MO0311RCKPRPCS.003, MO0402DQRIRPPR.003	Drained/undrained status unknown.
76.5	76.5	5		5	71.5	21.1	0.19	TSw1	Tptrn	ESF/ECRB/Borehole	UE-25 NRG #4	NRG-4-527.0-SNL-A	527.0	25.4	50.8	saturated	22	2.0	1.00E-05		ISRM T and ASTM D 2664-86	NBR	4.02	Triaxial data	MO0311RCKPRPCS.003, MO0402DQRIRPPR.003	Drained/undrained status unknown.
108.9	108.9	5		5	103.9	22.6	0.23	TSw1	Tptrn	ESF/ECRB/Borehole	UE-25 NRG #4	NRG-4-527.0-SNL-B	527.0	25.4	50.8	saturated	22	2.0	1.00E-05		ISRM T and ASTM D 2664-86	NBR	6.81	Triaxial data	MO0311RCKPRPCS.003, MO0402DQRIRPPR.003	Drained/undrained status unknown.
113.6	113.6	5		5	108.6	23.4	0.16	TSw1	Tptrn	ESF/ECRB/Borehole	UE-25 NRG #4	NRG-4-527.0-SNL-D	527.0	25.4	50.8	saturated	22	2.0	1.00E-05		ISRM T and ASTM D 2664-86	NBR	4.95	Triaxial data	MO0311RCKPRPCS.003, MO0402DQRIRPPR.003	Drained/undrained status unknown.
77.1	77.1	5		5	72.1	12.3	0.45	TSw1	Tptrn	ESF/ECRB/Borehole	USW NRG-6	NRG-6-416.0-SNL-F	416.0	25.4	50.8	saturated	22	2.0	1.00E-05			NBR	11.2	Triaxial data	MO0311RCKPRPCS.003, MO0402DQRIRPPR.003	Drained/undrained status unknown.
39.6	39.6	5		5	34.6	13.7		TSw1	Tptrn	ESF/ECRB/Borehole	USW NRG-6	NRG-6-416.0-SNL-G	416.0	25.4	50.8	saturated	22	2.0	1.00E-05			NBR	NA	Triaxial data	MO0311RCKPRPCS.003, MO0402DQRIRPPR.003	Drained/undrained status unknown.
58.8	58.8	5		5	53.8	16.3	0.21	TSw1	Tptrn	ESF/ECRB/Borehole	USW NRG-6	NRG-6-416.0-SNL-I	416.0	25.4	50.8	saturated	22	2.0	1.00E-05			NBR	5.3	Triaxial data	MO0311RCKPRPCS.003, MO0402DQRIRPPR.003	Drained/undrained status unknown.
84.7	84.7	5		5	79.7	17.1	0.21	TSw1	Tptrn	ESF/ECRB/Borehole	USW NRG-6	NRG-6-416.0-SNL-H	416.0	25.4	50.8	saturated	22	2.0	1.00E-05			NBR	7	Triaxial data	MO0311RCKPRPCS.003, MO0402DQRIRPPR.003	Drained/undrained status unknown.
99.3	99.3	5	0	5	94.3	20	0.20	TSw1	Tptrn	ESF/ECRB/Borehole	USW NRG-6	NRG-6-394.6-SNL-A	394.6	50.8	101.6	saturated	22	2.0	1.00E-05		ISRM T and ASTM D 2664	NBR	6.71	Triaxial data	MO0311RCKPRPCS.003, MO0402DQRIRPPR.003	Drained test.
116.1	116.1	5	0	5	111.1	25.4	0.22	TSw1	Tptrn	ESF/ECRB/Borehole	USW NRG-6	NRG-6-326.0-SNL-A	326.0	50.8	101.6	saturated	22	2.0	1.00E-05		ISRM T and ASTM D 2664	NBR	4.91	Triaxial data	MO0311RCKPRPCS.003, MO0402DQRIRPPR.003	Drained test.
70.5	70.5	5	0	5	65.5	14	0.24	TSw1	Tptrn	ESF/ECRB/Borehole	USW NRG-7a	NRG-7/7A-454.6-SNL-A	454.6	50.8	101.6	saturated	22	2.0	1.00E-05		ISRM T and ASTM D 2664	NBR	9.39	Triaxial data	MO0311RCKPRPCS.003, MO0402DQRIRPPR.003	Drained test.
73.1	73.1	5	0	5	68.1	16.1	0.14	TSw1	Tptrn	ESF/ECRB/Borehole	USW NRG-7a	NRG-7/7A-427.6-SNL-A	427.6	50.8	101.6	saturated	22	2.0	1.00E-05		ISRM T and ASTM D 2664	NBR	9.04	Triaxial data	MO0311RCKPRPCS.003, MO0402DQRIRPPR.003	Drained test.
110.2	110.2	5		5	105.2	20.6	0.21	TSw1	Tptrn	ESF/ECRB/Borehole	USW NRG-7a	NRG-7/7A-344.4-SNL-H	344.4	25.4	50.8	saturated	22	2.0	1.00E-05		TP-219 ASTM D 2664 ISRM T	NBR	6.91	Triaxial data	MO0311RCKPRPCS.003, MO0402DQRIRPPR.003	Drained/undrained status unknown.
75.9	75.9	5		5	70.9	22.5	0.20	TSw1	Tptrn	ESF/ECRB/Borehole	USW NRG-7a	NRG-7/7A-344.4-SNL-G	344.4	25.4	50.8	saturated	22	2.0	1.00E-05		TP-219 ASTM D 2664 ISRM T	NBR	3.41	Triaxial data	MO0311RCKPRPCS.003, MO0402DQRIRPPR.003	Drained/undrained status unknown.
56.5	56.5	5		5	51.5	24.7	0.17	TSw1	Tptrn	ESF/ECRB/Borehole	USW NRG-7a	NRG-7/7A-344.4-SNL-E	344.4	25.4	50.8	saturated	22	2.0	1.00E-05		TP-219 ASTM D 2664 ISRM T	NBR	3.94	Triaxial data	MO0311RCKPRPCS.003, MO0402DQRIRPPR.003	Drained/undrained status unknown.
163.9	163.9	5		5	158.9	28.7	0.23	TSw1	Tptrn	ESF/ECRB/Borehole	USW NRG-7a	NRG-7/7A-344.4-SNL-F	344.4	25.4	50.8	saturated	22	2.0	1.00E-05		TP-219 ASTM D 2664 ISRM T	NBR	6.11	Triaxial data	MO0311RCKPRPCS.003, MO0402DQRIRPPR.003	Drained/undrained status unknown.
104.5	104.5	5	0	5	99.5	29	0.24	TSw1	Tptrn	ESF/ECRB/Borehole	USW NRG-7a	NRG-7/7A-345.0-SNL-A	345.0	50.8	101.6	saturated	22	2.0	1.00E-05		ISRM T and ASTM D 2664	NBR	3.97	Triaxial data	MO0311RCKPRPCS.003, MO0402DQRIRPPR.003	Drained test.
88.8	88.8	5		5	83.8	24.3	0.18	TSw1	Tptrn	ESF/ECRB/Borehole	USW SD-12	SD-12-339.4-SNL-A	339.4	50.8	101.6	saturated	22	2.0	1.00E-05		ISRM T and ASTM D 2664-86	NBR	6.34	Triaxial data	MO0311RCKPRPCS.003, MO0402DQRIRPPR.003	Drained/undrained status unknown.
87.4	87.4	5		5	82.4	24.9	0.21	TSw1	Tptrn	ESF/ECRB/Borehole	USW SD-12	SD-12-370.1-SNL-A	370.1	50.8	101.6	saturated	22	2.0	1.00E-05		ISRM T and ASTM D 2664-86	NBR	4.95	Triaxial data	MO0311RCKPRPCS.003, MO0402DQRIRPPR.003	Drained/undrained status unknown.
99.4	99.4	5		5	94.4	25.2	0.20	TSw1	Tptrn	ESF/ECRB/Borehole	USW SD-12	SD-12-410.2-SNL-A	410.2	50.8	101.6	saturated	22	2.0	1.00E-05		ISRM T and ASTM D 2664-86	NBR	N/A	Triaxial data	MO0311RCKPRPCS.003, MO0402DQRIRPPR.003	Drained/undrained status unknown.
114.7	114.7	5	0	5	109.7	23.2	0.32	TSw2	Tptpll	ESF/ECRB/Borehole	USW G-1	G1-1179.6 SL	1179.6	26.1	50.1 to 51.3	saturated	22	2.0	1.00E-05			SNL	6.9	Triaxial Data	MO0311RCKPRPCS.003, MO0402DQRIRPPR.003	Drained test.
152.6	152.6	5	0	5	147.6	30.8	0.22	TSw2	Tptpln	ESF/ECRB/Borehole	USW NRG-7a	NRG-7/7A-1399.1-SNL-A	1399.1	50.8	101.6	saturated	22	2.0	1.00E-05		ISRM T and ASTM D 2664	NBR	5.43	Triaxial data	MO0311RCKPRPCS.003, MO0402DQRIRPPR.003	Drained/undrained status unknown.
216.1	216.1	5		5	211.1	35.9	0.28	TSw2	Tptpln	ESF/ECRB/Borehole	USW SD-12	SD-12-1073.3-SNL-B	1073.3	50.8	101.6	saturated	22	2.0	1.00E-05		ISRM T and ASTM D 2664-86	NBR	8.21	Triaxial Data	MO0311RCKPRPCS.003, MO0402DQRIRPPR.003	Drained/undrained status unknown.
280.6	280.6	5		5	275.6	36.1	0.22	TSw2	Tptpln	ESF/ECRB/Borehole	USW SD-12	SD-12-1112.1-SNL-B	1112.1	50.8	101.6	saturated	22	2.0	1.00E-05		ISRM T and ASTM D 2664-86	NBR	7.80	Triaxial Data	MO0311RCKPRPCS.003, MO0402DQRIRPPR.003	Drained/undrained status unknown.
160.4	160.4	5	0	5	155.4	33.7	0.17	TSw2	Tptpmn	Busted Butte	Busted Butte	10AE29Y		50.8	101.6	dry	22	2.0	1.00E-05			SNL	5.7	Triaxial Data	MO0311RCKPRPCS.003, MO0402DQRIRPPR.003	Drained test.
174	174	5	0	5	169	35.5	0.21	TSw2	Tptpmn	Busted Butte	Busted Butte	10AE45W		50.8	101.6	saturated	22	2.0	1.00E-05			SNL	6.7	Triaxial Data	MO0311RCKPRPCS.003, MO0402DQRIRPPR.003	Drained test.
174.7	174.7	5	0	5	169.7	36.8	0.20	TSw2	Tptpmn	Busted Butte	Busted Butte	10AE14X		50.8	101.6	saturated	22	2.0	1.00E-05			SNL	5.2	Triaxial Data	MO0311RCKPRPCS.003, MO0402DQRIRPPR.003	Drained test.
203.7	203.7	5	0	5	198.7	37.1	0.21	TSw2	Tptpmn	Busted Butte	Busted Butte	10AE23Z		50.8	101.6	saturated	22	2.0	1.00E-05			SNL	6.7	Triaxial Data	MO0311RCKPRPCS.003, MO0402DQRIRPPR.003	Drained test.
225.2	225.2	5	0	5	220.2	37.9	0.21	TSw2	Tptpmn	Busted Butte	Busted Butte	10AE9X		50.8	101.6	dry	22	2.0	1.00E-05			SNL	7.3	Triaxial Data	MO0311RCKPRPCS.003, MO0402DQRIRPPR.003	Drained test.
203.6	203.6	5	0	5	198.6	40.7	0.20	TSw2	Tptpmn	Busted Butte	Busted Butte	10AE52W		50.8	101.6	dry	22	2.0	1.00E-05			SNL	6.7	Triaxial Data	MO0311RCKPRPCS.003, MO0402DQRIRPPR.003	Drained test.
161	161	5	0	5	156	40.5	0.16	TSw2	Tptpmn	ESF/ECRB/Borehole	USW G-4	G4-686.6-B	686.6	25.32	50.90	saturated	22	2.0	1.00E-05			Terra Tek	13.3	Triaxial Data	MO0311RCKPRPCS.003, MO0402DQRIRPPR.003	Drained test.
92	92	5	0	5	87	43.6	0.30	TSw2	Tptpmn	ESF/ECRB/Borehole	USW G-4	G4-686.6-E	686.6	25.35	50.88	saturated	22	2.0	1.00E-05			Terra Tek	1.8	Triaxial Data	MO0311RCKPRPCS.003, MO0402DQRIRPPR.003	Drained test.
250.8	250.8	5	0	5	245.8	33.9	0.21	TSw2	Tptpmn	ESF/ECRB/Borehole	USW NRG-7a	NRG-7/7A-861.7-SNL-A	861.7	50.8	101.6	saturated	22	2.0	1.00E-05		ISRM T and ASTM D 2664	NBR	8.83	Triaxial Data	MO0311RCKPRPCS.003, MO0402DQRIRPPR.003	Drained test.
255.1	255.1	5		5	250.1	34	0.18	TSw2	Tptpmn	ESF/ECRB/Borehole	USW NRG-7a	NRG-7/7A-865.4-SNL-G	865.4	25.4	50.8	saturated	22	2.0	1.00E-05			NBR	8.10	Triaxial Data	MO0311RCKPRPCS.003, MO0402DQRIRPPR.003	Drained/undrained status unknown.
322.3	322.3	5		5	317.3	34.5	0.21	TSw2	Tptpmn	ESF/ECRB/Borehole	USW NRG-7a	NRG-7/7A-865.4-SNL-F	865.4	25.4	50.8	saturated	22	2.0	1.00E-05			NBR	10.28	Triaxial Data	MO0311RCKPRPCS.003, MO0402DQRIRPPR.003	Drained/undrained status unknown.
259.8	259.8	5		5	254.8	35	0.20	TSw2	Tptpmn	ESF/ECRB/Borehole	USW NRG-7a	NRG-7/7A-865.4-SNL-C	865.4	25.4	50.8	saturated	22	2.0	1.00E-05			NBR	7.93	Triaxial Data	MO0311RCKPRPCS.003, MO0402DQRIRPPR.003	Drained/undrained status unknown.
231.6	231.6	5		5	226.6	36.8	0.21	TSw2	Tptpmn	ESF/ECRB/Borehole	USW NRG-7a	NRG-7/7A-865.4-SNL-H	865.4	25.4	50.8	saturated	22	2.0	1.00E-05			NBR	6.50	Triaxial Data	MO0311RCKPRPCS.003, MO0402DQRIRPPR.003	Drained/undrained status unknown.
335.7	335.7	5		5	330.7	34.5	0.20	TSw2	Tptpmn	ESF/ECRB/Borehole	USW SD-12	SD-12-745.6-SNL-B	745.6	50.8	101.6	saturated	22	2.0	1.00E-05		ISRM T and ASTM D 2664-86	NBR	8.79	Triaxial Data	MO0311RCKPRPCS.003, MO0402DQRIRPPR.003	Drained/undrained status unknown.

Table A-1 Intact Rock Mechanical Properties Data - Strength and Elastic Properties Data

Axial Stress, σ_1 (MPa)	Axial Stress, effective σ_1' (MPa)	Confining Pressure (MPa) σ_3	Pore Pressure (MPa)	Confining Pressure, Effective (MPa), σ_3'	Differential Strength, (MPa) $\sigma_1 - \sigma_3$	Young's Modulus (GPa)	Poisson's Ratio	TM Unit	Litho-stratigraphic Unit	General Location	Sample Location	Specimen Number	Depth (ft)	Specimen Diameter (mm)	Specimen Length (mm)	Specimen Saturation	Specimen Temperature (deg. C)	l/d Ratio	Strain Rate (1/s)	Specimen Orientation (degree)	Test Standard	Laboratory	Failure Strain (millistrain)	Rock Property	Source DTN	Notes
248.9	243.9	10	5	5	243.9	22.3	0.15	TSw2	Tptpmn	ESF/ECRB/Borehole	USW SD-9	SD-9-832.8-SNL-B	832.8	50.8	101.6	saturated	150	2.0	1.00E-06		ISRM T and ASTM D 2664-86	NBR	10.88	Triaxial Data	MO0311RCKPRPCS.003, MO0402DQRIRPPR.003	Undrained test w/ constant Pore pressure of 5 MPa.
234.9	229.9	10	5	5	229.9	29.4	0.20	TSw2	Tptpmn	ESF/ECRB/Borehole	USW SD-9	SD-9-828.9-SNL-A	828.9	50.8	101.6	saturated	150	2.0	1.00E-06		ISRM T and ASTM D 2664-86	NBR	8.76	Triaxial Data	MO0311RCKPRPCS.003, MO0402DQRIRPPR.003	Undrained test w/ constant Pore pressure of 5 MPa.
277.7	272.7	10	5	5	272.7	32.3	0.23	TSw2	Tptpmn	ESF/ECRB/Borehole	USW SD-9	SD-9-842.1-SNL-B	842.1	50.8	101.6	saturated	150	2.0	1.00E-06		ISRM T and ASTM D 2664-86	NBR	9.57	Triaxial Data	MO0311RCKPRPCS.003, MO0402DQRIRPPR.003	Undrained test w/ constant Pore pressure of 5 MPa.
213.3	208.3	10	5	5	208.3	32.5	0.26	TSw2	Tptpmn	ESF/ECRB/Borehole	USW SD-9	SD-9-764.8-SNL-B	764.8	50.8	101.6	saturated	150	2.0	1.00E-06		ISRM T and ASTM D 2664-86	NBR	6.99	Triaxial Data	MO0311RCKPRPCS.003, MO0402DQRIRPPR.003	Undrained test w/ constant Pore pressure of 5 MPa.
207.3	202.3	10	5	5	202.3	33.5	0.18	TSw2	Tptpmn	ESF/ECRB/Borehole	USW SD-9	SD-9-774.6-SNL-C	774.6	50.8	101.6	saturated	150	2.0	1.00E-06		ISRM T and ASTM D 2664-86	NBR	6.74	Triaxial Data	MO0311RCKPRPCS.003, MO0402DQRIRPPR.003	Undrained test w/ constant Pore pressure of 5 MPa.
339.2	334.2	10	5	5	334.2	35	0.23	TSw2	Tptpmn	ESF/ECRB/Borehole	USW SD-9	SD-9-815.9-SNL-B	815.9	50.8	101.6	saturated	150	2.0	1.00E-06		ISRM T and ASTM D 2664-86	NBR	11.5	Triaxial Data	MO0311RCKPRPCS.003, MO0402DQRIRPPR.003	Undrained test w/ constant Pore pressure of 5 MPa.
52.2	52.2	5		5	47.2	54.2	0.17	TSw3	Tptpv3	ESF/ECRB/Borehole	USW SD-12	SD-12-1279.7-SNL-A	1279.7	50.8	101.6	saturated	22	2.0	1.00E-05		ISRM T and ASTM D 2664-86	NBR	4.45	Triaxial data	MO0311RCKPRPCS.003, MO0402DQRIRPPR.003	Drained/undrained status unknown.
103	103	10	0	10	93	15.7		CFUn	Tcbm	ESF/ECRB/Borehole	USW G-1	4 758.9-759.2	2490-2491	25.4	50.8	dry	200	2.0	1.00E-04			SNL		Triaxial data	MO0311RCKPRPCS.003, MO0402DQRIRPPR.003	Drained test.
39.9	39.9	10	0	10	29.9	5.57		CHn	Tac	ESF/ECRB/Borehole	USW G-1	G11487.4 SL5	1487.4	25.4	50.0-51.3	saturated	22	2.0	1.00E-05			SNL	6.8	Triaxial data	MO0311RCKPRPCS.003, MO0402DQRIRPPR.003	Drained test.
41.4	41.4	10	0	10	31.4	6.16	0.22	CHn	Tac	ESF/ECRB/Borehole	USW G-1	G11487.4 SL5A	1487.4	25.4	50.0-51.3	saturated	22	2.0	1.00E-05			SNL	6.6	Triaxial data	MO0311RCKPRPCS.003, MO0402DQRIRPPR.003	Drained test.
26	26	10	0	10	16	3.14	0.3	CHn	Tptpv1	ESF/ECRB/Borehole	USW G-4	G4-1400.6-D	1400.6	25.32	50.88	saturated	22	2.0	1.00E-05			Terra Tek	20.0	Triaxial data	MO0311RCKPRPCS.003, MO0402DQRIRPPR.003	Drained test.
42	42	10	0	10	32	4.35	0.3	CHn	Tptpv1	ESF/ECRB/Borehole	USW G-4	G4-1400.6-G	1400.6	25.32	50.88	saturated	22	2.0	1.00E-05			Terra Tek	16.0	Triaxial data	MO0311RCKPRPCS.003, MO0402DQRIRPPR.003	Drained test.
71.4	71.4	10		10	61.4	24	0.19	PTn	Tpcpv2	ESF/ECRB/Borehole	USW SD-12	SD-12-250.0-SNL-A	250.0	50.8	101.6	saturated	22	2.0	1.00E-05		ISRM T and ASTM D 2664-86	NBR	8.64	Triaxial data	MO0311RCKPRPCS.003, MO0402DQRIRPPR.003	Drained/undrained status unknown.
17.3	17.3	10		10	7.3			PTn	Tpp	ESF/ECRB/Borehole	USW SD-12	SD-12-282.5-SNL-A	282.5	50.8	101.6	saturated	22	2.0	1.00E-05		ISRM T and ASTM D 2664-86	NBR		Triaxial data	MO0311RCKPRPCS.003	Drained/undrained status unknown.
157.9	157.9	10	0	10	147.9	22.3	0.10	TCw	Tpcpll	ESF/ECRB/Borehole	USW NRG-6	NRG-6-46.4-SNL-A	46.4	50.8	101.6	saturated	22	2.0	1.00E-05		ISRM T and ASTM D 2664	NBR	8.99	Triaxial data	MO0311RCKPRPCS.003, MO0402DQRIRPPR.003	Drained test.
343.4	343.4	10		10	333.4	35.6	0.21	TCw	Tpcpll	ESF/ECRB/Borehole	USW NRG-6	NRG-6-22.2-SNL-D	22.2	25.4	50.8	saturated	22	2.0	1.00E-05			NBR	11.98	Triaxial data	MO0311RCKPRPCS.003, MO0402DQRIRPPR.003	
439.7	439.7	10		10	429.7	36.9	0.23	TCw	Tpcpll	ESF/ECRB/Borehole	USW NRG-6	NRG-6-22.2-SNL-B	22.2	25.4	50.8	saturated	22	2.0	1.00E-05			NBR	14.06	Triaxial data	MO0311RCKPRPCS.003, MO0402DQRIRPPR.003	
434.6	434.6	10		10	424.6	38.1	0.20	TCw	Tpcpll	ESF/ECRB/Borehole	USW NRG-6	NRG-6-22.2-SNL-C	22.2	25.4	50.8	saturated	22	2.0	1.00E-05			NBR	13.04	Triaxial data	MO0311RCKPRPCS.003, MO0402DQRIRPPR.003	
417.3	417.3	10		10	407.3	38.3	0.21	TCw	Tpcpll	ESF/ECRB/Borehole	USW NRG-6	NRG-6-22.2-SNL-E	22.2	25.4	50.8	saturated	22	2.0	1.00E-05			NBR	13.33	Triaxial data	MO0311RCKPRPCS.003, MO0402DQRIRPPR.003	
406	406	10	0	10	396	43.9	0.30	TCw	Tpcpln	ESF/ECRB/Borehole	UE-25 a #1	87.6	87.6	56	L:D = 2:1	ambient	22	2.0	1.00E-04			SNL		Triaxial data	MO0311RCKPRPCS.003, MO0402DQRIRPPR.003	Drained test.
183.1	183.1	10	0	10	173.1	18.8	0.17	TCw	Tpcpln	ESF/ECRB/Borehole	USW NRG-6	NRG-6-122.7-SNL-A	122.7	50.8	101.6	saturated	22	2.0	1.00E-05		ISRM T and ASTM D 2664	NBR	8.7	Triaxial data	MO0311RCKPRPCS.003, MO0402DQRIRPPR.003	Drained test.
410.4	410.4	10		10	400.4	38.7	0.21	TCw	Tpcpln	ESF/ECRB/Borehole	USW SD-12	SD-12-176.1-SNL-A	176.1	50.8	101.6	saturated	22	2.0	1.00E-05		ISRM T and ASTM D 2664-86	NBR	8.1	Triaxial data	MO0311RCKPRPCS.003, MO0402DQRIRPPR.003	Drained/undrained status unknown.
418.2	418.2	10		10	408.2	39.2	0.23	TCw	Tpcpln	ESF/ECRB/Borehole	USW SD-12	SD-12-161.7-SNL-A	161.7	50.8	101.6	saturated	22	2.0	1.00E-05		ISRM T and ASTM D 2664-86	NBR	8.71	Triaxial data	MO0311RCKPRPCS.003, MO0402DQRIRPPR.003	Drained/undrained status unknown.
152.2	152.2	10		10	142.2	54	0.26	TCw	Tpcpln	ESF/ECRB/Borehole	USW SD-12	SD-12-137.3-SNL-A	137.3	50.8	101.6	saturated	22	2.0	1.00E-05		ISRM T and ASTM D 2664-86	NBR	3.17	Triaxial data	MO0311RCKPRPCS.003, MO0402DQRIRPPR.003	Drained/undrained status unknown.
309.9	309.9	10		10	299.9	36.8	0.21	TCw	Tpcpmn	ESF/ECRB/Borehole	UE-25 NRG #3	NRG-3-265.7-SNL-G	265.7	25.4	50.8	saturated	22	2.0	1.00E-05			NER	9.10	Triaxial data	MO0311RCKPRPCS.003, MO0402DQRIRPPR.003	Drained/undrained status unknown.
369	369	10		10	359.0	37.1	0.21	TCw	Tpcpmn	ESF/ECRB/Borehole	UE-25 NRG #3	NRG-3-265.7-SNL-C	265.7	25.4	50.8	saturated	22	2.0	1.00E-05			NER	11.25	Triaxial data	MO0311RCKPRPCS.003, MO0402DQRIRPPR.003	Drained/undrained status unknown.
339.1	339.1	10		10	329.1	37.5	0.20	TCw	Tpcpmn	ESF/ECRB/Borehole	UE-25 NRG #3	NRG-3-265.7-SNL-E	265.7	25.4	50.8	saturated	22	2.0	1.00E-05			NER	9.75	Triaxial data	MO0311RCKPRPCS.003, MO0402DQRIRPPR.003	Drained/undrained status unknown.
291.4	291.4	10		10	281.4	39.3	0.19	TCw	Tpcpmn	ESF/ECRB/Borehole	UE-25 NRG #3	NRG-3-263.3-SNL-D	263.3	25.4	50.8	saturated	22	2.0	1.00E-05			NER	7.64	Triaxial data	MO0311RCKPRPCS.003, MO0402DQRIRPPR.003	Drained/undrained status unknown. Values are a few percent less than their ultimate value
245.5	245.5	10		10	235.5	27.4	0.12	TCw	Tpcpmn	ESF/ECRB/Borehole	USW SD-12	SD-12-32.0-SNL-A	32.0	50.8	101.6	saturated	22	2.0	1.00E-05		ISRM T and ASTM D 2664-86	NBR	8.64	Triaxial data	MO0311RCKPRPCS.003, MO0402DQRIRPPR.003	Drained/undrained status unknown.
227.9	227.9	10	0	10	217.9	22.3	0.11	TSw1	Tptpul	ESF/ECRB/Borehole	USW NRG-7a	NRG-7/7A-672.0-SNL-A	672.0	50.8	101.6	saturated	22	2.0	1.00E-05		ISRM T and ASTM D 2664	NER	9.26	Triaxial Data	MO0311RCKPRPCS.003, MO0402DQRIRPPR.003	Drained test.
133	133	10		10	123.0	23	0.20	TSw1	Tptrn	ESF/ECRB/Borehole	UE-25 NRG #4	NRG-4-527.0-SNL-I	527.0	25.4	50.8	saturated	22	2.0	1.00E-05		ISRM T and ASTM D 2664	NBR	6.57	Triaxial data	MO0311RCKPRPCS.003, MO0402DQRIRPPR.003	Drained/undrained status unknown.
131.4	131.4	10		10	121.4	25.3	0.19	TSw1	Tptrn	ESF/ECRB/Borehole	UE-25 NRG #4	NRG-4-527.0-SNL-H	527.0	25.4	50.8	saturated	22	2.0	1.00E-05		ISRM T and ASTM D 2664	NBR	6.02	Triaxial data	MO0311RCKPRPCS.003, MO0402DQRIRPPR.003	Drained/undrained status unknown.
160.8	160.8	10		10	150.8	25.5	0.18	TSw1	Tptrn	ESF/ECRB/Borehole	UE-25 NRG #4	NRG-4-527.0-SNL-C	527.0	25.4	50.8	saturated	22	2.0	1.00E-05		ISRM T and ASTM D 2664	NBR	6.82	Triaxial data	MO0311RCKPRPCS.003, MO0402DQRIRPPR.003	Drained/undrained status unknown.
142.1	142.1	10		10	132.1	25.8	0.19	TSw1	Tptrn	ESF/ECRB/Borehole	UE-25 NRG #4	NRG-4-527.0-SNL-F	527.0	25.4	50.8	saturated	22	2.0	1.00E-05		ISRM T and ASTM D 2664	NBR	5.74	Triaxial data	MO0311RCKPRPCS.003, MO0402DQRIRPPR.003	Drained/undrained status unknown.
61.1	61.1	10		10	51.1	8.4	0.22	TSw1	Tptrn	ESF/ECRB/Borehole	USW NRG-6	NRG-6-416.0-SNL-E	416.0	25.4	50.8	saturated	22	2.0	1.00E-05			NBR	9.8	Triaxial data	MO0311RCKPRPCS.003, MO0402DQRIRPPR.003	Drained/undrained status unknown.
93.6	93.6	10	0	10	83.6	17.5	0.19	TSw1	Tptrn	ESF/ECRB/Borehole	USW NRG-6	NRG-6-362.0-SNL-A	362.0	50.8	101.6	saturated	22	2.0	1.00E-05		ISRM T and ASTM D 2664	NBR	7.29	Triaxial data	MO0311RCKPRPCS.003, MO0402DQRIRPPR.003	Drained test.
119.9	119.9	10		10	109.9	17.9	0.34	TSw1	Tptrn	ESF/ECRB/Borehole	USW NRG-6	NRG-6-416.0-SNL-B	416.0	25.4	50.8	saturated	22	2.0	1.00E-05			NBR	8.6	Triaxial data	MO0311RCKPRPCS.003, MO0402DQRIRPPR.003	Drained/undrained status unknown.
147.9	147.9	10		10	137.9	19.3	0.30	TSw1	Tptrn	ESF/ECRB/Borehole	USW NRG-6	NRG-6-416.0-SNL-C	416.0	25.4	50.8	saturated	22	2.0	1.00E-05			NBR	9.1	Triaxial data	MO0311RCKPRPCS.003, MO0402DQRIRPPR.003	Drained/undrained status unknown.
30.1	30.1	10		10	20.1	21	0.28	TSw1	Tptrn	ESF/ECRB/Borehole	USW NRG-6	NRG-6-416.0-SNL-D	416.0	25.4	50.8	saturated	22	2.0	1.00E-05			NBR	1.1	Triaxial data	MO0311RCKPRPCS.003, MO0402DQRIRPPR.003	Drained/undrained status unknown.
228.5	228.5	10	0	10	218.5	28.4	0.21	TSw1	Tptrn	ESF/ECRB/Borehole	USW NRG-6	NRG-6-290.5-SNL-A	290.5	50.8	101.6	saturated	22	2.0	1.00E-05		ISRM T and ASTM D 2664	NBR	8.03	Triaxial data	MO0311RCKPRPCS.003, MO0402DQRIRPPR.003	Drained test.
88.4	88.4	10	0	10	78.4	17.8	0.20	TSw1	Tptrn	ESF/ECRB/Borehole	USW NRG-7a	NRG-7/7A-411.4-SNL-A	411.4	50.8	101.6	saturated	22	2.0	1.00E-05		ISRM T and ASTM D 2664	NBR	4.72	Triaxial data	MO0311RCKPRPCS.003, MO0402DQRIRPPR.003	Drained test.
139.3	139.3	10	0	10	129.3	19.8	0.33	TSw1	Tptrn	ESF/ECRB/Borehole	USW NRG-7a	NRG-7/7A-470.2-SNL-A	470.2	50.8	101.6	saturated	22	2.0	1.00E-05		ISRM T and ASTM D 2664	NBR	8.37	Triaxial data	MO0311RCKPRPCS.003, MO0402DQRIRPPR.003	Drained test.
103.3	103.3	10	0	10	93.3	20.3	0.22	TSw1	Tptrn	ESF/ECRB/Borehole	USW NRG-7a	NRG-7/7A-441.0-SNL-A	441.0	50.8	101.6	saturated	22	2.0	1.00E-05		ISRM T and ASTM D 2664	NBR	7.96	Triaxial data	MO0311RCKPRPCS.003, MO0402DQRIRPPR.003	Drained test.
139.1	139.1	10		10	129.1	25.5	0.15	TSw1	Tptrn	ESF/ECRB/Borehole	USW NRG-7a	NRG-7/7A-344.4-SNL-B	344.4	25.4	50.8	saturated	22	2.0	1.00E-05		TP-219 ASTM D 2664 ISRM U	NBR	8.28	Triaxial data	MO0311RCKPRPCS.003, MO0402DQRIRPPR.003	Drained/undrained status unknown.
185	185	10		10	175	27.3	0.21	TSw1	Tptrn	ESF/ECRB/Borehole	USW NRG-7a	NRG-7/7A-344.4-SNL-A	344.4	25.4	50.8	saturated	22	2.0	1.00E-05		TP-219 ASTM D 2664 ISRM U	NBR	7.67	Triaxial data	MO0311RCKPRPCS.003, MO0402DQRIRPPR.003	Drained/undrained status unknown.
208.3	208.3	10		10	198.3	29.4	0.15	TSw1	Tptrn	ESF/ECRB/Borehole	USW NRG-7a	NRG-7/7A-344.4-SNL-D	344.4	25.4	50.8	saturated	22	2.0	1.00E-05		TP-219 ASTM D 2664 ISRM U	NBR	7.96	Triaxial data	MO0311RCKPRPCS.003, MO0402DQRIRPPR.003	Drained/undrained status unknown.
60.4	60.4	10		10	50.4	2	0.02	TSw1	Tptrn	ESF/ECRB/Borehole	USW SD-12	SD-12-429.2-SNL-A	429.2	50.8	101.6	saturated	22	2.0	1.00E-05		ISRM T and ASTM D 2664-86	NBR	8.73	Triaxial data	MO0311RCKPRPCS.003, MO0402DQRIRPPR.003	Drained/undrained status unknown.
102.9	102.9	10		10	92.9	25.6	0.22	TSw1	Tptrn	ESF/ECRB/Borehole	USW SD-12	SD-12-401.5-SNL-A	401.5	50.8	101.6	saturated	22	2.0	1.00E-05		ISRM T and ASTM D 2664-86	NER	2.86	Triaxial data	MO0311RCKPRPCS.003, MO0402DQRIRPPR.003	Drained/undrained status unknown.
124.6	124.6	10		10	114.6	25.8	0.20	TSw1	Tptrn	ESF/ECRB/Borehole	USW SD-12	SD-12-343.4-SNL-A	343.4	50.8	101.6	saturated	22	2.0	1.00E-05		ISRM T and ASTM D 2664-86	NER	6.02	Triaxial data	MO0311RCKPRPCS.003, MO0402DQRIRPPR.003	Drained/undrained status unknown.
129.3	129.3	10	0	10	119.3	25.6	0.30	TSw2	Tptpll	ESF/ECRB/Borehole	USW G-1	G1-1189.0 SL	1189.0	26.1	50.1 to 51.3	saturated	22	2.0	1.00E-05			SNL	6.6	Triaxial Data	MO0311RCKPRPCS.003, MO0402DQRIRPPR.003	Drained test.
107	107	10	0	10	97	14.1	0.21	TSw2	Tptpll	ESF/ECRB/Borehole	USW G-4	G4-965.2-B	965.2	25.32	50.88	saturated	22	2.0	1.00E-05			Terra Tek	11.0	Triaxial Data	MO0311RCKPRPCS.003, MO0402DQRIRPPR.003	Drained test.
257	257	10	0	10	247	32.7	0.28	TSw2	Tptpll	ESF/ECRB/Borehole	USW G-4	G4-965.2-E	965.2	25.32	50.88	saturated	22	2.0	1.00E-05			Terra Tek	9.6	Triaxial Data	MO0311RCKPRPCS.003, MO0402DQRIRPPR.003	Drained test.
216.9	216.9	10	0	10	206.9	29.6	0.20	TSw2	Tptpll	ESF/ECRB/Borehole	USW NRG-7a	NRG-7/7A-977.8-SNL-A	977.8	50.8	101.6	saturated	22	2.0	1.00E-05		ISRM T and ASTM D 2664	NBR	8.50	Triaxial Data	MO0311RCKPRPCS.003, MO0402DQRIRPPR.003	Drained test.
422	422	10	0	10	412	73	0.23	TSw2	Tptpln	ESF/ECRB/Borehole	UE-25 a #1	1250	1250.0	56	L:D = 2:1 or greater	ambient	22	2.0	1.00E-04			SNL		Triaxial Data	MO0311RCKPRPCS.003, MO0402DQRIRPPR.003	Drained test.
261.8	261.8	10	0	10	251.8	39.6	0.26	TSw2	Tptpln	ESF/ECRB/Borehole	USW NRG-7a	NRG-7/7A-1400.5-SNL-B	1400.5	50.8	101.6	saturated	22	2.0	1.00E-05		ISRM T and ASTM D 2664	NBR	8.05	Triaxial Data	MO0311RCKPRPCS.003, MO0402DQRIRPPR.003	Drained test.
288.9	288.9	10		10	278.9	32.9	0.21	TSw2	Tptpln	ESF/ECRB/Borehole	USW SD-12	SD-12-1118.9-SNL-B	1118.9	50.8	101.6	saturated	22	2.0	1.00E-05		ISRM T and ASTM D 2664-86	NBR	8.74	Triaxial Data	MO0311RCKPRPCS.003, MO0402DQRIRPPR.003	Drained/undrained status unknown.
246.1	246.1	10		10	236.1	34	0.23	TSw2	Tptpln	ESF/ECRB/Borehole	USW SD-12	SD-12-1077.1-SNL-B	1077.1	50.8	101.6	saturated	22	2.0	1.00E-05		ISRM T and ASTM D 2664-86	NBR	8.00	Triaxial Data	MO0311RCKPRPCS.003, MO0402DQRIRPPR.003	Drained/undrained status unknown.

Table A-1 Intact Rock Mechanical Properties Data - Strength and Elastic Properties Data

Axial Stress, σ_1 (MPa)	Axial Stress, effective σ_1' (MPa)	Confining Pressure (MPa) σ_3	Pore Pressure (MPa)	Confining Pressure, Effective (MPa), σ_3'	Differential Strength, (MPa) σ_1-σ_3	Young's Modulus (GPa)	Poisson's Ratio	TM Unit	Litho-stratigraphic Unit	General Location	Sample Location	Specimen Number	Depth (ft)	Specimen Diameter (mm)	Specimen Length (mm)	Specimen Saturation	Specimen Temperature (deg. C)	l/d Ratio	Strain Rate (1/s)	Specimen Orientation (degree)	Test Standard	Laboratory	Failure Strain (millistrain)	Rock Property	Source DTN	Notes
274.5	269.5	15	5	10	264.5	43.9	0.12	TSw2	Tptpln	ESF/ECRB/Borehole	USW SD-9	SD-9-1325.4-SNL-A	1325.4	50.8	101.6	saturated	150	2.0	1.00E-06		ISRM T and ASTM D 2664-86	NBR	7.51	Triaxial Data	MO0311RCKPRPCS.003, MO0402DQRIRPPR.003	Undrained test w/ const. Pore pressure of 5 MPa.
163.6	163.6	10	0	10	153.6			TSw2	Tptpmn	Busted Butte	Busted Butte	10AE3Z		50.8	101.6	saturated	22	2.0	1.00E-05			SNL	N/A	Triaxial Data	MO0311RCKPRPCS.003, MO0402DQRIRPPR.003	Drained test.
49.7	49.7	10	0	10	39.7	21.7	0.11	TSw2	Tptpmn	Busted Butte	Busted Butte	10-AE-8Y		50	100	saturated	20	2.0	1.00E-05			RE/SPEC	2.37	Triaxial Data	MO0311RCKPRPCS.003, MO0402DQRIRPPR.003	Drained test.
171	171	10	0	10	161	28.07	0.12	TSw2	Tptpmn	Busted Butte	Busted Butte	10/AE/18/Z		50.8	101.6	saturated	22	2.0	1.03E-05			Terra Tek	N/A	Triaxial Data	MO0311RCKPRPCS.003, MO0402DQRIRPPR.003	Drained test.
191.6	191.6	10	0	10	181.6	29.7	0.15	TSw2	Tptpmn	Busted Butte	Busted Butte	10-AE-12Y		50	100	saturated	20	2.0	1.00E-05			RE/SPEC	7.74	Triaxial Data	MO0311RCKPRPCS.003, MO0402DQRIRPPR.003	Drained test.
127.3	127.3	10	0	10	117.3	30	0.18	TSw2	Tptpmn	Busted Butte	Busted Butte	10AE15Y		50.8	101.6	saturated	22	2.0	1.00E-05			SNL	4.6	Triaxial Data	MO0311RCKPRPCS.003, MO0402DQRIRPPR.003	Drained test.
191	191	10	0	10	181	30.75	0.19	TSw2	Tptpmn	Busted Butte	Busted Butte	10/AE/10/Y		50.8	101.6	saturated	22	2.0	9.83E-06			Terra Tek	N/A	Triaxial Data	MO0311RCKPRPCS.003, MO0402DQRIRPPR.003	Drained test.
196.5	196.5	10	0	10	186.5	32.5	0.19	TSw2	Tptpmn	Busted Butte	Busted Butte	10AE12Z		50.8	101.6	saturated	22	2.0	1.00E-05			SNL	7.6	Triaxial Data	MO0311RCKPRPCS.003, MO0402DQRIRPPR.003	Drained test.
115	115	10	0	10	105	32.72	0.21	TSw2	Tptpmn	Busted Butte	Busted Butte	10/AE/26/W		50.8	101.6	saturated	22	2.0	1.00E-05			Terra Tek	N/A	Triaxial Data	MO0311RCKPRPCS.003, MO0402DQRIRPPR.003	Drained test.
198	198	10	0	10	188	32.8	0.18	TSw2	Tptpmn	Busted Butte	Busted Butte	10AE50Y		50.8	101.6	dry	22	2.0	1.00E-05			SNL	7.7	Triaxial Data	MO0311RCKPRPCS.003, MO0402DQRIRPPR.003	Drained test.
203.3	203.3	10	0	10	193.3	32.9	0.18	TSw2	Tptpmn	Busted Butte	Busted Butte	10AE20Z		50.8	101.6	saturated	22	2.0	1.00E-05			SNL	8.7	Triaxial Data	MO0311RCKPRPCS.003, MO0402DQRIRPPR.003	Drained test.
230.1	230.1	10	0	10	220.1	33	0.14	TSw2	Tptpmn	Busted Butte	Busted Butte	10-AE-14Y		50	100	saturated	20	2.0	1.00E-05			RE/SPEC	7.75	Triaxial Data	MO0311RCKPRPCS.003, MO0402DQRIRPPR.003	Drained test.
192.8	192.8	10	0	10	182.8	33.1	0.24	TSw2	Tptpmn	Busted Butte	Busted Butte	10AE43W		50.8	101.6	dry	22	2.0	1.00E-05			SNL	9.7	Triaxial Data	MO0311RCKPRPCS.003, MO0402DQRIRPPR.003	Drained test.
122	122	10	0	10	112	34.6	0.13	TSw2	Tptpmn	Busted Butte	Busted Butte	BB-10-AE-49Y		50.8	101.60	dry	150	2.0	1.00E-05		RSI TP-04e	RE/SPEC	3.18	Triaxial Data	MO0311RCKPRPCS.003, MO0402DQRIRPPR.003	Effective confining pressure shown.
161.7	161.7	10	0	10	151.7	35.2	0.19	TSw2	Tptpmn	Busted Butte	Busted Butte	10AE42X		50.8	101.6	saturated	22	2.0	1.00E-05			SNL	6.0	Triaxial Data	MO0311RCKPRPCS.003, MO0402DQRIRPPR.003	Drained test.
229	229	10	0	10	219	37.2	0.14	TSw2	Tptpmn	Busted Butte	Busted Butte	BB-10-AE-13Y		50.8	101.60	dry	150	2.0	1.00E-05		RSI TP-04e	R/E/SPEC	7.15	Triaxial Data	MO0311RCKPRPCS.003, MO0402DQRIRPPR.003	Effective confining pressure shown.
238	238	10	0	10	228	37.5	0.16	TSw2	Tptpmn	Busted Butte	Busted Butte	BB-10-AE-43X		50.8	101.60	dry	150	2.0	1.00E-05		RSI TP-04e	RE/SPEC	6.58	Triaxial Data	MO0311RCKPRPCS.003, MO0402DQRIRPPR.003	Effective confining pressure shown.
314.5	314.5	10	0	10	304.5	40.8	0.19	TSw2	Tptpmn	Busted Butte	Busted Butte	10AE25Z		50.8	101.6	dry	22	2.0	1.00E-05			SNL	8.1	Triaxial Data	MO0311RCKPRPCS.003, MO0402DQRIRPPR.003	Drained test.
370	370	10	0	10	360	3.5	0.25	TSw2	Tptpmn	ESF/ECRB/Borehole	USW G-4	G4-686.6-F	686.6	25.35	50.90	saturated	22	2.0	1.00E-05			Terra Tek	11.8	Triaxial Data	MO0311RCKPRPCS.003, MO0402DQRIRPPR.003	Drained test.
354	354	10	0	10	344	3.8	0.23	TSw2	Tptpmn	ESF/ECRB/Borehole	USW G-4	G4-686.6-C	686.6	25.32	50.88	saturated	22	2.0	1.00E-05			Terra Tek	10.8	Triaxial Data	MO0311RCKPRPCS.003, MO0402DQRIRPPR.003	Drained test.
147.1	147.1	10	0	10	137.1	21.4	0.27	TSw2	Tptpmn	ESF/ECRB/Borehole	USW NRG-7a	NRG-7/7A-805.6-SNL-A	805.6	50.8	101.6	saturated	22	2.0	1.00E-05		ISRM T and ASTM D 2664	NBR	5.05	Triaxial Data	MO0311RCKPRPCS.003, MO0402DQRIRPPR.003	Drained test.
135.3	135.3	10	0	10	125.3	23.4	0.33	TSw2	Tptpmn	ESF/ECRB/Borehole	USW NRG-7a	NRG-7/7A-827.4-SNL-A	827.4	50.8	101.6	saturated	22	2.0	1.00E-05		ISRM T and ASTM D 2664	NBR	6.46	Triaxial Data	MO0311RCKPRPCS.003, MO0402DQRIRPPR.003	Drained test.
235.5	235.5	10		10	225.5	32	0.25	TSw2	Tptpmn	ESF/ECRB/Borehole	USW NRG-7a	NRG-7/7A-865.4-SNL-D	865.4	25.4	50.8	saturated	22	2.0	1.00E-05			NBR	8.18	Triaxial Data	MO0311RCKPRPCS.003, MO0402DQRIRPPR.003	Drained/undrained status unknown.
325.2	325.2	10		10	315.2	32.3	0.19	TSw2	Tptpmn	ESF/ECRB/Borehole	USW NRG-7a	NRG-7/7A-865.4-SNL-A	865.4	25.4	50.8	saturated	22	2.0	1.00E-05			NBR	12.24	Triaxial Data	MO0311RCKPRPCS.003, MO0402DQRIRPPR.003	Drained/undrained status unknown.
354	354	10		10	344.0	34	0.21	TSw2	Tptpmn	ESF/ECRB/Borehole	USW NRG-7a	NRG-7/7A-865.4-SNL-B	865.4	25.4	50.8	saturated	22	2.0	1.00E-05			NBR	11.80	Triaxial Data	MO0311RCKPRPCS.003, MO0402DQRIRPPR.003	Drained/undrained status unknown.
316.7	316.7	10		10	306.7	34.1	0.22	TSw2	Tptpmn	ESF/ECRB/Borehole	USW NRG-7a	NRG-7/7A-865.4-SNL-E	865.4	25.4	50.8	saturated	22	2.0	1.00E-05			NBR	9.84	Triaxial Data	MO0311RCKPRPCS.003, MO0402DQRIRPPR.003	Drained/undrained status unknown.
282.8	282.8	10		10	272.8	34.1	0.20	TSw2	Tptpmn	ESF/ECRB/Borehole	USW SD-12	SD-12-762.6-SNL-B	762.6	50.8	101.6	saturated	22	2.0	1.00E-05		ISRM T and ASTM D 2664-86	NER	8.80	Triaxial Data	MO0311RCKPRPCS.003, MO0402DQRIRPPR.003	Drained/undrained status unknown.
243.5	238.5	15	5	10	233.5	27.7	0.20	TSw2	Tptpmn	ESF/ECRB/Borehole	USW SD-9	SD-9-828.9-SNL-B	828.9	50.8	101.6	saturated	150	2.0	1.00E-06		ISRM T and ASTM D 2664-86	NER	11.09	Triaxial Data	MO0311RCKPRPCS.003, MO0402DQRIRPPR.003	Undrained test w/ constant Pore pressure of 5 MPa.
214.7	209.7	15	5	10	204.7	29.7	0.17	TSw2	Tptpmn	ESF/ECRB/Borehole	USW SD-9	SD-9-836.3-SNL-B	836.3	50.8	101.6	saturated	150	2.0	1.00E-06		ISRM T and ASTM D 2664-86	NER	8.29	Triaxial Data	MO0311RCKPRPCS.003, MO0402DQRIRPPR.003	Undrained test w/ constant Pore pressure of 5 MPa.
205.8	200.8	15	5	10	195.8	31	0.18	TSw2	Tptpmn	ESF/ECRB/Borehole	USW SD-9	SD-9-766.0-SNL-A	766.0	50.8	101.6	saturated	150	2.0	1.00E-06		ISRM T and ASTM D 2664-86	NER	6.8	Triaxial Data	MO0311RCKPRPCS.003, MO0402DQRIRPPR.003	Undrained test w/ constant Pore pressure of 5 MPa.
329.4	324.4	15	5	10	319.4	34.5	0.22	TSw2	Tptpmn	ESF/ECRB/Borehole	USW SD-9	SD-9-817.1-SNL-A	817.1	50.8	101.6	saturated	150	2.0	1.00E-06		ISRM T and ASTM D 2664-86	NER	10.76	Triaxial Data	MO0311RCKPRPCS.003, MO0402DQRIRPPR.003	Undrained test w/ constant Pore pressure of 5 MPa.
275.9	270.9	15	5	10	265.9	34.6	0.22	TSw2	Tptpmn	ESF/ECRB/Borehole	USW SD-9	SD-9-775.8-SNL-A	775.8	50.8	101.6	saturated	150	2.0	1.00E-06		ISRM T and ASTM D 2664-86	NBR	9.54	Triaxial Data	MO0311RCKPRPCS.003, MO0402DQRIRPPR.003	Undrained test w/ constant Pore pressure of 5 MPa.
37	37	10	0	10	27			TSw3	Tptpv3	ESF/ECRB/Borehole	USW G-2	G2-1646.8-C	1646.8	25.3	50.8	saturated	22	2.0	1.00E-05			Terra Tek	5.0	Triaxial data	MO0311RCKPRPCS.003	Drained test.
42	42	10	0	10	32			TSw3	Tptpv3	ESF/ECRB/Borehole	USW G-2	G2-1646.8-B	1646.8	25.3	50.8	saturated	22	2.0	1.00E-05			Terra Tek	3.8	Triaxial data	MO0311RCKPRPCS.003	Drained test.
63	63	10	0	10	53			TSw3	Tptpv3	ESF/ECRB/Borehole	USW G-2	G2-1659.2-B	1659.2	25.3	50.8	saturated	22	2.0	1.00E-05			Terra Tek	4.6	Triaxial data	MO0311RCKPRPCS.003	Drained test.
78	78	10	0	10	68			TSw3	Tptpv3	ESF/ECRB/Borehole	USW G-2	G2-1659.2-A	1659.2	25.3	50.9	saturated	22	2.0	1.00E-05			Terra Tek	5.3	Triaxial Test	MO0311RCKPRPCS.003	Drained test.
80	80	10		10	70	32.9	0.17	TSw3	Tptpv3	ESF/ECRB/Borehole	USW SD-12	SD-12-1284.2-SNL-A	1284.2	50.8	101.6	saturated	22	2.0	1.00E-05		ISRM T and ASTM D 2664-86	NBR	8.59	Triaxial data	MO0311RCKPRPCS.003, MO0402DQRIRPPR.003	Drained/undrained status unknown.
95.5	90.5	17.5	5	12.5	83	17.8		CFUn	Tcbm	ESF/ECRB/Borehole	USW G-1	6 758.9-759.2	2490-2491	25.4	50.8	saturated	200	2.0	1.00E-04			SNL		Triaxial data	MO0311RCKPRPCS.003, MO0402DQRIRPPR.003	Pore fluids pressure (MPa) = 5.
206.9	206.9	13.8		13.8	193.1			TCw	Tpcpmn	ESF/ECRB/Borehole	UE-25 NRG-1	136.8-144.4FT.-01,-01	136.8-144.4	61.1	129.0	ambient	22	2.1	1.00E-04		ASTM D 2664-86	USBR	14	Triaxial data	MO0311RCKPRPCS.003	Drained/undrained status unknown.
170.3	170.3	13.8		13.8	156.5			TCw	Tpcpul	ESF/ECRB/Borehole	UE-25 NRG-1	80.8-89.5FT.,-02,-01	80.8-89.5	61.2	127.6	ambient	22	2.1	1.00E-04		ASTM D 2664-86	USBR	9	Triaxial data	MO0311RCKPRPCS.003	Drained/undrained status unknown.
165	165	20	0	20	145	19.24	0.23	CFUn	Tcbm	ESF/ECRB/Borehole	UE-25 a #1	2421	2421.0	56	L:D = 2:1	ambient	22	2.0	1.00E-04			SNL		Triaxial data	MO0311RCKPRPCS.003, MO0402DQRIRPPR.003	Drained test.
196	196	20	0	20	176	27.01	0.20	CFUn	Tcpm	ESF/ECRB/Borehole	UE-25 a #1	1968	1968.0	56	L:D = 2:1	ambient	22	2.0	1.00E-04			SNL		Triaxial data	MO0311RCKPRPCS.003, MO0402DQRIRPPR.003	Drained test.
46.1	46.1	20	0	20	26.1	7.99	0.22	CHn	Tac	ESF/ECRB/Borehole	UE-25 a #1	1605	1605.0	56	L:D = 2:1	ambient	22	2.0	1.00E-04			SNL		Triaxial data	MO0311RCKPRPCS.003, MO0402DQRIRPPR.003	Drained test.
90.3	90.3	20	0	20	70.3	9.57	0.25	CHn	Tac	ESF/ECRB/Borehole	UE-25 a #1	1662	1662.0	56	L:D = 2:1	ambient	22	2.0	1.00E-04			SNL		Triaxial data	MO0311RCKPRPCS.003, MO0402DQRIRPPR.003	Drained test.
37.1	37.1	20	0	20	17.1	3.92	0.18	CHn	Tac	ESF/ECRB/Borehole	USW G-1	G11487.4 SL6	1487.4	25.4	50.0-51.3	saturated	22	2.0	1.00E-05			SNL	7.1	Triaxial data	MO0311RCKPRPCS.003, MO0402DQRIRPPR.003	Drained test.
54.4	54.4	20	0	20	34.4	6.24	0.17	CHn	Tac	ESF/ECRB/Borehole	USW G-1	G11487.4 SL6A	1487.4	25.4	50.0-51.3	saturated	22	2.0	1.00E-05			SNL	6.4	Triaxial data	MO0311RCKPRPCS.003, MO0402DQRIRPPR.003	Drained test.
895	895	20	0	20	875	58.3	0.22	TCw	Tpcpln	ESF/ECRB/Borehole	UE-25 a #1	87.6	87.6	56	L:D = 2:1	ambient	22	2.0	1.00E-04			SNL		Triaxial data	MO0311RCKPRPCS.003, MO0402DQRIRPPR.003	Drained test.
638	638	20	0	20	618	59.9	0.21	TSw2	Tptpln	ESF/ECRB/Borehole	UE-25 a #1	1250	1250.0	56	L:D = 2:1 or greater	ambient	22	2.0	1.00E-04			SNL		Triaxial Data	MO0311RCKPRPCS.003, MO0402DQRIRPPR.003	Drained test.
176.3	176.3	20	0	20	156.3	19.8	0.20	TSw2	Tptpmn	Busted Butte	Busted Butte	10-AE-47Z		50	100	saturated	20	2.0	1.00E-05			R/E/SPEC	7.77	Triaxial Data	MO0311RCKPRPCS.003, MO0402DQRIRPPR.003	Drained test.
212	212	20	0	20	192	28.38	0.16	TSw2	Tptpmn	Busted Butte	Busted Butte	10/AE/15/X		50.8	101.6	saturated	22	2.0	1.18E-05			Terra Tek	N/A	Triaxial Data	MO0311RCKPRPCS.003, MO0402DQRIRPPR.003	Drained test.
232	232	20	0	20	212	29.58	0.20	TSw2	Tptpmn	Busted Butte	Busted Butte	10/AE/9/W		50.8	101.6	saturated	22	2.0	9.65E-06			Terra Tek	N/A	Triaxial Data	MO0311RCKPRPCS.003, MO0402DQRIRPPR.003	Drained test.
180	180	20	0	20	160	31.17	0.21	TSw2	Tptpmn	Busted Butte	Busted Butte	10/AE/42/W		50.8	101.6	saturated	22	2.0	9.12E-06			Terra Tek	N/A	Triaxial Data	MO0311RCKPRPCS.003, MO0402DQRIRPPR.003	Drained test.
272.4	272.4	20	0	20	252.4	31.5	0.15	TSw2	Tptpmn	Busted Butte	Busted Butte	10-AE-15W		50	100	saturated	20	2.0	1.00E-05			R/E/SPEC	10.18	Triaxial Data	MO0311RCKPRPCS.003, MO0402DQRIRPPR.003	Drained test.
160.7	160.7	20.7	0	20.7	140	22.1	0.28	CFUn	Tcbm	ESF/ECRB/Borehole	UE-25 a #1	2491	2491.0	56	L:D = 2:1	ambient	22	2.0	1.00E-04			SNL		Triaxial data	MO0311RCKPRPCS.003, MO0402DQRIRPPR.003	Drained test.
106.7	103.3	24.1	3.4	20.7	86	13.8		CFUn	Tcbm	ESF/ECRB/Borehole	USW G-1	1 758.9-759.2	2490-2491	25.4	50.8	saturated	200	2.0	1.00E-04			SNL		Triaxial data	MO0311RCKPRPCS.003, MO0402DQRIRPPR.003	Pore fluids pressure (MPa) = 3.4.
139.7	139.7	20.7	0	20.7	119	17.6		CFUn	Tcbm	ESF/ECRB/Borehole	USW G-1	2 758.9-759.2	2490-2491	25.4	50.8	dry	200	2.0	1.00E-04			SNL		Triaxial data	MO0311RCKPRPCS.003, MO0402DQRIRPPR.003	Drained test.
168.7	168.7	20.7	0	20.7	148	20.5		CFUn	Tcbm	ESF/ECRB/Borehole	USW G-1	5 758.9-759.2	2490-2491	25.4	50.8	dry	200	2.0	1.00E-04			SNL		Triaxial data	MO0311RCKPRPCS.003, MO0402DQRIRPPR.003	Drained test.
227.7	227.7	20.7	0	20.7	207	31	0.25	CFUn	Tcpm	ESF/ECRB/Borehole	UE-25 a #1	1985	1985.0	56	L:D = 2:1	ambient	22	2.0	1.00E-04			SNL		Triaxial data	MO0311RCKPRPCS.003, MO0402DQRIRPPR.003	Drained test.
88.2	88.2	20.7	0	20.7	67.5	8.5	0.27	CHn	Tac	ESF/ECRB/Borehole	UE-25 a #1	1634	1634.0	56	L:D = 2:1	ambient	22	2.0	1.00E-04			SNL		Triaxial data	MO0311RCKPRPCS.003, MO0402DQRIRPPR.003	Drained test.
125.7	125.7	20.7	0	20.7	105			TCw	Tpcpln	ESF/ECRB/Borehole	UE-25 a #1	185	185.0	56	L:D = 2:1	ambient	200	2.0	1.00E-04			SNL		Triaxial data	MO0311RCKPRPCS.003, MO0402DQRIRPPR.003	Drained test.
153.7	153.7	20.7		20.7	133	23.9	0.15	TSw2	Tptpmn	ESF/ECRB/Borehole	UE-25 a #1	739	739.0	56	L:D = 2:1	ambient	200	2.0	1.00E-04			SNL		Triaxial Data	MO0311RCKPRPCS.003, MO0402DQRIRPPR.003	Drained test.
433	433	27.6		27.6	405.4			TCw	Tpcpmn	ESF/ECRB/Borehole	UE-25 NRG-1	136.8-144.4FT.-02,-01	136.8-144.4	61.2	123.9	ambient	22	2.0	1.00E-04		ASTM D 2664-86	USBR	13	Triaxial data	MO0311RCKPRPCS.003	Drained/undrained status unknown.

Table A-1 Intact Rock Mechanical Properties Data - Strength and Elastic Properties Data

Axial Stress, σ_1 (MPa)	Axial Stress, effective σ_1' (MPa)	Confining Pressure (MPa) σ_3	Pore Pressure (MPa)	Confining Pressure, Effective (MPa), σ_3'	Differential Strength, (MPa) $\sigma_1'-\sigma_3'$	Young's Modulus (GPa)	Poisson's Ratio	TM Unit	Litho-stratigraphic Unit	General Location	Sample Location	Specimen Number	Depth (ft)	Specimen Diameter (mm)	Specimen Length (mm)	Specimen Saturation	Specimen Temperature (deg. C)	l/d Ratio	Strain Rate (1/s)	Specimen Orientation (degree)	Test Standard	Laboratory	Failure Strain (millistrain)	Rock Property	Source DTN	Notes
227.6	227.6	27.6		27.6	200.0			TCw	Tpcpul	ESF/ECRB/Borehole	UE-25 NRG-1	89.5-97.8FT.-03,-02	89.5-97.8	61.1	130.7	ambient	22	2.1	1.00E-04		ASTM D 2664-86	USBR	13	Triaxial data	MO0311RCKPRPCS.003	Drained/undrained status unknown.
233.1	233.1	41.4		41.4	191.7			TCw	Tpcpmn	ESF/ECRB/Borehole	UE-25 NRG-1	136.8-144.4FT.-03,-01	136.8-144.4	61.2	132.9	ambient	22	2.2	1.00E-04		ASTM D 2664-86	USBR	9	Triaxial data	MO0311RCKPRPCS.003	Drained/undrained status unknown
253.8	253.8	41.4		41.4	212.4			TCw	Tpcpul	ESF/ECRB/Borehole	UE-25 NRG-1	80.8-89.5FT.-03,-01	80.8-89.5	61.2	138.1	ambient	22	2.3	1.00E-04		ASTM D 2664-86	USBR	11	Triaxial data	MO0311RCKPRPCS.003	Drained/undrained status unknown. Membrane leaked prior to failure.
224	224	50	0	50	174	18.74	0.19	CFUn	Tduc	ESF/ECRB/Borehole	UE-25 a #1	2401	2401.0	56	L:D = 2:1	ambient	22	2.0	1.00E-04			SNL		Triaxial data	MO0311RCKPRPCS.003, MO0402DQRIRPPR.003	Drained test.
399	399	100	0	100	299	21.95	0.20	CFUn	Tcprn	ESF/ECRB/Borehole	UE-25 a #1	1948	1948.0	56	L:D = 2:1	ambient	22	2.0	1.00E-04			SNL		Triaxial data	MO0311RCKPRPCS.003, MO0402DQRIRPPR.003	Drained test.
N/A	N/A	10	N/A	N/A	18.9	4.28		CHn	Tac	ESF/ECRB/Borehole	USW G-1	G11668.1 SL24C	1668.1	25.4	50.0-51.3	saturated	22	2.0	1.00E-05			SNL	4.9	Triaxial data	MO0311RCKPRPCS.003, MO0402DQRIRPPR.003	Undrained test without pore pressure monitoring.
N/A	N/A	10	N/A	N/A	26.8	6.01	0.36	CHn	Tac	ESF/ECRB/Borehole	USW G-1	G11668.1 SL24D	1668.1	25.4	50.0-51.3	saturated	22	2.0	1.00E-05			SNL	5.7	Triaxial data	MO0311RCKPRPCS.003, MO0402DQRIRPPR.003	Undrained test without pore pressure monitoring.
N/A	N/A	10	N/A	N/A	25.4	6.85	0.34	CHn	Tac	ESF/ECRB/Borehole	USW G-1	G11487.4 SL3	1487.4	25.4	50.0-51.3	saturated	22	2.0	1.00E-05			SNL	4.5	Triaxial data	MO0311RCKPRPCS.003, MO0402DQRIRPPR.003	Undrained test without pore pressure monitoring.
N/A	N/A	10	N/A	N/A	61.3	7.2	0.27	CHn	Tac	ESF/ECRB/Borehole	USW G-1	G11665.5 SL12	1665.5	25.4	50.0-51.3	ambient	22	2.0	1.00E-05			SNL	11	Triaxial data	MO0311RCKPRPCS.003, MO0402DQRIRPPR.003	Undrained test without pore pressure monitoring.
N/A	N/A	10	N/A	N/A	57.6	7.34	0.28	CHn	Tac	ESF/ECRB/Borehole	USW G-1	G11665.5 SL12A	1665.5	25.4	50.0-51.3	ambient	22	2.0	1.00E-05			SNL	9.9	Triaxial data	MO0311RCKPRPCS.003, MO0402DQRIRPPR.003	Undrained test without pore pressure monitoring.
N/A	N/A	20	N/A	N/A	26.7	7.38	0.45	CHn	Tac	ESF/ECRB/Borehole	USW G-1	G11487.4 SL4	1487.4	25.4	50.0-51.3	saturated	22	2.0	1.00E-05			SNL	5.0	Triaxial data	MO0311RCKPRPCS.003, MO0402DQRIRPPR.003	Undrained test without pore pressure monitoring.
N/A	N/A	10	N/A	N/A	26	7.79	0.34	CHn	Tac	ESF/ECRB/Borehole	USW G-1	G11487.4 SL3A	1487.4	25.4	50.0-51.3	saturated	22	2.0	1.00E-05			SNL	4.1	Triaxial data	MO0311RCKPRPCS.003, MO0402DQRIRPPR.003	Undrained test without pore pressure monitoring.
N/A	N/A	20	N/A	N/A	36.1	7.93		CHn	Tac	ESF/ECRB/Borehole	USW G-1	G11487.4 SL4A	1487.4	25.4	50.0-51.3	saturated	22	2.0	1.00E-05			SNL	5.2	Triaxial data	MO0311RCKPRPCS.003, MO0402DQRIRPPR.003	Undrained test without pore pressure monitoring.
N/A	N/A	10	N/A	N/A	27.6	8.48	0.30	CHn	Tac	ESF/ECRB/Borehole	USW G-1	G11665.5 SL9A	1665.5	25.4	50.0-51.3	saturated	22	2.0	1.00E-05			SNL	5.9	Triaxial data	MO0311RCKPRPCS.003, MO0402DQRIRPPR.003	Undrained test without pore pressure monitoring.
N/A	N/A	10	N/A	N/A	35.7	8.9	0.31	CHn	Tac	ESF/ECRB/Borehole	USW G-1	G11665.5 SL9	1665.5	25.4	50.0-51.3	saturated	22	2.0	1.00E-05			SNL	5.0	Triaxial data	MO0311RCKPRPCS.003, MO0402DQRIRPPR.003	Undrained test without pore pressure monitoring.
N/A	N/A	20	N/A	N/A	34.8	9.31		CHn	Tac	ESF/ECRB/Borehole	USW G-1	G11665.5 SL10	1665.5	25.4	50.0-51.3	saturated	22	2.0	1.00E-05			SNL	5.4	Triaxial data	MO0311RCKPRPCS.003, MO0402DQRIRPPR.003	Undrained test without pore pressure monitoring.
N/A	N/A	20	N/A	N/A	36.2	9.72	0.25	CHn	Tac	ESF/ECRB/Borehole	USW G-1	G11665.5 SL10A	1665.5	25.4	50.0-51.3	saturated	22	2.0	1.00E-05			SNL	4.9	Triaxial data	MO0311RCKPRPCS.003, MO0402DQRIRPPR.003	Undrained test without pore pressure monitoring.
N/A	N/A	5	N/A	N/A	72.5	19.2	0.14	TSw2	Tptpll	ESF/ECRB/Borehole	USW G-1	G1-1154.9 SLB	1154.9	26.1	50.1 to 51.3	saturated	22	2.0	1.00E-05			SNL	5.9	Triaxial Data	MO0311RCKPRPCS.003, MO0402DQRIRPPR.003	Undrained test.
N/A	N/A	5	N/A	N/A	219.3	35.6	0.30	TSw2	Tptpll	ESF/ECRB/Borehole	USW G-1	G1-1163.6 SL	1163.6	26.1	50.1 to 51.3	saturated	2:2	2.0	1.00E-05			SNL	7.4	Triaxial Data	MO0311RCKPRPCS.003, MO0402DQRIRPPR.003	Undrained test.
217.23174	212.73174	5	4.5	0.5	216.73174	42.2	0.30	TSw2	Tptpmn	ESF/HD	ESF-HD-WH-38-117-A	01025484	NA	50.8254	101.6508	saturated	125	2.0	1.00E-06			NER	8.52	Unaxial Data	SN0505L0212303.005	Undrained test
166.07864	161.57864	5	4.5	0.5	165.57864	32.7	0.15	TSw2	Tptpmn	ESF/HD	ESF-HD-WH-39-9.0-A	01025492	NA	50.8254	101.6254	saturated	125	2.0	1.00E-06			NER	5.64	Unaxial Data	SN0505L0212303.005	Undrained test
203.5	199	5	4.5	0.5	203	39.7	0.23	TSw2	Tptpmn	ESF/HD	ESF-HD-WH-40-10.8-A	01025491	NA	50.7492	101.473	saturated	125	2.0	1.00E-06			NER	4.87	Unaxial Data	SN0505L0212303.005	Undrained test
184.5	180	5	4.5	0.5	184	35.9	0.18	TSw2	Tptpmn	ESF/HD	ESF-HD-WH-40-28.4-A	01025503	NA	50.7492	101.7016	saturated	125	2.0	1.00E-06			NER	5.51	Unaxial Data	SN0505L0212303.005	Undrained test
229.5	225	5	4.5	0.5	229	41.1	0.24	TSw2	Tptpmn	ESF/HD	ESF-HD-WH-44-16.9-A	01025508	NA	50.7492	101.5492	saturated	125	2.0	1.00E-06			NER	7.58	Unaxial Data	SN0505L0212303.005	Undrained test
214.5	210	5	4.5	0.5	214	36.3	0.16	TSw2	Tptpmn	ESF/HD	ESF-HD-WH-4394-4-A	01025522	NA	50.8254	101.5746	saturatec	125	2.0	1.00E-06			NER	6.03	Unaxial Dat	SN0505L0212303.005	Undrained test

Notes: The data from G-Tunnel and CFun unit are presented in this table; however, these data are not used in the analysis.
All blanks, N/A, NA, or "-" are indicating that either the formation is not available or not applicable unless otherwise specified.

Table A-2. Intact Rock Mechanical Properties Data - Dynamic Elastic Data

Dynamic Young's Modulus (GPa)	Dynamic Poisson's Ratio	TM Unit	Litho-stratigraphic Unit	Sample Location	Specimen Number	Test Standard	Laboratory	Specimen Diameter (mm)	Specimen Length (mm)	Specimen Saturation	Specimen Temperature (deg. C)	L/D Ratio	Strain Rate (1/s)	Confining Pressure /Normal Stress (MPa)	DTN	Notes
8.31	0.010	CFUn	Tcplc	UE-25 UZ#16	25096 (-1667.8)	ultrasonic pulse	PBT, Inc.	25.4	51.84	Air	ambient	2.04	NA	0.7	MO0402DQRIRPPR.003	
8.35	0.011	CFUn	Tcplc	UE-25 UZ#16	25096 (-1667.8)	ultrasonic pulse	PBT, Inc.	25.4	51.84	Air	ambient	2.04	NA	0.7	MO0402DQRIRPPR.003	
9.42	0.057	CFUn	Tcplc	UE-25 UZ#16	25096 (-1667.8)	ultrasonic pulse	PBT, Inc.	25.4	51.84	Air	ambient	2.04	NA	2.1	MO0402DQRIRPPR.003	
10.70	0.096	CFUn	Tcplc	UE-25 UZ#16	25096 (-1667.8)	ultrasonic pulse	PBT, Inc.	25.4	51.84	Air	ambient	2.04	NA	4.1	MO0402DQRIRPPR.003	
11.60	0.108	CFUn	Tcplc	UE-25 UZ#16	25096 (-1667.8)	ultrasonic pulse	PBT, Inc.	25.4	51.84	Air	ambient	2.04	NA	6.9	MO0402DQRIRPPR.003	
9.92	0.370	CFUn	Tcplc	UE-25 UZ#16	25096 (-1667.8)	ultrasonic pulse	PBT, Inc.	25.4	51.84	Wtr	ambient	2.04	NA	0.7	MO0402DQRIRPPR.003	
10.00	0.370	CFUn	Tcplc	UE-25 UZ#16	25096 (-1667.8)	ultrasonic pulse	PBT, Inc.	25.4	51.84	Wtr	ambient	2.04	NA	0.7	MO0402DQRIRPPR.003	
10.10	0.366	CFUn	Tcplc	UE-25 UZ#16	25096 (-1667.8)	ultrasonic pulse	PBT, Inc.	25.4	51.84	Wtr	ambient	2.04	NA	2.1	MO0402DQRIRPPR.003	
10.20	0.366	CFUn	Tcplc	UE-25 UZ#16	25096 (-1667.8)	ultrasonic pulse	PBT, Inc.	25.4	51.84	Wtr	ambient	2.04	NA	4.1	MO0402DQRIRPPR.003	
10.40	0.365	CFUn	Tcplc	UE-25 UZ#16	25096 (-1667.8)	ultrasonic pulse	PBT, Inc.	25.4	51.84	Wtr	ambient	2.04	NA	6.9	MO0402DQRIRPPR.003	
12.90		CFUn	Tcplv	UE-25 UZ#16	25094 (-1681.8)	ultrasonic pulse	PBT, Inc.	25.4	89.29	Air	ambient	3.52	NA	0.7	MO0402DQRIRPPR.003	
13.00		CFUn	Tcplv	UE-25 UZ#16	25094 (-1681.8)	ultrasonic pulse	PBT, Inc.	25.4	89.29	Air	ambient	3.52	NA	0.7	MO0402DQRIRPPR.003	
15.40		CFUn	Tcplv	UE-25 UZ#16	25094 (-1681.8)	ultrasonic pulse	PBT, Inc.	25.4	89.29	Air	ambient	3.52	NA	2.1	MO0402DQRIRPPR.003	
17.00	0.033	CFUn	Tcplv	UE-25 UZ#16	25094 (-1681.8)	ultrasonic pulse	PBT, Inc.	25.4	89.29	Air	ambient	3.52	NA	4.1	MO0402DQRIRPPR.003	
18.30	0.043	CFUn	Tcplv	UE-25 UZ#16	25094 (-1681.8)	ultrasonic pulse	PBT, Inc.	25.4	89.29	Air	ambient	3.52	NA	6.9	MO0402DQRIRPPR.003	
15.60	0.332	CFUn	Tcplv	UE-25 UZ#16	25094 (-1681.8)	ultrasonic pulse	PBT, Inc.	25.4	89.29	Wtr	ambient	3.52	NA	0.7	MO0402DQRIRPPR.003	
15.50	0.334	CFUn	Tcplv	UE-25 UZ#16	25094 (-1681.8)	ultrasonic pulse	PBT, Inc.	25.4	89.29	Wtr	ambient	3.52	NA	0.7	MO0402DQRIRPPR.003	
15.70	0.327	CFUn	Tcplv	UE-25 UZ#16	25094 (-1681.8)	ultrasonic pulse	PBT, Inc.	25.4	89.29	Wtr	ambient	3.52	NA	2.1	MO0402DQRIRPPR.003	
16.60	0.314	CFUn	Tcplv	UE-25 UZ#16	25094 (-1681.8)	ultrasonic pulse	PBT, Inc.	25.4	89.29	Wtr	ambient	3.52	NA	4.1	MO0402DQRIRPPR.003	
17.90	0.291	CFUn	Tcplv	UE-25 UZ#16	25094 (-1681.8)	ultrasonic pulse	PBT, Inc.	25.4	89.29	Wtr	ambient	3.52	NA	6.9	MO0402DQRIRPPR.003	
26.00	0.098	CFUn	Tcpm	UE-25 UZ#16	25055 (-1611.2)	ultrasonic pulse	PBT, Inc.	25.4	89.1	Air	ambient	3.51	NA	0.7	MO0402DQRIRPPR.003	
26.70	0.122	CFUn	Tcpm	UE-25 UZ#16	25055 (-1611.2)	ultrasonic pulse	PBT, Inc.	25.4	89.1	Air	ambient	3.51	NA	0.7	MO0402DQRIRPPR.003	
37.30	0.175	CFUn	Tcpm	UE-25 UZ#16	25056 (-1627.2)	ultrasonic pulse	PBT, Inc.	25.4	98.72	Air	ambient	3.89	NA	0.7	MO0402DQRIRPPR.003	
37.70	0.166	CFUn	Tcpm	UE-25 UZ#16	25056 (-1627.2)	ultrasonic pulse	PBT, Inc.	25.4	98.72	Air	ambient	3.89	NA	0.7	MO0402DQRIRPPR.003	
27.30	0.126	CFUn	Tcpm	UE-25 UZ#16	25055 (-1611.2)	ultrasonic pulse	PBT, Inc.	25.4	89.1	Air	ambient	3.51	NA	2.1	MO0402DQRIRPPR.003	
38.50	0.140	CFUn	Tcpm	UE-25 UZ#16	25056 (-1627.2)	ultrasonic pulse	PBT, Inc.	25.4	98.72	Air	ambient	3.89	NA	2.1	MO0402DQRIRPPR.003	
27.90	0.150	CFUn	Tcpm	UE-25 UZ#16	25055 (-1611.2)	ultrasonic pulse	PBT, Inc.	25.4	89.1	Air	ambient	3.51	NA	4.1	MO0402DQRIRPPR.003	
40.20	0.134	CFUn	Tcpm	UE-25 UZ#16	25056 (-1627.2)	ultrasonic pulse	PBT, Inc.	25.4	98.72	Air	ambient	3.89	NA	4.1	MO0402DQRIRPPR.003	
28.40	0.156	CFUn	Tcpm	UE-25 UZ#16	25055 (-1611.2)	ultrasonic pulse	PBT, Inc.	25.4	89.1	Air	ambient	3.51	NA	6.9	MO0402DQRIRPPR.003	
41.10	0.126	CFUn	Tcpm	UE-25 UZ#16	25056 (-1627.2)	ultrasonic pulse	PBT, Inc.	25.4	98.72	Air	ambient	3.89	NA	6.9	MO0402DQRIRPPR.003	
28.60	0.281	CFUn	Tcpm	UE-25 UZ#16	25055 (-1611.2)	ultrasonic pulse	PBT, Inc.	25.4	89.1	Wtr	ambient	3.51	NA	0.7	MO0402DQRIRPPR.003	
28.00	0.288	CFUn	Tcpm	UE-25 UZ#16	25055 (-1611.2)	ultrasonic pulse	PBT, Inc.	25.4	89.1	Wtr	ambient	3.51	NA	0.7	MO0402DQRIRPPR.003	
39.10	0.286	CFUn	Tcpm	UE-25 UZ#16	25056 (-1627.2)	ultrasonic pulse	PBT, Inc.	25.4	98.72	Wtr	ambient	3.89	NA	0.7	MO0402DQRIRPPR.003	
39.20	0.286	CFUn	Tcpm	UE-25 UZ#16	25056 (-1627.2)	ultrasonic pulse	PBT, Inc.	25.4	98.72	Wtr	ambient	3.89	NA	0.7	MO0402DQRIRPPR.003	
28.90	0.274	CFUn	Tcpm	UE-25 UZ#16	25055 (-1611.2)	ultrasonic pulse	PBT, Inc.	25.4	89.1	Wtr	ambient	3.51	NA	2.1	MO0402DQRIRPPR.003	
41.60	0.254	CFUn	Tcpm	UE-25 UZ#16	25056 (-1627.2)	ultrasonic pulse	PBT, Inc.	25.4	98.72	Wtr	ambient	3.89	NA	2.1	MO0402DQRIRPPR.003	CT scan showed a large lithophysal cavity, causing the low value
29.60	0.265	CFUn	Tcpm	UE-25 UZ#16	25055 (-1611.2)	ultrasonic pulse	PBT, Inc.	25.4	89.1	Wtr	ambient	3.51	NA	4.1	MO0402DQRIRPPR.003	
41.60	0.255	CFUn	Tcpm	UE-25 UZ#16	25056 (-1627.2)	ultrasonic pulse	PBT, Inc.	25.4	98.72	Wtr	ambient	3.89	NA	4.1	MO0402DQRIRPPR.003	
30.00	0.266	CFUn	Tcpm	UE-25 UZ#16	25055 (-1611.2)	ultrasonic pulse	PBT, Inc.	25.4	89.1	Wtr	ambient	3.51	NA	6.9	MO0402DQRIRPPR.003	
41.70	0.253	CFUn	Tcpm	UE-25 UZ#16	25056 (-1627.2)	ultrasonic pulse	PBT, Inc.	25.4	98.72	Wtr	ambient	3.89	NA	6.9	MO0402DQRIRPPR.003	
13.80	0.155	CFUn	Tcpuc	UE-25 UZ#16	25054 (-1558.7)	ultrasonic pulse	PBT, Inc.	25.4	88.72	Air	ambient	3.49	NA	0.7	MO0402DQRIRPPR.003	
13.90	0.158	CFUn	Tcpuc	UE-25 UZ#16	25054 (-1558.7)	ultrasonic pulse	PBT, Inc.	25.4	88.72	Air	ambient	3.49	NA	0.7	MO0402DQRIRPPR.003	
7.51	0.180	CFUn	Tcpuc	UE-25 UZ#16	25053 (-1509.4)	ultrasonic pulse	PBT, Inc.	25.4	108.74	Air	ambient	4.28	NA	0.7	MO0402DQRIRPPR.003	
7.50	0.180	CFUn	Tcpuc	UE-25 UZ#16	25053 (-1509.4)	ultrasonic pulse	PBT, Inc.	25.4	108.74	Air	ambient	4.28	NA	0.7	MO0402DQRIRPPR.003	
14.50	0.180	CFUn	Tcpuc	UE-25 UZ#16	25054 (-1558.7)	ultrasonic pulse	PBT, Inc.	25.4	88.72	Air	ambient	3.49	NA	2.1	MO0402DQRIRPPR.003	
7.82	0.221	CFUn	Tcpuc	UE-25 UZ#16	25053 (-1509.4)	ultrasonic pulse	PBT, Inc.	25.4	108.74	Air	ambient	4.28	NA	2.1	MO0402DQRIRPPR.003	
15.20	0.196	CFUn	Tcpuc	UE-25 UZ#16	25054 (-1558.7)	ultrasonic pulse	PBT, Inc.	25.4	88.72	Air	ambient	3.49	NA	4.1	MO0402DQRIRPPR.003	
8.64	0.204	CFUn	Tcpuc	UE-25 UZ#16	25053 (-1509.4)	ultrasonic pulse	PBT, Inc.	25.4	108.74	Air	ambient	4.28	NA	4.1	MO0402DQRIRPPR.003	
15.90	0.209	CFUn	Tcpuc	UE-25 UZ#16	25054 (-1558.7)	ultrasonic pulse	PBT, Inc.	25.4	88.72	Air	ambient	3.49	NA	6.9	MO0402DQRIRPPR.003	
9.35	0.213	CFUn	Tcpuc	UE-25 UZ#16	25053 (-1509.4)	ultrasonic pulse	PBT, Inc.	25.4	108.74	Air	ambient	4.28	NA	6.9	MO0402DQRIRPPR.003	
14.50	0.132	CHn	Tac	UE-25 UZ#16	24031 (-1264.5)	ultrasonic pulse	PBT, Inc.	25.4	36.32	air dried	ambient	1.43	NA	0.7	MO0402DQRIRPPR.003	
14.60	0.142	CHn	Tac	UE-25 UZ#16	24031 (-1264.5)	ultrasonic pulse	PBT, Inc.	25.4	36.32	air dried	ambient	1.43	NA	0.7	MO0402DQRIRPPR.003	
16.80	0.169	CHn	Tac	UE-25 UZ#16	24031 (-1264.5)	ultrasonic pulse	PBT, Inc.	25.4	36.32	air dried	ambient	1.43	NA	2.1	MO0402DQRIRPPR.003	
18.00	0.176	CHn	Tac	UE-25 UZ#16	24031 (-1264.5)	ultrasonic pulse	PBT, Inc.	25.4	36.32	air dried	ambient	1.43	NA	4.1	MO0402DQRIRPPR.003	
20.00	0.195	CHn	Tac	UE-25 UZ#16	24031 (-1264.5)	ultrasonic pulse	PBT, Inc.	25.4	36.32	air dried	ambient	1.43	NA	6.9	MO0402DQRIRPPR.003	
15.00	0.111	CHn	Tac	UE-25 UZ#16	24030 (-1243.9)	ultrasonic pulse	PBT, Inc.	25.4	53.52	air dried	ambient	2.11	NA	0.7	MO0402DQRIRPPR.003	
15.10	0.122	CHn	Tac	UE-25 UZ#16	24030 (-1243.9)	ultrasonic pulse	PBT, Inc.	25.4	53.52	air dried	ambient	2.11	NA	0.7	MO0402DQRIRPPR.003	
14.40	0.175	CHn	Tac	UE-25 UZ#16	24034 (-1309.2)	ultrasonic pulse	PBT, Inc.	25.4	48.95	air dried	ambient	1.93	NA	0.7	MO0402DQRIRPPR.003	
14.60	0.194	CHn	Tac	UE-25 UZ#16	24034 (-1309.2)	ultrasonic pulse	PBT, Inc.	25.4	48.95	air dried	ambient	1.93	NA	0.7	MO0402DQRIRPPR.003	
15.10	0.119	CHn	Tac	UE-25 UZ#16	24030 (-1243.9)	ultrasonic pulse	PBT, Inc.	25.4	53.52	air dried	ambient	2.11	NA	2.1	MO0402DQRIRPPR.003	
16.90	0.156	CHn	Tac	UE-25 UZ#16	24034 (-1309.2)	ultrasonic pulse	PBT, Inc.	25.4	48.95	air dried	ambient	1.93	NA	2.1	MO0402DQRIRPPR.003	
15.60	0.156	CHn	Tac	UE-25 UZ#16	24030 (-1243.9)	ultrasonic pulse	PBT, Inc.	25.4	53.52	air dried	ambient	2.11	NA	4.1	MO0402DQRIRPPR.003	
17.20	0.180	CHn	Tac	UE-25 UZ#16	24034 (-1309.2)	ultrasonic pulse	PBT, Inc.	25.4	48.95	air dried	ambient	1.93	NA	4.1	MO0402DQRIRPPR.003	
16.20	0.144	CHn	Tac	UE-25 UZ#16	24030 (-1243.9)	ultrasonic pulse	PBT, Inc.	25.4	53.52	air dried	ambient	2.11	NA	6.9	MO0402DQRIRPPR.003	
18.00	0.171	CHn	Tac	UE-25 UZ#16	24034 (-1309.2)	ultrasonic pulse	PBT, Inc.	25.4	48.95	air dried	ambient	1.93	NA	6.9	MO0402DQRIRPPR.003	
19.40	0.129	CHn	Tac	UE-25 UZ#16	24032 (-1293.4)	ultrasonic pulse	PBT, Inc.	25.4	78.92	air dried	ambient	3.11	NA	0.7	MO0402DQRIRPPR.003	
19.40	0.124	CHn	Tac	UE-25 UZ#16	24032 (-1293.4)	ultrasonic pulse	PBT, Inc.	25.4	78.92	air dried	ambient	3.11	NA	0.7	MO0402DQRIRPPR.003	

Table A-2. Intact Rock Mechanical Properties Data - Dynamic Elastic Data

Dynamic Young's Modulus (GPa)	Dynamic Poisson's Ratio	TM Unit	Litho-stratigraphic Unit	Sample Location	Specimen Number	Test Standard	Laboratory	Specimen Diameter (mm)	Specimen Length (mm)	Specimen Saturation	Specimen Temperature (deg. C)	L/D Ratio	Strain Rate (1/s)	Confining Pressure /Normal Stress (MPa)	DTN	Notes
11.20	0.098	CHn	Tac	UE-25 UZ#16	25051 (-1449.4)	ultrasonic pulse	PBT, Inc.	25.4	79.21	air dried	ambient	3.12	NA	0.7	MO0402DQRIRPPR.003	
11.40	0.094	CHn	Tac	UE-25 UZ#16	25051 (-1449.4)	ultrasonic pulse	PBT, Inc.	25.4	79.21	air dried	ambient	3.12	NA	0.7	MO0402DQRIRPPR.003	
14.80	0.108	CHn	Tac	UE-25 UZ#16	24032 (-1276.8)	ultrasonic pulse	PBT, Inc.	25.4	83.24	air dried	ambient	3.28	NA	0.7	MO0402DQRIRPPR.003	
14.80	0.106	CHn	Tac	UE-25 UZ#16	24032 (-1276.8)	ultrasonic pulse	PBT, Inc.	25.4	83.24	air dried	ambient	3.28	NA	0.7	MO0402DQRIRPPR.003	
11.20	0.162	CHn	Tac	UE-25 UZ#16	25050 (-1384.1)	ultrasonic pulse	PBT, Inc.	25.4	93.84	air dried	ambient	3.69	NA	0.7	MO0402DQRIRPPR.003	
11.30	0.176	CHn	Tac	UE-25 UZ#16	25050 (-1384.1)	ultrasonic pulse	PBT, Inc.	25.4	93.84	air dried	ambient	3.69	NA	0.7	MO0402DQRIRPPR.003	
20.40	0.142	CHn	Tac	UE-25 UZ#16	24032 (-1293.4)	ultrasonic pulse	PBT, Inc.	25.4	78.92	air dried	ambient	3.11	NA	2.1	MO0402DQRIRPPR.003	
12.40	0.075	CHn	Tac	UE-25 UZ#16	25051 (-1449.4)	ultrasonic pulse	PBT, Inc.	25.4	79.21	air dried	ambient	3.12	NA	2.1	MO0402DQRIRPPR.003	
15.80	0.107	CHn	Tac	UE-25 UZ#16	24032 (-1276.8)	ultrasonic pulse	PBT, Inc.	25.4	83.24	air dried	ambient	3.28	NA	2.1	MO0402DQRIRPPR.003	
12.30	0.169	CHn	Tac	UE-25 UZ#16	25050 (-1384.1)	ultrasonic pulse	PBT, Inc.	25.4	93.84	air dried	ambient	3.69	NA	2.1	MO0402DQRIRPPR.003	
20.50	0.151	CHn	Tac	UE-25 UZ#16	24032 (-1293.4)	ultrasonic pulse	PBT, Inc.	25.4	78.92	air dried	ambient	3.11	NA	4.1	MO0402DQRIRPPR.003	
13.20	0.119	CHn	Tac	UE-25 UZ#16	25051 (-1449.4)	ultrasonic pulse	PBT, Inc.	25.4	79.21	air dried	ambient	3.12	NA	4.1	MO0402DQRIRPPR.003	
16.10	0.128	CHn	Tac	UE-25 UZ#16	24032 (-1276.8)	ultrasonic pulse	PBT, Inc.	25.4	83.24	air dried	ambient	3.28	NA	4.1	MO0402DQRIRPPR.003	
12.60	0.174	CHn	Tac	UE-25 UZ#16	25050 (-1384.1)	ultrasonic pulse	PBT, Inc.	25.4	93.84	air dried	ambient	3.69	NA	4.1	MO0402DQRIRPPR.003	
20.90	0.155	CHn	Tac	UE-25 UZ#16	24032 (-1293.4)	ultrasonic pulse	PBT, Inc.	25.4	78.92	air dried	ambient	3.11	NA	6.9	MO0402DQRIRPPR.003	
13.80	0.157	CHn	Tac	UE-25 UZ#16	25051 (-1449.4)	ultrasonic pulse	PBT, Inc.	25.4	79.21	air dried	ambient	3.12	NA	6.9	MO0402DQRIRPPR.003	
16.30	0.129	CHn	Tac	UE-25 UZ#16	24032 (-1276.8)	ultrasonic pulse	PBT, Inc.	25.4	83.24	air dried	ambient	3.28	NA	6.9	MO0402DQRIRPPR.003	
12.80	0.170	CHn	Tac	UE-25 UZ#16	25050 (-1384.1)	ultrasonic pulse	PBT, Inc.	25.4	93.84	air dried	ambient	3.69	NA	6.9	MO0402DQRIRPPR.003	
15.80		CHn	Tac	USW G-4	G4-1617.5-SNL-B	cyclic loading	NER	55	210	room dry	room temp.	3.82		atmospheric	MO0402DQRIRPPR.003	Strain Amplitude = 2.7 microstrain; @ 0.1 Hz
15.80		CHn	Tac	USW G-4	G4-1617.5-SNL-B	cyclic loading	NER	55	210	room dry	room temp.	3.82		atmospheric	MO0402DQRIRPPR.003	Strain Amplitude = 2.7 microstrain; @ 0.1 Hz
15.80		CHn	Tac	USW G-4	G4-1617.5-SNL-B	cyclic loading	NER	55	210	room dry	room temp.	3.82		atmospheric	MO0402DQRIRPPR.003	Strain Amplitude = 2.7 microstrain; @ 0.1 Hz
18.70	0.044	CHn	Tacbt	UE-25 UZ#16	25052 (-1483.4)	ultrasonic pulse	PBT, Inc.	25.4	98.45	air dried	ambient	3.88	NA	0.7	MO0402DQRIRPPR.003	
19.10	0.084	CHn	Tacbt	UE-25 UZ#16	25052 (-1483.4)	ultrasonic pulse	PBT, Inc.	25.4	98.45	air dried	ambient	3.88	NA	0.7	MO0402DQRIRPPR.003	
20.70	0.110	CHn	Tacbt	UE-25 UZ#16	25052 (-1483.4)	ultrasonic pulse	PBT, Inc.	25.4	98.45	air dried	ambient	3.88	NA	2.1	MO0402DQRIRPPR.003	
21.40	0.137	CHn	Tacbt	UE-25 UZ#16	25052 (-1483.4)	ultrasonic pulse	PBT, Inc.	25.4	98.45	air dried	ambient	3.88	NA	4.1	MO0402DQRIRPPR.003	
22.00	0.145	CHn	Tacbt	UE-25 UZ#16	25052 (-1483.4)	ultrasonic pulse	PBT, Inc.	25.4	98.45	air dried	ambient	3.88	NA	6.9	MO0402DQRIRPPR.003	
19.00	0.066	CHn	Tptpv1	UE-25 UZ#16	24029 (-1182.7)	ultrasonic pulse	PBT, Inc.	25.4	28.27	air dried	room temp.	1.11	NA	0.7	MO0402DQRIRPPR.003	
18.90	0.071	CHn	Tptpv1	UE-25 UZ#16	24029 (-1182.7)	ultrasonic pulse	PBT, Inc.	25.4	28.27	air dried	room temp.	1.11	NA	0.7	MO0402DQRIRPPR.003	
19.60	0.007	CHn	Tptpv1	UE-25 UZ#16	24029 (-1182.7)	ultrasonic pulse	PBT, Inc.	25.4	28.27	air dried	room temp.	1.11	NA	2.1	MO0402DQRIRPPR.003	
20.30	0.040	CHn	Tptpv1	UE-25 UZ#16	24029 (-1182.7)	ultrasonic pulse	PBT, Inc.	25.4	28.27	air dried	room temp.	1.11	NA	4.1	MO0402DQRIRPPR.003	
20.80	0.019	CHn	Tptpv1	UE-25 UZ#16	24029 (-1182.7)	ultrasonic pulse	PBT, Inc.	25.4	28.27	air dried	room temp.	1.11	NA	6.9	MO0402DQRIRPPR.003	
2.28	0.087	PTn	Tpbt2	UE-25 UZ#16	21124 (-216.0)	ultrasonic pulse	PBT, Inc.	25.4	33.72	air dried	room temp.	1.33	NA	0.7	MO0402DQRIRPPR.003	
2.26	0.090	PTn	Tpbt2	UE-25 UZ#16	21124 (-216.0)	ultrasonic pulse	PBT, Inc.	25.4	33.72	air dried	room temp.	1.33	NA	0.7	MO0402DQRIRPPR.003	
2.67	0.209	PTn	Tpbt2	UE-25 UZ#16	21124 (-216.0)	ultrasonic pulse	PBT, Inc.	25.4	33.72	air dried	room temp.	1.33	NA	2.1	MO0402DQRIRPPR.003	
3.15	0.234	PTn	Tpbt2	UE-25 UZ#16	21124 (-216.0)	ultrasonic pulse	PBT, Inc.	25.4	33.72	air dried	room temp.	1.33	NA	4.1	MO0402DQRIRPPR.003	
3.56	0.251	PTn	Tpbt2	UE-25 UZ#16	21124 (-216.0)	ultrasonic pulse	PBT, Inc.	25.4	33.72	air dried	room temp.	1.33	NA	6.9	MO0402DQRIRPPR.003	
3.69	0.303	PTn	Tpbt2	UE-25 UZ#16	23821 (-191.8)	ultrasonic pulse	PBT, Inc.	25.4	74.85	Air	ambient	2.95	NA	0.7	MO0402DQRIRPPR.003	
3.69	0.304	PTn	Tpbt2	UE-25 UZ#16	23821 (-191.8)	ultrasonic pulse	PBT, Inc.	25.4	74.85	Air	ambient	2.95	NA	0.7	MO0402DQRIRPPR.003	
3.82	0.346	PTn	Tpbt2	UE-25 UZ#16	23821 (-191.8)	ultrasonic pulse	PBT, Inc.	25.4	74.85	Air	ambient	2.95	NA	2.1	MO0402DQRIRPPR.003	
3.86	0.363	PTn	Tpbt2	UE-25 UZ#16	23821 (-191.8)	ultrasonic pulse	PBT, Inc.	25.4	74.85	Air	ambient	2.95	NA	4.1	MO0402DQRIRPPR.003	
3.93	0.380	PTn	Tpbt2	UE-25 UZ#16	23821 (-191.8)	ultrasonic pulse	PBT, Inc.	25.4	74.85	Air	ambient	2.95	NA	6.9	MO0402DQRIRPPR.003	
6.36	0.187	PTn	Tpbt3	UE-25 UZ#16	21122 (-176.3)	ultrasonic pulse	PBT, Inc.	25.4	62.7	Air	ambient	2.47	NA	0.7	MO0402DQRIRPPR.003	
6.33	0.180	PTn	Tpbt3	UE-25 UZ#16	21122 (-176.3)	ultrasonic pulse	PBT, Inc.	25.4	62.7	Air	ambient	2.47	NA	0.7	MO0402DQRIRPPR.003	
7.33	0.195	PTn	Tpbt3	UE-25 UZ#16	21122 (-176.3)	ultrasonic pulse	PBT, Inc.	25.4	62.7	Air	ambient	2.47	NA	2.1	MO0402DQRIRPPR.003	
8.12	0.236	PTn	Tpbt3	UE-25 UZ#16	21122 (-176.3)	ultrasonic pulse	PBT, Inc.	25.4	62.7	Air	ambient	2.47	NA	4.1	MO0402DQRIRPPR.003	
8.49	0.236	PTn	Tpbt3	UE-25 UZ#16	21122 (-176.3)	ultrasonic pulse	PBT, Inc.	25.4	62.7	Air	ambient	2.47	NA	6.9	MO0402DQRIRPPR.003	
2.79	0.150	PTn	Tpbt4	UE-25 UZ#16	21120 (-162.0)	ultrasonic pulse	PBT, Inc.	25.4	68.86	Air	ambient	2.71	NA	0.7	MO0402DQRIRPPR.003	
2.79	0.149	PTn	Tpbt4	UE-25 UZ#16	21120 (-162.0)	ultrasonic pulse	PBT, Inc.	25.4	68.86	Air	ambient	2.71	NA	0.7	MO0402DQRIRPPR.003	
3.12	0.021	PTn	Tpbt4	UE-25 UZ#16	26825 (-162.0)	ultrasonic pulse	PBT, Inc.	25.4	68.86	Air	ambient	2.71	NA	0.7	MO0402DQRIRPPR.003	
3.13	0.021	PTn	Tpbt4	UE-25 UZ#16	26825 (-162.0)	ultrasonic pulse	PBT, Inc.	25.4	68.86	Air	ambient	2.71	NA	0.7	MO0402DQRIRPPR.003	
2.91	0.190	PTn	Tpbt4	UE-25 UZ#16	21120 (-162.0)	ultrasonic pulse	PBT, Inc.	25.4	68.86	Air	ambient	2.71	NA	2.1	MO0402DQRIRPPR.003	
3.00	0.234	PTn	Tpbt4	UE-25 UZ#16	21120 (-162.0)	ultrasonic pulse	PBT, Inc.	25.4	68.86	Air	ambient	2.71	NA	4.1	MO0402DQRIRPPR.003	
3.57	0.163	PTn	Tpbt4	UE-25 UZ#16	21120 (-162.0)	ultrasonic pulse	PBT, Inc.	25.4	68.86	Air	ambient	2.71	NA	6.9	MO0402DQRIRPPR.003	
3.46	0.123	PTn	Tpbt4	UE-25 UZ#16	26825 (-162.0)	ultrasonic pulse	PBT, Inc.	25.4	68.86	Air	ambient	2.71	NA	2.1	MO0402DQRIRPPR.003	
3.03	0.239	PTn	Tpbt4	UE-25 UZ#16	26825 (-162.0)	ultrasonic pulse	PBT, Inc.	25.4	68.86	Air	ambient	2.71	NA	4.1	MO0402DQRIRPPR.003	
3.67	0.180	PTn	Tpbt4	UE-25 UZ#16	26825 (-162.0)	ultrasonic pulse	PBT, Inc.	25.4	68.86	Air	ambient	2.71	NA	6.9	MO0402DQRIRPPR.003	
6.80		PTn	Tpcpv1	USW G-4	G4-135.0-SNL-B	Resonant Bar	NER	13	201	room dry	room temp.	15.46		atmospheric	MO0402DQRIRPPR.003	Strain Amplitude = 2.7 microstrain; @ 0.1 Hz
5.96	0.149	PTn	Tpy	UE-25 UZ#16	21121 (-171.0)	ultrasonic pulse	PBT, Inc.	25.4	76.54	air dried	room temp.	3.01	NA	0.7	MO0402DQRIRPPR.003	
6.00	0.150	PTn	Tpy	UE-25 UZ#16	21121 (-171.0)	ultrasonic pulse	PBT, Inc.	25.4	76.54	air dried	room temp.	3.01	NA	0.7	MO0402DQRIRPPR.003	
6.21	0.188	PTn	Tpy	UE-25 UZ#16	21121 (-171.0)	ultrasonic pulse	PBT, Inc.	25.4	76.54	air dried	room temp.	3.01	NA	2.1	MO0402DQRIRPPR.003	
6.30	0.197	PTn	Tpy	UE-25 UZ#16	21121 (-171.0)	ultrasonic pulse	PBT, Inc.	25.4	76.54	air dried	room temp.	3.01	NA	4.1	MO0402DQRIRPPR.003	
6.37	0.204	PTn	Tpy	UE-25 UZ#16	21121 (-171.0)	ultrasonic pulse	PBT, Inc.	25.4	76.54	air dried	room temp.	3.01	NA	6.9	MO0402DQRIRPPR.003	
43.10	0.051	TCw	Tpcpll	UE-25 UZ#16	21114 (-54.2)	ultrasonic pulse	PBT, Inc.	25.4	65.27	Air	ambient	2.57	NA	0.7	MO0402DQRIRPPR.003	
44.20	0.073	TCw	Tpcpll	UE-25 UZ#16	21114 (-54.2)	ultrasonic pulse	PBT, Inc.	25.4	65.27	Air	ambient	2.57	NA	0.7	MO0402DQRIRPPR.003	
22.00		TCw	Tpcpll	UE-25 UZ#16	21115 (-46.3)	ultrasonic pulse	PBT, Inc.	25.4	82.72	Air	ambient	3.26	NA	0.7	MO0402DQRIRPPR.003	
24.90		TCw	Tpcpll	UE-25 UZ#16	21115 (-46.3)	ultrasonic pulse	PBT, Inc.	25.4	82.72	Air	ambient	3.26	NA	0.7	MO0402DQRIRPPR.003	
46.60	0.114	TCw	Tpcpll	UE-25 UZ#16	21114 (-54.2)	ultrasonic pulse	PBT, Inc.	25.4	65.27	Air	ambient	2.57	NA	2.1	MO0402DQRIRPPR.003	
32.10	0.114	TCw	Tpcpll	UE-25 UZ#16	21115 (-46.3)	ultrasonic pulse	PBT, Inc.	25.4	82.72	Air	ambient	3.26	NA	2.1	MO0402DQRIRPPR.003	

Table A-2. Intact Rock Mechanical Properties Data - Dynamic Elastic Data

Dynamic Young's Modulus (GPa)	Dynamic Poisson's Ratio	TM Unit	Litho-stratigraphic Unit	Sample Location	Specimen Number	Test Standard	Laboratory	Specimen Diameter (mm)	Specimen Length (mm)	Specimen Saturation	Specimen Temperature (deg. C)	L/D Ratio	Strain Rate (1/s)	Confining Pressure /Normal Stress (MPa)	DTN	Notes
45.50	0.079	TCw	Tpcpll	UE-25 UZ#16	21114 (-54.2)	ultrasonic pulse	PBT, Inc.	25.4	65.27	Air	ambient	2.57	NA	4.1	MO0402DQRIRPPR.003	
34.00	0.157	TCw	Tpcpll	UE-25 UZ#16	21115 (-46.3)	ultrasonic pulse	PBT, Inc.	25.4	82.72	Air	ambient	3.26	NA	4.1	MO0402DQRIRPPR.003	
47.30	0.127	TCw	Tpcpll	UE-25 UZ#16	21114 (-54.2)	ultrasonic pulse	PBT, Inc.	25.4	65.27	Air	ambient	2.57	NA	6.9	MO0402DQRIRPPR.003	
43.60	0.149	TCw	Tpcpln	UE-25 UZ#16	21118 (-134.9)	ultrasonic pulse	PBT, Inc.	25.4	93.55	Air	ambient	3.68	NA	0.7	MO0402DQRIRPPR.003	
43.90	0.152	TCw	Tpcpln	UE-25 UZ#16	21118 (-134.9)	ultrasonic pulse	PBT, Inc.	25.4	93.55	Air	ambient	3.68	NA	0.7	MO0402DQRIRPPR.003	
38.70	0.130	TCw	Tpcpln	UE-25 UZ#16	21117 (-100.5)	ultrasonic pulse	PBT, Inc.	25.4	98.6	Air	ambient	3.88	NA	0.7	MO0402DQRIRPPR.003	
38.50	0.132	TCw	Tpcpln	UE-25 UZ#16	21117 (-100.5)	ultrasonic pulse	PBT, Inc.	25.4	98.6	Air	ambient	3.88	NA	0.7	MO0402DQRIRPPR.003	
43.70	0.127	TCw	Tpcpln	UE-25 UZ#16	21116 (-79.8)	ultrasonic pulse	PBT, Inc.	25.4	71.22	Air	ambient	2.80	NA	0.7	MO0402DQRIRPPR.003	
43.90	0.126	TCw	Tpcpln	UE-25 UZ#16	21116 (-79.8)	ultrasonic pulse	PBT, Inc.	25.4	71.22	Air	ambient	2.80	NA	0.7	MO0402DQRIRPPR.003	
45.40	0.149	TCw	Tpcpln	UE-25 UZ#16	21118 (-134.9)	ultrasonic pulse	PBT, Inc.	25.4	93.55	Air	ambient	3.68	NA	2.1	MO0402DQRIRPPR.003	
39.30	0.134	TCw	Tpcpln	UE-25 UZ#16	21117 (-100.5)	ultrasonic pulse	PBT, Inc.	25.4	98.6	Air	ambient	3.88	NA	2.1	MO0402DQRIRPPR.003	
46.00	0.168	TCw	Tpcpln	UE-25 UZ#16	21118 (-134.9)	ultrasonic pulse	PBT, Inc.	25.4	93.55	Air	ambient	3.68	NA	4.1	MO0402DQRIRPPR.003	
39.50	0.151	TCw	Tpcpln	UE-25 UZ#16	21117 (-100.5)	ultrasonic pulse	PBT, Inc.	25.4	98.6	Air	ambient	3.88	NA	4.1	MO0402DQRIRPPR.003	
46.60	0.173	TCw	Tpcpln	UE-25 UZ#16	21118 (-134.9)	ultrasonic pulse	PBT, Inc.	25.4	93.55	Air	ambient	3.68	NA	6.9	MO0402DQRIRPPR.003	
39.70	0.151	TCw	Tpcpln	UE-25 UZ#16	21117 (-100.5)	ultrasonic pulse	PBT, Inc.	25.4	98.6	Air	ambient	3.88	NA	6.9	MO0402DQRIRPPR.003	
44.30	0.120	TCw	Tpcpln	UE-25 UZ#16	21116 (-79.8)	ultrasonic pulse	PBT, Inc.	25.4	71.22	Air	ambient	2.80	NA	2.1	MO0402DQRIRPPR.003	
44.40	0.151	TCw	Tpcpln	UE-25 UZ#16	21116 (-79.8)	ultrasonic pulse	PBT, Inc.	25.4	71.22	Air	ambient	2.80	NA	4.1	MO0402DQRIRPPR.003	
44.40	0.151	TCw	Tpcpln	UE-25 UZ#16	21116 (-79.8)	ultrasonic pulse	PBT, Inc.	25.4	71.22	Air	ambient	2.80	NA	6.9	MO0402DQRIRPPR.003	
35.70		TCw	Tpcpmn	USW GU-3	GU-3-165.35-SNL-B-2	Resonant Bar	NER	13	201	room dry	room temp.	15.46		atmospheric	MO0402DQRIRPPR.003	Strain Amplitude = 2.7 microstrain; @ 0.1 Hz
33.51	0.270	TCw	Tpcpmn	UE25-NRG-1	136.8-144.4FT,-01-01	-	USGS	61.14	129.07	as received	room temp.	2.11	NA	0	MO0402DQRIRPPR.003	
37.16	0.270	TCw	Tpcpmn	UE25-NRG-1	136.8-144.4FT,-04-01	-	USGS	61.21	132.51	as received	room temp.	2.16	NA	0	MO0402DQRIRPPR.003	
35.58	0.290	TCw	Tpcpmn	UE25-NRG-1	136.8-144.4FT,-02-01	-	USGS	61.19	123.88	as received	room temp.	2.02	NA	0	MO0402DQRIRPPR.003	
27.85	0.330	TCw	Tpcpmn	UE25-NRG-1	123.8-130.1FT,-05-01	-	USGS	61.16	126.29	as received	room temp.	2.06	NA	0	MO0402DQRIRPPR.003	
34.06	0.330	TCw	Tpcpmn	UE25-NRG-1	123.8-130.1FT,-01-02	-	USGS	61.19	126.62	as received	room temp.	2.07	NA	0	MO0402DQRIRPPR.003	
32.13	0.290	TCw	Tpcpmn	UE25-NRG-1	136.8-144.4FT,-01-01	-	USGS	61.14	129.07	as received	room temp.	2.11	NA	0.68	MO0402DQRIRPPR.003	
35.51	0.280	TCw	Tpcpmn	UE25-NRG-1	136.8-144.4FT,-04-01	-	USGS	61.21	132.51	as received	room temp.	2.16	NA	0.68	MO0402DQRIRPPR.003	
19.51	0.310	TCw	Tpcpmn	UE25-NRG-1	136.8-144.4FT,-02-01	-	USGS	61.19	123.88	as received	room temp.	2.02	NA	0.68	MO0402DQRIRPPR.003	
27.44	0.350	TCw	Tpcpmn	UE25-NRG-1	123.8-130.1FT,-05-01	-	USGS	61.16	126.29	as received	room temp.	2.06	NA	0.68	MO0402DQRIRPPR.003	
33.72	0.320	TCw	Tpcpmn	UE25-NRG-1	123.8-130.1FT,-01-02	-	USGS	61.19	126.62	as received	room temp.	2.07	NA	0.68	MO0402DQRIRPPR.003	
31.44	0.240	TCw	Tpcpmn	UE25-NRG-1	136.8-144.4FT,-03-01	-	USGS	61.16	135.15	as received	room temp.	2.21	NA	0	MO0402DQRIRPPR.003	
29.99	0.260	TCw	Tpcpmn	UE25-NRG-1	123.8-130.1FT,-02-02	-	USGS	61.16	139.04	as received	room temp.	2.27	NA	0	MO0402DQRIRPPR.003	
29.85	0.280	TCw	Tpcpmn	UE25-NRG-1	136.8-144.4FT,-03-01	-	USGS	61.16	135.15	as received	room temp.	2.21	NA	0.68	MO0402DQRIRPPR.003	
30.68	0.280	TCw	Tpcpmn	UE25-NRG-1	123.8-130.1FT,-02-02	-	USGS	61.16	139.04	as received	room temp.	2.27	NA	0.68	MO0402DQRIRPPR.003	
39.10		TCw	Tpcpmn	USW GU-3	GU-3-211.3-SNL-B	cyclic loading	NER	55	210	room dry	room temp.	3.82		atmospheric	MO0402DQRIRPPR.003	Strain Amplitude = 2.7 microstrain; @ 0.1 Hz
36.10		TCw	Tpcpmn	USW GU-3	GU-3-211.3-SNL-B	cyclic loading	NER	55	210	room dry	room temp.	3.82		atmospheric	MO0402DQRIRPPR.003	Strain Amplitude = 2.7 microstrain; @ 0.1 Hz
35.30		TCw	Tpcpmn	USW GU-3	GU-3-211.3-SNL-B	cyclic loading	NER	55	210	room dry	room temp.	3.82		atmospheric	MO0402DQRIRPPR.003	Strain Amplitude = 2.7 microstrain; @ 0.1 Hz
34.70		TCw	Tpcpmn	USW GU-3	GU-3-211.3-SNL-B	cyclic loading	NER	55	210	room dry	room temp.	3.82		atmospheric	MO0402DQRIRPPR.003	Strain Amplitude = 2.7 microstrain; @ 0.1 Hz
16.62	0.380	TCw	Tpcpul	UE25-NRG-1	89.5-97.8FT,-05,-01	-	USGS	61.19	111.4	as received	room temp.	1.82	NA	0	MO0402DQRIRPPR.003	
23.51	0.300	TCw	Tpcpul	UE25-NRG-1	89.5-97.8FT,-03-02	-	USGS	61.09	130.68	as received	room temp.	2.14	NA	0	MO0402DQRIRPPR.003	
22.75	0.300	TCw	Tpcpul	UE25-NRG-1	38.0-47.1FT,-01-01	-	USGS	61.16	132.05	as received	room temp.	2.16	NA	0	MO0402DQRIRPPR.003	
21.65	0.370	TCw	Tpcpul	UE25-NRG-1	105.1-115.1FT,-01,-01	-	USGS	61.14	122.35	as received	room temp.	2.00	NA	0	MO0402DQRIRPPR.003	
21.93	0.340	TCw	Tpcpul	UE25-NRG-1	80.8-89.5FT,-02-01	-	USGS	61.16	127.56	as received	room temp.	2.09	NA	0	MO0402DQRIRPPR.003	
22.27	0.310	TCw	Tpcpul	UE25-NRG-1	89.5-97.8FT,-03-02	-	USGS	61.09	130.68	as received	room temp.	2.14	NA	0.68	MO0402DQRIRPPR.003	CT scan showed a large lithophysal cavity, causing the low value
22.96	0.310	TCw	Tpcpul	UE25-NRG-1	38.0-47.1FT,-01-01	-	USGS	61.16	132.05	as received	room temp.	2.16	NA	0.68	MO0402DQRIRPPR.003	
21.58	0.330	TCw	Tpcpul	UE25-NRG-1	89.5-97.8FT,-05,-01	-	USGS	61.19	111.4	as received	room temp.	1.82	NA	0.68	MO0402DQRIRPPR.003	
25.65	0.340	TCw	Tpcpul	UE25-NRG-1	105.1-115.1FT,-01,-01	-	USGS	61.14	122.35	as received	room temp.	2.00	NA	0.68	MO0402DQRIRPPR.003	
21.58	0.340	TCw	Tpcpul	UE25-NRG-1	80.8-89.5FT,-02-01	-	USGS	61.16	127.56	as received	room temp.	2.09	NA	0.68	MO0402DQRIRPPR.003	
25.72	0.280	TCw	Tpcpul	UE25-NRG-1	80.8-89.5FT,-03-01	-	USGS	61.16	138.07	as received	room temp.	2.26	NA	0	MO0402DQRIRPPR.003	
24.27	0.270	TCw	Tpcpul	UE25-NRG-1	89.5-97.8FT,-06,-01	-	USGS	61.16	139.04	as received	room temp.	2.27	NA	0	MO0402DQRIRPPR.003	
23.99	0.300	TCw	Tpcpul	UE25-NRG-1	80.8-89.5FT,-03-01	-	USGS	61.16	138.07	as received	room temp.	2.26	NA	0.68	MO0402DQRIRPPR.003	

Table A-2. Intact Rock Mechanical Properties Data - Dynamic Elastic Data

Dynamic Young's Modulus (GPa)	Dynamic Poisson's Ratio	TM Unit	Litho-stratigraphic Unit	Sample Location	Specimen Number	Test Standard	Laboratory	Specimen Diameter (mm)	Specimen Length (mm)	Specimen Saturation	Specimen Temperature (deg. C)	L/D Ratio	Strain Rate (1/s)	Confining Pressure /Normal Stress (MPa)	DTN	Notes
23.30	0.280	TCw	Tpcpul	UE25-NRG-1	89.5-97.8FT,-06,-01	-	USGS	61.16	139.04	as received	room temp.	2.27	NA	0.68	MO0402DQRIRPPR.003	
22.27	0.330	TCw	Tpcrn	UE25-NRG-1	21.8-30.6FT,-01-03	-	USGS	61.24	124.69	as received	room temp.	2.04	NA	0	MO0402DQRIRPPR.003	
18.62	0.360	TCw	Tpcrn	UE25-NRG-1	16.2-21.8FT,-03	-	USGS	61.29	124.87	as received	room temp.	2.04	NA	0	MO0402DQRIRPPR.003	
22.75	0.320	TCw	Tpcrn	UE25-NRG-1	21.8-30.6FT,-01-03	-	USGS	61.24	124.69	as received	room temp.	2.04	NA	0.68	MO0402DQRIRPPR.003	
20.13	0.340	TCw	Tpcrn	UE25-NRG-1	16.2-21.8FT,-03	-	USGS	61.29	124.87	as received	room temp.	2.04	NA	0.68	MO0402DQRIRPPR.003	
17.93	0.350	TCw	Tpcrn	UE25-NRG-1	9.5-16.2FT,-01	-	USGS	61.06	134.72	as received	room temp.	2.21	NA	0	MO0402DQRIRPPR.003	
18.90	0.350	TCw	Tpcrn	UE25-NRG-1	9.5-16.2FT,-01	-	USGS	61.06	134.72	as received	room temp.	2.21	NA	0.68	MO0402DQRIRPPR.003	
27.00	0.094	TSw1	Tptpul	UE-25 UZ#16	21132 (-377.8)	ultrasonic pulse	PBT, Inc.	25.4	45.2	air dried	room temp.	1.78	NA	0.7	MO0402DQRIRPPR.003	
27.20	0.107	TSw1	Tptpul	UE-25 UZ#16	21132 (-377.8)	ultrasonic pulse	PBT, Inc.	25.4	45.2	air dried	room temp.	1.78	NA	0.7	MO0402DQRIRPPR.003	
27.90	0.106	TSw1	Tptpul	UE-25 UZ#16	21132 (-377.8)	ultrasonic pulse	PBT, Inc.	25.4	45.2	air dried	room temp.	1.78	NA	2.1	MO0402DQRIRPPR.003	
28.40	0.137	TSw1	Tptpul	UE-25 UZ#16	21132 (-377.8)	ultrasonic pulse	PBT, Inc.	25.4	45.2	air dried	room temp.	1.78	NA	4.1	MO0402DQRIRPPR.003	
29.00	0.144	TSw1	Tptpul	UE-25 UZ#16	21132 (-377.8)	ultrasonic pulse	PBT, Inc.	25.4	45.2	air dried	room temp.	1.78	NA	6.9	MO0402DQRIRPPR.003	
39.10	0.074	TSw1	Tptpul	UE-25 UZ#16	21137 (-533.1)	ultrasonic pulse	PBT, Inc.	25.4	54.2	air dried	room temp.	2.13	NA	0.7	MO0402DQRIRPPR.003	
39.70	0.086	TSw1	Tptpul	UE-25 UZ#16	21137 (-533.1)	ultrasonic pulse	PBT, Inc.	25.4	54.2	air dried	room temp.	2.13	NA	0.7	MO0402DQRIRPPR.003	
35.60	0.000	TSw1	Tptpul	UE-25 UZ#16	21336 (-495)	ultrasonic pulse	PBT, Inc.	25.4	47.0	air dried	room temp.	1.85	NA	0.7	MO0402DQRIRPPR.003	
36.30	0.015	TSw1	Tptpul	UE-25 UZ#16	21336 (-495)	ultrasonic pulse	PBT, Inc.	25.4	47.0	air dried	room temp.	1.85	NA	0.7	MO0402DQRIRPPR.003	
40.30	0.061	TSw1	Tptpul	UE-25 UZ#16	21137 (-533.1)	ultrasonic pulse	PBT, Inc.	25.4	54.2	air dried	room temp.	2.13	NA	2.1	MO0402DQRIRPPR.003	
37.20		TSw1	Tptpul	UE-25 UZ#16	21336 (-495)	ultrasonic pulse	PBT, Inc.	25.4	47.0	air dried	room temp.	1.85	NA	2.1	MO0402DQRIRPPR.003	
41.10	0.099	TSw1	Tptpul	UE-25 UZ#16	21137 (-533.1)	ultrasonic pulse	PBT, Inc.	25.4	54.2	air dried	room temp.	2.13	NA	4.1	MO0402DQRIRPPR.003	
38.90		TSw1	Tptpul	UE-25 UZ#16	21336 (-495)	ultrasonic pulse	PBT, Inc.	25.4	47.0	air dried	room temp.	1.85	NA	4.1	MO0402DQRIRPPR.003	
42.00	0.103	TSw1	Tptpul	UE-25 UZ#16	21137 (-533.1)	ultrasonic pulse	PBT, Inc.	25.4	54.2	air dried	room temp.	2.13	NA	6.9	MO0402DQRIRPPR.003	
40.40		TSw1	Tptpul	UE-25 UZ#16	21336 (-495)	ultrasonic pulse	PBT, Inc.	25.4	47.0	air dried	room temp.	1.85	NA	6.9	MO0402DQRIRPPR.003	
21.00	0.177	TSw1	Tptpul	UE-25 UZ#16	21335 (-457.9)	ultrasonic pulse	PBT, Inc.	25.4	73.0	air dried	room temp.	2.87	NA	0.7	MO0402DQRIRPPR.003	
20.80	0.179	TSw1	Tptpul	UE-25 UZ#16	21335 (-457.9)	ultrasonic pulse	PBT, Inc.	25.4	73.0	air dried	room temp.	2.87	NA	0.7	MO0402DQRIRPPR.003	
31.70	0.101	TSw1	Tptpul	UE-25 UZ#16	21134 (-450)	ultrasonic pulse	PBT, Inc.	25.4	98.76	air dried	room temp.	3.89	NA	0.7	MO0402DQRIRPPR.003	
31.90	0.098	TSw1	Tptpul	UE-25 UZ#16	21134 (-450)	ultrasonic pulse	PBT, Inc.	25.4	98.76	air dried	room temp.	3.89	NA	0.7	MO0402DQRIRPPR.003	
24.50	0.189	TSw1	Tptpul	UE-25 UZ#16	21133 (-419.9)	ultrasonic pulse	PBT, Inc.	25.4	101.4	air dried	room temp.	3.99	NA	0.7	MO0402DQRIRPPR.003	
24.70	0.197	TSw1	Tptpul	UE-25 UZ#16	21133 (-419.9)	ultrasonic pulse	PBT, Inc.	25.4	101.4	air dried	room temp.	3.99	NA	0.7	MO0402DQRIRPPR.003	
21.90	0.162	TSw1	Tptpul	UE-25 UZ#16	21335 (-457.9)	ultrasonic pulse	PBT, Inc.	25.4	73.0	air dried	room temp.	2.87	NA	2.1	MO0402DQRIRPPR.003	
34.40	0.101	TSw1	Tptpul	UE-25 UZ#16	21134 (-450)	ultrasonic pulse	PBT, Inc.	25.4	98.76	air dried	room temp.	3.89	NA	2.1	MO0402DQRIRPPR.003	
25.30	0.177	TSw1	Tptpul	UE-25 UZ#16	21133 (-419.9)	ultrasonic pulse	PBT, Inc.	25.4	101.4	air dried	room temp.	3.99	NA	2.1	MO0402DQRIRPPR.003	
23.40	0.184	TSw1	Tptpul	UE-25 UZ#16	21335 (-457.9)	ultrasonic pulse	PBT, Inc.	25.4	73.0	air dried	room temp.	2.87	NA	4.1	MO0402DQRIRPPR.003	
36.50	0.097	TSw1	Tptpul	UE-25 UZ#16	21134 (-450)	ultrasonic pulse	PBT, Inc.	25.4	98.76	air dried	room temp.	3.89	NA	4.1	MO0402DQRIRPPR.003	
25.90	0.190	TSw1	Tptpul	UE-25 UZ#16	21133 (-419.9)	ultrasonic pulse	PBT, Inc.	25.4	101.4	air dried	room temp.	3.99	NA	4.1	MO0402DQRIRPPR.003	Large solution cavities
24.30	0.192	TSw1	Tptpul	UE-25 UZ#16	21335 (-457.9)	ultrasonic pulse	PBT, Inc.	25.4	73.0	air dried	room temp.	2.87	NA	6.9	MO0402DQRIRPPR.003	Large solution cavities
37.10	0.072	TSw1	Tptpul	UE-25 UZ#16	21134 (-450)	ultrasonic pulse	PBT, Inc.	25.4	98.76	air dried	room temp.	3.89	NA	6.9	MO0402DQRIRPPR.003	
26.40	0.192	TSw1	Tptpul	UE-25 UZ#16	21133 (-419.9)	ultrasonic pulse	PBT, Inc.	25.4	101.4	air dried	room temp.	3.99	NA	6.9	MO0402DQRIRPPR.003	
24.10	0.137	TSw1	Tptrn	UE-25 UZ#16	21126 (-250.1)	ultrasonic pulse	PBT, Inc.	25.4	47.3	air dried	room temp.	1.86	NA	0.7	MO0402DQRIRPPR.003	
24.20	0.143	TSw1	Tptrn	UE-25 UZ#16	21126 (-250.1)	ultrasonic pulse	PBT, Inc.	25.4	47.3	air dried	room temp.	1.86	NA	0.7	MO0402DQRIRPPR.003	
27.10	0.180	TSw1	Tptrn	UE-25 UZ#16	21126 (-250.1)	ultrasonic pulse	PBT, Inc.	25.4	47.3	air dried	room temp.	1.86	NA	2.1	MO0402DQRIRPPR.003	
29.00	0.193	TSw1	Tptrn	UE-25 UZ#16	21126 (-250.1)	ultrasonic pulse	PBT, Inc.	25.4	47.3	air dried	room temp.	1.86	NA	4.1	MO0402DQRIRPPR.003	Large solution cavities
30.20	0.189	TSw1	Tptrn	UE-25 UZ#16	21126 (-250.1)	ultrasonic pulse	PBT, Inc.	25.4	47.3	air dried	room temp.	1.86	NA	6.9	MO0402DQRIRPPR.003	
17.30	0.207	TSw1	Tptrn	UE-25 UZ#16	23822 (-264.4)	ultrasonic pulse	PBT, Inc.	25.4	88.81	air dried	room temp.	3.50	NA	0.7	MO0402DQRIRPPR.003	
17.40	0.213	TSw1	Tptrn	UE-25 UZ#16	23822 (-264.4)	ultrasonic pulse	PBT, Inc.	25.4	88.81	air dried	room temp.	3.50	NA	0.7	MO0402DQRIRPPR.003	
21.70	0.123	TSw1	Tptrn	UE-25 UZ#16	23823 (-325.5)	ultrasonic pulse	PBT, Inc.	25.4	89.55	air dried	room temp.	3.53	NA	0.7	MO0402DQRIRPPR.003	
21.90	0.135	TSw1	Tptrn	UE-25 UZ#16	23823 (-325.5)	ultrasonic pulse	PBT, Inc.	25.4	89.55	air dried	room temp.	3.53	NA	0.7	MO0402DQRIRPPR.003	
21.80	0.182	TSw1	Tptrn	UE-25 UZ#16	21128 (-278.8)	ultrasonic pulse	PBT, Inc.	25.4	97.89	air dried	room temp.	3.85	NA	0.7	MO0402DQRIRPPR.003	
21.90	0.191	TSw1	Tptrn	UE-25 UZ#16	21128 (-278.8)	ultrasonic pulse	PBT, Inc.	25.4	97.89	air dried	room temp.	3.85	NA	0.7	MO0402DQRIRPPR.003	Large solution cavities
24.80	0.201	TSw1	Tptrn	UE-25 UZ#16	21129 (-302)	ultrasonic pulse	PBT, Inc.	25.4	98.45	air dried	room temp.	3.88	NA	0.7	MO0402DQRIRPPR.003	
24.80	0.197	TSw1	Tptrn	UE-25 UZ#16	21129 (-302)	ultrasonic pulse	PBT, Inc.	25.4	98.45	air dried	room temp.	3.88	NA	0.7	MO0402DQRIRPPR.003	
21.00	0.194	TSw1	Tptrn	UE-25 UZ#16	23822 (-264.4)	ultrasonic pulse	PBT, Inc.	25.4	88.81	air dried	room temp.	3.50	NA	2.1	MO0402DQRIRPPR.003	
23.10	0.119	TSw1	Tptrn	UE-25 UZ#16	23823 (-325.5)	ultrasonic pulse	PBT, Inc.	25.4	89.65	air dried	room temp.	3.53	NA	2.1	MO0402DQRIRPPR.003	
23.20	0.200	TSw1	Tptrn	UE-25 UZ#16	21128 (-278.8)	ultrasonic pulse	PBT, Inc.	25.4	97.89	air dried	room temp.	3.85	NA	2.1	MO0402DQRIRPPR.003	
26.40	0.188	TSw1	Tptrn	UE-25 UZ#16	21129 (-302)	ultrasonic pulse	PBT, Inc.	25.4	98.45	air dried	room temp.	3.88	NA	2.1	MO0402DQRIRPPR.003	
22.60	0.209	TSw1	Tptrn	UE-25 UZ#16	23822 (-264.4)	ultrasonic pulse	PBT, Inc.	25.4	88.81	air dried	room temp.	3.50	NA	4.1	MO0402DQRIRPPR.003	
24.00	0.138	TSw1	Tptrn	UE-25 UZ#16	23823 (-325.5)	ultrasonic pulse	PBT, Inc.	25.4	89.65	air dried	room temp.	3.53	NA	4.1	MO0402DQRIRPPR.003	
24.00	0.197	TSw1	Tptrn	UE-25 UZ#16	21128 (-278.8)	ultrasonic pulse	PBT, Inc.	25.4	97.89	air dried	room temp.	3.85	NA	4.1	MO0402DQRIRPPR.003	
27.70	0.203	TSw1	Tptrn	UE-25 UZ#16	21129 (-302)	ultrasonic pulse	PBT, Inc.	25.4	98.45	air dried	room temp.	3.88	NA	4.1	MO0402DQRIRPPR.003	
23.80	0.215	TSw1	Tptrn	UE-25 UZ#16	23822 (-264.4)	ultrasonic pulse	PBT, Inc.	25.4	88.81	air dried	room temp.	3.50	NA	6.9	MO0402DQRIRPPR.003	
25.10	0.145	TSw1	Tptrn	UE-25 UZ#16	23823 (-325.5)	ultrasonic pulse	PBT, Inc.	25.4	89.65	air dried	room temp.	3.53	NA	6.9	MO0402DQRIRPPR.003	
24.70	0.201	TSw1	Tptrn	UE-25 UZ#16	21128 (-278.8)	ultrasonic pulse	PBT, Inc.	25.4	97.89	air dried	room temp.	3.85	NA	6.9	MO0402DQRIRPPR.003	
28.90	0.207	TSw1	Tptrn	UE-25 UZ#16	21129 (-302)	ultrasonic pulse	PBT, Inc.	25.4	98.45	air dried	room temp.	3.88	NA	6.9	MO0402DQRIRPPR.003	
10.70		TSw1	Tptrn	USW GU-1	G1-409.9-SNL-B	cyclic loading	NER	55	210	room dry	room temp.	3.82		atmospheric	MO0402DQRIRPPR.003	Strain Amplitude = 2.7 microstrain; @ 0.1 Hz
10.50		TSw1	Tptrn	USW GU-1	G1-409.9-SNL-B	cyclic loading	NER	55	210	room dry	room temp.	3.82		atmospheric	MO0402DQRIRPPR.003	Strain Amplitude = 2.7 microstrain; @ 0.1 Hz
11.00		TSw1	Tptrn	USW GU-1	G1-409.9-SNL-B	cyclic loading	NER	55	210	room dry	room temp.	3.82		atmospheric	MO0402DQRIRPPR.003	Strain Amplitude = 2.7 microstrain; @ 0.1 Hz
11.90		TSw1	Tptrn	USW GU-1	G1-409.9-SNL-B	cyclic loading	NER	55	210	room dry	room temp.	3.82		atmospheric	MO0402DQRIRPPR.003	Strain Amplitude = 2.7 microstrain; @ 0.1 Hz
33.60	0.044	TSw2	Tptpll	UE-25 UZ#16	26829 (-899.3)	ultrasonic pulse	PBT, Inc.	25.4	39.7	air dried	room temp.	1.56	NA	0.7	MO0402DQRIRPPR.003	
33.60	0.034	TSw2	Tptpll	UE-25 UZ#16	26829 (-899.3)	ultrasonic pulse	PBT, Inc.	25.4	39.7	air dried	room temp.	1.56	NA	0.7	MO0402DQRIRPPR.003	

Table A-2. Intact Rock Mechanical Properties Data - Dynamic Elastic Data

Dynamic Young's Modulus (GPa)	Dynamic Poisson's Ratio	TM Unit	Litho-stratigraphic Unit	Sample Location	Specimen Number	Test Standard	Laboratory	Specimen Diameter (mm)	Specimen Length (mm)	Specimen Saturation	Specimen Temperature (deg. C)	L/D Ratio	Strain Rate (1/s)	Confining Pressure /Normal Stress (MPa)	DTN	Notes
34.90	0.014	TSw2	Tptpll	UE-25 UZ#16	26829 (-899.3)	ultrasonic pulse	PBT, Inc.	25.4	39.7	air dried	room temp.	1.56	NA	2.1	MO0402DQRIRPPR.003	
35.70	0.071	TSw2	Tptpll	UE-25 UZ#16	26829 (-899.3)	ultrasonic pulse	PBT, Inc.	25.4	39.7	air dried	room temp.	1.56	NA	4.1	MO0402DQRIRPPR.003	
36.30	0.082	TSw2	Tptpll	UE-25 UZ#16	26829 (-899.3)	ultrasonic pulse	PBT, Inc.	25.4	39.7	air dried	room temp.	1.56	NA	6.9	MO0402DQRIRPPR.003	
34.40	0.022	TSw2	Tptpll	UE-25 UZ#16	22215 (-784.1)	ultrasonic pulse	PBT, Inc.	25.4	51.2	air dried	room temp.	2.02	NA	0.7	MO0402DQRIRPPR.003	
34.60	0.024	TSw2	Tptpll	UE-25 UZ#16	22215 (-784.1)	ultrasonic pulse	PBT, Inc.	25.4	51.2	air dried	room temp.	2.02	NA	0.7	MO0402DQRIRPPR.003	
36.30	0.056	TSw2	Tptpll	UE-25 UZ#16	22215 (-784.1)	ultrasonic pulse	PBT, Inc.	25.4	51.2	air dried	room temp.	2.02	NA	2.1	MO0402DQRIRPPR.003	
37.80	0.098	TSw2	Tptpll	UE-25 UZ#16	22215 (-784.1)	ultrasonic pulse	PBT, Inc.	25.4	51.2	air dried	room temp.	2.02	NA	4.1	MO0402DQRIRPPR.003	
38.50	0.112	TSw2	Tptpll	UE-25 UZ#16	22215 (-784.1)	ultrasonic pulse	PBT, Inc.	25.4	51.2	air dried	room temp.	2.02	NA	6.9	MO0402DQRIRPPR.003	
34.50	0.113	TSw2	Tptpll	UE-25 UZ#16	24022 (-912)	ultrasonic pulse	PBT, Inc.	25.4	108.5	air dried	room temp.	4.27	NA	0.7	MO0402DQRIRPPR.003	
35.00	0.116	TSw2	Tptpll	UE-25 UZ#16	24022 (-912)	ultrasonic pulse	PBT, Inc.	25.4	108.5	air dried	room temp.	4.27	NA	0.7	MO0402DQRIRPPR.003	
28.70	0.132	TSw2	Tptpll	UE-25 UZ#16	22216 (-870.2)	ultrasonic pulse	PBT, Inc.	25.4	109.8	air dried	room temp.	4.32	NA	0.7	MO0402DQRIRPPR.003	
28.90	0.135	TSw2	Tptpll	UE-25 UZ#16	22216 (-870.2)	ultrasonic pulse	PBT, Inc.	25.4	109.8	air dried	room temp.	4.32	NA	0.7	MO0402DQRIRPPR.003	
35.40	0.195	TSw2	Tptpll	UE-25 UZ#16	22214 (-763.9)	ultrasonic pulse	PBT, Inc.	25.4	122.5	air dried	room temp.	4.82	NA	0.7	MO0402DQRIRPPR.003	
35.70	0.199	TSw2	Tptpll	UE-25 UZ#16	22214 (-763.9)	ultrasonic pulse	PBT, Inc.	25.4	122.5	air dried	room temp.	4.82	NA	0.7	MO0402DQRIRPPR.003	
36.50	0.115	TSw2	Tptpll	UE-25 UZ#16	24022 (-912)	ultrasonic pulse	PBT, Inc.	25.4	108.5	air dried	room temp.	4.27	NA	2.1	MO0402DQRIRPPR.003	
29.10	0.128	TSw2	Tptpll	UE-25 UZ#16	22216 (-870.2)	ultrasonic pulse	PBT, Inc.	25.4	109.8	air dried	room temp.	4.32	NA	2.1	MO0402DQRIRPPR.003	
37.30	0.186	TSw2	Tptpll	UE-25 UZ#16	22214 (-763.9)	ultrasonic pulse	PBT, Inc.	25.4	122.5	air dried	room temp.	4.82	NA	2.1	MO0402DQRIRPPR.003	
36.90	0.131	TSw2	Tptpll	UE-25 UZ#16	24022 (-912)	ultrasonic pulse	PBT, Inc.	25.4	108.5	air dried	room temp.	4.27	NA	4.1	MO0402DQRIRPPR.003	
29.60	0.148	TSw2	Tptpll	UE-25 UZ#16	22216 (-870.2)	ultrasonic pulse	PBT, Inc.	25.4	109.8	air dried	room temp.	4.32	NA	4.1	MO0402DQRIRPPR.003	
37.50	0.195	TSw2	Tptpll	UE-25 UZ#16	22214 (-763.9)	ultrasonic pulse	PBT, Inc.	25.4	122.5	air dried	room temp.	4.82	NA	4.1	MO0402DQRIRPPR.003	
37.10	0.140	TSw2	Tptpll	UE-25 UZ#16	24022 (-912)	ultrasonic pulse	PBT, Inc.	25.4	108.5	air dried	room temp.	4.27	NA	6.9	MO0402DQRIRPPR.003	
29.90	0.153	TSw2	Tptpll	UE-25 UZ#16	22216 (-870.2)	ultrasonic pulse	PBT, Inc.	25.4	109.8	air dried	room temp.	4.32	NA	6.9	MO0402DQRIRPPR.003	
38.00	0.196	TSw2	Tptpll	UE-25 UZ#16	22214 (-763.9)	ultrasonic pulse	PBT, Inc.	25.4	122.5	air dried	room temp.	4.82	NA	6.9	MO0402DQRIRPPR.003	
39.90	0.132	TSw2	Tptpln	UE-25 UZ#16	24025 (-1038.8)	ultrasonic pulse	PBT, Inc.	25.4	77.4	air dried	room temp.	3.05	NA	0.7	MO0402DQRIRPPR.003	
40.30	0.137	TSw2	Tptpln	UE-25 UZ#16	24025 (-1038.8)	ultrasonic pulse	PBT, Inc.	25.4	77.4	air dried	room temp.	3.05	NA	0.7	MO0402DQRIRPPR.003	
41.30	0.132	TSw2	Tptpln	UE-25 UZ#16	24026 (-1092.8)	ultrasonic pulse	PBT, Inc.	25.4	112.7	air dried	room temp.	4.44	NA	0.7	MO0402DQRIRPPR.003	
42.20	0.135	TSw2	Tptpln	UE-25 UZ#16	24026 (-1092.8)	ultrasonic pulse	PBT, Inc.	25.4	112.7	air dried	room temp.	4.44	NA	0.7	MO0402DQRIRPPR.003	
40.50	0.155	TSw2	Tptpln	UE-25 UZ#16	24024 (-1015.1)	ultrasonic pulse	PBT, Inc.	25.4	115.2	air dried	room temp.	4.54	NA	0.7	MO0402DQRIRPPR.003	
40.70	0.162	TSw2	Tptpln	UE-25 UZ#16	24024 (-1015.1)	ultrasonic pulse	PBT, Inc.	25.4	115.2	air dried	room temp.	4.54	NA	0.7	MO0402DQRIRPPR.003	
41.90	0.150	TSw2	Tptpln	UE-25 UZ#16	24023 (-955.6)	ultrasonic pulse	PBT, Inc.	25.4	122.1	air dried	room temp.	4.81	NA	0.7	MO0402DQRIRPPR.003	
41.80	0.150	TSw2	Tptpln	UE-25 UZ#16	24023 (-955.6)	ultrasonic pulse	PBT, Inc.	25.4	122.1	air dried	room temp.	4.81	NA	0.7	MO0402DQRIRPPR.003	
40.80	0.148	TSw2	Tptpln	UE-25 UZ#16	24025 (-1038.8)	ultrasonic pulse	PBT, Inc.	25.4	77.4	air dried	room temp.	3.05	NA	2.1	MO0402DQRIRPPR.003	
42.30	0.150	TSw2	Tptpln	UE-25 UZ#16	24026 (-1092.8)	ultrasonic pulse	PBT, Inc.	25.4	112.7	air dried	room temp.	4.44	NA	2.1	MO0402DQRIRPPR.003	
41.50	0.140	TSw2	Tptpln	UE-25 UZ#16	24024 (-1015.1)	ultrasonic pulse	PBT, Inc.	25.4	115.2	air dried	room temp.	4.54	NA	2.1	MO0402DQRIRPPR.003	
42.70	0.155	TSw2	Tptpln	UE-25 UZ#16	24023 (-955.6)	ultrasonic pulse	PBT, Inc.	25.4	122.1	air dried	room temp.	4.81	NA	2.1	MO0402DQRIRPPR.003	
41.00	0.158	TSw2	Tptpln	UE-25 UZ#16	24025 (-1038.8)	ultrasonic pulse	PBT, Inc.	25.4	77.4	air dried	room temp.	3.05	NA	4.1	MO0402DQRIRPPR.003	
42.60	0.156	TSw2	Tptpln	UE-25 UZ#16	24026 (-1092.8)	ultrasonic pulse	PBT, Inc.	25.4	112.7	air dried	room temp.	4.44	NA	4.1	MO0402DQRIRPPR.003	
41.70	0.153	TSw2	Tptpln	UE-25 UZ#16	24024 (-1015.1)	ultrasonic pulse	PBT, Inc.	25.4	115.2	air dried	room temp.	4.54	NA	4.1	MO0402DQRIRPPR.003	
42.80	0.169	TSw2	Tptpln	UE-25 UZ#16	24023 (-955.6)	ultrasonic pulse	PBT, Inc.	25.4	122.1	air dried	room temp.	4.81	NA	4.1	MO0402DQRIRPPR.003	
41.50	0.162	TSw2	Tptpln	UE-25 UZ#16	24025 (-1038.8)	ultrasonic pulse	PBT, Inc.	25.4	77.4	air dried	room temp.	3.05	NA	6.9	MO0402DQRIRPPR.003	
42.00	0.135	TSw2	Tptpln	UE-25 UZ#16	24026 (-1092.8)	ultrasonic pulse	PBT, Inc.	25.4	112.7	air dried	room temp.	4.44	NA	6.9	MO0402DQRIRPPR.003	
42.00	0.154	TSw2	Tptpln	UE-25 UZ#16	24024 (-1015.1)	ultrasonic pulse	PBT, Inc.	25.4	115.2	air dried	room temp.	4.54	NA	6.9	MO0402DQRIRPPR.003	
43.30	0.169	TSw2	Tptpln	UE-25 UZ#16	24023 (-955.6)	ultrasonic pulse	PBT, Inc.	25.4	122.1	air dried	room temp.	4.81	NA	6.9	MO0402DQRIRPPR.003	
44.42	0.212	TSw2	Tptpmn	Busted Butte	10/AE/78A; 10/AE/78B	-	NER	25.4	25.4	dry	room temp.	1.00		0	MO0402DQRIRPPR.003	
50.20	0.211	TSw2	Tptpmn	Busted Butte	10/AE/78A; 10/AE/78B	-	NER	25.4	25.4	dry	room temp.	1.00		0	MO0402DQRIRPPR.003	
	0.238	TSw2	Tptpmn	Busted Butte	10/AE/78A; 10/AE/78B	-	NER	25.4	25.4	dry	room temp.	1.00		0	MO0402DQRIRPPR.003	
39.00	0.129	TSw2	Tptpmn	UE-25 UZ#16	22212 (-624.1)	ultrasonic pulse	PBT, Inc.	25.4	106.3	air dried	room temp.	4.19	NA	0.7	MO0402DQRIRPPR.003	
39.50	0.126	TSw2	Tptpmn	UE-25 UZ#16	22212 (-624.1)	ultrasonic pulse	PBT, Inc.	25.4	106.3	air dried	room temp.	4.19	NA	0.7	MO0402DQRIRPPR.003	
42.40	0.124	TSw2	Tptpmn	UE-25 UZ#16	22213 (-659.2)	ultrasonic pulse	PBT, Inc.	25.4	119.4	air dried	room temp.	4.70	NA	0.7	MO0402DQRIRPPR.003	
42.20	0.113	TSw2	Tptpmn	UE-25 UZ#16	22213 (-659.2)	ultrasonic pulse	PBT, Inc.	25.4	119.4	air dried	room temp.	4.70	NA	0.7	MO0402DQRIRPPR.003	
36.20		TSw2	Tptpmn	Busted Butte	BB-10-AE-67-SNL	Waveform Inversion	NER	15	40	room dry	room temp.	2.67		atmospheric	MO0402DQRIRPPR.003	@ 45,000 Hz
37.40		TSw2	Tptpmn	Busted Butte	BB-10-AE-67-SNL	Waveform Inversion	NER	15	40	room dry	room temp.	2.67		atmospheric	MO0402DQRIRPPR.003	@ 65,000 Hz
37.00		TSw2	Tptpmn	Busted Butte	BB-10-AE-67-SNL	Waveform Inversion	NER	15	40	room dry	room temp.	2.67		atmospheric	MO0402DQRIRPPR.003	@ 85,000 Hz
35.80		TSw2	Tptpmn	Busted Butte	BB-10-AE-67-SNL	Waveform Inversion	NER	15	40	room dry	room temp.	2.67		atmospheric	MO0402DQRIRPPR.003	@ 105,000 Hz
40.20		TSw2	Tptpmn	Busted Butte	BB-10-AE-67-SNL	Resonant Bar	NER	13	201	room dry	room temp.	15.46		atmospheric	MO0402DQRIRPPR.003	@ 20,280 Hz
39.00		TSw2	Tptpmn	Busted Butte	BB-10-AE-67-SNL	Resonant Bar	NER	13	201	room dry	room temp.	15.46		atmospheric	MO0402DQRIRPPR.003	@ 30,155 Hz
38.70		TSw2	Tptpmn	Busted Butte	BB-10-AE-67-SNL	Resonant Bar	NER	13	201	room dry	room temp.	15.46		atmospheric	MO0402DQRIRPPR.003	@ 40,050 Hz
37.70		TSw2	Tptpmn	Busted Butte	BB-10-AE-67-SNL	Resonant Bar	NER	13	201	room dry	room temp.	15.46		atmospheric	MO0402DQRIRPPR.003	@ 49,667 Hz
40.10	0.130	TSw2	Tptpmn	UE-25 UZ#16	22212 (-624.1)	ultrasonic pulse	PBT, Inc.	25.4	106.3	air dried	room temp.	4.19	NA	2.1	MO0402DQRIRPPR.003	
43.20	0.131	TSw2	Tptpmn	UE-25 UZ#16	22213 (-659.2)	ultrasonic pulse	PBT, Inc.	25.4	119.4	air dried	room temp.	4.70	NA	2.1	MO0402DQRIRPPR.003	
40.50	0.145	TSw2	Tptpmn	UE-25 UZ#16	22212 (-624.1)	ultrasonic pulse	PBT, Inc.	25.4	106.3	air dried	room temp.	4.19	NA	4.1	MO0402DQRIRPPR.003	
43.70	0.145	TSw2	Tptpmn	UE-25 UZ#16	22213 (-659.2)	ultrasonic pulse	PBT, Inc.	25.4	119.4	air dried	room temp.	4.70	NA	4.1	MO0402DQRIRPPR.003	
40.80	0.148	TSw2	Tptpmn	UE-25 UZ#16	22212 (-624.1)	ultrasonic pulse	PBT, Inc.	25.4	106.3	air dried	room temp.	4.19	NA	6.9	MO0402DQRIRPPR.003	
44.10	0.145	TSw2	Tptpmn	UE-25 UZ#16	22213 (-659.2)	ultrasonic pulse	PBT, Inc.	25.4	119.4	air dried	room temp.	4.70	NA	6.9	MO0402DQRIRPPR.003	
39.10	0.220	TSw2	Tptpmn	USW GU-3	GU-3 760.9-3A	-	SANDIA	25.35	50.83	saturated	room temp.	2.01	NA	atmospheric	MO0402DQRIRPPR.003	Large solution cavities

Table A-2. Intact Rock Mechanical Properties Data - Dynamic Elastic Data

Dynamic Young's Modulus (GPa)	Dynamic Poisson's Ratio	TM Unit	Litho-stratigraphic Unit	Sample Location	Specimen Number	Test Standard	Laboratory	Specimen Diameter (mm)	Specimen Length (mm)	Specimen Saturation	Specimen Temperature (deg. C)	L/D Ratio	Strain Rate (1/s)	Confining Pressure /Normal Stress (MPa)	DTN	Notes
39.90	0.250	TSw2	Tptpmn	USW GU-3	GU-3 760.9-3A	-	SANDIA	25.35	50.83	saturated	room temp.	2.01	NA	atmospheric	MO0402DQRIRPPR.003	
41.30	0.250	TSw2	Tptpmn	USW GU-3	GU-3 760.9-3A	-	SANDIA	25.35	50.83	saturated	room temp.	2.01	NA	atmospheric	MO0402DQRIRPPR.003	
39.10	0.220	TSw2	Tptpmn	USW GU-3	GU-3 760.9-2B	-	SANDIA	25.37	50.88	saturated	room temp.	2.01	NA	atmospheric	MO0402DQRIRPPR.003	
39.90	0.210	TSw2	Tptpmn	USW GU-3	GU-3 760.9-2B	-	SANDIA	25.37	50.88	saturated	room temp.	2.01	NA	atmospheric	MO0402DQRIRPPR.003	
40.60	0.210	TSw2	Tptpmn	USW GU-3	GU-3 760.9-2B	-	SANDIA	25.37	50.88	saturated	room temp.	2.01	NA	atmospheric	MO0402DQRIRPPR.003	
39.10	0.230	TSw2	Tptpmn	USW GU-3	GU-3 760.9-3B	-	SANDIA	25.37	50.88	saturated	room temp.	2.01	NA	atmospheric	MO0402DQRIRPPR.003	
39.30	0.220	TSw2	Tptpmn	USW GU-3	GU-3 760.9-3B	-	SANDIA	25.37	50.88	saturated	room temp.	2.01	NA	atmospheric	MO0402DQRIRPPR.003	
39.70	0.230	TSw2	Tptpmn	USW GU-3	GU-3 760.9-3B	-	SANDIA	25.37	50.88	saturated	room temp.	2.01	NA	atmospheric	MO0402DQRIRPPR.003	
39.50	0.220	TSw2	Tptpmn	USW GU-3	GU-3 760.9-4A	-	SANDIA	25.37	50.88	saturated	room temp.	2.01	NA	atmospheric	MO0402DQRIRPPR.003	
42.00	0.190	TSw2	Tptpmn	USW GU-3	GU-3 760.9-4A	-	SANDIA	25.37	50.88	saturated	room temp.	2.01	NA	atmospheric	MO0402DQRIRPPR.003	Large solution cavities
42.00	0.220	TSw2	Tptpmn	USW GU-3	GU-3 760.9-4A	-	SANDIA	25.37	50.88	saturated	room temp.	2.01	NA	atmospheric	MO0402DQRIRPPR.003	
38.30	0.210	TSw2	Tptpmn	USW GU-3	GU-3 760.9-5A	-	SANDIA	25.35	50.85	saturated	room temp.	2.01	NA	atmospheric	MO0402DQRIRPPR.003	
39.20	0.210	TSw2	Tptpmn	USW GU-3	GU-3 760.9-5A	-	SANDIA	25.35	50.85	saturated	room temp.	2.01	NA	atmospheric	MO0402DQRIRPPR.003	
39.90	0.230	TSw2	Tptpmn	USW GU-3	GU-3 760.9-5A	-	SANDIA	25.35	50.85	saturated	room temp.	2.01	NA	atmospheric	MO0402DQRIRPPR.003	
36.20	0.190	TSw2	Tptpmn	USW GU-3	GU-3 760.9-4B	-	SANDIA	25.37	50.90	saturated	room temp.	2.01	NA	atmospheric	MO0402DQRIRPPR.003	
37.70	0.180	TSw2	Tptpmn	USW GU-3	GU-3 760.9-4B	-	SANDIA	25.37	50.90	saturated	room temp.	2.01	NA	atmospheric	MO0402DQRIRPPR.003	
38.50	0.210	TSw2	Tptpmn	USW GU-3	GU-3 760.9-4B	-	SANDIA	25.37	50.90	saturated	room temp.	2.01	NA	atmospheric	MO0402DQRIRPPR.003	
36.40	0.230	TSw2	Tptpmn	USW GU-3	GU-3 760.9-5B	-	SANDIA	25.35	50.88	saturated	room temp.	2.01	NA	atmospheric	MO0402DQRIRPPR.003	
37.00	0.190	TSw2	Tptpmn	USW GU-3	GU-3 760.9-5B	-	SANDIA	25.35	50.88	saturated	room temp.	2.01	NA	atmospheric	MO0402DQRIRPPR.003	
38.00	0.200	TSw2	Tptpmn	USW GU-3	GU-3 760.9-5B	-	SANDIA	25.35	50.88	saturated	room temp.	2.01	NA	atmospheric	MO0402DQRIRPPR.003	
39.00	0.250	TSw2	Tptpmn	USW GU-3	GU-3 760.9-1A	-	SANDIA	25.35	50.90	saturated	room temp.	2.01	NA	atmospheric	MO0402DQRIRPPR.003	
41.40	0.200	TSw2	Tptpmn	USW GU-3	GU-3 760.9-1A	-	SANDIA	25.35	50.90	saturated	room temp.	2.01	NA	atmospheric	MO0402DQRIRPPR.003	
42.60	0.230	TSw2	Tptpmn	USW GU-3	GU-3 760.9-1A	-	SANDIA	25.35	50.90	saturated	room temp.	2.01	NA	atmospheric	MO0402DQRIRPPR.003	
39.00	0.230	TSw2	Tptpmn	USW GU-3	GU-3 760.9-1B	-	SANDIA	25.35	50.90	saturated	room temp.	2.01	NA	atmospheric	MO0402DQRIRPPR.003	
39.50	0.210	TSw2	Tptpmn	USW GU-3	GU-3 760.9-1B	-	SANDIA	25.35	50.90	saturated	room temp.	2.01	NA	atmospheric	MO0402DQRIRPPR.003	Large solution cavities
40.50	0.240	TSw2	Tptpmn	USW GU-3	GU-3 760.9-1B	-	SANDIA	25.35	50.90	saturated	room temp.	2.01	NA	atmospheric	MO0402DQRIRPPR.003	
38.50	0.230	TSw2	Tptpmn	USW GU-3	GU-3 760.9-2A	-	SANDIA	25.35	50.90	saturated	room temp.	2.01	NA	atmospheric	MO0402DQRIRPPR.003	
38.20	0.210	TSw2	Tptpmn	USW GU-3	GU-3 760.9-2A	-	SANDIA	25.35	50.90	saturated	room temp.	2.01	NA	atmospheric	MO0402DQRIRPPR.003	
39.10	0.240	TSw2	Tptpmn	USW GU-3	GU-3 760.9-2A	-	SANDIA	25.35	50.90	saturated	room temp.	2.01	NA	atmospheric	MO0402DQRIRPPR.003	
35.70		TSw2	Tptpmn	Busted Butte	BB-10-AE-67-SNL	Waveform Inversion	NER	15	40	saturated	room temp.	2.67		atmospheric	MO0402DQRIRPPR.003	@ 45,000 Hz
36.10		TSw2	Tptpmn	Busted Butte	BB-10-AE-67-SNL	Waveform Inversion	NER	15	40	saturated	room temp.	2.67		atmospheric	MO0402DQRIRPPR.003	@ 65,000 Hz
36.50		TSw2	Tptpmn	Busted Butte	BB-10-AE-67-SNL	Waveform Inversion	NER	15	40	saturated	room temp.	2.67		atmospheric	MO0402DQRIRPPR.003	@ 85,000 Hz
35.90		TSw2	Tptpmn	Busted Butte	BB-10-AE-67-SNL	Waveform Inversion	NER	15	40	saturated	room temp.	2.67		atmospheric	MO0402DQRIRPPR.003	@ 105,000 Hz
40.60		TSw2	Tptpmn	Busted Butte	BB-10-AE-67-SNL	Resonant Bar	NER	13	201	saturated	room temp.	15.46		atmospheric	MO0402DQRIRPPR.003	@ 19,700 Hz
39.90		TSw2	Tptpmn	Busted Butte	BB-10-AE-67-SNL	Resonant Bar	NER	13	201	saturated	room temp.	15.46		atmospheric	MO0402DQRIRPPR.003	@ 29,400 Hz
40.00		TSw2	Tptpmn	Busted Butte	BB-10-AE-67-SNL	Resonant Bar	NER	13	201	saturated	room temp.	15.46		atmospheric	MO0402DQRIRPPR.003	@ 39,000 Hz
40.40		TSw2	Tptpmn	Busted Butte	BB-10-AE-67-SNL	Resonant Bar	NER	13	201	saturated	room temp.	15.46		atmospheric	MO0402DQRIRPPR.003	@ 48,400 Hz
41.89	0.200	TSw2	Tptpmn	Busted Butte	BB-10AE-11Y-SNL	-	NER	50.8	101.6	dry	ambient	2.00	NA	0	MO0402DQRIRPPR.003	
43.21	0.210	TSw2	Tptpmn	Busted Butte	BB-10AE-11Z-SNL	-	NER	50.8	101.6	dry	ambient	2.00	NA	0	MO0402DQRIRPPR.003	
40.83	0.220	TSw2	Tptpmn	Busted Butte	BB-10AE-49W-SNL	-	NER	50.8	101.6	dry	ambient	2.00	NA	0	MO0402DQRIRPPR.003	Large solution cavities
44.10	0.200	TSw2	Tptpmn	Busted Butte	BB-10AE-5X-SNL	-	NER	50.8	101.6	dry	ambient	2.00	NA	0	MO0402DQRIRPPR.003	
44.25	0.210	TSw2	Tptpmn	Busted Butte	BB-10AE-6Y-SNL	-	NER	50.8	101.6	dry	ambient	2.00	NA	0	MO0402DQRIRPPR.003	
38.30		TSw2	Tptpmn	Busted Butte	BB-10-AE-67-SNL	cyclic loading	NER	55	210	room dry	room temp.	3.82		atmospheric	MO0402DQRIRPPR.003	Strain Amplitude = 2.7 microstrain; @ 0.1 Hz
38.30		TSw2	Tptpmn	Busted Butte	BB-10-AE-67-SNL	cyclic loading	NER	55	210	room dry	room temp.	3.82		atmospheric	MO0402DQRIRPPR.003	Strain Amplitude = 7.3 microstrain; @ 0.1 Hz
38.50		TSw2	Tptpmn	Busted Butte	BB-10-AE-67-SNL	cyclic loading	NER	55	210	room dry	room temp.	3.82		atmospheric	MO0402DQRIRPPR.003	Strain Amplitude = 15.3 microstrain; @ 0.1 Hz
38.40		TSw2	Tptpmn	Busted Butte	BB-10-AE-67-SNL	cyclic loading	NER	55	210	room dry	room temp.	3.82		atmospheric	MO0402DQRIRPPR.003	Strain Amplitude = 53.1 microstrain; @ 0.1 Hz
38.20		TSw2	Tptpmn	Busted Butte	BB-10-AE-67-SNL	cyclic loading	NER	55	210	room dry	room temp.	3.82		atmospheric	MO0402DQRIRPPR.003	Strain Amplitude = 80.7 microstrain; @ 0.1 Hz
41.52	0.230	TSw2	Tptpmn	Busted Butte	BB-10AE-11Y-SNL	-	NER	50.8	101.6	saturated	ambient	2.00	NA	0	MO0402DQRIRPPR.003	
42.93	0.240	TSw2	Tptpmn	Busted Butte	BB-10AE-11Z-SNL	-	NER	50.8	101.6	saturated	ambient	2.00	NA	0	MO0402DQRIRPPR.003	
44.30	0.230	TSw2	Tptpmn	Busted Butte	BB-10AE-24Z-SNL	-	NER	50.8	101.6	saturated	ambient	2.00	NA	0	MO0402DQRIRPPR.003	
38.52	0.280	TSw2	Tptpmn	Busted Butte	BB-10AE-49W-SNL	-	NER	50.8	101.6	saturated	ambient	2.00	NA	0	MO0402DQRIRPPR.003	
44.73	0.230	TSw2	Tptpmn	Busted Butte	BB-10AE-5X-SNL	-	NER	50.8	101.6	saturated	ambient	2.00	NA	0	MO0402DQRIRPPR.003	
45.34	0.230	TSw2	Tptpmn	Busted Butte	BB-10AE-6Y-SNL	-	NER	50.8	101.6	saturated	ambient	2.00	NA	0	MO0402DQRIRPPR.003	
36.00		TSw2	Tptpmn	Busted Butte	BB-10-AE-67-SNL	cyclic loading	NER	55	210	saturated	room temp.	3.82		atmospheric	MO0402DQRIRPPR.003	Strain Amplitude = 6.1 microstrain; @ 0.1 Hz
36.30		TSw2	Tptpmn	Busted Butte	BB-10-AE-67-SNL	cyclic loading	NER	55	210	saturated	room temp.	3.82		atmospheric	MO0402DQRIRPPR.003	Strain Amplitude = 10.1 microstrain; @ 0.1 Hz
36.20		TSw2	Tptpmn	Busted Butte	BB-10-AE-67-SNL	cyclic loading	NER	55	210	saturated	room temp.	3.82		atmospheric	MO0402DQRIRPPR.003	Strain Amplitude = 17.4 microstrain; @ 0.1 Hz
36.10		TSw2	Tptpmn	Busted Butte	BB-10-AE-67-SNL	cyclic loading	NER	55	210	saturated	room temp.	3.82		atmospheric	MO0402DQRIRPPR.003	Strain Amplitude = 31.0 microstrain; @ 0.1 Hz
36.10		TSw2	Tptpmn	Busted Butte	BB-10-AE-67-SNL	cyclic loading	NER	55	210	saturated	room temp.	3.82		atmospheric	MO0402DQRIRPPR.003	Strain Amplitude = 70.3 microstrain; @ 0.1 Hz
53.30	0.182	TSw3	Tptpv3	UE-25 UZ#16	24027 (-1124.1)	ultrasonic pulse	PBT, Inc.	25.4	56.6	air dried	room temp.	2.23	NA	0.7	MO0402DQRIRPPR.003	
53.90	0.196	TSw3	Tptpv3	UE-25 UZ#16	24027 (-1124.1)	ultrasonic pulse	PBT, Inc.	25.4	56.6	air dried	room temp.	2.23	NA	0.7	MO0402DQRIRPPR.003	
57.50	0.132	TSw3	Tptpv3	UE-25 UZ#16	24027 (-1124.1)	ultrasonic pulse	PBT, Inc.	25.4	56.6	air dried	room temp.	2.23	NA	2.1	MO0402DQRIRPPR.003	
57.90	0.160	TSw3	Tptpv3	UE-25 UZ#16	24027 (-1124.1)	ultrasonic pulse	PBT, Inc.	25.4	56.6	air dried	room temp.	2.23	NA	4.1	MO0402DQRIRPPR.003	
58.10	0.160	TSw3	Tptpv3	UE-25 UZ#16	24027 (-1124.1)	ultrasonic pulse	PBT, Inc.	25.4	56.6	air dried	room temp.	2.23	NA	6.9	MO0402DQRIRPPR.003	

Notes: The data from CFun unit are presented in this table; however, these data are not used in the analysis.
All blanks, NA, or "-" are indicating the information is not available unless otherwise specified.

Table A-3. Intact Rock Mechanical Properties Data - Indirect Tensile Strength Data

Porosity (%)	Tensile Strength (MPa)	TM Unit	Litho stratigraphic Unit	Location	Depth (ft)	DTN	Test Procedure	Laboratory	Specimen Length (in)	Specimen Diameter (in)	Specimen Temperature (deg. C)	Length/ Diameter Ratio	Specimen Saturation	Specimen Mass (grams)	Apparent Specimen Unit Weight (lbm/ft^3)	Maximum Applied Load (lbf)	Strain Rate (1/s)	Testing Group
46.5	0.3	PTn	Tpbt2	USW NRG-6	222	MO0401DQRIRPTS.003	ASTM D 3967-93	New England Research	1.52	2.03	Ambient	0.75	Room Dry				10^{-5}	221121
59.4	0.2	PTn	Tpbt2	USW NRG-6	241.5	MO0401DQRIRPTS.003	ASTM D 3967-93	New England Research	1.52	2.03	Ambient	0.75	Room Dry				10^{-5}	221121
55.2	0.1	PTn	Tpbt2	USW-NRG-7/7A	268.6	MO0401DQRIRPTS.003	ASTM D 3967-93	New England Research	1.52	2.03	Ambient	0.75	Saturated				10^{-5}	231121
37.0	0.8	PTn	Tpbt2	UE-25-NRG-4	458.7	MO0401DQRIRPTS.003	ASTM D 3967-93	New England Research	1.52	2.03	Ambient	0.75	Saturated				10^{-5}	231121
46.1	0.1	PTn	Tpbt2	UE-25-NRG-4	469.0	MO0401DQRIRPTS.003	ASTM D 3967-93	New England Research	1.52	2.03	Ambient	0.75	Saturated				10^{-5}	231121
55.7	0.3	PTn	Tpbt3	USW NRG-6	174	MO0401DQRIRPTS.003	ASTM D 3967-93	New England Research	1.52	2.03	Ambient	0.75	Room Dry				10^{-5}	221121
41.2	0.5	PTn	Tpcpv1	USW-NRG-7/7A	91.0	MO0401DQRIRPTS.003	ASTM D 3967-93	New England Research	1.52	2.03	Ambient	0.75	Saturated				10^{-5}	231121
27.9	5.1	PTn	Tpcpv2	USW-NRG-7/7A	73.7	MO0401DQRIRPTS.003	ASTM D 3967-93	New England Research	1.52	2.03	Ambient	0.75	Saturated				10^{-5}	231121
37.0	1.2	PTn	Tpcpv2	USW-NRG-7/7A	77.7	MO0401DQRIRPTS.003	ASTM D 3967-93	New England Research	1.52	2.03	Ambient	0.75	Saturated				10^{-5}	231121
29.7	4.5	PTn	Tpcpv2	USW NRG-6	145.7	MO0401DQRIRPTS.003	ASTM D 3967-93	New England Research	1.52	2.03	Ambient	0.75	Saturated				10^{-5}	231121
40.8	1.9	PTn	Tpcpv2	USW NRG-6	151.2	MO0401DQRIRPTS.003	ASTM D 3967-93	New England Research	1.52	2.03	Ambient	0.75	Saturated				10^{-5}	231121
55.6	0.4	PTn	Tpp	USW NRG-6	182.2	MO0401DQRIRPTS.003	ASTM D 3967-93	New England Research	1.52	2.03	Ambient	0.75	Room Dry				10^{-5}	221121
52.3	0.1	PTn	Tpp	USW-NRG-7/7A	174.1	MO0401DQRIRPTS.003	ASTM D 3967-93	New England Research	1.52	2.03	Ambient	0.75	Saturated				10^{-5}	231121
53.9	0.02	PTn	Tpp	USW-NRG-7/7A	182.5	MO0401DQRIRPTS.003	ASTM D 3967-93	New England Research	1.52	2.03	Ambient	0.75	Saturated				10^{-5}	231121
54.3	0.03	PTn	Tpp	USW-NRG-7/7A	182.5	MO0401DQRIRPTS.003	ASTM D 3967-93	New England Research	1.52	2.03	Ambient	0.75	Saturated				10^{-5}	231121
52.2	0.1	PTn	Tpp	USW-NRG-7/7A	182.5	MO0401DQRIRPTS.003	ASTM D 3967-93	New England Research	1.52	2.03	Ambient	0.75	Saturated				10^{-5}	231121
48.7	0.02	PTn	Tpp	USW-NRG-7/7A	224.4	MO0401DQRIRPTS.003	ASTM D 3967-93	New England Research	1.52	2.03	Ambient	0.75	Saturated				10^{-5}	231121
50.9	0.1	PTn	Tpp	USW-NRG-7/7A	244.7	MO0401DQRIRPTS.003	ASTM D 3967-93	New England Research	1.52	2.03	Ambient	0.75	Saturated				10^{-5}	231121
54.6	0.2	PTn	Tpp	USW-NRG-7/7A	244.7	MO0401DQRIRPTS.003	ASTM D 3967-93	New England Research	1.52	2.03	Ambient	0.75	Saturated				10^{-5}	231121
50.1	0.1	PTn	Tpp	UE-25-NRG-4	382.9	MO0401DQRIRPTS.003	ASTM D 3967-93	New England Research	1.52	2.03	Ambient	0.75	Saturated				10^{-5}	231121
55.2	0.2	PTn	Tpp	UE-25-NRG-4	428.4	MO0401DQRIRPTS.003	ASTM D 3967-93	New England Research	1.52	2.03	Ambient	0.75	Saturated				10^{-5}	231121
51.0	0.2	PTn	Tpp	UE-25-NRG-4	433.2	MO0401DQRIRPTS.003	ASTM D 3967-93	New England Research	1.52	2.03	Ambient	0.75	Saturated				10^{-5}	231121
54.0	0.2	PTn	Tpp	UE-25-NRG-4	439.4	MO0401DQRIRPTS.003	ASTM D 3967-93	New England Research	1.52	2.03	Ambient	0.75	Saturated				10^{-5}	231121
45.4	0.7	PTn	Tpp	UE-25-NRG-4	456.0	MO0401DQRIRPTS.003	ASTM D 3967-93	New England Research	1.52	2.03	Ambient	0.75	Saturated				10^{-5}	231121
31.3	3.0	PTn	Tpy	USW-NRG-7/7A	135.3	MO0401DQRIRPTS.003	ASTM D 3967-93	New England Research	1.52	2.03	Ambient	0.75	Saturated				10^{-5}	231121
5.5	13.2	TCw	Tpcpll	USW NRG-6	23.4	MO0401DQRIRPTS.003	ASTM D 3967-93	New England Research	1.52	2.03	Ambient	0.75	Saturated				10^{-5}	231121
5.6	16	TCw	Tpcpll	USW NRG-6	23.4	MO0401DQRIRPTS.003	ASTM D 3967-93	New England Research	1.52	2.03	Ambient	0.75	Saturated				10^{-5}	231121
17.3	7.4	TCw	Tpcpll	UE-25 NRG #3	292.4	MO0401DQRIRPTS.003	ASTM D 3967-93	New England Research	1.52	2.03	Ambient	0.75	Saturated				10^{-5}	231121
8.8	10.6	TCw	Tpcpln	USW-NRG-7/7A	18.0	MO0401DQRIRPTS.003	ASTM D 3967-93	New England Research	1.52	2.03	Ambient	0.75	Saturated				10^{-5}	231121
6.6	9.4	TCw	Tpcpln	USW-NRG-7/7A	24.4	MO0401DQRIRPTS.003	ASTM D 3967-93	New England Research	1.52	2.03	Ambient	0.75	Saturated				10^{-5}	231121
6.9	9.9	TCw	Tpcpln	USW-NRG-7/7A	24.4	MO0401DQRIRPTS.003	ASTM D 3967-93	New England Research	1.52	2.03	Ambient	0.75	Saturated				10^{-5}	231121
8.5	13.0	TCw	Tpcpln	USW-NRG-7/7A	41.4	MO0401DQRIRPTS.003	ASTM D 3967-93	New England Research	1.52	2.03	Ambient	0.75	Saturated				10^{-5}	231121
13.7	13.4	TCw	Tpcpln	USW-NRG-7/7A	47.4	MO0401DQRIRPTS.003	ASTM D 3967-93	New England Research	1.52	2.03	Ambient	0.75	Saturated				10^{-5}	231121
16.6	11.8	TCw	Tpcpln	USW-NRG-7/7A	55.4	MO0401DQRIRPTS.003	ASTM D 3967-93	New England Research	1.52	2.03	Ambient	0.75	Saturated				10^{-5}	231121
7.3	10.6	TCw	Tpcpln	USW NRG-6	98.1	MO0401DQRIRPTS.003	ASTM D 3967-93	New England Research	1.52	2.03	Ambient	0.75	Saturated				10^{-5}	231121
7.4	11.3	TCw	Tpcpln	USW NRG-6	98.1	MO0401DQRIRPTS.003	ASTM D 3967-93	New England Research	1.52	2.03	Ambient	0.75	Saturated				10^{-5}	231121
10.4	8.2	TCw	Tpcpln	USW NRG-6	111	MO0401DQRIRPTS.003	ASTM D 3967-93	New England Research	1.52	2.03	Ambient	0.75	Saturated				10^{-5}	231121
11.1	12.1	TCw	Tpcpln	USW NRG-6	111	MO0401DQRIRPTS.003	ASTM D 3967-93	New England Research	1.52	2.03	Ambient	0.75	Saturated				10^{-5}	231121
7.4	10.9	TCw	Tpcpln	UE-25 NRG #2	171.0	MO0401DQRIRPTS.003	ASTM D 3967-93	New England Research	1.52	2.03	Ambient	0.75	Saturated				10^{-5}	231121
7.4	13.3	TCw	Tpcpln	UE-25 NRG #2	171.7	MO0401DQRIRPTS.003	ASTM D 3967-93	New England Research	1.52	2.03	Ambient	0.75	Saturated				10^{-5}	231121
9.3	8.2	TCw	Tpcpln	UE-25 NRG #2	172.0	MO0401DQRIRPTS.003	ASTM D 3967-93	New England Research	1.52	2.03	Ambient	0.75	Saturated				10^{-5}	231121
6.4	12.4	TCw	Tpcpln	UE-25 NRG #2	176.1	MO0401DQRIRPTS.003	ASTM D 3967-93	New England Research	1.52	2.03	Ambient	0.75	Saturated				10^{-5}	231121
7.4	12.0	TCw	Tpcpln	UE-25 NRG #2	178.5	MO0401DQRIRPTS.003	ASTM D 3967-93	New England Research	1.52	2.03	Ambient	0.75	Saturated				10^{-5}	231121
8.2	12.6	TCw	Tpcpln	UE-25 NRG #2	180.5	MO0401DQRIRPTS.003	ASTM D 3967-93	New England Research	1.52	2.03	Ambient	0.75	Saturated				10^{-5}	231121
7.4	9.3	TCw	Tpcpln	UE-25 NRG #2	188.8	MO0401DQRIRPTS.003	ASTM D 3967-93	New England Research	1.52	2.03	Ambient	0.75	Saturated				10^{-5}	231121
6.9	8.4	TCw	Tpcpln	UE-25 NRG #2	196.9	MO0401DQRIRPTS.003	ASTM D 3967-93	New England Research	1.52	2.03	Ambient	0.75	Saturated				10^{-5}	231121
7.2	9.6	TCw	Tpcpln	UE-25 NRG #2	199.0	MO0401DQRIRPTS.003	ASTM D 3967-93	New England Research	1.52	2.03	Ambient	0.75	Saturated				10^{-5}	231121
	18.9	TCw	Tpcpmn	UE25-NRG-1	123.4-123.5	MO0401DQRIRPTS.003	ASTM D 3967-93	USBR	1.26	2.41	Ambient	0.52	Saturated	218.56	144.5	13074	10^{-5}	231121
	17.4	TCw	Tpcpmn	UE25-NRG-1	123.5-123.6	MO0401DQRIRPTS.003	ASTM D 3967-93	USBR	1.27	2.41	Ambient	0.53	Saturated	218.26	143.2	12189	10^{-5}	231121
	16.8	TCw	Tpcpmn	UE25-NRG-1	123.6-123.7	MO0401DQRIRPTS.003	ASTM D 3967-93	USBR	1.33	2.41	Ambient	0.55	Saturated	228.23	143	12292	10^{-5}	231121
	7.2	TCw	Tpcpmn	UE25-NRG-1	127.9-128.0	MO0401DQRIRPTS.003	ASTM D 3967-93	USBR	1.38	2.41	Ambient	0.57	Saturated	239.24	145.1	5441	10^{-5}	231121
	15.1	TCw	Tpcpmn	UE25-NRG-1	129.1-129.2	MO0401DQRIRPTS.003	ASTM D 3967-93	USBR	1.25	2.41	Ambient	0.52	Saturated	205.71	137.5	10387	10^{-5}	231121
	19.1	TCw	Tpcpmn	UE25-NRG-1	129.7-129.8	MO0401DQRIRPTS.003	ASTM D 3967-93	USBR	1.29	2.41	Ambient	0.53	Saturated	222.16	144.2	13477	10^{-5}	231121
	14.9	TCw	Tpcpmn	UE25-NRG-1	129.9-130.0	MO0401DQRIRPTS.003	ASTM D 3967-93	USBR	1.39	2.41	Ambient	0.58	Saturated	239.27	143.8	11389	10^{-5}	231121
	16.3	TCw	Tpcpmn	UE25-NRG-1	130.95-131.1	MO0401DQRIRPTS.003	ASTM D 3967-93	USBR	1.37	2.41	Ambient	0.57	Saturated	236.16	144.3	12213	10^{-5}	231121
	14.1	TCw	Tpcpmn	UE25-NRG-1	131.1-131.2	MO0401DQRIRPTS.003	ASTM D 3967-93	USBR	1.3	2.41	Ambient	0.54	Saturated	224.67	144.7	10064	10^{-5}	231121
	17.5	TCw	Tpcpmn	UE25-NRG-1	131.3-131.45	MO0401DQRIRPTS.003	ASTM D 3967-93	USBR	1.36	2.41	Ambient	0.56	Saturated	235.99	144.9	13092	10^{-5}	231121
	15.7	TCw	Tpcpmn	UE25-NRG-1	131.45-131.55	MO0401DQRIRPTS.003	ASTM D 3967-93	USBR	1.4	2.41	Ambient	0.58	Saturated	244.81	146.1	12036	10^{-5}	231121

Table A-3. Intact Rock Mechanical Properties Data - Indirect Tensile Strength Data

Porosity (%)	Tensile Strength (MPa)	TM Unit	Litho stratigraphic Unit	Location	Depth (ft)	DTN	Test Procedure	Laboratory	Specimen Length (in)	Specimen Diameter (in)	Specimen Temperature (deg. C)	Length/ Diameter Ratio	Specimen Saturation	Specimen Mass (grams)	Apparent Specimen Unit Weight (lbm/ft^3)	Maximum Applied Load (lbf)	Strain Rate (1/s)	Testing Group
	13.7	TCw	Tpcpmn	UE25-NRG-1	146.6-146.75	MO0401DQRIRPTS.003	ASTM D 3967-93	USBR	1.33	2.42	Ambient	0.55	Saturated	234.67	145.8	10033	10^{-5}	231121
	15.3	TCw	Tpcpmn	UE25-NRG-1	146.75-146.85	MO0401DQRIRPTS.003	ASTM D 3967-93	USBR	1.32	2.42	Ambient	0.55	Saturated	231.5	144.9	11175	10^{-5}	231121
12.2	10.2	TCw	Tpcpmn	UE-25 NRG #3	218.0	MO0401DQRIRPTS.003	ASTM D 3967-93	New England Research	1.52	2.03	Ambient	0.75	Saturated				10^{-5}	231121
14.1	5.3	TCw	Tpcpmn	UE-25 NRG #3	226.7	MO0401DQRIRPTS.003	ASTM D 3967-93	New England Research	1.52	2.03	Ambient	0.75	Saturated				10^{-5}	231121
8.5	14.8	TCw	Tpcpmn	UE-25 NRG #3	256.0	MO0401DQRIRPTS.003	ASTM D 3967-93	New England Research	1.52	2.03	Ambient	0.75	Saturated				10^{-5}	231121
	11.5	TCw	Tpcpul	UE25-NRG-1	37.8-37.9	MO0401DQRIRPTS.003	ASTM D 3967-93	USBR	1.33	2.41	Ambient	0.55	Saturated	213.18	133.5	8433	10^{-5}	231121
	8.1	TCw	Tpcpul	UE25-NRG-1	68.7-68.8	MO0401DQRIRPTS.003	ASTM D 3967-93	USBR	1.2	2.41	Ambient	0.5	Saturated	191.36	133.6	5355	10^{-5}	231121
	6.2	TCw	Tpcpul	UE25-NRG-1	68.8-68.9	MO0401DQRIRPTS.003	ASTM D 3967-93	USBR	1.16	2.41	Ambient	0.48	Saturated	178.01	127.8	3981	10^{-5}	231121
	13.6	TCw	Tpcpul	UE25-NRG-1	76.45-76.55	MO0401DQRIRPTS.003	ASTM D 3967-93	USBR	1.35	2.41	Ambient	0.56	Saturated	218.33	134.7	10088	10^{-5}	231121
	7.7	TCw	Tpcpul	UE25-NRG-1	77.7-77.8	MO0401DQRIRPTS.003	ASTM D 3967-93	USBR	1.32	2.41	Ambient	0.55	Saturated	211.88	134.1	5612	10^{-5}	231121
	9.6	TCw	Tpcpul	UE25-NRG-1	77.95-78.05	MO0401DQRIRPTS.003	ASTM D 3967-93	USBR	1.36	2.41	Ambient	0.56	Saturated	213.66	131.5	7126	10^{-5}	231121
	8.8	TCw	Tpcpul	UE25-NRG-1	78.1-78.2	MO0401DQRIRPTS.003	ASTM D 3967-93	USBR	1.45	2.41	Ambient	0.6	Saturated	226.59	130.8	7004	10^{-5}	231121
	8.5	TCw	Tpcpul	UE25-NRG-1	87.8-87.9	MO0401DQRIRPTS.003	ASTM D 3967-93	USBR	1.29	2.41	Ambient	0.53	Saturated	205.68	133.5	5990	10^{-5}	231121
	11.5	TCw	Tpcpul	UE25-NRG-1	87.9-88.0	MO0401DQRIRPTS.003	ASTM D 3967-93	USBR	1.37	2.41	Ambient	0.57	Saturated	226.12	138.2	8635	10^{-5}	231121
	10.0	TCw	Tpcpul	UE25-NRG-1	89.7-89.8	MO0401DQRIRPTS.003	ASTM D 3967-93	USBR	1.26	2.41	Ambient	0.52	Saturated	206.55	136.6	6937	10^{-5}	231121
	9.5	TCw	Tpcpul	UE25-NRG-1	89.8-89.9	MO0401DQRIRPTS.003	ASTM D 3967-93	USBR	1.39	2.41	Ambient	0.58	Saturated	217.28	130.9	7212	10^{-5}	231121
	8.5	TCw	Tpcpul	UE25-NRG-1	91.1-91.2	MO0401DQRIRPTS.003	ASTM D 3967-93	USBR	1.43	2.41	Ambient	0.59	Saturated	221.27	129.5	6668	10^{-5}	231121
	11.1	TCw	Tpcpul	UE25-NRG-1	93.85-93.95	MO0401DQRIRPTS.003	ASTM D 3967-93	USBR	1.32	2.41	Ambient	0.55	Saturated	215.36	136.6	8024	10^{-5}	231121
	10.2	TCw	Tpcpul	UE25-NRG-1	100.2-100.3	MO0401DQRIRPTS.003	ASTM D 3967-93	USBR	1.34	2.41	Ambient	0.56	Saturated	218.78	136.4	7517	10^{-5}	231121
	11.6	TCw	Tpcpul	UE25-NRG-1	100.3-100.4	MO0401DQRIRPTS.003	ASTM D 3967-93	USBR	1.33	2.41	Ambient	0.55	Saturated	217.9	136.5	8494	10^{-5}	231121
13.7	9.1	TCw	Tpcpul	UE-25 NRG #3	119.6	MO0401DQRIRPTS.003	ASTM D 3967-93	New England Research	1.52	2.03	Ambient	0.75	Saturated				10^{-5}	231121
16.4	8.9	TCw	Tpcpul	UE-25 NRG #3	136.1	MO0401DQRIRPTS.003	ASTM D 3967-93	New England Research	1.52	2.03	Ambient	0.75	Saturated				10^{-5}	231121
15.1	10.3	TCw	Tpcpul	UE-25 NRG #3	136.1	MO0401DQRIRPTS.003	ASTM D 3967-93	New England Research	1.52	2.03	Ambient	0.75	Saturated				10^{-5}	231121
15.5	10.2	TCw	Tpcpul	UE-25 NRG #3	195.7	MO0401DQRIRPTS.003	ASTM D 3967-93	New England Research	1.52	2.03	Ambient	0.75	Saturated				10^{-5}	231121
	9.8	TCw	Tpcpul	UE25-NRG-1	31.25-31.35	MO0401DQRIRPTS.003	ASTM D 3967-93	USBR	1.56	2.41	Ambient	0.65	Saturated	255.96	137.3	8354	10^{-5}	231121
	11.5	TCw	Tpcpul	UE25-NRG-1	31.6-31.75	MO0401DQRIRPTS.003	ASTM D 3967-93	USBR	1.68	2.41	Ambient	0.7	Saturated	271.98	134.9	10644	10^{-5}	231121
	11.3	TCw	Tpcpul	UE25-NRG-1	94.05-94.15	MO0401DQRIRPTS.003	ASTM D 3967-93	USBR	1.51	2.41	Ambient	0.63	Saturated	244.8	135.7	9349	10^{-5}	231121
	12.2	TCw	Tpcpul	UE25-NRG-1	100.5-100.65	MO0401DQRIRPTS.003	ASTM D 3967-93	USBR	1.71	2.41	Ambient	0.71	Saturated	271.4	132.8	11456	10^{-5}	231121
	12.3	TCw	Tpcrn	UE25-NRG-1	11.3-11.4	MO0401DQRIRPTS.003	ASTM D 3967-93	USBR	1.11	2.41	Ambient	0.46	Saturated	178.27	134.1	7499	10^{-5}	231121
	8.5	TCw	Tpcrn	UE25-NRG-1	12.8-12.9	MO0401DQRIRPTS.003	ASTM D 3967-93	USBR	1.2	2.41	Ambient	0.5	Saturated	189.31	132.5	5551	10^{-5}	231121
	9.7	TCw	Tpcrn	UE25-NRG-1	15.05-15.15	MO0401DQRIRPTS.003	ASTM D 3967-93	USBR	1.26	2.4	Ambient	0.53	Saturated	198.04	132.4	6681	10^{-5}	231121
	8.2	TCw	Tpcrn	UE25-NRG-1	15.15-15.25	MO0401DQRIRPTS.003	ASTM D 3967-93	USBR	1.34	2.41	Ambient	0.56	Saturated	207.65	130.1	5990	10^{-5}	231121
	9.8	TCw	Tpcrn	UE25-NRG-1	15.30-15.4	MO0401DQRIRPTS.003	ASTM D 3967-93	USBR	1.39	2.4	Ambient	0.58	Saturated	224.33	135.6	7456	10^{-5}	231121
	8.9	TCw	Tpcrn	UE25-NRG-1	15.5-15.6	MO0401DQRIRPTS.003	ASTM D 3967-93	USBR	1.42	2.4	Ambient	0.59	Saturated	221.77	131.8	6931	10^{-5}	231121
	9.6	TCw	Tpcrn	UE25-NRG-1	15.6-15.7	MO0401DQRIRPTS.003	ASTM D 3967-93	USBR	1.39	2.41	Ambient	0.58	Saturated	220.87	133.4	7309	10^{-5}	231121
	12.4	TCw	Tpcrn	UE25-NRG-1	20.95-21.05	MO0401DQRIRPTS.003	ASTM D 3967-93	USBR	1.29	2.41	Ambient	0.54	Saturated	207.09	133.7	8824	10^{-5}	231121
	13.4	TCw	Tpcrn	UE25-NRG-1	21.05-21.15	MO0401DQRIRPTS.003	ASTM D 3967-93	USBR	1.24	2.41	Ambient	0.52	Saturated	199.85	134.6	9160	10^{-5}	231121
39.1	3.0	TCw	Tpcrn	UE-25 NRG #3	15.4	MO0401DQRIRPTS.003	ASTM D 3967-93	New England Research	1.52	2.03	Ambient	0.75	Saturated				10^{-5}	231121
33.2	2.6	TCw	Tpcrn	UE-25 NRG #3	32.1	MO0401DQRIRPTS.003	ASTM D 3967-93	New England Research	1.52	2.03	Ambient	0.75	Saturated				10^{-5}	231121
25.2	3.3	TCw	Tpcrn	UE-25 NRG #3	42.6	MO0401DQRIRPTS.003	ASTM D 3967-93	New England Research	1.52	2.03	Ambient	0.75	Saturated				10^{-5}	231121
24.1	3.9	TCw	Tpcrn	UE-25 NRG #3	48.0	MO0401DQRIRPTS.003	ASTM D 3967-93	New England Research	1.52	2.03	Ambient	0.75	Saturated				10^{-5}	231121
24.7	4.0	TCw	Tpcrn	UE-25 NRG #3	55.7	MO0401DQRIRPTS.003	ASTM D 3967-93	New England Research	1.52	2.03	Ambient	0.75	Saturated				10^{-5}	231121
13.5	10.1	TCw	Tpcrn	UE-25 NRG #3	87.3	MO0401DQRIRPTS.003	ASTM D 3967-93	New England Research	1.52	2.03	Ambient	0.75	Saturated				10^{-5}	231121
13.3	11.7	TCw	Tpcrn	UE-25 NRG #3	93.8	MO0401DQRIRPTS.003	ASTM D 3967-93	New England Research	1.52	2.03	Ambient	0.75	Saturated				10^{-5}	231121
9.8	8.7	TCw	Tpcrn	UE-25 NRG #2a	172.1	MO0401DQRIRPTS.003	ASTM D 3967-93	New England Research	1.52	2.03	Ambient	0.75	Saturated				10^{-5}	231121
44.0	3.8	TCw	Tpcrn	UE-25 NRG #2a	177.0	MO0401DQRIRPTS.003	ASTM D 3967-93	New England Research	1.52	2.03	Ambient	0.75	Saturated				10^{-5}	231121
44.5	3.8	TCw	Tpcrn	UE-25 NRG #2a	177.0	MO0401DQRIRPTS.003	ASTM D 3967-93	New England Research	1.52	2.03	Ambient	0.75	Saturated				10^{-5}	231121
29.9	3.8	TCw	Tpcrn	UE-25 NRG #2a	209.3	MO0401DQRIRPTS.003	ASTM D 3967-93	New England Research	1.52	2.03	Ambient	0.75	Saturated				10^{-5}	231121
26.4	5.8	TCw	Tpcrn	UE-25 NRG #2a	218.8	MO0401DQRIRPTS.003	ASTM D 3967-93	New England Research	1.52	2.03	Ambient	0.75	Saturated				10^{-5}	231121
24.7	5.6	TCw	Tpcrn	UE-25 NRG #2a	223.1	MO0401DQRIRPTS.003	ASTM D 3967-93	New England Research	1.52	2.03	Ambient	0.75	Saturated				10^{-5}	231121
24.4	5.6	TCw	Tpcrn	UE-25 NRG #2a	234.9	MO0401DQRIRPTS.003	ASTM D 3967-93	New England Research	1.52	2.03	Ambient	0.75	Saturated				10^{-5}	231121
28.0	2.7	TCw	Tpcrn	UE-25 NRG #2a	238.4	MO0401DQRIRPTS.003	ASTM D 3967-93	New England Research	1.52	2.03	Ambient	0.75	Saturated				10^{-5}	231121
18.7	3.6	TSw1	Tptpul	USW-NRG-7/7A	520.0	MO0401DQRIRPTS.003	ASTM D 3967-93	New England Research	1.52	2.03	Ambient	0.75	Saturated				10^{-5}	231121
21.8	5.7	TSw1	Tptpul	USW-NRG-7/7A	533.4	MO0401DQRIRPTS.003	ASTM D 3967-93	New England Research	1.52	2.03	Ambient	0.75	Saturated				10^{-5}	231121
16.5	2.1	TSw1	Tptpul	USW-NRG-7/7A	566.9	MO0401DQRIRPTS.003	ASTM D 3967-93	New England Research	1.52	2.03	Ambient	0.75	Saturated				10^{-5}	231121
21.2	3.9	TSw1	Tptpul	USW-NRG-7/7A	595.2	MO0401DQRIRPTS.003	ASTM D 3967-93	New England Research	1.52	2.03	Ambient	0.75	Saturated				10^{-5}	231121
19.2	3.5	TSw1	Tptpul	USW-NRG-7/7A	605.5	MO0401DQRIRPTS.003	ASTM D 3967-93	New England Research	1.52	2.03	Ambient	0.75	Saturated				10^{-5}	231121
21.1	4.0	TSw1	Tptpul	USW-NRG-7/7A	625.2	MO0401DQRIRPTS.003	ASTM D 3967-93	New England Research	1.52	2.03	Ambient	0.75	Saturated				10^{-5}	231121

Table A-3. Intact Rock Mechanical Properties Data - Indirect Tensile Strength Data

Porosity (%)	Tensile Strength (MPa)	TM Unit	Litho stratigraphic Unit	Location	Depth (ft)	DTN	Test Procedure	Laboratory	Specimen Length (in)	Specimen Diameter (in)	Specimen Temperature (deg. C)	Length/ Diameter Ratio	Specimen Saturation	Specimen Mass (grams)	Apparent Specimen Unit Weight (lbm/ft^3)	Maximum Applied Load (lbf)	Strain Rate (1/s)	Testing Group
13.6	5.1	TSw1	Tptpul	USW-NRG-6	640.0	MO0401DQRIRPTS.003	ASTM D 3967-93	New England Research	1.52	2.03	Ambient	0.75	Saturated				10^{-5}	231121
15.6	6.4	TSw1	Tptpul	USW-NRG-7/7A	640.4	MO0401DQRIRPTS.003	ASTM D 3967-93	New England Research	1.52	2.03	Ambient	0.75	Saturated				10^{-5}	231121
15.7	4.3	TSw1	Tptpul	USW-NRG-7/7A	653.5	MO0401DQRIRPTS.003	ASTM D 3967-93	New England Research	1.52	2.03	Ambient	0.75	Saturated				10^{-5}	231121
17.7	4.8	TSw1	Tptpul	USW-NRG-7/7A	653.5	MO0401DQRIRPTS.003	ASTM D 3967-93	New England Research	1.52	2.03	Ambient	0.75	Saturated				10^{-5}	231121
13.5	11.2	TSw1	Tptpul	USW-NRG-7/7A	665.3	MO0401DQRIRPTS.003	ASTM D 3967-93	New England Research	1.52	2.03	Ambient	0.75	Saturated				10^{-5}	231121
16.6	2.7	TSw1	Tptpul	USW-NRG-7/7A	680.1	MO0401DQRIRPTS.003	ASTM D 3967-93	New England Research	1.52	2.03	Ambient	0.75	Saturated				10^{-5}	231121
12.4	9.0	TSw1	Tptpul	USW-NRG-7/7A	680.1	MO0401DQRIRPTS.003	ASTM D 3967-93	New England Research	1.52	2.03	Ambient	0.75	Saturated				10^{-5}	231121
11.9	8.7	TSw1	Tptpul	usw-NRG-6	687.5	MO0401DQRIRPTS.003	ASTM D 3967-93	New England Research	1.52	2.03	Ambient	0.75	Saturated				10^{-5}	231121
15.2	3.6	TSw1	Tptpul	USW-NRG-7/7A	698.4	MO0401DQRIRPTS.003	ASTM D 3967-93	New England Research	1.52	2.03	Ambient	0.75	Saturated				10^{-5}	231121
11.3	12.9	TSw1	Tptpul	USW-NRG-7/7A	698.4	MO0401DQRIRPTS.003	ASTM D 3967-93	New England Research	1.52	2.03	Ambient	0.75	Saturated				10^{-5}	231121
14.0	1.9	TSw1	Tptpul	USW-NRG-7/7A	708.4	MO0401DQRIRPTS.003	ASTM D 3967-93	New England Research	1.52	2.03	Ambient	0.75	Saturated				10^{-5}	231121
18.7	3.9	TSw1	Tptpul	USW-NRG-7/7A	716.4	MO0401DQRIRPTS.003	ASTM D 3967-93	New England Research	1.52	2.03	Ambient	0.75	Saturated				10^{-5}	231121
15.1	8.5	TSw1	Tptpul	USW-NRG-7/7A	716.4	MO0401DQRIRPTS.003	ASTM D 3967-93	New England Research	1.52	2.03	Ambient	0.75	Saturated				10^{-5}	231121
13.8	5.2	TSw1	Tptrl	USW-NRG-6	462.3	MO0401DQRIRPTS.003	ASTM D 3967-93	New England Research	1.52	2.03	Ambient	0.75	Saturated				10^{-5}	231121
12.4	5.3	TSw1	Tptrl	USW-NRG-7/7A	479.4	MO0401DQRIRPTS.003	ASTM D 3967-93	New England Research	1.52	2.03	Ambient	0.75	Saturated				10^{-5}	231121
20.2	3.4	TSw1	Tptrl	USW-NRG-7/7A	488.4	MO0401DQRIRPTS.003	ASTM D 3967-93	New England Research	1.52	2.03	Ambient	0.75	Saturated				10^{-5}	231121
10.6	5.1	TSw1	Tptrl	USW-NRG-7/7A	490.6	MO0401DQRIRPTS.003	ASTM D 3967-93	New England Research	1.52	2.03	Ambient	0.75	Saturated				10^{-5}	231121
16.4	7.3	TSw1	Tptrl	USW-NRG-7/7A	507.4	MO0401DQRIRPTS.003	ASTM D 3967-93	New England Research	1.52	2.03	Ambient	0.75	Saturated				10^{-5}	231121
20.1	3.7	TSw1	Tptrl	UE-25-NRG-4	691.8	MO0401DQRIRPTS.003	ASTM D 3967-93	New England Research	1.52	2.03	Ambient	0.75	Saturated				10^{-5}	231121
22.2	3.7	TSw1	Tptrl	UE-25-NRG-4	691.8	MO0401DQRIRPTS.003	ASTM D 3967-93	New England Research	1.52	2.03	Ambient	0.75	Saturated				10^{-5}	231121
10.1	8.4	TSw1	Tptrn	USW NRG-6	276.2	MO0401DQRIRPTS.003	ASTM D 3967-93	New England Research	1.52	2.03	Ambient	0.75	Room Dry				10^{-5}	221121
10.6	9.3	TSw1	Tptrn	USW NRG-6	304.4	MO0401DQRIRPTS.003	ASTM D 3967-93	New England Research	1.52	2.03	Ambient	0.75	Saturated				10^{-5}	231121
14.1	7.6	TSw1	Tptrn	USW NRG-6	318.2	MO0401DQRIRPTS.003	ASTM D 3967-93	New England Research	1.52	2.03	Ambient	0.75	Saturated				10^{-5}	231121
10.1	9.3	TSw1	Tptrn	USW-NRG-7/7A	322.9	MO0401DQRIRPTS.003	ASTM D 3967-93	New England Research	1.52	2.03	Ambient	0.75	Saturated				10^{-5}	231121
21.3	6.3	TSw1	Tptrn	USW-NRG-7/7A	334.5	MO0401DQRIRPTS.003	ASTM D 3967-93	New England Research	1.52	2.03	Ambient	0.75	Saturated				10^{-5}	231121
10.5	10.5	TSw1	Tptrn	USW-NRG-7/7A	350.3	MO0401DQRIRPTS.003	ASTM D 3967-93	New England Research	1.52	2.03	Ambient	0.75	Saturated				10^{-5}	231121
15.9	5.3	TSw1	Tptrn	USW NRG-6	355.4	MO0401DQRIRPTS.003	ASTM D 3967-93	New England Research	1.52	2.03	Ambient	0.75	Saturated				10^{-5}	231121
16.9	6.8	TSw1	Tptrn	USW-NRG-7/7A	362.8	MO0401DQRIRPTS.003	ASTM D 3967-93	New England Research	1.52	2.03	Ambient	0.75	Saturated				10^{-5}	231121
14.5	6.6	TSw1	Tptrn	USW NRG-6	373.6	MO0401DQRIRPTS.003	ASTM D 3967-93	New England Research	1.52	2.03	Ambient	0.75	Saturated				10^{-5}	231121
18.9	1.6	TSw1	Tptrn	USW-NRG-7/7A	388.6	MO0401DQRIRPTS.003	ASTM D 3967-93	New England Research	1.52	2.03	Ambient	0.75	Saturated				10^{-5}	231121
17.0	2.3	TSw1	Tptrn	USW-NRG-7/7A	388.6	MO0401DQRIRPTS.003	ASTM D 3967-93	New England Research	1.52	2.03	Ambient	0.75	Saturated				10^{-5}	231121
12.4	6.5	TSw1	Tptrn	USW NRG-6	392.6	MO0401DQRIRPTS.003	ASTM D 3967-93	New England Research	1.52	2.03	Ambient	0.75	Saturated				10^{-5}	231121
11.4	6.8	TSw1	Tptrn	USW NRG-6	395.0	MO0401DQRIRPTS.003	ASTM D 3967-93	New England Research	1.52	2.03	Ambient	0.75	Saturated				10^{-5}	231121
11.8	4.7	TSw1	Tptrn	USW NRG-6	397.5	MO0401DQRIRPTS.003	ASTM D 3967-93	New England Research	1.52	2.03	Ambient	0.75	Saturated				10^{-5}	231121
12.2	5.1	TSw1	Tptrn	USW NRG-6	407.0	MO0401DQRIRPTS.003	ASTM D 3967-93	New England Research	1.52	2.03	Ambient	0.75	Saturated				10^{-5}	231121
16.5	4.9	TSw1	Tptrn	USW-NRG-7/7A	407.3	MO0401DQRIRPTS.003	ASTM D 3967-93	New England Research	1.52	2.03	Ambient	0.75	Saturated				10^{-5}	231121
16.7	6.1	TSw1	Tptrn	USW-NRG-7/7A	407.3	MO0401DQRIRPTS.003	ASTM D 3967-93	New England Research	1.52	2.03	Ambient	0.75	Saturated				10^{-5}	231121
16.8	5.9	TSw1	Tptrn	USW-NRG-7/7A	409.9	MO0401DQRIRPTS.003	ASTM D 3967-93	New England Research	1.52	2.03	Ambient	0.75	Saturated				10^{-5}	231121
17.1	6.2	TSw1	Tptrn	USW-NRG-7/7A	409.9	MO0401DQRIRPTS.003	ASTM D 3967-93	New England Research	1.52	2.03	Ambient	0.75	Saturated				10^{-5}	231121
14.3	4.7	TSw1	Tptrn	USW-NRG-7/7A	417.9	MO0401DQRIRPTS.003	ASTM D 3967-93	New England Research	1.52	2.03	Ambient	0.75	Saturated				10^{-5}	231121
14.2	4.1	TSw1	Tptrn	USW NRG-6	421.5	MO0401DQRIRPTS.003	ASTM D 3967-93	New England Research	1.52	2.03	Ambient	0.75	Saturated				10^{-5}	231121
12.2	3.9	TSw1	Tptrn	USW-NRG-7/7A	422.0	MO0401DQRIRPTS.003	ASTM D 3967-93	New England Research	1.52	2.03	Ambient	0.75	Saturated				10^{-5}	231121
12.6	4.0	TSw1	Tptrn	USW NRG-6	427	MO0401DQRIRPTS.003	ASTM D 3967-93	New England Research	1.52	2.03	Ambient	0.75	Saturated				10^{-5}	231121
14.4	7.0	TSw1	Tptrn	USW-NRG-7/7A	428.7	MO0401DQRIRPTS.003	ASTM D 3967-93	New England Research	1.52	2.03	Ambient	0.75	Saturated				10^{-5}	231121
15.4	4.9	TSw1	Tptrn	USW-NRG-7/7A	436.4	MO0401DQRIRPTS.003	ASTM D 3967-93	New England Research	1.52	2.03	Ambient	0.75	Saturated				10^{-5}	231121
13.6	5.4	TSw1	Tptrn	USW-NRG-7/7A	436.4	MO0401DQRIRPTS.003	ASTM D 3967-93	New England Research	1.52	2.03	Ambient	0.75	Saturated				10^{-5}	231121
15.0	4.7	TSw1	Tptrn	USW-NRG-7/7A	443.2	MO0401DQRIRPTS.003	ASTM D 3967-93	New England Research	1.52	2.03	Ambient	0.75	Saturated				10^{-5}	231121
14.3	5.3	TSw1	Tptrn	USW-NRG-7/7A	450.1	MO0401DQRIRPTS.003	ASTM D 3967-93	New England Research	1.52	2.03	Ambient	0.75	Saturated				10^{-5}	231121
10.5	4.8	TSw1	Tptrn	USW-NRG-7/7A	461.0	MO0401DQRIRPTS.003	ASTM D 3967-93	New England Research	1.52	2.03	Ambient	0.75	Saturated				10^{-5}	231121
12.2	4.0	TSw1	Tptrn	USW-NRG-7/7A	465.7	MO0401DQRIRPTS.003	ASTM D 3967-93	New England Research	1.52	2.03	Ambient	0.75	Saturated				10^{-5}	231121
12.2	5.1	TSw1	Tptrn	USW-NRG-7/7A	465.7	MO0401DQRIRPTS.003	ASTM D 3967-93	New England Research	1.52	2.03	Ambient	0.75	Saturated				10^{-5}	231121
11.2	4.4	TSw1	Tptrn	USW-NRG-7/7A	469.4	MO0401DQRIRPTS.003	ASTM D 3967-93	New England Research	1.52	2.03	Ambient	0.75	Saturated				10^{-5}	231121
12.1	4.2	TSw1	Tptrn	USW-NRG-7/7A	472.9	MO0401DQRIRPTS.003	ASTM D 3967-93	New England Research	1.52	2.03	Ambient	0.75	Saturated				10^{-5}	231121
6.8	7.7	TSw1	Tptrn	UE-25-NRG-4	489.4	MO0401DQRIRPTS.003	ASTM D 3967-93	New England Research	1.52	2.03	Ambient	0.75	Saturated				10^{-5}	231121
14.2	9.0	TSw1	Tptrn	UE-25-NRG-4	504.5	MO0401DQRIRPTS.003	ASTM D 3967-93	New England Research	1.52	2.03	Ambient	0.75	Saturated				10^{-5}	231121
13.4	9.3	TSw1	Tptrn	UE-25-NRG-4	504.5	MO0401DQRIRPTS.003	ASTM D 3967-93	New England Research	1.52	2.03	Ambient	0.75	Saturated				10^{-5}	231121
12.8	6.7	TSw1	Tptrn	UE-25-NRG-4	515.5	MO0401DQRIRPTS.003	ASTM D 3967-93	New England Research	1.52	2.03	Ambient	0.75	Saturated				10^{-5}	231121
14.9	8.6	TSw1	Tptrn	UE-25-NRG-4	525.0	MO0401DQRIRPTS.003	ASTM D 3967-93	New England Research	1.52	2.03	Ambient	0.75	Saturated				10^{-5}	231121

Table A-3. Intact Rock Mechanical Properties Data - Indirect Tensile Strength Data

Porosity (%)	Tensile Strength (MPa)	TM Unit	Litho stratigraphic Unit	Location	Depth (ft)	DTN	Test Procedure	Laboratory	Specimen Length (in)	Specimen Diameter (in)	Specimen Temperature (deg. C)	Length/ Diameter Ratio	Specimen Saturation	Specimen Mass (grams)	Apparent Specimen Unit Weight (lbm/ft^3)	Maximum Applied Load (lbf)	Strain Rate (1/s)	Testing Group
16.8	8.2	TSw1	Tptrn	UE-25-NRG-4	530.4	MO0401DQRIRPTS.003	ASTM D 3967-93	New England Research	1.52	2.03	Ambient	0.75	Saturated				10^{-5}	231121
18.2	7.5	TSw1	Tptrn	UE-25-NRG-4	535.3	MO0401DQRIRPTS.003	ASTM D 3967-93	New England Research	1.52	2.03	Ambient	0.75	Saturated				10^{-5}	231121
22.8	2.8	TSw1	Tptrn	UE-25-NRG-4	541.0	MO0401DQRIRPTS.003	ASTM D 3967-93	New England Research	1.52	2.03	Ambient	0.75	Saturated				10^{-5}	231121
19.0	4.8	TSw1	Tptrn	UE-25-NRG-4	546.0	MO0401DQRIRPTS.003	ASTM D 3967-93	New England Research	1.52	2.03	Ambient	0.75	Saturated				10^{-5}	231121
19.6	5.8	TSw1	Tptrn	UE-25-NRG-4	550.0	MO0401DQRIRPTS.003	ASTM D 3967-93	New England Research	1.52	2.03	Ambient	0.75	Saturated				10^{-5}	231121
17.7	3.0	TSw1	Tptrn	UE-25-NRG-4	587.4	MO0401DQRIRPTS.003	ASTM D 3967-93	New England Research	1.52	2.03	Ambient	0.75	Saturated				10^{-5}	231121
16.7	4.2	TSw1	Tptrn	UE-25-NRG-4	587.4	MO0401DQRIRPTS.003	ASTM D 3967-93	New England Research	1.52	2.03	Ambient	0.75	Saturated				10^{-5}	231121
19.6	2.3	TSw1	Tptrn	UE-25-NRG-4	591.7	MO0401DQRIRPTS.003	ASTM D 3967-93	New England Research	1.52	2.03	Ambient	0.75	Saturated				10^{-5}	231121
16.6	2.7	TSw1	Tptrn	UE-25-NRG-4	597.0	MO0401DQRIRPTS.003	ASTM D 3967-93	New England Research	1.52	2.03	Ambient	0.75	Saturated				10^{-5}	231121
15.6	3.4	TSw1	Tptrn	UE-25-NRG-4	602.9	MO0401DQRIRPTS.003	ASTM D 3967-93	New England Research	1.52	2.03	Ambient	0.75	Saturated				10^{-5}	231121
18.1	2.8	TSw1	Tptrn	UE-25-NRG-4	607.6	MO0401DQRIRPTS.003	ASTM D 3967-93	New England Research	1.52	2.03	Ambient	0.75	Saturated				10^{-5}	231121
15.1	4.3	TSw1	Tptrn	UE-25-NRG-4	612.5	MO0401DQRIRPTS.003	ASTM D 3967-93	New England Research	1.52	2.03	Ambient	0.75	Saturated				10^{-5}	231121
15.2	3.6	TSw1	Tptrn	UE-25-NRG-4	617.4	MO0401DQRIRPTS.003	ASTM D 3967-93	New England Research	1.52	2.03	Ambient	0.75	Saturated				10^{-5}	231121
13.4	3.6	TSw1	Tptrn	UE-25-NRG-4	617.4	MO0401DQRIRPTS.003	ASTM D 3967-93	New England Research	1.52	2.03	Ambient	0.75	Saturated				10^{-5}	231121
14.9	4.0	TSw1	Tptrn	UE-25-NRG-4	617.4	MO0401DQRIRPTS.003	ASTM D 3967-93	New England Research	1.52	2.03	Ambient	0.75	Saturated				10^{-5}	231121
10.0	7.9	TSw2	Tptpll	USW-NRG-6	848.0	MO0401DQRIRPTS.003	ASTM D 3967-93	New England Research	1.52	2.03	Ambient	0.75	Saturated				10^{-5}	231121
10.9	11.0	TSw2	Tptpll	USW-NRG-7/7A	879.2	MO0401DQRIRPTS.003	ASTM D 3967-93	New England Research	1.52	2.03	Ambient	0.75	Saturated				10^{-5}	231121
8.8	14.3	TSw2	Tptpll	USW-NRG-7/7A	879.2	MO0401DQRIRPTS.003	ASTM D 3967-93	New England Research	1.52	2.03	Ambient	0.75	Saturated				10^{-5}	231121
8.9	12.1	TSw2	Tptpll	USW-NRG-7/7A	881.0	MO0401DQRIRPTS.003	ASTM D 3967-93	New England Research	1.52	2.03	Ambient	0.75	Saturated				10^{-5}	231121
10.5	8.8	TSw2	Tptpll	USW-NRG-6	908.2	MO0401DQRIRPTS.003	ASTM D 3967-93	New England Research	1.52	2.03	Ambient	0.75	Saturated				10^{-5}	231121
12.4	4.0	TSw2	Tptpll	USW-NRG-6	934.0	MO0401DQRIRPTS.003	ASTM D 3967-93	New England Research	1.52	2.03	Ambient	0.75	Saturated				10^{-5}	231121
12.6	10.8	TSw2	Tptpll	USW-NRG-6	934.0	MO0401DQRIRPTS.003	ASTM D 3967-93	New England Research	1.52	2.03	Ambient	0.75	Saturated				10^{-5}	231121
16.4	5.3	TSw2	Tptpll	USW-NRG-6	956.8	MO0401DQRIRPTS.003	ASTM D 3967-93	New England Research	1.52	2.03	Ambient	0.75	Saturated				10^{-5}	231121
12.8	11.2	TSw2	Tptpll	USW-NRG-7/7A	958.7	MO0401DQRIRPTS.003	ASTM D 3967-93	New England Research	1.52	2.03	Ambient	0.75	Saturated				10^{-5}	231121
12.0	11.5	TSw2	Tptpll	USW-NRG-7/7A	958.7	MO0401DQRIRPTS.003	ASTM D 3967-93	New England Research	1.52	2.03	Ambient	0.75	Saturated				10^{-5}	231121
14.1	3.2	TSw2	Tptpll	USW-NRG-6	963.3	MO0401DQRIRPTS.003	ASTM D 3967-93	New England Research	1.52	2.03	Ambient	0.75	Saturated				10^{-5}	231121
13.5	7.5	TSw2	Tptpll	USW-NRG-6	969.3	MO0401DQRIRPTS.003	ASTM D 3967-93	New England Research	1.52	2.03	Ambient	0.75	Saturated				10^{-5}	231121
10.4	11.7	TSw2	Tptpll	USW-NRG-6	971.4	MO0401DQRIRPTS.003	ASTM D 3967-93	New England Research	1.52	2.03	Ambient	0.75	Saturated				10^{-5}	231121
11.8	5.5	TSw2	Tptpll	USW-NRG-7/7A	976.4	MO0401DQRIRPTS.003	ASTM D 3967-93	New England Research	1.52	2.03	Ambient	0.75	Saturated				10^{-5}	231121
13.5	6.3	TSw2	Tptpll	USW-NRG-7/7A	976.4	MO0401DQRIRPTS.003	ASTM D 3967-93	New England Research	1.52	2.03	Ambient	0.75	Saturated				10^{-5}	231121
11.5	5.2	TSw2	Tptpll	USW-NRG-7/7A	979.6	MO0401DQRIRPTS.003	ASTM D 3967-93	New England Research	1.52	2.03	Ambient	0.75	Saturated				10^{-5}	231121
12.6	6.2	TSw2	Tptpll	USW-NRG-7/7A	1046.8	MO0401DQRIRPTS.003	ASTM D 3967-93	New England Research	1.52	2.03	Ambient	0.75	Saturated				10^{-5}	231121
10.4	10.2	TSw2	Tptpll	USW-NRG-7/7A	1090.3	MO0401DQRIRPTS.003	ASTM D 3967-93	New England Research	1.52	2.03	Ambient	0.75	Saturated				10^{-5}	231121
9.9	10.4	TSw2	Tptpll	USW-NRG-7/7A	1090.3	MO0401DQRIRPTS.003	ASTM D 3967-93	New England Research	1.52	2.03	Ambient	0.75	Saturated				10^{-5}	231121
15.5	6.6	TSw2	Tptpll	USW-NRG-7/7A	1098.3	MO0401DQRIRPTS.003	ASTM D 3967-93	New England Research	1.52	2.03	Ambient	0.75	Saturated				10^{-5}	231121
10.7	7.0	TSw2	Tptpll	USW-NRG-7/7A	1129.3	MO0401DQRIRPTS.003	ASTM D 3967-93	New England Research	1.52	2.03	Ambient	0.75	Saturated				10^{-5}	231121
12.5	5.3	TSw2	Tptpll	USW-NRG-7/7A	1180.0	MO0401DQRIRPTS.003	ASTM D 3967-93	New England Research	1.52	2.03	Ambient	0.75	Saturated				10^{-5}	231121
11.4	8.6	TSw2	Tptpll	USW-NRG-7/7A	1188.7	MO0401DQRIRPTS.003	ASTM D 3967-93	New England Research	1.52	2.03	Ambient	0.75	Saturated				10^{-5}	231121
14.7	9.2	TSw2	Tptpll	USW-NRG-7/7A	1230.2	MO0401DQRIRPTS.003	ASTM D 3967-93	New England Research	1.52	2.03	Ambient	0.75	Saturated				10^{-5}	231121
9.0	9.0	TSw2	Tptpln	USW-NRG-7/7A	1263.7	MO0401DQRIRPTS.003	ASTM D 3967-93	New England Research	1.52	2.03	Ambient	0.75	Saturated				10^{-5}	231121
10.9	9.9	TSw2	Tptpln	USW-NRG-7/7A	1263.7	MO0401DQRIRPTS.003	ASTM D 3967-93	New England Research	1.52	2.03	Ambient	0.75	Saturated				10^{-5}	231121
9.8	13.7	TSw2	Tptpln	USW-NRG-7/7A	1263.7	MO0401DQRIRPTS.003	ASTM D 3967-93	New England Research	1.52	2.03	Ambient	0.75	Saturated				10^{-5}	231121
9.7	8.8	TSw2	Tptpln	USW-NRG-7/7A	1307.0	MO0401DQRIRPTS.003	ASTM D 3967-93	New England Research	1.52	2.03	Ambient	0.75	Saturated				10^{-5}	231121
9.7	10.9	TSw2	Tptpln	USW-NRG-7/7A	1307.0	MO0401DQRIRPTS.003	ASTM D 3967-93	New England Research	1.52	2.03	Ambient	0.75	Saturated				10^{-5}	231121
8.3	4.8	TSw2	Tptpln	USW-NRG-7/7A	1348.8	MO0401DQRIRPTS.003	ASTM D 3967-93	New England Research	1.52	2.03	Ambient	0.75	Saturated				10^{-5}	231121
9	5.9	TSw2	Tptpln	USW-NRG-7/7A	1348.8	MO0401DQRIRPTS.003	ASTM D 3967-93	New England Research	1.52	2.03	Ambient	0.75	Saturated				10^{-5}	231121
11.2	7.6	TSw2	Tptpln	USW-NRG-7/7A	1353.7	MO0401DQRIRPTS.003	ASTM D 3967-93	New England Research	1.52	2.03	Ambient	0.75	Saturated				10^{-5}	231121
7.7	7.6	TSw2	Tptpln	USW-NRG-7/7A	1363.5	MO0401DQRIRPTS.003	ASTM D 3967-93	New England Research	1.52	2.03	Ambient	0.75	Saturated				10^{-5}	231121
7.7	6.1	TSw2	Tptpln	USW-NRG-7/7A	1385.0	MO0401DQRIRPTS.003	ASTM D 3967-93	New England Research	1.52	2.03	Ambient	0.75	Saturated				10^{-5}	231121
7.8	6.3	TSw2	Tptpln	USW-NRG-7/7A	1385.0	MO0401DQRIRPTS.003	ASTM D 3967-93	New England Research	1.52	2.03	Ambient	0.75	Saturated				10^{-5}	231121
9.9	4.8	TSw2	Tptpln	USW-NRG-7/7A	1402.7	MO0401DQRIRPTS.003	ASTM D 3967-93	New England Research	1.52	2.03	Ambient	0.75	Saturated				10^{-5}	231121
3.8	7.6	TSw2	Tptpln	USW-NRG-7/7A	1409.0	MO0401DQRIRPTS.003	ASTM D 3967-93	New England Research	1.52	2.03	Ambient	0.75	Saturated				10^{-5}	231121
9.7	14.5	TSw2	Tptpmn	USW-NRG-6	742.3	MO0401DQRIRPTS.003	ASTM D 3967-93	New England Research	1.52	2.03	Ambient	0.75	Saturated				10^{-5}	231121
10.3	13	TSw2	Tptpmn	USW-NRG-6	742.9	MO0401DQRIRPTS.003	ASTM D 3967-93	New England Research	1.52	2.03	Ambient	0.75	Saturated				10^{-5}	231121
14.8	9.3	TSw2	Tptpmn	USW-NRG-7/7A	762.1	MO0401DQRIRPTS.003	ASTM D 3967-93	New England Research	1.52	2.03	Ambient	0.75	Saturated				10^{-5}	231121
11.9	7.9	TSw2	Tptpmn	USW-NRG-6	773.5	MO0401DQRIRPTS.003	ASTM D 3967-93	New England Research	1.52	2.03	Ambient	0.75	Saturated				10^{-5}	231121
9.6	12.5	TSw2	Tptpmn	USW-NRG-6	784.8	MO0401DQRIRPTS.003	ASTM D 3967-93	New England Research	1.52	2.03	Ambient	0.75	Saturated				10^{-5}	231121
9.3	14.1	TSw2	Tptpmn	USW-NRG-6	785.6	MO0401DQRIRPTS.003	ASTM D 3967-93	New England Research	1.52	2.03	Ambient	0.75	Saturated				10^{-5}	231121

Table A-3. Intact Rock Mechanical Properties Data - Indirect Tensile Strength Data

Porosity (%)	Tensile Strength (MPa)	TM Unit	Litho stratigraphic Unit	Location	Depth (ft)	DTN	Test Procedure	Laboratory	Specimen Length (in)	Specimen Diameter (in)	Specimen Temperature (deg. C)	Length/ Diameter Ratio	Specimen Saturation	Specimen Mass (grams)	Apparent Specimen Unit Weight (lbm/ft^3)	Maximum Applied Load (lbf)	Strain Rate (1/s)	Testing Group
19.2	4.3	TSw2	Tptpmn	UE-25-NRG#5	788.6	MO0401DQRIRPTS.003	ASTM D 3967-93	New England Research	1.52	2.03	Ambient	0.75	Saturated				10^{-5}	231121
15.9	6.1	TSw2	Tptpmn	USW-NRG-7/7A	828.4	MO0401DQRIRPTS.003	ASTM D 3967-93	New England Research	1.52	2.03	Ambient	0.75	Saturated				10^{-5}	231121
11.5	7.7	TSw2	Tptpmn	UE-25-NRG#5	832.9	MO0401DQRIRPTS.003	ASTM D 3967-93	New England Research	1.52	2.03	Ambient	0.75	Saturated				10^{-5}	231121
13.2	5.7	TSw2	Tptpmn	UE-25-NRG#5	847.2	MO0401DQRIRPTS.003	ASTM D 3967-93	New England Research	1.52	2.03	Ambient	0.75	Saturated				10^{-5}	231121
11.0	11.6	TSw2	Tptpmn	USW-NRG-7/7A	855.0	MO0401DQRIRPTS.003	ASTM D 3967-93	New England Research	1.52	2.03	Ambient	0.75	Saturated				10^{-5}	231121
9.9	16.8	TSw2	Tptpmn	UE-25-NRG#5	887.2	MO0401DQRIRPTS.003	ASTM D 3967-93	New England Research	1.52	2.03	Ambient	0.75	Saturated				10^{-5}	231121
9.0	15.9	TSw2	Tptpmn	UE-25-NRG#5	888.8	MO0401DQRIRPTS.003	ASTM D 3967-93	New England Research	1.52	2.03	Ambient	0.75	Saturated				10^{-5}	231121
10.5	12.9	TSw2	Tptpmn	UE-25-NRG#5	891.9	MO0401DQRIRPTS.003	ASTM D 3967-93	New England Research	1.52	2.03	Ambient	0.75	Saturated				10^{-5}	231121
1.3	4.1	TSw3	Tptpv3	USW-NRG-7/7A	1437.8	MO0401DQRIRPTS.003	ASTM D 3967-93	New England Research	1.52	2.03	Ambient	0.75	Saturated				10^{-5}	231121
1.4	3.6	TSw3	Tptpv3	USW-NRG-7/7A	1448.5	MO0401DQRIRPTS.003	ASTM D 3967-93	New England Research	1.52	2.03	Ambient	0.75	Saturated				10^{-5}	231121
1.2	4.2	TSw3	Tptpv3	USW-NRG-7/7A	1448.5	MO0401DQRIRPTS.003	ASTM D 3967-93	New England Research	1.52	2.03	Ambient	0.75	Saturated				10^{-5}	231121
35.8	2.7	UO	Tmr	UE-25-NRG #2b	2.7	MO0401DQRIRPTS.003	ASTM D 3967-93	New England Research	1.52	2.03	Ambient	0.75	Saturated				10^{-5}	231121
43.5	0.4	UO	Tmr	UE-25-NRG #2b	43.2	MO0401DQRIRPTS.003	ASTM D 3967-93	New England Research	1.52	2.03	Ambient	0.75	Saturated				10^{-5}	231121
44.3	0.6	UO	Tmr	UE-25-NRG #2b	46.1	MO0401DQRIRPTS.003	ASTM D 3967-93	New England Research	1.52	2.03	Ambient	0.75	Saturated				10^{-5}	231121
46.6	0.5	UO	Tpki	UE-25 NRG #2a	90.0	MO0401DQRIRPTS.003	ASTM D 3967-93	New England Research	1.52	2.03	Ambient	0.75	Saturated				10^{-5}	231121
50.4	0.9	UO	Tpki	UE-25 NRG #2a	96.0	MO0401DQRIRPTS.003	ASTM D 3967-93	New England Research	1.52	2.03	Ambient	0.75	Saturated				10^{-5}	231121
49.1	1.0	UO	Tpki	UE-25 NRG #2a	98.4	MO0401DQRIRPTS.003	ASTM D 3967-93	New England Research	1.52	2.03	Ambient	0.75	Saturated				10^{-5}	231121
45.2	0.8	UO	Tpki	UE-25 NRG #2a	105.6	MO0401DQRIRPTS.003	ASTM D 3967-93	New England Research	1.52	2.03	Ambient	0.75	Saturated				10^{-5}	231121
44.5	0.4	UO	Tpki	UE-25 NRG #2a	127.5	MO0401DQRIRPTS.003	ASTM D 3967-93	New England Research	1.52	2.03	Ambient	0.75	Saturated				10^{-5}	231121
46.1	0.6	UO	Tpki	UE-25 NRG #2a	127.5	MO0401DQRIRPTS.003	ASTM D 3967-93	New England Research	1.52	2.03	Ambient	0.75	Saturated				10^{-5}	231121

Note: All blanks or NA are indicating the information is either not available or not applicable unless otherwise specified.

APPENDIX B
SUMMARIES OF INTACT ROCK MECHANICAL PROPERTIES DATA

Table B-1. Summary of Intact rock Mechanical Properties Data - Compressive Strength and All Static Elastic Properties

Thermo-Mechanical Unit	Litho-stratigraphic Unit	Testing Group Code	Count	Mean	St. Error (SE)	Mean ± 1 SE	Mean ± 1 SE (%)	Standard Deviation (SD)	Uncertainty of the SD	SD+Uncertainty of SD (SD*)	Mean± 1 SD*	Mean± 1 SD* (%)	Median	Minimum	Maximum	Range
Compressive Strength (MPa)																
UO	Tmr	231221	5	7.60	3.34	7.60 ± 3.34	7.60 ± 44%	7.48	2.64	10.12	7.60 ± 10.12	7.60 ± 133%	6.50	1.80	20.30	18.50
	Tpki	231221	7	5.94	1.03	5.94 ± 1.03	5.94 ± 17%	2.72	0.78	3.50	5.94 ± 3.50	5.94 ± 59%	6.50	1.10	9.80	8.70
TCw	Tpcrn	221221	3	100.30	18.01	100.30 ± 18.01	100.30 ± 18%	31.19	15.59	46.78	100.30 ± 46.78	100.30 ± 47%	115.80	64.40	120.70	56.30
		231221	18	36.02	7.77	36.02 ± 7.77	36.02 ± 22%	32.98	5.66	38.64	36.02 ± 38.64	36.02 ± 107%	24.05	10.40	132.90	122.50
	Tpcpul	221221	3	92.10	13.00	92.10 ± 13.00	92.10 ± 14%	22.51	11.26	33.77	92.10 ± 33.77	92.10 ± 37%	100.00	66.70	109.60	42.90
		221233	1	170.30	NA	170.30 ± NA	170.30 ± NA	NA	NA	NA	170.30 ± NA	170.30 ± NA	170.30	170.30	170.30	NA
		221234	1	227.60	NA	227.60 ± NA	227.60 ± NA	NA	NA	NA	227.60 ± NA	227.60 ± NA	227.60	227.60	227.60	NA
		221321	1	65.60	NA	65.60 ± NA	65.60 ± NA	NA	NA	NA	65.60 ± NA	65.60 ± NA	65.60	65.60	65.60	NA
		221334	1	253.80	NA	253.80 ± NA	253.80 ± NA	NA	NA	NA	253.80 ± NA	253.80 ± NA	253.80	253.80	253.80	NA
		231221	5	62.14	11.87	62.14 ± 11.87	62.14 ± 19%	26.54	9.38	35.92	62.14 ± 35.92	62.14 ± 58%	75.00	32.50	85.50	53.00
	Tpcpmn	131222	4	227.38	34.13	227.38 ± 34.13	227.38 ± 15%	68.25	27.86	96.11	227.38 ± 96.11	227.38 ± 42%	227.70	158.20	295.90	137.70
		131223	4	327.35	17.00	327.35 ± 17.00	327.35 ± 5%	34.01	13.88	47.89	327.35 ± 47.89	327.35 ± 15%	324.50	291.40	369.00	77.60
		221221	3	232.13	22.31	232.13 ± 22.31	232.13 ± 10%	38.65	19.32	57.97	232.13 ± 57.97	232.13 ± 25%	223.40	198.60	274.40	75.80
		221233	1	206.90	NA	206.90 ± NA	206.90 ± NA	NA	NA	NA	206.90 ± NA	206.90 ± NA	206.90	206.90	206.90	NA
		221234	2	333.05	99.95	333.05 ± 99.95	333.05 ± 30%	141.35	99.95	241.30	333.05 ± 241.30	333.05 ± 72%	333.05	233.10	433.00	199.90
		221321	1	128.90	NA	128.90 ± NA	128.90 ± NA	NA	NA	NA	128.90 ± NA	128.90 ± NA	128.90	128.90	128.90	NA
		231221	8	167.19	22.67	167.19 ± 22.67	167.19 ± 14%	64.12	17.14	81.25	167.19 ± 81.25	167.19 ± 49%	183.55	71.90	244.00	172.10
		231222	2	319.25	70.25	319.25 ± 70.25	319.25 ± 22%	99.35	70.25	169.60	319.25 ± 169.60	319.25 ± 53%	319.25	249.00	389.50	140.50
		231223	1	245.50	NA	245.50 ± NA	245.50 ± NA	NA	NA	NA	245.50 ± NA	245.50 ± NA	245.50	245.50	245.50	NA
	Tpcpll	131221	4	311.55	10.02	311.55 ± 10.02	311.55 ± 3%	20.05	8.18	28.23	311.55 ± 28.23	311.55 ± 9%	314.80	284.20	332.40	48.20
		131222	4	372.65	21.88	372.65 ± 21.88	372.65 ± 6%	43.77	17.87	61.63	372.65 ± 61.63	372.65 ± 17%	393.35	307.10	396.80	89.70
		131223	4	408.75	22.30	408.75 ± 22.30	408.75 ± 5%	44.61	18.21	62.82	408.75 ± 62.82	408.75 ± 15%	425.95	343.40	439.70	96.30
		231221	5	186.74	50.47	186.74 ± 50.47	186.74 ± 27%	112.86	39.90	152.76	186.74 ± 152.76	186.74 ± 82%	121.10	75.40	313.60	238.20
		231222	1	125.30	NA	125.30 ± NA	125.30 ± NA	NA	NA	NA	125.30 ± NA	125.30 ± NA	125.30	125.30	125.30	NA
		231223	1	157.90	NA	157.90 ± NA	157.90 ± NA	NA	NA	NA	157.90 ± NA	157.90 ± NA	157.90	157.90	157.90	NA
	Tpcpln	221231	1	364.00	NA	364.00 ± NA	364.00 ± NA	NA	NA	NA	364.00 ± NA	364.00 ± NA	364.00	364.00	364.00	NA
		221233	1	406.00	NA	406.00 ± NA	406.00 ± NA	NA	NA	NA	406.00 ± NA	406.00 ± NA	406.00	406.00	406.00	NA
		221234	1	895.00	NA	895.00 ± NA	895.00 ± NA	NA	NA	NA	895.00 ± NA	895.00 ± NA	895.00	895.00	895.00	NA
		222234	1	125.70	NA	125.70 ± NA	125.70 ± NA	NA	NA	NA	125.70 ± NA	125.70 ± NA	125.70	125.70	125.70	NA
		231221	20	172.33	12.99	172.33 ± 12.99	172.33 ± 8%	58.09	9.42	67.52	172.33 ± 67.52	172.33 ± 39%	154.75	78.20	278.40	200.20
		231222	3	260.53	57.98	260.53 ± 57.98	260.53 ± 22%	100.43	50.22	150.65	260.53 ± 150.65	260.53 ± 58%	313.60	144.70	323.30	178.60
		231223	4	290.98	71.50	290.98 ± 71.50	290.98 ± 25%	143.00	58.38	201.37	290.98 ± 201.37	290.98 ± 69%	296.75	152.20	418.20	266.00
PTn	Tpcpv2	231221	4	28.18	11.80	28.18 ± 11.80	28.18 ± 42%	23.60	9.64	33.24	28.18 ± 33.24	28.18 ± 118%	19.80	11.30	61.80	50.50
		231223	1	71.40	NA	71.40 ± NA	71.40 ± NA	NA	NA	NA	71.40 ± NA	71.40 ± NA	71.40	71.40	71.40	NA
	Tpcpv1	231221	4	5.05	0.71	5.05 ± 0.71	5.05 ± 14%	1.41	0.58	1.99	5.05 ± 1.99	5.05 ± 39%	4.70	3.90	6.90	3.00
	Tpbt4	221221	1	3.50	NA	3.50 ± NA	3.50 ± NA	NA	NA	NA	3.50 ± NA	3.50 ± NA	3.50	3.50	3.50	NA
		221231	1	7.03	NA	7.03 ± NA	7.03 ± NA	NA	NA	NA	7.03 ± NA	7.03 ± NA	7.03	7.03	7.03	NA
		231221	1	1.20	NA	1.20 ± NA	1.20 ± NA	NA	NA	NA	1.20 ± NA	1.20 ± NA	1.20	1.20	1.20	NA
	Tpy	231221	5	19.30	3.13	19.30 ± 3.13	19.30 ± 16%	6.99	2.47	9.46	19.30 ± 9.46	19.30 ± 49%	21.00	7.80	26.20	18.40
	Tpbt3	221221	2	5.10	0.80	5.10 ± 0.80	5.10 ± 16%	1.13	0.80	1.93	5.10 ± 1.93	5.10 ± 38%	5.10	4.30	5.90	1.60
		231221	2	1.80	1.00	1.80 ± 1.00	1.80 ± 56%	1.41	1.00	2.41	1.80 ± 2.41	1.80 ± 134%	1.80	0.80	2.80	2.00
		231222	1	13.30	NA	13.30 ± NA	13.30 ± NA	NA	NA	NA	13.30 ± NA	13.30 ± NA	13.30	13.30	13.30	NA
	Tpp	221221	2	3.70	0.40	3.70 ± 0.40	3.70 ± 11%	0.57	0.40	0.97	3.70 ± 0.97	3.70 ± 26%	3.70	3.30	4.10	0.80
		231221	10	3.19	0.77	3.19 ± 0.77	3.19 ± 24%	2.45	0.58	3.02	3.19 ± 3.02	3.19 ± 95%	2.20	1.30	9.40	8.10
		231223	1	17.30	NA	17.30 ± NA	17.30 ± NA	NA	NA	NA	17.30 ± NA	17.30 ± NA	17.30	17.30	17.30	NA
	Tpbt2	221221	3	3.20	0.82	3.20 ± 0.82	3.20 ± 26%	1.42	0.71	2.13	3.20 ± 2.13	3.20 ± 66%	2.70	2.10	4.80	2.70
		231221	6	2.92	0.94	2.92 ± 0.94	2.92 ± 32%	2.30	0.73	3.03	2.92 ± 3.03	2.92 ± 104%	1.85	0.80	6.40	5.60
	Tptrv3	231221	2	4.25	1.55	4.25 ± 1.55	4.25 ± 36%	2.19	1.55	3.74	4.25 ± 3.74	4.25 ± 88%	4.25	2.70	5.80	3.10

Table B-1. Summary of Intact rock Mechanical Properties Data - Compressive Strength and All Static Elastic Properties

Thermo-Mechanical Unit	Litho-stratigraphic Unit	Testing Group Code	Count	Mean	St. Error (SE)	Mean ± 1 SE	Mean ± 1 SE (%)	Standard Deviation (SD)	Uncertainty of the SD	SD+Uncertainty of SD (SD*)	Mean± 1 SD*	Mean± 1 SD* (%)	Median	Minimum	Maximum	Range
TSw1	Tptrn	131221	10	103.68	11.39	103.68 ± 11.39	103.68 ± 11%	36.02	8.49	44.50	103.68 ± 44.50	103.68 ± 43%	93.40	62.60	162.00	99.40
		131222	13	86.40	8.89	86.40 ± 8.89	86.40 ± 10%	32.06	6.54	38.60	86.40 ± 38.60	86.40 ± 45%	77.10	39.60	163.90	124.30
		131223	11	132.61	15.20	132.61 ± 15.20	132.61 ± 11%	50.42	11.27	61.69	132.61 ± 61.69	132.61 ± 47%	139.10	30.10	208.30	178.20
		221221	5	63.34	16.37	63.34 ± 16.37	63.34 ± 26%	36.60	12.94	49.54	63.34 ± 49.54	63.34 ± 78%	64.00	26.50	114.30	87.80
		231221	53	61.98	4.27	61.98 ± 4.27	61.98 ± 7%	31.06	3.05	34.11	61.98 ± 34.11	61.98 ± 55%	55.50	25.70	148.40	122.70
		231222	8	92.39	5.50	92.39 ± 5.50	92.39 ± 6%	15.56	4.16	19.72	92.39 ± 19.72	92.39 ± 21%	94.05	70.50	116.10	45.60
		231223	8	117.63	17.90	117.63 ± 17.90	117.63 ± 15%	50.62	13.53	64.15	117.63 ± 64.15	117.63 ± 55%	103.10	60.40	228.50	168.10
	Tptrl	231221	3	26.73	5.34	26.73 ± 5.34	26.73 ± 20%	9.25	4.63	13.88	26.73 ± 13.88	26.73 ± 52%	26.90	17.40	35.90	18.50
		231222	1	67.10	NA	67.10 ± NA	67.10 ± NA	NA	NA	NA	67.10 ± NA	67.10 ± NA	67.10	67.10	67.10	NA
	Tptf	131211	2	116.00	1.00	116.00 ± 1.00	116.00 ± 1%	1.41	1.00	2.41	116.00 ± 2.41	116.00 ± 2%	116.00	115.00	117.00	2.00
		131221	5	176.80	16.80	176.80 ± 16.80	176.80 ± 10%	37.57	13.28	50.86	176.80 ± 50.86	176.80 ± 29%	167.00	130.00	220.00	90.00
		231221	1	157.00	NA	157.00 ± NA	157.00 ± NA	NA	NA	NA	157.00 ± NA	157.00 ± NA	157.00	157.00	157.00	NA
	Tptpul	221221	2	47.50	10.20	47.50 ± 10.20	47.50 ± 21%	14.42	10.20	24.62	47.50 ± 24.62	47.50 ± 52%	47.50	37.30	57.70	20.40
		231221	8	65.21	15.70	65.21 ± 15.70	65.21 ± 24%	44.40	11.87	56.27	65.21 ± 56.27	65.21 ± 86%	60.90	15.70	149.40	133.70
		231222	2	94.40	17.50	94.40 ± 17.50	94.40 ± 19%	24.75	17.50	42.25	94.40 ± 42.25	94.40 ± 45%	94.40	76.90	111.90	35.00
		231223	1	227.90	NA	227.90 ± NA	227.90 ± NA	NA	NA	NA	227.90 ± NA	227.90 ± NA	227.90	227.90	227.90	NA
		312111	3	30.47	5.47	30.47 ± 5.47	30.47 ± 18%	9.47	4.74	14.21	30.47 ± 14.21	30.47 ± 47%	34.80	19.60	37.00	17.40
		312221	1	17.70	NA	17.70 ± NA	17.70 ± NA	NA	NA	NA	17.70 ± NA	17.70 ± NA	17.70	17.70	17.70	NA
		321111	3	24.03	5.00	24.03 ± 5.00	24.03 ± 21%	8.66	4.33	12.99	24.03 ± 12.99	24.03 ± 54%	22.10	16.50	33.50	17.00
		321211	8	28.65	4.26	28.65 ± 4.26	28.65 ± 15%	12.04	3.22	15.26	28.65 ± 15.26	28.65 ± 53%	27.00	13.50	53.00	39.50
		321221	1	19.40	NA	19.40 ± NA	19.40 ± NA	NA	NA	NA	19.40 ± NA	19.40 ± NA	19.40	19.40	19.40	0.00
		331211	4	18.75	7.55	18.75 ± 7.55	18.75 ± 40%	15.10	6.16	21.26	18.75 ± 21.26	18.75 ± 113%	12.15	9.40	41.30	31.90
		331221	11	16.12	1.43	16.12 ± 1.43	16.12 ± 9%	4.73	1.06	5.79	16.12 ± 5.79	16.12 ± 36%	14.90	10.30	27.80	17.50
TSw2	Tptpmn	111321	30	146.46	10.47	146.46 ± 10.47	146.46 ± 7%	57.33	7.53	64.86	146.46 ± 64.86	146.46 ± 44%	155.10	31.90	236.00	204.10
		131211	2	236.60	6.50	236.60 ± 6.50	236.60 ± 3%	9.19	6.50	15.69	236.60 ± 15.69	236.60 ± 7%	236.60	230.10	243.10	13.00
		131221	30	222.70	7.74	222.70 ± 7.74	222.70 ± 3%	42.42	5.57	47.99	222.70 ± 47.99	222.70 ± 22%	224.30	113.30	326.10	212.80
		131222	6	220.30	33.31	220.30 ± 33.31	220.30 ± 15%	81.58	25.80	107.38	220.30 ± 107.38	220.30 ± 49%	243.35	92.00	322.30	230.30
		131223	6	325.90	19.82	325.90 ± 19.82	325.90 ± 6%	48.54	15.35	63.89	325.90 ± 63.89	325.90 ± 20%	339.60	235.50	370.00	134.50
		131231	3	294.10	12.53	294.10 ± 12.53	294.10 ± 4%	21.70	10.85	32.55	294.10 ± 32.55	294.10 ± 11%	283.10	280.10	319.10	39.00
		211211	4	150.88	25.09	150.88 ± 25.09	150.88 ± 17%	50.18	20.48	70.66	150.88 ± 70.66	150.88 ± 47%	169.95	78.10	185.50	107.40
		211221	4	122.58	17.66	122.58 ± 17.66	122.58 ± 14%	35.32	14.42	49.74	122.58 ± 49.74	122.58 ± 41%	118.60	87.00	166.10	79.10
		211222	3	196.40	19.05	196.40 ± 19.05	196.40 ± 10%	32.99	16.50	49.49	196.40 ± 49.49	196.40 ± 25%	203.60	160.40	225.20	64.80
		211223	3	235.10	39.73	235.10 ± 39.73	235.10 ± 17%	68.81	34.41	103.22	235.10 ± 103.22	235.10 ± 44%	198.00	192.80	314.50	121.70
		212211	9	105.67	11.51	105.67 ± 11.51	105.67 ± 11%	34.54	8.63	43.17	105.67 ± 43.17	105.67 ± 41%	103.00	45.00	152.00	107.00
		212221	2	90.50	18.50	90.50 ± 18.50	90.50 ± 20%	26.16	18.50	44.66	90.50 ± 44.66	90.50 ± 49%	90.50	72.00	109.00	37.00
		212223	3	196.33	37.26	196.33 ± 37.26	196.33 ± 19%	64.53	32.27	96.80	196.33 ± 96.80	196.33 ± 49%	229.00	122.00	238.00	116.00
		212231	2	101.50	72.50	101.50 ± 72.50	101.50 ± 71%	102.53	72.50	175.03	101.50 ± 175.03	101.50 ± 172%	101.50	29.00	174.00	145.00
		221221	16	176.35	16.46	176.35 ± 16.46	176.35 ± 9%	65.82	12.02	77.84	176.35 ± 77.84	176.35 ± 44%	173.90	71.30	324.10	252.80
		221231	1	138.00	NA	138.00 ± NA	138.00 ± NA	NA	NA	NA	138.00 ± NA	138.00 ± NA	138.00	138.00	138.00	NA
		221321	36	139.58	9.68	139.58 ± 9.68	139.58 ± 7%	58.07	6.94	65.01	139.58 ± 65.01	139.58 ± 47%	143.20	34.30	245.70	211.40
		222234	1	153.70	NA	153.70 ± NA	153.70 ± NA	NA	NA	NA	153.70 ± NA	153.70 ± NA	153.70	153.70	153.70	NA
		231211	10	103.65	10.14	103.65 ± 10.14	103.65 ± 10%	32.07	7.56	39.63	103.65 ± 39.63	103.65 ± 38%	95.85	45.30	149.00	103.70
		231221	42	164.58	10.13	164.58 ± 10.13	164.58 ± 6%	65.62	7.25	72.87	164.58 ± 72.87	164.58 ± 44%	161.55	38.40	288.90	250.50
		231222	5	227.78	30.39	227.78 ± 30.39	227.78 ± 13%	67.95	24.02	91.97	227.78 ± 91.97	227.78 ± 40%	203.70	174.00	335.70	161.70
		231223	14	169.00	14.86	169.00 ± 14.86	169.00 ± 9%	55.61	10.91	66.51	169.00 ± 66.51	169.00 ± 39%	167.30	49.70	282.80	233.10
		231224	5	214.54	17.77	214.54 ± 17.77	214.54 ± 8%	39.73	14.05	53.78	214.54 ± 53.78	214.54 ± 25%	212.00	176.30	272.40	96.10
		231231	4	113.20	21.43	113.20 ± 21.43	113.20 ± 19%	42.86	17.50	60.35	113.20 ± 60.35	113.20 ± 53%	107.85	68.10	169.00	100.90
		232211	11	196.79	7.79	196.79 ± 7.79	196.79 ± 4%	25.85	5.78	31.63	196.79 ± 31.63	196.79 ± 16%	203.50	148.30	229.50	81.20
		232212	6	253.55	20.04	253.55 ± 20.04	253.55 ± 8%	49.09	15.52	64.61	253.55 ± 64.61	253.55 ± 25%	241.90	207.30	339.20	131.90
		232213	5	253.86	22.52	253.86 ± 22.52	253.86 ± 9%	50.36	17.80	68.16	253.86 ± 68.16	253.86 ± 27%	243.50	205.80	329.40	123.60
		232221	4	117.38	10.33	117.38 ± 10.33	117.38 ± 9%	20.67	8.44	29.11	117.38 ± 29.11	117.38 ± 25%	122.15	89.40	135.80	46.40
		232222	3	121.10	34.22	121.10 ± 34.22	121.10 ± 28%	59.27	29.64	88.91	121.10 ± 88.91	121.10 ± 73%	150.20	52.90	160.20	107.30
		321221	1	159.60	NA	159.60 ± NA	159.60 ± NA	NA	NA	NA	159.60 ± NA	159.60 ± NA	159.60	159.60	159.60	NA
		331221	22	105.94	6.63	105.94 ± 6.63	105.94 ± 6%	31.11	4.80	35.91	105.94 ± 35.91	105.94 ± 34%	95.76	58.86	170.80	111.94

Table B-1. Summary of Intact rock Mechanical Properties Data - Compressive Strength and All Static Elastic Properties

Thermo-Mechanical Unit	Litho-stratigraphic Unit	Testing Group Code	Count	Mean	St. Error (SE)	Mean ± 1 SE	Mean ± 1 SE (%)	Standard Deviation (SD)	Uncertainty of the SD	SD+Uncertainty of SD (SD*)	Mean± 1 SD*	Mean± 1 SD* (%)	Median	Minimum	Maximum	Range
TSw2	Tptpll	121221	16	194.69	9.50	194.69 ± 9.50	194.69 ± 5%	37.99	6.94	44.93	194.69 ± 44.93	194.69 ± 23%	195.75	110.90	261.70	150.80
		131211	2	130.60	7.50	130.60 ± 7.50	130.60 ± 6%	10.61	7.50	18.11	130.60 ± 18.11	130.60 ± 14%	130.60	123.10	138.10	15.00
		131221	30	112.99	9.38	112.99 ± 9.38	112.99 ± 8%	51.38	6.75	58.12	112.99 ± 58.12	112.99 ± 51%	121.10	3.00	187.10	184.10
		131222	3	138.83	44.06	138.83 ± 44.06	138.83 ± 32%	76.32	38.16	114.48	138.83 ± 114.48	138.83 ± 82%	114.70	77.50	224.30	146.80
		131223	3	164.43	46.73	164.43 ± 46.73	164.43 ± 28%	80.94	40.47	121.41	164.43 ± 121.41	164.43 ± 74%	129.30	107.00	257.00	150.00
		211221	7	175.93	7.32	175.93 ± 7.32	175.93 ± 4%	19.38	5.59	24.97	175.93 ± 24.97	175.93 ± 14%	175.20	152.20	205.20	53.00
		212221	6	213.18	4.80	213.18 ± 4.80	213.18 ± 2%	11.75	3.72	15.46	213.18 ± 15.46	213.18 ± 7%	213.25	200.30	226.30	26.00
		221221	59	153.12	5.22	153.12 ± 5.22	153.12 ± 3%	40.06	3.72	43.78	153.12 ± 43.78	153.12 ± 29%	153.20	50.90	246.60	195.70
		231221	15	123.01	12.28	123.01 ± 12.28	123.01 ± 10%	47.57	8.99	56.57	123.01 ± 56.57	123.01 ± 46%	135.10	31.60	179.10	147.50
		231223	1	216.90	NA	216.90 ± NA	216.90 ± NA	NA	NA	NA	216.90 ± NA	216.90 ± NA	216.90	216.90	216.90	NA
		312111	2	31.65	0.55	31.65 ± 0.55	31.65 ± 2%	0.78	0.55	1.33	31.65 ± 1.33	31.65 ± 4%	31.65	31.10	32.20	1.10
		312221	5	122.72	33.98	122.72 ± 33.98	122.72 ± 28%	75.98	26.86	102.84	122.72 ± 102.84	122.72 ± 84%	162.00	28.30	196.10	167.80
		321211	7	34.57	6.57	34.57 ± 6.57	34.57 ± 19%	17.39	5.02	22.41	34.57 ± 22.41	34.57 ± 65%	33.10	13.30	67.40	54.10
		321221	25	121.24	7.74	121.24 ± 7.74	121.24 ± 6%	38.69	5.58	44.27	121.24 ± 44.27	121.24 ± 37%	124.70	28.10	180.00	151.90
		331211	1	15.70	NA	15.70 ± NA	15.70 ± NA	NA	NA	NA	15.70 ± NA	15.70 ± NA	15.70	15.70	15.70	NA
		331221	1	38.00	NA	38.00 ± NA	38.00 ± NA	NA	NA	NA	38.00 ± NA	38.00 ± NA	38.00	38.00	38.00	NA
		421221	5	60.70	11.09	60.70 ± 11.09	60.70 ± 18%	24.80	8.77	33.57	60.70 ± 33.57	60.70 ± 55%	65.60	27.00	92.20	65.20
	Tptpln	131211	3	126.13	40.98	126.13 ± 40.98	126.13 ± 32%	70.97	35.49	106.46	126.13 ± 106.46	126.13 ± 84%	156.70	45.00	176.70	131.70
		131221	10	104.40	11.94	104.40 ± 11.94	104.40 ± 11%	37.77	8.90	46.67	104.40 ± 46.67	104.40 ± 45%	109.70	31.10	152.10	121.00
		131231	4	149.58	5.52	149.58 ± 5.52	149.58 ± 4%	11.03	4.50	15.54	149.58 ± 15.54	149.58 ± 10%	153.55	133.90	157.30	23.40
		221221	2	171.55	1.35	171.55 ± 1.35	171.55 ± 1%	1.91	1.35	3.26	171.55 ± 3.26	171.55 ± 2%	171.55	170.20	172.90	2.70
		221231	1	166.00	NA	166.00 ± NA	166.00 ± NA	NA	NA	NA	166.00 ± NA	166.00 ± NA	166.00	166.00	166.00	NA
		221233	1	422.00	NA	422.00 ± NA	422.00 ± NA	NA	NA	NA	422.00 ± NA	422.00 ± NA	422.00	422.00	422.00	NA
		221234	1	638.00	NA	638.00 ± NA	638.00 ± NA	NA	NA	NA	638.00 ± NA	638.00 ± NA	638.00	638.00	638.00	NA
		231221	10	155.51	9.60	155.51 ± 9.60	155.51 ± 6%	30.35	7.15	37.50	155.51 ± 37.50	155.51 ± 24%	160.35	82.90	192.90	110.00
		231222	3	216.43	36.95	216.43 ± 36.95	216.43 ± 17%	64.00	32.00	96.00	216.43 ± 96.00	216.43 ± 44%	216.10	152.60	280.60	128.00
		231223	3	265.60	12.50	265.60 ± 12.50	265.60 ± 5%	21.65	10.83	32.48	265.60 ± 32.48	265.60 ± 12%	261.80	246.10	288.90	42.80
		232213	1	274.50	NA	274.50 ± NA	274.50 ± NA	NA	NA	NA	274.50 ± NA	274.50 ± NA	274.50	274.50	274.50	NA
TSw3	Tptpv3	131223	4	55.00	9.51	55.00 ± 9.51	55.00 ± 17%	19.03	7.77	26.79	55.00 ± 26.79	55.00 ± 49%	52.50	37.00	78.00	41.00
		221221	2	45.80	4.00	45.80 ± 4.00	45.80 ± 9%	5.66	4.00	9.66	45.80 ± 9.66	45.80 ± 21%	45.80	41.80	49.80	8.00
		231221	1	16.40	NA	16.40 ± NA	16.40 ± NA	NA	NA	NA	16.40 ± NA	16.40 ± NA	16.40	16.40	16.40	NA
		231222	1	52.20	NA	52.20 ± NA	52.20 ± NA	NA	NA	NA	52.20 ± NA	52.20 ± NA	52.20	52.20	52.20	NA
		231223	1	80.00	NA	80.00 ± NA	80.00 ± NA	NA	NA	NA	80.00 ± NA	80.00 ± NA	80.00	80.00	80.00	NA
CHn1	Tptpv2	131221	2	91.65	1.15	91.65 ± 1.15	91.65 ± 1%	1.63	1.15	2.78	91.65 ± 2.78	91.65 ± 3%	91.65	90.50	92.80	2.30
		221221	1	90.20	NA	90.20 ± NA	90.20 ± NA	NA	NA	NA	90.20 ± NA	90.20 ± NA	90.20	90.20	90.20	NA
	Tptpv1	131211	2	10.10	2.00	10.10 ± 2.00	10.10 ± 20%	2.83	2.00	4.83	10.10 ± 4.83	10.10 ± 48%	10.10	8.10	12.10	4.00
		131221	5	12.90	2.13	12.90 ± 2.13	12.90 ± 17%	4.76	1.68	6.45	12.90 ± 6.45	12.90 ± 50%	14.10	6.10	19.10	13.00
		131222	2	28.00	6.00	28.00 ± 6.00	28.00 ± 21%	8.49	6.00	14.49	28.00 ± 14.49	28.00 ± 52%	28.00	22.00	34.00	12.00
		131223	2	34.00	8.00	34.00 ± 8.00	34.00 ± 24%	11.31	8.00	19.31	34.00 ± 19.31	34.00 ± 57%	34.00	26.00	42.00	16.00
		131231	3	12.10	2.08	12.10 ± 2.08	12.10 ± 17%	3.61	1.80	5.41	12.10 ± 5.41	12.10 ± 45%	13.10	8.10	15.10	7.00
	Tpbt1	131211	3	27.67	0.33	27.67 ± 0.33	27.67 ± 1%	0.58	0.29	0.87	27.67 ± 0.87	27.67 ± 3%	28.00	27.00	28.00	1.00
		131221	4	27.25	3.01	27.25 ± 3.01	27.25 ± 11%	6.02	2.46	8.48	27.25 ± 8.48	27.25 ± 31%	26.00	22.00	35.00	13.00
		231221	1	20.50	NA	20.50 ± NA	20.50 ± NA	NA	NA	NA	20.50 ± NA	20.50 ± NA	20.50	20.50	20.50	NA
	Tac	121221	2	36.95	4.15	36.95 ± 4.15	36.95 ± 11%	5.87	4.15	10.02	36.95 ± 10.02	36.95 ± 27%	36.95	32.80	41.10	8.30
		121223	2	69.45	1.85	69.45 ± 1.85	69.45 ± 3%	2.62	1.85	4.47	69.45 ± 4.47	69.45 ± 6%	69.45	67.60	71.30	3.70
		131211	2	20.80	0.80	20.80 ± 0.80	20.80 ± 4%	1.13	0.80	1.93	20.80 ± 1.93	20.80 ± 9%	20.80	20.00	21.60	1.60
		131221	34	27.46	1.52	27.46 ± 1.52	27.46 ± 6%	8.87	1.09	9.96	27.46 ± 9.96	27.46 ± 36%	24.90	14.30	53.10	38.80
		131223	8	37.71	1.74	37.71 ± 1.74	37.71 ± 5%	4.91	1.31	6.23	37.71 ± 6.23	37.71 ± 17%	37.20	28.90	45.70	16.80
		131224	6	50.88	3.11	50.88 ± 3.11	50.88 ± 6%	7.62	2.41	10.04	50.88 ± 10.04	50.88 ± 20%	54.60	37.10	56.20	19.10
		131231	2	24.15	0.65	24.15 ± 0.65	24.15 ± 3%	0.92	0.65	1.57	24.15 ± 1.57	24.15 ± 6%	24.15	23.50	24.80	1.30
		221231	2	44.25	3.45	44.25 ± 3.45	44.25 ± 8%	4.88	3.45	8.33	44.25 ± 8.33	44.25 ± 19%	44.25	40.80	47.70	6.90
		221234	3	74.87	14.40	74.87 ± 14.40	74.87 ± 19%	24.93	12.47	37.40	74.87 ± 37.40	74.87 ± 50%	88.20	46.10	90.30	44.20
		231221	2	24.60	1.90	24.60 ± 1.90	24.60 ± 8%	2.69	1.90	4.59	24.60 ± 4.59	24.60 ± 19%	24.60	22.70	26.50	3.80

Table B-1. Summary of Intact rock Mechanical Properties Data - Compressive Strength and All Static Elastic Properties

Thermo-Mechanical Unit	Litho-stratigraphic Unit	Testing Group Code	Count	Mean	St. Error (SE)	Mean ± 1 SE	Mean ± 1 SE (%)	Standard Deviation (SD)	Uncertainty of the SD	SD+Uncertainty of SD (SD*)	Mean± 1 SD*	Mean± 1 SD* (%)	Median	Minimum	Maximum	Range
CHn2	Tacbt	131221	8	35.04	7.23	35.04 ± 7.23	35.04 ± 21%	20.45	5.47	25.92	35.04 ± 25.92	35.04 ± 74%	30.40	14.90	70.70	55.80
CFUn	Tcpm	221234	3	274.23	63.05	274.23 ± 63.05	274.23 ± 23%	109.21	54.60	163.81	274.23 ± 163.81	274.23 ± 60%	227.70	196.00	399.00	203.00
	Tcplc	221231	1	130.00	NA	130.00 ± NA	130.00 ± NA	NA	NA	NA	130.00 ± NA	130.00 ± NA	130.00	130.00	130.00	NA
	Tcplv	221231	1	32.20	NA	32.20 ± NA	32.20 ± NA	NA	NA	NA	32.20 ± NA	32.20 ± NA	32.20	32.20	32.20	NA
	Tcpbt	131221	8	27.25	5.68	27.25 ± 5.68	27.25 ± 21%	16.08	4.30	20.37	27.25 ± 20.37	27.25 ± 75%	21.10	11.70	47.50	35.80
	Tcbuv	131221	11	24.58	2.90	24.58 ± 2.90	24.58 ± 12%	9.61	2.15	11.75	24.58 ± 11.75	24.58 ± 48%	24.10	4.73	41.70	36.97
	Tcbuc	131221	18	30.45	1.23	30.45 ± 1.23	30.45 ± 4%	5.21	0.89	6.10	30.45 ± 6.10	30.45 ± 20%	29.85	16.70	38.00	21.30
		221234	1	224.00	NA	224.00 ± NA	224.00 ± NA	NA	NA	NA	224.00 ± NA	224.00 ± NA	224.00	224.00	224.00	NA
	Tcbm	112232	1	92.00	NA	92.00 ± NA	92.00 ± NA	NA	NA	NA	92.00 ± NA	92.00 ± NA	92.00	92.00	92.00	NA
		112233	1	103.00	NA	103.00 ± NA	103.00 ± NA	NA	NA	NA	103.00 ± NA	103.00 ± NA	103.00	103.00	103.00	NA
		112234	2	154.20	14.50	154.20 ± 14.50	154.20 ± 9%	20.51	14.50	35.01	154.20 ± 35.01	154.20 ± 23%	154.20	139.70	168.70	29.00
		131221	17	56.64	4.62	56.64 ± 4.62	56.64 ± 8%	19.06	3.37	22.43	56.64 ± 22.43	56.64 ± 40%	58.00	36.70	117.00	80.30
		132232	1	75.00	NA	75.00 ± NA	75.00 ± NA	NA	NA	NA	75.00 ± NA	75.00 ± NA	75.00	75.00	75.00	NA
		132233	1	95.50	NA	95.50 ± NA	95.50 ± NA	NA	NA	NA	95.50 ± NA	95.50 ± NA	95.50	95.50	95.50	NA
		132234	1	106.70	NA	106.70 ± NA	106.70 ± NA	NA	NA	NA	106.70 ± NA	106.70 ± NA	106.70	106.70	106.70	NA
		221231	1	54.00	NA	54.00 ± NA	54.00 ± NA	NA	NA	NA	54.00 ± NA	54.00 ± NA	54.00	54.00	54.00	NA
		221234	2	162.85	2.15	162.85 ± 2.15	162.85 ± 1%	3.04	2.15	5.19	162.85 ± 5.19	162.85 ± 3%	162.85	160.70	165.00	4.30
	Tcblv	131221	8	96.85	10.34	96.85 ± 10.34	96.85 ± 11%	29.23	7.81	37.05	96.85 ± 37.05	96.85 ± 38%	92.40	67.10	153.10	86.00
	Tcbbt	131221	4	69.68	3.11	69.68 ± 3.11	69.68 ± 4%	6.22	2.54	8.76	69.68 ± 8.76	69.68 ± 13%	72.35	60.40	73.60	13.20
	Tctuv	131221	7	52.20	2.80	52.20 ± 2.80	52.20 ± 5%	7.40	2.14	9.54	52.20 ± 9.54	52.20 ± 18%	50.30	45.20	63.90	18.70
	Tctuc	131221	4	57.65	8.17	57.65 ± 8.17	57.65 ± 14%	16.34	6.67	23.02	57.65 ± 23.02	57.65 ± 40%	56.20	42.00	76.20	34.20
	Tctm	131221	4	87.03	11.31	87.03 ± 11.31	87.03 ± 13%	22.62	9.24	31.86	87.03 ± 31.86	87.03 ± 37%	82.50	68.10	115.00	46.90
	Tctlc	131221	4	70.85	11.10	70.85 ± 11.10	70.85 ± 16%	22.21	9.07	31.28	70.85 ± 31.28	70.85 ± 44%	75.90	40.90	90.70	49.80
	Tctlv	131211	2	20.50	6.00	20.50 ± 6.00	20.50 ± 29%	8.49	6.00	14.49	20.50 ± 14.49	20.50 ± 71%	20.50	14.50	26.50	12.00
		131221	22	34.98	2.64	34.98 ± 2.64	34.98 ± 8%	12.38	1.91	14.29	34.98 ± 14.29	34.98 ± 41%	31.65	17.40	64.70	47.30
		131231	5	27.50	2.25	27.50 ± 2.25	27.50 ± 8%	5.02	1.78	6.80	27.50 ± 6.80	27.50 ± 25%	25.30	22.10	33.10	11.00

Table B-1. Summary of Intact rock Mechanical Properties Data - Compressive Strength and All Static Elastic Properties

Thermo-Mechanical Unit	Litho-stratigraphic Unit	Testing Group Code	Count	Mean	St. Error (SE)	Mean ± 1 SE	Mean ± 1 SE (%)	Standard Deviation (SD)	Uncertainty of the SD	SD+Uncertainty of SD (SD*)	Mean± 1 SD*	Mean± 1 SD* (%)	Median	Minimum	Maximum	Range
Young's Modulus (GPa)																
UO	Tmr	231221	5	3.36	1.20	3.36 ± 1.20	3.36 ± 36%	2.69	0.95	3.64	3.36 ± 3.64	3.36 ± 108%	3.70	0.70	7.20	6.50
	Tpki	231221	7	3.77	0.58	3.77 ± 0.58	3.77 ± 15%	1.54	0.44	1.99	3.77 ± 1.99	3.77 ± 53%	4.00	0.70	5.10	4.40
TCw	Tpcrn	221221	3	23.83	1.21	23.83 ± 1.21	23.83 ± 5%	2.09	1.04	3.13	23.83 ± 3.13	23.83 ± 13%	24.20	21.58	25.71	4.13
		231221	17	15.16	2.03	15.16 ± 2.03	15.16 ± 13%	8.39	1.48	9.87	15.16 ± 9.87	15.16 ± 65%	12.60	6.50	38.20	31.70
	Tpcpul	221221	3	26.24	2.22	26.24 ± 13.00	26.24 ± 50%	3.84	1.92	5.76	26.24 ± 5.76	26.24 ± 22%	25.85	22.61	30.26	7.65
		221233	0	NA	NA	NA ± NA	NA ± NA	NA	NA	NA	NA ± NA	NA ± NA	NA	NA	NA	NA
		221234	0	NA	NA	NA ± NA	NA ± NA	NA	NA	NA	NA ± NA	NA ± NA	NA	NA	NA	NA
		221321	1	23.16	NA	23.16 ± NA	23.16 ± NA	NA	NA	NA	23.16 ± NA	23.16 ± NA	23.16	23.16	23.16	NA
		221334	0	NA	NA	NA ± NA	NA ± NA	NA	NA	NA	NA ± NA	NA ± NA	NA	NA	NA	NA
		231221	5	23.72	3.08	23.72 ± 11.87	23.72 ± 50%	6.89	2.44	9.33	23.72 ± 9.33	23.72 ± 39%	27.00	14.80	29.60	14.80
	Tpcpmn	131222	4	35.08	2.76	35.08 ± 34.13	35.08 ± 97%	5.52	2.25	7.77	35.08 ± 7.77	35.08 ± 22%	36.95	27.00	39.40	12.40
		131223	4	37.68	0.56	37.68 ± 17.00	37.68 ± 45%	1.12	0.46	1.58	37.68 ± 1.58	37.68 ± 4%	37.30	36.80	39.30	2.50
		221221	2	35.40	3.00	35.40 ± 22.31	35.40 ± 63%	4.24	3.00	7.24	35.40 ± 7.24	35.40 ± 20%	35.40	32.40	38.40	6.00
		221233	0	NA	NA	NA ± NA	NA ± NA	NA	NA	NA	NA ± NA	NA ± NA	NA	NA	NA	NA
		221234	0	NA	NA	NA ± NA	NA ± NA	NA	NA	NA	NA ± NA	NA ± NA	NA	NA	NA	NA
		221321	1	28.88	NA	28.88 ± NA	28.88 ± NA	NA	NA	NA	28.88 ± NA	28.88 ± NA	28.88	28.88	28.88	NA
		231221	8	35.81	2.60	35.81 ± 22.67	35.81 ± 63%	7.35	1.96	9.31	35.81 ± 9.31	35.81 ± 26%	38.95	20.00	41.40	21.40
		231222	2	35.40	7.50	35.40 ± 70.25	35.40 ± 198%	10.61	7.50	18.11	35.40 ± 18.11	35.40 ± 51%	35.40	27.90	42.90	15.00
		231223	1	27.40	NA	27.40 ± NA	27.40 ± NA	NA	NA	NA	27.40 ± NA	27.40 ± NA	27.40	27.40	27.40	NA
	Tpcpll	131221	4	36.93	0.23	36.93 ± 10.02	36.93 ± 27%	0.46	0.19	0.64	36.93 ± 0.64	36.93 ± 2%	36.95	36.40	37.40	1.00
		131222	4	36.73	0.25	36.73 ± 21.88	36.73 ± 60%	0.50	0.20	0.70	36.73 ± 0.70	36.73 ± 2%	36.60	36.30	37.40	1.10
		131223	4	37.23	0.62	37.23 ± 22.30	37.23 ± 60%	1.25	0.51	1.76	37.23 ± 1.76	37.23 ± 5%	37.50	35.60	38.30	2.70
		231221	5	32.82	2.53	32.82 ± 50.47	32.82 ± 154%	5.65	2.00	7.65	32.82 ± 7.65	32.82 ± 23%	33.50	24.60	39.00	14.40
		231222	1	24.40	NA	24.40 ± NA	24.40 ± NA	NA	NA	NA	24.40 ± NA	24.40 ± NA	24.40	24.40	24.40	NA
		231223	1	22.30	NA	22.30 ± NA	22.30 ± NA	NA	NA	NA	22.30 ± NA	22.30 ± NA	22.30	22.30	22.30	NA
	Tpcpln	221231	1	57.50	NA	57.50 ± NA	57.50 ± NA	NA	NA	NA	57.50 ± NA	57.50 ± NA	57.50	57.50	57.50	NA
		221233	1	43.90	NA	43.90 ± NA	43.90 ± NA	NA	NA	NA	43.90 ± NA	43.90 ± NA	43.90	43.90	43.90	NA
		221234	1	58.30	NA	58.30 ± NA	58.30 ± NA	NA	NA	NA	58.30 ± NA	58.30 ± NA	58.30	58.30	58.30	NA
		222234	0	NA	NA	NA ± NA	NA ± NA	NA	NA	NA	NA ± NA	NA ± NA	NA	NA	NA	NA
		231221	20	33.84	1.35	33.84 ± 12.99	33.84 ± 38%	6.05	0.98	7.03	33.84 ± 7.03	33.84 ± 21%	35.75	21.40	40.10	18.70
		231222	3	32.73	4.94	32.73 ± 57.98	32.73 ± 177%	8.56	4.28	12.84	32.73 ± 12.84	32.73 ± 39%	36.10	23.00	39.10	16.10
		231223	4	37.68	7.22	37.68 ± 71.50	37.68 ± 190%	14.45	5.90	20.34	37.68 ± 20.34	37.68 ± 54%	38.95	18.80	54.00	35.20
PTn	Tpcpv2	231221	4	7.63	2.66	7.63 ± 11.80	7.63 ± 155%	5.32	2.17	7.50	7.63 ± 7.50	7.63 ± 98%	6.80	2.10	14.80	12.70
		231223	1	24.00	NA	24.00 ± NA	24.00 ± NA	NA	NA	NA	24.00 ± NA	24.00 ± NA	24.00	24.00	24.00	NA
	Tpcpv1	231221	4	2.53	0.83	2.53 ± 0.71	2.53 ± 28%	1.67	0.68	2.35	2.53 ± 2.35	2.53 ± 93%	2.95	0.30	3.90	3.60
	Tpbt4	221221	1	2.90	NA	2.90 ± NA	2.90 ± NA	NA	NA	NA	2.90 ± NA	2.90 ± NA	2.90	2.90	2.90	NA
		221231	1	0.41	NA	0.41 ± NA	0.41 ± NA	NA	NA	NA	0.41 ± NA	0.41 ± NA	0.41	0.41	0.41	NA
		231221	1	0.20	NA	0.20 ± NA	0.20 ± NA	NA	NA	NA	0.20 ± NA	0.20 ± NA	0.20	0.20	0.20	NA
	Tpy	231221	5	5.24	1.36	5.24 ± 3.13	5.24 ± 60%	3.05	1.08	4.13	5.24 ± 4.13	5.24 ± 79%	4.90	2.30	9.20	6.90
	Tpbt3	221221	2	1.80	0.60	1.80 ± 0.80	1.80 ± 44%	0.85	0.60	1.45	1.80 ± 1.45	1.80 ± 80%	1.80	1.20	2.40	1.20
		231221	2	1.30	1.10	1.30 ± 1.00	1.30 ± 77%	1.56	1.10	2.66	1.30 ± 2.66	1.30 ± 204%	1.30	0.20	2.40	2.20
		231222	0	NA	NA	NA ± NA	NA ± NA	NA	NA	NA	NA ± NA	NA ± NA	NA	NA	NA	NA
	Tpp	221221	2	1.05	0.25	1.05 ± 0.40	1.05 ± 38%	0.35	0.25	0.60	1.05 ± 0.60	1.05 ± 57%	1.05	0.80	1.30	0.50
		231221	10	0.98	0.21	0.98 ± 0.77	0.98 ± 79%	0.66	0.16	0.82	0.98 ± 0.82	0.98 ± 83%	0.75	0.30	2.10	1.80
		231223	0	NA	NA	NA ± NA	NA ± NA	NA	NA	NA	NA ± NA	NA ± NA	NA	NA	NA	NA
	Tpbt2	221221	3	0.90	0.31	0.90 ± 0.82	0.90 ± 91%	0.53	0.26	0.79	0.90 ± 0.79	0.90 ± 88%	0.70	0.50	1.50	1.00
		231221	6	0.67	0.28	0.67 ± 0.94	0.67 ± 140%	0.68	0.22	0.90	0.67 ± 0.90	0.67 ± 135%	0.50	0.01	1.70	1.69
	Tptrv3	231221	2	0.99	0.92	0.99 ± 1.55	0.99 ± 157%	1.29	0.92	2.21	0.99 ± 2.21	0.99 ± 224%	0.99	0.07	1.90	1.83

Table B-1. Summary of Intact rock Mechanical Properties Data - Compressive Strength and All Static Elastic Properties

Thermo-Mechanical Unit	Litho-stratigraphic Unit	Testing Group Code	Count	Mean	St. Error (SE)	Mean ± 1 SE	Mean ± 1 SE (%)	Standard Deviation (SD)	Uncertainty of the SD	SD+Uncertainty of SD (SD*)	Mean± 1 SD*	Mean± 1 SD* (%)	Median	Minimum	Maximum	Range
TSw1	Tptrn	131221	10	28.22	2.87	28.22 ± 11.39	28.22 ± 40%	9.08	2.14	11.21	28.22 ± 11.21	28.22 ± 40%	26.75	17.60	43.50	25.90
		131222	13	19.80	1.32	19.80 ± 8.89	19.80 ± 45%	4.77	0.97	5.74	19.80 ± 5.74	19.80 ± 29%	20.60	12.30	28.70	16.40
		131223	11	22.58	1.76	22.58 ± 15.20	22.58 ± 67%	5.83	1.30	7.13	22.58 ± 7.13	22.58 ± 32%	25.30	8.40	29.40	21.00
		221221	5	21.32	2.67	21.32 ± 16.37	21.32 ± 77%	5.98	2.11	8.10	21.32 ± 8.10	21.32 ± 38%	19.80	14.80	28.30	13.50
		231221	53	20.95	1.33	20.95 ± 4.27	20.95 ± 20%	9.66	0.95	10.60	20.95 ± 10.60	20.95 ± 51%	19.70	9.20	59.90	50.70
		231222	8	22.36	1.82	22.36 ± 5.50	22.36 ± 25%	5.16	1.38	6.54	22.36 ± 6.54	22.36 ± 29%	24.60	14.00	29.00	15.00
		231223	8	19.65	2.90	19.65 ± 17.90	19.65 ± 91%	8.19	2.19	10.38	19.65 ± 10.38	19.65 ± 53%	20.05	2.00	28.40	26.40
	Tptrl	231221	3	9.13	1.37	9.13 ± 5.34	9.13 ± 58%	2.38	1.19	3.56	9.13 ± 3.56	9.13 ± 39%	10.30	6.40	10.70	4.30
		231222	1	14.40	NA	14.40 ± NA	14.40 ± NA	NA	NA	NA	14.40 ± NA	14.40 ± NA	14.40	14.40	14.40	NA
	Tptf	131211	2	42.00	0.10	42.00 ± 1.00	42.00 ± 2%	0.14	0.10	0.24	42.00 ± 0.24	42.00 ± 1%	42.00	41.90	42.10	0.20
		131221	5	48.84	5.18	48.84 ± 16.80	48.84 ± 34%	11.58	4.10	15.68	48.84 ± 15.68	48.84 ± 32%	46.30	38.60	68.30	29.70
		231221	1	54.70	NA	54.70 ± NA	54.70 ± NA	NA	NA	NA	54.70 ± NA	54.70 ± NA	54.70	54.70	54.70	NA
	Tptpul	221221	2	19.70	1.40	19.70 ± 10.20	19.70 ± 52%	1.98	1.40	3.38	19.70 ± 3.38	19.70 ± 17%	19.70	18.30	21.10	2.80
		231221	8	20.41	3.24	20.41 ± 15.70	20.41 ± 77%	9.16	2.45	11.60	20.41 ± 11.60	20.41 ± 57%	21.90	6.00	33.30	27.30
		231222	2	25.10	7.30	25.10 ± 17.50	25.10 ± 70%	10.32	7.30	17.62	25.10 ± 17.62	25.10 ± 70%	25.10	17.80	32.40	14.60
		231223	1	22.30	NA	22.30 ± NA	22.30 ± NA	NA	NA	NA	22.30 ± NA	22.30 ± NA	22.30	22.30	22.30	NA
		312111	3	10.30	1.86	10.30 ± 5.47	10.30 ± 53%	3.22	1.61	4.83	10.30 ± 4.83	10.30 ± 47%	9.90	7.30	13.70	6.40
		312221	1	6.70	NA	6.70 ± NA	6.70 ± NA	NA	NA	NA	6.70 ± NA	6.70 ± NA	6.70	6.70	6.70	NA
		321111	3	15.93	2.39	15.93 ± 5.00	15.93 ± 31%	4.15	2.07	6.22	15.93 ± 6.22	15.93 ± 39%	14.90	12.40	20.50	8.10
		321211	8	13.10	1.58	13.10 ± 4.26	13.10 ± 33%	4.46	1.19	5.65	13.10 ± 5.65	13.10 ± 43%	14.10	5.80	19.50	13.70
		321221	1	7.30	NA	7.30 ± NA	7.30 ± NA	NA	NA	NA	7.30 ± NA	7.30 ± NA	7.30	7.30	7.30	NA
		331211	4	8.30	2.46	8.30 ± 7.55	8.30 ± 91%	4.92	2.01	6.92	8.30 ± 6.92	8.30 ± 83%	6.30	5.00	15.60	10.60
		331221	11	14.72	1.17	14.72 ± 1.43	14.72 ± 10%	3.89	0.87	4.77	14.72 ± 4.77	14.72 ± 32%	15.80	7.20	21.50	14.30
TSw2	Tptpmn	111321	30	24.02	0.75	24.02 ± 10.47	24.02 ± 44%	4.13	0.54	4.67	24.02 ± 4.67	24.02 ± 19%	25.10	6.80	27.80	21.00
		131211	2	35.55	1.95	35.55 ± 2.60	35.55 ± 7%	2.76	1.95	4.71	35.55 ± 4.71	35.55 ± 13%	35.55	33.60	37.50	3.90
		131221	30	34.90	1.02	34.90 ± 7.74	34.90 ± 22%	5.58	0.73	6.32	34.90 ± 6.32	34.90 ± 18%	33.80	28.10	47.30	19.20
		131222	6	37.40	1.57	37.40 ± 33.31	37.40 ± 89%	3.85	1.22	5.07	37.40 ± 5.07	37.40 ± 14%	35.90	34.00	43.60	9.60
		131223	6	34.23	0.89	34.23 ± 19.82	34.23 ± 58%	2.17	0.69	2.86	34.23 ± 2.86	34.23 ± 8%	34.05	32.00	38.00	6.00
		131231	3	36.60	1.33	36.60 ± 12.53	36.60 ± 34%	2.31	1.15	3.46	36.60 ± 3.46	36.60 ± 9%	37.40	34.00	38.40	4.40
		211211	4	37.98	2.24	37.98 ± 25.09	37.98 ± 66%	4.48	1.83	6.31	37.98 ± 6.31	37.98 ± 17%	38.80	32.10	42.20	10.10
		211221	4	40.55	2.51	40.55 ± 17.66	40.55 ± 44%	5.01	2.05	7.06	40.55 ± 7.06	40.55 ± 17%	41.40	33.70	45.70	12.00
		211222	3	37.43	2.03	37.43 ± 19.05	37.43 ± 51%	3.52	1.76	5.28	37.43 ± 5.28	37.43 ± 14%	37.90	33.70	40.70	7.00
		211223	3	35.57	2.62	35.57 ± 39.73	35.57 ± 112%	4.53	2.27	6.80	35.57 ± 6.80	35.57 ± 19%	33.10	32.80	40.80	8.00
		212211	9	50.72	12.74	50.72 ± 11.51	50.72 ± 23%	38.23	9.56	47.79	50.72 ± 47.79	50.72 ± 94%	37.70	33.10	152.40	119.30
		212221	2	37.60	0.10	37.60 ± 18.50	37.60 ± 49%	0.14	0.10	0.24	37.60 ± 0.24	37.60 ± 1%	37.60	37.50	37.70	0.20
		212223	3	36.43	0.92	36.43 ± 37.26	36.43 ± 102%	1.59	0.80	2.39	36.43 ± 2.39	36.43 ± 7%	37.20	34.60	37.50	2.90
		212231	2	26.10	12.10	26.10 ± 72.50	26.10 ± 278%	17.11	12.10	29.21	26.10 ± 29.21	26.10 ± 112%	26.10	14.00	38.20	24.20
		221221	16	36.76	0.87	36.76 ± 16.46	36.76 ± 45%	3.48	0.63	4.11	36.76 ± 4.11	36.76 ± 11%	37.60	28.90	43.10	14.20
		221231	1	40.40	NA	40.40 ± NA	40.40 ± NA	NA	NA	NA	40.40 ± NA	40.40 ± NA	40.40	40.40	40.40	NA
		221321	36	32.08	0.62	32.08 ± 9.68	32.08 ± 30%	3.74	0.45	4.19	32.08 ± 4.19	32.08 ± 13%	33.15	20.10	37.00	16.90
		222234	1	23.90	NA	23.90 ± NA	23.90 ± NA	NA	NA	NA	23.90 ± NA	23.90 ± NA	23.90	23.90	23.90	NA
		231211	10	36.35	1.64	36.35 ± 10.14	36.35 ± 28%	5.19	1.22	6.41	36.35 ± 6.41	36.35 ± 18%	36.90	26.10	44.50	18.40
		231221	41	32.53	1.05	32.53 ± 10.13	32.53 ± 31%	6.74	0.75	7.50	32.53 ± 7.50	32.53 ± 23%	34.17	13.40	45.70	32.30
		231222	5	35.56	0.62	35.56 ± 30.39	35.56 ± 85%	1.40	0.49	1.89	35.56 ± 1.89	35.56 ± 5%	35.50	33.90	37.10	3.20
		231223	13	29.65	1.30	29.65 ± 14.86	29.65 ± 50%	4.69	0.96	5.65	29.65 ± 5.65	29.65 ± 19%	30.75	21.40	35.20	13.80
		231224	5	28.09	2.15	28.09 ± 17.77	28.09 ± 63%	4.80	1.70	6.50	28.09 ± 6.50	28.09 ± 23%	29.58	19.80	31.50	11.70
		231231	4	32.53	2.06	32.53 ± 21.43	32.53 ± 66%	4.12	1.68	5.80	32.53 ± 5.80	32.53 ± 18%	33.20	26.90	36.80	9.90
		232211	11	35.74	1.34	35.74 ± 7.81	35.74 ± 22%	4.45	0.99	5.44	35.74 ± 5.44	35.74 ± 15%	35.90	29.60	42.20	12.60
		232212	6	30.83	1.86	30.83 ± 20.04	30.83 ± 65%	4.57	1.44	6.01	30.83 ± 6.01	30.83 ± 19%	32.40	22.30	35.00	12.70
		232213	5	31.50	1.35	31.50 ± 22.52	31.50 ± 71%	3.02	1.07	4.09	31.50 ± 4.09	31.50 ± 13%	31.00	27.70	34.60	6.90
		232221	4	30.98	1.10	30.98 ± 10.33	30.98 ± 33%	2.21	0.90	3.11	30.98 ± 3.11	30.98 ± 10%	31.60	28.00	32.70	4.70
		232222	3	28.60	6.33	28.60 ± 34.22	28.60 ± 120%	10.96	5.48	16.44	28.60 ± 16.44	28.60 ± 57%	33.90	16.00	35.90	19.90
		321221	1	32.40	NA	32.40 ± NA	32.40 ± NA	NA	NA	NA	32.40 ± NA	32.40 ± NA	32.40	32.40	32.40	NA
		331221	22	38.26	1.21	38.26 ± 6.63	38.26 ± 17%	5.66	0.87	6.53	38.26 ± 6.53	38.26 ± 17%	38.25	25.30	46.00	20.70

Table B-1. Summary of Intact rock Mechanical Properties Data - Compressive Strength and All Static Elastic Properties

Thermo-Mechanical Unit	Litho-stratigraphic Unit	Testing Group Code	Count	Mean	St. Error (SE)	Mean ± 1 SE	Mean ± 1 SE (%)	Standard Deviation (SD)	Uncertainty of the SD	SD+Uncertainty of SD (SD*)	Mean± 1 SD*	Mean± 1 SD* (%)	Median	Minimum	Maximum	Range
TSw2	Tptpll	121221	16	32.26	0.73	32.26 ± 9.50	32.26 ± 29%	2.91	0.53	3.44	32.26 ± 3.44	32.26 ± 11%	32.55	26.00	38.10	12.10
		131211	2	27.40	5.40	27.40 ± 7.50	27.40 ± 27%	7.64	5.40	13.04	27.40 ± 13.04	27.40 ± 48%	27.40	22.00	32.80	10.80
		131221	28	28.20	1.44	28.20 ± 9.38	28.20 ± 33%	7.63	1.04	8.66	28.20 ± 8.66	28.20 ± 31%	30.60	2.44	38.10	35.66
		131222	3	26.00	4.94	26.00 ± 44.06	26.00 ± 169%	8.55	4.28	12.83	26.00 ± 12.83	26.00 ± 49%	23.20	19.20	35.60	16.40
		131223	3	24.13	5.42	24.13 ± 46.73	24.13 ± 194%	9.39	4.69	14.08	24.13 ± 14.08	24.13 ± 58%	25.60	14.10	32.70	18.60
		211221	7	36.09	0.84	36.09 ± 7.32	36.09 ± 20%	2.22	0.64	2.86	36.09 ± 2.86	36.09 ± 8%	36.70	32.70	38.40	5.70
		212221	6	37.13	0.58	37.13 ± 4.80	37.13 ± 13%	1.42	0.45	1.87	37.13 ± 1.87	37.13 ± 5%	37.15	35.30	39.40	4.10
		221221	59	34.52	0.49	34.52 ± 5.22	34.52 ± 15%	3.75	0.35	4.09	34.52 ± 4.09	34.52 ± 12%	34.80	24.50	41.30	16.80
		231221	15	29.97	1.66	29.97 ± 12.28	29.97 ± 41%	6.43	1.21	7.64	29.97 ± 7.64	29.97 ± 25%	31.30	16.90	37.60	20.70
		231223	1	29.60	NA	29.60 ± NA	29.60 ± NA	NA	NA	NA	29.60 ± NA	29.60 ± NA	29.60	29.60	29.60	NA
		312111	2	6.80	0.30	6.80 ± 0.55	6.80 ± 8%	0.42	0.30	0.72	6.80 ± 0.72	6.80 ± 11%	6.80	6.50	7.10	0.60
		312221	5	28.96	6.29	28.96 ± 33.98	28.96 ± 117%	14.08	4.98	19.05	28.96 ± 19.05	28.96 ± 66%	34.20	7.10	40.50	33.40
		321211	7	11.81	1.93	11.81 ± 6.57	11.81 ± 56%	5.11	1.48	6.59	11.81 ± 6.59	11.81 ± 56%	12.00	5.00	21.00	16.00
		321221	25	33.65	1.63	33.65 ± 7.74	33.65 ± 23%	8.13	1.17	9.30	33.65 ± 9.30	33.65 ± 28%	36.30	9.60	41.60	32.00
		331211	1	5.30	NA	5.30 ± NA	5.30 ± NA	NA	NA	NA	5.30 ± NA	5.30 ± NA	5.30	5.30	5.30	NA
		331221	1	10.90	NA	10.90 ± NA	10.90 ± NA	NA	NA	NA	10.90 ± NA	10.90 ± NA	10.90	10.90	10.90	NA
		421221	5	31.60	2.43	31.60 ± 11.09	31.60 ± 35%	5.43	1.92	7.35	31.60 ± 7.35	31.60 ± 23%	33.80	25.30	37.50	12.20
	Tptpln	131211	3	33.00	5.29	33.00 ± 40.98	33.00 ± 124%	9.17	4.58	13.75	33.00 ± 13.75	33.00 ± 42%	35.30	22.90	40.80	17.90
		131221	10	29.72	2.29	29.72 ± 11.96	29.72 ± 40%	7.25	1.71	8.96	29.72 ± 8.96	29.72 ± 30%	32.40	16.60	36.30	19.70
		131231	4	32.75	2.51	32.75 ± 5.52	32.75 ± 17%	5.02	2.05	7.06	32.75 ± 7.06	32.75 ± 22%	32.90	27.70	37.50	9.80
		221221	2	35.05	0.65	35.05 ± 1.35	35.05 ± 4%	0.92	0.65	1.57	35.05 ± 1.57	35.05 ± 4%	35.05	34.40	35.70	1.30
		221231	1	61.80	NA	61.80 ± NA	61.80 ± NA	NA	NA	NA	61.80 ± NA	61.80 ± NA	61.80	61.80	61.80	NA
		221233	1	73.00	NA	73.00 ± NA	73.00 ± NA	NA	NA	NA	73.00 ± NA	73.00 ± NA	73.00	73.00	73.00	NA
		221234	1	59.90	NA	59.90 ± NA	59.90 ± NA	NA	NA	NA	59.90 ± NA	59.90 ± NA	59.90	59.90	59.90	NA
		231221	10	37.78	1.43	37.78 ± 9.60	37.78 ± 25%	4.53	1.07	5.59	37.78 ± 5.59	37.78 ± 15%	38.80	30.40	44.40	14.00
		231222	3	34.27	1.73	34.27 ± 36.95	34.27 ± 108%	3.00	1.50	4.51	34.27 ± 4.51	34.27 ± 13%	35.90	30.80	36.10	5.30
		231223	3	35.50	2.07	35.50 ± 12.50	35.50 ± 35%	3.59	1.80	5.39	35.50 ± 5.39	35.50 ± 15%	34.00	32.90	39.60	6.70
		232213	1	43.90	NA	43.90 ± NA	43.90 ± NA	NA	NA	NA	43.90 ± NA	43.90 ± NA	43.90	43.90	43.90	NA
TSw3	Tptpv3	131223	0	NA	NA	NA ± 9.51	NA ± NA	NA	NA	NA	NA ± NA	NA ± NA	NA	NA	NA	NA
		221221	2	34.25	2.35	34.25 ± 4.00	34.25 ± 12%	3.32	2.35	5.67	34.25 ± 5.67	34.25 ± 17%	34.25	31.90	36.60	4.70
		231221	1	25.20	NA	25.20 ± NA	25.20 ± NA	NA	NA	NA	25.20 ± NA	25.20 ± NA	25.20	25.20	25.20	NA
		231222	1	54.20	NA	54.20 ± NA	54.20 ± NA	NA	NA	NA	54.20 ± NA	54.20 ± NA	54.20	54.20	54.20	NA
		231223	1	32.90	NA	32.90 ± NA	32.90 ± NA	NA	NA	NA	32.90 ± NA	32.90 ± NA	32.90	32.90	32.90	NA
CHn1	Tptpv2	131221	2	16.45	0.35	16.45 ± 1.15	16.45 ± 7%	0.49	0.35	0.84	16.45 ± 0.84	16.45 ± 5%	16.45	16.10	16.80	0.70
		221221	1	16.70	NA	16.70 ± NA	16.70 ± NA	NA	NA	NA	16.70 ± NA	16.70 ± NA	16.70	16.70	16.70	NA
	Tptpv1	131211	2	2.26	0.85	2.26 ± 2.00	2.26 ± 89%	1.20	0.85	2.04	2.26 ± 2.04	2.26 ± 90%	2.26	1.41	3.10	1.69
		131221	5	2.40	0.35	2.40 ± 2.13	2.40 ± 89%	0.79	0.28	1.07	2.40 ± 1.07	2.40 ± 45%	2.25	1.53	3.70	2.17
		131222	2	3.39	0.29	3.39 ± 6.00	3.39 ± 177%	0.41	0.29	0.70	3.39 ± 0.70	3.39 ± 21%	3.39	3.10	3.68	0.58
		131223	2	3.75	0.60	3.75 ± 8.00	3.75 ± 214%	0.86	0.60	1.46	3.75 ± 1.46	3.75 ± 39%	3.75	3.14	4.35	1.21
		131231	3	2.70	0.48	2.70 ± 2.08	2.70 ± 77%	0.84	0.42	1.26	2.70 ± 1.26	2.70 ± 47%	2.96	1.76	3.37	1.61
	Tpbt1	131211	3	12.17	1.02	12.17 ± 0.33	12.17 ± 3%	1.76	0.88	2.64	12.17 ± 2.64	12.17 ± 22%	11.20	11.10	14.20	3.10
		131221	4	9.25	1.16	9.25 ± 3.01	9.25 ± 33%	2.32	0.95	3.27	9.25 ± 3.27	9.25 ± 35%	9.75	6.30	11.20	4.90
		231221	1	3.90	NA	3.90 ± NA	3.90 ± NA	NA	NA	NA	3.90 ± NA	3.90 ± NA	3.90	3.90	3.90	NA
	Tac	121221	2	7.31	0.81	7.31 ± 4.15	7.31 ± 57%	1.15	0.81	1.96	7.31 ± 1.96	7.31 ± 27%	7.31	6.50	8.12	1.62
		121223	2	7.27	0.07	7.27 ± 1.85	7.27 ± 25%	0.10	0.07	0.17	7.27 ± 0.17	7.27 ± 2%	7.27	7.20	7.34	0.14
		131211	2	7.45	0.41	7.45 ± 0.80	7.45 ± 11%	0.59	0.41	1.00	7.45 ± 1.00	7.45 ± 13%	7.45	7.03	7.86	0.83
		131221	33	7.07	0.37	7.07 ± 1.53	7.07 ± 22%	2.13	0.27	2.40	7.07 ± 2.40	7.07 ± 34%	6.60	3.51	12.80	9.29
		131223	8	6.76	0.55	6.76 ± 1.74	6.76 ± 26%	1.56	0.42	1.98	6.76 ± 1.98	6.76 ± 29%	6.51	4.28	8.90	4.62
		131224	6	7.42	0.87	7.42 ± 3.11	7.42 ± 42%	2.13	0.67	2.81	7.42 ± 2.81	7.42 ± 38%	7.66	3.92	9.72	5.80
		131231	2	5.43	0.02	5.43 ± 0.65	5.43 ± 12%	0.03	0.02	0.05	5.43 ± 0.05	5.43 ± 1%	5.43	5.41	5.45	0.04
		221231	2	13.16	0.86	13.16 ± 3.45	13.16 ± 26%	1.22	0.86	2.09	13.16 ± 2.09	13.16 ± 16%	13.16	12.29	14.02	1.73
		221234	3	8.69	0.47	8.69 ± 14.29	8.69 ± 164%	0.81	0.40	1.21	8.69 ± 1.21	8.69 ± 14%	8.50	7.99	9.57	1.58
		231221	2	6.50	0.40	6.50 ± 1.90	6.50 ± 29%	0.57	0.40	0.97	6.50 ± 0.97	6.50 ± 15%	6.50	6.10	6.90	0.80

Table B-1. Summary of Intact rock Mechanical Properties Data - Compressive Strength and All Static Elastic Properties

Thermo-Mechanical Unit	Litho-stratigraphic Unit	Testing Group Code	Count	Mean	St. Error (SE)	Mean ± 1 SE	Mean ± 1 SE (%)	Standard Deviation (SD)	Uncertainty of the SD	SD+Uncertainty of SD (SD*)	Mean± 1 SD*	Mean± 1 SD* (%)	Median	Minimum	Maximum	Range
CHn2	Tacbt	131221	8	6.92	1.46	6.92 ± 7.24	6.92 ± 105%	4.13	1.10	5.23	6.92 ± 5.23	6.92 ± 76%	6.38	2.52	12.70	10.18
CFUn	Tcpm	221234	3	26.65	2.62	26.65 ± 36.93	26.65 ± 139%	4.54	2.27	6.80	26.65 ± 6.80	26.65 ± 26%	27.01	21.95	31.00	9.05
	Tcplc	221231	1	47.90	NA	47.90 ± NA	47.90 ± NA	NA	NA	NA	47.90 ± NA	47.90 ± NA	47.90	47.90	47.90	NA
	Tcplv	221231	1	7.84	NA	7.84 ± NA	7.84 ± NA	NA	NA	NA	7.84 ± NA	7.84 ± NA	7.84	7.84	7.84	NA
	Tcpbt	131221	8	6.83	1.10	6.83 ± 5.68	6.83 ± 83%	3.11	0.83	3.94	6.83 ± 3.94	6.83 ± 58%	6.92	3.14	11.50	8.36
	Tcbuv	131221	11	6.58	1.25	6.58 ± 2.90	6.58 ± 44%	4.13	0.92	5.06	6.58 ± 5.06	6.58 ± 77%	5.76	2.03	15.80	13.77
	Tcbuc	131221	18	7.67	0.60	7.67 ± 1.23	7.67 ± 16%	2.54	0.44	2.97	7.67 ± 2.97	7.67 ± 39%	8.53	2.64	10.20	7.56
		221234	1	18.74	NA	18.74 ± NA	18.74 ± NA	NA	NA	NA	18.74 ± NA	18.74 ± NA	18.74	18.74	18.74	NA
	Tcbm	112232	1	16.50	NA	16.50 ± NA	16.50 ± NA	NA	NA	NA	16.50 ± NA	16.50 ± NA	16.50	16.50	16.50	NA
		112233	1	15.70	NA	15.70 ± NA	15.70 ± NA	NA	NA	NA	15.70 ± NA	15.70 ± NA	15.70	15.70	15.70	NA
		112234	2	19.05	1.45	19.05 ± 14.50	19.05 ± 76%	2.05	1.45	3.50	19.05 ± 3.50	19.05 ± 18%	19.05	17.60	20.50	2.90
		131221	16	14.18	1.05	14.18 ± 4.63	14.18 ± 33%	4.19	0.77	4.96	14.18 ± 4.96	14.18 ± 35%	14.85	3.82	20.80	16.98
		132232	1	13.10	NA	13.10 ± NA	13.10 ± NA	NA	NA	NA	13.10 ± NA	13.10 ± NA	13.10	13.10	13.10	NA
		132233	1	17.80	NA	17.80 ± NA	17.80 ± NA	NA	NA	NA	17.80 ± NA	17.80 ± NA	17.80	17.80	17.80	NA
		132234	1	13.80	NA	13.80 ± NA	13.80 ± NA	NA	NA	NA	13.80 ± NA	13.80 ± NA	13.80	13.80	13.80	NA
		221231	1	6.37	NA	6.37 ± NA	6.37 ± NA	NA	NA	NA	6.37 ± NA	6.37 ± NA	6.37	6.37	6.37	NA
		221234	2	20.67	1.43	20.67 ± 2.50	20.67 ± 12%	2.02	1.43	3.45	20.67 ± 3.45	20.67 ± 17%	20.67	19.24	22.10	2.86
	Tcblv	131221	8	18.64	2.09	18.64 ± 10.33	18.64 ± 55%	5.90	1.58	7.48	18.64 ± 7.48	18.64 ± 40%	18.15	11.60	28.90	17.30
	Tcbbt	131221	4	16.68	1.72	16.68 ± 3.09	16.68 ± 19%	3.44	1.40	4.84	16.68 ± 4.84	16.68 ± 29%	17.80	11.70	19.40	7.70
	Tctuv	131221	7	10.32	1.11	10.32 ± 2.80	10.32 ± 27%	2.94	0.85	3.79	10.32 ± 3.79	10.32 ± 37%	10.40	6.66	14.50	7.84
	Tctuc	131221	4	14.63	0.25	14.63 ± 8.17	14.63 ± 56%	0.51	0.21	0.71	14.63 ± 0.71	14.63 ± 5%	14.55	14.20	15.20	1.00
	Tctm	131221	4	19.88	0.61	19.88 ± 11.31	19.88 ± 57%	1.23	0.50	1.73	19.88 ± 1.73	19.88 ± 9%	19.95	18.30	21.30	3.00
	Tctlc	131221	4	18.33	2.85	18.33 ± 11.10	18.33 ± 61%	5.70	2.33	8.03	18.33 ± 8.03	18.33 ± 44%	20.35	10.10	22.50	12.40
	Tctlv	131211	2	7.65	0.61	7.65 ± 6.00	7.65 ± 78%	0.86	0.61	1.47	7.65 ± 1.47	7.65 ± 19%	7.65	7.04	8.26	1.22
		131221	22	7.84	0.51	7.84 ± 2.64	7.84 ± 34%	2.40	0.37	2.77	7.84 ± 2.77	7.84 ± 35%	7.64	2.61	12.40	9.79
		131231	5	8.54	1.41	8.54 ± 2.25	8.54 ± 26%	3.15	1.11	4.26	8.54 ± 4.26	8.54 ± 50%	8.76	5.17	13.40	8.23

Table B-1. Summary of Intact rock Mechanical Properties Data - Compressive Strength and All Static Elastic Properties

Thermo-Mechanical Unit	Litho-stratigraphic Unit	Testing Group Code	Count	Mean	St. Error (SE)	Mean ± 1 SE	Mean ± 1 SE (%)	Standard Deviation (SD)	Uncertainty of the SD	SD+Uncertainty of SD (SD*)	Mean± 1 SD*	Mean± 1 SD* (%)	Median	Minimum	Maximum	Range
Poisson's Ratio																
UO	Tmr	231221	5	0.03	0.01	0.03 ± 0.01	0.03 ± 27%	0.03	0.01	0.03	0.03 ± 0.03	0.03 ± 100%	0.02	0.01	0.07	0.06
	Tpki	231221	7	0.19	0.05	0.19 ± 0.05	0.19 ± 28%	0.14	0.04	0.18	0.19 ± 0.18	0.19 ± 95%	0.15	0.05	0.48	0.43
TCw	Tpcrn	221221	3	0.16	0.01	0.16 ± 0.01	0.16 ± 5%	0.02	0.01	0.02	0.16 ± 0.02	0.16 ± 14%	0.16	0.15	0.18	0.03
		231221	17	0.20	0.01	0.20 ± 0.01	0.20 ± 4%	0.03	0.01	0.04	0.20 ± 0.04	0.20 ± 20%	0.20	0.15	0.29	0.14
	Tpcpul	221221	3	0.17	0.01	0.17 ± 0.01	0.17 ± 7%	0.02	0.01	0.03	0.17 ± 0.03	0.17 ± 18%	0.17	0.15	0.19	0.04
		221233	0	NA	NA	NA ± NA	NA ± NA	NA	NA	NA	NA ± NA	NA ± NA	NA	NA	NA	NA
		221234	0	NA	NA	NA ± NA	NA ± NA	NA	NA	NA	NA ± NA	NA ± NA	NA	NA	NA	NA
		221321	1	0.15	NA	0.15 ± NA	0.15 ± NA	NA	NA	NA	0.15 ± NA	0.15 ± NA	0.15	0.15	0.15	NA
		221334	0	NA	NA	NA ± NA	NA ± NA	NA	NA	NA	NA ± NA	NA ± NA	NA	NA	NA	NA
		231221	5	0.19	0.01	0.19 ± 0.01	0.19 ± 5%	0.02	0.01	0.03	0.19 ± 0.03	0.19 ± 16%	0.20	0.15	0.20	0.05
	Tpcpmn	131222	4	0.24	0.02	0.24 ± 0.02	0.24 ± 9%	0.04	0.02	0.06	0.24 ± 0.06	0.24 ± 26%	0.23	0.20	0.29	0.09
		131223	4	0.20	0.00	0.20 ± 0.00	0.20 ± 2%	0.01	0.00	0.01	0.20 ± 0.01	0.20 ± 7%	0.21	0.19	0.21	0.02
		221221	2	0.18	0.00	0.18 ± 0.00	0.18 ± 0%	0.00	0.00	0.00	0.18 ± 0.00	0.18 ± 0%	0.18	0.18	0.18	0.00
		221233	0	NA	NA	NA ± NA	NA ± NA	NA	NA	NA	NA ± NA	NA ± NA	NA	NA	NA	NA
		221234	0	NA	NA	NA ± NA	NA ± NA	NA	NA	NA	NA ± NA	NA ± NA	NA	NA	NA	NA
		221321	1	0.17	NA	0.17 ± NA	0.17 ± NA	NA	NA	NA	0.17 ± NA	0.17 ± NA	0.17	0.17	0.17	NA
		231221	7	0.20	0.01	0.20 ± 0.01	0.20 ± 3%	0.02	0.00	0.02	0.20 ± 0.02	0.20 ± 11%	0.20	0.17	0.22	0.05
		231222	2	0.16	0.03	0.16 ± 0.03	0.16 ± 19%	0.04	0.03	0.07	0.16 ± 0.07	0.16 ± 45%	0.16	0.13	0.19	0.06
		231223	1	0.12	NA	0.12 ± NA	0.12 ± NA	NA	NA	NA	0.12 ± NA	0.12 ± NA	0.12	0.12	0.12	NA
	Tpcpll	131221	4	0.21	0.00	0.21 ± 0.00	0.21 ± 2%	0.01	0.00	0.01	0.21 ± 0.01	0.21 ± 6%	0.22	0.20	0.22	0.02
		131222	4	0.21	0.00	0.21 ± 0.00	0.21 ± 2%	0.01	0.00	0.01	0.21 ± 0.01	0.21 ± 6%	0.22	0.20	0.22	0.02
		131223	4	0.21	0.01	0.21 ± 0.01	0.21 ± 3%	0.01	0.01	0.02	0.21 ± 0.02	0.21 ± 8%	0.21	0.20	0.23	0.03
		231221	5	0.24	0.02	0.24 ± 0.02	0.24 ± 8%	0.04	0.02	0.06	0.24 ± 0.06	0.24 ± 25%	0.22	0.22	0.32	0.10
		231222	1	0.07	NA	0.07 ± NA	0.07 ± NA	NA	NA	NA	0.07 ± NA	0.07 ± NA	0.07	0.07	0.07	NA
		231223	1	0.10	NA	0.10 ± NA	0.10 ± NA	NA	NA	NA	0.10 ± NA	0.10 ± NA	0.10	0.10	0.10	NA
	Tpcpln	221231	1	0.31	NA	0.31 ± NA	0.31 ± NA	NA	NA	NA	0.31 ± NA	0.31 ± NA	0.31	0.31	0.31	NA
		221233	1	0.30	NA	0.30 ± NA	0.30 ± NA	NA	NA	NA	0.30 ± NA	0.30 ± NA	0.30	0.30	0.30	NA
		221234	1	0.22	NA	0.22 ± NA	0.22 ± NA	NA	NA	NA	0.22 ± NA	0.22 ± NA	0.22	0.22	0.22	NA
		222234	0	NA	NA	NA ± NA	NA ± NA	NA	NA	NA	NA ± NA	NA ± NA	NA	NA	NA	NA
		231221	20	0.21	0.00	0.21 ± 0.00	0.21 ± 2%	0.02	0.00	0.02	0.21 ± 0.02	0.21 ± 12%	0.20	0.17	0.25	0.08
		231222	3	0.19	0.02	0.19 ± 0.02	0.19 ± 9%	0.03	0.01	0.04	0.19 ± 0.04	0.19 ± 22%	0.21	0.16	0.21	0.05
		231223	4	0.22	0.02	0.22 ± 0.02	0.22 ± 9%	0.04	0.02	0.05	0.22 ± 0.05	0.22 ± 24%	0.22	0.17	0.26	0.09
PTn	Tpcpv2	231221	4	0.10	0.02	0.10 ± 0.02	0.10 ± 17%	0.03	0.01	0.05	0.10 ± 0.05	0.10 ± 47%	0.11	0.06	0.13	0.07
		231223	1	0.19	NA	0.19 ± NA	0.19 ± NA	NA	NA	NA	0.19 ± NA	0.19 ± NA	0.19	0.19	0.19	NA
	Tpcpv1	231221	4	0.10	0.04	0.10 ± 0.04	0.10 ± 39%	0.08	0.03	0.11	0.10 ± 0.11	0.10 ± 111%	0.08	0.03	0.21	0.18
	Tpbt4	221221	1	0.16	NA	0.16 ± NA	0.16 ± NA	NA	NA	NA	0.16 ± NA	0.16 ± NA	0.16	0.16	0.16	NA
		221231	1	0.28	NA	0.28 ± NA	0.28 ± NA	NA	NA	NA	0.28 ± NA	0.28 ± NA	0.28	0.28	0.28	NA
		231221	1	0.17	NA	0.17 ± NA	0.17 ± NA	NA	NA	NA	0.17 ± NA	0.17 ± NA	0.17	0.17	0.17	NA
	Tpy	231221	5	0.16	0.00	0.16 ± 0.00	0.16 ± 3%	0.01	0.00	0.01	0.16 ± 0.01	0.16 ± 8%	0.15	0.15	0.17	0.02
	Tpbt3	221221	2	0.17	0.05	0.17 ± 0.05	0.17 ± 27%	0.06	0.05	0.11	0.17 ± 0.11	0.17 ± 66%	0.17	0.12	0.21	0.09
		231221	1	0.28	NA	0.28 ± NA	0.28 ± NA	NA	NA	NA	0.28 ± NA	0.28 ± NA	0.28	0.28	0.28	NA
		231222	0	NA	NA	NA ± NA	NA ± NA	NA	NA	NA	NA ± NA	NA ± NA	NA	NA	NA	NA
	Tpp	221221	2	0.29	0.06	0.29 ± 0.06	0.29 ± 19%	0.08	0.06	0.13	0.29 ± 0.13	0.29 ± 47%	0.29	0.23	0.34	0.11
		231221	9	0.26	0.03	0.26 ± 0.03	0.26 ± 12%	0.09	0.02	0.12	0.26 ± 0.12	0.26 ± 46%	0.26	0.09	0.39	0.30
		231223	0	NA	NA	NA ± NA	NA ± NA	NA	NA	NA	NA ± NA	NA ± NA	NA	NA	NA	NA
	Tpbt2	221221	3	0.25	0.02	0.25 ± 0.02	0.25 ± 8%	0.03	0.02	0.05	0.25 ± 0.05	0.25 ± 21%	0.23	0.23	0.29	0.06
		231221	6	0.21	0.04	0.21 ± 0.04	0.21 ± 20%	0.10	0.03	0.13	0.21 ± 0.13	0.21 ± 65%	0.17	0.13	0.40	0.27
	Tptrv3	231221	2	0.23	0.08	0.23 ± 0.08	0.23 ± 33%	0.11	0.08	0.18	0.23 ± 0.18	0.23 ± 80%	0.23	0.15	0.30	0.15

Table B-1. Summary of Intact rock Mechanical Properties Data - Compressive Strength and All Static Elastic Properties

Thermo-Mechanical Unit	Litho-stratigraphic Unit	Testing Group Code	Count	Mean	St. Error (SE)	Mean ± 1 SE	Mean ± 1 SE (%)	Standard Deviation (SD)	Uncertainty of the SD	SD+Uncertainty of SD (SD*)	Mean± 1 SD*	Mean± 1 SD* (%)	Median	Minimum	Maximum	Range
TSw1	Tptrn	131221	10	0.20	0.02	0.20 ± 0.02	0.20 ± 8%	0.05	0.01	0.06	0.20 ± 0.06	0.20 ± 32%	0.19	0.13	0.27	0.14
		131222	12	0.21	0.02	0.21 ± 0.02	0.21 ± 11%	0.08	0.02	0.10	0.21 ± 0.10	0.21 ± 46%	0.21	0.13	0.45	0.32
		131223	11	0.22	0.02	0.22 ± 0.02	0.22 ± 8%	0.06	0.01	0.08	0.22 ± 0.08	0.22 ± 34%	0.20	0.15	0.34	0.19
		221221	4	0.25	0.02	0.25 ± 0.02	0.25 ± 9%	0.04	0.02	0.06	0.25 ± 0.06	0.25 ± 25%	0.24	0.21	0.30	0.09
		231221	53	0.25	0.01	0.25 ± 0.01	0.25 ± 3%	0.06	0.01	0.07	0.25 ± 0.07	0.25 ± 27%	0.24	0.14	0.43	0.29
		231222	8	0.20	0.01	0.20 ± 0.01	0.20 ± 6%	0.03	0.01	0.04	0.20 ± 0.04	0.20 ± 20%	0.21	0.14	0.24	0.10
		231223	8	0.20	0.03	0.20 ± 0.03	0.20 ± 15%	0.08	0.02	0.11	0.20 ± 0.11	0.20 ± 54%	0.21	0.02	0.33	0.31
	Tptrl	231221	2	0.30	0.01	0.30 ± 0.01	0.30 ± 5%	0.02	0.01	0.04	0.30 ± 0.04	0.30 ± 12%	0.30	0.28	0.31	0.03
		231222	1	0.28	NA	0.28 ± NA	0.28 ± NA	NA	NA	NA	0.28 ± NA	0.28 ± NA	0.28	0.28	0.28	NA
	Tptf	131211	2	0.26	0.00	0.26 ± 0.00	0.26 ± 0%	0.00	0.00	0.00	0.26 ± 0.00	0.26 ± 0%	0.26	0.26	0.26	0.00
		131221	4	0.24	0.02	0.24 ± 0.02	0.24 ± 10%	0.05	0.02	0.07	0.24 ± 0.07	0.24 ± 29%	0.24	0.19	0.30	0.11
		231221	1	0.34	NA	0.34 ± NA	0.34 ± NA	NA	NA	NA	0.34 ± NA	0.34 ± NA	0.34	0.34	0.34	NA
	Tptpul	221221	0	NA	NA	NA ± NA	NA ± NA	NA	NA	NA	NA ± NA	NA ± NA	NA	NA	NA	NA
		231221	8	0.25	0.05	0.25 ± 0.05	0.25 ± 18%	0.13	0.03	0.16	0.25 ± 0.16	0.25 ± 65%	0.22	0.09	0.46	0.37
		231222	2	0.31	0.12	0.31 ± 0.12	0.31 ± 38%	0.16	0.12	0.28	0.31 ± 0.28	0.31 ± 91%	0.31	0.19	0.42	0.23
		231223	1	0.11	NA	0.11 ± NA	0.11 ± NA	NA	NA	NA	0.11 ± NA	0.11 ± NA	0.11	0.11	0.11	NA
		312111	0	NA	NA	NA ± NA	NA ± NA	NA	NA	NA	NA ± NA	NA ± NA	NA	NA	NA	NA
		312221	0	NA	NA	NA ± NA	NA ± NA	NA	NA	NA	NA ± NA	NA ± NA	NA	NA	NA	NA
		321111	1	0.21	NA	0.21 ± NA	0.21 ± NA	NA	NA	NA	0.21 ± NA	0.21 ± NA	0.21	0.21	0.21	0.00
		321211	4	0.26	0.07	0.26 ± 0.07	0.26 ± 26%	0.13	0.05	0.19	0.26 ± 0.19	0.26 ± 74%	0.25	0.14	0.39	0.25
		321221	0	NA	NA	NA ± NA	NA ± NA	NA	NA	NA	NA ± NA	NA ± NA	NA	NA	NA	NA
		331211	3	0.17	0.07	0.17 ± 0.07	0.17 ± 41%	0.12	0.06	0.19	0.17 ± 0.19	0.17 ± 108%	0.24	0.03	0.25	0.22
		331221	10	0.16	0.01	0.16 ± 0.01	0.16 ± 6%	0.03	0.01	0.04	0.16 ± 0.04	0.16 ± 24%	0.14	0.13	0.21	0.08
TSw2	Tptpmn	111321	0	NA	NA	NA ± NA	NA ± NA	NA	NA	NA	NA ± NA	NA ± NA	NA	NA	NA	NA
		131211	2	0.16	0.05	0.16 ± 0.05	0.16 ± 29%	0.06	0.05	0.11	0.16 ± 0.11	0.16 ± 70%	0.16	0.11	0.20	0.09
		131221	30	0.21	0.01	0.21 ± 0.01	0.21 ± 3%	0.03	0.00	0.04	0.21 ± 0.04	0.21 ± 18%	0.21	0.14	0.29	0.15
		131222	6	0.21	0.02	0.21 ± 0.02	0.21 ± 9%	0.05	0.02	0.06	0.21 ± 0.06	0.21 ± 30%	0.21	0.16	0.30	0.14
		131223	6	0.23	0.01	0.23 ± 0.01	0.23 ± 4%	0.02	0.01	0.03	0.23 ± 0.03	0.23 ± 14%	0.23	0.19	0.25	0.06
		131231	3	0.27	0.01	0.27 ± 0.01	0.27 ± 4%	0.02	0.01	0.03	0.27 ± 0.03	0.27 ± 11%	0.28	0.25	0.29	0.04
		211211	4	0.17	0.02	0.17 ± 0.02	0.17 ± 10%	0.03	0.01	0.05	0.17 ± 0.05	0.17 ± 29%	0.18	0.12	0.20	0.08
		211221	4	0.23	0.03	0.23 ± 0.03	0.23 ± 14%	0.07	0.03	0.09	0.23 ± 0.09	0.23 ± 41%	0.21	0.18	0.32	0.14
		211222	3	0.19	0.01	0.19 ± 0.01	0.19 ± 6%	0.02	0.01	0.03	0.19 ± 0.03	0.19 ± 16%	0.20	0.17	0.21	0.04
		211223	3	0.20	0.02	0.20 ± 0.02	0.20 ± 9%	0.03	0.02	0.05	0.20 ± 0.05	0.20 ± 24%	0.19	0.18	0.24	0.06
		212211	9	0.12	0.03	0.12 ± 0.03	0.12 ± 25%	0.09	0.02	0.11	0.12 ± 0.11	0.12 ± 93%	0.10	0.04	0.33	0.29
		212221	2	0.14	0.02	0.14 ± 0.02	0.14 ± 11%	0.02	0.02	0.04	0.14 ± 0.04	0.14 ± 27%	0.14	0.12	0.15	0.03
		212223	3	0.14	0.01	0.14 ± 0.01	0.14 ± 6%	0.02	0.01	0.02	0.14 ± 0.02	0.14 ± 16%	0.14	0.13	0.16	0.03
		212231	2	0.26	0.11	0.26 ± 0.11	0.26 ± 42%	0.16	0.11	0.27	0.26 ± 0.27	0.26 ± 102%	0.26	0.15	0.37	0.22
		221221	16	0.20	0.01	0.20 ± 0.01	0.20 ± 5%	0.04	0.01	0.05	0.20 ± 0.05	0.20 ± 23%	0.19	0.17	0.34	0.17
		221231	1	0.22	NA	0.22 ± NA	0.22 ± NA	NA	NA	NA	0.22 ± NA	0.22 ± NA	0.22	0.22	0.22	NA
		221321	36	0.18	0.01	0.18 ± 0.01	0.18 ± 4%	0.04	0.01	0.05	0.18 ± 0.05	0.18 ± 28%	0.17	0.12	0.39	0.27
		222234	1	0.15	NA	0.15 ± NA	0.15 ± NA	NA	NA	NA	0.15 ± NA	0.15 ± NA	0.15	0.15	0.15	NA
		231211	9	0.15	0.02	0.15 ± 0.02	0.15 ± 15%	0.07	0.02	0.08	0.15 ± 0.08	0.15 ± 56%	0.16	0.01	0.23	0.22
		231221	41	0.19	0.01	0.19 ± 0.01	0.19 ± 3%	0.04	0.00	0.04	0.19 ± 0.04	0.19 ± 22%	0.20	0.07	0.30	0.23
		231222	5	0.21	0.00	0.21 ± 0.00	0.21 ± 1%	0.01	0.00	0.01	0.21 ± 0.01	0.21 ± 4%	0.21	0.20	0.21	0.01
		231223	13	0.19	0.02	0.19 ± 0.02	0.19 ± 9%	0.06	0.01	0.07	0.19 ± 0.07	0.19 ± 38%	0.19	0.11	0.33	0.22
		231224	5	0.18	0.01	0.18 ± 0.01	0.18 ± 7%	0.03	0.01	0.04	0.18 ± 0.04	0.18 ± 20%	0.20	0.15	0.21	0.06
		231231	4	0.20	0.01	0.20 ± 0.01	0.20 ± 6%	0.02	0.01	0.03	0.20 ± 0.03	0.20 ± 17%	0.19	0.18	0.23	0.05
		232211	11	0.20	0.01	0.20 ± 0.01	0.20 ± 7%	0.05	0.01	0.06	0.20 ± 0.06	0.20 ± 27%	0.20	0.15	0.30	0.15
		232212	6	0.21	0.02	0.21 ± 0.02	0.21 ± 8%	0.04	0.01	0.05	0.21 ± 0.05	0.21 ± 25%	0.22	0.15	0.26	0.11
		232213	5	0.20	0.01	0.20 ± 0.01	0.20 ± 5%	0.02	0.01	0.03	0.20 ± 0.03	0.20 ± 16%	0.20	0.17	0.22	0.05
		232221	0	NA	NA	NA ± NA	NA ± NA	NA	NA	NA	NA ± NA	NA ± NA	NA	NA	NA	NA
		232222	0	NA	NA	NA ± NA	NA ± NA	NA	NA	NA	NA ± NA	NA ± NA	NA	NA	NA	NA
		321221	1	NA	NA	NA ± NA	NA ± NA	NA	NA	NA	NA ± NA	NA ± NA	NA	NA	NA	NA
		331221	20	0.22	0.01	0.22 ± 0.01	0.22 ± 3%	0.03	0.00	0.03	0.22 ± 0.03	0.22 ± 14%	0.22	0.17	0.27	0.10

Table B-1. Summary of Intact rock Mechanical Properties Data - Compressive Strength and All Static Elastic Properties

Thermo-Mechanical Unit	Litho-stratigraphic Unit	Testing Group Code	Count	Mean	St. Error (SE)	Mean ± 1 SE	Mean ± 1 SE (%)	Standard Deviation (SD)	Uncertainty of the SD	SD+Uncertainty of SD (SD*)	Mean± 1 SD*	Mean± 1 SD* (%)	Median	Minimum	Maximum	Range
TSw2	Tptpll	121221	16	0.17	0.01	0.17 ± 0.01	0.17 ± 3%	0.02	0.00	0.02	0.17 ± 0.02	0.17 ± 14%	0.17	0.12	0.20	0.09
		131211	2	0.16	0.05	0.16 ± 0.05	0.16 ± 29%	0.06	0.05	0.11	0.16 ± 0.11	0.16 ± 70%	0.16	0.11	0.20	0.09
		131221	24	0.21	0.01	0.21 ± 0.01	0.21 ± 6%	0.06	0.01	0.07	0.21 ± 0.07	0.21 ± 35%	0.19	0.11	0.36	0.25
		131222	3	0.25	0.06	0.25 ± 0.06	0.25 ± 22%	0.10	0.05	0.15	0.25 ± 0.15	0.25 ± 58%	0.30	0.14	0.32	0.18
		131223	3	0.26	0.03	0.26 ± 0.03	0.26 ± 10%	0.05	0.02	0.07	0.26 ± 0.07	0.26 ± 27%	0.28	0.21	0.30	0.09
		211221	7	0.17	0.00	0.17 ± 0.00	0.17 ± 2%	0.01	0.00	0.01	0.17 ± 0.01	0.17 ± 8%	0.17	0.16	0.19	0.03
		212221	0	NA	NA	NA ± NA	NA ± NA	NA	NA	NA	NA ± NA	NA ± NA	NA	NA	NA	NA
		221221	57	0.19	0.00	0.19 ± 0.00	0.19 ± 1%	0.02	0.00	0.02	0.19 ± 0.02	0.19 ± 11%	0.19	0.14	0.23	0.09
		231221	15	0.22	0.02	0.22 ± 0.02	0.22 ± 8%	0.07	0.01	0.08	0.22 ± 0.08	0.22 ± 36%	0.23	0.11	0.40	0.29
		231223	1	0.20	NA	0.20 ± NA	0.20 ± NA	NA	NA	NA	0.20 ± NA	0.20 ± NA	0.20	0.20	0.20	NA
		312111	0	NA	NA	NA ± NA	NA ± NA	NA	NA	NA	NA ± NA	NA ± NA	NA	NA	NA	NA
		312221	4	0.19	0.06	0.19 ± 0.06	0.19 ± 29%	0.11	0.05	0.16	0.19 ± 0.16	0.19 ± 81%	0.16	0.10	0.35	0.25
		321211	3	0.25	0.05	0.25 ± 0.05	0.25 ± 19%	0.08	0.04	0.12	0.25 ± 0.12	0.25 ± 49%	0.20	0.20	0.34	0.14
		321221	24	0.19	0.01	0.19 ± 0.01	0.19 ± 4%	0.04	0.01	0.04	0.19 ± 0.04	0.19 ± 22%	0.19	0.10	0.32	0.22
		331211	0	NA	NA	NA ± NA	NA ± NA	NA	NA	NA	NA ± NA	NA ± NA	NA	NA	NA	NA
		331221	0	NA	NA	NA ± NA	NA ± NA	NA	NA	NA	NA ± NA	NA ± NA	NA	NA	NA	NA
		421221	0	NA	NA	NA ± NA	NA ± NA	NA	NA	NA	NA ± NA	NA ± NA	NA	NA	NA	NA
	Tptpln	131211	3	0.24	0.02	0.24 ± 0.02	0.24 ± 7%	0.03	0.02	0.05	0.24 ± 0.05	0.24 ± 19%	0.25	0.21	0.27	0.06
		131221	10	0.22	0.01	0.22 ± 0.01	0.22 ± 5%	0.04	0.01	0.04	0.22 ± 0.04	0.22 ± 20%	0.22	0.18	0.30	0.12
		131231	2	0.28	0.03	0.28 ± 0.03	0.28 ± 11%	0.04	0.03	0.07	0.28 ± 0.07	0.28 ± 26%	0.28	0.25	0.31	0.06
		221221	2	0.22	0.01	0.22 ± 0.01	0.22 ± 7%	0.02	0.01	0.04	0.22 ± 0.04	0.22 ± 17%	0.22	0.20	0.23	0.03
		221231	1	0.30	NA	0.30 ± NA	0.30 ± NA	NA	NA	NA	0.30 ± NA	0.30 ± NA	0.30	0.30	0.30	NA
		221233	1	0.23	NA	0.23 ± NA	0.23 ± NA	NA	NA	NA	0.23 ± NA	0.23 ± NA	0.23	0.23	0.23	NA
		221234	1	0.21	NA	0.21 ± NA	0.21 ± NA	NA	NA	NA	0.21 ± NA	0.21 ± NA	0.21	0.21	0.21	NA
		231221	10	0.22	0.01	0.22 ± 0.01	0.22 ± 6%	0.04	0.01	0.05	0.22 ± 0.05	0.22 ± 22%	0.21	0.14	0.28	0.14
		231222	3	0.24	0.02	0.24 ± 0.02	0.24 ± 8%	0.03	0.02	0.05	0.24 ± 0.05	0.24 ± 22%	0.22	0.22	0.28	0.06
		231223	3	0.23	0.01	0.23 ± 0.01	0.23 ± 6%	0.03	0.01	0.04	0.23 ± 0.04	0.23 ± 16%	0.23	0.21	0.26	0.05
		232213	1	0.12	NA	0.12 ± NA	0.12 ± NA	NA	NA	NA	0.12 ± NA	0.12 ± NA	0.12	0.12	0.12	NA
TSw3	Tptpv3	131223	0	NA	NA	NA ± NA	NA ± NA	NA	NA	NA	NA ± NA	NA ± NA	NA	NA	NA	NA
		221221	1	0.18	NA	0.18 ± NA	0.18 ± NA	NA	NA	NA	0.18 ± NA	0.18 ± NA	0.18	0.18	0.18	NA
		231221	1	0.39	NA	0.39 ± NA	0.39 ± NA	NA	NA	NA	0.39 ± NA	0.39 ± NA	0.39	0.39	0.39	NA
		231222	1	0.17	NA	0.17 ± NA	0.17 ± NA	NA	NA	NA	0.17 ± NA	0.17 ± NA	0.17	0.17	0.17	NA
		231223	1	0.17	NA	0.17 ± NA	0.17 ± NA	NA	NA	NA	0.17 ± NA	0.17 ± NA	0.17	0.17	0.17	NA
CHn1	Tptpv2	131221	2	0.20	0.01	0.20 ± 0.01	0.20 ± 8%	0.02	0.01	0.04	0.20 ± 0.04	0.20 ± 19%	0.20	0.18	0.21	0.03
		221221	1	0.22	NA	0.22 ± NA	0.22 ± NA	NA	NA	NA	0.22 ± NA	0.22 ± NA	0.22	0.22	0.22	NA
	Tptpv1	131211	2	0.17	0.00	0.17 ± 0.00	0.17 ± 0%	0.00	0.00	0.00	0.17 ± 0.00	0.17 ± 0%	0.17	0.17	0.17	0.00
		131221	5	0.18	0.01	0.18 ± 0.01	0.18 ± 6%	0.03	0.01	0.03	0.18 ± 0.03	0.18 ± 19%	0.18	0.14	0.21	0.07
		131222	2	0.21	0.00	0.21 ± 0.00	0.21 ± 2%	0.01	0.00	0.01	0.21 ± 0.01	0.21 ± 6%	0.21	0.20	0.21	0.01
		131223	2	0.30	0.00	0.30 ± 0.00	0.30 ± 0%	0.00	0.00	0.00	0.30 ± 0.00	0.30 ± 0%	0.30	0.30	0.30	0.00
		131231	3	0.18	0.04	0.18 ± 0.04	0.18 ± 23%	0.07	0.04	0.11	0.18 ± 0.11	0.18 ± 60%	0.16	0.12	0.26	0.14
	Tpbt1	131211	2	0.11	0.00	0.11 ± 0.00	0.11 ± 5%	0.01	0.00	0.01	0.11 ± 0.01	0.11 ± 11%	0.11	0.10	0.11	0.01
		131221	4	0.20	0.03	0.20 ± 0.03	0.20 ± 17%	0.07	0.03	0.09	0.20 ± 0.09	0.20 ± 47%	0.23	0.10	0.24	0.14
		231221	1	0.11	NA	0.11 ± NA	0.11 ± NA	NA	NA	NA	0.11 ± NA	0.11 ± NA	0.11	0.11	0.11	NA
	Tac	121221	2	0.30	0.01	0.30 ± 0.01	0.30 ± 3%	0.01	0.01	0.02	0.30 ± 0.02	0.30 ± 8%	0.30	0.29	0.31	0.02
		121223	2	0.28	0.00	0.28 ± 0.00	0.28 ± 2%	0.01	0.00	0.01	0.28 ± 0.01	0.28 ± 4%	0.28	0.27	0.28	0.01
		131211	2	0.22	0.01	0.22 ± 0.01	0.22 ± 2%	0.01	0.01	0.01	0.22 ± 0.01	0.22 ± 6%	0.22	0.21	0.22	0.01
		131221	24	0.16	0.02	0.16 ± 0.02	0.16 ± 11%	0.08	0.01	0.10	0.16 ± 0.10	0.16 ± 61%	0.12	0.07	0.36	0.29
		131223	6	0.31	0.02	0.31 ± 0.02	0.31 ± 7%	0.05	0.02	0.07	0.31 ± 0.07	0.31 ± 21%	0.33	0.22	0.36	0.14
		131224	4	0.26	0.06	0.26 ± 0.06	0.26 ± 25%	0.13	0.05	0.18	0.26 ± 0.18	0.26 ± 70%	0.22	0.17	0.45	0.28
		131231	1	0.33	NA	0.33 ± NA	0.33 ± NA	NA	NA	NA	0.33 ± NA	0.33 ± NA	0.33	0.33	0.33	NA
		221231	2	0.17	0.03	0.17 ± 0.03	0.17 ± 18%	0.04	0.03	0.07	0.17 ± 0.07	0.17 ± 43%	0.17	0.14	0.20	0.06
		221234	3	0.25	0.01	0.25 ± 0.01	0.25 ± 6%	0.03	0.01	0.04	0.25 ± 0.04	0.25 ± 15%	0.25	0.22	0.27	0.05
		231221	2	0.20	0.11	0.20 ± 0.11	0.20 ± 55%	0.16	0.11	0.27	0.20 ± 0.27	0.20 ± 133%	0.20	0.09	0.31	0.22

Table B-1. Summary of Intact rock Mechanical Properties Data - Compressive Strength and All Static Elastic Properties

Thermo-Mechanical Unit	Litho-stratigraphic Unit	Testing Group Code	Count	Mean	St. Error (SE)	Mean ± 1 SE	Mean ± 1 SE (%)	Standard Deviation (SD)	Uncertainty of the SD	SD+Uncertainty of SD (SD*)	Mean± 1 SD*	Mean± 1 SD* (%)	Median	Minimum	Maximum	Range
CHn2	Tacbt	131221	8	0.25	0.03	0.25 ± 0.03	0.25 ± 12%	0.09	0.02	0.11	0.25 ± 0.11	0.25 ± 45%	0.24	0.14	0.37	0.23
CFUn	Tcpm	221234	3	0.22	0.02	0.22 ± 0.02	0.22 ± 8%	0.03	0.01	0.04	0.22 ± 0.04	0.22 ± 20%	0.20	0.20	0.25	0.05
	Tcplc	221231	1	0.30	NA	0.30 ± NA	0.30 ± NA	NA	NA	NA	0.30 ± NA	0.30 ± NA	0.30	0.30	0.30	NA
	Tcplv	221231	1	0.18	NA	0.18 ± NA	0.18 ± NA	NA	NA	NA	0.18 ± NA	0.18 ± NA	0.18	0.18	0.18	NA
	Tcpbt	131221	7	0.18	0.06	0.18 ± 0.06	0.18 ± 32%	0.16	0.05	0.20	0.18 ± 0.20	0.18 ± 109%	0.11	0.05	0.43	0.38
	Tcbuv	131221	10	0.09	0.01	0.09 ± 0.01	0.09 ± 16%	0.04	0.01	0.05	0.09 ± 0.05	0.09 ± 61%	0.09	0.03	0.18	0.15
	Tcbuc	131221	13	0.13	0.00	0.13 ± 0.00	0.13 ± 4%	0.02	0.00	0.02	0.13 ± 0.02	0.13 ± 15%	0.13	0.11	0.16	0.05
		221234	1	0.19	NA	0.19 ± NA	0.19 ± NA	NA	NA	NA	0.19 ± NA	0.19 ± NA	0.19	0.19	0.19	NA
	Tcbm	112232	0	NA	NA	NA ± NA	NA ± NA	NA	NA	NA	NA ± NA	NA ± NA	NA	NA	NA	NA
		112233	0	NA	NA	NA ± NA	NA ± NA	NA	NA	NA	NA ± NA	NA ± NA	NA	NA	NA	NA
		112234	0	NA	NA	NA ± NA	NA ± NA	NA	NA	NA	NA ± NA	NA ± NA	NA	NA	NA	NA
		131221	10	0.12	0.01	0.12 ± 0.01	0.12 ± 5%	0.02	0.00	0.02	0.12 ± 0.02	0.12 ± 20%	0.12	0.09	0.14	0.05
		132232	0	NA	NA	NA ± NA	NA ± NA	NA	NA	NA	NA ± NA	NA ± NA	NA	NA	NA	NA
		132233	0	NA	NA	NA ± NA	NA ± NA	NA	NA	NA	NA ± NA	NA ± NA	NA	NA	NA	NA
		132234	0	NA	NA	NA ± NA	NA ± NA	NA	NA	NA	NA ± NA	NA ± NA	NA	NA	NA	NA
		221231	1	0.05	NA	0.05 ± NA	0.05 ± NA	NA	NA	NA	0.05 ± NA	0.05 ± NA	0.05	0.05	0.05	NA
		221234	2	0.26	0.03	0.26 ± 0.03	0.26 ± 10%	0.04	0.03	0.06	0.26 ± 0.06	0.26 ± 24%	0.26	0.23	0.28	0.05
	Tcblv	131221	8	0.14	0.01	0.14 ± 0.01	0.14 ± 9%	0.03	0.01	0.04	0.14 ± 0.04	0.14 ± 31%	0.14	0.08	0.19	0.11
	Tcbbt	131221	4	0.13	0.01	0.13 ± 0.01	0.13 ± 9%	0.03	0.01	0.04	0.13 ± 0.04	0.13 ± 27%	0.14	0.10	0.16	0.06
	Tctuv	131221	7	0.13	0.01	0.13 ± 0.01	0.13 ± 8%	0.03	0.01	0.04	0.13 ± 0.04	0.13 ± 27%	0.12	0.11	0.18	0.07
	Tctuc	131221	4	0.27	0.05	0.27 ± 0.05	0.27 ± 18%	0.10	0.04	0.13	0.27 ± 0.13	0.27 ± 50%	0.26	0.17	0.38	0.21
	Tctm	131221	4	0.25	0.01	0.25 ± 0.01	0.25 ± 5%	0.02	0.01	0.03	0.25 ± 0.03	0.25 ± 14%	0.26	0.22	0.27	0.05
	Tctlc	131221	3	0.18	0.06	0.18 ± 0.06	0.18 ± 31%	0.10	0.05	0.14	0.18 ± 0.14	0.18 ± 79%	0.23	0.07	0.24	0.17
	Tctlv	131211	2	0.22	0.08	0.22 ± 0.08	0.22 ± 36%	0.11	0.08	0.19	0.22 ± 0.19	0.22 ± 88%	0.22	0.14	0.30	0.16
		131221	19	0.19	0.02	0.19 ± 0.02	0.19 ± 8%	0.07	0.01	0.08	0.19 ± 0.08	0.19 ± 42%	0.18	0.07	0.31	0.24
		131231	1	0.09	NA	0.09 ± NA	0.09 ± NA	NA	NA	NA	0.09 ± NA	0.09 ± NA	0.09	0.09	0.09	0.00

Source: Appendix A, Table A-1

Notes:
1.Standard error (SE) is computed using following equation:
SE= Mean/SQRT(No. of tests)
2.Uncertainty of the standard deviation is computed using following equation:
Uncertainty = Standard deviation/(SQRT(2*No. of tests-1))
3. SD* stands for standard deviation plus uncertainty of the standard deviation.
4. Explanation of testing group code is presented in Table 6-3 of document.

Table B-2. Summary of Intact Rock Dynamic Elastic Properties Data

Thermo-Mechanical Unit	Litho-stratigraphic Unit	Code	Count	Mean	Standard Deviation (SD)	Mean ± SE	Mean ± SE (%)	Standard Error (SE)	Median	Minimum	Maximum	Range
Dynamic Young's Modulus (GPa)												
TCw	Tpcrn	2212N1	4	20.94	1.92	20.9 ± 1.0	20.9 ± 5%	0.96	21.20	18.62	22.75	4.13
		2213N1	2	18.42	0.69	18.4 ± 0.5	18.4 ± 3%	0.49	18.42	17.93	18.90	0.97
	Tpcpul	2212N1	10	22.05	2.27	22.1 ± 0.7	22.1 ± 3%	0.72	22.10	16.62	25.65	9.03
		2213N1	4	24.32	1.02	24.3 ± 0.5	24.3 ± 2%	0.51	24.13	23.30	25.72	2.42
	Tpcpmn	1213N1	1	35.70	NA	35.7 ± NA	35.7 ± NA	NA	35.70	35.70	35.70	0.00
		2212N1	10	31.65	5.31	31.6 ± 1.7	31.6 ± 5%	1.68	33.62	19.51	37.16	17.65
		2213N1	8	33.40	3.39	33.4 ± 1.2	33.4 ± 4%	1.20	33.07	29.85	39.10	9.25
	Tpcpll	1213N1	4	33.55	11.73	33.6 ± 5.9	33.6 ± 17%	5.87	34.00	22.00	44.20	22.20
		1213N2	5	41.10	7.41	41.1 ± 3.3	41.1 ± 8%	3.31	45.50	32.10	47.30	15.20
	Tpcpln	1213N1	6	42.05	2.68	42.1 ± 1.1	42.1 ± 3%	1.09	43.65	38.50	43.90	5.40
		1213N2	9	43.29	2.95	43.3 ± 1.0	43.3 ± 2%	0.98	44.40	39.30	46.60	7.30
PTn	Tpcpv1	1213N1	1	6.80	NA	6.8 ± NA	6.8 ± NA	NA	6.80	6.80	6.80	0.00
	Tpbt4	1213N1	4	2.96	0.19	3.0 ± 0.1	3.0 ± 3%	0.10	2.96	2.79	3.13	0.34
		1213N2	6	3.27	0.33	3.3 ± 0.1	3.3 ± 4%	0.13	3.25	2.91	3.67	0.76
	Tpy	1213N1	2	5.98	0.03	6.0 ± 0.0	6.0 ± 0%	0.02	5.98	5.96	6.00	0.04
		1213N2	3	6.29	0.08	6.3 ± 0.0	6.3 ± 1%	0.05	6.30	6.21	6.37	0.16
	Tpbt3	1212N1	2	6.35	0.02	6.3 ± 0.0	6.3 ± 0%	0.01	6.35	6.33	6.36	0.03
		1212N2	3	7.98	0.59	8.0 ± 0.3	8.0 ± 4%	0.34	8.12	7.33	8.49	1.16
	Tpbt2	1211N1	2	2.27	0.01	2.3 ± 0.0	2.3 ± 0%	0.01	2.27	2.26	2.28	0.02
		1211N2	3	3.13	0.45	3.1 ± 0.3	3.1 ± 8%	0.26	3.15	2.67	3.56	0.89
		1213N1	2	3.69	0.00	3.7 ± 0.0	3.7 ± 0%	0.00	3.69	3.69	3.69	0.00
		1213N2	3	3.87	0.06	3.9 ± 0.0	3.9 ± 1%	0.03	3.86	3.82	3.93	0.11
TSw1	Tptrn	1212N1	2	24.15	0.07	24.2 ± 0.1	24.2 ± 0%	0.05	24.15	24.10	24.20	0.10
		1212N2	3	28.77	1.56	28.8 ± 0.9	28.8 ± 3%	0.90	29.00	27.10	30.20	3.10
		1213N1	8	21.45	2.85	21.5 ± 1.0	21.5 ± 5%	1.01	21.85	17.30	24.80	7.50
		1213N2	12	24.54	2.22	24.5 ± 0.6	24.5 ± 3%	0.64	24.00	21.00	28.90	7.90
		2213N1	4	11.03	0.62	11.0 ± 0.3	11.0 ± 3%	0.31	10.85	10.50	11.90	1.40
	Tptpul	1211N1	2	27.10	0.14	27.1 ± 0.1	27.1 ± 0%	0.10	27.10	27.00	27.20	0.20
		1211N2	3	28.43	0.55	28.4 ± 0.3	28.4 ± 1%	0.32	28.40	27.90	29.00	1.10
		1212N1	4	37.68	2.03	37.7 ± 1.0	37.7 ± 3%	1.01	37.70	35.60	39.70	4.10
		1212N2	6	39.98	1.70	40.0 ± 0.7	40.0 ± 2%	0.70	40.35	37.20	42.00	4.80
		1213N1	6	25.77	4.96	25.8 ± 2.0	25.8 ± 8%	2.02	24.60	20.80	31.90	11.10
		1213N2	9	28.36	5.93	28.4 ± 2.0	28.4 ± 7%	1.98	25.90	21.90	37.10	15.20
TSw2	Tptpmn	1111N1	2	47.31	4.09	47.3 ± 2.9	47.3 ± 6%	2.89	47.31	44.42	50.20	5.78
		1213N1	12	38.76	2.12	38.8 ± 0.6	38.8 ± 2%	0.61	38.85	35.80	42.40	6.60
		1213N2	6	42.07	1.79	42.1 ± 0.7	42.1 ± 2%	0.73	42.00	40.10	44.10	4.00
		1312N1	30	39.35	1.55	39.4 ± 0.3	39.4 ± 1%	0.28	39.15	36.20	42.60	6.40
		1313N1	8	38.14	2.25	38.1 ± 0.8	38.1 ± 2%	0.80	38.20	35.70	40.60	4.90
		2112N1	5	42.86	1.47	42.9 ± 0.7	42.9 ± 2%	0.66	43.21	40.83	44.25	3.42
		2213N1	5	38.34	0.11	38.3 ± 0.1	38.3 ± 0%	0.05	38.30	38.20	38.50	0.30
		2312N1	6	42.89	2.54	42.9 ± 1.0	42.9 ± 2%	1.04	43.62	38.52	45.34	6.82
		2313N1	5	36.14	0.11	36.1 ± 0.1	36.1 ± 0%	0.05	36.10	36.00	36.30	0.30
	Tptpll	1211N1	2	33.60	0.00	33.6 ± 0.0	33.6 ± 0%	0.00	33.60	33.60	33.60	0.00
		1211N2	3	35.63	0.70	35.6 ± 0.4	35.6 ± 1%	0.41	35.70	34.90	36.30	1.40
		1212N1	2	34.50	0.14	34.5 ± 0.1	34.5 ± 0%	0.10	34.50	34.40	34.60	0.20
		1212N2	3	37.53	1.12	37.5 ± 0.6	37.5 ± 2%	0.65	37.80	36.30	38.50	2.20
		1213N1	6	33.03	3.30	33.0 ± 1.3	33.0 ± 4%	1.35	34.75	28.70	35.70	7.00
		1213N2	9	34.66	3.87	34.7 ± 1.3	34.7 ± 4%	1.29	36.90	29.10	38.00	8.90
	Tptpln	1213N1	8	41.08	0.84	41.1 ± 0.3	41.1 ± 1%	0.30	41.00	39.90	42.20	2.30
		1213N2	12	42.02	0.76	42.0 ± 0.2	42.0 ± 1%	0.22	42.00	40.80	43.30	2.50
TSw3	Tptpv3	1212N1	2	53.60	0.42	53.6 ± 0.3	53.6 ± 1%	0.30	53.60	53.30	53.90	0.60
		1212N2	3	57.83	0.31	57.8 ± 0.2	57.8 ± 0%	0.18	57.90	57.50	58.10	0.60
CHn	Tptpv1	1211N1	2	18.95	0.07	19.0 ± 0.0	19.0 ± 0%	0.05	18.95	18.90	19.00	0.10
		1211N2	3	19.72	0.60	19.7 ± 0.3	19.7 ± 2%	0.35	20.30	19.60	20.80	1.20
	Tac	1211N1	2	14.55	0.07	14.6 ± 0.0	14.6 ± 0%	0.05	14.55	14.50	14.60	0.10
		1211N2	3	18.27	1.62	18.3 ± 0.9	18.3 ± 5%	0.93	18.00	16.80	20.00	3.20
		1212N1	4	14.78	0.33	14.8 ± 0.2	14.8 ± 1%	0.17	14.80	14.40	15.10	0.70
		1212N2	6	16.50	1.07	16.5 ± 0.4	16.5 ± 3%	0.44	16.55	15.10	18.00	2.90
		1213N1	8	14.19	3.57	14.2 ± 1.3	14.2 ± 9%	1.26	13.10	11.20	19.40	8.20
		1213N2	12	15.59	3.34	15.6 ± 1.0	15.6 ± 6%	0.96	14.80	12.30	20.90	8.60
		2213N1	3	15.80	0.00	15.8 ± 0.0	15.8 ± 0%	0.00	15.80	15.80	15.80	0.00
	Tacbt	1213N1	2	18.90	0.28	18.9 ± 0.2	18.9 ± 1%	0.20	18.90	18.70	19.10	0.40
		1213N2	3	20.40	1.18	20.4 ± 0.7	20.4 ± 3%	0.68	20.70	19.10	21.40	2.30

Table B-2. Summary of Intact Rock Dynamic Elastic Properties Data

Thermo-Mechanical Unit	Litho-stratigraphic Unit	Code	Count	Mean	Standard Deviation (SD)	Mean ± SE	Mean ± SE (%)	Standard Error (SE)	Median	Minimum	Maximum	Range
Dynamic Poisson's Ratio												
TCw	Tpcrn	2212N1	4	0.34	0.02	0.34 ± 0.01	0.34 ± 3%	0.01	0.34	0.32	0.36	0.04
		2213N1	2	0.35	0.00	0.35 ± 0.00	0.35 ± 0%	0.00	0.35	0.35	0.35	0.00
	Tpcpul	2212N1	10	0.33	0.03	0.33 ± 0.01	0.33 ± 3%	0.01	0.34	0.30	0.38	0.08
		2213N1	4	0.28	0.01	0.28 ± 0.01	0.28 ± 2%	0.01	0.28	0.27	0.30	0.03
	Tpcpmn	1213N1	0	NA	NA	NA ± NA	NA ± NA	NA	NA	0.00	0.00	0.00
		2212N1	10	0.30	0.03	0.30 ± 0.01	0.30 ± 3%	0.01	0.30	0.27	0.35	0.08
		2213N1	4	0.27	0.02	0.27 ± 0.01	0.27 ± 4%	0.01	0.27	0.24	0.28	0.04
	Tpcpll	1213N1	2	0.06	0.02	0.06 ± 0.01	0.06 ± 18%	0.01	0.06	0.05	0.07	0.02
		1213N2	5	0.12	0.03	0.12 ± 0.01	0.12 ± 11%	0.01	0.11	0.08	0.16	0.08
	Tpcpln	1213N1	6	0.14	0.01	0.14 ± 0.00	0.14 ± 3%	0.00	0.13	0.13	0.15	0.03
		1213N2	9	0.15	0.02	0.15 ± 0.01	0.15 ± 4%	0.01	0.15	0.12	0.17	0.05
PTn	Tpcpv1	1213N1	0	NA	NA	NA ± NA	NA ± NA	NA	NA	NA	NA	NA
	Tpbt4	1213N1	4	0.09	0.07	0.09 ± 0.04	0.09 ± 43%	0.04	0.09	0.02	0.15	0.13
		1213N2	6	0.19	0.04	0.19 ± 0.02	0.19 ± 10%	0.02	0.19	0.12	0.24	0.12
	Tpy	1213N1	2	0.15	0.00	0.15 ± 0.00	0.15 ± 0%	0.00	0.15	0.15	0.15	0.00
		1213N2	3	0.20	0.01	0.20 ± 0.00	0.20 ± 2%	0.00	0.20	0.19	0.20	0.02
	Tpbt3	1212N1	2	0.18	0.00	0.18 ± 0.00	0.18 ± 2%	0.00	0.18	0.18	0.19	0.01
		1212N2	3	0.22	0.02	0.22 ± 0.01	0.22 ± 6%	0.01	0.24	0.20	0.24	0.04
	Tpbt2	1211N1	2	0.09	0.00	0.09 ± 0.00	0.09 ± 2%	0.00	0.09	0.09	0.09	0.00
		1211N2	3	0.23	0.02	0.23 ± 0.01	0.23 ± 5%	0.01	0.23	0.21	0.25	0.04
		1213N1	2	0.30	0.00	0.30 ± 0.00	0.30 ± 0%	0.00	0.30	0.30	0.30	0.00
		1213N2	3	0.36	0.02	0.36 ± 0.01	0.36 ± 3%	0.01	0.36	0.35	0.38	0.03
TSw1	Tptrn	1212N1	2	0.14	0.00	0.14 ± 0.00	0.14 ± 2%	0.00	0.14	0.14	0.14	0.01
		1212N2	3	0.19	0.01	0.19 ± 0.00	0.19 ± 2%	0.00	0.19	0.18	0.19	0.01
		1213N1	8	0.18	0.03	0.18 ± 0.01	0.18 ± 7%	0.01	0.19	0.12	0.21	0.09
		1213N2	12	0.18	0.03	0.18 ± 0.01	0.18 ± 5%	0.01	0.20	0.12	0.22	0.10
		2213N1	0	NA	NA	NA ± NA	NA ± NA	NA	NA	NA	NA	NA
	Tptpul	1211N1	2	0.10	0.01	0.10 ± 0.01	0.10 ± 7%	0.01	0.10	0.09	0.11	0.01
		1211N2	3	0.13	0.02	0.13 ± 0.01	0.13 ± 9%	0.01	0.14	0.11	0.14	0.04
		1212N1	4	0.04	0.04	0.04 ± 0.02	0.04 ± 49%	0.02	0.04	0.00	0.09	0.09
		1212N2	3	0.09	0.02	0.09 ± 0.01	0.09 ± 15%	0.01	0.10	0.06	0.10	0.04
		1213N1	6	0.16	0.05	0.16 ± 0.02	0.16 ± 12%	0.02	0.18	0.10	0.20	0.10
		1213N2	9	0.15	0.05	0.15 ± 0.02	0.15 ± 10%	0.02	0.18	0.07	0.19	0.12
TSw2	Tptpmn	1111N1	3	0.22	0.02	0.22 ± 0.01	0.22 ± 4%	0.01	0.21	0.21	0.24	0.03
		1213N1	4	0.12	0.01	0.12 ± 0.00	0.12 ± 3%	0.00	0.13	0.11	0.13	0.02
		1213N2	6	0.14	0.01	0.14 ± 0.00	0.14 ± 2%	0.00	0.15	0.13	0.15	0.02
		1312N1	30	0.22	0.02	0.22 ± 0.00	0.22 ± 2%	0.00	0.22	0.18	0.25	0.07
		1313N1	0	NA	NA	NA ± NA	NA ± NA	NA	NA	NA	NA	NA
		2112N1	5	0.21	0.01	0.21 ± 0.00	0.21 ± 2%	0.00	0.21	0.20	0.22	0.02
		2213N1	0	NA	NA	NA ± NA	NA ± NA	NA	NA	NA	NA	NA
		2312N1	6	0.24	0.02	0.24 ± 0.01	0.24 ± 3%	0.01	0.23	0.23	0.28	0.05
		2313N1	0	NA	NA	NA ± NA	NA ± NA	NA	NA	NA	NA	NA
	Tptpll	1211N1	2	0.04	0.01	0.04 ± 0.00	0.04 ± 12%	0.00	0.04	0.03	0.04	0.01
		1211N2	3	0.06	0.04	0.06 ± 0.02	0.06 ± 38%	0.02	0.07	0.01	0.08	0.07
		1212N1	2	0.02	0.00	0.02 ± 0.00	0.02 ± 6%	0.00	0.02	0.02	0.02	0.00
		1212N2	3	0.09	0.03	0.09 ± 0.02	0.09 ± 19%	0.02	0.10	0.06	0.11	0.06
		1213N1	6	0.15	0.04	0.15 ± 0.02	0.15 ± 11%	0.02	0.13	0.11	0.20	0.09
		1213N2	9	0.15	0.03	0.15 ± 0.01	0.15 ± 7%	0.01	0.15	0.12	0.20	0.08
	Tptpln	1213N1	8	0.14	0.01	0.14 ± 0.00	0.14 ± 3%	0.00	0.14	0.13	0.16	0.03
		1213N2	12	0.15	0.01	0.15 ± 0.00	0.15 ± 2%	0.00	0.15	0.14	0.17	0.03
TSw3	Tptpv3	1212N1	2	0.19	0.01	0.19 ± 0.01	0.19 ± 4%	0.01	0.19	0.18	0.20	0.01
		1212N2	3	0.15	0.02	0.15 ± 0.01	0.15 ± 6%	0.01	0.16	0.13	0.16	0.03
CHn	Tptpv1	1211N1	2	0.07	0.00	0.07 ± 0.00	0.07 ± 4%	0.00	0.07	0.07	0.07	0.01
		1211N2	3	0.04	0.02	0.04 ± 0.01	0.04 ± 23%	0.01	0.02	0.01	0.04	0.03
	Tac	1211N1	2	0.14	0.01	0.14 ± 0.00	0.14 ± 4%	0.00	0.14	0.13	0.14	0.01
		1211N2	3	0.18	0.01	0.18 ± 0.01	0.18 ± 4%	0.01	0.18	0.17	0.20	0.03
		1212N1	4	0.15	0.04	0.15 ± 0.02	0.15 ± 13%	0.02	0.15	0.11	0.19	0.08
		1212N2	6	0.15	0.02	0.15 ± 0.01	0.15 ± 6%	0.01	0.16	0.12	0.18	0.06
		1213N1	8	0.12	0.03	0.12 ± 0.01	0.12 ± 9%	0.01	0.12	0.09	0.18	0.08
		1213N2	12	0.14	0.03	0.14 ± 0.01	0.14 ± 6%	0.01	0.15	0.07	0.17	0.10
		2213N1	0	NA	NA	NA ± NA	NA ± NA	NA	NA	NA	NA	NA
	Tacbt	1213N1	2	0.06	0.03	0.06 ± 0.02	0.06 ± 32%	0.02	0.06	0.04	0.08	0.04
		1213N2	3	0.11	0.03	0.11 ± 0.02	0.11 ± 14%	0.02	0.11	0.08	0.14	0.05

Source: Appendix A, Table A-2.

Note:
1. Standard error (SE) is computed using following equation:
SE= Mean/SQRT(No. of tests)

Table B-3. Summary of Intact rock Mechanical Properties Data - Indirect Tensile Strength

Thermo-Mechanical Unit	Litho-stratigraphic Unit	Testing Group	No. of Tests	Mean	Standard Error (SE)	Mean ± 1 SE	Mean ± 1 SE (%)	Standard Deviation (SD)	Median	Minimum	Maximum	Range
Tensile Strength (MPa)												
UO	Tmr	231121	3	1.23	0.74	1.2 ± 0.74	1.2 ± 60%	1.27	0.60	0.40	2.70	2.30
	Tpki	231121	6	0.70	0.10	0.7 ± 0.10	0.7 ± 14%	0.24	0.70	0.40	1.00	0.60
TCw	Tpcrn	231121	24	7.14	0.72	7.1 ± 0.72	7.1 ± 10%	3.52	6.99	2.60	13.44	10.84
	Tpcpul	231121	23	9.99	0.35	10.0 ± 0.35	10.0 ± 3%	1.67	10.00	6.23	13.58	7.34
	Tpcpmn	231121	16	14.52	0.97	14.5 ± 0.97	14.5 ± 7%	3.88	15.22	5.30	19.08	13.78
	Tpcpll	231121	3	12.20	2.53	12.2 ± 2.53	12.2 ± 21%	4.39	13.20	7.40	16.00	8.60
	Tpcpln	231121	19	10.89	0.40	10.9 ± 0.40	10.9 ± 4%	1.73	10.90	8.20	13.40	5.20
PTn	Tpcpv2	231121	4	3.18	0.96	3.2 ± 0.96	3.2 ± 30%	1.91	3.20	1.20	5.10	3.90
	Tpcpv1	231121	1	0.50	NA	0.5 ± NA	0.5 ± NA	NA	0.50	0.50	0.50	NA
	Tpy	231121	1	3.00	NA	3.0 ± NA	3.0 ± NA	NA	3.00	3.00	3.00	NA
	Tpbt3	221121	1	0.30	NA	0.3 ± NA	0.3 ± NA	NA	0.30	0.30	0.30	NA
	Tpp	221121	1	0.40	NA	0.4 ± NA	0.4 ± NA	NA	0.40	0.40	0.40	NA
		231121	12	0.16	0.05	0.2 ± 0.05	0.2 ± 32%	0.18	0.10	0.02	0.70	0.68
	Tpbt2	221121	2	0.25	0.05	0.3 ± 0.05	0.3 ± 20%	0.07	0.25	0.20	0.30	0.10
		231121	3	0.33	0.23	0.3 ± 0.23	0.3 ± 70%	0.40	0.10	0.10	0.80	0.70
TSw1	Tptrn	221121	1	8.40	NA	8.4 ± NA	8.4 ± NA	NA	8.40	8.40	8.40	NA
		231121	52	5.43	0.29	5.4 ± 0.29	5.4 ± 5%	2.07	5.00	1.60	10.50	8.90
	Tptrl	231121	7	4.81	0.51	4.8 ± 0.51	4.8 ± 11%	1.36	5.10	3.40	7.30	3.90
	Tptpul	231121	19	5.57	0.71	5.6 ± 0.71	5.6 ± 13%	3.10	4.30	1.90	12.90	11.00
TSw2	Tptpmn	231121	14	10.88	1.07	10.9 ± 1.07	10.9 ± 10%	4.02	12.05	4.30	16.80	12.50
	Tptpll	231121	24	8.33	0.60	8.3 ± 0.60	8.3 ± 7%	2.93	8.25	3.20	14.30	11.10
	Tptpln	231121	13	7.92	0.71	7.9 ± 0.71	7.9 ± 9%	2.55	7.60	4.80	13.70	8.90
TSw3	Tptpv3	231121	3	3.97	0.19	4.0 ± 0.19	4.0 ± 5%	0.32	4.10	3.60	4.20	0.60
Porosity												
UO	Tmr	231121	3	41.20	2.71	41.2 ± 2.71	41.2 ± 7%	4.69	43.50	35.80	44.30	8.50
	Tpki	231121	6	46.98	0.94	47.0 ± 0.94	47.0 ± 2%	2.30	46.35	44.50	50.40	5.90
TCw	Tpcrn	231121	15	26.99	2.66	27.0 ± 2.66	27.0 ± 0.10	10.30	25.20	9.80	44.50	34.70
	Tpcpul	231121	4	15.18	0.56	15.2 ± 0.56	15.2 ± 0.04	1.12	15.30	13.70	16.40	2.70
	Tpcpmn	231121	3	11.60	1.64	11.6 ± 1.64	11.6 ± 0.14	2.85	12.20	8.50	14.10	5.60
	Tpcpll	231121	3	9.47	3.92	9.5 ± 3.92	9.5 ± 41%	6.78	5.60	5.50	17.30	11.80
	Tpcpln	231121	19	8.68	0.61	8.7 ± 0.61	8.7 ± 7%	2.64	7.40	6.40	16.60	10.20
PTn	Tpcpv2	231121	4	33.85	3.04	33.9 ± 3.04	33.9 ± 9%	6.08	33.35	27.90	40.80	12.90
	Tpcpv1	231121	1	41.20	NA	41.2 ± NA	41.2 ± NA	NA	41.20	41.20	41.20	NA
	Tpy	231121	1	31.30	NA	31.3 ± NA	31.3 ± NA	NA	31.30	31.30	31.30	NA
	Tpbt3	221121	1	55.70	NA	55.7 ± NA	55.7 ± NA	NA	55.70	55.70	55.70	NA
	Tpp	221121	1	55.60	NA	55.6 ± NA	55.6 ± NA	NA	55.60	55.60	55.60	NA
		231121	12	51.88	0.83	51.9 ± 0.83	51.9 ± 2%	2.86	52.25	45.40	55.20	9.80
	Tpbt2	221121	2	52.95	6.45	53.0 ± 6.45	53.0 ± 12%	9.12	52.95	46.50	59.40	12.90
		231121	3	46.10	5.25	46.1 ± 5.25	46.1 ± 11%	9.10	46.10	37.00	55.20	18.20
TSw1	Tptrn	221121	1	10.10	NA	10.1 ± NA	10.1 ± NA	NA	10.10	10.10	10.10	NA
		231121	52	14.81	0.43	14.8 ± 0.43	14.8 ± 3%	3.09	14.70	6.80	22.80	16.00
	Tptrl	231121	7	16.53	1.68	16.5 ± 1.68	16.5 ± 10%	4.44	16.40	10.60	22.20	11.60
	Tptpul	231121	19	16.31	0.73	16.3 ± 0.73	16.3 ± 4%	3.19	15.70	11.30	21.80	10.50
TSw2	Tptpmn	231121	14	11.84	0.79	11.8 ± 0.79	11.8 ± 7%	2.96	10.75	9.00	19.20	10.20
	Tptpll	231121	24	11.99	0.40	12.0 ± 0.40	12.0 ± 3%	1.96	11.90	8.80	16.40	7.60
	Tptpln	231121	13	8.81	0.52	8.8 ± 0.52	8.8 ± 6%	1.89	9.00	3.80	11.20	7.40
TSw3	Tptpv3	231121	3	1.30	0.06	1.3 ± 0.06	1.3 ± 4%	0.10	1.30	1.20	1.40	0.20

Source: Appendix A, Table A-3

Note:
1. Standard error (SE) is computed using following equation:
   SE= Mean/SQRT(No. of tests)

APPENDIX C
SUMMARY OF ALL LABORATORY DATA

Specimen Inventory Number	Tests In Each Lithostratigraphic Unit	GFM 2000 Layer	Testing Group	Max. Depth (ft)	Equivalent Specimen Diameter - D (mm)	Specimen Temperature (deg. C)	Specimen Saturation	Effective Confining Pressure, (MPa), s3'	Effective Axial Stress, s1' (MPa)	Young's Modulus (GPa)	Poisson's Ratio
Group 1	5										
1	1	02_UO_Tmr	231221	2.7	50.8	22	saturated	0	20.30	7.20	0.07
2	2	02_UO_Tmr	231221	42.3	50.8	22	saturated	0	7.00	3.70	0.05
3	3	02_UO_Tmr	231221	46.1	50.8	22	saturated	0	6.50	4.30	0.02
4	4	02_UO_Tmr	231221	86.9	50.8	22	saturated	0	2.40	0.90	0.02
5	5	02_UO_Tmr	231221	87.6	50.8	22	saturated	0	1.80	0.70	0.01
							Average:	0	7.60	3.36	0.03
							Std. Dev.:	0	7.48	2.69	0.03
Group 2	3										
1	1	02_UO_Tmr	231121		51.6	Ambient	Saturated	-2.70	0.0		
2	2	02_UO_Tmr	231121		51.6	Ambient	Saturated	-0.40	0.0		
3	3	02_UO_Tmr	231121		51.6	Ambient	Saturated	-0.60	0.0		
							Average:	-1.23	0.00		
							Std_Dev:	1.27			
Group 1	7										
6	1	03_UO_Tpki	231221	105.6	50.80	22	saturated	0	7.20	4.90	0.14
7	2	03_UO_Tpki	231221	127.0	50.80	22	saturated	0	6.50	3.70	0.20
8	3	03_UO_Tpki	231221	136.1	50.80	22	saturated	0	9.80	5.10	0.15
9	4	03_UO_Tpki	231221	145.3	50.80	22	saturated	0	1.10	0.70	0.48
10	5	03_UO_Tpki	231221	90.0	50.80	22	saturated	0	4.10	3.10	0.05
11	6	03_UO_Tpki	231221	96.0	50.80	22	saturated	0	6.20	4.90	0.17
12	7	03_UO_Tpki	231221	98.4	50.80	22	saturated	0	6.70	4.00	0.12
							Average:	0	5.94	3.77	0.19
							Std. Dev.:	0	2.72	1.54	0.14
Group 2	6										
4	1	03_UO_Tpki	231121		51.6	Ambient	Saturated	-0.50	0.0		
5	2	03_UO_Tpki	231121		51.6	Ambient	Saturated	-0.90	0.0		
6	3	03_UO_Tpki	231121		51.6	Ambient	Saturated	-1.00	0.0		
7	4	03_UO_Tpki	231121		51.6	Ambient	Saturated	-0.80	0.0		
8	5	03_UO_Tpki	231121		51.6	Ambient	Saturated	-0.40	0.0		
9	6	03_UO_Tpki	231121		51.6	Ambient	Saturated	-0.60	0.0		
							Average:	-0.70	0.00		
							Std_Dev:	0.24			
Group 1	18										
13	1	04_TCw_Tpcrn	231221	172.1	50.80	22	saturated	0	110.60	38.20	0.23
14	2	04_TCw_Tpcrn	231221	199.4	50.80	22	saturated	0	17.50	8.90	0.20
15	3	04_TCw_Tpcrn	231221	203.9	50.80	22	saturated	0	31.10	13.80	0.17
16	4	04_TCw_Tpcrn	231221	209.3	50.80	22	saturated	0	22.20	11.50	0.19
17	5	04_TCw_Tpcrn	231221	213.0	50.80	22	saturated	0	23.60	11.40	0.19
18	6	04_TCw_Tpcrn	231221	218.8	50.80	22	saturated	0	25.50	13.80	0.21
19	7	04_TCw_Tpcrn	231221	223.1	50.80	22	saturated	0	19.90	9.70	0.24
20	8	04_TCw_Tpcrn	231221	226.4	50.80	22	saturated	0	24.50	11.50	0.24
21	9	04_TCw_Tpcrn	231221	234.9	50.80	22	saturated	0	10.40	6.50	0.16
22	10	04_TCw_Tpcrn	231221	238.4	50.80	22	saturated	0	20.20	10.30	0.29
23	11	04_TCw_Tpcrn	231221	254.5	50.80	22	saturated	0	53.20	17.50	0.22
24	12	04_TCw_Tpcrn	231221	21.4	50.80	22	saturated	0	18.80		
25	13	04_TCw_Tpcrn	231221	32.1	50.80	22	saturated	0	13.10	9.70	0.21
26	14	04_TCw_Tpcrn	231221	38.9	50.80	22	saturated	0	39.70	17.60	0.20
27	15	04_TCw_Tpcrn	231221	42.6	50.80	22	saturated	0	27.10	12.60	0.15
28	16	04_TCw_Tpcrn	231221	48.0	50.80	22	saturated	0	36.60	15.00	0.19
29	17	04_TCw_Tpcrn	231221	55.7	50.80	22	saturated	0	21.50	16.40	0.17
30	18	04_TCw_Tpcrn	231221	93.8	50.80	22	saturated	0	132.90	33.40	0.22
							Average:	0	36.02	15.16	0.20
							Std. Dev.:	0	32.98	8.39	0.03
Group 2	3										
31	1	04_TCw_Tpcrn	221221	21.8	61.3	22	ambient	0	120.70	24.20	0.18
32	2	04_TCw_Tpcrn	221221	21.8-30.6	61.3	22	ambient	0	115.80	25.71	0.16

Specimen Inventory Number	Tests In Each Lithostratigraphic Unit	GFM 2000 Layer	Testing Group	Max. Depth (ft)	Equivalent Specimen Diameter - D (mm)	Specimen Temperature (deg. C)	Specimen Saturation	Effective Confining Pressure, (MPa), s3'	Effective Axial Stress, s1' (MPa)	Young's Modulus (GPa)	Poisson's Ratio
33	3	04_TCw_Tpcrn	221221	9.5-16.2	61.1	22	ambient	0	64.40	21.58	0.15
							Average:	0	100.30	23.83	0.16
							Std. Dev.:	0	31.19	2.09	0.02
Group 3	24										
10	1	04_TCw_Tpcrn	231121		61.2	Ambient	Saturated	-12.31	0.0		
11	2	04_TCw_Tpcrn	231121		61.2	Ambient	Saturated	-8.50	0.0		
12	3	04_TCw_Tpcrn	231121		61.0	Ambient	Saturated	-9.70	0.0		
13	4	04_TCw_Tpcrn	231121		61.2	Ambient	Saturated	-8.17	0.0		
14	5	04_TCw_Tpcrn	231121		61.0	Ambient	Saturated	-9.78	0.0		
15	6	04_TCw_Tpcrn	231121		61.0	Ambient	Saturated	-8.95	0.0		
16	7	04_TCw_Tpcrn	231121		61.2	Ambient	Saturated	-9.61	0.0		
17	8	04_TCw_Tpcrn	231121		61.2	Ambient	Saturated	-12.42	0.0		
18	9	04_TCw_Tpcrn	231121		61.2	Ambient	Saturated	-13.44	0.0		
19	10	04_TCw_Tpcrn	231121		51.6	Ambient	Saturated	-3.00	0.0		
20	11	04_TCw_Tpcrn	231121		51.6	Ambient	Saturated	-2.60	0.0		
21	12	04_TCw_Tpcrn	231121		51.6	Ambient	Saturated	-3.30	0.0		
22	13	04_TCw_Tpcrn	231121		51.6	Ambient	Saturated	-3.90	0.0		
23	14	04_TCw_Tpcrn	231121		51.6	Ambient	Saturated	-4.00	0.0		
24	15	04_TCw_Tpcrn	231121		51.6	Ambient	Saturated	-10.10	0.0		
25	16	04_TCw_Tpcrn	231121		51.6	Ambient	Saturated	-11.70	0.0		
26	17	04_TCw_Tpcrn	231121		51.6	Ambient	Saturated	-8.70	0.0		
27	18	04_TCw_Tpcrn	231121		51.6	Ambient	Saturated	-3.80	0.0		
28	19	04_TCw_Tpcrn	231121		51.6	Ambient	Saturated	-3.80	0.0		
29	20	04_TCw_Tpcrn	231121		51.6	Ambient	Saturated	-3.80	0.0		
30	21	04_TCw_Tpcrn	231121		51.6	Ambient	Saturated	-5.80	0.0		
31	22	04_TCw_Tpcrn	231121		51.6	Ambient	Saturated	-5.60	0.0		
32	23	04_TCw_Tpcrn	231121		51.6	Ambient	Saturated	-5.60	0.0		
33	24	04_TCw_Tpcrn	231121		51.6	Ambient	Saturated	-2.70	0.0		
							Average:	-7.14	0.00		
							Std_Dev:	3.52			
Group 1	5										
34	1	07_TCw_Tpcpul	231221	123.2	50.80	22	saturated	0	83.40	29.60	0.20
35	2	07_TCw_Tpcpul	231221	142.3	50.80	22	saturated	0	34.30	14.80	0.18
36	3	07_TCw_Tpcpul	231221	154.4	50.80	22	saturated	0	32.50	17.90	0.15
37	4	07_TCw_Tpcpul	231221	187.1	50.80	22	saturated	0	75.00	29.30	0.20
38	5	07_TCw_Tpcpul	231221	195.7	50.80	22	saturated	0	85.50	27.00	0.20
							Average:	0	62.14	23.72	0.19
							Std. Dev.:	0	26.54	6.89	0.02
Group 2	3										
39	1	07_TCw_Tpcpul	221221	105.1-115.1	61.1	22	ambient	0	109.60	30.26	0.17
40	2	07_TCw_Tpcpul	221221	38.0-47.1	61.2	22	ambient	0	66.70	22.61	0.15
41	3	07_TCw_Tpcpul	221221	89.5-97.8	61.2	22	ambient	0	100.00	25.85	0.19
							Average:	0	92.10	26.24	0.17
							Std. Dev.:	0	22.51	3.84	0.02
Group 3	1										
42	1	07_TCw_Tpcpul	221233	80.8-89.5	61.2	22	ambient	13.8	170.30		
							Average:	13.80	170.30		
							Std. Dev.:				
Group 4	1										
43	1	07_TCw_Tpcpul	221234	89.5-97.8	61.1	22	ambient	27.6	227.60		
							Average:	27.60	227.60		
							Std. Dev.:				
Group 5	1										

Specimen Inventory Number	Tests In Each Lithostratigraphic Unit	GFM 2000 Layer	Testing Group	Max. Depth (ft)	Equivalent Specimen Diameter - D (mm)	Specimen Temperature (deg. C)	Specimen Saturation	Effective Confining Pressure, (MPa), s3'	Effective Axial Stress, s1' (MPa)	Young's Modulus (GPa)	Poisson's Ratio
44	1	07_TCw_Tpcpul	221321	89.5-97.8	61.2	22	ambient	0	65.60	23.16	0.15
							Average:	0.00	65.60	23.16	0.15
							Std. Dev.:				
Group 6	1										
45	1	07_TCw_Tpcpul	221334	80.8-89.5	61.2	22	ambient	41.4	253.80		
							Average:	41.40	253.80		
							Std. Dev.:				
Group 7	23										
34	1	07_TCw_Tpcpul	231121		61.2	Ambient	Saturated	-11.52	0.0		
35	2	07_TCw_Tpcpul	231121		61.2	Ambient	Saturated	-8.14	0.0		
36	3	07_TCw_Tpcpul	231121		61.2	Ambient	Saturated	-6.23	0.0		
37	4	07_TCw_Tpcpul	231121		61.2	Ambient	Saturated	-13.58	0.0		
38	5	07_TCw_Tpcpul	231121		61.2	Ambient	Saturated	-7.74	0.0		
39	6	07_TCw_Tpcpul	231121		61.2	Ambient	Saturated	-9.57	0.0		
40	7	07_TCw_Tpcpul	231121		61.2	Ambient	Saturated	-8.82	0.0		
41	8	07_TCw_Tpcpul	231121		61.2	Ambient	Saturated	-8.48	0.0		
42	9	07_TCw_Tpcpul	231121		61.2	Ambient	Saturated	-11.51	0.0		
43	10	07_TCw_Tpcpul	231121		61.2	Ambient	Saturated	-10.00	0.0		
44	11	07_TCw_Tpcpul	231121		61.2	Ambient	Saturated	-9.46	0.0		
45	12	07_TCw_Tpcpul	231121		61.2	Ambient	Saturated	-8.52	0.0		
46	13	07_TCw_Tpcpul	231121		61.2	Ambient	Saturated	-11.10	0.0		
47	14	07_TCw_Tpcpul	231121		61.2	Ambient	Saturated	-10.22	0.0		
48	15	07_TCw_Tpcpul	231121		61.2	Ambient	Saturated	-11.60	0.0		
49	16	07_TCw_Tpcpul	231121		51.6	Ambient	Saturated	-9.10	0.0		
50	17	07_TCw_Tpcpul	231121		51.6	Ambient	Saturated	-8.90	0.0		
51	18	07_TCw_Tpcpul	231121		51.6	Ambient	Saturated	-10.30	0.0		
52	19	07_TCw_Tpcpul	231121		51.6	Ambient	Saturated	-10.20	0.0		
53	20	07_TCw_Tpcpul	231121		61.2	Ambient	Saturated	-9.78	0.0		
54	21	07_TCw_Tpcpul	231121		61.2	Ambient	Saturated	-11.51	0.0		
55	22	07_TCw_Tpcpul	231121		61.2	Ambient	Saturated	-11.30	0.0		
56	23	07_TCw_Tpcpul	231121		61.2	Ambient	Saturated	-12.22	0.0		
							Average:	-9.99	0.00		
							Std_Dev:	1.67			
Group 1	4										
46	1	08_TCw_Tpcpmn	131222	263.3	25.4	22	saturated	5	158.20	27.00	0.29
47	2	08_TCw_Tpcpmn	131222	265.7	25.4	22	saturated	5	295.90	37.40	0.20
48	3	08_TCw_Tpcpmn	131222	265.7	25.4	22	saturated	5	275.10	36.50	0.20
49	4	08_TCw_Tpcpmn	131222	265.7	25.4	22	saturated	5	180.30	39.40	0.25
							Average:	5	227.38	35.08	0.24
							Std. Dev.:	0	68.25	5.52	0.04
Group 2	4										
50	1	08_TCw_Tpcpmn	131223	263.3	25.4	22	saturated	10	291.40	39.30	0.19
51	2	08_TCw_Tpcpmn	131223	265.7	25.4	22	saturated	10	369.00	37.10	0.21
52	3	08_TCw_Tpcpmn	131223	265.7	25.4	22	saturated	10	339.10	37.50	0.20
53	4	08_TCw_Tpcpmn	131223	265.7	25.4	22	saturated	10	309.90	36.80	0.21
							Average:	10	327.35	37.68	0.20
							Std. Dev.:	0	34.01	1.12	0.01
Group 3	3										
54	1	08_TCw_Tpcpmn	221221	123.8-130.1	61.2	22	ambient	0	198.60	38.40	0.18
55	2	08_TCw_Tpcpmn	221221	123.8-130.1	61.2	22	ambient	0	223.40	32.40	0.18
56	3	08_TCw_Tpcpmn	221221	136.8-144.4	61.2	22	ambient	0	274.40		
							Average:	0	232.13	35.40	0.18
							Std. Dev.:	0	38.65	4.24	0.00
Group 4	1										

Specimen Inventory Number	Tests In Each Lithostratigraphic Unit	GFM 2000 Layer	Testing Group	Max. Depth (ft)	Equivalent Specimen Diameter - D (mm)	Specimen Temperature (deg. C)	Specimen Saturation	Effective Confining Pressure, (MPa), s3'	Effective Axial Stress, s1' (MPa)	Young's Modulus (GPa)	Poisson's Ratio
57	1	08_TCw_Tpcpmn	221233	136.8-144.4	61.1	22	ambient	13.8	206.90		
							Average:	13.80	206.90		
							Std. Dev.:				
Group 5	2										
58	1	08_TCw_Tpcpmn	221234	136.8-144.4	61.2	22	ambient	27.6	433.00		
59	2	08_TCw_Tpcpmn	221234	136.8-144.4	61.2	22	ambient	41.4	233.10		
							Average:	34.5	333.05		
							Std. Dev.:	9.758	141.35		
Group 6	1										
60	1	08_TCw_Tpcpmn	221321	123.8-130.1	61.2	22	ambient	0	128.90	28.88	0.17
							Average:	0.00	128.90	28.88	0.17
							Std. Dev.:				
Group 7	8										
61	1	08_TCw_Tpcpmn	231221	208.9	50.80	22	saturated	0	71.90	20.00	0.17
62	2	08_TCw_Tpcpmn	231221	218.0	50.80	22	saturated	0	105.20	36.30	0.20
63	3	08_TCw_Tpcpmn	231221	226.7	50.80	22	saturated	0	108.90	30.10	
64	4	08_TCw_Tpcpmn	231221	256.0	50.80	22	saturated	0	230.90	41.40	0.21
65	5	08_TCw_Tpcpmn	231221	257.6	50.80	22	saturated	0	174.30	38.40	0.19
66	6	08_TCw_Tpcpmn	231221	257.6	50.80	22	saturated	0	192.80	39.50	0.20
67	7	08_TCw_Tpcpmn	231221	263.3	50.80	22	saturated	0	244.00	39.60	0.22
68	8	08_TCw_Tpcpmn	231221	60.5	50.8	22	saturated	0	209.50	41.20	0.21
							Average:	0	167.19	35.81	0.20
							Std. Dev.:	0	64.12	7.35	0.02
Group 8	2										
69	1	08_TCw_Tpcpmn	231222	16.1	50.8	22	saturated	5	389.50	42.90	0.19
70	2	08_TCw_Tpcpmn	231222	80.0	50.8	22	saturated	5	249.00	27.90	0.13
							Average:	5	319.25	35.40	0.16
							Std. Dev.:	0	99.35	10.61	0.04
Group 9	1										
71	1	08_TCw_Tpcpmn	231223	32.0	50.8	22	saturated	10	245.50	27.40	0.12
							Average:	10.00	245.50		
							Std. Dev.:				
Group 10	16										
57	1	08_TCw_Tpcpmn	231121		61.2	Ambient	Saturated	-18.85	0.0		
58	2	08_TCw_Tpcpmn	231121		61.2	Ambient	Saturated	-17.44	0.0		
59	3	08_TCw_Tpcpmn	231121		61.2	Ambient	Saturated	-16.79	0.0		
60	4	08_TCw_Tpcpmn	231121		61.2	Ambient	Saturated	-7.20	0.0		
61	5	08_TCw_Tpcpmn	231121		61.2	Ambient	Saturated	-15.13	0.0		
62	6	08_TCw_Tpcpmn	231121		61.2	Ambient	Saturated	-19.08	0.0		
63	7	08_TCw_Tpcpmn	231121		61.2	Ambient	Saturated	-14.92	0.0		
64	8	08_TCw_Tpcpmn	231121		61.2	Ambient	Saturated	-16.28	0.0		
65	9	08_TCw_Tpcpmn	231121		61.2	Ambient	Saturated	-14.13	0.0		
66	10	08_TCw_Tpcpmn	231121		61.2	Ambient	Saturated	-17.53	0.0		
67	11	08_TCw_Tpcpmn	231121		61.2	Ambient	Saturated	-15.66	0.0		
68	12	08_TCw_Tpcpmn	231121		61.5	Ambient	Saturated	-13.65	0.0		
69	13	08_TCw_Tpcpmn	231121		61.5	Ambient	Saturated	-15.31	0.0		
70	14	08_TCw_Tpcpmn	231121		51.6	Ambient	Saturated	-10.20	0.0		
71	15	08_TCw_Tpcpmn	231121		51.6	Ambient	Saturated	-5.30	0.0		
72	16	08_TCw_Tpcpmn	231121		51.6	Ambient	Saturated	-14.80	0.0		
							Average:	-14.52	0.00		
							Std_Dev:	3.88			
Group 1	4										
75	1	09_TCw_Tpcpll	131221	22.2	25.4	22	saturated	0	315.80	37.20	0.21
76	2	09_TCw_Tpcpll	131221	22.2	25.4	22	saturated	0	284.20	37.40	0.20

Specimen Inventory Number	Tests In Each Lithostratigraphic Unit	GFM 2000 Layer	Testing Group	Max. Depth (ft)	Equivalent Specimen Diameter - D (mm)	Specimen Temperature (deg. C)	Specimen Saturation	Effective Confining Pressure, (MPa), s3'	Effective Axial Stress, s1' (MPa)	Young's Modulus (GPa)	Poisson's Ratio
77	3	09_TCw_Tpcpll	131221	22.2	25.4	22	saturated	0	313.80	36.40	0.22
78	4	09_TCw_Tpcpll	131221	22.2	25.4	22	saturated	0	332.40	36.70	0.22
							Average:	0	311.55	36.93	0.21
							Std. Dev.:	0	20.05	0.46	0.01
Group 2	4										
79	1	09_TCw_Tpcpll	131222	22.2	25.4	22	saturated	5	395.50	36.40	0.22
80	2	09_TCw_Tpcpll	131222	22.2	25.4	22	saturated	5	391.20	37.40	0.22
81	3	09_TCw_Tpcpll	131222	22.2	25.4	22	saturated	5	396.80	36.80	0.21
82	4	09_TCw_Tpcpll	131222	22.2	25.4	22	saturated	5	307.10	36.30	0.20
							Average:	5	372.65	36.73	0.21
							Std. Dev.:	0	43.77	0.50	0.01
Group 3	4										
83	1	09_TCw_Tpcpll	131223	22.2	25.4	22	saturated	10	439.70	36.90	0.23
84	2	09_TCw_Tpcpll	131223	22.2	25.4	22	saturated	10	434.60	38.10	0.20
85	3	09_TCw_Tpcpll	131223	22.2	25.4	22	saturated	10	343.40	35.60	0.21
86	4	09_TCw_Tpcpll	131223	22.2	25.4	22	saturated	10	417.30	38.30	0.21
							Average:	10	408.75	37.23	0.21
							Std. Dev.:	0	44.61	1.25	0.01
Group 4	5										
72	1	09_TCw_Tpcpll	231221	289.2	50.8	22	saturated	0	121.10	33.50	0.23
73	2	09_TCw_Tpcpll	231221	292.4	50.8	22	saturated	0	119.90	30.30	0.32
74	3	09_TCw_Tpcpll	231221	297.1	50.8	22	saturated	0	75.40	24.60	0.22
87	4	09_TCw_Tpcpll	231221	22.2	50.8	22	saturated	0	313.60	36.70	0.22
88	5	09_TCw_Tpcpll	231221	23.4	50.8	22	saturated	0	303.70	39.00	0.22
							Average:	0	186.74	32.82	0.24
							Std. Dev.:	0	112.86	5.65	0.04
Group 5	1										
89	1	09_TCw_Tpcpll	231222	5.7	50.8	22	saturated	5	125.30	24.40	0.07
							Average:	5.00	125.30		
							Std. Dev.:				
Group 6	1										
90	1	09_TCw_Tpcpll	231223	46.4	50.8	22	saturated	10	157.90	22.30	0.10
							Average:	10.00	157.90		
							Std. Dev.:				
Group 7	3										
73	1	09_TCw_Tpcpll	231121		51.6	Ambient	Saturated	-13.20	0.0		
74	2	09_TCw_Tpcpll	231121		51.6	Ambient	Saturated	-16.00	0.0		
75	3	09_TCw_Tpcpll	231121		51.6	Ambient	Saturated	-7.40	0.0		
							Average:	-12.2	0.00		
							Std_Dev:	4.39			
Group 1	1										
91	1	10_TCw_Tpcpln	221231	87.6	56	22	ambient	0	364.00	57.50	0.31
							Average:	0.00	364.00	57.50	0.31
							Std. Dev.:				
Group 2	1										
92	1	10_TCw_Tpcpln	221233	87.6	56	22	ambient	10	406.00	43.90	0.30
							Average:	10.00	406.00	43.90	0.30
							Std. Dev.:				
Group 3	1										
93	1	10_TCw_Tpcpln	221234	87.6	56	22	ambient	20	895.00	58.30	0.22
							Average:	20.00	895.00	58.30	0.22
							Std. Dev.:				
Group 4	1										
94	1	10_TCw_Tpcpln	222234	185.0	56	200	ambient	20.7	125.70		
							Average:	20.70	125.70		
							Std. Dev.:				
Group 5	20										

Specimen Inventory Number	Tests In Each Lithostratigraphic Unit	GFM 2000 Layer	Testing Group	Max. Depth (ft)	Equivalent Specimen Diameter - D (mm)	Specimen Temperature (deg. C)	Specimen Saturation	Effective Confining Pressure, (MPa), s3'	Effective Axial Stress, s1' (MPa)	Young's Modulus (GPa)	Poisson's Ratio
95	1	10_TCw_Tpcpln	231221	170.4	50.80	22	saturated	0	117.50	40.10	0.19
96	2	10_TCw_Tpcpln	231221	174.0	50.80	22	saturated	0	141.80	38.70	0.20
97	3	10_TCw_Tpcpln	231221	178.0	50.80	22	saturated	0	142.70	39.80	0.20
98	4	10_TCw_Tpcpln	231221	179.5	50.80	22	saturated	0	215.80	40.10	0.22
99	5	10_TCw_Tpcpln	231221	180.0	50.80	22	saturated	0	149.10	37.10	0.20
100	6	10_TCw_Tpcpln	231221	188.3	50.80	22	saturated	0	209.20	39.80	0.20
101	7	10_TCw_Tpcpln	231221	196.2	50.80	22	saturated	0	185.60	36.50	0.22
102	8	10_TCw_Tpcpln	231221	200.0	50.80	22	saturated	0	145.30	38.70	0.23
103	9	10_TCw_Tpcpln	231221	111.0	50.80	22	saturated	0	78.20	23.10	0.21
104	10	10_TCw_Tpcpln	231221	111.0	50.8	22	saturated	0	114.10	26.50	0.21
105	11	10_TCw_Tpcpln	231221	98.1	50.8	22	saturated	0	245.60	30.00	0.24
106	12	10_TCw_Tpcpln	231221	98.1	50.8	22	saturated	0	242.20	29.20	0.25
108	13	10_TCw_Tpcpln	231221	18.0	50.8	22	saturated	0	84.60	28.70	0.18
109	14	10_TCw_Tpcpln	231221	33.5	50.8	22	saturated	0	160.40	35.00	0.21
110	15	10_TCw_Tpcpln	231221	41.4	50.8	22	saturated	0	135.00	31.50	0.18
111	16	10_TCw_Tpcpln	231221	47.4	50.8	22	saturated	0	228.10	28.10	0.20
112	17	10_TCw_Tpcpln	231221	55.4	50.8	22	saturated	0	143.30	21.40	0.20
113	18	10_TCw_Tpcpln	231221	144.7	50.8	22	saturated	0	278.40	39.00	0.18
114	19	10_TCw_Tpcpln	231221	165.8	50.8	22	saturated	0	169.80	34.30	0.17
115	20	10_TCw_Tpcpln	231221	195.3	50.8	22	saturated	0	259.90	39.10	0.21
							Average:	0	172.33	33.84	0.21
							Std. Dev.:	0	58.09	6.05	0.02
Group 6	3										
116	1	10_TCw_Tpcpln	231222	156.0	50.8	22	saturated	5	313.60	39.10	0.21
117	2	10_TCw_Tpcpln	231222	167.9	50.8	22	saturated	5	144.70	23.00	0.16
118	3	10_TCw_Tpcpln	231222	202.9	50.8	22	saturated	5	323.30	36.10	0.21
							Average:	5	260.53	32.73	0.19
							Std. Dev.:	0	100.43	8.56	0.03
Group 7	4										
107	1	10_TCw_Tpcpln	231223	122.7	50.8	22	saturated	10	183.10	18.80	0.17
119	2	10_TCw_Tpcpln	231223	137.3	50.8	22	saturated	10	152.20	54.00	0.26
120	3	10_TCw_Tpcpln	231223	161.7	50.8	22	saturated	10	418.20	39.20	0.23
121	4	10_TCw_Tpcpln	231223	176.1	50.8	22	saturated	10	410.40	38.70	0.21
							Average:	10	290.98	37.68	0.22
							Std. Dev.:	0	143.00	14.45	0.04
Group 8	19										
76	1	10_TCw_Tpcpln	231121		51.6	Ambient	Saturated	-10.60	0.0		
77	2	10_TCw_Tpcpln	231121		51.6	Ambient	Saturated	-9.40	0.0		
78	3	10_TCw_Tpcpln	231121		51.6	Ambient	Saturated	-9.90	0.0		
79	4	10_TCw_Tpcpln	231121		51.6	Ambient	Saturated	-13.00	0.0		
80	5	10_TCw_Tpcpln	231121		51.6	Ambient	Saturated	-13.40	0.0		
81	6	10_TCw_Tpcpln	231121		51.6	Ambient	Saturated	-11.80	0.0		
82	7	10_TCw_Tpcpln	231121		51.6	Ambient	Saturated	-10.60	0.0		
83	8	10_TCw_Tpcpln	231121		51.6	Ambient	Saturated	-11.30	0.0		
84	9	10_TCw_Tpcpln	231121		51.6	Ambient	Saturated	-8.20	0.0		
85	10	10_TCw_Tpcpln	231121		51.6	Ambient	Saturated	-12.10	0.0		
86	11	10_TCw_Tpcpln	231121		51.6	Ambient	Saturated	-10.90	0.0		
87	12	10_TCw_Tpcpln	231121		51.6	Ambient	Saturated	-13.30	0.0		
88	13	10_TCw_Tpcpln	231121		51.6	Ambient	Saturated	-8.20	0.0		
89	14	10_TCw_Tpcpln	231121		51.6	Ambient	Saturated	-12.40	0.0		
90	15	10_TCw_Tpcpln	231121		51.6	Ambient	Saturated	-12.00	0.0		
91	16	10_TCw_Tpcpln	231121		51.6	Ambient	Saturated	-12.60	0.0		
92	17	10_TCw_Tpcpln	231121		51.6	Ambient	Saturated	-9.30	0.0		
93	18	10_TCw_Tpcpln	231121		51.6	Ambient	Saturated	-8.40	0.0		
94	19	10_TCw_Tpcpln	231121		51.6	Ambient	Saturated	-9.60	0.0		
							Average:	-10.89	0.00		
							Std_Dev:	1.73			
Group 1	4										
122	1	12_TCw_Tpcpv2	231221	143.5	50.80	22	saturated	0	61.80	14.80	0.13

Specimen Inventory Number	Tests In Each Lithostratigraphic Unit	GFM 2000 Layer	Testing Group	Max. Depth (ft)	Equivalent Specimen Diameter - D (mm)	Specimen Temperature (deg. C)	Specimen Saturation	Effective Confining Pressure, (MPa), s3'	Effective Axial Stress, s1' (MPa)	Young's Modulus (GPa)	Poisson's Ratio
123	2	12_TCw_Tpcpv2	231221	151.2	50.80	22	saturated	0	11.30	5.90	0.13
124	3	12_TCw_Tpcpv2	231221	73.7	50.8	22	saturated	0	27.40	7.70	0.09
125	4	12_TCw_Tpcpv2	231221	77.7	50.8	22	saturated	0	12.20	2.10	0.06
							Average:	0	28.18	7.63	0.10
							Std. Dev.:	0	23.60	5.32	0.03
Group 2	1										
126	1	12_TCw_Tpcpv2	231223	250.0	50.8	22	saturated	10	71.40	24.00	0.19
							Average:	10	71.40	24.00	0.19
							Std. Dev.:				
Group 3	4										
95	1	12_TCw_Tpcpv2	231121		51.6	Ambient	Saturated	-5.10	0.0		
96	2	12_TCw_Tpcpv2	231121		51.6	Ambient	Saturated	-1.20	0.0		
97	3	12_TCw_Tpcpv2	231121		51.6	Ambient	Saturated	-4.50	0.0		
98	4	12_TCw_Tpcpv2	231121		51.6	Ambient	Saturated	-1.90	0.0		
							Average:	-3.18	0.00		
							Std_Dev:	1.91			
Group 1	4										
127	1	13_PTn_Tpcpv1	231221	84.4	50.8	22	saturated	0	6.90	3.70	0.10
128	2	13_PTn_Tpcpv1	231221	91.0	50.8	22	saturated	0	5.40	3.90	0.06
129	3	13_PTn_Tpcpv1	231221	97.9	50.8	22	saturated	0	3.90	0.30	0.21
130	4	13_PTn_Tpcpv1	231221	85.8	50.8	22	saturated	0	4.00	2.20	0.03
							Average:	0	5.05	2.53	0.10
							Std. Dev.:	0	1.41	1.67	0.08
Group 2	1										
99	1	13_PTn_Tpcpv1	231121		51.6	Ambient	Saturated	-0.50	0.0		
							Average:	-0.50	0.00		
							Std_Dev:				
Group 1	2										
132	1	14_PTn_Tpbt4	221221	161.4	50.80	22	ambient	0	3.50	2.90	0.16
131	2	14_PTn_Tpbt4	221231	212.7	56	22	ambient	0	7.03	0.41	0.28
							Average:	0	5.27	1.66	0.22
							Std. Dev.:	0	2.50	1.76	0.08
Group 2	1										
133	3	14_PTn_Tpbt4	231221	105.0	50.8	22	saturated	0	1.20	0.20	0.17
							Average:	0.00	1.20	0.20	0.17
							Std_Dev:				
Group 1	5										
134	1	15_PTn_Tpy	231221	119.4	50.8	22	saturated	0	22.80	9.20	0.15
135	2	15_PTn_Tpy	231221	130.0	50.8	22	saturated	0	21.00	2.30	0.17
136	3	15_PTn_Tpy	231221	135.3	50.8	22	saturated	0	26.20	4.90	0.16
137	4	15_PTn_Tpy	231221	109.5	50.8	22	saturated	0	18.70	7.40	0.15
138	5	15_PTn_Tpy	231221	138.7	50.8	22	saturated	0	7.80	2.40	0.15
							Average:	0	19.30	5.24	0.16
							Std. Dev.:	0	6.99	3.05	0.01
Group 2	1										
100	1	15_PTn_Tpy	231121		51.6	Ambient	Saturated	-3.00	0.0		
							Average:	-3.00	0.00		
							Std_Dev:				
Group 1	2										
139	1	16_PTn_Tpbt3	221221	169.5	50.8	22	ambient	0	5.90	2.40	0.12
140	2	16_PTn_Tpbt3	221221	174.0	50.8	22	ambient	0	4.30	1.20	0.21
							Average:	0	5.10	1.80	0.17
							Std. Dev.:	0	1.13	0.85	0.06
Group 2	2										
141	1	16_PTn_Tpbt3	231221	169.1	50.8	22	saturated	0	0.80	0.20	0.28
142	2	16_PTn_Tpbt3	231221	267.1	50.8	22	saturated	0	2.80	2.40	
							Average:	0	1.80	1.30	0.28

Specimen Inventory Number	Tests In Each Lithostratigraphic Unit	GFM 2000 Layer	Testing Group	Max. Depth (ft)	Equivalent Specimen Diameter - D (mm)	Specimen Temperature (deg. C)	Specimen Saturation	Effective Confining Pressure, (MPa), s3'	Effective Axial Stress, s1' (MPa)	Young's Modulus (GPa)	Poisson's Ratio
							Std. Dev.:	0	1.41	1.56	
Group 3	1										
143	1	16_PTn_Tpbt3	231222	276.9	50.8	22	saturated	5	13.30		
							Average:	5.00	13.30		
							Std_Dev:				
Group 4	1										
101	1	16_PTn_Tpbt3	221121		51.6	Ambient	Room Dry	-0.30	0.0		
							Average:	-0.30	0.00		
							Std_Dev:				
Group 1	1										
149	1	17_PTn_Tpp	221221	182.2	50.80	22	ambient	0	3.30	0.80	0.23
150	2	17_PTn_Tpp	221221	187.0	50.80	22	ambient	0	4.10	1.30	0.34
							Average:	0	3.70	1.05	0.29
							Std. Dev.:	0	0.57	0.35	0.08
Group 2	10										
144	1	17_PTn_Tpp	231221	416.6	50.8	22	saturated	0	4.90	1.90	0.28
145	2	17_PTn_Tpp	231221	422.3	50.8	22	saturated	0	1.80	0.70	
146	3	17_PTn_Tpp	231221	428.4	50.8	22	saturated	0	3.50	1.20	0.18
147	4	17_PTn_Tpp	231221	433.2	50.8	22	saturated	0	3.30	0.80	0.36
148	5	17_PTn_Tpp	231221	456.0	50.8	22	saturated	0	9.40	2.10	0.09
151	6	17_PTn_Tpp	231221	174.1	50.8	22	saturated	0	1.80	0.30	0.19
152	7	17_PTn_Tpp	231221	213.6	50.8	22	saturated	0	1.50	0.30	0.25
153	8	17_PTn_Tpp	231221	249.7	50.8	22	saturated	0	2.30	0.60	0.31
154	9	17_PTn_Tpp	231221	254.0	50.8	22	saturated	0	2.10	0.40	0.26
156	10	17_PTn_Tpp	231221	215.7	50.8	22	saturated	0	1.30	1.50	0.39
							Average:	0	3.19	0.98	0.26
							Std. Dev.:	0	2.45	0.66	0.09
Group 3	1										
155	1	17_PTn_Tpp	231223	282.5	50.8	22	saturated	10	17.30		
							Average:	10.00	17.30		
							Std_Dev:				
Group 4	1										
102	1	17_PTn_Tpp	221121		51.6	Ambient	Room Dry	-0.40	0.0		
							Average:	-0.40	0.00		
							Std_Dev:				
Group 5	12										
103	1	17_PTn_Tpp	231121		51.6	Ambient	Saturated	-0.10	0.0		
104	2	17_PTn_Tpp	231121		51.6	Ambient	Saturated	-0.02	0.0		
105	3	17_PTn_Tpp	231121		51.6	Ambient	Saturated	-0.03	0.0		
106	4	17_PTn_Tpp	231121		51.6	Ambient	Saturated	-0.10	0.0		
107	5	17_PTn_Tpp	231121		51.6	Ambient	Saturated	-0.02	0.0		
108	6	17_PTn_Tpp	231121		51.6	Ambient	Saturated	-0.10	0.0		
109	7	17_PTn_Tpp	231121		51.6	Ambient	Saturated	-0.20	0.0		
110	8	17_PTn_Tpp	231121		51.6	Ambient	Saturated	-0.10	0.0		
111	9	17_PTn_Tpp	231121		51.6	Ambient	Saturated	-0.20	0.0		
112	10	17_PTn_Tpp	231121		51.6	Ambient	Saturated	-0.20	0.0		
113	11	17_PTn_Tpp	231121		51.6	Ambient	Saturated	-0.20	0.0		
114	12	17_PTn_Tpp	231121		51.6	Ambient	Saturated	-0.70	0.0		
							Average:	-0.16	0.00		
							Std_Dev:	0.18			
Group 1	3										
160	1	18_PTn_Tpbt2	221221	222.0	50.8	22	ambient	0	4.80	1.50	0.23
161	2	18_PTn_Tpbt2	221221	227.9	50.80	22	ambient	0	2.70	0.70	0.23
162	3	18_PTn_Tpbt2	221221	241.5	50.80	22	ambient	0	2.10	0.50	0.29
							Average:	0	3.20	0.90	0.25
							Std. Dev.:	0	1.42	0.53	0.03
Group 2	6										
157	1	18_PTn_Tpbt2	231221	458.7	50.8	22	saturated	0	5.20	0.80	0.15

Specimen Inventory Number	Tests In Each Lithostratigraphic Unit	GFM 2000 Layer	Testing Group	Max. Depth (ft)	Equivalent Specimen Diameter - D (mm)	Specimen Temperature (deg. C)	Specimen Saturation	Effective Confining Pressure, (MPa), s3'	Effective Axial Stress, s1' (MPa)	Young's Modulus (GPa)	Poisson's Ratio
158	2	18_PTn_Tpbt2	231221	466.8	50.8	22	saturated	0	6.40	1.70	0.14
159	3	18_PTn_Tpbt2	231221	469.0	50.8	22	saturated	0	2.00	0.20	0.19
163	4	18_PTn_Tpbt2	231221	268.6	50.8	22	saturated	0	0.80	0.10	0.13
164	5	18_PTn_Tpbt2	231221	310.6	50.8	22	saturated	0	1.70	1.20	0.40
165	6	18_PTn_Tpbt2	231221	235.0	50.8	22	saturated	0	1.40	0.01	0.24
							Average:	0	2.92	0.67	0.21
							Std. Dev.:	0	2.30	0.68	0.10
Group 3	2										
115	1	18_PTn_Tpbt2	221121		51.6	Ambient	Room Dry	-0.30	0.0		
116	2	18_PTn_Tpbt2	221121		51.6	Ambient	Room Dry	-0.20	0.0		
							Average:	-0.25	0.00		
							Std_Dev:	0.07			
Group 4	3										
117	1	18_PTn_Tpbt2	231121		51.6	Ambient	Saturated	-0.10	0.0		
118	2	18_PTn_Tpbt2	231121		51.6	Ambient	Saturated	-0.80	0.0		
119	3	18_PTn_Tpbt2	231121		51.6	Ambient	Saturated	-0.10	0.0		
							Average:	-0.33	0.00		
							Std_Dev:	0.40			
Group 1	2										
166	1	19_PTn_Tptrv3	231221	292.4	50.8	22	saturated	0	5.80	1.90	0.30
167	2	19_PTn_Tptrv3	231221	258.5	50.8	22	saturated	0	2.70	0.07	0.15
							Average:	0	4.25	0.99	0.23
							Std. Dev.:	0	2.19	1.29	0.11
Group 1	10										
196	1	22_TSw1_Tptrn	131221	818.4	25.2	22	saturated	0	160.00	37.80	0.24
194	2	22_TSw1_Tptrn	131221	797.0	25.3	22	saturated	0	162.00	43.50	0.25
195	3	22_TSw1_Tptrn	131221	797.0	25.3	22	saturated	0	130.00	39.60	0.26
200	4	22_TSw1_Tptrn	131221	519.4	25.35	22	saturated	0	67.70	21.20	0.13
201	5	22_TSw1_Tptrn	131221	519.4	25.35	22	saturated	0	62.60	22.20	0.27
199	6	22_TSw1_Tptrn	131221	484.7	25.37	22	saturated	0	72.80	17.60	0.19
235	7	22_TSw1_Tptrn	131221	344.4	25.4	22	saturated	0	106.20	26.30	0.17
236	8	22_TSw1_Tptrn	131221	344.4	25.4	22	saturated	0	89.50	19.10	0.15
237	9	22_TSw1_Tptrn	131221	344.4	25.4	22	saturated	0	97.30	27.70	0.18
238	10	22_TSw1_Tptrn	131221	344.4	25.4	22	saturated	0	88.70	27.20	0.15
							Average:	0	103.68	28.22	0.20
							Std. Dev.:	0	36.02	9.08	0.05
Group 2	13										
168	1	22_TSw1_Tptrn	131222	527.0	25.4	22	saturated	5	76.50	21.10	0.19
169	2	22_TSw1_Tptrn	131222	527.0	25.4	22	saturated	5	108.90	22.60	0.23
170	3	22_TSw1_Tptrn	131222	527.0	25.4	22	saturated	5	113.60	23.40	0.16
171	4	22_TSw1_Tptrn	131222	527.0	25.4	22	saturated	5	90.00	19.70	0.17
172	5	22_TSw1_Tptrn	131222	527.0	25.4	22	saturated	5	67.50	14.70	0.13
208	6	22_TSw1_Tptrn	131222	416.0	25.4	22	saturated	5	77.10	12.30	0.45
209	7	22_TSw1_Tptrn	131222	416.0	25.4	22	saturated	5	39.60	13.70	
210	8	22_TSw1_Tptrn	131222	416.0	25.4	22	saturated	5	84.70	17.10	0.21
211	9	22_TSw1_Tptrn	131222	416.0	25.4	22	saturated	5	58.80	16.30	0.21
239	10	22_TSw1_Tptrn	131222	344.4	25.4	22	saturated	5	56.50	24.70	0.17
240	11	22_TSw1_Tptrn	131222	344.4	25.4	22	saturated	5	163.90	28.70	0.23
241	12	22_TSw1_Tptrn	131222	344.4	25.4	22	saturated	5	75.90	22.50	0.20
242	13	22_TSw1_Tptrn	131222	344.4	25.4	22	saturated	5	110.20	20.60	0.21
							Average:	5	86.40	19.80	0.21
							Std. Dev.:	0	32.06	4.77	0.08
Group 3	11										
173	1	22_TSw1_Tptrn	131223	527.0	25.4	22	saturated	10	160.80	25.50	0.18
174	2	22_TSw1_Tptrn	131223	527.0	25.4	22	saturated	10	142.10	25.80	0.19
175	3	22_TSw1_Tptrn	131223	527.0	25.4	22	saturated	10	131.40	25.30	0.19
176	4	22_TSw1_Tptrn	131223	527.0	25.4	22	saturated	10	133.00	23.00	0.20

Specimen Inventory Number	Tests In Each Lithostratigraphic Unit	GFM 2000 Layer	Testing Group	Max. Depth (ft)	Equivalent Specimen Diameter - D (mm)	Specimen Temperature (deg. C)	Specimen Saturation	Effective Confining Pressure, (MPa), s3'	Effective Axial Stress, s1' (MPa)	Young's Modulus (GPa)	Poisson's Ratio
212	5	22_TSw1_Tptrn	131223	416.0	25.4	22	saturated	10	119.90	17.90	0.34
213	6	22_TSw1_Tptrn	131223	416.0	25.4	22	saturated	10	147.90	19.30	0.30
214	7	22_TSw1_Tptrn	131223	416.0	25.4	22	saturated	10	30.10	21.00	0.28
215	8	22_TSw1_Tptrn	131223	416.0	25.4	22	saturated	10	61.10	8.40	0.22
243	9	22_TSw1_Tptrn	131223	344.4	25.4	22	saturated	10	185.00	27.30	0.21
244	10	22_TSw1_Tptrn	131223	344.4	25.4	22	saturated	10	139.10	25.50	0.15
245	11	22_TSw1_Tptrn	131223	344.4	25.4	22	saturated	10	208.30	29.40	0.15
							Average:	10	132.61	22.58	0.22
							Std. Dev.:	0	50.42	5.83	0.06
Group 4	5										
203	1	22_TSw1_Tptrn	221221	484.7	57.1	22	ambient	0	26.50	16.90	0.30
204	2	22_TSw1_Tptrn	221221	528.4	57.10	22	ambient	0	64.00	19.80	
202	3	22_TSw1_Tptrn	221221	484.7	57.15	22	ambient	0	30.50	14.80	0.21
205	4	22_TSw1_Tptrn	221221	528.4	57.18	22	ambient	0	114.30	28.30	0.21
206	5	22_TSw1_Tptrn	221221	528.4	57.20	22	ambient	0	81.40	26.80	0.26
							Average:	0	63.34	21.32	0.25
							Std. Dev.:	0	36.60	5.98	0.04
Group 5	53										
177	1	22_TSw1_Tptrn	231221	508.4	50.8	22	saturated	0	102.60	32.30	0.22
178	2	22_TSw1_Tptrn	231221	515.5	50.8	22	saturated	0	98.50	31.60	0.22
179	3	22_TSw1_Tptrn	231221	525.0	50.8	22	saturated	0	97.90	27.30	0.21
180	4	22_TSw1_Tptrn	231221	530.4	50.8	22	saturated	0	67.10	21.60	0.20
181	5	22_TSw1_Tptrn	231221	535.3	50.8	22	saturated	0	55.40	22.30	0.22
182	6	22_TSw1_Tptrn	231221	541.0	50.8	22	saturated	0	33.20	14.60	0.34
183	7	22_TSw1_Tptrn	231221	546.0	50.8	22	saturated	0	56.80	19.20	0.26
184	8	22_TSw1_Tptrn	231221	550.0	50.8	22	saturated	0	61.90	20.80	0.22
185	9	22_TSw1_Tptrn	231221	582.4	50.8	22	saturated	0	26.20	13.20	0.28
186	10	22_TSw1_Tptrn	231221	591.7	50.8	22	saturated	0	31.80	9.20	0.26
187	11	22_TSw1_Tptrn	231221	597.0	50.8	22	saturated	0	33.30	15.60	0.29
188	12	22_TSw1_Tptrn	231221	602.9	50.8	22	saturated	0	34.10	13.60	0.27
189	13	22_TSw1_Tptrn	231221	607.6	50.8	22	saturated	0	43.70	11.40	0.27
190	14	22_TSw1_Tptrn	231221	612.5	50.8	22	saturated	0	47.90	17.20	0.32
191	15	22_TSw1_Tptrn	231221	623.8	50.8	22	saturated	0	43.40	14.90	0.27
192	16	22_TSw1_Tptrn	231221	627.7	50.8	22	saturated	0	32.00	11.20	0.20
193	17	22_TSw1_Tptrn	231221	655.8	50.8	22	saturated	0	31.10	14.50	0.41
197	18	22_TSw1_Tptrn	231221	797.0	50.8	22	saturated	0	143.00	57.10	0.28
216	19	22_TSw1_Tptrn	231221	276.2	50.80	22	saturated	0	118.60	33.20	0.21
217	20	22_TSw1_Tptrn	231221	304.4	50.80	22	saturated	0	102.20	28.10	0.21
218	21	22_TSw1_Tptrn	231221	316.3	50.80	22	saturated	0	79.20	22.00	0.26
219	22	22_TSw1_Tptrn	231221	318.2	50.80	22	saturated	0	77.20	22.40	0.27
220	23	22_TSw1_Tptrn	231221	328.7	50.80	22	saturated	0	73.20	21.50	0.29
221	24	22_TSw1_Tptrn	231221	328.7	50.80	22	saturated	0	72.80	23.80	0.24
222	25	22_TSw1_Tptrn	231221	354.4	50.80	22	saturated	0	32.40	17.00	0.15
223	26	22_TSw1_Tptrn	231221	372.6	50.80	22	saturated	0	33.30	15.10	0.16
224	27	22_TSw1_Tptrn	231221	373.1	50.80	22	saturated	0	68.80	21.20	0.25
225	28	22_TSw1_Tptrn	231221	391.6	50.80	22	saturated	0	58.30	20.60	0.22
226	29	22_TSw1_Tptrn	231221	395.2	50.80	22	saturated	0	48.40	21.80	0.21
227	30	22_TSw1_Tptrn	231221	397.0	50.80	22	saturated	0	60.40	20.60	0.29
228	31	22_TSw1_Tptrn	231221	407.2	50.80	22	saturated	0	56.80	20.10	0.27
229	32	22_TSw1_Tptrn	231221	420.8	50.80	22	saturated	0	36.20	12.20	0.33
230	33	22_TSw1_Tptrn	231221	427.0	50.80	22	saturated	0	43.40	14.20	0.19
246	34	22_TSw1_Tptrn	231221	334.5	50.8	22	saturated	0	63.30	22.40	0.19
247	35	22_TSw1_Tptrn	231221	350.3	50.8	22	saturated	0	148.40	34.30	0.17
248	36	22_TSw1_Tptrn	231221	369.5	50.8	22	saturated	0	45.20	22.90	0.19
249	37	22_TSw1_Tptrn	231221	380.8	50.8	22	saturated	0	61.00	19.90	0.22
250	38	22_TSw1_Tptrn	231221	396.6	50.8	22	saturated	0	33.90	13.10	0.26
251	39	22_TSw1_Tptrn	231221	417.9	50.8	22	saturated	0	27.90	9.80	0.16
252	40	22_TSw1_Tptrn	231221	422.0	50.8	22	saturated	0	60.80	19.00	0.18
253	41	22_TSw1_Tptrn	231221	428.7	50.8	22	saturated	0	55.50	21.80	0.20

Specimen Inventory Number	Tests In Each Lithostratigraphic Unit	GFM 2000 Layer	Testing Group	Max. Depth (ft)	Equivalent Specimen Diameter - D (mm)	Specimen Temperature (deg. C)	Specimen Saturation	Effective Confining Pressure, (MPa), s3'	Effective Axial Stress, s1' (MPa)	Young's Modulus (GPa)	Poisson's Ratio
254	42	22_TSw1_Tptrn	231221	443.2	50.8	22	saturated	0	66.30	17.90	0.31
255	43	22_TSw1_Tptrn	231221	450.1	50.8	22	saturated	0	25.70	17.20	0.28
256	44	22_TSw1_Tptrn	231221	461.0	50.8	22	saturated	0	52.60	13.70	0.36
257	45	22_TSw1_Tptrn	231221	469.4	50.8	22	saturated	0	53.90	18.40	0.43
258	46	22_TSw1_Tptrn	231221	472.9	50.8	22	saturated	0	54.20	15.50	0.23
265	47	22_TSw1_Tptrn	231221	354.1	50.8	22	saturated	0	44.40	17.80	0.19
266	48	22_TSw1_Tptrn	231221	406.1	50.8	22	saturated	0	48.40	19.70	0.25
273	49	22_TSw1_Tptrn	231221	311.1	50.8	22	saturated	0	142.70	32.30	0.18
274	50	22_TSw1_Tptrn	231221	338.6	50.8	22	saturated	0	74.30	25.50	0.24
275	51	22_TSw1_Tptrn	231221	405.6	50.8	22	saturated	0	32.80	14.80	0.31
198	52	22_TSw1_Tptrn	231221	797.0	50.9	22	saturated	0	125.00	59.90	0.31
207	53	22_TSw1_Tptrn	231221	519.4	50.93	22	saturated	0	67.50	13.00	0.14
							Average:	0	61.98	20.95	0.25
							Std. Dev.:	0	31.06	9.66	0.06
Group 6	8										
231	1	22_TSw1_Tptrn	231222	326.0	50.8	22	saturated	5	116.10	25.40	0.22
232	2	22_TSw1_Tptrn	231222	394.6	50.8	22	saturated	5	99.30	20.00	0.20
259	3	22_TSw1_Tptrn	231222	345.0	50.8	22	saturated	5	104.50	29.00	0.24
260	4	22_TSw1_Tptrn	231222	427.6	50.8	22	saturated	5	73.10	16.10	0.14
261	5	22_TSw1_Tptrn	231222	454.6	50.8	22	saturated	5	70.50	14.00	0.24
267	6	22_TSw1_Tptrn	231222	339.4	50.8	22	saturated	5	88.80	24.30	0.18
268	7	22_TSw1_Tptrn	231222	370.1	50.8	22	saturated	5	87.40	24.90	0.21
269	8	22_TSw1_Tptrn	231222	410.2	50.8	22	saturated	5	99.40	25.20	0.20
							Average:	5	92.39	22.36	0.20
							Std. Dev.:	0	15.56	5.16	0.03
Group 7	8										
233	1	22_TSw1_Tptrn	231223	290.5	50.8	22	saturated	10	228.50	28.40	0.21
234	2	22_TSw1_Tptrn	231223	362.0	50.8	22	saturated	10	93.60	17.50	0.19
262	3	22_TSw1_Tptrn	231223	411.4	50.8	22	saturated	10	88.40	17.80	0.20
263	4	22_TSw1_Tptrn	231223	441.0	50.8	22	saturated	10	103.30	20.30	0.22
264	5	22_TSw1_Tptrn	231223	470.2	50.8	22	saturated	10	139.30	19.80	0.33
270	6	22_TSw1_Tptrn	231223	343.4	50.8	22	saturated	10	124.60	25.80	0.20
271	7	22_TSw1_Tptrn	231223	401.5	50.8	22	saturated	10	102.90	25.60	0.22
272	8	22_TSw1_Tptrn	231223	429.2	50.8	22	saturated	10	60.40	2.00	0.02
							Average:	10	117.63	19.65	0.20
							Std. Dev.:	0	50.62	8.19	0.08
Group 8	1										
120	1	22_TSw1_Tptrn	221121		51.6	Ambient	Room Dry	-8.40	0.0		
							Average:	-8.40	0.00		
							Std_Dev:				
Group 9	52										
121	1	22_TSw1_Tptrn	231121		51.6	Ambient	Saturated	-9.30	0.0		
122	2	22_TSw1_Tptrn	231121		51.6	Ambient	Saturated	-7.60	0.0		
123	3	22_TSw1_Tptrn	231121		51.6	Ambient	Saturated	-9.30	0.0		
124	4	22_TSw1_Tptrn	231121		51.6	Ambient	Saturated	-6.30	0.0		
125	5	22_TSw1_Tptrn	231121		51.6	Ambient	Saturated	-10.50	0.0		
126	6	22_TSw1_Tptrn	231121		51.6	Ambient	Saturated	-5.30	0.0		
127	7	22_TSw1_Tptrn	231121		51.6	Ambient	Saturated	-6.80	0.0		
128	8	22_TSw1_Tptrn	231121		51.6	Ambient	Saturated	-6.60	0.0		
129	9	22_TSw1_Tptrn	231121		51.6	Ambient	Saturated	-1.60	0.0		
130	10	22_TSw1_Tptrn	231121		51.6	Ambient	Saturated	-2.30	0.0		
131	11	22_TSw1_Tptrn	231121		51.6	Ambient	Saturated	-6.50	0.0		
132	12	22_TSw1_Tptrn	231121		51.6	Ambient	Saturated	-6.80	0.0		
133	13	22_TSw1_Tptrn	231121		51.6	Ambient	Saturated	-4.70	0.0		
134	14	22_TSw1_Tptrn	231121		51.6	Ambient	Saturated	-5.10	0.0		
135	15	22_TSw1_Tptrn	231121		51.6	Ambient	Saturated	-4.90	0.0		
136	16	22_TSw1_Tptrn	231121		51.6	Ambient	Saturated	-6.10	0.0		
137	17	22_TSw1_Tptrn	231121		51.6	Ambient	Saturated	-5.90	0.0		
138	18	22_TSw1_Tptrn	231121		51.6	Ambient	Saturated	-6.20	0.0		

Specimen Inventory Number	Tests In Each Lithostratigraphic Unit	GFM 2000 Layer	Testing Group	Max. Depth (ft)	Equivalent Specimen Diameter - D (mm)	Specimen Temperature (deg. C)	Specimen Saturation	Effective Confining Pressure, (MPa), s3'	Effective Axial Stress, s1' (MPa)	Young's Modulus (GPa)	Poisson's Ratio
139	19	22_TSw1_Tptrn	231121		51.6	Ambient	Saturated	-4.70	0.0		
140	20	22_TSw1_Tptrn	231121		51.6	Ambient	Saturated	-4.10	0.0		
141	21	22_TSw1_Tptrn	231121		51.6	Ambient	Saturated	-3.90	0.0		
142	22	22_TSw1_Tptrn	231121		51.6	Ambient	Saturated	-4.00	0.0		
143	23	22_TSw1_Tptrn	231121		51.6	Ambient	Saturated	-7.00	0.0		
144	24	22_TSw1_Tptrn	231121		51.6	Ambient	Saturated	-4.90	0.0		
145	25	22_TSw1_Tptrn	231121		51.6	Ambient	Saturated	-5.40	0.0		
146	26	22_TSw1_Tptrn	231121		51.6	Ambient	Saturated	-4.70	0.0		
147	27	22_TSw1_Tptrn	231121		51.6	Ambient	Saturated	-5.30	0.0		
148	28	22_TSw1_Tptrn	231121		51.6	Ambient	Saturated	-4.80	0.0		
149	29	22_TSw1_Tptrn	231121		51.6	Ambient	Saturated	-4.00	0.0		
150	30	22_TSw1_Tptrn	231121		51.6	Ambient	Saturated	-5.10	0.0		
151	31	22_TSw1_Tptrn	231121		51.6	Ambient	Saturated	-4.40	0.0		
152	32	22_TSw1_Tptrn	231121		51.6	Ambient	Saturated	-4.20	0.0		
153	33	22_TSw1_Tptrn	231121		51.6	Ambient	Saturated	-7.70	0.0		
154	34	22_TSw1_Tptrn	231121		51.6	Ambient	Saturated	-9.00	0.0		
155	35	22_TSw1_Tptrn	231121		51.6	Ambient	Saturated	-9.30	0.0		
156	36	22_TSw1_Tptrn	231121		51.6	Ambient	Saturated	-6.70	0.0		
157	37	22_TSw1_Tptrn	231121		51.6	Ambient	Saturated	-8.60	0.0		
158	38	22_TSw1_Tptrn	231121		51.6	Ambient	Saturated	-8.20	0.0		
159	39	22_TSw1_Tptrn	231121		51.6	Ambient	Saturated	-7.50	0.0		
160	40	22_TSw1_Tptrn	231121		51.6	Ambient	Saturated	-2.80	0.0		
161	41	22_TSw1_Tptrn	231121		51.6	Ambient	Saturated	-4.80	0.0		
162	42	22_TSw1_Tptrn	231121		51.6	Ambient	Saturated	-5.80	0.0		
163	43	22_TSw1_Tptrn	231121		51.6	Ambient	Saturated	-3.00	0.0		
164	44	22_TSw1_Tptrn	231121		51.6	Ambient	Saturated	-4.20	0.0		
165	45	22_TSw1_Tptrn	231121		51.6	Ambient	Saturated	-2.30	0.0		
166	46	22_TSw1_Tptrn	231121		51.6	Ambient	Saturated	-2.70	0.0		
167	47	22_TSw1_Tptrn	231121		51.6	Ambient	Saturated	-3.40	0.0		
168	48	22_TSw1_Tptrn	231121		51.6	Ambient	Saturated	-2.80	0.0		
169	49	22_TSw1_Tptrn	231121		51.6	Ambient	Saturated	-4.30	0.0		
170	50	22_TSw1_Tptrn	231121		51.6	Ambient	Saturated	-3.60	0.0		
171	51	22_TSw1_Tptrn	231121		51.6	Ambient	Saturated	-3.60	0.0		
172	52	22_TSw1_Tptrn	231121		51.6	Ambient	Saturated	-4.00	0.0		
							Average:	-5.43	0.00		
							Std_Dev:	2.07			
Group 1	3										
276	1	23_TSw1_Tptrl	231221	664.4	50.8	22	saturated	0	26.90	10.70	
277	2	23_TSw1_Tptrl	231221	667.8	50.8	22	saturated	0	17.40	6.40	0.31
278	3	23_TSw1_Tptrl	231221	695.8	50.8	22	saturated	0	35.90	10.30	0.28
				664.4			Average:	0	26.73	9.13	0.30
							Std. Dev.:	0	9.25	2.38	0.02
Group 2	1										
279	1	23_TSw1_Tptrl	231222	483.3	50.8	22	saturated	5	67.10	14.40	0.28
				483.3			Average:	5	67.10	14.40	0.28
							Std. Dev.:				
Group 3	7										
173	1	23_TSw1_Tptrl	231121		51.6	Ambient	Saturated	-5.20	0.0		
174	2	23_TSw1_Tptrl	231121		51.6	Ambient	Saturated	-5.30	0.0		
175	3	23_TSw1_Tptrl	231121		51.6	Ambient	Saturated	-3.40	0.0		
176	4	23_TSw1_Tptrl	231121		51.6	Ambient	Saturated	-5.10	0.0		
177	5	23_TSw1_Tptrl	231121		51.6	Ambient	Saturated	-7.30	0.0		
178	6	23_TSw1_Tptrl	231121		51.6	Ambient	Saturated	-3.70	0.0		
179	7	23_TSw1_Tptrl	231121		51.6	Ambient	Saturated	-3.70	0.0		
							Average:	-4.81	0.00		
							Std_Dev:	1.36			
Group 1	2										
280	1	24_TSw1_Tptf	131211	948.4	25.2	22	saturated	0	115.00	41.90	0.26
281	2	24_TSw1_Tptf	131211	948.4	25.3	22	saturated	0	117.00	42.10	0.26

Specimen Inventory Number	Tests In Each Lithostratigraphic Unit	GFM 2000 Layer	Testing Group	Max. Depth (ft)	Equivalent Specimen Diameter - D (mm)	Specimen Temperature (deg. C)	Specimen Saturation	Effective Confining Pressure, (MPa), s3'	Effective Axial Stress, s1' (MPa)	Young's Modulus (GPa)	Poisson's Ratio
				948.4			Average:	0	116.00	42.00	0.26
							Std. Dev.:	0	1.41	0.14	0.00
Group 2	5										
282	1	24_TSw1_Tptf	131221	948.4	25.3	22	saturated	0	167.00	42.00	0.30
283	2	24_TSw1_Tptf	131221	948.4	25.3	22	saturated	0	157.00	49.00	0.26
284	3	24_TSw1_Tptf	131221	949.6	25.3	22	saturated	0	220.00	38.60	0.19
285	4	24_TSw1_Tptf	131221	969.0	25.3	22	saturated	0	130.00	68.30	
286	5	24_TSw1_Tptf	131221	969.0	25.3	22	saturated	0	210.00	46.30	0.21
				948.4			Average:	0	176.80	48.84	0.24
							Std. Dev.:	0	37.57	11.58	0.05
Group 3	1										
287	1	24_TSw1_Tptf	231221	969.0	50.9	22	saturated	0	157.00	54.70	0.34
							Average:	0	157.00	54.70	0.34
							Std. Dev.:				
Group 1	2										
319	1	25_TSw1_Tptpul	221221	633.9	57.15	22	ambient	0	37.30	18.30	
320	2	25_TSw1_Tptpul	221221	634.4	57.23	22	ambient	0	57.70	21.10	
							Average:	0	47.50	19.70	
							Std. Dev.:	0	14.42	1.98	
Group 2	8										
321	1	25_TSw1_Tptpul	231221	488.0	50.80	22	saturated	0	149.40	33.30	0.21
322	2	25_TSw1_Tptpul	231221	662.2	50.80	22	saturated	0	50.40	29.20	0.38
323	3	25_TSw1_Tptpul	231221	687.5	50.80	22	saturated	0	95.80	24.60	0.12
324	4	25_TSw1_Tptpul	231221	525.9	50.8	22	saturated	0	21.10	13.00	0.35
325	5	25_TSw1_Tptpul	231221	546.2	50.8	22	saturated	0	15.70	6.00	0.46
326	6	25_TSw1_Tptpul	231221	649.6	50.8	22	saturated	0	36.10	13.40	0.20
327	7	25_TSw1_Tptpul	231221	692.5	50.8	22	saturated	0	81.80	19.70	0.09
331	8	25_TSw1_Tptpul	231221	725.6	50.8	22	saturated	0	71.40	24.10	0.22
							Average:	0	65.21	20.41	0.25
							Std. Dev.:	0	44.40	9.16	0.13
Group 3	2										
328	1	25_TSw1_Tptpul	231222	671.4	50.8	22	saturated	5	111.90	32.40	0.19
329	2	25_TSw1_Tptpul	231222	717.7	50.8	22	saturated	5	76.90	17.80	0.42
							Average:	5	94.40	25.10	0.31
							Std. Dev.:	0	24.75	10.32	0.16
Group 4	1										
330	1	25_TSw1_Tptpul	231223	672.0	50.8	22	saturated	10	227.90	22.30	0.11
							Average:	10	227.90	22.30	0.11
							Std. Dev.:				
Group 5	3										
298	1	25_TSw1_Tptpul	312111		288	**190**	dry	0	19.60	7.30	
306	2	25_TSw1_Tptpul	312111		289	**190**	dry	0	34.80	9.90	
299	3	25_TSw1_Tptpul	312111		289	**200**	dry	0	37.00	13.70	
							Average:	0	30.47	10.30	
							Std. Dev.:	0	9.47	3.22	
Group 6	1										
312	1	25_TSw1_Tptpul	312221		146.5	**200**	dry	0	17.70	6.70	
							Average:	0	17.70	6.70	
							Std. Dev.:				
Group 7	3										
307	1	25_TSw1_Tptpul	321111		289	24	ambient	0	22.10	14.90	0.21
308	2	25_TSw1_Tptpul	321111		289	24	ambient	0	33.50	20.50	
309	3	25_TSw1_Tptpul	321111		289	24	ambient	0	16.50	12.40	
							Average:	0	24.03	15.93	0.21
							Std. Dev.:	0	8.66	4.15	
Group 8	8										
314	1	25_TSw1_Tptpul	321211		145.50	22	ambient	0	36.30	14.50	0.14

Specimen Inventory Number	Tests In Each Lithostratigraphic Unit	GFM 2000 Layer	Testing Group	Max. Depth (ft)	Equivalent Specimen Diameter - D (mm)	Specimen Temperature (deg. C)	Specimen Saturation	Effective Confining Pressure, (MPa), s3'	Effective Axial Stress, s1' (MPa)	Young's Modulus (GPa)	Poisson's Ratio
313	2	25_TSw1_Tptpul	321211		145.60	22	ambient	0	27.80	10.60	0.35
311	3	25_TSw1_Tptpul	321211		145.80	22	ambient	0	53.00	16.90	0.14
315	4	25_TSw1_Tptpul	321211		146.80	22	ambient	0	28.80	15.00	
300	5	25_TSw1_Tptpul	321211		288	24	ambient	0	13.50	5.80	0.39
301	6	25_TSw1_Tptpul	321211		289	24	ambient	0	17.70	8.80	
302	7	25_TSw1_Tptpul	321211		289	24	ambient	0	25.90	13.70	
310	8	25_TSw1_Tptpul	321211		289	24	ambient	0	26.20	19.50	
							Average:	0	28.65	13.10	0.26
							Std. Dev.:	0	12.04	4.46	0.13
Group 9	1										
316	1	25_TSw1_Tptpul	321221		146.8	24	ambient	0	19.40	7.30	
							Average:	0	19.40	7.30	
							Std. Dev.:				
Group 10	4										
317	1	25_TSw1_Tptpul	331211		146.80	22	saturated	0	41.30	15.60	0.25
303	2	25_TSw1_Tptpul	331211		288	24	saturated	0	12.70	6.70	
304	3	25_TSw1_Tptpul	331211		288	24	saturated	0	9.40	5.00	0.24
305	4	25_TSw1_Tptpul	331211		288	24	saturated	0	11.60	5.90	0.03
							Average:	0	18.75	8.30	0.17
							Std. Dev.:	0	15.10	4.92	0.12
Group 11	11										
288	1	25_TSw1_Tptpul	331221		266.7	22	saturated	0	14.50	14.20	0.14
289	2	25_TSw1_Tptpul	331221		266.7	22	saturated	0	10.30	10.90	0.14
290	3	25_TSw1_Tptpul	331221		266.7	22	saturated	0	12.40	11.90	0.16
291	4	25_TSw1_Tptpul	331221		266.7	22	saturated	0	12.00	12.90	0.14
292	5	25_TSw1_Tptpul	331221		266.7	22	saturated	0	18.20	16.60	0.14
293	6	25_TSw1_Tptpul	331221		266.7	22	saturated	0	17.40	16.80	0.18
294	7	25_TSw1_Tptpul	331221		266.7	22	saturated	0	18.50	15.80	0.13
295	8	25_TSw1_Tptpul	331221		266.7	22	saturated	0	17.50	18.30	0.13
296	9	25_TSw1_Tptpul	331221		266.7	22	saturated	0	13.80	15.80	0.21
297	10	25_TSw1_Tptpul	331221		266.7	22	saturated	0	27.80	21.50	0.21
318	11	25_TSw1_Tptpul	331221		146.3	24	saturated	0	14.90	7.20	
							Average:	0	16.12	14.72	0.16
							Std. Dev.:	0	4.73	3.89	0.03
Group 12	19										
180	1	25_TSw1_Tptpul	231121		51.6	Ambient	Saturated	-3.60	0.0		
181	2	25_TSw1_Tptpul	231121		51.6	Ambient	Saturated	-5.70	0.0		
182	3	25_TSw1_Tptpul	231121		51.6	Ambient	Saturated	-2.10	0.0		
183	4	25_TSw1_Tptpul	231121		51.6	Ambient	Saturated	-3.90	0.0		
184	5	25_TSw1_Tptpul	231121		51.6	Ambient	Saturated	-3.50	0.0		
185	6	25_TSw1_Tptpul	231121		51.6	Ambient	Saturated	-4.00	0.0		
186	7	25_TSw1_Tptpul	231121		51.6	Ambient	Saturated	-5.10	0.0		
187	8	25_TSw1_Tptpul	231121		51.6	Ambient	Saturated	-6.40	0.0		
188	9	25_TSw1_Tptpul	231121		51.6	Ambient	Saturated	-4.30	0.0		
189	10	25_TSw1_Tptpul	231121		51.6	Ambient	Saturated	-4.80	0.0		
190	11	25_TSw1_Tptpul	231121		51.6	Ambient	Saturated	-11.20	0.0		
191	12	25_TSw1_Tptpul	231121		51.6	Ambient	Saturated	-2.70	0.0		
192	13	25_TSw1_Tptpul	231121		51.6	Ambient	Saturated	-9.00	0.0		
193	14	25_TSw1_Tptpul	231121		51.6	Ambient	Saturated	-8.70	0.0		
194	15	25_TSw1_Tptpul	231121		51.6	Ambient	Saturated	-3.60	0.0		
195	16	25_TSw1_Tptpul	231121		51.6	Ambient	Saturated	-12.90	0.0		
196	17	25_TSw1_Tptpul	231121		51.6	Ambient	Saturated	-1.90	0.0		
197	18	25_TSw1_Tptpul	231121		51.6	Ambient	Saturated	-3.90	0.0		
198	19	25_TSw1_Tptpul	231121		51.6	Ambient	Saturated	-8.50	0.0		
							Average:	-5.57	0.00		
							Std_Dev:	3.10			
Group 1	30										
495	1	26_TSw2_Tptpmn	111321		25.4	22	dry	0	170.50	25.40	

Specimen Inventory Number	Tests In Each Lithostratigraphic Unit	GFM 2000 Layer	Testing Group	Max. Depth (ft)	Equivalent Specimen Diameter - D (mm)	Specimen Temperature (deg. C)	Specimen Saturation	Effective Confining Pressure, (MPa), s3'	Effective Axial Stress, s1' (MPa)	Young's Modulus (GPa)	Poisson's Ratio
496	2	26_TSw2_Tptpmn	111321		25.4	22	dry	0	47.90	6.80	
497	3	26_TSw2_Tptpmn	111321		25.4	22	dry	0	96.00	23.30	
498	4	26_TSw2_Tptpmn	111321		25.4	22	dry	0	135.60	24.60	
499	5	26_TSw2_Tptpmn	111321		25.4	22	dry	0	204.00	26.80	
500	6	26_TSw2_Tptpmn	111321		25.4	22	dry	0	191.10	27.80	
501	7	26_TSw2_Tptpmn	111321		25.4	22	dry	0	221.20	27.10	
502	8	26_TSw2_Tptpmn	111321		25.4	22	dry	0	58.90	17.90	
503	9	26_TSw2_Tptpmn	111321		25.4	22	dry	0	150.50	21.20	
504	10	26_TSw2_Tptpmn	111321		25.4	22	dry	0	192.60	27.50	
505	11	26_TSw2_Tptpmn	111321		25.4	22	dry	0	164.50	25.00	
506	12	26_TSw2_Tptpmn	111321		25.4	22	dry	0	201.60	26.70	
507	13	26_TSw2_Tptpmn	111321		25.4	22	dry	0	205.80	27.30	
508	14	26_TSw2_Tptpmn	111321		25.4	22	dry	0	151.90	26.10	
509	15	26_TSw2_Tptpmn	111321		25.4	22	dry	0	158.30	27.10	
510	16	26_TSw2_Tptpmn	111321		25.4	22	dry	0	236.00	26.40	
511	17	26_TSw2_Tptpmn	111321		25.4	22	dry	0	149.00	25.40	
512	18	26_TSw2_Tptpmn	111321		25.4	22	dry	0	128.40	24.20	
513	19	26_TSw2_Tptpmn	111321		25.4	22	dry	0	213.40	25.90	
514	20	26_TSw2_Tptpmn	111321		25.4	22	dry	0	132.40	23.10	
515	21	26_TSw2_Tptpmn	111321		25.4	22	dry	0	116.80	22.70	
516	22	26_TSw2_Tptpmn	111321		25.4	22	dry	0	213.00	26.60	
517	23	26_TSw2_Tptpmn	111321		25.4	22	dry	0	168.30	23.20	
518	24	26_TSw2_Tptpmn	111321		25.4	22	dry	0	51.30	22.50	
519	25	26_TSw2_Tptpmn	111321		25.4	22	dry	0	63.00	23.90	
520	26	26_TSw2_Tptpmn	111321		25.4	22	dry	0	31.90	21.00	
521	27	26_TSw2_Tptpmn	111321		25.4	22	dry	0	76.30	19.00	
522	28	26_TSw2_Tptpmn	111321		25.4	22	dry	0	166.60	25.20	
523	29	26_TSw2_Tptpmn	111321		25.4	22	dry	0	123.00	23.30	
524	30	26_TSw2_Tptpmn	111321		25.4	22	dry	0	174.10	27.70	
							Average:	0	146.46	24.02	
							Std. Dev.:	0	57.33	4.13	
Group 2	2										
535	1	26_TSw2_Tptpmn	131211	742.8	25.32	22	saturated	0.1	243.10	37.50	0.20
536	2	26_TSw2_Tptpmn	131211	742.8	25.32	22	saturated	0.1	230.10	33.60	0.11
							Average:	0.1	236.60	35.55	0.16
							Std. Dev.:	0	9.19	2.76	0.06
Group 3	30										
539	1	26_TSw2_Tptpmn	131221	686.6	25.30	22	saturated	0.1	180.10	33.10	0.21
545	2	26_TSw2_Tptpmn	131221	749.0	25.30	22	saturated	0.1	268.10	33.50	0.29
546	3	26_TSw2_Tptpmn	131221	749.0	25.30	22	saturated	0.1	188.10	34.10	0.27
537	4	26_TSw2_Tptpmn	131221	686.6	25.32	22	saturated	0.1	270.10	36.20	0.18
538	5	26_TSw2_Tptpmn	131221	686.6	25.32	22	saturated	0.1	326.10	40.70	0.17
540	6	26_TSw2_Tptpmn	131221	742.8	25.32	22	saturated	0.1	235.10	35.60	0.21
541	7	26_TSw2_Tptpmn	131221	742.8	25.32	22	saturated	0.1	256.10	36.80	0.21
542	8	26_TSw2_Tptpmn	131221	742.8	25.32	22	saturated	0.1	279.10	34.60	0.21
544	9	26_TSw2_Tptpmn	131221	748.6	25.32	22	saturated	0.1	190.10	32.30	0.21
543	10	26_TSw2_Tptpmn	131221	748.6	25.35	22	saturated	0.1	196.10	32.20	0.16
554	11	26_TSw2_Tptpmn	131221	760.9	25.35	22	saturated	0	210.30	30.20	0.19
555	12	26_TSw2_Tptpmn	131221	760.9	25.35	22	saturated	0	234.40	28.60	0.29
556	13	26_TSw2_Tptpmn	131221	760.9	25.35	22	saturated	0	215.50	29.00	0.22
558	14	26_TSw2_Tptpmn	131221	760.9	25.35	22	saturated	0	245.20	30.60	0.23
562	15	26_TSw2_Tptpmn	131221	760.9	25.35	22	saturated	0	229.70	30.70	0.22
563	16	26_TSw2_Tptpmn	131221	760.9	25.35	22	saturated	0	226.40	30.00	0.21
557	17	26_TSw2_Tptpmn	131221	760.9	25.37	22	saturated	0	221.40	30.20	0.22
559	18	26_TSw2_Tptpmn	131221	760.9	25.37	22	saturated	0	222.20	30.80	0.21
560	19	26_TSw2_Tptpmn	131221	760.9	25.37	22	saturated	0	205.20	29.30	0.19
561	20	26_TSw2_Tptpmn	131221	760.9	25.37	22	saturated	0	183.50	28.10	0.16
332	21	26_TSw2_Tptpmn	131221		25.4	22	saturated	0	203.20	45.80	0.22
333	22	26_TSw2_Tptpmn	131221		25.4	22	saturated	0	132.20	44.20	0.21

Specimen Inventory Number	Tests In Each Lithostratigraphic Unit	GFM 2000 Layer	Testing Group	Max. Depth (ft)	Equivalent Specimen Diameter - D (mm)	Specimen Temperature (deg. C)	Specimen Saturation	Effective Confining Pressure, (MPa), s3'	Effective Axial Stress, s1' (MPa)	Young's Modulus (GPa)	Poisson's Ratio
334	23	26_TSw2_Tptpmn	131221		25.4	22	saturated	0	113.30	34.90	0.21
335	24	26_TSw2_Tptpmn	131221		25.4	22	saturated	0	274.30	47.30	0.19
336	25	26_TSw2_Tptpmn	131221		25.4	22	saturated	0	198.60	42.50	0.14
337	26	26_TSw2_Tptpmn	131221		25.4	22	saturated	0	241.30	47.20	0.19
572	27	26_TSw2_Tptpmn	131221	865.4	25.4	22	saturated	0	215.80	34.30	0.20
573	28	26_TSw2_Tptpmn	131221	865.4	25.4	22	saturated	0	232.00	33.50	0.19
574	29	26_TSw2_Tptpmn	131221	865.4	25.4	22	saturated	0	239.10	34.90	0.22
575	30	26_TSw2_Tptpmn	131221	865.4	25.4	22	saturated	0	248.50	35.70	0.21
							Average:	0.03	222.70	34.90	0.21
							Std. Dev.:	0.05	42.42	5.58	0.03
Group 4	6										
547	1	26_TSw2_Tptpmn	131222	686.6	25.32	22	saturated	5	161.00	40.50	0.16
548	2	26_TSw2_Tptpmn	131222	686.6	25.35	22	saturated	5	92.00	43.60	0.30
576	3	26_TSw2_Tptpmn	131222	865.4	25.4	22	saturated	5	259.80	35.00	0.20
577	4	26_TSw2_Tptpmn	131222	865.4	25.4	22	saturated	5	322.30	34.50	0.21
578	5	26_TSw2_Tptpmn	131222	865.4	25.4	22	saturated	5	255.10	34.00	0.18
579	6	26_TSw2_Tptpmn	131222	865.4	25.4	22	saturated	5	231.60	36.80	0.21
							Average:	5	220.30	37.40	0.21
							Std. Dev.:	0	81.58	3.85	0.05
Group 5	6										
549	1	26_TSw2_Tptpmn	131223	686.6	25.32	22	saturated	10	354.00	38.00	0.23
550	2	26_TSw2_Tptpmn	131223	686.6	25.35	22	saturated	10	370.00	35.00	0.25
580	3	26_TSw2_Tptpmn	131223	865.4	25.4	22	saturated	10	325.20	32.30	0.19
581	4	26_TSw2_Tptpmn	131223	865.4	25.4	22	saturated	10	354.00	34.00	0.21
582	5	26_TSw2_Tptpmn	131223	865.4	25.4	22	saturated	10	235.50	32.00	0.25
583	6	26_TSw2_Tptpmn	131223	865.4	25.4	22	saturated	10	316.70	34.10	0.22
							Average:	10	325.90	34.23	0.23
							Std. Dev.:	0	48.54	2.17	0.02
Group 6	3										
551	1	26_TSw2_Tptpmn	131231	742.8	25.32	22	saturated	0.1	319.10	37.40	0.29
552	2	26_TSw2_Tptpmn	131231	742.8	25.32	22	saturated	0.1	283.10	34.00	0.28
553	3	26_TSw2_Tptpmn	131231	742.8	25.32	22	saturated	0.1	280.10	38.40	0.25
							Average:	0.1	294.10	36.60	0.27
							Std. Dev.:	0	21.70	2.31	0.02
Group 7	4										
338	1	26_TSw2_Tptpmn	211211		50.8	22	dry	0	78.10	32.10	0.12
339	2	26_TSw2_Tptpmn	211211		50.8	22	dry	0	157.10	37.00	0.18
340	3	26_TSw2_Tptpmn	211211		50.8	22	dry	0	185.50	42.20	0.20
341	4	26_TSw2_Tptpmn	211211		50.8	22	dry	0	182.80	40.60	0.17
							Average:	0	150.88	37.98	0.17
							Std. Dev.:	0	50.18	4.48	0.03
Group 8	4										
342	1	26_TSw2_Tptpmn	211221		50.8	22	dry	0	166.10	41.90	0.18
343	2	26_TSw2_Tptpmn	211221		50.8	22	dry	0	135.20	33.70	0.24
344	3	26_TSw2_Tptpmn	211221		50.8	22	dry	0	87.00	45.70	0.32
345	4	26_TSw2_Tptpmn	211221		50.8	22	dry	0	102.00	40.90	0.18
							Average:	0	122.58	40.55	0.23
							Std. Dev.:	0	35.32	5.01	0.07
Group 9	3										
346	1	26_TSw2_Tptpmn	211222		50.8	22	dry	5	160.40	33.70	0.17
347	2	26_TSw2_Tptpmn	211222		50.8	22	dry	5	203.60	40.70	0.20
348	3	26_TSw2_Tptpmn	211222		50.8	22	dry	5	225.20	37.90	0.21
							Average:	5	196.40	37.43	0.19
							Std. Dev.:	0	32.99	3.52	0.02
Group 10	3										
349	1	26_TSw2_Tptpmn	211223		50.8	22	dry	10	314.50	40.80	0.19
350	2	26_TSw2_Tptpmn	211223		50.8	22	dry	10	192.80	33.10	0.24
351	3	26_TSw2_Tptpmn	211223		50.8	22	dry	10	198.00	32.80	0.18

Specimen Inventory Number	Tests In Each Lithostratigraphic Unit	GFM 2000 Layer	Testing Group	Max. Depth (ft)	Equivalent Specimen Diameter - D (mm)	Specimen Temperature (deg. C)	Specimen Saturation	Effective Confining Pressure, (MPa), s3'	Effective Axial Stress, s1' (MPa)	Young's Modulus (GPa)	Poisson's Ratio
							Average:	10	235.10	35.57	0.20
							Std. Dev.:	0	68.81	4.53	0.03
Group 11	9										
352	1	26_TSw2_Tptpmn	212211		50.8	150	dry	0	115.00	39.30	0.10
353	2	26_TSw2_Tptpmn	212211		50.8	150	dry	0	85.00	41.80	0.04
354	3	26_TSw2_Tptpmn	212211		50.8	150	dry	0	152.00	36.70	0.14
355	4	26_TSw2_Tptpmn	212211		50.8	150	dry	0	148.00	37.70	0.13
356	5	26_TSw2_Tptpmn	212211		50.8	150	dry	0	103.00	42.00	0.11
358	6	26_TSw2_Tptpmn	212211		50.8	150	dry	0	78.00	33.10	0.05
359	7	26_TSw2_Tptpmn	212211		50.8	150	dry	0	129.00	36.30	0.06
360	8	26_TSw2_Tptpmn	212211		50.8	150	dry	0	96.00	37.20	0.09
357	9	26_TSw2_Tptpmn	212211		50.9	150	dry	0	45.00	152.40	0.33
							Average:	0	105.67	50.72	0.12
							Std. Dev.:	0	34.54	38.23	0.09
Group 12	2										
361	1	26_TSw2_Tptpmn	212221		50.8	150	dry	0	109.00	37.50	0.15
362	2	26_TSw2_Tptpmn	212221		50.8	150	dry	0	72.00	37.70	0.12
							Average:	0	90.50	37.60	0.14
							Std. Dev.:	0	26.16	0.14	0.02
Group 13	3										
363	1	26_TSw2_Tptpmn	212223		50.8	150	dry	10	229.00	37.20	0.14
364	2	26_TSw2_Tptpmn	212223		50.8	150	dry	10	238.00	37.50	0.16
365	3	26_TSw2_Tptpmn	212223		50.8	150	dry	10	122.00	34.60	0.13
							Average:	10	196.33	36.43	0.14
							Std. Dev.:	0	64.53	1.59	0.02
Group 14	2										
366	1	26_TSw2_Tptpmn	212231		50.8	150	dry	0	174.00	38.20	0.15
367	2	26_TSw2_Tptpmn	212231		50.8	150	dry	0	29.00	14.00	0.37
							Average:	0	101.50	26.10	0.26
							Std. Dev.:	0	102.53	17.11	0.16
Group 15	16										
442	1	26_TSw2_Tptpmn	221221		38.1	22	ambient	0	123.10	34.50	0.34
443	2	26_TSw2_Tptpmn	221221		38.1	22	ambient	0	175.60	40.00	0.19
444	3	26_TSw2_Tptpmn	221221		38.1	22	ambient	0	159.00	31.60	0.17
445	4	26_TSw2_Tptpmn	221221		38.1	22	ambient	0	268.30	37.40	0.20
447	5	26_TSw2_Tptpmn	221221		38.1	22	ambient	0	179.40	43.10	0.18
448	6	26_TSw2_Tptpmn	221221		38.1	22	ambient	0	201.00	38.50	0.21
449	7	26_TSw2_Tptpmn	221221		38.1	22	ambient	0	232.60	38.20	0.19
450	8	26_TSw2_Tptpmn	221221		38.1	22	ambient	0	114.10	39.30	0.19
451	9	26_TSw2_Tptpmn	221221		38.1	22	ambient	0	97.20	36.20	0.22
452	10	26_TSw2_Tptpmn	221221		38.1	22	ambient	0	178.00	37.80	0.20
453	11	26_TSw2_Tptpmn	221221		38.1	22	ambient	0	128.00	34.50	0.19
454	12	26_TSw2_Tptpmn	221221		38.1	22	ambient	0	71.30	40.20	0.17
455	13	26_TSw2_Tptpmn	221221		38.1	22	ambient	0	324.10	37.80	0.19
456	14	26_TSw2_Tptpmn	221221		38.1	22	ambient	0	172.20	28.90	0.18
457	15	26_TSw2_Tptpmn	221221		38.1	22	ambient	0	158.60	34.80	0.22
458	16	26_TSw2_Tptpmn	221221		38.1	22	ambient	0	239.10	35.40	0.18
							Average:	0	176.35	36.76	0.20
							Std. Dev.:	0	65.82	3.48	0.04
Group 16	1										
525	1	26_TSw2_Tptpmn	221231	723.0	56	22	ambient	0	138.00	40.40	0.22
							Average:	0	138.00	40.40	0.22
							Std. Dev.:				
Group 17	36										
481	1	26_TSw2_Tptpmn	221321		38.1	22	ambient	0	78.70	26.60	0.39
482	2	26_TSw2_Tptpmn	221321		38.1	22	ambient	0	159.20	28.90	0.18
483	3	26_TSw2_Tptpmn	221321		38.1	22	ambient	0	51.80	20.10	0.25
484	4	26_TSw2_Tptpmn	221321		38.1	22	ambient	0	144.90	37.00	0.26

Specimen Inventory Number	Tests In Each Lithostratigraphic Unit	GFM 2000 Layer	Testing Group	Max. Depth (ft)	Equivalent Specimen Diameter - D (mm)	Specimen Temperature (deg. C)	Specimen Saturation	Effective Confining Pressure, (MPa), s3'	Effective Axial Stress, s1' (MPa)	Young's Modulus (GPa)	Poisson's Ratio
485	5	26_TSw2_Tptpmn	221321		38.1	22	ambient	0	240.50	34.00	0.18
486	6	26_TSw2_Tptpmn	221321		38.1	22	ambient	0	245.70	34.40	0.19
487	7	26_TSw2_Tptpmn	221321		38.1	22	ambient	0	191.40	32.90	0.18
488	8	26_TSw2_Tptpmn	221321		38.1	22	ambient	0	34.30	33.40	0.17
489	9	26_TSw2_Tptpmn	221321		38.1	22	ambient	0	113.90	32.30	0.17
490	10	26_TSw2_Tptpmn	221321		38.1	22	ambient	0	175.40	34.40	0.19
491	11	26_TSw2_Tptpmn	221321		38.1	22	ambient	0	38.70	24.20	0.12
492	12	26_TSw2_Tptpmn	221321		38.1	22	ambient	0	137.00	34.20	0.17
493	13	26_TSw2_Tptpmn	221321		38.1	22	ambient	0	80.50	34.30	0.16
494	14	26_TSw2_Tptpmn	221321		38.1	22	ambient	0	183.50	35.40	0.17
459	15	26_TSw2_Tptpmn	221321		41.9	22	ambient	0	171.50	35.90	0.18
460	16	26_TSw2_Tptpmn	221321		41.9	22	ambient	0	113.20	36.30	0.16
461	17	26_TSw2_Tptpmn	221321		41.9	22	ambient	0	190.80	33.50	0.15
462	18	26_TSw2_Tptpmn	221321		41.9	22	ambient	0	149.50	32.70	0.16
463	19	26_TSw2_Tptpmn	221321		41.9	22	ambient	0	79.40	31.50	0.16
464	20	26_TSw2_Tptpmn	221321		41.9	22	ambient	0	118.40	29.10	0.15
465	21	26_TSw2_Tptpmn	221321		41.9	22	ambient	0	171.00	30.10	0.16
466	22	26_TSw2_Tptpmn	221321		41.9	22	ambient	0	141.50	32.60	0.22
467	23	26_TSw2_Tptpmn	221321		41.9	22	ambient	0	161.20	32.30	0.19
468	24	26_TSw2_Tptpmn	221321		41.9	22	ambient	0	75.10	25.70	0.18
469	25	26_TSw2_Tptpmn	221321		41.9	22	ambient	0	218.90	30.70	0.16
470	26	26_TSw2_Tptpmn	221321		41.9	22	ambient	0	232.10	31.60	0.17
471	27	26_TSw2_Tptpmn	221321		41.9	22	ambient	0	243.80	30.20	0.16
472	28	26_TSw2_Tptpmn	221321		41.9	22	ambient	0	179.80	29.80	0.15
473	29	26_TSw2_Tptpmn	221321		41.9	22	ambient	0	150.50	27.30	0.17
474	30	26_TSw2_Tptpmn	221321		41.9	22	ambient	0	108.90	36.70	0.16
475	31	26_TSw2_Tptpmn	221321		41.9	22	ambient	0	83.40	34.70	0.15
476	32	26_TSw2_Tptpmn	221321		41.9	22	ambient	0	126.80	33.70	0.15
477	33	26_TSw2_Tptpmn	221321		41.9	22	ambient	0	82.80	33.90	0.16
478	34	26_TSw2_Tptpmn	221321		41.9	22	ambient	0	123.30	35.40	0.15
479	35	26_TSw2_Tptpmn	221321		41.9	22	ambient	0	76.50	33.40	0.17
480	36	26_TSw2_Tptpmn	221321		41.9	22	ambient	0	151.00	35.70	0.17
							Average:	0	139.58	32.08	0.18
							Std. Dev.:	0	58.07	3.74	0.04
Group 18	1										
526	1	26_TSw2_Tptpmn	222234	739.0	56	200	ambient	20.7	153.70	23.90	0.15
							Average:	20.7	153.70	23.90	0.15
							Std. Dev.:				
Group 19	10										
368	1	26_TSw2_Tptpmn	231211		50.8	22	saturated	0	94.30	42.10	0.21
369	2	26_TSw2_Tptpmn	231211		50.8	22	saturated	0	149.00	44.50	0.23
370	3	26_TSw2_Tptpmn	231211		50.8	22	saturated	0	145.80	37.10	0.18
371	4	26_TSw2_Tptpmn	231211		50.8	22	saturated	0	134.90	36.70	0.19
372	5	26_TSw2_Tptpmn	231211		50.8	22	saturated	0	97.40	34.10	0.11
373	6	26_TSw2_Tptpmn	231211		50.8	22	saturated	0	87.20	33.60	0.12
374	7	26_TSw2_Tptpmn	231211		50.8	22	saturated	0	108.50	38.10	0.16
375	8	26_TSw2_Tptpmn	231211		50.8	22	saturated	0	45.30	26.10	
376	9	26_TSw2_Tptpmn	231211		50.8	22	saturated	0	81.20	32.40	0.01
377	10	26_TSw2_Tptpmn	231211		50.8	22	saturated	0	92.90	38.80	0.13
							Average:	0	103.65	36.35	0.15
							Std. Dev.:	0	32.07	5.19	0.07
Group 20	42										
381	1	26_TSw2_Tptpmn	231221		50	20	saturated	0	53.70	18.60	0.07
382	2	26_TSw2_Tptpmn	231221		50	20	saturated	0	107.00	28.60	0.14
383	3	26_TSw2_Tptpmn	231221		50	20	saturated	0	62.40	21.70	0.11
378	4	26_TSw2_Tptpmn	231221		50.8	22	saturated	0	109.00	28.71	0.17
379	5	26_TSw2_Tptpmn	231221		50.8	22	saturated	0	143.00	34.17	0.18
380	6	26_TSw2_Tptpmn	231221		50.8	22	saturated	0	153.00	31.52	0.20
384	7	26_TSw2_Tptpmn	231221		50.8	22	saturated	0	126.80	34.60	0.21

Specimen Inventory Number	Tests In Each Lithostratigraphic Unit	GFM 2000 Layer	Testing Group	Max. Depth (ft)	Equivalent Specimen Diameter - D (mm)	Specimen Temperature (deg. C)	Specimen Saturation	Effective Confining Pressure, (MPa), s3'	Effective Axial Stress, s1' (MPa)	Young's Modulus (GPa)	Poisson's Ratio
385	8	26_TSw2_Tptpmn	231221		50.8	22	saturated	0	143.20	35.90	0.20
386	9	26_TSw2_Tptpmn	231221		50.8	22	saturated	0	158.40	37.40	0.20
387	10	26_TSw2_Tptpmn	231221		50.8	22	saturated	0	200.50	45.70	0.20
388	11	26_TSw2_Tptpmn	231221		50.8	22	saturated	0	111.70	34.60	0.21
389	12	26_TSw2_Tptpmn	231221		50.8	22	saturated	0	104.30	34.60	0.20
527	13	26_TSw2_Tptpmn	231221	847.2	50.8	22	saturated	0	84.20	35.20	0.21
528	14	26_TSw2_Tptpmn	231221	849.4	50.8	22	saturated	0	240.80	37.00	0.19
529	15	26_TSw2_Tptpmn	231221	861.2	50.8	22	saturated	0	55.30	17.10	0.23
530	16	26_TSw2_Tptpmn	231221	873.4	50.8	22	saturated	0	38.40	13.40	0.30
531	17	26_TSw2_Tptpmn	231221	887.2	50.8	22	saturated	0	240.90	40.50	0.20
532	18	26_TSw2_Tptpmn	231221	888.8	50.8	22	saturated	0	288.90	39.40	0.19
533	19	26_TSw2_Tptpmn	231221	891.9	50.8	22	saturated	0	253.50	38.30	0.15
534	20	26_TSw2_Tptpmn	231221	896.5	50.8	22	saturated	0	184.70	39.10	0.10
564	21	26_TSw2_Tptpmn	231221	720.7	50.80	22	saturated	0	235.50	37.10	0.19
565	22	26_TSw2_Tptpmn	231221	742.3	50.80	22	saturated	0	162.30	30.60	0.20
566	23	26_TSw2_Tptpmn	231221	742.9	50.80	22	saturated	0	212.80	32.40	0.22
567	24	26_TSw2_Tptpmn	231221	762.9	50.80	22	saturated	0	112.10	29.20	0.18
568	25	26_TSw2_Tptpmn	231221	773.5	50.80	22	saturated	0	117.40	36.20	0.23
569	26	26_TSw2_Tptpmn	231221	784.8	50.80	22	saturated	0	223.00	29.70	0.17
570	27	26_TSw2_Tptpmn	231221	785.6	50.80	22	saturated	0	218.60	30.10	0.16
571	28	26_TSw2_Tptpmn	231221	806.8	50.80	22	saturated	0	261.90	31.70	0.16
584	29	26_TSw2_Tptpmn	231221	777.0	50.8	22	saturated	0	143.80	32.90	0.22
585	30	26_TSw2_Tptpmn	231221	800.2	50.8	22	saturated	0	179.20		
586	31	26_TSw2_Tptpmn	231221	806.3	50.8	22	saturated	0	225.40	36.70	0.19
587	32	26_TSw2_Tptpmn	231221	818.5	50.8	22	saturated	0	126.30	33.10	0.20
588	33	26_TSw2_Tptpmn	231221	859.2	50.8	22	saturated	0	118.80	38.80	0.20
592	34	26_TSw2_Tptpmn	231221	734.7	50.8	22	saturated	0	193.30	31.90	0.18
593	35	26_TSw2_Tptpmn	231221	781.1	50.8	22	saturated	0	198.20	36.70	0.21
596	36	26_TSw2_Tptpmn	231221	761.5	50.8	22	saturated	0	231.50	33.90	0.21
597	37	26_TSw2_Tptpmn	231221	768.7	50.8	22	saturated	0	254.50	36.90	0.20
598	38	26_TSw2_Tptpmn	231221	771.7	50.8	22	saturated	0	160.80	34.80	0.19
599	39	26_TSw2_Tptpmn	231221	774.6	50.8	22	saturated	0	60.10	16.80	0.19
600	40	26_TSw2_Tptpmn	231221	826.7	50.8	22	saturated	0	224.90	31.90	0.21
601	41	26_TSw2_Tptpmn	231221	832.8	50.8	22	saturated	0	183.30	29.80	0.19
602	42	26_TSw2_Tptpmn	231221	842.1	50.8	22	saturated	0	208.90	36.30	0.20
							Average:	0	164.58	32.53	0.19
							Std. Dev.:	0	65.62	6.74	0.04
Group 21	5										
390	1	26_TSw2_Tptpmn	231222		50.8	22	saturated	5	174.70	36.80	0.20
391	2	26_TSw2_Tptpmn	231222		50.8	22	saturated	5	203.70	37.10	0.21
392	3	26_TSw2_Tptpmn	231222		50.8	22	saturated	5	174.00	35.50	0.21
589	4	26_TSw2_Tptpmn	231222	861.7	50.8	22	saturated	5	250.80	33.90	0.21
594	5	26_TSw2_Tptpmn	231222	745.6	50.8	22	saturated	5	335.70	34.50	0.20
							Average:	5	227.78	35.56	0.21
							Std. Dev.:	0	67.95	1.40	0.01
Group 22	14										
396	1	26_TSw2_Tptpmn	231223		50	20	saturated	10	191.60	29.70	0.15
398	2	26_TSw2_Tptpmn	231223		50	20	saturated	10	230.10	33.00	0.14
403	3	26_TSw2_Tptpmn	231223		50	20	saturated	10	49.70	21.70	0.11
393	4	26_TSw2_Tptpmn	231223		50.8	22	saturated	10	191.00	30.75	0.19
394	5	26_TSw2_Tptpmn	231223		50.8	22	saturated	10	171.00	28.07	0.12
395	6	26_TSw2_Tptpmn	231223		50.8	22	saturated	10	115.00	32.72	0.21
397	7	26_TSw2_Tptpmn	231223		50.8	22	saturated	10	196.50	32.50	0.19
399	8	26_TSw2_Tptpmn	231223		50.8	22	saturated	10	127.30	30.00	0.18
400	9	26_TSw2_Tptpmn	231223		50.8	22	saturated	10	203.30	32.90	0.18
401	10	26_TSw2_Tptpmn	231223		50.8	22	saturated	10	163.60		
402	11	26_TSw2_Tptpmn	231223		50.8	22	saturated	10	161.70	35.20	0.19
590	12	26_TSw2_Tptpmn	231223	805.6	50.8	22	saturated	10	147.10	21.40	0.27
591	13	26_TSw2_Tptpmn	231223	827.4	50.8	22	saturated	10	135.30	23.40	0.33

Specimen Inventory Number	Tests In Each Lithostratigraphic Unit	GFM 2000 Layer	Testing Group	Max. Depth (ft)	Equivalent Specimen Diameter - D (mm)	Specimen Temperature (deg. C)	Specimen Saturation	Effective Confining Pressure, (MPa), s3'	Effective Axial Stress, s1' (MPa)	Young's Modulus (GPa)	Poisson's Ratio
595	14	26_TSw2_Tptpmn	231223	762.6	50.8	22	saturated	10	282.80	34.10	0.20
							Average:	10	169.00	29.65	0.19
							Std. Dev.:	0	55.61	4.69	0.06
Group 23	5										
407	1	26_TSw2_Tptpmn	231224		50	20	saturated	20	272.40	31.50	0.15
408	2	26_TSw2_Tptpmn	231224		50	20	saturated	20	176.30	19.80	0.20
404	3	26_TSw2_Tptpmn	231224		50.8	22	saturated	20	212.00	28.38	0.16
405	4	26_TSw2_Tptpmn	231224		50.8	22	saturated	20	180.00	31.17	0.21
406	5	26_TSw2_Tptpmn	231224		50.8	22	saturated	20	232.00	29.58	0.20
							Average:	20	214.54	28.09	0.18
							Std. Dev.:	0	39.73	4.80	0.03
Group 24	4										
409	1	26_TSw2_Tptpmn	231231		50.8	22	saturated	0	120.20	33.30	0.18
410	2	26_TSw2_Tptpmn	231231		50.8	22	saturated	0	169.00	36.80	0.19
411	3	26_TSw2_Tptpmn	231231		50.8	22	saturated	0	95.50	33.10	0.23
412	4	26_TSw2_Tptpmn	231231		50.8	22	saturated	0	68.10	26.90	0.18
							Average:	0	113.20	32.53	0.20
							Std. Dev.:	0	42.86	4.12	0.02
Group 25	11										
610	1	26_TSw2_Tptpmn	232211	NA	50.75	125	saturated	0.5	203.50	39.70	0.23
611	2	26_TSw2_Tptpmn	232211	NA	50.75	125	saturated	0.5	184.50	35.90	0.18
612	3	26_TSw2_Tptpmn	232211	NA	50.75	125	saturated	0.5	229.50	41.10	0.24
608	4	26_TSw2_Tptpmn	232211	NA	50.83	125	saturated	0.5	217.23	42.20	0.30
609	5	26_TSw2_Tptpmn	232211	NA	50.83	125	saturated	0.5	166.08	32.70	0.15
613	6	26_TSw2_Tptpmn	232211	NA	50.83	125	saturated	0.5	214.50	36.30	0.16
603	7	26_TSw2_Tptpmn	232211	764.8	50.8	150	saturated	1	226.90	31.20	0.20
604	8	26_TSw2_Tptpmn	232211	774.6	50.8	150	saturated	1	148.30	33.30	0.15
605	9	26_TSw2_Tptpmn	232211	775.8	50.8	150	saturated	1	176.70	39.90	0.23
606	10	26_TSw2_Tptpmn	232211	832.8	50.8	150	saturated	1	192.80	29.60	0.20
607	11	26_TSw2_Tptpmn	232211	842.1	50.8	150	saturated	1	204.70	31.20	0.20
							Average:	0.727	196.79	35.74	0.20
							Std. Dev.:	0.261	25.85	4.45	0.05
Group 26	6										
614	1	26_TSw2_Tptpmn	232212	764.8	50.8	150	saturated	5	213.30	32.50	0.26
615	2	26_TSw2_Tptpmn	232212	774.6	50.8	150	saturated	5	207.30	33.50	0.18
616	3	26_TSw2_Tptpmn	232212	815.9	50.8	150	saturated	5	339.20	35.00	0.23
617	4	26_TSw2_Tptpmn	232212	828.9	50.8	150	saturated	5	234.90	29.40	0.20
618	5	26_TSw2_Tptpmn	232212	832.8	50.8	150	saturated	5	248.90	22.30	0.15
619	6	26_TSw2_Tptpmn	232212	842.1	50.8	150	saturated	5	277.70	32.30	0.23
							Average:	5	253.55	30.83	0.21
							Std. Dev.:	0	49.09	4.57	0.04
Group 27	5										
620	1	26_TSw2_Tptpmn	232213	766.0	50.8	150	saturated	10	205.80	31.00	0.18
621	2	26_TSw2_Tptpmn	232213	775.8	50.8	150	saturated	10	275.90	34.60	0.22
622	3	26_TSw2_Tptpmn	232213	817.1	50.8	150	saturated	10	329.40	34.50	0.22
623	4	26_TSw2_Tptpmn	232213	828.9	50.8	150	saturated	10	243.50	27.70	0.20
624	5	26_TSw2_Tptpmn	232213	836.3	50.8	150	saturated	10	214.70	29.70	0.17
							Average:	10	253.86	31.50	0.20
							Std. Dev.:	0	50.36	3.02	0.02
Group 28	4										
413	1	26_TSw2_Tptpmn	232221		50.8	150	saturated	0	129.70	32.60	
414	2	26_TSw2_Tptpmn	232221		50.8	150	saturated	0	135.80	30.60	
415	3	26_TSw2_Tptpmn	232221		50.8	150	saturated	0	114.60	32.70	
416	4	26_TSw2_Tptpmn	232221		50.8	150	saturated	0	89.40	28.00	
							Average:	0	117.38	30.98	
							Std. Dev.:	0	20.67	2.21	
Group 29	3										
417	1	26_TSw2_Tptpmn	232222		50.8	150	saturated	5	160.20	33.90	

Specimen Inventory Number	Tests In Each Lithostratigraphic Unit	GFM 2000 Layer	Testing Group	Max. Depth (ft)	Equivalent Specimen Diameter - D (mm)	Specimen Temperature (deg. C)	Specimen Saturation	Effective Confining Pressure, (MPa), s3'	Effective Axial Stress, s1' (MPa)	Young's Modulus (GPa)	Poisson's Ratio
418	2	26_TSw2_Tptpmn	232222		50.8	150	saturated	5	52.90	16.00	
419	3	26_TSw2_Tptpmn	232222		50.8	150	saturated	5	150.20	35.90	
							Average:	5	121.10	28.60	
							Std. Dev.:	0	59.27	10.96	
Group 30	1										
446	1	26_TSw2_Tptpmn	321221		145.5	24	ambient	0	159.60	32.40	0.17
							Average:	0	159.60	32.40	0.17
							Std. Dev.:				
Group 31	22										
420	1	26_TSw2_Tptpmn	331221		82.6	22	saturated	0	160.70	43.80	0.22
423	2	26_TSw2_Tptpmn	331221		82.6	22	saturated	0	140.70	42.90	0.23
426	3	26_TSw2_Tptpmn	331221		82.6	22	saturated	0	58.86	32.30	0.21
436	4	26_TSw2_Tptpmn	331221		82.6	22	saturated	0	141.70	43.90	0.23
437	5	26_TSw2_Tptpmn	331221		82.6	22	saturated	0	99.76	38.80	0.19
438	6	26_TSw2_Tptpmn	331221		82.6	22	saturated	0	130.60	44.50	0.25
439	7	26_TSw2_Tptpmn	331221		82.6	22	saturated	0	87.69	37.60	0.22
440	8	26_TSw2_Tptpmn	331221		82.6	22	saturated	0	124.30	46.00	0.24
441	9	26_TSw2_Tptpmn	331221		82.6	22	saturated	0	131.80	44.00	0.22
421	10	26_TSw2_Tptpmn	331221		127.0	22	saturated	0	134.30	41.20	
424	11	26_TSw2_Tptpmn	331221		127.0	22	saturated	0	85.84	39.80	0.25
425	12	26_TSw2_Tptpmn	331221		127.0	22	saturated	0	170.80	45.10	0.20
427	13	26_TSw2_Tptpmn	331221		127.0	22	saturated	0	90.41	30.60	0.27
428	14	26_TSw2_Tptpmn	331221		127.0	22	saturated	0	98.81	37.70	0.21
430	15	26_TSw2_Tptpmn	331221		127.0	22	saturated	0	59.91	25.30	
431	16	26_TSw2_Tptpmn	331221		127.0	22	saturated	0	84.25	32.10	0.18
432	17	26_TSw2_Tptpmn	331221		127.0	22	saturated	0	92.40	35.70	0.18
433	18	26_TSw2_Tptpmn	331221		127.0	22	saturated	0	98.16	36.30	0.20
434	19	26_TSw2_Tptpmn	331221		127.0	22	saturated	0	89.77	33.00	0.22
435	20	26_TSw2_Tptpmn	331221		127.0	22	saturated	0	69.67	31.60	0.17
422	21	26_TSw2_Tptpmn	331221		228.6	22	saturated	0	86.92	37.40	0.22
429	22	26_TSw2_Tptpmn	331221		228.6	22	saturated	0	93.36	42.10	0.21
							Average:	0	105.94	38.26	0.22
							Std. Dev.:	0	31.11	5.66	0.03
Group 32	14										
199	1	26_TSw2_Tptpmn	231121		51.6	Ambient	Saturated	-14.50	0.0		
200	2	26_TSw2_Tptpmn	231121		51.6	Ambient	Saturated	-13.00	0.0		
201	3	26_TSw2_Tptpmn	231121		51.6	Ambient	Saturated	-9.30	0.0		
202	4	26_TSw2_Tptpmn	231121		51.6	Ambient	Saturated	-7.90	0.0		
203	5	26_TSw2_Tptpmn	231121		51.6	Ambient	Saturated	-12.50	0.0		
204	6	26_TSw2_Tptpmn	231121		51.6	Ambient	Saturated	-14.10	0.0		
205	7	26_TSw2_Tptpmn	231121		51.6	Ambient	Saturated	-4.30	0.0		
206	8	26_TSw2_Tptpmn	231121		51.6	Ambient	Saturated	-6.10	0.0		
207	9	26_TSw2_Tptpmn	231121		51.6	Ambient	Saturated	-7.70	0.0		
208	10	26_TSw2_Tptpmn	231121		51.6	Ambient	Saturated	-5.70	0.0		
209	11	26_TSw2_Tptpmn	231121		51.6	Ambient	Saturated	-11.60	0.0		
210	12	26_TSw2_Tptpmn	231121		51.6	Ambient	Saturated	-16.80	0.0		
211	13	26_TSw2_Tptpmn	231121		51.6	Ambient	Saturated	-15.90	0.0		
212	14	26_TSw2_Tptpmn	231121		51.6	Ambient	Saturated	-12.90	0.0		
							Average:	-10.88	0.00		
							Std_Dev:	4.02			
Group 1	16										
626	1	27_TSw2_Tptpll	121221		26.09	25	ambient	0	209.80	32.90	0.16
625	2	27_TSw2_Tptpll	121221		26.12	25	ambient	0	230.00	32.40	0.17
627	3	27_TSw2_Tptpll	121221		26.12	25	ambient	0	203.50	33.50	0.20
628	4	27_TSw2_Tptpll	121221		26.14	25	ambient	0	220.30	32.70	0.18
634	5	27_TSw2_Tptpll	121221		26.17	25	ambient	0	192.70	34.60	0.17
630	6	27_TSw2_Tptpll	121221		26.20	25	ambient	0	174.10	29.60	0.17
631	7	27_TSw2_Tptpll	121221		26.20	25	ambient	0	146.90	29.10	0.16
632	8	27_TSw2_Tptpll	121221		26.20	25	ambient	0	110.90	26.00	0.12

Specimen Inventory Number	Tests In Each Lithostratigraphic Unit	GFM 2000 Layer	Testing Group	Max. Depth (ft)	Equivalent Specimen Diameter - D (mm)	Specimen Temperature (deg. C)	Specimen Saturation	Effective Confining Pressure, (MPa), s3'	Effective Axial Stress, s1' (MPa)	Young's Modulus (GPa)	Poisson's Ratio
637	9	27_TSw2_Tptpll	121221		26.20	25	ambient	0	198.70	31.20	0.17
638	10	27_TSw2_Tptpll	121221		26.21	25	ambient	0	261.70	38.10	0.20
629	11	27_TSw2_Tptpll	121221		26.22	25	ambient	0	179.60	29.70	0.16
636	12	27_TSw2_Tptpll	121221		26.23	25	ambient	0	213.20	33.60	0.18
635	13	27_TSw2_Tptpll	121221		26.24	25	ambient	0	179.50	32.40	0.16
639	14	27_TSw2_Tptpll	121221		26.24	25	ambient	0	154.20	33.00	0.19
633	15	27_TSw2_Tptpll	121221		26.25	25	ambient	0	192.80	31.00	0.18
640	16	27_TSw2_Tptpll	121221		26.25	25	ambient	0	247.20	36.40	0.18
							Average:	0	194.69	32.26	0.17
							Std. Dev.:	0	37.99	2.91	0.02
Group 2	2										
784	1	27_TSw2_Tptpll	131211	1002.4	25.32	22	saturated	0.1	123.10	22.00	0.11
785	2	27_TSw2_Tptpll	131211	1002.4	25.32	22	saturated	0.1	138.10	32.80	0.20
							Average:	0.1	130.60	27.40	0.16
							Std. Dev.:	0	10.61	7.64	0.06
Group 3	30										
772	1	27_TSw2_Tptpll	131221	1297.6	25.2	22	saturated	0	3.00		
780	2	27_TSw2_Tptpll	131221	1579.1	25.2	22	saturated	0	175.00	31.80	0.17
773	3	27_TSw2_Tptpll	131221	1297.6	25.3	22	saturated	0	7.00		
774	4	27_TSw2_Tptpll	131221	1561.3	25.3	22	saturated	0	85.00	22.10	0.11
775	5	27_TSw2_Tptpll	131221	1561.3	25.3	22	saturated	0	73.00	22.00	0.17
776	6	27_TSw2_Tptpll	131221	1561.3	25.3	22	saturated	0	86.00	22.70	
777	7	27_TSw2_Tptpll	131221	1561.3	25.3	22	saturated	0	61.00	23.60	
778	8	27_TSw2_Tptpll	131221	1579.1	25.3	22	saturated	0	170.00	33.90	0.17
779	9	27_TSw2_Tptpll	131221	1579.1	25.3	22	saturated	0	97.00	18.80	0.18
781	10	27_TSw2_Tptpll	131221	1579.1	25.3	22	saturated	0	96.00	20.50	0.19
782	11	27_TSw2_Tptpll	131221	1587.8	25.3	22	saturated	0	165.00	35.90	0.20
783	12	27_TSw2_Tptpll	131221	1587.8	25.3	22	saturated	0	155.00	35.50	0.16
789	13	27_TSw2_Tptpll	131221	1002.4	25.30	22	saturated	0.1	179.10	33.60	0.32
790	14	27_TSw2_Tptpll	131221	1002.4	25.30	22	saturated	0.1	137.10	31.10	
791	15	27_TSw2_Tptpll	131221	1065.8	25.30	22	saturated	0.1	12.10	2.44	
794	16	27_TSw2_Tptpll	131221	911.3	25.30	22	saturated	0.1	160.10	37.60	0.36
786	17	27_TSw2_Tptpll	131221	1001.9	25.32	22	saturated	0.1	99.10	22.80	0.19
787	18	27_TSw2_Tptpll	131221	1001.9	25.32	22	saturated	0.1	170.10	32.70	0.20
788	19	27_TSw2_Tptpll	131221	1001.9	25.32	22	saturated	0.1	147.10	31.80	0.18
793	20	27_TSw2_Tptpll	131221	910.7	25.32	22	saturated	0.1	131.10	30.10	0.18
796	21	27_TSw2_Tptpll	131221	911.3	25.32	22	saturated	0.1	118.10	26.00	0.19
797	22	27_TSw2_Tptpll	131221	965.2	25.32	22	saturated	0.1	187.10	38.00	0.21
798	23	27_TSw2_Tptpll	131221	965.2	25.32	22	saturated	0.1	131.10	31.10	0.18
799	24	27_TSw2_Tptpll	131221	965.2	25.32	22	saturated	0.1	148.10	33.10	0.19
792	25	27_TSw2_Tptpll	131221	1065.8	25.35	22	saturated	0.1	124.10	26.70	0.21
795	26	27_TSw2_Tptpll	131221	911.3	25.35	22	saturated	0.1	88.10	24.80	0.15
764	27	27_TSw2_Tptpll	131221	1021.8	26.1	22	saturated	0.1	75.30	25.50	0.25
765	28	27_TSw2_Tptpll	131221	1060.8	26.1	22	saturated	0.1	142.90	38.10	0.32
766	29	27_TSw2_Tptpll	131221	1096.0	26.1	22	saturated	0.1	59.90	24.90	0.15
767	30	27_TSw2_Tptpll	131221	1154.9	26.1	22	saturated	0.1	106.30	32.50	0.33
							Average:	0.060	112.99	28.20	0.21
							Std. Dev.:	0.050	51.38	7.63	0.06
Group 4	3										
768	1	27_TSw2_Tptpll	131222	1154.9	26.1	22	saturated	5	77.50	19.20	0.14
769	2	27_TSw2_Tptpll	131222	1163.6	26.1	22	saturated	5	224.30	35.60	0.30
770	3	27_TSw2_Tptpll	131222	1179.6	26.1	22	saturated	5	114.70	23.20	0.32
							Average:	5	138.83	26.00	0.25
							Std. Dev.:	0	76.32	8.55	0.10
Group 5	3										
800	1	27_TSw2_Tptpll	131223	965.2	25.32	22	saturated	10	107.00	14.10	0.21
801	2	27_TSw2_Tptpll	131223	965.2	25.32	22	saturated	10	257.00	32.70	0.28
771	3	27_TSw2_Tptpll	131223	1189.0	26.1	22	saturated	10	129.30	25.60	0.30
							Average:	10	164.43	24.13	0.26

Specimen Inventory Number	Tests In Each Lithostratigraphic Unit	GFM 2000 Layer	Testing Group	Max. Depth (ft)	Equivalent Specimen Diameter - D (mm)	Specimen Temperature (deg. C)	Specimen Saturation	Effective Confining Pressure, (MPa), s3'	Effective Axial Stress, s1' (MPa)	Young's Modulus (GPa)	Poisson's Ratio
							Std. Dev.:	0	80.94	9.39	0.05
Group 6	7										
644	1	27_TSw2_Tptpll	211221		51.00	25	dry	0	165.60	37.30	0.18
643	2	27_TSw2_Tptpll	211221		51.02	25	dry	0	175.20	36.70	0.16
641	3	27_TSw2_Tptpll	211221		51.03	25	dry	0	205.20	37.80	0.19
645	4	27_TSw2_Tptpll	211221		51.03	25	dry	0	197.20	38.40	0.19
642	5	27_TSw2_Tptpll	211221		51.05	25	dry	0	176.70	36.40	0.17
646	6	27_TSw2_Tptpll	211221		51.05	25	dry	0	152.20	32.70	0.17
647	7	27_TSw2_Tptpll	211221		51.05	25	dry	0	159.40	33.30	0.17
							Average:	0	175.93	36.09	0.17
							Std. Dev.:	0	19.38	2.22	0.01
Group 7	6										
649	1	27_TSw2_Tptpll	212221		51.00	200	dry	0	217.70	36.80	
650	2	27_TSw2_Tptpll	212221		51.03	200	dry	0	200.50	37.50	
648	3	27_TSw2_Tptpll	212221		51.04	200	dry	0	208.80	39.40	
653	4	27_TSw2_Tptpll	212221		51.04	200	dry	0	225.50	36.10	
651	5	27_TSw2_Tptpll	212221		51.05	200	dry	0	200.30	35.30	
652	6	27_TSw2_Tptpll	212221		51.05	200	dry	0	226.30	37.70	
							Average:	0	213.18	37.13	
							Std. Dev.:	0	11.75	1.42	
Group 8	59										
802	1	27_TSw2_Tptpll	221221	853.4	57.05	22	ambient	0	144.90	26.80	
803	2	27_TSw2_Tptpll	221221	874.6	57.18	22	ambient	0	50.90	24.50	
686	3	27_TSw2_Tptpll	221221		50.88	25	ambient	0	133.40	35.80	0.17
683	4	27_TSw2_Tptpll	221221		50.90	25	ambient	0	201.00	37.40	0.21
685	5	27_TSw2_Tptpll	221221		50.91	25	ambient	0	135.70	35.30	0.20
693	6	27_TSw2_Tptpll	221221		50.94	25	ambient	0	114.90	29.00	0.14
706	7	27_TSw2_Tptpll	221221		50.96	25	ambient	0	191.10	34.80	0.18
684	8	27_TSw2_Tptpll	221221		50.97	25	ambient	0	187.90	36.70	0.20
694	9	27_TSw2_Tptpll	221221		50.97	25	ambient	0	203.80	40.20	0.19
695	10	27_TSw2_Tptpll	221221		50.97	25	ambient	0	168.50	38.00	0.22
696	11	27_TSw2_Tptpll	221221		50.97	25	ambient	0	198.70	37.90	0.21
700	12	27_TSw2_Tptpll	221221		50.98	25	ambient	0	145.60	33.50	0.20
709	13	27_TSw2_Tptpll	221221		50.98	25	ambient	0	104.80	30.90	0.16
698	14	27_TSw2_Tptpll	221221		50.99	25	ambient	0	228.70	40.00	0.20
701	15	27_TSw2_Tptpll	221221		50.99	25	ambient	0	170.30	37.90	0.20
703	16	27_TSw2_Tptpll	221221		50.99	25	ambient	0	162.00	35.20	0.19
704	17	27_TSw2_Tptpll	221221		50.99	25	ambient	0	137.60	34.80	0.16
707	18	27_TSw2_Tptpll	221221		50.99	25	ambient	0	88.60	30.60	0.21
654	19	27_TSw2_Tptpll	221221		51.00	25	ambient	0	246.60	40.70	0.20
655	20	27_TSw2_Tptpll	221221		51.00	25	ambient	0	208.10	38.70	0.20
659	21	27_TSw2_Tptpll	221221		51.00	25	ambient	0	202.10	37.60	0.19
660	22	27_TSw2_Tptpll	221221		51.00	25	ambient	0	109.20	30.90	0.17
662	23	27_TSw2_Tptpll	221221		51.00	25	ambient	0	161.70	37.00	0.19
664	24	27_TSw2_Tptpll	221221		51.00	25	ambient	0	213.60	37.30	0.18
665	25	27_TSw2_Tptpll	221221		51.00	25	ambient	0	168.50	35.50	0.20
697	26	27_TSw2_Tptpll	221221		51.00	25	ambient	0	119.20	33.00	0.23
681	27	27_TSw2_Tptpll	221221		51.01	25	ambient	0	153.20	32.10	0.19
657	28	27_TSw2_Tptpll	221221		51.02	25	ambient	0	242.50	41.30	0.20
658	29	27_TSw2_Tptpll	221221		51.02	25	ambient	0	149.50	36.60	0.18
679	30	27_TSw2_Tptpll	221221		51.02	25	ambient	0	121.90	30.50	0.16
680	31	27_TSw2_Tptpll	221221		51.02	25	ambient	0	115.20	29.80	0.17
656	32	27_TSw2_Tptpll	221221		51.03	25	ambient	0	123.90	33.90	0.18
663	33	27_TSw2_Tptpll	221221		51.03	25	ambient	0	135.20	36.00	0.18
667	34	27_TSw2_Tptpll	221221		51.03	25	ambient	0	118.60	33.10	0.16
668	35	27_TSw2_Tptpll	221221		51.03	25	ambient	0	162.80	34.60	0.18
676	36	27_TSw2_Tptpll	221221		51.03	25	ambient	0	92.40	26.60	0.21
688	37	27_TSw2_Tptpll	221221		51.03	25	ambient	0	154.00	35.90	0.20
705	38	27_TSw2_Tptpll	221221		51.03	25	ambient	0	130.00	32.20	0.21

Specimen Inventory Number	Tests In Each Lithostratigraphic Unit	GFM 2000 Layer	Testing Group	Max. Depth (ft)	Equivalent Specimen Diameter - D (mm)	Specimen Temperature (deg. C)	Specimen Saturation	Effective Confining Pressure, (MPa), s3'	Effective Axial Stress, s1' (MPa)	Young's Modulus (GPa)	Poisson's Ratio
661	39	27_TSw2_Tptpll	221221		51.04	25	ambient	0	163.60	34.70	0.17
675	40	27_TSw2_Tptpll	221221		51.04	25	ambient	0	157.20	32.50	0.19
678	41	27_TSw2_Tptpll	221221		51.04	25	ambient	0	87.40	27.30	0.16
687	42	27_TSw2_Tptpll	221221		51.04	25	ambient	0	137.70	34.70	0.21
689	43	27_TSw2_Tptpll	221221		51.04	25	ambient	0	194.50	40.40	0.19
708	44	27_TSw2_Tptpll	221221		51.04	25	ambient	0	122.00	37.00	0.18
670	45	27_TSw2_Tptpll	221221		51.05	25	ambient	0	133.70	32.50	0.18
671	46	27_TSw2_Tptpll	221221		51.05	25	ambient	0	121.20	31.40	0.16
672	47	27_TSw2_Tptpll	221221		51.05	25	ambient	0	113.70	32.50	0.17
673	48	27_TSw2_Tptpll	221221		51.05	25	ambient	0	114.40	28.70	0.16
674	49	27_TSw2_Tptpll	221221		51.05	25	ambient	0	143.20	35.00	0.18
677	50	27_TSw2_Tptpll	221221		51.05	25	ambient	0	164.90	34.70	0.18
690	51	27_TSw2_Tptpll	221221		51.05	25	ambient	0	196.60	37.20	0.20
691	52	27_TSw2_Tptpll	221221		51.05	25	ambient	0	155.90	36.40	0.17
692	53	27_TSw2_Tptpll	221221		51.05	25	ambient	0	164.30	39.10	0.19
702	54	27_TSw2_Tptpll	221221		51.05	25	ambient	0	158.10	37.30	0.17
682	55	27_TSw2_Tptpll	221221		51.06	25	ambient	0	109.90	31.10	0.16
699	56	27_TSw2_Tptpll	221221		51.06	25	ambient	0	142.50	33.00	0.16
666	57	27_TSw2_Tptpll	221221		51.07	25	ambient	0	192.60	36.50	0.20
669	58	27_TSw2_Tptpll	221221		51.07	25	ambient	0	175.80	34.40	0.19
710	59	27_TSw2_Tptpll	221221		51.07	25	ambient	0	188.30	37.70	0.19
							Average:	0	153.12	34.52	0.19
							Std. Dev.:	0	40.06	3.75	0.02
Group 9	15										
804	1	27_TSw2_Tptpll	231221	1017.8	50.80	22	saturated	0	84.90	27.40	0.23
805	2	27_TSw2_Tptpll	231221	848.0	50.80	22	saturated	0	175.50	34.60	0.19
806	3	27_TSw2_Tptpll	231221	953.2	50.80	22	saturated	0	31.60	16.90	0.11
807	4	27_TSw2_Tptpll	231221	963.3	50.80	22	saturated	0	56.30	19.30	0.31
808	5	27_TSw2_Tptpll	231221	971.4	50.80	22	saturated	0	97.30	27.40	0.19
809	6	27_TSw2_Tptpll	231221	985.7	50.80	22	saturated	0	177.30	37.60	0.25
810	7	27_TSw2_Tptpll	231221	1230.2	50.8	22	saturated	0	117.20	29.80	0.23
811	8	27_TSw2_Tptpll	231221	1236.7	50.8	22	saturated	0	61.00	21.80	0.40
711	9	27_TSw2_Tptpll	231221		51.00	25	saturated	0	121.00	28.40	0.23
712	10	27_TSw2_Tptpll	231221		51.00	25	saturated	0	135.40	34.70	0.16
713	11	27_TSw2_Tptpll	231221		51.03	25	saturated	0	179.10	35.50	0.18
716	12	27_TSw2_Tptpll	231221		51.03	25	saturated	0	158.10	34.20	0.20
717	13	27_TSw2_Tptpll	231221		51.04	25	saturated	0	135.10	31.30	0.23
714	14	27_TSw2_Tptpll	231221		51.05	25	saturated	0	150.70	34.60	0.23
715	15	27_TSw2_Tptpll	231221		51.05	25	saturated	0	164.70	36.10	0.19
							Average:	0	123.01	29.97	0.22
							Std. Dev.:	0	47.57	6.43	0.07
Group 10	1										
812	188	27_TSw2_Tptpll	231223	977.8	50.8	22	saturated	10	216.90	29.60	0.20
							Average:	10	216.90	29.60	0.20
							Std. Dev.:				
Group 11	2										
752	1	27_TSw2_Tptpll	312111		289	195	dry	0	32.20	7.10	
750	2	27_TSw2_Tptpll	312111		289	200	dry	0	31.10	6.50	
							Average:	0	31.65	6.80	
							Std. Dev.:	0	0.78	0.42	
Group 12	5										
718	1	27_TSw2_Tptpll	312221		81.89	200	dry	0	54.10	23.10	0.35
720	2	27_TSw2_Tptpll	312221		81.89	200	dry	0	196.10	39.90	0.10
721	3	27_TSw2_Tptpll	312221		81.89	200	dry	0	173.10	40.50	0.19
719	4	27_TSw2_Tptpll	312221		81.94	200	dry	0	162.00	34.20	0.13
761	5	27_TSw2_Tptpll	312221		146.9	200	dry	0	28.30	7.10	
							Average:	0	122.72	28.96	0.19
							Std. Dev.:	0	75.98	14.08	0.11

Specimen Inventory Number	Tests In Each Lithostratigraphic Unit	GFM 2000 Layer	Testing Group	Max. Depth (ft)	Equivalent Specimen Diameter - D (mm)	Specimen Temperature (deg. C)	Specimen Saturation	Effective Confining Pressure, (MPa), s3'	Effective Axial Stress, s1' (MPa)	Young's Modulus (GPa)	Poisson's Ratio
Group 13	7										
760	1	27_TSw2_Tptpll	321211		145.70	22	ambient	0	34.20	14.60	0.20
759	2	27_TSw2_Tptpll	321211		145.80	22	ambient	0	67.40	21.00	0.20
757	3	27_TSw2_Tptpll	321211		146.20	22	ambient	0	43.60	12.40	
758	4	27_TSw2_Tptpll	321211		146.80	22	ambient	0	33.10	12.00	0.34
751	5	27_TSw2_Tptpll	321211		288	24	ambient	0	21.70	8.50	
753	6	27_TSw2_Tptpll	321211		288	24	ambient	0	28.70	9.20	
754	7	27_TSw2_Tptpll	321211		288	24	ambient	0	13.30	5.00	
							Average:	0	34.57	11.81	0.25
							Std. Dev.:	0	17.39	5.11	0.08
Group 14	25										
762	1	27_TSw2_Tptpll	321221		146.3	24	ambient	0	28.10	9.60	0.32
756	2	27_TSw2_Tptpll	321221		146.6	24	ambient	0	44.90	12.50	
743	3	27_TSw2_Tptpll	321221		81.86	25	ambient	0	122.10	36.30	0.20
739	4	27_TSw2_Tptpll	321221		81.89	25	ambient	0	139.80	35.40	0.23
725	5	27_TSw2_Tptpll	321221		81.92	25	ambient	0	169.00	39.10	0.18
722	6	27_TSw2_Tptpll	321221		81.94	25	ambient	0	149.60	36.30	0.20
726	7	27_TSw2_Tptpll	321221		81.94	25	ambient	0	124.60	35.50	0.19
728	8	27_TSw2_Tptpll	321221		81.99	25	ambient	0	138.90	29.40	0.16
729	9	27_TSw2_Tptpll	321221		81.99	25	ambient	0	179.50	36.50	0.20
731	10	27_TSw2_Tptpll	321221		81.99	25	ambient	0	61.00	23.00	0.17
740	11	27_TSw2_Tptpll	321221		81.99	25	ambient	0	180.00	39.90	0.20
735	12	27_TSw2_Tptpll	321221		82.22	25	ambient	0	120.80	33.60	0.17
734	13	27_TSw2_Tptpll	321221		82.24	25	ambient	0	145.00	38.30	0.19
736	14	27_TSw2_Tptpll	321221		82.27	25	ambient	0	150.80	41.50	0.19
730	15	27_TSw2_Tptpll	321221		120.60	25	ambient	0	108.70	33.70	0.18
738	16	27_TSw2_Tptpll	321221		120.60	25	ambient	0	124.70	36.60	0.19
741	17	27_TSw2_Tptpll	321221		120.60	25	ambient	0	97.70	35.90	0.22
742	18	27_TSw2_Tptpll	321221		120.60	25	ambient	0	111.30	36.40	0.21
744	19	27_TSw2_Tptpll	321221		120.60	25	ambient	0	141.30	41.60	0.22
723	20	27_TSw2_Tptpll	321221		120.70	25	ambient	0	151.30	39.70	0.21
724	21	27_TSw2_Tptpll	321221		120.70	25	ambient	0	105.90	35.00	0.19
727	22	27_TSw2_Tptpll	321221		120.70	25	ambient	0	128.30	39.00	0.19
732	23	27_TSw2_Tptpll	321221		120.70	25	ambient	0	64.40	25.80	0.10
733	24	27_TSw2_Tptpll	321221		120.70	25	ambient	0	114.30	31.60	0.16
737	25	27_TSw2_Tptpll	321221		120.70	25	ambient	0	128.90	39.10	0.20
							Average:	0	121.24	33.65	0.19
							Std. Dev.:	0	38.69	8.13	0.04
Group 15	1										
755	1	27_TSw2_Tptpll	331211		288	24	saturated	0	15.70	5.30	
							Average:	0	15.70	5.30	
							Std. Dev.:				
Group 16	1										
763	1	27_TSw2_Tptpll	331221		146.9	24	saturated	0	38.00	10.90	
							Average:	0	38.00	10.90	
							Std. Dev.:				
Group 17	5										
747	1	27_TSw2_Tptpll	421221		217	25	ambient	0	47.00	26.40	
745	2	27_TSw2_Tptpll	421221		223	25	ambient	0	27.00	25.30	
748	3	27_TSw2_Tptpll	421221		223	25	ambient	0	71.70	35.00	
746	4	27_TSw2_Tptpll	421221		231	25	ambient	0	65.60	33.80	
749	5	27_TSw2_Tptpll	421221		245	25	ambient	0	92.20	37.50	
							Average:	0	60.70	31.60	
							Std. Dev.:	0	24.80	5.43	
18	24										
213	1	27_TSw2_Tptpll	231121	27	51.6	Ambient	Saturated	-7.90	0.0		
214	2	27_TSw2_Tptpll	231121	27	51.6	Ambient	Saturated	-11.00	0.0		
215	3	27_TSw2_Tptpll	231121	27	51.6	Ambient	Saturated	-14.30	0.0		

Specimen Inventory Number	Tests In Each Lithostratigraphic Unit	GFM 2000 Layer	Testing Group	Max. Depth (ft)	Equivalent Specimen Diameter - D (mm)	Specimen Temperature (deg. C)	Specimen Saturation	Effective Confining Pressure, (MPa), s3'	Effective Axial Stress, s1' (MPa)	Young's Modulus (GPa)	Poisson's Ratio
216	4	27_TSw2_Tptpll	231121	27	51.6	Ambient	Saturated	-12.10	0.0		
217	5	27_TSw2_Tptpll	231121	27	51.6	Ambient	Saturated	-8.80	0.0		
218	6	27_TSw2_Tptpll	231121	27	51.6	Ambient	Saturated	-4.00	0.0		
219	7	27_TSw2_Tptpll	231121	27	51.6	Ambient	Saturated	-10.80	0.0		
220	8	27_TSw2_Tptpll	231121	27	51.6	Ambient	Saturated	-5.30	0.0		
221	9	27_TSw2_Tptpll	231121	27	51.6	Ambient	Saturated	-11.20	0.0		
222	10	27_TSw2_Tptpll	231121	27	51.6	Ambient	Saturated	-11.50	0.0		
223	11	27_TSw2_Tptpll	231121	27	51.6	Ambient	Saturated	-3.20	0.0		
224	12	27_TSw2_Tptpll	231121	27	51.6	Ambient	Saturated	-7.50	0.0		
225	13	27_TSw2_Tptpll	231121	27	51.6	Ambient	Saturated	-11.70	0.0		
226	14	27_TSw2_Tptpll	231121	27	51.6	Ambient	Saturated	-5.50	0.0		
227	15	27_TSw2_Tptpll	231121	27	51.6	Ambient	Saturated	-6.30	0.0		
228	16	27_TSw2_Tptpll	231121	27	51.6	Ambient	Saturated	-5.20	0.0		
229	17	27_TSw2_Tptpll	231121	27	51.6	Ambient	Saturated	-6.20	0.0		
230	18	27_TSw2_Tptpll	231121	27	51.6	Ambient	Saturated	-10.20	0.0		
231	19	27_TSw2_Tptpll	231121	27	51.6	Ambient	Saturated	-10.40	0.0		
232	20	27_TSw2_Tptpll	231121	27	51.6	Ambient	Saturated	-6.60	0.0		
233	21	27_TSw2_Tptpll	231121	27	51.6	Ambient	Saturated	-7.00	0.0		
234	22	27_TSw2_Tptpll	231121	27	51.6	Ambient	Saturated	-5.30	0.0		
235	23	27_TSw2_Tptpll	231121	27	51.6	Ambient	Saturated	-8.60	0.0		
236	24	27_TSw2_Tptpll	231121	27	51.6	Ambient	Saturated	-9.20	0.0		
							Average:	-8.33	0.00		
							Std_Dev:	2.93			
Group 1	3										
816	1	28_TSw2_Tptpln	131211	1218.2	26.1	22	saturated	0.1	176.70	40.80	0.25
817	2	28_TSw2_Tptpln	131211	1223.7	26.1	22	saturated	0.1	156.70	35.30	0.21
818	3	28_TSw2_Tptpln	131211	1279.5	26.1	22	saturated	0.1	45.00	22.90	0.27
							Average:	0.1	126.13	33.00	0.24
							Std. Dev.:	0	70.97	9.17	0.03
Group 2	10										
823	1	28_TSw2_Tptpln	131221	1307.2	25.27	22	saturated	0.1	104.10	30.20	0.23
824	2	28_TSw2_Tptpln	131221	1307.2	25.27	22	saturated	0.1	79.10	22.80	0.20
825	3	28_TSw2_Tptpln	131221	1307.2	25.27	22	saturated	0.1	31.10	20.00	0.30
826	4	28_TSw2_Tptpln	131221	1307.2	25.27	22	saturated	0.1	65.10	16.60	0.24
827	5	28_TSw2_Tptpln	131221	1307.2	25.27	22	saturated	0.1	98.10	34.90	0.20
828	6	28_TSw2_Tptpln	131221	1050.4	25.35	22	saturated	0	131.30	35.50	0.18
829	7	28_TSw2_Tptpln	131221	1050.4	25.35	22	saturated	0	147.70	36.10	0.19
830	8	28_TSw2_Tptpln	131221	1050.4	25.35	22	saturated	0	152.10	36.30	0.19
831	9	28_TSw2_Tptpln	131221	1067.8	25.35	22	saturated	0	115.30	32.70	0.24
832	10	28_TSw2_Tptpln	131221	1067.8	25.35	22	saturated	0	120.10	32.10	0.24
							Average:	0.050	104.40	29.72	0.22
							Std. Dev.:	0.053	37.77	7.25	0.04
Group 3	4										
819	1	28_TSw2_Tptpln	131231	1222.1	26.1	22	saturated	0.1	157.30	29.20	0.31
820	2	28_TSw2_Tptpln	131231	1222.1	26.1	22	saturated	0.1	133.90	27.70	
821	3	28_TSw2_Tptpln	131231	1223.7	26.1	22	saturated	0.1	157.30	37.50	0.25
822	4	28_TSw2_Tptpln	131231	1262.4	26.1	22	saturated	0.1	149.80	36.60	
							Average:	0.1	149.58	32.75	0.28
							Std. Dev.:	0	11.03	5.02	0.04
Group 4	2										
833	1	28_TSw2_Tptpln	221221	1067.8	57.18	22	ambient	0	172.90	34.40	0.20
834	2	28_TSw2_Tptpln	221221	1067.8	57.18	22	ambient	0	170.20	35.70	0.23
							Average:	0	171.55	35.05	0.22
							Std. Dev.:	0	1.91	0.92	0.02
Group 5	1										
813	1	28_TSw2_Tptpln	221231	1250.0	56	22	ambient	0	166.00	61.80	0.30
							Average:	0	166.00	61.80	0.30
							Std. Dev.:				

Specimen Inventory Number	Tests In Each Lithostratigraphic Unit	GFM 2000 Layer	Testing Group	Max. Depth (ft)	Equivalent Specimen Diameter - D (mm)	Specimen Temperature (deg. C)	Specimen Saturation	Effective Confining Pressure, (MPa), s3'	Effective Axial Stress, s1' (MPa)	Young's Modulus (GPa)	Poisson's Ratio
Group 6	1										
814	1	28_TSw2_Tptpln	221233	1250.0	56	22	ambient	10	422.00	73.00	0.23
							Average:	10	422.00	73.00	0.23
							Std. Dev.:				
Group 7	1										
815	1	28_TSw2_Tptpln	221234	1250.0	56	22	ambient	20	638.00	59.90	0.21
							Average:	20	638.00	59.90	0.21
							Std. Dev.:				
Group 8	10										
835	1	28_TSw2_Tptpln	231221	1252.3	50.8	22	saturated	0	82.90	30.40	0.14
836	2	28_TSw2_Tptpln	231221	1257.8	50.8	22	saturated	0	169.30	41.80	0.20
837	3	28_TSw2_Tptpln	231221	1259.1	50.8	22	saturated	0	172.50	40.60	0.21
838	4	28_TSw2_Tptpln	231221	1265.2	50.8	22	saturated	0	192.90	40.70	0.21
839	5	28_TSw2_Tptpln	231221	1314.8	50.8	22	saturated	0	173.40	37.70	0.21
842	6	28_TSw2_Tptpln	231221	1107.1	50.8	22	saturated	0	162.00	34.50	0.23
843	7	28_TSw2_Tptpln	231221	1209.0	50.8	22	saturated	0	128.00	31.90	0.28
848	8	28_TSw2_Tptpln	231221	1243.0	50.8	22	saturated	0	158.70	35.90	0.19
849	9	28_TSw2_Tptpln	231221	1298.0	50.8	22	saturated	0	158.70	39.90	0.25
850	10	28_TSw2_Tptpln	231221	1346.5	50.8	22	saturated	0	156.70	44.40	0.25
							Average:	0	155.51	37.78	0.22
							Std. Dev.:	0	30.35	4.53	0.04
Group 9	3										
840	1	28_TSw2_Tptpln	231222	1399.1	50.8	22	saturated	5	152.60	30.80	0.22
844	2	28_TSw2_Tptpln	231222	1073.3	50.8	22	saturated	5	216.10	35.90	0.28
845	3	28_TSw2_Tptpln	231222	1112.1	50.8	22	saturated	5	280.60	36.10	0.22
							Average:	5	216.43	34.27	0.24
							Std. Dev.:	0	64.00	3.00	0.03
Group 10	3										
841	1	28_TSw2_Tptpln	231223	1400.5	50.8	22	saturated	10	261.80	39.60	0.26
846	2	28_TSw2_Tptpln	231223	1077.1	50.8	22	saturated	10	246.10	34.00	0.23
847	3	28_TSw2_Tptpln	231223	1118.9	50.8	22	saturated	10	288.90	32.90	0.21
							Average:	10	265.60	35.50	0.23
							Std. Dev.:	0	21.65	3.59	0.03
Group 11	1										
851	1	28_TSw2_Tptpln	232213	1325.4	50.8	150	saturated	10	274.50	43.90	0.12
							Average:	10	274.50	43.90	0.12
							Std. Dev.:				
Group 12	13										
237	1	28_TSw2_Tptpln	231121		51.6	Ambient	Saturated	-9.00	0.0		
238	2	28_TSw2_Tptpln	231121		51.6	Ambient	Saturated	-9.90	0.0		
239	3	28_TSw2_Tptpln	231121		51.6	Ambient	Saturated	-13.70	0.0		
240	4	28_TSw2_Tptpln	231121		51.6	Ambient	Saturated	-8.80	0.0		
241	5	28_TSw2_Tptpln	231121		51.6	Ambient	Saturated	-10.90	0.0		
242	6	28_TSw2_Tptpln	231121		51.6	Ambient	Saturated	-4.80	0.0		
243	7	28_TSw2_Tptpln	231121		51.6	Ambient	Saturated	-5.90	0.0		
244	8	28_TSw2_Tptpln	231121		51.6	Ambient	Saturated	-7.60	0.0		
245	9	28_TSw2_Tptpln	231121		51.6	Ambient	Saturated	-7.60	0.0		
246	10	28_TSw2_Tptpln	231121		51.6	Ambient	Saturated	-6.10	0.0		
247	11	28_TSw2_Tptpln	231121		51.6	Ambient	Saturated	-6.30	0.0		
248	12	28_TSw2_Tptpln	231121		51.6	Ambient	Saturated	-4.80	0.0		
249	13	28_TSw2_Tptpln	231121		51.6	Ambient	Saturated	-7.60	0.0		
							Average:	-7.92	0.00		
							Std_Dev:	2.55			
Group 1	4										
852	1	29_TSw3_Tptpv3	131223	1646.8	25.3	22	saturated	10	42.00		
853	2	29_TSw3_Tptpv3	131223	1646.8	25.3	22	saturated	10	37.00		
854	3	29_TSw3_Tptpv3	131223	1659.2	25.3	22	saturated	10	78.00		
855	4	29_TSw3_Tptpv3	131223	1659.2	25.3	22	saturated	10	63.00		

Specimen Inventory Number	Tests In Each Lithostratigraphic Unit	GFM 2000 Layer	Testing Group	Max. Depth (ft)	Equivalent Specimen Diameter - D (mm)	Specimen Temperature (deg. C)	Specimen Saturation	Effective Confining Pressure, (MPa), s3'	Effective Axial Stress, s1' (MPa)	Young's Modulus (GPa)	Poisson's Ratio
							Average:	10	55.00		
							Std. Dev.:	0	19.03		
Group 2	2										
856	1	29_TSw3_Tptpv3	221221	1195.1	57.15	22	ambient	0	49.80	36.60	
857	2	29_TSw3_Tptpv3	221221	1197.5	57.15	22	ambient	0	41.80	31.90	0.18
							Average:	0	45.80	34.25	0.18
							Std. Dev.:	0	5.66	3.32	
Group 3	1										
858	3	29_TSw3_Tptpv3	231221	1299.9	50.8	22	saturated	0	16.40	25.20	0.39
							Average:	0	16.40	25.20	0.39
							Std. Dev.:				
Group 4	1										
859	1	29_TSw3_Tptpv3	231222	1279.7	50.8	22	saturated	5	52.20	54.20	0.17
							Average:	5	52.20	54.20	0.17
							Std. Dev.:				
Group 5	1										
860	1	29_TSw3_Tptpv3	231223	1284.2	50.8	22	saturated	10	80.00	32.90	0.17
							Average:	10	80.00	32.90	0.17
							Std. Dev.:				
Group 1	2										
861	1	30_CHn1_Tptpv2	131221	1280.6	25.37	22	saturated	0	92.80	16.80	0.18
862	2	30_CHn1_Tptpv2	131221	1280.6	25.35	22	saturated	0	90.50	16.10	0.21
							Average:	0	91.65	16.45	0.20
							Std. Dev.:	0	1.63	0.49	0.02
Group 2	1										
863	1	30_CHn1_Tptpv2	221221	1280.6	57.15	22	ambient	0	90.20	16.70	0.22
							Average:	0	90.20	16.70	0.22
							Std. Dev.:				
Group 1	2										
864	1	31_CHn1_Tptpv1	131211	1369.1	25.27	22	saturated	0.1	8.10	1.41	0.17
865	2	31_CHn1_Tptpv1	131211	1369.1	25.27	22	saturated	0.1	12.10	3.10	0.17
							Average:	0.1	10.10	2.26	0.17
							Std. Dev.:	0	2.83	1.20	0.00
Group 2	5										
868	1	31_CHn1_Tptpv1	131221	1369.1	25.25	22	saturated	0.1	6.10	1.53	0.19
866	2	31_CHn1_Tptpv1	131221	1369.1	25.27	22	saturated	0.1	11.10	2.21	0.21
867	3	31_CHn1_Tptpv1	131221	1369.1	25.30	22	saturated	0.1	14.10	3.70	0.14
869	4	31_CHn1_Tptpv1	131221	1400.6	25.30	22	saturated	0.1	19.10	2.32	0.18
870	5	31_CHn1_Tptpv1	131221	1400.6	25.32	22	saturated	0.1	14.10	2.25	0.18
							Average:	0.1	12.90	2.40	0.18
							Std. Dev.:	0.00	4.76	0.79	0.03
Group 3	2										
871	1	31_CHn1_Tptpv1	131222	1400.6	25.32	22	saturated	5	22.00	3.10	0.21
872	2	31_CHn1_Tptpv1	131222	1400.6	25.32	22	saturated	5	34.00	3.68	0.20
							Average:	5	28.00	3.39	0.21
							Std. Dev.:	0	8.49	0.41	0.01
Group 4	2										
873	1	31_CHn1_Tptpv1	131223	1400.6	25.32	22	saturated	10	26.00	3.14	0.30
874	2	31_CHn1_Tptpv1	131223	1400.6	25.32	22	saturated	10	42.00	4.35	0.30
							Average:	10	34.00	3.75	0.30
							Std. Dev.:	0	11.31	0.86	0.00
Group 5	3										
875	1	31_CHn1_Tptpv1	131231	1369.1	25.27	22	saturated	0.1	13.10	2.96	0.26
876	2	31_CHn1_Tptpv1	131231	1369.1	25.27	22	saturated	0.1	8.10	1.76	0.16
877	3	31_CHn1_Tptpv1	131231	1369.1	25.30	22	saturated	0.1	15.10	3.37	0.12
							Average:	0.1	12.10	2.70	0.18
							Std. Dev.:	0	3.61	0.84	0.07

Specimen Inventory Number	Tests In Each Lithostratigraphic Unit	GFM 2000 Layer	Testing Group	Max. Depth (ft)	Equivalent Specimen Diameter - D (mm)	Specimen Temperature (deg. C)	Specimen Saturation	Effective Confining Pressure, (MPa), s3'	Effective Axial Stress, s1' (MPa)	Young's Modulus (GPa)	Poisson's Ratio
Group 1	3										
878	1	32_CHn1_Tpbt1	131211	1748.0	25.3	22	saturated	0	28.00	14.20	0.10
879	2	32_CHn1_Tpbt1	131211	1748.0	25.3	22	saturated	0	27.00	11.20	
880	3	32_CHn1_Tpbt1	131211	1748.0	25.3	22	saturated	0	28.00	11.10	0.11
							Average:	0	27.67	12.17	0.11
							Std. Dev.:	0	0.58	1.76	0.01
Group 2	4										
881	1	32_CHn1_Tpbt1	131221	1725.1	25.3	22	saturated	0	22.00	6.30	0.24
882	2	32_CHn1_Tpbt1	131221	1725.1	25.3	22	saturated	0	29.00	8.50	0.10
883	3	32_CHn1_Tpbt1	131221	1748.0	25.3	22	saturated	0	23.00	11.00	0.22
884	4	32_CHn1_Tpbt1	131221	1748.0	25.3	22	saturated	0	35.00	11.20	0.23
							Average:	0	27.25	9.25	0.20
							Std. Dev.:	0	6.02	2.32	0.07
Group 3	1										
885	1	32_CHn1_Tpbt1	231221	1477.2	50.8	22	saturated	0	20.50	3.90	0.11
							Average:	0	20.50	3.90	0.11
							Std. Dev.:				
Group 1	2										
891	1	33_CHn1_Tac	121221	1665.5	25.4	22	ambient	0.1	41.10	8.12	0.29
892	2	33_CHn1_Tac	121221	1665.5	25.4	22	ambient	0.1	32.80	6.50	0.31
							Average:	0.1	36.95	7.31	0.30
							Std. Dev.:	0	5.87	1.15	0.01
Group 2	2										
893	1	33_CHn1_Tac	121223	1665.5	25.4	22	ambient	10	71.30	7.20	0.27
894	2	33_CHn1_Tac	121223	1665.5	25.4	22	ambient	10	67.60	7.34	0.28
							Average:	10	69.45	7.27	0.28
							Std. Dev.:	0	2.62	0.10	0.01
Group 3	2										
895	1	33_CHn1_Tac	131211	1668.1	25.4	22	saturated	0.1	21.60	7.86	0.21
896	2	33_CHn1_Tac	131211	1668.1	25.4	22	saturated	0.1	20.00	7.03	0.22
							Average:	0.1	20.80	7.45	0.22
							Std. Dev.:	0.0	1.13	0.59	0.01
Group 4	34										
913	1	33_CHn1_Tac	131221	1442.0	25.4	22	saturated	0.1	21.80	6.40	
914	2	33_CHn1_Tac	131221	1442.0	25.4	22	saturated	0.1	22.10	5.79	
915	3	33_CHn1_Tac	131221	1487.4	25.4	22	saturated	0.1	27.50		
916	4	33_CHn1_Tac	131221	1487.4	25.4	22	saturated	0.1	23.00	4.87	
917	5	33_CHn1_Tac	131221	1519.9	25.4	22	saturated	0.1	19.00	4.93	
918	6	33_CHn1_Tac	131221	1519.9	25.4	22	saturated	0.1	20.80	5.14	
919	7	33_CHn1_Tac	131221	1550.4	25.4	22	saturated	0.1	36.00	7.03	
920	8	33_CHn1_Tac	131221	1550.4	25.4	22	saturated	0.1	30.60	7.45	
921	9	33_CHn1_Tac	131221	1594.8	25.4	22	saturated	0.1	14.30	3.51	
922	10	33_CHn1_Tac	131221	1594.8	25.4	22	saturated	0.1	15.40	4.23	0.19
923	11	33_CHn1_Tac	131221	1617.0	25.4	22	saturated	0.1	26.60	7.86	0.26
924	12	33_CHn1_Tac	131221	1617.0	25.4	22	saturated	0.1	19.50	7.17	0.25
925	13	33_CHn1_Tac	131221	1665.5	25.4	22	saturated	0.1	26.30	6.86	0.18
926	14	33_CHn1_Tac	131221	1665.5	25.4	22	saturated	0.1	34.20	9.52	
927	15	33_CHn1_Tac	131221	1668.1	25.4	22	saturated	0.1	25.50	6.15	0.36
928	16	33_CHn1_Tac	131221	1668.1	25.4	22	saturated	0.1	16.80	4.92	0.18
929	17	33_CHn1_Tac	131221	1719.7	25.4	22	saturated	0.1	20.20	5.83	0.29
930	18	33_CHn1_Tac	131221	1719.7	25.4	22	saturated	0.1	27.50	7.93	0.30
897	19	33_CHn1_Tac	131221	1441.9	25.4	23	saturated	0	24.30	6.03	0.09
898	20	33_CHn1_Tac	131221	1441.9	25.4	23	saturated	0	34.20	8.84	0.07
899	21	33_CHn1_Tac	131221	1487.5	25.4	23	saturated	0	23.20	5.45	0.09
900	22	33_CHn1_Tac	131221	1487.5	25.4	23	saturated	0	45.30	9.42	0.09
901	23	33_CHn1_Tac	131221	1520.0	25.4	23	saturated	0	29.60	4.41	0.17
902	24	33_CHn1_Tac	131221	1520.0	25.4	23	saturated	0	22.60	5.61	0.10
903	25	33_CHn1_Tac	131221	1550.5	25.4	23	saturated	0	40.60	9.12	0.07

Specimen Inventory Number	Tests In Each Lithostratigraphic Unit	GFM 2000 Layer	Testing Group	Max. Depth (ft)	Equivalent Specimen Diameter - D (mm)	Specimen Temperature (deg. C)	Specimen Saturation	Effective Confining Pressure, (MPa), s3'	Effective Axial Stress, s1' (MPa)	Young's Modulus (GPa)	Poisson's Ratio
904	26	33_CHn1_Tac	131221	1550.5	25.4	23	saturated	0	53.10	12.80	0.07
905	27	33_CHn1_Tac	131221	1594.8	25.4	23	saturated	0	22.30	6.37	0.10
906	28	33_CHn1_Tac	131221	1594.8	25.4	23	saturated	0	22.30	6.60	0.09
907	29	33_CHn1_Tac	131221	1617.1	25.4	23	saturated	0	26.60	9.41	0.10
908	30	33_CHn1_Tac	131221	1617.1	25.4	23	saturated	0	42.70	11.00	0.10
909	31	33_CHn1_Tac	131221	1665.3	25.4	23	saturated	0	23.70	6.39	0.18
910	32	33_CHn1_Tac	131221	1665.3	25.4	23	saturated	0	37.60	9.85	0.14
911	33	33_CHn1_Tac	131221	1719.8	25.4	23	saturated	0	23.70	6.81	0.21
912	34	33_CHn1_Tac	131221	1719.8	25.4	23	saturated	0	34.60	9.52	0.10
							Average:	0.05	27.46	7.07	0.16
							Std. Dev.:	0.05	8.87	2.13	0.08
Group 5	8										
931	1	33_CHn1_Tac	131223	1487.4	25.4	22	saturated	10	35.40	6.85	0.34
932	2	33_CHn1_Tac	131223	1487.4	25.4	22	saturated	10	36.00	7.79	0.34
933	3	33_CHn1_Tac	131223	1487.4	25.4	22	saturated	10	39.90	5.57	
934	4	33_CHn1_Tac	131223	1487.4	25.4	22	saturated	10	41.40	6.16	0.22
935	5	33_CHn1_Tac	131223	1665.5	25.4	22	saturated	10	45.70	8.90	0.31
936	6	33_CHn1_Tac	131223	1665.5	25.4	22	saturated	10	37.60	8.48	0.30
937	7	33_CHn1_Tac	131223	1668.1	25.4	22	saturated	10	28.90	4.28	
938	8	33_CHn1_Tac	131223	1668.1	25.4	22	saturated	10	36.80	6.01	0.36
							Average:	10	37.71	6.76	0.31
							Std. Dev.:	0	4.91	1.56	0.05
Group 6	6										
939	1	33_CHn1_Tac	131224	1487.4	25.4	22	saturated	20	46.70	7.38	0.45
940	2	33_CHn1_Tac	131224	1487.4	25.4	22	saturated	20	56.10	7.93	
941	3	33_CHn1_Tac	131224	1487.4	25.4	22	saturated	20	37.10	3.92	0.18
942	4	33_CHn1_Tac	131224	1487.4	25.4	22	saturated	20	54.40	6.24	0.17
943	5	33_CHn1_Tac	131224	1665.5	25.4	22	saturated	20	54.80	9.31	
944	6	33_CHn1_Tac	131224	1665.5	25.4	22	saturated	20	56.20	9.72	0.25
							Average:	20	50.88	7.42	0.26
							Std. Dev.:	0	7.62	2.13	0.13
Group 7	2										
945	1	33_CHn1_Tac	131231	1668.1	25.4	22	saturated	0.1	24.80	5.41	0.33
946	2	33_CHn1_Tac	131231	1668.1	25.4	22	saturated	0.1	23.50	5.45	
							Average:	0.1	24.15	5.43	0.33
							Std. Dev.:	0	0.92	0.03	
Group 8	2										
886	1	33_CHn1_Tac	221231	1490.0	56	22	ambient	0	47.70	12.29	0.14
887	2	33_CHn1_Tac	221231	1692.0	56	22	ambient	0	40.80	14.02	0.20
							Average:	0	44.25	13.16	0.17
							Std. Dev.:	0	4.88	1.22	0.04
Group 9	3										
888	1	33_CHn1_Tac	221234	1605.0	56	22	ambient	20	46.10	7.99	0.22
889	2	33_CHn1_Tac	221234	1634.0	56	22	ambient	20.7	88.20	8.50	0.27
890	3	33_CHn1_Tac	221234	1662.0	56	22	ambient	20	90.30	9.57	0.25
							Average:	20.23	74.87	8.69	0.25
							Std. Dev.:	0.40	24.93	0.81	0.03
Group 10	2										
947	1	33_CHn1_Tac	231221	1499.9	50.8	22	saturated	0	26.50	6.90	0.09
948	2	33_CHn1_Tac	231221	1560.8	50.8	22	saturated	0	22.70	6.10	0.31
							Average:	0	24.60	6.50	0.20
							Std. Dev.:	0	2.69	0.57	0.16
Group 1	8										
953	1	34_CHn1_Tacbt	131221	1741.8	25.4	22	saturated	0.1	39.20	8.41	0.27
954	2	34_CHn1_Tacbt	131221	1741.8	25.4	22	saturated	0.1	42.10	8.14	0.32
955	3	34_CHn1_Tacbt	131221	1784.8	25.4	22	saturated	0.1	15.50	2.55	0.34
956	4	34_CHn1_Tacbt	131221	1784.8	25.4	22	saturated	0.1	14.90	2.52	0.37
949	5	34_CHn1_Tacbt	131221	1741.8	25.4	23	saturated	0	55.50	12.40	0.14

Specimen Inventory Number	Tests In Each Lithostratigraphic Unit	GFM 2000 Layer	Testing Group	Max. Depth (ft)	Equivalent Specimen Diameter - D (mm)	Specimen Temperature (deg. C)	Specimen Saturation	Effective Confining Pressure, (MPa), s3'	Effective Axial Stress, s1' (MPa)	Young's Modulus (GPa)	Poisson's Ratio
950	6	34_CHn1_Tacbt	131221	1741.8	25.4	23	saturated	0	70.70	12.70	0.15
951	7	34_CHn1_Tacbt	131221	1784.8	25.4	23	saturated	0	20.80	4.05	0.21
952	8	34_CHn1_Tacbt	131221	1784.8	25.4	23	saturated	0	21.60	4.61	0.20
							Average:	0.050	35.04	6.92	0.25
							Std. Dev.:	0.053	20.45	4.13	0.09

APPENDIX D
RESULTS OF TUNNEL MAPPING USING ROCK MASS RATING METHOD

Source: BSC 2004. *Rock Mass Quality Ratings and Classifications of the Combined ESF, Heated Drift and ECRB Cross-Drift*. [DIRS 176608], Appendix B.

Location	Thermal Mechanical and Lithostratigraphic Unit Designation	Begin Station (m)	End Station (m)	RQD	Mean Intact UCS, σ_{ci} (MPa)	Hoek & Brown Intact Material Constant, mi	Unit Weight of Rock Mass, γ (MN/m^3)	Depth of Tunnel, H (m)	RQD Index	C	Js	Jcd	JwR	AJO	RMR Rating = (RQD Index+C+Js+Jcd+JwR+AJ0)	RMR' = (RQD Index+C+Js+Jcd+JwR)	Geological Strength Index, GSI = (RMR' - 5)
CD	25_TSw1_Tptpul	0	5	65.0	58.22	10.60	0.021	176	13	7	15	22	15	-12	60	72	67
CD	25_TSw1_Tptpul	5	10	52.0	58.22	10.60	0.021	176	13	7	20	20	15	-12	63	75	70
CD	25_TSw1_Tptpul	10	15	62.2	58.22	10.60	0.021	175	13	7	10	25	15	-12	58	70	65
CD	25_TSw1_Tptpul	15	20	36.0	58.22	10.60	0.021	176	8	7	20	21	15	-12	59	71	66
CD	25_TSw1_Tptpul	20	25	32.4	58.22	10.60	0.021	176	8	7	15	21	15	-12	54	66	61
CD	25_TSw1_Tptpul	25	30	56.4	58.22	10.60	0.021	175	13	7	15	25	15	0	75	75	70
CD	25_TSw1_Tptpul	30	35	66.8	58.22	10.60	0.021	175	13	7	15	22	15	0	72	72	67
CD	25_TSw1_Tptpul	35	40	54.8	58.22	10.60	0.021	175	13	7	15	22	15	-5	67	72	67
CD	25_TSw1_Tptpul	40	45	63.6	58.22	10.60	0.021	175	13	7	15	23	15	0	73	73	68
CD	25_TSw1_Tptpul	45	50	67.0	58.22	10.60	0.021	175	13	7	10	18	15	-5	58	63	58
CD	25_TSw1_Tptpul	50	55	59.4	58.22	10.60	0.021	175	13	7	20	18	15	-12	61	73	68
CD	25_TSw1_Tptpul	55	60	30.2	58.22	10.60	0.021	175	8	7	15	18	15	-12	51	63	58
CD	25_TSw1_Tptpul	60	65	34.4	58.22	10.60	0.021	175	8	7	20	16	15	-12	54	66	61
CD	25_TSw1_Tptpul	65	70	52.0	58.22	10.60	0.021	175	13	7	20	13	15	0	68	68	63
CD	25_TSw1_Tptpul	70	75	28.6	58.22	10.60	0.021	175	8	7	20	21	15	0	71	71	66
CD	25_TSw1_Tptpul	75	80	43.4	58.22	10.60	0.021	175	8	7	20	13	15	0	63	63	58
CD	25_TSw1_Tptpul	80	85	60.8	58.22	10.60	0.021	175	13	7	20	21	15	-12	64	76	71
CD	25_TSw1_Tptpul	85	90	42.6	58.22	10.60	0.021	175	8	7	20	14	15	-12	52	64	59
CD	25_TSw1_Tptpul	90	95	37.8	58.22	10.60	0.021	175	8	7	15	14	15	-12	47	59	54
CD	25_TSw1_Tptpul	95	100	49.0	58.22	10.60	0.021	175	8	7	20	21	15	-12	59	71	66
CD	25_TSw1_Tptpul	100	105	35.0	58.22	10.60	0.021	175	8	7	20	18	15	0	68	68	63
CD	25_TSw1_Tptpul	105	110	18.8	58.22	10.60	0.021	175	5	7	15	21	15	0	63	63	58
CD	25_TSw1_Tptpul	110	115	28.8	58.22	10.60	0.021	175	8	7	15	21	15	0	66	66	61
CD	25_TSw1_Tptpul	115	120	32.8	58.22	10.60	0.021	175	8	7	15	20	15	0	65	65	60
CD	25_TSw1_Tptpul	120	125	20.8	58.22	10.60	0.021	175	5	7	15	20	15	0	62	62	57
CD	25_TSw1_Tptpul	125	130	24.4	58.22	10.60	0.021	176	5	7	20	23	15	0	70	70	65
CD	25_TSw1_Tptpul	130	135	51.4	58.22	10.60	0.021	176	13	7	20	25	15	0	80	80	75
CD	25_TSw1_Tptpul	135	140	19.2	58.22	10.60	0.021	176	5	7	15	20	15	-12	50	62	57
CD	25_TSw1_Tptpul	140	145	11.0	58.22	10.60	0.021	176	5	7	15	18	15	-12	48	60	55
CD	25_TSw1_Tptpul	145	150	36.0	58.22	10.60	0.021	176	8	7	15	18	15	-12	51	63	58
CD	25_TSw1_Tptpul	150	155	30.0	58.22	10.60	0.021	177	8	7	20	25	15	-12	63	75	70
CD	25_TSw1_Tptpul	155	160	31.0	58.22	10.60	0.021	177	8	7	20	25	15	-12	63	75	70
CD	25_TSw1_Tptpul	160	165	11.0	58.22	10.60	0.021	178	5	7	20	25	15	-12	60	72	67
CD	25_TSw1_Tptpul	165	170	25.4	58.22	10.60	0.021	180	8	7	20	25	15	-12	63	75	70
CD	25_TSw1_Tptpul	170	175	70.6	58.22	10.60	0.021	181	13	7	20	25	15	-12	68	80	75
CD	25_TSw1_Tptpul	175	180	44.8	58.22	10.60	0.021	182	8	7	20	23	15	-12	61	73	68
CD	25_TSw1_Tptpul	180	185	32.6	58.22	10.60	0.021	183	8	7	15	23	15	0	68	68	63
CD	25_TSw1_Tptpul	185	190	69.0	58.22	10.60	0.021	184	13	7	0	23	15	0	58	58	53
CD	25_TSw1_Tptpul	190	195	26.2	58.22	10.60	0.021	184	8	7	10	25	15	0	65	65	60

Location	Thermal Mechanical and Lithostratigraphic Unit Designation	Begin Station (m)	End Station (m)	RQD	Mean Intact UCS, σ_{ci} (MPa)	Hoek & Brown Intact Material Constant, mi	Unit Weight of Rock Mass, γ (MN/m^3)	Depth of Tunnel, H (m)	RQD Index	C	Js	Jcd	JwR	AJO	RMR Rating = (RQD Index+C+Js+Jcd+JwR+AJ0)	RMR' = (RQD Index+C+Js+Jcd+JwR)	Geological Strength Index, GSI = (RMR' - 5)
CD	25_TSw1_Tptpul	195	200	61.2	58.22	10.60	0.021	185	13	7	15	21	15	0	71	71	66
CD	25_TSw1_Tptpul	200	205	43.8	58.22	10.60	0.021	186	8	7	10	20	15	0	60	60	55
CD	25_TSw1_Tptpul	205	210	16.6	58.22	10.60	0.021	187	5	7	10	20	15	0	57	57	52
CD	25_TSw1_Tptpul	210	215	40.2	58.22	10.60	0.021	188	8	7	20	26	15	0	76	76	71
CD	25_TSw1_Tptpul	215	220	24.8	58.22	10.60	0.021	189	5	7	20	25	15	0	72	72	67
CD	25_TSw1_Tptpul	220	225	48.8	58.22	10.60	0.021	190	8	7	20	20	15	0	70	70	65
CD	25_TSw1_Tptpul	225	230	36.4	58.22	10.60	0.021	192	8	7	10	22	15	0	62	62	57
CD	25_TSw1_Tptpul	230	235	34.4	58.22	10.60	0.021	194	8	7	15	16	15	-12	49	61	56
CD	25_TSw1_Tptpul	235	240	29.2	58.22	10.60	0.021	196	8	7	15	19	15	-12	52	64	59
CD	25_TSw1_Tptpul	240	245	29.0	58.22	10.60	0.021	198	8	7	15	19	15	-12	52	64	59
CD	25_TSw1_Tptpul	245	250	38.2	58.22	10.60	0.021	200	8	7	15	20	15	-12	53	65	60
CD	25_TSw1_Tptpul	250	255	29.6	58.22	10.60	0.021	201	8	7	8	24	15	0	62	62	57
CD	25_TSw1_Tptpul	255	260	22.2	58.22	10.60	0.021	203	5	7	20	21	15	-12	56	68	63
CD	25_TSw1_Tptpul	260	265	30.0	58.22	10.60	0.021	205	8	7	20	21	15	-12	59	71	66
CD	25_TSw1_Tptpul	265	270	38.8	58.22	10.60	0.021	207	8	7	10	25	15	0	65	65	60
CD	25_TSw1_Tptpul	270	275	35.4	58.22	10.60	0.021	209	8	7	10	25	15	0	65	65	60
CD	25_TSw1_Tptpul	275	280	34.2	58.22	10.60	0.021	211	8	7	10	25	15	0	65	65	60
CD	25_TSw1_Tptpul	280	285	67.2	58.22	10.60	0.021	213	13	7	20	24	15	0	79	79	74
CD	25_TSw1_Tptpul	285	290	59.2	58.22	10.60	0.021	215	13	7	20	24	15	0	79	79	74
CD	25_TSw1_Tptpul	290	295	45.4	58.22	10.60	0.021	216	8	7	15	24	15	-12	57	69	64
CD	25_TSw1_Tptpul	295	300	47.6	58.22	10.60	0.021	215	8	7	20	23	15	-12	61	73	68
CD	25_TSw1_Tptpul	300	305	62.2	58.22	10.60	0.021	215	13	7	20	23	15	-12	66	78	73
CD	25_TSw1_Tptpul	305	310	85.0	58.22	10.60	0.021	214	17	7	20	23	15	-5	77	82	77
CD	25_TSw1_Tptpul	310	315	69.4	58.22	10.60	0.021	214	13	7	20	23	15	-12	66	78	73
CD	25_TSw1_Tptpul	315	320	10.0	58.22	10.60	0.021	214	5	7	20	23	15	-12	58	70	65
CD	25_TSw1_Tptpul	320	325	47.6	58.22	10.60	0.021	213	8	7	20	23	15	-12	61	73	68
CD	25_TSw1_Tptpul	325	330	65.6	58.22	10.60	0.021	213	13	7	20	23	15	-12	66	78	73
CD	25_TSw1_Tptpul	330	335	70.2	58.22	10.60	0.021	212	13	7	20	23	15	-12	66	78	73
CD	25_TSw1_Tptpul	335	340	93.8	58.22	10.60	0.021	212	20	7	20	23	15	-5	80	85	80
CD	25_TSw1_Tptpul	340	345	90.0	58.22	10.60	0.021	212	17	7	20	23	15	-12	70	82	77
CD	25_TSw1_Tptpul	345	350	86.2	58.22	10.60	0.021	211	17	7	20	23	15	-5	77	82	77
CD	25_TSw1_Tptpul	350	355	40.8	58.22	10.60	0.021	211	8	7	20	23	15	-5	68	73	68
CD	25_TSw1_Tptpul	355	360	51.6	58.22	10.60	0.021	210	13	7	20	23	15	-12	66	78	73
CD	25_TSw1_Tptpul	360	365	59.2	58.22	10.60	0.021	210	13	7	20	23	15	0	78	78	73
CD	25_TSw1_Tptpul	365	370	54.8	58.22	10.60	0.021	209	13	7	20	16	15	-5	66	71	66
CD	25_TSw1_Tptpul	370	375	48.4	58.22	10.60	0.021	209	8	7	20	21	15	-12	59	71	66
CD	25_TSw1_Tptpul	375	380	57.0	58.22	10.60	0.021	207	13	7	20	23	15	0	78	78	73
CD	25_TSw1_Tptpul	380	385	80.8	58.22	10.60	0.021	205	17	7	20	23	15	-12	70	82	77
CD	25_TSw1_Tptpul	385	390	60.4	58.22	10.60	0.021	204	13	7	20	21	15	0	76	76	71

Location	Thermal Mechanical and Lithostratigraphic Unit Designation	Begin Station (m)	End Station (m)	RQD	Mean Intact UCS, σ_{ci} (MPa)	Hoek & Brown Intact Material Constant, mi	Unit Weight of Rock Mass, γ (MN/m^3)	Depth of Tunnel, H (m)	RQD Index	C	Js	Jcd	JwR	AJO	RMR Rating = (RQD Index+C+Js+Jcd+JwR+AJ0)	RMR' = (RQD Index+C+Js+Jcd+JwR)	Geological Strength Index, GSI = (RMR' - 5)
CD	25_TSw1_Tptpul	390	395	53.2	58.22	10.60	0.021	202	13	7	20	21	15	-2	74	76	71
CD	25_TSw1_Tptpul	395	400	59.8	58.22	10.60	0.021	201	13	7	20	21	15	-12	64	76	71
CD	25_TSw1_Tptpul	400	405	69.2	58.22	10.60	0.021	200	13	7	15	17	15	-12	55	67	62
CD	25_TSw1_Tptpul	405	410	49.6	58.22	10.60	0.021	198	8	7	20	19	15	-12	57	69	64
CD	25_TSw1_Tptpul	410	415	40.6	58.22	10.60	0.021	197	8	7	20	19	15	0	69	69	64
CD	25_TSw1_Tptpul	415	420	20.0	58.22	10.60	0.021	196	5	7	20	22	15	0	69	69	64
CD	25_TSw1_Tptpul	420	425	26.6	58.22	10.60	0.021	194	8	7	20	20	15	-12	58	70	65
CD	25_TSw1_Tptpul	425	430	28.8	58.22	10.60	0.021	193	8	7	20	21	15	-12	59	71	66
CD	25_TSw1_Tptpul	430	435	44.4	58.22	10.60	0.021	192	8	7	20	21	15	-12	59	71	66
CD	25_TSw1_Tptpul	435	440	44.8	58.22	10.60	0.021	190	8	7	15	19	15	-12	52	64	59
CD	25_TSw1_Tptpul	440	445	34.4	58.22	10.60	0.021	189	8	7	15	19	15	-12	52	64	59
CD	25_TSw1_Tptpul	445	450	45.2	58.22	10.60	0.021	188	8	7	20	22	15	-12	60	72	67
CD	25_TSw1_Tptpul	450	455	32.8	58.22	10.60	0.021	186	8	7	20	12	15	-12	50	62	57
CD	25_TSw1_Tptpul	455	460	50.6	58.22	10.60	0.021	186	13	7	20	22	15	-12	65	77	72
CD	25_TSw1_Tptpul	460	465	52.2	58.22	10.60	0.021	185	13	7	20	20	15	-5	70	75	70
CD	25_TSw1_Tptpul	465	470	57.2	58.22	10.60	0.021	185	13	7	20	22	15	0	77	77	72
CD	25_TSw1_Tptpul	470	475	40.6	58.22	10.60	0.021	184	8	7	20	20	15	-5	65	70	65
CD	25_TSw1_Tptpul	475	480	48.2	58.22	10.60	0.021	184	8	7	20	22	15	-5	67	72	67
CD	25_TSw1_Tptpul	480	485	56.2	58.22	10.60	0.021	185	13	7	20	22	15	-5	72	77	72
CD	25_TSw1_Tptpul	485	490	29.2	58.22	10.60	0.021	186	8	7	20	22	15	-5	67	72	67
CD	25_TSw1_Tptpul	490	495	25.2	58.22	10.60	0.021	187	8	7	20	22	15	-12	60	72	67
CD	25_TSw1_Tptpul	495	500	38.8	58.22	10.60	0.021	188	8	7	20	22	15	0	72	72	67
CD	25_TSw1_Tptpul	500	505	18.2	58.22	10.60	0.021	189	5	7	20	22	15	-12	57	69	64
CD	25_TSw1_Tptpul	505	510	27.0	58.22	10.60	0.021	191	8	7	20	22	15	-5	67	72	67
CD	25_TSw1_Tptpul	510	515	35.4	58.22	10.60	0.021	192	8	7	20	22	15	-5	67	72	67
CD	25_TSw1_Tptpul	515	520	41.0	58.22	10.60	0.021	193	8	7	20	22	15	-5	67	72	67
CD	25_TSw1_Tptpul	520	525	23.4	58.22	10.60	0.021	194	5	7	20	22	15	-5	64	69	64
CD	25_TSw1_Tptpul	525	530	18.0	58.22	10.60	0.021	195	5	7	20	17	15	-5	59	64	59
CD	25_TSw1_Tptpul	530	535	16.6	58.22	10.60	0.021	196	5	7	20	22	15	-10	59	69	64
CD	25_TSw1_Tptpul	535	540	11.6	58.22	10.60	0.021	198	5	7	20	22	15	-12	57	69	64
CD	25_TSw1_Tptpul	540	545	10.0	58.22	10.60	0.021	200	5	7	20	20	15	0	67	67	62
CD	25_TSw1_Tptpul	545	550	26.8	58.22	10.60	0.021	202	8	7	15	14	15	-12	47	59	54
CD	25_TSw1_Tptpul	550	555	14.8	58.22	10.60	0.021	203	5	7	15	18	15	-5	55	60	55
CD	25_TSw1_Tptpul	555	560	37.6	58.22	10.60	0.021	205	8	7	20	19	15	-5	64	69	64
CD	25_TSw1_Tptpul	560	565	15.6	58.22	10.60	0.021	207	5	7	15	22	15	-12	52	64	59
CD	25_TSw1_Tptpul	565	570	16.8	58.22	10.60	0.021	209	5	7	20	25	15	-12	60	72	67
CD	25_TSw1_Tptpul	570	575	14.6	58.22	10.60	0.021	211	5	7	20	25	15	-12	60	72	67
CD	25_TSw1_Tptpul	575	580	25.2	58.22	10.60	0.021	214	8	7	20	25	15	-12	63	75	70
CD	25_TSw1_Tptpul	580	585	27.6	58.22	10.60	0.021	216	8	7	20	25	15	-12	63	75	70

Location	Thermal Mechanical and Lithostratigraphic Unit Designation	Begin Station (m)	End Station (m)	RQD	Mean Intact UCS, σ_{ci} (MPa)	Hoek & Brown Intact Material Constant, mi	Unit Weight of Rock Mass, γ (MN/m^3)	Depth of Tunnel, H (m)	RQD Index	C	Js	Jcd	JwR	AJO	RMR Rating = (RQD Index+C+Js+Jcd+JwR+AJ0)	RMR' = (RQD Index+C+Js+Jcd+JwR)	Geological Strength Index, GSI = (RMR' - 5)
CD	25_TSw1_Tptpul	585	590	30.0	58.22	10.60	0.021	218	8	7	10	24	15	-12	52	64	59
CD	25_TSw1_Tptpul	590	595	15.0	58.22	10.60	0.021	220	5	7	15	18	15	-12	48	60	55
CD	25_TSw1_Tptpul	595	600	21.4	58.22	10.60	0.021	223	5	7	15	18	15	-12	48	60	55
CD	25_TSw1_Tptpul	600	605	35.8	58.22	10.60	0.021	225	8	7	15	20	15	-12	53	65	60
CD	25_TSw1_Tptpul	605	610	20.0	58.22	10.60	0.021	227	5	7	15	23	15	-12	53	65	60
CD	25_TSw1_Tptpul	610	615	10.0	58.22	10.60	0.021	229	5	7	8	23	15	-12	46	58	53
CD	25_TSw1_Tptpul	615	620	10.4	58.22	10.60	0.021	231	5	7	8	23	15	-12	46	58	53
CD	25_TSw1_Tptpul	620	625	20.2	58.22	10.60	0.021	234	5	7	15	23	15	-12	53	65	60
CD	25_TSw1_Tptpul	625	630	37.6	58.22	10.60	0.021	236	8	7	15	20	15	-12	53	65	60
CD	25_TSw1_Tptpul	630	635	41.2	58.22	10.60	0.021	238	8	7	15	23	15	-12	56	68	63
CD	25_TSw1_Tptpul	635	640	52.6	58.22	10.60	0.021	240	13	7	8	20	15	-12	51	63	58
CD	25_TSw1_Tptpul	640	645	47.2	58.22	10.60	0.021	242	8	7	0	20	15	-12	38	50	45
CD	25_TSw1_Tptpul	645	650	68.0	58.22	10.60	0.021	245	13	7	10	23	15	-12	56	68	63
CD	25_TSw1_Tptpul	650	655	41.4	58.22	10.60	0.021	247	8	7	15	23	15	-12	56	68	63
CD	25_TSw1_Tptpul	655	660	27.2	58.22	10.60	0.021	249	8	7	8	23	15	-12	49	61	56
CD	25_TSw1_Tptpul	660	665	27.6	58.22	10.60	0.021	251	8	7	8	21	15	-12	47	59	54
CD	25_TSw1_Tptpul	665	670	27.2	58.22	10.60	0.021	251	8	7	0	20	15	-5	45	50	45
CD	25_TSw1_Tptpul	670	675	39.4	58.22	10.60	0.021	251	8	7	0	22	15	-5	47	52	47
CD	25_TSw1_Tptpul	675	680	23.2	58.22	10.60	0.021	251	5	7	8	19	15	-12	42	54	49
CD	25_TSw1_Tptpul	680	685	31.0	58.22	10.60	0.021	252	8	7	10	21	15	-12	49	61	56
CD	25_TSw1_Tptpul	685	690	31.2	58.22	10.60	0.021	252	8	7	10	15	15	-12	43	55	50
CD	25_TSw1_Tptpul	690	695	17.2	58.22	10.60	0.021	252	5	7	10	23	15	-12	48	60	55
CD	25_TSw1_Tptpul	695	700	39.0	58.22	10.60	0.021	252	8	7	10	16	15	-12	44	56	51
CD	25_TSw1_Tptpul	700	705	10.0	58.22	10.60	0.021	251	5	7	10	21	15	-12	46	58	53
CD	25_TSw1_Tptpul	705	710	11.0	58.22	10.60	0.021	250	5	7	15	21	15	-12	51	63	58
CD	25_TSw1_Tptpul	710	715	12.4	58.22	10.60	0.021	250	5	7	10	16	15	-12	41	53	48
CD	25_TSw1_Tptpul	715	720	10.0	58.22	10.60	0.021	249	5	7	15	19	15	-12	49	61	56
CD	25_TSw1_Tptpul	720	725	18.6	58.22	10.60	0.021	248	5	7	15	16	15	-12	46	58	53
CD	25_TSw1_Tptpul	725	730	25.4	58.22	10.60	0.021	247	8	7	15	16	15	-12	49	61	56
CD	25_TSw1_Tptpul	730	735	23.2	58.22	10.60	0.021	246	5	7	8	18	15	-12	41	53	48
CD	25_TSw1_Tptpul	735	740	22.6	58.22	10.60	0.021	246	5	7	10	21	15	-12	46	58	53
CD	25_TSw1_Tptpul	740	745	14.4	58.22	10.60	0.021	245	5	7	15	21	15	-10	53	63	58
CD	25_TSw1_Tptpul	745	750	20.0	58.22	10.60	0.021	244	5	7	8	21	15	-12	44	56	51
CD	25_TSw1_Tptpul	750	755	11.0	58.22	10.60	0.021	243	5	7	15	21	15	-10	53	63	58
CD	25_TSw1_Tptpul	755	760	10.0	58.22	10.60	0.021	243	5	7	8	21	15	-12	44	56	51
CD	25_TSw1_Tptpul	760	765	22.6	58.22	10.60	0.021	243	5	7	15	23	15	-12	53	65	60
CD	25_TSw1_Tptpul	765	770	16.0	58.22	10.60	0.021	242	5	7	10	16	15	-12	41	53	48
CD	25_TSw1_Tptpul	770	775	39.2	58.22	10.60	0.021	242	8	7	15	20	15	-12	53	65	60
CD	25_TSw1_Tptpul	775	780	36.2	58.22	10.60	0.021	242	8	7	10	16	15	-12	44	56	51

Location	Thermal Mechanical and Lithostratigraphic Unit Designation	Begin Station (m)	End Station (m)	RQD	Mean Intact UCS, σ_{ci} (MPa)	Hoek & Brown Intact Material Constant, mi	Unit Weight of Rock Mass, γ (MN/m^3)	Depth of Tunnel, H (m)	RQD Index	C	Js	Jcd	JwR	AJO	RMR Rating = (RQD Index+C+Js+Jcd+JwR+AJ0)	RMR' = (RQD Index+C+Js+Jcd+JwR)	Geological Strength Index, GSI = (RMR' - 5)
CD	25_TSw1_Tptpul	780	785	36.2	58.22	10.60	0.021	243	8	7	15	18	15	-12	51	63	58
CD	25_TSw1_Tptpul	785	790	35.2	58.22	10.60	0.021	243	8	7	15	21	15	-12	54	66	61
CD	25_TSw1_Tptpul	790	795	39.8	58.22	10.60	0.021	244	8	7	15	21	15	-12	54	66	61
CD	25_TSw1_Tptpul	795	800	31.6	58.22	10.60	0.021	244	8	7	15	19	15	-12	52	64	59
CD	25_TSw1_Tptpul	800	805	10.4	58.22	10.60	0.021	245	5	7	10	22	15	-10	49	59	54
CD	25_TSw1_Tptpul	805	810	10.0	58.22	10.60	0.021	246	5	7	10	21	15	-10	48	58	53
CD	25_TSw1_Tptpul	810	815	12.2	58.22	10.60	0.021	246	5	7	10	24	15	-12	49	61	56
CD	25_TSw1_Tptpul	815	820	31.4	58.22	10.60	0.021	247	8	7	10	21	15	-12	49	61	56
CD	25_TSw1_Tptpul	820	825	23.6	58.22	10.60	0.021	248	5	7	8	18	15	0	53	53	48
CD	25_TSw1_Tptpul	825	830	10.0	58.22	10.60	0.021	248	5	7	15	18	15	-12	48	60	55
CD	25_TSw1_Tptpul	830	835	10.4	58.22	10.60	0.021	249	5	7	10	18	15	-12	43	55	50
CD	25_TSw1_Tptpul	835	840	11.4	58.22	10.60	0.021	249	5	7	15	19	15	-12	49	61	56
CD	25_TSw1_Tptpul	840	845	23.0	58.22	10.60	0.021	250	5	7	15	20	15	-5	57	62	57
CD	25_TSw1_Tptpul	845	850	24.4	58.22	10.60	0.021	251	5	7	15	20	15	-5	57	62	57
CD	25_TSw1_Tptpul	850	855	20.0	58.22	10.60	0.021	251	5	7	15	22	15	-5	59	64	59
CD	25_TSw1_Tptpul	855	860	38.0	58.22	10.60	0.021	251	8	7	10	20	15	-12	48	60	55
CD	25_TSw1_Tptpul	860	865	20.0	58.22	10.60	0.021	251	5	7	15	14	15	-12	44	56	51
CD	25_TSw1_Tptpul	865	870	18.0	58.22	10.60	0.021	251	5	7	10	18	15	-12	43	55	50
CD	25_TSw1_Tptpul	870	875	21.8	58.22	10.60	0.021	251	5	7	10	21	15	-12	46	58	53
CD	25_TSw1_Tptpul	875	880	15.6	58.22	10.60	0.021	250	5	7	8	20	15	-10	45	55	50
CD	25_TSw1_Tptpul	880	885	14.2	58.22	10.60	0.021	250	5	7	15	21	15	0	63	63	58
CD	25_TSw1_Tptpul	885	890	36.8	58.22	10.60	0.021	250	8	7	15	19	15	-5	59	64	59
CD	25_TSw1_Tptpul	890	895	21.6	58.22	10.60	0.021	249	5	7	8	21	15	-10	46	56	51
CD	25_TSw1_Tptpul	895	900	17.0	58.22	10.60	0.021	249	5	7	8	20	15	-12	43	55	50
CD	25_TSw1_Tptpul	900	905	13.0	58.22	10.60	0.021	249	5	7	15	20	15	-12	50	62	57
CD	25_TSw1_Tptpul	905	910	18.4	58.22	10.60	0.021	249	5	7	8	16	15	-12	39	51	46
CD	25_TSw1_Tptpul	910	915	34.4	58.22	10.60	0.021	248	8	7	15	21	15	-12	54	66	61
CD	25_TSw1_Tptpul	915	920	35.6	58.22	10.60	0.021	248	8	7	8	22	15	0	60	60	55
CD	25_TSw1_Tptpul	920	925	15.4	58.22	10.60	0.021	248	5	7	8	21	15	-12	44	56	51
CD	25_TSw1_Tptpul	925	930	33.4	58.22	10.60	0.021	248	8	7	8	18	15	-5	51	56	51
CD	25_TSw1_Tptpul	930	935	25.2	58.22	10.60	0.021	247	8	7	8	19	15	-12	45	57	52
CD	25_TSw1_Tptpul	935	940	25.6	58.22	10.60	0.021	247	8	7	8	21	15	-12	47	59	54
CD	25_TSw1_Tptpul	940	945	37.2	58.22	10.60	0.021	247	8	7	8	21	15	-12	47	59	54
CD	25_TSw1_Tptpul	945	950	20.8	58.22	10.60	0.021	246	5	7	8	21	15	0	56	56	51
CD	25_TSw1_Tptpul	950	955	33.0	58.22	10.60	0.021	246	8	7	0	21	15	-5	46	51	46
CD	25_TSw1_Tptpul	955	960	33.2	58.22	10.60	0.021	245	8	7	15	22	15	-12	55	67	62
CD	25_TSw1_Tptpul	960	965	41.6	58.22	10.60	0.021	245	8	7	10	21	15	-12	49	61	56
CD	25_TSw1_Tptpul	965	970	12.8	58.22	10.60	0.021	244	5	7	10	21	15	-10	48	58	53
CD	25_TSw1_Tptpul	970	975	27.6	58.22	10.60	0.021	244	8	7	10	21	15	-12	49	61	56

Location	Thermal Mechanical and Lithostratigraphic Unit Designation	Begin Station (m)	End Station (m)	RQD	Mean Intact UCS, σ_{ci} (MPa)	Hoek & Brown Intact Material Constant, mi	Unit Weight of Rock Mass, γ (MN/m^3)	Depth of Tunnel, H (m)	RQD Index	C	Js	Jcd	JwR	AJO	RMR Rating = (RQD Index+C+Js+Jcd+JwR+AJ0)	RMR' = (RQD Index+C+Js+Jcd+JwR)	Geological Strength Index, GSI = (RMR' - 5)
CD	25_TSw1_Tptpul	975	980	27.6	58.22	10.60	0.021	244	8	7	8	18	15	-12	44	56	51
CD	25_TSw1_Tptpul	980	985	46.8	58.22	10.60	0.021	243	8	7	15	20	15	-12	53	65	60
CD	25_TSw1_Tptpul	985	990	39.4	58.22	10.60	0.021	243	8	7	15	21	15	-12	54	66	61
CD	25_TSw1_Tptpul	990	995	59.0	58.22	10.60	0.021	242	13	7	10	21	15	-12	54	66	61
CD	25_TSw1_Tptpul	995	1000	34.4	58.22	10.60	0.021	242	8	7	10	21	15	-12	49	61	56
CD	25_TSw1_Tptpul	1000	1005	45.2	58.22	10.60	0.021	241	8	7	10	21	15	-12	49	61	56
CD	25_TSw1_Tptpul	1005	1010	35.6	58.22	10.60	0.021	241	8	7	8	19	15	-12	45	57	52
CD	25_TSw1_Tptpul	1010	1015	44.0	58.22	10.60	0.021	240	8	7	0	21	15	-12	39	51	46
CD	26_TSw2_Tptpmn	1015	1020	33.4	167.9	19.68	0.022	240	8	12	15	22	15	-12	60	72	67
CD	26_TSw2_Tptpmn	1020	1025	37.4	167.9	19.68	0.022	240	8	12	0	18	15	-12	41	53	48
CD	26_TSw2_Tptpmn	1025	1030	52.0	167.9	19.68	0.022	240	13	12	10	22	15	-5	67	72	67
CD	26_TSw2_Tptpmn	1030	1035	44.8	167.9	19.68	0.022	239	8	12	15	20	15	-12	58	70	65
CD	26_TSw2_Tptpmn	1035	1040	59.4	167.9	19.68	0.022	242	13	12	15	17	15	-12	60	72	67
CD	26_TSw2_Tptpmn	1040	1045	61.4	167.9	19.68	0.022	244	13	12	10	16	15	-12	54	66	61
CD	26_TSw2_Tptpmn	1045	1050	45.8	167.9	19.68	0.022	246	8	12	15	14	15	-12	52	64	59
CD	26_TSw2_Tptpmn	1050	1055	56.8	167.9	19.68	0.022	248	13	12	10	16	15	-12	54	66	61
CD	26_TSw2_Tptpmn	1055	1060	61.2	167.9	19.68	0.022	250	13	12	15	16	15	-12	59	71	66
CD	26_TSw2_Tptpmn	1060	1065	81.8	167.9	19.68	0.022	252	17	12	15	22	15	-12	69	81	76
CD	26_TSw2_Tptpmn	1065	1070	47.8	167.9	19.68	0.022	255	8	12	15	14	15	-12	52	64	59
CD	26_TSw2_Tptpmn	1070	1075	51.6	167.9	19.68	0.022	257	13	12	10	18	15	-12	56	68	63
CD	26_TSw2_Tptpmn	1075	1080	60.0	167.9	19.68	0.022	259	13	12	15	18	15	-12	61	73	68
CD	26_TSw2_Tptpmn	1080	1085	55.2	167.9	19.68	0.022	261	13	12	10	18	15	-12	56	68	63
CD	26_TSw2_Tptpmn	1085	1090	41.6	167.9	19.68	0.022	263	8	12	10	18	15	-12	51	63	58
CD	26_TSw2_Tptpmn	1090	1095	40.4	167.9	19.68	0.022	266	8	12	8	16	15	-12	47	59	54
CD	26_TSw2_Tptpmn	1095	1100	53.6	167.9	19.68	0.022	268	13	12	15	20	15	-12	63	75	70
CD	26_TSw2_Tptpmn	1100	1105	64.6	167.9	19.68	0.022	270	13	12	15	21	15	-12	64	76	71
CD	26_TSw2_Tptpmn	1105	1110	49.6	167.9	19.68	0.022	272	8	12	15	23	15	-12	61	73	68
CD	26_TSw2_Tptpmn	1110	1115	60.0	167.9	19.68	0.022	274	13	12	10	22	15	-12	60	72	67
CD	26_TSw2_Tptpmn	1115	1120	40.0	167.9	19.68	0.022	276	8	12	10	20	15	-10	55	65	60
CD	26_TSw2_Tptpmn	1120	1125	68.4	167.9	19.68	0.022	278	13	12	10	22	15	-5	67	72	67
CD	26_TSw2_Tptpmn	1125	1130	47.4	167.9	19.68	0.022	280	8	12	15	22	15	-12	60	72	67
CD	26_TSw2_Tptpmn	1130	1135	40.8	167.9	19.68	0.022	280	8	12	10	22	15	-10	57	67	62
CD	26_TSw2_Tptpmn	1135	1140	30.0	167.9	19.68	0.022	280	8	12	10	18	15	-5	58	63	58
CD	26_TSw2_Tptpmn	1140	1145	32.2	167.9	19.68	0.022	280	8	12	15	24	15	-10	64	74	69
CD	26_TSw2_Tptpmn	1145	1150	81.2	167.9	19.68	0.022	280	17	12	10	21	15	-12	63	75	70
CD	26_TSw2_Tptpmn	1150	1155	81.6	167.9	19.68	0.022	280	17	12	15	22	15	-12	69	81	76
CD	26_TSw2_Tptpmn	1155	1160	83.8	167.9	19.68	0.022	280	17	12	10	19	15	0	73	73	68
CD	26_TSw2_Tptpmn	1160	1165	74.8	167.9	19.68	0.022	280	13	12	15	20	15	-12	63	75	70
CD	26_TSw2_Tptpmn	1165	1170	56.8	167.9	19.68	0.022	280	13	12	10	18	15	-12	56	68	63

Location	Thermal Mechanical and Lithostratigraphic Unit Designation	Begin Station (m)	End Station (m)	RQD	Mean Intact UCS, σ_{ci} (MPa)	Hoek & Brown Intact Material Constant, mi	Unit Weight of Rock Mass, γ (MN/m^3)	Depth of Tunnel, H (m)	RQD Index	C	Js	Jcd	JwR	AJO	RMR Rating = (RQD Index+C+Js+Jcd+JwR+AJ0)	RMR' = (RQD Index+C+Js+Jcd+JwR)	Geological Strength Index, GSI = (RMR' - 5)
CD	26_TSw2_Tptpmn	1170	1175	38.2	167.9	19.68	0.022	280	8	12	8	18	15	0	61	61	56
CD	26_TSw2_Tptpmn	1175	1180	57.6	167.9	19.68	0.022	280	13	12	15	22	15	-12	65	77	72
CD	26_TSw2_Tptpmn	1180	1185	82.4	167.9	19.68	0.022	279	17	12	15	20	15	-12	67	79	74
CD	26_TSw2_Tptpmn	1185	1190	45.0	167.9	19.68	0.022	278	8	12	10	19	15	-12	52	64	59
CD	26_TSw2_Tptpmn	1190	1195	64.0	167.9	19.68	0.022	277	13	12	10	20	15	-12	58	70	65
CD	26_TSw2_Tptpmn	1195	1200	66.8	167.9	19.68	0.022	276	13	12	10	20	15	-12	58	70	65
CD	26_TSw2_Tptpmn	1200	1205	75.6	167.9	19.68	0.022	275	17	12	10	17	15	-12	59	71	66
CD	26_TSw2_Tptpmn	1205	1210	59.6	167.9	19.68	0.022	274	13	12	10	18	15	-12	56	68	63
CD	26_TSw2_Tptpmn	1210	1215	73.0	167.9	19.68	0.022	273	13	12	10	22	15	-5	67	72	67
CD	26_TSw2_Tptpmn	1215	1220	58.2	167.9	19.68	0.022	271	13	12	10	22	15	-5	67	72	67
CD	26_TSw2_Tptpmn	1220	1225	65.4	167.9	19.68	0.022	271	13	12	15	20	15	-12	63	75	70
CD	26_TSw2_Tptpmn	1225	1230	50.2	167.9	19.68	0.022	271	13	12	15	22	15	-12	65	77	72
CD	26_TSw2_Tptpmn	1230	1235	56.4	167.9	19.68	0.022	270	13	12	10	22	15	-5	67	72	67
CD	26_TSw2_Tptpmn	1235	1240	72.0	167.9	19.68	0.022	270	13	12	10	21	15	-12	59	71	66
CD	26_TSw2_Tptpmn	1240	1245	78.0	167.9	19.68	0.022	269	17	12	10	20	15	-12	62	74	69
CD	26_TSw2_Tptpmn	1245	1250	64.0	167.9	19.68	0.022	269	13	12	10	19	15	-12	57	69	64
CD	26_TSw2_Tptpmn	1250	1255	73.0	167.9	19.68	0.022	269	13	12	10	22	15	-5	67	72	67
CD	26_TSw2_Tptpmn	1255	1260	55.2	167.9	19.68	0.022	268	13	12	8	22	15	-12	58	70	65
CD	26_TSw2_Tptpmn	1260	1265	51.0	167.9	19.68	0.022	269	13	12	10	18	15	-12	56	68	63
CD	26_TSw2_Tptpmn	1265	1270	39.4	167.9	19.68	0.022	270	8	12	8	21	15	-12	52	64	59
CD	26_TSw2_Tptpmn	1270	1275	59.2	167.9	19.68	0.022	271	13	12	10	19	15	-12	57	69	64
CD	26_TSw2_Tptpmn	1275	1280	42.0	167.9	19.68	0.022	272	8	12	10	22	15	-12	55	67	62
CD	26_TSw2_Tptpmn	1280	1285	64.8	167.9	19.68	0.022	273	13	12	10	20	15	-12	58	70	65
CD	26_TSw2_Tptpmn	1285	1290	78.6	167.9	19.68	0.022	274	17	12	15	22	15	-12	69	81	76
CD	26_TSw2_Tptpmn	1290	1295	78.6	167.9	19.68	0.022	275	17	12	10	20	15	-12	62	74	69
CD	26_TSw2_Tptpmn	1295	1300	41.2	167.9	19.68	0.022	276	8	12	10	18	15	-12	51	63	58
CD	26_TSw2_Tptpmn	1300	1305	55.2	167.9	19.68	0.022	277	13	12	8	22	15	-12	58	70	65
CD	26_TSw2_Tptpmn	1305	1310	72.0	167.9	19.68	0.022	278	13	12	8	22	15	-12	58	70	65
CD	26_TSw2_Tptpmn	1310	1315	52.4	167.9	19.68	0.022	279	13	12	8	22	15	-12	58	70	65
CD	26_TSw2_Tptpmn	1315	1320	5.4	167.9	19.68	0.022	280	5	12	8	16	15	-12	44	56	51
CD	26_TSw2_Tptpmn	1320	1325	13.8	167.9	19.68	0.022	281	5	12	8	16	15	-12	44	56	51
CD	26_TSw2_Tptpmn	1325	1330	30.8	167.9	19.68	0.022	282	8	12	10	16	15	0	61	61	56
CD	26_TSw2_Tptpmn	1330	1335	51.0	167.9	19.68	0.022	284	13	12	15	21	15	-12	64	76	71
CD	26_TSw2_Tptpmn	1335	1340	69.0	167.9	19.68	0.022	285	13	12	15	22	15	-12	65	77	72
CD	26_TSw2_Tptpmn	1340	1345	69.2	167.9	19.68	0.022	286	13	12	15	19	15	-12	62	74	69
CD	26_TSw2_Tptpmn	1345	1350	45.6	167.9	19.68	0.022	287	8	12	15	14	15	-12	52	64	59
CD	26_TSw2_Tptpmn	1350	1355	66.6	167.9	19.68	0.022	288	13	12	15	17	15	-12	60	72	67
CD	26_TSw2_Tptpmn	1355	1360	57.8	167.9	19.68	0.022	289	13	12	10	19	15	-12	57	69	64
CD	26_TSw2_Tptpmn	1360	1365	60.6	167.9	19.68	0.022	290	13	12	15	16	15	-12	59	71	66

Location	Thermal Mechanical and Lithostratigraphic Unit Designation	Begin Station (m)	End Station (m)	RQD	Mean Intact UCS, σ_{ci} (MPa)	Hoek & Brown Intact Material Constant, mi	Unit Weight of Rock Mass, γ (MN/m^3)	Depth of Tunnel, H (m)	RQD Index	C	Js	Jcd	JwR	AJO	RMR Rating = (RQD Index+C+Js+Jcd+JwR+AJ0)	RMR' = (RQD Index+C+Js+Jcd+JwR)	Geological Strength Index, GSI = (RMR' - 5)
CD	26_TSw2_Tptpmn	1365	1370	44.6	167.9	19.68	0.022	291	8	12	10	20	15	-5	60	65	60
CD	26_TSw2_Tptpmn	1370	1375	77.0	167.9	19.68	0.022	292	17	12	10	21	15	-12	63	75	70
CD	26_TSw2_Tptpmn	1375	1380	83.6	167.9	19.68	0.022	293	17	12	10	23	15	-12	65	77	72
CD	26_TSw2_Tptpmn	1380	1385	70.0	167.9	19.68	0.022	294	13	12	10	16	15	-12	54	66	61
CD	26_TSw2_Tptpmn	1385	1390	70.0	167.9	19.68	0.022	295	13	12	10	19	15	-12	57	69	64
CD	26_TSw2_Tptpmn	1390	1395	62.0	167.9	19.68	0.022	296	13	12	8	19	15	-5	62	67	62
CD	26_TSw2_Tptpmn	1395	1400	72.8	167.9	19.68	0.022	297	13	12	10	20	15	-12	58	70	65
CD	26_TSw2_Tptpmn	1400	1405	82.0	167.9	19.68	0.022	298	17	12	10	21	15	0	75	75	70
CD	26_TSw2_Tptpmn	1405	1410	94.0	167.9	19.68	0.022	298	20	12	15	20	15	-12	70	82	77
CD	26_TSw2_Tptpmn	1410	1415	75.2	167.9	19.68	0.022	297	17	12	15	19	15	-12	66	78	73
CD	26_TSw2_Tptpmn	1415	1420	83.4	167.9	19.68	0.022	297	17	12	10	18	15	0	72	72	67
CD	26_TSw2_Tptpmn	1420	1425	88.8	167.9	19.68	0.022	297	17	12	20	14	15	-12	66	78	73
CD	26_TSw2_Tptpmn	1425	1430	70.8	167.9	19.68	0.022	296	13	12	10	14	15	-12	52	64	59
CD	26_TSw2_Tptpmn	1430	1435	69.2	167.9	19.68	0.022	296	13	12	15	19	15	-12	62	74	69
CD	26_TSw2_Tptpmn	1435	1440	88.8	167.9	19.68	0.022	295	17	12	15	19	15	-12	66	78	73
CD	27_TSw2_Tptpll	1440	1445	74.0	167.9	19.68	0.022	295	13	12	15	23	15	-12	66	78	73
CD	27_TSw2_Tptpll	1445	1450	48.8	167.9	19.68	0.022	295	8	12	15	18	15	0	68	68	63
CD	27_TSw2_Tptpll	1450	1455	60.8	167.9	19.68	0.022	294	13	12	10	14	15	-12	52	64	59
CD	27_TSw2_Tptpll	1455	1460	63.8	167.9	19.68	0.022	294	13	12	10	18	15	-12	56	68	63
CD	27_TSw2_Tptpll	1460	1465	47.2	167.9	19.68	0.022	293	8	12	15	20	15	-12	58	70	65
CD	27_TSw2_Tptpll	1465	1470	NA	167.9	19.68	0.022	293	NA	NA	NA	NA	NA	NA	NA	NA	NA
CD	27_TSw2_Tptpll	1470	1475	NA	167.9	19.68	0.022	292	NA	NA	NA	NA	NA	NA	NA	NA	NA
CD	27_TSw2_Tptpll	1475	1480	NA	167.9	19.68	0.022	292	NA	NA	NA	NA	NA	NA	NA	NA	NA
CD	27_TSw2_Tptpll	1480	1485	NA	167.9	19.68	0.022	291	NA	NA	NA	NA	NA	NA	NA	NA	NA
CD	27_TSw2_Tptpll	1485	1490	NA	167.9	19.68	0.022	291	NA	NA	NA	NA	NA	NA	NA	NA	NA
CD	27_TSw2_Tptpll	1490	1495	49.2	167.9	19.68	0.022	291	8	12	8	16	15	0	59	59	54
CD	27_TSw2_Tptpll	1495	1500	32.4	167.9	19.68	0.022	291	8	12	8	18	15	0	61	61	56
CD	27_TSw2_Tptpll	1500	1505	21.0	167.9	19.68	0.022	290	5	12	15	21	15	-12	56	68	63
CD	27_TSw2_Tptpll	1505	1510	25.6	167.9	19.68	0.022	289	8	12	15	21	15	-12	59	71	66
CD	27_TSw2_Tptpll	1510	1515	67.2	167.9	19.68	0.022	288	13	12	15	21	15	-12	64	76	71
CD	27_TSw2_Tptpll	1515	1520	46.8	167.9	19.68	0.022	287	8	12	10	21	15	-12	54	66	61
CD	27_TSw2_Tptpll	1520	1525	25.2	167.9	19.68	0.022	285	8	12	10	21	15	-12	54	66	61
CD	27_TSw2_Tptpll	1525	1530	28.4	167.9	19.68	0.022	284	8	12	10	21	15	-12	54	66	61
CD	27_TSw2_Tptpll	1530	1535	10.2	167.9	19.68	0.022	283	5	12	10	16	15	-12	46	58	53
CD	27_TSw2_Tptpll	1535	1540	37.2	167.9	19.68	0.022	282	8	12	10	23	15	-12	56	68	63
CD	27_TSw2_Tptpll	1540	1545	10.2	167.9	19.68	0.022	281	5	12	10	23	15	-12	53	65	60
CD	27_TSw2_Tptpll	1545	1550	33.6	167.9	19.68	0.022	280	8	12	10	23	15	-12	56	68	63
CD	27_TSw2_Tptpll	1550	1555	45.8	167.9	19.68	0.022	279	8	12	10	23	15	-12	56	68	63
CD	27_TSw2_Tptpll	1555	1560	45.2	167.9	19.68	0.022	278	8	12	10	23	15	-12	56	68	63

Location	Thermal Mechanical and Lithostratigraphic Unit Designation	Begin Station (m)	End Station (m)	RQD	Mean Intact UCS, σ_{ci} (MPa)	Hoek & Brown Intact Material Constant, mi	Unit Weight of Rock Mass, γ (MN/m^3)	Depth of Tunnel, H (m)	RQD Index	C	Js	Jcd	JwR	AJO	RMR Rating = (RQD Index+C+Js+Jcd+JwR+AJ0)	RMR' = (RQD Index+C+Js+Jcd+JwR)	Geological Strength Index, GSI = (RMR' - 5)
CD	27_TSw2_Tptpll	1560	1565	19.8	167.9	19.68	0.022	277	5	12	10	23	15	-12	53	65	60
CD	27_TSw2_Tptpll	1565	1570	21.2	167.9	19.68	0.022	276	5	12	10	23	15	-12	53	65	60
CD	27_TSw2_Tptpll	1570	1575	21.2	167.9	19.68	0.022	275	5	12	10	23	15	-12	53	65	60
CD	27_TSw2_Tptpll	1575	1580	30.0	167.9	19.68	0.022	274	8	12	10	16	15	0	61	61	56
CD	27_TSw2_Tptpll	1580	1585	28.6	167.9	19.68	0.022	273	8	12	10	16	15	0	61	61	56
CD	27_TSw2_Tptpll	1585	1590	22.4	167.9	19.68	0.022	272	5	12	10	21	15	0	63	63	58
CD	27_TSw2_Tptpll	1590	1595	29.4	167.9	19.68	0.022	273	8	12	10	21	15	0	66	66	61
CD	27_TSw2_Tptpll	1595	1600	26.6	167.9	19.68	0.022	275	8	12	15	16	15	0	66	66	61
CD	27_TSw2_Tptpll	1600	1605	36.4	167.9	19.68	0.022	278	8	12	10	23	15	-12	56	68	63
CD	27_TSw2_Tptpll	1605	1610	19.8	167.9	19.68	0.022	280	5	12	10	23	15	-12	53	65	60
CD	27_TSw2_Tptpll	1610	1615	43.4	167.9	19.68	0.022	282	8	12	10	23	15	-12	56	68	63
CD	27_TSw2_Tptpll	1615	1620	41.4	167.9	19.68	0.022	284	8	12	10	23	15	-12	56	68	63
CD	27_TSw2_Tptpll	1620	1625	62.0	167.9	19.68	0.022	287	13	12	10	23	15	-12	61	73	68
CD	27_TSw2_Tptpll	1625	1630	63.8	167.9	19.68	0.022	289	13	12	10	23	15	-12	61	73	68
CD	27_TSw2_Tptpll	1630	1635	62.0	167.9	19.68	0.022	291	13	12	10	23	15	-12	61	73	68
CD	27_TSw2_Tptpll	1635	1640	40.4	167.9	19.68	0.022	293	8	12	10	23	15	-12	56	68	63
CD	27_TSw2_Tptpll	1640	1645	41.0	167.9	19.68	0.022	296	8	12	10	23	15	-12	56	68	63
CD	27_TSw2_Tptpll	1645	1650	30.6	167.9	19.68	0.022	298	8	12	10	19	15	-12	52	64	59
CD	27_TSw2_Tptpll	1650	1655	27.6	167.9	19.68	0.022	300	8	12	10	18	15	0	63	63	58
CD	27_TSw2_Tptpll	1655	1660	54.8	167.9	19.68	0.022	302	13	12	10	18	15	0	68	68	63
CD	27_TSw2_Tptpll	1660	1665	36.0	167.9	19.68	0.022	305	8	12	10	21	15	0	66	66	61
CD	27_TSw2_Tptpll	1665	1670	58.2	167.9	19.68	0.022	307	13	12	10	21	15	0	71	71	66
CD	27_TSw2_Tptpll	1670	1675	44.0	167.9	19.68	0.022	309	8	12	10	21	15	0	66	66	61
CD	27_TSw2_Tptpll	1675	1680	31.6	167.9	19.68	0.022	311	8	12	10	16	15	-12	49	61	56
CD	27_TSw2_Tptpll	1680	1685	56.2	167.9	19.68	0.022	313	13	12	8	16	15	-12	52	64	59
CD	27_TSw2_Tptpll	1685	1690	15.0	167.9	19.68	0.022	315	5	12	8	16	15	-12	44	56	51
CD	27_TSw2_Tptpll	1690	1695	11.4	167.9	19.68	0.022	316	5	12	8	19	15	-12	47	59	54
CD	27_TSw2_Tptpll	1695	1700	22.4	167.9	19.68	0.022	317	5	12	10	19	15	-12	49	61	56
CD	27_TSw2_Tptpll	1700	1705	43.2	167.9	19.68	0.022	318	8	12	10	16	15	-12	49	61	56
CD	27_TSw2_Tptpll	1705	1710	36.8	167.9	19.68	0.022	320	8	12	10	16	15	-12	49	61	56
CD	27_TSw2_Tptpll	1710	1715	44.8	167.9	19.68	0.022	321	8	12	8	16	15	0	59	59	54
CD	27_TSw2_Tptpll	1715	1720	41.4	167.9	19.68	0.022	322	8	12	8	16	15	0	59	59	54
CD	27_TSw2_Tptpll	1720	1725	61.2	167.9	19.68	0.022	323	13	12	8	18	15	0	66	66	61
CD	27_TSw2_Tptpll	1725	1730	42.4	167.9	19.68	0.022	325	8	12	8	18	15	-12	49	61	56
CD	27_TSw2_Tptpll	1730	1735	36.6	167.9	19.68	0.022	326	8	12	10	18	15	-12	51	63	58
CD	27_TSw2_Tptpll	1735	1740	14.8	167.9	19.68	0.022	327	5	12	8	18	15	-12	46	58	53
CD	27_TSw2_Tptpll	1740	1745	31.4	167.9	19.68	0.022	328	8	12	8	18	15	-12	49	61	56
CD	27_TSw2_Tptpll	1745	1750	53.2	167.9	19.68	0.022	329	13	12	8	18	15	-12	54	66	61
CD	27_TSw2_Tptpll	1750	1755	35.2	167.9	19.68	0.022	330	8	12	10	18	15	-12	51	63	58

Location	Thermal Mechanical and Lithostratigraphic Unit Designation	Begin Station (m)	End Station (m)	RQD	Mean Intact UCS, σ_{ci} (MPa)	Hoek & Brown Intact Material Constant, mi	Unit Weight of Rock Mass, γ (MN/m^3)	Depth of Tunnel, H (m)	RQD Index	C	Js	Jcd	JwR	AJO	RMR Rating = (RQD Index+C+Js+Jcd+JwR+AJ0)	RMR' = (RQD Index+C+Js+Jcd+JwR)	Geological Strength Index, GSI = (RMR' - 5)
CD	27_TSw2_Tptpll	1755	1760	18.8	167.9	19.68	0.022	331	5	12	10	21	15	-12	51	63	58
CD	27_TSw2_Tptpll	1760	1765	44.4	167.9	19.68	0.022	332	8	12	10	21	15	-12	54	66	61
CD	27_TSw2_Tptpll	1765	1770	23.8	167.9	19.68	0.022	332	5	12	10	18	15	-12	48	60	55
CD	27_TSw2_Tptpll	1770	1775	22.0	167.9	19.68	0.022	333	5	12	8	18	15	-12	46	58	53
CD	27_TSw2_Tptpll	1775	1780	22.2	167.9	19.68	0.022	334	5	12	8	18	15	-12	46	58	53
CD	27_TSw2_Tptpll	1780	1785	35.4	167.9	19.68	0.022	335	8	12	8	18	15	-12	49	61	56
CD	27_TSw2_Tptpll	1785	1790	51.6	167.9	19.68	0.022	336	13	12	8	18	15	-12	54	66	61
CD	27_TSw2_Tptpll	1790	1795	56.0	167.9	19.68	0.022	337	13	12	8	18	15	-12	54	66	61
CD	27_TSw2_Tptpll	1795	1800	32.2	167.9	19.68	0.022	338	8	12	8	16	15	-12	47	59	54
CD	27_TSw2_Tptpll	1800	1805	31.6	167.9	19.68	0.022	339	8	12	10	16	15	-12	49	61	56
CD	27_TSw2_Tptpll	1805	1810	42.8	167.9	19.68	0.022	340	8	12	10	16	15	-12	49	61	56
CD	27_TSw2_Tptpll	1810	1815	32.8	167.9	19.68	0.022	341	8	12	10	18	15	0	63	63	58
CD	27_TSw2_Tptpll	1815	1820	35.6	167.9	19.68	0.022	342	8	12	15	21	15	-12	59	71	66
CD	27_TSw2_Tptpll	1820	1825	35.8	167.9	19.68	0.022	343	8	12	15	21	15	-12	59	71	66
CD	27_TSw2_Tptpll	1825	1830	77.6	167.9	19.68	0.022	344	17	12	15	21	15	-12	68	80	75
CD	27_TSw2_Tptpll	1830	1835	57.6	167.9	19.68	0.022	344	13	12	8	18	15	-12	54	66	61
CD	27_TSw2_Tptpll	1835	1840	45.8	167.9	19.68	0.022	345	8	12	15	21	15	-12	59	71	66
CD	27_TSw2_Tptpll	1840	1845	73.0	167.9	19.68	0.022	346	13	12	15	23	15	-12	66	78	73
CD	27_TSw2_Tptpll	1845	1850	62.4	167.9	19.68	0.022	346	13	12	15	20	15	-5	70	75	70
CD	27_TSw2_Tptpll	1850	1855	66.6	167.9	19.68	0.022	347	13	12	15	20	15	-12	63	75	70
CD	27_TSw2_Tptpll	1855	1860	71.8	167.9	19.68	0.022	348	13	12	15	21	15	-12	64	76	71
CD	27_TSw2_Tptpll	1860	1865	51.4	167.9	19.68	0.022	348	13	12	15	18	15	-12	61	73	68
CD	27_TSw2_Tptpll	1865	1870	34.8	167.9	19.68	0.022	349	8	12	15	20	15	-12	58	70	65
CD	27_TSw2_Tptpll	1870	1875	78.4	167.9	19.68	0.022	349	17	12	15	20	15	-12	67	79	74
CD	27_TSw2_Tptpll	1875	1880	51.4	167.9	19.68	0.022	350	13	12	15	19	15	-12	62	74	69
CD	27_TSw2_Tptpll	1880	1885	47.6	167.9	19.68	0.022	351	8	12	15	19	15	-12	57	69	64
CD	27_TSw2_Tptpll	1885	1890	40.8	167.9	19.68	0.022	351	8	12	10	18	15	-12	51	63	58
CD	27_TSw2_Tptpll	1890	1895	36.4	167.9	19.68	0.022	352	8	12	10	18	15	-12	51	63	58
CD	27_TSw2_Tptpll	1895	1900	61.0	167.9	19.68	0.022	353	13	12	15	19	15	-12	62	74	69
CD	27_TSw2_Tptpll	1900	1905	58.4	167.9	19.68	0.022	353	13	12	10	12	15	0	62	62	57
CD	27_TSw2_Tptpll	1905	1910	54.6	167.9	19.68	0.022	354	13	12	10	16	15	0	66	66	61
CD	27_TSw2_Tptpll	1910	1915	54.6	167.9	19.68	0.022	355	13	12	10	20	15	-12	58	70	65
CD	27_TSw2_Tptpll	1915	1920	40.6	167.9	19.68	0.022	355	8	12	8	16	15	0	59	59	54
CD	27_TSw2_Tptpll	1920	1925	61.4	167.9	19.68	0.022	356	13	12	8	13	15	0	61	61	56
CD	27_TSw2_Tptpll	1925	1930	33.6	167.9	19.68	0.022	356	8	12	10	16	15	0	61	61	56
CD	27_TSw2_Tptpll	1930	1935	35.6	167.9	19.68	0.022	357	8	12	10	16	15	-12	49	61	56
CD	27_TSw2_Tptpll	1935	1940	48.2	167.9	19.68	0.022	357	8	12	15	14	15	-12	52	64	59
CD	27_TSw2_Tptpll	1940	1945	43.6	167.9	19.68	0.022	358	8	12	15	16	15	-12	54	66	61
CD	27_TSw2_Tptpll	1945	1950	43.4	167.9	19.68	0.022	358	8	12	10	16	15	-12	49	61	56

Location	Thermal Mechanical and Lithostratigraphic Unit Designation	Begin Station (m)	End Station (m)	RQD	Mean Intact UCS, σ_{ci} (MPa)	Hoek & Brown Intact Material Constant, mi	Unit Weight of Rock Mass, γ (MN/m^3)	Depth of Tunnel, H (m)	RQD Index	C	Js	Jcd	JwR	AJO	RMR Rating = (RQD Index+C+Js+Jcd+JwR+AJ0)	RMR' = (RQD Index+C+Js+Jcd+JwR)	Geological Strength Index, GSI = (RMR' - 5)
CD	27_TSw2_Tptpll	1950	1955	56.6	167.9	19.68	0.022	359	13	12	10	18	15	-12	56	68	63
CD	27_TSw2_Tptpll	1955	1960	37.2	167.9	19.68	0.022	359	8	12	10	21	15	-12	54	66	61
CD	27_TSw2_Tptpll	1960	1965	42.4	167.9	19.68	0.022	360	8	12	10	21	15	-12	54	66	61
CD	27_TSw2_Tptpll	1965	1970	57.8	167.9	19.68	0.022	360	13	12	10	19	15	-12	57	69	64
CD	27_TSw2_Tptpll	1970	1975	63.0	167.9	19.68	0.022	361	13	12	10	19	15	-12	57	69	64
CD	27_TSw2_Tptpll	1975	1980	57.6	167.9	19.68	0.022	361	13	12	10	19	15	-12	57	69	64
CD	27_TSw2_Tptpll	1980	1985	60.8	167.9	19.68	0.022	362	13	12	10	19	15	-12	57	69	64
CD	27_TSw2_Tptpll	1985	1990	67.6	167.9	19.68	0.022	363	13	12	10	19	15	-12	57	69	64
CD	27_TSw2_Tptpll	1990	1995	28.6	167.9	19.68	0.022	362	8	12	15	19	15	-12	57	69	64
CD	27_TSw2_Tptpll	1995	2000	16.2	167.9	19.68	0.022	362	5	12	15	19	15	-12	54	66	61
CD	27_TSw2_Tptpll	2000	2005	11.6	167.9	19.68	0.022	362	5	12	10	18	15	0	60	60	55
CD	27_TSw2_Tptpll	2005	2010	18.4	167.9	19.68	0.022	361	5	12	10	16	15	-12	46	58	53
CD	27_TSw2_Tptpll	2010	2015	55.2	167.9	19.68	0.022	361	13	12	10	19	15	-12	57	69	64
CD	27_TSw2_Tptpll	2015	2020	34.2	167.9	19.68	0.022	361	8	12	10	18	15	-12	51	63	58
CD	27_TSw2_Tptpll	2020	2025	17.4	167.9	19.68	0.022	361	5	12	10	19	15	-12	49	61	56
CD	27_TSw2_Tptpll	2025	2030	38.6	167.9	19.68	0.022	360	8	12	15	19	15	-12	57	69	64
CD	27_TSw2_Tptpll	2030	2035	42.4	167.9	19.68	0.022	360	8	12	15	19	15	-12	57	69	64
CD	27_TSw2_Tptpll	2035	2040	23.2	167.9	19.68	0.022	360	5	12	10	19	15	-12	49	61	56
CD	27_TSw2_Tptpll	2040	2045	28.8	167.9	19.68	0.022	360	8	12	8	19	15	-12	50	62	57
CD	27_TSw2_Tptpll	2045	2050	18.8	167.9	19.68	0.022	359	5	12	10	19	15	-12	49	61	56
CD	27_TSw2_Tptpll	2050	2055	44.4	167.9	19.68	0.022	359	8	12	15	19	15	-12	57	69	64
CD	27_TSw2_Tptpll	2055	2060	48.4	167.9	19.68	0.022	359	8	12	15	19	15	-12	57	69	64
CD	27_TSw2_Tptpll	2060	2065	61.4	167.9	19.68	0.022	358	13	12	15	19	15	-12	62	74	69
CD	27_TSw2_Tptpll	2065	2070	56.6	167.9	19.68	0.022	358	13	12	15	19	15	-12	62	74	69
CD	27_TSw2_Tptpll	2070	2075	66.6	167.9	19.68	0.022	356	13	12	15	19	15	-12	62	74	69
CD	27_TSw2_Tptpll	2075	2080	58.6	167.9	19.68	0.022	353	13	12	15	19	15	-12	62	74	69
CD	27_TSw2_Tptpll	2080	2085	57.2	167.9	19.68	0.022	351	13	12	15	19	15	-12	62	74	69
CD	27_TSw2_Tptpll	2085	2090	70.0	167.9	19.68	0.022	349	13	12	15	19	15	-12	62	74	69
CD	27_TSw2_Tptpll	2090	2095	NA	167.9	19.68	0.022	NA	NA	NA	NA	NA	NA	NA	NA	NA	NA
CD	27_TSw2_Tptpll	2095	2100	NA	167.9	19.68	0.022	NA	NA	NA	NA	NA	NA	NA	NA	NA	NA
CD	27_TSw2_Tptpll	2100	2105	42.0	167.9	19.68	0.022	342	8	12	8	19	15	0	62	62	57
CD	27_TSw2_Tptpll	2105	2110	41.0	167.9	19.68	0.022	339	8	12	8	21	15	-12	52	64	59
CD	27_TSw2_Tptpll	2110	2115	24.6	167.9	19.68	0.022	337	5	12	8	16	15	-12	44	56	51
CD	27_TSw2_Tptpll	2115	2120	54.4	167.9	19.68	0.022	335	13	12	8	18	15	-12	54	66	61
CD	27_TSw2_Tptpll	2120	2125	62.8	167.9	19.68	0.022	332	13	12	15	21	15	-12	64	76	71
CD	27_TSw2_Tptpll	2125	2130	72.8	167.9	19.68	0.022	330	13	12	15	21	15	-12	64	76	71
CD	27_TSw2_Tptpll	2130	2135	10.0	167.9	19.68	0.022	328	5	12	8	21	15	-12	49	61	56
CD	27_TSw2_Tptpll	2135	2140	56.2	167.9	19.68	0.022	325	13	12	8	21	15	-12	57	69	64
CD	27_TSw2_Tptpll	2140	2145	37.2	167.9	19.68	0.022	323	8	12	15	19	15	-12	57	69	64

Location	Thermal Mechanical and Lithostratigraphic Unit Designation	Begin Station (m)	End Station (m)	RQD	Mean Intact UCS, σ_{ci} (MPa)	Hoek & Brown Intact Material Constant, mi	Unit Weight of Rock Mass, γ (MN/m^3)	Depth of Tunnel, H (m)	RQD Index	C	Js	Jcd	JwR	AJO	RMR Rating = (RQD Index+C+Js+Jcd+JwR+AJ0)	RMR' = (RQD Index+C+Js+Jcd+JwR)	Geological Strength Index, GSI = (RMR' - 5)
CD	27_TSw2_Tptpll	2145	2150	42.2	167.9	19.68	0.022	321	8	12	15	19	15	-12	57	69	64
CD	27_TSw2_Tptpll	2150	2155	41.4	167.9	19.68	0.022	319	8	12	20	16	15	-12	59	71	66
CD	27_TSw2_Tptpll	2155	2160	33.8	167.9	19.68	0.022	317	8	12	10	20	15	0	65	65	60
CD	27_TSw2_Tptpll	2160	2165	26.8	167.9	19.68	0.022	314	8	12	8	16	15	0	59	59	54
CD	27_TSw2_Tptpll	2165	2170	44.2	167.9	19.68	0.022	312	8	12	15	21	15	-12	59	71	66
CD	27_TSw2_Tptpll	2170	2175	49.0	167.9	19.68	0.022	310	8	12	10	21	15	0	66	66	61
CD	27_TSw2_Tptpll	2175	2180	56.4	167.9	19.68	0.022	308	13	12	15	16	15	-12	59	71	66
CD	27_TSw2_Tptpll	2180	2185	63.0	167.9	19.68	0.022	306	13	12	15	16	15	-12	59	71	66
CD	27_TSw2_Tptpll	2185	2190	46.2	167.9	19.68	0.022	304	8	12	15	16	15	-12	54	66	61
CD	27_TSw2_Tptpll	2190	2195	54.8	167.9	19.68	0.022	302	13	12	15	16	15	-12	59	71	66
CD	27_TSw2_Tptpll	2195	2200	44.0	167.9	19.68	0.022	300	8	12	15	16	15	-12	54	66	61
CD	27_TSw2_Tptpll	2200	2205	38.6	167.9	19.68	0.022	298	8	12	15	16	15	-12	54	66	61
CD	27_TSw2_Tptpll	2205	2210	44.4	167.9	19.68	0.022	296	8	12	15	19	15	-12	57	69	64
CD	27_TSw2_Tptpll	2210	2215	24.0	167.9	19.68	0.022	294	5	12	10	19	15	0	61	61	56
CD	27_TSw2_Tptpll	2215	2220	32.4	167.9	19.68	0.022	292	8	12	10	19	15	-5	59	64	59
CD	27_TSw2_Tptpll	2220	2225	43.6	167.9	19.68	0.022	289	8	12	15	22	15	-12	60	72	67
CD	27_TSw2_Tptpll	2225	2230	50.2	167.9	19.68	0.022	287	13	12	10	19	15	0	69	69	64
CD	27_TSw2_Tptpll	2230	2235	51.8	167.9	19.68	0.022	285	13	12	10	21	15	0	71	71	66
CD	27_TSw2_Tptpll	2235	2240	59.6	167.9	19.68	0.022	284	13	12	10	21	15	-12	59	71	66
CD	27_TSw2_Tptpll	2240	2245	37.0	167.9	19.68	0.022	282	8	12	10	21	15	-12	54	66	61
CD	27_TSw2_Tptpll	2245	2250	62.0	167.9	19.68	0.022	281	13	12	10	21	15	0	71	71	66
CD	27_TSw2_Tptpll	2250	2255	77.6	167.9	19.68	0.022	279	17	12	15	19	15	-12	66	78	73
CD	27_TSw2_Tptpll	2255	2260	57.0	167.9	19.68	0.022	278	13	12	15	21	15	-12	64	76	71
CD	27_TSw2_Tptpll	2260	2265	50.2	167.9	19.68	0.022	276	13	12	15	19	15	-12	62	74	69
CD	27_TSw2_Tptpll	2265	2270	31.4	167.9	19.68	0.022	275	8	12	10	19	15	0	64	64	59
CD	27_TSw2_Tptpll	2270	2275	41.6	167.9	19.68	0.022	273	8	12	10	19	15	0	64	64	59
CD	27_TSw2_Tptpll	2275	2280	54.8	167.9	19.68	0.022	272	13	12	10	18	15	-12	56	68	63
CD	27_TSw2_Tptpll	2280	2285	48.2	167.9	19.68	0.022	270	8	12	10	20	15	-12	53	65	60
CD	27_TSw2_Tptpll	2285	2290	43.0	167.9	19.68	0.022	269	8	12	10	20	15	-12	53	65	60
CD	27_TSw2_Tptpll	2290	2295	27.0	167.9	19.68	0.022	268	8	12	10	19	15	0	64	64	59
CD	27_TSw2_Tptpll	2295	2300	29.6	167.9	19.68	0.022	266	8	12	10	23	15	-12	56	68	63
CD	27_TSw2_Tptpll	2300	2305	10.0	167.9	19.68	0.022	265	5	12	10	17	15	0	59	59	54
CD	27_TSw2_Tptpll	2305	2310	42.4	167.9	19.68	0.022	263	8	12	10	17	15	0	62	62	57
CD	27_TSw2_Tptpll	2310	2315	26.6	167.9	19.68	0.022	262	8	12	10	17	15	0	62	62	57
CD	27_TSw2_Tptpll	2315	2320	21.8	167.9	19.68	0.022	261	5	12	15	21	15	-12	56	68	63
CD	27_TSw2_Tptpll	2320	2325	32.8	167.9	19.68	0.022	260	8	12	10	21	15	0	66	66	61
CD	28_TSw2_Tptpln	2325	2330	11.2	167.9	19.68	0.022	260	5	12	10	16	15	0	58	58	53
CD	28_TSw2_Tptpln	2330	2335	18.8	167.9	19.68	0.022	259	5	12	10	21	15	-12	51	63	58
CD	28_TSw2_Tptpln	2335	2340	18.8	167.9	19.68	0.022	258	5	12	10	21	15	-12	51	63	58

Location	Thermal Mechanical and Lithostratigraphic Unit Designation	Begin Station (m)	End Station (m)	RQD	Mean Intact UCS, σ_{ci} (MPa)	Hoek & Brown Intact Material Constant, mi	Unit Weight of Rock Mass, γ (MN/m^3)	Depth of Tunnel, H (m)	RQD Index	C	Js	Jcd	JwR	AJO	RMR Rating = (RQD Index+C+Js+Jcd+JwR+AJ0)	RMR' = (RQD Index+C+Js+Jcd+JwR)	Geological Strength Index, GSI = (RMR' - 5)
CD	28_TSw2_Tptpln	2340	2345	46.0	167.9	19.68	0.022	257	8	12	10	21	15	-12	54	66	61
CD	28_TSw2_Tptpln	2345	2350	32.4	167.9	19.68	0.022	256	8	12	20	21	15	-12	64	76	71
CD	28_TSw2_Tptpln	2350	2355	86.8	167.9	19.68	0.022	255	17	12	10	16	15	-12	58	70	65
CD	28_TSw2_Tptpln	2355	2360	88.4	167.9	19.68	0.022	254	17	12	10	16	15	-12	58	70	65
CD	28_TSw2_Tptpln	2360	2365	72.6	167.9	19.68	0.022	252	13	12	10	16	15	-12	54	66	61
CD	28_TSw2_Tptpln	2365	2370	95.0	167.9	19.68	0.022	251	20	12	10	17	15	-12	62	74	69
CD	28_TSw2_Tptpln	2370	2375	77.8	167.9	19.68	0.022	250	17	12	10	17	15	0	71	71	66
CD	28_TSw2_Tptpln	2375	2380	73.4	167.9	19.68	0.022	249	13	12	10	17	15	-12	55	67	62
CD	28_TSw2_Tptpln	2380	2385	87.8	167.9	19.68	0.022	248	17	12	15	21	15	-12	68	80	75
CD	28_TSw2_Tptpln	2385	2390	84.6	167.9	19.68	0.022	246	17	12	10	17	15	-12	59	71	66
CD	28_TSw2_Tptpln	2390	2395	78.0	167.9	19.68	0.022	245	17	12	15	18	15	-12	65	77	72
CD	28_TSw2_Tptpln	2395	2400	66.0	167.9	19.68	0.022	243	13	12	10	20	15	-12	58	70	65
CD	28_TSw2_Tptpln	2400	2405	81.8	167.9	19.68	0.022	241	17	12	10	16	15	0	70	70	65
CD	28_TSw2_Tptpln	2405	2410	76.0	167.9	19.68	0.022	239	17	12	15	14	15	-12	61	73	68
CD	28_TSw2_Tptpln	2410	2415	74.6	167.9	19.68	0.022	237	13	12	10	22	15	-5	67	72	67
CD	28_TSw2_Tptpln	2415	2420	59.0	167.9	19.68	0.022	235	13	12	15	14	15	-12	57	69	64
CD	28_TSw2_Tptpln	2420	2425	59.4	167.9	19.68	0.022	233	13	12	15	14	15	-12	57	69	64
CD	28_TSw2_Tptpln	2425	2430	78.6	167.9	19.68	0.022	231	17	12	15	14	15	-12	61	73	68
CD	28_TSw2_Tptpln	2430	2435	72.8	167.9	19.68	0.022	229	13	12	10	16	15	-12	54	66	61
CD	28_TSw2_Tptpln	2435	2440	91.8	167.9	19.68	0.022	227	20	12	15	19	15	-12	69	81	76
CD	28_TSw2_Tptpln	2440	2445	67.2	167.9	19.68	0.022	225	13	12	15	19	15	-12	62	74	69
CD	28_TSw2_Tptpln	2445	2450	82.8	167.9	19.68	0.022	223	17	12	15	19	15	-12	66	78	73
CD	28_TSw2_Tptpln	2450	2455	67.4	167.9	19.68	0.022	221	13	12	15	19	15	-12	62	74	69
CD	28_TSw2_Tptpln	2455	2460	69.0	167.9	19.68	0.022	220	13	12	15	19	15	-12	62	74	69
CD	28_TSw2_Tptpln	2460	2465	64.6	167.9	19.68	0.022	218	13	12	10	22	15	-12	60	72	67
CD	28_TSw2_Tptpln	2465	2470	28.8	167.9	19.68	0.022	216	8	12	10	22	15	-12	55	67	62
CD	28_TSw2_Tptpln	2470	2475	83.8	167.9	19.68	0.022	215	17	12	15	22	15	-12	69	81	76
CD	28_TSw2_Tptpln	2475	2480	57.4	167.9	19.68	0.022	213	13	12	15	19	15	-12	62	74	69
CD	28_TSw2_Tptpln	2480	2485	48.0	167.9	19.68	0.022	212	8	12	10	19	15	-12	52	64	59
CD	28_TSw2_Tptpln	2485	2490	69.4	167.9	19.68	0.022	210	13	12	15	19	15	-12	62	74	69
CD	28_TSw2_Tptpln	2490	2495	58.6	167.9	19.68	0.022	209	13	12	8	20	15	-12	56	68	63
CD	28_TSw2_Tptpln	2495	2500	38.4	167.9	19.68	0.022	207	8	12	8	20	15	-12	51	63	58
CD	28_TSw2_Tptpln	2500	2505	68.2	167.9	19.68	0.022	206	13	12	15	19	15	-12	62	74	69
CD	28_TSw2_Tptpln	2505	2510	66.0	167.9	19.68	0.022	204	13	12	15	20	15	-12	63	75	70
CD	28_TSw2_Tptpln	2510	2515	66.8	167.9	19.68	0.022	203	13	12	15	21	15	-12	64	76	71
CD	28_TSw2_Tptpln	2515	2520	77.4	167.9	19.68	0.022	202	17	12	10	21	15	-5	70	75	70
CD	28_TSw2_Tptpln	2520	2525	51.4	167.9	19.68	0.022	201	13	12	10	20	15	0	70	70	65
CD	28_TSw2_Tptpln	2525	2530	39.2	167.9	19.68	0.022	200	8	12	10	22	15	-5	62	67	62
CD	28_TSw2_Tptpln	2530	2535	12.6	167.9	19.68	0.022	199	5	12	15	18	15	-12	53	65	60

Location	Thermal Mechanical and Lithostratigraphic Unit Designation	Begin Station (m)	End Station (m)	RQD	Mean Intact UCS, σ_{ci} (MPa)	Hoek & Brown Intact Material Constant, mi	Unit Weight of Rock Mass, γ (MN/m^3)	Depth of Tunnel, H (m)	RQD Index	C	Js	Jcd	JwR	AJO	RMR Rating = (RQD Index+C+Js+Jcd+JwR+AJ0)	RMR' = (RQD Index+C+Js+Jcd+JwR)	Geological Strength Index, GSI = (RMR' - 5)
CD	28_TSw2_Tptpln	2535	2540	10.0	167.9	19.68	0.022	198	5	12	10	18	15	-12	48	60	55
CD	28_TSw2_Tptpln	2540	2545	NA	167.9	19.68	0.022	197	NA	NA	NA	NA	NA	NA	NA	NA	NA
CD	28_TSw2_Tptpln	2545	2550	NA	167.9	19.68	0.022	196	NA	NA	NA	NA	NA	NA	NA	NA	NA
CD	28_TSw2_Tptpln	2550	2555	NA	167.9	19.68	0.022	195	NA	NA	NA	NA	NA	NA	NA	NA	NA
CD	28_TSw2_Tptpln	2555	2560	NA	167.9	19.68	0.022	194	NA	NA	NA	NA	NA	NA	NA	NA	NA
CD	28_TSw2_Tptpln	2560	2565	NA	167.9	19.68	0.022	193	NA	NA	NA	NA	NA	NA	NA	NA	NA
CD	28_TSw2_Tptpln	2565	2570	NA	167.9	19.68	0.022	192	NA	NA	NA	NA	NA	NA	NA	NA	NA
CD	28_TSw2_Tptpln	2570	2575	NA	167.9	19.68	0.022	190	NA	NA	NA	NA	NA	NA	NA	NA	NA
CD	28_TSw2_Tptpln	2575	2580	NA	167.9	19.68	0.022	190	NA	NA	NA	NA	NA	NA	NA	NA	NA
CD	28_TSw2_Tptpln	2580	2585	NA	167.9	19.68	0.022	189	NA	NA	NA	NA	NA	NA	NA	NA	NA
CD	25_TSw1_Tptpul	2585	2590	NA	58.22	10.60	0.022	188	NA	NA	NA	NA	NA	NA	NA	NA	NA
CD	25_TSw1_Tptpul	2590	2595	NA	58.22	10.60	0.022	188	NA	NA	NA	NA	NA	NA	NA	NA	NA
CD	25_TSw1_Tptpul	2595	2600	NA	58.22	10.60	0.022	187	NA	NA	NA	NA	NA	NA	NA	NA	NA
CD	25_TSw1_Tptpul	2600	2605	26.2	58.22	10.60	0.022	186	8	7	15	23	15	-5	63	68	63
CD	25_TSw1_Tptpul	2605	2610	44.8	58.22	10.60	0.022	186	8	7	15	18	15	0	63	63	58
CD	25_TSw1_Tptpul	2610	2615	57.2	58.22	10.60	0.022	185	13	7	15	18	15	0	68	68	63
CD	25_TSw1_Tptpul	2615	2620	50.0	58.22	10.60	0.022	185	13	7	15	18	15	0	68	68	63
CD	25_TSw1_Tptpul	2620	2625	31.0	58.22	10.60	0.022	184	8	7	15	24	15	0	69	69	64
CD	25_TSw1_Tptpul	2625	2630	41.4	58.22	10.60	0.022	183	8	7	15	24	15	0	69	69	64
CD	25_TSw1_Tptpul	2630	2635	35.0	58.22	10.60	0.022	183	8	7	15	24	15	0	69	69	64
CD	25_TSw1_Tptpul	2635	2640	52.0	58.22	10.60	0.022	182	13	7	15	24	15	0	74	74	69
CD	25_TSw1_Tptpul	2640	2645	52.2	58.22	10.60	0.022	182	13	7	15	21	15	0	71	71	66
CD	25_TSw1_Tptpul	2645	2650	42.4	58.22	10.60	0.022	182	8	7	15	21	15	0	66	66	61
CD	25_TSw1_Tptpul	2650	2655	55.8	58.22	10.60	0.022	181	13	7	15	21	15	0	71	71	66
CD	25_TSw1_Tptpul	2655	2660	30.0	58.22	10.60	0.022	181	8	7	8	18	15	-12	44	56	51
CD	25_TSw1_Tptpul	2660	2665	28.4	58.22	10.60	0.022	181	8	7	15	22	15	-5	62	67	62
ESF	07_TCw_Tpcpul	00+60	00+65	35.0	127.54	18.50	0.021	35.3	8	7	8	16	15	0	59	54	49
ESF	07_TCw_Tpcpul	00+65	00+70	95.0	127.54	18.50	0.021	37.3	20	7	15	17	15	0	79	74	69
ESF	07_TCw_Tpcpul	00+70	00+75	75.0	127.54	18.50	0.021	39.3	13	7	10	20	15	-5	65	65	60
ESF	07_TCw_Tpcpul	00+75	00+80	92.0	127.54	18.50	0.021	40.4	20	7	8	12	15	-5	62	62	57
ESF	07_TCw_Tpcpul	00+80	00+85	90.0	127.54	18.50	0.021	40.8	17	7	8	12	15	-5	59	59	54
ESF	07_TCw_Tpcpul	00+85	00+90	100.0	127.54	18.50	0.021	41.2	20	7	15	18	15	-5	75	75	70
ESF	07_TCw_Tpcpul	00+90	00+95	96.0	127.54	18.50	0.021	41.6	20	7	15	14	15	-5	71	71	66
ESF	07_TCw_Tpcpul	00+95	01+00	99.0	127.54	18.50	0.021	42	20	7	15	13	15	-5	70	70	65
ESF	08_TCw_Tpcpmn	01+00	01+05	97.0	127.54	18.50	0.021	42.4	20	12	15	15	15	-5	72	77	72
ESF	08_TCw_Tpcpmn	01+05	01+10	93.0	127.54	18.50	0.021	42.5	20	12	15	17	15	-5	74	79	74
ESF	08_TCw_Tpcpmn	01+10	01+14	99.0	127.54	18.50	0.021	42.4	20	12	15	15	15	-5	72	77	72
ESF	08_TCw_Tpcpmn	01+14	01+19	100.0	127.54	18.50	0.021	42.3	20	12	15	22	15	-5	79	84	79
ESF	08_TCw_Tpcpmn	01+19	01+24	82.0	127.54	18.50	0.021	42.2	17	12	10	12	15	-5	61	66	61

Location	Thermal Mechanical and Lithostratigraphic Unit Designation	Begin Station (m)	End Station (m)	RQD	Mean Intact UCS, σ_{ci} (MPa)	Hoek & Brown Intact Material Constant, mi	Unit Weight of Rock Mass, γ (MN/m^3)	Depth of Tunnel, H (m)	RQD Index	C	Js	Jcd	JwR	AJO	RMR Rating = (RQD Index+C+Js+Jcd+JwR+AJ0)	RMR' = (RQD Index+C+Js+Jcd+JwR)	Geological Strength Index, GSI = (RMR' - 5)
ESF	08_TCw_Tpcpmn	01+24	01+29	77.0	127.54	18.50	0.021	42.1	17	12	15	13	15	-5	67	72	67
ESF	08_TCw_Tpcpmn	01+29	01+34	83.0	127.54	18.50	0.021	42	17	12	15	15	15	-5	69	74	69
ESF	08_TCw_Tpcpmn	01+34	01+39	96.0	127.54	18.50	0.021	41.9	20	12	20	23	15	-5	85	90	85
ESF	08_TCw_Tpcpmn	01+39	01+44	97.0	127.54	18.50	0.021	41.8	20	12	15	18	15	-5	75	80	75
ESF	08_TCw_Tpcpmn	01+44	01+49	94.0	127.54	18.50	0.021	41.3	20	12	15	21	15	-5	78	83	78
ESF	08_TCw_Tpcpmn	01+49	01+54	75.0	127.54	18.50	0.021	40.6	13	12	10	10	15	-5	55	60	55
ESF	08_TCw_Tpcpmn	01+53	01+58	80.0	127.54	18.50	0.021	39.9	17	12	15	25	15	-5	79	84	79
ESF	08_TCw_Tpcpmn	01+58	01+63	81.0	127.54	18.50	0.021	39	17	12	10	10	15	-5	59	64	59
ESF	08_TCw_Tpcpmn	01+63	01+68	98.0	127.54	18.50	0.021	38.2	20	12	15	21	15	-5	78	83	78
ESF	08_TCw_Tpcpmn	01+68	01+73	99.0	127.54	18.50	0.021	37.4	20	12	15	21	15	-5	78	83	78
ESF	08_TCw_Tpcpmn	01+73	01+78	99.0	127.54	18.50	0.021	36.6	20	12	15	22	15	-5	79	84	79
ESF	08_TCw_Tpcpmn	01+78	01+83	98.0	127.54	18.50	0.021	35.8	20	12	20	25	15	-5	87	92	87
ESF	08_TCw_Tpcpmn	01+83	01+88	92.0	127.54	18.50	0.021	35	20	12	15	17	15	-5	74	79	74
ESF	09_TCw_Tpcpll	01+88	01+93	72.0	127.54	18.50	0.021	34.2	13	12	10	19	15	-5	64	69	64
ESF	09_TCw_Tpcpll	01+93	01+98	10.0	127.54	18.50	0.021	33.7	5	12	15	26	15	-5	60	73	68
ESF		01+98	02+01	NA		125.64	7.140	33.4	NA	NA	NA	NA	NA	NA	NA	NA	NA
ESF		02+01	02+66	NA		125.64	0.013	27.1	NA	NA	NA	NA	NA	NA	NA	NA	NA
ESF	03_UO_Tpki	02+66	02+71	NA	7.14	125.64	0.013	26.7	NA	NA	NA	NA	NA	NA	NA	NA	NA
ESF	03_UO_Tpki	02+71	02+76	100.0	7.14	125.64	0.013	26.2	20	4	20	30	15	0	89	89	84
ESF	03_UO_Tpki	02+76	02+81	93.0	7.14	125.64	0.013	25.8	20	4	20	0	15	-2	57	59	54
ESF	03_UO_Tpki	02+81	02+86	99.0	7.14	125.64	0.013	25.4	20	4	15	0	15	-5	49	54	49
ESF	03_UO_Tpki	02+86	02+91	100.0	7.14	125.64	0.013	25.6	20	4	20	14	15	0	73	73	68
ESF	03_UO_Tpki	02+91	02+96	100.0	7.14	125.64	0.013	25.9	20	4	20	0	15	-5	54	59	54
ESF	03_UO_Tpki	02+96	03+01	100.0	7.14	125.64	0.013	26.2	20	4	15	13	15	0	67	67	62
ESF	03_UO_Tpki	03+01	03+06	100.0	7.14	125.64	0.013	26.4	20	4	20	30	15	0	89	89	84
ESF	03_UO_Tpki	03+06	03+11	100.0	7.14	125.64	0.013	26.7	20	4	20	30	15	0	89	89	84
ESF	03_UO_Tpki	03+11	03+16	99.0	7.14	125.64	0.013	27	20	4	20	30	15	0	89	89	84
ESF	03_UO_Tpki	03+16	03+20	100.0	7.14	125.64	0.013	27.3	20	4	20	30	15	0	89	89	84
ESF	03_UO_Tpki	03+20	03+25	100.0	7.14	125.64	0.013	27.6	20	4	20	30	15	0	89	89	84
ESF	03_UO_Tpki	03+25	03+30	100.0	7.14	125.64	0.013	27.8	20	4	20	10	15	-5	64	69	64
ESF	03_UO_Tpki	03+30	03+35	95.0	7.14	125.64	0.013	28.2	20	4	20	8	15	-5	62	67	62
ESF		03+35	03+40	100.0	127.54	125.64	0.013	28.5	20	4	20	30	15	0	89	89	84
ESF		03+40	03+45	100.0	127.54	125.64	0.013	28.8	20	4	10	10	15	-5	54	59	54
ESF		03+45	03+50	98.0	127.54	18.50	0.013	29.1	20	4	15	20	15	-5	77	74	69
ESF		03+50	03+55	100.0	127.54	18.50	0.021	29.5	20	4	15	20	15	-5	77	74	69
ESF	04_TCw_Tpcrn	03+55	03+60	100.0	127.54	18.50	0.021	29.9	20	4	15	20	15	-5	77	74	69
ESF	04_TCw_Tpcrn	03+60	03+65	76.0	127.54	18.50	0.021	30.3	17	4	10	20	15	-5	69	66	61
ESF	04_TCw_Tpcrn	03+65	03+70	94.0	127.54	18.50	0.021	30.7	20	4	10	20	15	-12	65	69	64
ESF	04_TCw_Tpcrn	03+70	03+75	99.0	127.54	18.50	0.021	31.1	20	4	15	25	15	-5	82	79	74

Location	Thermal Mechanical and Lithostratigraphic Unit Designation	Begin Station (m)	End Station (m)	RQD	Mean Intact UCS, σ_{ci} (MPa)	Hoek & Brown Intact Material Constant, mi	Unit Weight of Rock Mass, γ (MN/m^3)	Depth of Tunnel, H (m)	RQD Index	C	Js	Jcd	JwR	AJO	RMR Rating = (RQD Index+C+Js+Jcd+JwR+AJ0)	RMR' = (RQD Index+C+Js+Jcd+JwR)	Geological Strength Index, GSI = (RMR' - 5)
ESF	04_TCw_Tpcrn	03+75	03+80	94.0	127.54	18.50	0.021	31.3	20	4	20	30	15	-2	95	89	84
ESF	04_TCw_Tpcrn	03+80	03+85	100.0	127.54	18.50	0.021	31.6	20	4	20	30	15	-2	95	89	84
ESF	04_TCw_Tpcrn	03+85	03+90	100.0	127.54	18.50	0.021	31.8	20	4	15	20	15	-5	77	74	69
ESF	05_TCw_Tpcrn2	03+90	03+95	100.0	127.54	18.50	0.021	32.1	20	4	20	25	15	-5	87	84	79
ESF	05_TCw_Tpcrn2	03+95	04+00	96.0	127.54	18.50	0.021	32.3	20	4	15	25	15	-5	82	79	74
ESF	05_TCw_Tpcrn2	04+00	04+05	97.0	127.54	18.50	0.021	32.5	20	4	20	25	15	-5	87	84	79
ESF	05_TCw_Tpcrn2	04+05	04+10	99.0	127.54	18.50	0.021	32.8	20	4	15	25	15	-5	82	79	74
ESF	05_TCw_Tpcrn2	04+10	04+15	100.0	127.54	18.50	0.021	33	20	4	10	20	15	-5	72	69	64
ESF	05_TCw_Tpcrn2	04+15	04+20	83.0	127.54	18.50	0.021	33.2	17	4	15	18	15	-5	72	69	64
ESF	05_TCw_Tpcrn2	04+20	04+25	91.0	127.54	18.50	0.021	33.6	20	4	15	25	15	-12	75	79	74
ESF	05_TCw_Tpcrn2	04+25	04+30	92.0	127.54	18.50	0.021	34	20	4	10	17	15	-5	69	66	61
ESF	06_TCw_Tpcrn1	04+30	04+35	93.0	127.54	18.50	0.021	34.5	20	4	10	17	15	-5	69	66	61
ESF	06_TCw_Tpcrn1	04+35	04+40	59.0	127.54	18.50	0.021	34.9	13	4	8	8	15	-5	51	48	43
ESF	07_TCw_Tpcpul	04+40	04+45	36.0	127.54	18.50	0.021	35.4	8	7	8	10	15	-5	48	48	43
ESF	07_TCw_Tpcpul	04+45	04+50	49.0	127.54	18.50	0.021	35.8	8	7	8	20	15	-5	58	58	53
ESF	07_TCw_Tpcpul	04+50	04+55	83.0	127.54	18.50	0.021	36.2	17	7	10	24	15	-12	66	73	68
ESF	07_TCw_Tpcpul	04+55	04+60	69.0	127.54	18.50	0.021	36.7	13	7	15	25	15	-5	75	75	70
ESF	07_TCw_Tpcpul	04+60	04+65	88.0	127.54	18.50	0.021	37.1	17	7	15	25	15	-5	79	79	74
ESF	07_TCw_Tpcpul	04+65	04+70	96.0	127.54	18.50	0.021	37.7	20	7	20	21	15	-12	76	83	78
ESF	07_TCw_Tpcpul	04+70	04+75	93.0	127.54	18.50	0.021	38.2	20	7	15	19	15	-12	69	76	71
ESF	07_TCw_Tpcpul	04+75	04+80	90.0	127.54	18.50	0.021	38.8	17	7	15	25	15	-5	79	79	74
ESF	07_TCw_Tpcpul	04+80	04+85	98.0	127.54	18.50	0.021	39.4	20	7	15	25	15	-5	82	82	77
ESF	07_TCw_Tpcpul	04+85	04+90	92.0	127.54	18.50	0.021	39.9	20	7	10	15	15	-5	67	67	62
ESF	07_TCw_Tpcpul	04+90	04+95	84.0	127.54	18.50	0.021	40.5	17	7	10	15	15	-12	57	64	59
ESF	07_TCw_Tpcpul	04+95	05+00	84.0	127.54	18.50	0.021	41	17	7	15	16	15	-5	70	70	65
ESF	07_TCw_Tpcpul	05+00	05+05	70.0	127.54	18.50	0.021	41.5	13	7	8	10	15	-10	48	53	48
ESF	07_TCw_Tpcpul	05+05	05+10	79.0	127.54	18.50	0.021	42	17	7	10	18	15	-5	67	67	62
ESF	07_TCw_Tpcpul	05+10	05+15	61.0	127.54	18.50	0.021	42.9	13	7	10	15	15	-5	60	60	55
ESF	07_TCw_Tpcpul	05+15	05+20	90.0	127.54	18.50	0.021	43.8	17	7	10	15	15	-5	64	64	59
ESF	07_TCw_Tpcpul	05+20	05+25	37.0	127.54	18.50	0.021	44.6	8	7	8	10	15	-12	41	48	43
ESF	07_TCw_Tpcpul	05+25	05+30	56.0	127.54	18.50	0.021	45.5	13	7	10	17	15	-10	57	62	57
ESF	07_TCw_Tpcpul	05+30	05+35	81.0	127.54	18.50	0.021	46.4	17	7	15	20	15	-10	69	74	69
ESF	07_TCw_Tpcpul	05+35	05+40	73.0	127.54	18.50	0.021	47.2	13	7	10	20	15	-5	65	65	60
ESF	07_TCw_Tpcpul	05+40	05+45	10.0	127.54	18.50	0.021	47.9	5	7	5	10	15	-5	42	42	37
ESF	07_TCw_Tpcpul	05+45	05+50	10.0	127.54	18.50	0.021	48.7	5	7	5	10	15	-5	42	42	37
ESF	08_TCw_Tpcpmn	05+50	05+55	10.0	127.54	18.50	0.021	49.5	5	12	8	10	15	-5	45	50	45
ESF	08_TCw_Tpcpmn	05+55	05+60	10.0	127.54	18.50	0.021	50.8	5	12	10	15	15	-12	45	57	52
ESF	08_TCw_Tpcpmn	05+60	05+65	50.0	127.54	18.50	0.021	52.1	8	12	7	10	15	-5	47	52	47
ESF	08_TCw_Tpcpmn	05+65	05+70	88.0	127.54	18.50	0.021	53	17	12	10	25	15	-5	74	79	74

Location	Thermal Mechanical and Lithostratigraphic Unit Designation	Begin Station (m)	End Station (m)	RQD	Mean Intact UCS, σ_{ci} (MPa)	Hoek & Brown Intact Material Constant, mi	Unit Weight of Rock Mass, γ (MN/m^3)	Depth of Tunnel, H (m)	RQD Index	C	Js	Jcd	JwR	AJO	RMR Rating = (RQD Index+C+Js+Jcd+JwR+AJ0)	RMR' = (RQD Index+C+Js+Jcd+JwR)	Geological Strength Index, GSI = (RMR' - 5)
ESF	08_TCw_Tpcpmn	05+70	05+75	82.0	127.54	18.50	0.021	53.9	17	12	8	20	15	-12	60	72	67
ESF	08_TCw_Tpcpmn	05+75	05+80	100.0	127.54	18.50	0.021	54.9	20	12	10	16	15	-12	61	73	68
ESF	08_TCw_Tpcpmn	05+80	05+85	84.0	127.54	18.50	0.021	55.8	17	12	10	16	15	-12	58	70	65
ESF	09_TCw_Tpcpll	05+85	05+90	99.0	127.54	18.50	0.021	56.7	20	12	15	25	15	0	87	87	82
ESF	09_TCw_Tpcpll	05+90	05+95	80.0	127.54	18.50	0.021	57.6	17	12	5	10	15	0	59	59	54
ESF	09_TCw_Tpcpll	05+95	06+00	87.0	127.54	18.50	0.021	58.6	17	12	15	25	15	0	84	84	79
ESF	09_TCw_Tpcpll	06+00	06+05	99.0	127.54	18.50	0.021	60.2	20	12	15	25	15	0	87	87	82
ESF	09_TCw_Tpcpll	06+05	06+10	80.0	127.54	18.50	0.021	61.8	17	12	15	25	15	0	84	84	79
ESF	09_TCw_Tpcpll	06+10	06+15	65.0	127.54	18.50	0.021	63.4	13	12	15	25	15	0	80	80	75
ESF	09_TCw_Tpcpll	06+15	06+20	53.6	127.54	18.50	0.021	65	13	12	8	25	15	0	73	73	68
ESF	10_TCw_Tpcpln	06+20	06+25	67.0	127.54	18.50	0.021	66.6	13	12	15	25	15	-5	75	80	75
ESF	10_TCw_Tpcpln	06+25	06+30	89.0	127.54	18.50	0.021	68.2	17	12	15	25	15	-12	72	84	79
ESF	10_TCw_Tpcpln	06+30	06+35	84.0	127.54	18.50	0.021	69.8	17	12	10	25	15	-12	67	79	74
ESF	10_TCw_Tpcpln	06+35	06+40	100.0	127.54	18.50	0.021	71.7	20	12	15	25	15	-12	75	87	82
ESF	10_TCw_Tpcpln	06+40	06+45	73.0	127.54	18.50	0.021	73.4	13	12	15	25	15	-12	68	80	75
ESF	10_TCw_Tpcpln	06+45	06+50	80.0	127.54	18.50	0.021	75	17	12	NA	NA	NA	NA	NA	NA	NA
ESF	10_TCw_Tpcpln	06+50	06+55	67.0	127.54	18.50	0.021	76.5	13	12	15	25	15	-12	68	80	75
ESF	10_TCw_Tpcpln	06+55	06+60	50.0	127.54	18.50	0.021	78	8	12	NA	NA	NA	NA	NA	NA	NA
ESF	10_TCw_Tpcpln	06+60	06+65	20.0	127.54	18.50	0.021	79.5	5	12	15	25	15	-12	60	72	67
ESF	10_TCw_Tpcpln	06+65	06+70	50.0	127.54	18.50	0.021	81	8	12	15	25	15	-12	63	75	70
ESF	10_TCw_Tpcpln	06+70	06+75	64.0	127.54	18.50	0.021	82.5	13	12	15	20	15	0	75	75	70
ESF	10_TCw_Tpcpln	06+75	06+80	29.0	127.54	18.50	0.021	84	8	12	8	10	15	-2	51	53	48
ESF	10_TCw_Tpcpln	06+80	06+85	43.0	127.54	18.50	0.021	85.5	8	12	8	0	15	-2	41	43	38
ESF	10_TCw_Tpcpln	06+85	06+90	76.0	127.54	18.50	0.021	86.9	17	12	15	10	15	0	69	69	64
ESF	10_TCw_Tpcpln	06+90	06+95	78.0	127.54	18.50	0.021	87.7	17	12	15	13	15	-5	67	72	67
ESF	10_TCw_Tpcpln	06+95	07+00	73.0	127.54	18.50	0.021	87.9	13	12	15	20	15	-12	63	75	70
ESF	10_TCw_Tpcpln	07+00	07+05	47.0	127.54	18.50	0.021	88.7	8	12	15	25	15	-12	63	75	70
ESF	10_TCw_Tpcpln	07+05	07+10	52.0	127.54	18.50	0.021	89	13	12	15	25	15	-12	68	80	75
ESF	10_TCw_Tpcpln	07+10	07+15	91.0	127.54	18.50	0.021	88.9	20	12	15	25	15	0	87	87	82
ESF	10_TCw_Tpcpln	07+15	07+20	84.0	127.54	18.50	0.021	88.9	17	12	15	25	15	0	84	84	79
ESF	10_TCw_Tpcpln	07+20	07+25	81.0	127.54	18.50	0.021	88.9	17	12	15	25	15	-12	72	84	79
ESF	10_TCw_Tpcpln	07+25	07+30	97.0	127.54	18.50	0.021	88.9	20	12	15	25	15	-12	75	87	82
ESF	10_TCw_Tpcpln	07+30	07+35	91.0	127.54	18.50	0.021	88.9	20	12	15	25	15	-10	77	87	82
ESF	10_TCw_Tpcpln	07+35	07+40	85.0	127.54	18.50	0.021	88.9	17	12	15	25	15	-5	79	84	79
ESF	10_TCw_Tpcpln	07+40	07+45	66.0	127.54	18.50	0.021	88.9	13	12	15	20	15	-10	65	75	70
ESF	10_TCw_Tpcpln	07+45	07+50	90.0	127.54	18.50	0.021	88.9	17	12	10	25	15	-12	67	79	74
ESF	10_TCw_Tpcpln	07+50	07+55	93.0	127.54	18.50	0.013	89.1	20	12	15	25	15	-2	85	87	82
ESF	10_TCw_Tpcpln	07+55	07+60	97.0	127.54	18.50	0.013	89.5	20	12	15	25	15	-5	82	87	82
ESF	10_TCw_Tpcpln	07+60	07+65	95.0	127.54	18.50	0.013	89.9	20	12	15	25	15	-10	77	87	82

Location	Thermal Mechanical and Lithostratigraphic Unit Designation	Begin Station (m)	End Station (m)	RQD	Mean Intact UCS, σ_{ci} (MPa)	Hoek & Brown Intact Material Constant, mi	Unit Weight of Rock Mass, γ (MN/m^3)	Depth of Tunnel, H (m)	RQD Index	C	Js	Jcd	JwR	AJO	RMR Rating = (RQD Index+C+Js+Jcd+JwR+AJ0)	RMR' = (RQD Index+C+Js+Jcd+JwR)	Geological Strength Index, GSI = (RMR' - 5)
ESF	10_TCw_Tpcpln	07+65	07+70	82.0	127.54	18.50	0.013	90.3	17	12	15	20	15	-10	69	79	74
ESF	10_TCw_Tpcpln	07+70	07+75	95.0	127.54	18.50	0.013	90.3	20	12	15	25	15	-5	82	87	82
ESF	12_PTn_Tpcpv2	07+75	07+80	91.0	6.37	17.64	0.013	90.1	20	4	15	18	15	-10	62	72	67
ESF	12_PTn_Tpcpv2	07+80	07+85	91.0	6.37	17.64	0.013	89.9	20	4	15	17	15	-5	66	71	66
ESF	12_PTn_Tpcpv2	07+85	07+90	97.0	6.37	17.64	0.013	89.6	20	4	20	14	15	-12	61	73	68
ESF	13_PTn_Tpcpv1	07+90	07+95	99.0	6.37	17.64	0.013	89.3	20	4	20	14	15	-12	61	73	68
ESF	13_PTn_Tpcpv1	07+95	08+00	100.0	6.37	17.64	0.013	89	20	4	20	16	15	-2	73	75	70
ESF	13_PTn_Tpcpv1	08+00	08+05	99.0	6.37	17.64	0.013	88.8	20	4	20	12	15	-2	69	71	66
ESF	13_PTn_Tpcpv1	08+05	08+10	100.0	6.37	17.64	0.013	88.4	20	4	15	16	15	-2	68	70	65
ESF	13_PTn_Tpcpv1	08+10	08+15	100.0	6.37	17.64	0.013	88.1	20	4	15	20	15	-2	72	74	69
ESF	13_PTn_Tpcpv1	08+15	08+20	100.0	6.37	17.64	0.013	87.8	20	4	15	16	15	-2	68	70	65
ESF	13_PTn_Tpcpv1	08+20	08+25	100.0	6.37	17.64	0.013	87.6	20	4	15	15	15	-5	64	69	64
ESF	13_PTn_Tpcpv1	08+25	08+30	100.0	6.37	17.64	0.013	88.2	20	4	20	18	15	-5	72	77	72
ESF	13_PTn_Tpcpv1	08+30	08+35	99.0	6.37	17.64	0.013	88.7	20	4	20	23	15	-10	72	82	77
ESF	13_PTn_Tpcpv1	08+35	08+40	100.0	6.37	17.64	0.013	89.2	20	4	20	25	15	-10	74	84	79
ESF	13_PTn_Tpcpv1	08+40	08+45	100.0	6.37	17.64	0.013	90.1	20	4	20	25	15	-10	74	84	79
ESF	13_PTn_Tpcpv1	08+45	08+50	100.0	6.37	17.64	0.013	91.7	20	4	20	20	15	-5	74	79	74
ESF	13_PTn_Tpcpv1	08+50	08+55	100.0	6.37	17.64	0.013	93.2	20	4	20	17	15	-5	71	76	71
ESF	13_PTn_Tpcpv1	08+55	08+60	100.0	6.37	17.64	0.013	94.8	20	4	15	17	15	-10	61	71	66
ESF	13_PTn_Tpcpv1	08+60	08+65	99.0	6.37	17.64	0.013	96.3	20	4	15	17	15	-10	61	71	66
ESF	13_PTn_Tpcpv1	08+65	08+70	100.0	6.37	17.64	0.013	97.8	20	4	20	17	15	-2	74	76	71
ESF	16_PTn_Tpbt3	08+70	08+75	100.0	6.37	150.97	0.013	125	20	4	20	25	15	-2	82	84	79
ESF	16_PTn_Tpbt3	08+75	08+80	100.0	6.37	150.97	0.013	125	20	4	20	25	15	-2	82	84	79
ESF	16_PTn_Tpbt3	08+80	08+85	NA	6.37	150.97	0.013		NA	NA	NA	NA	NA	NA	NA	NA	NA
ESF	16_PTn_Tpbt3	08+85	08+90	NA	6.37	150.97	0.013		NA	NA	NA	NA	NA	NA	NA	NA	NA
ESF	16_PTn_Tpbt3	08+90	08+95	NA	6.37	150.97	0.013		NA	NA	NA	NA	NA	NA	NA	NA	NA
ESF	17_PTn_Tpp	08+95	09+00	NA	6.37	150.97	0.013		NA	NA	NA	NA	NA	NA	NA	NA	NA
ESF	17_PTn_Tpp	09+00	09+05	NA	6.37	150.97	0.013		NA	NA	NA	NA	NA	NA	NA	NA	NA
ESF	17_PTn_Tpp	09+05	09+10	NA	6.37	150.97	0.013		NA	NA	NA	NA	NA	NA	NA	NA	NA
ESF	17_PTn_Tpp	09+10	09+15	NA	6.37	150.97	0.013		NA	NA	NA	NA	NA	NA	NA	NA	NA
ESF	17_PTn_Tpp	09+15	09+20	NA	6.37	150.97	0.013		NA	NA	NA	NA	NA	NA	NA	NA	NA
ESF	17_PTn_Tpp	09+20	09+25	NA	6.37	150.97	0.013		NA	NA	NA	NA	NA	NA	NA	NA	NA
ESF	17_PTn_Tpp	09+25	09+30	NA	6.37	150.97	0.013		NA	NA	NA	NA	NA	NA	NA	NA	NA
ESF	17_PTn_Tpp	09+30	09+35	NA	6.37	150.97	0.013		NA	NA	NA	NA	NA	NA	NA	NA	NA
ESF	17_PTn_Tpp	09+35	09+40	NA	6.37	150.97	0.013		NA	NA	NA	NA	NA	NA	NA	NA	NA
ESF	17_PTn_Tpp	09+40	09+45	NA	6.37	150.97	0.013		NA	NA	NA	NA	NA	NA	NA	NA	NA
ESF	17_PTn_Tpp	09+45	09+50	NA	6.37	150.97	0.013		NA	NA	NA	NA	NA	NA	NA	NA	NA
ESF	17_PTn_Tpp	09+50	09+55	NA	6.37	150.97	0.013		NA	NA	NA	NA	NA	NA	NA	NA	NA
ESF	17_PTn_Tpp	09+55	09+60	NA	6.37	150.97	0.013		NA	NA	NA	NA	NA	NA	NA	NA	NA

Location	Thermal Mechanical and Lithostratigraphic Unit Designation	Begin Station (m)	End Station (m)	RQD	Mean Intact UCS, σ_{ci} (MPa)	Hoek & Brown Intact Material Constant, mi	Unit Weight of Rock Mass, γ (MN/m^3)	Depth of Tunnel, H (m)	RQD Index	C	Js	Jcd	JwR	AJO	RMR Rating = (RQD Index+C+Js+Jcd+JwR+AJ0)	RMR' = (RQD Index+C+Js+Jcd+JwR)	Geological Strength Index, GSI = (RMR' - 5)
ESF	17_PTn_Tpp	09+60	09+65	NA	6.37	150.97	0.013		NA	NA	NA	NA	NA	NA	NA	NA	NA
ESF	17_PTn_Tpp	09+65	09+70	NA	6.37	150.97	0.013		NA	NA	NA	NA	NA	NA	NA	NA	NA
ESF	17_PTn_Tpp	09+70	09+75	NA	6.37	150.97	0.013		NA	NA	NA	NA	NA	NA	NA	NA	NA
ESF	17_PTn_Tpp	09+75	09+80	NA	6.37	150.97	0.013		NA	NA	NA	NA	NA	NA	NA	NA	NA
ESF	17_PTn_Tpp	09+80	09+85	NA	6.37	150.97	0.013		NA	NA	NA	NA	NA	NA	NA	NA	NA
ESF	17_PTn_Tpp	09+85	09+90	NA	6.37	150.97	0.013		NA	NA	NA	NA	NA	NA	NA	NA	NA
ESF	17_PTn_Tpp	09+90	09+95	NA	6.37	150.97	0.013		NA	NA	NA	NA	NA	NA	NA	NA	NA
ESF	17_PTn_Tpp	09+95	10+00	NA	6.37	150.97	0.013		NA	NA	NA	NA	NA	NA	NA	NA	NA
ESF	17_PTn_Tpp	10+00	10+05	96.0	6.37	150.97	0.013	125	20	4	15	18	15	0	72	72	67
ESF	17_PTn_Tpp	10+05	10+10	100.0	6.37	150.97	0.013	127	20	4	15	25	15	0	79	79	74
ESF	17_PTn_Tpp	10+10	10+15	100.0	6.37	150.97	0.013	128	20	4	20	25	15	0	84	84	79
ESF	17_PTn_Tpp	10+15	10+20	100.0	6.37	150.97	0.013	130	20	4	20	25	15	0	84	84	79
ESF	18_PTn_Tpbt2	10+20	10+25	100.0	6.37	150.97	0.013	131	20	4	20	25	15	0	84	84	79
ESF	18_PTn_Tpbt2	10+25	10+30	96.0	6.37	150.97	0.013	133	20	4	20	25	15	0	84	84	79
ESF	18_PTn_Tpbt2	10+30	10+35	97.0	6.37	150.97	0.013	134	20	4	15	20	15	0	74	74	69
ESF	18_PTn_Tpbt2	10+35	10+40	91.0	6.37	150.97	0.013	136	20	4	20	20	15	0	79	79	74
ESF	18_PTn_Tpbt2	10+40	10+45	96.0	6.37	150.97	0.013	137	20	4	15	20	15	-2	72	74	69
ESF	18_PTn_Tpbt2	10+45	10+50	100.0	6.37	150.97	0.013	139	20	4	15	20	15	-5	69	74	69
ESF	19_PTn_Tptrv3	10+50	10+55	100.0	6.37	17.64	0.013	139	20	4	15	18	15	-2	70	72	67
ESF	19_PTn_Tptrv3	10+55	10+60	98.0	6.37	17.64	0.013	139	20	4	15	20	15	0	74	74	69
ESF	20_PTn_Tptrv2	10+60	10+65	87.0	6.37	17.64	0.013	139	17	4	15	15	15	-10	56	66	61
ESF	20_PTn_Tptrv2	10+65	10+70	74.0	6.37	17.64	0.021	138	13	4	15	15	15	-10	52	62	57
ESF	20_PTn_Tptrv2	10+70	10+75	68.0	6.37	17.64	0.021	138	13	4	15	8	15	-12	43	55	50
ESF	21_TSw1_Tptrv1	10+75	10+80	56.0	58.22	10.60	0.021	138	13	7	15	8	15	-10	48	58	53
ESF	21_TSw1_Tptrv1	10+80	10+85	51.0	58.22	10.60	0.021	137	13	7	15	8	15	-12	46	58	53
ESF	21_TSw1_Tptrv1	10+85	10+90	48.0	58.22	10.60	0.021	137	8	7	10	10	15	-12	38	50	45
ESF	21_TSw1_Tptrv1	10+90	10+95	74.0	58.22	10.60	0.021	137	13	7	15	20	15	-12	58	70	65
ESF	21_TSw1_Tptrv1	10+95	11+00	75.0	58.22	10.60	0.021	138	13	7	15	0	15	10	60	50	45
ESF	21_TSw1_Tptrv1	11+00	11+05	76.0	58.22	10.60	0.021	139	17	7	15	25	15	0	79	79	74
ESF	21_TSw1_Tptrv1	11+05	11+10	52.0	58.22	10.60	0.021	140	13	7	10	25	15	-5	65	70	65
ESF	21_TSw1_Tptrv1	11+10	11+15	54.0	58.22	10.60	0.021	141	13	7	15	25	15	-12	63	75	70
ESF	21_TSw1_Tptrv1	11+15	11+20	48.0	58.22	10.60	0.021	142	8	7	0	0	15	-12	18	30	25
ESF	21_TSw1_Tptrv1	11+20	11+25	52.0	58.22	10.60	0.021	142	13	7	8	9	15	0	52	52	47
ESF	21_TSw1_Tptrv1	11+25	11+30	46.0	58.22	10.60	0.021	143	8	7	20	14	15	-5	59	64	59
ESF	21_TSw1_Tptrv1	11+30	11+35	10.0	58.22	10.60	0.021	144	5	7	20	13	15	0	60	60	55
ESF	21_TSw1_Tptrv1	11+35	11+40	18.0	58.22	10.60	0.021	145	5	7	10	15	15	-5	47	52	47
ESF	21_TSw1_Tptrv1	11+40	11+45	78.0	58.22	10.60	0.021	150	17	7	10	13	15	-5	57	62	57
ESF	21_TSw1_Tptrv1	11+45	11+50	73.0	58.22	10.60	0.021	150	13	7	NA	NA	NA	NA	NA	NA	NA
ESF	21_TSw1_Tptrv1	11+50	11+55	NA	58.22	10.60	0.021		NA	7	NA	NA	NA	NA	NA	NA	NA

Location	Thermal Mechanical and Lithostratigraphic Unit Designation	Begin Station (m)	End Station (m)	RQD	Mean Intact UCS, σ_{ci} (MPa)	Hoek & Brown Intact Material Constant, mi	Unit Weight of Rock Mass, γ (MN/m^3)	Depth of Tunnel, H (m)	RQD Index	C	Js	Jcd	JwR	AJO	RMR Rating = (RQD Index+C+Js+Jcd+JwR+AJ0)	RMR' = (RQD Index+C+Js+Jcd+JwR)	Geological Strength Index, GSI = (RMR' - 5)
ESF	21_TSw1_Tptrv1	11+55	11+60	NA	58.22	10.60	0.021		NA	7	NA	NA	NA	NA	NA	NA	NA
ESF	21_TSw1_Tptrv1	11+60	11+65	NA	58.22	10.60	0.021		NA	7	NA	NA	NA	NA	NA	NA	NA
ESF	21_TSw1_Tptrv1	11+65	11+70	NA	58.22	10.60	0.021		NA	7	NA	NA	NA	NA	NA	NA	NA
ESF	21_TSw1_Tptrv1	11+70	11+75	NA	58.22	10.60	0.021		NA	7	NA	NA	NA	NA	NA	NA	NA
ESF	21_TSw1_Tptrv1	11+75	11+80	15.0	58.22	10.60	0.021		5	7	NA	NA	NA	NA	NA	NA	NA
ESF	22_TSw1_Tptrn	11+80	11+85	70.0	58.22	10.60	0.021	150	13	7	10	21	15	-12	54	66	61
ESF	22_TSw1_Tptrn	11+85	11+90	98.0	58.22	10.60	0.021	150	20	7	15	16	15	-12	61	73	68
ESF	22_TSw1_Tptrn	11+90	11+95	99.0	58.22	10.60	0.021	150	20	7	20	24	15	-10	76	86	81
ESF	22_TSw1_Tptrn	11+95	12+00	93.0	58.22	10.60	0.021	149	20	7	10	15	15	-12	55	67	62
ESF	22_TSw1_Tptrn	12+00	12+05	99.0	58.22	10.60	0.021	149	20	7	15	17	15	-5	69	74	69
ESF	22_TSw1_Tptrn	12+05	12+10	82.0	58.22	10.60	0.021	148	17	7	15	12	15	-5	61	66	61
ESF	22_TSw1_Tptrn	12+10	12+15	78.0	58.22	10.60	0.021	148	17	7	15	19	15	-12	61	73	68
ESF	22_TSw1_Tptrn	12+15	12+20	78.0	58.22	10.60	0.021	148	17	7	10	19	15	0	68	68	63
ESF	22_TSw1_Tptrn	12+20	12+25	51.0	58.22	10.60	0.021	147	13	7	15	18	15	-12	56	68	63
ESF	22_TSw1_Tptrn	12+25	12+30	58.0	58.22	10.60	0.021	148	13	7	15	13	15	-12	51	63	58
ESF	22_TSw1_Tptrn	12+30	12+35	65.0	58.22	10.60	0.021	149	13	7	10	13	15	-5	53	58	53
ESF	22_TSw1_Tptrn	12+35	12+40	60.0	58.22	10.60	0.021	151	13	7	15	23	15	-5	68	73	68
ESF	22_TSw1_Tptrn	12+40	12+45	59.0	58.22	10.60	0.021	152	13	7	15	17	15	-12	55	67	62
ESF	22_TSw1_Tptrn	12+45	12+50	93.0	58.22	10.60	0.021	154	20	7	15	19	15	-10	66	76	71
ESF	22_TSw1_Tptrn	12+50	12+55	95.0	58.22	10.60	0.021	156	20	7	15	17	15	-5	69	74	69
ESF	22_TSw1_Tptrn	12+55	12+60	90.0	58.22	10.60	0.021	157	17	7	15	19	15	-12	61	73	68
ESF	22_TSw1_Tptrn	12+60	12+65	83.0	58.22	10.60	0.021	157	17	7	15	13	15	-12	55	67	62
ESF	22_TSw1_Tptrn	12+65	12+70	84.0	58.22	10.60	0.021	157	17	7	15	18	15	0	72	72	67
ESF	22_TSw1_Tptrn	12+70	12+75	98.0	58.22	10.60	0.021	158	20	7	15	25	15	-5	77	82	77
ESF	22_TSw1_Tptrn	12+75	12+80	87.0	58.22	10.60	0.021	159	17	7	15	25	15	-12	67	79	74
ESF	22_TSw1_Tptrn	12+80	12+85	96.0	58.22	10.60	0.021	160	20	7	20	16	15	-5	73	78	73
ESF	22_TSw1_Tptrn	12+85	12+90	88.0	58.22	10.60	0.021	161	17	7	15	17	15	-12	59	71	66
ESF	22_TSw1_Tptrn	12+90	12+95	60.0	58.22	10.60	0.021	162	13	7	10	15	15	-12	48	60	55
ESF	22_TSw1_Tptrn	12+95	13+00	53.0	58.22	10.60	0.021	162	13	7	10	18	15	0	63	63	58
ESF	22_TSw1_Tptrn	13+00	13+05	84.0	58.22	10.60	0.021	162	17	7	15	18	15	0	72	72	67
ESF	22_TSw1_Tptrn	13+05	13+10	63.0	58.22	10.60	0.021	162	13	7	10	10	15	0	55	55	50
ESF	22_TSw1_Tptrn	13+10	13+15	30.0	58.22	10.60	0.021	161	8	7	8	12	15	0	50	50	45
ESF	22_TSw1_Tptrn	13+15	13+20	32.0	58.22	10.60	0.021	162	8	7	8	12	15	0	50	50	45
ESF	22_TSw1_Tptrn	13+20	13+25	33.0	58.22	10.60	0.021	163	8	7	8	12	15	0	50	50	45
ESF	22_TSw1_Tptrn	13+25	13+30	85.0	58.22	10.60	0.021	165	17	7	15	21	15	0	75	75	70
ESF	22_TSw1_Tptrn	13+30	13+35	78.0	58.22	10.60	0.021	165	17	7	15	13	15	0	67	67	62
ESF	22_TSw1_Tptrn	13+35	13+40	96.0	58.22	10.60	0.021	166	20	7	20	20	15	-12	70	82	77
ESF	22_TSw1_Tptrn	13+40	13+45	96.0	58.22	10.60	0.021	166	20	7	20	10	15	0	72	72	67
ESF	22_TSw1_Tptrn	13+45	13+50	86.0	58.22	10.60	0.021	167	17	7	10	10	15	0	59	59	54

Location	Thermal Mechanical and Lithostratigraphic Unit Designation	Begin Station (m)	End Station (m)	RQD	Mean Intact UCS, σ_{ci} (MPa)	Hoek & Brown Intact Material Constant, mi	Unit Weight of Rock Mass, γ (MN/m^3)	Depth of Tunnel, H (m)	RQD Index	C	Js	Jcd	JwR	AJO	RMR Rating = (RQD Index+C+Js+Jcd+JwR+AJ0)	RMR' = (RQD Index+C+Js+Jcd+JwR)	Geological Strength Index, GSI = (RMR' - 5)
ESF	22_TSw1_Tptrn	13+50	13+55	84.0	58.22	10.60	0.021	167	17	7	NA	NA	NA	NA	NA	NA	NA
ESF	22_TSw1_Tptrn	13+55	13+60	85.0	58.22	10.60	0.021	168	17	7	20	20	15	-12	67	79	74
ESF	22_TSw1_Tptrn	13+60	13+65	80.0	58.22	10.60	0.021	169	17	7	15	20	15	-5	69	74	69
ESF	22_TSw1_Tptrn	13+65	13+70	98.0	58.22	10.60	0.021	170	20	7	15	17	15	-12	62	74	69
ESF	22_TSw1_Tptrn	13+70	13+75	96.0	58.22	10.60	0.021	171	20	7	15	12	15	-5	64	69	64
ESF	22_TSw1_Tptrn	13+75	13+80	79.0	58.22	10.60	0.021	172	17	7	20	14	15	-5	68	73	68
ESF	22_TSw1_Tptrn	13+80	13+85	98.0	58.22	10.60	0.021	173	20	7	15	15	15	-5	67	72	67
ESF	22_TSw1_Tptrn	13+85	13+90	57.0	58.22	10.60	0.021	174	13	7	15	15	15	-5	60	65	60
ESF	22_TSw1_Tptrn	13+90	13+95	85.0	58.22	10.60	0.021	175	17	7	10	12	15	0	61	61	56
ESF	22_TSw1_Tptrn	13+95	14+00	93.0	58.22	10.60	0.021	176	20	7	20	10	15	0	72	72	67
ESF	22_TSw1_Tptrn	14+00	14+05	100.0	58.22	10.60	0.021	177	20	7	20	10	15	0	72	72	67
ESF	22_TSw1_Tptrn	14+05	14+10	96.0	58.22	10.60	0.021	179	20	7	20	10	15	0	72	72	67
ESF	22_TSw1_Tptrn	14+10	14+15	81.0	58.22	10.60	0.021	179	17	7	20	8	15	0	67	67	62
ESF	22_TSw1_Tptrn	14+15	14+20	98.0	58.22	10.60	0.021	181	20	7	20	8	15	0	70	70	65
ESF	22_TSw1_Tptrn	14+20	14+25	96.0	58.22	10.60	0.021	182	20	7	15	22	15	-5	74	79	74
ESF	22_TSw1_Tptrn	14+25	14+30	92.0	58.22	10.60	0.021	183	20	7	15	22	15	-5	74	79	74
ESF	22_TSw1_Tptrn	14+30	14+35	94.0	58.22	10.60	0.021	184	20	7	10	13	15	-5	60	65	60
ESF	22_TSw1_Tptrn	14+35	14+40	74.0	58.22	10.60	0.021	185	13	7	15	17	15	-5	62	67	62
ESF	22_TSw1_Tptrn	14+40	14+45	76.0	58.22	10.60	0.021	186	17	7	20	17	15	0	76	76	71
ESF	22_TSw1_Tptrn	14+45	14+50	100.0	58.22	10.60	0.021	187	20	7	20	21	15	-12	71	83	78
ESF	22_TSw1_Tptrn	14+50	14+55	97.0	58.22	10.60	0.021	188	20	7	15	16	15	-12	61	73	68
ESF	22_TSw1_Tptrn	14+55	14+60	98.0	58.22	10.60	0.021	188	20	7	15	16	15	-12	61	73	68
ESF	22_TSw1_Tptrn	14+60	14+65	100.0	58.22	10.60	0.021	189	20	7	15	17	15	0	74	74	69
ESF	22_TSw1_Tptrn	14+65	14+70	77.0	58.22	10.60	0.021	190	17	7	15	15	15	-12	57	69	64
ESF	22_TSw1_Tptrn	14+70	14+75	92.0	58.22	10.60	0.021	190	20	7	20	17	15	-12	67	79	74
ESF	22_TSw1_Tptrn	14+75	14+80	82.0	58.22	10.60	0.021	191	17	7	15	18	15	-12	60	72	67
ESF	22_TSw1_Tptrn	14+80	14+85	97.0	58.22	10.60	0.021	192	20	7	20	16	15	-12	66	78	73
ESF	22_TSw1_Tptrn	14+85	14+90	94.0	58.22	10.60	0.021	193	20	7	20	16	15	0	78	78	73
ESF	22_TSw1_Tptrn	14+90	14+95	92.0	58.22	10.60	0.021	193	20	7	20	20	15	0	82	82	77
ESF	22_TSw1_Tptrn	14+95	15+00	85.0	58.22	10.60	0.021	194	17	7	15	19	15	0	73	73	68
ESF	22_TSw1_Tptrn	15+00	15+05	92.0	58.22	10.60	0.021	195	20	7	10	12	15	0	64	64	59
ESF	22_TSw1_Tptrn	15+05	15+10	77.0	58.22	10.60	0.021	196	17	7	15	11	15	-12	53	65	60
ESF	22_TSw1_Tptrn	15+10	15+15	83.0	58.22	10.60	0.021	196	17	7	10	23	15	-5	67	72	67
ESF	22_TSw1_Tptrn	15+15	15+20	82.0	58.22	10.60	0.021	197	17	7	10	23	15	-5	67	72	67
ESF	22_TSw1_Tptrn	15+20	15+25	85.0	58.22	10.60	0.021	198	17	7	15	25	15	-12	67	79	74
ESF	22_TSw1_Tptrn	15+25	15+30	66.0	58.22	10.60	0.021	198	13	7	10	17	15	-12	50	62	57
ESF	22_TSw1_Tptrn	15+30	15+35	84.0	58.22	10.60	0.021	199	17	7	15	10	15	0	64	64	59
ESF	22_TSw1_Tptrn	15+35	15+40	73.0	58.22	10.60	0.021	200	13	7	15	22	15	0	72	72	67
ESF	22_TSw1_Tptrn	15+40	15+45	94.0	58.22	10.60	0.021	199	20	7	20	11	15	0	73	73	68

Location	Thermal Mechanical and Lithostratigraphic Unit Designation	Begin Station (m)	End Station (m)	RQD	Mean Intact UCS, σ_{ci} (MPa)	Hoek & Brown Intact Material Constant, mi	Unit Weight of Rock Mass, γ (MN/m^3)	Depth of Tunnel, H (m)	RQD Index	C	Js	Jcd	JwR	AJO	RMR Rating = (RQD Index+C+Js+Jcd+JwR+AJ0)	RMR' = (RQD Index+C+Js+Jcd+JwR)	Geological Strength Index, GSI = (RMR' - 5)
ESF	22_TSw1_Tptrn	15+45	15+50	86.0	58.22	10.60	0.021	199	17	7	20	11	15	0	70	70	65
ESF	22_TSw1_Tptrn	15+50	15+55	81.0	58.22	10.60	0.021	199	17	7	15	13	15	0	67	67	62
ESF	22_TSw1_Tptrn	15+55	15+60	98.0	58.22	10.60	0.021	199	20	7	NA	NA	NA	NA	NA	NA	NA
ESF	22_TSw1_Tptrn	15+60	15+65	97.0	58.22	10.60	0.021	198	20	7	20	19	15	0	81	81	76
ESF	22_TSw1_Tptrn	15+65	15+70	97.0	58.22	10.60	0.021	198	20	7	20	5	15	-12	55	67	62
ESF	22_TSw1_Tptrn	15+70	15+75	96.0	58.22	10.60	0.021	198	20	7	20	13	15	0	75	75	70
ESF	22_TSw1_Tptrn	15+75	15+80	94.0	58.22	10.60	0.021	197	20	7	10	25	15	-5	72	77	72
ESF	22_TSw1_Tptrn	15+80	15+85	93.0	58.22	10.60	0.021	197	20	7	15	24	15	-12	69	81	76
ESF	22_TSw1_Tptrn	15+85	15+90	100.0	58.22	10.60	0.021	198	20	7	20	18	15	-12	68	80	75
ESF	22_TSw1_Tptrn	15+90	15+95	96.0	58.22	10.60	0.021	198	20	7	15	17	15	-12	62	74	69
ESF	22_TSw1_Tptrn	15+95	16+00	81.0	58.22	10.60	0.021	199	17	7	20	11	15	-12	58	70	65
ESF	22_TSw1_Tptrn	16+00	16+05	92.0	58.22	10.60	0.021	200	20	7	20	11	15	0	73	73	68
ESF	22_TSw1_Tptrn	16+05	16+10	93.0	58.22	10.60	0.021	200	20	7	20	20	15	-12	70	82	77
ESF	22_TSw1_Tptrn	16+10	16+15	97.0	58.22	10.60	0.021	199	20	7	20	17	15	-12	67	79	74
ESF	22_TSw1_Tptrn	16+15	16+20	89.0	58.22	10.60	0.021	198	17	7	15	20	15	-12	62	74	69
ESF	22_TSw1_Tptrn	16+20	16+25	95.0	58.22	10.60	0.021	196	20	7	20	7	15	0	69	69	64
ESF	22_TSw1_Tptrn	16+25	16+30	90.0	58.22	10.60	0.021	195	17	7	20	9	15	0	68	68	63
ESF	22_TSw1_Tptrn	16+30	16+35	93.0	58.22	10.60	0.021	194	20	7	20	9	15	-12	59	71	66
ESF	22_TSw1_Tptrn	16+35	16+40	100.0	58.22	10.60	0.021	193	20	7	20	10	15	-12	60	72	67
ESF	22_TSw1_Tptrn	16+40	16+45	99.0	58.22	10.60	0.021	192	20	7	20	8	15	0	70	70	65
ESF	22_TSw1_Tptrn	16+45	16+50	97.0	58.22	10.60	0.021	192	20	7	20	11	15	0	73	73	68
ESF	22_TSw1_Tptrn	16+50	16+55	96.0	58.22	10.60	0.021	191	20	7	20	16	15	0	78	78	73
ESF	22_TSw1_Tptrn	16+55	16+60	96.0	58.22	10.60	0.021	190	20	7	15	20	15	-12	65	77	72
ESF	22_TSw1_Tptrn	16+60	16+65	88.0	58.22	10.60	0.021	189	17	7	15	15	15	-12	57	69	64
ESF	22_TSw1_Tptrn	16+65	16+70	95.0	58.22	10.60	0.021	188	20	7	15	13	15	0	70	70	65
ESF	22_TSw1_Tptrn	16+70	16+75	87.0	58.22	10.60	0.021	187	17	7	15	18	15	-5	67	72	67
ESF	22_TSw1_Tptrn	16+75	16+80	88.0	58.22	10.60	0.021	187	17	7	15	23	15	0	77	77	72
ESF	22_TSw1_Tptrn	16+80	16+85	87.0	58.22	10.60	0.021	187	17	7	20	11	15	0	70	70	65
ESF	22_TSw1_Tptrn	16+85	16+90	90.0	58.22	10.60	0.021	186	17	7	15	18	15	0	72	72	67
ESF	22_TSw1_Tptrn	16+90	16+95	86.0	58.22	10.60	0.021	186	17	7	20	10	15	0	69	69	64
ESF	22_TSw1_Tptrn	16+95	17+00	87.0	58.22	10.60	0.021	186	17	7	15	13	15	0	67	67	62
ESF	22_TSw1_Tptrn	17+00	17+05	77.0	58.22	10.60	0.021	185	17	7	20	7	15	-12	54	66	61
ESF	22_TSw1_Tptrn	17+05	17+10	39.0	58.22	10.60	0.021	185	8	7	15	7	15	0	52	52	47
ESF	23_TSw1_Tptrl	17+10	17+15	76.0	58.22	10.60	0.021	185	17	4	15	20	15	-12	62	71	66
ESF	23_TSw1_Tptrl	17+15	17+20	77.0	58.22	10.60	0.021	184	17	4	15	20	15	-12	62	71	66
ESF	23_TSw1_Tptrl	17+20	17+25	61.0	58.22	10.60	0.021	184	13	4	15	20	15	0	70	67	62
ESF	23_TSw1_Tptrl	17+25	17+30	59.0	58.22	10.60	0.021	184	13	4	15	11	15	-12	49	58	53
ESF	23_TSw1_Tptrl	17+30	17+35	53.0	58.22	10.60	0.021	184	13	4	15	16	15	-12	54	63	58
ESF	23_TSw1_Tptrl	17+35	17+40	59.0	58.22	10.60	0.021	184	13	4	20	19	15	-5	69	71	66

Location	Thermal Mechanical and Lithostratigraphic Unit Designation	Begin Station (m)	End Station (m)	RQD	Mean Intact UCS, σ_{ci} (MPa)	Hoek & Brown Intact Material Constant, mi	Unit Weight of Rock Mass, γ (MN/m^3)	Depth of Tunnel, H (m)	RQD Index	C	Js	Jcd	JwR	AJO	RMR Rating = (RQD Index+C+Js+Jcd+JwR+AJ0)	RMR' = (RQD Index+C+Js+Jcd+JwR)	Geological Strength Index, GSI = (RMR' - 5)
ESF	23_TSw1_Tptrl	17+40	17+45	60.0	58.22	10.60	0.021	183	13	4	15	17	15	0	67	64	59
ESF	23_TSw1_Tptrl	17+45	17+50	43.0	58.22	10.60	0.021	183	8	4	20	16	15	-12	54	63	58
ESF	23_TSw1_Tptrl	17+50	17+55	45.0	58.22	10.60	0.021	184	8	4	0	17	15	0	47	44	39
ESF	23_TSw1_Tptrl	17+55	17+60	59.0	58.22	10.60	0.021	184	13	4	15	18	15	0	68	65	60
ESF	23_TSw1_Tptrl	17+60	17+65	36.0	58.22	10.60	0.021	184	8	4	8	15	15	0	53	50	45
ESF	23_TSw1_Tptrl	17+65	17+70	35.0	58.22	10.60	0.021	184	8	4	15	17	15	0	62	59	54
ESF	23_TSw1_Tptrl	17+70	17+75	31.0	58.22	10.60	0.021	184	8	4	15	11	15	0	56	53	48
ESF	23_TSw1_Tptrl	17+75	17+80	32.0	58.22	10.60	0.021	184	8	4	20	16	15	-12	54	63	58
ESF	23_TSw1_Tptrl	17+80	17+85	57.0	58.22	10.60	0.021	184	13	4	20	16	15	-12	59	68	63
ESF	23_TSw1_Tptrl	17+85	17+90	33.0	58.22	10.60	0.021	184	8	4	20	20	15	-12	58	67	62
ESF	23_TSw1_Tptrl	17+90	17+95	37.0	58.22	10.60	0.021	184	8	4	20	20	15	0	70	67	62
ESF	25_TSw1_Tptpul	17+95	18+00	55.0	58.22	10.60	0.021	184	13	7	10	25	15	-12	58	70	65
ESF	25_TSw1_Tptpul	18+00	18+05	36.0	58.22	10.60	0.021	184	8	7	20	25	15	-12	63	75	70
ESF	25_TSw1_Tptpul	18+05	18+10	47.0	58.22	10.60	0.021	185	8	7	10	17	15	-5	52	57	52
ESF	25_TSw1_Tptpul	18+10	18+15	54.0	58.22	10.60	0.021	184	13	7	10	20	15	-12	53	65	60
ESF	25_TSw1_Tptpul	18+15	18+20	52.0	58.22	10.60	0.021	184	13	7	20	21	15	0	76	76	71
ESF	25_TSw1_Tptpul	18+20	18+25	29.0	58.22	10.60	0.021	184	8	7	15	15	15	-12	48	60	55
ESF	25_TSw1_Tptpul	18+25	18+30	12.0	58.22	10.60	0.021	183	5	7	0	0	15	-12	15	27	22
ESF	25_TSw1_Tptpul	18+30	18+35	38.0	58.22	10.60	0.021	183	8	7	8	14	15	0	52	52	47
ESF	25_TSw1_Tptpul	18+35	18+40	32.0	58.22	10.60	0.021	183	8	7	8	14	15	0	52	52	47
ESF	25_TSw1_Tptpul	18+40	18+45	48.0	58.22	10.60	0.021	183	8	7	8	14	15	0	52	52	47
ESF	25_TSw1_Tptpul	18+45	18+50	41.0	58.22	10.60	0.021	183	8	7	15	15	15	-5	55	60	55
ESF	25_TSw1_Tptpul	18+50	18+55	61.0	58.22	10.60	0.021	183	13	7	10	14	15	0	59	59	54
ESF	25_TSw1_Tptpul	18+55	18+60	33.0	58.22	10.60	0.021	182	8	7	15	12	15	0	57	57	52
ESF	25_TSw1_Tptpul	18+60	18+65	29.0	58.22	10.60	0.021	181	8	7	20	11	15	0	61	61	56
ESF	25_TSw1_Tptpul	18+65	18+70	21.0	58.22	10.60	0.021	180	5	7	8	14	15	0	49	49	44
ESF	25_TSw1_Tptpul	18+70	18+75	10.0	58.22	10.60	0.021	179	5	7	8	14	15	0	49	49	44
ESF	25_TSw1_Tptpul	18+75	18+80	46.0	58.22	10.60	0.021	178	8	7	10	16	15	-12	44	56	51
ESF	25_TSw1_Tptpul	18+80	18+85	15.0	58.22	10.60	0.021	177	5	7	10	16	15	-12	41	53	48
ESF	25_TSw1_Tptpul	18+85	18+90	15.0	58.22	10.60	0.021	177	5	7	10	16	15	-12	41	53	48
ESF	25_TSw1_Tptpul	18+90	18+95	30.0	58.22	10.60	0.021	177	8	7	10	16	15	-12	44	56	51
ESF	25_TSw1_Tptpul	18+95	19+00	15.0	58.22	10.60	0.021	178	5	7	10	16	15	-12	41	53	48
ESF	25_TSw1_Tptpul	19+00	19+05	40.0	58.22	10.60	0.021	177	8	7	10	16	15	-12	44	56	51
ESF	25_TSw1_Tptpul	19+05	19+10	40.0	58.22	10.60	0.021	177	8	7	15	18	15	0	63	63	58
ESF	25_TSw1_Tptpul	19+10	19+15	61.0	58.22	10.60	0.021	176	13	7	15	16	15	0	66	66	61
ESF	25_TSw1_Tptpul	19+15	19+20	42.0	58.22	10.60	0.021	176	8	7	15	17	15	-12	50	62	57
ESF	25_TSw1_Tptpul	19+20	19+25	19.0	58.22	10.60	0.021	176	5	7	15	17	15	-12	47	59	54
ESF	25_TSw1_Tptpul	19+25	19+30	38.0	58.22	10.60	0.021	176	8	7	20	17	15	0	67	67	62
ESF	25_TSw1_Tptpul	19+30	19+35	47.0	58.22	10.60	0.021	176	8	7	20	14	15	-12	52	64	59

Location	Thermal Mechanical and Lithostratigraphic Unit Designation	Begin Station (m)	End Station (m)	RQD	Mean Intact UCS, σ_{ci} (MPa)	Hoek & Brown Intact Material Constant, mi	Unit Weight of Rock Mass, γ (MN/m^3)	Depth of Tunnel, H (m)	RQD Index	C	Js	Jcd	JwR	AJO	RMR Rating = (RQD Index+C+Js+Jcd+JwR+AJ0)	RMR' = (RQD Index+C+Js+Jcd+JwR)	Geological Strength Index, GSI = (RMR' - 5)
ESF	25_TSw1_Tptpul	19+35	19+40	67.0	58.22	10.60	0.021	176	13	7	20	14	15	-12	57	69	64
ESF	25_TSw1_Tptpul	19+40	19+45	36.0	58.22	10.60	0.021	176	8	7	15	9	15	-12	42	54	49
ESF	25_TSw1_Tptpul	19+45	19+50	19.0	58.22	10.60	0.021	175	5	7	15	9	15	-12	39	51	46
ESF	25_TSw1_Tptpul	19+50	19+55	34.0	58.22	10.60	0.021	174	8	7	15	19	15	-12	52	64	59
ESF	25_TSw1_Tptpul	19+55	19+60	21.0	58.22	10.60	0.021	174	5	7	15	20	15	-12	50	62	57
ESF	25_TSw1_Tptpul	19+60	19+65	67.0	58.22	10.60	0.021	174	13	7	0	24	15	-5	54	59	54
ESF	25_TSw1_Tptpul	19+65	19+70	43.0	58.22	10.60	0.021	175	8	7	0	24	15	-5	49	54	49
ESF	25_TSw1_Tptpul	19+70	19+75	53.0	58.22	10.60	0.021	175	13	7	NA	NA	NA	NA	NA	NA	NA
ESF	25_TSw1_Tptpul	19+75	19+80	54.0	58.22	10.60	0.021	175	13	7	15	18	15	-12	56	68	63
ESF	25_TSw1_Tptpul	19+80	19+85	80.0	58.22	10.60	0.021	176	17	7	0	17	15	-5	51	56	51
ESF	25_TSw1_Tptpul	19+85	19+90	88.0	58.22	10.60	0.021	176	17	7	15	21	15	-5	70	75	70
ESF	25_TSw1_Tptpul	19+90	19+95	70.0	58.22	10.60	0.021	176	13	7	10	24	15	-12	57	69	64
ESF	25_TSw1_Tptpul	19+95	20+00	73.0	58.22	10.60	0.021	176	13	7	15	20	15	-12	58	70	65
ESF	25_TSw1_Tptpul	20+00	20+05	82.0	58.22	10.60	0.021	176	17	7	15	15	15	-12	57	69	64
ESF	25_TSw1_Tptpul	20+05	20+10	60.0	58.22	10.60	0.021	176	13	7	15	19	15	-5	64	69	64
ESF	25_TSw1_Tptpul	20+10	20+15	75.0	58.22	10.60	0.021	176	13	7	20	30	15	-5	80	85	80
ESF	25_TSw1_Tptpul	20+15	20+20	58.0	58.22	10.60	0.021	177	13	7	20	30	15	-5	80	85	80
ESF	25_TSw1_Tptpul	20+20	20+25	60.0	58.22	10.60	0.021	177	13	7	8	12	15	0	55	55	50
ESF	25_TSw1_Tptpul	20+25	20+30	64.0	58.22	10.60	0.021	177	13	7	10	20	15	0	65	65	60
ESF	25_TSw1_Tptpul	20+30	20+35	41.0	58.22	10.60	0.021	177	8	7	10	20	15	-5	55	60	55
ESF	25_TSw1_Tptpul	20+35	20+40	45.0	58.22	10.60	0.021	177	8	7	15	21	15	0	66	66	61
ESF	25_TSw1_Tptpul	20+40	20+45	78.0	58.22	10.60	0.021	177	17	7	20	15	15	0	74	74	69
ESF	25_TSw1_Tptpul	20+45	20+50	81.0	58.22	10.60	0.021	178	17	7	10	13	15	0	62	62	57
ESF	25_TSw1_Tptpul	20+50	20+55	55.0	58.22	10.60	0.021	178	13	7	15	21	15	0	71	71	66
ESF	25_TSw1_Tptpul	20+55	20+60	44.0	58.22	10.60	0.021	178	8	7	15	17	15	-5	57	62	57
ESF	25_TSw1_Tptpul	20+60	20+65	60.0	58.22	10.60	0.021	179	13	7	8	18	15	-5	56	61	56
ESF	25_TSw1_Tptpul	20+65	20+70	88.0	58.22	10.60	0.021	179	17	7	20	13	15	-12	60	72	67
ESF	25_TSw1_Tptpul	20+70	20+75	54.0	58.22	10.60	0.021	180	13	7	10	13	15	0	58	58	53
ESF	25_TSw1_Tptpul	20+75	20+80	53.0	58.22	10.60	0.021	180	13	7	10	13	15	0	58	58	53
ESF	25_TSw1_Tptpul	20+80	20+85	62.0	58.22	10.60	0.021	180	13	7	15	24	15	0	74	74	69
ESF	25_TSw1_Tptpul	20+85	20+90	42.0	58.22	10.60	0.021	180	8	7	8	24	15	-5	57	62	57
ESF	25_TSw1_Tptpul	20+90	20+95	42.0	58.22	10.60	0.021	180	8	7	8	21	15	-5	54	59	54
ESF	25_TSw1_Tptpul	20+95	21+00	79.0	58.22	10.60	0.021	180	17	7	10	26	15	-5	70	75	70
ESF	25_TSw1_Tptpul	21+00	21+05	77.0	58.22	10.60	0.021	180	17	7	20	23	15	0	82	82	77
ESF	25_TSw1_Tptpul	21+05	21+10	69.0	58.22	10.60	0.021	181	13	7	15	17	15	0	67	67	62
ESF	25_TSw1_Tptpul	21+10	21+15	68.0	58.22	10.60	0.021	181	13	7	10	17	15	-5	57	62	57
ESF	25_TSw1_Tptpul	21+15	21+20	80.0	58.22	10.60	0.021	182	17	7	10	22	15	-5	66	71	66
ESF	25_TSw1_Tptpul	21+20	21+25	40.0	58.22	10.60	0.021	183	8	7	8	21	15	-5	54	59	54
ESF	25_TSw1_Tptpul	21+25	21+30	62.0	58.22	10.60	0.021	183	13	7	8	21	15	0	64	64	59

Location	Thermal Mechanical and Lithostratigraphic Unit Designation	Begin Station (m)	End Station (m)	RQD	Mean Intact UCS, σ_{ci} (MPa)	Hoek & Brown Intact Material Constant, mi	Unit Weight of Rock Mass, γ (MN/m^3)	Depth of Tunnel, H (m)	RQD Index	C	Js	Jcd	JwR	AJO	RMR Rating = (RQD Index+C+Js+Jcd+JwR+AJ0)	RMR' = (RQD Index+C+Js+Jcd+JwR)	Geological Strength Index, GSI = (RMR' - 5)
ESF	25_TSw1_Tptpul	21+30	21+35	58.0	58.22	10.60	0.021	183	13	7	8	21	15	0	64	64	59
ESF	25_TSw1_Tptpul	21+35	21+40	70.0	58.22	10.60	0.021	183	13	7	8	21	15	0	64	64	59
ESF	25_TSw1_Tptpul	21+40	21+45	43.0	58.22	10.60	0.021	184	8	7	10	20	15	0	60	60	55
ESF	25_TSw1_Tptpul	21+45	21+50	50.0	58.22	10.60	0.021	184	8	7	10	15	15	0	55	55	50
ESF	25_TSw1_Tptpul	21+50	21+55	49.0	58.22	10.60	0.021	184	8	7	8	23	15	-5	56	61	56
ESF	25_TSw1_Tptpul	21+55	21+60	49.0	58.22	10.60	0.021	185	8	7	0	22	15	-5	47	52	47
ESF	25_TSw1_Tptpul	21+60	21+65	71.0	58.22	10.60	0.021	185	13	7	20	14	15	-5	64	69	64
ESF	25_TSw1_Tptpul	21+65	21+70	53.0	58.22	10.60	0.021	185	13	7	15	10	15	-5	55	60	55
ESF	25_TSw1_Tptpul	21+70	21+75	50.0	58.22	10.60	0.021	186	8	7	0	20	15	0	50	50	45
ESF	25_TSw1_Tptpul	21+75	21+80	29.0	58.22	10.60	0.021	186	8	7	0	20	15	0	50	50	45
ESF	25_TSw1_Tptpul	21+80	21+85	45.0	58.22	10.60	0.021	186	8	7	0	20	15	0	50	50	45
ESF	25_TSw1_Tptpul	21+85	21+90	52.0	58.22	10.60	0.021	187	13	7	0	20	15	0	55	55	50
ESF	25_TSw1_Tptpul	21+90	21+95	49.0	58.22	10.60	0.021	187	8	7	8	12	15	0	50	50	45
ESF	25_TSw1_Tptpul	21+95	22+00	19.0	58.22	10.60	0.021	187	5	7	NA	NA	NA	NA	NA	NA	NA
ESF	25_TSw1_Tptpul	22+00	22+05	54.0	58.22	10.60	0.021	188	13	7	0	18	15	0	53	53	48
ESF	25_TSw1_Tptpul	22+05	22+10	41.0	58.22	10.60	0.021	188	8	7	15	18	15	0	63	63	58
ESF	25_TSw1_Tptpul	22+10	22+15	55.0	58.22	10.60	0.021	188	13	7	15	18	15	0	68	68	63
ESF	25_TSw1_Tptpul	22+15	22+20	28.0	58.22	10.60	0.021	189	8	7	15	14	15	-5	54	59	54
ESF	25_TSw1_Tptpul	22+20	22+25	25.0	58.22	10.60	0.021	189	5	7	0	17	15	0	44	44	39
ESF	25_TSw1_Tptpul	22+25	22+30	20.0	58.22	10.60	0.021	189	5	7	0	20	15	0	47	47	42
ESF	25_TSw1_Tptpul	22+30	22+35	38.0	58.22	10.60	0.021	189	8	7	0	16	15	-5	41	46	41
ESF	25_TSw1_Tptpul	22+35	22+40	31.0	58.22	10.60	0.021	190	8	7	0	16	15	-5	41	46	41
ESF	25_TSw1_Tptpul	22+40	22+45	30.0	58.22	10.60	0.021	190	8	7	0	15	15	0	45	45	40
ESF	25_TSw1_Tptpul	22+45	22+50	30.0	58.22	10.60	0.021	190	8	7	0	15	15	0	45	45	40
ESF	25_TSw1_Tptpul	22+50	22+55	36.0	58.22	10.60	0.021	191	8	7	0	19	15	-5	44	49	44
ESF	25_TSw1_Tptpul	22+55	22+60	38.0	58.22	10.60	0.021	191	8	7	0	19	15	-5	44	49	44
ESF	25_TSw1_Tptpul	22+60	22+65	20.0	58.22	10.60	0.021	191	5	7	0	19	15	-5	41	46	41
ESF	25_TSw1_Tptpul	22+65	22+70	37.0	58.22	10.60	0.021	192	8	7	0	13	15	0	43	43	38
ESF	25_TSw1_Tptpul	22+70	22+75	14.0	58.22	10.60	0.021	192	5	7	0	13	15	0	40	40	35
ESF	25_TSw1_Tptpul	22+75	22+80	30.0	58.22	10.60	0.021	192	8	7	8	16	15	0	54	54	49
ESF	25_TSw1_Tptpul	22+80	22+85	46.0	58.22	10.60	0.021	192	8	7	10	16	15	0	56	56	51
ESF	25_TSw1_Tptpul	22+85	22+90	28.0	58.22	10.60	0.021	193	8	7	0	16	15	-5	41	46	41
ESF	25_TSw1_Tptpul	22+90	22+95	41.0	58.22	10.60	0.021	193	8	7	15	15	15	-5	55	60	55
ESF	25_TSw1_Tptpul	22+95	23+00	41.0	58.22	10.60	0.021	193	8	7	0	18	15	0	48	48	43
ESF	25_TSw1_Tptpul	23+00	23+05	37.0	58.22	10.60	0.021	194	8	7	8	9	15	0	47	47	42
ESF	25_TSw1_Tptpul	23+05	23+10	56.0	58.22	10.60	0.021	195	13	7	8	20	15	0	63	63	58
ESF	25_TSw1_Tptpul	23+10	23+15	62.0	58.22	10.60	0.021	196	13	7	0	17	15	0	52	52	47
ESF	25_TSw1_Tptpul	23+15	23+20	72.0	58.22	10.60	0.021	197	13	7	0	15	15	0	50	50	45
ESF	25_TSw1_Tptpul	23+20	23+25	71.0	58.22	10.60	0.021	197	13	7	0	15	15	0	50	50	45

Location	Thermal Mechanical and Lithostratigraphic Unit Designation	Begin Station (m)	End Station (m)	RQD	Mean Intact UCS, σ_{ci} (MPa)	Hoek & Brown Intact Material Constant, mi	Unit Weight of Rock Mass, γ (MN/m^3)	Depth of Tunnel, H (m)	RQD Index	C	Js	Jcd	JwR	AJO	RMR Rating = (RQD Index+C+Js+Jcd+JwR+AJ0)	RMR' = (RQD Index+C+Js+Jcd+JwR)	Geological Strength Index, GSI = (RMR' - 5)
ESF	25_TSw1_Tptpul	23+25	23+30	70.0	58.22	10.60	0.021	198	13	7	15	17	15	0	67	67	62
ESF	25_TSw1_Tptpul	23+30	23+35	63.0	58.22	10.60	0.021	198	13	7	15	21	15	0	71	71	66
ESF	25_TSw1_Tptpul	23+35	23+40	71.0	58.22	10.60	0.021	199	13	7	10	20	15	-5	60	65	60
ESF	25_TSw1_Tptpul	23+40	23+45	54.0	58.22	10.60	0.021	199	13	7	8	23	15	-5	61	66	61
ESF	25_TSw1_Tptpul	23+45	23+50	75.0	58.22	10.60	0.021	200	13	7	10	15	15	0	60	60	55
ESF	25_TSw1_Tptpul	23+50	23+55	73.0	58.22	10.60	0.021	201	13	7	0	20	15	-5	50	55	50
ESF	25_TSw1_Tptpul	23+55	23+60	75.0	58.22	10.60	0.021	201	13	7	15	11	15	-5	56	61	56
ESF	25_TSw1_Tptpul	23+60	23+65	59.0	58.22	10.60	0.021	203	13	7	8	16	15	-5	54	59	54
ESF	25_TSw1_Tptpul	23+65	23+70	73.0	58.22	10.60	0.021	205	13	7	15	13	15	0	63	63	58
ESF	25_TSw1_Tptpul	23+70	23+75	67.0	58.22	10.60	0.021	208	13	7	15	13	15	0	63	63	58
ESF	25_TSw1_Tptpul	23+75	23+80	54.0	58.22	10.60	0.021	209	13	7	8	7	15	0	50	50	45
ESF	25_TSw1_Tptpul	23+80	23+85	81.0	58.22	10.60	0.021	211	17	7	20	16	15	0	75	75	70
ESF	25_TSw1_Tptpul	23+85	23+90	78.0	58.22	10.60	0.021	212	17	7	8	7	15	-5	49	54	49
ESF	25_TSw1_Tptpul	23+90	23+95	91.0	58.22	10.60	0.021	214	20	7	0	25	15	-5	62	67	62
ESF	25_TSw1_Tptpul	23+95	24+00	59.0	58.22	10.60	0.021	216	13	7	0	11	15	0	46	46	41
ESF	25_TSw1_Tptpul	24+00	24+05	58.0	58.22	10.60	0.021	217	13	7	0	11	15	0	46	46	41
ESF	25_TSw1_Tptpul	24+05	24+10	34.0	58.22	10.60	0.021	219	8	7	0	11	15	0	41	41	36
ESF	25_TSw1_Tptpul	24+10	24+15	67.0	58.22	10.60	0.021	220	13	7	0	13	15	0	48	48	43
ESF	25_TSw1_Tptpul	24+15	24+20	52.0	58.22	10.60	0.021	222	13	7	8	15	15	-5	53	58	53
ESF	25_TSw1_Tptpul	24+20	24+25	44.0	58.22	10.60	0.021	225	8	7	0	13	15	-5	38	43	38
ESF	25_TSw1_Tptpul	24+25	24+30	55.0	58.22	10.60	0.021	227	13	7	0	18	15	0	53	53	48
ESF	25_TSw1_Tptpul	24+30	24+35	66.0	58.22	10.60	0.021	230	13	7	0	21	15	0	56	56	51
ESF	25_TSw1_Tptpul	24+35	24+40	66.0	58.22	10.60	0.021	233	13	7	0	14	15	-5	44	49	44
ESF	25_TSw1_Tptpul	24+40	24+45	38.0	58.22	10.60	0.021	235	8	7	8	24	15	-5	57	62	57
ESF	25_TSw1_Tptpul	24+45	24+50	56.0	58.22	10.60	0.021	238	13	7	0	24	15	-5	54	59	54
ESF	25_TSw1_Tptpul	24+50	24+55	52.0	58.22	10.60	0.021	241	13	7	8	21	15	-5	59	64	59
ESF	25_TSw1_Tptpul	24+55	24+60	37.0	58.22	10.60	0.021	244	8	7	8	21	15	-5	54	59	54
ESF	25_TSw1_Tptpul	24+60	24+65	60.0	58.22	10.60	0.021	246	13	7	15	17	15	0	67	67	62
ESF	25_TSw1_Tptpul	24+65	24+70	26.0	58.22	10.60	0.021	249	8	7	0	14	15	0	44	44	39
ESF	25_TSw1_Tptpul	24+70	24+75	67.0	58.22	10.60	0.021	251	13	7	10	18	15	-5	58	63	58
ESF	25_TSw1_Tptpul	24+75	24+80	38.0	58.22	10.60	0.021	254	8	7	8	13	15	0	51	51	46
ESF	25_TSw1_Tptpul	24+80	24+85	23.0	58.22	10.60	0.021	256	5	7	8	9	15	0	44	44	39
ESF	25_TSw1_Tptpul	24+85	24+90	51.0	58.22	10.60	0.021	259	13	7	10	15	15	0	60	60	55
ESF	25_TSw1_Tptpul	24+90	24+95	66.0	58.22	10.60	0.021	262	13	7	10	15	15	0	60	60	55
ESF	25_TSw1_Tptpul	24+95	25+00	57.0	58.22	10.60	0.021	265	13	7	8	10	15	0	53	53	48
ESF	25_TSw1_Tptpul	25+00	25+05	37.0	58.22	10.60	0.021	267	8	7	8	9	15	0	47	47	42
ESF	25_TSw1_Tptpul	25+05	25+10	64.0	58.22	10.60	0.021	270	13	7	10	16	15	0	61	61	56
ESF	25_TSw1_Tptpul	25+10	25+15	65.0	58.22	10.60	0.021	273	13	7	10	16	15	-5	56	61	56
ESF	25_TSw1_Tptpul	25+15	25+20	57.0	58.22	10.60	0.021	275	13	7	15	20	15	0	70	70	65

Location	Thermal Mechanical and Lithostratigraphic Unit Designation	Begin Station (m)	End Station (m)	RQD	Mean Intact UCS, σ_{ci} (MPa)	Hoek & Brown Intact Material Constant, mi	Unit Weight of Rock Mass, γ (MN/m^3)	Depth of Tunnel, H (m)	RQD Index	C	Js	Jcd	JwR	AJO	RMR Rating = (RQD Index+C+Js+Jcd+JwR+AJ0)	RMR' = (RQD Index+C+Js+Jcd+JwR)	Geological Strength Index, GSI = (RMR' - 5)
ESF	25_TSw1_Tptpul	25+20	25+25	72.0	58.22	10.60	0.021	277	13	7	8	14	15	-5	52	57	52
ESF	25_TSw1_Tptpul	25+25	25+30	62.0	58.22	10.60	0.021	279	13	7	10	17	15	-5	57	62	57
ESF	25_TSw1_Tptpul	25+30	25+35	70.0	58.22	10.60	0.021	281	13	7	15	14	15	-5	59	64	59
ESF	25_TSw1_Tptpul	25+35	25+40	46.0	58.22	10.60	0.021	282	8	7	15	11	15	-5	51	56	51
ESF	25_TSw1_Tptpul	25+40	25+45	71.0	58.22	10.60	0.021	284	13	7	10	14	15	-5	54	59	54
ESF	25_TSw1_Tptpul	25+45	25+50	74.0	58.22	10.60	0.021	286	13	7	15	19	15	-10	59	69	64
ESF	25_TSw1_Tptpul	25+50	25+55	75.0	58.22	10.60	0.021	288	13	7	15	19	15	-10	59	69	64
ESF	25_TSw1_Tptpul	25+55	25+60	54.0	58.22	10.60	0.021	290	13	7	10	18	15	0	63	63	58
ESF	25_TSw1_Tptpul	25+60	25+65	69.0	58.22	10.60	0.021	291	13	7	10	18	15	0	63	63	58
ESF	25_TSw1_Tptpul	25+65	25+70	56.0	58.22	10.60	0.021	292	13	7	10	12	15	0	57	57	52
ESF	25_TSw1_Tptpul	25+70	25+75	42.0	58.22	10.60	0.021	293	8	7	10	12	15	0	52	52	47
ESF	25_TSw1_Tptpul	25+75	25+80	69.0	58.22	10.60	0.021	294	13	7	10	20	15	0	65	65	60
ESF	25_TSw1_Tptpul	25+80	25+85	49.0	58.22	10.60	0.021	295	8	7	8	18	15	-5	51	56	51
ESF	25_TSw1_Tptpul	25+85	25+90	61.0	58.22	10.60	0.021	295	13	7	0	19	15	-5	49	54	49
ESF	25_TSw1_Tptpul	25+90	25+95	82.0	58.22	10.60	0.021	296	17	7	10	15	15	0	64	64	59
ESF	25_TSw1_Tptpul	25+95	26+00	81.0	58.22	10.60	0.021	297	17	7	10	16	15	0	65	65	60
ESF	25_TSw1_Tptpul	26+00	26+05	84.0	58.22	10.60	0.021	298	17	7	10	21	15	-12	58	70	65
ESF	25_TSw1_Tptpul	26+05	26+10	71.0	58.22	10.60	0.021	298	13	7	10	19	15	-12	52	64	59
ESF	25_TSw1_Tptpul	26+10	26+15	81.0	58.22	10.60	0.021	298	17	7	10	12	15	-10	51	61	56
ESF	25_TSw1_Tptpul	26+15	26+20	65.0	58.22	10.60	0.021	297	13	7	8	20	15	-5	58	63	58
ESF	25_TSw1_Tptpul	26+20	26+25	83.0	58.22	10.60	0.021	297	17	7	10	22	15	0	71	71	66
ESF	25_TSw1_Tptpul	26+25	26+30	71.0	58.22	10.60	0.021	296	13	7	15	15	15	-5	60	65	60
ESF	25_TSw1_Tptpul	26+30	26+35	75.0	58.22	10.60	0.021	296	13	7	8	20	15	-12	51	63	58
ESF	25_TSw1_Tptpul	26+35	26+40	71.0	58.22	10.60	0.021	295	13	7	10	18	15	-12	51	63	58
ESF	25_TSw1_Tptpul	26+40	26+45	59.0	58.22	10.60	0.021	294	13	7	0	18	15	-12	41	53	48
ESF	25_TSw1_Tptpul	26+45	26+50	66.0	58.22	10.60	0.021	294	13	7	0	18	15	-12	41	53	48
ESF	25_TSw1_Tptpul	26+50	26+55	73.0	58.22	10.60	0.021	293	13	7	10	20	15	-12	53	65	60
ESF	25_TSw1_Tptpul	26+55	26+60	66.0	58.22	10.60	0.021	291	13	7	10	20	15	-12	53	65	60
ESF	25_TSw1_Tptpul	26+60	26+65	55.0	58.22	10.60	0.021	289	13	7	10	14	15	-10	49	59	54
ESF	25_TSw1_Tptpul	26+65	26+70	70.0	58.22	10.60	0.021	287	13	7	15	19	15	-5	64	69	64
ESF	25_TSw1_Tptpul	26+70	26+75	69.0	58.22	10.60	0.021	286	13	7	15	19	15	-12	57	69	64
ESF	25_TSw1_Tptpul	26+75	26+80	52.0	58.22	10.60	0.021	284	13	7	10	16	15	-12	49	61	56
ESF	25_TSw1_Tptpul	26+80	26+85	43.0	58.22	10.60	0.021	281	8	7	10	18	15	-10	48	58	53
ESF	25_TSw1_Tptpul	26+85	26+90	77.0	58.22	10.60	0.021	279	17	7	8	24	15	-5	66	71	66
ESF	25_TSw1_Tptpul	26+90	26+95	55.0	58.22	10.60	0.021	276	13	7	0	19	15	-5	49	54	49
ESF	25_TSw1_Tptpul	26+95	27+00	68.0	58.22	10.60	0.021	274	13	7	15	18	15	-12	56	68	63
ESF	25_TSw1_Tptpul	27+00	27+05	42.0	58.22	10.60	0.021	271	8	7	10	14	15	-5	49	54	49
ESF	25_TSw1_Tptpul	27+05	27+10	62.0	58.22	10.60	0.021	269	13	7	10	14	15	-5	54	59	54
ESF	26_TSw2_Tptpmn	27+10	27+15	77.0	167.9	19.68	0.021	266	17	12	15	12	15	-12	59	71	66

Location	Thermal Mechanical and Lithostratigraphic Unit Designation	Begin Station (m)	End Station (m)	RQD	Mean Intact UCS, σ_{ci} (MPa)	Hoek & Brown Intact Material Constant, mi	Unit Weight of Rock Mass, γ (MN/m^3)	Depth of Tunnel, H (m)	RQD Index	C	Js	Jcd	JwR	AJO	RMR Rating = (RQD Index+C+Js+Jcd+JwR+AJ0)	RMR' = (RQD Index+C+Js+Jcd+JwR)	Geological Strength Index, GSI = (RMR' - 5)
ESF	26_TSw2_Tptpmn	27+15	27+20	85.0	167.9	19.68	0.021	263	17	12	8	19	15	-10	61	71	66
ESF	26_TSw2_Tptpmn	27+20	27+25	50.0	167.9	19.68	0.022	261	8	12	10	17	15	-12	50	62	57
ESF	26_TSw2_Tptpmn	27+25	27+30	90.0	167.9	19.68	0.022	258	17	12	10	21	15	-5	70	75	70
ESF	26_TSw2_Tptpmn	27+30	27+35	71.0	167.9	19.68	0.022	255	13	12	10	21	15	-5	66	71	66
ESF	26_TSw2_Tptpmn	27+35	27+40	63.0	167.9	19.68	0.022	253	13	12	0	18	15	-10	48	58	53
ESF	26_TSw2_Tptpmn	27+40	27+45	58.0	167.9	19.68	0.022	250	13	12	8	21	15	-12	57	69	64
ESF	26_TSw2_Tptpmn	27+45	27+50	55.0	167.9	19.68	0.022	247	13	12	8	16	15	-10	54	64	59
ESF	26_TSw2_Tptpmn	27+50	27+55	68.0	167.9	19.68	0.022	245	13	12	8	16	15	-10	54	64	59
ESF	26_TSw2_Tptpmn	27+55	27+60	89.0	167.9	19.68	0.022	243	17	12	8	17	15	-12	57	69	64
ESF	26_TSw2_Tptpmn	27+60	27+65	76.0	167.9	19.68	0.022	240	17	12	10	21	15	-12	63	75	70
ESF	26_TSw2_Tptpmn	27+65	27+70	74.0	167.9	19.68	0.022	238	13	12	15	18	15	-10	63	73	68
ESF	26_TSw2_Tptpmn	27+70	27+75	61.0	167.9	19.68	0.022	236	13	12	8	16	15	-12	52	64	59
ESF	26_TSw2_Tptpmn	27+75	27+80	90.0	167.9	19.68	0.022	233	17	12	8	19	15	-5	66	71	66
ESF	26_TSw2_Tptpmn	27+80	27+85	65.0	167.9	19.68	0.022	231	13	12	15	13	15	-12	56	68	63
ESF	26_TSw2_Tptpmn	27+85	27+90	92.0	167.9	19.68	0.022	229	20	12	15	22	15	-12	72	84	79
ESF	26_TSw2_Tptpmn	27+90	27+95	67.0	167.9	19.68	0.022	226	13	12	0	13	15	-5	48	53	48
ESF	26_TSw2_Tptpmn	27+95	28+00	56.0	167.9	19.68	0.022	223	13	12	15	18	15	-10	63	73	68
ESF	26_TSw2_Tptpmn	28+00	28+05	62.0	167.9	19.68	0.022	221	13	12	15	24	15	-12	67	79	74
ESF	26_TSw2_Tptpmn	28+05	28+10	51.0	167.9	19.68	0.022	220	13	12	8	20	15	-12	56	68	63
ESF	26_TSw2_Tptpmn	28+10	28+15	59.0	167.9	19.68	0.022	220	13	12	8	20	15	-12	56	68	63
ESF	26_TSw2_Tptpmn	28+15	28+20	57.0	167.9	19.68	0.022	221	13	12	10	20	15	-12	58	70	65
ESF	26_TSw2_Tptpmn	28+20	28+25	39.0	167.9	19.68	0.022	222	8	12	8	13	15	-12	44	56	51
ESF	26_TSw2_Tptpmn	28+25	28+30	59.0	167.9	19.68	0.022	223	13	12	10	12	15	-12	50	62	57
ESF	26_TSw2_Tptpmn	28+30	28+35	58.0	167.9	19.68	0.022	224	13	12	10	16	15	-12	54	66	61
ESF	26_TSw2_Tptpmn	28+35	28+40	51.0	167.9	19.68	0.022	225	13	12	10	21	15	-12	59	71	66
ESF	26_TSw2_Tptpmn	28+40	28+45	49.0	167.9	19.68	0.022	226	8	12	8	13	15	-12	44	56	51
ESF	26_TSw2_Tptpmn	28+45	28+50	72.0	167.9	19.68	0.022	227	13	12	10	22	15	-5	67	72	67
ESF	26_TSw2_Tptpmn	28+50	28+55	73.0	167.9	19.68	0.022	227	13	12	10	11	15	-5	56	61	56
ESF	26_TSw2_Tptpmn	28+55	28+60	73.0	167.9	19.68	0.022	228	13	12	15	19	15	-12	62	74	69
ESF	26_TSw2_Tptpmn	28+60	28+65	65.0	167.9	19.68	0.022	229	13	12	15	19	15	-10	64	74	69
ESF	26_TSw2_Tptpmn	28+65	28+70	57.0	167.9	19.68	0.022	230	13	12	8	22	15	-12	58	70	65
ESF	26_TSw2_Tptpmn	28+70	28+75	57.0	167.9	19.68	0.022	232	13	12	15	15	15	-5	65	70	65
ESF	26_TSw2_Tptpmn	28+75	28+80	22.0	167.9	19.68	0.022	234	5	12	15	16	15	-12	51	63	58
ESF	26_TSw2_Tptpmn	28+80	28+85	57.0	167.9	19.68	0.022	237	13	12	15	18	15	-5	68	73	68
ESF	26_TSw2_Tptpmn	28+85	28+90	66.0	167.9	19.68	0.022	239	13	12	15	20	15	-12	63	75	70
ESF	26_TSw2_Tptpmn	28+90	28+95	40.0	167.9	19.68	0.022	241	8	12	0	20	15	-10	45	55	50
ESF	26_TSw2_Tptpmn	28+95	29+00	53.0	167.9	19.68	0.022	243	13	12	10	20	15	-12	58	70	65
ESF	26_TSw2_Tptpmn	29+00	29+05	82.0	167.9	19.68	0.022	246	17	12	15	21	15	-12	68	80	75
ESF	26_TSw2_Tptpmn	29+05	29+10	70.0	167.9	19.68	0.022	248	13	12	10	13	15	-5	58	63	58

Location	Thermal Mechanical and Lithostratigraphic Unit Designation	Begin Station (m)	End Station (m)	RQD	Mean Intact UCS, σ_{ci} (MPa)	Hoek & Brown Intact Material Constant, mi	Unit Weight of Rock Mass, γ (MN/m^3)	Depth of Tunnel, H (m)	RQD Index	C	Js	Jcd	JwR	AJO	RMR Rating = (RQD Index+C+Js+Jcd+JwR+AJ0)	RMR' = (RQD Index+C+Js+Jcd+JwR)	Geological Strength Index, GSI = (RMR' - 5)
ESF	26_TSw2_Tptpmn	29+10	29+15	58.0	167.9	19.68	0.022	250	13	12	15	21	15	-12	64	76	71
ESF	26_TSw2_Tptpmn	29+15	29+20	50.0	167.9	19.68	0.022	253	8	12	10	20	15	-5	60	65	60
ESF	26_TSw2_Tptpmn	29+20	29+25	42.0	167.9	19.68	0.022	255	8	12	15	19	15	-12	57	69	64
ESF	26_TSw2_Tptpmn	29+25	29+30	42.0	167.9	19.68	0.022	257	8	12	15	25	15	-12	63	75	70
ESF	26_TSw2_Tptpmn	29+30	29+35	73.0	167.9	19.68	0.022	259	13	12	15	21	15	-5	71	76	71
ESF	26_TSw2_Tptpmn	29+35	29+40	76.0	167.9	19.68	0.022	261	17	12	8	24	15	-5	71	76	71
ESF	26_TSw2_Tptpmn	29+40	29+45	79.0	167.9	19.68	0.022	263	17	12	15	20	15	-12	67	79	74
ESF	26_TSw2_Tptpmn	29+45	29+50	69.0	167.9	19.68	0.022	266	13	12	15	20	15	-12	63	75	70
ESF	26_TSw2_Tptpmn	29+50	29+55	78.0	167.9	19.68	0.022	268	17	12	8	22	15	-12	62	74	69
ESF	26_TSw2_Tptpmn	29+55	29+60	48.0	167.9	19.68	0.022	270	8	12	10	24	15	-12	57	69	64
ESF	26_TSw2_Tptpmn	29+60	29+65	54.0	167.9	19.68	0.022	272	13	12	15	14	15	-12	57	69	64
ESF	26_TSw2_Tptpmn	29+65	29+70	60.0	167.9	19.68	0.022	274	13	12	15	18	15	-12	61	73	68
ESF	26_TSw2_Tptpmn	29+70	29+75	80.0	167.9	19.68	0.022	276	17	12	15	20	15	-5	74	79	74
ESF	26_TSw2_Tptpmn	29+75	29+80	68.0	167.9	19.68	0.022	278	13	12	15	22	15	-5	72	77	72
ESF	26_TSw2_Tptpmn	29+80	29+85	75.0	167.9	19.68	0.022	280	13	12	8	24	15	-5	67	72	67
ESF	26_TSw2_Tptpmn	29+85	29+90	77.0	167.9	19.68	0.022	282	17	12	15	20	15	0	79	79	74
ESF	26_TSw2_Tptpmn	29+90	29+95	78.0	167.9	19.68	0.022	281	17	12	15	23	15	-5	77	82	77
ESF	26_TSw2_Tptpmn	29+95	30+00	60.0	167.9	19.68	0.022	280	13	12	10	23	15	0	73	73	68
ESF	26_TSw2_Tptpmn	30+00	30+05	48.0	167.9	19.68	0.022	279	8	12	10	10	15	-12	43	55	50
ESF	26_TSw2_Tptpmn	30+05	30+10	79.0	167.9	19.68	0.022	277	17	12	15	19	15	-5	73	78	73
ESF	26_TSw2_Tptpmn	30+10	30+15	85.0	167.9	19.68	0.022	276	17	12	10	21	15	-12	63	75	70
ESF	26_TSw2_Tptpmn	30+15	30+20	83.0	167.9	19.68	0.022	275	17	12	15	15	15	0	74	74	69
ESF	26_TSw2_Tptpmn	30+20	30+25	60.0	167.9	19.68	0.022	273	13	12	15	18	15	-12	61	73	68
ESF	26_TSw2_Tptpmn	30+25	30+30	55.0	167.9	19.68	0.022	272	13	12	10	15	15	-12	53	65	60
ESF	26_TSw2_Tptpmn	30+30	30+35	48.0	167.9	19.68	0.022	270	8	12	15	22	15	-12	60	72	67
ESF	26_TSw2_Tptpmn	30+35	30+40	64.0	167.9	19.68	0.022	269	13	12	20	13	15	-12	61	73	68
ESF	26_TSw2_Tptpmn	30+40	30+45	80.0	167.9	19.68	0.022	268	17	12	10	22	15	-12	64	76	71
ESF	26_TSw2_Tptpmn	30+45	30+50	52.0	167.9	19.68	0.022	266	13	12	10	17	15	-12	55	67	62
ESF	26_TSw2_Tptpmn	30+50	30+55	51.0	167.9	19.68	0.022	265	13	12	10	20	15	-12	58	70	65
ESF	26_TSw2_Tptpmn	30+55	30+60	66.0	167.9	19.68	0.022	265	13	12	10	11	15	-12	49	61	56
ESF	26_TSw2_Tptpmn	30+60	30+65	53.0	167.9	19.68	0.022	264	13	12	10	20	15	-12	58	70	65
ESF	26_TSw2_Tptpmn	30+65	30+70	79.0	167.9	19.68	0.022	264	17	12	15	18	15	-5	72	77	72
ESF	26_TSw2_Tptpmn	30+70	30+75	93.0	167.9	19.68	0.022	263	20	12	8	21	15	-5	71	76	71
ESF	26_TSw2_Tptpmn	30+75	30+80	91.0	167.9	19.68	0.022	263	20	12	10	23	15	-5	75	80	75
ESF	26_TSw2_Tptpmn	30+80	30+85	89.0	167.9	19.68	0.022	262	17	12	20	20	15	-12	72	84	79
ESF	26_TSw2_Tptpmn	30+85	30+90	94.0	167.9	19.68	0.022	262	20	12	15	22	15	-12	72	84	79
ESF	26_TSw2_Tptpmn	30+90	30+95	80.0	167.9	19.68	0.022	261	17	12	15	16	15	-12	63	75	70
ESF	26_TSw2_Tptpmn	30+95	31+00	79.0	167.9	19.68	0.022	261	17	12	8	22	15	0	74	74	69
ESF	26_TSw2_Tptpmn	31+00	31+05	66.0	167.9	19.68	0.022	260	13	12	10	19	15	-12	57	69	64

Location	Thermal Mechanical and Lithostratigraphic Unit Designation	Begin Station (m)	End Station (m)	RQD	Mean Intact UCS, σ_{ci} (MPa)	Hoek & Brown Intact Material Constant, mi	Unit Weight of Rock Mass, γ (MN/m^3)	Depth of Tunnel, H (m)	RQD Index	C	Js	Jcd	JwR	AJO	RMR Rating = (RQD Index+C+Js+Jcd+JwR+AJ0)	RMR' = (RQD Index+C+Js+Jcd+JwR)	Geological Strength Index, GSI = (RMR' - 5)
ESF	26_TSw2_Tptpmn	31+05	31+10	33.0	167.9	19.68	0.022	259	8	12	10	19	15	-12	52	64	59
ESF	26_TSw2_Tptpmn	31+10	31+15	76.0	167.9	19.68	0.022	259	17	12	20	17	15	-12	69	81	76
ESF	26_TSw2_Tptpmn	31+15	31+20	29.0	167.9	19.68	0.022	259	8	12	20	17	15	-10	62	72	67
ESF	26_TSw2_Tptpmn	31+20	31+25	70.0	167.9	19.68	0.022	259	13	12	15	26	15	-12	69	81	76
ESF	26_TSw2_Tptpmn	31+25	31+30	64.0	167.9	19.68	0.022	260	13	12	15	25	15	-12	68	80	75
ESF	26_TSw2_Tptpmn	31+30	31+35	83.0	167.9	19.68	0.022	260	17	12	15	20	15	-5	74	79	74
ESF	26_TSw2_Tptpmn	31+35	31+40	80.0	167.9	19.68	0.022	260	17	12	15	20	15	-12	67	79	74
ESF	26_TSw2_Tptpmn	31+40	31+45	59.0	167.9	19.68	0.022	260	13	12	15	20	15	-5	70	75	70
ESF	26_TSw2_Tptpmn	31+45	31+50	92.0	167.9	19.68	0.022	260	20	12	15	15	15	-12	65	77	72
ESF	26_TSw2_Tptpmn	31+50	31+55	64.0	167.9	19.68	0.022	260	13	12	15	13	15	-12	56	68	63
ESF	26_TSw2_Tptpmn	31+55	31+60	56.0	167.9	19.68	0.022	260	13	12	10	15	15	-12	53	65	60
ESF	26_TSw2_Tptpmn	31+60	31+65	61.0	167.9	19.68	0.022	260	13	12	10	13	15	-12	51	63	58
ESF	26_TSw2_Tptpmn	31+65	31+70	44.0	167.9	19.68	0.022	260	8	12	15	21	15	-12	59	71	66
ESF	26_TSw2_Tptpmn	31+70	31+75	65.0	167.9	19.68	0.022	260	13	12	10	18	15	-12	56	68	63
ESF	26_TSw2_Tptpmn	31+75	31+80	70.0	167.9	19.68	0.022	258	13	12	10	18	15	-5	63	68	63
ESF	26_TSw2_Tptpmn	31+80	31+85	80.0	167.9	19.68	0.022	256	17	12	10	20	15	-12	62	74	69
ESF	26_TSw2_Tptpmn	31+85	31+90	57.0	167.9	19.68	0.022	254	13	12	8	18	15	-12	54	66	61
ESF	26_TSw2_Tptpmn	31+90	31+95	80.0	167.9	19.68	0.022	251	17	12	10	22	15	-5	71	76	71
ESF	26_TSw2_Tptpmn	31+95	32+00	60.0	167.9	19.68	0.022	249	13	12	10	22	15	-5	67	72	67
ESF	26_TSw2_Tptpmn	32+00	32+05	43.0	167.9	19.68	0.022	247	8	12	10	22	15	-12	55	67	62
ESF	26_TSw2_Tptpmn	32+05	32+10	80.0	167.9	19.68	0.022	244	17	12	8	19	15	-5	66	71	66
ESF	26_TSw2_Tptpmn	32+10	32+15	86.0	167.9	19.68	0.022	242	17	12	15	22	15	-12	69	81	76
ESF	26_TSw2_Tptpmn	32+15	32+20	60.0	167.9	19.68	0.022	240	13	12	15	22	15	-10	67	77	72
ESF	26_TSw2_Tptpmn	32+20	32+25	95.0	167.9	19.68	0.022	238	20	12	15	23	15	-12	73	85	80
ESF	26_TSw2_Tptpmn	32+25	32+30	77.0	167.9	19.68	0.022	235	17	12	15	22	15	-12	69	81	76
ESF	26_TSw2_Tptpmn	32+30	32+35	71.0	167.9	19.68	0.022	233	13	12	20	16	15	-5	71	76	71
ESF	26_TSw2_Tptpmn	32+35	32+40	75.0	167.9	19.68	0.022	235	13	12	20	20	15	-12	68	80	75
ESF	26_TSw2_Tptpmn	32+40	32+45	85.0	167.9	19.68	0.022	237	17	12	15	22	15	-5	76	81	76
ESF	26_TSw2_Tptpmn	32+45	32+50	88.0	167.9	19.68	0.022	238	17	12	15	20	15	-12	67	79	74
ESF	26_TSw2_Tptpmn	32+50	32+55	68.0	167.9	19.68	0.022	240	13	12	10	22	15	0	72	72	67
ESF	26_TSw2_Tptpmn	32+55	32+60	62.0	167.9	19.68	0.022	241	13	12	15	20	15	0	75	75	70
ESF	26_TSw2_Tptpmn	32+60	32+65	49.0	167.9	19.68	0.022	243	8	12	15	15	15	0	65	65	60
ESF	26_TSw2_Tptpmn	32+65	32+70	76.0	167.9	19.68	0.022	244	17	12	10	22	15	-5	71	76	71
ESF	26_TSw2_Tptpmn	32+70	32+75	51.0	167.9	19.68	0.022	246	13	12	15	24	15	-12	67	79	74
ESF	26_TSw2_Tptpmn	32+75	32+80	45.0	167.9	19.68	0.022	247	8	12	10	20	15	-12	53	65	60
ESF	26_TSw2_Tptpmn	32+80	32+85	71.0	167.9	19.68	0.022	248	13	12	8	23	15	-10	61	71	66
ESF	26_TSw2_Tptpmn	32+85	32+90	63.0	167.9	19.68	0.022	250	13	12	15	22	15	-5	72	77	72
ESF	26_TSw2_Tptpmn	32+90	32+95	81.0	167.9	19.68	0.022	251	17	12	20	14	15	-5	73	78	73
ESF	26_TSw2_Tptpmn	32+95	33+00	73.0	167.9	19.68	0.022	253	13	12	15	24	15	-12	67	79	74

Location	Thermal Mechanical and Lithostratigraphic Unit Designation	Begin Station (m)	End Station (m)	RQD	Mean Intact UCS, σ_{ci} (MPa)	Hoek & Brown Intact Material Constant, mi	Unit Weight of Rock Mass, γ (MN/m^3)	Depth of Tunnel, H (m)	RQD Index	C	Js	Jcd	JwR	AJO	RMR Rating = (RQD Index+C+Js+Jcd+JwR+AJ0)	RMR' = (RQD Index+C+Js+Jcd+JwR)	Geological Strength Index, GSI = (RMR' - 5)
ESF	26_TSw2_Tptpmn	33+00	33+05	82.0	167.9	19.68	0.022	255	17	12	15	20	15	-12	67	79	74
ESF	26_TSw2_Tptpmn	33+05	33+10	45.0	167.9	19.68	0.022	257	8	12	0	15	15	-5	45	50	45
ESF	26_TSw2_Tptpmn	33+10	33+15	66.0	167.9	19.68	0.022	259	13	12	15	16	15	-5	66	71	66
ESF	26_TSw2_Tptpmn	33+15	33+20	55.0	167.9	19.68	0.022	261	13	12	10	16	15	-5	61	66	61
ESF	26_TSw2_Tptpmn	33+20	33+25	83.0	167.9	19.68	0.022	263	17	12	10	16	15	-5	65	70	65
ESF	26_TSw2_Tptpmn	33+25	33+30	47.0	167.9	19.68	0.022	265	8	12	8	16	15	0	59	59	54
ESF	26_TSw2_Tptpmn	33+30	33+35	69.0	167.9	19.68	0.022	267	13	12	15	14	15	-5	64	69	64
ESF	26_TSw2_Tptpmn	33+35	33+40	69.0	167.9	19.68	0.022	268	13	12	15	18	15	-5	68	73	68
ESF	26_TSw2_Tptpmn	33+40	33+45	57.0	167.9	19.68	0.022	270	13	12	15	14	15	-5	64	69	64
ESF	26_TSw2_Tptpmn	33+45	33+50	55.0	167.9	19.68	0.022	272	13	12	15	20	15	-5	70	75	70
ESF	26_TSw2_Tptpmn	33+50	33+55	50.0	167.9	19.68	0.022	274	8	12	15	15	15	-12	53	65	60
ESF	26_TSw2_Tptpmn	33+55	33+60	76.0	167.9	19.68	0.022	275	17	12	15	15	15	-5	69	74	69
ESF	26_TSw2_Tptpmn	33+60	33+65	66.0	167.9	19.68	0.022	276	13	12	20	15	15	-10	65	75	70
ESF	26_TSw2_Tptpmn	33+65	33+70	70.0	167.9	19.68	0.022	276	13	12	20	15	15	-5	70	75	70
ESF	26_TSw2_Tptpmn	33+70	33+75	70.0	167.9	19.68	0.022	276	13	12	0	24	15	-5	59	64	59
ESF	26_TSw2_Tptpmn	33+75	33+80	70.0	167.9	19.68	0.022	277	13	12	15	22	15	-12	65	77	72
ESF	26_TSw2_Tptpmn	33+80	33+85	71.0	167.9	19.68	0.022	277	13	12	10	20	15	-12	58	70	65
ESF	26_TSw2_Tptpmn	33+85	33+90	85.0	167.9	19.68	0.022	278	17	12	15	21	15	-12	68	80	75
ESF	26_TSw2_Tptpmn	33+90	33+95	77.0	167.9	19.68	0.022	278	17	12	15	25	15	-12	72	84	79
ESF	26_TSw2_Tptpmn	33+95	34+00	74.0	167.9	19.68	0.022	279	13	12	15	16	15	-5	66	71	66
ESF	26_TSw2_Tptpmn	34+00	34+05	47.0	167.9	19.68	0.022	279	8	12	8	11	15	-12	42	54	49
ESF	26_TSw2_Tptpmn	34+05	34+10	57.0	167.9	19.68	0.022	279	13	12	10	21	15	-12	59	71	66
ESF	26_TSw2_Tptpmn	34+10	34+15	42.0	167.9	19.68	0.022	280	8	12	15	10	15	-12	48	60	55
ESF	26_TSw2_Tptpmn	34+15	34+20	66.0	167.9	19.68	0.022	279	13	12	10	20	15	-12	58	70	65
ESF	26_TSw2_Tptpmn	34+20	34+25	64.0	167.9	19.68	0.022	276	13	12	10	20	15	-12	58	70	65
ESF	26_TSw2_Tptpmn	34+25	34+30	63.0	167.9	19.68	0.022	273	13	12	10	17	15	-10	57	67	62
ESF	26_TSw2_Tptpmn	34+30	34+35	56.0	167.9	19.68	0.022	270	13	12	10	20	15	-12	58	70	65
ESF	26_TSw2_Tptpmn	34+35	34+40	69.0	167.9	19.68	0.022	268	13	12	10	18	15	-12	56	68	63
ESF	26_TSw2_Tptpmn	34+40	34+45	80.0	167.9	19.68	0.022	266	17	12	15	24	15	-12	71	83	78
ESF	26_TSw2_Tptpmn	34+45	34+50	56.0	167.9	19.68	0.022	264	13	12	15	22	15	-12	65	77	72
ESF	26_TSw2_Tptpmn	34+50	34+55	59.0	167.9	19.68	0.022	262	13	12	15	18	15	-12	61	73	68
ESF	26_TSw2_Tptpmn	34+55	34+60	57.0	167.9	19.68	0.022	259	13	12	15	16	15	-2	69	71	66
ESF	26_TSw2_Tptpmn	34+60	34+65	73.0	167.9	19.68	0.022	257	13	12	15	13	15	0	68	68	63
ESF	26_TSw2_Tptpmn	34+65	34+70	63.0	167.9	19.68	0.022	255	13	12	10	13	15	0	63	63	58
ESF	26_TSw2_Tptpmn	34+70	34+75	72.0	167.9	19.68	0.022	253	13	12	10	8	15	-12	46	58	53
ESF	26_TSw2_Tptpmn	34+75	34+80	72.0	167.9	19.68	0.022	251	13	12	15	16	15	-12	59	71	66
ESF	26_TSw2_Tptpmn	34+80	34+85	57.0	167.9	19.68	0.022	249	13	12	10	23	15	-12	61	73	68
ESF	26_TSw2_Tptpmn	34+85	34+90	55.0	167.9	19.68	0.022	247	13	12	10	20	15	-12	58	70	65
ESF	26_TSw2_Tptpmn	34+90	34+95	52.0	167.9	19.68	0.022	245	13	12	10	19	15	-12	57	69	64

Location	Thermal Mechanical and Lithostratigraphic Unit Designation	Begin Station (m)	End Station (m)	RQD	Mean Intact UCS, σ_{ci} (MPa)	Hoek & Brown Intact Material Constant, mi	Unit Weight of Rock Mass, γ (MN/m^3)	Depth of Tunnel, H (m)	RQD Index	C	Js	Jcd	JwR	AJO	RMR Rating = (RQD Index+C+Js+Jcd+JwR+AJ0)	RMR' = (RQD Index+C+Js+Jcd+JwR)	Geological Strength Index, GSI = (RMR' - 5)
ESF	26_TSw2_Tptpmn	34+95	35+00	64.0	167.9	19.68	0.022	243	13	12	15	20	15	-12	63	75	70
ESF	26_TSw2_Tptpmn	35+00	35+05	50.0	167.9	19.68	0.022	241	8	12	10	20	15	-12	53	65	60
ESF	26_TSw2_Tptpmn	35+05	35+10	39.0	167.9	19.68	0.022	239	8	12	10	14	15	-5	54	59	54
ESF	26_TSw2_Tptpmn	35+10	35+15	68.0	167.9	19.68	0.022	237	13	12	10	13	15	-10	53	63	58
ESF	26_TSw2_Tptpmn	35+15	35+20	51.0	167.9	19.68	0.022	235	13	12	15	11	15	-12	54	66	61
ESF	26_TSw2_Tptpmn	35+20	35+25	80.0	167.9	19.68	0.022	233	17	12	15	20	15	-12	67	79	74
ESF	26_TSw2_Tptpmn	35+25	35+30	64.0	167.9	19.68	0.022	231	13	12	15	19	15	-10	64	74	69
ESF	26_TSw2_Tptpmn	35+30	35+35	63.0	167.9	19.68	0.022	229	13	12	15	16	15	-12	59	71	66
ESF	26_TSw2_Tptpmn	35+35	35+40	59.0	167.9	19.68	0.022	227	13	12	10	22	15	-12	60	72	67
ESF	26_TSw2_Tptpmn	35+40	35+45	57.0	167.9	19.68	0.022	228	13	12	15	22	15	-12	65	77	72
ESF	26_TSw2_Tptpmn	35+45	35+50	36.0	167.9	19.68	0.022	230	8	12	10	21	15	-12	54	66	61
ESF	26_TSw2_Tptpmn	35+50	35+55	33.0	167.9	19.68	0.022	231	8	12	10	22	15	-10	57	67	62
ESF	26_TSw2_Tptpmn	35+55	35+60	49.0	167.9	19.68	0.022	233	8	12	10	17	15	-12	50	62	57
ESF	26_TSw2_Tptpmn	35+60	35+65	62.0	167.9	19.68	0.022	234	13	12	15	21	15	-12	64	76	71
ESF	26_TSw2_Tptpmn	35+65	35+70	73.0	167.9	19.68	0.022	236	13	12	8	17	15	-5	60	65	60
ESF	26_TSw2_Tptpmn	35+70	35+75	77.0	167.9	19.68	0.022	238	17	12	15	19	15	-12	66	78	73
ESF	26_TSw2_Tptpmn	35+75	35+80	84.0	167.9	19.68	0.022	240	17	12	15	21	15	-12	68	80	75
ESF	26_TSw2_Tptpmn	35+80	35+85	73.0	167.9	19.68	0.022	242	13	12	10	18	15	-5	63	68	63
ESF	26_TSw2_Tptpmn	35+85	35+90	54.0	167.9	19.68	0.022	244	13	12	10	18	15	-5	63	68	63
ESF	26_TSw2_Tptpmn	35+90	35+95	14.0	167.9	19.68	0.022	246	5	12	10	7	15	-12	37	49	44
ESF	26_TSw2_Tptpmn	35+95	36+00	36.0	167.9	19.68	0.022	248	8	12	8	22	15	-12	53	65	60
ESF	26_TSw2_Tptpmn	36+00	36+05	26.0	167.9	19.68	0.022	247	8	12	10	21	15	-12	54	66	61
ESF	26_TSw2_Tptpmn	36+05	36+10	28.0	167.9	19.68	0.022	246	8	12	10	14	15	-5	54	59	54
ESF	26_TSw2_Tptpmn	36+10	36+15	42.0	167.9	19.68	0.022	244	8	12	10	18	15	-5	58	63	58
ESF	26_TSw2_Tptpmn	36+15	36+20	30.0	167.9	19.68	0.022	243	8	12	10	15	15	-5	55	60	55
ESF	26_TSw2_Tptpmn	36+20	36+25	42.0	167.9	19.68	0.022	241	8	12	10	20	15	-5	60	65	60
ESF	26_TSw2_Tptpmn	36+25	36+30	51.0	167.9	19.68	0.022	240	13	12	10	24	15	-12	62	74	69
ESF	26_TSw2_Tptpmn	36+30	36+35	63.0	167.9	19.68	0.022	240	13	12	10	21	15	0	71	71	66
ESF	26_TSw2_Tptpmn	36+35	36+40	58.0	167.9	19.68	0.022	239	13	12	15	21	15	-12	64	76	71
ESF	26_TSw2_Tptpmn	36+40	36+45	64.0	167.9	19.68	0.022	239	13	12	15	17	15	-10	62	72	67
ESF	26_TSw2_Tptpmn	36+45	36+50	73.0	167.9	19.68	0.022	238	13	12	15	22	15	-12	65	77	72
ESF	26_TSw2_Tptpmn	36+50	36+55	50.0	167.9	19.68	0.022	238	8	12	15	18	15	-5	63	68	63
ESF	26_TSw2_Tptpmn	36+55	36+60	78.0	167.9	19.68	0.022	237	17	12	10	15	15	-5	64	69	64
ESF	26_TSw2_Tptpmn	36+60	36+65	40.0	167.9	19.68	0.022	236	8	12	10	20	15	-12	53	65	60
ESF	26_TSw2_Tptpmn	36+65	36+70	50.0	167.9	19.68	0.022	234	8	12	15	15	15	-12	53	65	60
ESF	26_TSw2_Tptpmn	36+70	36+75	49.0	167.9	19.68	0.022	232	8	12	15	19	15	-5	64	69	64
ESF	26_TSw2_Tptpmn	36+75	36+80	45.0	167.9	19.68	0.022	229	8	12	10	21	15	-12	54	66	61
ESF	26_TSw2_Tptpmn	36+80	36+85	58.0	167.9	19.68	0.022	227	13	12	8	21	15	-5	64	69	64
ESF	26_TSw2_Tptpmn	36+85	36+90	82.0	167.9	19.68	0.022	225	17	12	20	16	15	-12	68	80	75

Location	Thermal Mechanical and Lithostratigraphic Unit Designation	Begin Station (m)	End Station (m)	RQD	Mean Intact UCS, σ_{ci} (MPa)	Hoek & Brown Intact Material Constant, mi	Unit Weight of Rock Mass, γ (MN/m^3)	Depth of Tunnel, H (m)	RQD Index	C	Js	Jcd	JwR	AJO	RMR Rating = (RQD Index+C+Js+Jcd+JwR+AJ0)	RMR' = (RQD Index+C+Js+Jcd+JwR)	Geological Strength Index, GSI = (RMR' - 5)
ESF	26_TSw2_Tptpmn	36+90	36+95	77.0	167.9	19.68	0.022	223	17	12	10	20	15	-5	69	74	69
ESF	26_TSw2_Tptpmn	36+95	37+00	65.0	167.9	19.68	0.022	221	13	12	15	12	15	-5	62	67	62
ESF	26_TSw2_Tptpmn	37+00	37+05	57.0	167.9	19.68	0.022	219	13	12	15	21	15	-10	66	76	71
ESF	26_TSw2_Tptpmn	37+05	37+10	87.0	167.9	19.68	0.022	216	17	12	10	20	15	-12	62	74	69
ESF	26_TSw2_Tptpmn	37+10	37+15	64.0	167.9	19.68	0.022	214	13	12	10	19	15	-12	57	69	64
ESF	26_TSw2_Tptpmn	37+15	37+20	48.0	167.9	19.68	0.022	212	8	12	15	13	15	-5	58	63	58
ESF	26_TSw2_Tptpmn	37+20	37+25	65.0	167.9	19.68	0.022	210	13	12	10	17	15	-5	62	67	62
ESF	26_TSw2_Tptpmn	37+25	37+30	74.0	167.9	19.68	0.022	212	13	12	15	20	15	-12	63	75	70
ESF	26_TSw2_Tptpmn	37+30	37+35	72.0	167.9	19.68	0.022	213	13	12	15	20	15	-12	63	75	70
ESF	26_TSw2_Tptpmn	37+35	37+40	77.0	167.9	19.68	0.022	214	17	12	15	15	15	-5	69	74	69
ESF	26_TSw2_Tptpmn	37+40	37+45	41.0	167.9	19.68	0.022	215	8	12	10	18	15	-5	58	63	58
ESF	26_TSw2_Tptpmn	37+45	37+50	61.0	167.9	19.68	0.022	217	13	12	15	20	15	-5	70	75	70
ESF	26_TSw2_Tptpmn	37+50	37+55	69.0	167.9	19.68	0.022	218	13	12	15	21	15	-5	71	76	71
ESF	26_TSw2_Tptpmn	37+55	37+60	69.0	167.9	19.68	0.022	218	13	12	15	20	15	-5	70	75	70
ESF	26_TSw2_Tptpmn	37+60	37+65	78.0	167.9	19.68	0.022	218	17	12	15	20	15	-12	67	79	74
ESF	26_TSw2_Tptpmn	37+65	37+70	72.0	167.9	19.68	0.022	218	13	12	15	21	15	-12	64	76	71
ESF	26_TSw2_Tptpmn	37+70	37+75	64.0	167.9	19.68	0.022	218	13	12	10	23	15	-5	68	73	68
ESF	26_TSw2_Tptpmn	37+75	37+80	96.0	167.9	19.68	0.022	217	20	12	15	15	15	-5	72	77	72
ESF	26_TSw2_Tptpmn	37+80	37+85	91.0	167.9	19.68	0.022	217	20	12	10	19	15	-12	64	76	71
ESF	26_TSw2_Tptpmn	37+85	37+90	93.0	167.9	19.68	0.022	219	20	12	15	19	15	-12	69	81	76
ESF	26_TSw2_Tptpmn	37+90	37+95	87.0	167.9	19.68	0.022	221	17	12	15	19	15	-10	68	78	73
ESF	26_TSw2_Tptpmn	37+95	38+00	86.0	167.9	19.68	0.022	222	17	12	15	23	15	-12	70	82	77
ESF	26_TSw2_Tptpmn	38+00	38+05	69.0	167.9	19.68	0.022	224	13	12	10	14	15	-5	59	64	59
ESF	26_TSw2_Tptpmn	38+05	38+10	92.0	167.9	19.68	0.022	226	20	12	15	17	15	-12	67	79	74
ESF	26_TSw2_Tptpmn	38+10	38+15	89.0	167.9	19.68	0.022	227	17	12	10	23	15	-12	65	77	72
ESF	26_TSw2_Tptpmn	38+15	38+20	72.0	167.9	19.68	0.022	229	13	12	10	20	15	0	70	70	65
ESF	26_TSw2_Tptpmn	38+20	38+25	40.0	167.9	19.68	0.022	230	8	12	15	15	15	-12	53	65	60
ESF	26_TSw2_Tptpmn	38+25	38+30	48.0	167.9	19.68	0.022	231	8	12	15	15	15	-12	53	65	60
ESF	26_TSw2_Tptpmn	38+30	38+35	66.0	167.9	19.68	0.022	233	13	12	10	20	15	-12	58	70	65
ESF	26_TSw2_Tptpmn	38+35	38+40	89.0	167.9	19.68	0.022	234	17	12	15	20	15	-12	67	79	74
ESF	26_TSw2_Tptpmn	38+40	38+45	91.0	167.9	19.68	0.022	235	20	12	20	20	15	-12	75	87	82
ESF	26_TSw2_Tptpmn	38+45	38+50	78.0	167.9	19.68	0.022	235	17	12	15	16	15	-12	63	75	70
ESF	26_TSw2_Tptpmn	38+50	38+55	96.0	167.9	19.68	0.022	235	20	12	15	17	15	-12	67	79	74
ESF	26_TSw2_Tptpmn	38+55	38+60	90.0	167.9	19.68	0.022	235	17	12	15	15	15	-12	62	74	69
ESF	26_TSw2_Tptpmn	38+60	38+65	77.0	167.9	19.68	0.022	234	17	12	15	14	15	-5	68	73	68
ESF	26_TSw2_Tptpmn	38+65	38+70	75.0	167.9	19.68	0.022	234	13	12	10	13	15	-12	51	63	58
ESF	26_TSw2_Tptpmn	38+70	38+75	59.0	167.9	19.68	0.022	234	13	12	15	20	15	-5	70	75	70
ESF	26_TSw2_Tptpmn	38+75	38+80	79.0	167.9	19.68	0.022	234	17	12	10	20	15	-5	69	74	69
ESF	26_TSw2_Tptpmn	38+80	38+85	70.0	167.9	19.68	0.022	234	13	12	15	11	15	-5	61	66	61

Location	Thermal Mechanical and Lithostratigraphic Unit Designation	Begin Station (m)	End Station (m)	RQD	Mean Intact UCS, σ_{ci} (MPa)	Hoek & Brown Intact Material Constant, mi	Unit Weight of Rock Mass, γ (MN/m^3)	Depth of Tunnel, H (m)	RQD Index	C	Js	Jcd	JwR	AJO	RMR Rating = (RQD Index+C+Js+Jcd+JwR+AJ0)	RMR' = (RQD Index+C+Js+Jcd+JwR)	Geological Strength Index, GSI = (RMR' - 5)
ESF	26_TSw2_Tptpmn	38+85	38+90	72.0	167.9	19.68	0.022	234	13	12	15	25	15	-12	68	80	75
ESF	26_TSw2_Tptpmn	38+90	38+95	89.0	167.9	19.68	0.022	234	17	12	15	14	15	0	73	73	68
ESF	26_TSw2_Tptpmn	38+95	39+00	73.0	167.9	19.68	0.022	234	13	12	15	17	15	-12	60	72	67
ESF	26_TSw2_Tptpmn	39+00	39+05	64.0	167.9	19.68	0.022	234	13	12	15	20	15	-12	63	75	70
ESF	26_TSw2_Tptpmn	39+05	39+10	54.0	167.9	19.68	0.022	233	13	12	10	22	15	0	72	72	67
ESF	26_TSw2_Tptpmn	39+10	39+15	55.0	167.9	19.68	0.022	231	13	12	15	20	15	-5	70	75	70
ESF	26_TSw2_Tptpmn	39+15	39+20	66.0	167.9	19.68	0.022	229	13	12	15	20	15	-12	63	75	70
ESF	26_TSw2_Tptpmn	39+20	39+25	71.0	167.9	19.68	0.022	228	13	12	8	20	15	-12	56	68	63
ESF	26_TSw2_Tptpmn	39+25	39+30	65.0	167.9	19.68	0.022	226	13	12	15	18	15	-12	61	73	68
ESF	26_TSw2_Tptpmn	39+30	39+35	55.0	167.9	19.68	0.022	224	13	12	10	19	15	0	69	69	64
ESF	26_TSw2_Tptpmn	39+35	39+40	59.0	167.9	19.68	0.022	223	13	12	10	18	15	-12	56	68	63
ESF	26_TSw2_Tptpmn	39+40	39+45	43.0	167.9	19.68	0.022	221	8	12	10	19	15	-12	52	64	59
ESF	26_TSw2_Tptpmn	39+45	39+50	55.0	167.9	19.68	0.022	219	13	12	10	21	15	-12	59	71	66
ESF	26_TSw2_Tptpmn	39+50	39+55	50.0	167.9	19.68	0.022	218	8	12	10	18	15	-5	58	63	58
ESF	26_TSw2_Tptpmn	39+55	39+60	72.0	167.9	19.68	0.022	217	13	12	8	22	15	-5	65	70	65
ESF	26_TSw2_Tptpmn	39+60	39+65	57.0	167.9	19.68	0.022	215	13	12	10	23	15	-12	61	73	68
ESF	26_TSw2_Tptpmn	39+65	39+70	71.0	167.9	19.68	0.022	215	13	12	10	21	15	-12	59	71	66
ESF	26_TSw2_Tptpmn	39+70	39+75	66.0	167.9	19.68	0.022	215	13	12	0	20	15	0	60	60	55
ESF	26_TSw2_Tptpmn	39+75	39+80	59.0	167.9	19.68	0.022	215	13	12	15	19	15	-5	69	74	69
ESF	26_TSw2_Tptpmn	39+80	39+85	65.0	167.9	19.68	0.022	214	13	12	15	20	15	-12	63	75	70
ESF	26_TSw2_Tptpmn	39+85	39+90	67.0	167.9	19.68	0.022	214	13	12	15	22	15	-5	72	77	72
ESF	26_TSw2_Tptpmn	39+90	39+95	73.0	167.9	19.68	0.022	214	13	12	10	23	15	-12	61	73	68
ESF	26_TSw2_Tptpmn	39+95	40+00	66.0	167.9	19.68	0.022	214	13	12	8	19	15	0	67	67	62
ESF	26_TSw2_Tptpmn	40+00	40+05	64.0	167.9	19.68	0.022	214	13	12	15	16	15	-12	59	71	66
ESF	26_TSw2_Tptpmn	40+05	40+10	81.0	167.9	19.68	0.022	214	17	12	15	16	15	-12	63	75	70
ESF	26_TSw2_Tptpmn	40+10	40+15	42.0	167.9	19.68	0.022	214	8	12	10	20	15	-12	53	65	60
ESF	26_TSw2_Tptpmn	40+15	40+20	54.0	167.9	19.68	0.022	215	13	12	10	20	15	-12	58	70	65
ESF	26_TSw2_Tptpmn	40+20	40+25	45.0	167.9	19.68	0.022	216	8	12	10	22	15	-5	62	67	62
ESF	26_TSw2_Tptpmn	40+25	40+30	72.0	167.9	19.68	0.022	218	13	12	15	18	15	-5	68	73	68
ESF	26_TSw2_Tptpmn	40+30	40+35	57.0	167.9	19.68	0.022	220	13	12	10	18	15	0	68	68	63
ESF	26_TSw2_Tptpmn	40+35	40+40	43.0	167.9	19.68	0.022	223	8	12	8	16	15	-5	54	59	54
ESF	26_TSw2_Tptpmn	40+40	40+45	40.0	167.9	19.68	0.022	225	8	12	15	20	15	-12	58	70	65
ESF	26_TSw2_Tptpmn	40+45	40+50	44.0	167.9	19.68	0.022	228	8	12	15	20	15	-12	58	70	65
ESF	26_TSw2_Tptpmn	40+50	40+55	53.0	167.9	19.68	0.022	230	13	12	10	11	15	-5	56	61	56
ESF	26_TSw2_Tptpmn	40+55	40+60	80.0	167.9	19.68	0.022	232	17	12	10	20	15	-12	62	74	69
ESF	26_TSw2_Tptpmn	40+60	40+65	69.0	167.9	19.68	0.022	235	13	12	15	18	15	-5	68	73	68
ESF	26_TSw2_Tptpmn	40+65	40+70	71.0	167.9	19.68	0.022	237	13	12	15	22	15	-12	65	77	72
ESF	26_TSw2_Tptpmn	40+70	40+75	35.0	167.9	19.68	0.022	239	8	12	10	22	15	-12	55	67	62
ESF	26_TSw2_Tptpmn	40+75	40+80	70.0	167.9	19.68	0.022	242	13	12	15	20	15	-12	63	75	70

Location	Thermal Mechanical and Lithostratigraphic Unit Designation	Begin Station (m)	End Station (m)	RQD	Mean Intact UCS, σ_{ci} (MPa)	Hoek & Brown Intact Material Constant, mi	Unit Weight of Rock Mass, γ (MN/m^3)	Depth of Tunnel, H (m)	RQD Index	C	Js	Jcd	JwR	AJO	RMR Rating = (RQD Index+C+Js+Jcd+JwR+AJ0)	RMR' = (RQD Index+C+Js+Jcd+JwR)	Geological Strength Index, GSI = (RMR' - 5)
ESF	26_TSw2_Tptpmn	40+80	40+85	79.0	167.9	19.68	0.022	243	17	12	20	22	15	-12	74	86	81
ESF	26_TSw2_Tptpmn	40+85	40+90	60.0	167.9	19.68	0.022	245	13	12	15	22	15	-5	72	77	72
ESF	26_TSw2_Tptpmn	40+90	40+95	64.0	167.9	19.68	0.022	247	13	12	10	16	15	-12	54	66	61
ESF	26_TSw2_Tptpmn	40+95	41+00	74.0	167.9	19.68	0.022	248	13	12	10	19	15	-5	64	69	64
ESF	26_TSw2_Tptpmn	41+00	41+05	59.0	167.9	19.68	0.022	250	13	12	10	14	15	-5	59	64	59
ESF	26_TSw2_Tptpmn	41+05	41+10	69.0	167.9	19.68	0.022	251	13	12	10	22	15	-5	67	72	67
ESF	26_TSw2_Tptpmn	41+10	41+15	58.0	167.9	19.68	0.022	253	13	12	10	20	15	0	70	70	65
ESF	26_TSw2_Tptpmn	41+15	41+20	30.0	167.9	19.68	0.022	255	8	12	10	19	15	-5	59	64	59
ESF	26_TSw2_Tptpmn	41+20	41+25	20.0	167.9	19.68	0.022	256	5	12	10	25	15	-5	62	67	62
ESF	26_TSw2_Tptpmn	41+25	41+30	46.0	167.9	19.68	0.022	258	8	12	8	22	15	-12	53	65	60
ESF	26_TSw2_Tptpmn	41+30	41+35	71.0	167.9	19.68	0.022	259	13	12	10	19	15	-2	67	69	64
ESF	26_TSw2_Tptpmn	41+35	41+40	68.0	167.9	19.68	0.022	261	13	12	10	22	15	-12	60	72	67
ESF	26_TSw2_Tptpmn	41+40	41+45	67.0	167.9	19.68	0.022	262	13	12	15	15	15	-5	65	70	65
ESF	26_TSw2_Tptpmn	41+45	41+50	62.0	167.9	19.68	0.022	263	13	12	15	18	15	-12	61	73	68
ESF	26_TSw2_Tptpmn	41+50	41+55	64.0	167.9	19.68	0.022	263	13	12	10	19	15	-5	64	69	64
ESF	26_TSw2_Tptpmn	41+55	41+60	81.0	167.9	19.68	0.022	262	17	12	15	20	15	-12	67	79	74
ESF	26_TSw2_Tptpmn	41+60	41+65	65.0	167.9	19.68	0.022	261	13	12	15	18	15	-10	63	73	68
ESF	26_TSw2_Tptpmn	41+65	41+70	44.0	167.9	19.68	0.022	260	8	12	8	17	15	-12	48	60	55
ESF	26_TSw2_Tptpmn	41+70	41+75	35.0	167.9	19.68	0.022	260	8	12	8	17	15	-12	48	60	55
ESF	26_TSw2_Tptpmn	41+75	41+80	35.0	167.9	19.68	0.022	259	8	12	10	20	15	-12	53	65	60
ESF	26_TSw2_Tptpmn	41+80	41+85	84.0	167.9	19.68	0.022	258	17	12	10	20	15	-12	62	74	69
ESF	26_TSw2_Tptpmn	41+85	41+90	86.0	167.9	19.68	0.022	257	17	12	10	25	15	-5	74	79	74
ESF	26_TSw2_Tptpmn	41+90	41+95	56.0	167.9	19.68	0.022	257	13	12	15	18	15	-12	61	73	68
ESF	26_TSw2_Tptpmn	41+95	42+00	65.0	167.9	19.68	0.022	256	13	12	15	19	15	-12	62	74	69
ESF	26_TSw2_Tptpmn	42+00	42+05	26.0	167.9	19.68	0.022	255	8	12	10	19	15	-12	52	64	59
ESF	26_TSw2_Tptpmn	42+05	42+10	32.0	167.9	19.68	0.022	255	8	12	10	20	15	-12	53	65	60
ESF	26_TSw2_Tptpmn	42+10	42+15	40.0	167.9	19.68	0.022	253	8	12	8	23	15	-12	54	66	61
ESF	26_TSw2_Tptpmn	42+15	42+20	43.0	167.9	19.68	0.022	251	8	12	15	18	15	-12	56	68	63
ESF	26_TSw2_Tptpmn	42+20	42+25	35.0	167.9	19.68	0.022	248	8	12	8	17	15	-5	55	60	55
ESF	26_TSw2_Tptpmn	42+25	42+30	68.0	167.9	19.68	0.022	246	13	12	10	20	15	0	70	70	65
ESF	26_TSw2_Tptpmn	42+30	42+35	86.0	167.9	19.68	0.022	243	17	12	10	23	15	-5	72	77	72
ESF	26_TSw2_Tptpmn	42+35	42+40	54.0	167.9	19.68	0.022	241	13	12	10	21	15	0	71	71	66
ESF	26_TSw2_Tptpmn	42+40	42+45	87.0	167.9	19.68	0.022	238	17	12	10	20	15	-12	62	74	69
ESF	26_TSw2_Tptpmn	42+45	42+50	81.0	167.9	19.68	0.022	236	17	12	10	18	15	0	72	72	67
ESF	26_TSw2_Tptpmn	42+50	42+55	35.0	167.9	19.68	0.022	233	8	12	8	21	15	-12	52	64	59
ESF	26_TSw2_Tptpmn	42+55	42+60	59.0	167.9	19.68	0.022	231	13	12	10	12	15	0	62	62	57
ESF	26_TSw2_Tptpmn	42+60	42+65	63.0	167.9	19.68	0.022	228	13	12	8	20	15	-12	56	68	63
ESF	26_TSw2_Tptpmn	42+65	42+70	54.0	167.9	19.68	0.022	226	13	12	8	14	15	0	62	62	57
ESF	26_TSw2_Tptpmn	42+70	42+75	41.0	167.9	19.68	0.022	225	8	12	10	20	15	-5	60	65	60

Location	Thermal Mechanical and Lithostratigraphic Unit Designation	Begin Station (m)	End Station (m)	RQD	Mean Intact UCS, σ_{ci} (MPa)	Hoek & Brown Intact Material Constant, mi	Unit Weight of Rock Mass, γ (MN/m^3)	Depth of Tunnel, H (m)	RQD Index	C	Js	Jcd	JwR	AJO	RMR Rating = (RQD Index+C+Js+Jcd+JwR+AJ0)	RMR' = (RQD Index+C+Js+Jcd+JwR)	Geological Strength Index, GSI = (RMR' - 5)
ESF	26_TSw2_Tptpmn	42+75	42+80	54.0	167.9	19.68	0.022	225	13	12	10	20	15	-12	58	70	65
ESF	26_TSw2_Tptpmn	42+80	42+85	63.0	167.9	19.68	0.022	225	13	12	10	18	15	0	68	68	63
ESF	26_TSw2_Tptpmn	42+85	42+90	49.0	167.9	19.68	0.022	225	8	12	8	21	15	0	64	64	59
ESF	26_TSw2_Tptpmn	42+90	42+95	57.0	167.9	19.68	0.022	225	13	12	15	17	15	-12	60	72	67
ESF	26_TSw2_Tptpmn	42+95	43+00	60.0	167.9	19.68	0.022	226	13	12	15	17	15	-5	67	72	67
ESF	26_TSw2_Tptpmn	43+00	43+05	42.0	167.9	19.68	0.022	226	8	12	0	17	15	0	52	52	47
ESF	26_TSw2_Tptpmn	43+05	43+10	69.0	167.9	19.68	0.022	226	13	12	10	19	15	-12	57	69	64
ESF	26_TSw2_Tptpmn	43+10	43+15	62.0	167.9	19.68	0.022	226	13	12	10	22	15	-5	67	72	67
ESF	26_TSw2_Tptpmn	43+15	43+20	61.0	167.9	19.68	0.022	227	13	12	10	20	15	-12	58	70	65
ESF	26_TSw2_Tptpmn	43+20	43+25	67.0	167.9	19.68	0.022	227	13	12	10	21	15	-12	59	71	66
ESF	26_TSw2_Tptpmn	43+25	43+30	80.0	167.9	19.68	0.022	227	17	12	8	23	15	-5	70	75	70
ESF	26_TSw2_Tptpmn	43+30	43+35	64.0	167.9	19.68	0.022	227	13	12	10	18	15	-12	56	68	63
ESF	26_TSw2_Tptpmn	43+35	43+40	69.0	167.9	19.68	0.022	227	13	12	10	18	15	-12	56	68	63
ESF	26_TSw2_Tptpmn	43+40	43+45	52.0	167.9	19.68	0.022	227	13	12	10	18	15	-10	58	68	63
ESF	26_TSw2_Tptpmn	43+45	43+50	67.0	167.9	19.68	0.022	228	13	12	15	15	15	-5	65	70	65
ESF	26_TSw2_Tptpmn	43+50	43+55	57.0	167.9	19.68	0.022	228	13	12	10	17	15	-12	55	67	62
ESF	26_TSw2_Tptpmn	43+55	43+60	40.0	167.9	19.68	0.022	228	8	12	15	20	15	-12	58	70	65
ESF	26_TSw2_Tptpmn	43+60	43+65	50.0	167.9	19.68	0.022	228	8	12	0	21	15	0	56	56	51
ESF	26_TSw2_Tptpmn	43+65	43+70	45.0	167.9	19.68	0.022	228	8	12	15	17	15	-12	55	67	62
ESF	26_TSw2_Tptpmn	43+70	43+75	72.0	167.9	19.68	0.022	229	13	12	15	22	15	-12	65	77	72
ESF	26_TSw2_Tptpmn	43+75	43+80	62.0	167.9	19.68	0.022	229	13	12	10	20	15	0	70	70	65
ESF	26_TSw2_Tptpmn	43+80	43+85	41.0	167.9	19.68	0.022	229	8	12	10	14	15	0	59	59	54
ESF	26_TSw2_Tptpmn	43+85	43+90	60.0	167.9	19.68	0.022	229	13	12	10	19	15	-5	64	69	64
ESF	26_TSw2_Tptpmn	43+90	43+95	66.0	167.9	19.68	0.022	229	13	12	8	22	15	0	70	70	65
ESF	26_TSw2_Tptpmn	43+95	44+00	65.0	167.9	19.68	0.022	228	13	12	10	23	15	0	73	73	68
ESF	26_TSw2_Tptpmn	44+00	44+05	57.0	167.9	19.68	0.022	227	13	12	10	21	15	0	71	71	66
ESF	26_TSw2_Tptpmn	44+05	44+10	41.0	167.9	19.68	0.022	226	8	12	10	14	15	-12	47	59	54
ESF	26_TSw2_Tptpmn	44+10	44+15	48.0	167.9	19.68	0.022	226	8	12	10	19	15	-5	59	64	59
ESF	26_TSw2_Tptpmn	44+15	44+20	54.0	167.9	19.68	0.022	225	13	12	8	11	15	0	59	59	54
ESF	26_TSw2_Tptpmn	44+20	44+25	60.0	167.9	19.68	0.022	224	13	12	NA	NA	NA	NA	NA	NA	NA
ESF	26_TSw2_Tptpmn	44+25	44+30	59.0	167.9	19.68	0.022	224	13	12	10	19	15	-5	64	69	64
ESF	26_TSw2_Tptpmn	44+30	44+35	17.0	167.9	19.68	0.022	223	5	12	10	20	15	-12	50	62	57
ESF	26_TSw2_Tptpmn	44+35	44+40	47.0	167.9	19.68	0.022	223	8	12	10	20	15	-5	60	65	60
ESF	26_TSw2_Tptpmn	44+40	44+45	53.0	167.9	19.68	0.022	222	13	12	8	18	15	0	66	66	61
ESF	26_TSw2_Tptpmn	44+45	44+50	41.0	167.9	19.68	0.022	221	8	12	8	16	15	0	59	59	54
ESF	26_TSw2_Tptpmn	44+50	44+55	38.0	167.9	19.68	0.022	221	8	12	8	18	15	0	61	61	56
ESF	26_TSw2_Tptpmn	44+55	44+60	61.0	167.9	19.68	0.022	222	13	12	10	18	15	-12	56	68	63
ESF	26_TSw2_Tptpmn	44+60	44+65	80.0	167.9	19.68	0.022	224	17	12	0	12	15	-5	51	56	51
ESF	26_TSw2_Tptpmn	44+65	44+70	58.0	167.9	19.68	0.022	226	13	12	8	19	15	-5	62	67	62

Location	Thermal Mechanical and Lithostratigraphic Unit Designation	Begin Station (m)	End Station (m)	RQD	Mean Intact UCS, σ_{ci} (MPa)	Hoek & Brown Intact Material Constant, mi	Unit Weight of Rock Mass, γ (MN/m^3)	Depth of Tunnel, H (m)	RQD Index	C	Js	Jcd	JwR	AJO	RMR Rating = (RQD Index+C+Js+Jcd+JwR+AJ0)	RMR' = (RQD Index+C+Js+Jcd+JwR)	Geological Strength Index, GSI = (RMR' - 5)
ESF	26_TSw2_Tptpmn	44+70	44+75	67.0	167.9	19.68	0.022	228	13	12	15	19	15	-12	62	74	69
ESF	26_TSw2_Tptpmn	44+75	44+80	46.0	167.9	19.68	0.022	229	8	12	8	18	15	-12	49	61	56
ESF	26_TSw2_Tptpmn	44+80	44+85	40.0	167.9	19.68	0.022	231	8	12	10	17	15	-5	57	62	57
ESF	26_TSw2_Tptpmn	44+85	44+90	60.0	167.9	19.68	0.022	233	13	12	10	20	15	-12	58	70	65
ESF	26_TSw2_Tptpmn	44+90	44+95	40.0	167.9	19.68	0.022	235	8	12	15	13	15	-5	58	63	58
ESF	26_TSw2_Tptpmn	44+95	45+00	43.0	167.9	19.68	0.022	236	8	12	8	18	15	0	61	61	56
ESF	26_TSw2_Tptpmn	45+00	45+05	49.0	167.9	19.68	0.022	238	8	12	8	18	15	-12	49	61	56
ESF	26_TSw2_Tptpmn	45+05	45+10	81.0	167.9	19.68	0.022	240	17	12	10	18	15	-5	67	72	67
ESF	26_TSw2_Tptpmn	45+10	45+15	82.0	167.9	19.68	0.022	242	17	12	10	18	15	-12	60	72	67
ESF	26_TSw2_Tptpmn	45+15	45+20	65.0	167.9	19.68	0.022	242	13	12	10	17	15	-12	55	67	62
ESF	26_TSw2_Tptpmn	45+20	45+25	79.0	167.9	19.68	0.022	241	17	12	10	17	15	-12	59	71	66
ESF	26_TSw2_Tptpmn	45+25	45+30	81.0	167.9	19.68	0.022	240	17	12	10	17	15	-12	59	71	66
ESF	26_TSw2_Tptpmn	45+30	45+35	83.0	167.9	19.68	0.022	239	17	12	10	16	15	-12	58	70	65
ESF	26_TSw2_Tptpmn	45+35	45+40	96.0	167.9	19.68	0.022	238	20	12	15	18	15	-12	68	80	75
ESF	26_TSw2_Tptpmn	45+40	45+45	97.0	167.9	19.68	0.022	238	20	12	15	22	15	-5	79	84	79
ESF	26_TSw2_Tptpmn	45+45	45+50	80.0	167.9	19.68	0.022	237	17	12	10	14	15	0	68	68	63
ESF	26_TSw2_Tptpmn	45+50	45+55	88.0	167.9	19.68	0.022	236	17	12	15	15	15	-12	62	74	69
ESF	26_TSw2_Tptpmn	45+55	45+60	77.0	167.9	19.68	0.022	236	17	12	10	18	15	-12	60	72	67
ESF	26_TSw2_Tptpmn	45+60	45+65	70.0	167.9	19.68	0.022	235	13	12	10	19	15	0	69	69	64
ESF	26_TSw2_Tptpmn	45+65	45+70	96.0	167.9	19.68	0.022	234	20	12	15	16	15	-12	66	78	73
ESF	26_TSw2_Tptpmn	45+70	45+75	65.0	167.9	19.68	0.022	234	13	12	15	19	15	-12	62	74	69
ESF	26_TSw2_Tptpmn	45+75	45+80	56.0	167.9	19.68	0.022	233	13	12	10	14	15	-12	52	64	59
ESF	26_TSw2_Tptpmn	45+80	45+85	76.0	167.9	19.68	0.022	232	17	12	15	15	15	0	74	74	69
ESF	26_TSw2_Tptpmn	45+85	45+90	82.0	167.9	19.68	0.022	230	17	12	15	20	15	-12	67	79	74
ESF	26_TSw2_Tptpmn	45+90	45+95	71.0	167.9	19.68	0.022	229	13	12	10	19	15	-5	64	69	64
ESF	26_TSw2_Tptpmn	45+95	46+00	67.0	167.9	19.68	0.022	228	13	12	10	18	15	-12	56	68	63
ESF	26_TSw2_Tptpmn	46+00	46+05	59.0	167.9	19.68	0.022	227	13	12	10	14	15	0	64	64	59
ESF	26_TSw2_Tptpmn	46+05	46+10	70.0	167.9	19.68	0.022	225	13	12	15	14	15	-5	64	69	64
ESF	26_TSw2_Tptpmn	46+10	46+15	65.0	167.9	19.68	0.022	224	13	12	10	20	15	0	70	70	65
ESF	26_TSw2_Tptpmn	46+15	46+20	77.0	167.9	19.68	0.022	222	17	12	15	13	15	-5	67	72	67
ESF	26_TSw2_Tptpmn	46+20	46+25	76.0	167.9	19.68	0.022	221	17	12	8	19	15	0	71	71	66
ESF	26_TSw2_Tptpmn	46+25	46+30	94.0	167.9	19.68	0.022	220	20	12	15	16	15	-12	66	78	73
ESF	26_TSw2_Tptpmn	46+30	46+35	83.0	167.9	19.68	0.022	218	17	12	15	16	15	-12	63	75	70
ESF	26_TSw2_Tptpmn	46+35	46+40	68.0	167.9	19.68	0.022	218	13	12	15	19	15	-12	62	74	69
ESF	26_TSw2_Tptpmn	46+40	46+45	28.0	167.9	19.68	0.022	219	8	12	0	25	15	-12	48	60	55
ESF	26_TSw2_Tptpmn	46+45	46+50	56.0	167.9	19.68	0.022	220	13	12	10	24	15	-12	62	74	69
ESF	26_TSw2_Tptpmn	46+50	46+55	67.0	167.9	19.68	0.022	221	13	12	8	19	15	-12	55	67	62
ESF	26_TSw2_Tptpmn	46+55	46+60	57.0	167.9	19.68	0.022	223	13	12	15	22	15	-12	65	77	72
ESF	26_TSw2_Tptpmn	46+60	46+65	40.0	167.9	19.68	0.022	224	8	12	10	19	15	0	64	64	59

Location	Thermal Mechanical and Lithostratigraphic Unit Designation	Begin Station (m)	End Station (m)	RQD	Mean Intact UCS, σ_{ci} (MPa)	Hoek & Brown Intact Material Constant, mi	Unit Weight of Rock Mass, γ (MN/m^3)	Depth of Tunnel, H (m)	RQD Index	C	Js	Jcd	JwR	AJO	RMR Rating = (RQD Index+C+Js+Jcd+JwR+AJ0)	RMR' = (RQD Index+C+Js+Jcd+JwR)	Geological Strength Index, GSI = (RMR' - 5)
ESF	26_TSw2_Tptpmn	46+65	46+70	47.0	167.9	19.68	0.022	225	8	12	10	26	15	-12	59	71	66
ESF	26_TSw2_Tptpmn	46+70	46+75	34.0	167.9	19.68	0.022	227	8	12	0	21	15	-5	51	56	51
ESF	26_TSw2_Tptpmn	46+75	46+80	62.0	167.9	19.68	0.022	228	13	12	8	18	15	0	66	66	61
ESF	26_TSw2_Tptpmn	46+80	46+85	72.0	167.9	19.68	0.022	230	13	12	10	17	15	0	67	67	62
ESF	26_TSw2_Tptpmn	46+85	46+90	61.0	167.9	19.68	0.022	231	13	12	15	21	15	-12	64	76	71
ESF	26_TSw2_Tptpmn	46+90	46+95	74.0	167.9	19.68	0.022	232	13	12	8	19	15	0	67	67	62
ESF	26_TSw2_Tptpmn	46+95	47+00	65.0	167.9	19.68	0.022	234	13	12	10	18	15	-12	56	68	63
ESF	26_TSw2_Tptpmn	47+00	47+05	57.0	167.9	19.68	0.022	236	13	12	8	19	15	0	67	67	62
ESF	26_TSw2_Tptpmn	47+05	47+10	88.0	167.9	19.68	0.022	238	17	12	10	19	15	-12	61	73	68
ESF	26_TSw2_Tptpmn	47+10	47+15	73.0	167.9	19.68	0.022	240	13	12	0	19	15	0	59	59	54
ESF	26_TSw2_Tptpmn	47+15	47+20	35.0	167.9	19.68	0.022	242	8	12	0	14	15	0	49	49	44
ESF	26_TSw2_Tptpmn	47+20	47+25	51.0	167.9	19.68	0.022	244	13	12	0	18	15	0	58	58	53
ESF	26_TSw2_Tptpmn	47+25	47+30	40.0	167.9	19.68	0.022	246	8	12	0	21	15	0	56	56	51
ESF	26_TSw2_Tptpmn	47+30	47+35	41.0	167.9	19.68	0.022	249	8	12	10	25	15	-10	60	70	65
ESF	26_TSw2_Tptpmn	47+35	47+40	50.0	167.9	19.68	0.022	251	8	12	8	17	15	0	60	60	55
ESF	26_TSw2_Tptpmn	47+40	47+45	32.0	167.9	19.68	0.022	254	8	12	8	17	15	0	60	60	55
ESF	26_TSw2_Tptpmn	47+45	47+50	32.0	167.9	19.68	0.022	256	8	12	8	17	15	0	60	60	55
ESF	26_TSw2_Tptpmn	47+50	47+55	61.0	167.9	19.68	0.022	259	13	12	0	17	15	-12	45	57	52
ESF	26_TSw2_Tptpmn	47+55	47+60	55.0	167.9	19.68	0.022	261	13	12	0	20	15	0	60	60	55
ESF	26_TSw2_Tptpmn	47+60	47+65	32.0	167.9	19.68	0.022	262	8	12	10	20	15	-5	60	65	60
ESF	26_TSw2_Tptpmn	47+65	47+70	66.0	167.9	19.68	0.022	262	13	12	8	19	15	-12	55	67	62
ESF	26_TSw2_Tptpmn	47+70	47+75	58.0	167.9	19.68	0.022	263	13	12	8	20	15	0	68	68	63
ESF	26_TSw2_Tptpmn	47+75	47+80	56.0	167.9	19.68	0.022	263	13	12	15	14	15	-5	64	69	64
ESF	26_TSw2_Tptpmn	47+80	47+85	46.0	167.9	19.68	0.022	264	8	12	0	14	15	-12	37	49	44
ESF	26_TSw2_Tptpmn	47+85	47+90	23.0	167.9	19.68	0.022	264	5	12	0	14	15	0	46	46	41
ESF	26_TSw2_Tptpmn	47+90	47+95	50.0	167.9	19.68	0.022	264	8	12	8	17	15	-12	48	60	55
ESF	26_TSw2_Tptpmn	47+95	48+00	46.0	167.9	19.68	0.022	264	8	12	8	18	15	0	61	61	56
ESF	26_TSw2_Tptpmn	48+00	48+05	50.0	167.9	19.68	0.022	264	8	12	0	14	15	0	49	49	44
ESF	26_TSw2_Tptpmn	48+05	48+10	48.0	167.9	19.68	0.022	264	8	12	15	11	15	-5	56	61	56
ESF	26_TSw2_Tptpmn	48+10	48+15	40.0	167.9	19.68	0.022	264	8	12	10	11	15	-5	51	56	51
ESF	26_TSw2_Tptpmn	48+15	48+20	60.0	167.9	19.68	0.022	264	13	12	8	21	15	-12	57	69	64
ESF	26_TSw2_Tptpmn	48+20	48+25	74.0	167.9	19.68	0.022	263	13	12	8	19	15	0	67	67	62
ESF	26_TSw2_Tptpmn	48+25	48+30	52.0	167.9	19.68	0.022	261	13	12	0	18	15	0	58	58	53
ESF	26_TSw2_Tptpmn	48+30	48+35	29.0	167.9	19.68	0.022	259	8	12	0	14	15	0	49	49	44
ESF	26_TSw2_Tptpmn	48+35	48+40	33.0	167.9	19.68	0.022	257	8	12	8	15	15	-12	46	58	53
ESF	26_TSw2_Tptpmn	48+40	48+45	36.0	167.9	19.68	0.022	256	8	12	8	15	15	0	58	58	53
ESF	26_TSw2_Tptpmn	48+45	48+50	47.0	167.9	19.68	0.022	254	8	12	8	15	15	0	58	58	53
ESF	26_TSw2_Tptpmn	48+50	48+55	51.0	167.9	19.68	0.022	252	13	12	8	17	15	-12	53	65	60
ESF	26_TSw2_Tptpmn	48+55	48+60	63.0	167.9	19.68	0.022	251	13	12	8	18	15	-12	54	66	61

Location	Thermal Mechanical and Lithostratigraphic Unit Designation	Begin Station (m)	End Station (m)	RQD	Mean Intact UCS, σ_{ci} (MPa)	Hoek & Brown Intact Material Constant, mi	Unit Weight of Rock Mass, γ (MN/m^3)	Depth of Tunnel, H (m)	RQD Index	C	Js	Jcd	JwR	AJO	RMR Rating = (RQD Index+C+Js+Jcd+JwR+AJ0)	RMR' = (RQD Index+C+Js+Jcd+JwR)	Geological Strength Index, GSI = (RMR' - 5)
ESF	26_TSw2_Tptpmn	48+60	48+65	43.0	167.9	19.68	0.022	250	8	12	10	18	15	-5	58	63	58
ESF	26_TSw2_Tptpmn	48+65	48+70	45.0	167.9	19.68	0.022	248	8	12	0	18	15	-12	41	53	48
ESF	26_TSw2_Tptpmn	48+70	48+75	18.0	167.9	19.68	0.022	247	5	12	8	20	15	-5	55	60	55
ESF	26_TSw2_Tptpmn	48+75	48+80	26.0	167.9	19.68	0.022	246	8	12	0	21	15	-5	51	56	51
ESF	26_TSw2_Tptpmn	48+80	48+85	21.0	167.9	19.68	0.022	244	5	12	8	16	15	-12	44	56	51
ESF	26_TSw2_Tptpmn	48+85	48+90	10.0	167.9	19.68	0.022	242	5	12	0	14	15	0	46	46	41
ESF	26_TSw2_Tptpmn	48+90	48+95	28.0	167.9	19.68	0.022	239	8	12	0	17	15	0	52	52	47
ESF	26_TSw2_Tptpmn	48+95	49+00	30.0	167.9	19.68	0.022	237	8	12	0	16	15	-5	46	51	46
ESF	26_TSw2_Tptpmn	49+00	49+05	45.0	167.9	19.68	0.022	235	8	12	0	18	15	-5	48	53	48
ESF	26_TSw2_Tptpmn	49+05	49+10	41.0	167.9	19.68	0.022	232	8	12	0	14	15	-12	37	49	44
ESF	26_TSw2_Tptpmn	49+10	49+15	51.0	167.9	19.68	0.022	230	13	12	0	17	15	0	57	57	52
ESF	26_TSw2_Tptpmn	49+15	49+20	32.0	167.9	19.68	0.022	228	8	12	15	14	15	-12	52	64	59
ESF	26_TSw2_Tptpmn	49+20	49+25	51.0	167.9	19.68	0.022	226	13	12	8	15	15	-12	51	63	58
ESF	26_TSw2_Tptpmn	49+25	49+30	50.0	167.9	19.68	0.022	224	8	12	8	17	15	-12	48	60	55
ESF	26_TSw2_Tptpmn	49+30	49+35	33.0	167.9	19.68	0.022	222	8	12	15	14	15	-5	59	64	59
ESF	26_TSw2_Tptpmn	49+35	49+40	69.0	167.9	19.68	0.022	220	13	12	10	16	15	-12	54	66	61
ESF	26_TSw2_Tptpmn	49+40	49+45	26.0	167.9	19.68	0.022	219	8	12	0	17	15	0	52	52	47
ESF	26_TSw2_Tptpmn	49+45	49+50	13.0	167.9	19.68	0.022	219	5	12	0	16	15	0	48	48	43
ESF	26_TSw2_Tptpmn	49+50	49+55	27.0	167.9	19.68	0.022	219	8	12	0	16	15	0	51	51	46
ESF	26_TSw2_Tptpmn	49+55	49+60	48.0	167.9	19.68	0.022	219	8	12	8	20	15	-12	51	63	58
ESF	26_TSw2_Tptpmn	49+60	49+65	41.0	167.9	19.68	0.022	219	8	12	8	16	15	0	59	59	54
ESF	26_TSw2_Tptpmn	49+65	49+70	32.0	167.9	19.68	0.022	220	8	12	8	16	15	-12	47	59	54
ESF	26_TSw2_Tptpmn	49+70	49+75	29.0	167.9	19.68	0.022	220	8	12	10	16	15	-12	49	61	56
ESF	26_TSw2_Tptpmn	49+75	49+80	46.0	167.9	19.68	0.022	220	8	12	8	16	15	-12	47	59	54
ESF	26_TSw2_Tptpmn	49+80	49+85	40.0	167.9	19.68	0.022	219	8	12	8	19	15	-12	50	62	57
ESF	26_TSw2_Tptpmn	49+85	49+90	30.0	167.9	19.68	0.022	217	8	12	8	16	15	-12	47	59	54
ESF	26_TSw2_Tptpmn	49+90	49+95	46.0	167.9	19.68	0.022	216	8	12	8	16	15	0	59	59	54
ESF	26_TSw2_Tptpmn	49+95	50+00	35.0	167.9	19.68	0.022	214	8	12	10	18	15	-5	58	63	58
ESF	26_TSw2_Tptpmn	50+00	50+05	31.0	167.9	19.68	0.022	212	8	12	8	19	15	-12	50	62	57
ESF	26_TSw2_Tptpmn	50+05	50+10	40.0	167.9	19.68	0.022	213	8	12	8	18	15	-12	49	61	56
ESF	26_TSw2_Tptpmn	50+10	50+15	17.0	167.9	19.68	0.022	213	5	12	10	23	15	-10	55	65	60
ESF	26_TSw2_Tptpmn	50+15	50+20	61.0	167.9	19.68	0.022	213	13	12	10	16	15	-5	61	66	61
ESF	26_TSw2_Tptpmn	50+20	50+25	55.0	167.9	19.68	0.022	214	13	12	8	16	15	-12	52	64	59
ESF	26_TSw2_Tptpmn	50+25	50+30	64.0	167.9	19.68	0.022	214	13	12	10	16	15	-10	56	66	61
ESF	26_TSw2_Tptpmn	50+30	50+35	62.0	167.9	19.68	0.022	214	13	12	8	16	15	-12	52	64	59
ESF	26_TSw2_Tptpmn	50+35	50+40	61.0	167.9	19.68	0.022	215	13	12	8	16	15	0	64	64	59
ESF	26_TSw2_Tptpmn	50+40	50+45	68.0	167.9	19.68	0.022	215	13	12	10	17	15	-5	62	67	62
ESF	26_TSw2_Tptpmn	50+45	50+50	64.0	167.9	19.68	0.022	215	13	12	10	14	15	-5	59	64	59
ESF	26_TSw2_Tptpmn	50+50	50+55	50.0	167.9	19.68	0.022	216	8	12	10	19	15	-12	52	64	59

Location	Thermal Mechanical and Lithostratigraphic Unit Designation	Begin Station (m)	End Station (m)	RQD	Mean Intact UCS, σ_{ci} (MPa)	Hoek & Brown Intact Material Constant, mi	Unit Weight of Rock Mass, γ (MN/m^3)	Depth of Tunnel, H (m)	RQD Index	C	Js	Jcd	JwR	AJO	RMR Rating = (RQD Index+C+Js+Jcd+JwR+AJ0)	RMR' = (RQD Index+C+Js+Jcd+JwR)	Geological Strength Index, GSI = (RMR' - 5)
ESF	26_TSw2_Tptpmn	50+55	50+60	59.0	167.9	19.68	0.022	216	13	12	8	18	15	-12	54	66	61
ESF	26_TSw2_Tptpmn	50+60	50+65	71.0	167.9	19.68	0.022	216	13	12	10	16	15	-5	61	66	61
ESF	26_TSw2_Tptpmn	50+65	50+70	49.0	167.9	19.68	0.022	216	8	12	8	16	15	-5	54	59	54
ESF	26_TSw2_Tptpmn	50+70	50+75	67.0	167.9	19.68	0.022	215	13	12	8	16	15	-12	52	64	59
ESF	26_TSw2_Tptpmn	50+75	50+80	56.0	167.9	19.68	0.022	214	13	12	8	18	15	-12	54	66	61
ESF	26_TSw2_Tptpmn	50+80	50+85	49.0	167.9	19.68	0.022	214	8	12	8	11	15	-5	49	54	49
ESF	26_TSw2_Tptpmn	50+85	50+90	66.0	167.9	19.68	0.022	213	13	12	8	13	15	-12	49	61	56
ESF	26_TSw2_Tptpmn	50+90	50+95	52.0	167.9	19.68	0.022	213	13	12	15	18	15	-12	61	73	68
ESF	26_TSw2_Tptpmn	50+95	51+00	51.0	167.9	19.68	0.022	212	13	12	10	13	15	-12	51	63	58
ESF	26_TSw2_Tptpmn	51+00	51+05	34.0	167.9	19.68	0.022	211	8	12	10	16	15	-5	56	61	56
ESF	26_TSw2_Tptpmn	51+05	51+10	53.0	167.9	19.68	0.022	211	13	12	10	14	15	-5	59	64	59
ESF	26_TSw2_Tptpmn	51+10	51+15	68.0	167.9	19.68	0.022	212	13	12	15	20	15	-12	63	75	70
ESF	26_TSw2_Tptpmn	51+15	51+20	59.0	167.9	19.68	0.022	213	13	12	10	18	15	-5	63	68	63
ESF	26_TSw2_Tptpmn	51+20	51+25	58.0	167.9	19.68	0.022	214	13	12	8	22	15	-12	58	70	65
ESF	26_TSw2_Tptpmn	51+25	51+30	61.0	167.9	19.68	0.022	215	13	12	10	14	15	-5	59	64	59
ESF	26_TSw2_Tptpmn	51+30	51+35	65.0	167.9	19.68	0.022	218	13	12	15	14	15	-5	64	69	64
ESF	26_TSw2_Tptpmn	51+35	51+40	54.0	167.9	19.68	0.022	220	13	12	10	19	15	-12	57	69	64
ESF	26_TSw2_Tptpmn	51+40	51+45	84.0	167.9	19.68	0.022	223	17	12	10	20	15	-12	62	74	69
ESF	26_TSw2_Tptpmn	51+45	51+50	87.0	167.9	19.68	0.022	225	17	12	10	21	15	-12	63	75	70
ESF	26_TSw2_Tptpmn	51+50	51+55	59.0	167.9	19.68	0.022	227	13	12	10	16	15	-12	54	66	61
ESF	26_TSw2_Tptpmn	51+55	51+60	66.0	167.9	19.68	0.022	230	13	12	15	17	15	-12	60	72	67
ESF	26_TSw2_Tptpmn	51+60	51+65	38.0	167.9	19.68	0.022	232	8	12	8	13	15	-12	44	56	51
ESF	26_TSw2_Tptpmn	51+65	51+70	61.0	167.9	19.68	0.022	234	13	12	15	19	15	-12	62	74	69
ESF	26_TSw2_Tptpmn	51+70	51+75	60.0	167.9	19.68	0.022	237	13	12	15	11	15	-5	61	66	61
ESF	26_TSw2_Tptpmn	51+75	51+80	36.0	167.9	19.68	0.022	239	8	12	15	12	15	-5	57	62	57
ESF	26_TSw2_Tptpmn	51+80	51+85	26.0	167.9	19.68	0.022	241	8	12	10	20	15	-12	53	65	60
ESF	26_TSw2_Tptpmn	51+85	51+90	62.0	167.9	19.68	0.022	244	13	12	10	18	15	-12	56	68	63
ESF	26_TSw2_Tptpmn	51+90	51+95	69.0	167.9	19.68	0.022	245	13	12	10	18	15	0	68	68	63
ESF	26_TSw2_Tptpmn	51+95	52+00	73.0	167.9	19.68	0.022	247	13	12	10	18	15	-12	56	68	63
ESF	26_TSw2_Tptpmn	52+00	52+05	60.0	167.9	19.68	0.022	249	13	12	15	12	15	-12	55	67	62
ESF	26_TSw2_Tptpmn	52+05	52+10	80.0	167.9	19.68	0.022	250	17	12	10	16	15	-12	58	70	65
ESF	26_TSw2_Tptpmn	52+10	52+15	71.0	167.9	19.68	0.022	252	13	12	10	16	15	-12	54	66	61
ESF	26_TSw2_Tptpmn	52+15	52+20	60.0	167.9	19.68	0.022	254	13	12	10	21	15	-12	59	71	66
ESF	26_TSw2_Tptpmn	52+20	52+25	64.0	167.9	19.68	0.022	256	13	12	10	19	15	-12	57	69	64
ESF	26_TSw2_Tptpmn	52+25	52+30	81.0	167.9	19.68	0.022	257	17	12	8	16	15	-12	56	68	63
ESF	26_TSw2_Tptpmn	52+30	52+35	50.0	167.9	19.68	0.022	259	8	12	0	18	15	-5	48	53	48
ESF	26_TSw2_Tptpmn	52+35	52+40	55.0	167.9	19.68	0.022	261	13	12	15	13	15	-5	63	68	63
ESF	26_TSw2_Tptpmn	52+40	52+45	70.0	167.9	19.68	0.022	262	13	12	8	16	15	-12	52	64	59
ESF	26_TSw2_Tptpmn	52+45	52+50	73.0	167.9	19.68	0.022	263	13	12	15	11	15	-12	54	66	61

Location	Thermal Mechanical and Lithostratigraphic Unit Designation	Begin Station (m)	End Station (m)	RQD	Mean Intact UCS, σ_{ci} (MPa)	Hoek & Brown Intact Material Constant, mi	Unit Weight of Rock Mass, γ (MN/m^3)	Depth of Tunnel, H (m)	RQD Index	C	Js	Jcd	JwR	AJO	RMR Rating = (RQD Index+C+Js+Jcd+JwR+AJ0)	RMR' = (RQD Index+C+Js+Jcd+JwR)	Geological Strength Index, GSI = (RMR' - 5)
ESF	26_TSw2_Tptpmn	52+50	52+55	63.0	167.9	19.68	0.022	263	13	12	10	17	15	-12	55	67	62
ESF	26_TSw2_Tptpmn	52+55	52+60	76.0	167.9	19.68	0.022	263	17	12	10	13	15	-12	55	67	62
ESF	26_TSw2_Tptpmn	52+60	52+65	63.0	167.9	19.68	0.022	264	13	12	10	16	15	-12	54	66	61
ESF	26_TSw2_Tptpmn	52+65	52+70	60.0	167.9	19.68	0.022	264	13	12	8	15	15	-12	51	63	58
ESF	26_TSw2_Tptpmn	52+70	52+75	78.0	167.9	19.68	0.022	264	17	12	8	18	15	-12	58	70	65
ESF	26_TSw2_Tptpmn	52+75	52+80	70.0	167.9	19.68	0.022	264	13	12	10	19	15	-12	57	69	64
ESF	26_TSw2_Tptpmn	52+80	52+85	80.0	167.9	19.68	0.022	265	17	12	15	20	15	-12	67	79	74
ESF	26_TSw2_Tptpmn	52+85	52+90	86.0	167.9	19.68	0.022	265	17	12	10	20	15	-12	62	74	69
ESF	26_TSw2_Tptpmn	52+90	52+95	83.0	167.9	19.68	0.022	265	17	12	15	23	15	-12	70	82	77
ESF	26_TSw2_Tptpmn	52+95	53+00	79.0	167.9	19.68	0.022	265	17	12	15	19	15	-12	66	78	73
ESF	26_TSw2_Tptpmn	53+00	53+05	82.0	167.9	19.68	0.022	265	17	12	15	18	15	-12	65	77	72
ESF	26_TSw2_Tptpmn	53+05	53+10	51.0	167.9	19.68	0.022	265	13	12	15	14	15	-12	57	69	64
ESF	26_TSw2_Tptpmn	53+10	53+15	54.0	167.9	19.68	0.022	265	13	12	15	22	15	-12	65	77	72
ESF	26_TSw2_Tptpmn	53+15	53+20	65.0	167.9	19.68	0.022	265	13	12	10	19	15	0	69	69	64
ESF	26_TSw2_Tptpmn	53+20	53+25	67.0	167.9	19.68	0.022	265	13	12	15	20	15	-12	63	75	70
ESF	26_TSw2_Tptpmn	53+25	53+30	58.0	167.9	19.68	0.022	265	13	12	15	11	15	0	66	66	61
ESF	26_TSw2_Tptpmn	53+30	53+35	54.0	167.9	19.68	0.022	265	13	12	15	17	15	-12	60	72	67
ESF	26_TSw2_Tptpmn	53+35	53+40	65.0	167.9	19.68	0.022	265	13	12	8	17	15	-12	53	65	60
ESF	26_TSw2_Tptpmn	53+40	53+45	76.0	167.9	19.68	0.022	265	17	12	10	20	15	-12	62	74	69
ESF	26_TSw2_Tptpmn	53+45	53+50	73.0	167.9	19.68	0.022	265	13	12	15	21	15	-12	64	76	71
ESF	26_TSw2_Tptpmn	53+50	53+55	61.0	167.9	19.68	0.022	265	13	12	10	17	15	-12	55	67	62
ESF	26_TSw2_Tptpmn	53+55	53+60	57.0	167.9	19.68	0.022	265	13	12	10	17	15	-12	55	67	62
ESF	26_TSw2_Tptpmn	53+60	53+65	62.0	167.9	19.68	0.022	265	13	12	10	22	15	-5	67	72	67
ESF	26_TSw2_Tptpmn	53+65	53+70	78.0	167.9	19.68	0.022	265	17	12	15	17	15	-12	64	76	71
ESF	26_TSw2_Tptpmn	53+70	53+75	68.0	167.9	19.68	0.022	264	13	12	15	17	15	0	72	72	67
ESF	26_TSw2_Tptpmn	53+75	53+80	78.0	167.9	19.68	0.022	263	17	12	15	17	15	-5	71	76	71
ESF	26_TSw2_Tptpmn	53+80	53+85	51.0	167.9	19.68	0.022	261	13	12	20	16	15	-5	71	76	71
ESF	26_TSw2_Tptpmn	53+85	53+90	47.0	167.9	19.68	0.022	260	8	12	15	9	15	-5	54	59	54
ESF	26_TSw2_Tptpmn	53+90	53+95	73.0	167.9	19.68	0.022	258	13	12	15	9	15	0	64	64	59
ESF	26_TSw2_Tptpmn	53+95	54+00	80.0	167.9	19.68	0.022	257	17	12	10	19	15	-12	61	73	68
ESF	26_TSw2_Tptpmn	54+00	54+05	70.0	167.9	19.68	0.022	255	13	12	10	14	15	-12	52	64	59
ESF	26_TSw2_Tptpmn	54+05	54+10	60.0	167.9	19.68	0.022	253	13	12	15	11	15	-5	61	66	61
ESF	26_TSw2_Tptpmn	54+10	54+15	50.0	167.9	19.68	0.022	252	8	12	10	8	15	-12	41	53	48
ESF	26_TSw2_Tptpmn	54+15	54+20	36.0	167.9	19.68	0.022	250	8	12	8	12	15	-5	50	55	50
ESF	26_TSw2_Tptpmn	54+20	54+25	64.0	167.9	19.68	0.022	249	13	12	10	20	15	-12	58	70	65
ESF	26_TSw2_Tptpmn	54+25	54+30	63.0	167.9	19.68	0.022	247	13	12	10	14	15	0	64	64	59
ESF	26_TSw2_Tptpmn	54+30	54+35	71.0	167.9	19.68	0.022	246	13	12	10	19	15	-12	57	69	64
ESF	26_TSw2_Tptpmn	54+35	54+40	79.0	167.9	19.68	0.022	244	17	12	15	18	15	-12	65	77	72
ESF	26_TSw2_Tptpmn	54+40	54+45	69.0	167.9	19.68	0.022	242	13	12	15	16	15	-5	66	71	66

Location	Thermal Mechanical and Lithostratigraphic Unit Designation	Begin Station (m)	End Station (m)	RQD	Mean Intact UCS, σ_{ci} (MPa)	Hoek & Brown Intact Material Constant, mi	Unit Weight of Rock Mass, γ (MN/m^3)	Depth of Tunnel, H (m)	RQD Index	C	Js	Jcd	JwR	AJO	RMR Rating = (RQD Index+C+Js+Jcd+JwR+AJ0)	RMR' = (RQD Index+C+Js+Jcd+JwR)	Geological Strength Index, GSI = (RMR' - 5)
ESF	26_TSw2_Tptpmn	54+45	54+50	71.0	167.9	19.68	0.022	240	13	12	10	17	15	0	67	67	62
ESF	26_TSw2_Tptpmn	54+50	54+55	88.0	167.9	19.68	0.022	238	17	12	10	20	15	0	74	74	69
ESF	26_TSw2_Tptpmn	54+55	54+60	88.0	167.9	19.68	0.022	236	17	12	15	14	15	0	73	73	68
ESF	26_TSw2_Tptpmn	54+60	54+65	97.0	167.9	19.68	0.022	234	20	12	15	20	15	-12	70	82	77
ESF	26_TSw2_Tptpmn	54+65	54+70	83.0	167.9	19.68	0.022	232	17	12	15	18	15	-12	65	77	72
ESF	26_TSw2_Tptpmn	54+70	54+75	90.0	167.9	19.68	0.022	231	17	12	15	20	15	-12	67	79	74
ESF	26_TSw2_Tptpmn	54+75	54+80	90.0	167.9	19.68	0.022	229	17	12	15	18	15	-12	65	77	72
ESF	26_TSw2_Tptpmn	54+80	54+85	69.0	167.9	19.68	0.022	227	13	12	15	17	15	-5	67	72	67
ESF	26_TSw2_Tptpmn	54+85	54+90	71.0	167.9	19.68	0.022	225	13	12	15	19	15	-12	62	74	69
ESF	26_TSw2_Tptpmn	54+90	54+95	81.0	167.9	19.68	0.022	224	17	12	15	14	15	-12	61	73	68
ESF	26_TSw2_Tptpmn	54+95	55+00	78.0	167.9	19.68	0.022	225	17	12	15	14	15	-5	68	73	68
ESF	26_TSw2_Tptpmn	55+00	55+05	75.0	167.9	19.68	0.022	226	13	12	15	20	15	-12	63	75	70
ESF	26_TSw2_Tptpmn	55+05	55+10	81.0	167.9	19.68	0.022	227	17	12	15	19	15	-12	66	78	73
ESF	26_TSw2_Tptpmn	55+10	55+15	84.0	167.9	19.68	0.022	228	17	12	15	17	15	-12	64	76	71
ESF	26_TSw2_Tptpmn	55+15	55+20	93.0	167.9	19.68	0.022	229	20	12	15	19	15	-12	69	81	76
ESF	26_TSw2_Tptpmn	55+20	55+25	76.0	167.9	19.68	0.022	230	17	12	15	16	15	-12	63	75	70
ESF	26_TSw2_Tptpmn	55+25	55+30	82.0	167.9	19.68	0.022	231	17	12	15	9	15	-12	56	68	63
ESF	26_TSw2_Tptpmn	55+30	55+35	69.0	167.9	19.68	0.022	232	13	12	15	14	15	-12	57	69	64
ESF	26_TSw2_Tptpmn	55+35	55+40	56.0	167.9	19.68	0.022	233	13	12	10	11	15	0	61	61	56
ESF	26_TSw2_Tptpmn	55+40	55+45	57.0	167.9	19.68	0.022	234	13	12	15	13	15	-5	63	68	63
ESF	26_TSw2_Tptpmn	55+45	55+50	67.0	167.9	19.68	0.022	235	13	12	15	21	15	-12	64	76	71
ESF	26_TSw2_Tptpmn	55+50	55+55	62.0	167.9	19.68	0.022	235	13	12	10	23	15	-12	61	73	68
ESF	26_TSw2_Tptpmn	55+55	55+60	63.0	167.9	19.68	0.022	235	13	12	15	24	15	-12	67	79	74
ESF	26_TSw2_Tptpmn	55+60	55+65	58.0	167.9	19.68	0.022	235	13	12	10	9	15	-5	54	59	54
ESF	26_TSw2_Tptpmn	55+65	55+70	61.0	167.9	19.68	0.022	235	13	12	15	21	15	-12	64	76	71
ESF	26_TSw2_Tptpmn	55+70	55+75	81.0	167.9	19.68	0.022	236	17	12	10	16	15	0	70	70	65
ESF	26_TSw2_Tptpmn	55+75	55+80	83.0	167.9	19.68	0.022	236	17	12	15	14	15	0	73	73	68
ESF	26_TSw2_Tptpmn	55+80	55+85	47.0	167.9	19.68	0.022	236	8	12	10	14	15	0	59	59	54
ESF	26_TSw2_Tptpmn	55+85	55+90	51.0	167.9	19.68	0.022	237	13	12	15	16	15	-12	59	71	66
ESF	26_TSw2_Tptpmn	55+90	55+95	53.0	167.9	19.68	0.022	237	13	12	15	14	15	-12	57	69	64
ESF	26_TSw2_Tptpmn	55+95	56+00	53.0	167.9	19.68	0.022	237	13	12	10	11	15	-12	49	61	56
ESF	26_TSw2_Tptpmn	56+00	56+05	54.0	167.9	19.68	0.022	238	13	12	15	14	15	-12	57	69	64
ESF	26_TSw2_Tptpmn	56+05	56+10	75.0	167.9	19.68	0.022	238	13	12	15	14	15	-12	57	69	64
ESF	26_TSw2_Tptpmn	56+10	56+15	61.0	167.9	19.68	0.022	238	13	12	10	14	15	-12	52	64	59
ESF	26_TSw2_Tptpmn	56+15	56+20	72.0	167.9	19.68	0.022	238	13	12	15	13	15	-12	56	68	63
ESF	26_TSw2_Tptpmn	56+20	56+25	51.0	167.9	19.68	0.022	237	13	12	10	12	15	-12	50	62	57
ESF	26_TSw2_Tptpmn	56+25	56+30	77.0	167.9	19.68	0.022	235	17	12	10	17	15	-12	59	71	66
ESF	26_TSw2_Tptpmn	56+30	56+35	81.0	167.9	19.68	0.022	234	17	12	10	14	15	-12	56	68	63
ESF	26_TSw2_Tptpmn	56+35	56+40	47.0	167.9	19.68	0.022	232	8	12	10	16	15	0	61	61	56

Location	Thermal Mechanical and Lithostratigraphic Unit Designation	Begin Station (m)	End Station (m)	RQD	Mean Intact UCS, σ_{ci} (MPa)	Hoek & Brown Intact Material Constant, mi	Unit Weight of Rock Mass, γ (MN/m^3)	Depth of Tunnel, H (m)	RQD Index	C	Js	Jcd	JwR	AJO	RMR Rating = (RQD Index+C+Js+Jcd+JwR+AJ0)	RMR' = (RQD Index+C+Js+Jcd+JwR)	Geological Strength Index, GSI = (RMR' - 5)
ESF	26_TSw2_Tptpmn	56+40	56+45	79.0	167.9	19.68	0.022	231	17	12	15	12	15	-12	59	71	66
ESF	26_TSw2_Tptpmn	56+45	56+50	58.0	167.9	19.68	0.022	230	13	12	10	12	15	-12	50	62	57
ESF	26_TSw2_Tptpmn	56+50	56+55	74.0	167.9	19.68	0.022	228	13	12	15	16	15	-12	59	71	66
ESF	26_TSw2_Tptpmn	56+55	56+60	67.0	167.9	19.68	0.022	227	13	12	15	13	15	-12	56	68	63
ESF	26_TSw2_Tptpmn	56+60	56+65	46.0	167.9	19.68	0.022	225	8	12	10	18	15	-12	51	63	58
ESF	26_TSw2_Tptpmn	56+65	56+70	74.0	167.9	19.68	0.022	224	13	12	15	18	15	-5	68	73	68
ESF	26_TSw2_Tptpmn	56+70	56+75	49.0	167.9	19.68	0.022	222	8	12	10	16	15	0	61	61	56
ESF	26_TSw2_Tptpmn	56+75	56+80	67.0	167.9	19.68	0.022	221	13	12	10	19	15	0	69	69	64
ESF	26_TSw2_Tptpmn	56+80	56+85	66.0	167.9	19.68	0.022	219	13	12	15	14	15	-5	64	69	64
ESF	26_TSw2_Tptpmn	56+85	56+90	46.0	167.9	19.68	0.022	217	8	12	10	11	15	0	56	56	51
ESF	26_TSw2_Tptpmn	56+90	56+95	33.0	167.9	19.68	0.022	216	8	12	10	22	15	-12	55	67	62
ESF	26_TSw2_Tptpmn	56+95	57+00	45.0	167.9	19.68	0.022	214	8	12	10	22	15	-12	55	67	62
ESF	26_TSw2_Tptpmn	57+00	57+05	57.0	167.9	19.68	0.022	213	13	12	0	14	15	-12	42	54	49
ESF	26_TSw2_Tptpmn	57+05	57+10	47.0	167.9	19.68	0.022	211	8	12	15	20	15	-12	58	70	65
ESF	26_TSw2_Tptpmn	57+10	57+15	49.0	167.9	19.68	0.022	209	8	12	10	24	15	-5	64	69	64
ESF	26_TSw2_Tptpmn	57+15	57+20	37.0	167.9	19.68	0.022	208	8	12	10	19	15	-12	52	64	59
ESF	26_TSw2_Tptpmn	57+20	57+25	37.0	167.9	19.68	0.022	206	8	12	8	25	15	-12	56	68	63
ESF	27_TSw2_Tptpll	57+25	57+30	47.0	167.9	19.68	0.022	204	8	12	15	16	15	-12	54	66	61
ESF	27_TSw2_Tptpll	57+30	57+35	45.0	167.9	19.68	0.022	203	8	12	15	25	15	-12	63	75	70
ESF	27_TSw2_Tptpll	57+35	57+40	30.0	167.9	19.68	0.022	202	8	12	15	24	15	-12	62	74	69
ESF	27_TSw2_Tptpll	57+40	57+45	14.0	167.9	19.68	0.022	201	5	12	15	19	15	-12	54	66	61
ESF	27_TSw2_Tptpll	57+45	57+50	10.0	167.9	19.68	0.022	201	5	12	8	20	15	-12	48	60	55
ESF	27_TSw2_Tptpll	57+50	57+55	15.0	167.9	19.68	0.022	200	5	12	10	19	15	-12	49	61	56
ESF	27_TSw2_Tptpll	57+55	57+60	25.0	167.9	19.68	0.022	199	5	12	15	19	15	-12	54	66	61
ESF	27_TSw2_Tptpll	57+60	57+65	16.0	167.9	19.68	0.022	199	5	12	15	18	15	-12	53	65	60
ESF	27_TSw2_Tptpll	57+65	57+70	10.0	167.9	19.68	0.022	198	5	12	15	23	15	-12	58	70	65
ESF	27_TSw2_Tptpll	57+70	57+75	12.0	167.9	19.68	0.022	197	5	12	10	17	15	-5	54	59	54
ESF	27_TSw2_Tptpll	57+75	57+80	25.0	167.9	19.68	0.022	196	5	12	15	21	15	-5	63	68	63
ESF	27_TSw2_Tptpll	57+80	57+85	14.0	167.9	19.68	0.022	196	5	12	15	12	15	-12	47	59	54
ESF	27_TSw2_Tptpll	57+85	57+90	10.0	167.9	19.68	0.022	195	5	12	15	15	15	-12	50	62	57
ESF	27_TSw2_Tptpll	57+90	57+95	22.0	167.9	19.68	0.022	194	5	12	15	11	15	-12	46	58	53
ESF	27_TSw2_Tptpll	57+95	58+00	16.0	167.9	19.68	0.022	194	5	12	8	19	15	-12	47	59	54
ESF	27_TSw2_Tptpll	58+00	58+05	21.0	167.9	19.68	0.022	194	5	12	8	14	15	-12	42	54	49
ESF	27_TSw2_Tptpll	58+05	58+10	10.0	167.9	19.68	0.022	194	5	12	0	19	15	-12	39	51	46
ESF	27_TSw2_Tptpll	58+10	58+15	10.0	167.9	19.68	0.022	194	5	12	8	13	15	-12	41	53	48
ESF	27_TSw2_Tptpll	58+15	58+20	24.0	167.9	19.68	0.022	195	5	12	8	18	15	-12	46	58	53
ESF	27_TSw2_Tptpll	58+20	58+25	54.0	167.9	19.68	0.022	196	13	12	8	19	15	-12	55	67	62
ESF	27_TSw2_Tptpll	58+25	58+30	20.0	167.9	19.68	0.022	197	5	12	10	19	15	-12	49	61	56
ESF	27_TSw2_Tptpll	58+30	58+35	23.0	167.9	19.68	0.022	198	5	12	15	14	15	-5	56	61	56

Location	Thermal Mechanical and Lithostratigraphic Unit Designation	Begin Station (m)	End Station (m)	RQD	Mean Intact UCS, σ_{ci} (MPa)	Hoek & Brown Intact Material Constant, mi	Unit Weight of Rock Mass, γ (MN/m^3)	Depth of Tunnel, H (m)	RQD Index	C	Js	Jcd	JwR	AJO	RMR Rating = (RQD Index+C+Js+Jcd+JwR+AJ0)	RMR' = (RQD Index+C+Js+Jcd+JwR)	Geological Strength Index, GSI = (RMR' - 5)
ESF	27_TSw2_Tptpll	58+35	58+40	44.0	167.9	19.68	0.022	199	8	12	15	12	15	-5	57	62	57
ESF	27_TSw2_Tptpll	58+40	58+45	44.0	167.9	19.68	0.022	200	8	12	15	19	15	-12	57	69	64
ESF	27_TSw2_Tptpll	58+45	58+50	50.0	167.9	19.68	0.022	201	8	12	15	21	15	-12	59	71	66
ESF	27_TSw2_Tptpll	58+50	58+55	38.0	167.9	19.68	0.022	202	8	12	15	19	15	-12	57	69	64
ESF	27_TSw2_Tptpll	58+55	58+60	13.0	167.9	19.68	0.022	203	5	12	20	17	15	-12	57	69	64
ESF	27_TSw2_Tptpll	58+60	58+65	10.0	167.9	19.68	0.022	202	5	12	15	19	15	-12	54	66	61
ESF	27_TSw2_Tptpll	58+65	58+70	36.0	167.9	19.68	0.022	201	8	12	15	9	15	-12	47	59	54
ESF	27_TSw2_Tptpll	58+70	58+75	18.0	167.9	19.68	0.022	200	5	12	10	13	15	-12	43	55	50
ESF	27_TSw2_Tptpll	58+75	58+80	43.0	167.9	19.68	0.022	198	8	12	8	13	15	-12	44	56	51
ESF	27_TSw2_Tptpll	58+80	58+85	36.0	167.9	19.68	0.022	197	8	12	10	19	15	-12	52	64	59
ESF	27_TSw2_Tptpll	58+85	58+90	64.0	167.9	19.68	0.022	196	13	12	10	19	15	0	69	69	64
ESF	27_TSw2_Tptpll	58+90	58+95	62.0	167.9	19.68	0.022	195	13	12	15	17	15	-12	60	72	67
ESF	27_TSw2_Tptpll	58+95	59+00	67.0	167.9	19.68	0.022	194	13	12	15	17	15	-12	60	72	67
ESF	27_TSw2_Tptpll	59+00	59+05	41.0	167.9	19.68	0.022	193	8	12	15	17	15	0	67	67	62
ESF	27_TSw2_Tptpll	59+05	59+10	39.0	167.9	19.68	0.022	191	8	12	10	17	15	-12	50	62	57
ESF	27_TSw2_Tptpll	59+10	59+15	26.0	167.9	19.68	0.022	190	8	12	15	17	15	-12	55	67	62
ESF	27_TSw2_Tptpll	59+15	59+20	46.0	167.9	19.68	0.022	189	8	12	10	17	15	0	62	62	57
ESF	27_TSw2_Tptpll	59+20	59+25	42.0	167.9	19.68	0.022	189	8	12	15	19	15	-12	57	69	64
ESF	27_TSw2_Tptpll	59+25	59+30	49.0	167.9	19.68	0.022	188	8	12	15	17	15	-12	55	67	62
ESF	27_TSw2_Tptpll	59+30	59+35	61.0	167.9	19.68	0.022	188	13	12	15	17	15	-12	60	72	67
ESF	27_TSw2_Tptpll	59+35	59+40	42.0	167.9	19.68	0.022	188	8	12	15	17	15	-12	55	67	62
ESF	27_TSw2_Tptpll	59+40	59+45	58.0	167.9	19.68	0.022	187	13	12	15	17	15	-12	60	72	67
ESF	26_TSw2_Tptpmn	59+45	59+50	88.0	167.9	19.68	0.022	186	17	12	10	17	15	-12	59	71	66
ESF	26_TSw2_Tptpmn	59+50	59+55	96.0	167.9	19.68	0.022	185	20	12	15	17	15	-12	67	79	74
ESF	26_TSw2_Tptpmn	59+55	59+60	92.0	167.9	19.68	0.022	184	20	12	15	17	15	-12	67	79	74
ESF	26_TSw2_Tptpmn	59+60	59+65	89.0	167.9	19.68	0.022	183	17	12	15	17	15	-12	64	76	71
ESF	26_TSw2_Tptpmn	59+65	59+70	93.0	167.9	19.68	0.022	182	20	12	15	17	15	-12	67	79	74
ESF	26_TSw2_Tptpmn	59+70	59+75	64.0	167.9	19.68	0.022	181	13	12	15	17	15	-12	60	72	67
ESF	26_TSw2_Tptpmn	59+75	59+80	83.0	167.9	19.68	0.022	180	17	12	15	14	15	-12	61	73	68
ESF	26_TSw2_Tptpmn	59+80	59+85	73.0	167.9	19.68	0.022	180	13	12	15	17	15	-12	60	72	67
ESF	26_TSw2_Tptpmn	59+85	59+90	79.0	167.9	19.68	0.022	180	17	12	15	17	15	-12	64	76	71
ESF	26_TSw2_Tptpmn	59+90	59+95	81.0	167.9	19.68	0.022	179	17	12	10	19	15	-12	61	73	68
ESF	26_TSw2_Tptpmn	59+95	60+00	76.0	167.9	19.68	0.022	179	17	12	10	19	15	-12	61	73	68
ESF	26_TSw2_Tptpmn	60+00	60+05	83.0	167.9	19.68	0.022	179	17	12	10	19	15	-12	61	73	68
ESF	26_TSw2_Tptpmn	60+05	60+10	76.0	167.9	19.68	0.022	180	17	12	15	17	15	-12	64	76	71
ESF	26_TSw2_Tptpmn	60+10	60+15	59.0	167.9	19.68	0.022	182	13	12	15	14	15	-12	57	69	64
ESF	26_TSw2_Tptpmn	60+15	60+20	61.0	167.9	19.68	0.022	183	13	12	15	14	15	-12	57	69	64
ESF	26_TSw2_Tptpmn	60+20	60+25	58.0	167.9	19.68	0.022	184	13	12	15	16	15	-12	59	71	66
ESF	26_TSw2_Tptpmn	60+25	60+30	62.0	167.9	19.68	0.022	185	13	12	15	12	15	-12	55	67	62

Location	Thermal Mechanical and Lithostratigraphic Unit Designation	Begin Station (m)	End Station (m)	RQD	Mean Intact UCS, σ_{ci} (MPa)	Hoek & Brown Intact Material Constant, mi	Unit Weight of Rock Mass, γ (MN/m^3)	Depth of Tunnel, H (m)	RQD Index	C	Js	Jcd	JwR	AJO	RMR Rating = (RQD Index+C+Js+Jcd+JwR+AJ0)	RMR' = (RQD Index+C+Js+Jcd+JwR)	Geological Strength Index, GSI = (RMR' - 5)
ESF	26_TSw2_Tptpmn	60+30	60+35	34.0	167.9	19.68	0.022	186	8	12	8	14	15	-12	45	57	52
ESF	26_TSw2_Tptpmn	60+35	60+40	46.0	167.9	19.68	0.022	188	8	12	10	15	15	-12	48	60	55
ESF	26_TSw2_Tptpmn	60+40	60+45	47.0	167.9	19.68	0.022	189	8	12	8	16	15	-12	47	59	54
ESF	26_TSw2_Tptpmn	60+45	60+50	49.0	167.9	19.68	0.022	191	8	12	8	17	15	-12	48	60	55
ESF	26_TSw2_Tptpmn	60+50	60+55	73.0	167.9	19.68	0.022	192	13	12	15	14	15	-12	57	69	64
ESF	26_TSw2_Tptpmn	60+55	60+60	61.0	167.9	19.68	0.022	194	13	12	10	16	15	-5	61	66	61
ESF	26_TSw2_Tptpmn	60+60	60+65	62.0	167.9	19.68	0.022	196	13	12	10	19	15	-12	57	69	64
ESF	26_TSw2_Tptpmn	60+65	60+70	74.0	167.9	19.68	0.022	198	13	12	10	19	15	-12	57	69	64
ESF	26_TSw2_Tptpmn	60+70	60+75	65.0	167.9	19.68	0.022	200	13	12	8	17	15	-5	60	65	60
ESF	26_TSw2_Tptpmn	60+75	60+80	61.0	167.9	19.68	0.022	202	13	12	10	14	15	-12	52	64	59
ESF	26_TSw2_Tptpmn	60+80	60+85	71.0	167.9	19.68	0.022	204	13	12	10	18	15	-12	56	68	63
ESF	26_TSw2_Tptpmn	60+85	60+90	10.0	167.9	19.68	0.022	206	5	12	10	20	15	-12	50	62	57
ESF	26_TSw2_Tptpmn	60+90	60+95	51.0	167.9	19.68	0.022	207	13	12	15	17	15	-12	60	72	67
ESF	26_TSw2_Tptpmn	60+95	61+00	85.0	167.9	19.68	0.022	209	17	12	10	19	15	-12	61	73	68
ESF	26_TSw2_Tptpmn	61+00	61+05	68.0	167.9	19.68	0.022	210	13	12	8	16	15	-12	52	64	59
ESF	26_TSw2_Tptpmn	61+05	61+10	44.0	167.9	19.68	0.022	211	8	12	8	17	15	-12	48	60	55
ESF	26_TSw2_Tptpmn	61+10	61+15	58.0	167.9	19.68	0.022	212	13	12	10	22	15	-12	60	72	67
ESF	26_TSw2_Tptpmn	61+15	61+20	41.0	167.9	19.68	0.022	213	8	12	0	17	15	-5	47	52	47
ESF	26_TSw2_Tptpmn	61+20	61+25	51.0	167.9	19.68	0.022	214	13	12	8	20	15	-12	56	68	63
ESF	26_TSw2_Tptpmn	61+25	61+30	58.0	167.9	19.68	0.022	215	13	12	8	20	15	-12	56	68	63
ESF	26_TSw2_Tptpmn	61+30	61+35	35.0	167.9	19.68	0.022	216	8	12	10	14	15	-5	54	59	54
ESF	26_TSw2_Tptpmn	61+35	61+40	30.0	167.9	19.68	0.022	217	8	12	10	18	15	-12	51	63	58
ESF	26_TSw2_Tptpmn	61+40	61+45	43.0	167.9	19.68	0.022	218	8	12	10	20	15	-12	53	65	60
ESF	26_TSw2_Tptpmn	61+45	61+50	49.0	167.9	19.68	0.022	219	8	12	10	17	15	-12	50	62	57
ESF	26_TSw2_Tptpmn	61+50	61+55	31.0	167.9	19.68	0.022	219	8	12	8	12	15	-12	43	55	50
ESF	26_TSw2_Tptpmn	61+55	61+60	66.0	167.9	19.68	0.022	219	13	12	10	19	15	-12	57	69	64
ESF	26_TSw2_Tptpmn	61+60	61+65	50.0	167.9	19.68	0.022	219	8	12	10	18	15	-12	51	63	58
ESF	26_TSw2_Tptpmn	61+65	61+70	44.0	167.9	19.68	0.022	219	8	12	10	18	15	-12	51	63	58
ESF	26_TSw2_Tptpmn	61+70	61+75	59.0	167.9	19.68	0.022	219	13	12	10	16	15	-12	54	66	61
ESF	26_TSw2_Tptpmn	61+75	61+80	52.0	167.9	19.68	0.022	219	13	12	8	20	15	-12	56	68	63
ESF	26_TSw2_Tptpmn	61+80	61+85	54.0	167.9	19.68	0.022	219	13	12	10	21	15	-12	59	71	66
ESF	26_TSw2_Tptpmn	61+85	61+90	43.0	167.9	19.68	0.022	218	8	12	10	21	15	-12	54	66	61
ESF	26_TSw2_Tptpmn	61+90	61+95	31.0	167.9	19.68	0.022	217	8	12	10	9	15	-5	49	54	49
ESF	26_TSw2_Tptpmn	61+95	62+00	50.0	167.9	19.68	0.022	215	8	12	8	14	15	-12	45	57	52
ESF	26_TSw2_Tptpmn	62+00	62+05	64.0	167.9	19.68	0.022	214	13	12	10	19	15	-12	57	69	64
ESF	26_TSw2_Tptpmn	62+05	62+10	71.0	167.9	19.68	0.022	212	13	12	10	18	15	-12	56	68	63
ESF	26_TSw2_Tptpmn	62+10	62+15	48.0	167.9	19.68	0.022	210	8	12	10	20	15	-12	53	65	60
ESF	26_TSw2_Tptpmn	62+15	62+20	28.0	167.9	19.68	0.022	208	8	12	10	20	15	-12	53	65	60
ESF	26_TSw2_Tptpmn	62+20	62+25	20.0	167.9	19.68	0.022	207	5	12	10	20	15	-12	50	62	57

Location	Thermal Mechanical and Lithostratigraphic Unit Designation	Begin Station (m)	End Station (m)	RQD	Mean Intact UCS, σ_{ci} (MPa)	Hoek & Brown Intact Material Constant, mi	Unit Weight of Rock Mass, γ (MN/m^3)	Depth of Tunnel, H (m)	RQD Index	C	Js	Jcd	JwR	AJO	RMR Rating = (RQD Index+C+Js+Jcd+JwR+AJ0)	RMR' = (RQD Index+C+Js+Jcd+JwR)	Geological Strength Index, GSI = (RMR' - 5)
ESF	26_TSw2_Tptpmn	62+25	62+30	18.0	167.9	19.68	0.022	205	5	12	10	20	15	-12	50	62	57
ESF	26_TSw2_Tptpmn	62+30	62+35	48.0	167.9	19.68	0.022	204	8	12	8	14	15	-12	45	57	52
ESF	26_TSw2_Tptpmn	62+35	62+40	54.0	167.9	19.68	0.022	202	13	12	10	21	15	-12	59	71	66
ESF	26_TSw2_Tptpmn	62+40	62+45	22.0	167.9	19.68	0.022	201	5	12	10	16	15	-12	46	58	53
ESF	26_TSw2_Tptpmn	62+45	62+50	54.0	167.9	19.68	0.022	200	13	12	15	19	15	-12	62	74	69
ESF	26_TSw2_Tptpmn	62+50	62+55	85.0	167.9	19.68	0.022	199	17	12	15	18	15	-12	65	77	72
ESF	26_TSw2_Tptpmn	62+55	62+60	83.0	167.9	19.68	0.022	197	17	12	10	19	15	-10	63	73	68
ESF	26_TSw2_Tptpmn	62+60	62+65	99.0	167.9	19.68	0.022	196	20	12	15	15	15	-12	65	77	72
ESF	26_TSw2_Tptpmn	62+65	62+70	56.0	167.9	19.68	0.022	195	13	12	15	15	15	-12	58	70	65
ESF	26_TSw2_Tptpmn	62+70	62+75	43.0	167.9	19.68	0.022	193	8	12	10	13	15	-12	46	58	53
ESF	26_TSw2_Tptpmn	62+75	62+80	53.0	167.9	19.68	0.022	191	13	12	10	15	15	-12	53	65	60
ESF	26_TSw2_Tptpmn	62+80	62+85	54.0	167.9	19.68	0.022	190	13	12	0	18	15	-12	46	58	53
ESF	26_TSw2_Tptpmn	62+85	62+90	55.0	167.9	19.68	0.022	188	13	12	0	18	15	-12	46	58	53
ESF	26_TSw2_Tptpmn	62+90	62+95	65.0	167.9	19.68	0.022	186	13	12	10	15	15	-12	53	65	60
ESF	26_TSw2_Tptpmn	62+95	63+00	75.0	167.9	19.68	0.022	184	13	12	10	15	15	-12	53	65	60
ESF	26_TSw2_Tptpmn	63+00	63+05	65.0	167.9	19.68	0.022	182	13	12	10	16	15	-12	54	66	61
ESF	26_TSw2_Tptpmn	63+05	63+10	47.0	167.9	19.68	0.022	181	8	12	10	17	15	-12	50	62	57
ESF	25_TSw1_Tptpul	63+10	63+15	74.0	58.22	10.60	0.021	179	13	7	10	13	15	-12	46	58	53
ESF	25_TSw1_Tptpul	63+15	63+20	72.0	58.22	10.60	0.021	177	13	7	15	16	15	-12	54	66	61
ESF	25_TSw1_Tptpul	63+20	63+25	43.0	58.22	10.60	0.021	175	8	7	8	15	15	-12	41	53	48
ESF	26_TSw2_Tptpmn	63+25	63+30	28.0	167.9	19.68	0.021	173	8	12	8	13	15	-12	44	56	51
ESF	25_TSw1_Tptpul	63+30	63+35	48.0	58.22	10.60	0.021	172	8	7	10	18	15	-12	46	58	53
ESF	25_TSw1_Tptpul	63+35	63+40	79.0	58.22	10.60	0.021	171	17	7	15	21	15	-12	63	75	70
ESF	25_TSw1_Tptpul	63+40	63+45	70.0	58.22	10.60	0.021	169	13	7	15	19	15	-12	57	69	64
ESF	25_TSw1_Tptpul	63+45	63+50	47.0	58.22	10.60	0.021	168	8	7	15	16	15	-12	49	61	56
ESF	25_TSw1_Tptpul	63+50	63+55	35.0	58.22	10.60	0.021	166	8	7	15	17	15	-5	57	62	57
ESF	25_TSw1_Tptpul	63+55	63+60	69.0	58.22	10.60	0.021	165	13	7	15	16	15	-5	61	66	61
ESF	25_TSw1_Tptpul	63+60	63+65	82.0	58.22	10.60	0.021	164	17	7	10	16	15	-5	60	65	60
ESF	25_TSw1_Tptpul	63+65	63+70	79.0	58.22	10.60	0.021	162	17	7	15	12	15	-12	54	66	61
ESF	25_TSw1_Tptpul	63+70	63+75	40.0	58.22	10.60	0.021	161	8	7	10	14	15	-12	42	54	49
ESF	25_TSw1_Tptpul	63+75	63+80	79.0	58.22	10.60	0.021	160	17	7	10	9	15	-5	53	58	53
ESF	25_TSw1_Tptpul	63+80	63+85	78.0	58.22	10.60	0.021	159	17	7	15	14	15	-5	63	68	63
ESF	25_TSw1_Tptpul	63+85	63+90	73.0	58.22	10.60	0.021	158	13	7	10	15	15	-12	48	60	55
ESF	25_TSw1_Tptpul	63+90	63+95	61.0	58.22	10.60	0.021	157	13	7	15	16	15	-5	61	66	61
ESF	25_TSw1_Tptpul	63+95	64+00	66.0	58.22	10.60	0.021	155	13	7	10	21	15	-5	61	66	61
ESF	25_TSw1_Tptpul	64+00	64+05	22.0	58.22	10.60	0.021	154	5	7	10	14	15	-5	46	51	46
ESF	25_TSw1_Tptpul	64+05	64+10	44.0	58.22	10.60	0.021	153	8	7	0	23	15	-5	48	53	48
ESF	25_TSw1_Tptpul	64+10	64+15	21.0	58.22	10.60	0.021	152	5	7	0	18	15	-5	40	45	40
ESF	25_TSw1_Tptpul	64+15	64+20	45.0	58.22	10.60	0.021	151	8	7	10	22	15	-5	57	62	57

Location	Thermal Mechanical and Lithostratigraphic Unit Designation	Begin Station (m)	End Station (m)	RQD	Mean Intact UCS, σ_{ci} (MPa)	Hoek & Brown Intact Material Constant, mi	Unit Weight of Rock Mass, γ (MN/m^3)	Depth of Tunnel, H (m)	RQD Index	C	Js	Jcd	JwR	AJO	RMR Rating = (RQD Index+C+Js+Jcd+JwR+AJ0)	RMR' = (RQD Index+C+Js+Jcd+JwR)	Geological Strength Index, GSI = (RMR' - 5)
ESF	25_TSw1_Tptpul	64+20	64+25	35.0	58.22	10.60	0.021	150	8	7	0	23	15	-5	48	53	48
ESF	25_TSw1_Tptpul	64+25	64+30	36.0	58.22	10.60	0.021	149	8	7	0	18	15	-5	43	48	43
ESF	25_TSw1_Tptpul	64+30	64+35	45.0	58.22	10.60	0.021	148	8	7	8	21	15	-12	47	59	54
ESF	25_TSw1_Tptpul	64+35	64+40	34.0	58.22	10.60	0.021	147	8	7	0	22	15	-12	40	52	47
ESF	25_TSw1_Tptpul	64+40	64+45	26.0	58.22	10.60	0.021	146	8	7	8	16	15	-5	49	54	49
ESF	25_TSw1_Tptpul	64+45	64+50	34.0	58.22	10.60	0.021	145	8	7	0	18	15	-5	43	48	43
ESF	25_TSw1_Tptpul	64+50	64+55	27.0	58.22	10.60	0.021	144	8	7	0	20	15	-5	45	50	45
ESF	25_TSw1_Tptpul	64+55	64+60	48.0	58.22	10.60	0.021	143	8	7	0	20	15	-5	45	50	45
ESF	23_TSw1_Tptrl	64+60	64+65	30.0	58.22	10.60	0.021	142	8	4	0	20	15	-5	45	47	42
ESF	23_TSw1_Tptrl	64+65	64+70	23.0	58.22	10.60	0.021	142	5	4	8	18	15	-5	48	50	45
ESF	23_TSw1_Tptrl	64+70	64+75	19.0	58.22	10.60	0.021	141	5	4	10	20	15	-5	52	54	49
ESF	23_TSw1_Tptrl	64+75	64+80	61.0	58.22	10.60	0.021	141	13	4	10	19	15	-12	52	61	56
ESF	23_TSw1_Tptrl	64+80	64+85	44.0	58.22	10.60	0.021	140	8	4	10	18	15	-5	53	55	50
ESF	23_TSw1_Tptrl	64+85	64+90	73.0	58.22	10.60	0.021	139	13	4	10	18	15	-12	51	60	55
ESF	23_TSw1_Tptrl	64+90	64+95	59.0	58.22	10.60	0.021	138	13	4	10	20	15	-12	53	62	57
ESF	23_TSw1_Tptrl	64+95	65+00	50.0	58.22	10.60	0.021	137	8	4	10	22	15	-5	57	59	54
ESF	23_TSw1_Tptrl	65+00	65+05	51.0	58.22	10.60	0.021	136	13	4	8	17	15	-5	55	57	52
ESF	23_TSw1_Tptrl	65+05	65+10	92.0	58.22	10.60	0.021	134	20	4	8	19	15	-12	57	66	61
ESF	22_TSw1_Tptrn	65+10	65+15	75.0	58.22	10.60	0.021	133	13	7	15	22	15	-5	67	72	67
ESF	22_TSw1_Tptrn	65+15	65+20	93.0	58.22	10.60	0.021	132	20	7	15	16	15	-5	68	73	68
ESF	22_TSw1_Tptrn	65+20	65+25	89.0	58.22	10.60	0.021	132	17	7	15	14	15	-5	63	68	63
ESF	23_TSw1_Tptrl	65+25	65+30	60.0	58.22	10.60	0.021	131	13	4	15	14	15	-12	52	61	56
ESF	22_TSw1_Tptrn	65+30	65+35	56.0	58.22	10.60	0.021	131	13	7	0	18	15	-5	48	53	48
ESF	22_TSw1_Tptrn	65+35	65+40	89.0	58.22	10.60	0.021	130	17	7	15	18	15	-5	67	72	67
ESF	22_TSw1_Tptrn	65+40	65+45	91.0	58.22	10.60	0.021	130	20	7	8	17	15	-12	55	67	62
ESF	22_TSw1_Tptrn	65+45	65+50	76.0	58.22	10.60	0.021	130	17	7	15	17	15	-12	59	71	66
ESF	22_TSw1_Tptrn	65+50	65+55	82.0	58.22	10.60	0.021	129	17	7	15	21	15	-12	63	75	70
ESF	22_TSw1_Tptrn	65+55	65+60	81.0	58.22	10.60	0.021	129	17	7	15	18	15	-5	67	72	67
ESF	22_TSw1_Tptrn	65+60	65+65	79.0	58.22	10.60	0.021	129	17	7	15	21	15	-5	70	75	70
ESF	22_TSw1_Tptrn	65+65	65+70	99.0	58.22	10.60	0.021	129	20	7	15	19	15	-5	71	76	71
ESF	22_TSw1_Tptrn	65+70	65+75	93.0	58.22	10.60	0.021	128	20	7	15	18	15	-5	70	75	70
ESF	22_TSw1_Tptrn	65+75	65+80	95.0	58.22	10.60	0.021	128	20	7	15	20	15	-12	65	77	72
ESF	22_TSw1_Tptrn	65+80	65+85	83.0	58.22	10.60	0.021	127	17	7	10	15	15	-5	59	64	59
ESF	22_TSw1_Tptrn	65+85	65+90	93.0	58.22	10.60	0.021	126	20	7	15	20	15	-12	65	77	72
ESF	22_TSw1_Tptrn	65+90	65+95	100.0	58.22	10.60	0.021	125	20	7	15	22	15	-12	67	79	74
ESF	22_TSw1_Tptrn	65+95	66+00	88.0	58.22	10.60	0.021	124	17	7	10	23	15	-5	67	72	67
ESF	22_TSw1_Tptrn	66+00	66+05	99.0	58.22	10.60	0.021	124	20	7	20	17	15	-12	67	79	74
ESF	22_TSw1_Tptrn	66+05	66+10	93.0	58.22	10.60	0.021	123	20	7	10	20	15	-5	67	72	67
ESF	22_TSw1_Tptrn	66+10	66+15	81.0	58.22	10.60	0.021	123	17	7	15	16	15	-5	65	70	65

Location	Thermal Mechanical and Lithostratigraphic Unit Designation	Begin Station (m)	End Station (m)	RQD	Mean Intact UCS, σ_{ci} (MPa)	Hoek & Brown Intact Material Constant, mi	Unit Weight of Rock Mass, γ (MN/m^3)	Depth of Tunnel, H (m)	RQD Index	C	Js	Jcd	JwR	AJO	RMR Rating = (RQD Index+C+Js+Jcd+JwR+AJ0)	RMR' = (RQD Index+C+Js+Jcd+JwR)	Geological Strength Index, GSI = (RMR' - 5)
ESF	22_TSw1_Tptrn	66+15	66+20	98.0	58.22	10.60	0.021	123	20	7	15	22	15	-12	67	79	74
ESF	22_TSw1_Tptrn	66+20	66+25	86.0	58.22	10.60	0.021	123	17	7	8	16	15	-5	58	63	58
ESF	22_TSw1_Tptrn	66+25	66+30	99.0	58.22	10.60	0.021	123	20	7	10	19	15	-2	69	71	66
ESF	22_TSw1_Tptrn	66+30	66+35	95.0	58.22	10.60	0.021	123	20	7	10	18	15	-5	65	70	65
ESF	21_TSw1_Tptrv1	66+35	66+40	95.0	58.22	10.60	0.021	122	20	7	10	22	15	-2	72	74	69
ESF	20_PTn_Tptrv2	66+40	66+45	96.0	6.37	17.64	0.013	122	20	4	15	26	15	-12	68	80	75
ESF	19_PTn_Tptrv3	66+45	66+50	NA	6.37	17.64	0.013		20	4	NA	NA	NA	NA	NA	NA	NA
ESF		66+50	66+97	NA	6.37	17.64	0.013		20	4	NA	NA	NA	NA	NA	NA	NA
ESF	13_PTn_Tpcpv1	66+97	67+10	NA	6.37	17.64	0.013		20	4	NA	NA	NA	NA	NA	NA	NA
ESF	13_PTn_Tpcpv1	67+10	67+15	NA	6.37	17.64	0.013		20	4	NA	NA	NA	NA	NA	NA	NA
ESF	13_PTn_Tpcpv1	67+15	67+20	NA	6.37	17.64	0.013		20	4	NA	NA	NA	NA	NA	NA	NA
ESF	13_PTn_Tpcpv1	67+20	67+25	100.0	6.37	17.64	0.013	106	20	4	15	20	15	-12	62	74	69
ESF	12_PTn_Tpcpv2	67+25	67+30	92.0	6.37	17.64	0.021	105	20	4	10	22	15	-12	59	71	66
ESF	10_TCw_Tpcpln	67+30	67+35	88.0	127.54	18.50	0.021	104	17	12	15	24	15	-12	71	83	78
ESF	10_TCw_Tpcpln	67+35	67+40	86.0	127.54	18.50	0.021	103	17	12	10	22	15	-12	64	76	71
ESF	10_TCw_Tpcpln	67+40	67+45	88.0	127.54	18.50	0.021	102	17	12	10	22	15	-12	64	76	71
ESF	10_TCw_Tpcpln	67+45	67+50	96.0	127.54	18.50	0.021	101	20	12	15	22	15	-12	72	84	79
ESF	10_TCw_Tpcpln	67+50	67+55	95.0	127.54	18.50	0.021	99.9	20	12	20	20	15	-12	75	87	82
ESF	10_TCw_Tpcpln	67+55	67+60	76.0	127.54	18.50	0.021	98.9	17	12	20	20	15	-12	72	84	79
ESF	12_PTn_Tpcpv2	67+60	67+65	92.0	6.37	17.64	0.013	98.1	20	4	15	15	15	-12	57	69	64
ESF	10_TCw_Tpcpln	67+65	67+70	97.0	127.54	18.50	0.013	98.1	20	12	15	19	15	-12	69	81	76
ESF	10_TCw_Tpcpln	67+70	67+75	85.0	127.54	18.50	0.021	98	17	12	15	14	15	-12	61	73	68
ESF	10_TCw_Tpcpln	67+75	67+80	69.0	127.54	18.50	0.021	97.9	13	12	10	11	15	-5	56	61	56
ESF	10_TCw_Tpcpln	67+80	67+85	81.0	127.54	18.50	0.021	97.9	17	12	15	19	15	-5	73	78	73
ESF	22_TSw1_Tptrn	67+85	67+90	42.0	58.22	10.60	0.021	97.6	8	7	0	9	15	-5	34	39	34
ESF	25_TSw1_Tptpul	67+90	67+95	47.0	58.22	10.60	0.021	97.2	8	7	0	18	15	-5	43	48	43
ESF	25_TSw1_Tptpul	67+95	68+00	29.0	58.22	10.60	0.021	96.9	8	7	0	18	15	-5	43	48	43
ESF	25_TSw1_Tptpul	68+00	68+05	23.0	58.22	10.60	0.021	96.5	5	7	0	19	15	-5	41	46	41
ESF	25_TSw1_Tptpul	68+05	68+10	24.0	58.22	10.60	0.021	96.2	5	7	0	19	15	-5	41	46	41
ESF	25_TSw1_Tptpul	68+10	68+15	50.0	58.22	10.60	0.021	95.8	8	7	10	18	15	-12	46	58	53
ESF	25_TSw1_Tptpul	68+15	68+20	45.0	58.22	10.60	0.021	95.5	8	7	10	18	15	-12	46	58	53
ESF	25_TSw1_Tptpul	68+20	68+25	38.0	58.22	10.60	0.021	95.1	8	7	0	16	15	-5	41	46	41
ESF	25_TSw1_Tptpul	68+25	68+30	34.0	58.22	10.60	0.021	96.9	8	7	0	16	15	-5	41	46	41
ESF	25_TSw1_Tptpul	68+30	68+35	38.0	58.22	10.60	0.021	98.7	8	7	10	18	15	-5	53	58	53
ESF	25_TSw1_Tptpul	68+35	68+40	35.0	58.22	10.60	0.021	101	8	7	10	19	15	-5	54	59	54
ESF	25_TSw1_Tptpul	68+40	68+45	33.0	58.22	10.60	0.021	102	8	7	8	16	15	-5	49	54	49
ESF	25_TSw1_Tptpul	68+45	68+50	77.0	58.22	10.60	0.021	104	17	7	0	17	15	-5	51	56	51
ESF	23_TSw1_Tptrl	68+50	68+55	42.0	58.22	10.60	0.021	105	8	4	10	18	15	-5	53	55	50

Location	Thermal Mechanical and Lithostratigraphic Unit Designation	Begin Station (m)	End Station (m)	RQD	Mean Intact UCS, σ_{ci} (MPa)	Hoek & Brown Intact Material Constant, mi	Unit Weight of Rock Mass, γ (MN/m^3)	Depth of Tunnel, H (m)	RQD Index	C	Js	Jcd	JwR	AJO	RMR Rating = (RQD Index+C+Js+Jcd+JwR+AJ0)	RMR' = (RQD Index+C+Js+Jcd+JwR)	Geological Strength Index, GSI = (RMR' - 5)
ESF	23_TSw1_Tptrl	68+55	68+60	74.0	58.22	10.60	0.021	107	13	4	10	21	15	-12	54	63	58
ESF	23_TSw1_Tptrl	68+60	68+65	40.0	58.22	10.60	0.021	108	8	4	0	23	15	0	53	50	45
ESF	23_TSw1_Tptrl	68+65	68+70	67.0	58.22	10.60	0.021	110	13	4	0	16	15	-5	46	48	43
ESF	23_TSw1_Tptrl	68+70	68+75	96.0	58.22	10.60	0.021	111	20	4	15	12	15	-5	64	66	61
ESF	23_TSw1_Tptrl	68+75	68+80	55.0	58.22	10.60	0.021	113	13	4	10	19	15	-5	59	61	56
ESF	23_TSw1_Tptrl	68+80	68+85	77.0	58.22	10.60	0.021	114	17	4	10	22	15	-5	66	68	63
ESF	23_TSw1_Tptrl	68+85	68+90	87.0	58.22	10.60	0.021	115	17	4	20	16	15	-5	70	72	67
ESF	22_TSw1_Tptrn	68+90	68+95	87.0	58.22	10.60	0.021	117	17	7	15	17	15	-5	66	71	66
ESF	22_TSw1_Tptrn	68+95	69+00	80.0	58.22	10.60	0.021	118	17	7	15	17	15	-5	66	71	66
ESF	22_TSw1_Tptrn	69+00	69+05	92.0	58.22	10.60	0.021	120	20	7	0	22	15	-5	59	64	59
ESF	22_TSw1_Tptrn	69+05	69+10	87.0	58.22	10.60	0.021	121	17	7	0	22	15	-5	56	61	56
ESF	22_TSw1_Tptrn	69+10	69+15	77.0	58.22	10.60	0.021	123	17	7	15	14	15	-12	56	68	63
ESF	22_TSw1_Tptrn	69+15	69+20	58.0	58.22	10.60	0.021	125	13	7	0	16	15	-5	46	51	46
ESF	22_TSw1_Tptrn	69+20	69+25	84.0	58.22	10.60	0.021	127	17	7	15	19	15	-12	61	73	68
ESF	22_TSw1_Tptrn	69+25	69+30	93.0	58.22	10.60	0.021	129	20	7	15	19	15	-12	64	76	71
ESF	22_TSw1_Tptrn	69+30	69+35	64.0	58.22	10.60	0.021	131	13	7	15	18	15	-12	56	68	63
ESF	22_TSw1_Tptrn	69+35	69+40	93.0	58.22	10.60	0.021	133	20	7	8	23	15	-10	63	73	68
ESF	22_TSw1_Tptrn	69+40	69+45	76.0	58.22	10.60	0.021	134	17	7	15	20	15	-12	62	74	69
ESF	22_TSw1_Tptrn	69+45	69+50	73.0	58.22	10.60	0.021	134	13	7	15	12	15	-12	50	62	57
ESF	22_TSw1_Tptrn	69+50	69+55	97.0	58.22	10.60	0.021	133	20	7	15	17	15	-12	62	74	69
ESF	22_TSw1_Tptrn	69+55	69+60	98.0	58.22	10.60	0.021	132	20	7	15	16	15	-12	61	73	68
ESF	22_TSw1_Tptrn	69+60	69+65	98.0	58.22	10.60	0.021	130	20	7	15	18	15	-12	63	75	70
ESF	22_TSw1_Tptrn	69+65	69+70	78.0	58.22	10.60	0.021	129	17	7	8	17	15	-5	59	64	59
ESF	22_TSw1_Tptrn	69+70	69+75	76.0	58.22	10.60	0.021	128	17	7	10	22	15	-12	59	71	66
ESF	22_TSw1_Tptrn	69+75	69+80	66.0	58.22	10.60	0.021	127	13	7	15	10	15	-12	48	60	55
ESF	22_TSw1_Tptrn	69+80	69+85	51.0	58.22	10.60	0.021	126	13	7	10	19	15	-10	54	64	59
ESF	22_TSw1_Tptrn	69+85	69+90	77.0	58.22	10.60	0.021	125	17	7	10	21	15	-12	58	70	65
ESF	22_TSw1_Tptrn	69+90	69+95	82.0	58.22	10.60	0.021	124	17	7	10	21	15	-5	65	70	65
ESF	21_TSw1_Tptrv1	69+95	70+00	59.0	58.22	10.60	0.021	123	13	7	8	20	15	-2	61	63	58
ESF	20_PTn_Tptrv2	70+00	70+05	96.0	6.37	17.64	0.013	122	20	4	15	19	15	-12	61	73	68
ESF	20_PTn_Tptrv2	70+05	70+10	98.0	6.37	17.64	0.013		20	4	NA	NA	NA	NA	NA	NA	NA
ESF	20_PTn_Tptrv2	70+10	70+15	100.0	6.37	17.64	0.013		20	4	NA	NA	NA	NA	NA	NA	NA
ESF	20_PTn_Tptrv2	70+15	70+20	100.0	6.37	17.64	0.013		20	4	NA	NA	NA	NA	NA	NA	NA
ESF	20_PTn_Tptrv2	70+20	70+25	99.0	6.37	17.64	0.013		20	4	NA	NA	NA	NA	NA	NA	NA
ESF	18_PTn_Tpbt2	70+25	70+30	NA	6.37	150.97	0.013		NA	4	NA	NA	NA	NA	NA	NA	NA
ESF	18_PTn_Tpbt2	70+30	70+35	NA	6.37	150.97	0.013		NA	4	NA	NA	NA	NA	NA	NA	NA
ESF	18_PTn_Tpbt2	70+35	70+40	NA	6.37	150.97	0.013		NA	4	NA	NA	NA	NA	NA	NA	NA
ESF	18_PTn_Tpbt2	70+40	70+45	NA	6.37	150.97	0.013		NA	4	NA	NA	NA	NA	NA	NA	NA
ESF	18_PTn_Tpbt2	70+45	70+50	NA	6.37	150.97	0.013		NA	4	NA	NA	NA	NA	NA	NA	NA

Location	Thermal Mechanical and Lithostratigraphic Unit Designation	Begin Station (m)	End Station (m)	RQD	Mean Intact UCS, σ_{ci} (MPa)	Hoek & Brown Intact Material Constant, mi	Unit Weight of Rock Mass, γ (MN/m^3)	Depth of Tunnel, H (m)	RQD Index	C	Js	Jcd	JwR	AJO	RMR Rating = (RQD Index+C+Js+Jcd+JwR+AJ0)	RMR' = (RQD Index+C+Js+Jcd+JwR)	Geological Strength Index, GSI = (RMR' - 5)
ESF	18_PTn_Tpbt2	70+50	70+55	NA	6.37	150.97	0.013		NA	4	NA	NA	NA	NA	NA	NA	NA
ESF	26_TSw2_Tptpmn	70+55	70+60	56.0	167.9	19.68	0.022	98.7	13	12	0	16	15	0	56	56	51
ESF	26_TSw2_Tptpmn	70+60	70+65	51.0	167.9	19.68	0.022	96.5	13	12	0	16	15	-12	44	56	51
ESF	26_TSw2_Tptpmn	70+65	70+70	66.0	167.9	19.68	0.022	94.8	13	12	15	16	15	-12	59	71	66
ESF	26_TSw2_Tptpmn	70+70	70+75	65.0	167.9	19.68	0.022	95.5	13	12	0	16	15	-12	44	56	51
ESF	26_TSw2_Tptpmn	70+75	70+80	57.0	167.9	19.68	0.022	96.1	13	12	10	15	15	-12	53	65	60
ESF	26_TSw2_Tptpmn	70+80	70+85	60.0	167.9	19.68	0.022	96.8	13	12	8	13	15	-5	56	61	56
ESF	26_TSw2_Tptpmn	70+85	70+90	70.0	167.9	19.68	0.022	96.2	13	12	10	16	15	-12	54	66	61
ESF	26_TSw2_Tptpmn	70+90	70+95	69.0	167.9	19.68	0.022	95.6	13	12	10	16	15	-12	54	66	61
ESF	26_TSw2_Tptpmn	70+95	71+00	62.0	167.9	19.68	0.022	94.9	13	12	10	21	15	-12	59	71	66
ESF	26_TSw2_Tptpmn	71+00	71+05	64.0	167.9	19.68	0.022	94.3	13	12	10	22	15	-12	60	72	67
ESF	26_TSw2_Tptpmn	71+05	71+10	67.0	167.9	19.68	0.022	93.6	13	12	10	23	15	-5	68	73	68
ESF	26_TSw2_Tptpmn	71+10	71+15	NA	167.9	19.68	0.022		20	12	NA	NA	NA	NA	NA	NA	NA
ESF	26_TSw2_Tptpmn	71+15	71+35	NA	167.9	19.68	0.022		20	12	NA	NA	NA	NA	NA	NA	NA
ESF	26_TSw2_Tptpmn	71+35	71+40	NA	167.9	19.68	0.022		20	12	NA	NA	NA	NA	NA	NA	NA
ESF	26_TSw2_Tptpmn	71+40	71+45	26.0	167.9	19.68	0.022		8	12	NA	NA	NA	NA	NA	NA	NA
ESF	26_TSw2_Tptpmn	71+45	71+50	38.0	167.9	19.68	0.022	88	8	12	10	14	15	-12	47	59	54
ESF	26_TSw2_Tptpmn	71+50	71+55	59.0	167.9	19.68	0.022	87.8	13	12	10	19	15	-12	57	69	64
ESF	26_TSw2_Tptpmn	71+55	71+60	48.0	167.9	19.68	0.022	87.6	8	12	8	19	15	-12	50	62	57
ESF	26_TSw2_Tptpmn	71+60	71+65	63.0	167.9	19.68	0.022	87.4	13	12	15	18	15	-12	61	73	68
ESF	26_TSw2_Tptpmn	71+65	71+70	60.0	167.9	19.68	0.022	87.1	13	12	10	21	15	-12	59	71	66
ESF	25_TSw1_Tptpul	71+70	71+75	48.0	58.22	10.60	0.021	86.9	8	7	10	19	15	-12	47	59	54
ESF	25_TSw1_Tptpul	71+75	71+80	25.0	58.22	10.60	0.021	86.7	5	7	10	19	15	-12	44	56	51
ESF	25_TSw1_Tptpul	71+80	71+85	24.0	58.22	10.60	0.021	86.5	5	7	15	23	15	-12	53	65	60
ESF	25_TSw1_Tptpul	71+85	71+90	30.0	58.22	10.60	0.021	86.3	8	7	15	23	15	-12	56	68	63
ESF	25_TSw1_Tptpul	71+90	71+95	11.0	58.22	10.60	0.021	86.5	5	7	0	23	15	-5	45	50	45
ESF	25_TSw1_Tptpul	71+95	72+00	10.0	58.22	10.60	0.021	86.7	5	7	10	22	15	-12	47	59	54
ESF	25_TSw1_Tptpul	72+00	72+05	55.0	58.22	10.60	0.021	86.9	13	7	15	16	15	-5	61	66	61
ESF	25_TSw1_Tptpul	72+05	72+10	15.0	58.22	10.60	0.021	87.6	5	7	10	18	15	-5	50	55	50
ESF	25_TSw1_Tptpul	72+10	72+15	70.0	58.22	10.60	0.021	88.2	13	7	10	19	15	-5	59	64	59
ESF	25_TSw1_Tptpul	72+15	72+20	60.0	58.22	10.60	0.021	88.8	13	7	8	22	15	-5	60	65	60
ESF	25_TSw1_Tptpul	72+20	72+25	31.0	58.22	10.60	0.021	89.5	8	7	10	13	15	-5	48	53	48
ESF	25_TSw1_Tptpul	72+25	72+30	34.0	58.22	10.60	0.021	90.1	8	7	8	16	15	-5	49	54	49
ESF	25_TSw1_Tptpul	72+30	72+35	32.0	58.22	10.60	0.021	90.8	8	7	15	15	15	-5	55	60	55
ESF	25_TSw1_Tptpul	72+35	72+40	29.0	58.22	10.60	0.021	91.4	8	7	8	17	15	-5	50	55	50
ESF	25_TSw1_Tptpul	72+40	72+45	15.0	58.22	10.60	0.021	92	5	7	0	19	15	-5	41	46	41
ESF	25_TSw1_Tptpul	72+45	72+50	35.0	58.22	10.60	0.021	92.7	8	7	0	17	15	-5	42	47	42
ESF	25_TSw1_Tptpul	72+50	72+55	29.0	58.22	10.60	0.021	94.2	8	7	0	20	15	-12	38	50	45
ESF	25_TSw1_Tptpul	72+55	72+60	61.0	58.22	10.60	0.021	96.3	13	7	0	20	15	-12	43	55	50

Location	Thermal Mechanical and Lithostratigraphic Unit Designation	Begin Station (m)	End Station (m)	RQD	Mean Intact UCS, σ_{ci} (MPa)	Hoek & Brown Intact Material Constant, mi	Unit Weight of Rock Mass, γ (MN/m^3)	Depth of Tunnel, H (m)	RQD Index	C	Js	Jcd	JwR	AJO	RMR Rating = (RQD Index+C+Js+Jcd+JwR+AJ0)	RMR' = (RQD Index+C+Js+Jcd+JwR)	Geological Strength Index, GSI = (RMR' - 5)
ESF	25_TSw1_Tptpul	72+60	72+65	52.0	58.22	10.60	0.021	98.3	13	7	8	16	15	-5	54	59	54
ESF	25_TSw1_Tptpul	72+65	72+70	26.0	58.22	10.60	0.021	101	8	7	0	15	15	-5	40	45	40
ESF	25_TSw1_Tptpul	72+70	72+75	42.0	58.22	10.60	0.021	103	8	7	0	16	15	-5	41	46	41
ESF	25_TSw1_Tptpul	72+75	72+80	18.0	58.22	10.60	0.021	105	5	7	0	16	15	-5	38	43	38
ESF	25_TSw1_Tptpul	72+80	72+85	25.0	58.22	10.60	0.021	107	5	7	0	20	15	-5	42	47	42
ESF	25_TSw1_Tptpul	72+85	72+90	50.0	58.22	10.60	0.021	110	8	7	0	18	15	-5	43	48	43
ESF	25_TSw1_Tptpul	72+90	72+95	36.0	58.22	10.60	0.021	112	8	7	0	19	15	-5	44	49	44
ESF	25_TSw1_Tptpul	72+95	73+00	42.0	58.22	10.60	0.021	114	8	7	0	23	15	-5	48	53	48
ESF	25_TSw1_Tptpul	73+00	73+05	49.0	58.22	10.60	0.021	116	8	7	0	24	15	-5	49	54	49
ESF	23_TSw1_Tptrl	73+05	73+10	38.0	58.22	10.60	0.021	119	8	4	15	20	15	-12	53	62	57
ESF	23_TSw1_Tptrl	73+10	73+15	51.0	58.22	10.60	0.021	120	13	4	10	17	15	-5	57	59	54
ESF	23_TSw1_Tptrl	73+15	73+20	58.0	58.22	10.60	0.021	121	13	4	8	19	15	-12	50	59	54
ESF	23_TSw1_Tptrl	73+20	73+25	59.0	58.22	10.60	0.021	121	13	4	10	25	15	-5	65	67	62
ESF	23_TSw1_Tptrl	73+25	73+30	64.0	58.22	10.60	0.021	122	13	4	10	16	15	-5	56	58	53
ESF	23_TSw1_Tptrl	73+30	73+35	47.0	58.22	10.60	0.021	123	8	4	8	25	15	-12	51	60	55
ESF	23_TSw1_Tptrl	73+35	73+40	68.0	58.22	10.60	0.021	124	13	4	10	16	15	-12	49	58	53
ESF	23_TSw1_Tptrl	73+40	73+45	90.0	58.22	10.60	0.021	125	17	4	15	13	15	-12	55	64	59
ESF	22_TSw1_Tptrn	73+45	73+50	91.0	58.22	10.60	0.021	126	20	7	15	13	15	-12	58	70	65
ESF	22_TSw1_Tptrn	73+50	73+55	94.0	58.22	10.60	0.021	127	20	7	15	13	15	-12	58	70	65
ESF	22_TSw1_Tptrn	73+55	73+60	93.0	58.22	10.60	0.021	128	20	7	15	15	15	-12	60	72	67
ESF	22_TSw1_Tptrn	73+60	73+65	92.0	58.22	10.60	0.021	129	20	7	0	23	15	-5	60	65	60
ESF	22_TSw1_Tptrn	73+65	73+70	83.0	58.22	10.60	0.021	130	17	7	10	13	15	-12	50	62	57
ESF	22_TSw1_Tptrn	73+70	73+75	98.0	58.22	10.60	0.021	130	20	7	15	17	15	-12	62	74	69
ESF	22_TSw1_Tptrn	73+75	73+80	94.0	58.22	10.60	0.021	127	20	7	10	22	15	-12	62	74	69
ESF	22_TSw1_Tptrn	73+80	73+85	58.0	58.22	10.60	0.021	125	13	7	8	15	15	-12	46	58	53
ESF	22_TSw1_Tptrn	73+85	73+90	94.0	58.22	10.60	0.021	123	20	7	15	19	15	-12	64	76	71
ESF	22_TSw1_Tptrn	73+90	73+95	82.0	58.22	10.60	0.021	122	17	7	8	11	15	-5	53	58	53
ESF	22_TSw1_Tptrn	73+95	74+00	100.0	58.22	10.60	0.021	121	20	7	10	12	15	-5	59	64	59
ESF	22_TSw1_Tptrn	74+00	74+05	96.0	58.22	10.60	0.021	120	20	7	10	23	15	-5	70	75	70
ESF	22_TSw1_Tptrn	74+05	74+10	92.0	58.22	10.60	0.021	118	20	7	10	24	15	-12	64	76	71
ESF	22_TSw1_Tptrn	74+10	74+15	91.0	58.22	10.60	0.021	117	20	7	15	23	15	-12	68	80	75
ESF	22_TSw1_Tptrn	74+15	74+20	72.0	58.22	10.60	0.021	116	13	7	15	16	15	-12	54	66	61
ESF	22_TSw1_Tptrn	74+20	74+25	69.0	58.22	10.60	0.021	114	13	7	10	16	15	-5	56	61	56
ESF	22_TSw1_Tptrn	74+25	74+30	82.0	58.22	10.60	0.021	113	17	7	10	21	15	-10	60	70	65
ESF	22_TSw1_Tptrn	74+30	74+35	78.0	58.22	10.60	0.021	112	17	7	10	14	15	-5	58	63	58
ESF	22_TSw1_Tptrn	74+35	74+40	76.0	58.22	10.60	0.021	110	17	7	10	10	15	-5	54	59	54
ESF		74+40	74+50	NA	58.22	10.60	0.021		NA	7	NA	NA	NA	NA	NA	NA	NA
ESF	18_PTn_Tpbt2	74+50	74+75	NA	6.37	150.97	0.013		NA	4	NA	NA	NA	NA	NA	NA	NA
ESF		74+75	74+95	NA	6.37	17.64	0.013		NA	4	NA	NA	NA	NA	NA	NA	NA

Location	Thermal Mechanical and Lithostratigraphic Unit Designation	Begin Station (m)	End Station (m)	RQD	Mean Intact UCS, σ_{ci} (MPa)	Hoek & Brown Intact Material Constant, mi	Unit Weight of Rock Mass, γ (MN/m^3)	Depth of Tunnel, H (m)	RQD Index	C	Js	Jcd	JwR	AJO	RMR Rating = (RQD Index+C+Js+Jcd+JwR+AJ0)	RMR' = (RQD Index+C+Js+Jcd+JwR)	Geological Strength Index, GSI = (RMR' - 5)
ESF	14_PTn_Tpbt4	74+95	75+00	NA	6.37	17.64	0.013		NA	4	NA	NA	NA	NA	NA	NA	NA
ESF	14_PTn_Tpbt4	75+00	75+05	99.0	6.37	17.64	0.013		20	4	NA	NA	NA	NA	NA	NA	NA
ESF	13_PTn_Tpcpv1	75+05	75+10	90.0	6.37	17.64	0.013		17	4	NA	NA	NA	NA	NA	NA	NA
ESF	12_PTn_Tpcpv2	75+10	75+15	77.0	6.37	17.64	0.013	83.6	17	4	10	15	15	-5	56	61	56
ESF	10_TCw_Tpcpln	75+15	75+20	67.0	127.54	18.50	0.021	81.8	13	12	10	16	15	-12	54	66	61
ESF	10_TCw_Tpcpln	75+20	75+25	52.0	127.54	18.50	0.021	79.9	13	12	8	15	15	-5	58	63	58
ESF	10_TCw_Tpcpln	75+25	75+30	62.0	127.54	18.50	0.021	78.1	13	12	8	17	15	-5	60	65	60
ESF	10_TCw_Tpcpln	75+30	75+35	66.0	127.54	18.50	0.021	76.2	13	12	10	13	15	-12	51	63	58
ESF	10_TCw_Tpcpln	75+35	75+40	92.0	127.54	18.50	0.021	74.4	20	12	8	22	15	-12	65	77	72
ESF	10_TCw_Tpcpln	75+40	75+45	79.0	127.54	18.50	0.021	72.6	17	12	10	22	15	-12	64	76	71
ESF	10_TCw_Tpcpln	75+45	75+50	68.0	127.54	18.50	0.021	70.7	13	12	10	22	15	-12	60	72	67
ESF	10_TCw_Tpcpln	75+50	75+55	64.0	127.54	18.50	0.021	68.9	13	12	10	12	15	-5	57	62	57
ESF	10_TCw_Tpcpln	75+55	75+60	85.0	127.54	18.50	0.021	67.5	17	12	15	15	15	-12	62	74	69
ESF	10_TCw_Tpcpln	75+60	75+65	86.0	127.54	18.50	0.021	66.3	17	12	10	15	15	-5	64	69	64
ESF	10_TCw_Tpcpln	75+65	75+70	85.0	127.54	18.50	0.021	64.8	17	12	10	18	15	-5	67	72	67
ESF	10_TCw_Tpcpln	75+70	75+75	81.0	127.54	18.50	0.021	63.3	17	12	10	14	15	-5	63	68	63
ESF	10_TCw_Tpcpln	75+75	75+80	91.0	127.54	18.50	0.021	61.8	20	12	15	8	15	-5	65	70	65
ESF	10_TCw_Tpcpln	75+80	75+85	89.0	127.54	18.50	0.021	60.4	17	12	15	22	15	-12	69	81	76
ESF	10_TCw_Tpcpln	75+85	75+90	87.0	127.54	18.50	0.021	58.9	17	12	15	15	15	-12	62	74	69
ESF	10_TCw_Tpcpln	75+90	75+95	85.0	127.54	18.50	0.021	57.4	17	12	15	16	15	-12	63	75	70
ESF	10_TCw_Tpcpln	75+95	76+00	95.0	127.54	18.50	0.021	55.9	20	12	15	16	15	-12	66	78	73
ESF	10_TCw_Tpcpln	76+00	76+05	87.0	127.54	18.50	0.021	54.4	17	12	15	13	15	-5	67	72	67
ESF	08_TCw_Tpcpmn	76+05	76+10	95.0	127.54	18.50	0.021	52.9	20	12	10	12	15	-12	57	69	64
ESF	08_TCw_Tpcpmn	76+10	76+15	84.0	127.54	18.50	0.021	51.4	17	12	8	23	15	-5	70	75	70
ESF	08_TCw_Tpcpmn	76+15	76+20	85.0	127.54	18.50	0.021	50.1	17	12	15	16	15	-12	63	75	70
ESF	08_TCw_Tpcpmn	76+20	76+25	93.0	127.54	18.50	0.021	49	20	12	8	23	15	-5	73	78	73
ESF	08_TCw_Tpcpmn	76+25	76+30	79.0	127.54	18.50	0.021	48	17	12	8	23	15	-2	73	75	70
ESF	08_TCw_Tpcpmn	76+30	76+35	71.0	127.54	18.50	0.021	47.1	13	12	15	15	15	-12	58	70	65
ESF	08_TCw_Tpcpmn	76+35	76+40	88.0	127.54	18.50	0.021	46.2	17	12	20	19	15	-12	71	83	78
ESF	08_TCw_Tpcpmn	76+40	76+45	60.0	127.54	18.50	0.021	45.2	13	12	10	20	15	-12	58	70	65
ESF	08_TCw_Tpcpmn	76+45	76+50	87.0	127.54	18.50	0.021	44.3	17	12	10	10	15	-5	59	64	59
ESF	08_TCw_Tpcpmn	76+50	76+55	64.0	127.54	18.50	0.021	43.4	13	12	10	18	15	-5	63	68	63
ESF	08_TCw_Tpcpmn	76+55	76+60	80.0	127.54	18.50	0.021	42.5	17	12	15	15	15	-5	69	74	69
ESF	08_TCw_Tpcpmn	76+60	76+65	57.0	127.54	18.50	0.021	41.5	13	12	15	14	15	-12	57	69	64
ESF	08_TCw_Tpcpmn	76+65	76+70	80.0	127.54	18.50	0.021	40.6	17	12	0	18	15	0	62	62	57
ESF	08_TCw_Tpcpmn	76+70	76+75	78.0	127.54	18.50	0.021	39.7	17	12	15	16	15	-12	63	75	70
ESF	08_TCw_Tpcpmn	76+75	76+80	76.0	127.54	18.50	0.021	38.8	17	12	10	15	15	-5	64	69	64
ESF	08_TCw_Tpcpmn	76+80	76+85	84.0	127.54	18.50	0.021	38.1	17	12	15	16	15	-5	70	75	70
ESF	08_TCw_Tpcpmn	76+85	76+90	77.0	127.54	18.50	0.021	37.6	17	12	8	16	15	-5	63	68	63

Location	Thermal Mechanical and Lithostratigraphic Unit Designation	Begin Station (m)	End Station (m)	RQD	Mean Intact UCS, σ_{ci} (MPa)	Hoek & Brown Intact Material Constant, mi	Unit Weight of Rock Mass, γ (MN/m^3)	Depth of Tunnel, H (m)	RQD Index	C	Js	Jcd	JwR	AJO	RMR Rating = (RQD Index+C+Js+Jcd+JwR+AJ0)	RMR' = (RQD Index+C+Js+Jcd+JwR)	Geological Strength Index, GSI = (RMR' - 5)
ESF	08_TCw_Tpcpmn	76+90	76+95	87.0	127.54	18.50	0.021	37	17	12	10	16	15	-5	65	70	65
ESF	08_TCw_Tpcpmn	76+95	77+00	67.0	127.54	18.50	0.021	36.4	13	12	10	22	15	-12	60	72	67
ESF	08_TCw_Tpcpmn	77+00	77+05	80.0	127.54	18.50	0.021	35.8	17	12	10	14	15	-12	56	68	63
ESF	08_TCw_Tpcpmn	77+05	77+10	75.0	127.54	18.50	0.021	35.2	13	12	8	15	15	-5	58	63	58
ESF	08_TCw_Tpcpmn	77+10	77+15	45.0	127.54	18.50	0.021	34.6	8	12	10	17	15	-5	57	62	57
ESF	08_TCw_Tpcpmn	77+15	77+20	54.0	127.54	18.50	0.021	34	13	12	0	17	15	-5	52	57	52
ESF	08_TCw_Tpcpmn	77+20	77+25	60.0	127.54	18.50	0.021	33.4	13	12	10	19	15	-12	57	69	64
ESF	08_TCw_Tpcpmn	77+25	77+30	49.0	127.54	18.50	0.021	32.8	8	12	10	14	15	-5	54	59	54
ESF	08_TCw_Tpcpmn	77+30	77+35	84.0	127.54	18.50	0.021	32.2	17	12	NA	NA	NA	NA	NA	NA	NA
ESF	08_TCw_Tpcpmn	77+35	77+40	80.0	127.54	18.50	0.021	31.6	17	12	10	20	15	-12	62	74	69
ESF	08_TCw_Tpcpmn	77+40	77+45	51.0	127.54	18.50	0.021	31.5	13	12	15	22	15	-5	72	77	72
ESF	08_TCw_Tpcpmn	77+45	77+50	94.0	127.54	18.50	0.021	31.2	20	12	15	22	15	-12	72	84	79
ESF	08_TCw_Tpcpmn	77+50	77+55	74.0	127.54	18.50	0.021	30.8	13	12	10	20	15	-12	58	70	65
ESF	08_TCw_Tpcpmn	77+55	77+60	64.0	127.54	18.50	0.021	30.5	13	12	10	18	15	-12	56	68	63
ESF	08_TCw_Tpcpmn	77+60	77+65	61.0	127.54	18.50	0.021	30.1	13	12	15	12	15	-5	62	67	62
ESF	08_TCw_Tpcpmn	77+65	77+70	58.0	127.54	18.50	0.021	29.8	13	12	10	20	15	-12	58	70	65
ESF	08_TCw_Tpcpmn	77+70	77+75	52.0	127.54	18.50	0.021	29.5	13	12	10	18	15	-12	56	68	63
ESF	08_TCw_Tpcpmn	77+75	77+80	45.0	127.54	18.50	0.021	29.1	8	12	10	18	15	-12	51	63	58
ESF	08_TCw_Tpcpmn	77+80	77+85	56.0	127.54	18.50	0.021	28.8	13	12	10	18	15	-12	56	68	63
ESF	08_TCw_Tpcpmn	77+85	77+90	49.0	127.54	18.50	0.021	28.5	8	12	15	14	15	-12	52	64	59
ESF	08_TCw_Tpcpmn	77+90	77+95	59.0	127.54	18.50	0.021	28.1	13	12	10	19	15	-12	57	69	64
ESF	08_TCw_Tpcpmn	77+95	78+00	83.0	127.54	18.50	0.021	27.8	17	12	10	18	15	-5	67	72	67
ESF	08_TCw_Tpcpmn	78+00	78+05	46.0	127.54	18.50	0.021	27	8	12	10	15	15	-5	55	60	55
ESF	08_TCw_Tpcpmn	78+05	78+10	61.0	127.54	18.50	0.021	25.9	13	12	10	17	15	-5	62	67	62
ESF	08_TCw_Tpcpmn	78+10	78+15	78.0	127.54	18.50	0.021	24.7	17	12	15	14	15	-12	61	73	68
ESF	08_TCw_Tpcpmn	78+15	78+20	76.0	127.54	18.50	0.021	23.6	17	12	10	13	15	-5	62	67	62
ESF	08_TCw_Tpcpmn	78+20	78+25	37.0	127.54	18.50	0.021	22.5	8	12	10	18	15	-5	58	63	58
ESF	08_TCw_Tpcpmn	78+25	78+30	62.0	127.54	18.50	0.021	21.3	13	12	8	18	15	-5	61	66	61
ESF	08_TCw_Tpcpmn	78+30	78+35	63.0	127.54	18.50	0.021	20.2	13	12	10	21	15	-12	59	71	66
ESF	08_TCw_Tpcpmn	78+35	78+40	75.0	127.54	18.50	0.021	19.1	13	12	10	21	15	-12	59	71	66
ESF	07_TCw_Tpcpul	78+40	78+45	68.0	127.54	18.50	0.021	18	13	7	10	21	15	-5	66	66	61
ESF	07_TCw_Tpcpul	78+45	78+50	72.0	127.54	18.50	0.021	17.1	13	7	15	18	15	-5	68	68	63
ESF	07_TCw_Tpcpul	78+50	78+55	47.0	127.54	18.50	0.021	16.2	8	7	15	21	15	-5	66	66	61
ESF	07_TCw_Tpcpul	78+55	78+60	70.0	127.54	18.50	0.021	15.3	13	7	20	22	15	-5	77	77	72
ESF	07_TCw_Tpcpul	78+60	78+65	39.0	127.54	18.50	0.021	14.2	8	7	10	24	15	0	69	64	59
ESF	07_TCw_Tpcpul	78+65	78+70	60.0	127.54	18.50	0.021	6.54	13	7	10	24	15	-5	69	69	64
ESF	07_TCw_Tpcpul	78+70	78+75	69.0	127.54	18.50	0.021	5.58	13	7	10	21	15	-12	59	66	61
HD	26_TSw2_Tptpmn	0	5	80.0	167.9	19.68	0.022	233	17	12	8	18	15	-12	58	70	65
HD	26_TSw2_Tptpmn	5	10		167.9	19.68	0.022	233	Not Rate								

Location	Thermal Mechanical and Lithostratigraphic Unit Designation	Begin Station (m)	End Station (m)	RQD	Mean Intact UCS, σ_{ci} (MPa)	Hoek & Brown Intact Material Constant, mi	Unit Weight of Rock Mass, γ (MN/m^3)	Depth of Tunnel, H (m)	RQD Index d	C	Js	Jcd	JwR	AJO	RMR Rating = (RQD Index+C+Js+Jcd+JwR+AJ0)	RMR' = (RQD Index+C+Js+Jcd+JwR)	Geological Strength Index, GSI = (RMR' - 5)
HD	26_TSw2_Tptpmn	10	15	78.0	167.9	19.68	0.022	233	17	12	8	18	15	-5	65	70	65
HD	26_TSw2_Tptpmn	15	20	69.0	167.9	19.68	0.022	233	13	12	8	18	15	-5	61	66	61
HD	26_TSw2_Tptpmn	20	25	90.0	167.9	19.68	0.022	234	17	12	10	23	15	-5	72	77	72
HD	26_TSw2_Tptpmn	25	30	76.0	167.9	19.68	0.022	234	17	12	8	23	15	-5	70	75	70
HD	26_TSw2_Tptpmn	30	35	77.0	167.9	19.68	0.022	235	17	12	15	22	15	-12	69	81	76
HD	26_TSw2_Tptpmn	35	40	67.0	167.9	19.68	0.022	236	13	12	15	22	15	-12	65	77	72
HD	26_TSw2_Tptpmn	40	45	83.0	167.9	19.68	0.022	237	17	12	15	24	15	-12	71	83	78
HD	26_TSw2_Tptpmn	45	50	58.0	167.9	19.68	0.022	237	13	12	8	23	15	-5	66	71	66
HD	26_TSw2_Tptpmn	50	55	59.0	167.9	19.68	0.022	236	13	12	8	23	15	-12	59	71	66
HD	26_TSw2_Tptpmn	55	60	54.0	167.9	19.68	0.022	236	13	12	8	23	15	-12	59	71	66

APPENDIX E
CUMULATIVE FREQUENCY DISTRIBUTION VERSUS GSI INDEX FOR LITHOSTRATIGRAPHIC ZONES

NOTE: Cumulative Frequency Distribution for GSI Index Obtained from ESF, ECRB, and HD Tunnel Mapping Data and Manual Readings of GSI Index Values Corresponding to Five Rock Mass Categories Established at 5, 20, 40, 70, and 90% of Cumulative GSI Frequency Occurrence

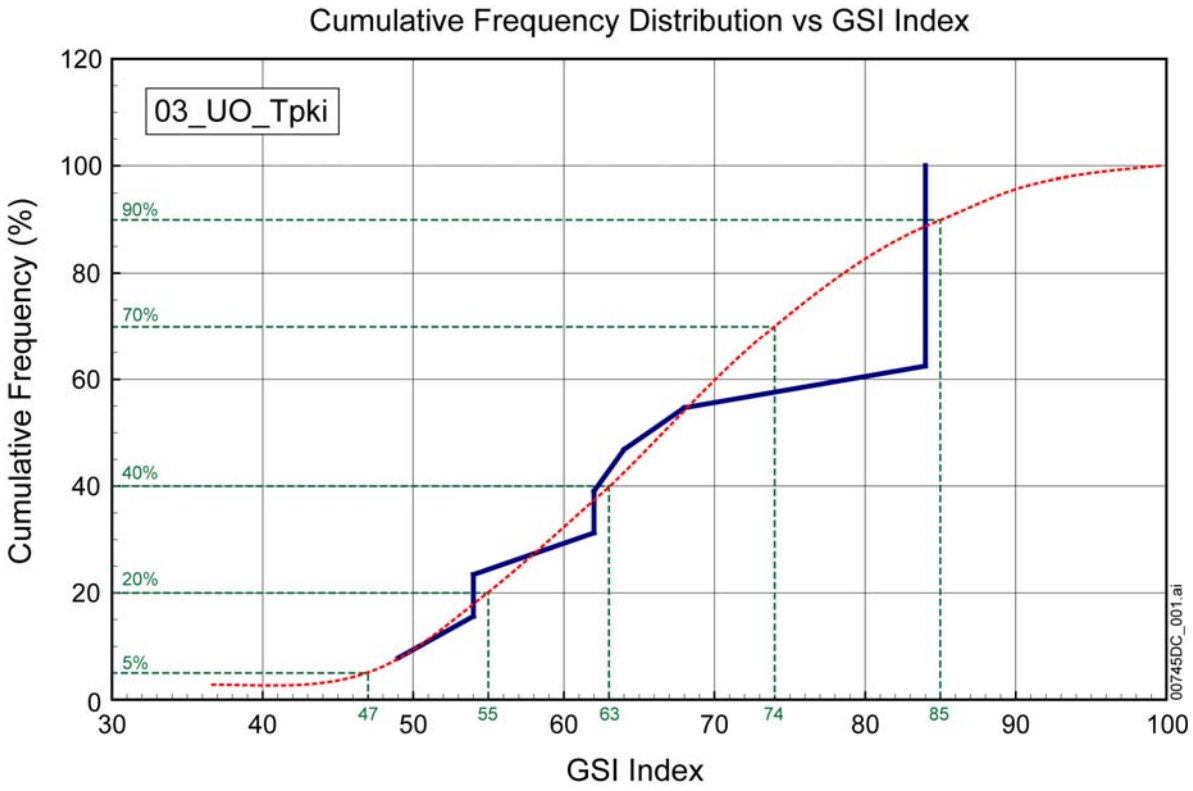

Figure E-1. Cumulative Frequency Distribution versus GSI Index at UO_Tpki Zone

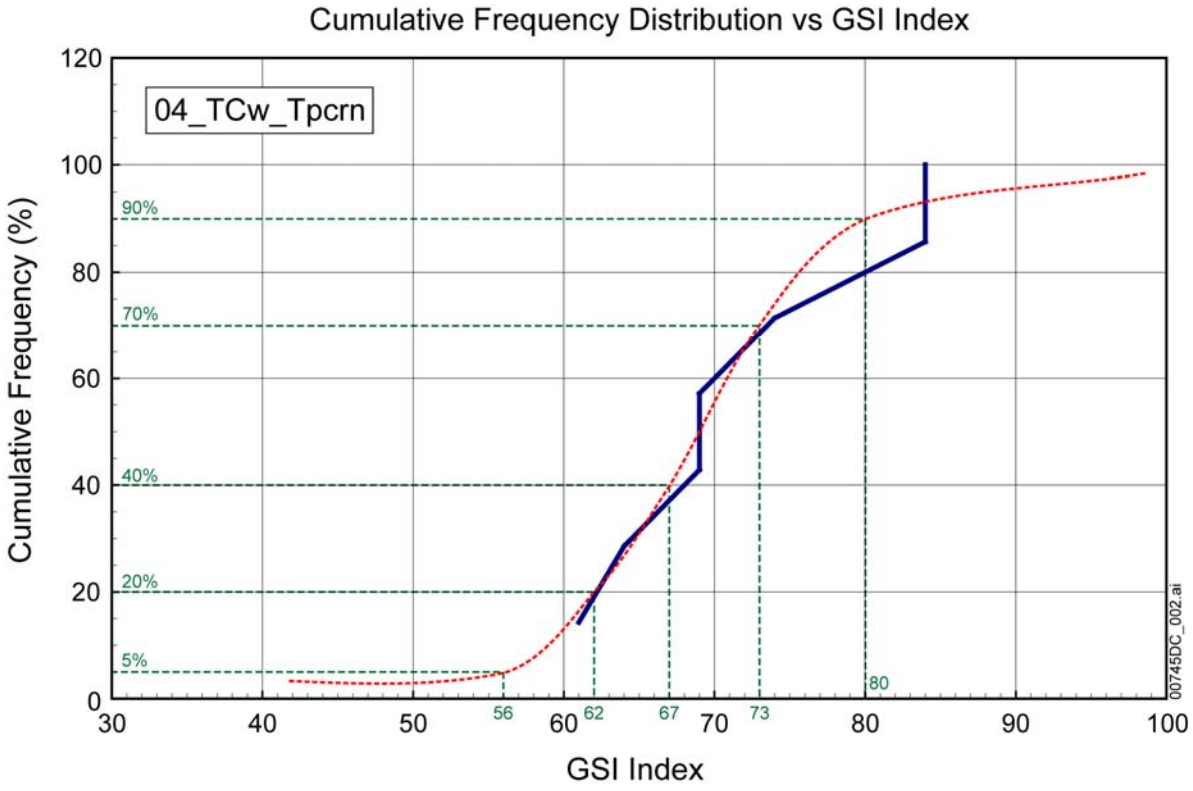

Figure E-2. Cumulative Frequency Distribution versus GSI Index at TCw_Tpcrn Zone

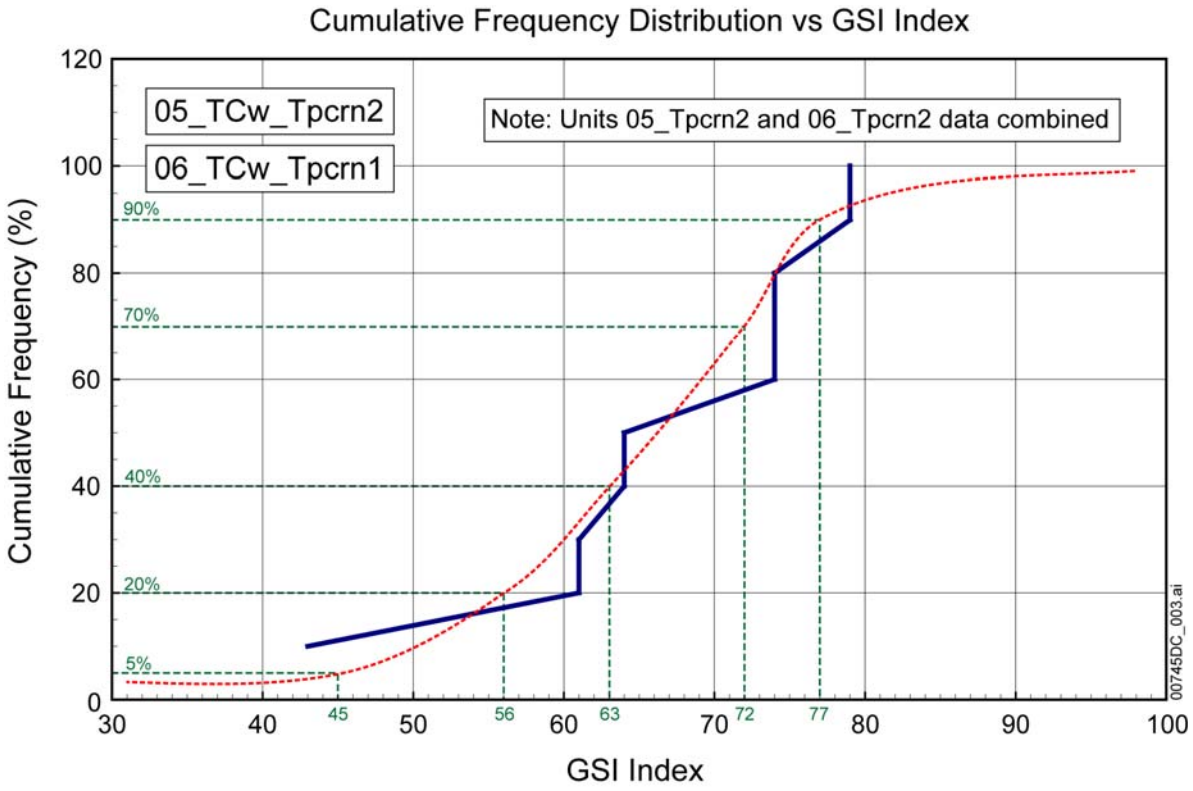

Figure E-3. Cumulative Frequency Distribution versus GSI Index at TCw_Tpcrn1 and Tpcrn2 Zones

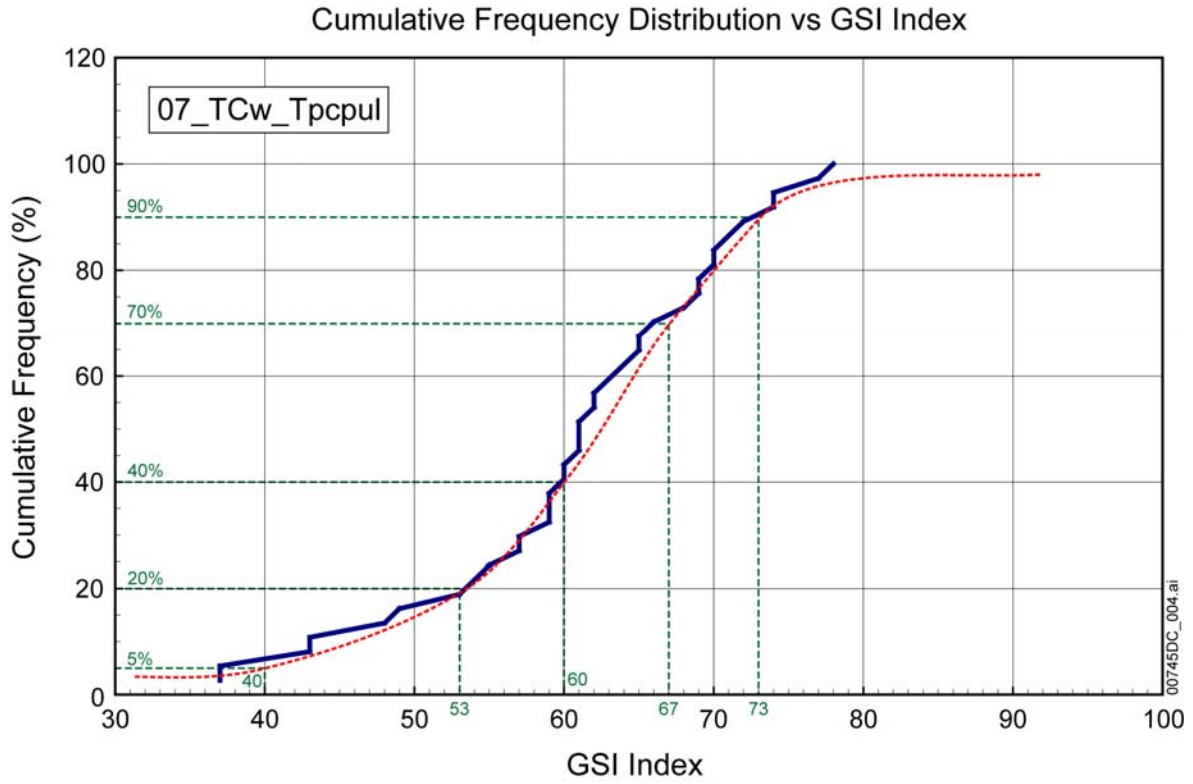

Figure E-4. Cumulative Frequency Distribution versus GSI Index at TCw_Tpcpul Zone

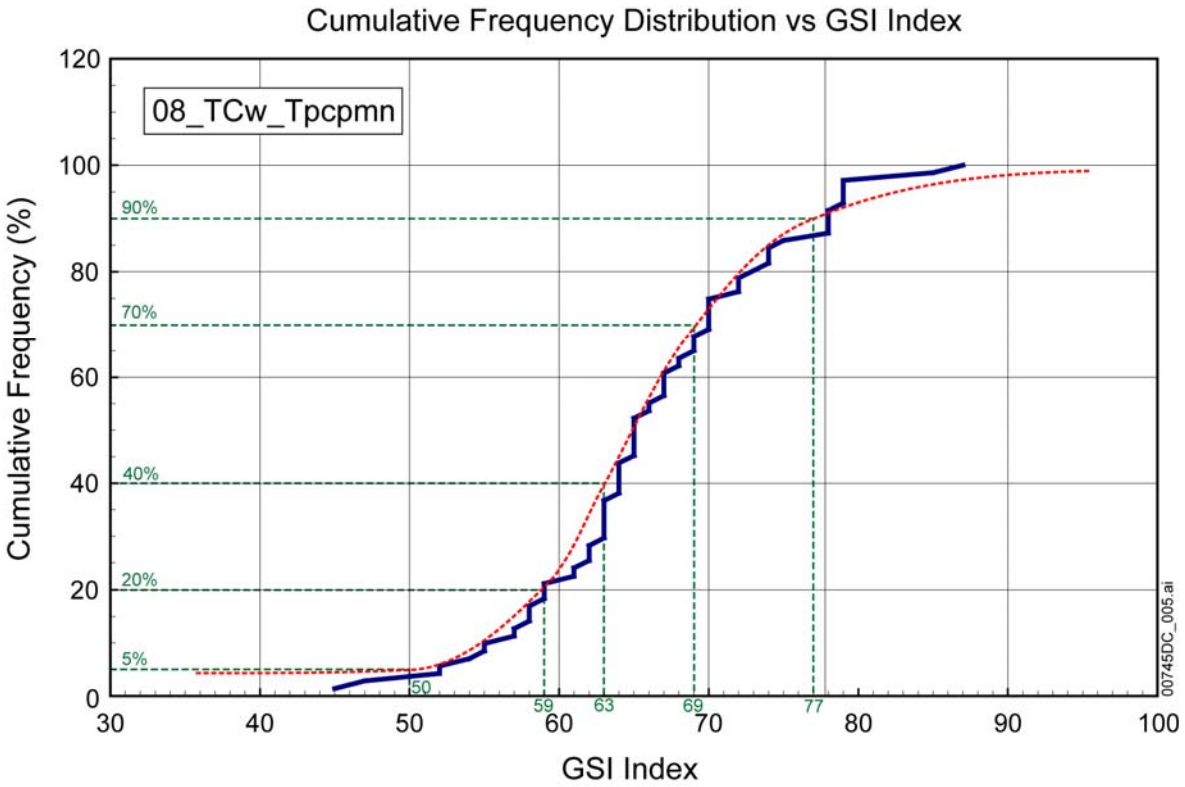

Figure E-5. Cumulative Frequency Distribution versus GSI Index at TCw_Tpcpmn Zone

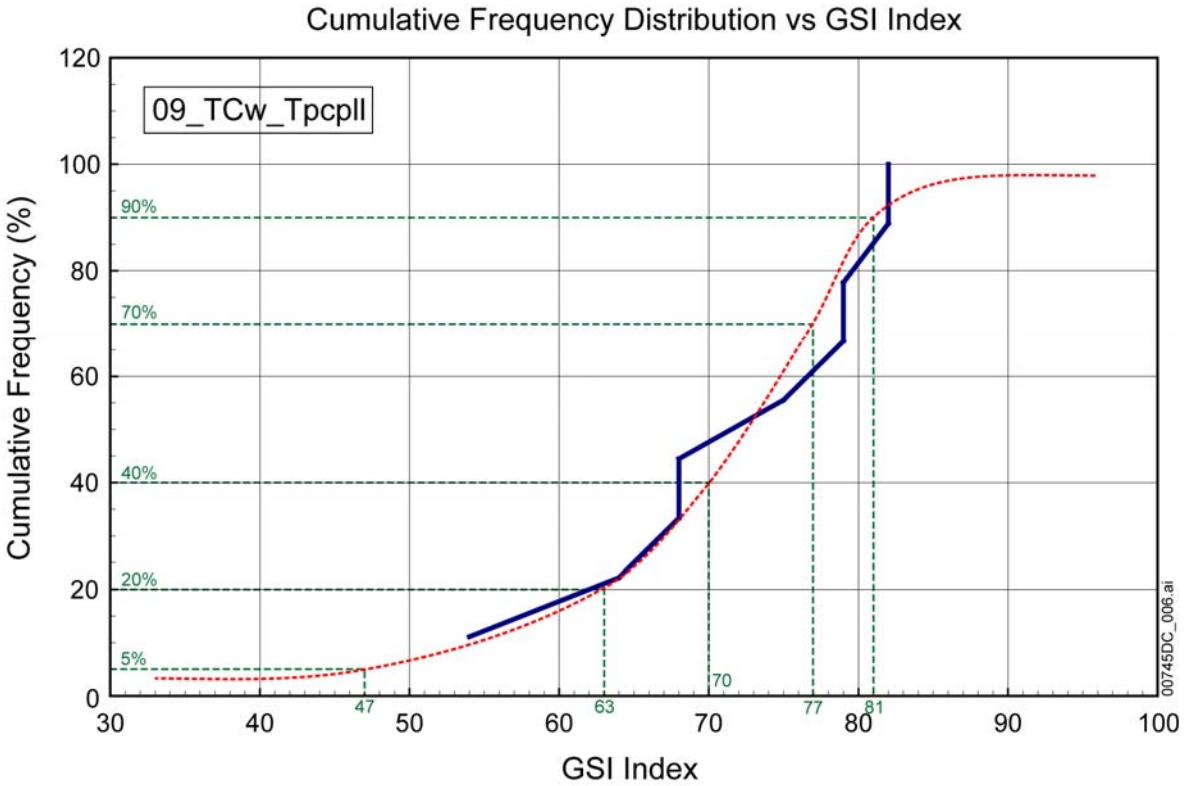

Figure E-6. Cumulative Frequency Distribution versus GSI Index at TCw_Tpcpll Zone

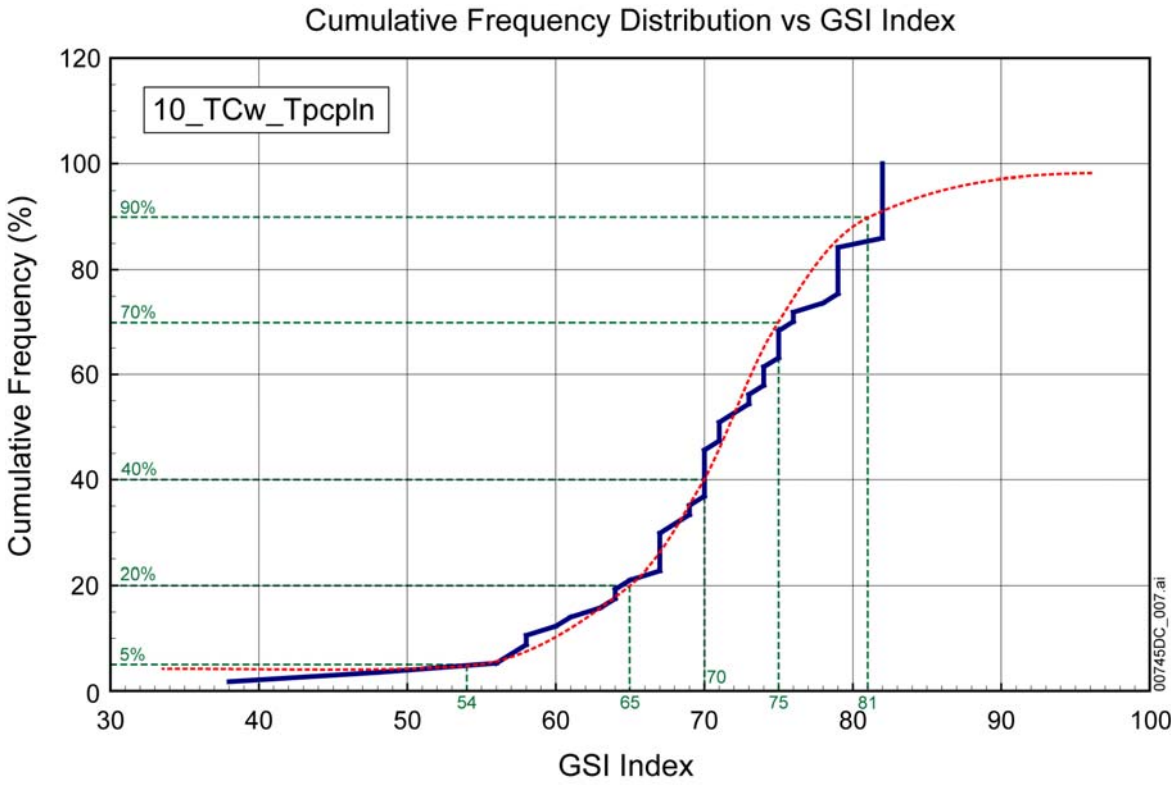

Figure E-7. Cumulative Frequency Distribution versus GSI Index at TCw_Tpcpln Zone

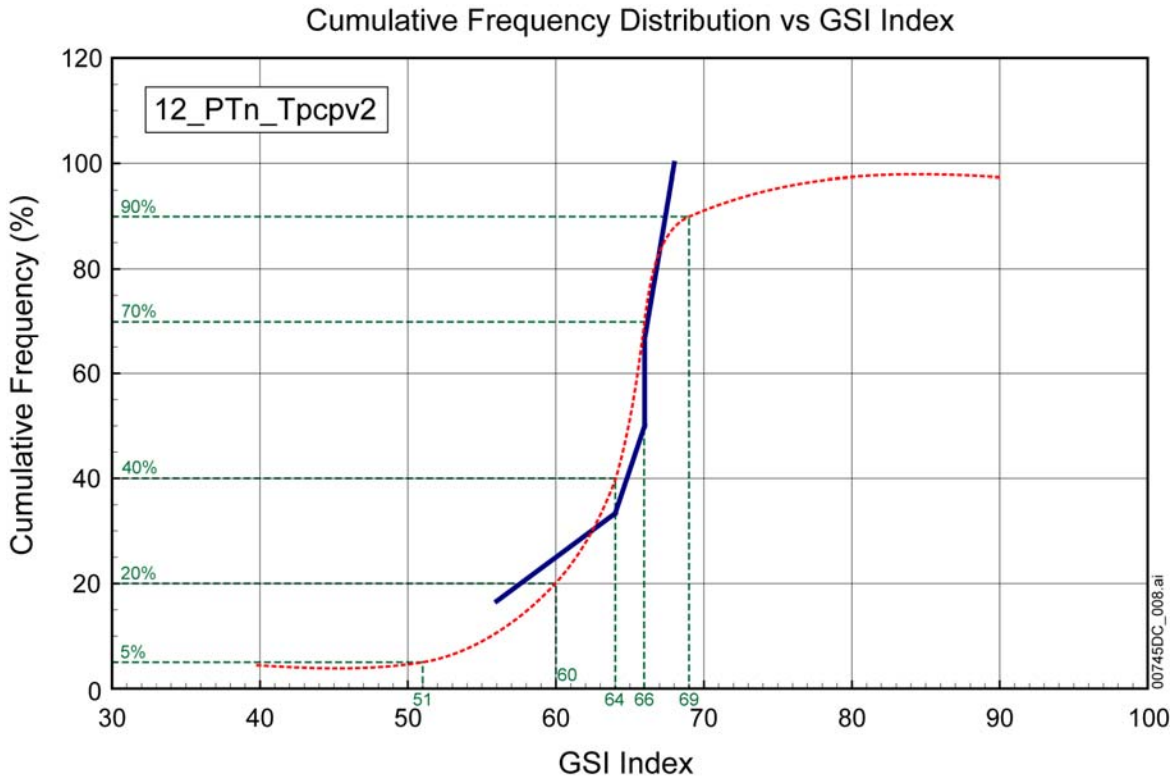

Figure E-8. Cumulative Frequency Distribution versus GSI Index at PTn_Tpcpv2 Zone

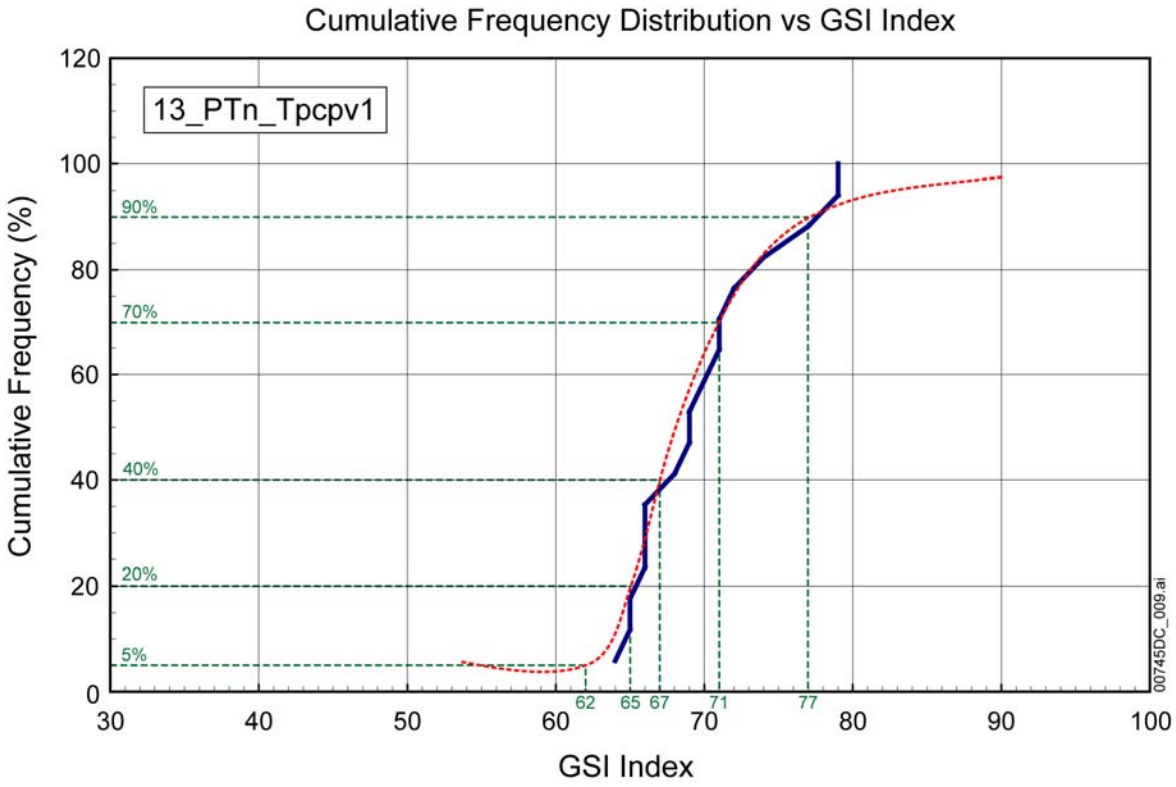

Figure E-9. Cumulative Frequency Distribution versus GSI Index at PTn_Tpcpv1 Zone

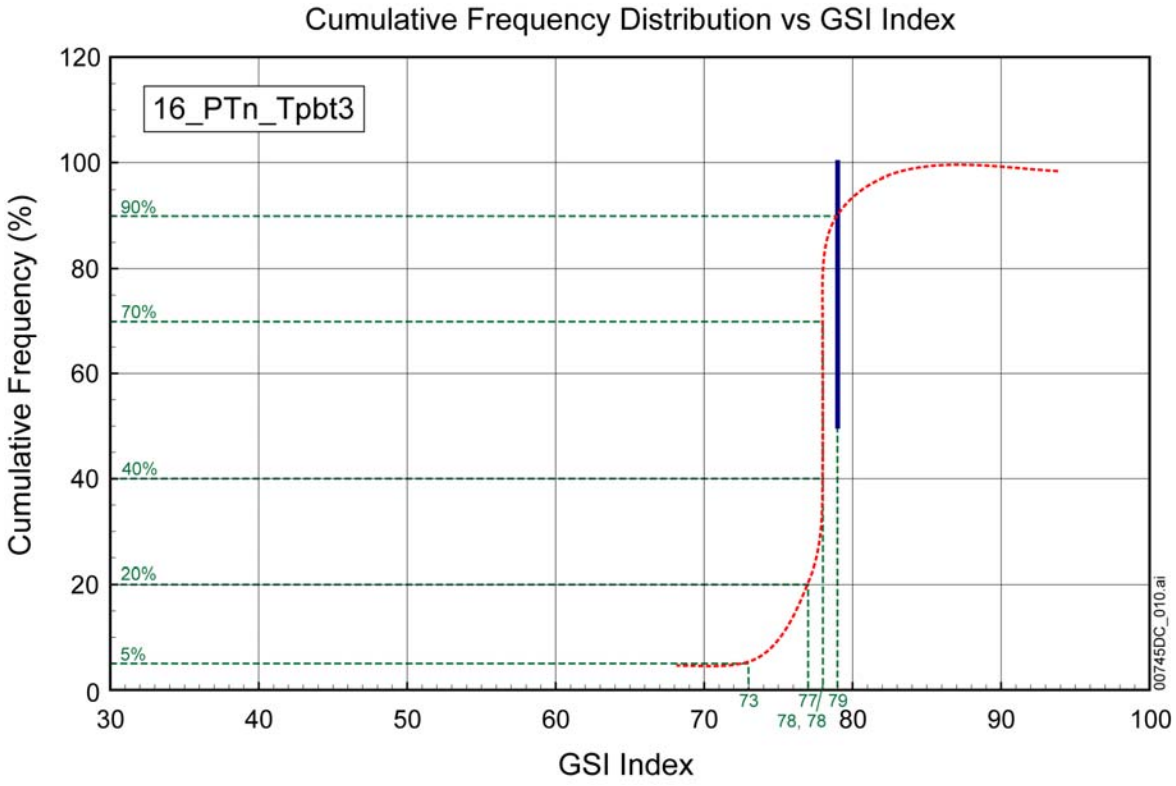

Figure E-10. Cumulative Frequency Distribution versus GSI Index at PTn_Tpbt3 Zone

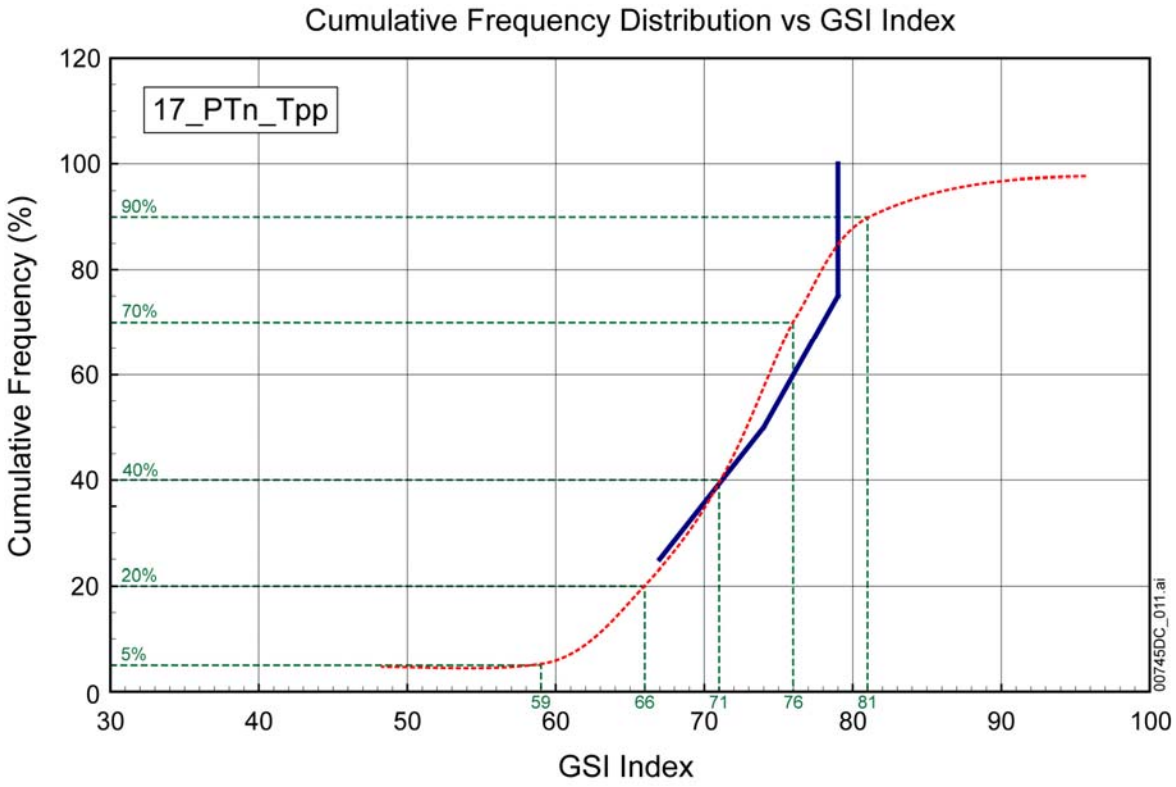

Figure E-11. Cumulative Frequency Distribution versus GSI Index at PTn_Tpp Zone

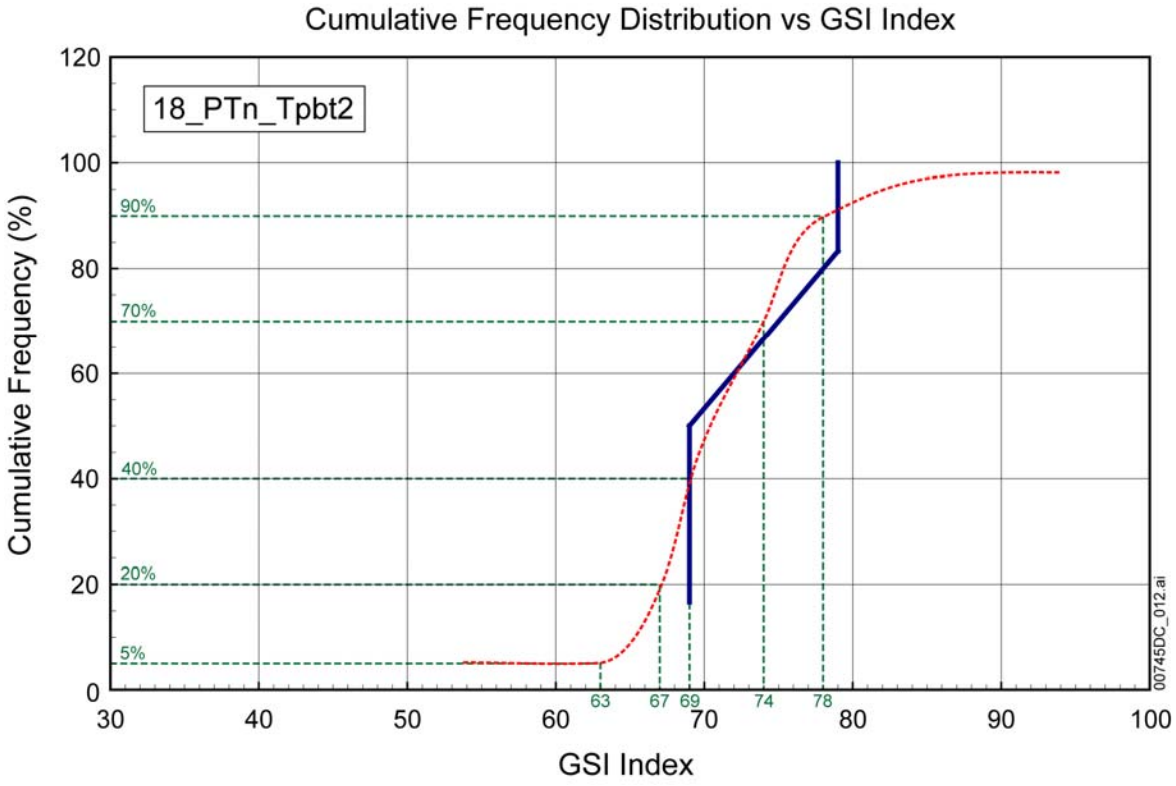

Figure E-12. Cumulative Frequency Distribution versus GSI Index at PTn_Tpbt2 Zone

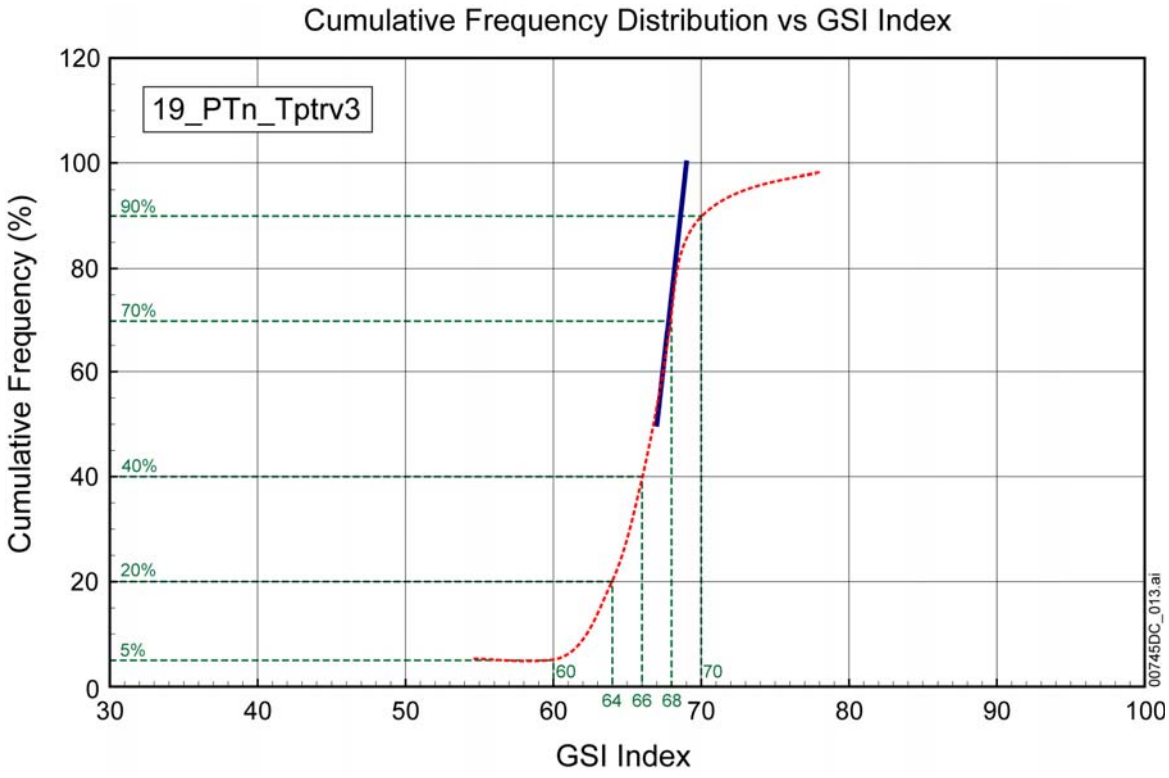

Figure E-13. Cumulative Frequency Distribution versus GSI Index at PTn_Tptrv3 Zone

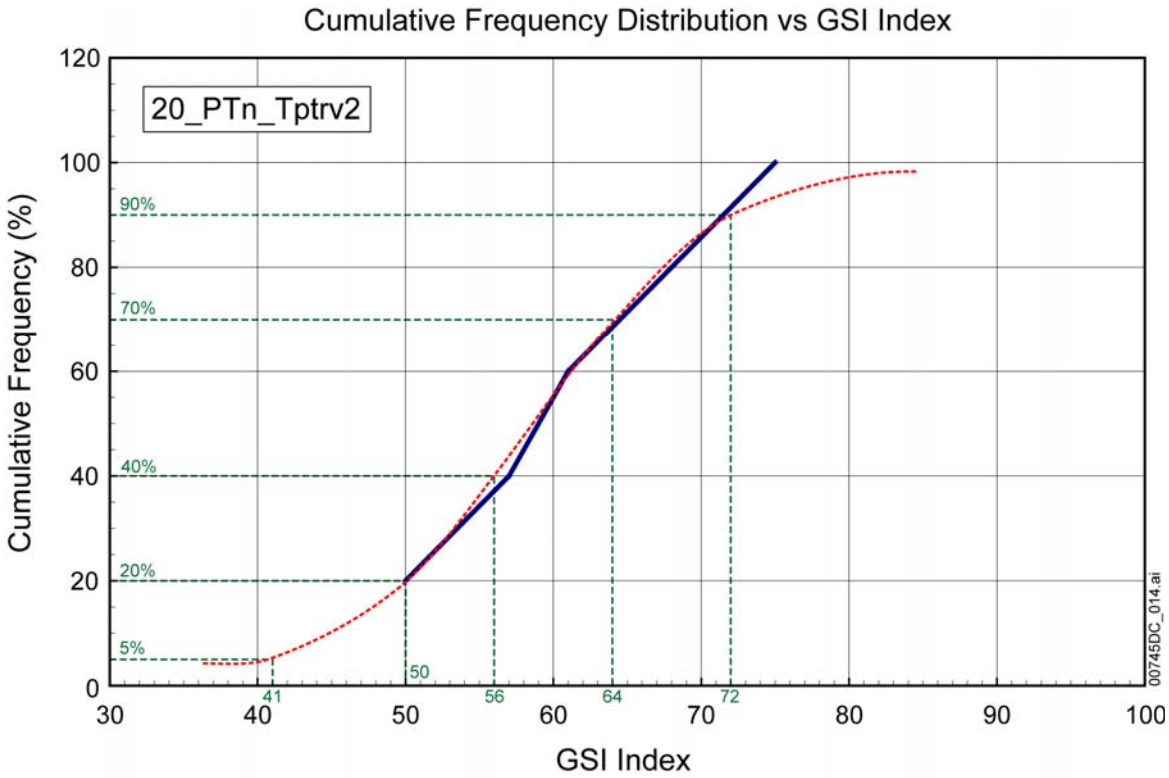

Figure E-14. Cumulative Frequency Distribution versus GSI Index at PTn_Tptrv2 Zone

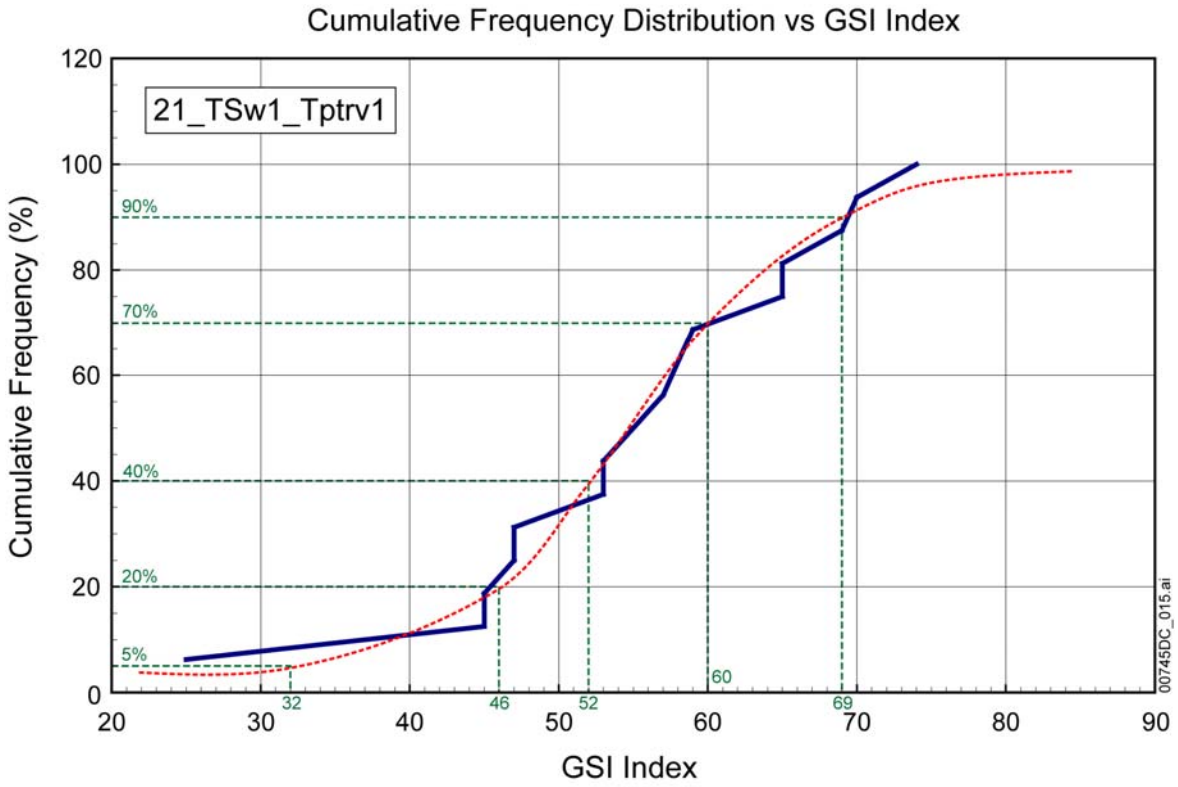

Figure E-15. Cumulative Frequency Distribution versus GSI Index at PTn_Tptrv1 Zone

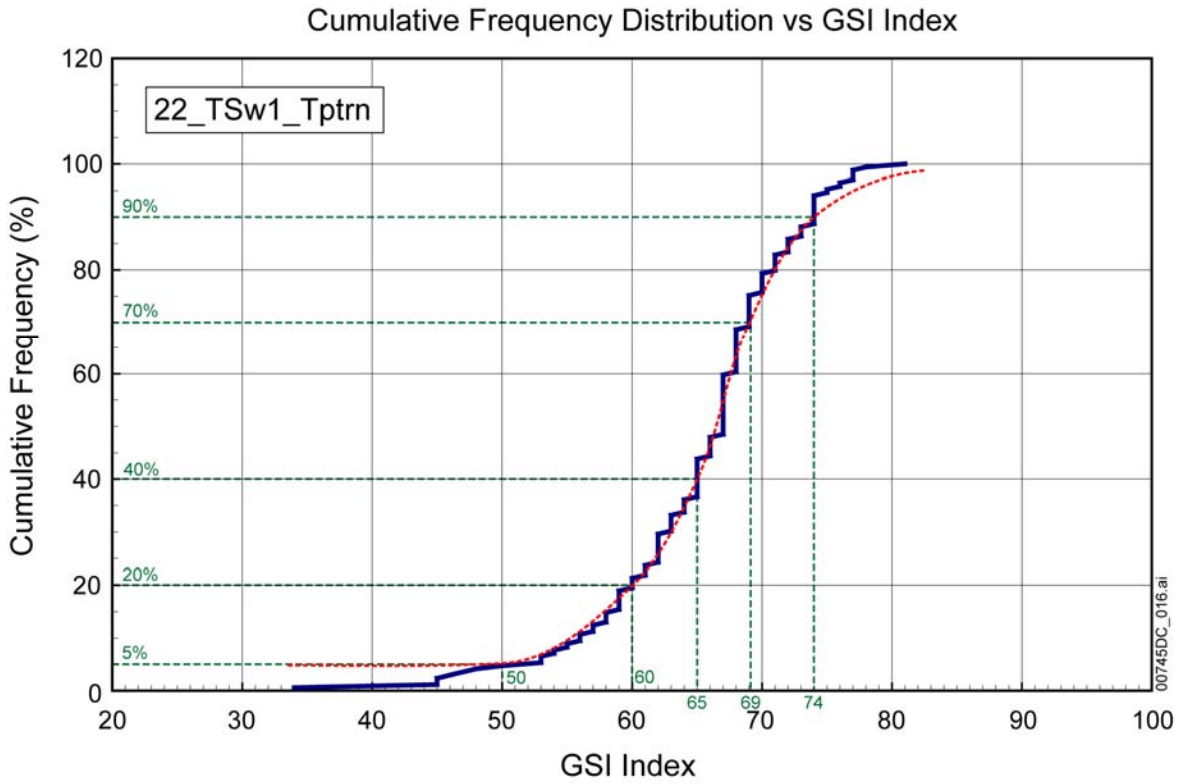

Figure E-16. Cumulative Frequency Distribution versus GSI Index at TSw1_Tptrn Zone

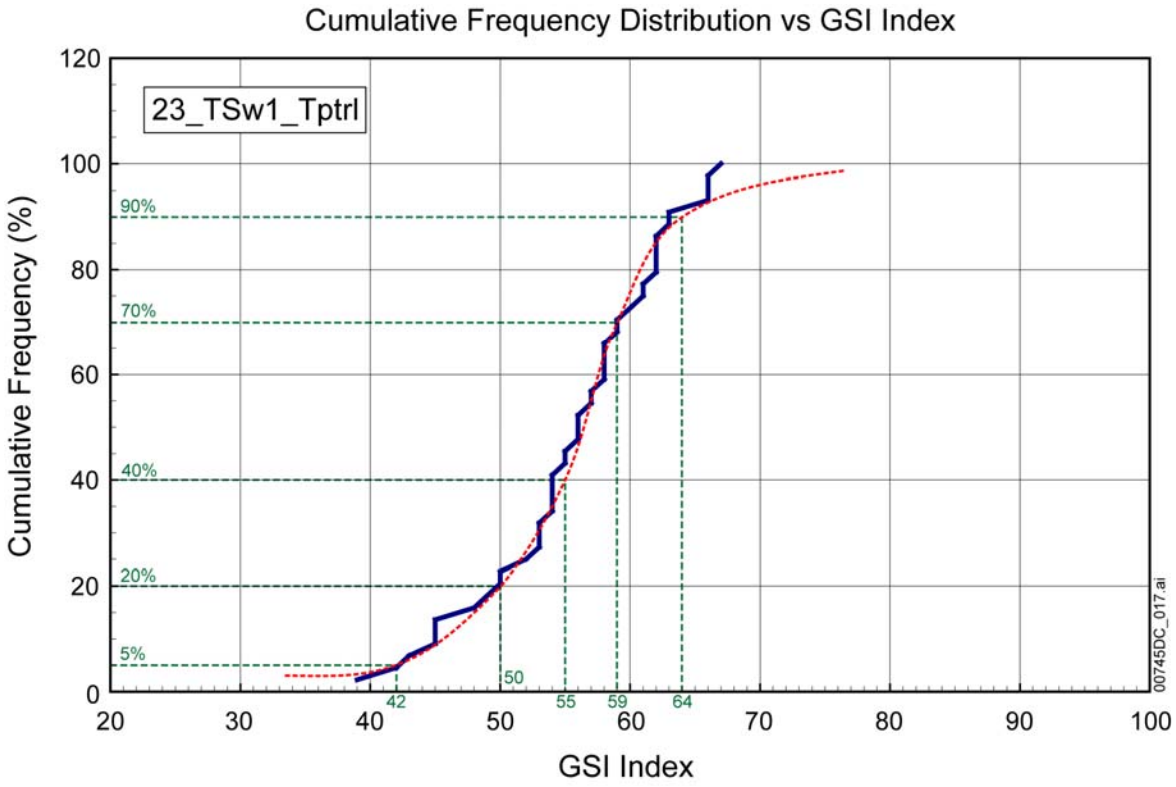

Figure E-17. Cumulative Frequency Distribution versus GSI Index at TSw1_Tptrl Zone

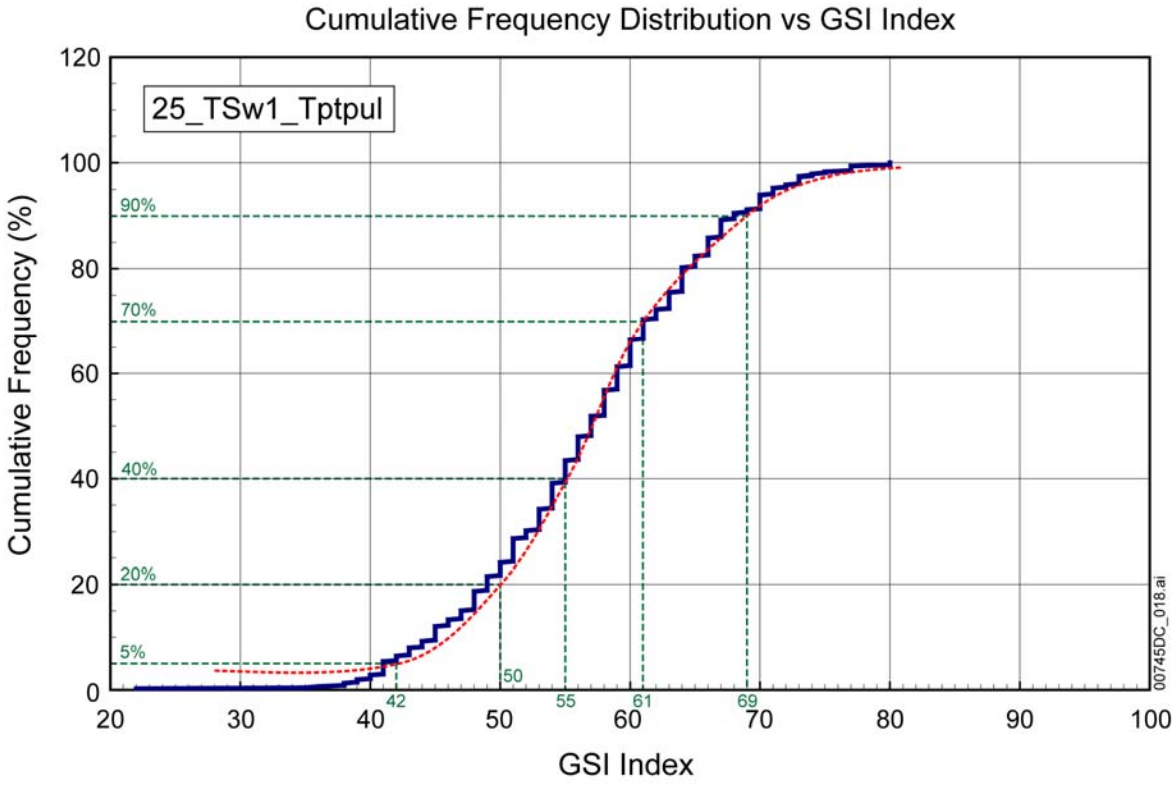

Figure E-18. Cumulative Frequency Distribution versus GSI Index at TSw1_Tptpul Zone

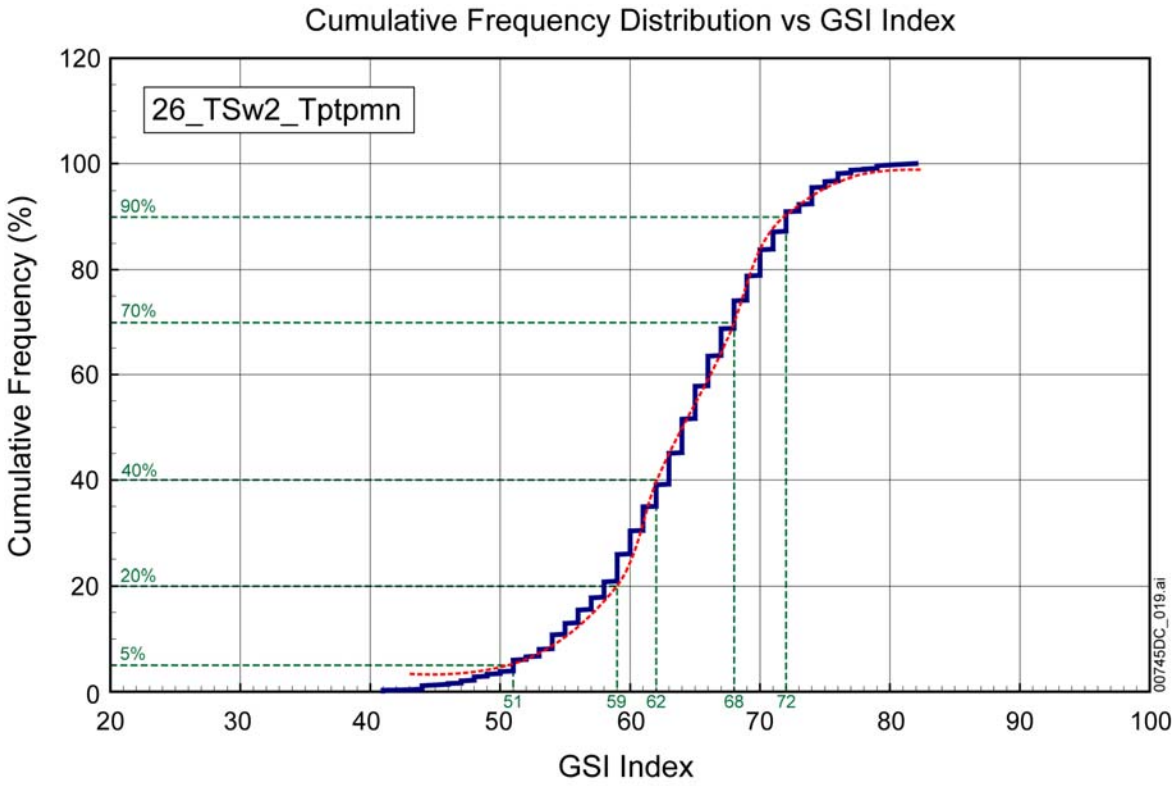

Figure E-19. Cumulative Frequency Distribution versus GSI Index at TSw2_Tptpmn Zone

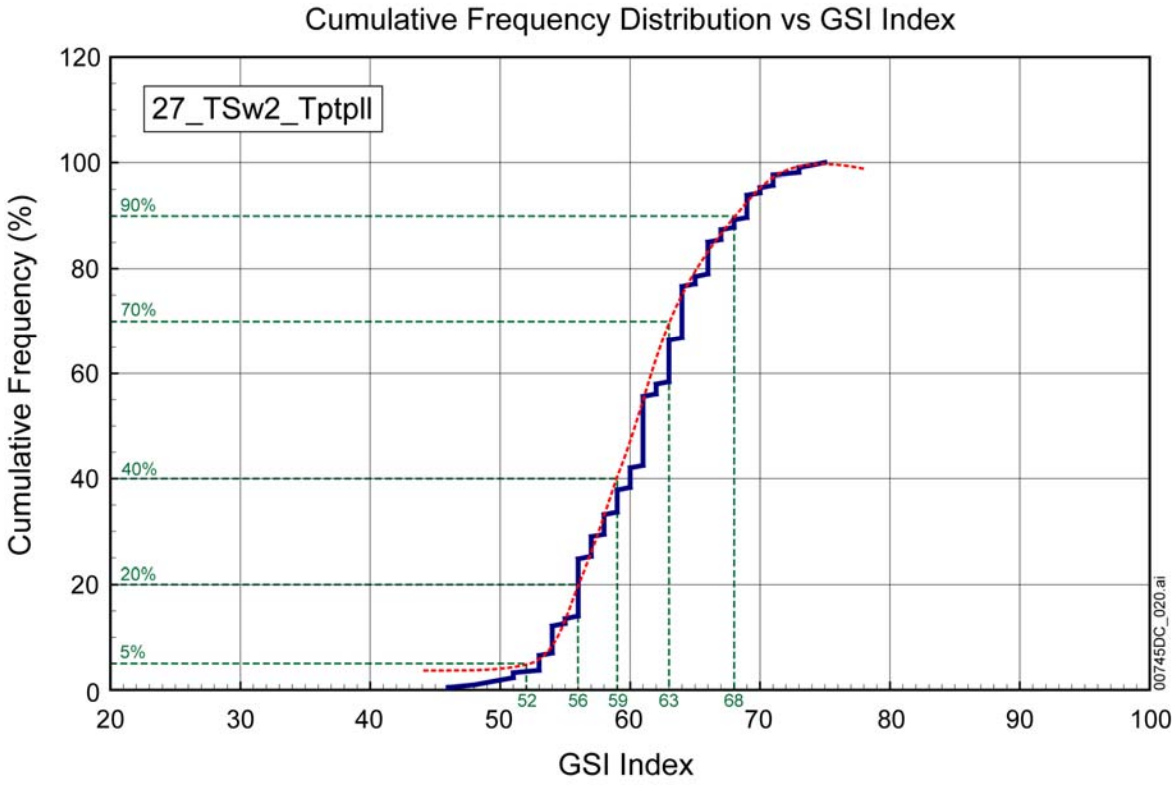

Figure E-20. Cumulative Frequency Distribution versus GSI Index at TSw2_Tptpll Zone

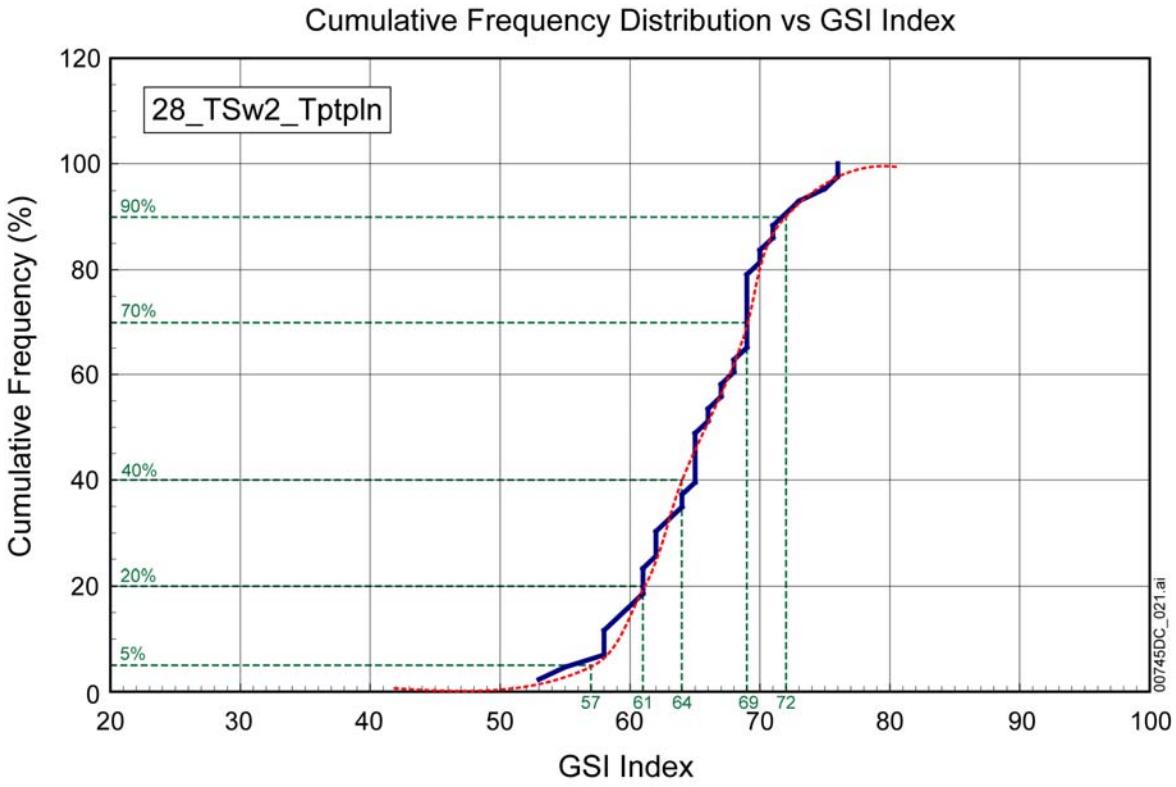

Figure E-21. Cumulative Frequency Distribution versus GSI Index at TSw2_Tptpln Zone

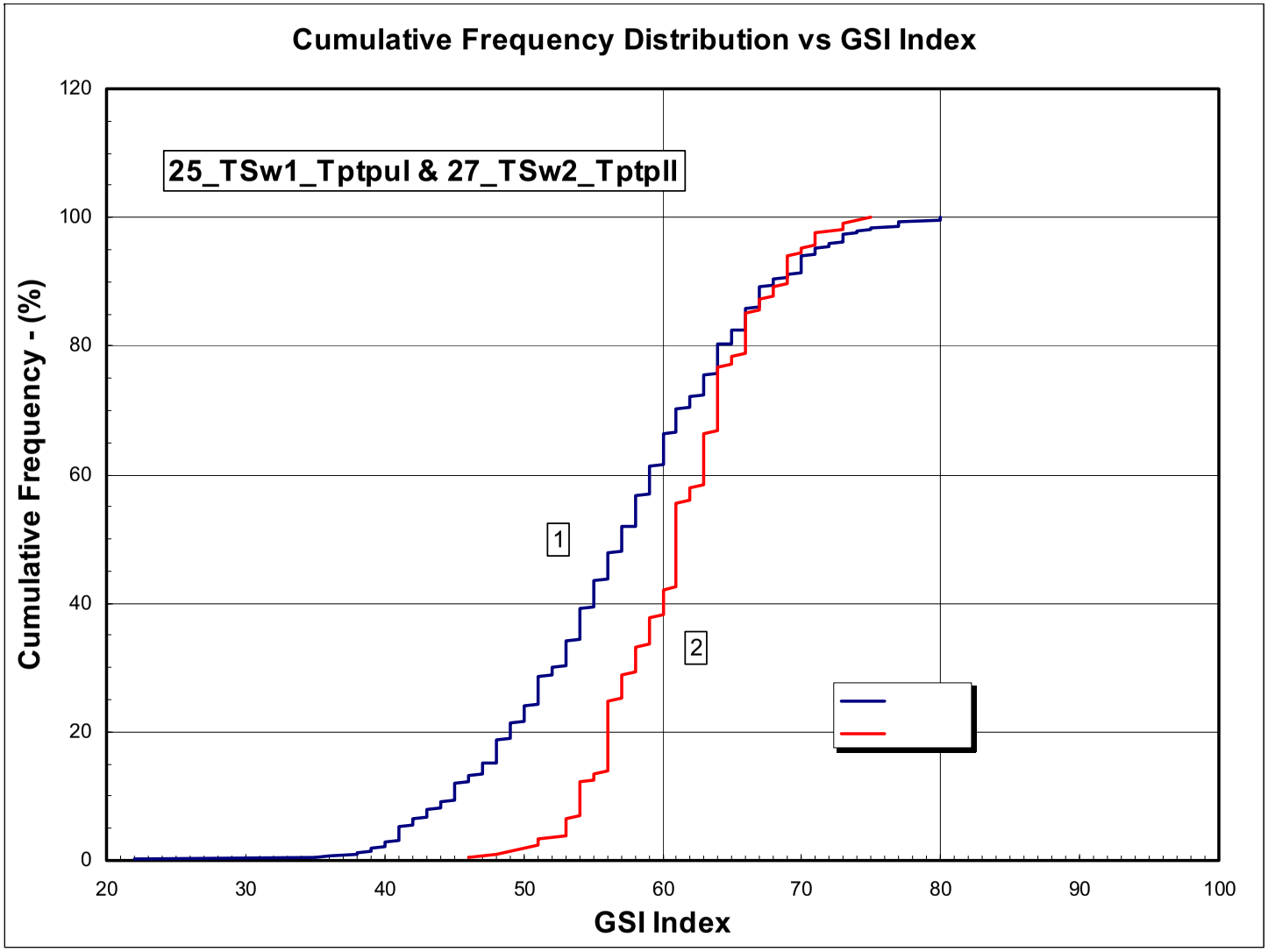

Figure E-22. Comparison of Cumulative Frequency Distribution versus GSI Index for RHH Lithophysal Zones

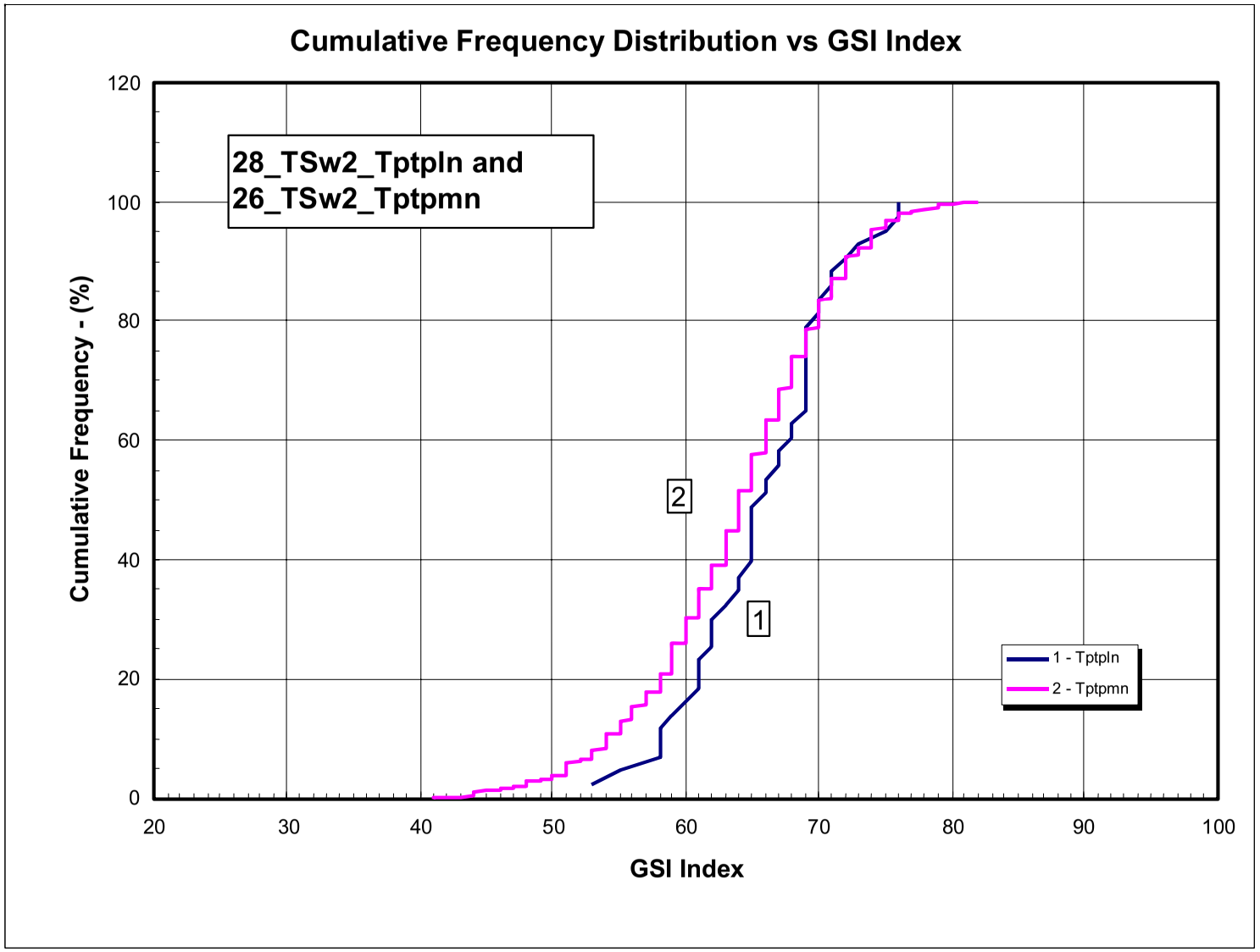

Figure E-23. Comparison of Cumulative Frequency Distribution versus GSI Index for RHH Nonlithophysal Zone

APPENDIX F
STATISTICAL ANALYSIS OF GSI INDEX

NOTE: Statistical Analysis of GSI Index Obtained from ESF, ECRB, and HD Tunnels

For Determining Statistical Distributions of the Observed GSI Index

The statistical analyses presented in this Appendix are based on intact rock data and tunnel mapping data presented in Appendices C and D, respectively. The source DTNs for this Appendix are provided in Appendices C and D.

Litho. Unit w No=03_UO_Tpki
GSI Distributions

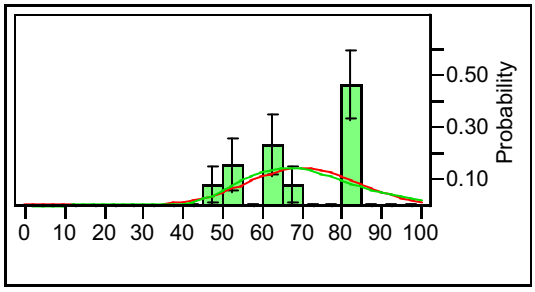

CDF Plot

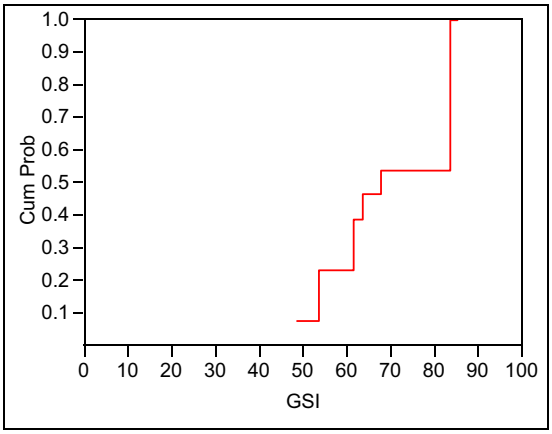

Normal(70.5385,13.824)

LogNormal(4.23749,0.20374)

Quantiles

100.0%	maximum	84.000
99.5%		84.000
97.5%		84.000
90.0%		84.000
75.0%	quartile	84.000
50.0%	median	68.000
25.0%	quartile	58.000
10.0%		51.000
2.5%		49.000
0.5%		49.000
0.0%	minimum	49.000

Moments

Mean	70.538462
Std Dev	13.823985
Std Err Mean	3.8340836
upper 95% Mean	78.892212
lower 95% Mean	62.184711
N	13
Sum Wgt	13
Sum	917
Variance	191.10256
Skewness	-0.22157
Kurtosis	-1.758812
CV	19.597798
N Missing	1

Fitted Normal Parameter Estimates

Type	Parameter	Estimate	Lower 95%	Upper 95%
Location	Mu	70.53846	62.18471	78.89221
Dispersion	Sigma	13.82399	9.91299	22.81974

Fitted LogNormal Parameter Estimates

Type	Parameter	Estimate	Lower 95%	Upper 95%
Scale	Mu	4.237488	4.114371	4.360606
Shape	Sigma	0.203738	0.153916	0.308728

Litho. Unit w No=04_TCw_Tpcrn
GSI Distributions

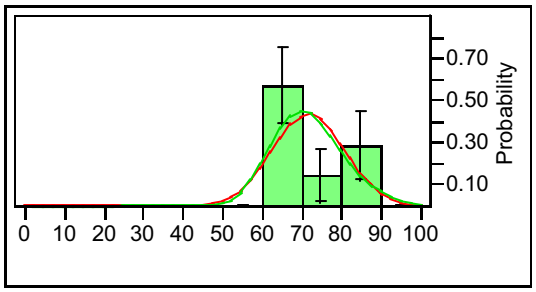

CDF Plot

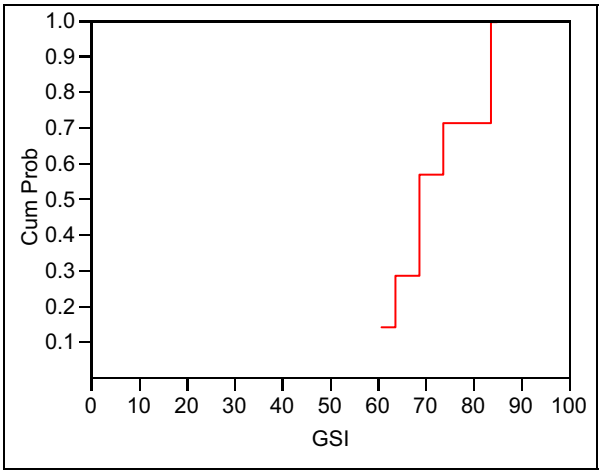

Normal(72.1429,9.08164)
LogNormal(4.27195,0.12457)

Quantiles

100.0%	maximum	84.000
99.5%		84.000
97.5%		84.000
90.0%		84.000
75.0%	quartile	84.000
50.0%	median	69.000
25.0%	quartile	64.000
10.0%		61.000
2.5%		61.000
0.5%		61.000
0.0%	minimum	61.000

Moments

Mean	72.142857
Std Dev	9.0816403
Std Err Mean	3.4325374
upper 95% Mean	80.541974
lower 95% Mean	63.743741
N	7
Sum Wgt	7
Sum	505
Variance	82.47619
Skewness	0.4220758
Kurtosis	-1.314481
CV	12.588412
N Missing	0

Fitted Normal
Parameter Estimates

Type	Parameter	Estimate	Lower 95%	Upper 95%
Location	Mu	72.14286	63.74374	80.54197
Dispersion	Sigma	9.08164	5.85215	19.99837

Fitted LogNormal
Parameter Estimates

Type	Parameter	Estimate	Lower 95%	Upper 95%
Scale	Mu	4.271953	4.156747	4.387159
Shape	Sigma	0.124568	0.085989	0.238600

Litho. Unit w No=05_TCw_Tpcrn2
GSI Distributions

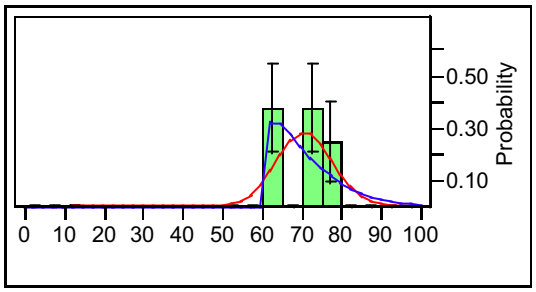

CDF Plot

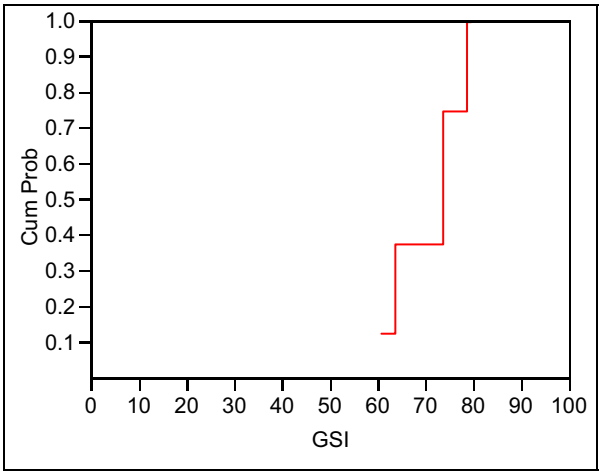

Normal(71.125,7.10005)

Beta(1.29978,8.55944,60.38,79.72)

Quantiles

100.0%	maximum	79.000
99.5%		79.000
97.5%		79.000
90.0%		79.000
75.0%	quartile	77.750
50.0%	median	74.000
25.0%	quartile	64.000
10.0%		61.000
2.5%		61.000
0.5%		61.000
0.0%	minimum	61.000

Moments

Mean	71.125
Std Dev	7.1000503
Std Err Mean	2.5102469
upper 95% Mean	77.060791
lower 95% Mean	65.189209
N	8
Sum Wgt	8
Sum	569
Variance	50.410714
Skewness	-0.379625
Kurtosis	-1.72127
CV	9.982496
N Missing	0

Fitted Normal
Parameter Estimates

Type	Parameter	Estimate	Lower 95%	Upper 95%
Location	Mu	71.12500	65.18921	77.06079
Dispersion	Sigma	7.10005	4.69437	14.45053

Fitted Beta
Parameter Estimates

Type	Parameter	Estimate	Lower 95%	Upper 95%
Shape	Alpha	1.29978	.	.
Shape	Beta	8.55944	.	.
Threshold	Theta	60.38003	.	.
Scale	Sigma	79.71997	.	.

Note: unable to converge on all confidence limits.

Litho. Unit w No=06_TCw_Tpcrn1
GSI Distributions

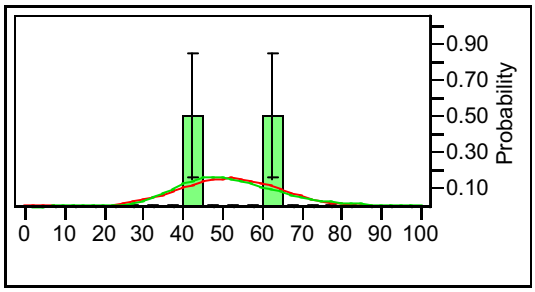

CDF Plot

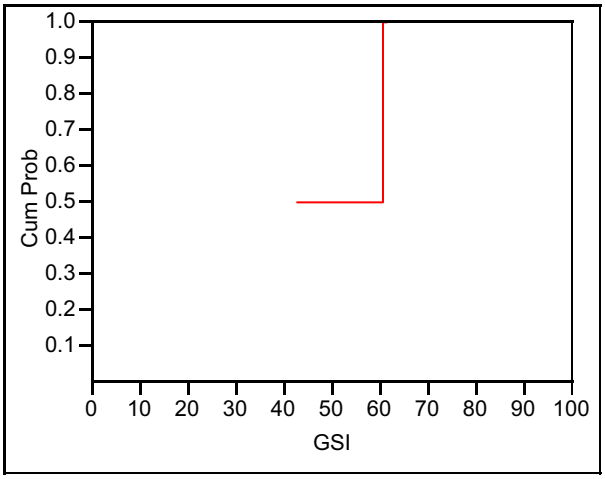

Normal(52,12.7279)

LogNormal(3.93604,0.24726)

Quantiles

100.0%	maximum	61.000
99.5%		61.000
97.5%		61.000
90.0%		61.000
75.0%	quartile	61.000
50.0%	median	52.000
25.0%	quartile	43.000
10.0%		43.000
2.5%		43.000
0.5%		43.000
0.0%	minimum	43.000

Moments

Mean	52
Std Dev	12.727922
Std Err Mean	9
upper 95% Mean	166.35584
lower 95% Mean	-62.35584
N	2
Sum Wgt	2
Sum	104
Variance	162
Skewness	.
Kurtosis	.
CV	24.476773
N Missing	0

Fitted Normal Parameter Estimates

Type	Parameter	Estimate	Lower 95%	Upper 95%
Location	Mu	52.00000	-62.3558	166.3558
Dispersion	Sigma	12.72792	5.6786	406.1500

Fitted LogNormal Parameter Estimates

Type	Parameter	Estimate	Lower 95%	Upper 95%
Scale	Mu	3.936037	1.714524	6.157550
Shape	Sigma	0.247257	0.126154	3.943061

Litho. Unit w No=07_TCw_Tpcpul
GSI Distributions

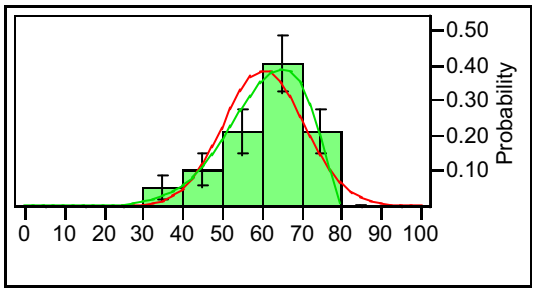

CDF Plot

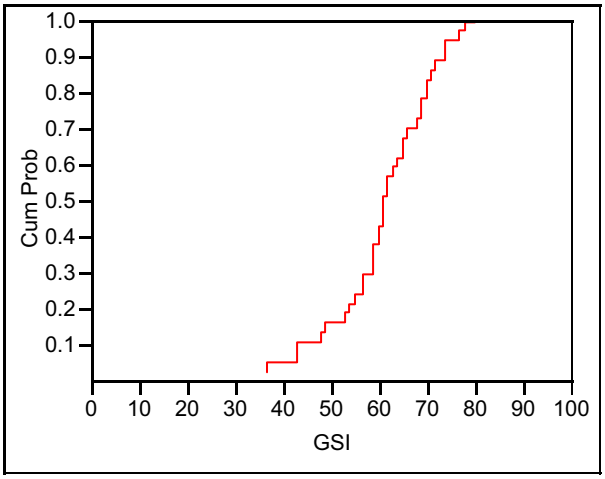

Normal(60.8649,10.3042)

Beta(8.41425,2.67596,-2.1339,83.0602)

Quantiles

100.0%	maximum	78.000
99.5%		78.000
97.5%		78.000
90.0%		74.000
75.0%	quartile	69.000
50.0%	median	61.000
25.0%	quartile	56.000
10.0%		43.000
2.5%		37.000
0.5%		37.000
0.0%	minimum	37.000

Moments

Mean	60.864865
Std Dev	10.304158
Std Err Mean	1.6939932
upper 95% Mean	64.300442
lower 95% Mean	57.429287
N	37
Sum Wgt	37
Sum	2252
Variance	106.17568
Skewness	-0.645876
Kurtosis	0.1491773
CV	16.929567
N Missing	0

Fitted Normal
Parameter Estimates

Type	Parameter	Estimate	Lower 95%	Upper 95%
Location	Mu	60.86486	57.42929	64.30044
Dispersion	Sigma	10.30416	8.37945	13.38469

Fitted Beta
Parameter Estimates

Type	Parameter	Estimate	Lower 95%	Upper 95%
Shape	Alpha	8.4143	.	.
Shape	Beta	2.6760	.	.
Threshold	Theta	-2.1339	.	.
Scale	Sigma	83.0602	.	.

Note: unable to converge on all confidence limits.

Litho. Unit w No=08_TCw_Tpcpmn
GSI Distributions

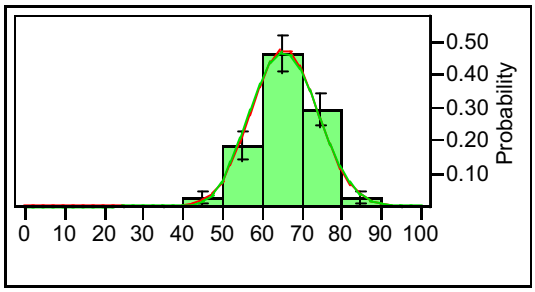

CDF Plot

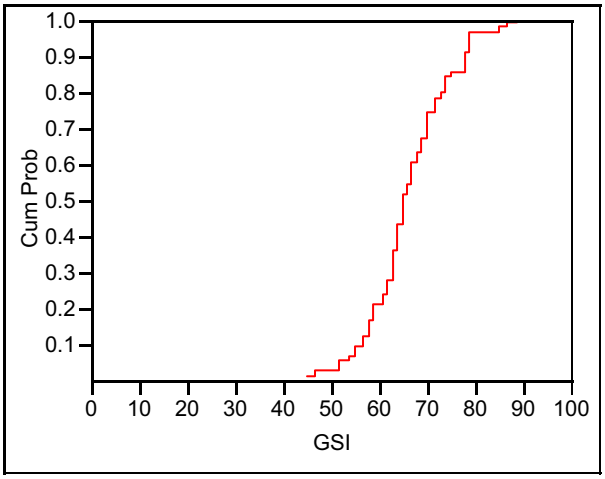

Normal(66.1972,8.33173)

Beta(15.4777,17.9638,21.0312,97.5836)

Quantiles

100.0%	maximum	87.000
99.5%		87.000
97.5%		85.400
90.0%		78.000
75.0%	quartile	72.000
50.0%	median	65.000
25.0%	quartile	62.000
10.0%		55.400
2.5%		46.600
0.5%		45.000
0.0%	minimum	45.000

Moments

Mean	66.197183
Std Dev	8.3317289
Std Err Mean	0.9887943
upper 95% Mean	68.169271
lower 95% Mean	64.225095
N	71
Sum Wgt	71
Sum	4700
Variance	69.417706
Skewness	0.0495858
Kurtosis	0.2031129
CV	12.586229
N Missing	1

Fitted Normal
Parameter Estimates

Type	Parameter	Estimate	Lower 95%	Upper 95%
Location	Mu	66.19718	64.22510	68.16927
Dispersion	Sigma	8.33173	7.15104	9.98305

Fitted Beta
Parameter Estimates

Type	Parameter	Estimate	Lower 95%	Upper 95%
Shape	Alpha	15.47770	.	.
Shape	Beta	17.96379	.	.
Threshold	Theta	21.03117	.	.
Scale	Sigma	97.58360	.	.

Note: unable to converge on all confidence limits.

Litho. Unit w No=09_TCw_Tpcpll
GSI Distributions

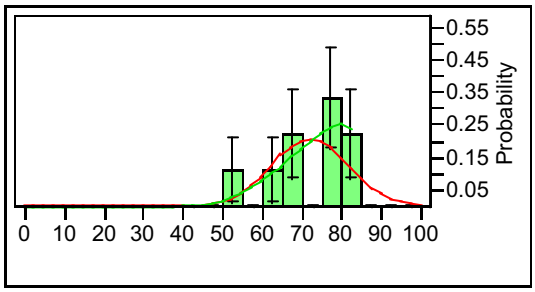

CDF Plot GSI

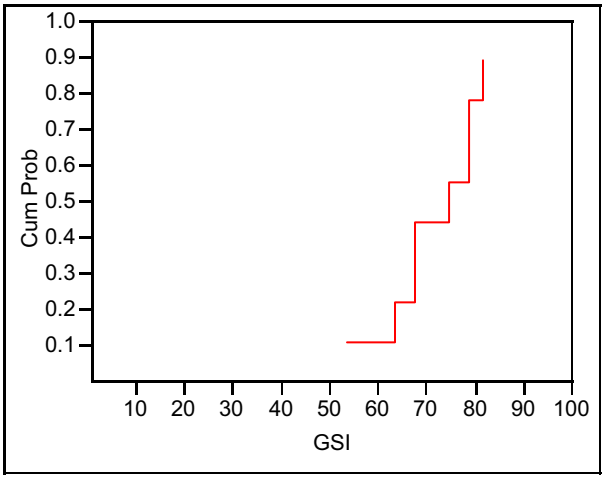

Normal(72.3333,9.52628)

Beta(3.57698,1.27318,37.7992,46.7037)

Quantiles

100.0%	maximum	82.000
99.5%		82.000
97.5%		82.000
90.0%		82.000
75.0%	quartile	80.500
50.0%	median	75.000
25.0%	quartile	66.000
10.0%		54.000
2.5%		54.000
0.5%		54.000
0.0%	minimum	54.000

Moments

Mean	72.333333
Std Dev	9.5262794
Std Err Mean	3.1754265
upper 95% Mean	79.65588
lower 95% Mean	65.010787
N	9
Sum Wgt	9
Sum	651
Variance	90.75
Skewness	-0.833833
Kurtosis	-0.019198
CV	13.169972
N Missing	0

Fitted Normal
Parameter Estimates

Type	Parameter	Estimate	Lower 95%	Upper 95%
Location	Mu	72.33333	65.01079	79.65588
Dispersion	Sigma	9.52628	6.43459	18.25017

Fitted Beta
Parameter Estimates

Type	Parameter	Estimate	Lower 95%	Upper 95%
Shape	Alpha	3.57698	.	.
Shape	Beta	1.27318	.	.
Threshold	Theta	37.79919	.	.
Scale	Sigma	46.70372	.	.

Note: unable to converge on all confidence limits.

Litho. Unit w No=10_TCw_Tpcpln
GSI Distributions

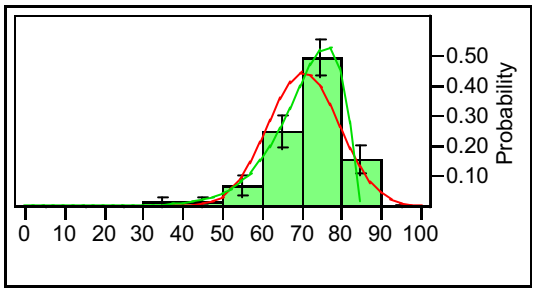

CDF Plot

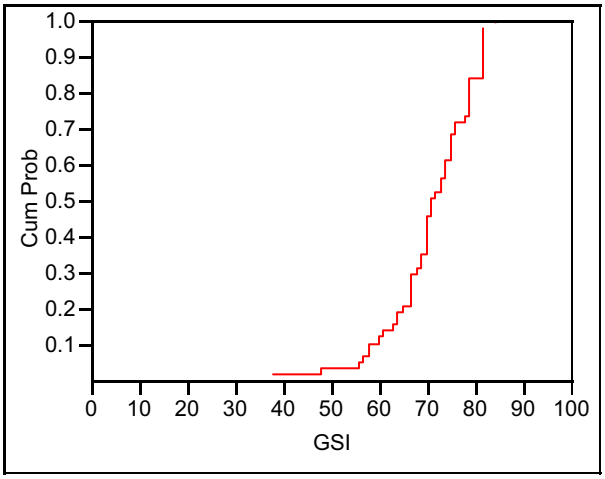

Normal(71.0175,9.03464)

Beta(53.1186,2.41033,-245.76,331.157)

Quantiles

100.0%	maximum	82.000
99.5%		82.000
97.5%		82.000
90.0%		82.000
75.0%	quartile	79.000
50.0%	median	71.000
25.0%	quartile	67.000
10.0%		58.000
2.5%		42.500
0.5%		38.000
0.0%	minimum	38.000

Moments

Mean	71.017544
Std Dev	9.0346382
Std Err Mean	1.1966671
upper 95% Mean	73.414756
lower 95% Mean	68.620332
N	57
Sum Wgt	57
Sum	4048
Variance	81.624687
Skewness	-1.178815
Kurtosis	2.2405083
CV	12.721699
N Missing	2

Fitted Normal
Parameter Estimates

Type	Parameter	Estimate	Lower 95%	Upper 95%
Location	Mu	71.01754	68.62033	73.41476
Dispersion	Sigma	9.03464	7.62754	11.08321

Fitted Beta
Parameter Estimates

Type	Parameter	Estimate	Lower 95%	Upper 95%
Shape	Alpha	53.119	.	.
Shape	Beta	2.410	.	.
Threshold	Theta	-245.764	.	.
Scale	Sigma	331.157	.	.

Note: unable to converge on all confidence limits.

Litho. Unit w No=12_PTn_Tpcpv2
GSI Distributions

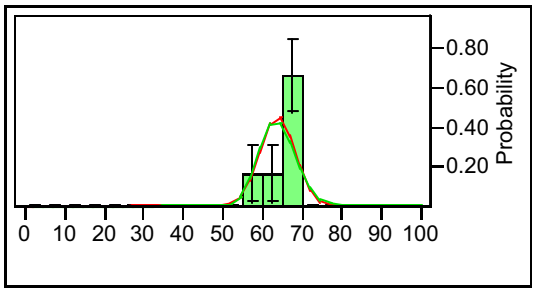

CDF Plot

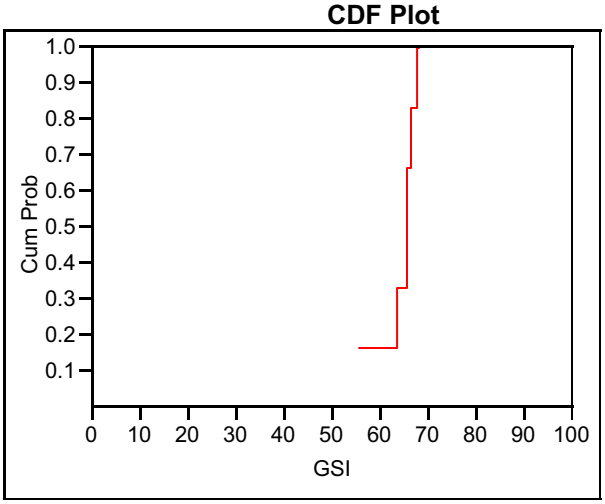

Normal(64.5,4.37035)
LogNormal(4.16462,0.07113)

Quantiles

100.0%	maximum	68.000
99.5%		68.000
97.5%		68.000
90.0%		68.000
75.0%	quartile	67.250
50.0%	median	66.000
25.0%	quartile	62.000
10.0%		56.000
2.5%		56.000
0.5%		56.000
0.0%	minimum	56.000

Moments

Mean	64.5
Std Dev	4.3703547
Std Err Mean	1.7841898
upper 95% Mean	69.086406
lower 95% Mean	59.913594
N	6
Sum Wgt	6
Sum	387
Variance	19.1
Skewness	-1.973075
Kurtosis	4.148735
CV	6.7757437
N Missing	0

Fitted Normal
Parameter Estimates

Type	Parameter	Estimate	Lower 95%	Upper 95%
Location	Mu	64.50000	59.91359	69.08641
Dispersion	Sigma	4.37035	2.72801	10.71879

Fitted LogNormal
Parameter Estimates

Type	Parameter	Estimate	Lower 95%	Upper 95%
Scale	Mu	4.164624	4.089973	4.239275
Shape	Sigma	0.071134	0.047806	0.148618

Litho. Unit w No=13_PTn_Tpcpv1
GSI Distributions

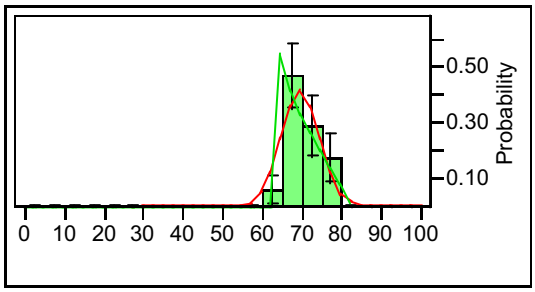

CDF Plot

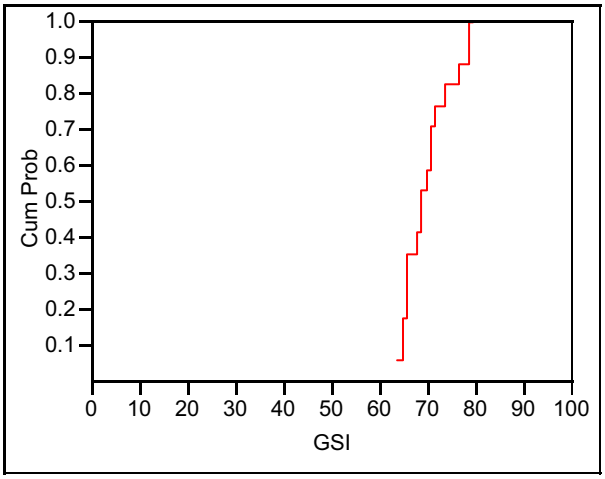

Normal(70.0588,4.82792)

Beta(0.89319,1.89683,63.9,19.1535)

Quantiles

100.0%	maximum	79.000
99.5%		79.000
97.5%		79.000
90.0%		79.000
75.0%	quartile	73.000
50.0%	median	69.000
25.0%	quartile	66.000
10.0%		64.800
2.5%		64.000
0.5%		64.000
0.0%	minimum	64.000

Moments

Mean	70.058824
Std Dev	4.8279212
Std Err Mean	1.1709429
upper 95% Mean	72.541112
lower 95% Mean	67.576535
N	17
Sum Wgt	17
Sum	1191
Variance	23.308824
Skewness	0.7183111
Kurtosis	-0.496932
CV	6.8912394
N Missing	4

Fitted Normal
Parameter Estimates

Type	Parameter	Estimate	Lower 95%	Upper 95%
Location	Mu	70.05882	67.57654	72.54111
Dispersion	Sigma	4.82792	3.59569	7.34775

Fitted Beta
Parameter Estimates

Type	Parameter	Estimate	Lower 95%	Upper 95%
Shape	Alpha	0.89319	.	.
Shape	Beta	1.89683	.	.
Threshold	Theta	63.90000	.	.
Scale	Sigma	19.15350	.	.

Note: unable to converge on all confidence limits.

Litho. Unit w No=16_PTn_Tpbt3
GSI Distributions

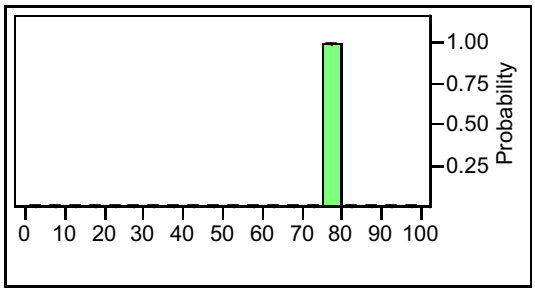

CDF Plot

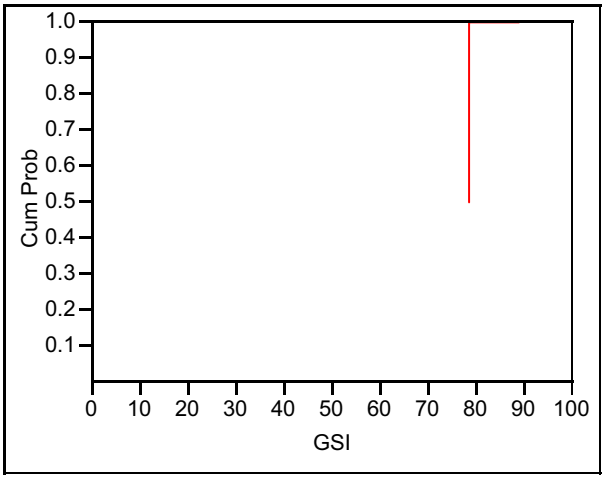

Normal(79,0)

Quantiles

100.0%	maximum	79.000
99.5%		79.000
97.5%		79.000
90.0%		79.000
75.0%	quartile	79.000
50.0%	median	79.000
25.0%	quartile	79.000
10.0%		79.000
2.5%		79.000
0.5%		79.000
0.0%	minimum	79.000

Moments

Mean	79
Std Dev	0
Std Err Mean	0
upper 95% Mean	79
lower 95% Mean	79
N	2
Sum Wgt	2
Sum	158
Variance	0
Skewness	.
Kurtosis	.
CV	0
N Missing	3

Fitted Normal
Parameter Estimates

Type	Parameter	Estimate	Lower 95%	Upper 95%
Location	Mu	79.00000	79.00000	79.00000
Dispersion	Sigma	0.00000	0.00000	0.00000

Litho. Unit w No=17_PTn_Tpp
GSI Distributions

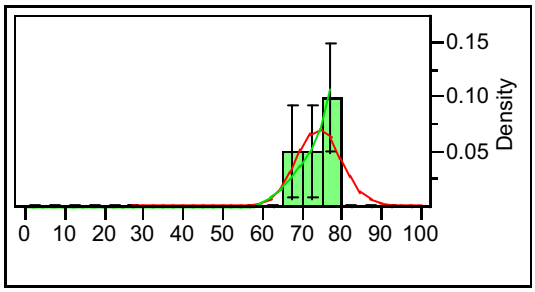

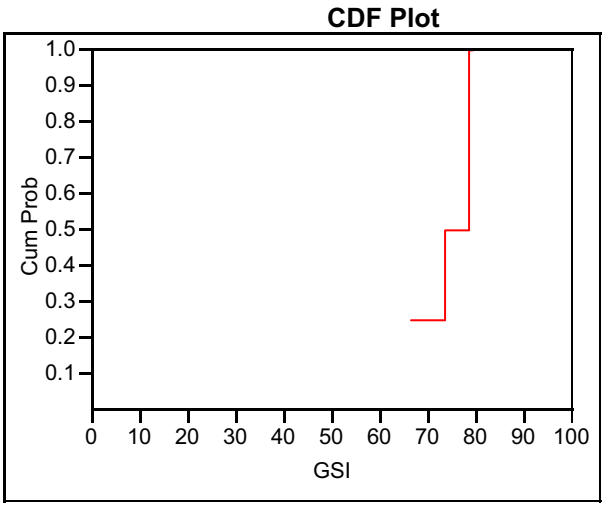

Normal(74.75,5.67891)

Beta(2.19314,0.66961,58.703,20.9648)

Quantiles

100.0%	maximum	79.000
99.5%		79.000
97.5%		79.000
90.0%		79.000
75.0%	quartile	79.000
50.0%	median	76.500
25.0%	quartile	68.750
10.0%		67.000
2.5%		67.000
0.5%		67.000
0.0%	minimum	67.000

Moments

Mean	74.75
Std Dev	5.6789083
Std Err Mean	2.8394542
upper 95% Mean	83.78641
lower 95% Mean	65.71359
N	4
Sum Wgt	4
Sum	299
Variance	32.25
Skewness	-1.137078
Kurtosis	0.1540773
CV	7.5972018
N Missing	21

Fitted Normal
Parameter Estimates

Type	Parameter	Estimate	Lower 95%	Upper 95%
Location	Mu	74.75000	65.71359	83.78641
Dispersion	Sigma	5.67891	3.21704	21.17408

Fitted Beta
Parameter Estimates

Type	Parameter	Estimate	Lower 95%	Upper 95%
Shape	Alpha	2.19314	.	.
Shape	Beta	0.66961	.	.
Threshold	Theta	58.70296	.	.
Scale	Sigma	20.96481	.	.

Note: unable to converge on all confidence limits.

Litho. Unit w No=18_PTn_Tpbt2
GSI Distributions

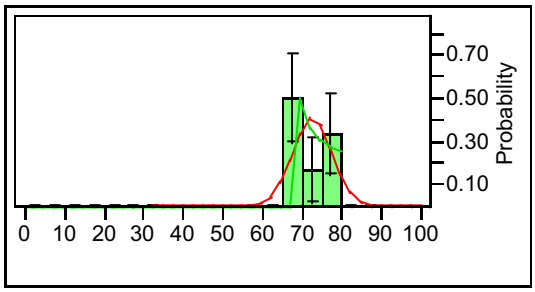

CDF Plot

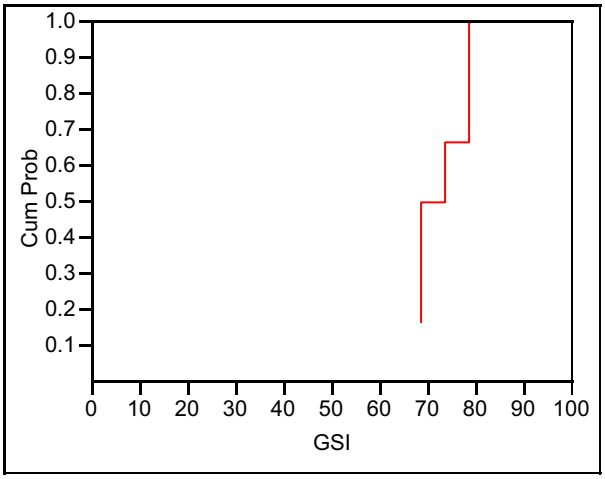

Normal(73.1667,4.91596)

Beta(0.64855,1.0172,68.1449,13.029)

Quantiles

100.0%	maximum	79.000
99.5%		79.000
97.5%		79.000
90.0%		79.000
75.0%	quartile	79.000
50.0%	median	71.500
25.0%	quartile	69.000
10.0%		69.000
2.5%		69.000
0.5%		69.000
0.0%	minimum	69.000

Moments

Mean	73.166667
Std Dev	4.9159604
Std Err Mean	2.0069324
upper 95% Mean	78.325651
lower 95% Mean	68.007683
N	6
Sum Wgt	6
Sum	439
Variance	24.166667
Skewness	0.4559393
Kurtosis	-2.390012
CV	6.7188525
N Missing	7

Fitted Normal
Parameter Estimates

Type	Parameter	Estimate	Lower 95%	Upper 95%
Location	Mu	73.16667	68.00768	78.32565
Dispersion	Sigma	4.91596	3.06858	12.05695

Fitted Beta
Parameter Estimates

Type	Parameter	Estimate	Lower 95%	Upper 95%
Shape	Alpha	0.64855	.	1.366033
Shape	Beta	1.01720	.	.
Threshold	Theta	68.14488	.	.
Scale	Sigma	13.02895	.	.

Note: unable to converge on all confidence limits.

Litho. Unit w No=19_PTn_Tptrv3
GSI Distributions

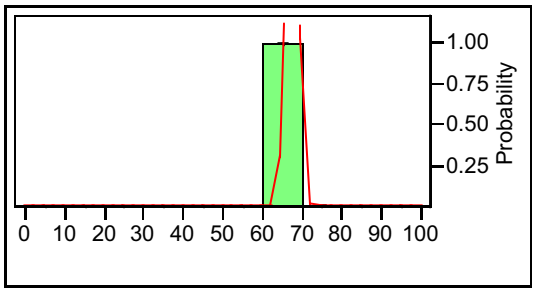

CDF Plot

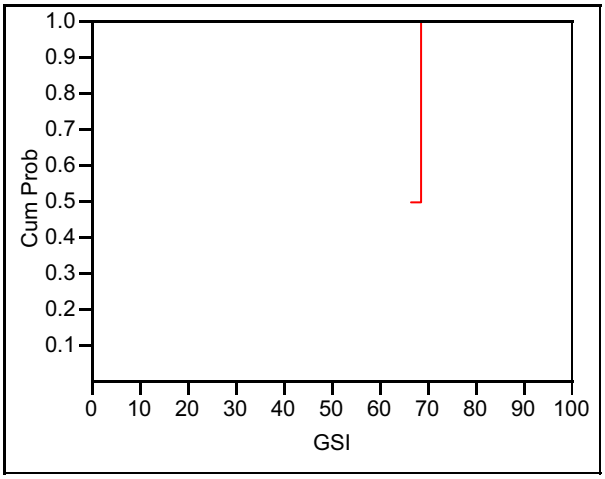

Normal(68,1.41421)

Quantiles

100.0%	maximum	69.000
99.5%		69.000
97.5%		69.000
90.0%		69.000
75.0%	quartile	69.000
50.0%	median	68.000
25.0%	quartile	67.000
10.0%		67.000
2.5%		67.000
0.5%		67.000
0.0%	minimum	67.000

Moments

Mean	68
Std Dev	1.4142136
Std Err Mean	1
upper 95% Mean	80.706205
lower 95% Mean	55.293795
N	2
Sum Wgt	2
Sum	136
Variance	2
Skewness	.
Kurtosis	.
CV	2.0797258
N Missing	1

Fitted Normal
Parameter Estimates

Type	Parameter	Estimate	Lower 95%	Upper 95%
Location	Mu	68.00000	55.29380	80.70620
Dispersion	Sigma	1.41421	0.63095	45.12778

Litho. Unit w No=20_PTn_Tptrv2
GSI Distributions

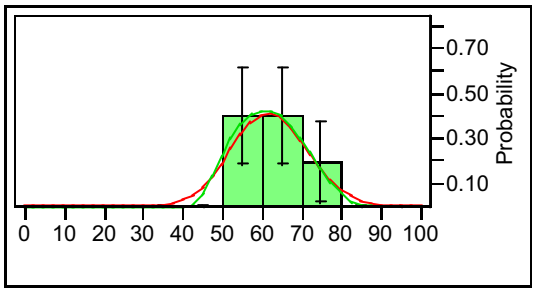

CDF Plot

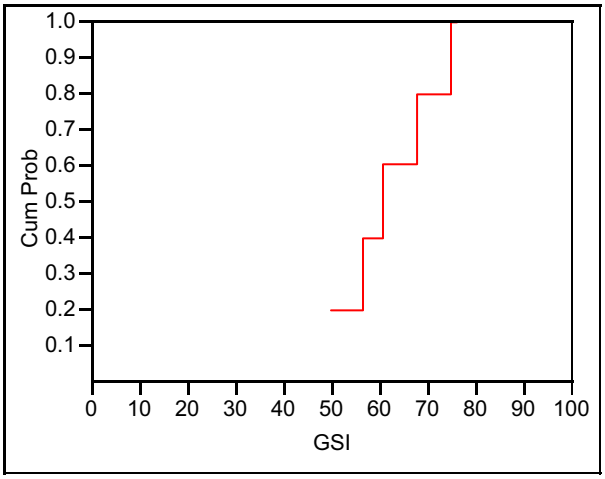

Normal(62.2,9.67988)

Beta(2.89768,3.58883,41.6106,46.0826)

Quantiles

100.0%	maximum	75.000
99.5%		75.000
97.5%		75.000
90.0%		75.000
75.0%	quartile	71.500
50.0%	median	61.000
25.0%	quartile	53.500
10.0%		50.000
2.5%		50.000
0.5%		50.000
0.0%	minimum	50.000

Moments

Mean	62.2
Std Dev	9.679876
Std Err Mean	4.3289722
upper 95% Mean	74.219154
lower 95% Mean	50.180846
N	5
Sum Wgt	5
Sum	311
Variance	93.7
Skewness	0.1534722
Kurtosis	-0.758603
CV	15.562502
N Missing	4

Fitted Normal
Parameter Estimates

Type	Parameter	Estimate	Lower 95%	Upper 95%
Location	Mu	62.20000	50.18085	74.21915
Dispersion	Sigma	9.67988	5.79953	27.81566

Fitted Beta
Parameter Estimates

Type	Parameter	Estimate	Lower 95%	Upper 95%
Shape	Alpha	2.89768	.	.
Shape	Beta	3.58883	.	.
Threshold	Theta	41.61061	.	.
Scale	Sigma	46.08258	.	.

Note: unable to converge on all confidence limits.

Litho. Unit w No=21_TSw1_Tptrv1
GSI Distributions

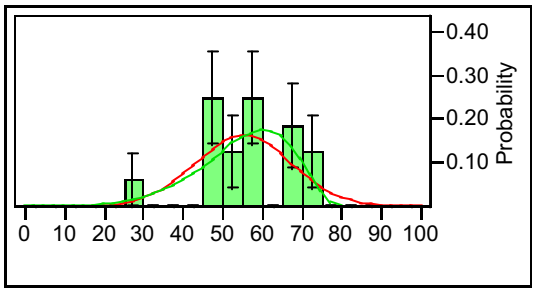

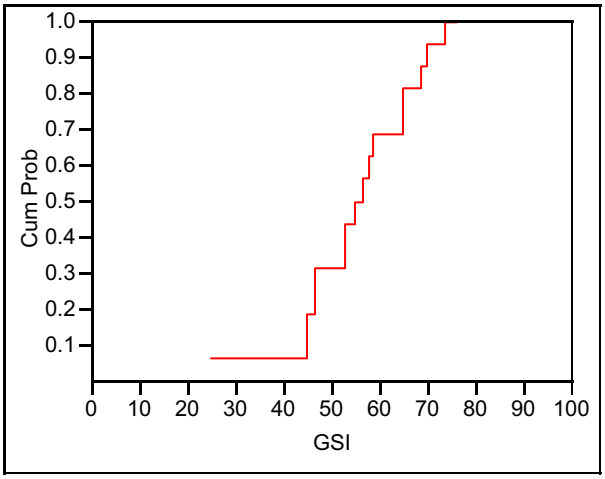

Normal(55.4375,12.2309)

Beta(18.3443,3.58176,-73.744,154.417)

Quantiles

100.0%	maximum	74.000
99.5%		74.000
97.5%		74.000
90.0%		71.200
75.0%	quartile	65.000
50.0%	median	56.000
25.0%	quartile	47.000
10.0%		39.000
2.5%		25.000
0.5%		25.000
0.0%	minimum	25.000

Moments

Mean	55.4375
Std Dev	12.230938
Std Err Mean	3.0577344
upper 95% Mean	61.954907
lower 95% Mean	48.920093
N	16
Sum Wgt	16
Sum	887
Variance	149.59583
Skewness	-0.74577
Kurtosis	1.218388
CV	22.062571
N Missing	7

Fitted Normal
Parameter Estimates

Type	Parameter	Estimate	Lower 95%	Upper 95%
Location	Mu	55.43750	48.92009	61.95491
Dispersion	Sigma	12.23094	9.03505	18.92971

Fitted Beta
Parameter Estimates

Type	Parameter	Estimate	Lower 95%	Upper 95%
Shape	Alpha	18.344	.	.
Shape	Beta	3.582	.	.
Threshold	Theta	-73.744	.	.
Scale	Sigma	154.417	.	.

Note: unable to converge on all confidence limits.

Litho. Unit w No=22_TSw1_Tptrn
GSI Distributions

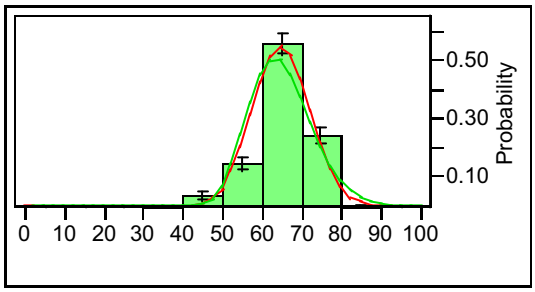

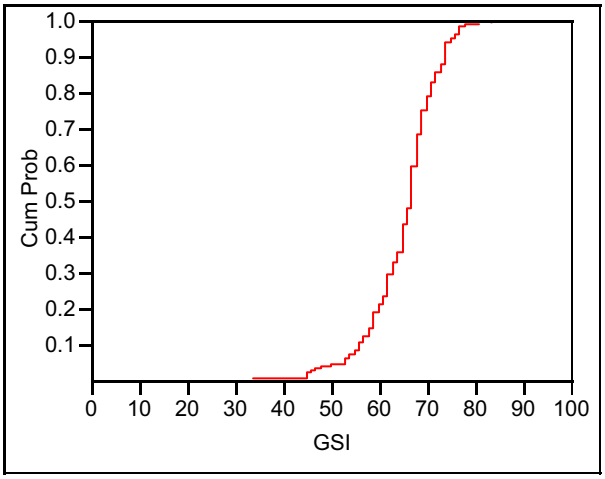

Normal(65.2426,7.29198)

LogNormal(4.17117,0.12203)

Quantiles

100.0%	maximum	81.000
99.5%		81.000
97.5%		77.000
90.0%		74.000
75.0%	quartile	69.500
50.0%	median	67.000
25.0%	quartile	62.000
10.0%		56.000
2.5%		45.250
0.5%		34.000
0.0%	minimum	34.000

Moments

Mean	65.242604
Std Dev	7.2919775
Std Err Mean	0.5609213
upper 95% Mean	66.349966
lower 95% Mean	64.135241
N	169
Sum Wgt	169
Sum	11026
Variance	53.172936
Skewness	-1.032162
Kurtosis	2.0461017
CV	11.176711
N Missing	2

Fitted Normal Parameter Estimates

Type	Parameter	Estimate	Lower 95%	Upper 95%
Location	Mu	65.24260	64.13524	66.34997
Dispersion	Sigma	7.29198	6.58865	8.16473

Fitted LogNormal Parameter Estimates

Type	Parameter	Estimate	Lower 95%	Upper 95%
Scale	Mu	4.171169	4.152638	4.189700
Shape	Sigma	0.122027	0.112051	0.134140

Litho. Unit w No=23_TSw1_Tptrl
GSI Distributions

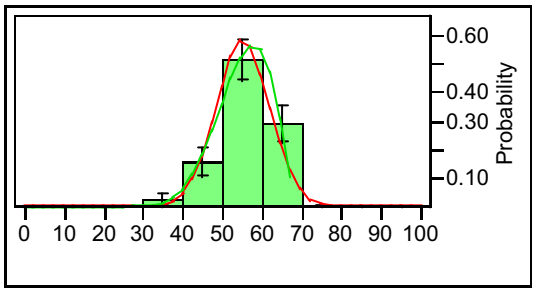

CDF Plot

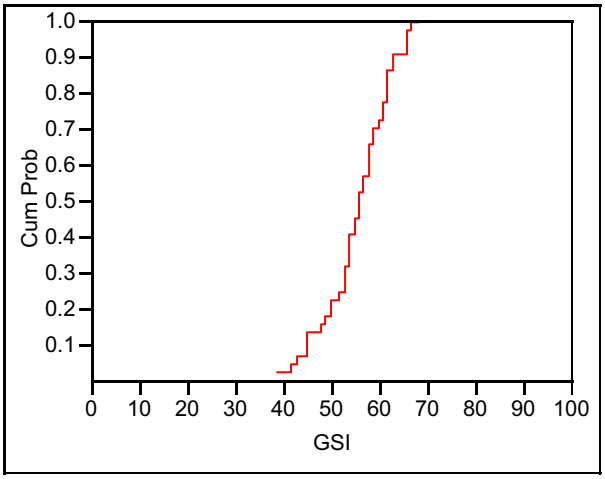

Normal(55.5909,6.85504)

Beta(5.5505,2.50041,25.3053,43.9393)

Quantiles

100.0%	maximum	67.000
99.5%		67.000
97.5%		66.875
90.0%		64.500
75.0%	quartile	61.000
50.0%	median	56.000
25.0%	quartile	52.250
10.0%		45.000
2.5%		39.375
0.5%		39.000
0.0%	minimum	39.000

Moments

Mean	55.590909
Std Dev	6.8550378
Std Err Mean	1.0334358
upper 95% Mean	57.675031
lower 95% Mean	53.506787
N	44
Sum Wgt	44
Sum	2446
Variance	46.991543
Skewness	-0.495171
Kurtosis	-0.221838
CV	12.331221
N Missing	0

Fitted Normal
Parameter Estimates

Type	Parameter	Estimate	Lower 95%	Upper 95%
Location	Mu	55.59091	53.50679	57.67503
Dispersion	Sigma	6.85504	5.66379	8.68551

Fitted Beta
Parameter Estimates

Type	Parameter	Estimate	Lower 95%	Upper 95%
Shape	Alpha	5.55050	.	.
Shape	Beta	2.50041	.	.
Threshold	Theta	25.30526	.	.
Scale	Sigma	43.93926	.	.

Note: unable to converge on all confidence limits.

Litho. Unit w No=25_TSw1_Tptpul
GSI Distributions

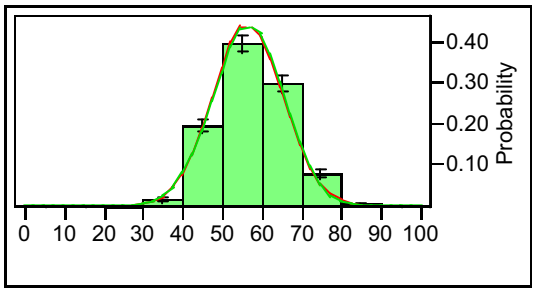

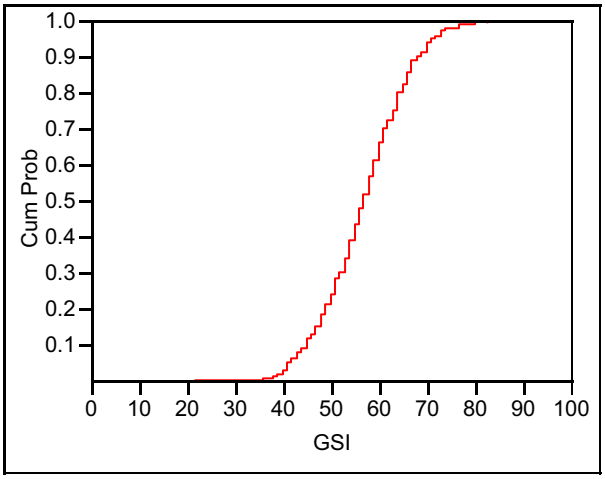

Normal(56.8344,8.98637)

Beta(56.2561,37.5923,-50.1,178.391)

Quantiles

100.0%	maximum	80.000
99.5%		80.000
97.5%		74.000
90.0%		68.000
75.0%	quartile	63.000
50.0%	median	57.000
25.0%	quartile	51.000
10.0%		45.000
2.5%		40.000
0.5%		35.330
0.0%	minimum	22.000

Moments

Mean	56.834409
Std Dev	8.9863701
Std Err Mean	0.4167329
upper 95% Mean	57.653326
lower 95% Mean	56.015491
N	465
Sum Wgt	465
Sum	26428
Variance	80.754848
Skewness	-0.082573
Kurtosis	-0.051976
CV	15.811496
N Missing	5

Fitted Normal
Parameter Estimates

Type	Parameter	Estimate	Lower 95%	Upper 95%
Location	Mu	56.83441	56.01549	57.65333
Dispersion	Sigma	8.98637	8.44354	9.60435

Fitted Beta
Parameter Estimates

Type	Parameter	Estimate	Lower 95%	Upper 95%
Shape	Alpha	56.256	.	.
Shape	Beta	37.592	.	.
Threshold	Theta	-50.100	.	.
Scale	Sigma	178.391	.	.

Note: unable to converge on all confidence limits.

Litho. Unit w No=26_TSw2_Tptpmn
GSI Distributions

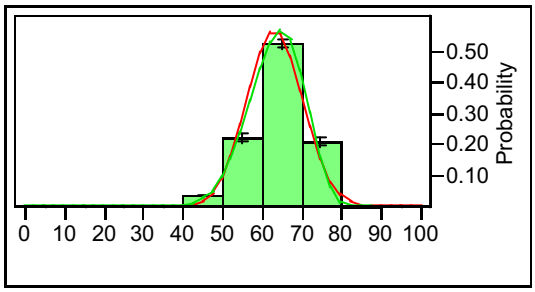

CDF Plot

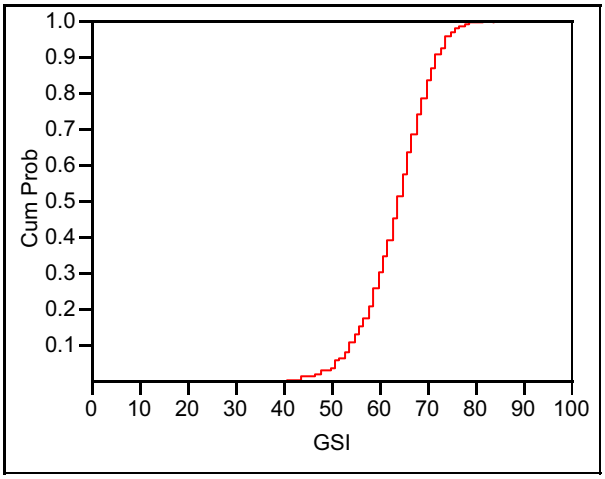

Normal(63.736,7.0364)

Beta(34.2652,9.55878,-25.531,114.17)

Quantiles

100.0%	maximum	82.000
99.5%		79.055
97.5%		76.000
90.0%		72.000
75.0%	quartile	69.000
50.0%	median	64.000
25.0%	quartile	59.000
10.0%		54.000
2.5%		48.000
0.5%		43.945
0.0%	minimum	41.000

Moments

Mean	63.736041
Std Dev	7.0363999
Std Err Mean	0.2506614
upper 95% Mean	64.228085
lower 95% Mean	63.243997
N	788
Sum Wgt	788
Sum	50224
Variance	49.510923
Skewness	-0.398569
Kurtosis	0.105274
CV	11.039907
N Missing	6

Fitted Normal
Parameter Estimates

Type	Parameter	Estimate	Lower 95%	Upper 95%
Location	Mu	63.73604	63.24400	64.22808
Dispersion	Sigma	7.03640	6.70532	7.40213

Fitted Beta
Parameter Estimates

Type	Parameter	Estimate	Lower 95%	Upper 95%
Shape	Alpha	34.265	.	.
Shape	Beta	9.559	.	.
Threshold	Theta	-25.531	.	.
Scale	Sigma	114.170	.	.

Note: unable to converge on all confidence limits.

Litho. Unit w No=27_TSw2_Tptpll
GSI Distributions

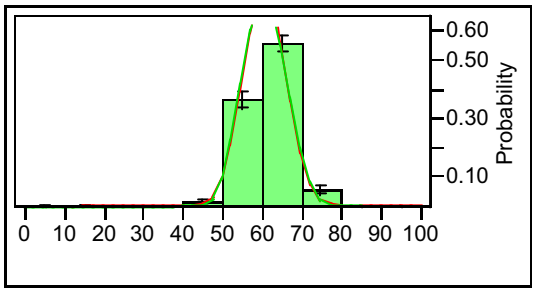

CDF Plot

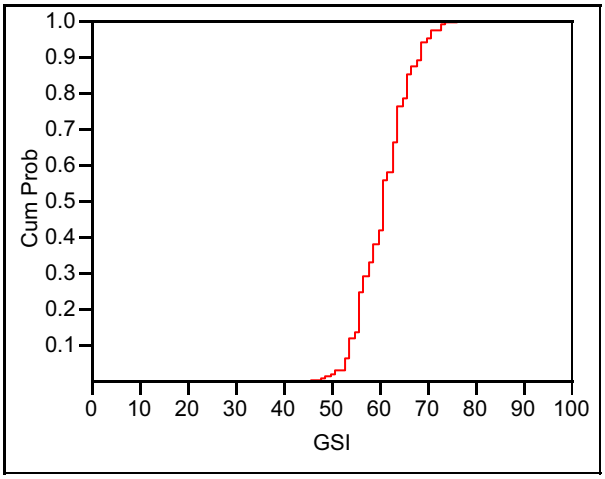

Normal(61.0935,5.40393)

Beta(9.02899,10.4089,38.3932,48.867)

Quantiles

100.0%	maximum	75.000
99.5%		74.925
97.5%		72.250
90.0%		69.000
75.0%	quartile	64.000
50.0%	median	61.000
25.0%	quartile	56.750
10.0%		54.000
2.5%		51.000
0.5%		46.150
0.0%	minimum	46.000

Moments

Mean	61.093458
Std Dev	5.403933
Std Err Mean	0.3694053
upper 95% Mean	61.821616
lower 95% Mean	60.3653
N	214
Sum Wgt	214
Sum	13074
Variance	29.202492
Skewness	0.0601178
Kurtosis	-0.263392
CV	8.8453547
N Missing	7

Fitted Normal
Parameter Estimates

Type	Parameter	Estimate	Lower 95%	Upper 95%
Location	Mu	61.09346	60.36530	61.82162
Dispersion	Sigma	5.40393	4.93587	5.97084

Fitted Beta
Parameter Estimates

Type	Parameter	Estimate	Lower 95%	Upper 95%
Shape	Alpha	9.02899	.	.
Shape	Beta	10.40894	.	.
Threshold	Theta	38.39317	.	.
Scale	Sigma	48.86705	.	.

Note: unable to converge on all confidence limits.

Litho. Unit w No=28_TSw2_Tptpln
GSI Distributions

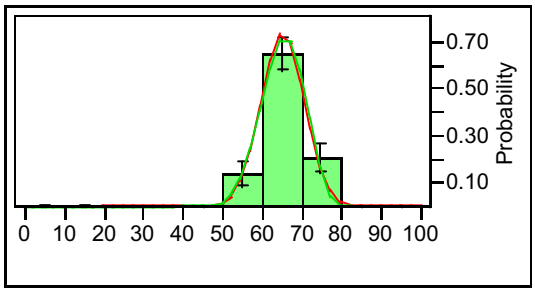

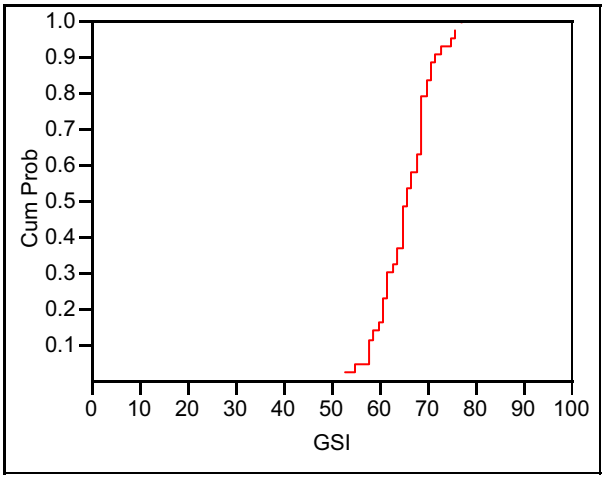

Normal(65.6977,5.40958)

Beta(9.86713,6.45138,38.2548,45.3857)

Quantiles

100.0%	maximum	76.000
99.5%		76.000
97.5%		76.000
90.0%		72.600
75.0%	quartile	69.000
50.0%	median	66.000
25.0%	quartile	62.000
10.0%		58.000
2.5%		53.200
0.5%		53.000
0.0%	minimum	53.000

Moments

Mean	65.697674
Std Dev	5.4095809
Std Err Mean	0.8249534
upper 95% Mean	67.362498
lower 95% Mean	64.032851
N	43
Sum Wgt	43
Sum	2825
Variance	29.263566
Skewness	-0.19703
Kurtosis	-0.263562
CV	8.2340524
N Missing	9

Fitted Normal
Parameter Estimates

Type	Parameter	Estimate	Lower 95%	Upper 95%
Location	Mu	65.69767	64.03285	67.36250
Dispersion	Sigma	5.40958	4.46042	6.87563

Fitted Beta
Parameter Estimates

Type	Parameter	Estimate	Lower 95%	Upper 95%
Shape	Alpha	9.86713	.	.
Shape	Beta	6.45138	.	.
Threshold	Theta	38.25476	.	.
Scale	Sigma	45.38568	.	.

Note: unable to converge on all confidence limits.

APPENDIX G
CHECK OF ROCLAB CALCULATION

H-B Principal Stress and Sig_n vs Tau Envelope Calculation

Source: Hoek, E.; Carranza-Torres, C.; and Corkum, B. 2002. "Hoek-Brown Failure Criterion – 2002 Edition." [5th North American Rock Mechanics Symposium and 17th Tunnelling Association of Canada Conference: NARMS-TAC 2002, July 7-10, University of Toronto]. Toronto, Ontario, Canada: Rocscience. Accessed March 17, 2003. TIC: 253954. [DIRS 162204].

22_TSw1_Tptrn

Hoek Brown Classification	
sigci	63.369 MPa
GSI	65
mi	11.587
D	0
Hoek Brown Criterion	
mb	3.31973
s	0.020468
a	0.501975
Failure Envelope Range	
Application	Tunnels
sig3max	3.27863 MPa
Unit Weight	0.022 MN/m3
Tunnel Depth	300 m
Mohr-Coulomb Fit	
c	1.82742 MPa
phi	48.7218 degrees
Rock Mass Parameters	
sigt	-0.390707 MPa
sigc	8.99662 MPa
sigcm	16.611 MPa
Em	18877.2 MPa

$$\sigma_1' = \sigma_3' + \sigma_{ci}\left(m_b \frac{\sigma_3'}{\sigma_{ci}} + s\right)^a \qquad \text{Eq. 2}$$

$$\sigma_n' = \frac{\sigma_1' + \sigma_3'}{2} - \frac{\sigma_1' - \sigma_3'}{2} \cdot \frac{\frac{d\sigma_1'}{d\sigma_3'} - 1}{\frac{d\sigma_1'}{d\sigma_3'} + 1} \qquad \text{Eq. 8}$$

$$\tau = \left(\sigma_1' - \sigma_3'\right) \frac{\sqrt{\frac{d\sigma_1'}{d\sigma_3'}}}{\frac{d\sigma_1'}{d\sigma_3'} + 1} \qquad \text{Eq. 9}$$

$$\frac{d\sigma_1'}{d\sigma_3'} = 1 + a m_b \left(\frac{m_b \sigma_3'}{\sigma_{ci}} + s\right)^{a-1} \qquad \text{Eq. 10}$$

22_TSw1_Tptrn

Principal Stresses				Normal & Shear Stresses	
Number	Minor Principal Stress (MPa)	Major principal stress - Calc'd (MPa)	(d_sig1'/d_sig3')	Sig_n'	
1	-0.390707	0	9154.973	-0.3906641	0.004083
2	-0.390707	0	9154.97	-0.3906641	0.004083
3	-0.353265	2.418927	38.17	-0.2824831	0.437275
4	-0.315822	3.610019	27.32	-0.1771789	0.724617
5	-0.27838	4.533627	22.50	-0.0736509	0.971208
6	-0.240938	5.318647	19.63	0.02850254	1.193892
7	-0.203496	6.01505	17.67	0.1295108	1.399972
8	-0.166053	6.648475	16.23	0.22952722	1.593490
9	-0.128611	7.234162	15.10	0.32866326	1.776994
10	-0.091169	7.782043	14.19	0.42700452	1.952226
11	-0.053727	8.299019	13.44	0.52461927	2.120446
12	-0.016284	8.790115	12.81	0.62156354	2.282607
13	0.021158	9.259127	12.26	0.7178843	2.439448
14	0.0586	9.709002	11.78	0.81362162	2.591564
15	0.096042	10.14209	11.36	0.90881018	2.739436
16	0.133485	10.56028	10.98	1.00348035	2.883466
17	0.170927	10.96516	10.65	1.09765898	3.023992
18	0.208369	11.35803	10.34	1.19137001	3.161302
19	0.245811	11.73999	10.06	1.28463496	3.295644
20	0.283254	12.112	9.81	1.37747329	3.427234
21	0.320696	12.47488	9.58	1.46990268	3.556261
22	0.358138	12.82933	9.36	1.56193932	3.682893
23	0.39558	13.17598	9.16	1.65359805	3.807277
24	0.433023	13.51538	8.97	1.74489256	3.929548
25	0.470465	13.84802	8.80	1.83583552	4.049825
26	0.507907	14.17433	8.63	1.92643869	4.168216
27	0.545349	14.49471	8.48	2.01671304	4.284819
28	0.582792	14.80951	8.34	2.10666878	4.399724
29	0.620234	15.11904	8.20	2.19631552	4.513011
30	0.657676	15.4236	8.07	2.28566223	4.624757

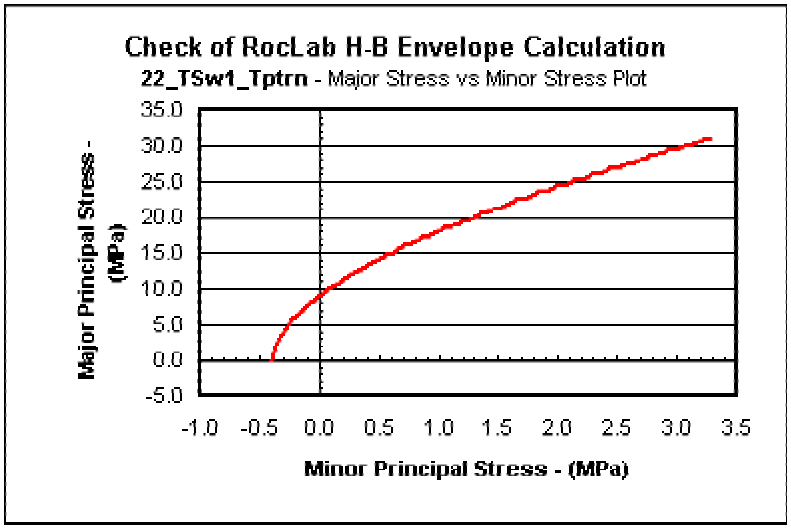

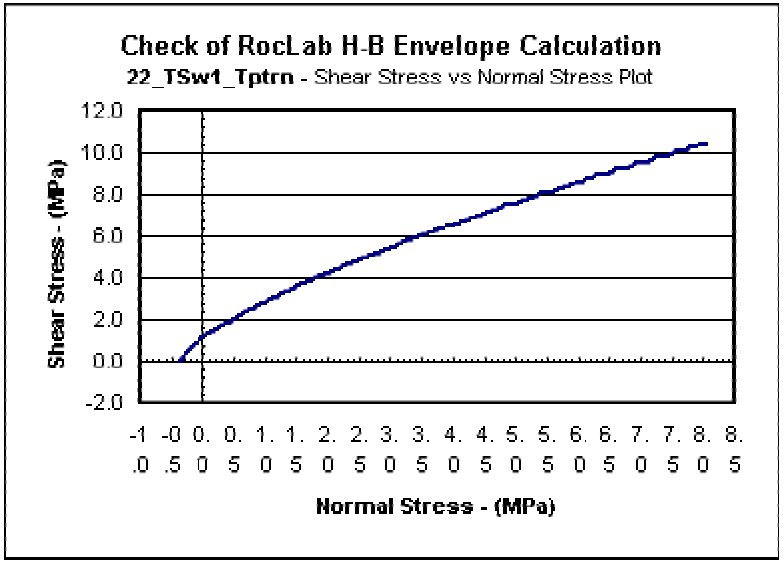

31	0.695118	15.72345	7.95	2.37471738	4.735031
32	0.732561	16.01883	7.83	2.46348894	4.843895
33	0.770003	16.30996	7.72	2.55198446	4.951409
34	0.807445	16.59705	7.62	2.64021105	5.057629
35	0.844887	16.88028	7.51	2.72817548	5.162604
36	0.88233	17.15983	7.42	2.81588415	5.266383
37	0.919772	17.43585	7.33	2.90334317	5.369010
38	0.957214	17.70851	7.24	2.99055834	5.470527
39	0.994656	17.97794	7.15	3.0775352	5.570972
40	1.032099	18.24426	7.07	3.16427902	5.670382
41	1.069541	18.5076	6.99	3.25079486	5.768793
42	1.106983	18.76808	6.92	3.33708755	5.866235
43	1.144425	19.02579	6.85	3.4231617	5.962741
44	1.181868	19.28085	6.78	3.50902176	6.058339
45	1.21931	19.53334	6.71	3.59467198	6.153056
46	1.256752	19.78335	6.64	3.68011645	6.246919
47	1.294194	20.03097	6.58	3.7653591	6.339953
48	1.331637	20.27628	6.52	3.8504037	6.432181
49	1.369079	20.51935	6.46	3.9352539	6.523625
50	1.406521	20.76025	6.41	4.0199132	6.614307
51	1.443963	20.99905	6.35	4.104385	6.704247
52	1.481406	21.23581	6.30	4.18867255	6.793464
53	1.518848	21.4706	6.24	4.272779	6.881978
54	1.55629	21.70347	6.19	4.35670742	6.969805
55	1.593732	21.93448	6.15	4.44046073	7.056962
56	1.631175	22.16368	6.10	4.52404179	7.143467
57	1.668617	22.39111	6.05	4.60745336	7.229334
58	1.706059	22.61684	6.01	4.69069811	7.314578
59	1.743501	22.84089	5.96	4.77377864	7.399214
60	1.780944	23.06333	5.92	4.85669745	7.483256
61	1.818386	23.28418	5.88	4.93945699	7.566716
62	1.855828	23.50349	5.84	5.02205962	7.649607
63	1.89327	23.7213	5.80	5.10450763	7.731942
64	1.930713	23.93764	5.76	5.18680325	7.813732
65	1.968155	24.15255	5.72	5.26894866	7.894990
66	2.005597	24.36606	5.68	5.35094597	7.975724

67	2.043039	24.5782	5.65	5.43279722	8.055948
68	2.080482	24.78902	5.61	5.51450442	8.135669
69	2.117924	24.99853	5.58	5.5960695	8.214899
70	2.155366	25.20676	5.54	5.67749436	8.293647
71	2.192808	25.41375	5.51	5.75878085	8.371922
72	2.230251	25.61952	5.48	5.83993075	8.449733
73	2.267693	25.82409	5.45	5.92094583	8.527088
74	2.305135	26.0275	5.42	6.00182779	8.603997
75	2.342577	26.22977	5.39	6.0825783	8.680467
76	2.38002	26.43091	5.36	6.16319898	8.756505
77	2.417462	26.63095	5.33	6.24369143	8.832120
78	2.454904	26.82992	5.30	6.3240572	8.907319
79	2.492346	27.02784	5.27	6.4042978	8.982109
80	2.529789	27.22471	5.24	6.4844147	9.056497
81	2.567231	27.42058	5.22	6.56440937	9.130489
82	2.604673	27.61545	5.19	6.6442832	9.204093
83	2.642115	27.80934	5.17	6.72403759	9.277315
84	2.679558	28.00227	5.14	6.80367389	9.350160
85	2.717	28.19426	5.12	6.88319342	9.422635
86	2.754442	28.38533	5.09	6.96259748	9.494745
87	2.791884	28.57549	5.07	7.04188732	9.566497
88	2.829326	28.76475	5.04	7.12106421	9.637896
89	2.866769	28.95314	5.02	7.20012934	9.708947
90	2.904211	29.14067	5.00	7.27908391	9.779656
91	2.941653	29.32735	4.97	7.35792909	9.850027
92	2.979095	29.5132	4.95	7.43666602	9.920066
93	3.016538	29.69823	4.93	7.51529582	9.989777
94	3.05398	29.88245	4.91	7.59381959	10.059166
95	3.091422	30.06588	4.89	7.6722384	10.128236
96	3.128864	30.24854	4.87	7.75055332	10.196993
97	3.166307	30.43042	4.85	7.82876537	10.265441
98	3.203749	30.61155	4.83	7.90687558	10.333584
99	3.241191	30.79193	4.81	7.98488493	10.401426
100	3.278633	30.97159	4.79	8.06279442	10.468971

Normal Stress vs. Shear Stress			Normal vs Tau Stress Checked Values	
Number	Normal stress (MPa)	Shear stress (MPa)	Normal stress (Calc'd) (MPa)	Shear stress (Calc'd) (MPa)
1	-0.390707	0	-0.390664	0.004083
2	-0.390707	0	-0.390664	0.004083
3	-0.282484	0.437274	-0.282483	0.437275
4	-0.177179	0.724616	-0.177179	0.724617
5	-0.073651	0.971207	-0.073651	0.971208
6	0.028502	1.193891	0.028503	1.193892
7	0.12951	1.399971	0.129511	1.399972
8	0.229527	1.593489	0.229527	1.593490
9	0.328663	1.776993	0.328663	1.776994
10	0.427004	1.952225	0.427005	1.952226
11	0.524619	2.120446	0.524619	2.120446
12	0.621563	2.282606	0.621564	2.282607
13	0.717884	2.439448	0.717884	2.439448
14	0.813621	2.591563	0.813622	2.591564
15	0.90881	2.739436	0.90881	2.739436
16	1.00348	2.883466	1.00348	2.883466
17	1.097659	3.023992	1.097659	3.023992
18	1.19137	3.161302	1.19137	3.161302
19	1.284635	3.295644	1.284635	3.295644
20	1.377473	3.427234	1.377473	3.427234
21	1.469902	3.556261	1.469903	3.556261
22	1.561939	3.682892	1.561939	3.682893
23	1.653598	3.807277	1.653598	3.807277
24	1.744892	3.929548	1.744893	3.929548
25	1.835835	4.049825	1.835836	4.049825
26	1.926438	4.168216	1.926439	4.168216
27	2.016713	4.284819	2.016713	4.284819
28	2.106668	4.399723	2.106669	4.399724
29	2.196315	4.513011	2.196316	4.513011
30	2.285662	4.624757	2.285662	4.624757
31	2.374717	4.73503	2.374717	4.735031
32	2.463489	4.843894	2.463489	4.843895

33	2.551984	4.951409	2.551984	4.951409
34	2.640211	5.057628	2.640211	5.057629
35	2.728175	5.162604	2.728175	5.162604
36	2.815884	5.266383	2.815884	5.266383
37	2.903343	5.36901	2.903343	5.369010
38	2.990558	5.470526	2.990558	5.470527
39	3.077535	5.570971	3.077535	5.570972
40	3.164279	5.670382	3.164279	5.670382
41	3.250794	5.768792	3.250795	5.768793
42	3.337087	5.866235	3.337088	5.866235
43	3.423161	5.96274	3.423162	5.962741
44	3.509021	6.058338	3.509022	6.058339
45	3.594672	6.153056	3.594672	6.153056
46	3.680116	6.246919	3.680116	6.246919
47	3.765359	6.339952	3.765359	6.339953
48	3.850403	6.43218	3.850404	6.432181
49	3.935253	6.523624	3.935254	6.523625
50	4.019913	6.614306	4.019913	6.614307
51	4.104384	6.704246	4.104385	6.704247
52	4.188672	6.793464	4.188673	6.793464
53	4.272778	6.881977	4.272779	6.881978
54	4.356707	6.969804	4.356707	6.969805
55	4.44046	7.056962	4.440461	7.056962
56	4.524041	7.143466	4.524042	7.143467
57	4.607453	7.229333	4.607453	7.229334
58	4.690698	7.314578	4.690698	7.314578
59	4.773778	7.399214	4.773779	7.399214
60	4.856697	7.483255	4.856697	7.483256
61	4.939456	7.566715	4.939457	7.566716
62	5.022059	7.649606	5.02206	7.649607
63	5.104507	7.731941	5.104508	7.731942
64	5.186803	7.813732	5.186803	7.813732
65	5.268948	7.894989	5.268949	7.894990
66	5.350945	7.975724	5.350946	7.975724
67	5.432797	8.055947	5.432797	8.055948
68	5.514504	8.135669	5.514504	8.135669

69	5.596069	8.214898	5.59607	8.214899
70	5.677494	8.293646	5.677494	8.293647
71	5.75878	8.371921	5.758781	8.371922
72	5.83993	8.449732	5.839931	8.449733
73	5.920945	8.527088	5.920946	8.527088
74	6.001827	8.603996	6.001828	8.603997
75	6.082578	8.680466	6.082578	8.680467
76	6.163198	8.756504	6.163199	8.756505
77	6.243691	8.832119	6.243691	8.832120
78	6.324056	8.907318	6.324057	8.907319
79	6.404297	8.982108	6.404298	8.982109
80	6.484414	9.056496	6.484415	9.056497
81	6.564409	9.130489	6.564409	9.130489
82	6.644282	9.204092	6.644283	9.204093
83	6.724037	9.277314	6.724038	9.277315
84	6.803673	9.350159	6.803674	9.350160
85	6.883193	9.422634	6.883193	9.422635
86	6.962597	9.494745	6.962597	9.494745
87	7.041886	9.566496	7.041887	9.566497
88	7.121063	9.637895	7.121064	9.637896
89	7.200128	9.708946	7.200129	9.708947
90	7.279083	9.779655	7.279084	9.779656
91	7.357928	9.850026	7.357929	9.850027
92	7.436665	9.920065	7.436666	9.920066
93	7.515295	9.989777	7.515296	9.989777
94	7.593819	10.05917	7.59382	10.059166
95	7.672237	10.12824	7.672238	10.128236
96	7.750552	10.19699	7.750553	10.196993
97	7.828764	10.26544	7.828765	10.265441
98	7.906875	10.33358	7.906876	10.333584
99	7.984884	10.40142	7.984885	10.401426
100	8.062793	10.46897	8.062794	10.468971

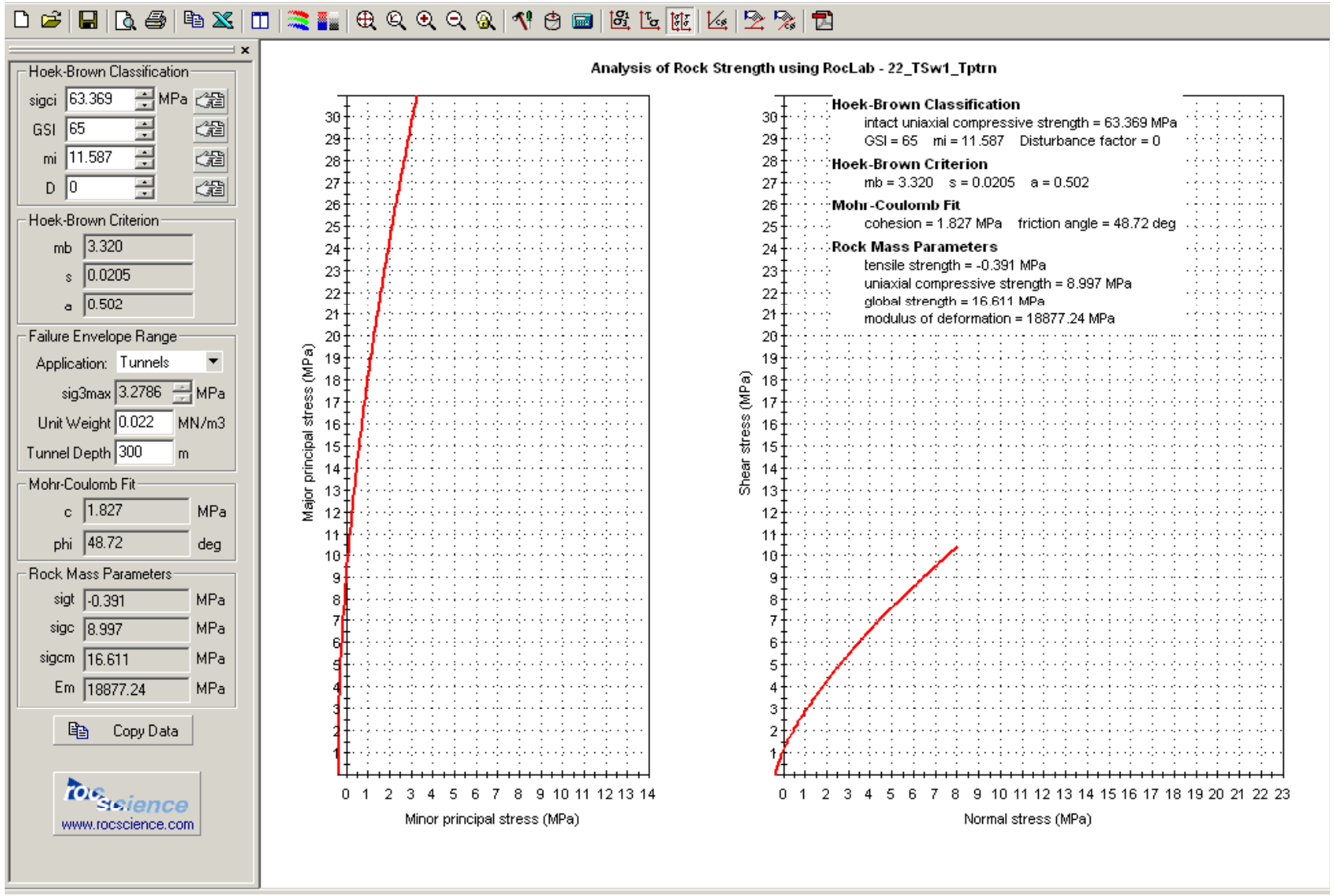

Note that the calculation results obtained using RocLab and Excel are identical.

Figure G-1. An example of graphical output obtained from the RocLab

APPENDIX H

LIST OF FILES CONTAINED ON CD INCLUDING ONE (1) CD

CD File List

File Name	File Size, KB	File type	Date and Time Created
Appendix_A	24	Microsoft Word	1/10/2007 7:38 AM
Appendix_B	24	Microsoft Word	1/10/2007 7:38 AM
Appendix_C	2,253	Microsoft Word	1/10/2007 7:39 AM
Appendix_D	3,722	Microsoft Word	1/10/2007 7:39 AM
Appendix_E	10,973	Microsoft Word	1/10/2007 7:40 AM
Appendix_F	384	Microsoft Word	1/10/2007 7:40 AM
Appendix_G	365	Microsoft Word	1/10/2007 7:40 AM
Rock Mass Strength Parameters - All_Plus Porosity_Based Data	96	Microsoft Excel	12/11/2006 2:54 PM
Sig_V and Stress Around Tunnel - 101606	127	Microsoft Excel	12/6/2006 1:38 PM
Surface and ESF Centerline Elevations - 101606	4,706	Microsoft Excel	12/12/2006 3:04 PM
Table A-1	497	Microsoft Excel	1/10/2007 7:42 AM
Table A-2	117	Microsoft Excel	1/10/2007 7:42 AM
Table A-3	257	Microsoft Excel	1/10/2007 7:42 AM
Table B-1	211	Microsoft Excel	1/10/2007 7:43 AM
Table B-2	53	Microsoft Excel	1/10/2007 7:43 AM
Table B-3	28	Microsoft Excel	1/10/2007 7:44 AM
Worksheet_Dynamic Data	270	Microsoft Excel	12/12/2006 2:12 PM
Worksheet_Indirect Tensile Strength Data	431	Microsoft Excel	12/12/2006 2:11 PM
Worksheet_Mohr-Coulomb Parameters	258	Microsoft Excel	12/12/2006 2:24 PM
Worksheet_Static Data	1,144	Microsoft Excel	12/11/2006 2:49 PM